Cranfield University

School of Applied Sciences

Integrated Earth System Sciences Institute

PhD Thesis

Academic Year 2005 - 2006

Mónica Rivas Casado

The use of geostatistics for hydromorphological assessment in rivers

Supervisor Professor Sue White

6 October 2006

This thesis is submitted in fulfilment of the requirements for the Degree of Doctor of Philosophy

The use of geostatistics for hydromorphological assessment in rivers

ABSTRACT

Assessment of river rehabilitation and restoration projects, as well as the monitoring of morphological changes in rivers requires collection of hydromorphological parameter data (i.e. depth, velocity and substrate). Field data collection is highly time and cost consuming and thus, effective and efficient monitoring programmes need to be designed. Interpolation techniques are often used to predict values of the variables under study at non measured locations. In this way, it is not necessary to collect detailed data sets of information. The accuracy of these predictions depends upon (i) the method used for the interpolation and/or extrapolation procedure and (ii) the sampling strategy applied for the collection of data. Even though the design of effective sampling strategies are of crucial importance when applying interpolation techniques, little work has been developed to determine the most effective way to collect hydromorphological data for this purpose.

This project aimed to define a set of guidelines for effective and efficient hydromorphological data collection in rivers and relate this to the type of river site that is being sampled and to the objective for which the data are being collected. The project is structured in three main sections: spatial problem, the scaling problem and the temporal problem. Spatial problem refers to the location and number of points that need to be collected. Scaling problems focus on the study of the river length that needs to be sampled to characterise the spatial variability of a river site, whilst temporal problems determine how often a river site needs to be sampled to characterise the temporal variability associated with changes in discharge. Intensive depth data sets have been collected at a total of 20 river sites. These data sets have been used to investigate the spatial, temporal and scaling problems through geostatistical theory.

Acknowledgements

Para mi padre, por el apoyo moral y económico de tantos años,
para mi madre, por estar siempre ahí.
para Dan, con la ilusión y el entusiasmo del primer día…
pero sobre todo, para Sue White y para Pat Bellamy,
sin cuyo apoyo y esfuerzo esto no hubiera sido posible.

Mónica Rivas Casado

I would like to thank CEH Wallingford for providing funding and logistical support for the development of this research project.

I would also like to thank Venkatesh Merwade, Helmut Mader, Ian Maddock and Gregor Laaha and the thesis committee members: Andrew Gill and Tim Hess.

Table of Contents

List of Appendices

List of Tables

Chapter 6

Chapter 7

Chapter 8

Chapter 9

List of Figures

Chapter 4

Chapter 5

Chapter 6

Chapter 7

Chapter 8

1

Introduction

1.1. The need for hydromorphological sampling and monitoring in rivers

1.2. The problems of current hydromorphological sampling strategies

1.3. Aim and objectives of this research project.

1.4. Layout of the thesis

1.5. The river sites

This chapter describes the need for hydromorphological data collection in rivers. It also briefly identifies and describes the main problems of current hydromorphological sampling strategies, states the aim and objectives of this research project and describes the contents of the thesis, chapter by chapter.

1.1. The need for hydromorphological sampling and monitoring in rivers

Rivers change their characteristics throughout their length, from the point of origin onwards, following what is described as the continuum concept (Vannote et al., 1980). This theory describes the structure and function of communities along a river system; physical, chemical and biological changes occur on a longitudinal gradient from the headwater to the lower reaches. Stream communities are located in those areas with physical and chemical characteristics for which they are biologically adapted. The characteristic producer and consumer communities at a given reach of the river continuum conform to the manner in which the river system utilizes its kinetic energy in achieving a dynamic balance. Figure 1.1 illustrates the continuum concept. Physical characteristics of the river change towards lower reaches and so, the communities of vertebrates, invertebrates and flora are different at each stage.

The river continuum concept has been commented and discussed from many aspects, a summary of which can be encountered in Statzner and Higler (1985). The simplified way of describing river dynamics used by Vannote et al (1980) presented the following limitations (Statzner and Higler, 1985): (i) the concept was developed for natural, unperturbed stream ecosystems, (ii) streams with characteristics different to those for which the concept was developed may deviate from the general pattern, (iii) the concept does not consider the various types of stream types and (iv) it does not

consider the variations that macroinvertebrate species might have on their diet according to age.

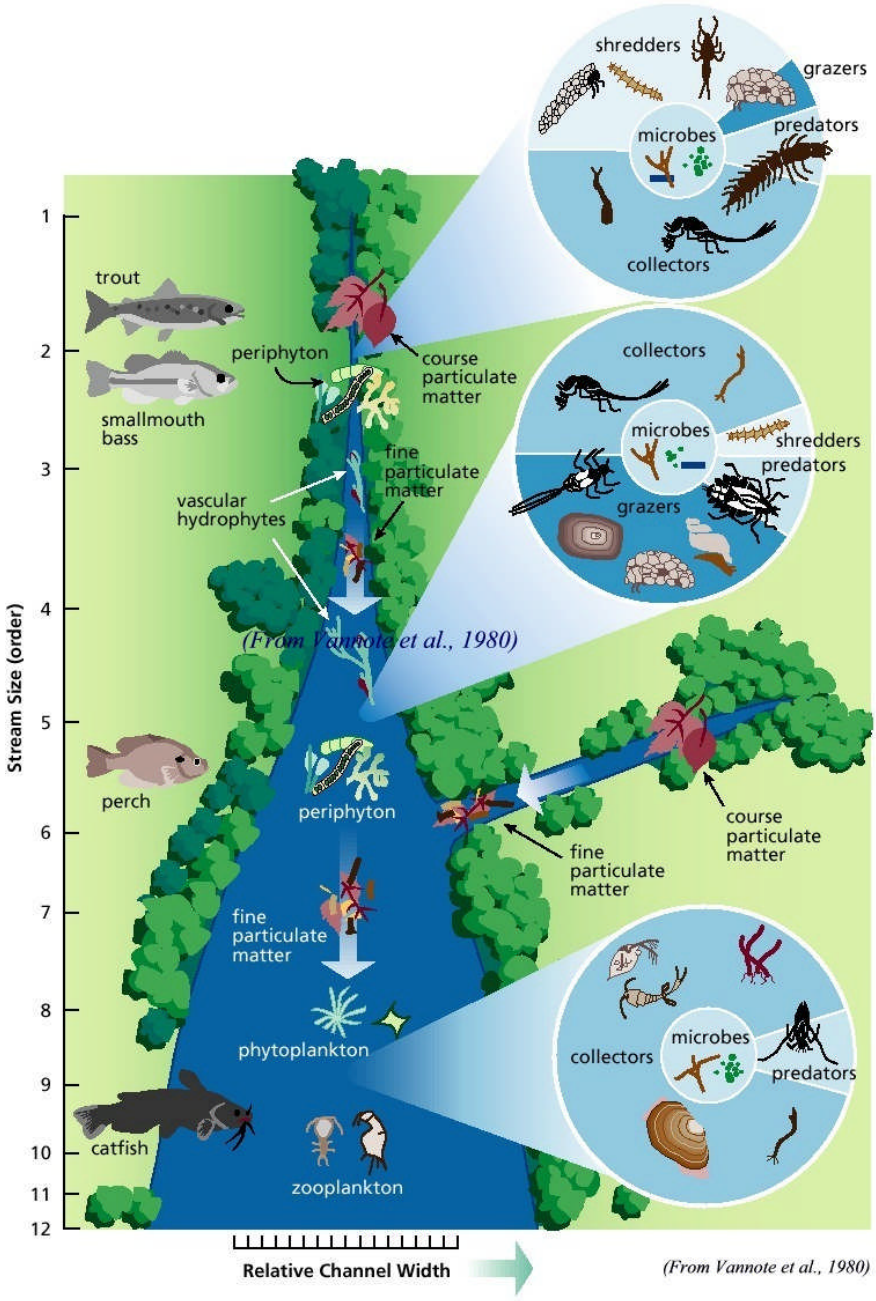

Figure 1.1: illustration of the continuum concept showing changes on the river from headwaters to lower reaches.

For the purpose of this study it will be considered that natural channels conform to the river continuum concept. Therefore, the comparison of physical, chemical and biological characteristics of a river reach with those expected from the continuum concept will help to determine the ecological quality of the system (i.e. its proximity to a pristine status). The study of the complete river is not possible as this would be

highly time and cost consuming. Instead, representative reaches of the river may be selected and characterised. The main variables used to describe or asses river reaches include; biological, chemical/physico-chemical and hydromorphological elements (Directive 2000/60.EC). The first group defines the community structure present at the site and it is defined by variables such as composition and abundance of aquatic flora, composition and abundance of benthic invertebrate fauna and composition & age structure of fish fauna, among others.

Chemical and physico-chemical elements define the water quality at the river reach under analysis. The main variables measured to identify the chemical / physico-chemical composition are: thermal conditions, oxygenation conditions, salinity, acidification status, nutrient concentration and presence of specific pollutants.

Finally, hydromorphological parameters define the shape and structure of the river channel, this is the physical structure described in the continuum, which provides information on the physical characteristics of the river and therefore, information on the potential stream communities that could be encountered at the site. Variables that are measured in this group are: river depth and width variation, structure & substrate of the river bed and structure of the riparian zone. Many other variables can be considered for river characterisation, such as: catchment characteristics (geology, climate, hydrology, flow regime, erosion rates) and habitat characteristics (i.e. mesohabitat types and flow types), among others.

Hydromorphological data are collected for three main purposes: modelling, river assessment and research studies. River models are developed to simulate the status of variables under interest for selected scenarios. The range of variables under interest depends on the final objective of the study and includes, for example, water quality (San Martin et al., 2004), fish habitat (Hardy & Addley, 2003) and consequences of changes in discharge or fluvial bank erosion (Darby et al., 2004). By modelling the status of the river site for a specific scenario (i.e. dam construction, increase in the pollution, flow change or river restoration) it is possible (i) to understand how the system will improve or degrade under specific conditions and (ii) to undertake decisions on river management and river appraisal methods. The development of these models may include either a hydraulic or a hydrodynamic component that

requires the description of the hydromorphological variables of the river site under study.

Assessment and monitoring of hydromorphological characteristics is carried out to analyse the physical status of a river system at a specific time or over a time period for ecological and management purposes. Some of the objectives for which hydromorphology is assessed are (i) to categorise the change of the river physical status according to consequences of anthropogenic measures that will be taken in the future or that have been undertaken in the past and (ii) to evaluate the remoteness of the river from a potential natural form (Bizjak & Mikos, 2004). Hence, the impact of dam constructions (Woo et al., 2004), flow regulation (Hauer et al., 2004) or the improvement achieved after developing a river restoration project (Muhar et al., 2004) are some of the changes that can be assessed through the monitoring of hydromorphology variables. These objectives are in agreement with those defined for model development. Therefore, assessment and monitoring of rivers is a useful tool to validate a model and determine whether the model results are simulating the system as expected.

Finally, hydromorphological data may be collected during the development of research projects. Research studies are carried out (i) to increase the knowledge of river dynamics described in the continuum concept and (ii) to propose new and more efficient methodologies for river characterisation - representation at chemical, physical and community structure level. This in turn will help to develop more accurate and sophisticated river models. Examples of studies that can be considered under these frameworks are provided by several authors (Alfredsen et al., 2004a, Alfredsen et al., 2004b, Hauer et al., 2004 and Magdaleno et al., 2004).

Hydromorphological data collection in rivers is necessary for many purposes, some of which have been described above. Effective and efficient sampling strategies need to be applied in each case in order (i) to reduce the time and economic costs and (ii) to achieve a specific accuracy level. The next section briefly states the problems of current hydromorphological sampling strategies and assesses whether they meet these two requirements.

1.2. The problems of current hydromorphological sampling strategies

Rivers occur in a wide range of forms and shapes determined by the catchment characteristics in which the river flows. Development of a common hydromorphological sampling strategy that can be easily applied for all rivers is difficult, if not impracticable, due to the variety of rivers that can be found. Current hydromorphological sampling strategies have been designed for specific purposes and river sites. These sampling strategies have been applied to other objectives or study areas without adaptation. As a result three main problems can be identified: spatial problems, scaling problems and temporal problems.

1.2.1. Spatial problems

Spatial problems describe the limitations of current sampling strategies when trying to characterise the hydromorphological features of a selected river reach at a specific time, as if a picture was taken. Five main spatial problems can be identified: (i) no consideration of the spatial variation of the river, (ii) lack of consensus on the sample strategy to be applied, (iii) inability to provide levels of accuracy for the characterised river reach, (iv) lack of consensus on the length of river reach to be sampled and (v) subjectivity in the determination of specific hydromorphological features.

Generally, hydromorphological features are measured by placing regularly or irregularly spaced cross-sections in the selected river reach. Cross-sections are distributed at the river site by analysing visible river features (e.g. mesohabitats, flow types or river bed shape) that describe the variability of the site. Information is collected at equidistantly distributed points across each cross-section and later on interpolated between cross-sections. The general and easy way of interpolating the collected data is by considering that the inter-cross-sectional space does not change between cross-sections (e.g. Waddle, 2001). This introduces errors in the characterisation of the site since (i) cross-sections can be located at intervals that do not represent all the spatial information and (ii) detail can be lost in the interpolation procedure.

An example of potential errors is shown in Figure 1.2, which identifies three cross-sections (red dots) placed in a river reach and their respective sampling points. The low concentration of suspended sediments in the river site allows visual determination of the river bed features and therefore, placing of the cross-sections in the adequate spots. However, if the turbidity was high enough to obscure the channel bed, the intermediate features defined by cross-section 2 may not be identified and therefore, cross-sections 1 and 3 could be considered sufficient for the hydromorphological characterisation, when they are not.

The lack of consensus on the sampling strategy to be applied implies that there is no agreement on the number of points that need to be collected and where they need to be located. It also reflects the variation in physical structure between different rivers. Therefore, many possible combinations of location and number of points may be applied at a selected river site. Figure 1.3 shows two sampling densities and two strategies for point distribution that could be implemented at the selected reach. Which one is better? The question does not have an easy answer as this will depend on the final objective for which the data are collected and the level of accuracy required from the study.

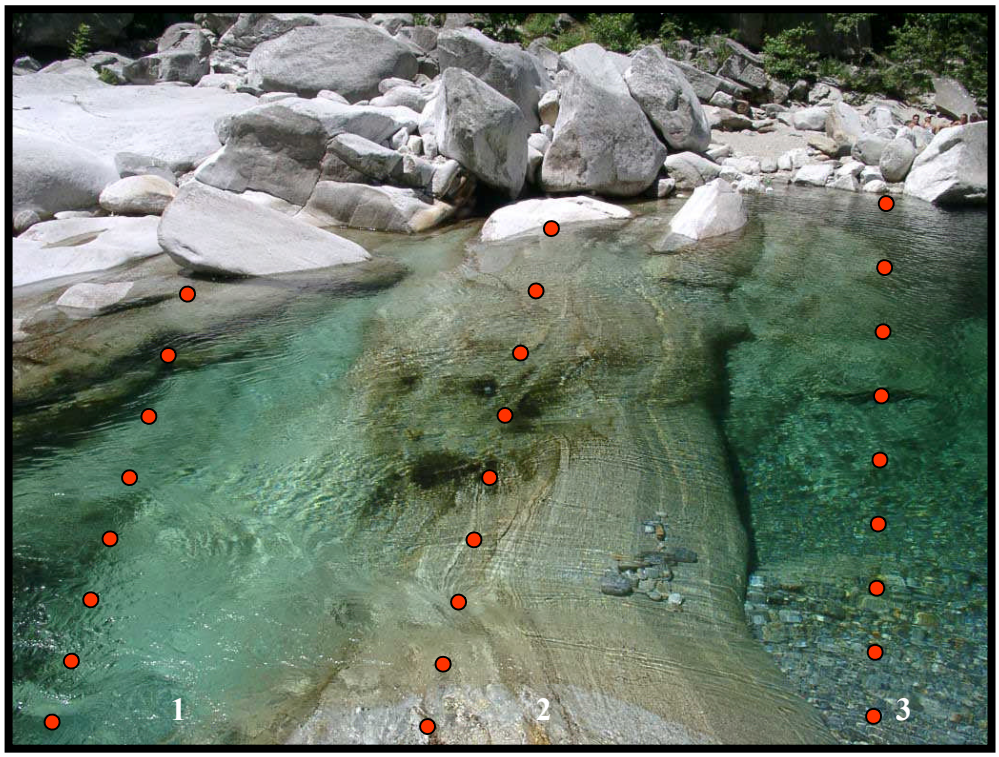

Figure 1.2: example of three equidistant cross-sections placed at the river site for the characterisation of hydromorphological features.

Current hydromorphological sampling strategies provide a simplified representation of the river site since parameters are measured at specific locations to either (i) obtain representative values of the reach features or (ii) to interpolate the results to the whole sampled reach later on. In the latter case, the error needs to be considered and accounted for when analysing the interpolated results. This can be achieved by determining the difference between the interpolated representation of the hydromorphological features and the true characteristics of the site. This difference between observed and predicted (interpolated) values is known as the prediction error. The accuracy level of the sampling and interpolated procedure can be obtained through the calculation of this prediction error. Accuracy values are not usually provided since (i) this requires more data collection to calculate the error between interpolated and measured values, (ii) it is assumed that the inter-cross-sectional variability is small or (iii) the interpolation technique applied does not allow the determination of the standard error of the predictions (e.g. Inverse Distance Weighting).

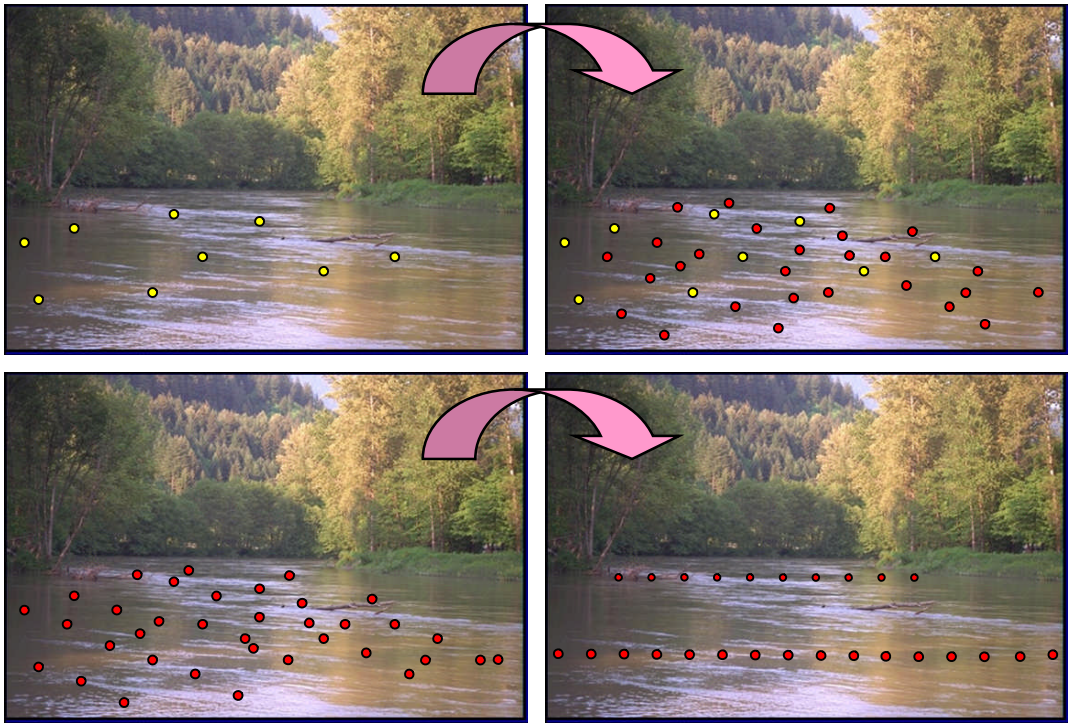

Figure 1.3: comparison of two sampling densities (top) and two strategies for point distribution (bottom) at a selected river site.

Finally, further issues associated with the lack of a common framework for hydromorphological characterisation of rivers are: (i) the lack of consensus on the

length of the river reach to be sampled and (ii) the subjectivity and lack of consensus on the determination of river features for hydromorphological characterisation (i.e. mesohabitat/habitat types and flow types).

1.2.2. Scaling problem

Several spatial scales can be identified in rivers according to the level of detail that is being analysed. These spatial scales are defined differently in relation to the objective for which they are being considered and to the author establishing the classification. Even though there are differences between classifications, it is clear that there is a need for development of a methodology that will allow scaling of information collected at a river site from small to large spatial scales (up-scaling) and vice versa (down-scaling) (Figure 1.4). This is known as the river-scaling concept (Habersack, 2000).

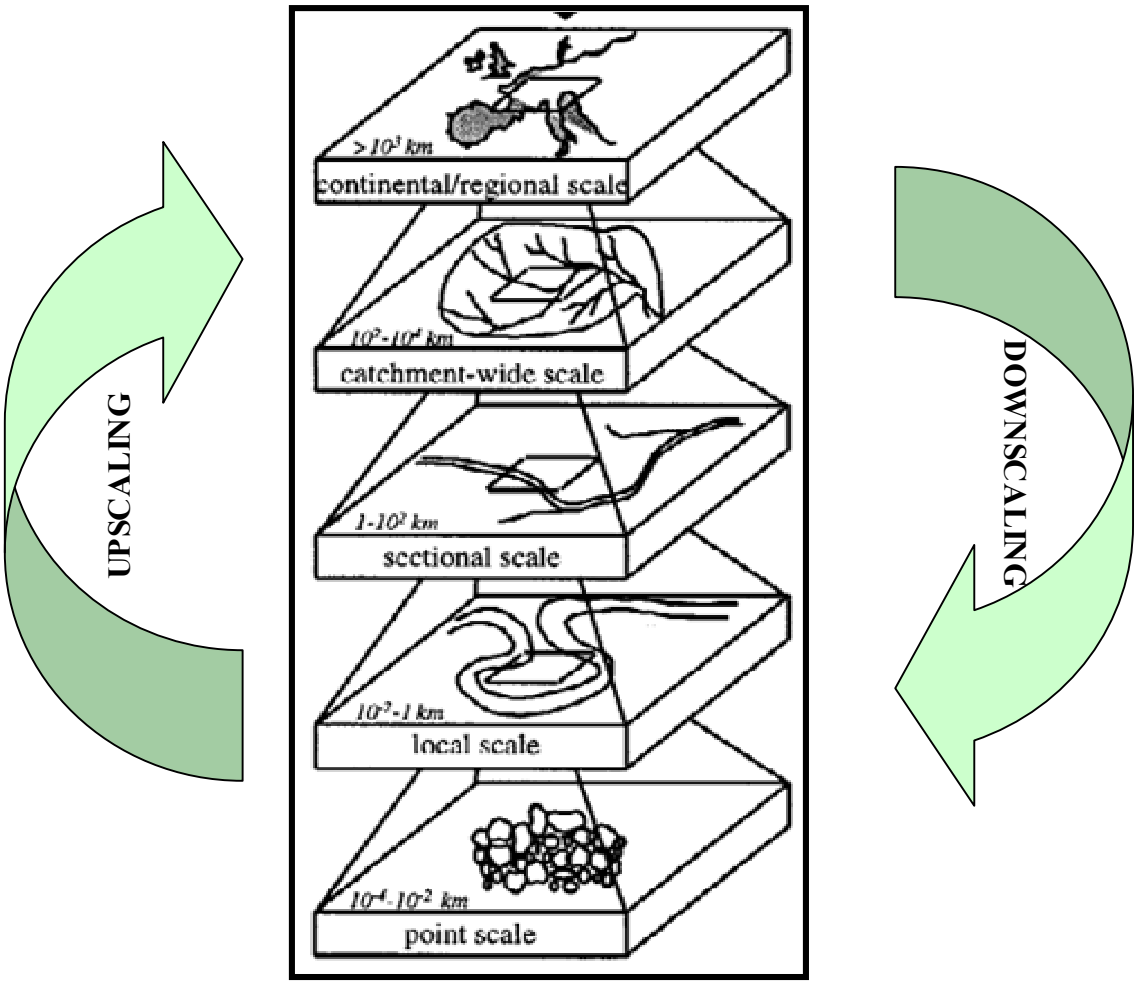

Figure 1.4: spatial scales defined by Habersack (2000). This is a diagrama of the full range of scales analysed for freshwater ecosystems. This does not imply that hydromorphological parameters are characterised at all the scales shown.

1.2.3. Temporal Problem

Monitoring of rivers is also carried out to study changes in river characteristics over time. Data are collected at the same river reach repeatedly over a time period and results obtained are analysed to determine if the river hydromorphology has improved or degraded. The difficulty of designing spatio-temporal sampling strategies for river monitoring is due to the need to achieve two main requirements: (i) the strategy applied needs to provide a satisfactory degree of information for a sampled time and (ii) the data needs to be collected in such a way that allows comparison between sampled times. The sampling strategy not only has to be efficient, defining the spatial variability of the reach for each sampled time, but also needs to be efficient in collecting data at those locations that are going to provide most information about hydromorphological change.

Figure 1.5 exemplifies the concept explained above. The visual hydromorphological features of the selected reach have been identified through the delineation of flow types (red dotted lines). Flow types are the features that can be observed in the water surface when walking along the river reach. With increasing discharge, the features identified will change and therefore, it is necessary to develop sampling strategies which address the requirements mentioned above in order to characterise these changes.

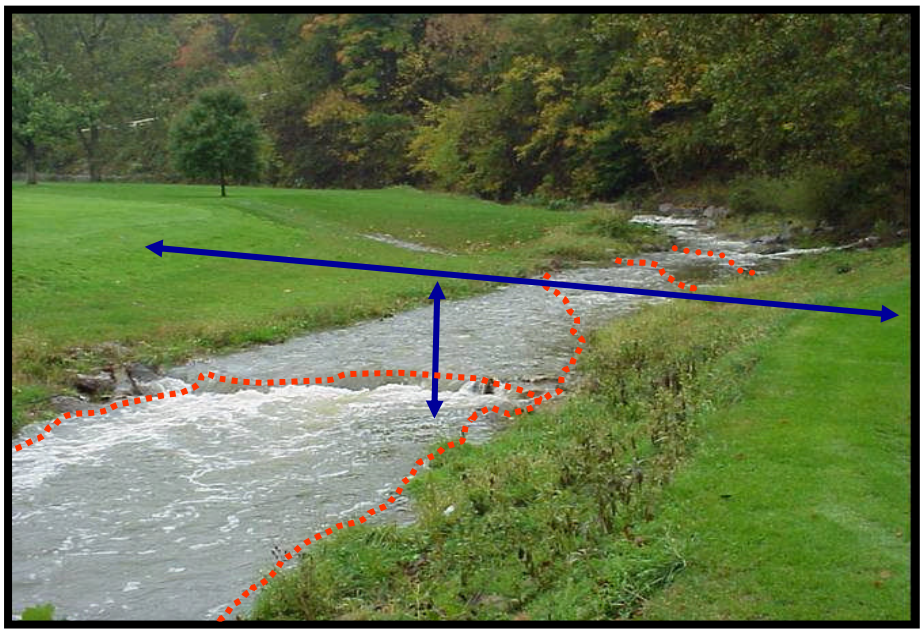

Figure 1.5 the spatio-temporal problem in hydromorphological monitoring. Changes in hydromorphological features (i.e. mesohabitat/flow types defined by the red lines); Change due to changes in flow (blue line).

1.3. Aim and objectives of this research project.

1.3.1. Overall Aim

The aim of the proposed project is to define a methodology for effective and efficient collection of hydromorphological data and to relate this to other characteristics of the site under observation. This can be expressed as the following research goal:

"To determine if it is possible to develop a set of guidelines for effective (cost-time-accuracy) collection of hydromorphological data for different purposes and relate this to other characteristics of the sites under observation."

1.3.2. Objectives

The specific objectives of the study were to:

a. identify the main limitations of current hydromorphological sampling strategies.
b. identify potential analytical tools to address the above limitations.
c. explore the application of geostatistical techniques for the resolution of the problems identified in current hydromorphological sampling strategies.
    i. compare different sampling strategies and determine the differences between them in terms of accuracy for nine selected indicators (spatial problem: methodological strategies).
    ii. compare different sampling densities and determine the differences between them in terms of accuracy for nine selected indicators (spatial problem: data density).
    iii. explore the application of the combined techniques of geostatistics and spectral analysis for the resolution of scaling problems (up-scaling/down-scaling).
    iv. assess the utility of the variogram for the identification of hydromorphological differences between river sites (spatial problem) and link the results with the

characteristics of the river sites for three different spatial scales (scaling problem).

v. Explore the hydromorphological changes occurring in two river sites due to changes in discharge.

d. create a set of guidelines for the development of effective and efficient hydromorphological sampling strategies in space, time and for the scaling concept linked with the observable characteristics of each river site.

1.4. Layout of the thesis

The thesis has been structured in nine chapters plus references and appendixes. The chapters which contain the data analysis (chapters 3 to 8) have been developed to facilitate the writing up of future scientific papers: introduction, methodology, results, discussion and conclusions. A brief description of the contents and purpose of each chapter is provided below.

Chapter 2 constitutes the literature review of the research project. It describes the current hydromorphological sampling strategies applied for data collection in rivers. It assesses the relevance of hydromorphological parameters in the Water Framework Directive and describes the requirements of hydromorphological data collection for its implementation. The problems listed in chapter 1 are described in detail and a set of appropriate solutions is proposed. Finally, in the discussion section, geostatistics is proposed as an approach to meet the objectives described in chapter 1.

The analysis developed in Chapter 3 has as its main objectives (i) to identify the differences when measuring depth parameters with two commonly used methods: a metric staff and a total station and (ii) to compare two possible ways of sampling depth values with the total station. This allows identification of the level of inaccuracy inherent to the equipment that is being used and to set a reference level of data error for further chapters.

Chapter 4 analyses the **spatial problem** by comparing five different **sampling strategies** for the collection of three hydromorphological parameters: depth, velocity

and substrate. The objective is to define which of these five sampling strategies gives better results when applying geostatistical techniques for prediction of values at non measured locations. Afterwards, levels of accuracy and implementation constraints are compared and a sampling strategy is recommended.

Chapter 5 focuses on the **spatial problem** and links the results with the **scaling concept**. The spatial pattern of depth is analysed for twelve river sites. The way that the rivers group together according to their spatial characteristics is then compared to the way that they group according to the characteristics defined for different spatial scales. Conclusions on how similar the rivers are according to their spatial pattern and the spatial scale analysed are used in chapter 6.

Chapter 6 continues with the analysis of **spatial problems** through consideration of **data density**. Chapter 4 provided a partial answer to the spatial problem as it only provided a solution to the spatial pattern for which data points need to be collected. Chapter 6 provides a set of guidelines to identify the sampling density at which the sampling strategy selected in chapter 4 could be implemented.

In Chapter 7 the different classifications and characterisations of river spatial scales are discussed. Here the possibility of applying a combination of geostatistical and spectral analysis to address the **scaling problem** i.e. the length of river which needs to be measured to correctly represent spatial variability over larger sections is considered. Conclusions are established on how far apart sampled reaches should be in order to interpolate the intermediate distance.

Chapter 8 focuses on the **temporal problem**. The analysis is developed considering the spatio-temporal character of the variables. Hydromorphological data collected or simulated for different discharges at two different river sites are analysed and conclusions are established on how data should be collected to obtain maximum information on hydromorphological changes due to changes in discharge.

Finally, chapter 9 summarises the conclusions established for each chapter and presents a discussion about the contribution to knowledge of this research project.

Recommendations for further research and potential applications of the findings are described.

In addition to the nine chapters described, appendices and a list of references have been included to support the study. A Compact Disk with a copy of the thesis in pdf format (for Acrobat reader) has been attached at the end of the thesis.

1.5. The river sites

Data for twenty river sites have been collected as part of this project or provided by different organisations to develop the analysis required for the objectives defined in section 1.3.2. Therefore, data have been collected with different equipment, different sampling strategies and for different objectives. Hence, these data sets were studied and analysed according to their characteristics: the data sets that had the best characteristics for analysis of each objective were selected.

Table 1.1 summarises the data sets available and provides a guide to the river sites that were analysed in each chapter. It also includes the name of the organisation that provided the data, as well as the location where the data was collected.

Table 1.1: river sites analysed in each chapter of this study. (HM and LM refer to Highly Modified and Low Modified, respectively). Catchment area refers to the area between the origin and the sampled site (except for the Brazos, Sulphur, Peris, Senni and Seiont site which are not included in Chapter 5 analysis and for which the full catchment area has been identified).

River site	Location	Data Source	Chapter in which data are used	Catchment area (km^2)	Reason for choice
Austrian channel	Vienna, Austria,	BOKU University	4	-	Artificial channel with alpine characteristics. Very detailed data set of depth and velocity.
Brazos	Texas, USA	Texas Water Development Board	7	16000	River length sampled adequate for the analysis of the scale problem.
Bere	Dorset, UK.	CEH	5, 8	48	Lowland site.
Blackwater	Surrey, UK	CEH	8	46	Lowland site with intensive depth data set. Site sampled up to the bankfull level.
Cruick	North East Scotland	CEH	5, 6	72	Upland site.
Highland Water	Hampshire, UK	CEH	5, 6	13	Lowland site.
Lambourn	Berkshire, UK	CEH	5, 6	185	Lowland site.
Leigh Brook	Gloucestershire, UK	Worcester College	4, 5, 6, 8	41	Depth, velocity, mesohabitat and flow type data available. at two different discharges.
Peris	North Wales	Data collected for thesis	3	10	Upland river site. High mesohabitat diversity.
Pang Fenced	Berkshire, UK	CEH	5, 6	84	Lowland site.
Pang Unfenced	Berkshire, UK	CEH	5, 6	84	Lowland site.
Pang Old Fenced	Berkshire, UK	CEH	5, 6	84	Lowland site.
Seiont	North Wales	Data collected for thesis	3	220	Upland river site. High mesohabitat diversity.
Senni	Brecon, Wales	CEH	5, 6	28	Upland river site. High mesohabitat diversity.
Sulphur	Texas, USA	Texas Water Development Board	7	891737	River length sampled adequate for the analysis of the scale problem.
Tame HM	Birmingham, UK	CEH	5, 6	183	Lowland site.
Tame LM	Birmingham, UK	CEH	5, 6	187	Lowland site.
Tarf	North East Scotland	CEH	5, 6	22	Upland site.
Windrush	Gloucestershire	CEH	3, 5, 6, 8	174	Lowland site

2

Hydromorphological sampling and monitoring of rivers: State of the art

Depth, velocity and substrate data sets need to be collected in rivers for different purposes. This chapter summarises the hydromorphological sampling strategies that are currently being applied for data collection. Problems and limitations of the sampling procedures are highlighted and a range of possible solutions considered. Geostatistical techniques are identified as the analytical methodology for this research project.

2.1. Current sampling and monitoring strategies of hydromorphological parameters in rivers.

Hydromorphological sampling strategies have been applied over time in order to obtain data sets for different purposes, such as assessing the habitat quality of rivers (Booker et al., 2004b), appraisal and impact assessment (Woo et al., 2004), habitat modelling (Waddle, 2001), hydraulic modelling (e.g. Hec-Ras software (Brunner, 2002)), planning habitat improvements and hydromorphological quality assessment of rivers (Raven et al., 1998), among others. Different methodologies have been applied for collection of hydromorphological data according to the spatial scale of the objective, the accuracy required in the measurements, the country where the study is being carried out and economic and temporal factors. Two main sources of hydromorphological sampling strategies can be identified; those developed for the assessment of hydromorphology in rivers and those developed for fish habitat models.

2.1.1. *Strategies derived from methods for hydromorphological assessment.*

Since a wide range of hydromorphological sampling strategies have been derived from methods for hydromorphological assessment and many of them are not documented, only the most relevant ones developed in Europe will be reviewed in this section, these are: River Habitat Survey (RHS) from the UK, the Systeme d'Evaluation de la Qualite du Milieu Physique (SEQ-MP) from France and the Landerarbeitsgemeinschaft Wasser (LAWA-vor-Ort) from Germany. Other European

countries such as Austria, Italy, Spain and Switzerland have developed hydromorphological sampling protocols for river habitat assessment but these methodologies are relatively recent and have very little documentation and development (Raven et al., 2002).

River Habitat Survey (RHS).

RHS is a methodology developed to broadly characterise and assess the physical structure of freshwater streams and rivers (Environment Agency, 2003). The need for the development of a system to assess the value of the physical structure of rivers was identified after reviewing the existing survey methods (Habscore and River Corridor survey, among others) none of which provided a system which could be directly applied, was simple to apply, representative of the structural diversity, capable of providing consistent data and results and statistically sound (Fox et al., 1998).

RHS characterises the physical structure along a 500 m length of river channel and data are collected at 10 equidistant "spot-check" reaches and a "sweep-up" summary (Raven et al., 2002). At each "spot-check" the following information is collected: predominant bank material, bank modifications, predominant substrate, channel modifications, flow type, land use within 5 m and 50 m of the banktop, banktop and bankface vegetation structure and channel dimensions. The "sweep-up" process is carried out along the 500 m and information regarding artificial features, the valley form, number of riffle-pools and point bars, land use, bank profiles, vegetation, channel and bank features, channel dimensions and features of special interest is collected.

The data collected following the RHS characterise the hydromorphological features of the rivers broadly. Objectives such as modelling will need more detailed data sets to obtain representative results and so the RHS data cannot be used. Aspects such as the mesohabitat types are briefly identified in the methodology and the lack of collection of depth-velocity data at a cross-section scale restricts the application of RHS data for other purposes.

The SEQ-MP method

The SEQ-MP method for hydromorphological assessment of rivers records information regarding channel geometry, substrate, channel vegetation, organic debris, flow, longitudinal continuity, structure - vegetation of river banks, description of the riparian zone and floodplain characteristics. Maps are used to determine the boundaries for the selection of individual survey units according to significant breaks in slope, valley form, junctions with large tributaries and major changes in land-use (Raven et al., 2002). The method describes broadly the hydromorphological features at the selected river site and, as in the RHS case the application of the method is difficult for purposes other than hydromorphological assessment of rivers.

The LAWA-vor-Ort method

The LAWA-vor-Ort method was developed to assess the hydromorphology of small and medium-size rivers. Hydromorphology is characterised through the measurement of 25 single attributes which are grouped into six main categories: development of the stream course, longitudinal profile, river-bed structure, cross-section profile, bank structure and riparian surroundings. The length of the stream surveyed is a function of the river width (Raven et al., 2002). The attributes are characterised according to options available, i.e. "low" and "very high" are options for flow diversity. Limitations defined in the methodologies described above are also present in the LAWA-vor-Ort method.

2.1.2. *Strategies derived from habitat models*

Hydromorphological sampling strategies defined for fish habitat simulation models have represented the basis of hydromorphological data collection in many studies (e.g. river restoration (Parasiewicz, 2001)). Random sampling (Parasiewicz, 1996), fractal geometry (Nestler & Sutton, 2000), geodetic sampling (Parasiewicz & Dunbar, 2001), stratified random reaches (Parasiewicz, 1996) and systematic sampling (Parasiewicz, 1996) are some of the strategies applied for the measurement of hydromorphological data for habitat modelling.

Fish habitat models require the description of hydraulic characteristics which can be obtained through (i) direct measurement of hydraulic factors, (ii) one dimensional hydraulic models, (iii) two and three dimensional hydraulic models and (iv) statistical hydraulic models (Harby et al., 2004). The first type relies on the direct measurement of hydromorphological parameters at specific locations and flow conditions of the river site under study. The second rely on reach sampling of hydromorphological parameters and the application of standard hydraulic equations. Two and three dimensional hydraulic models apply the principles of conservation of mass and momentum on a spatial computational grid, whilst statistical models provide estimates of frequency distributions of hydraulic variables. A brief description of the hydromorphological sampling strategies of the most common fish habitat models used is given below:

PHABSIM - RHABSIM

PHABSIM is a habitat model developed for the prediction of micro-habitat conditions in rivers as a function of streamflow. The suitability of these conditions for aquatic life is assessed by the software (Waddle, 2001). RHABSIM follows the same principles as PHABSIM but the software is more user friendly.

PHABSIM has two major sub-systems: river hydraulics simulation and physical habitat simulation. The habitat simulations are carried out for a selected study area which has been segmented according to one of three possible approaches that is selected according to the individual study objectives and may involve a combination of the above approaches.

Once the segmentation approach has been applied, cross-sections are placed within each study site using a stratified random or stratified systematic sampling scheme (Figure 2.1). Cross-sections are also placed at each hydraulic control (gauging point). The number of cross-sections at the river sites is determined according to habitat diversity, the extent of the study area and the resources available (U.S. Geological Survey , 2004).

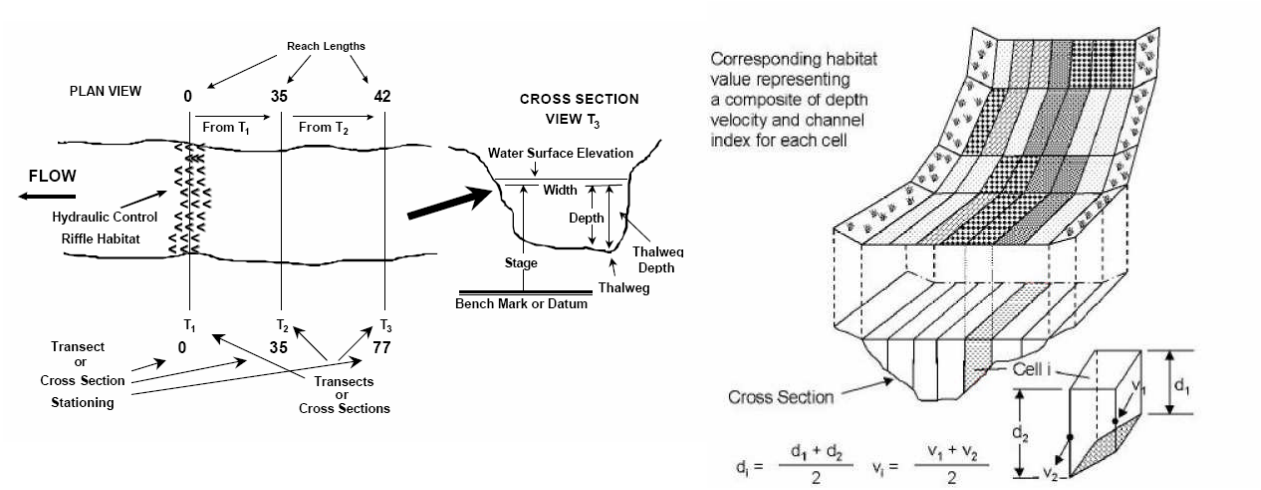

Figure 2.1: diagram representing the hydromorphological sampling strategy (left) and the habitat simulation concept applied in P-Habsim. (d) and (v) are depth and velocity, respectively. Image extracted from P-Habsim user manual (Waddle, 2001).

A topographic survey of channel morphology is carried out at each cross-section. Mean column velocities, substrate and cover are also measured at each topographical sampling point. Field notes describing the stream and water surface levels are recorded at each cross-section and data are collected at three different flows in order to model the physical habitat "correctly". The surveyor moves between cross-section by walking along the river banks.

The data collected are used to create the hydraulic and habitat simulations. Habitat modelling transforms the hydraulic simulation into the Weighted Usable Area index, which characterises the quantity and quality of available habitat for each cell across each cross-section.

RYHABSIM

Several habitat simulation programs, such as RYHABSIM, have been developed from the U.S.G.S version of PHABSIM, following the same basic principles for the determination of river habitat suitability but introducing specific modifications to the methodology.

RYHABSIM characterises hydromorphology through the measurement of cross sections separated by one channel width interval. Extra cross-sections are added

where flow is markedly non-uniform (Mosley & Jowett, 1985). Measurement points across the cross-section are equally spaced (around 15 to 20 points per cross-section). Depth and velocity (at 0.6 of total depth) are measured at each point. The number of points per cross-section is progressively reduced according to the width of the cross-section and additional points are located on changes in cross-slope or at deepest points to properly define the cross-sections. Water levels are measured at both banks on every cross-section and interpolated between banks. The river bed is mapped into areas according to the substrate. Values of depth and velocity are used to calculate the Weighted Usable Area (WUA).

MESOHABSIM

MESOHABSIM is a methodology developed for habitat simulation at larger scale levels (mesoscale) by setting the precision of hydraulic sampling to large units and increasing emphasis of system scale mapping (Parasiewicz, 2001). Physical attributes used for model calibration are commonly measured at only a few sampling sites and model predictions are then extrapolated to larger segments of rivers and streams. This is supported by rapid habitat mapping of a larger area to weight the spatial distribution of habitat features. Rapid habitat mapping consists of the visual characterisation of the habitat features of a river reach. Aerial photographs are used for this purpose. The biggest uncertainty associated with this method is the feasibility and accuracy of data sampling procedures.

CASIMIR – MESOCASIMIR

CASIMIR uses a similar methodology to PHABSIM but establishes the relationship between the physical habitat and biological variables through application of fuzzy rules. Hydromorphological parameters are obtained at cross-sectional level (Jorde et al., 2001). Water surface levels are either measured or calculated and a three dimensional digital river bed model is generated. Velocities are determined with an approach considering bottom roughness, water depth and water surface slope. Habitat suitability is calculated through fuzzy rules that consider the relationship between water depth, substrate, flow velocity and cover. Weighted Usable Area (WUA) is obtained from the habitat quality maps as an integral value. Figure 2.2 shows the

output of CASIMIR for a river site; habitat units are represented by rectangular cells that do not allow the identification of irregular shapes for habitat.

MESOCASIMIR was developed for the application of CASIMIR at mesoscale level. Depth, velocity and substrate are measured at each mesohabitat type by locating one sampling point in a representative zone for each mesohabitat type.

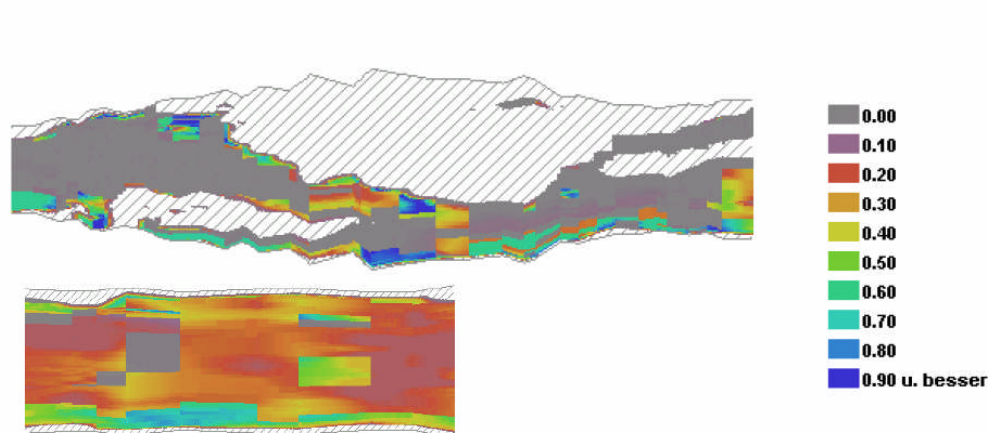

Figure 2.2: example of habitat suitability map for brown trout (Salmo trutta) obtained with CASIMIR. Image extracted from Jorde *et al* (2001). No scale of the sampled river site was provided. The output cells show the regularity of the predictions.

HAMOSOFT

The Habitat Modelling Software (HaMoSoft) is currently under development but a first version of the software is available (Mader et al., 2005). Up to now habitat models have assessed fish habitat by calculating the *Weighted Usable Area* (*WUA*), which is obtained from hydraulic simulation. *WUA* is calculated by averaging the velocity data in verticals or reaches. HaMoSoft assesses the fish habitat available at a river site through the analysis of Weighted Usable Volume (WUV). The main difference with existing models is that the measures or simulated velocity base data are not reduced to mean values in verticals or reaches.

The input data required consist of bathymetry of the river reach (3D terrain model), flow velocity data (point sampling, profile sampling or velocity data from 3D hydraulic models), substrate and cover data (longitudinal and lateral extension) (Mader et al., 2005). The model was developed to apply linear interpolation for the

prediction of hydromorphological parameters at non measured points. However, after analysing the first results of this study a geostatistical data processing module was included in the software. Geostatistical techniques are applied to obtain the depth and habitat distribution at the sampled river site. Finally, graphical outputs of the cross-sectional velocities and the *WUV* are produced.

HYDROSIGNATURE

Hydrosignature is a habitat model that divides the river site into cells using a Triangular Irregular Network (TIN) and calculates the number of different combinations of depth and velocity that exist (Le Coarer, Y. 2005, pers. Comm, April 2005). The output, called the Hydrosignature of the river site, consists of a diagram showing the combinations of depth and velocity available at a specific cross-section or river site. Figure 2.3. is a diagram of the Hydrosignature of the Leigh Brook river site. The output highlights the diversity of conditions present.

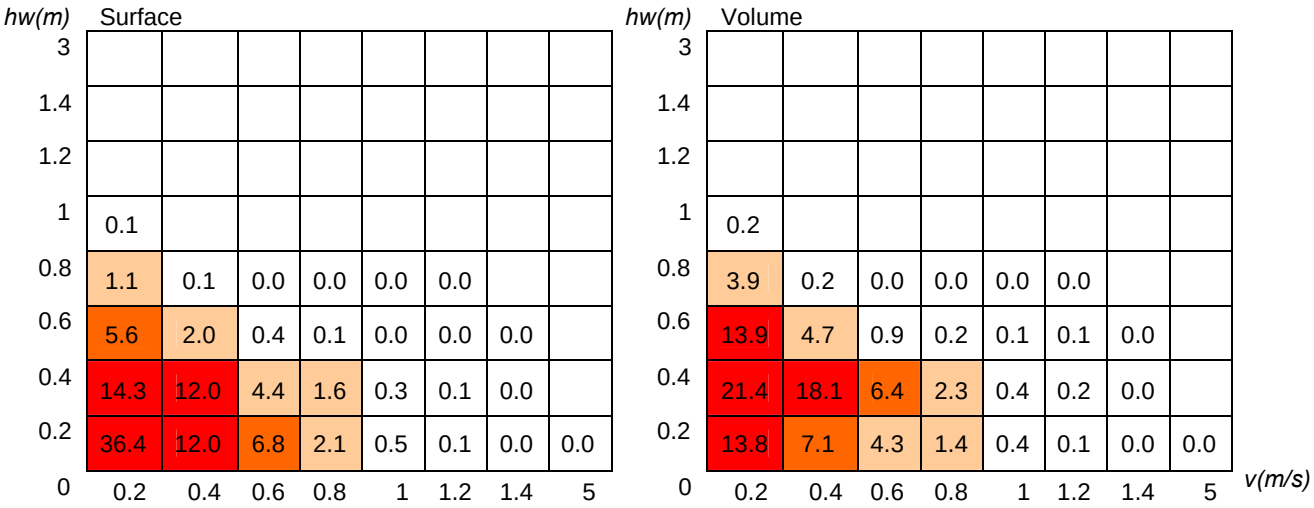

Figure 2.3: hydrosignature of the Leigh Brook river site. The habitat suitability is given by the number in each cell. The coloured scale indicates the degree of suitability. The hydrosignature is given for the total volume of the river site and for the surface characteristics.

Hydrosignature is also still under development. A first version of the software is available for downloading at the official web site (Le Coarer, 2005). However, the user manual needs to be completed. The input data are the hydraulic measurements of verticals described by their depth and average velocity (Scharl & Le

Coarer, 2005). Substrate and cover data are not required for the model to be implemented (Le Coarer, Y. 2005, pers. Comm, April).

The hydrosignature can be calculated with georeferenced and non georeferenced data. Depth and velocity data collection can be carried out following three different field data collection procedures: (i) depth and velocity are measured at unspecified locations, (ii) data is collected following cross-sections and (iii) data is collected following a Triangular Irregular Network (TIN). In the first case, vertical measurements of depth and velocities are collected at unspecified locations. In the second case, velocity and depth measurements are recorded along a cross-section: the distance between measured points is also recorded. Finally, in the last case, a Digital Elevation Model (DEM) is created to obtain topographical information, to apply advanced interpolation methods for depth and to implement 2D and 3D models for habitat assessment. Values of depth can be interpolated and predicted at non measured locations with an equation that considers the curvature of the river and the spatial variation of the parameter interpolated (Le Coarer, Y. 2005, pers. Comm, April).

2.2. The role of hydromorphology in the Water Framework Directive (WFD)

The implementation of the WFD (Directive 2000/60.EC) requires the development of monitoring programmes to obtain a comprehensive overview of water status. The monitoring programme will inform the classification of status, the long term changes in natural conditions, the changes in status of those bodies identified as being at risk and determine the causes of water bodies failing to achieve environmental objectives (Working Group 2.7, 2003).

These monitoring programmes may "quantify the temporal and spatial variability of quality elements and the parameters indicative of the quality elements in the water surface bodies being considered. Those that are very variable may require more sampling (and hence cost) than those that are more stable or predictable. Alternatively variability might be reduced or managed by an appropriate targeted or stratified sampling programme which collects data in a limited but well-defined sampling window" (Working Group 2.7, 2003). In addition, estimates of the confidence and

precision attained by the monitoring systems have to be accounted for so limits of how much uncertainty can be expected in the results of monitoring programmes. This can be compared with acceptable uncertainty or error levels.

Hydromorphological elements to be monitored are hydrological regime, river continuity and morphological conditions (river depth and width variation, structure and substrate of the river bed and structure of the riparian zone) (Chovanec et al., 2000 and Directive 2000/60.EC). There is no common sampling methodology consistent across the EU for the hydromorphological elements and the existing classification systems do not meet the requirements of the WFD (Working Group 2.7, 2003).

The need for a standardised way to assess morphological conditions of rivers in order to obtain a common interpretation of river quality and classification in future stream assessment in the whole of Europe has been identified (Buffagni & Erba, 2002). Details about hydromorphological monitoring requirements for the WFD can be found in a series of documents (Johnson, 2000; REFCOND, 2001; REFCOND, 2003; Owen et al., 2001 and Nixon, 2002).

Finally, the WFD requires the development of status maps (Working Group 2.7, 2003) that will be represented with GIS techniques. These maps shall cover the networks established for the purpose of monitoring and the results of the monitoring programmes carried out (Nixon, 2002) in order to propose a programme of measures in the River Basin Management Plans (Directive 2000/60.EC). The problem arises when trying to propose the programme of measures at a river basin scale from measurement obtained at a reach scale. Hence, the concept of river scaling (Habersack, 2000) needs to be considered in the development of the hydromorphological monitoring programme. The river scaling concept (RSC) (Habersack, 2000) is an integration of two procedures: down and up-scaling. The down-scaling procedure starts at a catchment scale and goes through sectional and local scale to point scale. The up-scaling procedure follows the down-scaling one in reverse, in order to aggregate the data for local scale, derive sectional results and suggest regional catchment management.

2.3. The problems identified

Three sources of uncertainty arising during the selection and application of hydromorphological sampling strategies have been identified: spatial, scaling and temporal (Table 2.1). These problems are summarised below:

Table 2.1: problems identified for design of hydromorphological sampling strategies.

Problem type	Limitations
Spatial	• No consensus on the sampling strategy to be followed or the number of points to be collected. • No consensus on the length of river to be sampled. • Loss of spatial information when applying linear interpolation between measured cross-sections in habitat models. • Need for quantifying the spatial variability of hydromorphological parameters. • Lack of consistency when defining *mesohabitat* types. • Lack of studies on comparison of sampling strategies. • Hydromorphological sampling strategies proposed have been designed for specific purposes. They cannot be used for different objectives. • No estimation of the level of accuracy/error associated with the current sampling strategies. • Need for the development of adequate sampling strategies
Scaling	• Need for data collection at high spatial scales. • The accuracy of the prediction declines with the extrapolation procedure. • Results may vary according to the sampling strategy. • Need for the development of adequate sampling strategies.
Temporal	• Temporal issues are not considered in some of the current sampling strategies. • Need for quantifying the temporal variability of hydromorphological parameters. • Need for the development of adequate sampling strategies. • Need to differentiate between different sources of hydromorphological variation.

2.3.1. *Spatial problems*

The use of interpolation techniques for the prediction of values at non measured locations and for the creation of maps of depth, velocity or substrate is widespread, especially in the context of habitat modelling. Little work has yet been carried out to determine the best location for sampling points for the application of interpolation. Furthermore, there is no consensus on which sampling strategy should be followed, where the sampling points should be located and how many points need to be collected.

Available hydromorphological sampling strategies for habitat models such as PHABSIM require data collection at cross-sections and consider that the variance between consecutive cross-sections is null. Thus, the less homogeneous the stream segment is in terms of geomorphologic characteristics, the less accurate the generalisation from study site simulations to the entire study area will be.

Other limitations associated with the PHABSIM software are the existence of different options available to select the sampling sites and their length. Sanz-Ronda et al. (2003) summarise different researchers' opinions regarding the best river length for the application of the PHABSIM methodology, which (i) is considered to be 35 times longer than the channel width under average flow conditions (Simonson et al., 1994 cited in Sanz-Ronda et al., 2003), (ii) should include three complete riffle-pool sequences or two consecutive meanders (Lyons, 1992 cited in Sanz-Ronda et al., 2003), (iii) may include 10% of habitat units (Overton et al. 1993 cited in Sanz-Ronda et al., 2003) and (iv) should analyse two randomly selected mesohabitats (Bovee, 1997). Additional to the lack of consistency in the sampling methodology, there is a difficulty in accurately defining and identifying the mesohabitat types (Sanz-Ronda et al., 2003) and in validating the model outputs.

Little work has been published regarding the accuracy of the predicted physical habitat when applying different sampling strategies and sets of equipment, an example of which is provided by Scruton et al. (1998) Previous works developed for the comparison of sampling strategies for habitat modelling stated that stratified sampling strategies (i.e. reaches) typically applied for this purpose are relatively crude and do not properly reflect the curvilinear distribution of hydromorphological parameters (Le Coarer & Dumont, 1995 cited in Parasiewicz, 2001).

Recent work has been carried out in order to improve the representation of the depth hydromorphological parameter in two and three dimensions (Legleiter & Kyriakidis, 2006, Merwade, 2002; Carter & Shankar, 1997 and Osting, 2004). The objective of these studies was to obtain a suitable representation of the river bathymetry for hydrodynamic models by creating rectangular bathymetric grids. Carter & Shankar (1997) state the increasing interest in using hydrodynamic models for habitat modelling and the importance of defining the problem domain (i.e. river bathymetry)

to obtain accurate results. The gridding methodology applied by Carter and Shankar (1997) is based on geostatistics (ordinary kriging). The geostatistical approach was preferred to triangulation techniques since (i) the technique is able to deal with irregular data, (ii) it is possible to consider a specific number of points for the prediction of values at non measured points, (iii) the spatial variability of the interpolated parameter is considered and (iv) the residual variance is minimised when interpolating. One problem needs to be highlighted in Carter and Shankar's (1997) study: anisotropy was not considered or analysed because they considered that "although there may be changes across the reach, the braids do not maintain a constant direction and an anisotropic direction will not be valid for all the data". The study of anisotropy is really necessary when applying geostatistical analysis and therefore results obtained in Carter & Shankar's (1997) study should be viewed with some caution.

Merwade (2002) solved the previous limitation for anisotropy analysis by developing a tool for straightening the river. The method recognised that (i) results of hydrodynamic models for instream flow studies are dependent on the accurate representation of river geometry and (ii) the river bathymetry is generally created with GIS by applying the interpolation module (Geostatistical Analyst). Current GIS interpolation tools have been designed for the land surface and do not allow the creation of adequate river bathymetry. According to Merwade (2002) this is due to the different behaviour of this parameter across and along the river. Further explanations for the inadequacy of GIS for river bed interpolation could be: (i) high degree of accuracy and detail is required for the bathymetry, (ii) lack of transparency when applying the interpolation processes and (iii) decrease of the accuracy when interpolating meandering areas (curvature) due to the distortion caused by points that are close in space but are not spatially correlated. Merwade (2002) developed a new GIS tool in order to (i) consider the river as a linear feature, (ii) transform it into a regular mesh for further data analysis and (iii) provide continuous information of the bathymetry at a resolution finer than the source of data (Osting, 2004). However, the project does not include any study regarding the sampling strategy and density required to apply the developed tools effectively.

Hydromorphological sampling strategies can be successfully designed when properly combining the number of points to be sampled and the sampling strategy with the interpolation technique to be applied. Furthermore, specific levels of accuracy or confidence intervals can be proposed for the prediction of values at non measured locations by comparing different interpolation techniques, different sampling strategies and a range of sampling densities. Similar studies have been developed in other research fields to define adequate sampling strategies (Webster & Oliver, 1992)

2.3.2. *Scaling*

One of the problems in fish habitat modelling is the need for data collection at high spatial scales which is time and cost consuming (Parasiewicz, 2001). Several strategies for mesoscale habitat mapping and/or modelling such as, MesoHabsim (Parasiewicz, 2001), MesoCasimir (Jorde et al., 2001) and Rapid Habitat Mapping (Maddock & Lander, 2002) are being developed in order to deal with the up-scaling concept (Habersack, 2000). The general approach is to consider impractical the application of models that increase the accuracy by increasing the number of sampled points (Parasiewicz, 2001). Thus, the strategy followed in order to reduce the effort to a feasible level is to take measurements at a few short sampling sites and extrapolate them to larger segments of rivers and streams.

The extrapolation or interpolation of collected values may introduce considerable errors if data have not been collected adequately for the interpolation technique that is going to be applied. Furthermore, the accuracy of a river-wide assessment strongly declines during the extrapolation procedure due to variations in stream morphology among sampled sites (Dolloff et al., 1997 cited in Parasiewicz, 2001) and results may vary according to the selected sampling strategy or location of the sampled locations (Gore & Nestler, 1998 and Williams, 1996 cited in Parasiewicz, 2001).

Research studies need to be undertaken to identify which sampling strategy should be used and how many points need to be collected in order to achieve a specific level of accuracy in the extrapolation procedure. Furthermore, further research has to be undertaken in order (i) to improve scaling methods in general (Habersack, 2000;

Nestler & Sutton, 2000 and Hilderbrand et al. 1999) so detailed river scaling can be developed and (ii) to determine whether existing methods can be up-scaled or an entirely new approach needs to be developed (Booker et al., 2004a).

2.3.3. *Temporal problems*

In addition to the spatial issues of data collection, it is necessary to consider the variation of the hydromorphological characteristics of rivers over time due to variations in flow. Work developed by Dunne & Leopold (1978 cited in Parasiewicz, 2001) indicates that as flow rises, the distribution of hydro-morphological units will change from riffle-pool towards homogeneous run-type habitats.

Temporal scale should play a major role in the design of sampling strategies for the monitoring of hydromorphological parameters of rivers. Monitoring of rivers can be undertaken to analyse the evolution of the quality (i.e. water quality, ecological status, hydromorphological parameters) of the river site over time. Therefore, it would be necessary for the sampling strategies applied (i) to maximise the information obtained from the river site at a specific time and (ii) to obtain comparable information between sampled times. Although temporal uncertainties are broadly recognised (Parasiewicz, 2001), some fish habitat models do not take these into account when calculating the physical habitat available in the river site. An example is PHABSIM, which assumes that the shape of the channel does not substantially change with discharge over the range of flows simulated (U.S. Geological Survey , 2004 and Leopold et al., 1964); when geomorphic changes are significant between data collection field trips, the data are treated as independent data sets.

2.4. Brief overview of analysis methods

2.4.1 *Solutions for the spatial problems*

Spatial problems can be analysed with the application of geostatistical analysis, which can be used as a tool (i) to determine the maximum or adequate distance between sampled points, (ii) to predict values of a selected variable at non measured points and (iii) to determine the level of accuracy of the predicted values. Geostatistics use the semivariogram (also called variogram) to represent the spatial pattern of variation of a

selected variable. Semivariograms have been proved to be a useful tool for detection of scales of spatial variability in the landscape (Meisel & Turner, 1998).

Software, such as ArcGIS, is a powerful tool for the interpolation (kriging) of collected data and creation of maps and 3D outputs. However, results may be erratic if the suitable parameters are not introduced in the dialogs. The spatial behaviour of the variance (variogram) for hydromorphological parameters can be analysed in order to identify an adequate sampling strategy for the application of kriging interpolation techniques. Several studies have been developed in soil science for this purpose (Webster & Oliver, 1992; Muller, 1999; Lark, 2002; Burgess & Webster, 1984; Burgess, 1980; Bogaert and Russo, 1999; Russo, 1984 and McBratney & Webster, 1983, among others), showing that this research issue has to be considered before interpolating.

Spatial variability of hydromorphological parameters can also be characterised with remote sensing techniques. Remote sensing allows the collection of information of a specific variable from a distance, without coming into physical contact with it. The energy reflected from the earth is measured with a sensor and the information is displayed either as a digital image or a photograph (Figure 2.4). These sensors can either be located in satellites, planes or other airborne structures. Gilvear & Bryant. R. (2003) give a very detailed description of remote sensing techniques that are currently being applied for the study of rivers.

Limitations of remote sensing are (Gilvear & Bryant. R., 2003): (i) results obtained depend upon the earth's location relative to the Sun, time, geometry of observation and waveband, (ii) scattering and distortion occurs due to atmospheric moisture, pollution and dust, (iii) the resolution of the methodology requires the application of special equipment for the analysis of small streams (<20m wide), (iv) many aerial photographs are necessary for the study of a river site which increases the cost of the technique, (v) aerial photographs need to be matched together to obtain the complete image of a river site; this produces mismatch in geometry results and (vi) no detail can be obtained when the scale is smaller than the pixel size of the image.

Figure 2.4: example of aerial photograph of a river reach. The patterns of the river site are shown with different colours.

Winterbottom & Gilvear (1997) analysed the potential for mapping depth in rivers within a shallow gravel-bed river using airborne multispectral imagery and aerial photography. Values of depth obtained from remote sensing were compared to depth data collected at several cross-sections. Although the methodology is useful for habitat mapping and quick characterisation of the river under study, results show that (i) at depths greater than 60 cm the error of the estimations increases as the intensity of the radiation decreases exponentially with distance, (ii) results depend upon the water turbidity, colour, substrate reflectance and water surface back-scatter and (iii) differences between measured and predicted water depth can be equal to or higher than 40 cm in shallow areas.

Multi-spectral video imaging systems have also been applied to classify water depth and mesohabitat types (Hardy et al., 1994 cited in Gilvear & Bryant. R., 2003). Limitations encountered when applying this methodology were: (i) erroneous values of depth when collecting information in areas with submerged/floating/emerging vegetation, (ii) errors associated to water turbidity and (iii) decreases of the level of accuracy in deep areas.

Artificial neural networks (ANN) have recently been applied as a tool for spatial interpolation (Rigol et al., 2001). ANN try to simulate the processes of brain cells

(neurons) (Russell & Norvig, 2003). This technique works with a collection of units that are connected through a specific pattern to allow communication between the units (Callan, 1999). The components necessary for the application of the technique are: (i) a set of simple processing units that constitute the input and the output variables, (ii) a pattern of connectivity between the units which will define their interactions, (iii) a set of rules for controlling the signals through the network and calculating the output signal and (iv) a set of learning rules to adapt the interaction between the network nodes.

The main advantages of ANN (Rigol et al., 2001) are: (i) the technique is able to incorporate additional data and expert knowledge within the estimation process to guide the interpolation, (ii) no critical assumption about the nature of the data is taken and (iii) non-linear modelling tasks can be handled. The main disadvantage is the failure to incorporate neighbourhood data and trend within the network structures. As an alternative to geostatistics (kriging), Rigol et al. (2001) propose feed-forward backpropagation ANN, with the advantages of (i) avoiding the need of specifying the variogram model and (ii) reproducing multiple anisotropic spatial structures.

Geostatistics is applied for the analysis of the spatial problem in this research project since Rigol et al. (2001) recognises the need for further studies on comparison of interpolation methods using identical data sets, little work has been yet developed and published on geostatistical interpolation techniques applied to hydromorphological parameters, aerial photographs are expensive to obtain and present limitations associated with the turbidity and depth of the river site and geostatistical techniques consider the spatial variability of the variable.

2.4.2 *Solutions for the scaling problem*

The scaling problem can be analysed with different methodologies such as stochastic and deterministic models, dimensional analysis (Habersack, 2000) or even habitat mapping surveys (Maddock & Lander, 2002).

Stochastic and deterministic techniques aggregate the results in order to derive average values for larger time-space scales. Deterministic models describe

relationships between different scales by distributing small-scale modelled values, resulting in a spatial or temporal pattern. Stochastic models apply covariance and distribution functions (Habersack, 2000).

Dimensional analysis uses fractals (or tessellation methods) to determine spatial and temporal structure (Nestler & Sutton, 2000). The methodology characterises the objects which repeat in space on a proportional scale following a regular or irregular pattern (Figure 2.5). The methodology is usually linked to remote sensing (i.e. analysis of satellite images (Emerson et al., 1999)) which provides the basis for pattern detection.

Fractals are present in the organisation of the river network structure at different scales (Rodriguez-Iturbe & Rinaldo, 2001) and therefore, it may be possible that this pattern is also repeated for hydromorphological features. Nikora et al. (1993) studied the fractal properties of single thread channels and concluded that the assumption that self-similar properties extend up to the largest river scales is incorrect.

Habitat mapping is a strategy followed in order to reduce the effort of data collection to a feasible level. Measurements taken at few short sampling sites are extrapolated to larger segments of rivers and streams (Parasiewicz, 2001), usually with the help of aerial photographs.

Parasiewicz (2003) identified three main types of up-scaling that need to be considered for management practices at the river and watershed scale: biological, spatial and temporal up-scaling. This indicates that when solving any of the spatial, scaling or temporal problems, the interrelation between them will need to be considered.

A combination of geostatiscal and spectral analysis has been selected to explore the spatial pattern of river depth along a river reach and link the results to the scaling concept in this project. Spectral analysis is based on the study of the fluctuations, cyclic patterns or periodic behaviour of a selected variable (e.g. sound waves, soil properties) across the space or time domain (Nielsen & Wendroth, 2003).

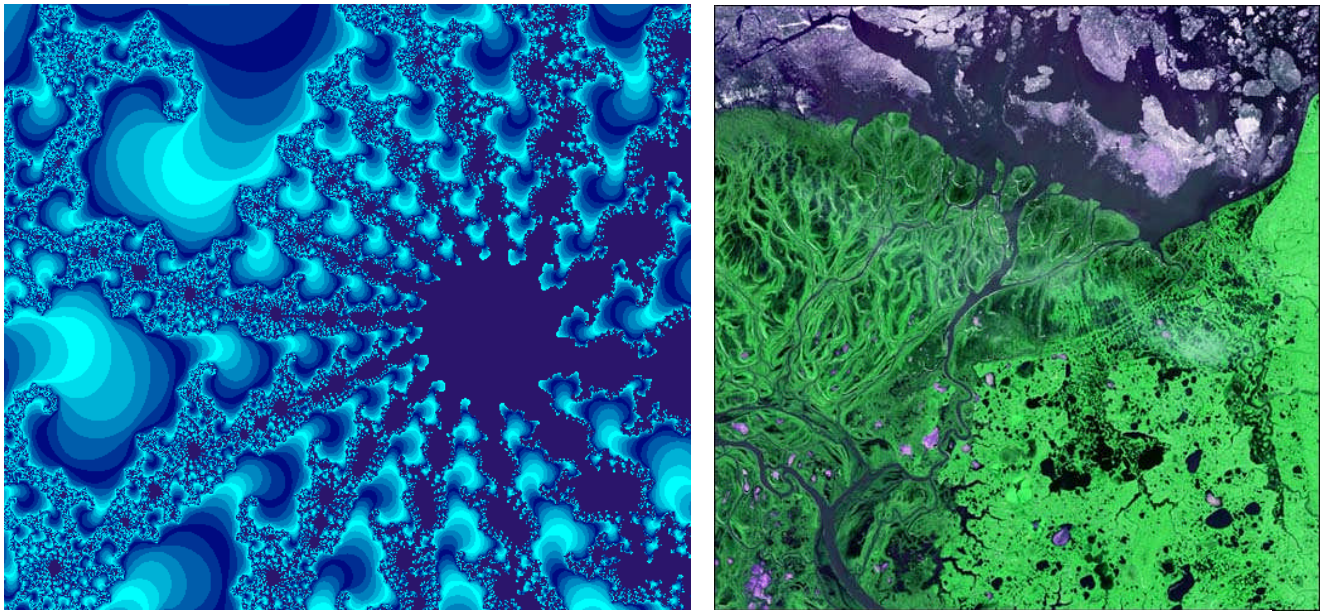

Figure 2.5: computer simulated fractal (left) and satellite image of a catchment area (right). Fractals can be identified in both images. The methodology characterises the objects which repeat in space on a proportional scale following a regular or irregular pattern

The methodology employed in Chapter 7 has been developed and based on a geostatistical approach in order to apply a consistent and comparable method of analysis for both spatial and scaling problems. In addition, geostatistical and spectral analysis have been selected since (i) fractal analysis has mainly been applied to river basin patterns and self-similar properties may not be extended to larger scales (ii) habitat mapping lacks consistency when determining the mesohabitats and does not allow the prediction of values at non measured points and (iii) remote sensing has limitations of data availability and interference due to water colour and water depth.

2.4.3 *Solutions for the temporal problem*

Temporal variability of hydromorphological parameters is mainly represented by changes in discharge, which modifies the vegetation, the channel morphology and the mesohabitat units of the river sites (Hilderbrand et al. 1999). Sampling strategies for the monitoring of rivers should: (i) maximise the information at a specific time and (ii) provide comparable information between sampled periods.

Temporal variability can be characterised through the application of spectral analysis (Webster & Oliver, 2001), geostatistical analysis (usually combined with spectral

analysis: i.e. (Skoien & Bloschl, 2003) or remote sensing (Gilvear & Bryant. R., 2003 and Gilvear et al., 1998).

Spectral analysis is useful for determining periodicity patterns of linear sequences (Webster & Oliver, 2001). Linear sequences can either be represented by a set of equally distributed spatial points that follow one single direction or by the value of a variable at a point that has been measured periodically over time. Data points need to be located in the same longitudinal profile and separated by equal distances in space when analysing spatial characteristics. If temporal characteristics are analysed, points need to be collected at equal time intervals. Spectral analysis requires large data series so cyclic patterns can be identified and thus, other methodologies have been preferred.

The temporal issues encountered with hydromorphological parameters are not associated with just a single point in space. Generally, the objective is to characterise the changes through time for a set of data collected, which includes many spatial points (Emery et al., 2003). Therefore, it is necessary to consider spatial and temporal components jointly. Figure 2.6 shows a diagram of the spatio-temporal problem; three different data sets have been collected at three different times at the same river site.

The sampling strategy applied has to be designed in such a way that the spatial variation of each time and the temporal variation of each sampled point can be compared.

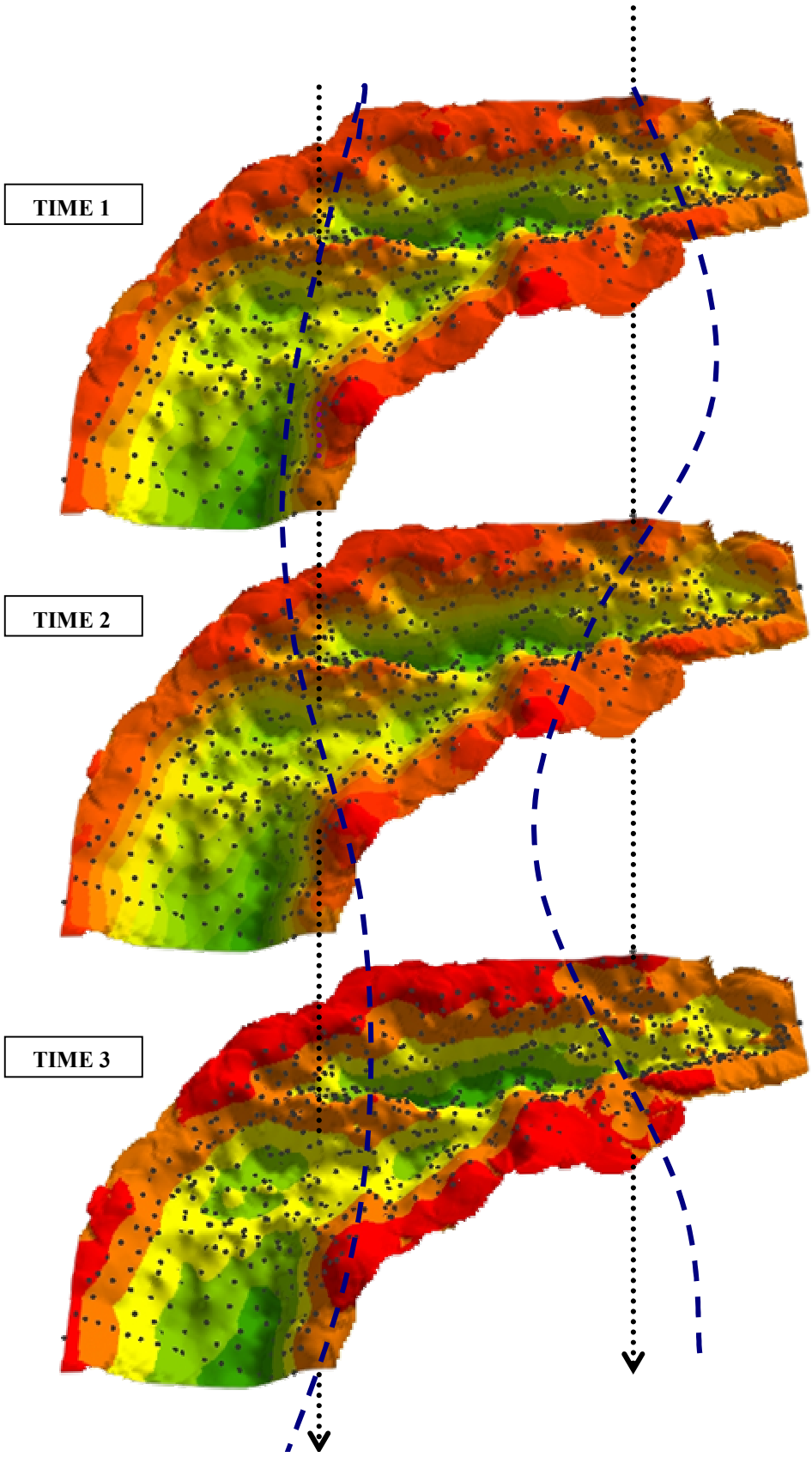

Figure 2.6: diagram of the spatio-temporal problem. The three images represent the interpolated surface of the depth variable for a sampled river site at a specific time. Each black dot is one measurement of depth. Each black dotted line informs on the location of a selected point at each time Dashed blue lines represent the hypothetical change of depth value in time for the selected sampled point. Depth not only varies in space (interpolated surface) but also in time (dashed blue lines).

Generally, space-time data are analysed with models developed for temporal or spatial distributions (Kyriakidis & Journel, 1999). Geostatistical analyses have usually been applied to either spatial or temporal analysis (Skoien & Bloschl, in press). Results are presented by either producing interpolated attribute maps of the parameters analysed for all the time instants of interest, so comparisons between times can be obtained (Kyriakidis & Journel, 1999), or prioritising time over space and modelling time series of the attribute of interest (Kyriakidis & Journel, 1999).

Recently, spatio-temporal geostatistical analyses have been successfully developed and applied in environmental sciences, some examples of which are referenced in Kyriakidis and Journel (1999). The spatial and temporal dimensions are combined in one single analysis and therefore, it is possible to compare the behaviour of the selected variable in both dimensions and to determine which one introduces a higher degree of variability.

Other methodologies for spatio-temporal analysis include spatio-temporal modelling via Gaussian process models (Banerjee et al., 2004) or Bayesian Maximum Entropy Space/Time analysis (Christakos, 2000). Christakos (2000) introduces the concept of "modern geostatistics" to solve the spatio-temporal limitations of geostatistics by recognising that the spatiotemporal geometry is not purely mathematical and relies on physical knowledge for the description of reality. Spatio-temporal geostatistics have been selected as a key methodology for this research project to combine results obtained for the spatial and scaling problems with the temporal dimension through a common analysis procedure.

2.5. Brief introduction to geostatistics

There are various techniques for generating surfaces from measured values. A brief introduction to these technique is given here.

Geostatistics is an interpolation technique that allows the prediction of a variable at non measured locations by determining its spatial variation pattern. Another interpolation technique available is the use of deterministic models (Table 2.2).

Table 2.2: description of deterministic interpolation techniques and their limitations (Jhonston et al., 2001)

Method	Interpolation Technique	Description	Limitations
Deterministic	Inverse Distance Weighting	The method assumes that each measured point has a local influence that diminishes with distance. Points closer to the prediction have higher weights than those farther away.	• Exact interpolation technique: maximum and minimum values in the interpolated surface can only occur at sample points. • The output is sensitive to clustering and the presence of outliers. • It assumes that the local variation can be captured through the neighbourhood.
	Global Polynomial Interpolation	This method fits a smooth surface that is defined by a polynomial function fitted to the input sample points. The result is a surface that varies slowly over the area of interest.	• Inexact interpolation technique: the predicted surface will not pass through all the measured points. • It is necessary to determine the degree of the polynomial function to be used. The more complex the polynomial, the more difficult it is to ascribe physical meaning to it. • The predicted values are susceptible to outliers, especially at the edges of the measured site.
	Local Polynomial Interpolation	This method works like Global Polynomial Interpolation but fitting many polynomials, each within specified overlapping neighbourhoods.	• Sensitive to the neighbourhood distance. • Same limitations as for the Global polynomial Interpolation technique.
	Radial Basis Functions	Exact interpolation technique: the predicted surface goes through each measured sample value. Splines, splines with tension, multiquadratic functions and inverse multiquadratic functions are some of the functions applied for the prediction of values at non measured locations. These methods are able to predict values above the maximum measured or below the minimum measured.	• This technique provides good results when the parameter predicted changes gradually in space. It is not adequate when there are large changes in a short horizontal distance.

Deterministic interpolation techniques obtain predictions from measured points based on either the extent of similarity (i.e. Inverse Distance Weighting) or the degree of smoothing (i.e. radial basis functions). Geostatistical interpolation (i.e. kriging) obtains predictions based on the statistical properties of the measured points, calculating the autocorrelation among measured points and accounting for the spatial configuration of the sample points around the prediction (Johnston et al., 2001). Since deterministic interpolation methods do not provide enough information regarding the spatial behaviour of the parameters analysed whilst kriging does, geostatiscal analysis and kriging interpolation have been selected as methodologies for this study. Figure 2.7 summarises the available interpolation techniques, a basic description of their procedure and the limitations for the scope of this research project.

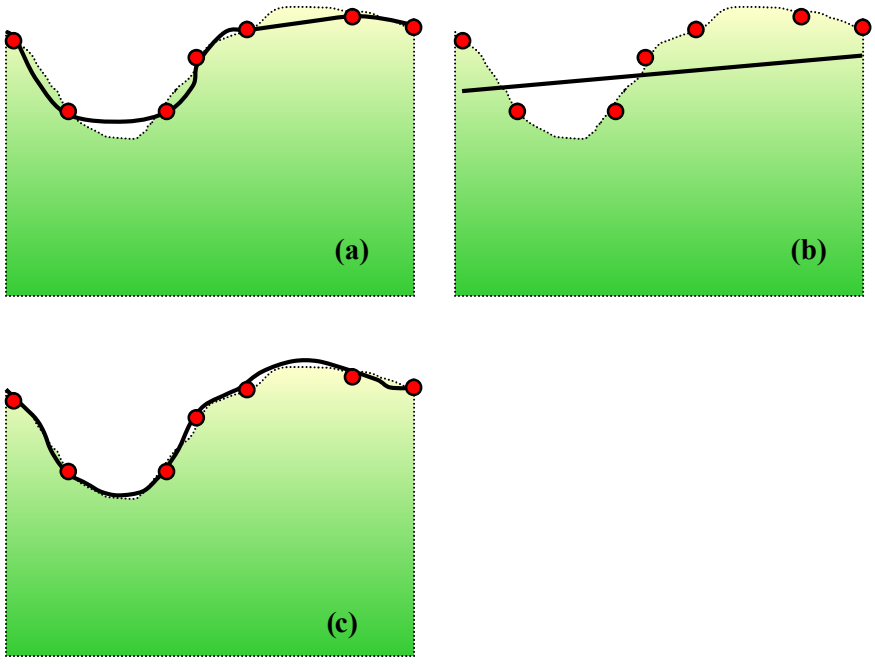

Figure 2.7: diagram representing the output of three deterministic interpolation techniques: (a) Inverse Distance Weighting, (b) Global Polynomial Interpolation and (c) Radial Basis Functions. Red points indicate sampled location, the dotted line represents the real surface and the black solid line the interpolated result. This diagram is just a simplification of the interpolated results (Johnston et al., 2001).

Geostatistics relies on spatial models and considers the spatial dependence of the variable studied; it assumes that the variable studied is random and is the outcome of one or more random processes. Spatial correlation is represented through a variogram in which the variance between measured values is estimated at increasing intervals of distance and in several directions (Webster & Oliver, 2001).

The experimental variogram is the first step for the calculation of the empirical variogram. Experimental variograms are a display of the variance (gamma) between pairs of points in relation to their relative distance (Figure 2.8), commonly called lag distance (h). The empirical variogram (Figure 2.8) is the result of fitting a continuous function to the experimental variogram. This function is fitted in order to describe the spatial variation so that values can be estimated or predicted at non sampled locations (Webster & Oliver, 2001).

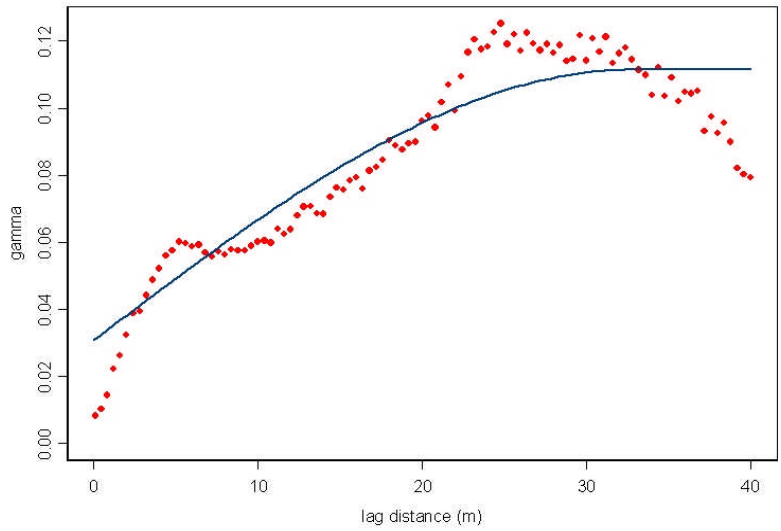

Figure 2.8: experimental (red dots) and empirical (blue line) variograms. Gamma represents the semivariance.

Three main parameters define the empirical variogram: range, sill and nugget (Figure 2.9). Range is the maximum distance over which pairs of observations remain correlated (Nielsen & Wendroth, 2003). Sill is the maximum value obtained for a transitional or bounded semivariogram. Nugget defines the spatially dependent variation that occurs over smaller distances than the smallest sampling interval and the measurement errors. Table 2.3 summarises possible models for the variogram modelling procedure.

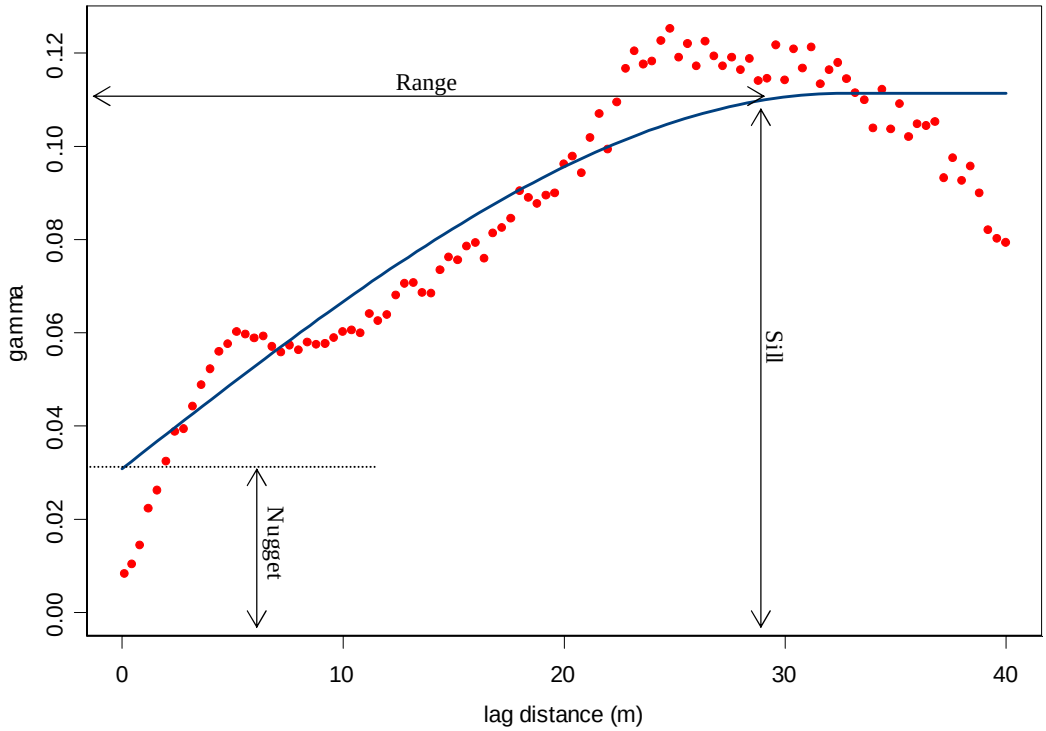

Figure 2.9: *variogram* parameters (sill, range and nugget).

Prediction of values at non measured points is obtained by interpolating with a kriging procedure. Kriging estimates the value of a random variable, Z, at one or more unsampled locations (Webster & Oliver, 2001). The estimation is done by applying a weighted average of data:

$$\hat{Z}(x_0) = \sum_{i=1}^{N} \lambda_i z(x_i)$$

Where:

N is the number of sampled points

$z(x_i)$ is the value of a sampled point at location x_i

$\hat{Z}(x_0)$ is the predicted value at location x_0

λ_i are the weights and meet the condition:

$$\sum_{i=1}^{N} \lambda_i = 1$$

Predicted values depend upon the empirical variogram modelled and therefore, the more accurate the variogram is, the better the predicted result. Accuracy of the fitted model for the variogram increases with the number of points collected (Webster &

Oliver, 1992). Webster and Oliver (1992) determined that 30-50 point-to-point (pairs of points), regarded by some authorities as adequate for the variogram calculation, were not enough for the prediction of non erratic variograms.

Table 2.3: authorized functions for the experimental *variogram* modelling procedure (Webster & Oliver, 2001). Parameters included in the equations are: a=range, c=sill, c_0=nugget, h=lag distance, α=curvature descriptor, ω=descriptor of the intensity of variation, r=distance parameter that defines the spatial extent of the model.

Classification	Model	Equation
Unbounded	Power function	$\gamma(h) = \omega h^{\alpha} \rightarrow for(0 < \alpha < 2)$
Bounded	Circular	$\gamma(h) = \left\{ c\left\{ 1 - \frac{2}{\pi}\cos^{-1}\left(\frac{h}{a}\right) + \left(\frac{2h}{\pi a}\right)\sqrt{1 - \frac{h^2}{a^2}} \right\} \rightarrow for(h \le a) \right.$ $\gamma(h) = c \rightarrow for(h > a)$
	Spherical	$\gamma(h) = \left\{ c\left\{ \left(\frac{3h}{2a}\right) - \frac{1}{2}\left(\frac{h}{a}\right)^3 \right\} \rightarrow for(h \le a) \right.$ $\gamma(h) = c \rightarrow for(h > a)$
	Pentaspherical	$\gamma(h) = \left\{ c\left\{ \left(\frac{15h}{8a}\right) - \frac{5}{4}\left(\frac{h}{a}\right)^3 + \frac{3}{8}\left(\frac{h}{a}\right)^5 \right\} \rightarrow for(h \le a) \right.$ $\gamma(h) = c \rightarrow for(h > a)$
	Exponential	$\gamma(h) = \left\{ c\left\{ 1 - \exp\left(-\frac{h}{r} \right)^3 \right\} \rightarrow for(h \ge 0) \right.$
	Gaussian	$\gamma(h) = \left\{ c\left\{ 1 - \exp\left(-\frac{h^2}{r^2} \right) \right\} \rightarrow for(h \ge 0) \right.$
	Pure Nugget	$\gamma(h) = \{ c_0 \{ 1 - \delta(h) \} \rightarrow for(h \ge 0)$
	Combined models	$\gamma(h) = \left\{ c_0 + c\left\{ 1 - \exp\left(-\frac{h^2}{r^2} \right) \right\} \rightarrow for(h \ge 0) \right.$

The approach selected for the PhD is geostatistics. Many analytical techniques have been explored and discussed for the resolution of spatial, scaling and temporal analysis. Although any of the analytical approaches mentioned could provide methods for analysis, it was necessary to find a common approach that was useful for the resolution of the three stated problems. Geostatitical techniques have been selected as the approach for this research project because: (i) geostatistics provides a viable and comparable analytical procedure for the spatial, scaling and temporal issues, (ii) the technique considers the spatial variation of the variable under study, (iii) it allows the

combination of spatio-temporal variables and (iv) little work has been published using this analytical tool for hydromorphological parameters.

2.6. Discussion and conclusions

Three different concepts need to be considered when defining effective and efficient hydromorphological sampling strategies for rivers: spatial patterns, the scaling concept and temporal changes.

The need to design effective and efficient sampling strategies for hydromorphology has been recognised in many studies. Several analytical tools have been applied for the resolution of similar issues in different research fields. However, little work has been done on applying those tools to hydromorphological parameters.

Further research projects need to be developed to determine the application of such methods to help us to understand the spatial and temporal pattern of hydromorphology, contributing to understanding of spatial issues, the scaling concept and the temporal variation. Furthermore, spatial, scaling and temporal issues are interrelated and therefore, research studies will need to be developed to find a solution that considers the correlation and interrelation of these processes. This research project has selected geostatistical analysis as the starting point and potential tool for the resolution of the mentioned concepts separately. Correlation or interrelation between processes will be difficult to establish if the spatial, scaling and temporal pattern are not first understood independently.

Geostatistics has been selected for the methodology of the research due to three main advantages: (i) geostatistical analysis and kriging interpolation techniques provide a common framework for the three problems identified, which will allow the comparison of results between spatial, scaling and temporal analysis, (ii) semivariograms (geostatistics) have been proved to be a useful tool to solve spatial, scaling and temporal issues in many research areas and (iii) little work has been developed and/or published on geostatistical interpolation techniques applied to hydromorphological parameters.

3

Comparison of the accuracy of depth measurements for two sampling strategies and two sets of equipment.

River depth is generally measured with either a metric staff or a total station. Measurements obtained with this equipment can differ due to the characteristics of the equipment. This chapter describes the differences between depth measurements associated with the type of equipment that is being used.

3.1. Introduction and objectives of Chapter 3.

3.1.1. *Data collection possibilities for the 3D characterisation of the channel bed: Two equipment types available: Total Station (TS) and the Metric Staff (MS).*

River depth can be determined with different methodologies such as aerial photographs, echosounds or a simple walk along the selected reach. Usually, the selected reach is waded to take direct measurements of depth at specific locations. Two main sets of equipment can be used for this purpose: the total station (TS) and the metric staff (MS).

TS are topographical equipment that provide x, y and z coordinates of a measured point. The measurements are obtained by placing the telescopic range pole (Figure 3.1) at the point that is going to be measured. Data collected are stored in the internal memory and downloaded with the appropriate software later on. Measurements of bed channel topography (TO) and water surface level (WSL) are required for the calculation of river depth, which is the result of subtracting TO from WSL. Figure 3.1 shows a diagram of the components of the TS and some pictures of the data collection procedure.

The MS is used to directly measure depth when wading in rivers. The measurements are obtained by placing the MS on the channel bed and recording the reading given by the water surface level. Figure 3.2 shows the MS located at two sample points.

(a)

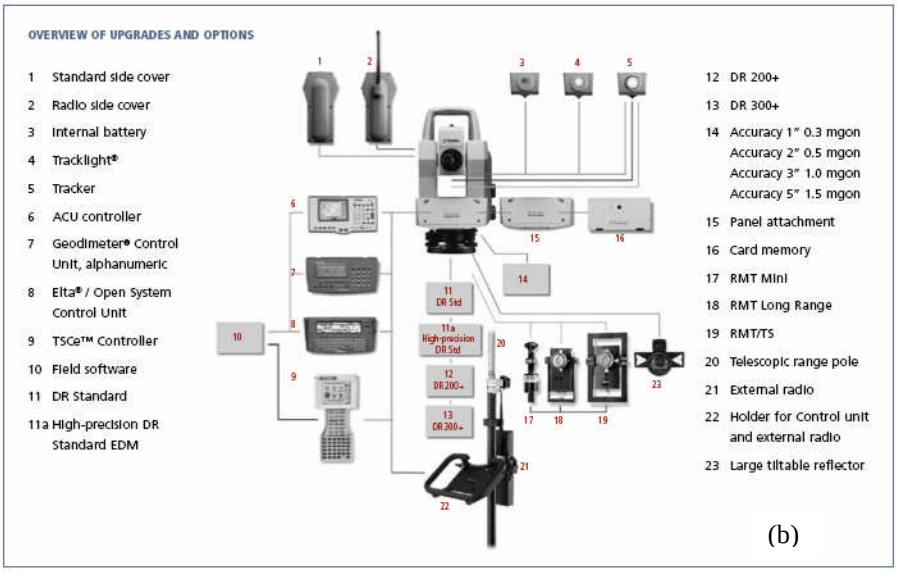

(b)

Figure 3.1: Depth data collection with the Total station (Trimble 5600). (a) Frontal view of the total station, (b) components of the total station, (c) total station placed in the river for data collection, (d) positioning of the telescopic range pole at a topographical point and (e) positioning of the telescopic range pole at the water surface level.

Both sets of equipment can be alternated during data collection in the field. The MS is generally used when no TS is available or for those locations where the measurements are impracticable with the TS. TO measurements cannot be obtained at locations

where depth is high (>2m), due to the difficulty accessing the location, and/or to the inadequate length of the telescopic range pole (Figure 3.3). Such points can be measured from the river bank with a MS long enough or with special equipment developed for the purpose.

A TS is preferable when high numbers of points need to be collected; the mechanisation of the process and the digital storage of the data allows increased data collection efficiency. The MS requires the writing down of depth measurements, as well as, the annotation of the distance between points to obtain the relative point coordinates. Also, measurements are difficult to take with the MS when the surface water velocity is high due to (i) the oscillations that the water surface produces around a reading (Figure 3.2) and (ii) the difficulty of maintaining the metric staff vertically; the problem with maintaining verticality with TS is overcome through use of levelling device. Thus, MS is preferable when relatively few points are measured, when there is not a TS available or when the river is not too deep to wade.

Figure 3.2: metric staff located at a point with low water surface velocity (left) and at a medium water surface velocity (right).

Since (i) water surface velocity makes the reading of depth when using the MS less accurate and (ii) this can have an effect on the increase in difference between

measurements taken with the two types of equipment, an analysis will be undertaken to determine how the flow characteristics affect the differences in depth readings obtained with both equipment types. Depth was measured with both types of equipment at areas with different water flow characteristics. These characteristics were assessed and associated with mesohabitats and flow types.

Figure 3.3: difficulties when measuring depth with the total station at deep points. The metric staff cannot be placed at deepest points because the data collector cannot walk any further (Windrush river site).

Chapters 4 and 6 have as main objectives the analysis of spatial patterns of river depth and the comparison of the accuracy level obtained with different sampling strategies/densities for eight defined indicators. In order to achieve these objectives, it is necessary to first understand the possible measurement error associated with the equipment that is being used. This Chapter focuses on providing a reference level to which the differences encountered between sampling strategies/densities considered can be compared. Differences between sampling strategies/densities will be significant if they are larger than the measurement error encountered.

3.1.2. *Heterotopic and Isotopic measurements with the TS*

WSL can be either collected following a heterotopic or an isotopic sampling strategy (Figure 3.4). In heterotopic sampling strategies, WSL is measured at different points

than the TO. WSL is interpolated (e.g. kriging) and predicted at the TO points. Depth is then calculated by subtracting TO from WSL. A second interpolation is required to predict depth value at non measured locations.

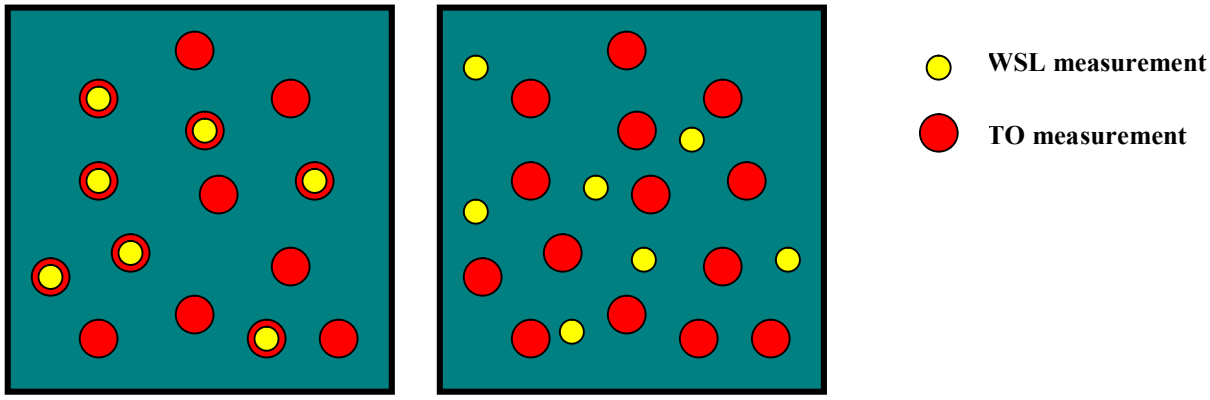

Figure 3.4: Isotopic (left) versus Heterotopic (right) sampling strategies for river depth.

WSL for heterotopic sampling strategies can be either measured at points located in the river channel or at points located at the river banks (Figure 3.5). The last option is less time consuming but may introduce higher errors when predicting WSL values at the TO locations. Since the data sets available for this study included river sites sampled in both ways, the differences between both sampling strategies were analysed.

In the isotopic case (Figure 3.4), TO and WSL are measured at the same vertical points. Depth is then calculated by subtracting TO from the WSL. Interpolation techniques are then applied to obtain depth measurements at non sampled locations. Data collected following isotopic sampling strategies have the potential of including errors in the positioning of the telescopic range pole when measuring the WSL; WSL and TO points may not be located on the same vertical line (Figure 3.6) due to (i) lack of visibility of the bed channel because of a high water turbidity or (ii) instability at the waded point due to high water velocities. Thus, it was necessary to analyse the approximate deviation between TO and WSL points in isotopic data sets in order to determine the practicality of isotopic sampling strategies.

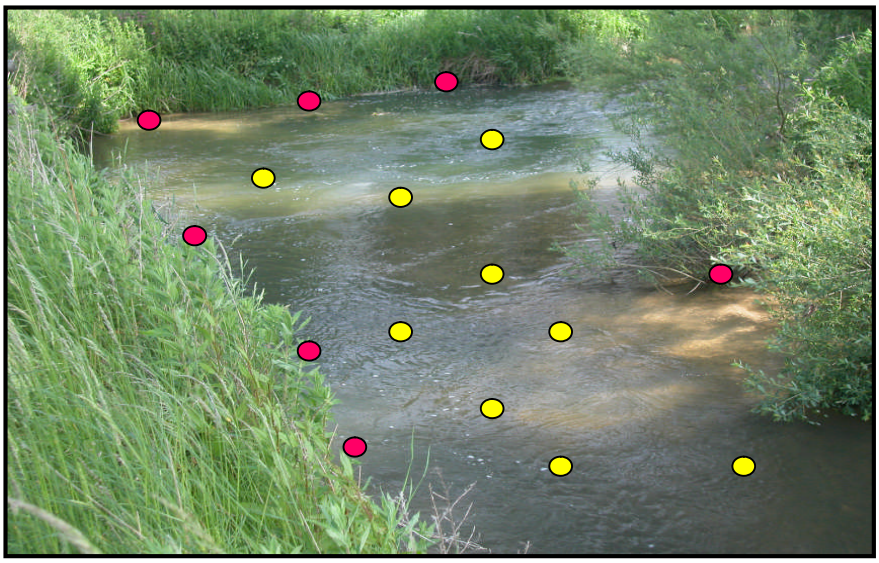

Figure 3.5: two possibilities for water surface level data collection: random along the reach (yellow dots) or following the river banks (red dots).

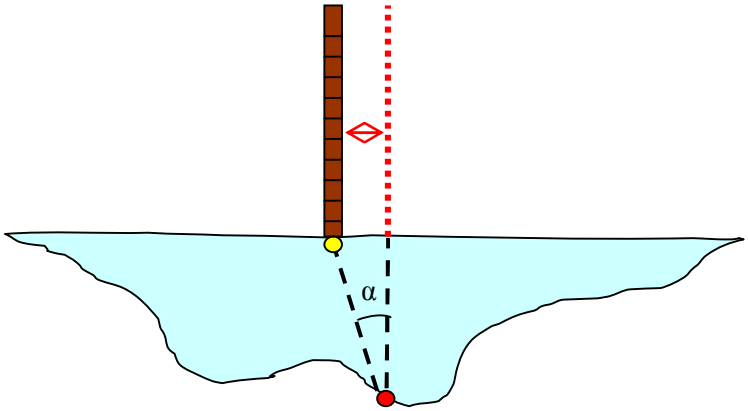

Figure 3.6: deviation of the telescopic range pole when measuring isotopic WSL and TO points.

3.1.3. *Prediction of WSL at non measured locations.*

WSL data collected following a heterotopic sampling strategy were predicted at the TO points measured to obtain the correspondent depth. This interpolation can either be implemented with kriging (geostatistics) or with descriptive geometry, also known as triangulation. Kriging requires the measurement of a high number of values of the variable that is going to be predicted so its spatial variation can be characterised. Descriptive geometry requires the measurement of fewer points for its application and considers that the variable measured behaves linearly and therefore, predictions can be obtained at non measured locations by defining the planes that link three measured

points (see section 3.2). These two methodologies were compared for the scope of this chapter.

Spatial WSL variation is considered low and thus, descriptive geometry can be applied to predict values at non measured locations. However, it is necessary to characterise the differences between various WSL sampling strategies in order to determine how far apart WSL points can be located along the bank for the application of descriptive geometry. Also, it is necessary to analyse if this methodology gives good predictions of WSL for points located in the river channel.

3.1.4. Objectives for Chapter 3.

The objectives of the data analysis included in this chapter are:

a. **first objective**: to determine the differences between depth measurements obtained with two sets of equipment: a TS and a MS.
b. **second objective:** to relate the differences between equipment to the mesohabitat and flow type characteristics of the sampled points.
c. **third objective:** determine the difference between depth calculated from heterotopic and isotopic sampling strategies.
d. **fourth objective:** to assess the level of deviation of the telescopic range pole of the total station, when trying to collect depth data following an isotopic sampling strategy.
e. **fifth objective**: to assess the differences between predicting WSL at non measured locations with triangulation and a kriging approach.

3.2. Methodology

Data were collected in SI units at three river sites (the Windrush, the Peris and the Seiont – see Appendix 1 for a full description of the river sites) using two different methods; a Trimble 5600 TS with autolock and a MS. The three sites were selected to compare results obtained at rivers with different hydromorphological characteristics. Sampling strategies applied at each river site were different since the data required different characteristics for each of the objectives listed. Hence, heterotopic, isotopic, MS and TS were combined in the data collection procedure.

Table 3.1 shows data collected at each river site for each sampling strategy, equipment and objective. The sampling strategies were applied during the same field visit (low flow). Therefore, it was assumed that no bed movement occurred during sampling.

The sampled reach at the Windrush river site is 30 m long, with one single mesohabitat type (a run). The reduced number of WSL points collected in the Windrush did not allow the application of interpolation techniques such as Kriging or Inverse Distance Weighting. The WSL data set was triangulated; six triangles, each of which defined a plane in the space, were created. The WSL value for each TO point was calculated by applying descriptive geometry (Ayres, 1958). The following sections describe the data analysis developed for each of the objectives.

Table 3.1: number of data points collected at the Windrush, Peris and Seiont river sites for each set of equipment and each sampling strategy (MS=Metric Staff, TS=Total Station). Note that points collected with both MS and TS have just been added once to the total. The objective column corresponds to the objectives identified in section 3.2.

River site	Objective	Variable	Heterotopic		Isotopic		Total
			MS	TS	MS	TS	
Windrush	a	TO	214	214	-	-	214
		WSL	-	9	-	-	9
Peris	a,b,c,d,e	TO	-	266	58	183	449
		WSL	-	193	-	183	376
Seiont	a,b,d,e	TO	-	-	106	106	106
		WSL	-	-		106	106

3.2.1. *Differences between depth measurements obtained with two sets of equipment: a total station and a metric staff.*

The differences between MS and TS measurements were calculated for specific indicators. The indicators selected were: Mean Squared Error (MSE), Mean Error (ME), descriptive statistics, frequency distribution (Kolmogorov Smirnov test), regression analysis and channel volume. A description of the selected indicators for the analysis in this chapter is given below:

Mean Squared Error (MSE): MSE is a measure of the difference between values measured with the TS and those measured with the MS. The MSE has been calculated

as expressed in equation (3.1) where y_i = depth TS; $\hat{y}_i$ = depth MS and N = total number of points sampled.

$$MSE = \frac{\sum_{i=1}^{N} (y_i - \hat{y}_i)^2}{N} \qquad (3.1)$$

Mean Error (ME): MSE provides the mean squared value of the difference between values measured with MS and values measured with TS. The ME has been calculated to provide a measure of the mean absolute difference between measured values. The following equation (3.2) was used for the calculation of ME. Where: y = depth TS; $\hat{y}$ = depth MS; N = total number of points.

$$\text{ME} = \frac{\sum_{i=1}^{N} |y_i - \hat{y}_i|}{N} \qquad (3.2)$$

Mean Difference between predicted and observed values was also calculated as an indicator of the error/difference between methodologies or equipments. Mean Difference was calculated as shown for the ME but without considering the absolute values of the differences. Therefore, Mean Difference presented positive or negative values whilst ME was always positive. Mean Difference has been calculated when it was necessary to identify which equipment/methodology provided higher estimations or readings of depth.

Descriptive statistics: maximum, minimum, average, median and standard deviation were calculated for the difference between depth measurements obtained with the MS and the TS. Box plots and histograms were plotted to complete the descriptive statistics analysis.

Regression analysis: a linear model was fitted for the depth values collected with the metric staff and those collected with the total station. The coefficient of determination or r-squared quantified the proportion of variation explained by the model created (Montgomery *et al,* 2001) indicating how similar the measured values of both

equipment types were. The slope and the intersection value of the regression line was also analysed.

The Pearsons correlation coefficient, as well as R-squared, measures a linear relationship but fails to detect any departure from the 45° line (Lin, 1989 and Nickerson, 1997). The concordance correlation coefficient (Lin, 1989) was calculated to evaluate the agreement between two readings (obtained with different equipment or sampling methodology) by measuring the variation from the 45° line through the origin (or concordance line). The concordance correlation coefficient is scaled between the range -1 and 1, as this gives a complete concordance with the 45° line. The concordance coefficient was calculated following equation 3.3:

$$\widehat{\rho}_c = \frac{2S_{12}}{S^2{}_1 + S^2{}_2 + (\bar{Y}_1 + \bar{Y}_2)^2} \qquad (3.3)$$

Where:

$$\bar{Y}_j = \frac{1}{n}\sum_{i=1}^{n} Y_{ij} \qquad S^2{}_j = \frac{1}{n}\sum_{i=1}^{n} (Y_{ij} - \bar{Y}_j)^2 \qquad S_{12} = \frac{1}{n}\sum_{i=1}^{n} (Y_{i1} - \bar{Y}_1)(Y_{i2} - \bar{Y}_2)$$

ρ_c is the concordance correlation coefficient,
Y_{ij} is the value of observation i with the equipment or methodology j (j= 1 and 2) and
n is the number of independent pairs of samples.

Frequency distribution (Kolmogorov Smirnov Test): frequency distribution of depth can be used to characterise the diversity of features present at a river site. A two sample non parametric test was applied in order to compare the depth distribution of measurements obtained with the MS and measurements obtained with the TS.

Channel Volume: since channel volume is an indicator of the potential capacity of the channel to hold suitable habitat for target species, it was necessary to determine if both types of equipment provide the same channel volume with the values measured. Channel volume, the two dimensional surface area (2D surface area is the mapped surface as if it was being observed from a aeroplane) and the 3D surface area (this is the are including all the changes in slope as if the wetted perimeter was being

calculated), were calculated for the depth values obtained with the TS and MS methods. The results obtained were compared.

3.2.2. *Relation between the differences of depth obtained with two equipment types and the mesohabitat/flow type characteristics of the sampled points.*

The differences between equipment were related to the mesohabitat and flow type where the measurements were subjected to General Linear Model (GLM) analysis. Surface velocity (flow type), mesohabitat type and substrate were recorded for each of the depth data points collected at the Peris and Seiont river sites.

Flow types and mesohabitats were defined as described below. The classification was developed by defining the more common features defined in the wide range of mesohabitat and flow type classifications. Flow types were assigned according to the typology used within the River Habitat Survey (Environment Agency, 2003). The flow types considered were Barely Perceptible Flow (BPF), Smooth, Unbroken standing Waves (UW), Broken standing Waves (BW) and Chute. Mesohabitats considered are listed below:

- No perceptible flow (NPF): no visible flow.
- Pool: smooth, low gradient water surface. Usually of limited downstream extent with shallower water evident both upstream and downstream.
- Riffle (RI): relatively steep water gradient, coarser bed material than local vicinity, some broken water. Usually of limited downstream extent with deeper water evident both upstream and downstream.
- Run: relatively smooth and low gradient water surface. Visible flow: clearly evident.
- Chute: bedrock slides, with water remaining in contact with the bed (velocity range > 0.45 ms^{-1}).

Substrate was visually identified and classified according to the dominant size type. The classes considered and their diameter were the following: not visible, clay (<1/256 mm), silt (1/256 mm to 1/16 mm), sand (1/16 mm to 2 mm), gravel (2 mm to 4 mm), pebble (4 mm to 64 mm), cobble (64 mm to 256 mm), boulder (>256 mm), bedrock and artificial.

3.2.3. *Differences between depths calculated with heterotopic and isotopic sampling strategies.*

WSL measured at heterotopic locations were predicted with geostatistical techniques (kriging) at the location of the isotopic WSL measured. The same statistics described in section 3.2.1 were calculated for the difference between predicted and measured WSL. Depth was calculated with both data sets (predicted and observed) for a total of 444 TO measured points at the Peris river site. The methodology applied in section 3.2.1. was applied to the difference between depth obtained with the isotopic and heterotopic data sets.

3.2.4. *Deviation of the position of the telescopic range pole between TO and WSL for isotopic measurements.*

Descriptive statistics were obtained for the value of horizontal distance (Figure 3.6) that separates the TO reading from the WSL reading. The analysis was carried out with the Seiont (106 points) and the Peris (183 points) data sets.

3.2.5. *Differences between prediction of WSL at non measured locations with Triangulation and Kriging approach.*

Different sampling densities were compared for the Peris and Seiont data sets to determine how far apart WSL points could be located along the river banks. WSL sampling strategies compared included WSL points collected every 2 m, 5 m, 10 m, 15 m and more than 20 m along both banks.

A total of 316 WSL points measured at the Peris and 106 measured at the Seiont were predicted with descriptive geometry with each sampling strategy. Statistics described in section 3.2.1 were calculated for the difference between measured and predicted WSL.

3.3. Results

3.3.1. *Differences between depth measurements obtained with two sets of equipment: a total station and a metric staff.*

MSE and Mean Difference: Results (Table 3.2) indicated that the Mean Difference was less than 1.3 cm for the Windrush and less than 3 cm for the Peris and Seiont data sets. The higher values of MSE and ME obtained for the Peris and Seiont could be due to the combination of mesohabitat, surface velocity, substrate and depth present at this river site.

Table 3.2: values of MSE and ME obtained for the Windrush, Peris and Seiont data sets.

River Site	MSE	Mean Difference (cm)
Windrush	0.115	1.21
Peris	0.0019	-2.77
Seiont	0.0017	-2.778

Descriptive statistics: the box plot for the Windrush showed that the mean difference between equipment was 0.4 cm and that the quartiles were between 1 cm and -1 cm. Similar interpretation can be obtained when analysing the histogram. Maximum and median differences identified were equal to 3.8 cm and 0.4 cm (Table 3.3) respectively. This indicated that measurements obtained with the TS were larger than those obtained with the MS, since the average difference obtained was positive.

Table 3.3: descriptive statistics calculated for the Windrush, the Seiont and the Peris (Depth TS – Depth MS) river sites.

Statistics	Windrush	Seiont	Peris
Total number of points	213	104	55
Maximum Difference (m)	0.03836	0.062	0.064
Minimum Difference (m)	-0.02126	-0.085	-0.080
Average Difference (m)	0.00395	-0.031	-0.027
Standard Deviation of Difference (m)	0.01124	0.025	0.026
Median of the differences (m)	0.00376	-0.028	-0.028

The values of descriptive statistics (Table 3.3) obtained for the Peris and Seiont river sites presented more extreme values than those obtained for the Windrush. Results for the Peris data sets showed that the averaged difference between values obtained with the TS and those obtained with the MS, was equal to 2.7 cm. The median value of the

difference between equipment was 2.8 cm, a value that was equal to that obtained for the Seiont river site. The maximum difference identified was 8 cm (negative value since MS gave a higher reading than the TS). The box plot did not show the existence of any extreme or outlier value for the Peris river site (Figure 3.7).

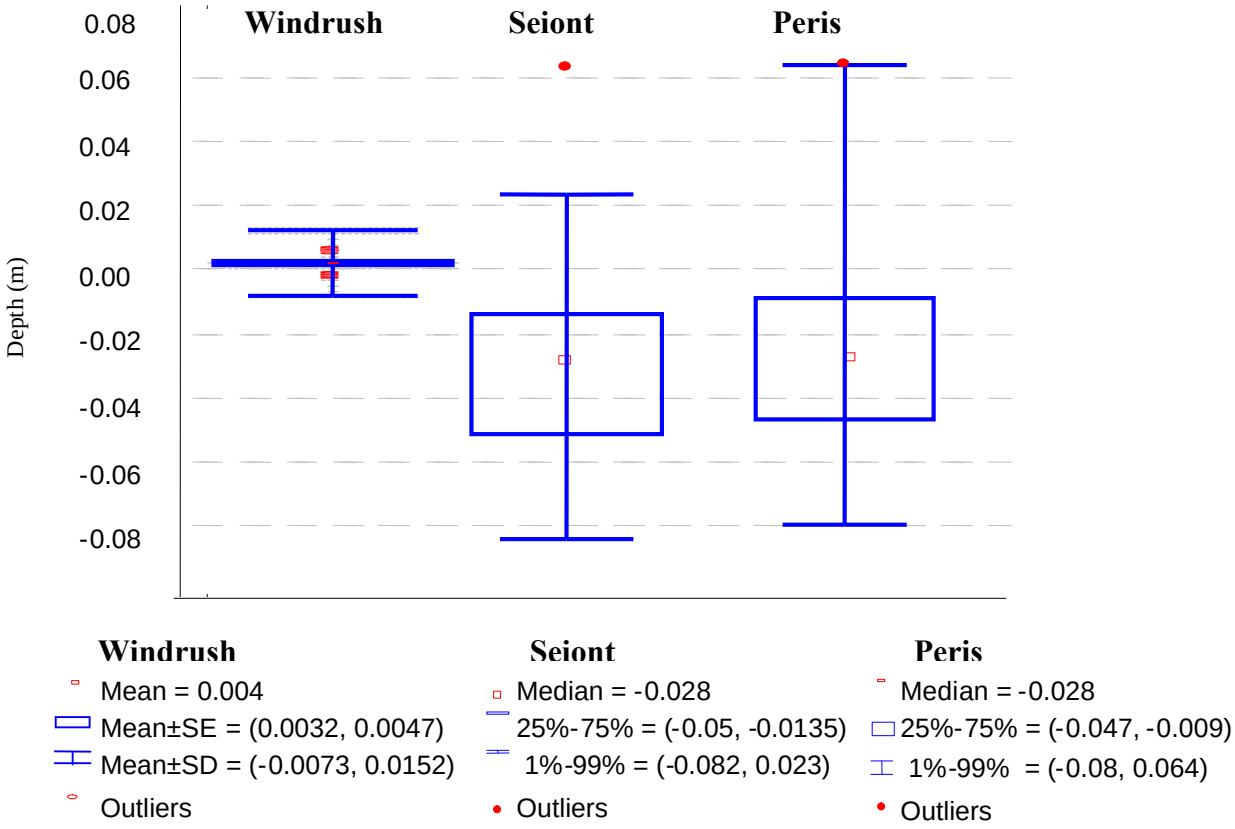

Figure 3.7: box-plot obtained for the difference between depth measured with the Total Station and depth measured with the Metric Staff. (Depth TS – Depth MT). From left to right the plots represent: the Windrush, the Seiont and the Peris data sets.

The descriptive statistics for the Seiont data set (Table 3.3) indicated that the averaged difference between equipment was 3.1 cm, with a maximum difference of 6 cm and a median of 2.8 cm. The box-plot results obtained for the Seiont indicated that higher differences between equipment types were encountered than in the Windrush.

Results showed that TS gave lower values than MS in 35%, 88% and 94% of the cases for the Windrush (data set with 214 points), Peris (data set with 58 points) and Seiont (data sets with 106 points) data sets respectively. There are two possible explanations for this behaviour: (i) the TS gives higher depth readings in some types of mesohabitats, which had a high representation in the studied area or (ii) TS systematically gives higher measurements due to the inherent characteristics of this

technique. Results also showed that differences between equipment were not systematic and they depended on other factors, such as depth, velocity surface, substrate and mesohabitat type.

Figure 3.8 (c) shows (i) that TS depth measurements were higher than MS depth measurements in deep areas for the Windrush and (ii) that higher differences between equipment were encountered in deep areas at the Windrush river site. A different pattern was identified for the Peris and Seiont data sets (Figure 3.8 (a) and (b)). The Seiont data set did not show differences between equipment in relation to the depth at the river site, whilst the Peris data set indicated that differences between equipment decrease with decreasing depth.

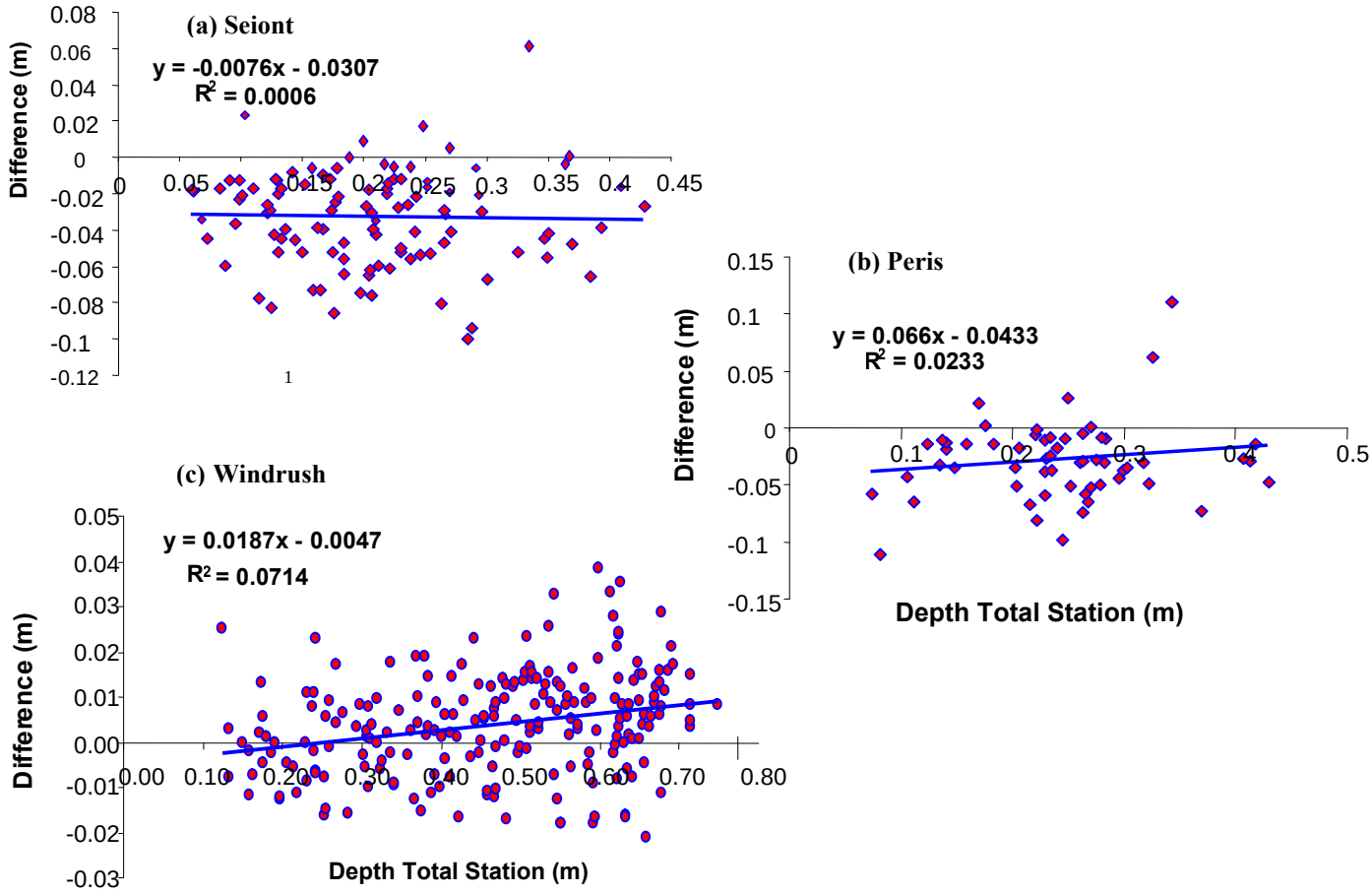

Figure 3.8: regression analysis of the difference between measurements equipment and a reference depth (total station depth). The difference between equipments corresponds to depth measured with the TS and depth measured with MT (depth TS – depth MT). The data sets analysed correspond to (a) Seiont, (b) Peris and (c) Windrush.

Regression analysis: the relationship between measurements obtained with TS and MS was established with a regression analysis. The value of the coefficient of

determination (Table 3.4) indicated that 99.53%, 82.71% and 90.9% of the variability, for the Windrush, the Peris and the Seiont respectively, were explained by the regression model when considering TS depth as the explanatory variable. The Windrush showed better agreement between values measured with the two techniques, whilst the Peris showed worst r-squared values. This may be due to the contrasts in the type of mesohabitat and flow types at the data collection sites. The same conclusion can be obtained by analysing the slope and the interception point. This indicated that TS depth values did not differ significantly from the MS depth values.

Table 3.4: results obtained for the regression analysis for two sets of equipment: TS and MT.

Regression analysis	Windrush	Peris	Seiont
R-squared	0.9953	0.8271	0.9098
Slope	0.9813	0.934	1.0076
Interception	0.0047	0.0433	0.0307
Concordance correlation coefficient	0.982	0.890	0.897

The concordance correlation coefficient was close to 1 for all the data sets analysed (Table 3.4). This indicated that the variation from the 45° line through the origin was small and that both sets of equipment provided very similar readings.

Frequency distribution (Kolmogorov Smirnov Test): results indicated that it can be accepted that both data sets collected at one specific river site, had similar distributions (K_s = 0.0419, p-value = 0.9898) for the Windrush and for the Peris (K_s = 0.2241, p-value = 0.1086), but they had different distributions for the Seiont (K_s = 0.217, p-value = 0.01).

Channel Volume: volumes of 79.29 m^3 and 78.51 m^3 were obtained for the TS and MS techniques, respectively, for the Windrush river site. The wetted surface areas were 193.93 m^2 for the TS and 194.21 m^2 for MS (two dimensional surface area equal to 191.25 m^2 in both analysis). The results obtained for the "channel volume" study showed that higher values of volume were obtained when using the TS equipment (due to the fact that depth measurements obtained are also greater). The same analysis was developed for two mesohabitats (chute and pool) in the Peris river site and one mesohabitat (run) in the Seiont. The results, which are summarised in Table 3.5,

indicated that the differences encountered between mesohabitats were not relevant since the surfaces and volumes obtained were very similar.

The maps obtained for the Windrush river site (Figure 3.9) indicated that MS depth values were higher than TS depth values in shallow areas (riffles), with the TS measurement being higher in deep areas. The Peris and Seiont rivers were analysed according to the mesohabitat type: one pool and one chute for the river Peris and a run for the river Seiont (Figure 3.9). The maps showed that MS usually presents higher values of depth than those obtained with the TS for the mesohabitats studied at the Peris and Seiont river sites.

Table 3.5: 2D surface area, 3D surface area and volume for the Peris-Seiont data sets.

River Site	Mesohabitat	Methodology	2D surface area (m^2)	3D surface area (m^2)	Volume (m^3)
Seiont	**Run**	**TS**	344.41	345.76	45.42
		MS	344.41	346.13	45.76
Peris	**Pool**	**TS**	13.43	14.01	1.40
		MS	13.63	14.29	1.53
Peris	**Chute**	**TS**	4.49	5.11	0.56
		MS	4.50	5.26	0.67

3.3.2. *Relation between the differences of depth obtained with two types of equipment and the mesohabitat/flow type characteristics of the sampled points.*

Figure 3.10 shows the combinations of depth, mesohabitat type, surface velocity and substrate obtained from the collected data. Some combinations were not represented due to the low probability of occurrence that they had at the studied sites. The results obtained for the Windrush river site, whose substrate was mainly dominated by a combination of gravel-and-silt and clay, did not show relevant differences between sets of equipment (Table 3.3). Differences between methodologies remained constant along the studied river site and so, no differences between substrate, surface velocity, depth and mesohabitat type were identified.

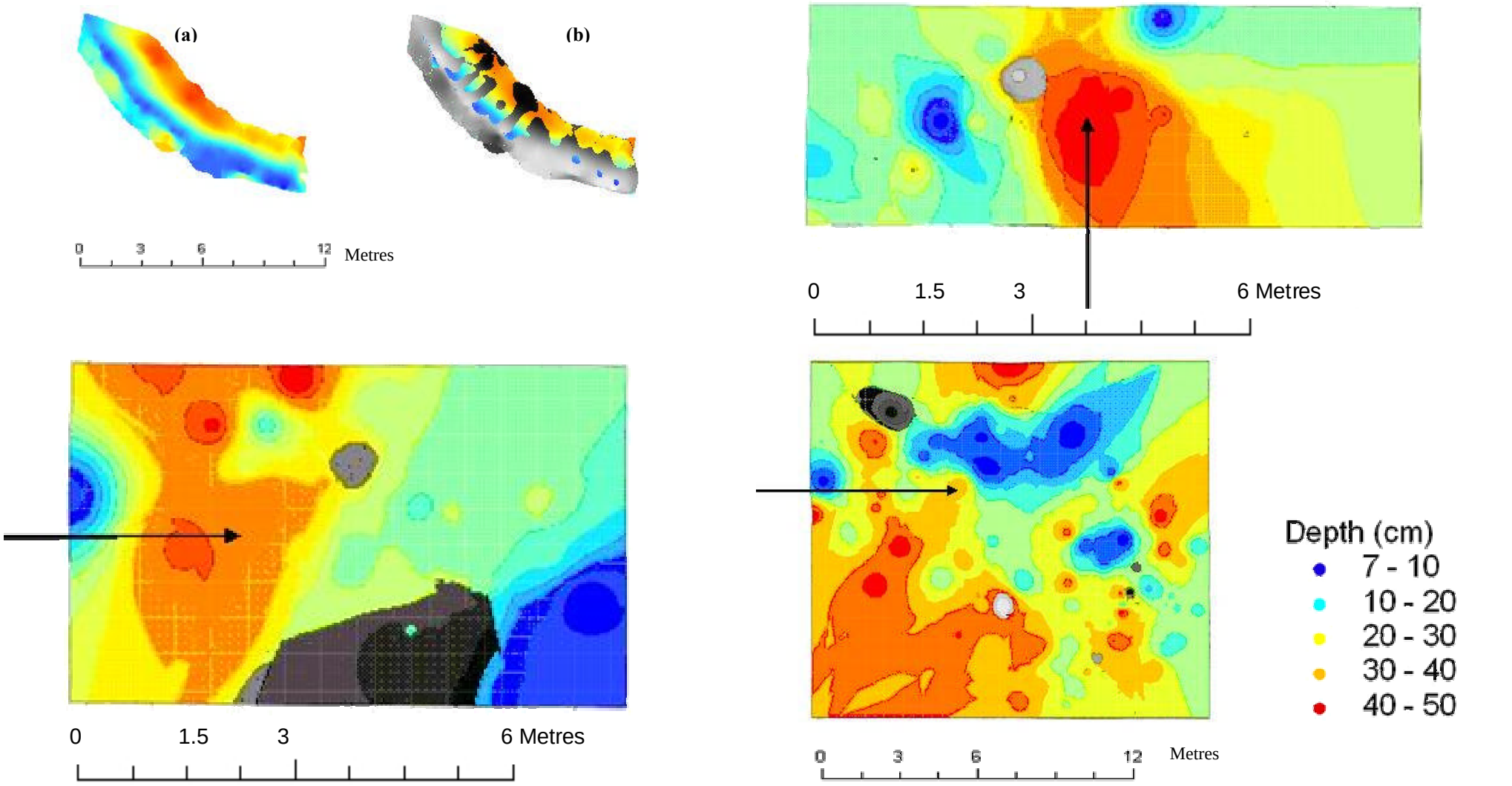

Figure 3.9: The plots represent the superposition of depth values obtained with TS (grey scale) and MS (coloured scale). Areas were MS gave a higher value than TS are coloured whilst areas where TS depth was higher than MS depth are represented in the grey scale. Representation of the depth values obtained with MS and TS equipment for the Windrush river site (top left): (a) shows MS only and (b) shows TS superposed on MS, the pool at the Peris river site (bottom left), the chute at the Peris river site (top right) and the run at the Seiont river site (bottom right). Shallow areas (≈7cm) are represented in red whilst deep areas are blue (≈50cm).

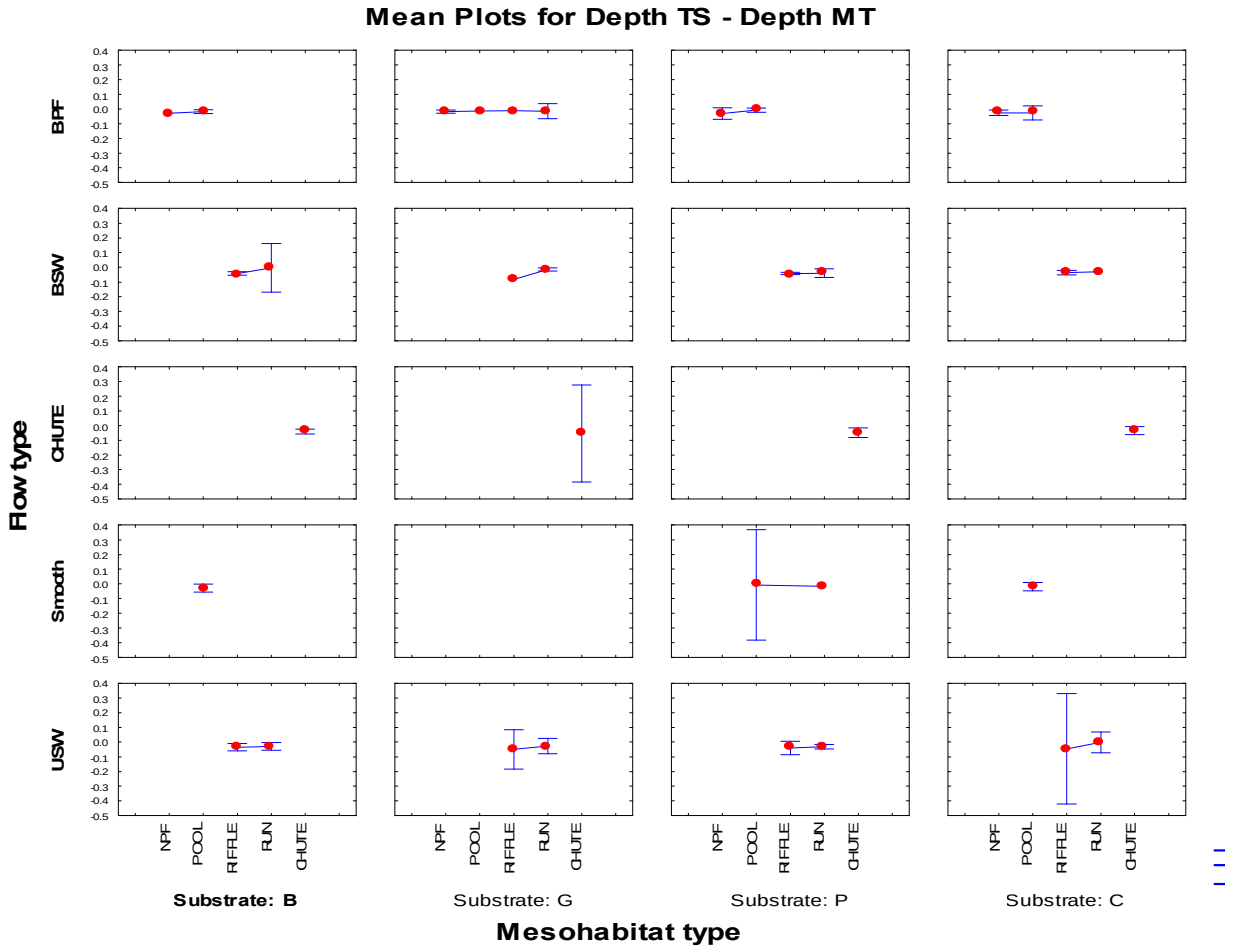

Figure 3.10: mean plot for the combinations of substrate, mesohabitat type and flow type represented by the three data sets (Windrush, Seiont and Peris). Each plot shows data from all river sites as relevant. The variables are coded as follows: No Perceptible Flow (NPF), Boulder (B), Gravel (G), Pebble (P) and Cobble (C), Barely Perceptible Flow (BPF), Broken Standing Waves (BW) and Unbroken Standing Waves (UW). Red dots show the mean value and blue lines the 0.95 confidence interval. Data has been joined for visual purposes.

Alternative grouping of the flow types were made and investigated. The difference between Depth TS - Depth MS was analysed for the different flow types to determine if there was evidence to reject the null hypothesis that differences between depth measurements obtained with TS and MS did not depend on the flow type. Flow type was classed as fast, slow and UW. The significance level (p=0.048) indicated that there was evidence to reject the null hypothesis (Figure 3.11). The p-values obtained for hierarchical nested GLM indicated that there was no evidence to reject the null hypothesis that considers differences in depth for the two methodologies at two river sites (p=0.55 for the mesohabitat test, p=0.17 for the surface velocity test and p=0.44 for the substrate test).

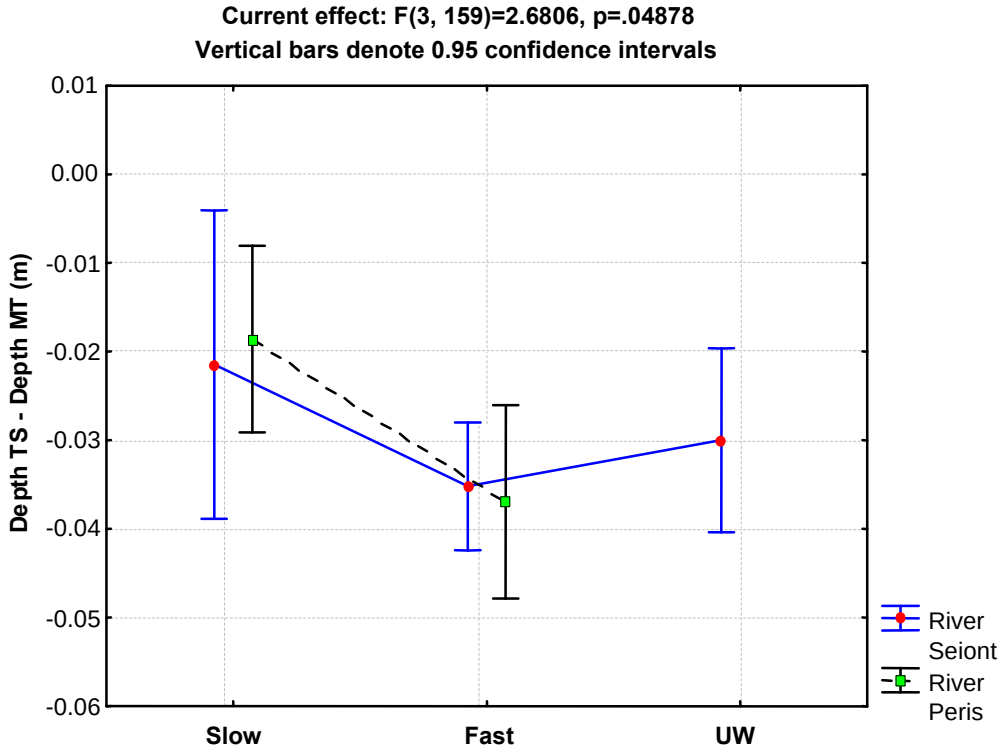

Figure 3.11: mean plot obtained from the GLM [(Depth TS-Depth MS) ~ flow type, where flow type is coded as slow, fast, unbroken standing waves] for the fast – slow flow types. Data has been joined for graphical purposes.

3.3.3. *Differences between depth calculated with heterotopic and isotopic sampling strategies.*

The geostatistical analysis of the WSL heterotopic data set was carried out in order to obtain predictions of WSL at the isotopic measured points. The anisotropy study, which analysed the change of the variogram characteristics according to the spatial direction being analysed, indicated that there were no differences in the spatial variance according to the direction analysed (Figure 3.12). The models analysed for the calculation of the variogram were the exponential, the spherical and the Gaussian. The values of range obtained were very high which indicates that there was a spatial relation between WSL measurements for long lag distances (more than 27 m) and that a reduced number of WSL data needed to be collected to predict values at non measured points. The Gaussian model was the best fitting model and was selected to predict WSL at the isotopic WSL points. Predicted points were compared to those measured at the same locations. The results are summarised below.

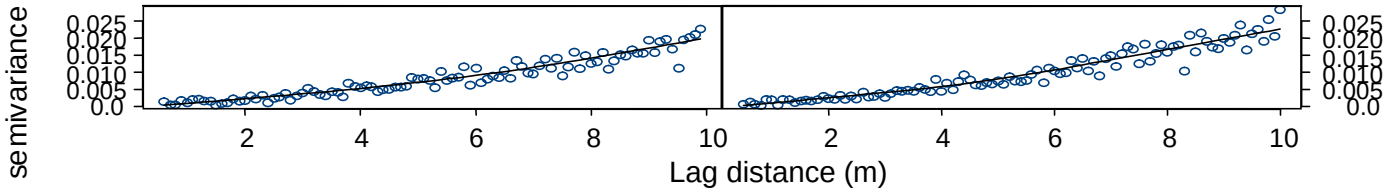

Figure 3.12: example of Anisotropy results for the heterotopic WSL collected at the Peris river site. Left hand image represents the variogram along the river and right hand image the variogram across the river. This example corresponds to an azimuth tolerance equal to 1.25; this means that the angle selected for neighbourhood search is very small and therefore, anisotropy would be easier to detect.

Descriptive statistics: Results show that there was a higher proportion of points where the predicted value was higher than the measured one (59.6 %). This indicated that heterotopic data sets tended to overestimate the WSL isotopic readings. The same pattern was observed for the differences of depth calculated with the original isotopic data set and the predicted one.

Results obtained when calculating depth with both methodologies showed that mean differences between data sets were equal to -1.2 cm, where the sign indicates that the predicted values are higher than the TS readings. Maximum differences were around 12.3 cm for overestimations of the predictions and 8.6 cm for underestimations of the predictions (Table 3.6). Therefore, the overestimations of the predicted values were higher than the underestimations. The absolute averaged difference (ME) was 3.3 cm. Maximum and minimum absolute differences were 12.36 cm and 0.014 cm respectively.

Table 3.6: descriptive statistics for the measured and predicted WSL (m) and depth (m). "Iso" refers to Isotopic and "Hetero" to Heterotopic.

Parameter	WSLHetero	WSLIso	WSL Iso-WSLHetero	DepthIso	DeptHetero	DepthIso-DepthHetero
Min	8.94	8.92	-0.12365	0.000	-0.0161	-0.1236
Mean	9.27	9.26	-0.01081	0.2025	0.2145	-0.0120
Median	9.24	9.22	-0.00805	0.2200	0.2201	-0.0093
Max	9.75	9.67	0.086224	0.4300	0.4708	0.0862
Total N	188	188	189	444	444	444
Std Dev.	0.19	0.18	0.040149	0.0859	0.0985	0.0398
SE Mean	0.01	0.01	0.00292	0.0063	0.0072	0.0029
Skewness	0.28	0.20	-0.108	-0.0138	-0.0816	-0.0936
Kurtosis	-0.86	-0.90	-0.08785	-0.1305	-0.1704	-0.0538

Regression analysis: results indicate that there is a strong correlation between predicted and observed values (R^2 = 0.95). The residuals plot indicated that the predicted WSL with the heterotopic data set were usually higher than the isotopic measurements when increasing the WSL value. Overestimations were encountered for predicted values in the deepest areas

whilst underestimations were found in shallower parts. Differences between sampling strategies were smaller for depths around 10 cm. The concordance correlation coefficient for depth and WSL was equal to 0.909 and 0.976, respectively. This indicated that there was a high agreement between the readings obtained with isotopic and heterotopic data sets since the variation from the 45° line through the origin was low.

Frequency distribution (Kolmogorov – Smirnov test): the results of the non-parametric test indicated that observed and predicted distribution of water surface level (Ks = 0.1277 and p-value = 0.0778) and depth (Ks=0.1202, p-value=0.1195) were not different.

Channel Volume: The total volume obtained (above plane 0 cm) differed by around 3 m^3 from the original isotopic depth data set to the predicted one (Table 3.7). Higher differences were encountered when calculating the volume above the plane of 10 cm, which indicates that volumes between the planes of 10 cm and 30 cm were introducing the majority of the variation**.** This may be due to the overestimation encountered when predicting the WSL and depth data with the heterotopic data set; the residual plot showed a wider range around 10 cm to 30 cm. The same pattern can be described for 2 dimensional and 3 dimensional areas.

The depth maps obtained with both sampling strategies (Figure 3.13) showed that deeper and shallower areas were identified in the heterotopic data set due to the differences obtained when predicting the WSL values.

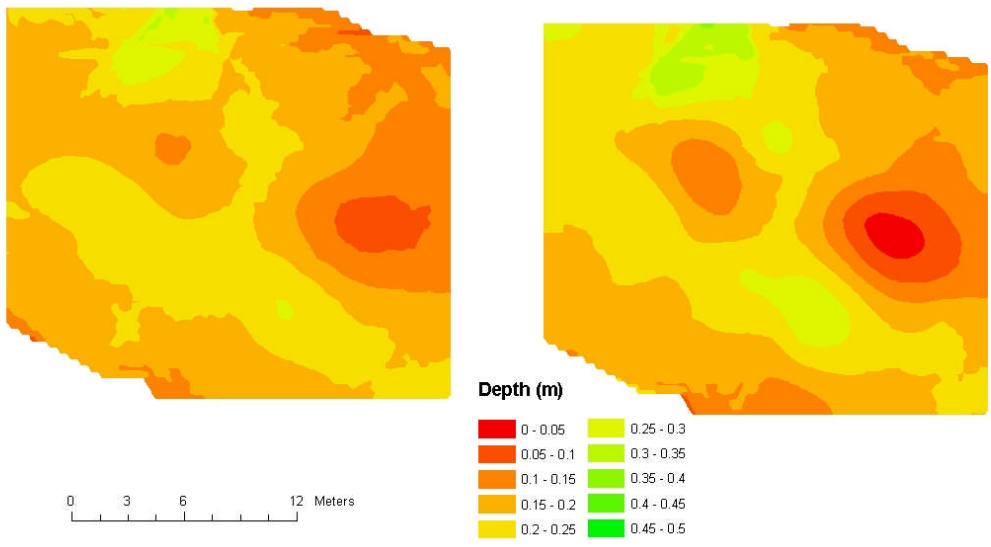

Figure 3.13: comparison between depth calculated with the isotopic (left) and heterotopic (right) data sets.

Table 3.7: 2D surface area, 3D surface area and volume obtained with the measured and predicted isotopic depth (m). Row "Plane" indicates at which depth the horizontal plane was located for the calculation of surface area and volume.

	Depth Heterotopic (m)					Depth Isotopic (m)					Depth isotopic-depth heterotopic (m)				
Plane (m)	**0**	**0.1**	**0.2**	**0.3**	**0.4**	**0**	**0.1**	**0.2**	**0.3**	**0.4**	**0**	**0.1**	**0.2**	**0.3**	**0.4**
2D AREA (m^2)	470.4	446.4	205.2	11.2	0	470.4	457.6	162	1.6	0	0	11.02	-43.3	-9.6	0
3D AREA (m^2)	471.4	447.3	205.7	11.3	0	471.6	458.5	162	1.6	0	0.3	11.22	-43.4	-9.7	0
VOLUME (m^3)	89.1	42.8	6.6	0.3	0	86.3	39.4	3.5	0.01	0	-2.8	-3.43	-3	-0.3	0

3.3.4. *Deviation of the position of the telescopic range pole between TO and WSL for isotopic measurements.*

The descriptive statistics obtained for the 183 and 106 points studied at the Peris and Seiont river sites, respectively, are presented in Figure 3.14. The results indicated that horizontal mean deviation of 10 cm can be observed between TO and WSL measurements. Note that there are few extreme values or outliers (Figure 3.14) that have not been deleted from the data set since they were not associated to any measurement error but to the difficulties of measuring the data in the field.

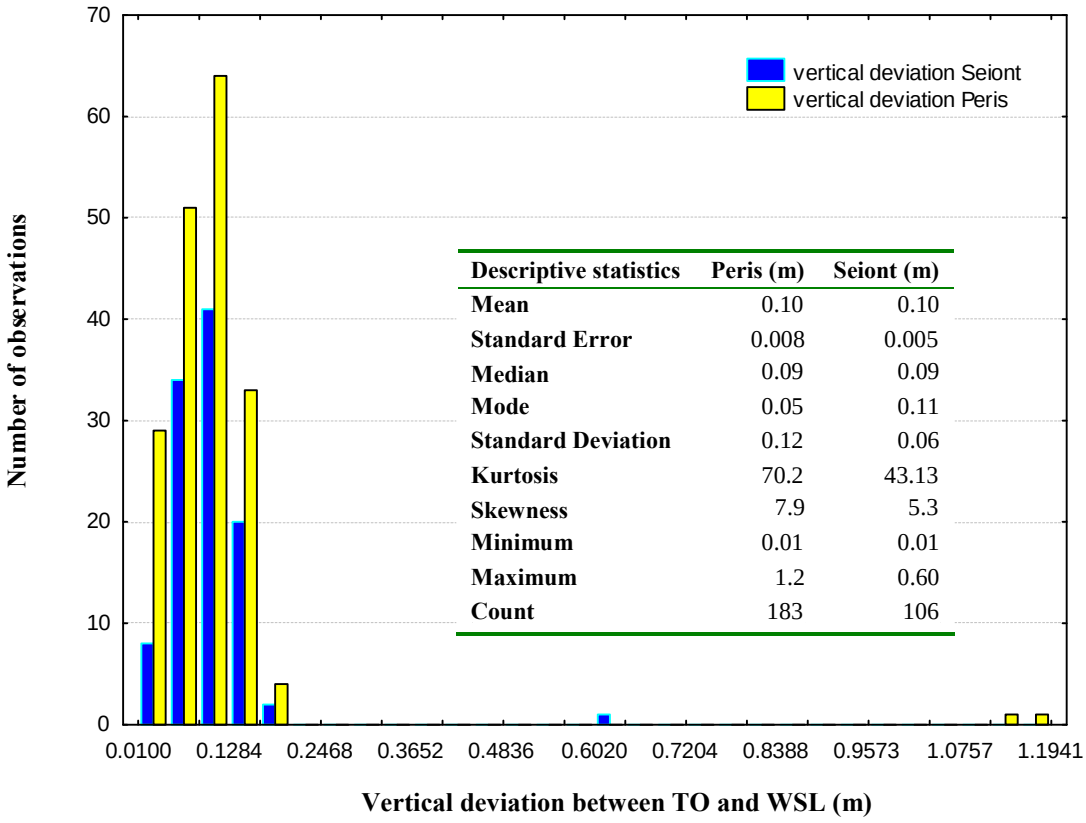

Figure 3.14: histograms and descriptive statistics for the vertical deviation between TO and WSL measurements in isotopic data sets. Note the extreme values for both data sets.

3.3.5. *Differences between prediction of WSL at non measured locations with Triangulation and Kriging approach*

The WSL sampling distances studied at the Peris river site were 2 m, 5 m, 10 m and 15 m, whilst only 5 m and 10 m distances were analysed at the Seiont river site due to the length of the sampled reach. Both data sets include the analysis of WSL predicted when only measuring four WSL points located at the extremes of the sampled area. The results obtained are now described.

Descriptive statistics:

Table 3.8 summarises the descriptive statistics obtained for both river sites. Results showed that (i) maximum absolute differences between predicted and observed values can be larger than 30 cm for some of the WSL sampling distances analysed, (ii) maximum and mean differences decreased when increasing the distance between WSL sampled points, (iii) mean differences between observed and predicted values were approximately 5 cm in the majority of the distances analysed and (iv) minimum and maximum differences between observed and predicted were approximately 1 cm and 6 cm, respectively. Mean values of difference (either absolute or not) between predicted and observed measurements were higher than the mean values of difference between heterotopic and isotopic sampling strategies presented in Table 3.6 and those obtained for the differences between depth measurements obtained with MS and TS.

Table 3.8: descriptive statistics for the differences between measured and predicted WSL (units in metres). Absolute values have been calculated to observe the global difference without considering if they are over or underestimations. Extremes refer to the maximum distance sampled at the site.

Descriptive Statistic		Peris					Seiont		
		2m	5m	10m	15m	Extremes	5m	10m	Extremes
STATISTICAL VALUE	Mean	-0.0238	-0.0490	-0.0440	-0.0328	-0.0094	-0.0265	-0.0253	-0.0244
	Standard Error	0.0033	0.0047	0.0034	0.0027	0.0035	0.0058	0.0028	0.0030
	Standard Deviation	0.0590	0.0837	0.0622	0.0486	0.0627	0.0594	0.0286	0.0314
	Minimum	-0.2196	-0.3200	-0.2308	-0.1839	-0.1450	-0.2573	-0.0899	-0.1003
	Maximum	0.1435	0.1341	0.1419	0.0990	0.1833	0.0748	0.0410	0.0517
	Count	316	316	316	316	316	106	106	106
ABSOLUTE Value	Mean	0.0445	0.0629	0.0561	0.0445	0.0514	0.0412	0.0297	0.0299
	Standard Error	0.0025	0.0041	0.0029	0.0021	0.0020	0.0048	0.0023	0.0025
	Standard Deviation	0.0454	0.0738	0.0521	0.0382	0.0371	0.0502	0.0240	0.0261
	Maximum	0.2196	0.3200	0.2308	0.1839	0.1832	0.2573	0.0899	0.1003

The analysis of box-plots obtained for both rivers showed that when increasing the number of WSL points included for the prediction of WSL, the range of extreme values increased whilst the mean of the predicted values remained relatively constant.

Conclusions that can be obtained from this analysis indicate that, for the river sites and sampling strategies analysed: (i) descriptive geometry tends to overestimate the observed measurements; (ii) distances of around 15 to 20 m between WSL points give WSL predictions that provide mean accuracy of around 5 cm; (iii) distance less than or equal to 5 m between WSL do not give as good predictions as distances of more than 10 m for the range of distances studied (from 2 to 20 m); and (iv) the higher the distance between WSL points, the better are the predictions.

Kolmogorov-Smirnov test: the non-parametric tests carried out for each river showed that all the predicted WSL distributions can be considered different to the observed one ($p<0.05$) and that the distributions of residuals did not belong to the same population ($p<0.05$).

Regression Analysis: in general the relation between observed and predicted values gave high values of R^2 for all the sampling distances analysed (Table 3.9). No pattern can be defined when comparing the R^2 values between them, although it was possible to identify an increase in the R^2 values between predictions and observed depth when decreasing the number of WSL collected. The R^2 for the residuals between observed and predicted were better distributed for distances between WSL points higher than 5 m. The same trend for the R^2 between predicted and observed values can be identified; better values of R^2 and better distributions of residuals were obtained when decreasing the number of WSL points included to obtain the WSL predictions.

Table 3.9: values of R^2 obtained for observed vs. predicted and observed vs. residuals for different WSL sampling distances.

Distance between WSL points	2 m	5 m	10 m	15 m	Extremes
Peris	0.7342	0.8249	0.9106	0.9438	0.9162
Seiont	-	0.5398	0.8813	-	0.8636

3.4. Discussion and Conclusions

Different analyses have been carried out in order to determine the differences between sampling equipment and techniques for depth measurements; metric staff vs. total station and heterotopic vs. isotopic data sets. Data have been collected at three different river sites: the Windrush, the Seiont and the Peris. The main conclusions obtained are summarised below:

Differences encountered between the two sets of equipment analysed (i.e. metric staff and total station) are slightly smaller than those differences encountered between depth obtained from heterotopic and isotopic data sets. Absolute mean differences between total station and metric staff are ≈0.4 cm for the Windrush river site and ≈3 cm for the Peris and Seiont river sites, whilst absolute averaged differences ≈3.3 cm are obtained between heterotopic and isotopic data sets. Maximum differences between measurements obtained with the total station and the metric staff are 3.8 cm for the Windrush and ≈6 cm for the Peris and Seiont. This difference reaches values of 12.3 cm when comparing heterotopic and isotopic depth data sets.

Larger differences than those encountered between measurements taken with total station and metric staff or between heterotopic and isotopic data sets can be observed when predicting WSL with descriptive geometry at non measured locations. Mean absolute differences (ME) are ≈5 cm, with maximum absolute differences that can be larger than 30 cm.

Descriptive geometry can be applied for the prediction of WSL at non measured points since WSL points are highly spatially related (i.e. spatial correlation can be appreciated over long distances (more than 27 m)). Thus, a reduced number of WSL points need to be collected to predict values at non measured points. However, it needs to be taken into account that the application of this methodology may contribute to increase the range of error (or difference) between depth values obtained with different equipment types and sampling strategies.

WSL predicted with descriptive geometry at non measured locations overestimates the observed measurements. Distances from 15 to 20 m between WSL points provide mean accuracy of ≈5 cm for the predicted locations; distance less than or equal to 5 m between WSL do not give as good an accuracy as distances of more than 10 m for the range of distances studied (from 2 to 20 m).The higher the distance between WSL points, the more

accurate the predictions are. This can be due to the fact that a higher number of planes are created when sampling points are every 5 m. Each plane is defined by three points and is in contact with either one or two more planes. Differences in the orientation of consecutive planes might increase the error in the prediction of WSL. Instead, when considering points that are separated by higher distances, the WSL becomes a smooth surface defined by a smaller number of planes. In this way, there are less changes in the orientation of each WSL plane defined.

Table 3.10 summarises the differences encountered between (i) two sets of equipment (MS & TS), (ii) heterotopic vs. isotopic data sets and (iii) observed vs. WSL values predicted with descriptive geometry. The values have been calculated by averaging the results of all the river sites analysed in each independent study. The differences encountered have been assumed to be independent and therefore, a total figure has been provided by adding up the differences encountered in each study.

Table 3.10: values of differences encountered for the three studies developed in chapter 3. TS vs. MS shows the averaged difference between depth measured with TS and depth measured with MS for all the river sites analysed. Heterotopic vs. Isotopic shows the difference between depth collected following these two sampling strategies. Triangulation refers to the difference between observed and predicted WSL with descriptive geometry when locating the WSL 10 m apart from each other.

Parameter	TS vs. MS (cm)	Heterotopic vs. Isotopic (cm)	Triangulation (cm)	Total (cm)
ME	2.25	3.3	4.29	9.84
Maximum absolute difference	6.20	12.36	16.03	34.6
Mean difference	2.00	1.08	3.40	6.48

Differences between metric staff and total station are not systematic; they depend on factors such as mesohabitat. TS depth measurements are higher than MS depth measurements in deep areas whilst MS provides larger readings in shallow areas. Differences between methodologies, MS and TS, are independent of the substrate where depth measurements are collected. However, these differences are not independent of the mesohabitat type at the measured location. Riffles and chutes are the features with highest differences between methodologies (≈4 cm) and are significantly different from runs and pools. Higher differences are presented for coarse materials (when analysing the trend of the substrate results) and high flow types. These results can be explained by the fact that it is more difficult to obtain accurate readings when using the metric staff in these systems. Thus, it is suggested to take measurements with MS in deep areas and measurements with TS at shallow points.

Depth differences between TS and MS can be calculated as differences in channel volume. The results show that differences in volume ≈3 m^3 are obtained for the sampled areas (80 m^2).

Difficulties in collecting isotopic data sets can be observed since deviations of 10 cm are encountered between WSL and TO isotopic points. This indicates that even isotopic data sets can be considered as heterotopic; a horizontal deviation of 10 cm between TO and WSL isotopic measurements can introduce high error in depth measurement. The shape of the channel may change considerably over distances ≈10 cm in areas with coarse material. Heterotopic data sets are therefore recommended for depth data collection since (i) the error introduced is not much larger than that obtained between sampling equipment (MS and TS) (ii) they are easier to collect and (iii) isotopic data sets have horizontal deviation between WSL and TO ≈ 10 cm.

4

Comparison of sampling strategies for depth, velocity and substrate

Monitoring of hydromorphological parameters is time and cost consuming. Interpolation techniques, such as kriging, are usually applied in order to predict values of the variable under study at non measured locations. This chapter focus on the comparison of the prediction error obtained with several sampling strategies when applying geostatistical interpolation techniques (kriging).

4.1. Introduction and objectives of Chapter 4

4.1.1. *Brief overview of the problem*

Hydromorphological variables are monitored for different purposes such as river restoration and habitat assessment. One of the difficulties of implementing monitoring programmes is the time and cost requirements of the sampling procedure. Efficient and effective sampling strategies need to be developed in order to reduce these constraints.

Time and economic requirements associated with data collection make the application of intensive sampling strategies impracticable. Thus, data are collected at some locations and then used to predict the value of the variable under interest at non measured locations. These predictions can either be obtained through remote sensing techniques, river mapping or interpolation procedures, among others. Even though interpolation techniques are commonly applied for the prediction of hydromorphological variables at non measured locations, little work has been done on determining which sampling strategy is adequate for their application.

4.1.2. *Objectives of Chapter 4*

This chapter aims to analyse the accuracy obtained with different sampling strategies when predicting values at non measured locations with geostatistical methods. The **first objective** of the study is to assess the prediction error of each sampling strategy when predicting values at non measured locations with geostatistics. The **second objective** is to study the spatial distribution of the error encountered for the predicted values and the **third objective** is to identify if the prediction error is equally distributed between mesohabitat types and flow types.

Two data sets were analysed: the first one was collected from a full-scale laboratory physical model of a natural channel run by the Department of Water Management at the University of Agricultural Sciences, Vienna (Hydrology and Hydraulic Engineering; BOKU) and the second was collected on the Leigh Brook river site (Worcester, UK) by the Department of Applied Sciences, Geography and Archeology at University College Worcester (see Appendix 1 for a detailed description of the river sites and the data collected). Five sampling strategies have been compared for the artificial Austrian channel through the calculation of nine indicators. Those sampling strategies that proved to be more successful have been compared for the Leigh Brook river site. The artificial Austrian channel was analysed first since it has a more detailed data set than the Leigh Brook.

The study was developed for three hydromorphological parameters (i.e. depth, velocity and substrate) for the Leigh Brook data set and only depth and velocity for the Austrian channel (substrate was not determined for this river site). Mesohabitat and flow types were characterised for both river sites.

4.2. *Notes on the data collected*

Flow types are defined by observing the characteristics of the water surface, whilst mesohabitat types are defined through the characterisation of depth, water surface velocity (i.e. flow types) and substrate. The diversity and number of mesohabitat or flow types provide information on the different biological conditions that are present.

Mesohabitat and flow types are qualitative variables and thus, they are associated with a degree of subjectivity. Results for the characterisation of a river site may vary depending on the experience/training of the surveyor and the range of features encountered at a site. The wide range of typologies available for the characterisation of mesohabitat and flow types (Bovee, 1997, Hawkins et al., 1993; Thomas and Bovee, 1993 cited in Bovee 1997, Frissell et al., 1986, Maddock, 1999, Borsany, P., Rowntree & Wadeson, 1998, Thomson et al., 2001, Brierley and Fryirs (2000 cited in Thomson et al., 2001) and Taylor et al. (2000 cited in Thomson et al., 2001) makes the selection of a typology for research projects difficult. Mesohabitat and flow type data collected for this research project were provided by Ian Maddock who had already developed his own typology for the characterisation of mesohabitats (Maddock, 1999). Figure 4.1 and Figure 4.2 show examples of the classes of mesohabitat and flow types identified at the Leigh Brook river site.

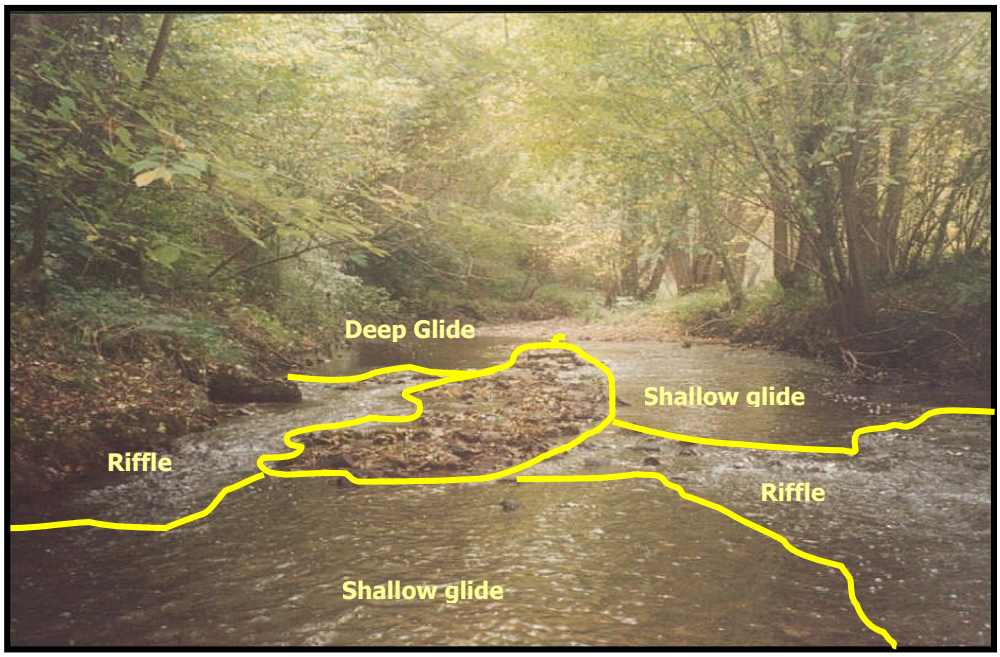

Figure 4.1: mesohabitat types identified at the Leigh Brook river site.

Substrate was classified by determining the dominant (>80%) substrate size present for the observed area. A second size was noted if it occupied > 20% of the bed area. Three sizes were noted if they occurred in approximately equal proportions. The classes considered and their diameters are fine (F), coarse (C), boulder (B) and bedrock (R). Fine includes clay, silt and sand sized particles (clay (<1/256mm), silt (1/256 mm to 1/16 mm), sand (1/16mm to 2mm)), coarse includes gravel and cobble-

sized particles (gravel (2mm to 4 mm), pebble (4mm to 64 mm), cobble (64mm to 256mm)), boulders represent particles >256mm and bedrock represents exposed rock.

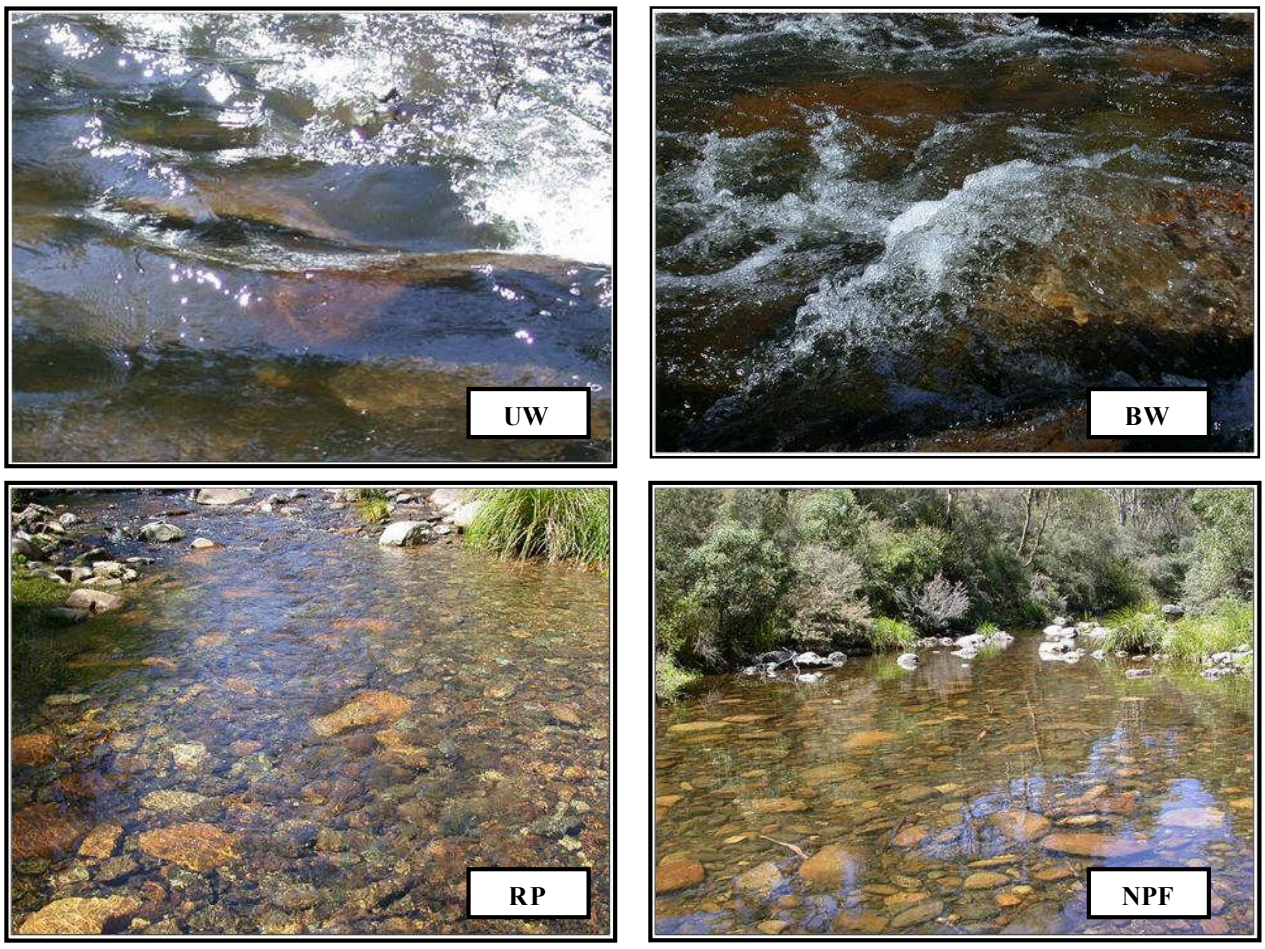

Figure 4.2: example of four flow types defined according to the River Habitat Survey. The abbreviations stand for Unbroken Standing Waves (UW), Rippled (RP), Broken Standing Waves (BW) and No Perceptible Flow (NPF).

4.3. Methodology

4.3.1. *The sampling strategies compared*

Five different sampling strategies were compared (Table 4.1 and Figure 4.3) for the Austrian channel. These sampling strategies were derived from the original data set which was based on a regular grid of 0.05 m x 0.07 m: (i) random grid points were created by random selection of points without replacement, (ii) stratified grids by selection of points included at a specific depth, velocity or Froude number interval, (iii) regular grids by dividing the sampled area into regular cells, (iv) regular transects by selection of equally spaced cross-sections and (v) irregular transects

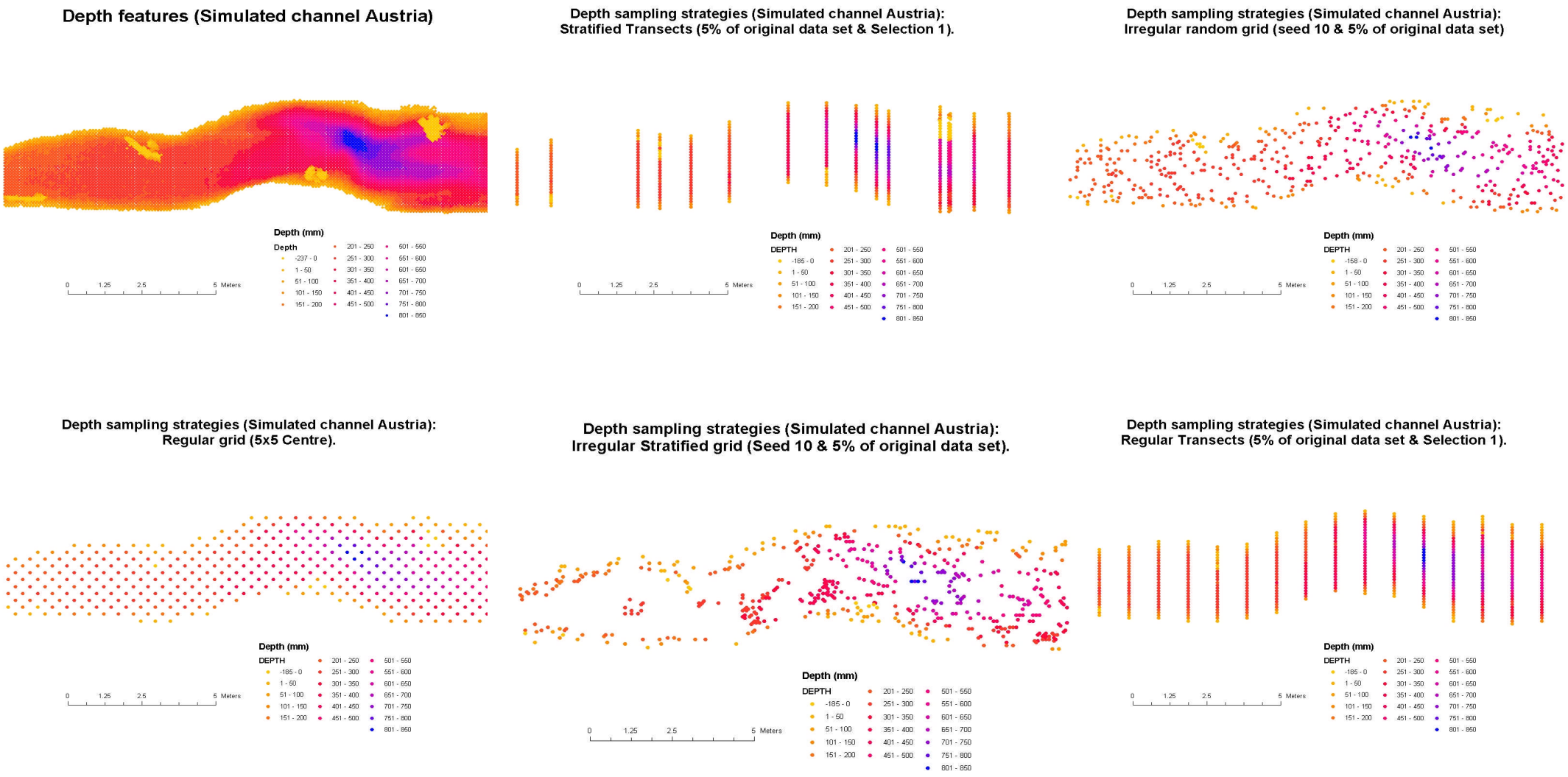

Figure 4.3: sampling strategies compared for the Austrian channel. Repetitions have been considered for some of the sampling strategies according to their characteristics. This image is an schematic diagram of the strategies compared for depth.

by identifying the mesohabitats at the river sites and locating the transects at "representative" sites of these mesohabitats.

Table 4.1: hydromorphological sampling strategies tested for the artificial Austrian channel (descriptions proposed after reviewing Parasiewicz, 1996; Parasiewicz and Dunbar, 2001 and Mader & Laaha, unpublished).

Sampling strategy		Description
Discrete cell representation	**Regular transects**	The study area (stream) is represented by a mosaic of cells. The stream is divided into regularly spaced cross sections. The hydromorphological parameters are sampled at regular distances within each cross section. The whole stream is represented by interpolation between transects.
	Stratified transects (Mesohabitat types)	The study area (stream) is represented by a mosaic of cells. The stream is divided into several-cross sections according to the morphological homogeneity of the habitat. The hydromorphological parameters are sampled according to their homogeneity in each cross section. Each cell represents a homogeneous hydromorphological unit. The whole stream is represented by interpolation between transects.
Grid	**Random Sampling**	The hydromorphological parameters are measured at points distributed in the studied area on an irregular grid. The whole stream representation is obtained by interpolation techniques.
	Regular Grid	The hydromorphological parameters are measured at points distributed in the studied area on a regular grid. The whole stream representation is obtained by interpolation techniques.
	Stratified Grid (Hydromorphological changes)	The hydromorphological parameters are measured at points distributed in the studied area according to the identified hydromorphological changes. The whole stream representation is obtained by interpolation techniques.

Different sampling densities were considered for each sampling strategy in order to identify the number of points to be selected for the definition of each sampling strategy. Subsets of data with different numbers of points were extracted from the original data set in order to compare the variogram characteristics (i.e. sill, range and nugget) obtained for each sampling strategy and variable (depth, velocity and Froude Number). Differences between the variograms of each sampling strategy were identified when decreasing the data sets to 428 points for the Leigh Brook and around 520 points for the Austrian channel. Thus, these used to define the size of the sampling data sets. Only 2583 points were selected for the data analysis for the Leigh Brook river site as those were the ones with measured values of velocity, depth and Froude number for the two flows considered. The study was carried out for the data obtained at both flows for the Leigh Brook river site ($Q=0.344\ m^3s^{-1}$ and $Q=0.517\ m3s^{-1}$).

The following points were also included in the analysis: (a) how the random selection of points, (b) how the intervals for the stratified sampling strategies and (c) how the

location of the regular transects affected the results by replicating the selection process of the subsets up to six times for the Austrian channel (Table 4.2). Results obtained were used to select the most successful sampling strategies for the repetition of the study at the Leigh Brook river site (Table 4.3). The six replications considered for the random sampling strategy at the Austrian channel were selected after observing the changes in variogram values obtained from a total of 10 different random selections of points created. Since values of sill, range and nugget did not present a high difference between randomly selected points, a reduced number of replications were selected.

4.3.2. *Depth*

The sampling strategies selected for the Austrian channel, their codes and the number of points used is shown in Figure 4.3 and Table 4.2. Two different sampling densities were compared (5% and 10% of the original data set) for each sampling strategy, with three replications for each sampling density. Transect sampling strategies have been replicated only twice due to the low number of transects that could be included with sampling densities of 5% and 10%. Replications analysed for regular grids considered two different distributions of points: corner and centre. Corner represents a regular grid defined by locating the points at the lower left corner of a 5 cm x 5 cm or a 3 cm x 3 cm (depending on the grid considered - see Table 4.3) grid and Centre located the points at the centre of each grid cell. The difficulties in selecting the same number of points following grids/transects and regular/irregular patterns introduced slight differences to the number of points considered for different the sampling strategies. This was considered when analysing the results.

A total of three sampling strategies were compared for the Leigh Brook river site (Table 4.3). Sampling densities selected for the Leigh Brook and Austrian channel are not comparable. Results obtained for the Leigh Brook river site will only be used to support those obtained for the Austrian channel since the artificial channel presented a more detailed data set.

Depth was measured in metres at the Leigh Brook river site and in millimetres at the Austrian channel. Variance, semivariance, Mean Squared Error and Mean Error were

calculated for the units in which data were collected in each case, unless the units of these parameters are specified.

Table 4.2: sampling strategies studied for depth hydromorphological parameter for the artificial Austrian channel.

Sampling strategy group	Sampling strategy	Percentage of original data set (sampling density)	Grid size - repetition sample (or random seed) / point location in the grid (cm).	Code	Num. Points
Grid	Regular	11.0	5x5-Centre	GRe5x5Ce	1151
		4.0	5x5-Corner	GRe5x5Co	409
		11.0	3x3-Centre	GRe3x3Ce	1151
		11.2	3x3-Corner	GRe3x3Co	1168
	Random	5.0	10	GRa5x10	522
		5.0	20	GRa5x20	522
		5.0	30	GRa5x30	522
		10.0	10	GRa10x10	1044
		10.0	20	GRa10x20	1044
		10.0	30	GRa10x30	1044
	Stratified	5.0	10	GStrat5x10	522
		5.0	20	GStrat5x20	522
		10.0	10	GStrat10x10	1044
		10.0	20	GStrat10x20	1044
Transects	Regular	5.0	1	TRe5x1	521
		5.0	2	TRe5x2	523
		10.0	1	TRe10x1	1044
		9.7	2	TRe10x2	1014
	Stratified	5.0	1	TStrat5x1	527
		4.9	2	TStrat5x2	517
		10.0	1	TStrat10x1	1050
		10.0	2	TStrat10x2	1052

Table 4.3: sampling strategies studied at the Leigh Brook river site for depth, velocity and Froude number measurements obtained at two flows (Q=0.344 m^3/s and Q=0.517 m3/).

Sampling strategy group	Sampling strategy	Percentage of original data set.	Abbreviation	Num. Points
Grid	Random	16.5	GRa	428
	Stratified	16.5	GStrat1	428
		16.5	GStrat2	428
Transects	Regular	16.5	TRe1	428
		16.5	TRe2	428

4.3.3. *Velocity*

The velocity data sets provided for the artificial Austrian channel were divided into depth layers in order to work with two dimensional data sets. Layers of velocity were defined by considering all the velocity values located at the same depth level (Figure 4.4), parallel to the bed channel. Those layers with less than 200 points were not analysed as it is necessary to have a high number of measured points (Webster & Oliver, 2001) in order to obtain accurate predictions with geostatistical techniques.

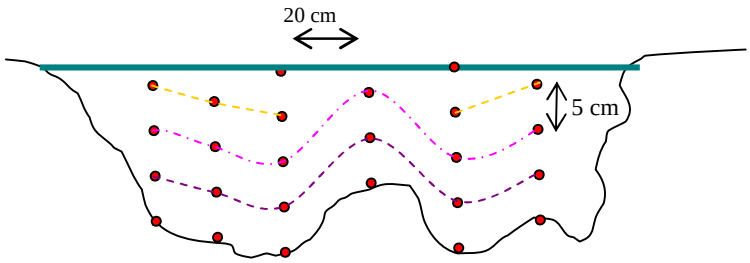

Figure 4.4: layers of velocity defined for the artificial Austrian channel, parallel to the bed channel (top).

The data characteristics only allowed the comparison of regular and stratified grid sampling strategies at the artificial Austrian channel (Table 4.4). Repetitions were considered for these two sampling strategies. Since the geostatistical analysis showed that the variogram was more stable for regular grids than for stratified ones, three repetitions for stratified sampling strategies and two repetitions for regular sampling strategies have been considered.

Table 4.4: percentage and number of points (referred to the original data set) included in each velocity sampling strategy analysed at the Austrian channel.

Sampling Strategy	Layer 1		Layer 2		Layer 3		Layer 4	
	%	No. of Points	%	No. of Points	%	No. of Points	%	No. of Points
Int5	70	159	75	170	74	149	69	136
Int10	60	136	59	133	62	126	60	117
Int20	42	95	42	95	47	94	37	73
RE50	50	112	50	113	50	101	50	96
RE25	25	58	25	56	25	53	25	51
Total number of pointa	100	227	100	226	100	203	100	197

Stratified grids were obtained by selecting the points which identify velocity changes of 5 ms^{-1} (Int5), 10 ms^{-1} (Int10) and 20 ms^{-1} (Int20). Regular grids were defined by selecting 50% (RE50) and 25% (RE25) of the original measured points. Conclusions about the differences between sampling strategies were established according to a series of indicators and the number of points included in each strategies. The same sampling strategies that were considered for the depth hydromorphological parameter (Table 4.3) were also considered for velocity at the Leigh Brook river site. Velocity data were collected in ms^{-1}. The results obtained were calculated in these units.

4.3.4. *Substrate*

Substrate data were only available for the Leigh Brook river site. Since substrate was measured at each depth sampled point, the same sampling strategies that were analysed for depth were considered for substrate (Table 4.3).

4.3.5. *The indicators*

Different indicators were calculated in order to compare sampling strategies when predicting hydromorphological parameters with geostatistical analysis (i.e. ordinary kriging). The indicators selected were quantitative and qualitative. The first type is the objective result of a mathematical equation whilst the second type is the result of subjective observations. The indicators were calculated for the straightened data sets.

Quantitative indicators

Variogram model assessment: Exponential, Gaussian and Spherical variogram models were compared. The goodness of fit was analysed through the Objective function (Cressie, 1993) and the percentage of variance accounted for. The smaller the value of the objective function, the better the fitted model. The "percentage of variance accounted for" is the *adjusted* R^2 *statistic*. The higher the percentage of variance accounted for, the better the fitted model at describing the measured data.

The azimuth and azimuth tolerance were determined after analysing the degree of anisotropy in the data set. The azimuth determines the direction for the search and selection of neighbours. The azimuth tolerance is a range in direction that also determines the search of neighbours. Values of azimuth tolerance are delimited by the interval 0° to 180°. The variogram created by the azimuth tolerance of 180° is called the omnidirectional variogram (Webster & Oliver, 2001). Other azimuth tolerances define directional variograms.

Anisotropy is present when the spatial behaviour of the parameter changes according to the direction analysed. This means that it is possible to identify different variograms according to the direction studied. The directions of main interest for this study are along and across the river. The variables analysed to determine the existence of anisotropy at a river site are range, sill and nugget. Different azimuth tolerances and lag distances were compared to determine at which point there was a compromise

between loss of directional information and capacity to represent anisotropy of the site (Webster & Oliver, 2001). The variance (or semivariance) obtained at specific lag distances have been compared for the two directions of interest to provide a quantitative reference for the determination of the "anisotropy level".

Mean Squared Error (MSE) and Mean Error (ME): The Objective function analyses the difference between observed values and fitted values for those points included in the variogram calculation. The MSE is a statistic that tests the capacity of the variogram to predict values from a validation data set, whilst ME also tests the capacity of the variogram to predict values but considers the mean absolute difference which gives a result that is directly related to the original data (Webster & Oliver, 2001).

Descriptive statistics: the mean, standard deviation, median, mode, minimum, maximum, skewness and Kurtosis values were calculated for the original data sets and the selected points for each sampling strategy analysed. The spatial distribution of the prediction errors was also analysed and related to the flow types/mesohabitat types identified at the Leigh Brook river site.

Frequency distribution: Frequency distributions of depth and velocity obtained for each sampling strategy were compared with those calculated for the original data set. A Kolmogorov-Smirnov test was carried out for this purpose.

Regression analysis: the relation between predicted and observed values were obtained through the application of linear regression analysis. Values of R-squared, slope and intercept were considered in the analysis.

Qualitative indicators

Mapping resolution: This indicator was used to determine which sampling strategies gave better approximations in terms of mapping resolution of the sampled area and to assess the differences that can be encountered between sampling strategies in terms of mapping resolution.

The variogram calculated with data from each sampling strategy was used to create an interpolated surface of the variable under study with ArcGIS 9 software. The resolution of each interpolated surface was compared with that obtained with the

original data set. Mapping resolution was not accepted as adequate when the map failed to differentiate the patterns shown in the original data set.

A regular grid was placed on top of each map to corroborate the differences encountered by visual assessment. The mean value of the points included in each cell was calculated and associated to the respective grid cell. The size of the cells was determined by the characteristics of the data sets collected. The area covered by the total grid was calculated and the sampling density of each sampling strategy was determined in relation to this area value. The size of the grid cells was obtained by dividing the total surface area between the total number of points in such a way that a mean of 2 points were included in each cell. Each river site and sampling strategy therefore had a specific grid cell dimension. Thus, results obtained for this indicator would not be comparable between river sites and sampling strategies.

Differences between grid cells of the original and predicted data sets were calculated by subtracting the mean values of the same grid cells. These differences were categorised with a binary system (0, 1), where 0 represents no difference between grid cell values and 1 represents the existence of differences between grid cell values. Two grid cells were considered different when the mean values of each cell differ more than twice the minimum standard error obtained for each hydromorphological parameter. The number of cells of each category was calculated to compare the results obtained for each sampling strategy.

Map of Standard Error: this indicator shows the distribution of the SE of the predictions across the interpolated surface obtained with each sampling strategy. The SE maps indicate which locations have the highest errors in prediction and which sampling strategies have higher errors. Maps that display a random pattern of SE were not considered suitable as spatial representations of the river site.

Predicted-Observed cross-sections and longitudinal profiles: The sampling strategies that gave better approximations to the original cross-section in terms of shape (i.e. depth) or trend (i.e. velocity) were visually identified. The percentage of times that a sampling strategy was more successful than the rest of the strategies was noted down to establish comparisons.

Channel Volume: the volume of the channel created by interpolating the data points defining each sampling strategy, as well as the wetted 2D and 3D surface areas were calculated for the studied sampling strategies with ArcGIS 9 software. Results obtained were compared with those obtained for the original data set.

4.4. Results

4.4.1. *Variogram model assessment*

DEPTH FOR THE AUSTRIAN CHANNEL

The variograms presented in Figure 4.5 are an example of the directional differences (azimuth tolerance of 30 degrees) detected. The variance is higher across than along the direction of river flow. This directional difference of variance decreases when increasing the azimuth tolerance since more area is considered for the determination of the neighbourhood of each variogram point. Anisotropy decreases when reaching azimuth tolerances $\cong 60°$, independently of the lag distance selected.

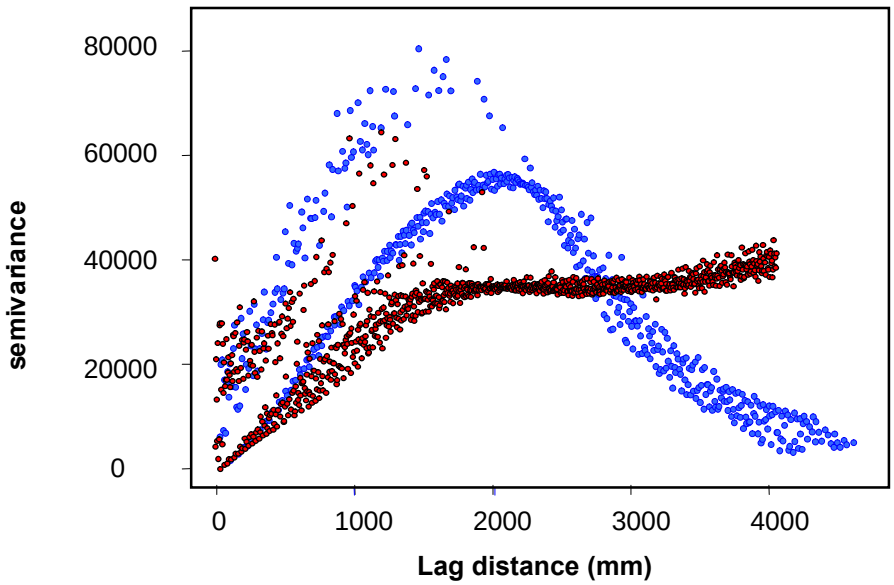

Figure 4.5: anisotropy study. Variograms for along (red) and across (blue) the river directions (Depth data set for the Austrian channel). In this example, azimuth tolerance is equal to 30 degrees.

The symmetry of the variogram representing the cross sectional direction (Figure 4.5) is due to the similarity of depth encountered at both ends of the measured cross sections. Thus, points that are very close have similar variances to points that are separated by the width of the cross section.

One requirement for the determination of the variogram is to have "sufficient" numbers of pairs of points to define a specific lag interval. Since the number of pairs of points available in the cross-sectional variogram decreased for lag intervals higher than 2.5 m (Figure 4.5), it can only be compared with the longitudinal variogram up to a lag of 2.5 m. Up to this distance the cross-sectional variogram was very similar in shape to that obtained for the longitudinal direction. Therefore, it can be assumed that the omnidirectional variogram defines the spatial behaviour of depth for both cross-sectional and longitudinal directions at the Austrian channel.

The directional variograms obtained for each sampling strategy were distorted (Figure 4.6 and Figure 4.7) in comparison to that obtained for the original data set. Cross-sectional variograms did show higher modifications than longitudinal variograms due to the fact that only few points were included for the calculation of the semivariance at a specific lag distance. Therefore, it is recommended to use the omnidirectional variogram to predict values across and along the river.

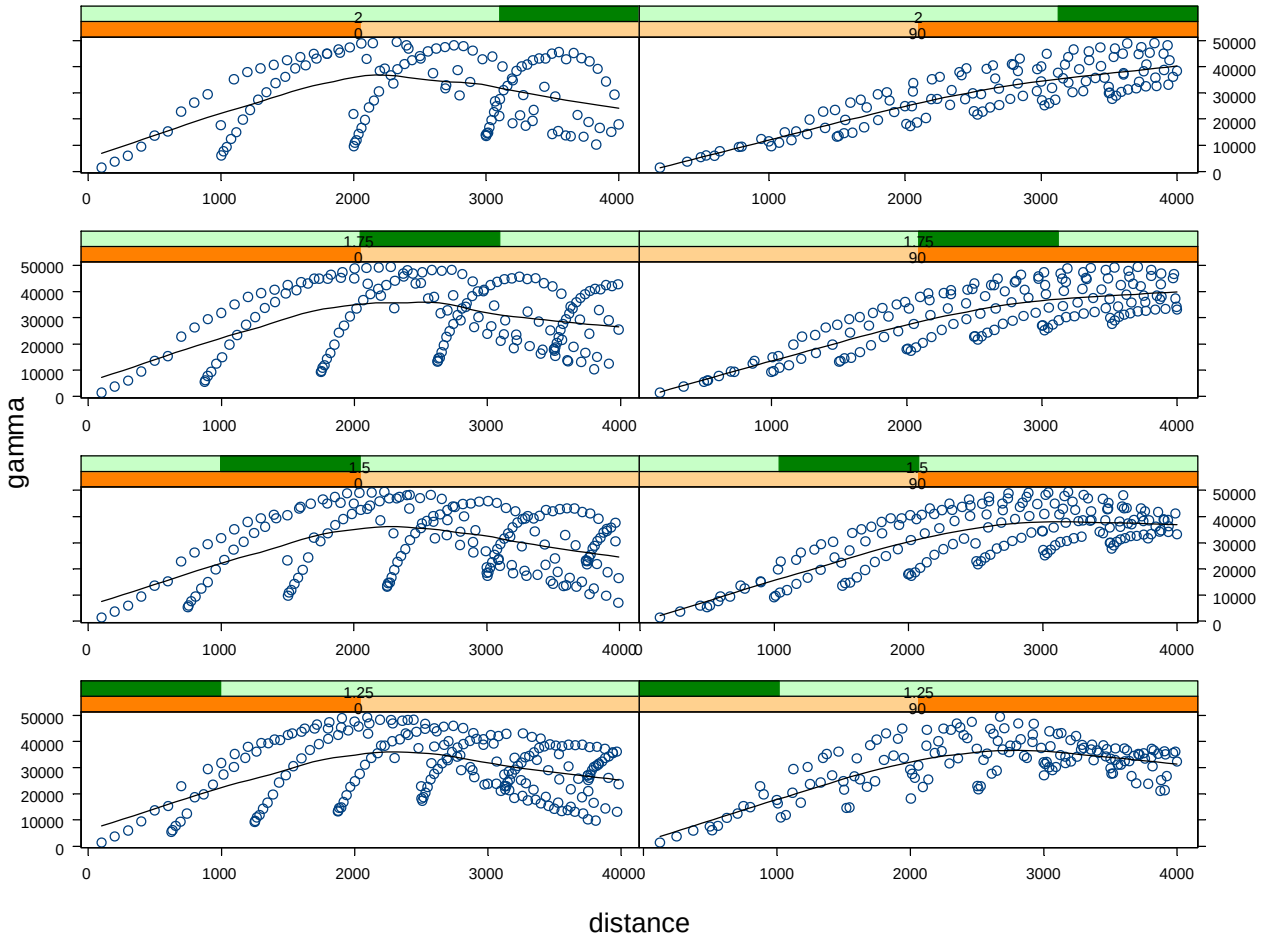

Figure 4.6: anisotropy for the sampling strategy defined by transects distributed regularly (including 10 % of the original depth data set). Direction 0 and 90 represent across and along the river, respectively (orange box). Numbers in the green box represent azimuth tolerance (values of 2, 1.75, 1.50 and 1.25 from top to bottom) . Depth data set for the Austrian channel. Distance is the Lag distance in mm and gamma represents the semivariance.

Strong directional differences were identified for sampling strategies defined by regular and stratified transects (Figure 4.6). Differences in the directional variograms were more dependent on the location of transects rather than the number of points included. Variograms with the same number of transects were different when locating those transects at different places; this did not happen (or at least it was not observed) with regular, stratified and random grids. Thus, grids should be preferred to transects for the determination of depth variograms. Random selection of points did not seem to affect the directional variograms and thus, differences identified can be associated to the number of points rather than to their location. The same principle is applied for stratified and regular grids.

The best fitted models were obtained for sampling strategies developed following random grids. The variance accounted for (Appendix 2) did not change between random grids with the same number of points but it changed when decreasing the number of points. This indicated that for random grids the number of points included in the analysis was more relevant than their location. The same principle can be observed in regular and stratified grids but not in transect sampling strategies.

Values of Range were between 4 m and 5 m, which indicated that spatial correlation for depth was lost at distances higher than this interval. Therefore, when defining sampling strategies for the Austrian channel it would be necessary to locate the points at distances smaller than 5 m. Values of sill were smaller than 0.02, which indicated that the variance between sampled points was not high. Finally, nugget values were $\cong$ 0 for all the sampling strategies.

VELOCITY FOR THE AUSTRIAN CHANNEL

The velocity data set presented differences in the variogram for both directions analysed. This was due to the distribution of the measured points in space. The velocity data set was collected following cross sections separated by 1 m intervals and thus, the variograms showed groups of points at 1 metre intervals (Figure 4.8). This indicated that the directional differences obtained were just the result of the lack of intermediate points between cross sections. The anisotropy was not so visible when considering higher azimuth tolerances. The cross-sectional variogram cannot be successfully determined due to the spatial distribution of the points and so, it was necessary to use the omnidirectional variogram in order to make predictions.

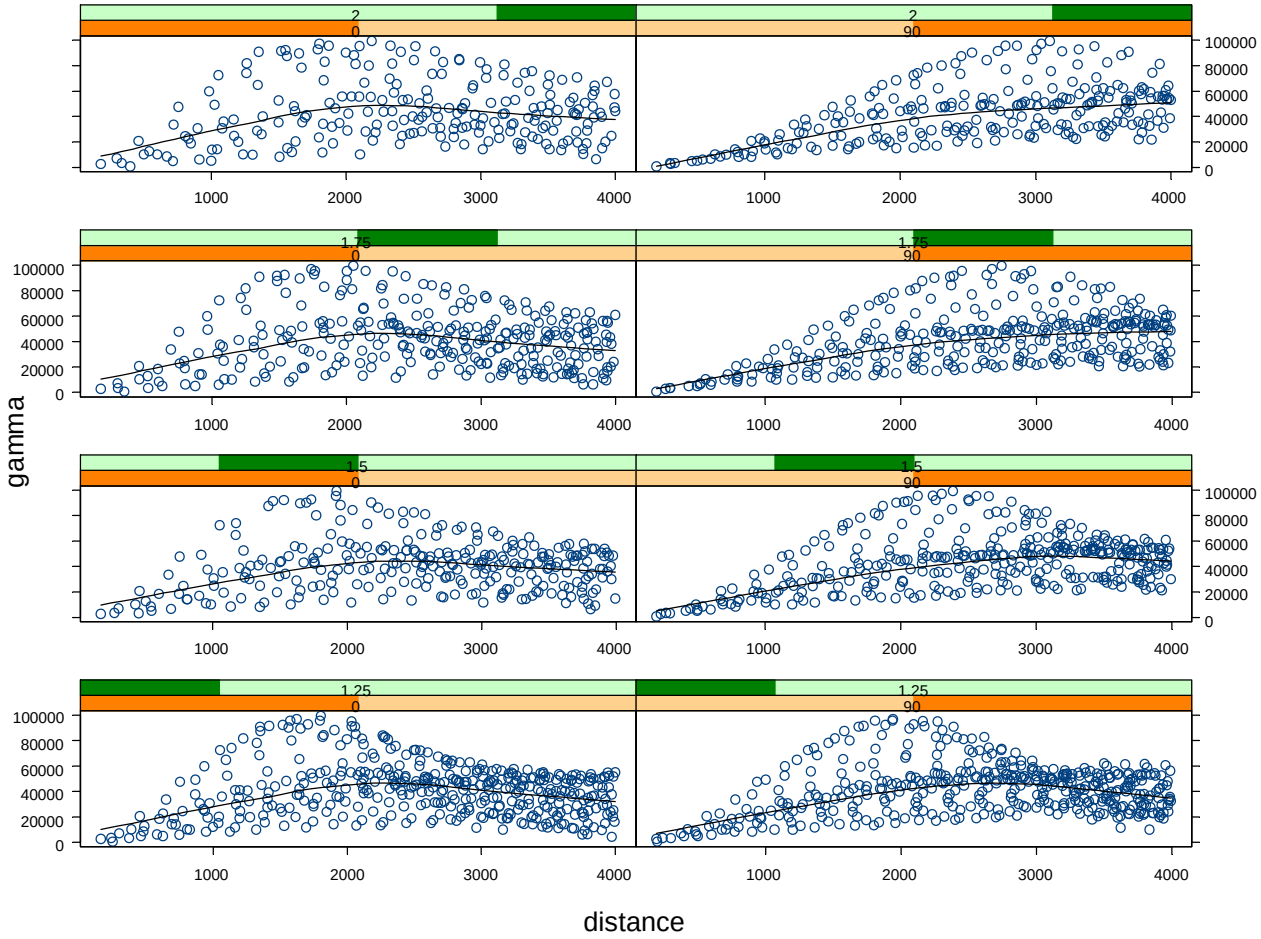

Figure 4.7: anisotropy for the sampling strategy defined by regular grid (3x3 Centre). Direction 0 and 90 represent across and along the river, respectively (orange box). Numbers in the green box represent azimuth tolerance (values of 2, 1.75, 1.50 and 1.25 from top to bottom). Depth data set for the Austrian channel. Distance is the Lag distance in mm and gamma represents the semivariance.

The lack of points separated by small distances can produce a bad estimation of the nugget (inherent variance of the parameter studied). It would be necessary to carry out a study at a micro scale level in order to determine the inherent variance of velocity measurements.

The variance explained by the variogram models fitted was very low in all the cases (from 0.8% up to 63%) (Appendix 2). This could be due to (i) a low number of points collected, (ii) a high distance between sampling points, (iii) a bad sampling strategy or (iv) a poor relationship between velocity and space. Values of percentage of variance accounted for were lower than those obtained for the depth data set.

The ranges obtained for the selected models were very small (from 0.482 m to 2.05 m), which indicates that the spatial relation between velocity measurements was small. Therefore, high sampling densities were necessary in order to obtain good predictions when kriging this variable. The sill was small for all the selected models (from 0.04 to 0.06), which indicated that the maximum variance between points was not high. The nugget or inherent variance of the parameter was 0 in the majority of the models.

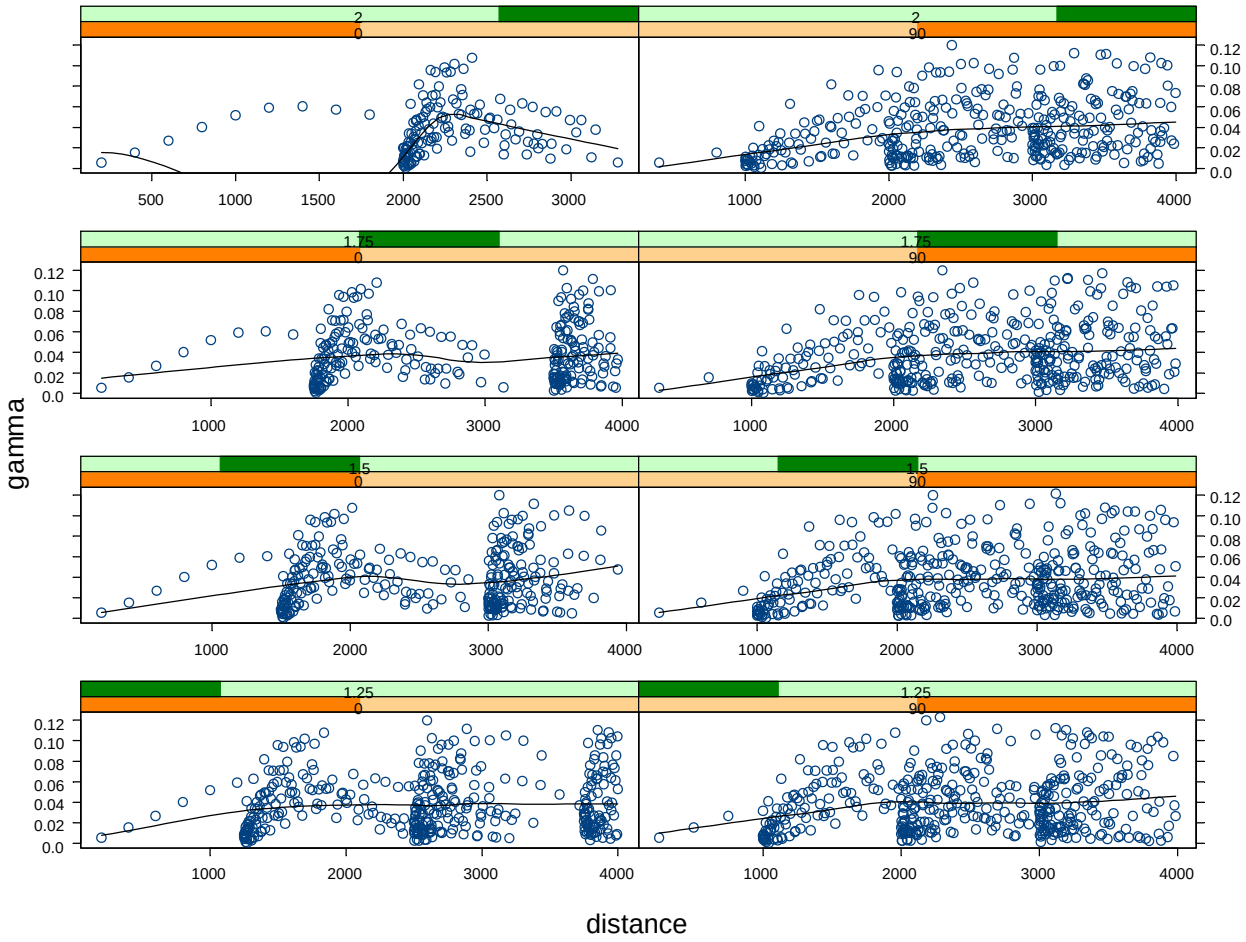

Figure 4.8: anisotropy for Velocity - Layer 1 (direction 0 = across the river & direction 90 = along the river). Values included in the green box indicate ratio of aperture for neighbourhood or azimuth tolerance and are: 2, 1.75, 1.5 and 1.25 from top to bottom. Austrian artificial channel. Distance represents lag distance and it is measured in mm. Gamma represents the semivariance.

THE LEIGH BROOK

The analysis of the variograms obtained for depth, velocity and Froude number at the Leigh Brook showed that the variance had the same behaviour along and across the river and so, no anisotropy was identified.

The exponential variogram presented the best results of "variance accounted for" (94.1% for depth at Q_1 and 95.6% for depth at Q_2) for depth and velocity (less than 60% in all cases for velocity – Appendix 2). The spherical model was the best variogram defining the spatial behaviour of Froude Number, with constant values of "variance accounted for" in all sampling strategies (57.6% for Froude at Q_1 and 69.6% Froude at Q_2).

The range (Table 4.5) was the parameter that best identified changes of the variogram shape, whilst sill and nugget values oscillated within a small interval. This suggests that the range could be a good variable to identify hydromorphological changes in rivers due to water abstraction. Grid sampling strategies presented the best approximations of range to the original variogram and thus, these sampling strategies can be considered as the ones that best define the variogram. Regular transects gave the worst approximations for range, sill and nugget.

Table 4.5: variogram descriptors for each sampling strategy and flow analysed at the Leigh Brook river site.

Variable	Flow	Variogram	GRa	Gstrat1	GStrat2	TRE1	TRE2	Original data set
Depth (m)	Q_1	Range	2.57	2.68	3.15	1.70	1.91	3.09
		Sill	0.019	0.019	0.023	0.018	0.017	0.019
		Nugget	0	0.0001	0	0.0006	0	0.0008
	Q_2	Range	3.22	3.21	3.26	2.02	1.86	3.33
		Sill	0.019	0.022	0.017	0.018	0.016	0.019
		Nugget	0	0.0016	0.0007	0.00017	0	0.0006
Velocity (ms^{-1})	Q_1	Range	3.16	5.44	8.73	1.79	2.21	5.00
		Sill	0.042	0.046	0.048	0.041	0.070	0.052
		Nugget	0.015	0.0144	0.019	0.008	0.006	0.016
	Q_2	Range	2.73	8.57	2.11	26.88	8480	6.26
		Sill	0.048	0.031	0.041	0.10	216.0	0.048
		Nugget	0.0034	0.011	0	0.015	0.022	0.013
Froude Number	Q_1	Range	9.80	8.99	7.04	95800	8.15	9.16
		Sill	0.022	0.038	0.022	176.0	0.037	0.042
		Nugget	0.013	0.010	0.010	0.0083	0.012	0.008
	Q_2	Range	9.24	6.144	10.13	50326.14	18.55	9.17
		Sill	0.027	0.033	0.041	126.00	0.065	0.050
		Nugget	0.017	0.0077	0.0063	0.011	0.012	0.0098

4.4.2. *Mean Squared Error and Mean Error*

DEPTH FOR THE AUSTRIAN CHANNEL

The MSE and ME for regular and stratified transects could not be calculated due to the distribution of points obtained with these sampling strategies. Best results were

obtained for regular and random grids. In general, stratified grids gave worse results than random and regular grids. The number of points included in each grid sampling strategy did not seem to affect the MSE and the ME value for random grids, although it slightly affected sampling strategies with regular grids and transects (Appendix 2).

VELOCITY FOR THE AUSTRIAN CHANNEL

MSE obtained for the velocity data set increased when decreasing the number of points measured (Appendix 2). Differences in the MSE value were not high between comparable sampling strategies (i.e. RE50%, Int10 and Int20). RE25% showed the worst results, which may indicate that the points were located at a distance higher than the variogram range and thus, the predictions were not good as there was no spatial relation between measured points.

Best results for all sampling strategies of velocity were provided by Int5, which included the higher number of points. RE50% showed better results than Int10 although it had a higher number of points. This indicated that the changes in the MSE values were not just associated with the number of points included but also to the location (sampling strategy) of those points.

ME was also higher for stratified sampling strategies than for comparable regular grid sampling strategies (Appendix 2). ME was between 0.008 ms^{-1} and 0.19 ms^{-1}. Higher values of ME were obtained for RE25 due to the low number of points included in this sampling strategy.

THE LEIGH BROOK

MSE obtained for all the predicted values were low for velocity (from 0.025 to 0.05), depth (from 0.00003 to 0.0016) and Froude Number (from 0.016 to 0.034) predictions, which indicated that the predictions were accurate. It needs to be noted that, even employing the same number of points for the variogram calculation of depth, velocity and Froude number, velocity gave higher errors in the predictions. This indicates that more points need to be collected when trying to define the spatial pattern of velocity.

Random grids were the best sampling strategies for velocity and Froude number measurements when analysing the MSE, whilst stratified grids and regular transects oscillated in their behaviour. TRE2 was the sampling strategy with the largest MSE and TRE1 the one with the smallest MSE for depth (Appendix 2) and velocity measurements. This pattern indicated that the results of "regular transect" sampling strategies depended on the location of the transects. Random or stratified grids, which were not so sensitive to the location of the points, are preferable for the prediction of depth and velocity values with geostatistical analysis.

ME obtained for the values predicted with the depth variogram were between 1 cm and 6 cm. The maximum mean errors were for TRE2 for depth measurement ($\cong$ 6 cm), whilst the minimum ME results were obtained for TRE1. Maximum errors or differences between observed and predicted reach values of 44 cm (depth at Q_1) and 51 cm (depth at Q_2) and were produced by the TRE2 sampling strategy.

Velocity predictions gave ME between 0.10 ms^{-1} and 0.17ms^{-1}. The maximum values of ME were with regular transects and smallest ME values were for random grids. The value of ME oscillated between stratified grids and regular transects. This made it difficult to propose a final pattern for these sampling strategies. The range of maximum values of ME was between 0.90 ms^{-1} and 1.33 ms^{-1}.

Froude number predictions presented smaller values of ME for random grids. The same lack of pattern between regular transects and stratified grids observed in velocity predictions appeared in the predictions of Froude number. ME values oscillated between 0.083 and 0.15, with maximum errors of 1.07.

4.4.3. *Descriptive Statistics*

Results for the Austrian channel and Leigh Brook river site indicated that the sample obtained were representative of the original data set in terms of depth and velocity. Results showed that the spatial location of extreme values was approximately the same for all the sampling strategies.

The GLM analysis carried out to identify the relationship between error and habitat type/flow type indicates that there was evidence to reject the null hypothesis H_o: all the habitat types/flow types have the same prediction error ($p<0.05$). This showed that

the prediction error of depth, velocity and Froude number was not evenly distributed between mesohabitat nor flow types.

The mean-plots (Appendix 2) obtained for the Leigh Brook river site indicated that the error increased from riffle to pool habitat types for depth, velocity and Froude number. Riffles and shallow glides had approximately the same range of absolute error (around 1 cm for depth, 0.03 ms^{-1} for velocity and 0.02 for Froude number) whilst deep glides and pools could be grouped together (with errors around 6 cm for depth, 0.10 ms^{-1} for velocity and 0.16 for Froude number). This pattern was observed for the habitat types identified for both discharges.

The relationships were not as clear between flow types; velocity and Froude number present higher errors for Unbroken standing Waves (UW) and Broken standing Waves (BW), whilst it was not possible to define a pattern for the error of predicted depth vs. flow type. The maps of prediction error obtained for the different sampling strategies presented the outliers and extreme values always at the same locations, which coincided with the location of BW and UW. The maps obtained also showed that there were more extreme/outlier values for stratified and regular transect sampling strategies. This indicated that the location of the extreme values was preserved for all sampling strategies whilst the value of error changes between them. The results obtained indicate that more points have to be collected in deep areas in order to identify the peaks of variability in the semivariogram. The variogram was able to identify a range of variability but the peaks were not well predicted, maximum differences (errors) were coincident with the deepest areas (peaks) when analysing the spatial distribution of the prediction errors. Higher sampling densities also need to be applied in areas with UW and BW when trying to define the velocity and Froude number variogram, as these areas also presented higher errors in the predictions.

4.4.4. *Frequency Distribution*

None of the sampling strategies analysed for the depth data sets gave frequency distributions similar to the original data set for the Austrian channel (Appendix 2). Comparable stratified sampling strategies (i.e. Int10 and Int20) presented differences from the frequency distribution of the original measured velocities. This indicated that

the sampling strategy and the number of points measured were a key influence on the determination of the "real" frequency distribution.

There was evidence to reject the null hypothesis (H_0: predicted and observed values provide the same frequency distribution) and consider the predicted data sets of velocity, depth and Froude number to be different to the measured ones (p=0) for the Leigh Brook. No conclusions could be established regarding differences between sampling strategies as the values of significance level were 0 for all the tests run.

4.4.5. *Regression Analysis*

DEPTH FOR THE AUSTRIAN CHANNEL

The maximum values of R^2 were obtained for random grids and stratified grids, whilst the lowest values belonged to regular and stratified transects (Appendix 2). Values of R^2 were affected by the number of points included in regular and stratified grid sampling strategies whilst the location of the points seemed to modify the R^2 value in random grids. Stratified and regular transects gave low values of R^2 since there was a lack of precision for certain intervals of depth; predictions were usually approximated to a constant value (around 200-300 mm depth – Figure 4.9). Plots of SE showed inconsistency in the distribution of the SE for regular grids, regular and stratified transects

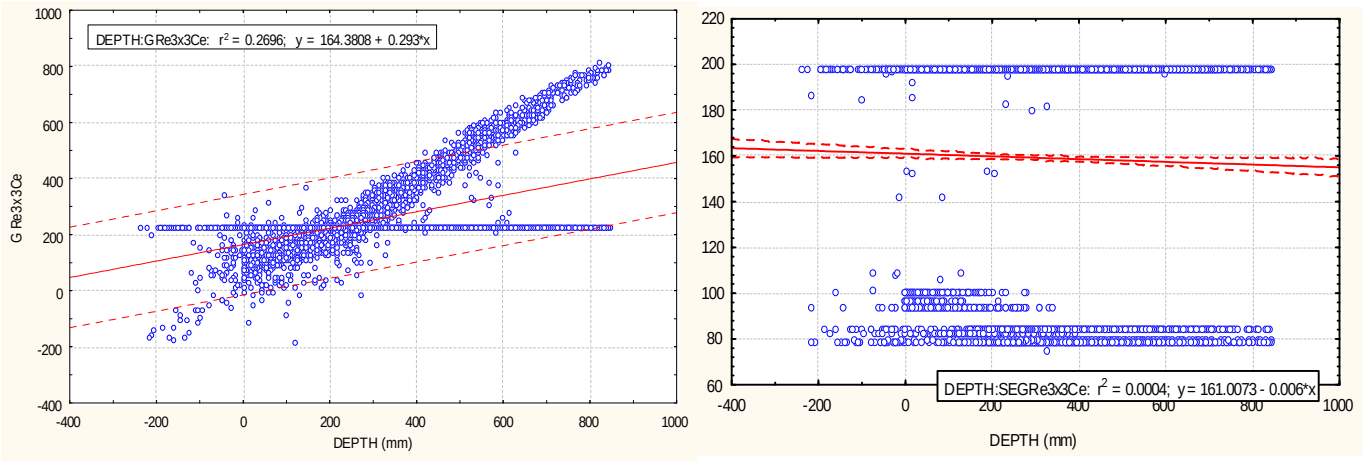

Figure 4.9: R-Squared for Regular Grid 3x3Ce (left) vs. original for depth (DEPTH) and plot of the Standard Error of the predictions for the same sampling strategy the Austrian channel. Red lines represent the fitted linear regression model with 95% confidence interval.

VELOCITY FOR THE AUSTRIAN CHANNEL

Regular grids provided better results than stratified sampling strategies with the same number of points. However, the differences were not notable as R^2 is significant at small values when the number of points analysed is high enough. The values of R^2 were between 0 and 0.98 and RE25% presented the worst results (Appendix 2).

THE LEIGH BROOK

Grid sampling strategies for depth predictions gave better values of R^2 ($R^2 \approx 0.7$) than regular transects ($R^2 \approx 0.6$). Random grids also provided better R^2 values ($R^2 \approx 0.55$) for Froude number, whilst stratified grids provided the worst relationship ($R^2 \approx 0.45$) for the same variable. Velocity did not show a clear pattern of preference between sampling strategies. Residual plots obtained did not present good distributions for stratified grid sampling strategy when predicting Froude number; values appeared in clusters.

4.4.6. *Mapping Resolution*

DEPTH FOR THE AUSTRIAN CHANNEL

Sampling strategies defined by grids gave better mapping resolution than those defined by transects. Stratified transects gave worse mapping resolutions than regular transects and regular grids predicted better maps than random and stratified grids. The number of points included in the sampling strategy and the location of the sampled points affected the mapping resolution for random grids whilst regular and stratified grids were just affected by the location of the points. Mapping resolution of transect sampling strategies were mainly affected by the location of the sampled transects (Figure 4.10).

VELOCITY FOR THE AUSTRIAN CHANNEL

Stratified sampling strategies gave similar or even better approximations of the real situations than those obtained with regular grids. RE25% did not give acceptable approximations of the real situation as the patterns of deep-shallow areas were not conserved. The analysis of the number of grid cells that represent significant change from the original situation (Table 4.6) supported the conclusions reached from visual comparison of maps. Note that sampling strategy RE25 provided the best results for

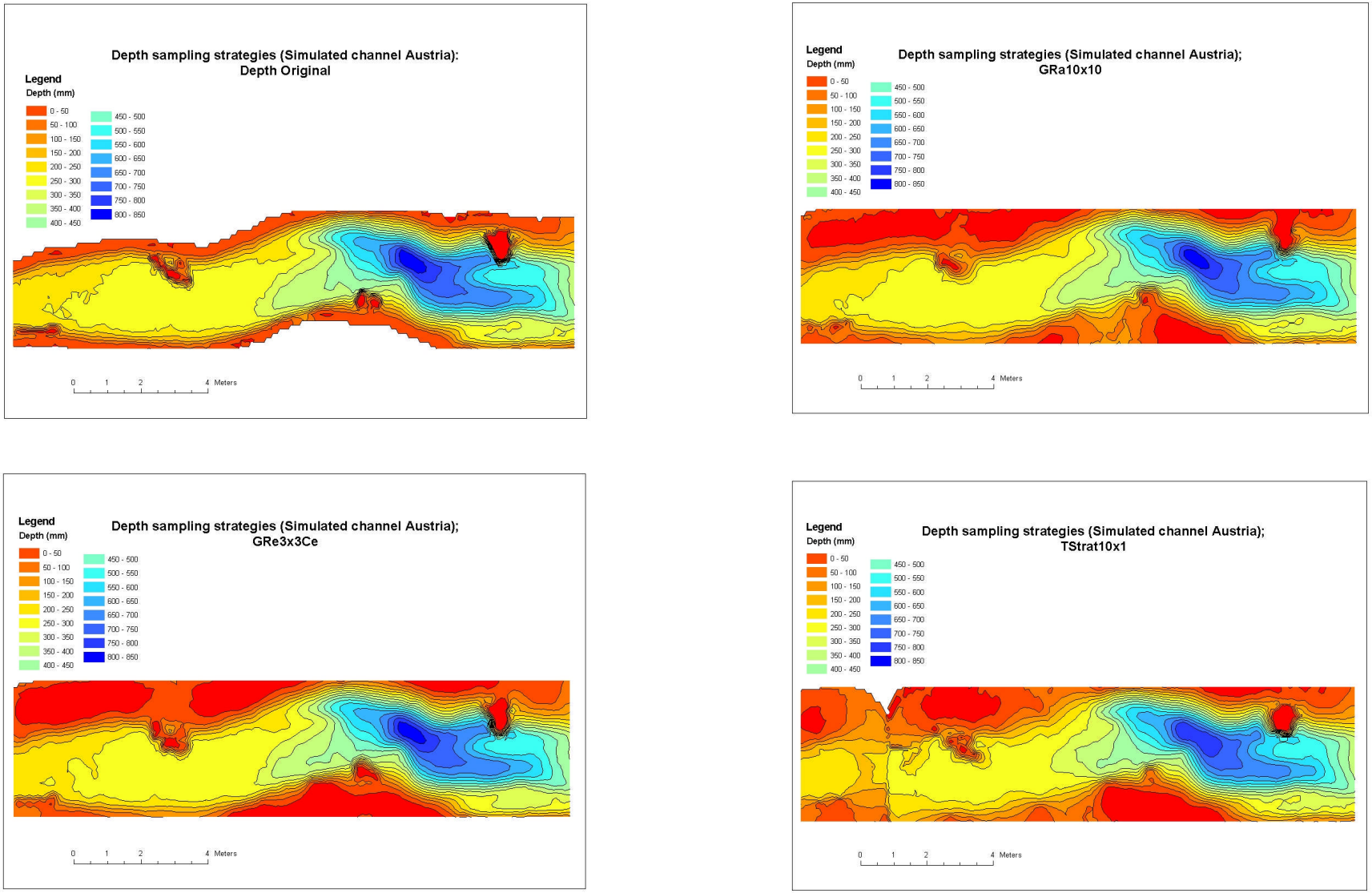

Figure 4.10: mapping resolution for depth original data set (top left), GRE3x3Ce (bottom left), GRa10x10 (top right) and TStrat10x1 (bottom right) at the Austrian channel.

the number of grid cells that were not changing. This is due to the fact that all the predictions obtained for the Re25 sampling strategy had the same value, which implies a constant value of prediction error. Therefore, the values obtained with this sampling strategy were not sufficiently representative of the original situation even though it gave low prediction errors.

Table 4.6: number of grid cells that presented significant change (mean +/- 2SE; SE=0.0122) from the original situation for the Velocity data sets for the Austrian channel.

Strategy	Layer 1	Layer 2	Layer 3	Layer 4
Re50	66	68	63	51
Re25	5	9	8	6
L1Int5	62	64	35	50
L1Int10	33	30	22	28
L1Int20	5	4	5	4

THE LEIGH BROOK

Sampling strategies that gave better spatial representations were those that followed regular and stratified grids. Random grids were more successful than stratified for velocity, depth and Froude number. Different results were obtained for the grid cell analysis (Table 4.7); stratified grids provided worse results on mapping resolution than random grids and regular transects for the velocity data set. Differences between depth sampling strategies were not consistent for the two discharges analysed. Froude Number and velocity data sets have a higher number of grid cells that have significant change from the original situation than depth (Table 4.7).

Table 4.7: sampling strategies studied at the Leigh Brook river site for depth, velocity and Froude number measurements obtained at two flows (Q=0.344 m^3s^{-1} and Q=0.517 $m3s^{-1}$).

Sampling strategy group	Sampling strategy	Number of significantly different grid cells Velocity		Number of significantly different grid cells Froude Number		Number of significantly different grid cells Depth		Abbreviation
Discharge m^3s^{-1}		**0.344**	**0.517**	**0.344**	**0.517**	**0.344**	**0.517**	
Grid	**Random**	20	16	31	30	2	1	GRa
		27	32	30	30	2	2	GStrat1
	Stratified	29	20	30	30	1	2	GStrat2
Transects	**Regular**	15	21	27	26	1	0	TRe1
		13	17	26	23	0	0	TRe2

4.4.7. *Standard Error Maps*

Results for the velocity data from the Austrian channel show that regular grids gave better approximations to the mapping distribution of errors obtained with the "real situation", as the original data set was collected following a regular grid. Results obtained for the depth data set showed that the pattern observed for mapping resolution, in terms of best and worst sampling strategies for the indicator, can be attributed to the standard error maps. Results obtained for the Leigh Brook river site show that regular and stratified grids were the sampling strategies that provide maps of SE with a closer pattern to that identified for the original data set. Random grids were more successful than stratified grids for the three hydromorphological variables analysed.

4.4.8. *Predicted-Observed cross-sections and longitudinal profiles*

DEPTH FOR THE AUSTRIAN CHANNEL

Sampling strategies defined by transects did not give good approximations to the values of depth (Figure 4.11). Some predictions along the longitudinal profile were very close to the measured values; these "good predictions" matched with the position of the selected transects used for the calculation of the semivariogram. This pattern was observed in each of the fifty longitudinal profiles created. Regular grids gave the best results when predicting longitudinal profiles, followed by stratified and random grids. Random grids presented more oscillations than the two first types of grids studied, but still gave very good approximations.

Differences between regular grids can be identified according to the location of the points selected when analysing the cross-sections created. Random grids did not give as good a numerical prediction as regular grids. Stratified grids gave worse predictions than regular and random grids, although the predictions were much better than those obtained with transects. Differences were also identified according to the number of points included; sampling strategies with higher number of points gave better predictions (Figure 4.11).

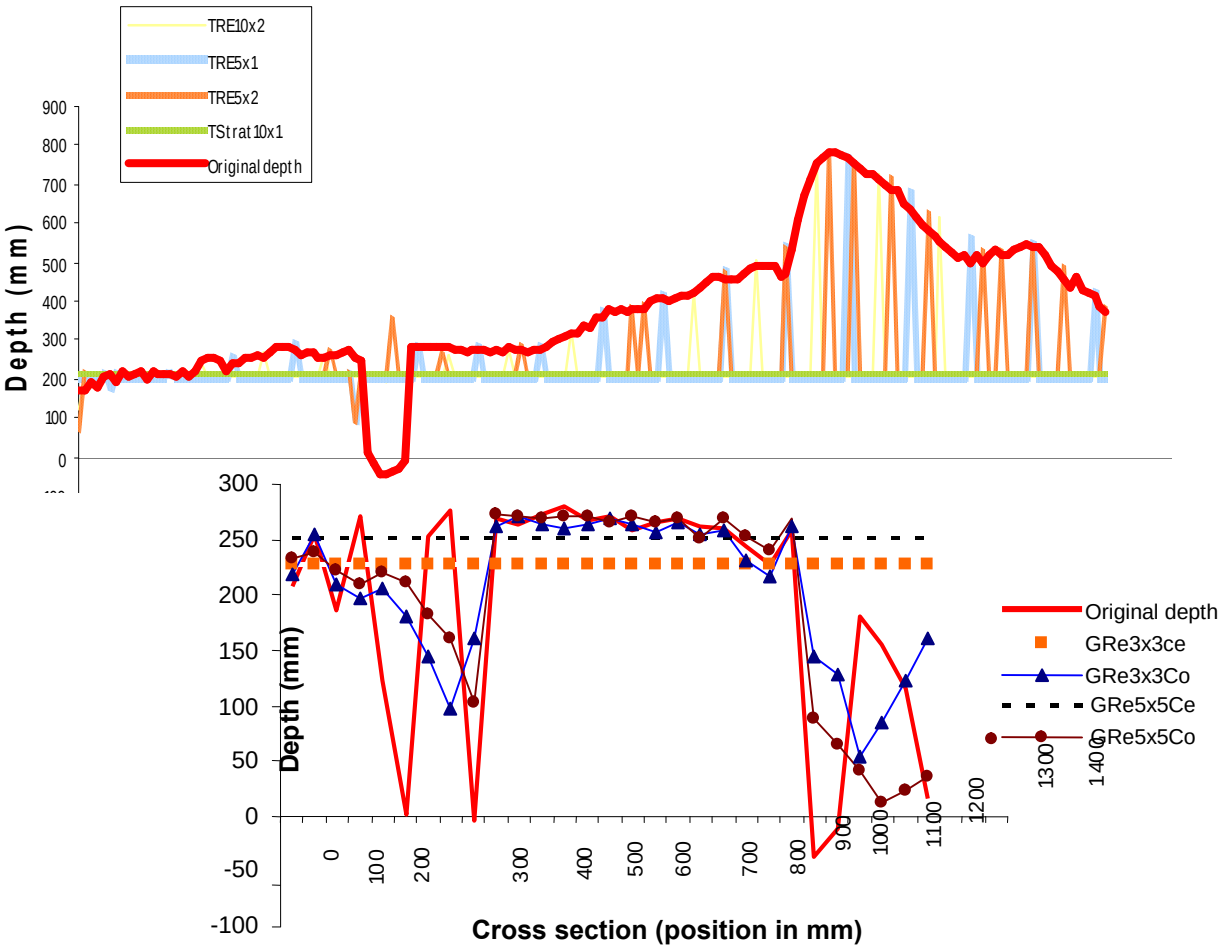

Figure 4.11: example of longitudinal profiles (top) and cross sections (bottom) predicted with the different sampling strategies studied for the Austrian channel.

VELOCITY FOR THE AUSTRIAN CHANNEL

Cross sections predicted from all the sampling strategies, except RE25% and Int20 gave good approximations of the measured cross sections (Figure 4.12). Approximations were better for longitudinal profiles than for cross-sections. There were not significant differences between comparable regular and stratified grids. The number of points included seemed more relevant than the sampling strategy applied when determining longitudinal profiles and cross-sections. However, conclusions could not be established for the longitudinal profiles as only two sections along the river were analysed for each layer.

THE LEIGH BROOK

Results showed that depth is better predicted with random grids for more than 95 of the 200 cross sections. Stratified grids were better than regular transects at 55 of the

200 cross-sections, whilst transect sampling strategies were good for only 40 cross sections. Transect sampling strategies predicted with high accuracy the value and shape of those cross-sections where transects were measured; the predictions were usually poor in value and shape in the remaining cross-sections.

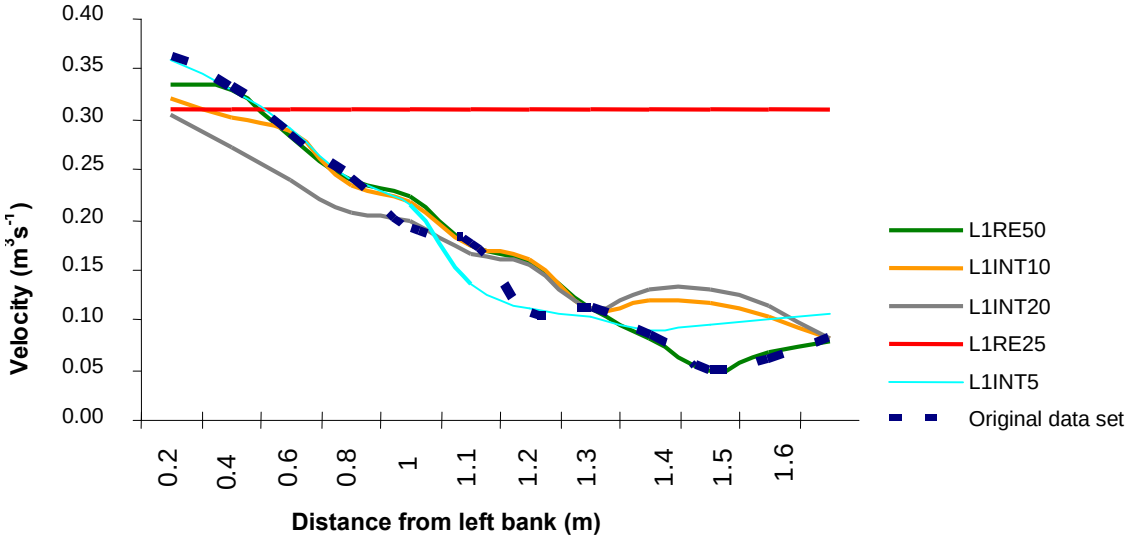

Figure 4.12: example of velocity predicted at one cross section (layer 1) for the Austrian channel.

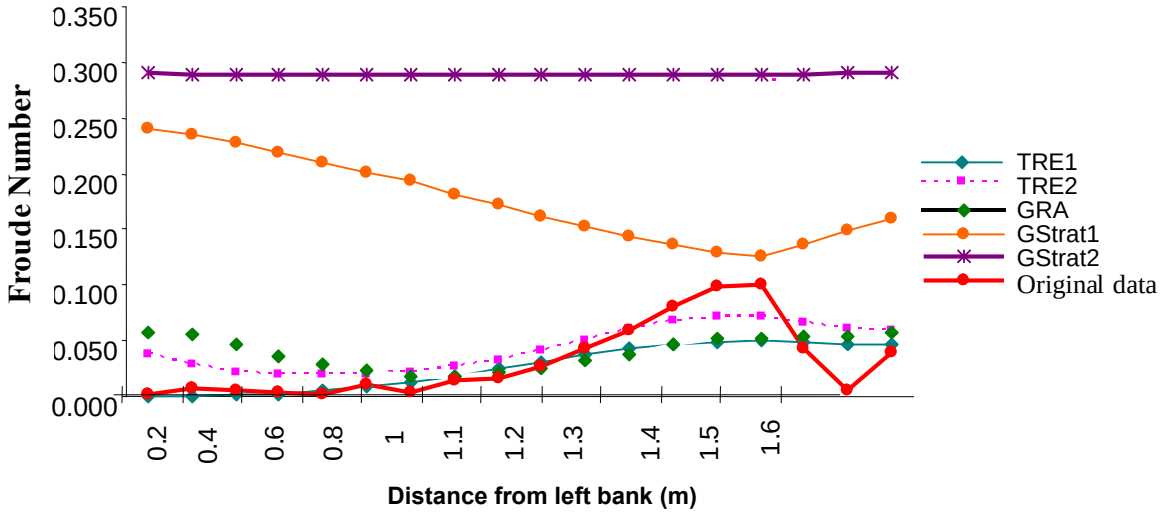

Figure 4.13: example of Froude Number predictions for different sampling strategies for the Leigh Brook river site.

Velocity prediction showed good approximations in value and shape adjustment at the 200 cross sections studied, although there were underestimations of the predicted values at all the cross sections and for all sampling strategies. Regular transect sampling strategies represented the majority of cases where the predictions were not adjusted in shape to the measured cross-section values; the two regular transect replicates studied gave different outputs. One replicate gave the best approximation of

all the sampling strategies and the other replicate gave the worst approximation. Since the results were so dissimilar, it could not be accepted that regular transects give good predictions to the "real situation" and so, it may be preferable to apply grid sampling strategies.

Froude number (Figure 4.13 & Appendix 2) values predicted for the cross-section did not approximate to the real observations as well as velocity predictions did. The majority of cross-sections do not present neither a good estimation of the real value nor an adjustment on shape. Regular transects gave better approximation than the other sampling strategies.

4.4.9. *Channel Volume*

AUSTRIAN CHANNEL

Results indicate that overestimations of 2 dimensional and 3 dimensional surface area were made from all sampling strategies except those defined by transects. Volume results did not significantly change between sampling strategies; that may indicate that volume is just affected by changes in the number of points collected rather than the sampling strategy applied. Best results were obtained with regular grids whilst underestimation was obtained with transects and overestimation with random grids.

THE LEIGH BROOK

Differences in volume between sampling strategies were higher than 100 m^3 between grids and transect sampling strategies. Transect strategies gave the most similar values of volume to those obtained with the whole data set. 2D and 3D wetted surfaces did not present high differences between sampling strategies although stratified sampling strategies gave more comparable values to those obtained with the original data set (Table 4.8).

Table 4.8: water volume, 2D surface and 3D surface (wetted surface) for each sampling strategy and flow studied.

Sampling strategy	Q_1			Q_2		
	Volume	2D Surface	3D surface	Volume	2D Surface	3D surface
Original Data set	562.72	2490.95	2504.15	479.11	2593.27	2606.01
GRa	868.64	3398.72	3407.44	723.69	3398.72	3406.54
Gstrat1	871.39	3371.14	3379.71	471.76	2172.74	2179.99
GStrat2	878.95	3322.96	3331.25	452.35	2182.35	2187.82
TRE1	867.04	3376.07	3385.32	825.28	3312.94	3321.01
TRE2	729.54	3376.07	3385.32	691.01	3312.94	3320.91

4.5. Discussion and Conclusions

DEPTH

It is recommended that the omnidirectional variogram be calculated when characterising the spatial pattern of depth. The anisotropy detected when comparing longitudinal and cross-sectional variograms is either due to (i) the symmetrical shape of the cross-sections or (ii) the sampling strategy applied. The omnidirectional variogram reduces both effects by considering all the information provided by points collected in both directions and by increasing the azimuth tolerance up to the maximum.

It is recommended that grid sampling strategies be applied when characterising the spatial pattern of depth rather than applying any type of transect sampling strategies. Results obtained with regular or stratified transects have been proved to be highly sensitive to the number of points sampled, as well as to the location of these transects.

In general, regular grids provided better results than random and stratified grid sampling strategies, the latter being the worst in the grid sampling range. However, the use of random grids should be prefered to the use of stratified and regular grids since (i) results obtained for random grids did not significantly differ from those obtained with regular grids and (ii) random sampling strategies (i.e. random walk) are less time consuming sampling strategies.

VELOCITY

It is recommended to collect high resolution data sets for velocity when trying to apply kriging interpolation techniques since (i) the spatial correlation between points can be lost at very short distances (between 0.5 m to 2 m for the Austrian channel and between 3 to 5 m for the Leigh Brook) and (ii) worse results were obtained for velocity than for depth when applying the same sampling strategy.

Velocity data collection is more cost and time consuming than depth and so, smaller sampling densities are usually applied for its characterisation. Thus, it is recommended to use different interpolation procedures to ordinary kriging for the prediction of velocity values at non measured locations when low sampling densities

are being applied (i.e. points are separated more than ≅ 3 m between each other). As an alternative option using three dimensional hydraulic modelling is suggested.

Results obtained with regular transect sampling strategies depend on the location of the transects for the majority of indicators and so, grid sampling strategies, which are not so sensitive to the location of the points, are preferable. Results obtained with irregular grids (i.e. random and stratified grids) do not significantly differ from those obtained with regular grids and so, it is recommended that irregular grids are applied as they are less time consuming. Stratified grids cannot be applied for velocity measurements as it is difficult to visually identify velocity changes at the river site. Instead, random grids are preferred as the sampling strategy.

Further analysis should be developed for different sampling densities and spatial scales in order to (i) determine the relationship between sampling density and specific accuracy levels in the predictions and (ii) define the spatial behaviour of velocity, depth and substrate at different spatial scales.

FROUDE NUMBER

It is recommended that grid sampling strategies are used for the calculation of the variogram since these sampling strategies better characterise the spatial pattern. Regular transects proved to be worse than grid sampling strategies for the characterisation of the spatial pattern.

It is recommended to space sampling points less than 9 m from each other when designing Froude Number sampling strategies as this is the point at which the spatial correlation between points is lost.

GENERAL CONCLUSIONS

The range is the variogram parameter that best identified changes in the variogram shape. This may indicate that the range is the best variogram parameter to identify hydromorphological changes in rivers due to water abstraction.

It is recommended to apply higher sampling densities in deep areas when measuring depth, and in broken-unbroken standing waves, when measuring velocity or Froude number. The prediction error (i.e. difference between observed and predicted values) is higher in deep glides and pool habitat types for depth, velocity and Froude number.

Higher errors are also located at unbroken and broken standing waves for velocity and Froude number. By increasing the sampling density in deep areas and at broken – unbroken standing waves, the peaks of variability in the semivariograms will be identified and therefore, higher levels of accuracy will be achieved when predicting hydromorphological parameters in these areas.

5

The link between spatial scales and depth spatial pattern

Comparable river sites among the available data sets for this research project need to be identified in order to define which sites are going to constitute the validation data sets for results obtained in Chapter 6. Chapter 5 identifies which river sites are comparable in terms of (i) catchment characteristics, (ii) reach characteristics, (iii) percentage of flow exceedance and (iv) spatial structure, among other criteria. Chapter 5 also includes a sensitivity analysis for the modelled variograms defining the spatial structure of the river sites.

5.1. Introduction and objectives of Chapter 5

Hydromorphological data from fourteen river sites were analysed. River sites were separated into validation and test data sets. The test data sets were analysed to provide a set of sampling strategies for the collection of hydromorphological parameters. Results were validated with the validation data sets. The **first objective** of Chapter 5 is to group the river sites according to (i) their catchment characteristics, (ii) their reach characteristics, (iii) the data collection procedure and (iv) their spatial structure.

Differences and similarities of spatial structure were determined through the analysis of the variogram characteristics. Several variables need to be determined for the fitting of the variogram model (e.g. lag distance and azimuth tolerance). The **second objective** of Chapter 5 focuses on the development of a sensitivity analysis of the variogram model for those variables that are required for its calculation. This will define the value of the variables for the variogram calculation and how sensitive the variogram model is to changes of these variables. The **third objective** of Chapter 5 is to fit the variogram model for each of the river sites.

The **fourth objective** of Chapter 5 is to analyse which physical descriptors of the river site and parameters used for the first objective have most influence in defining the variogram.

5.2. The river sites and the data collected at each site

Fourteen river sites were analysed in this Chapter. The majority of the river sites are lowland and thus, this research project will focus on the development of effective and efficient sampling strategies for this type of river. A few examples were included to represent river sites that were not typical lowland sites. These river sites were: Tame Less Modified, Tame Highly Modified and Tarf. The first two had a high degree of hydromorphological modification and the Tarf is an upland river.

5.3. Methodology

5.3.1. *Limitations of the available data sets and approach taken to address them.*

The data sets were collected for different purposes and by different surveyors. It was necessary to investigate these differences before proceeding to the data analysis. The limitations identified were:

Insufficient WSL data sets: in some cases the WSL data sets did not include enough points for the application of interpolation techniques (Webster & Oliver, 2001; Webster, 1992). Table 5.1 shows the interpolation technique applied to obtain the WSL at each river site according to the characteristics of the data set. Two approaches were selected: inverse distance weighting and descriptive geometry.

Short river length sampled: The reduced sample length of some rivers could result in a lack of information on river characteristics. Work developed by Ian Maddock (personal comment) showed that the distance necessary to characterise the spatial variability of a river site in terms of mesohabitat structures is between 50 m and 100 m. The sampled length of the river sites also affects the geostatistical analysis since the variogram cannot be accurately calculated for lag distances higher than the sampled distance. The variogram calculation was reduced to the minimum length sampled (i.e. 30 m) to provide comparable variogram results without losing the extra information provided by the points located at higher lag distances.

Table 5.1: limitations of the data sets analysed in chapter 5 (TO=Topographic, IDW=Inverse Distance Weighted and DG=Descriptive Geometry; Density in points per square metre). "Wet" refers to those points below the water surface level whilst "dry" points refer to those points above the WSL.

Site	Measured Discharge	Number of points wet	Mean Width dry & wet	Mean Width wet	Area dry & wet (m^2)	Area wet (m^2)	Sampled length (m)	Existence of Curvature	Method used for WSL calculation	Number of TO points sampled	Number of WSL points sampled	TO Sampling density (wet & dry) Points/m^2	TO Sampling density (wet) Points/m^2	Date WSL collection	Date TO collection	Q% LowFlows 2000	LowFlows 2000 Group
Pang Old fenced	0.27	299	7.6	5	236.9	155.75	31	no	IDW	474	7	2	3	14/05/2003	26/02/2003	90	**1**
Pang fenced	0.27	700	10.5	5.5	1154.8	611	110	no	IDW	1438	17	1.3	2.3	15/05/2003	not specified	91	**1**
Pang Unfenced	0.27	784	12.5	6.7	1333	725	107	yes	IDW	1468	21	1.1	2	14/05/2003	not specified	90	**1**
Lambourn	0.67	2200	7.5	7.5	345.25	345.25	46	no	DG	2205	4	6.4	6.4	16/07/2002	not specified	92	**1**
Leigh Brook	0.344	2983	8.1	8.1	1622.5	1622.5	200	no	-	2983	-	1.8	1.8	?	-	93	**1**
Bere 2000	0.36	924	6.9	5.8	559.8	415	80	yes	IDW	1546	47	2.8	3.7	07/09/2000	13/01/2000	79	**2**
Pang Old fenced	0.32	306	7.6	5	236.9	155	31	no	IDW	474	9	2	3	07/05/2003	26/02/2003	80	**2**
Pang Unfenced	0.32	801	12.5	6.7	1333	725	107	yes	IDW	1468	22	1.1	2	07/05/2003	not specified	80	**2**
Leigh Brook	0.517	2983	8.1	8.1	1622.5	1622.5	200	no	-	2983	-	1.8	1.8	?	-	82	**2**
Senni	0.44	894	8.8	8.8	352.25	352.25	40	no	IDW	895	24	2.7	2.5	18/10/2000	not specified	78	**2**
Highland Water	0.09	219	6.5	4	323.4	202.75	50	yes	IDW	501	16	1.54	2.5	18/03/1999	27/04/1999	43	**3**
Cruick	0.61	2382	5.6	5.6	1388	1388	246	yes	IDW	2431	83	6.7	6.7	11/08/2002	11/08/2002	51	**3**
Tarf	0.34	5045	5.5	5.5	1156.25	1156.25	212	yes	IDW	5486	281	4.74	4.7	17/09/2002	17/09/2002	50	**3**
Tarf	0.32													18/09/2002	18/09/2002	52	**3**
Tarf	0.30													19/09/2002	19/09/2002	54	**3**
Blackwater	0.46	4529	7.8	5.8	1210.9	909	155	yes	IDW	6100	111	5	6.7	14/05/2001	unknown	33	**3**
Tame LM	1.46	957	9.5	9.5	2368.61	1360	142	no	DG	1726	5	0.72	1.3	?	30/09/1999	43	**3**
Tame HM	2.52	1278	14.5	12	1348.59	1116	93	no	DG	1302	8	0.96	1.1	01/11/1999	not specified	20	**0**
Windrush	?	810	9.7	9.7	1228.25	1228.25	126	yes	IDW	1206	27	0.98	0.98	10/04/2003	10/04/2003	?	**?**

Different sampling strategies and sampling conditions: different sampling strategies (density and location of points) were applied at each river site. Data were also collected at different discharge conditions. Groups of comparable data sets were established according to the sampling densities of the river sites and to the percentage of flow exceedance at which they were sampled (Table 5.1) to minimise the following problems:

i. The total number of TO and WSL points was different for each river site and thus, the information was not directly comparable.
ii. Differences in the number of dry points (dry points = negative depth; wet points = positive depth) indicated that the river banks were not equally defined for all the river sites (Table 5.1 and Figure 5.1)
iii. The information provided by the data sets was not comparable in terms of water depth characterisation since the discharges at which the data were collected were different.

River sinuosity: interpolation techniques calculate the value of variables at unknown points through the analysis of the value of the neighbouring points. Curvilinear shapes create false neighbours, specially at the internal face of the curve, where points that are located a long distance away along the flow path are found relatively close in geometric space (Figure 5.2). This can be solved by straightening techniques (e.g. Brunner, 2002, Wadzuk, undated, Merwade, 2004, Merwade, 2002 and Legleiter & Kyriakidis, 2006). The straightening procedure was carried with the River Channel Morphology Model (RCMM) tool (Merwade, 2004; Merwade, 2002)

Data sets collected at different periods: the majority of WSL data sets were not collected simultaneously with the TO data sets. River sites that presented this limitation were carefully analysed since the TO could have changed between the TO sampling period and the WSL sampling period.

Lack of data : Velocity and substrate were only measured at the Leigh Brook river site. Therefore, only depth will be analysed in this chapter.

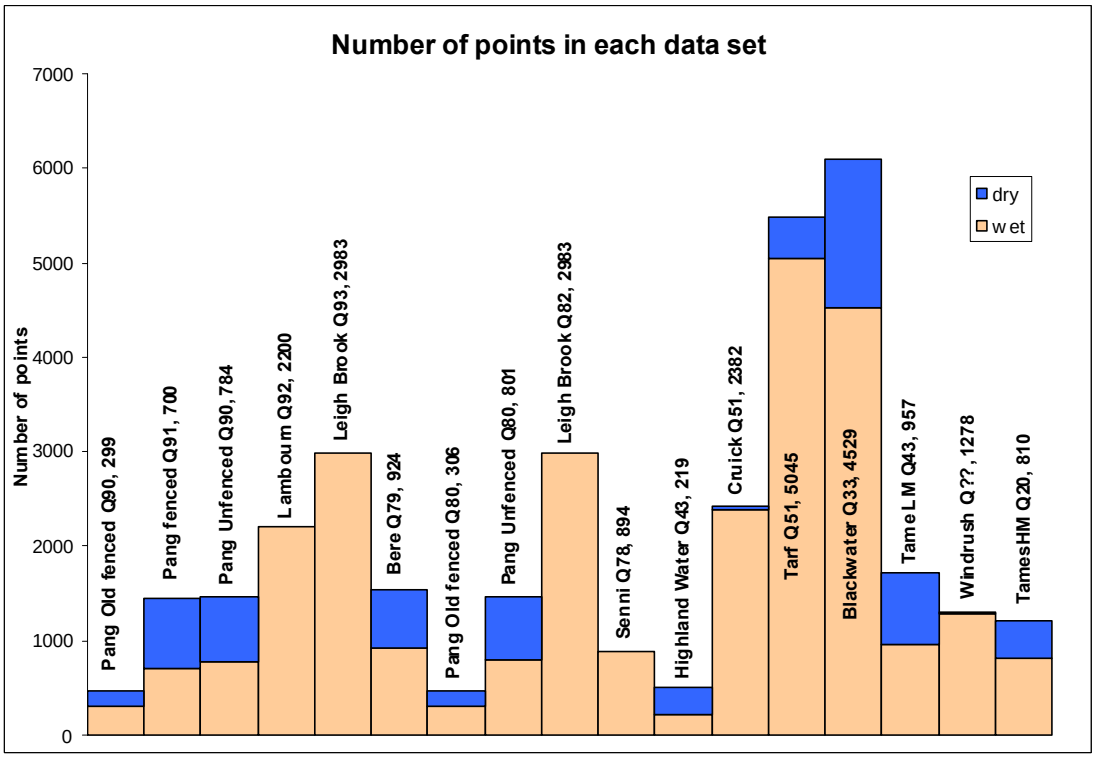

Figure 5.1: number of wet and dry points measured at each river site. The number given in the label refers to the number of wet points.

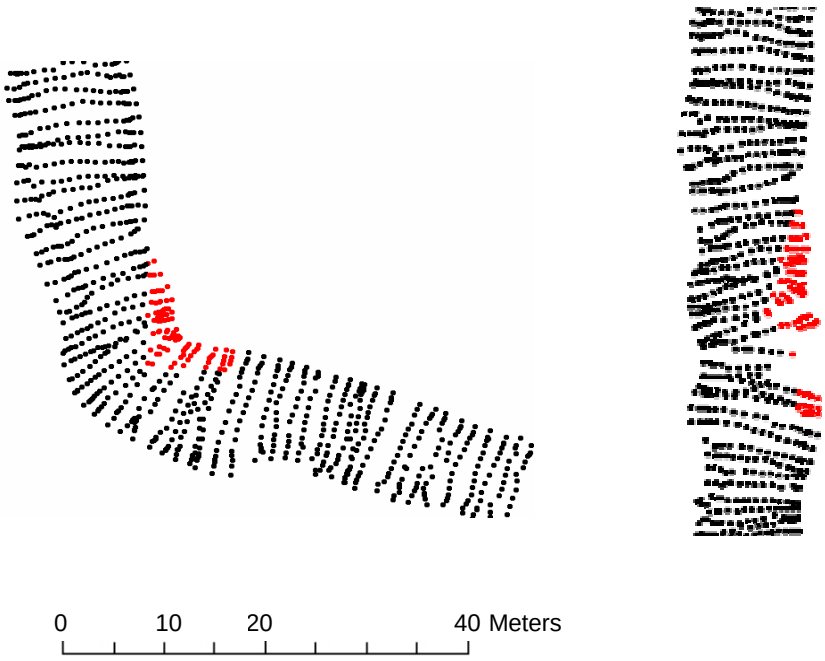

Figure 5.2: example of straightened river site (Bere river site). Note the differences in distances between the selected red points when straightening has been applied.

5.3.2. *Grouping the river sites to find comparable data sets and river sites*

Four different criteria were considered: (i) catchment characteristics, (ii) reach characteristics, (iii) percentage flow exceedance and (iv) depth spatial structure. Catchment and reach characteristics were defined through physical descriptors that were selected according to their relevance for the geostatistical analysis. Only variables that could have an influence on the variogram shape were considered. Percentage of flow exceedance was calculated from the discharge at which the data measurements were collected and spatial structure was determined after analysing the variogram obtained for each river site.

Comparable river sites in terms of (i) catchment characteristics, (ii) reach characteristics and (iii) spatial structure were defined using cluster analysis. Cluster analysis was developed by considering the Euclidean distance as a measure of dissimilarity between data points and Ward's method of cluster formation (Lattin et al., 2003). Ward's method has a tendency to produce equal sized clusters (i.e. clusters with approximately the same number of observations in each) that are convex and compact which is due to the strategy followed when identifying differences between data points for the cluster classification. Ward's approach seeks to join the two clusters whose merger leads to the smallest within cluster sum of squares (Lattin et al., 2003). Data were normalised for the performance of cluster analysis.

5.3.3. *The selected physical descriptors*

Physical descriptors were defined for different spatial scales which allowed the properties of depth spatial structure to be linked with the scaling concept defined in Chapter 1. Spatial scales for rivers have been defined in different studies (Rowntree & Wadeson, 1998; Thomson et al., 2001; Thomson et al., 2003; Wadeson & Rowentree, 1998; Maddock et al., 2001; Maddock & Bird, 1996; Muhar, 1996; Frissell et al., 1986; Petts & Amoros, 1996). Two spatial scales were selected for the determination of physical descriptors after reviewing the works listed above: catchment and reach scales. Spatial scales smaller than reach scale were not considered since the sampling densities applied for the data collection procedures did not allow characterisation at this level. The selected physical descriptors for the catchment and reach scales are shown in Table 5.2 and Table 5.3.

Catchment Scale

Table 5.2 summarises the catchment descriptors used in the Flood Estimation Handbook (FEH) (Bayliss, 1999). Descriptors included at this spatial scale were characteristics of the river catchment that could be derived from a map (ordnance survey) and that could have an influence on the variogram characteristics.

Table 5.2: physical descriptors included at the catchment scale.

Code	Catchment descriptor
AREA	Catchment drainage area (km^2). It influences the characteristics of the runoff and river discharge. This has an influence on the shape of the river (e.g. bankfull, maximum/minimum depth) and therefore on the slope of the variogram.
ALTBAR	Mean catchment altitude (m above sea level). This affects the slope of the river site, which is going to have an influence on the energy of the discharge and therefore, on the erosion/shape of the channel.
ASPBAR	Index representing the dominant aspect of catchment slopes. This variable was considered for the same reasons as for ALTBAR.
BFIHOST	Base flow index derived using the HOST classification. This may influence the shape of the channel through characteristics of the depth data sets.
DPLBAR	Index describing catchment size and drainage path configuration (km).
DPSBAR	Index of catchment steepness (m/km).
LDP	Longest drainage path (km).
SPRHOST	Standard percentage runoff (%) derived using the HOST classification.
QX	Exceedance flow for the X flow percentile. Corresponds to the flow at which WSL was collected. This will define the characteristics of the bankfull and depth data sets.
Flow Exceedance	Percentage of flow exceedance calculated from the measured flow during the data collection procedure.
QMin 0	Average Annual Mean Flow m^3s^{-1}
DistSorc	Distance from the river site to the origin of the river.
SOrd	Stream Order. The methodology applied for the determination of river orders is the one developed by Horton (Chow, 1964). Data were obtained from 1:25000 maps of the Ordnance Survey.
HSorc	Height of the river at the origin (m). HSorc and HSite give an approximation to the slope which has influence on the runoff, erosion rates, discharge and finally, channel shape.
HSite	Height of the river at the river site (m).

Reach Scale

Physical descriptors describing reach scale characteristics were derived from the data collected at the site. Table 5.3 summarises the physical descriptors selected for the reach scale. Cluster classes were identified in order to determine the river sites that were comparable in terms of these physical descriptors for the data sets with the dry and wet points and data sets with only the wet points.

Table 5.3: physical descriptors for the reach scale.

Code	Catchment descriptor
Subs	Substrate was categorised for the application of multivariate analysis. The classes and categorical values considered were: *Category 1-GravelCobble &Pebble, Category 2- Gravel-Cobble & Sand, Category 3-Gravel and Category 4-Gravel, Silt & Sand (*see Chapter 3 for the associated substrate sizes).
DV	Depth Variance of the data set. The variogram may be influenced by extreme values (maximum and minimum values of depth). This was represented with the depth variance.
Minimum Width	Minimum width identified. Maximum and minimum width were obtained through the analysis of the river banks in ArcGIS software.
Maximum Width	Maximum width identified.
Mean Depth	Average of all the depth points measured. Depth was calculated as the difference between the water surface level and the topography measurement.
Minimum Depth	Minimum depth collected. Negative values were obtained for the data sets that include dry points whilst positive values were obtained for the data sets with only wet points.
Maximum Depth	Maximum depth collected.
Hab	Number of mesohabitat types identified. The characterisation of the river sites into mesohabitats for the scope of this study was established following the types considered by Maddock (Maddock et al., 2001; Howard & Hemberger, 1991) which is based on Hawkins (1993) and Maddock & Bird (1996) and included all the types considered in the RHS methodology (see section 4.3 for more detail). For those river sites where mesohabitat types were not identified during the data collection, the number of habitats was determined by assessing the hydromorphological characteristics of the river site.
L	Reach length. Defines the length of the sampled river site following the central axis of the river once the reach has been straightened.
Sin	Sinuosity coefficient. Measures of sinuosity can be obtained by applying different criteria and equations (Howard & Hemberger, 1991). Sinuosity was measured as the path length divided by the straight-line distance, D, between the initial and final points of the measured path.
PoRiS	Averaged distance between consecutive pool or riffle features.

5.3.4. *Descriptive statistics*

Descriptive statistics were calculated to characterise and compare the different data sets collected and included: number of points, minimum and maximum depth, median, mean, standard deviation, 1st quartile and 3rd quartile. Analysis of normality was also carried out (Kolmogorov-Smirnov and chi-squared tests). Histograms, boxplots and QQplots were plotted. A comparison was established between duplicated data sets analysed for the same river site to determine the hydromorphological differences between discharges analysed for a single river site.

5.3.5. *Sensitivity analysis*

Four main variables need to be determined before proceeding to calculate the variogram: lag distance, azimuth tolerance, azimuth and maximum distance of

analysis. The lag distance is the interval for which the search of neighbours is carried out, the azimuth defines the direction of the search and the azimuth tolerance is the angle that determines the range of search at each side of the azimuth line. The maximum distance of analysis determines the distance at which the variogram provides information that has been calculated with an increasing and adequate number of pair of comparisons. Since the four variables are interrelated, it is necessary to fix three of the variables when carrying out a sensitivity analysis of the fourth one. The sensitivity analysis was carried out for each variable as follows:

Lag distance: the analysis included: (i) changes in the omnidirectional variogram shape (the experimental variogram not the modelled variogram) when changing the lag distance and (ii) the change in the number of pairs of points used for the variogram calculation when changing the lag distance. The objectives of these analyses were to determine (i) the smallest lag distance that can be considered (i.e. at which point analysis of the variogram can start) and (ii) the lag interval for the variogram calculation. The smallest lag distance depends on the sampling strategy applied. The selection of the lag distance for the variogram calculation is a balance between (i) selecting a lag distance that is well represented by the sampling strategy and (ii) selecting a lag distance that provides a sufficient number of pairs of points for the variogram calculation; the smaller the lag distance, the higher the number of points that will be represented on the experimental variogram; and the higher the lag distance, the higher the number of points that will be included in the calculation of each point of the experimental variogram. Seven lag distances were compared (i.e. 0.1 m, 0.3 m, 0.5 m, 0.7 m, 0.9 m, 1.5 m, 2 m). The analysis was carried out twice; the first time for the dry & wet points and the second time for the wet points only (i.e. wet points being below the WSL and dry points above the WSL).

Azimuth tolerance: the higher the azimuth tolerance, the wider the neighbourhood area is and the more information on directional behaviour is lost (Webster & Oliver, 2001). The differences between the cross-sectional and longitudinal variograms when changing the azimuth tolerance value were analysed. The decrease in directional information when increasing the number of comparisons was observed. The azimuth

tolerances considered for the sensitivity analysis went from 20° to 90° in intervals of 10°, 90° being the azimuth tolerance of the omnidirectional variogram.

The sensitivity analysis also considered the differences between results obtained for a specific azimuth direction (Figure 5.3) and the change in the number of pairs of points obtained when changing the azimuth tolerance (Figure 5.3). The lag distance and the azimuth direction were kept constant for the data analysis (i.e. 1 m lag distance and 0 azimuth direction). The values of lag distance and azimuth direction were chosen after iterative runs of sensitivity analysis.

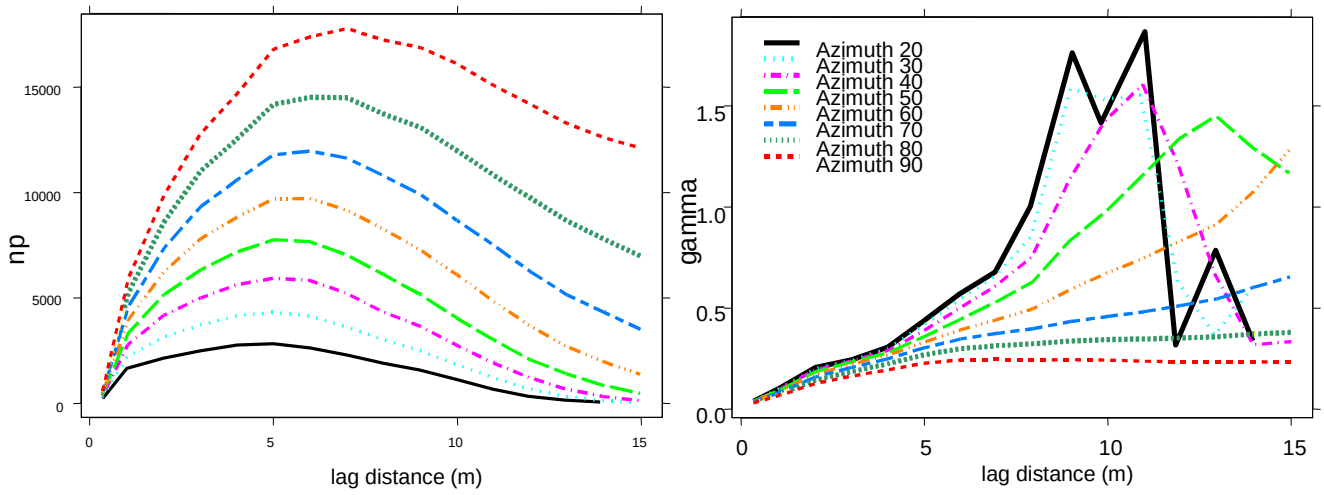

Figure 5.3: Example of output obtained for the sensitivity analysis of the azimuth tolerance: number of pairs of points (left) and experimental variogram (right) obtained for different azimuth tolerances analysed (Blackwater river site). "NP" is the number of pairs of points whilst gamma represents the semivariance. The legend on the right hand image is valid for both plots.

Azimuth or anisotropy analysis: the directional differences of depth spatial structure were analysed by comparing the variogram shape for four directions: 0, 45, 90 and 135 degrees. The azimuth tolerance for this study was fixed at 60, the lag distance at 1 m and the maximum distance of analysis at 50 m. The azimuth tolerance and the lag distance were selected after carrying out the sensitivity analysis for these parameters. The analysis also included the study of the change in number of pairs of points used in the variogram calculation for each azimuth direction.

Maximum distance of analysis: the number of pairs of points was analysed for all the variables previously included in the sensitivity analysis. The number of pairs of

points included in each directional variogram was compared and conclusions were established according to (i) results obtained in this comparison and (ii) results obtained in the previous sensitivity analysis. The maximum distance for which the variogram can be analysed corresponds to the distance at which the maximum number of pairs of points is identified (Bellamy, P. personal comment).

Sensitivity analysis for the empirical variogram: The variogram was modelled for a combination of lag distances (from 0.1 to 2 in steps of 0.1) and maximum distances (from 10 to 100 in steps of 10 m) to determine the effect of these two factors on the variogram variables. Only these two variables were considered since the number of total combinations of lag distance, azimuth tolerance, tolerance and maximum distance would be too high to clearly interpret the results

A total of 200 combinations were tested for each river site. The analysis was undertaken for both, (i) data sets with dry and wet points and (ii) data sets with only wet points for all the river sites. Two variogram models were analysed: the spherical and the exponential and results for each model were compared.

5.3.6. *Determining the effect of bankfull information in the variograms.*

The influence of wet and dry points on the variogram was analysed. This helped to understand whether the variogram provides information on the structure of banks at each river site. The analyses focused on the study of the variogram cloud. The variogram cloud is the scatter diagram that shows the semivariance for each pairs of points against the lag distance. It shows the spread of values at the different lags and it enables detection of outliers or anomalies. The tighter this distribution is, the stronger the spatial continuity in the data (Webster & Oliver, 2001).

Three variogram clouds (for (i) the dry points, (ii) the wet points and (iii) the dry and the wet points together.) were calculated and superimposed in one single plot. Figure 5.4 is an example of the output obtained. The analysis of these plots helped in understanding the influence that the wet and dry points had, either independently or by interaction, on the final variogram output.

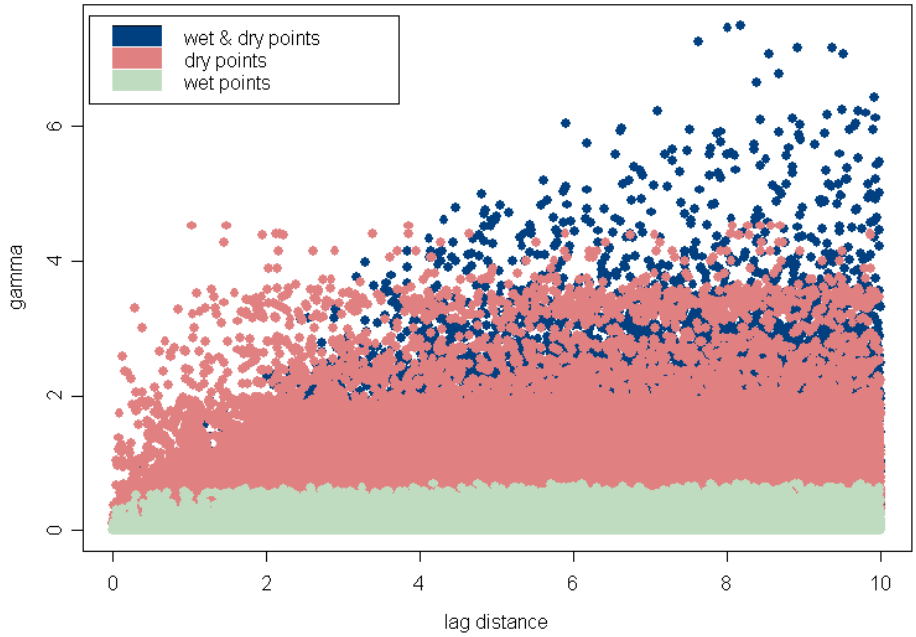

Figure 5.4: variogram cloud analysis for the Tame Less Modified data set.

5.3.7. *Geostatistical analysis*

The third objective of Chapter 5 is to calculate the variogram for all river sites considered for analysis. The model (either spherical or exponential) was selected through the analysis of the Objective function in Splus. The lag distance, azimuth, azimuth tolerance and the minimum/maximum distance were determined according to the results obtained for the sensitivity analysis. Range, sill and nugget values were obtained from each variogram. Conclusions on the spatial behaviour of the depth variable for each river site were obtained after analysing the results.

5.3.8. *Variables with more influence on the variogram*

The fourth objective of Chapter 5 is to determine which variables of those considered for this study were most related to the degree of spatial variation present at a river site. This determined the characteristics of the data set or the characteristics of the river site that need to be defined with higher accuracy in order to obtain lower errors in prediction (e.g. is the maximum depth value more important than the adequate characterisation of the frequency distribution?). Results may provide a set of guidelines for the design of effective-efficient sampling strategies: e.g. if maximum depth is one of the most relevant parameters for the variogram calculation, then pools will need to be sampled with more detail than other areas.

Several variables that could be related to the spatial structure of hydromorphological parameters at a site were selected. The list of variables selected did not pretend to be a comprehensive compendium of all the factors that could affect the spatial structure of a site, since this could be a whole new area of research by itself. The variables selected for the catchment and reach scales described in section5.3.3 were considered. A complementary set of variables describing the main characteristics of the data sets collected was analysed (Table 5.4). The parameters were calculated for data sets including wet and dry points and data sets including only wet points.

The correlation coefficients (Pearson's coefficient) were calculated for each variogram parameter (range, sill and nugget) and each descriptor considered (Table 5.2, Table 5.3 and Table 5.4). The variables that were significantly correlated were selected for more detailed study in Chapter 6. Multiple regression analysis was not possible as the descriptors are not independent.

Table 5.4: data sets parameters considered for the correlation analysis.

Code	Description
Stdev	Standard deviation of the depth values measured.
miD	Minimum depth measured.
FirstQ	First quartile interval.
MedianD	Median depth
meD	Mean depth
ThirdQ	Third quartile interval
maD	Maximum depth
DV	Variation for the depth data sets measured.
Skewness	Skewness coefficient for the depth depth
Kurtosis	Kurtosis coefficient for the depth distribution

5.4. Results

5.4.1. *Grouping the river sites to find comparable data sets and river sites*

The groups identified for each cluster analysis developed are shown in Figure 5.5 and Table 5.5. The flow exceedance classification provided information on which river sites were sampled at similar conditions and therefore, it had preference on the establishment of comparable river sites. The rest of the classification criteria were used to determine which river sites were comparable inside each group of percentage of flow exceedance. Two river sites were considered comparable when they were classified in the same group for the four classification criteria. The river sites that

were comparable for the 90% flow exceedance were Lambourn, Pang Old Fenced, Pang Unfenced and Pang Fenced. The Lambourn river site was selected as a validation data set since the other three river sites corresponded to the same system; the Pang.

Table 5.5: groups identified according to each selected criterion after developing the each cluster analysis (except for the classification obtained for the percentage of flow exceedance).

Site	Percentage of Flow Exceedance	Catchment scale	Reach Scale	Spatial structure	Sampling density
Pang Old fenced	1	1	1	1	3
Pang fenced	1	1	1	1	2.3
Pang Unfenced	1	1	1	1	2
Lambourn	1	1	1	1	6.4
Leigh Brook	1	2	2	1	1.8
Bere 2000	2	1	1	1	3.7
Pang Old fenced	2	1	1	1	3
Pang Unfenced	2	1	1	1	2
Leigh Brook	2	2	2	1	1.8
Senni	2	3	2	1	2.5
Highland Water	3	2	1	1	2.5
Cruick	3	2	2	1	6.7
Tarf	3	3	2	2	4.7
Blackwater	3	2	1	1	6.7
Tame LM	3	4	2	3	1.3
Tame HM	4	4	2	2	1.1
Windrush	4	-	2	2	0.98

Comparable river sites for the 80% flow exceedance classification were the Bere, Pang Old Fenced and Pang Unfenced. Sampling densities applied for the first two river sites were similar and, therefore, this pair of river sites constituted the test and validation data sets. The Bere was used as the validation data set. Only two river sites were comparable for the 40% flow exceedance interval: the Highland Water and the Blackwater. The sampling densities for these two river sites were not similar, with the Blackwater having a more detailed data set than the Highland Water. In this case, the Highland Water was used for validation. Conclusions were drawn taking into account the differences in sampling densities between these two river sites.

Note that the Windrush river site was not classified for catchment scale characteristics. This is because no discharge and percentage flow exceedance data were available. Note also that the variables for reach scale were defined for the data sets with dry and wet points and for the data sets with only wet points. The cluster

analysis for reach scale was performed with only variables related to the wet data sets since only these will be analysed in Chapter 6.

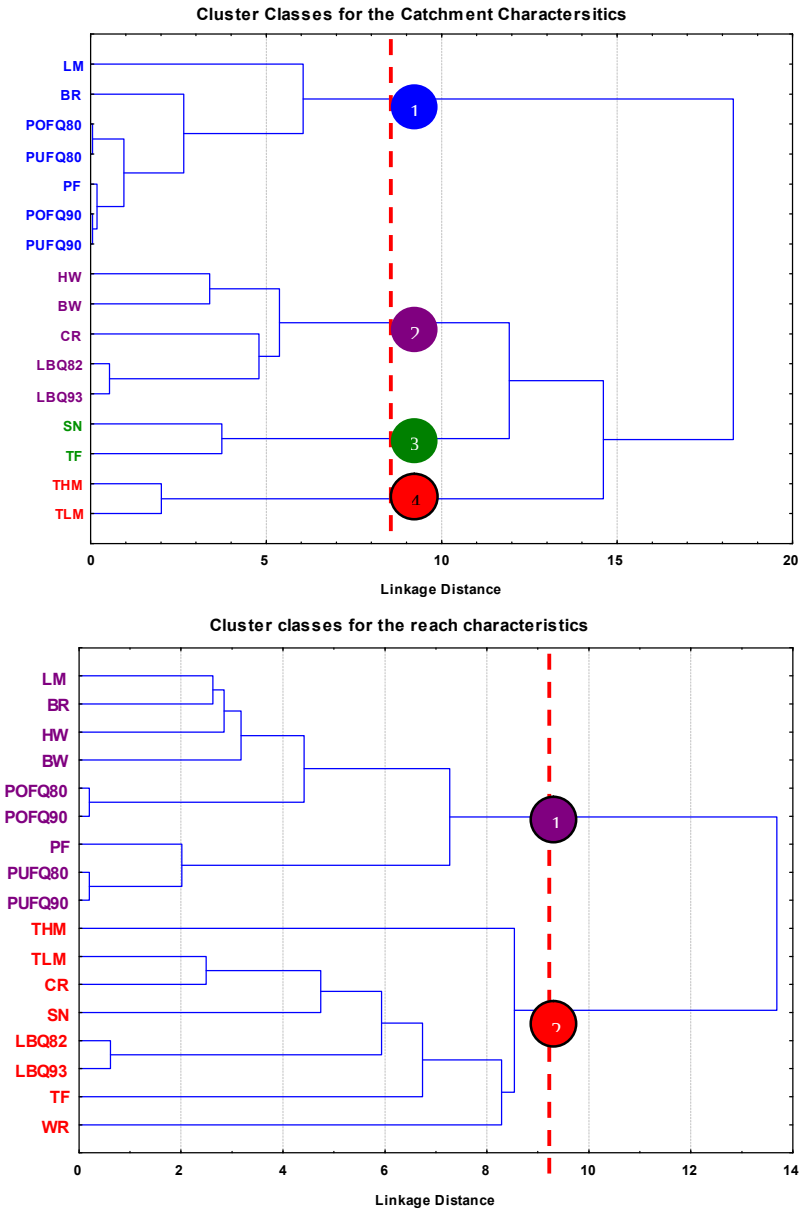

Figure 5.5: cluster classes identified for the catchment and reach physical descriptors. The numbers shown inside the circles show the groups identified at each cluster analysis. The abbreviations used for each river site are: BR=Bere, BW=Blackwater, CR=Cruick, HW=Highland Water, LB=Leigh Brook, LM=Lambourn, PF=Pang Fenced, POF=Pang Old Fenced, PUF=Pang Unfenced, SN=Senni, TF=Tarf and WR=Windrush. The numbers after the river name indicate the percentage of flow exceedance of those river sites that have been considered more than once in the data analysis. Vertical lines have been drawn according to the type of cluster analysis developed (Euclidean distances & Ward's method)

5.4.2. *Descriptive statistics*

Results for the analysis of the data sets including dry and wet points showed that depth values were not normally distributed at any of the river sites analysed. The same results were obtained for the data sets with only the wet points.

Results for the wet-dry data sets provide information on the characteristics of both the channel and data set (Appendix 3.1). Negative mean values of depth indicated that the river banks were more elevated (i.e. rivers more incised) than in those rivers with positive mean depth values (Appendix 3.1). The combination of positive and negative values of depth created frequency distributions with values either side of 0. River sites with higher proportions of negative values show higher river banks or a higher number of boulders. Those sites whose banks were considerably higher than the river bed were Highland Water, Pang, Tame and Windrush. These sites have a higher range of depth values.

Results for the wet points gave information on the topographical shape of the bed channel. Mean values of depth were between 0.15 m and 0.42 m. Deeper areas were encountered for (i) Leigh Brook and Pang Fenced for the 90% flow exceedance group, (ii) Senni and Leigh Brook for the 80% flow exceedance group and (iii) Tame LM and Cruick for the 40% flow exceedance rate. Appendix 3.1 contains all the graphical and numerical outputs obtained for the descriptive analysis.

5.4.3. *Sensitivity analysis*

Lag Distance: Table 5.6 shows the minimum lag distances encountered and the number of pairs of points separated by this distance. The final variograms modelled were not analysed for lag distances smaller than those in Table 5.6 since no values were available for the calculation of the variogram at such distances.

The selected lag distance should (i) be the same for all the data sets so comparable variograms are obtained, (ii) provide sufficient numbers of pairs of points for the calculation of the variogram values and (iii) provide sufficient intervals for the variogram. Figure 5.6 shows some examples of experimental variograms calculated with the same data set for different lag distances (results for all the river sites can be seen in Appendix 3.2). The smoothness of the variogram disappears as lag distance decreases due to an increase in the number of intervals considered for the variogram calculation. It is proposed that lag distances of 1 m be used for the data sets with wet points and distances of 0.5 m be used for the data sets with dry and wet points since (i) the number of pairs of points used for the calculation of each variogram value was

considerably lower for lag distances smaller than 0.2 m than for other lag distances analysed (Figure 5.6) and (ii) results for the experimental variograms were erratic when selecting lag distances smaller than 0.4 m.

Table 5.6: minimum lag distance encountered at each river site analysed. NPP indicates the number of pairs of points separated by the minimum lag distance.

Site	Min Lag Dry & wet	NPP Dry & Wet	Min Lag Wet	NPP Wet	Measured Discharge
Pang Old fenced	0.25	31	0.45	47	0.27
Pang fenced	0.30	34	0.5	32	0.27
Pang Unfenced	0.30	38	0.40	35	0.27
Lambourn	0.05	133	0.05	133	0.67
Leigh Brook	0.40	65	0.40	65	0.344
Bere 2000	0.05	42	0.14	34	0.36
Pang Old fenced	0.25	31	0.39	32	0.32
Pang Unfenced	0.30	34	0.40	35	0.32
Leigh Brook	0.40	65	0.40	65	0.517
Senni	0.15	61	0.15	61	0.44
Highland Water	0.35	35	0.80	31	0.09
Cruick	0.04	45	0.04	42	0.61
Tarf	0.01	38	0.01	36	0.34
Blackwater	0.01	49	0.05	224	0.46
Tame LM	0.05	37	0.80	46	1.46
Tame HM	0.10	61	0.74	32	2.52
Windrush	0.25	45	0.25	43	?

Azimuth tolerance: the selected azimuth tolerance should provide sufficient information about the cross-sectional anisotropy but it should avoid the influence of symmetry and the reduced number of pairs of points (Chapter 4). An azimuth tolerance of 60 degrees was selected because:

(i) Differences between variograms calculated for a specific azimuth direction decreased when increasing the azimuth tolerance from 60° to 90°. This reduced the effect of the anisotropy since cross-sectional and longitudinal variograms became more similar (Appendix 3.3).

(ii) The number of pairs of points available for the calculation of each value in the variogram decreased considerably for azimuth tolerances smaller than 40°. From 60° upwards the number of pairs of points increased, being more than 2000 for all the data sets (Appendix 3.3).

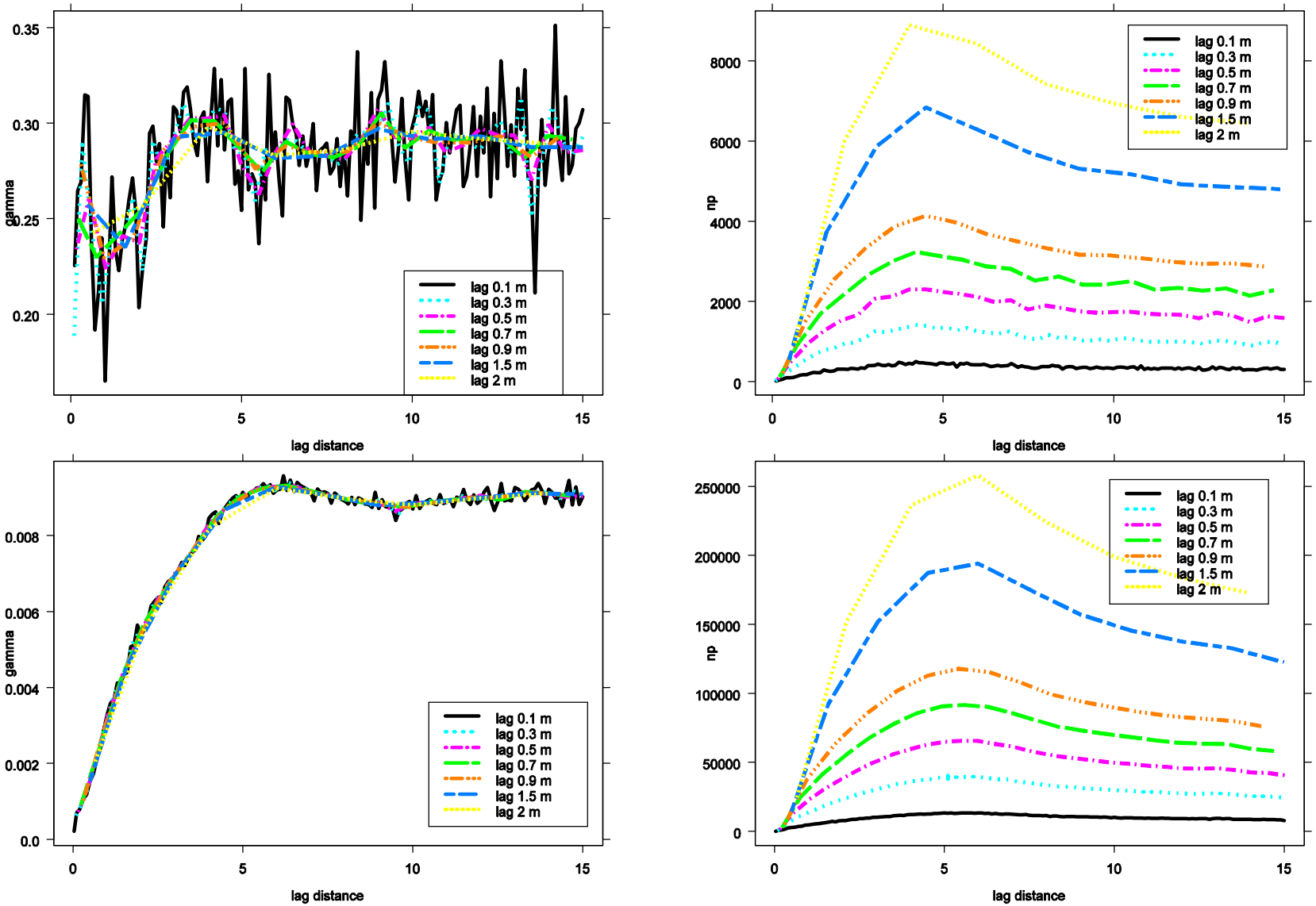

Figure 5.6: variogram calculated for different lag distances (left) for two river sites, the Highland Water (top) and the Lambourn (bottom). Graphs on the right represent the respective number of pairs of points (np) used for the calculation of each variogram value at each lag distance. Gamma represents the semivariance.

Azimuth or anisotropy analysis: the variograms were calculated for four azimuth directions (0°, 45°, 90°, 135°,) (Figure 5.7). Results showed that the cross-sectional variogram (90°) was more likely to be symmetric (Appendix 3.4), probably due to the symmetry of the channel cross-sections. Cross-sectional variograms presented a higher degree of variance than longitudinal variograms but the number of pairs of points included for the calculation of the variogram was considerably smaller; cross-sectional variograms were not as reliable as longitudinal variograms. Azimuth directions of 45 and 135 degrees did not present significant differences to the longitudinal variogram.

Maximum distance of analysis: variograms were calculated for all the data sets with the following characteristics: azimuth tolerance = 60, azimuth = longitudinal direction and lag distance = 0.5 m (dry and wet points) or 1 m (wet points). The distance for which the maximum number of pairs of points was identified has already been noted in Table 5.7. (Appendix 3.4). This is the maximum potential distance that was considered for the variogram interpretation.

Table 5.7: maximum number of pairs of points (NPP) and distance at which they were encountered for two azimuth directions (Direction 90 = across the river; Direction 0 = along the river).

Site	Distance (m) Max NP* Direction 0	Distance (m) Max NP* Direction 90	NP Direction 0	NP Direction 90	% Low Flows 2000
Pang Old fenced	5	4	5768	4297	1
Pang fenced	12	7	19508	11686	1
Pang Unfenced	10	7	18853	12873	1
Lambourn	7	5	109627	69932	1
Leigh Brook	8	5	46340	27804	1
Bere 2000	8	5	30048	18657	2
Pang Old fenced	5	4	5768	4297	2
Pang Unfenced	10	7	18853	12873	2
Leigh Brook	8	5	46340	27804	2
Senni	7	5	18715	12092	2
Highland Water	5	4	3942	2394	3
Cruick	9	3	25440	14047	3
Tarf	8	3	148315	86455	3
Blackwater	7	4	252143	154152	3
Tame LM	16	11	23502	14762	3
Windrush	9	6	14380	9718	0
TamesHM	16	13	17614	10931	0

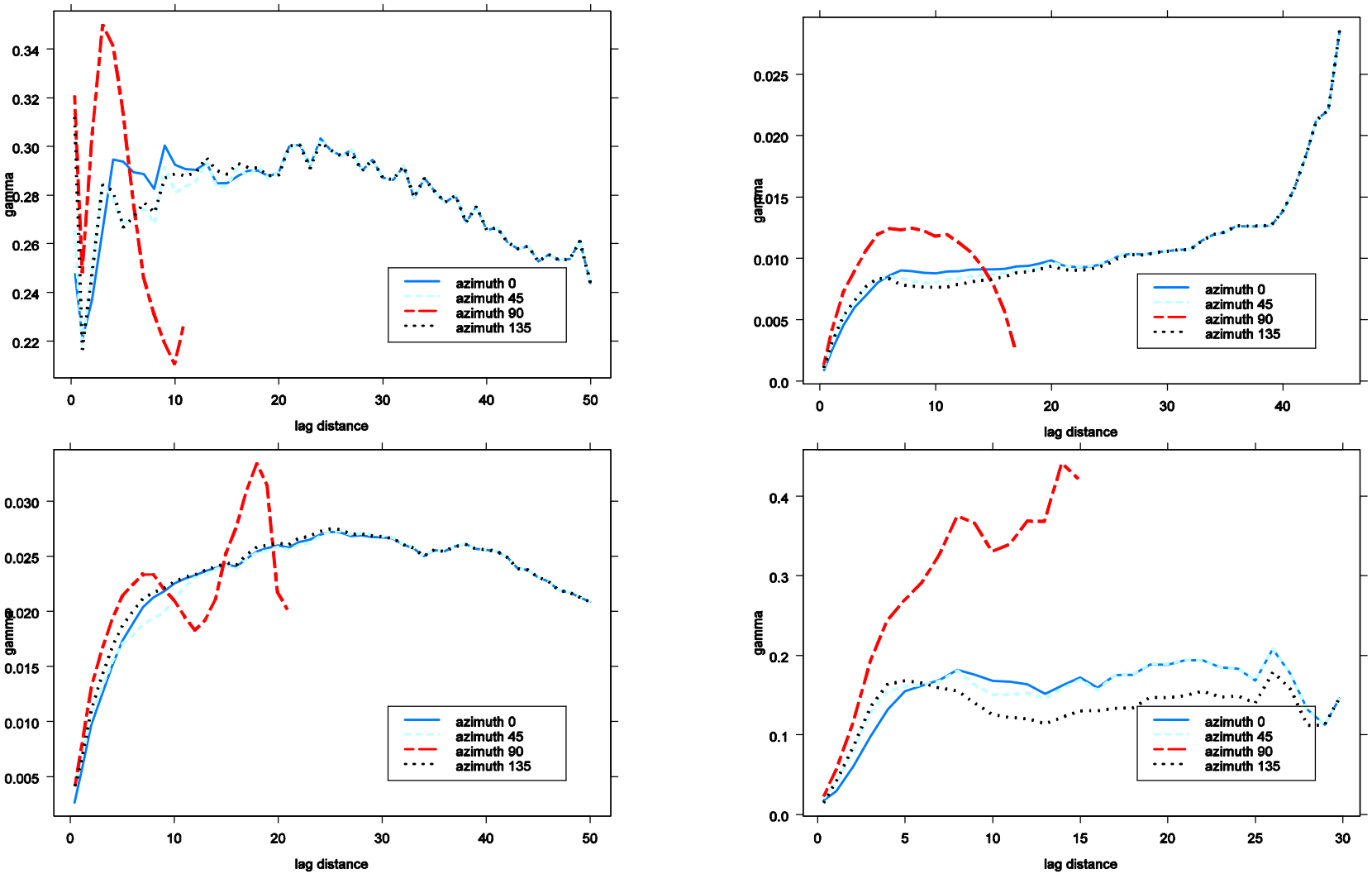

Figure 5.7: example of results obtained for the anisotropy study (wet & dry points). The rivers shown are Highland Water (top left), Lambourn (top right), Leigh Brook (bottom left) and Pang Old Fenced (bottom right). Results for all the river sites can be found in Appendix 3.4.

Sensitivity analysis for the empirical variogram: there were certain combinations of lag and maximum distance that provided distorted values of range, sill and nugget for the variogram fit (Figure 5.8 bottom). These combinations could not be identified at all the river sites and did not always correspond to the same lag and maximum distance. Extreme values encountered were always associated to bad fitting of the variogram model and either provided extreme high values of range (e.g 36584586 m for the Bere) or very low values (≅0) (Table 5.8).

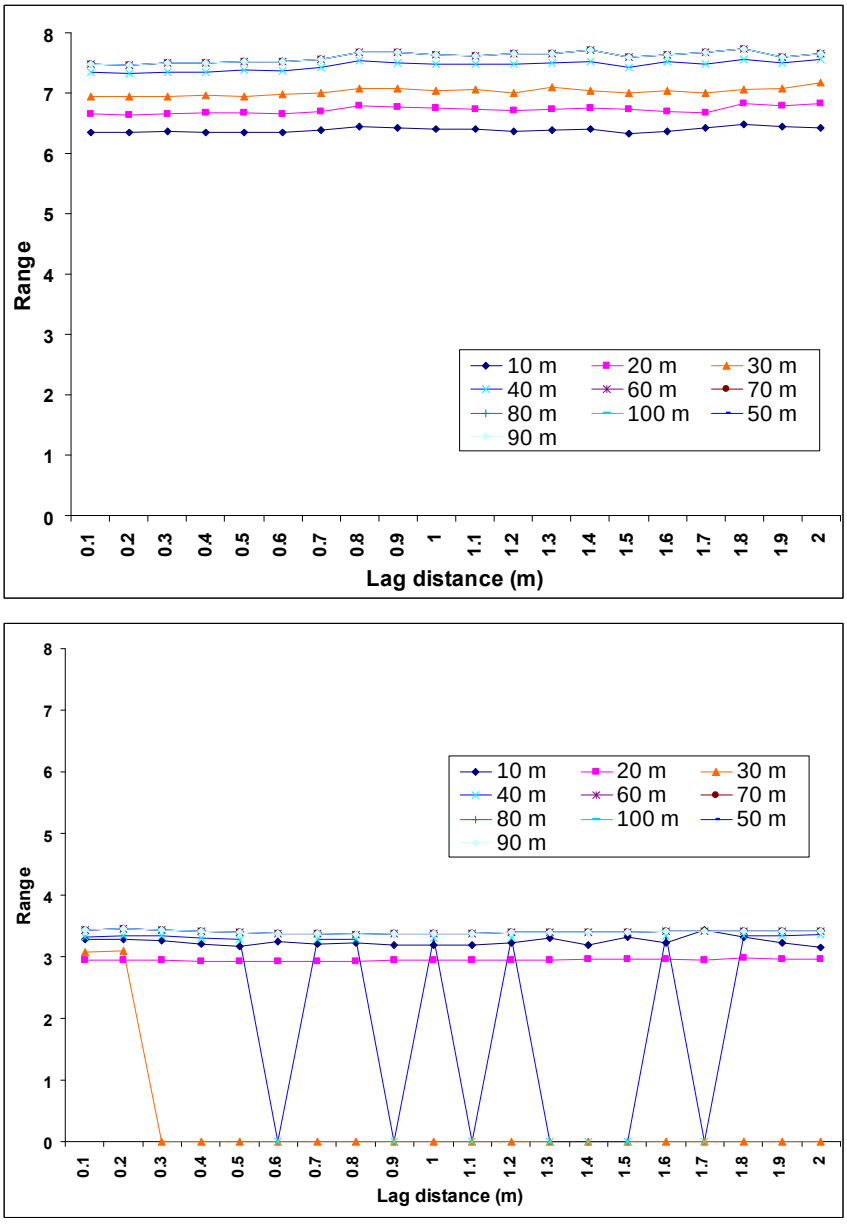

Figure 5.8: values of range obtained for the specified combinations of lag and maximum distance for the Lambourn river site. The top image represents the values obtained for the spherical variogram whilst the bottom image represents those obtained with the exponential. Each line represents a maximum distance selected. The legend defines which maximum distance was used for the variogram calculation.

Data sets with only wet points presented more cases of failure when fitting the variogram than data sets with dry and wet points. This may be due to the decrease of spatial variation between points: the variance between pairs of points remained more or less constant and thus, the points represented in the variogram followed a horizontal pattern which made it difficult to fit the variogram model. Those combinations that did not present extreme values of range, sill and nugget show consistency in the results obtained at the same river site (Figure 5.8).

Table 5.8: values of deviation encountered for each variogram parameter at each river site. "Total" refers to the deviation encountered for the total number of variograms calculated for the sensitivity analysis of the combinations of maximum distance and lag distance. "Selected" refers to the deviation calculated for the same criteria but excluding the extreme values of Range encountered. Only values for the spherical variogram have been considered.

DEVIATION	Range (m) Total	Sill Total	Nugget Total	Range (m) Selected	Sill Selected	Nugget Selected
Bere	2586960	902	0.04	0.09	0.00	0.00
Blackwater	4.08	0.11	0.10	0.13	0.00	0.00
Lambourn	0.43	0.00	0.00	0.43	0.00	0.00
Leigh Brook Q283	1.35	0.00	0.00	0.66	0.00	0.00
Leigh Brook Q294	4.01	0.01	0.01	1.33	0.00	0.00
Pang Fenced	692692	114	0.04	0.42	0.00	0.00
Pang Old Fenced Q281	0.08	0.00	0.00	0.08	0.00	0.00
Pang Old Fenced Q291	0.58	28.79	0.08	0.08	0.00	0.00
Pang Unfenced Q281	4645	38.93	0.04	5.60	0.04	0.00
Pang Unfenced Q291	2150	18.04	0.04	7.92	0.06	0.00
Senni	0.19	0.00	0.00	0.19	0.00	0.00
Cruick	0.58	28.79	7.09	7.09	0.00	0.00
Highland Water	125081	79.10	0.04	0.23	0.01	0.00
Tames HM	6.76	0.04	0.04	1.72	0.01	0.00
Tames LM	1.42	0.01	0.02	1.42	0.01	0.02
Tarf	7.14	0.00	0.00	4.41	0.00	0.00
Windrush	14.59	0.03	0.01	14.59	0.03	0.01

The adequate fitting of the variogram function is necessary to obtain smaller errors in the predictions and thus, special effort needs to be invested in determining if the empirical model represents the experimental variogram. The Objective function may be useful for this purpose but it may be misleading if there is not any reference value to be compared to. A sensitivity analysis is required for the fitting of the variogram model.

Results were more dependent on the maximum distance than on the lag distance (Figure 5.8 and Figure 5.9). Figure 5.9 shows a stable pattern for the range value from a maximum distance of 50 m to 100 m. This pattern was repeated for the three

variogram model parameters analysed: range, sill and nugget. Similar results were obtained for the majority of data sets (Appendix 3.5.1 to 3.5.5) although those intervals where the range was stable were not the same between river sites (Figure 5.9).

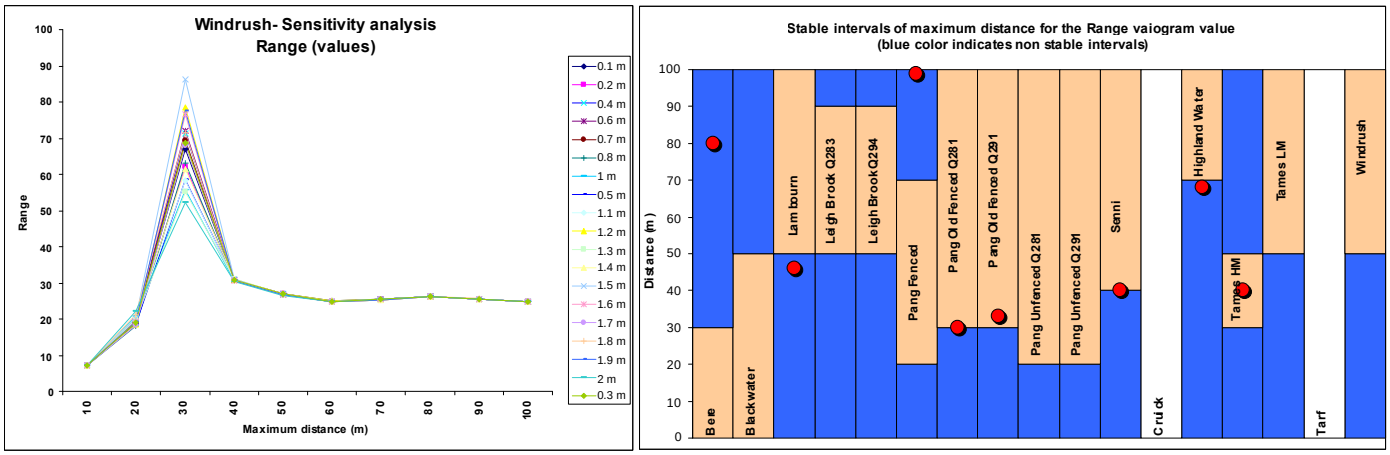

Figure 5.9: Left: changes in the range value for different lag distances and maximum distances for the Windrush river site (data set includes dry and wet points). Right: interval of maximum distance considered for which the variogram is stable. Orange areas indicate stable values of range, blue areas are non stable values and red dots show the distance sampled. Sampled distances higher than 100m have not been included in the plot.

The possibility of linking the distance at which the variogram stabilised with the sampled river length and the sampling density applied was considered. Results showed (Figure 5.9) that in general the variogram stabilised when reaching the total sampled distance (e.g. Lambourn, Pang Old Fenced, Senni, Highland Water). This may be due to the lack of ability to calculate the spatial pattern in areas that had not been sampled. River sites which presented stable values of spatial structure before the total length of sampled distance (e.g Bere, Blackwater, Leigh Brook and Pang Fenced) suggested that (i) either the spatial correlation of depth was smaller than the total sampled reach and therefore, the variogram was adequately defined or (ii) that values obtained for the variogram at non stable distances included a lot of noise due to the decrease in the number of pairs of points separated by a specific lag distance. The second option was more probable since the stable values were always encountered for distances greater than that at which the maximum number of pairs of points was identified. Since no pattern could be identified in the results for the combination of lag distance and maximum distance, it is suggested that the same criteria defined in the previous sections (maximum distance = 30 m) is applied.

It was observed that the exponential model always presented smaller values of range than the spherical model (Figure 5.8). Selection of different variogram models for the objective of Chapter 6 will result in misinterpretation of the results since it would not be possible to determine whether, the differences obtained between sampling densities are due to the fitted variogram model or to the sampling density applied. The spherical model will be selected for this purpose due to the fact that it presented fewer cases of failure in the sensitivity analysis (Figure 5.8).

Values of nugget and sill did not differ between models to the same extent as the range. Extreme values were produced using different combinations of lag and maximum distance for the two models tested and a higher rate of failure was observed for the exponential variogram.

5.4.4. *Determining the effect of bank-full information in the variogram.*

In general, wet points presented lower variance than dry points, except for the Windrush, Cruick, Lambourn and Tarf. This indicated that for these river sites, the spatial variability encountered for the bank information was smaller or similar to the spatial variability of the bed channel. The variogram cloud indicated the relationship between bed channel (wetted surface) and banks (dry points) since (i) it was able to differentiate them in terms of variance encountered and (ii) it was able to find the relationship between both sets of data. The variogram cloud can therefore be used as a tool for describing the shape characteristics of the river channel. Temporal changes in the shape of the river channel could also be detected through analysis of the variogram cloud. Results are summarised in Figure 5.10 and Appendix 3.6.

The differences encountered between the dry and wet variogram clouds indicated that it was necessary to develop the study separately for (i) wet points only to describe the spatial pattern of the wet channel and (ii) for wet & dry points to describe the spatial pattern of the river channel. The first analysis provided information on the usefulness of the variogram for the description of hydromorphological features such as changes in the physical habitat available for fish, whilst the second analysis informed on the suitability of the variogram for the description of the shape of the channel for structural purposes. Only data sets with wet points are analysed in Chapter 6.

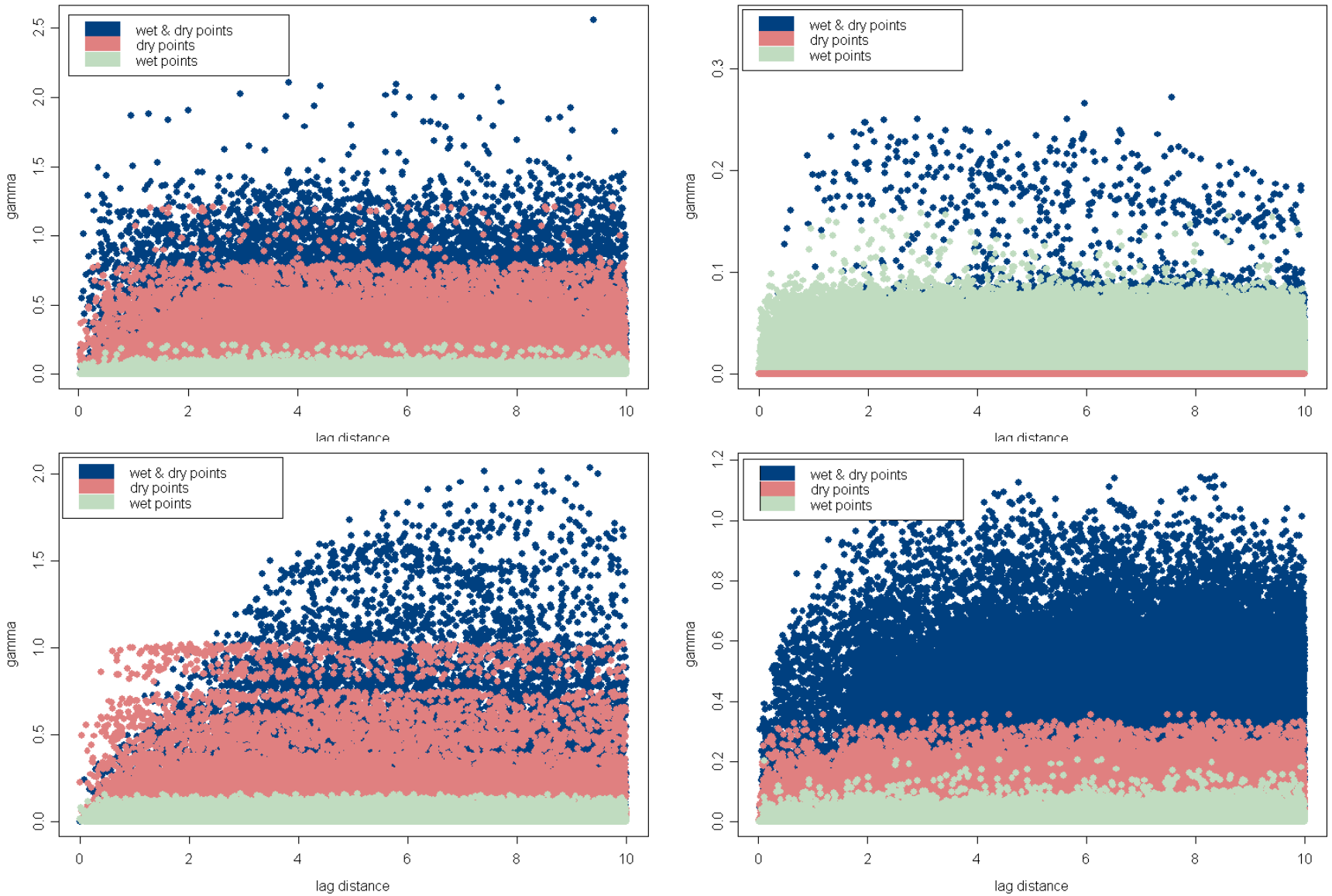

Figure 5.10: example of results obtained for the variogram cloud analysis. The rivers shown are Highland Water (top left), Lambourn (top right), Pang Old Fenced (bottom left) and Tames Highly Modified (bottom right). Blue represents the relation between wet & dry points, pink represents the relation between dry points and green shows the relation between wet points. Results for all the river sites can be found in Appendix 3.6.
results for the variogram cloud analysis.

5.4.5. *Geostatistical analysis*

The variogram results (Table 5.9 and Figure 5.11) showed that the spatial structure of the river sites did not have the same properties for all the data sets. Differences were encountered between river sites when considering (i) only wet points and (ii) dry and wet points. Variograms obtained with only wet points were also different to those obtained with wet & dry points. These differences in terms of variogram range were not consistent because (i) there were no significant differences between the spatial structure of the wetted channel and the spatial structure of the river with banks or (ii) the empirical variogram is not able to detect the differences between these two data sets.

The range (Table 5.9) indicated that the spatial correlation for depth was between 4 m to 30 m depending on the river site and data set analysed. This suggested that different sampling strategies should be applied for each river site according to their spatial structures. Results obtained for the sill variable (Table 5.9) were between 0.01 and 0.46. The sill had higher values for data sets with dry and wet points than for the same

Table 5.9: variogram values (i.e. range, sill and nugget) obtained for the data sets analysed. Spher and Exp refer to the spherical and exponential variogram model respectively.

River site	Selected Model		Wet				Dry & wet			
	Wet	Dry/wet	Range	Sill	Nugget	Objective	Range	Sill	Nugget	Objective
Bere	Spher	Spher	6.56	0.03	0.00	2442.03	4.98	0.10	0.02	603.56
Blackwater	Spher	Spher	2.46	0.01	0.00	2560.48	8.26	0.22	0.01	1632.51
Cruick	Exp	Exp	9.44	0.03	0.00	1011.28	9.18	0.03	0.00	949.80
Highland Water	Spher	Spher	4.79	0.02	0.00	181.94	5.27	0.10	0.20	139.25
Lambourn	Spher	Spher	6.83	0.01	0.00	3790.36	6.95	0.01	0.00	4908.52
Leigh Brook Q82	Exp	Exp	4.41	0.02	0.00	1017.88	4.41	0.02	0.00	1017.88
Leigh Brook Q93	Exp	Exp	5.07	0.03	0.00	1158.48	5.07	0.03	0.00	1158.48
Pang Fenced Q91	Spher	Spher	4.08	0.01	0.00	389.42	8.96	0.10	0.00	1605.16
Pang Old Fenced Q80	Spher	Spher	4.10	0.02	0.00	697.75	7.76	0.18	0.00	773.77
Pang Old Fenced Q90	Spher	Spher	4.23	0.02	0.00	766.91	7.76	0.18	0.00	773.77
Pang Unfenced Q80	Spher	Spher	5.64	0.01	0.00	444.99	10.61	0.10	0.00	2579.75
Pang Unfenced Q90	Spher	Spher	5.55	0.01	0.00	515.63	10.57	0.10	0.00	2601.24
Senni	Spher	Spher	6.27	0.04	0.01	809.86	6.30	0.04	0.01	761.78
Tames HM	Spher	Spher	15.09	0.01	0.00	1729.24	14.86	0.10	0.10	1077.56
Tames LM	Spher	Spher	13.17	0.46	0.07	2789.10	9.12	0.04	0.00	664.48
Tarf	Spher	Spher	13.37	0.00	0.01	9147.43	16.88	0.01	0.01	8007.83
Windrush	Spher	Spher	28.60	0.07	0.02	25410.17	26.23	0.07	0.03	26218.00

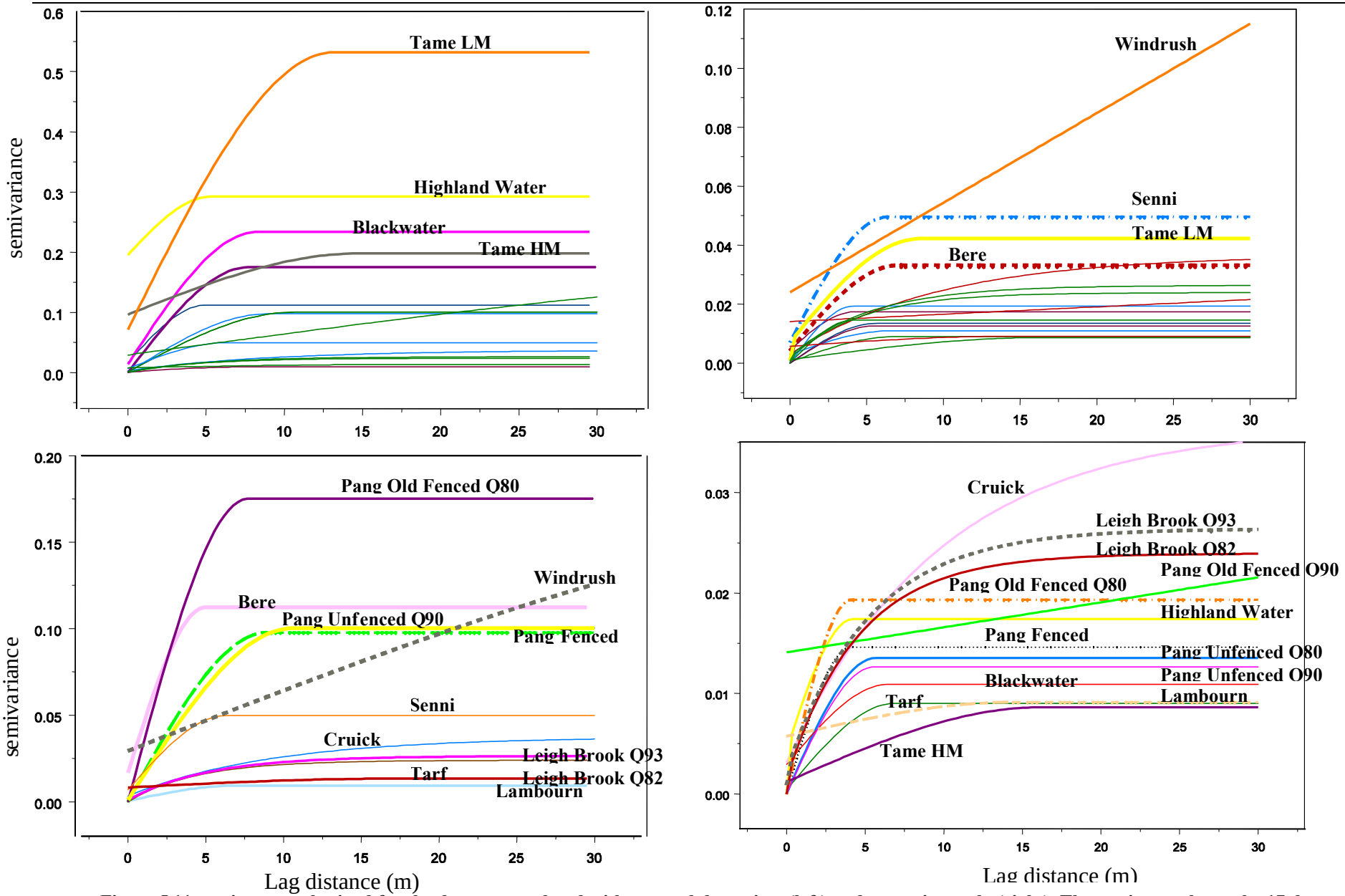

Figure 5.11: variograms obtained for the data sets analysed with wet and dry points (left) and wet points only (right). The top image shows the 17 data sets analysed. The bottom images are a detail of the variograms with lower values of range, sill and nugget represented in the top image.

river sites analysed with only the wet points. This indicated that higher spatial variation was encountered for the former due to the representation of the banks. Only one exception was encountered which corresponds to the Tame Less Modified river site. No obvious explanation can be found for this exception.

The empirical variogram did not give as much information on the spatial structure as the variogram cloud did. The empirical variogram was a "summary" of the results obtained for the variogram cloud and it simplified the spatial relationship between variance and lag distances by calculating the mean value of specific intervals. It is suggested to use the variogram cloud as a complementary tool to the empirical variogram when analysing the spatial pattern of hydromorphological variables.

Results for the nugget parameter (Table 5.9) were close to 0 for all the sites analysed. This indicated that the intrinsic spatial variance of depth was close to 0. However, it is necessary to note that the sampling strategies applied at the different river sites did not taken into account lag distances smaller than 0.2 m, which indicates that no conclusions can be established regarding the spatial structure of depth at microscale level. It is suggested that research studies are developed to analyse the spatial structure of depth at microscale level.

Nugget values did not show a consistent pattern of differences between data sets with only wet points and data sets with dry and wet points. In general, nugget values were higher for those data sets with dry and wet points. This may be due to the bank information introduced by the dry points but no conclusions could be established since the pattern was not observed for all the data sets.

Three cluster classes were obtained for the variogram model parameters for those data sets with only wet points and for the dry & wet points. Figure 5.12 shows the differences between both the classification obtained for dry and wet points and the classification obtained for only wet points. The river sites have been colour coded according to the groups obtained for the "wet points" data analysis. Results show that there are differences in the way that the river sites distribute in each of the cluster classes. Tame Low Modified is classified as a single group when considering wet points only and it is included in a more general group for the second analysis.

Blackwater and Pang Old Fenced form a single group for the wet and dry analysis whilst they are grouped with a higher number of river sites for the wet data analysis. Finally, for the wet and dry data analysis, the Highland Water is classified with the Tarf, Windrush and Tame Highly Modified group identified in the wet point data analysis.

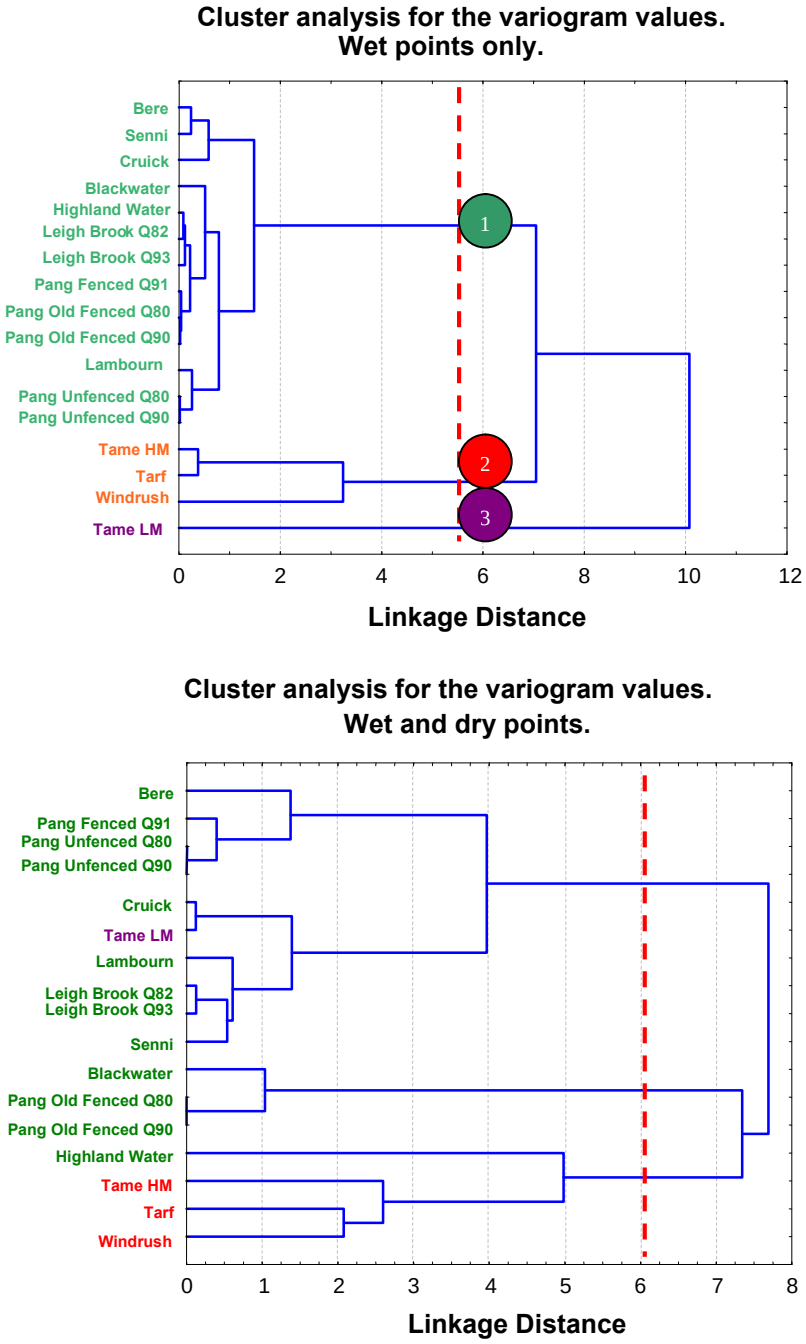

Figure 5.12: cluster analysis for the variogram values of the data sets including dry & wet points (bottom) and only the wet points (top). The number after the river name indicates the percentage of flow exceedance at which the data were collected. The rivers in each cluster class for the wet points analysis have been identified by a colour code. The rivers for the wet and dry analysis have been identified with the same colour as in the wet points analysis to identify the differences between cluster groups.

Multivariate analysis (cluster analysis in this case) is highly sensitive to the data used in the analysis. Results obtained are always associated with a degree of subjectivity on their interpretation. The groups identified for the "wet" and the "wet and dry" data set need to be interpreted according to the information obtained for the variogram analysis; wet points only inform the structure and characteristics of the bed channel whilst dry and wet points also include information on the structure and characteristics of the river banks. It is suggested that wet and dry points information should be used for classification purposes. It needs to be noted that for a correct classification of the river sites according to their spatial structure of bed channel and banks it would be necessary to collect comparable information for all the river sites. The groups identified in this study do not accomplish this criterion and therefore need to be carefully interpreted.

5.4.6. *Variables with more influences on the variogram*

Table 5.10 and Table 5.11 show the correlation values obtained for the reach scale and catchment scale physical descriptors. Those correlation coefficients that proved to be significant ($p<0.05$) have been highlighted in green. Both analyses (catchment and reach scale) showed a decrease in the number of significant correlation values when including the bank information in the variogram calculation.

Table 5.10: Pearson's coefficient (correlation coefficients) between the catchment descriptors and the variogram parameters. Wet refers to the data set with wet points only. Significant correlation values (P<0.05) have been highlighted in green.

Catchment Descriptors	Range Wet	Sill Wet	Nugget Wet	Range	Sill	Nugget
AREA	0.46	0.47	0.42	0.21	-0.14	-0.15
ALTBAR	0.44	-0.07	0.12	**0.54**	-0.43	-0.21
ASPBAR	-0.44	-0.23	-0.21	-0.44	-0.04	-0.12
BFIHOST	**-0.61**	-0.32	-0.40	-0.28	0.43	-0.45
DPLBAR	0.22	0.26	0.18	0.04	-0.09	-0.37
DPSBAR	0.12	-0.24	-0.09	0.10	**-0.50**	-0.17
LDP	0.11	0.19	0.08	-0.00	-0.03	-0.42
SPRHOST	**0.57**	0.23	0.31	0.28	**-0.51**	0.32
DistSorc	**0.81**	**0.59**	**0.56**	0.32	-0.36	0.14
Sord	**0.82**	**0.51**	**0.56**	**0.54**	-0.40	0.11
Hsorc	0.47	-0.05	0.11	0.43	**-0.53**	-0.12
Hsite	0.39	0.02	0.22	0.50	-0.30	-0.21
Qx	**0.74**	0.38	0.37	0.44	-0.12	0.18
Flow Exceedance	**-0.58**	-0.26	-0.29	-0.46	-0.11	**-0.52**
QMIN_0	**0.61**	**0.53**	**0.56**	0.26	-0.26	-0.05

Range appeared most strongly correlated with Stream Order (Table 5.10) for both the wet points and the wet & dry analysis for the catchment descriptors. High values of correlation were also encountered for the distance to the source and the flow at which the data were collected. Results for the dry and wet points indicated that the mean catchment altitude was significantly correlated to the variogram range. The continuum concept explains that rivers in their lower reaches have a wider cross-section, a higher flow and a higher sedimentation rate. The increase in the sedimentation rate gives uniformity to the bed channel (especially in respect of fine sediments). This uniformity results in lower roughness on the bed and therefore, a higher spatial correlation (i.e. a higher range).

Sill was significantly correlated to the distance to the source, the stream order and the average annual mean flow for the wet points analysis. These catchment descriptors did not coincide with the significant correlations identified for the wet and dry points analysis, where the index of catchment steepness, the standard percentage runoff and the height at the river source were the significant correlated catchment descriptors.

Table 5.11: Pearson's coefficient (correlation coefficients) between the reach descriptors and the variogram parameters. Wet refers to the data set with wet points only. Significant correlation values (P<0.05) have been highlighted in green.

Reach Descriptors	Range Wet	Sill Wet	Nugget Wet	Range	Sill	Nugget
Substrate	0.21	-0.16	-0.10	0.44	0.42	-0.03
Minimum Depth	0.28	-0.10	-0.09	0.01	-0.45	-0.13
Mean Depth	0.40	0.29	0.31	0.24	-0.37	-0.44
Maximum Depth	**0.72**	0.48	**0.58**	0.45	**-0.53**	-0.09
Mean Width	0.08	0.01	0.01	0.32	0.11	0.15
Minimum Width	0.16	0.00	0.00	0.24	0.08	0.12
Maximum Width	0.11	0.03	0.06	0.38	0.04	0.04
Depth Variation	**0.62**	0.38	0.47	-0.07	0.32	0.30
Number of habitat types	0.13	0.02	0.04	-0.08	**-0.72**	-0.17
Length of the reach	0.19	0.09	0.12	0.17	-0.44	-0.27
Reach Sinuosity	**0.77**	-0.07	0.14	**0.83**	-0.18	0.03
Pool – Riffle spacing	0.22	-0.03	0.11	0.32	**-0.52**	-0.25

Nugget was significantly correlated to the distance to the source, the stream order and the average annual mean flow for the data sets with only wet points. Percentage of flow exceedance was the only catchment physical descriptor that was significantly correlated with the nugget parameter for wet and dry points. The correlation was negative for this physical descriptor and thus, the higher the percentage of flow exceedance, the smaller the nugget value.

High correlations were encountered between the range (for the data sets with only wet points) and the following reach physical descriptors: reach sinuosity, maximum depth, and the depth variation. Reach sinuosity was also highly correlated with the range calculated with the data set including dry and wet points. This suggested that during the data collection procedure it was necessary to identify the deeper areas of a reach since they could have a strong influence on the modelling of the variogram; not so much effort needs to be invested on data collection in shallow areas.

There were fewer significant correlated values for the sill and the nugget variogram parameters. The number of habitat types was negatively correlated to the sill which indicated that the more diverse the habitat, the smaller the variation encountered. This suggested that the higher the number of habitats encountered, the higher the continuity between habitat types, and therefore, the smaller the sampling density that needs to be applied (i.e. this assumes the habitats are present at the site as a continuity, otherwise, it is necessary to characterise each habitat and thus, it would be necessary to increase the sampling density). River sites located near the river origin can present pools and riffles close together due to the substrate and the steepness present at the site. Instead, in lowland rivers the gradient between riffles and pools will be more smooth, going through intermediate habitats such as shallow glides and deep glides.

Table 5.12 shows correlations between variogram parameters and summary data statistics. High correlation coefficients were encountered between the range (calculated for the data sets that only include wet points) and the maximum depth and depth variation. The analysis showed that maximum depth values were more important than the determination of depth frequency distribution for the variogram calculation. This suggested that it is necessary to characterise the deepest areas of the river site in more detail (i.e. more effort needs to be invested in the characterisation of pools) in order to obtain representative values of maximum depth.

Note that for all correlation analysis carried out the highest correlation values identified belonged to the catchment or reach scale, with the former giving a higher number of high correlation values (i.e. >0.7).

Table 5.12: Pearson's coefficient (correlation coefficients) between the data descriptors and the variogram parameters. Wet refers to the data set with wet points only. Significant correlation values (P<0.05) have been highlighted in green.

Data Variables	Range Wet	Sill Wet	Nugget Wet	Range	Sill	Nugget
Stdev	**0.52**	0.41	0.47	-0.05	**0.52**	0.36
miD	0.28	-0.10	-0.09	0.01	-0.45	-0.13
FirstQ	0.15	0.13	0.10	0.16	-0.40	**-0.54**
MedianD	0.25	0.25	0.25	0.23	-0.09	-0.34
meD	0.40	0.29	0.31	0.24	-0.37	-0.44
ThirdQ	0.42	0.29	0.33	0.27	-0.05	-0.26
maD	**0.72**	0.48	**0.58**	0.45	**-0.53**	-0.09
DV	**0.62**	0.38	0.47	-0.07	0.32	0.30
Skewness	0.42	0.39	0.42	0.09	**-0.68**	-0.03
Kurtosis	0.33	**0.68**	**0.65**	0.08	0.20	-0.48

5.5. Conclusions

- River sites that will be used for the Test and Validation data sets for the analysis in Chapter 6 are as follows:

  - Group of 90 percent flow exceedance includes the river sites Lambourn, Pang Old Fenced, Pang Fenced and Pang Unfenced. The Lambourn was selected as a validation data set.
  - The 80 percent flow exceedance group is made up of the river sites Pang Old Fenced, Pang Unfenced and Bere. The latter one was selected as the validation data set.
  - Finally, the 40 percent flow exceedance group includes the Highland Water and the Blackwater. Highland Water was selected as a validation data set.

- The analysis developed in Chapter 6 will focus on data sets that include only wet points. Dry points will not be considered for the data analysis since the main interest is to determine the relationship between the variogram and the structure of the wetted channel.
- The variables used for variogram calculation will be: minimum number of pairs of points equal to 30, lag distance equal to 1 m, azimuth tolerance equal to 60° degrees, azimuth equal to 0° and maximum distance equal to 30 m. The variograms determined with these characteristics will be the basis for the prediction of regular grids in Chapter 6.

- The maximum distance that can be considered for variogram calculation is a limiting factor when determining the spatial structure. The maximum distance that can be considered is always smaller than the total distance sampled (from 50% to 33% of the total distance sampled). This means that the distance sampled needs to be longer (two to three times longer) than the maximum distance to be considered for the analysis of the spatial structure.
- The spatial structure along the river differs from that encountered for the cross-sectional direction. The cross-section presents more variability than the longitudinal profile due to (i) a reduced number of pairs of points available for the calculation and (ii) the symmetrical shape in this direction. The cross-sectional variogram is misleading when interpreting the spatial structure. It is suggested to give priority to the longitudinal variogram when analysing the spatial structure of depth at a river site. The longitudinal variogram will need to be calculated with a wide (>60) azimuth tolerance in order to include the information provided for the cross-sectional direction.
- It is necessary to develop a sensitivity analysis when fitting the variogram model. The sensitivity analysis should focus on the study of the number of pairs of points available, the lag distance, the maximum distance, the azimuth tolerance and the azimuth.
- Spherical and exponential variogram models can give different results for the same data. Chapter 6 will focus on the comparison of results of the spherical variograms obtained for different sampling densities and different river sites. Only one variogram model will be selected for the comparison of results obtained between river sites and sampling densities.
- The variogram cloud is able to detect differences between the spatial structure of the bed channel and the spatial structure of the river banks. This suggests that the variogram cloud could be used as a tool (i) to describe the hydromorphological characteristics (depth) of the channel and (ii) to detect the temporal changes in the hydromorphological characteristics of the river.
- The variogram cloud is more informative than the experimental variogram when studying the spatial structure of a site. The experimental variogram is an average of the values obtained in the variogram cloud. It is suggested that the variogram cloud is used as a complementary tool to the experimental variogram.

- The variogram has been able to detect differences in the spatial structure of the river sites. Results suggest that different sampling densities should be applied at each site; river sites with a high degree of variation in space will need higher sampling densities in order to obtain the same level of information in comparison with river sites with low spatial variation.
- During the data collection procedure it is necessary to invest special effort in characterising the deepest areas of the river site to be sampled since this could have an impact on the variogram calculation.
- The higher the hydromorphological uniformity and continuity of the river site, the lower the sampling density that needs to be applied.
- Catchment descriptors appear to be more correlated to the variogram values than the reach descriptors. This may suggest that characteristics at catchment level are more relevant than characteristics at reach level in determining the spatial structure of a river site.
- Further research projects should focus on the microscale level in order to analyse the spatial structure at this spatial scale and on the sensitivity analysis of the predictions.

6

Defining effective Sampling Densities

This chapter deals with the design of effective sampling densities for depth data collection. Three different tools will be provided in this chapter in order to relate the sampling density and the level of accuracy of predicted depth with geostatistical techniques. These tools are provided in terms of confidence intervals, graphs and plots that relate sampling density, river site and accuracy obtained. Results can be used to identify the sampling density required for a specific objective.

6.1. Introduction and objectives of Chapter 6

The spatial problem is constituted of two main components: the type of sampling strategy that needs to be applied and the sampling density that is required to obtain a specific level of accuracy in the predictions. Chapter 4 focused on the comparison of several sampling strategies. Chapter 6 will focus on the comparison of different sampling densities to meet the following objectives:

(i) the **first objective** is to determine which level of accuracy is associated with a specific sampling density where accuracy is measured by different indicators and

(ii) the **second objective** is to determine whether the accuracy depends upon the characteristics of the river site, in order that a common methodology for data collection could be developed.

6.2. Methodology

6.2.1. *Analytical procedure*

Fifteen sites were analysed in this Chapter. These river sites corresponded to those considered in Chapter 5 and were: Bere, Blackwater, Cruick. Highland Water, Lambourn, Leigh Brook (Q82 and Q93), Pang Fenced, Pang Unfenced (Q80 and Q90), Senni, Tame Less Modified, Tame Highly Modified, Tarf and Windrush.

Chapter 5 also includes the Pang Old Fenced river site, which was not considered in Chapter 6 (see below).

The depth data collected at these sites were used to create a 0.5 m x 0.5 m regular grid of depth. Points were randomly selected from the 0.5 m by 0.5 m regular grid to obtain different sampling densities. Nineteen different sampling densities per river site were obtained. The selected points were analysed with geostatistical techniques to obtain the variogram and to characterise the spatial structure of each data set. The variogram was used to predict the value of depth at all points on the 0.5 m x 0.5 m regular grid. The accuracy of the predicted values was assessed with a set of quantitative and qualitative indicators described in Chapter 4 (channel volume was not used). Pang Old fenced could not be included in the analysis since the 0.5 m x 0.5 m grid created did not represent the variability of depth at the site. The majority of depth points in the regular grid had very similar value.

6.2.2. *Comparison of two software packages: ArcGIS and SPLUS*

Depth predictions at the 0.5 m x 0.5 m regular grid could not be obtained with SPLUS software for all the river sites due to the different sampling strategies that were originally applied in data collection, which meant the resultant covariance matrix was not positive definite. This means that even though the mean sampling density for these river sites was high enough to properly calculate the variogram, some of the 0.5 m x 0.5 m regular grid points were not surrounded by measured points. Thus, predictions could not be properly obtained. Depth was predicted with ArcGIS software at these river sites, which were: Blackwater, Cruick, Highland Water, Lambourn, Tame Less Modified and Tarf. ArcGIS was able to solve this by combining geostatistical and extrapolation methods (see section 7.3.2 for more detail on limitations for this methodology).

Since two different methodologies and software were used to obtain the predictions on the regular grid, it was considered necessary to compare the results obtained with ArcGIS and SPLUS. The comparison was carried out for the following river sites: Bere, Pang Fenced, Pang Unfenced (both flows), Pang Old Fenced (both flows), Leigh Brook (both flows), Windrush, Senni and Tame Highly Modified. The

variogram was initially calculated with SPLUS as output from this software was more informative regarding the type of adjustment required to fit the variogram. Lag distance, maximum distance, azimuth tolerance, azimuth, range, sill and nugget were determined with SPLUS. These values were used in the geostatistical module of ArcGIS to define the variogram. Predictions were obtained with both software packages at the 0.5 m x 0.5 m points of the regular grid. A comparison of the predicted values was obtained through the calculation of the maximum absolute difference between predicted and observed values, the Standard Error (SE) and Mean Squared Error (MSE) of the predictions.

6.2.3. *The indicators defining the different objectives*

The different objectives for which hydromorphological sampling strategies may be applied are diverse and include purposes such as river restoration or morphological quality assessment. Each objective for which hydromorphological data are being collected should require a specific level of accuracy in the representation of the "real environment". There is a need to determine which sampling strategy and density is required for each objective. Since the list of purposes for which data are collected is wide and the level of accuracy selected is still associated with subjective criteria, a more practical approach was taken. A set of tables that relates the sampling density with the accuracy of the predicted values was produced so the end user can relate these variables. Accuracy was measured with the qualitative and quantitative indicators already described in previous chapters. Quantitative indicators (variogram assessment, frequency distribution, prediction error, mean squared error, regression analysis) were obtained for all the river sites analysed in Chapter 6 whilst qualitative indicators (cross-sections & longitudinal profiles, mapping resolution and SE maps) were only calculated for specific river sites as they are only qualitative.

6.2.4. *Finding a relationship between the river descriptors and the results obtained.*

The rivers analysed were grouped according to the criteria described in Chapter 5. General Linear Models were considered as an appropriate analysis technique to determine whether or not these groups were representative of the pattern that the indicators showed when decreasing the sampling density. However, the data violated

the assumptions of normality and homogeneity of variance. The normality assumption requires that the residuals (after fitting the model) are normally distributed. This was examined by looking at the QQ-plot and the histogram. Results obtained showed that the majority of the data did not follow a normal distribution and that the same indicator had a different distribution according to the river site being analysed. Thus, data transformations were not a feasible solution.

The homogeneity of variance assumption states that the variance in the different groups of the design is identical. This was checked visually through the inspection of the boxplots of each data group. Results indicated that the variances were not homogeneous for many of the indicators and that with the non normal residuals a General Linear Model was not an appropriate analysis.

A non-parametric alternative test (the Kruskal – Wallis test) was used to determine if there were differences between the groups and within them. This test compares several independent random samples and can be used as a non parametric alternative to the one way ANOVA. The analysis was repeated several times:

- To determine if there were differences between rivers grouped according to each grouping criterion mentioned in Chapter 5: (i) the flow exceedance criterion, (ii) the catchment descriptors, (iii) the reach descriptors, (iv) the spatial structure descriptors and (v) the final classification proposed.
- To compare differences between sampling densities within each of the groups obtained for each grouping criterion.

Finally, the coefficients of correlation (Pearson's coefficient) were obtained for the relationships between (i) each catchment descriptor, reach descriptor and spatial descriptor of each river site and (ii) the indicators analysed for each site, grouped according to the sampling density. This determines which descriptors had a higher

influence on the behaviour of the indicator analysed and therefore, which descriptors should have the highest relevance when designing the sampling strategy.

6.3. Results

6.3.1. *Comparison of two software packages: ArcGIS and SPLUS*

Figure 6.1 shows the difference between the depth values obtained with ArcGIS software packages and those obtained with SPLUS. The mean difference between methods corresponded to less than 10 cm for all the river sites analysed. Maximum difference reached values of up to 70 cm. Maximum differences were typically less than 30 cm. Minimum differences were all less than 20 cm. Table 6.1 shows the number of points with a positive and a negative difference between ArcGIS and SPLUS. The percentage of points associated with positive or negative differences was close to 50% for all the river sites, which indicated that no pattern of overestimation or underestimation could be identified between the methods. The Mean Squared Errors obtained are presented in Figure 6.2. Note the high MSE obtained for the Tame Highly Modified site, which is associated to the results shown in Figure 6.1. The high MSE was due to a large difference between predictions using SPLUS and predictions using ArcGIS depth values at the edge of the reach. These points did not have a high number of neighbours that can be used to calculate the predicted values and thus, higher errors were found.

The differences encountered between software packages indicated that (i) different processes were being applied to obtain the predictions, (ii) it was necessary to specify which software was used to obtain the predicted values and (iii) further studies were required to understand and identify the differences between the analytical procedures used. Statistical packages such as SPLUS or Genstat are recommended for the implementation of geostatistical analysis since the settings allow the user to control the interpolation processes and variables.

Even though differences were encountered between methodologies, this did not affect the purpose of the analysis. The predicted depth values may not represent the total variability of depth at a river site since the predictions at the 0.5 m x 0.5 m regular

grid were obtained from significantly smaller sampling densities (less points per square metre) for the majority of river sites. However, this representation provided at least as much information on the variability of depth as it was provided with the original situation and thus, it was assumed that the predicted values represented the variability of the sites.

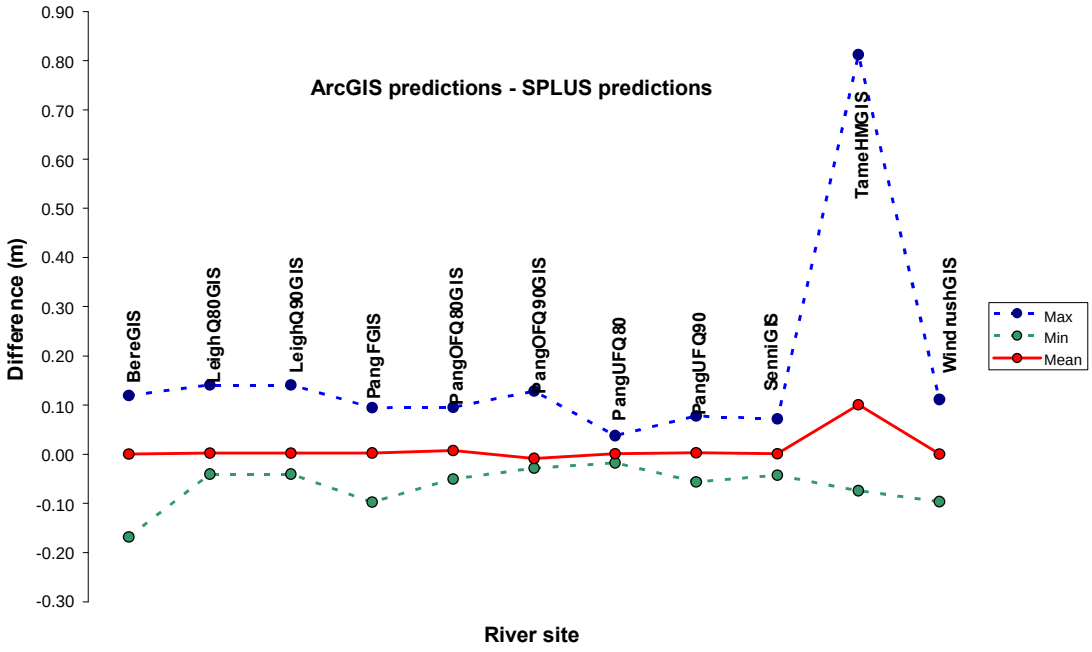

Figure 6.1: maximum (Max), minimum (min) and mean differences encountered between predictions obtained with ArcGIS and Splus software. Tame HM refers to Tame Highly Modified river site. Pang OF and Pang UF refer to Pang Old Fenced and Pang UnFenced. Q80 and Q90 refer to the flow exceedance group to which the river site belongs.

Table 6.1: number of points that provide a positive and negative difference between ArcGIS and SPLUS predictions. Tame HM refers to Tame Highly Modified river site. Pang OF and Pang UF refer to Pang Old Fenced and Pang UnFenced. Q80 and Q90 refer to the flow exceedance group to which the river site belongs.

River Site	Positive difference	Negative Difference	Total Number of points
Bere	848	812	1660
LeighQ80	3228	3262	6490
LeighQ90	3228	3262	6490
PangFenced	1210	1234	2444
PangOFQ80	298	322	620
PangOFQ90	71	552	623
PangUFQ80	1349	1551	2900
PangUFQ90	1309	1591	2900
Senni	698	711	1409
TameHM	2602	2023	4625
Windrush	2767	2146	4913

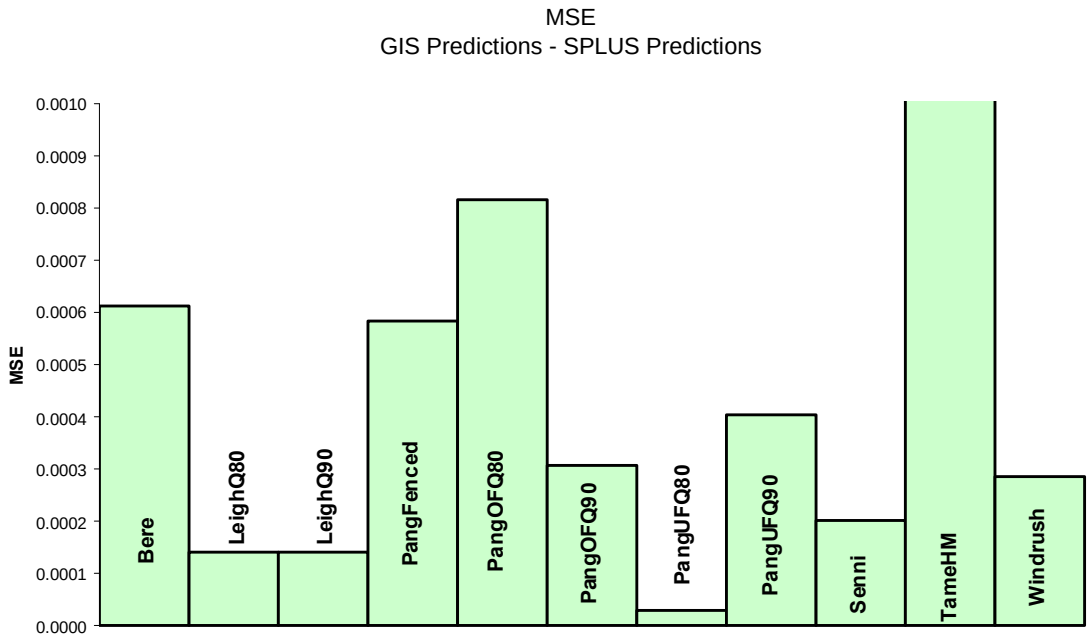

Figure 6.2: Mean Squared Error (MSE) obtained between ArcGIS predictions and SPLUS predictions for depth (measured in metres). Tame HM refers to Tame Highly Modified river site. Pang OF and Pang UF refer to Pang Old Fenced and Pang UnFenced. Q80 and Q90 refer to the flow exceedance group to which the river site belongs. Note that Tame Highly Modified exceeds the represented scale; its MSE value is 0.04.

6.3.2. *The indicators defining the different objectives*

Results for the quantitative indicators considered are shown in Figure 6.3 to Figure 6.6. The rivers analysed were ordered differently depending on the indicator that was being analysed. Thus, it was difficult to define a pattern that defines a river site for all the indicators; for the MSE between predicted and observed values (Figure 6.4), the rivers with highest errors were the Bere, the Pang Fenced and the Blackwater, in decreasing order. In contrast, different results were obtained when considering the p-value (Figure 6.5); the rivers with higher accuracy using this indicator were the Blackwater, the Leigh Brook, the Pang Fenced and the Tame Highly Modified in descending order.

The general pattern showed that the discrepancy in representing each river site increased when decreasing the sampling density and that the sampling density at which the dispersion started increasing differed according to the indicator considered. Thus, it could be observed that different sampling densities should be applied for different sampling objectives (indicators). To determine whether these differences were statistically significant, the Kruskal-Wallis test was used (section 6.3.3).

From the pattern observed in Figure 6.3 to Figure 6.6 it was possible to divide the quantitative indicators into two main categories; (i) indicators highly dependent on the sampling density and (ii) indicators less dependent on the sampling density. The first group included all the indicators that show a clear pattern change when decreasing the sampling density. The second group included all the indicators that did not show such a distinct pattern. Indicators highly dependent on the sampling density were: maximum difference between predicted and observed values (Figure 6.3), minimum difference between predicted and observed values (Figure 6.4), mean difference between predicted and observed values (Figure 6.4), Maximum Squared Error (Figure 6.4), MSE (Figure 6.4), p-value (Figure 6.5), R-squared (Figure 6.5) and objective function value.

Sampling densities need to be carefully chosen when trying to characterise indicators that change sharply with a change in sampling density. The pattern identified showed that the lower the sampling density, (i) the lower the accuracy of the indicators defining data characteristics (e.g. mean depth value) and (ii) the higher the value of the indicators describing the error of the predictions (e.g. maximum difference between predicted and observed values).

Table 6.2 shows the equation that was obtained to characterise the change of the indicator value in relation to the change in the sampling density (model fitted included all the river sites). These equations provide a guideline to understanding the behaviour of each indicator and they must not be interpreted as an exact relationship. Absolute maximum and minimum differences between observed and predicted values, as well as, maximum, minimum and mean squared error and objective function value showed an exponential relation between the value of the indicator and the sampling density selected. Mean difference between observed and predicted values also showed an exponential pattern when considering the absolute value of this indicator. R-squared and p-value indicators were not described by an exponential function; a logarithmic function better described the R-squared values whilst a polynomial function was used for the p-value. The equations obtained for each river site and indicator are presented in Appendix 4.1.

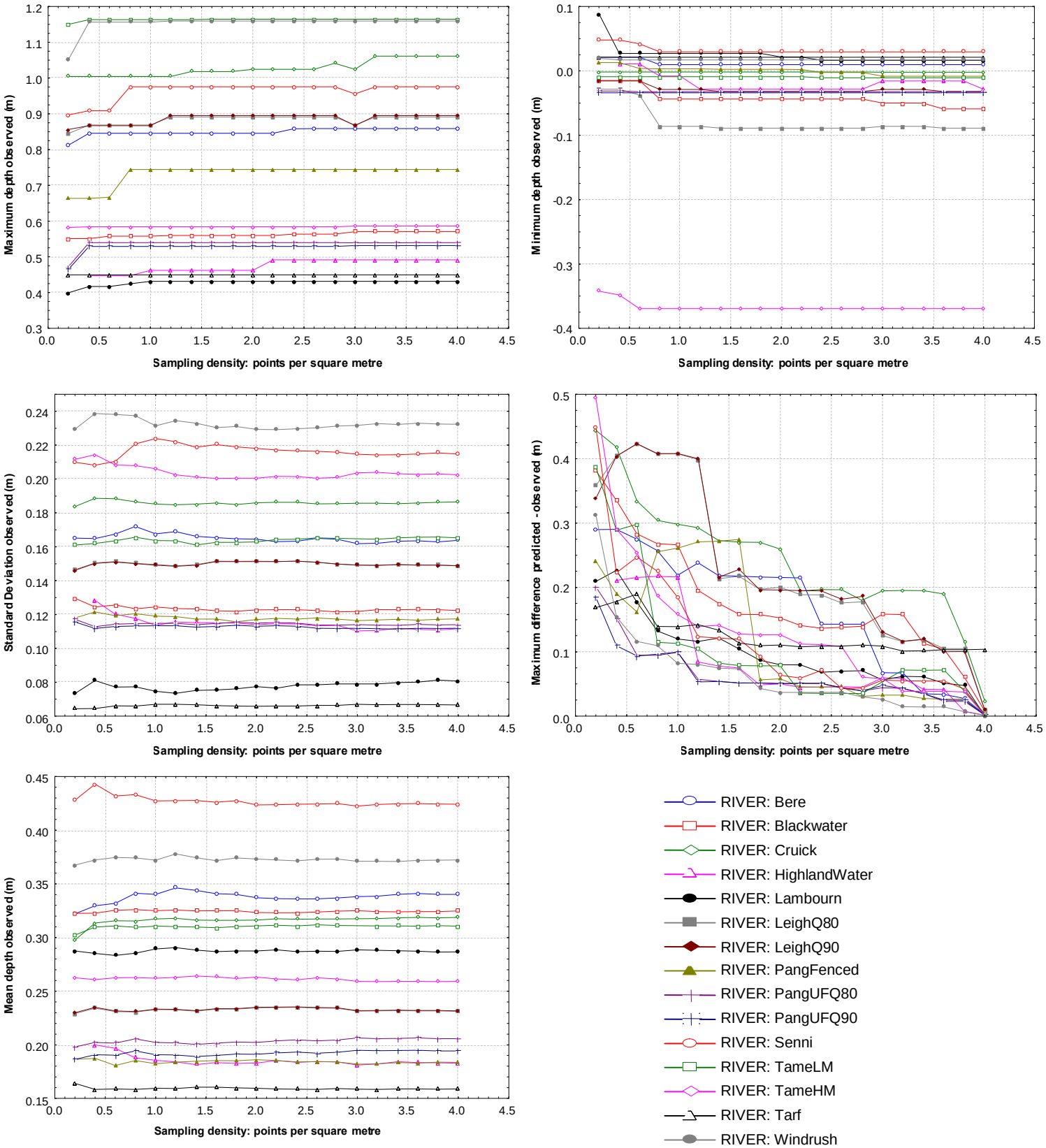

Figure 6.3: results obtained for five different indicators, 20 different sampling densities and 15 different river sites. The indicators represented are: maximum depth observed (m), minimum depth observed (m), Standard deviation of the observed data set, mean depth observed (m), and maximum difference between observed and predicted values (m). Note that the scales for each indicator are different and that some of the indicators represent the difference between original and predicted points, whilst others represent a characteristic of the data set that needs to be compared to the original value (e.g. mean depth observed).

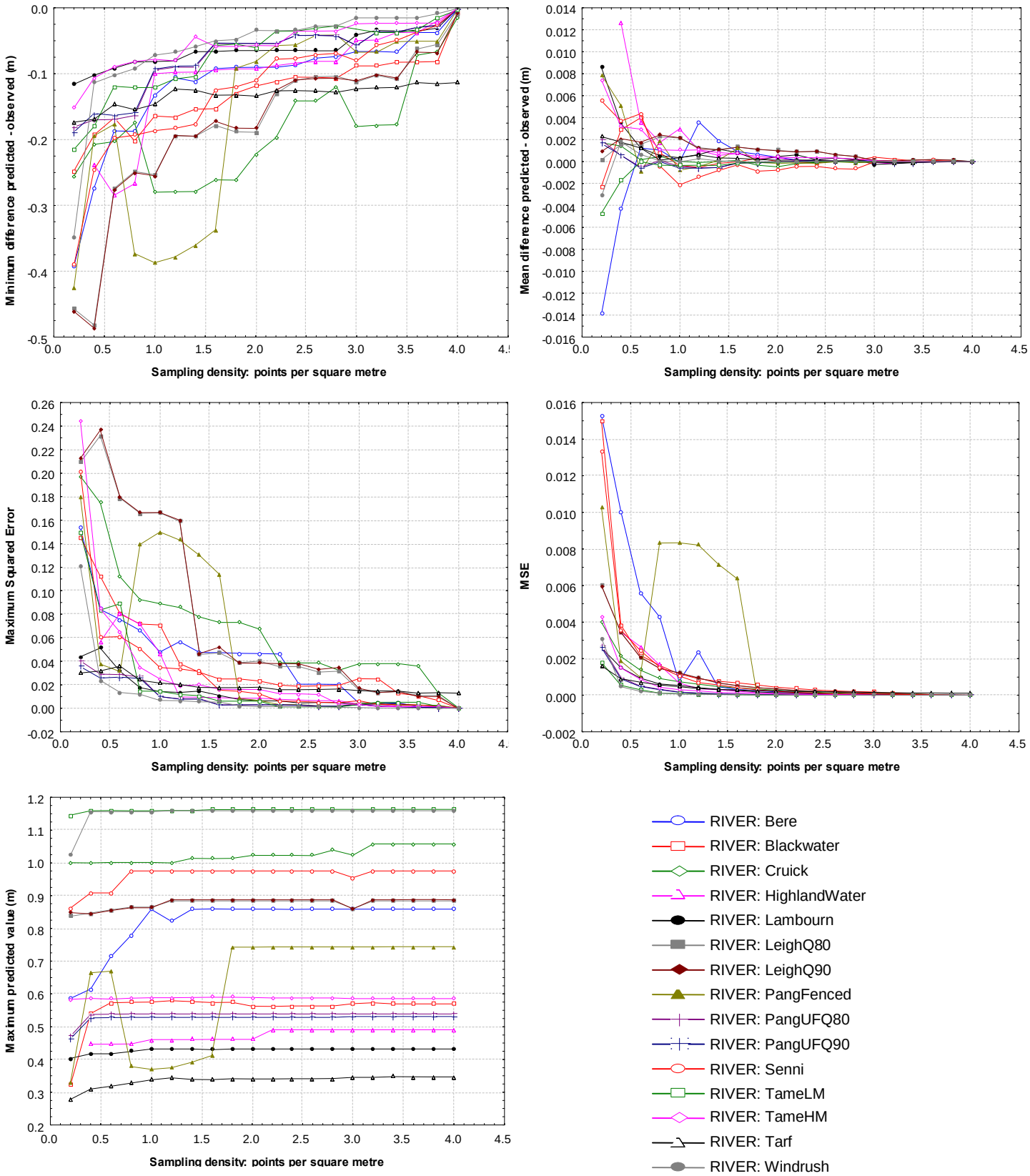

Figure 6.4: results obtained for five different indicators, 20 different sampling densities and 15 different river sites. The indicators represented are: minimum difference between predicted and observed (m), mean difference between predicted and observed (m), Maximum squared error, Mean Squared Error (MSE) and maximum predicted value. Note that the scales for each indicator are different and that some of the indicators represent the difference between original and predicted points, whilst others represent a characteristic of the data set that needs to be compared to the original value (e.g. maximum predicted and MSE).

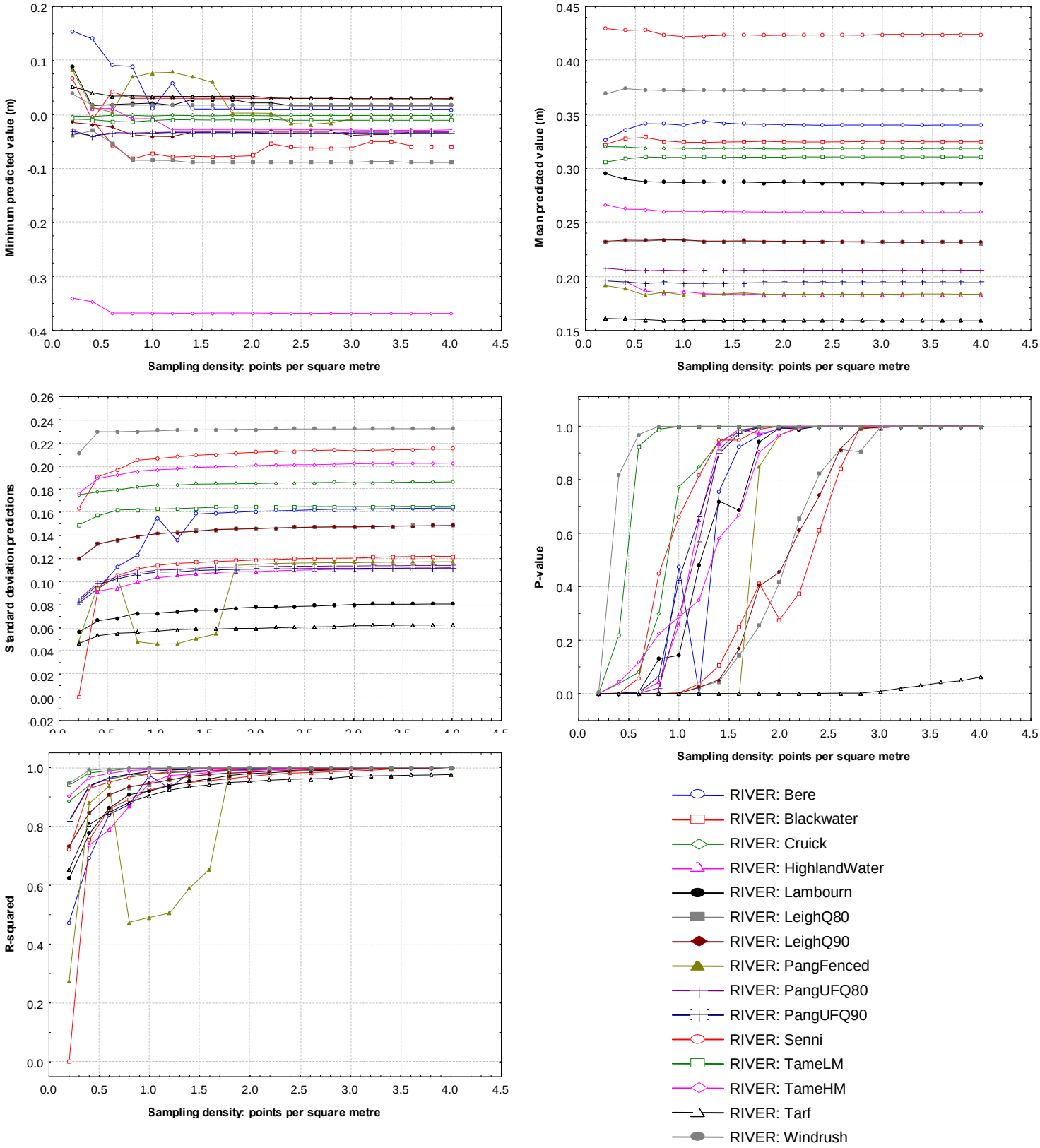

Figure 6.5: results obtained for five different indicators, 20 different sampling densities and 15 different river sites. The indicators represented are: minimum predicted value (m), mean predicted value (m), standard deviation of the predicted values, P-value and R-squared.

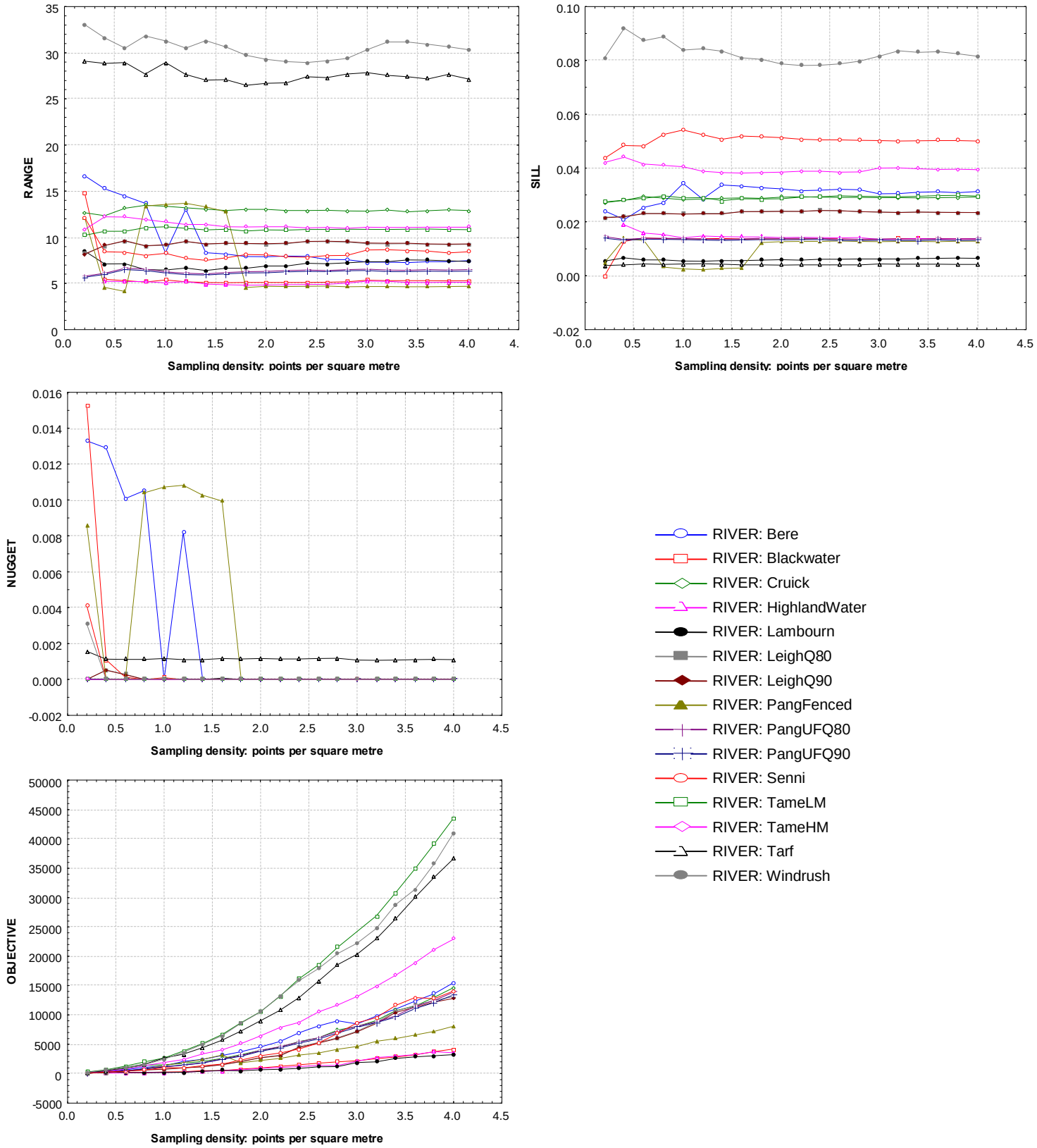

Figure 6.6: results obtained for four different indicators, 20 different sampling densities and 15 different river sites. The indicators represented are: range, sill, nugget and objective. Note that these indicators represent a characteristic of the data set that needs to be compared to the original value.

Table 6.2: equations obtained for the relation between the sampling density (x) and the indicator value (y) for those indicators that showed a clear pattern when changing the sampling density.

Indicator	Model	Equation	Correlation (r)
Maximum Difference	exponential	y=0.364*exp(-0.6684*x)	-0.6842
Minimum Difference	exponential	y=0.3013*exp(-0.6465*x)	-0.6687
Mean Difference	exponential	y=0.0379*exp(-3.2402*x)	-0.5218
Maximum Squared Error	exponential	y=0.1565*exp(-1.3306*x)	-0.6061
MSE	exponential	y=0.0046*exp(-1.8527*x)	-0.4833
P-value	polynomial	$y=-0.2033+0.6964*-0.044*x^2$	0.7687
R-squared	logarithmic	y=0.9125+0.1908*log10(x)	0.4763
Objective function	exponential	y=295.0299*exp(1.0559*x)	0.6522

The fact that some indicators did not visually show a strong relationship between sampling density and the indicator value might be related to the type of graphs presented in Figure 6.3 to Figure 6.6. Note that (i) the scales of each indicator are different and that (ii) some indicators represent the difference or error between predicted and observed values (e.g. maximum difference between predicted and observed values and MSE) whilst other indicators present characteristics of the data set (e.g. maximum depth of the observed data set) that need to be compared to the value obtained for the original data set (4 points/m^2). These comparisons are presented in Appendix 4.2.

Note that the objective function value increases when increasing the sampling density. The smaller the value of the objective function the better the variogram model was fitted. Higher sampling densities include more points for the calculation of the variogram function and therefore, provide better variogram models. However, this is associated with an increase of the objective function. The objective function fitting criterion is sensible from the point of view that the more pairs of observations there are the more weight the residual receives (Cressie, 1993). Further research is needed to determine what value of the objective function represents "good" fitting of the variogram model for a specific number of sampled points.

Results obtained for the quantitative indicators are presented in Appendix 4.2. A table was produced for each river site that related the sampling density applied with the value of the indicator obtained. The table was accompanied by pictures of the river site and its description so that the end user could appreciate how the decrease of the sampling density affected each indicator at each river site. In this way, when trying to determine the sampling density that is needed for a river site, it should be possible (i) to identify which river site of those presented in Appendix 4.2 is most similar to the

one that is going to be sampled, (ii) to define which indicator better describes the objectives for which data are being collected and (iii) to relate this to the sampling density that is needed for a specific level of accuracy. The final objective of this work was to produce a table for each type of river site. This will be discussed further in section 6.3.3.

Qualitative indicators were calculated for some of the river sites to have an idea of the behaviour of these parameters. Cross-section and longitudinal profiles were obtained for the Cruick river site, one of the sites that presented high maximum differences between observed and predicted values. Results were difficult to interpret since more than 250 cross sections and 20 profiles were obtained. The general pattern encountered showed that the shape of the cross-sections was predicted by all the sampling densities except for 0.2 points/m^2. The shape of the longitudinal profiles was more accurately predicted than those obtained for the cross-sections (0.2 points/m^2 being the only density not identifying the longitudinal pattern).

Depth maps were produced for the Bere, Highland Water and Lambourn at sampling densities 0.2 points/m^2, 1 points/m^2, 3.8 points/m^2 and 4 points/m^2, as a reference for the rest of the river sites included in the same group (Chapter 5 grouping criteria). Figure 6.7 to Figure 6.9 show the results obtained for the depth indicator. Depth patterns obtained with sampling densities $\geq$ 1 point/m^2 were similar to those obtained with the maximum sampling density (4 points/m^2), although small differences could be seen regarding the surface defined by each contour line and the volume associated with each depth class. Maps obtained for sampling densities smaller than 1 point/m^2 presented higher differences in terms of pattern. Shallow and deep areas were not properly represented, especially when considering the dry areas that appeared in some of the river sites represented. These areas were not adequately defined or represented when decreasing the sampling density down to 0.2 points/m^2. The lower the sampling density, the smaller the width of the river that could be predicted; the number of neighbours that were available to obtain the prediction at the edge of the river were not sufficient to obtain the complete profile of depth. The decrease in resolution and the lack of representation of specific patterns could have consequences for the assessment of the ecological suitability of a river site for specific species, whichever methodology is being considered.

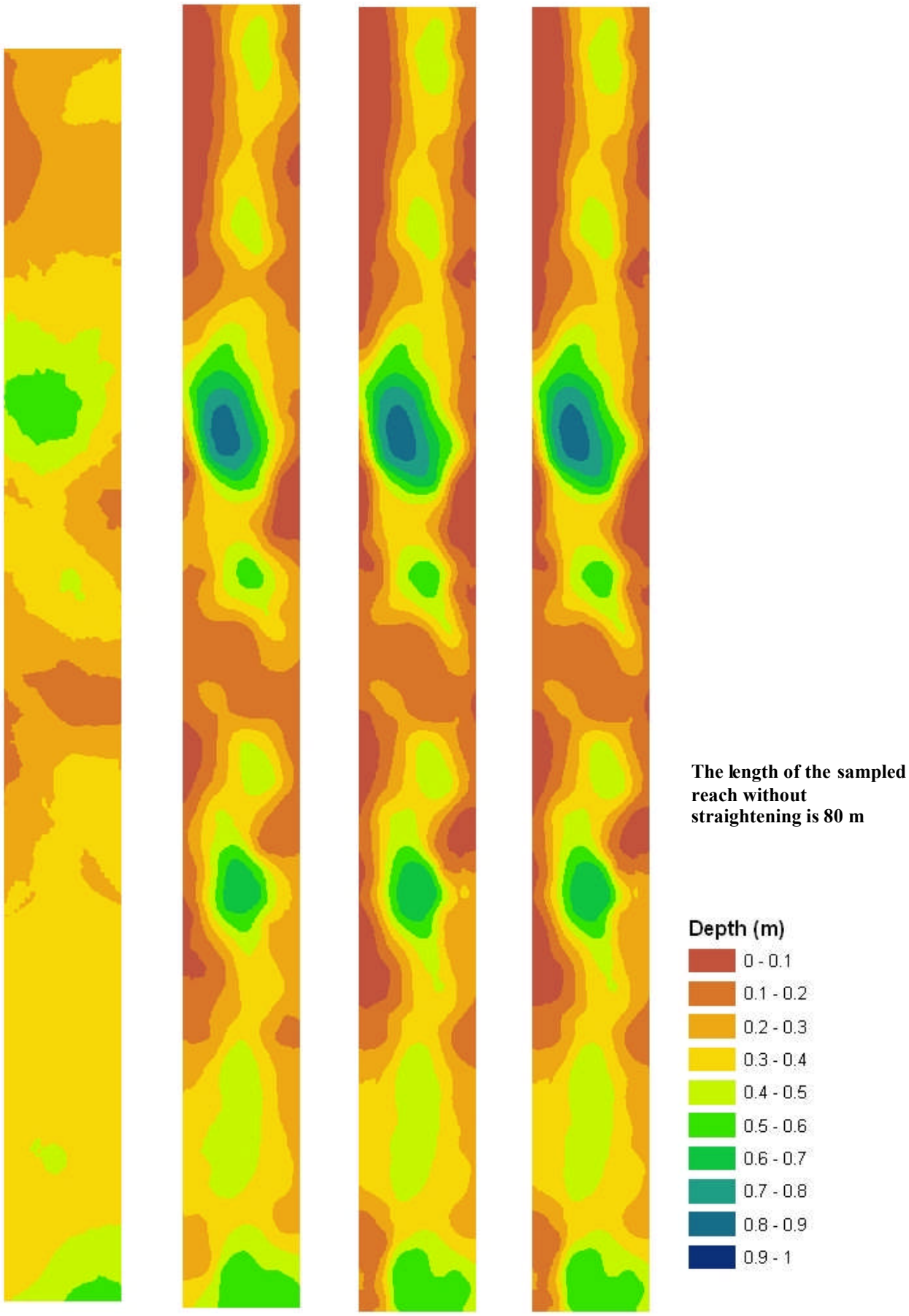

Figure 6.7: depth maps obtained for the Bere river site at four different sampling densities. From left to right: 0.2 points/m^2, 1 point/m^2, 3.8 points/m^2 and 4 points/m^2. Note the changes in depth pattern when decreasing the sampling density to the lowest value.

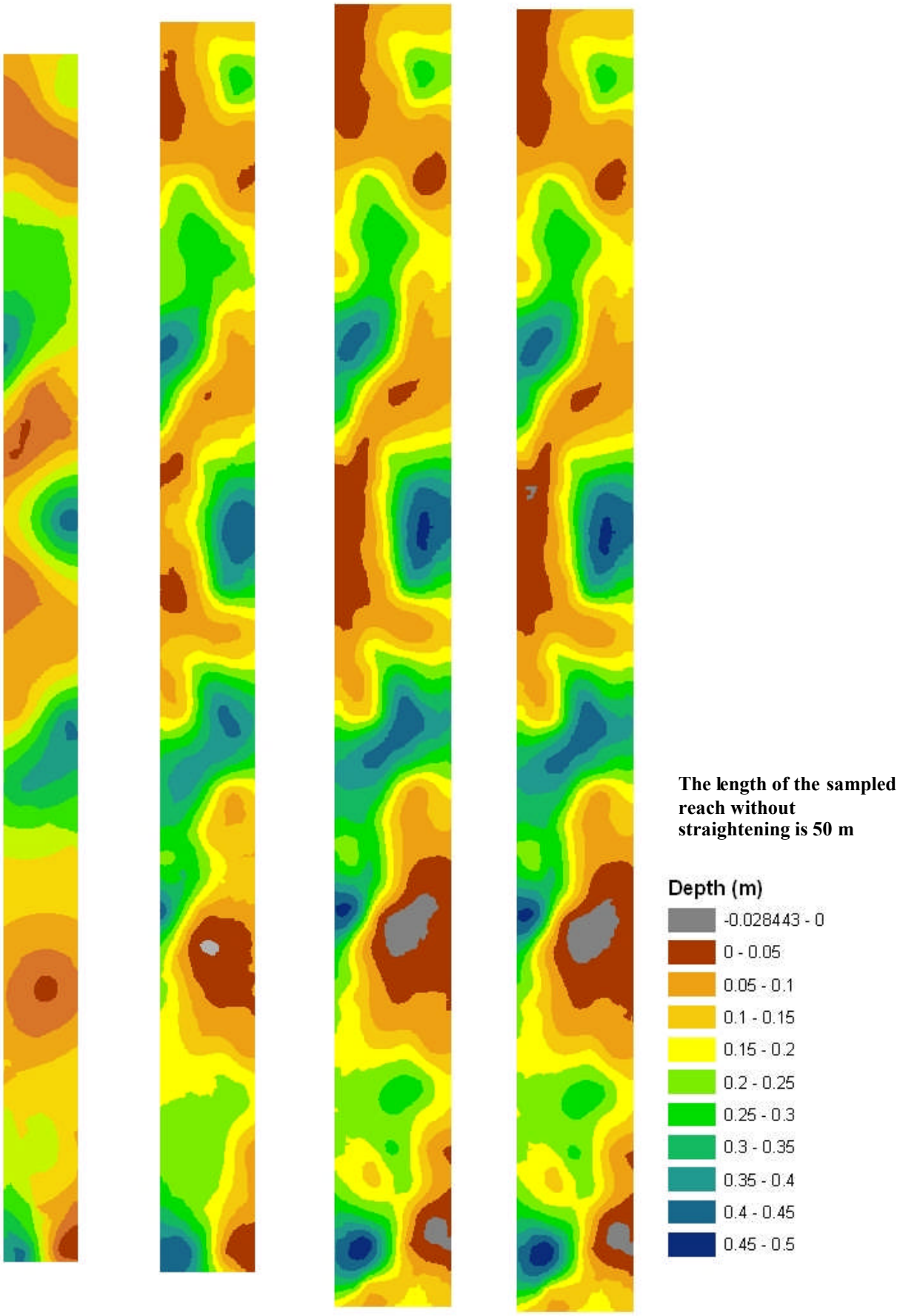

Figure 6.8: Depth maps obtained for the Highland Water river site at four different sampling densities. From left to right: 0.2 points/m^2, 1 point/m^2, 3.8 points/m^2 and 4 points/m^2. Note the changes in depth pattern when decreasing the sampling density to the lowest value.

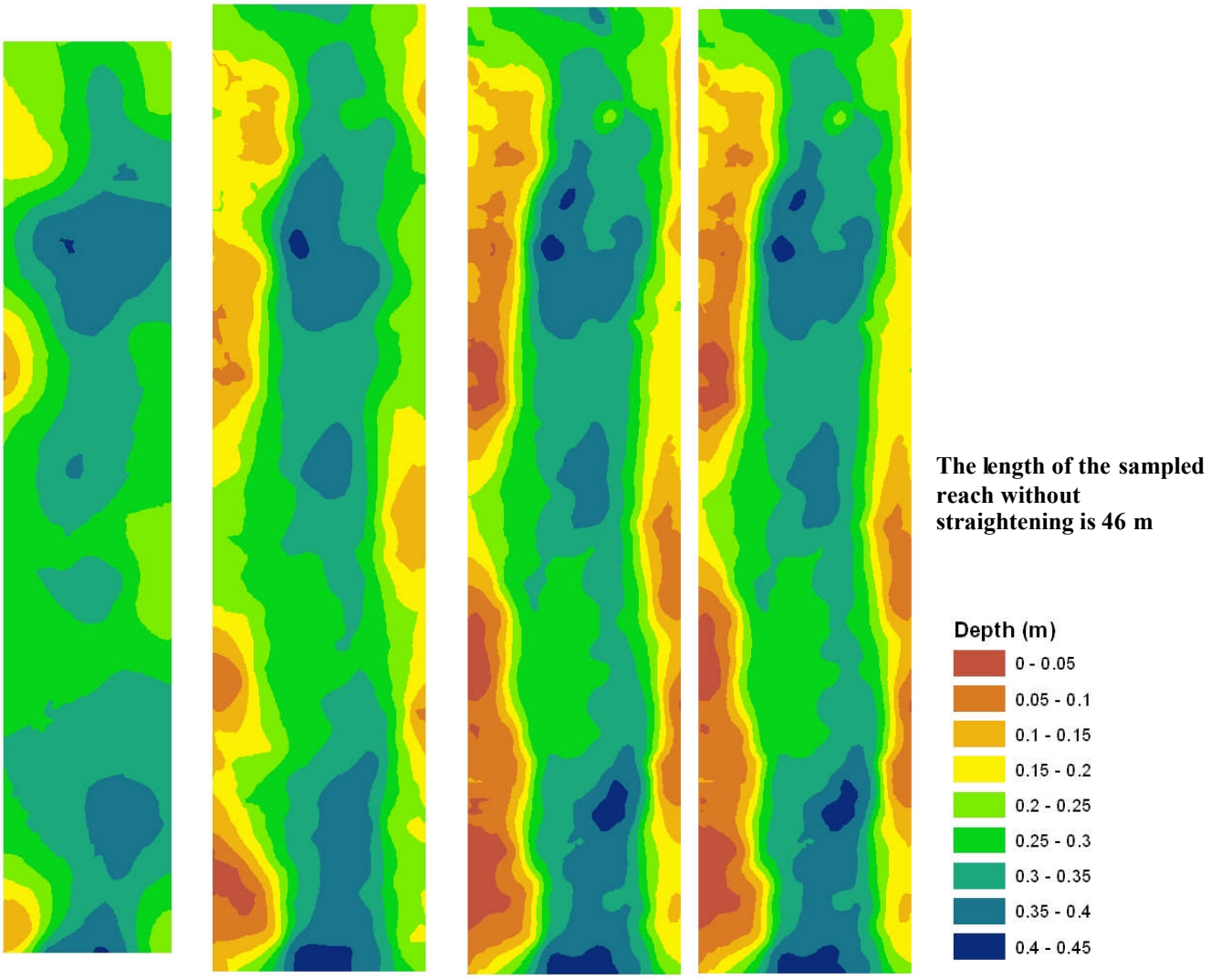

Figure 6.9: Depth maps obtained for the Lambourn river site at four different sampling densities. From left to right: 0.2 points/m^2, 1 point/m^2, 3.8 points/m^2 and 4 points/m^2. Note the changes in depth pattern when decreasing the sampling density to the lowest value.

SE maps, which were calculated for the Lambourn river site are shown in Figure 6.10. The highest values of SE were located around the edges, where the number of neighbours available to calculate the prediction was significantly smaller. The SE increased when decreasing the sampling density and it became larger in the centre of the river.

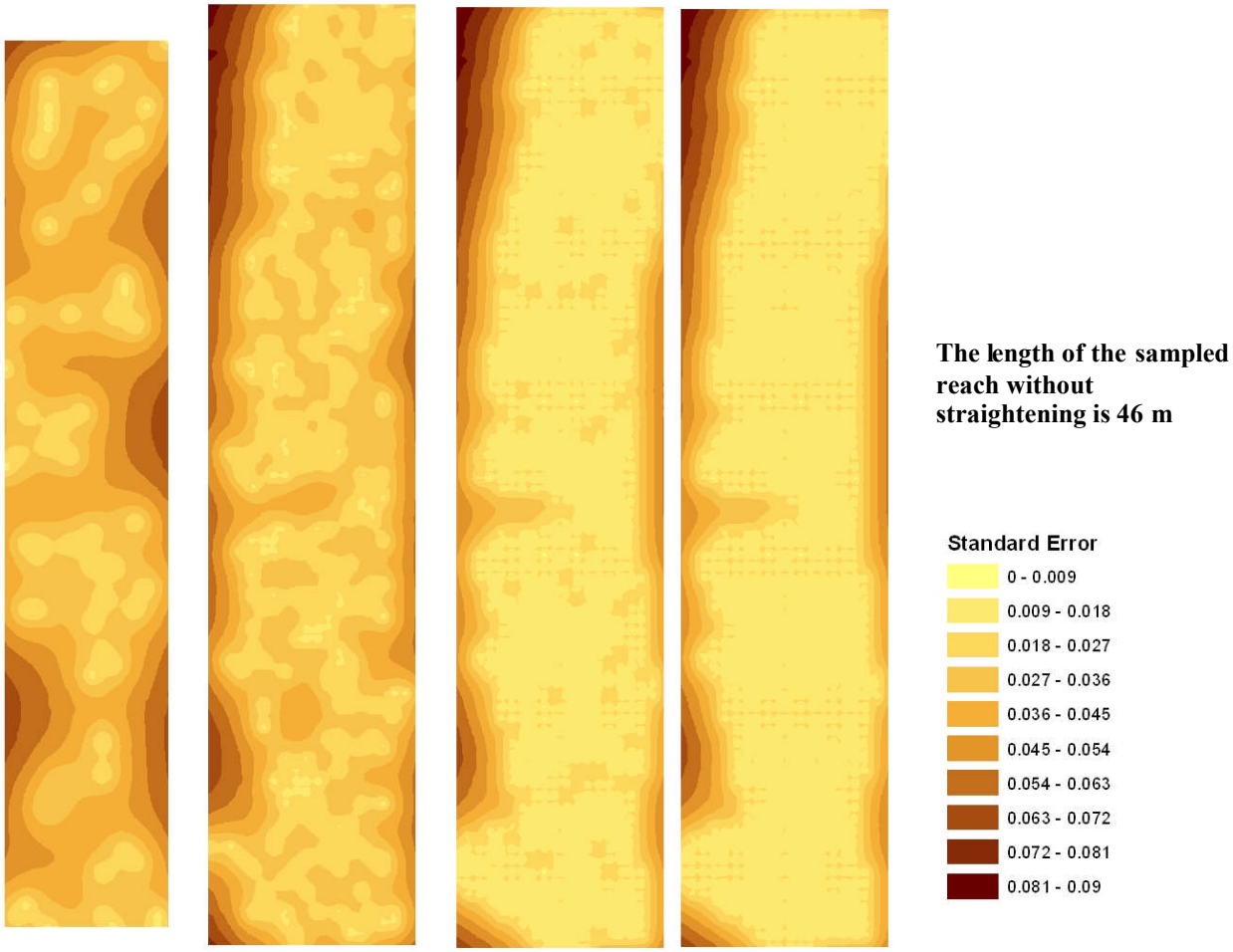

Figure 6.10: map of SE obtained for the Lambourn river site at four different sampling densities. From left to right: 0.2 points/m^2, 1 point/m^2, 3.8 points/m^2 and 4 points/m^2. Note the increase of the SE when decreasing the sampling density to the lowest value.

6.3.3. *Finding a relationship between the river descriptors and the results obtained.*

This section focus on (i) determining if the grouping criteria described in Chapter 5 can be used to identify differences in the behaviour of indicators when decreasing the sampling density and (ii) establishing the relationship between the indicators analysed and the physical characteristics described in Chapter 5. Table 6.3 shows the grouping criteria and the rivers included in each group.

Relation between the physical descriptors and the grouped river sites.

Results obtained for the Kruskal-Wallis test showed that the validation river sites selected in Chapter 5 were significantly different ($p<0.05$) to those sites that were selected as test data sets. However, these differences were encountered between validation and test data sets that were supposed to be similar (i.e. from the same group). Moreover, when comparing the validation data sets with their respective test data sets it was possible to observe that there were more similarities between the test data sets than the respective validation and test data sets. This showed that (i) the groups identified according to the general criteria (mainly based on the flow exceedance criteria) did not represent the variability encountered for the indicators, and that (ii) the grouping criteria selected was not representative for the development of a sampling methodology.

Table 6.3: groups identified according to each selected criterion described in Chapter 5. Q90 and Q80 refer to the flow exceedance at which data were collected. Codes in the catchment descriptors, reach descriptors and spatial structure columns correspond to the groups identified with multivariate techniques in Chapter 5. Finally, codes in the validation –test column show the rivers that have been used to develop the guidelines (test data sets = T) and those selected to validate these guidelines (validation = V). The number associated to the validation – test code shows the flow exceedance group that the river belongs to.

Site	Percentage of Flow Exceedance	Catchment scale	Reach Scale	Spatial structure	Validation-Test
Pang Old fenced	Q90	C1	R1	S1	T90
Pang fenced	Q90	C1	R1	S1	T90
Pang Unfenced	Q90	C1	R1	S1	T90
Lambourn	Q90	C1	R1	S1	V90
Leigh Brook	Q90	C2	R2	S1	-
Bere 2000	Q80	C1	R1	S1	V80
Pang Old fenced	Q80	C1	R1	S1	T80
Pang Unfenced	Q80	C1	R1	S1	T80
Leigh Brook	Q80	C2	R2	S1	-
Senni	Q80	C3	R2	S1	-
Highland Water	Q40	C2	R1	S1	V40
Cruick	Q40	C2	R2	S1	-
Tarf	Q40	C3	R2	S2	-
Blackwater	Q40	C2	R1	S1	T40
Tame LM	Q40	C4	R2	S3	-
Tame HM	Q0	C4	R2	S2	-
Windrush	Q0	-	R2	S2	-

For the majority of indicators analysed, the rivers included in group V80 and V90 were significantly different to those included in T80 and T90, respectively. These

indicators were: maximum depth, minimum depth, mean depth, standard deviation, maximum difference between predicted and observed values, mean difference between predicted and observed values, minimum depth predicted, sill and objective function. Moreover, there was no significant difference between groups T80, T90 and T40 for some of the indicators. This suggests that the differences between validation and test groups (e.g. T90 and V90) were higher than those encountered between different test groups (i.e. T40, T90 and T80), when it would have been expected to find the opposite result. Therefore, it could be concluded that the groups created in Chapter 5 did not identify nor explain the indicator behaviour when decreasing the sampling density. Therefore, the sampling strategies defined according to the general grouping criteria of Chapter 5 were not the best to characterise the effects of changes in sampling density on the selected indicators.

The same study was repeated for each of the individual grouping criteria considered (i.e. catchment descriptors, reach descriptors and spatial descriptors – Table 6.3) to complete the analysis. Results showed that there were not consistent differences between groups obtained for each grouping criteria (i.e. flow exceedance, catchment descriptors, reach descriptors and spatial descriptors) for some of the indicators. For example, rivers included in the flow exceedance Q80 group, were not different to those rivers included in the flow exceedance Q90 group for all the indicators analysed.

The grouping criteria that best identified the variability between the results obtained were those developed using the catchment descriptors, where a higher number of indicators had a different behaviour for each of the groups considered (the number of indicators that showed differences between the groups was as follows: 16 for the flow exceedance groups, 18 for the catchment descriptors, 13 for the reach descriptors and 13 for the spatial descriptors). The indicators that did not show significant differences between grouping criteria are shown in Table 6.4.

The Kruskal-Wallis tests carried out to determine if there were differences between results obtained for each sampling density within each group considered in Chapter 5 are summarised in Table 6.5, which shows at which sampling density each group is significantly different ($p<0.05$) to the original sampling density (4 points/ m^2). Those

indicators for which no significant difference was encountered were not included in Table 6.5. Table 6.5 summarises the results for all the grouping criteria considered.

Table 6.4: indicators that did not show significant differences between groups for the Kruskal-Wallis test (p<0.05). The codes for the indicators are as follow: MinTran=minimum depth of the data set to be interpolated, Mean Tran= mean depth of the data set to be interpolated, MaxDiff=maximum difference between predicted and observed values, MeanDiff= mean difference between predicted and observed values, MSE=Mean Squared Error, MinPred=Minimum value predicted, MeanPred= Mean value predicted, , P-value=p-value of the non parametric Kolmogorov-Smirnov test and R-squared = linear regression coefficient between predicted and observed values.

Grouping criteria	Flow Exceedance	Catchment descriptors	Reach descriptors	Spatial descriptors	Final grouping
Indicators not significantly different	MinTran MinPred Nugget	Nugget	MinPred MinTran MeanDiff P-value MSE Nugget	MinPred MinTran MeanTran MeanPred MaxDiff.	Nugget R-squared P-value

Table 6.5: sampling density (points/m^2) at which the Kruskal-Wallis test (p<0.05) starts identifying significant differences between the value of the indicator at the listed sampling density and the value obtained at sampling density 4 points/m^2. Q90 and Q80 refer to the flow exceedance at which data were collected. Codes in the catchment descriptors, reach descriptors and spatial structure columns correspond to the groups identified with multivariate techniques in Chapter 5. Finally, codes in the validation –test column show the rivers that have been used to develop the guidelines (test data sets = T) and those selected to validate these guidelines (validation = V). The number associated with the validation – test code shows the flow exceedance group that the river belongs to.

Grouping criteria	Flow Exceedance			Catchment descriptors				Reach descriptors		Spatial descriptors		Final grouping		
Code	**Q40**	**Q80**	**Q90**	**C1**	**C2**	**C3**	**C4**	**R1**	**R2**	**S1**	**S2**	**T40**	**T80**	**T90**
Maximum Difference	0.6	0.8	0.4	1	1	/	/	1.6	1.2	2	/	/	/	0.2
Minimum Difference	0.4	0.8	0.4	1	0.8	/	/	1.4	1.2	2	/	/	/	/
Maximum Squared Error	0.6	0.8	0.4	1	1	/	/	1.4	1.2	2	/	/	/	/
MSE	0.6	0.8	1	1.2	1	/	/	1.6	1.4	2	/	/	/	0.2
P-value	0.2	0.8	0.4	0.8	0.8	/	/	1.6	0.6	1.8	/	/	/	/
R-squared	0.4	0.8	1	1.2	1	/	/	1.6	1	2	/	/	/	0.2
Objective	0.2	0.8	0.4	0.8	0.4	/	/	1	1.4	1.6	0.2	/	/	/

In general, no differences were observed between consecutive values of sampling densities; the change in the value of the indicator could be visually identified (Figure 6.3 to Figure 6.6) but this difference was not statistically significant (p>0.05). However, when considering all the sampling strategies analysed, it was possible to observe that there was a statistically significant difference between sampling strategies that were not consecutive. Differences between sampling densities were not

significant for all the indicators as described in previous paragraphs. Only maximum difference, minimum difference, maximum squared error, mean squared error, p-value, R-squared and the objective function showed differences between some of the grouping criteria. Significant differences were encountered for a higher number of indicators when analysing the flow exceedance and reach physical descriptor grouping criterion. The highest sampling density at which differences started to be encountered for some of the indicators was 2 points/m^2. This suggests that special consideration needs to be placed on the value of the indicators when applying sampling densities smaller than 2 points/m^2.

Results showed that even though the sampling density at which the Kruskal-Wallis tests starts identifying significant differences differed between grouping criteria (Table 6.5), a similar pattern could be observed for all the groups considered: mean squared error and R-squared, followed by maximum squared error and maximum difference between observed and predicted values, were the indicators that were more sensitive to a decrease in sampling density and, therefore, the indicators that required a higher sampling density to be applied, if they were the objective for which data were being collected. In other words, when the objective of the data collection procedure is to decrease the error of the predicted values at specific locations in terms of MSE, maximum difference, R-squared or maximum squared error, higher sampling densities are required than when the objective is to statistically characterise the data set (e.g. to determine mean depth, minimum depth or maximum depth of the sampled reach).

Note that the Kruskal-Wallis test did not show differences between sampling densities for some of the indicators that showed a trend as the sampling density was being decreased. For these indicators it is recommended to observe the general trend (Figure 6.3 to Figure 6.6 and Appendix 4.2) and estimate what the potential results of decreasing the sampling density could be.

A table of confidence intervals was calculated for each indicator. The confidence interval was related to the sampling density to be applied, in such a way that the end user can identify the Standard Error that should be associated with each sampling density to obtain a specific level of confidence. Each confidence interval was calculated with equation 6.1:

$$CI=Z*SE \quad (6.1)$$

where,

CI is the confidence interval

Z is a function of the Level of Confidence (LOC) derived from the Normal Curve. It corresponds to the area that is under the two-tailed standard Normal distribution curve for a specific associated probability level (p-value) (e.g. for 95% CI the Z value is 1.96).

and SE is the Standard Error of the indicator that is being analysed at a specific sampling density.

Since there were no clear results on how to group the rivers according to the behaviour of the indicators at different sampling densities, a global table relating confidence interval with sampling density was created for each indicator. That is, the Confidence Interval (CI) calculated including the values obtained for a specific indicator and sampling density for all the river sites. These tables are presented in Appendix 4.3. The values shown in these tables are the CI that needs to be added to the value of the indicator obtained for a specific sampling density. Then, for data at a river site with a sampling density equal to 0.4 points/m^2, where the maximum predicted depth value is equal to 0.5 m (for example) and a 75% confidence in this "real" maximum depth is required, in this case a CI equal to 0.018 must be used (see table of maximum predicted depth in Appendix 4.3). Then, the maximum depth can be stated as 0.5 m ± 0.018 m. Note that these tables were designed in relation to the "real" situation equal to 4 points/m^2.

Confidence intervals differed in magnitude according to the indicator being analysed. For those indicators that were measured in depth units (m), which were: (i) maximum, minimum & mean depth observed, (ii) maximum, minimum & mean depth predicted, and (iii) maximum, minimum and mean difference between predicted and observed values, indicators defining maximum and minimum characteristics presented higher confidence intervals than mean indicators.

Correlation between the physical descriptors and the variogram model parameters.

A correlation matrix was calculated to analyse the relationship between the indicators and the physical descriptors listed in Chapter 5. The analysis was repeated for each sampling density tested, including all the river sites in each analysis. Pearson's coefficient was obtained and those descriptors that showed a significant correlation ($p<0.05$) with the indicators considered were identified. The correlation values that were statistically significant for the catchment and reach physical descriptors considered are summarised in Table 6.6 and Table 6.7. The interpretation of these results is presented in the following paragraphs.

Catchment Descriptors

Results for the catchment descriptors showed that just a few catchment physical descriptors (ASPBAR, DPSBAR, SPRHOST, Sord, HSorc, HSite and Qx – see Table 6.6 for explanation of these abbreviations) and indicators were correlated. Four main catchment descriptors seemed to be related to the degree of error in the predictions: mean catchment altitude, index of catchment steepness, height at the river source and height at the river site. Thus, it could be observed that, in general, the higher these physical descriptors were, the higher the error of the prediction was. In other words, the higher these values were, the smaller the correlation (Pearson's coefficient) between predicted and observed values was.

The four catchment descriptors associated with an increase in error of the predictions were associated with the steepness of the catchment where the data were collected. The degree of catchment steepness could also be expressed as the relationship between the height at the river site, the height at the river origin and the mean catchment altitude. According to the results, the steeper the catchment was, the higher the sampling density that needs to be applied. This can be explained by the fact that steeper catchments present longitudinal profiles characterised by coarser bed material and higher capacity to evacuate fine sediments. The bed channel therefore is usually composed of gravel and/or boulders, with little fine sediment. This means that the variability of depth in space is higher and, therefore, a higher number of points need to be measured to characterise depth variability with the variogram. Thus, higher sampling densities are required.

Table 6.6: catchment descriptors and indicators that proved to be significantly correlated (p<0.05). The value shown in the table is the Pearson's correlation coefficient (r).

Indicator \ Descriptor	Mean Catchment altitude (ALTBAR)	Index of catchment steepness (DPSBAR)	Standard percentage of runoff (SPRHOST)	Stream Order (Sord)	Height at river Source (HSorc)	Height at river site (HSite)	Flow exceedance (Qx)
Minimum observed depth	-	-	-	-	-	-	-.7944
Maximum difference predicted vs. observed	-	-	-	.5757	-	-	-
Minimum difference predicted vs. observed	-.8020	-.7203	-	-	-.6288	-.7380	-
Maximum Squared Error	.5780	-	.5232	.5656	-	-	-
Mean Squared Error	.9330	.7875	-	-	.7851	.8417	-
Minimum predicted value	-	-	-	-	-	-	-.7860
p-value	-.8224	-.6397	-	-	-.6825	-.6332	-
R-squared	-.8300	-.6424	-	-	-.6729	-.6479	-

Reach Descriptors.

A higher number of reach descriptors were found to be significantly correlated with the indicators than for the catchment descriptors (Table 6.7). This might indicate that the characterisation of the reach scale is more useful for the design of the sampling density (or strategy) suggesting that a field visit is necessary before detailed data are collected.

Indicators related to the quantification of error in the predicted values (i.e. maximum, minimum & mean difference between predicted and observed values and maximum & mean squared error) were correlated with the pool riffle spacing ($r \cong 0.80$), the type of substrate ($r \cong 0.50$), the depth variation of the reach ($r \cong 0.77$), the sinuosity ($r \cong 0.80$) and the maximum depth measured ($r \cong 0.70$). Indicators that defined data characteristics (e.g. maximum depth predicted) were more related to the actual characteristics of the river site (i.e. maximum, mean and depth variation). Finally, p-value and R-squared were more associated to the riffle-pool spacing.

Table 6.7: reach descriptors and indicators that proved to be significantly correlated (p<0.05). The value shown in the table is the Pearson's correlation coefficient.

Indicator \ Descriptor	Substrate	Mean Width	Depth Variation	Reach length	Sinuosity	Pool Riffle Spacing	Mean Depth	Maximum Depth
Maximum difference predicted vs. observed	-	-	-	0.53	-	0.83	-	-
Minimum difference predicted vs. observed	-	-	-	-	-	-0.84	-	-
Mean difference predicted vs. observed	0.52	-	0.77	-	0.80	-	-	0.67
Maximum Squared Error	-	-	-	-	-	0.84	-	-
Man Squared Error	-	-	-	-	-	0.84	-	-
Maximum predicted value	-	0.57	0.59	-	-	-	0.61	0.55
Mean predicted value	-	-	0.64	-	-	-	0.95	-
Standard deviation predicted values	-	0.56	0.87	-	-	-	0.80	0.77
p-value	-	-	-	-	-	-0.84	-	-
R-squared	-	-	-	-	-	-0.84	-	-

The relationship between the substrate and the error in predictions could be explained by the increase of depth variability when increasing the coarseness of the bed materials; when boulders and gravel are present, points that are separated by a small distance present higher differences in depth than two points separated by the same distance but located in a fine sediment channel. The same principle could be applied to the maximum depth and sinuosity criteria: the higher the maximum depth identified and the higher the sinuosity, the higher the error obtained. High maximum depths indicated an increase in variability of depth values; the sampling density needs to cover the whole range of depth from 0 to the maximum depth identified in order to calculate an accurate variogram. This, of course, is associated with the degree of variability of depth in space; if changes are gradual in space, smaller sampling densities are required. Sinuosity and pool-riffle spacing are the factors which control the spatial variability of this.

6.4. Discussion

This study has shown the degree of error associated to sampling density and the influence of the software package on the calculation of predicted values.

The reduction of depth sampling density results in a decrease in the accuracy of the data characterisation (e.g. mean depth) and an increase in the error of the predicted values (e.g. maximum difference between predicted and observed values). The

decrease in the sampling density affects each indicator analysed differently: some indicators show a higher variability between sampling densities than between river sites (e.g. mean squared error), whilst others show a higher variability between river sites than between sampling densities (e.g. mean depth). The general pattern shows that the accuracy of the predictions is reduced considerably when applying sampling densities with less than 2 points/m^2. Qualitative indicators decrease in accuracy for sampling densities less than 1 point/m^2, where the patterns of deep and shallow areas appear mixed, unclear and do not represent the "real situation".

Several options have been presented in this chapter in order to determine which sampling density is necessary to obtain a specific level of accuracy for a selected indicator when sampling a particular river site. These options are summarised in the following guidelines:

1. It is suggested that the characteristics of the river site that is going to be sampled are compared with the descriptions of the sites analysed in this project (Appendix 4.2) to find the river that best represents the reach that is going to be sampled. This river can be used as a reference to determine the sampling density that is required.
2. Then, it will be necessary to determine the objective for which data are being collected and the indicator (of those presented in Appendix 4.2) that best suits the final objective (e.g. calculation of the maximum depth of the river or calculation of the frequency distribution of depths).
3. Decide on the accuracy that is required for the type of study that is going to be undertaken and check how the value of the indicator changes for the reference river type when decreasing the sampling density.
4. Select the sampling density that provides a change in the indicator value that can be accepted for the purpose of the study. Obtain this information from the tables and plots provided in Appendix 4.2, the plots shown in Chapter 6 (Figure 6.3 to Figure 6.6) and the equations provided in Appendix 4.1 and Table 6.2.
5. Choose the confidence interval that is necessary for the final objective for which the data are being collected (e.g. river restoration) according to the sampling density that has been selected.

6. Calculate the value of the indicator selected and account for the confidence interval when providing the final result.
7. Alternatively, it is possible to select any of the criteria described (i.e. tables and plots in Appendix 4.2, equations in Appendix 4.1, confidence interval in Appendix 4.3., plots and equations in Chapter 6 - Figure 6.3 to Figure 6.6 and Table 6.2) to work backwards to the sampling density required or from the sampling density required to the described criteria.

When applying these guidelines several limitations need to be taken into account. The indicators, the confidence interval and the accuracy required need to be selected according to the objective for which the data are being collected (e.g. river restoration, hydromorphological assessment or quantification of habitat). However, little work has been developed in this study (i) to determine which accuracy is needed for each objective or (ii) to identify which indicator or indicators are best suited for each objective. Moreover, it is possible that there is not an adequate indicator that suits the final objective for which data are being collected. An example might be habitat quantification; it might be adequate to have information on how the volume of habitat available for fish decreases according to the sampling density. Further work could be developed in order to (i) include a higher number of indicators in the results obtained in Appendix 4.1. Appendix 4.2 and Appendix 4.3 and (ii) relate each indicator to each objective.

Results have been obtained by considering sampling density equal to 4 points/m^2 as representative of the real situation. It is necessary to take this into account when applying the proposed guidelines. Density equal to 4 points/m^2 corresponds to a distance of 0.5 m between sampled points distributed in a regular grid. Spatial variation at smaller distance has neither been considered nor characterised. Thus, information at smaller distances (e.g. sampling density equal to 5 or 6 points/m^2) has not been included in the final results. Further research will need to be developed to widen the range of sampling densities for which results have been obtained.

The guidelines have been proposed to test whether it was possible or not to develop a methodology that helped to characterise the accuracy obtained for different indicators at different sampling densities. The project has proven that it is possible to develop

the methodology, but further research needs to be carried out in order to consolidate the results obtained and to apply the methodology to a wider range of river sites. Further research projects need to account for the fact that (i) the analysis in this study has only been carried out once per sampling density and no replication has been considered and (ii) the range of river sites is limited to those available. The first limitation refers to the fact that points have been selected only once from the original regular grid of 0.5 m for 0.5 m through random selection of points. This was decided adequate as it was seen in previous chapters (Chapter 4) that multiple random selections of the points did not introduce a significant change in the indicators. Information on how the random selection process affects the variogram model parameters has been included in Appendix 4.4.

The second limitation is associated with the characteristics that define the river sites analysed. Differences in terms of morphological characteristics can be observed between the analysed river sites. This differentiation helps to classify the rivers according to their characteristics, so one of the sites can be selected as a reference when designing the sampling density of a new reach. However, these differences do not cover all the possible river types and so, situations will arise where the end user will not be able to find a river in Appendix 4.2 that matches the reach that needs to be sampled. Further research needs to be developed in order to widen the number of river types for which the methodology has been developed.

Regarding the different river types that need to be represented, it has to be noted that many river typologies have been developed over the past few decades, examples of which are described by Rosgen (1994). Three possibilities are available to solve the previous limitation: (i) to select one of these typologies and reproduce the methodology for each river type identified, (ii) to develop a summary of all the typologies and select a river corresponding to each type in each typology or (iii) create a new typology that characterises the river according to the behaviour of the indicators when decreasing the sampling density. An attempt to develop a typology that classifies the rivers according to the change of the descriptors when changing the sampling density has been described in this Chapter. Results indicated that not enough variability between river sites was encountered to define different types. This might be due to (i) a lack of adequate physical descriptors for the creation of the typology,

(ii) a restrictive statistical criteria applied when determining the differences between rivers ($p<0.05$) or (iii) a low degree of variability between river sites. It is suggested that a wider list of physical descriptors to be used and that river sites that are more representative of morphological and physical characteristics be selected. Analysis of different typologies can help to identify more indicators that could be useful for the creation of a new typology based on the change of the indicators according to changes in sampling density. This study has divided the physical descriptors into two main groups: catchment and reach descriptors. Catchment descriptors proved to be more successful when trying to classify the river sites into types. However, when analysing the indicators independently with the correlation values, reach descriptors appear to be more significant than catchment descriptors. Thus, it is suggested that analysis with more physical descriptors be developed for a wider range of river sites to determine if a suitable typology can be developed.

It is necessary to determine if it would also be possible to detect differences between river sites that show higher morphological variation in terms of physical descriptors. If this is possible, it will be useful to quantify these differences so it is possible to identify which variogram represents each river type and to use it as a target reference condition for hydromorphological characteristics.

Summarising, it is necessary to account for error when characterising depth in rivers. This chapter provides a tool to do so but the information and results presented here need to be interpreted only as guidelines and not as definitive conclusions. New results could be provided by developing or implementing a river typology so that a set of results (i.e. equations, confidence intervals, tables and plots presented in Appendix 4.1, Appendix 4.2, Appendix 4.3 and Chapter 6) can be provided for each river type

.

6.5. Conclusions

A decrease in the sampling density applied for depth data collection has consequences for the information provided by values predicted with geostatistical techniques. The lower the sampling density the higher the error obtained in the different indicators analysed. Three different tools have been developed to understand how the accuracy of each indicator changes when decreasing the sampling density. These tools are: confidence interval values, equations relating the indicator value with the sampling density and tables showing the relationship between sampling density and indicator value.

The tools provided are as simple guidelines for the selection of an adequate sampling strategy since they have been developed considering 4 points/m^2 as representative of the real situation. The three tools can be used separately, although it is preferred to combine the three of them for a more consistent result.

When determining the sampling density that is going to be applied it is necessary to identify the objective for which the data are being collected and the indicator that best defines that objective. Then, confidence intervals and accuracy levels can be selected to obtain the required sampling density. Different sampling densities need to be applied for different objectives.

A degree of error needs to be considered when calculating any of the indicators considered. This error is related to the sampling density applied as well as to the type of software selected for the prediction of depth values. The first type of error can be quantified through the application of the confidence intervals provided in this Chapter. The second source of error (from choice of software) reaches mean values of 10 cm, with maximum values that can be up to 70 cm.

Results obtained for sampling densities lower than 2 points/m^2 for quantitative indicators and 1 point/m^2 for qualitative indicators need to be carefully interpreted as these seem to be the thresholds at which the characteristics of the indicators are affected.

Further research is necessary to develop a typology that groups the river sites according to the behaviour of the indicators when changing the sampling density. The grouping criteria and physical descriptors selected in this study do not properly characterise the behaviour of the indicators. A strong relationship was encountered between reach descriptors and the variability of the indicators, which suggests that the data collection needed to define the adequate sampling strategy must be assessed in the field. More indicators, physical descriptors and river types need to be considered if the developed tools are to be applied at a more general level.

7

The Scaling Problem

This chapter focus on the scaling problem described in Chapter 2. Several classifications are available to determine spatial scales in rivers. This makes it difficult to select a specific sampling length for the analysis of the spatial structure with geostatistical techniques. The objectives of this chapter are to assess if spectral analysis is a useful tool for recognising patterns of periodicity (spatial scales) in rivers and to determine if the combination of spectral and geostatistical analysis is useful for the up-scaling of depth data.

7.1. Introduction and objectives of Chapter 7

The need to explore the spatial and temporal distribution of hydromorphological variables to facilitate scaling in data was identified in Chapter 2. Spatial scales for rivers have been defined in different studies (Rowntree & Wadeson, 1998; Thomson et al., 2001; Thomson et al., 2003; Wadeson & Rowentree, 1998; Maddock et al., 2001; Maddock & Bird, 1996; Muhar, 1996; Frissell et al., 1986; Petts & Amoros, 1996). Frisell et al (1986) considered six main system levels dependent on the spatial scale (watershed, stream, segment, reach, pool/riffle and microhabitat) and defined their spatial scale, the boundaries and the variables that should be measured at each level. The hierarchy is spatially nested; the system at one level forms the environment of its subsystems at lower levels and the spatio-temporal scales are defined through the description of variables related to geomorphic processes and forms (Frissell et al., 1986) (Table 7.1).

Petts & Amoros (1996) defined the fluvial hydrosystem approach, where the longitudinal and temporal dimensions focused on the downstream variation of flow, temperature, channel form, unidirectional fluxes of energy/material and biotic communities. The spatial-temporal scale was defined as a nested five level hierarchy of subsystems: drainage basin, functional sectors, functional sets, functional units and mesohabitats.

Maddock (Maddock, 1999; Maddock & Bird, 1996) considered a scale classification based on the proposals introduced by Frissell *et al* (1986) and Petts & Amoros (1996). The classes considered (drainage basin, type, sector, reach, site/reach and patch) are identified according to a scale defined by spatial, sensitivity and recovery characteristics. This classification can be reduced down to 3 main classes: reach or segment scale, macrohabitat/mesohabitat scale and microhabitat scale. Alternatively, Muhar (1996) modified the classification developed by Frissell (1986) and that given by Naiman *et al* (1992 in Muhar, 1996) into five classes: micro-habitat, macro-habitat, reach scale, segment scale and stream-system. Habersack (1997 in Habersack, 2000) provided a classification with five hierarchical levels according to spatial and geomorphological characteristics: regional-continental, catchment-wide, reach, local and point level.

Rowntree & Wadeson (1994, in Rowntree & Wadeson, 1998) developed a classification based on a geomorphological hierarchy. The classes identified were: catchment, zone, segment, reach, morphological units and hydraulic biotope. This approach has been considered limited by some authors (Newson and Newson, 2000 in Thomson et al., 2001) because important habitat variables (variation in substrate character, macrophytes and organic matter) are not readily taken into account. Finally, the River Styles Framework (Brierley and Fryirs, 2000 in Thomson et al., 2001) introduces the concept of ecology to previous classifications considering five different geo-ecological scales: catchment, landscape, river style, geomorphic unit and hydraulic unit. Table 7.1 summarises some of the spatial scales above described. Spatial scales were defined differently by each of the authors.

The **first objective** of chapter 7 is to assess if spectral analysis is a useful tool for recognising patterns of periodicity (spatial scales) in rivers. The **second objective** of this Chapter is to determine if a combination of spectral and geostatistical tools is useful for the up-scaling of depth pattern along the river.

Table 7.1: Hierarchical spatio-temporal classification (after Rowntree & Wadeson (1998) and Frissell et al. (1986))

System level (Frissell et al., 1986)	System level (Rowntree & Wadeson, 1998)	Lineal spatial scale (m) (Frissell et al., 1986)	Boundaries (Frissell et al., 1986)	Description (Rowntree & Wadeson, 1998)	Variables (Frissell et al., 1986)
Watershed	Catchment	>1000	Biogeoclimatic region, geology, topography, soils, climate, biota	Land surface which contributes water and sediment to any given stream network.	Biogeoclimatic region, geology, topography, soils, climate, biota
Stream	Zone	1000	Watershed class, long profile, slope, shape, network structure	Areas within the catchment which can be considered as homogeneous with respect to flood runoff and sediment production.	Watershed class, long profile, slope, shape, network structure
Segment	Segment	100	Stream class, channel floor lithology, channel floor slope, position in drainage network, valley sideslopes, potential	A length of channel along which there is no significant change in the imposed flow discharge or sediment load.	Stream class, channel floor lithology, channel floor slope, position in drainage network, valley sideslopes, potential
Reach	Reach	10	Segment class, bedrock relief, slope, morphogenic structure or process, channel pattern, local sideslopes floodplain, bank composition, riparian vegetation state.	A length of channel within which the constraints on channel form are uniform so that a characteristic assemblage of channel forms or morphological units occur; respective sequences of reaches of alternating characteristics may be grouped into macroreaches.	Segment class, bedrock relief, slope. Morphogenic structure or process, channel pattern, local sideslopes floodplain, bank composition, riparian vegetation state.
Pool/riffle	Morphological unit	1	Reach class, bed topography, water surface slope, morphogenic structure or process, substrates, bank configuration	The basic structures recognised by fluvial geomorphologists as comprising the channel morphology, formed from the erosion of bedrock (rapids, waterfalls, plunge pools, etc…) or from the deposition of alluvium (sand or gravel bars, riffles, pools…)	Reach class, bed topography, water surface slope, morphogenic structure or process, substrates, bank configuration
Microhabitat	Hydraulic biotope	0.1	Pool/riffle class, underlying substrate, overlying substrate, water depth, velocity, overhanging cover.	Spatially distinct instream flow environments determined by the temporally variable hydraulic and substrate characteristics associated with each morphological unit.	Underlaying substrate, overlying substrate, water depth, velocity, overhanging cover.

7.2. Methodology

7.2.1. *The river sites and the collected data set*

Two river sites were analysed for the scope of this Chapter; the Brazos and the Sulphur. The data set for the Brazos site included 37288 topographical data points collected along a 7.5 km reach. Maximum depth at the Brazos site is equal to 12.95 m, with a mean depth of 2.57 m and a variance equal to 1.83. Mean width is equal to 100 m which provides a depth-width ratio of 0.025. The sinuosity index is equal to 3.2.

The Sulphur data set had 8490 topographical data points collected along a 1.5 km reach. The maximum and mean depth at the Sulphur site is equal to 22.8 m and 12.86 m, respectively, with a variance equal to 22.13. Mean width is equal to 35 m, which provides width – depth ratio equal to 0.36. The sinuosity index is equal to 1.81.

Data were collected using a single beam depth sounder for both river sites. A more detailed description of both river sites is provided in Appendix 1.

7.2.2. *Detecting spatial scales*

i) De-trending the data sets

The data needed to be formatted before further analysis. The raw topographical data referred to the distance from a base horizontal line to the topographical (TO) point measured (Figure 7.1). Depth had to be calculated for all the measured points by considering the slope factor and the Water Surface Level (WSL).

The slope factor was taken into account by applying Equation 7.1 and Equation 7.2 where: TO is the raw topographical value, WSL is the Water Surface Level, DEPTH is the river depth at the measured TO point, LENGTH is the sampled length, SLOPE is the slope of the sampled length according to the measured water surface level, TO_1 is the de-trended TO value and N is the maximum TO_1 value recorded. WSL was calculated from the analysis of all the points located at the bank edges, where WSL was considered 0. WSL points where interpolated along the surface and depth

predicted at each TO point. WSL was assumed to be at the point were the single beam depth sounder was located.

$$TO_1 = (TO + LENGTH * SLOPE) \quad (7.1)$$

$$DEPTH = N - TO_1 \quad (7.2)$$

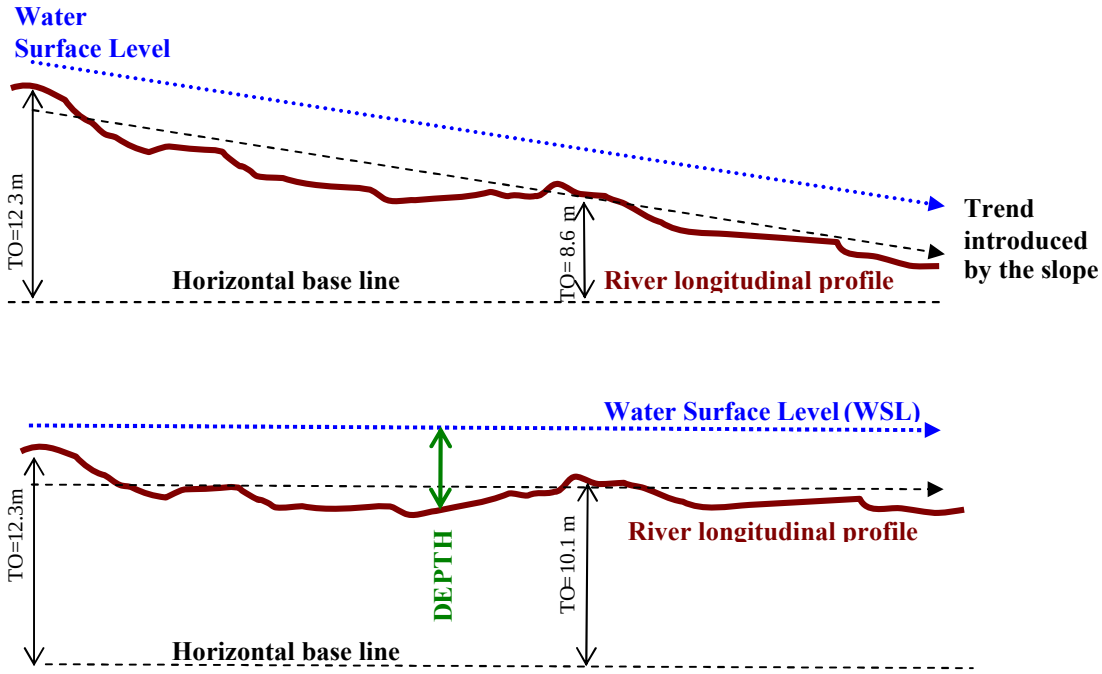

Figure 7.1: data transformation procedure to obtain depth at the Brazos and Sulphur river sites. The upper image shows the original data provided, the slope factor a longitudinal profile and the water surface level. The lower image shows the same information after transforming the TO data to Depth data.

ii) Sensitivity Analysis for the Variogram

The sensitivity analysis described in Chapter 5 was applied to the Brazos and Sulphur data sets. The objectives of the analysis were to (i) study the anisotropy level, (ii) determine the lag distance for the variogram calculation and (iii) define the maximum distance to be used in the variogram calculation. Sensitivity analysis for the azimuth tolerance was considered unnecessary according to the results obtained in Chapter 5. Seven lag distances (0.1 m, 0.3 m, 0.5 m, 0.7 m, 0.9 m, 1.5 m and 2 m) and four azimuth directions (0, 45, 90 and 135) were compared. The variogram was calculated for several maximum distances ranging from 20 m to the maximum sampled length of each river site with increments of 50 m.

iii) Spectral Analysis

Spectral analysis is used to recognise cyclical pattern of series of data by applying a modification of Fourier analysis {Chatfield, 1996}, which is based on approximating a function by a sum of sine and cosine terms, called the Fourier series representation. The periodogram, which is the output result of the spectral analysis, provides information on the pattern of the variation of the data set in the spectral domain {Webster & Oliver, 2001}. The spectrum and the variogram are complementary ways of viewing the spatial/temporal periodicity and estimating the period.

The calculation of the periodogram requires input values equally spaced and distributed along a longitudinal line. Since data collected did not meet these requirements, the variogram was calculated to predict depth values at the appropriate locations. The spherical model was used for this purpose, with a lag distance equal to 1.5 m, azimuth tolerance of 60 and maximum distance equal to 150 m. Depth values were predicted at three longitudinal profiles at each river site separated by 5 m intervals for the Sulphur and 10 m for the Brazos site. Points were predicted every 20 m along each longitudinal profile. Periodic cycles at distances smaller than 20 m were not considered within the scope of this study.

The Brazos river site was divided into reaches of 2000 m in length so that similar lengths were analysed for the Sulphur and Brazos river sites. Three different reaches, with three different longitudinal profiles, were analysed for the Brazos site.

7.2.3. *Comparison of sampled reach length*

The total length of the surveyed river was divided into equally spaced segments. Data included in the defined segments were consecutively classified into two groups: (i) a training data set and (ii) a test data set. The training data was used to calculate the variogram whilst the test data was used to validate the predictions obtained for the calculated variogram.

Accuracy obtained for the predicted values was assessed through the analysis of quantitative indicators, which were: variogram assessment, descriptive statistics, mean

squared error and mean error, frequency distribution and regression analysis. These indicators were described in detail in Chapter 5.

7.3. Results

7.3.1. Detecting spatial periodicity

i) De-trending the data sets

The slope factors obtained for the Sulphur and Brazos river sites were 0.0029 and 0.00012 respectively. The trend factor, which is defined by the slope, is smaller than 20% of the variance encountered for the depth data sets at both river sites. This indicated that the trend would not significantly affect the variogram results and therefore, it did not need to be taken into account. However, since spectral analysis was going to be carried out data were de-trended.

The descriptive statistics obtained for each river site after de-trending the raw data are presented in Table 7.2. The Sulphur river presents a deeper and narrower channel bed than the Brazos river site. The Kolmogorov-Smirnov test indicated that depth for both river sites did not follow a normal distribution but the skew and kurtosis were less than 1. Thus, data could be assumed to be normal for the purposes of this analysis.

Table 7.2: descriptive statistics obtained after de-trending the raw data set.

River Site	1st Qu	Median	Mean	3rd Qu.	Max	St Dev	Num. Points	Length	Width
Sulphur	8.47	11.43	11.92	15.43	25.98	4.84	8490	1395	36
Brazos	1.62	2.54	2.57	3.35	12.95	1.35	37288	7828	150

ii) Sensitivity Analysis for the Variogram

The minimum distance between pairs of points encountered for the Sulphur and Brazos sites were 0.75 m and 0.065 m, respectively. The variogram was not analysed for lag distances smaller than the minimum lag distances encountered since no information was available for the variogram calculation at such lag intervals.

Results indicated that for both river sites, a lag step size of 1.5 m offered a suitable balance between the number of pairs of points obtained for the variogram calculation

and the number of lags considered. Thus, the variogram was calculated with a lag step size equal to 1.5 m. The anisotropy analysis showed that no directional difference in the spatial pattern could be identified for the Brazos site and that only direction 135° presented differences to the others for the Sulphur site (Figure 7.2). This anisotropy started at intervals higher than 27 m, which coincided with the decrease in the number of pairs of points included in the calculation. The longitudinal direction was used for the variogram calculation of both river sites.

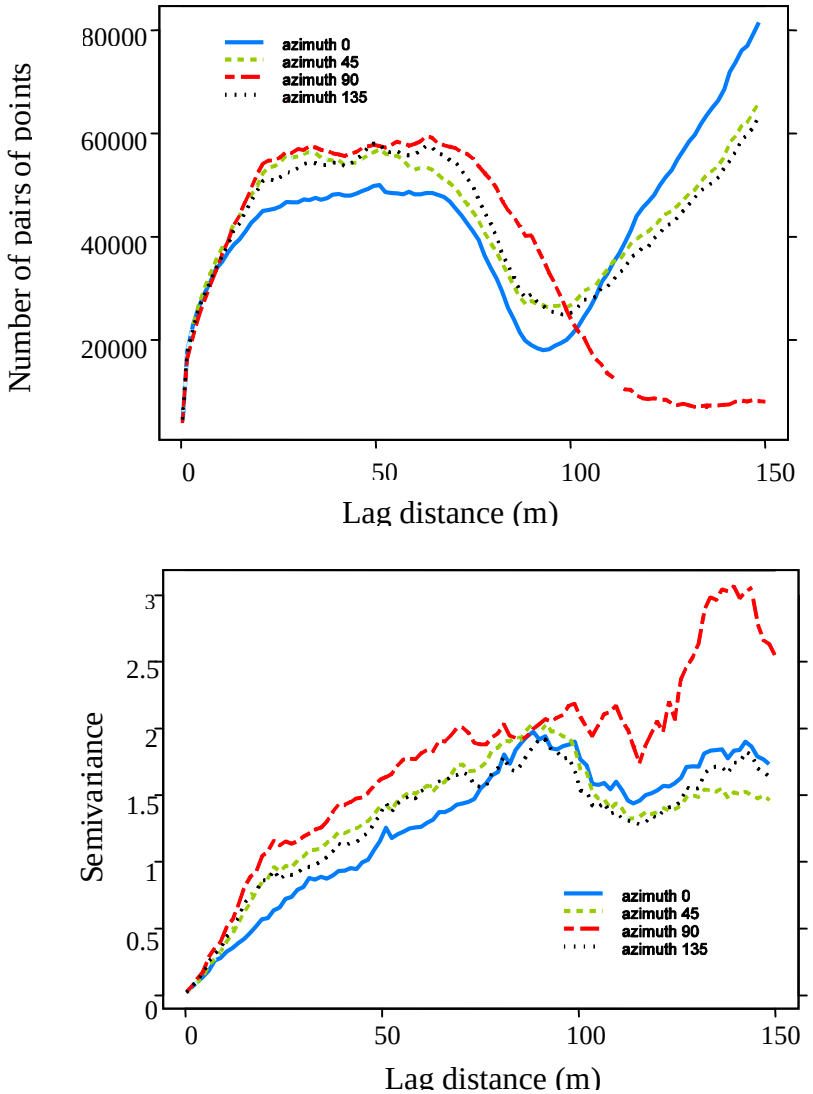

Figure 7.2: results for the anisotropy analysis for the Brazos site. The top plot shows the number of pairs of points obtained for each lag distance and the bottom plot shows the experimental variogram obtained for four different directions (0°,45°, 90° and 135°, 0 being the longitudinal direction)

The number of pairs of points available for the variogram calculation decreased for lag intervals equal to 90 m and 27 m for the Brazos and Sulphur sites, respectively. The number of points collected was high and thus, the number of pairs of points available for the variogram calculation remained significantly high (>2000) for intervals close to the total length sampled (≅80% sampled length). The resulting experimental variograms calculated for the total sampled distance are shown in Figure 7.3.

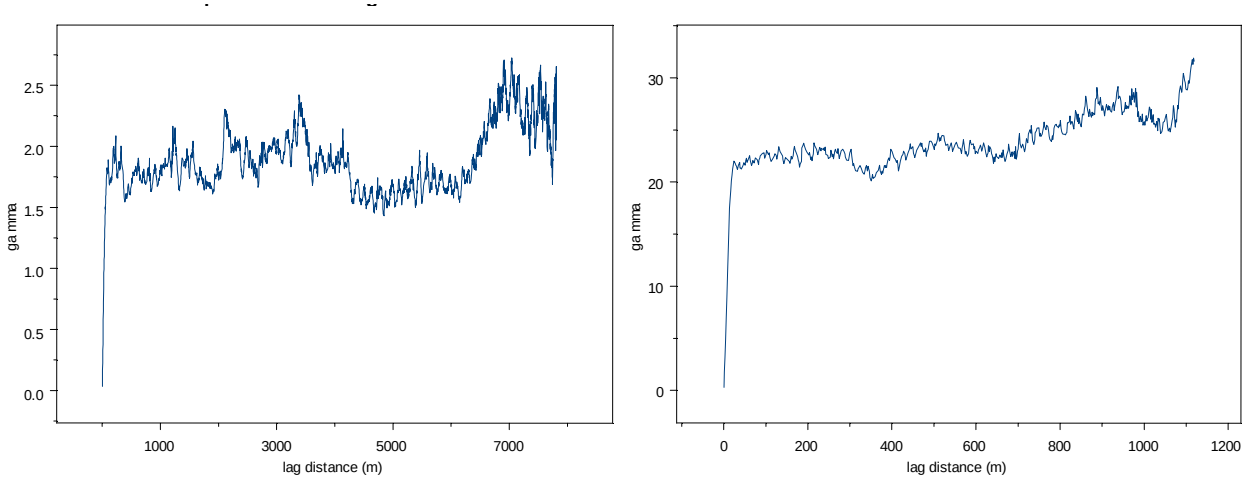

Figure 7.3: experimental variogram calculated for the Brazos (left) and the Sulphur (right) river sites. Note that the maximum distance for which the variogram has been calculated is different for each river site.

The experimental variogram obtained showed the difference in spatial pattern encountered between both river sites. The Sulphur river presented a higher value of variance (gamma) over a smaller range of distance than the Brazos river. This supported the results obtained with the descriptive statistics presented in Table 7.2. It was also possible to identify a sinusoidal pattern in both experimental variograms which suggested a repetition of the spatial characteristics. The variograms presented a monotonic increase in variance with increasing lag distance and fluctuated periodically.

The values of range, sill and nugget obtained for the maximum distances analysed showed that there were irregularities in the results obtained for some of the maximum distances considered (Figure 7.4). The irregularities encountered occur for maximum distances associated with a decreasing number of pairs of points. The range values

obtained for maximum distances of analysis from 50 m to 600 m (Figure 7.4) showed a more stable pattern than thase obtained for higher distances. A maximum distance of 150 m provided a good compromise between (i) the distance represented by the variogram and (ii) the number of pairs of points obtained for the calculations. Table 7.3 shows the number of pairs of points and the variogram values obtained for a maximum distance equal to (i) 150 m and (ii) the distance at which the maximum number of points was encountered.

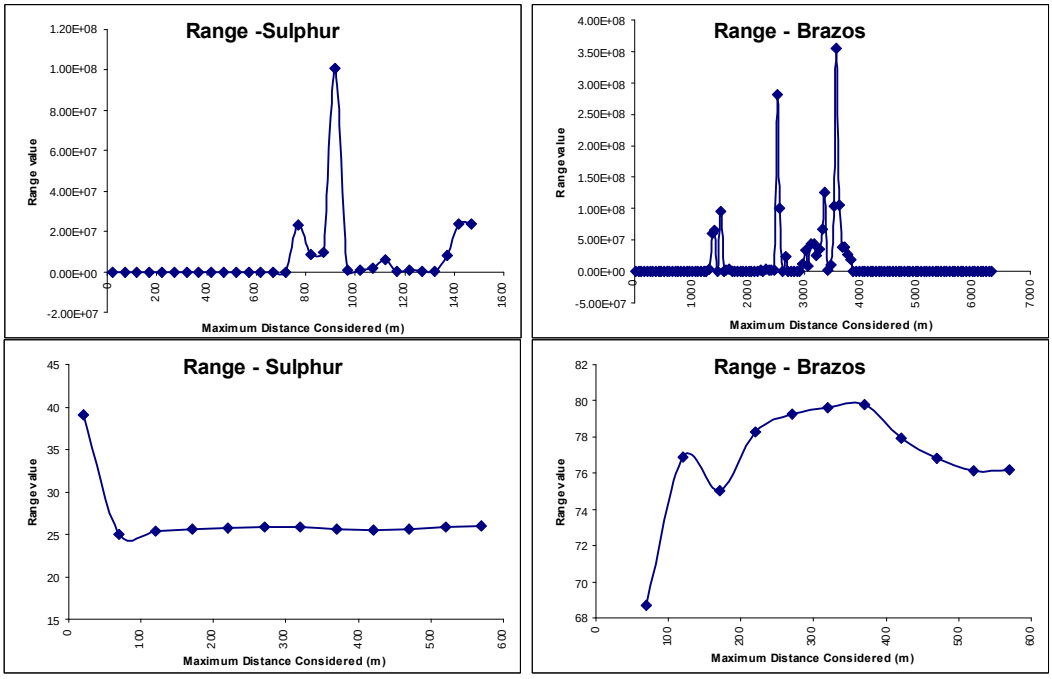

Figure 7.4: results obtained for the range when calculating the variogram for different maximum distances. The lower images are a detail of the values represented in the upper images.

Table 7.3: range, sill Nugget and Number of Pairs of Points obtained for the variogram calculated at two different distances; the distances at which the maximum number of pairs of points is encountered and the reference distance (150 m)

River Site	Range	Sill	Nugget	NPP	Distance
Sulphur	25.52	22.2	0	70494	150
Sulphur	39.13	32.19	0	87012	26
Brazos	75.23	1.73	0.016	292644	150
Brazos	68.69	1.63	0.013	371073	89

iii) Spectral Analysis

The periodogram, which is a measure of smoothness of the periodogram function, was computed for several bandwidths (i.e. 1, 10, 20, and 50). The higher the bandwidth, the less detail was provided by the periodogram (Figure 7.5). Bandwidth 1 represents the raw periodogram, without smoothing. The bandwidth needs to be narrower than the features that one wishes to reveal (Webster & Oliver, 2001). Choosing bandwidths of 10 seemed to show the principal features of the periodogram most clearly whilst the information provided by the raw periodogram was too detailed. The estimated periodogram was judged rather too smooth when using bandwidths above 20.

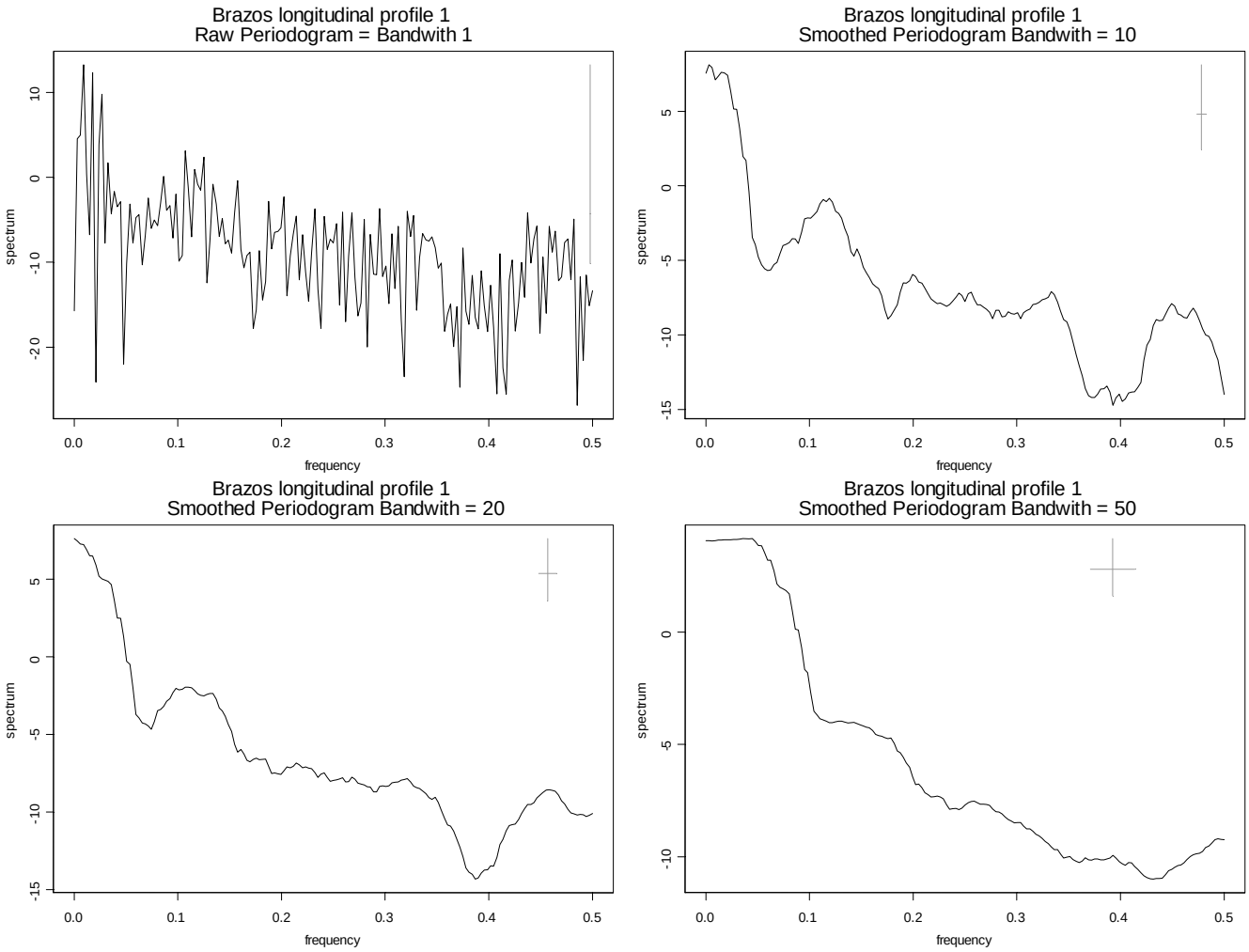

Figure 7.5: example of periodograms obtained for different bandwidths (1, 10, 20 and 50). The higher the bandwidth, the less detail is provided by the periodogram.

Peaks in the periodogram were identified from sampled lengths of 20 m up to the total sampled length. Figure 7.6 summarises the frequencies at which the peaks where identified, the corresponding wavelength (number of sampling intervals) and the extension of the cycle in terms of sampled river length for one of the longitudinal profiles analysed for the Sulphur site. Since the variograms were calculated for lag distances equal to 20 m and the periodograms were calculated with the variogram results, the sampling interval of the periodogram corresponds to 20 m. Frequency was transformed into sampled length through Equation 7.3, where L is the length of the cycle (m) and F is the frequency.

$$L = (1/F) * 20 \quad (7.3)$$

Thus, a peak identified at 0.014 cycles for the Sulphur river, corresponds to a wavelength of 71.42 sampling intervals or 1428 m, each sampling interval being 20 m. Each peak identified corresponds to the wavelength of a cycle of the spatial pattern defined by the variogram. The area under the spectrum curve represents the total variance of the observations from their mean value (Nielsen & Wendroth, 2003).

Results indicated that it was possible to recognise specific spatial occurrences for the longitudinal profiles analysed but that these occurrences were not common to both river sites. For the Brazos site, depth seemed to follow a pattern of repetition every 750 m, 500 m, 170 m and 110 m. Cycles of repetition could also be observed at smaller scales but they were not consistent between the analysed longitudinal profiles. For the Sulphur river site it was possible to identify common patterns of repetition of depth at 350 m, 87 m and 60 m.

The total length sampled for both river sites was divided into reaches of equal length. The spatial occurrences identified by the spectral analysis were used for this purpose. The pattern of repetition identified in the Brazos site at 750 m was not considered since it only allowed the creation of two reaches for the Sulphur river site.

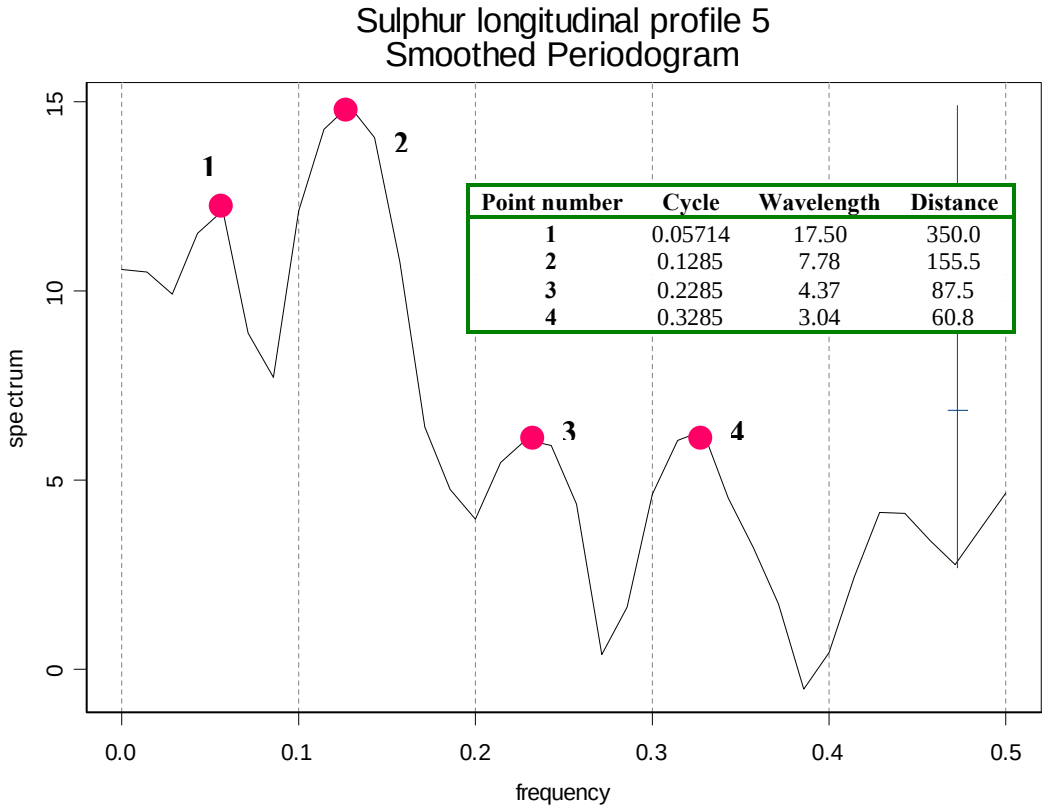

Figure 7.6: periodogram obtained for one of the longitudinal profiles analysed in the Sulphur river site. Values on the table show the cycle, wavelength and distance at which each peak has been identified.

7.3.2. Comparison of sampling reach length

The range, sill, nugget and objective function values were obtained for each training data set and compared with those obtained for the original data set (maximum distance = 150 m, lag distance = 1.5 m, azimuth tolerance = 60 and azimuth = longitudinal direction). The number of points and the variogram values obtained are shown in Table 7.4.

Results showed that for the Brazos river site reaches of 60 m, 87 m and 500 m length provided the best fits for the variogram functions, as indicated by the objective function value (Table 7.4). Thus, values of range, sill and nugget were closer to those obtained for the reference variogram. Similar results were obtained for the Sulphur river site (except for the 87 m reach length), where reaches of 350 m also presented a relatively good fit of the variogram function. For both river sites intermediate reaches of 110 m and 170 m provided irregularities in the modelling of the variogram function

(Figure 7.7). This may be explained by the fact that small distances (i.e. 60 m) allowed the division of the reach length into many equally spaced reaches, which provided a high number of pairs of points for all the lag distances of the variogram. Thus, the variogram can be calculated with more accuracy. Figure 7.7 shows the disturbances caused to the variogram when considering 60 m and 110 m length reaches for the Sulphur river site. The peak observed was present in all the variograms obtained for the Sulphur river site and it was always located at the lag distance that corresponds to the reach length. Similar results were encountered for the Brazos river site.

Table 7.4: range, sill and nugget values obtained for the variograms calculated for each of the spatial scales identified.

River	Reach length (m)	Range	Sill	Nugget	Objective
Sulphur	60	31.88	9.12	0	31928.4
	87	102.47	6.98	1.16	47155.7
	110	208.17	5.08	2.16	44709.3
	170	75317648	1064486	2.56	69083.3
	350	20.78	7.64	0	12652.9
	500	19.97	2.65	0.37	10391.8
	Reference – 150 m	**25.52**	**22.2**	**0**	**6966.2**
Brazos	60	90.74	1.27	0.017	31020.7
	87	99.09	1.69	0.028	25341.8
	110	2378321	10576.3	0	171029
	170	2163754	16240.1	0	55897.0
	350	175.21	0.62	0	64535.6
	500	89.65	1.12	0.007	29308.7
	Reference – 150 m	**75.23**	**1.73**	**0.016**	**24742.1**

Predictions of depth for the test data sets were not calculated since the statistical packages used (Genstat and SPlus) were not able to apply kriging to the training data sets. For example, the resulting SPLUS output indicated that the covariance matrix was not positive defined while calling subroutine ssukrige. This indicated that not enough neighbours were available for the prediction of depth values at non measured locations. The sampled reaches were separated from each other a longer distance than the variogram range value, the point at which the spatial correlation is lost. Thus, predictions could not be calculated.

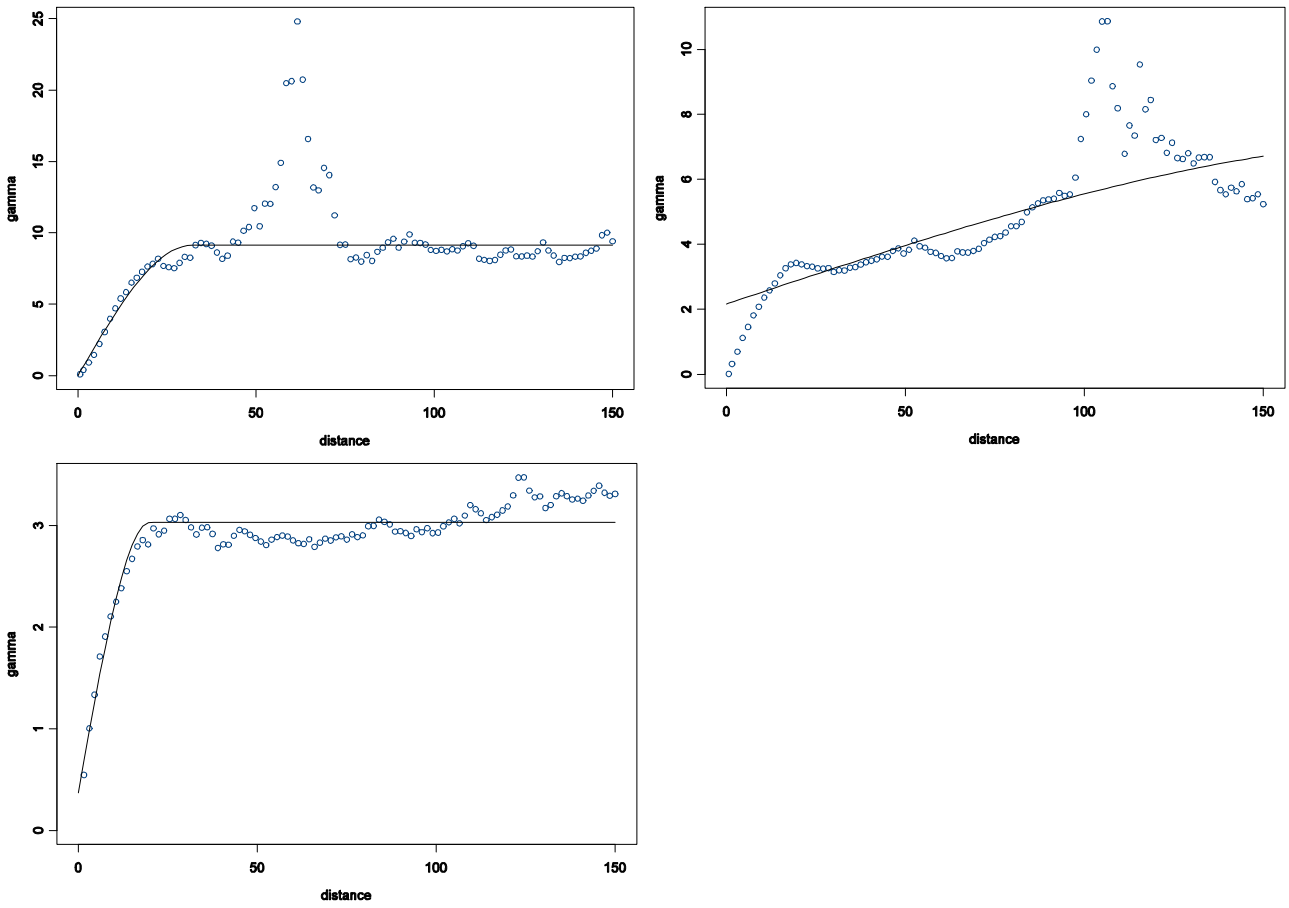

Figure 7.7: spherical variograms obtained for the training data sets of sampling distances 60 m (top left), 110 m (top right) and 500 m (bottom).

Different results were obtained when using the geostatistical extension of ArcGIS 9. Even though small differences were encountered between the range values fitted with ArcGIS and the other software used, ArcGIS was able to predict depth values for the test data sets by adjusting the area of the neighbourhood. This increased the number of data points, creating a positive definite covariance matrix. However, there remained the problem of lack of spatial correlation that was reflected as a high value for the error estimated at that point. This means that even though (i) the spatial correlation was lost at this point and (ii) the variance between pairs of points was constant, the neighbours selected were different at each new calculation of the depth value. Thus, it was still possible to observe some degree of variation in the predicted depth values where a constant value of depth should be expected. As stated by (Burrough & McDonnell, 1998), "the range of the variogram provides clear information about the size of the search window that should be used. If the distance from the data point to an unsampled point exceeds the range, then it is too far away to make any contribution; if all data points are further away than the range, the best estimate is the general mean".

Stochastic imaging (conditional simulation) helps to solve the problem (Journel 1996 in Burrough and McDonnell, 1998, Gomez Hernandez and Journel, 1992 in Burrough and McDonnell, 1998 and Deutsch and Journel, 1992 in Burrough and McDonnell, 1998). It combines the data at the observation points with the information from the variogram to compute the most likely outcomes as a function of the variogram parameters.

Results obtained with ArcGIS were not analysed since it was impossible to determine (or control) the methodology used within ArcGIS. Further studies are needed to investigate and compare the methodologies in ArcGIS with other statistical software packages.

7.4. Discussion and Conclusions

Application of spectral analysis allowed the detection of cyclical patterns in the longitudinal spatial dimension at both river sites. The spatial lengths (scales) defined by each cyclic pattern differ between river sites. This suggests that spatial scales might not correspond to a fixed sampling distance and that they need to be defined according to the characteristics of each river site.

The spatial scales identified for the Brazos and Sulphur river site with the spectral analysis did not correspond to those identified with geostatistics. However, the cyclic patterns corresponding to distances equal to 500 m coincide with the sampling distance proposed for some methodologies, such as River Habitat Survey. This indicates that the selection of reaches of 500 m could well be justified from a statistical point of view. Note also that in previous studies, Ian Maddock (personal comment) identified that the necessary distance to characterise the mesohabitats of a river site was between 50 m and 100 m. The cyclic patterns identified every 60 m and 110 m correspond to the distances that Maddock identified as adequate for the characterisation of habitat features.

Reaches equal to 60 m, 350 m and 500 m define variograms that better simulate obtained with the original data sets. This suggests that these distances were more adequate for the characterisation of depth spatial pattern at the Brazos and Sulphur

river site. To determine whether these distances could be associated with a repetition of patterns of hydromorphological features (e.g. mesohabitat and flow types), it was suggested that the study be repeated and results compared with aerial photographs taken during the data collection procedure.

Lack of information between measured reaches (i.e. non measured reaches that separate two consecutive measured reaches) have a consequence on the variogram calculation; variance values calculated for lag distances around the reach length break the continuity of the variogram model, providing extremely high values of variance. This is due to a decrease of the number of pairs of points available for these distance intervals.

Geostatistics is not a suitable tool for the up-scaling of depth data (pattern) in rivers since the spatial correlation of this parameter is lost at short lag distances (less than 80 m). In Chapter 5 it was concluded that there was a limitation regarding the sampled length, which was less than 250 m for all the river sites. There was a possibility that the spatial correlation between pairs of points was lost at higher distances than that encountered but was not identified by the variogram due to the shortness of the sampled reach. The lengths sampled at the Brazos and Sulphur river sites were long enough to mitigate this problem. The spatial correlation for depth is lost for distances smaller than 80 m, which determines the up-scaling distance for which predictions can be obtained. The possibility of obtaining predictions for higher distances is available in software packages like ArcGIS, where the neighbourhood area can be adapted to the requirements and conditional simulations can be implemented. Further research projects need to be developed in order to compare and determine the differences between predictions obtained with different software packages.

Finally, it is suggested that further research be developed which concentrates on developing a sinusoidal variogram function that models the spatial variance of the data collected. This will provide higher accuracy for the predictions and a characterisation of the spatial pattern for distances higher than the range determined by the spherical model, allowing the up-scaling processes to be implemented for larger distances.

8

The temporal problem

Temporal changes in rivers conditions affect results from monitoring of hydromorphological variables. To develop effective and efficient monitoring programmes it is necessary to understand how the hydromorphological features change over time. Little work has been developed on hydraulic functioning of hydromorphological features. This chapter focuses on the study of changes in hydromorphological parameters associated with changes in discharge. The chapter aims to determine which mesohabitat and flow types are more sensitive to discharge change and whether the monitoring of mesohabitat types are more relevant than flow types for this purpose. The chapter also investigates the suitability of the variogram for quantification of temporal changes in hydromorphology

8.1. Introduction and objectives of Chapter 8

Hydromorphological variables may change in time as well as space. Temporal changes can be caused by changes in discharge, changes in the sediment regime or vegetation changes. There is a need to determine which areas of a river are more sensitive to changes in discharge so that monitoring programmes can be designed efficiently. The **first objective** of this study is to identify which mesohabitat types and flow types better characterise hydromorphological changes due to variations in flow. The **second objective** is to determine if mesohabitat types are better than flow types for assessing hydromorphological changes associated to changes in discharge and the **third objective** is to determine if the variogram is able to identify temporal changes in depth due to changes in discharge.

8.2. The river sites and the data collected at each site

The Leigh Brook and the Windrush river sites were analysed (i) to determine changes in hydromorphological parameters due to discharge variation and (ii) to study the

relationship between these changes and mesohabitat and flow types. The analysis of the variogram at different discharges was carried out for the Cruick, Lambourn, Leigh Brook, Bere, PangOld Fenced, Senni, Blackwater, Highland Water, Tame Highly Modified, Tame Less Modified, Pang Fenced, Pang Unfenced, Windrush and Tarf. A complete description of these river sites is presented in Appendix 1. Details of the data collected and analysed are provided in the following sections.

8.3. Methodology

8.3.1. Hydromorphological changes due to variations in discharge for the Leigh Brook site.

Depth, substrate, velocity, mesohabitat and flow types were measured at the Leigh Brook river site for two different discharges: $Q_1 = 0.52\ m^3s^{-1}$ and $Q_2 = 0.34\ m^3s^{-1}$. A total of 2583 points were selected from the original data set for this analysis. The analysis of those points that dried out when decreasing the discharge was developed separately. The variables included in the analysis were defined by the rate of change encountered between the two discharges and were: mesohabitat change, depth change, velocity change, flow change and Froude number change (Table 8.1). Depth, velocity, Froude number and flow type were measured at each single point. Mesohabitat was determined for each cross-section by analysing the dominant mesohabitat type. Cross-sections were separated 1 m in the downstream direction. Points across each cross-section were collected at 0.5 m intervals.

Table 8.1: parameters identifying change that were included in the data analysis of Chapter 8. Note that the categories for the flow type change were quantified according to the code given to each type.

Parameter	Data Type	Units	Codes	Categories
Froude changes	Continuous	-	-	-
Depth changes	Continuous	m	-	-
Velocity changes	Continuous	ms^{-1}	-	-
Habitat Type Change	Binary	-	DG=Deep Glide; SG=Shallow Glide; RI=Rippled; POOL=Pool	0=no change; 1=Habitat Change
Flow Type Changes	Categorical	-	1=No flow (NO); 2=No perceptible flow (NPF);3=Smooth (SM); 4=Rippled (RP); 5=Unbroken Standing waves (UW); 6=Broken standing waves (BW); 7= Boulder (BO – no flow type characterisation)	0=no change; 1=increase of flow intensity of 1 unit, -1=decrease of flow intensity of 1 unit, 2= increase of flow intensity of 1 unit, -2=decrease of flow intensity of 1 unit

Two different situations were considered in this analysis: one identifying the changes from Q_1=0.52 m^3s^{-1} to Q_2=0.34 m^3s^{-1} and a second characterising the hydromorphological changes from Q_2 to Q_1. The first study was developed by taking the categorical parameters of the Q_1 as a reference, whilst the second study used those at Q_2. The relationships between the different quantitative parameters measured (velocity, depth and Froude change) and the categorical parameters (habitat and flow type) were established through the application of multiple regression techniques (general linear model). Descriptive statistics (QQ plots, histograms, Kolmogorov-Smirnov test and Chi-squared test) were calculated for each parameter to determine whether it was necessary to standardise the data set.

Discriminant function analysis was carried out to determine which variables among velocity change and depth change discriminated between the (i) mesohabitat and (ii) flow types encountered at Q_2. The variables included in the discriminant analysis are shown in Table 8.1. Each variable was standardized (i.e. normalised) prior to discriminant analysis. Maps of velocity, depth, Froude number, mesohabitat and flow type changes were created in order to associate the spatial distribution of quantitative parameters with mesohabitat and flow type changes.

The analysis for the Windrush site was developed to compare the results with those obtained for the Leigh Brook study explained above. Data were collected following the same methodology applied at the Leigh Brook river site (except for the fact that cross-sections were separated 2 m in the downstream direction instead of 1 m). Mesohabitat type, flow type and substrate were the categorical variables measured. Mesohabitat types identified were Riffle (RI), Shallow Glide (SG), Deep Glide (DG) and Pool. Flow types identified were Ripple (RP), Smooth (SM), No perceptible flow (NPF) and Unbroken standing Waves (UW). Substrate types identified were Gravel (G), Silt (SI), Sand (SA), Clay (CL) and Cobble (CO). Only depth was recorded as a quantitative variable. Points across each cross section were collected at 1 m intervals. Data were collected at two different flows: Q_1 = 1.4 m^3s^{-1} and Q_2 = 0.53 m^3s^{-1} along a 105 m reach. The cross-sections were not marked in the field and so, the location of the points collected at the two discharges did not match. Information from the first discharge was extrapolated to those points collected during the second discharge. The methodology applied for this purpose was based on the digitisation of polygons that

identified the mesohabitat types, flow types and substrate types of the data collected at the first discharge. The polygons were independently created for each criterion and were digitised with ArcGIS. Points collected during the second discharge described the habitat, flow and substrate type of the polygon in which they were included. Thus, each point of the data sets associated to the second discharge had two values of depth and two values of each categorical variable (mesohabitat, flow and substrate type) corresponding to the first and the second discharge. A total of 366 points, defining 42 cross-sections, were analysed. The methodology for the data analysis was the same for both the Leigh Brook and the Windrush.

Note that values representing Q_1 were obtained through the digitisation of polygons. These values might not represent the situation encountered during Q_1 since they were a product of an extrapolation methodology. Conclusions were drawn having regard to this limitation

8.3.2. The variogram as a tool to detect temporal changes

The variogram of depth was calculated for different discharges at each river site to analyse whether the range, sill and nugget were sensitive to changes in discharge. A plot relating discharge with each variogram model parameter was presented and conclusions were drawn having regard to results obtained in previous chapters. The analysis was carried out for (i) wet points and (ii) wet and dry points at each river site, wet points being those that had positive depth and dry points those whose depth value was negative. Note that the number of wet points decreased when decreasing the flow and therefore, changes in the variogram values may be due to this rather than to a sensitivity of the variogram to a change in discharge.

Values of depth used for the Windrush river site were simulated with the SSIIM CFD hydraulic model (Olsen, 1996; Olsen 2000) by staff at CEH. The model used a finite difference approach to solve the three-dimensional Navier-Stokes equations, with a two-equation k-ε turbulence closure model. The model had previously been applied to simulate hydraulics in several natural rivers (Olsen and Stokseth, 1995; Booker *et al.,* 2001; Harby and Alfredsen, 1998; Booker, 2003; Booker et al., 2004b). A calibration process was used to set roughness height (e.g. Booker 2003) by comparing observed

and calculated water surface elevations at a discharge of 1.1 m^3s^{-1}. This method assumes that there are no significant spatial changes in roughness. A roughness height of 0.1 m gave an average difference between observed and calculated of -0.00015 m for 20 measurements of water surface elevation. Having been calibrated using data from a high discharge the model was then run using the same value of roughness height for a discharge of 0.61 m^3s^{-1} and compared with 173 measurements of water surface elevation distributed throughout the reach. For this independent test of the roughness calibration 82% of the predictions were within 0.025 m of their corresponding observations. The procedure was repeated again for a discharge of 0.75 m^3s^{-1} using 136 measurements. For this simulation 90% of measured water levels were predicted to be within ± 0.025 m. The biggest differences between observed and calculated water levels for all simulations were under predictions of water level at discrete locations on a riffle.

8.3.3. Analysis of river width

Changes in channel width due to changes in discharge were analysed for the four discharges simulated at the Windrush river site (0.61 m^3s^{-1}, 0.75 m^3s^{-1}, 1.14 m^3s^{-1} and 1.37 m^3s^{-1}). Width was obtained at 586 cross-sections for the four discharges. The value of width at each cross-section was graphically compared between discharges. Differences encountered were analysed in relation to the morphological characteristics (e.g. channel shape, location of the cross-section in relation to the meander bend) at the site. Results were interpreted taking into account that the data was the product of a modelled environment and not field data

8.4. Results

8.4.1. Hydromorphological changes due to variations in discharge for the Leigh Brook river site.

1. Descriptive statistics

The QQ plots and histograms obtained for the depth, velocity and Froude number collected for the first discharge and for the quantitative variables characterising the

hydromorphological changes (depth change, velocity changes and Froude changes) indicated that the variables did not follow a Normal distribution. The Kolmogorov-Smirnov and Chi-square test provided evidence to reject the null hypothesis of Normality for all parameters tested.

Values of descriptive statistics for the continuous parameters are presented in Table 8.2. It is necessary to note that the two discharges analysed correspond to typical low flow conditions and so, the changes in hydromorphological parameters were not considerable (Table 8.2); only 9% of the data points changed their mesohabitat type and 39% their flow type (Figure 8.1). The values of change in depth, velocity and Froude Number were obtained as the difference between the value of the variable at Q_2 and the value of the variable at Q_1. In this way, positive values of change always indicated an increase of depth, velocity or Froude number, and negative values of change indicated a decrease in these parameters.

Table 8.2: descriptive statistics for the continuous parameters measured at the Leigh Brook river site. Values of change in depth, velocity or Froude Number were calculated considering an original discharge = 0.52 m^3s^{-1} and a final discharge = 0.34 m^3s^{-1} (decrease in discharge). Positive changes indicated an increase of the value of the parameter and negative changes a decrease.

Parameter	Mean	Median	Minimum	Maximum	Std.Dev.	Skewness	Kurtosis
Depth Change (m)	-0.039	-0.04	-0.50	0.58	0.06	0.5	7.9
Velocity change (m^3s^{-1})	-0.057	-0.04	-1.12	0.98	0.16	-0.04	6.5
Froude Change	-0.014	-0.01	-0.91	1.27	0.13	1.1	12.6
Depth 1st Flow (m)	0.245	0.21	0.00	0.94	0.15	0.8	0.7
Velocity 1st Flow (m^3s^{-1})	0.294	0.25	-0.39	1.53	0.25	0.8	0.9
Froude 1st Flow	0.212	0.16	-0.00	1.19	0.19	1.4	2.6
Depth 2nd Flow (m)	0.206	0.18	0.00	0.85	0.15	0.8	0.4
Velocity 2nd Flow (m^3s^{-1})	0.237	0.18	-0.24	1.51	0.23	1.1	1.8
Froude 2nd Flow	0.196	0.13	-0.00	1.35	0.21	1.8	4.0

Histograms were plotted in order to determine which mesohabitat and flow types were more prevalent at the Leigh Brook river site. Results (Figure 8.2) showed that shallow glides and riffles were the dominant mesohabitat types identified and rippled surfaces were the most common surface flow types for both discharges.

Figure 8.3 shows the mesohabitat types and flow types that were more affected by the discharge change; mesohabitat changes were considered equal to 1 when a change appeared and equal to 0 when no change was registered whilst the rate of flow change was calculated as the difference between flow type codes (positive changes indicated

increase of flow type intensity whilst negative changes indicated decrease of the flow type intensity).

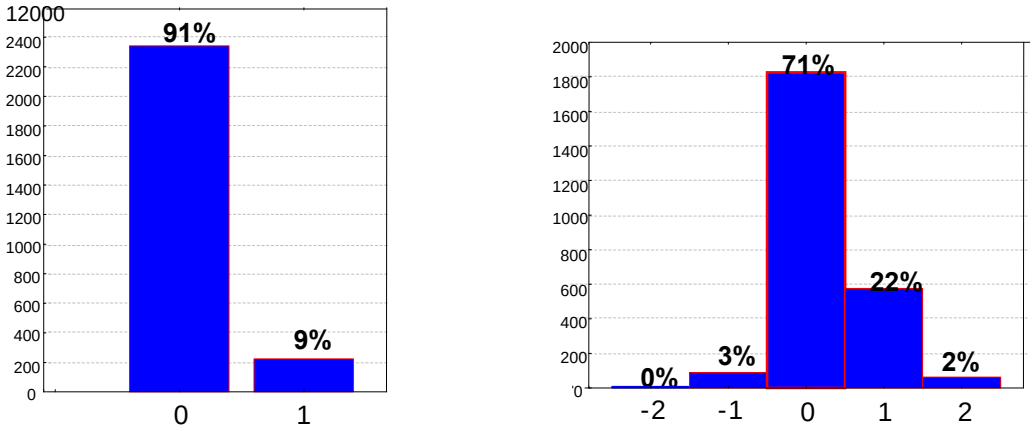

Figure 8.1: histogram and percentage of mesohabitat (left) and flow type (right) identified at the Leigh Brook river site. For the mesohabitat change: 0 is equal to no change and 1 indicates change. For the Flow type change: 0 indicates no change and 1, 2, -1, -2 indicate change of flow category, the category being indicated by the code in Table 8.1.

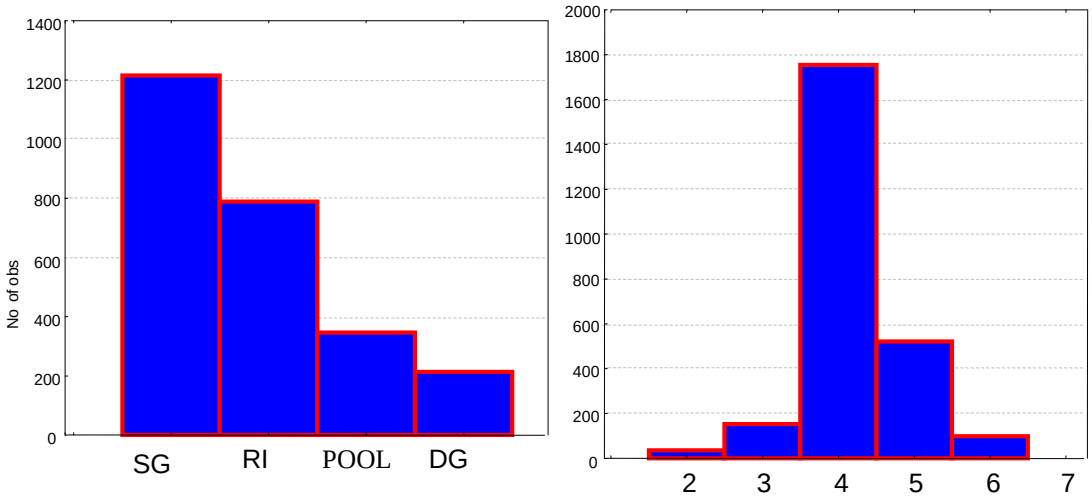

Figure 8.2: histograms obtained for the categorical parameters (habitat (left) and flow (right) types identified for Q=0.52 m^3s^{-1}). Results obtained for the first discharge (Q=0.344 m^3s^{-1}) did not present significant differences to those obtained for the second discharge. Table 8.1 summarises the flow type classification. SG = Shallow Glide, RI = Riffle and DG = Deep Glide.

The majority of the mesohabitat changes were in deep glides when decreasing the discharge. Three significantly different groups could be distinguished for the flow types: (1) unbroken standing waves & broken standing waves group, (2) smooth & rippled group and (3) no perceptible flow group. Higher changes were identified in no perceptible flow and rippled smooth flow types, which were strongly associated to the habitats identified with the highest rates of change (deep-shallow glide and pool mesohabitat types). Note that the plots shown in Figure 8.3 represent the mean and its 95% confidence interval and they were not the result of an analysis of variance. The flow and mesohabitat types in Figure 8.3 correspond to those identified for Q_1 ($0.52m^3s^{-1}$).

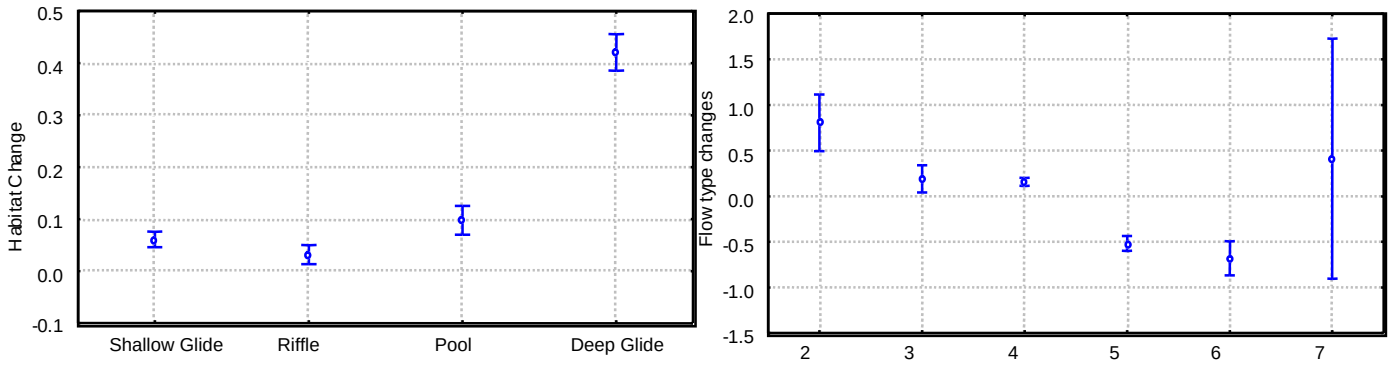

Figure 8.3: mean plot for mesohabitat (left) and surface flow type (right) changes. See Table 8.1 to identify the flow type codes. Vertical lines denote 95% confidence interval. Note that these plots represent the mean and the 95% confidence interval and they are not the result of an analysis of variance (i.e. the plots represent the raw data). Points included in the flow and mesohabitat type categories correspond to those identified as such for $Q_1=0.52m^3s^{-1}$.

Table 8.3 shows the percentage of points that changed from one mesohabitat type to another when increasing/decreasing the flow. The majority of habitats that changed when decreasing the discharge are transformed into shallow glides, those changes being more frequent from deep glides. Additionally, the discharge increment transformed the majority of affected points into shallow and deep glides. Thus, for these data, discharge increments transformed shallow areas into deeper and more smooth habitats (shallow & deep glides), whilst discharge decrements mainly transformed deep areas (deep glides & pools) into shallower and less smooth habitats (shallow glides). Comparing these results with these obtained in Figure 8.3 it was possible to conclude that when the discharge decreases the deepest areas (deep glides and pools) experienced higher changes whilst, when the flow increases, shallow areas (riffles-shallow glides) were more affected.

Table 8.3: percentage of points that change from the original mesohabitat to the mesohabitat at altered flow for the Leigh Brook river site.

		Original Situation Q=0.52 m^3s^{-1}			
		Deep Glide	**Pool**	**Riffle**	**Shallow Glide**
Final Situation Q=0.34m^3s^{-1}	**Deep Glide**	58	-	-	-
	Pool	-	90	-	-
	Riffle	3	-	97	6
	Shallow glide	39	10	3	94
		Original Situation Q=0.34 m^3s^{-1}			
		Deep Glide	**Pool**	**Riffle**	**Shallow Glide**
Final Situation Q=0.52m^3s^{-1}	**Deep Glide**	100	-	-	7
	Pool	-	100	-	3
	Riffle	-	-	91	2
	Shallow glide	-	-	9	88

Figure 8.4 shows that flow type usually increased when increasing the discharge and decreased the intensity when decreasing the discharge. Table 8.4 and Table 8.5 show the percentage of points that changed flow type when changing the discharge; increments of discharge (Table 8.5) transformed smooth and broken standing waves into rippled flow type and unbroken standing waves into smooth flow type. Table 8.4 shows the result of discharge decrements; rippled areas were transformed into no perceptible and smooth flow types, whilst smooth flow type was converted into no perceptible/rippled/unbroken standing waves. It is important to note that discharge changes in one direction (increase or decrease) produced flow type changes in two directions (increase and decrease of categorical value of flow type).

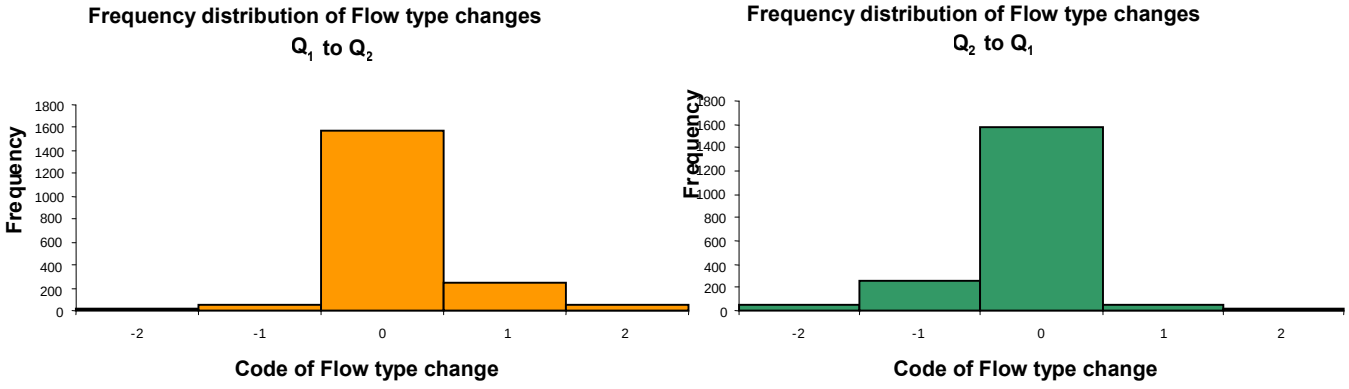

Figure 8.4: change of flow type from the original to the final situation. Negative values of change indicate a decrease on the intensity of flow type, whilst positive values indicate the opposite. Q_1= 0.34 m^3s^{-1} and Q_2 = 0.52 m^3s^{-1}.

Table 8.4: percentage of points that change from the original flow type ($Q=0.52 m^3s^{-1}$) to the flow type at reduced discharge ($Q=0.34 m^3s^{-1}$) for the Leigh Brook river site.

		Original Situation $Q=0.52\ m^3s^{-1}$						
		No flow (NO)	No perceptible flow (NPF)	Smooth (SM)	Rippled (RP)	Unbroken Standing (UW)	Broken Standing (BW)	BO
Final Situation $Q=0.34\ m^3s^{-1}$	NO	0	0	0	0	0	0	0
	NPF	0	83	27	2	0	0	0
	SM	0	11	36	12	0	0	0
	RP	0	6	14	85	0	0	0
	UW	0	0	23	0	100	0	0
	BW	0	0	0	1	0	100	0
	BO	0	0	0	0	0	0	100

Table 8.5: percentage of points that change from the flow type at the original ($Q=0.34 m^3s^{-1}$) to the flow type at increased discharge ($Q=0.52 m^3s^{-1}$) for the Leigh Brook river site.

		Original Situation $Q=0.34\ m^3s^{-1}$						
		No flow (NO)	No perceptible flow (NPF)	Smooth (SM)	Rippled (RP)	Unbroken Standing (UW)	Broken Standing (BW)	BO
Final Situation $Q=0.52\ m^3s^{-1}$	NO	0	0	0	0	0	0	0
	NPF	0	26	1	0	0	0	0
	SM	0	35	30	1	13	0	0
	RP	0	39	69	99	0	8	0
	UW	0	0	0	0	87	0	0
	BW	0	0	0	0	0	92	0
	BO	0	0	0	0	0	0	100

2. General Linear Model Analysis

The analysis of variance was based on the following hypotheses:

> **Ho:** the classes of each categorical parameter have the same rate of change for a specific hydromorphological variable (i.e. depth, velocity or Froude number).
>
> **H_1:** the classes of each categorical parameter do not have the same rate of change (there is at least one difference between them) for a specific hydromorphological variable (i.e. depth, velocity or Froude number).

The General Linear Model analysis tested the hypothesis between one categorical parameter and one quantitative parameter, creating the combination of tests presented in Table 8.6. The results indicated that the null hypothesis could be rejected for the following analysis when considering $Q_2=0.34\ m^3s^{-1}$ as the reference discharge to classify flow and mesohabitat types: depth vs. mesohabitat type, velocity vs. mesohabitat type, velocity vs. flow type and Froude number vs. mesohabitat type. If

discharge Q_1=0.52 m^3s^{-1} was considered for the classification, the null hypothesis was only rejected for the depth changes vs. flow type analysis (p=0.0053).

Table 8.6: analysis of variance between categorical and continuous parameters after standardisation. Red coloured p-values indicate rejection of null hypothesis.

	Velocity change	Depth Change	Froude Num. Change
Habitat Type	0	0	0.0029
Flow Type	0	0.1456	0.571

Figure 8.5 shows the LS means plot (plot of the least squares means which are the best linear-unbiased estimates of the marginal means for the design) obtained for the standardised parameters included in these analyses (mesohabitat and flow types classified according to Q_2=0.34 m^3s^{-1}). The LS mean plot of depth change vs. mesohabitat showed that depth changes were significantly different between deep glides and shallow glides, whilst pools and riffles did not present significant differences between them. Deep glides presented the higher depth changes followed by shallow glides. Deep glides could not be considered significantly different to riffles and pools, whilst shallow glides represented differences from both, riffles and pools. The mean depth changes were located between 0.037 m (riffles) and 0.048 m (shallow glide) (Table 8.7).

Since (a) the group made up of pool-riffles did not experience large depth changes with flow and (b) deep and shallow glides presented higher depth changes than the rest of the mesohabitat types, it was possible to conclude that depth changes for the Leigh Brook river site were mainly located at deep and shallow glides, which usually are habitats that link pools and riffles. Similar results were obtained when considering Q_1=0.52 m^3s^{-1} as the reference discharge for the mesohabitat and flow type classification.

Figure 8.5 shows two significantly different groups regarding velocity changes (Q_2 = 0.34 m^3s^{-1} was considered for the mesohabitat and flow type classification): the first one constituted by deep glides and riffles and the second one with pool and shallow glides. The results indicated that shallow and deep glides were those mesohabitat types that alternatively represented the maximum and minimum changes for the different quantitative parameters analysed. Velocity changes seemed to follow an

inverse pattern to depth changes; mesohabitat types that presented higher changes in depth did not have significant changes in velocity. The opposite situation was encountered when analysing mesohabitat types with small depth changes. Since shallow and deep glides were never included in the same group, it was possible to consider them as the extremes of the hydromorphological changes. Pools and riffles switched between extremes according to the parameter analysed, but it is difficult to establish a pattern in their grouping preferences.

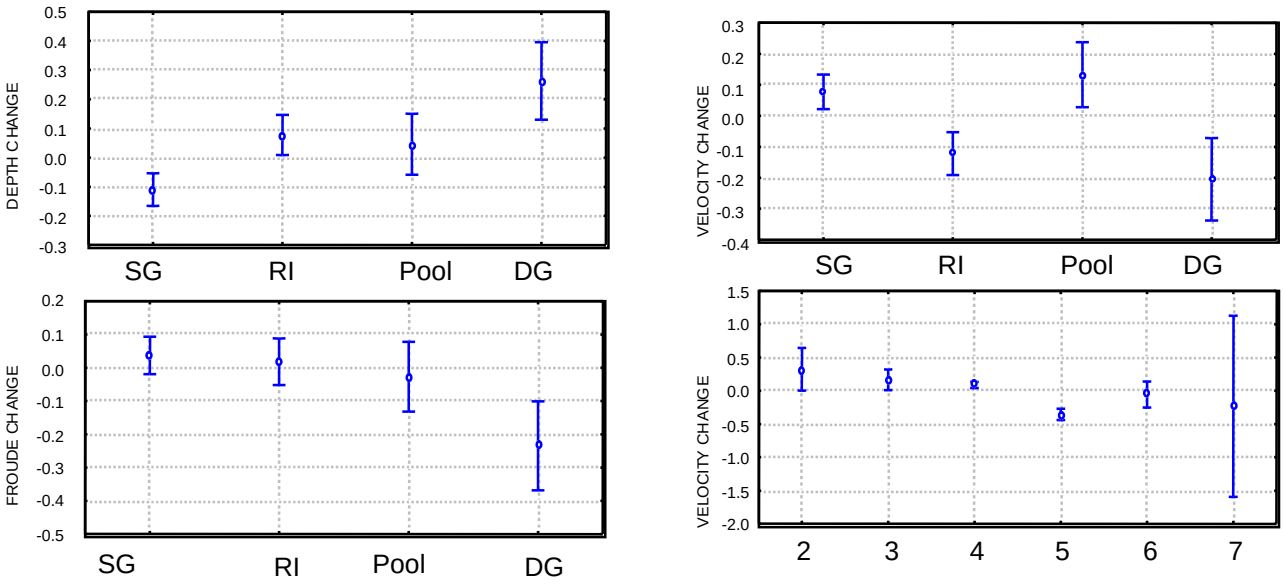

Figure 8.5: mean plots with 0.95 confidence interval obtained for the standardised parameters. Vertical lines denote the 95% confidence interval. Codes can be obtained from Table 8.1. Flow types are represented on the right bottom corner. The types represented correspond to those encountered at discharge 0.34 m^3s^{-1}.

Table 8.7: descriptive statistics for the different parameters of change grouped by mesohabitat types encountered at discharge = 0.52 m^3s^{-1} at the Leigh Brook river site. None standardised parameters.

	Descriptive Stat.	Shallow glide	Riffle	Pool	Deep glide
Depth Change (m)	**Absolute Mean**	0.048	0.037	0.039	0.026
	Absolute Maximum	0.33	0.37	0.58	0.19
	Std. Dev.	0.05	0.053	0.07	0.048
Velocity Change (m^3s^{-1})	**Absolute Mean**	0.045	0.076	0.036	0.089
	Absolute Maximum	0.762	1.12	0.780	0.707
	Std. Dev.	0.105	0.205	0.198	0.115
Froude Number Change	**Absolute Mean**	0.008	0.011	0.017	0.044
	Absolute Maximum	0.838	1.273	0.486	0.388
	Std. Dev.	0.089	0.198	0.103	0.067

Changes in Froude number encountered when considering Q_2=0.34m^3s^{-1} as a discharge reference for the mesohabitat and flow type classification, were different between at least two mesohabitat types (Table 8.2 and Figure 8.5). Pools, riffles and shallow glides did not present significant differences. Deep glides were different to the rest of the mesohabitat types although there was some overlapping between this mesohabitat and pools. Maximum Froude number changes were identified in deep glides and minimum changes in shallow glides, which supports the observations noted earlier regarding the representation of extremes values by these two mesohabitat types.

Depth and Froude number changes were not significantly different between flow types (Table 8.6) if Q_2=0.34 m^3s^{-1} was considered as the discharge reference for the mesohabitat and flow type classification. However, there were significant differences between flow types for the velocity change (Figure 8.5); unbroken standing waves were significantly different to the rest of the flow types which did not present significant differences between them. Differences between flow types were also encountered for depth changes when considering Q_2 =0.52 m^3s^{-1} as a discharge reference for the mesohabitat and flow type classification (Figure 8.6). However, the overlapping between flow types was considerable and just rippled flow type could be considered significantly different to the rest (except flow type 7).

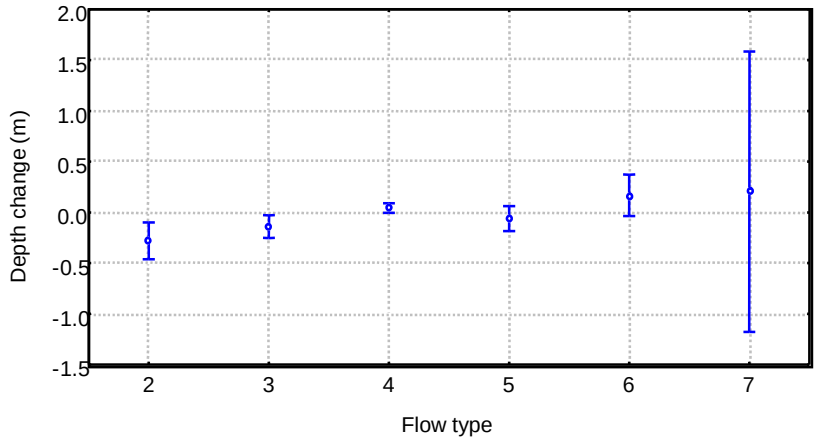

Figure 8.6: mean plot for flow type changes vs. depth change. Flow change from 0.52 m^3s^{-1} to 0.34m^3s^{-1}. See Table 8.1 to identify the code for each flow type. Vertical bars denote 95 % confidence interval.

Since mesohabitat types were able to identify changes in depth and velocity whilst flow types just determine differences in velocity, mesohabitat types seemed a better tool for rapid habitat assessment as more information could be extracted from their classification. Further studies should be carried out to determine the relationship between flow type and velocity; velocity measurements are time consuming and it would be necessary to determine if it is possible to establish a relationship between flow type (visually identified) and velocity at 0.6 x depth.

1. Factorial analysis.

The factorial General Linear Model designs contain variables representing combinations of the levels of 2 or more categorical predictors (e.g: the study of depth changes in relationship to mesohabitat and flow types, resulting in a 4 (habitat types) x 6 (flow types) design). The combinations studied were those between each of the continuous parameters (depth changes, velocity changes or Froude number change) and the 2 categorical ones (habitat type and flow type). The null hypothesis tested was H_0 = the classes of each combination of categorical parameters (i.e. flow type and mesohabitat type) have the same rate of change for a specific hydromorphological variable (i.e. depth, velocity or Froude Number). The combinations that gave evidence for rejecting the null hypothesis were: depth changes vs. mesohabitat x flow types (for Q_2=0.34m^3s^{-1}), Froude changes vs. flow x mesohabitat type (for Q_1=0.52m^3s^{-1}) and velocity changes vs. flow x mesohabitat type (for Q_1=0.52m^3s^{-1}) ($p<0.05$ in all cases).

Figure 8.7 shows the factorial combinations that gave evidence for rejecting the null hypothesis. Velocity changes were different between mesohabitat types for flow type 4 (rippled) and flow type 5 (unbroken standing waves). Rippled surfaces showed three significantly different groups when analysing the velocity changes; (1) deep glides & riffles,

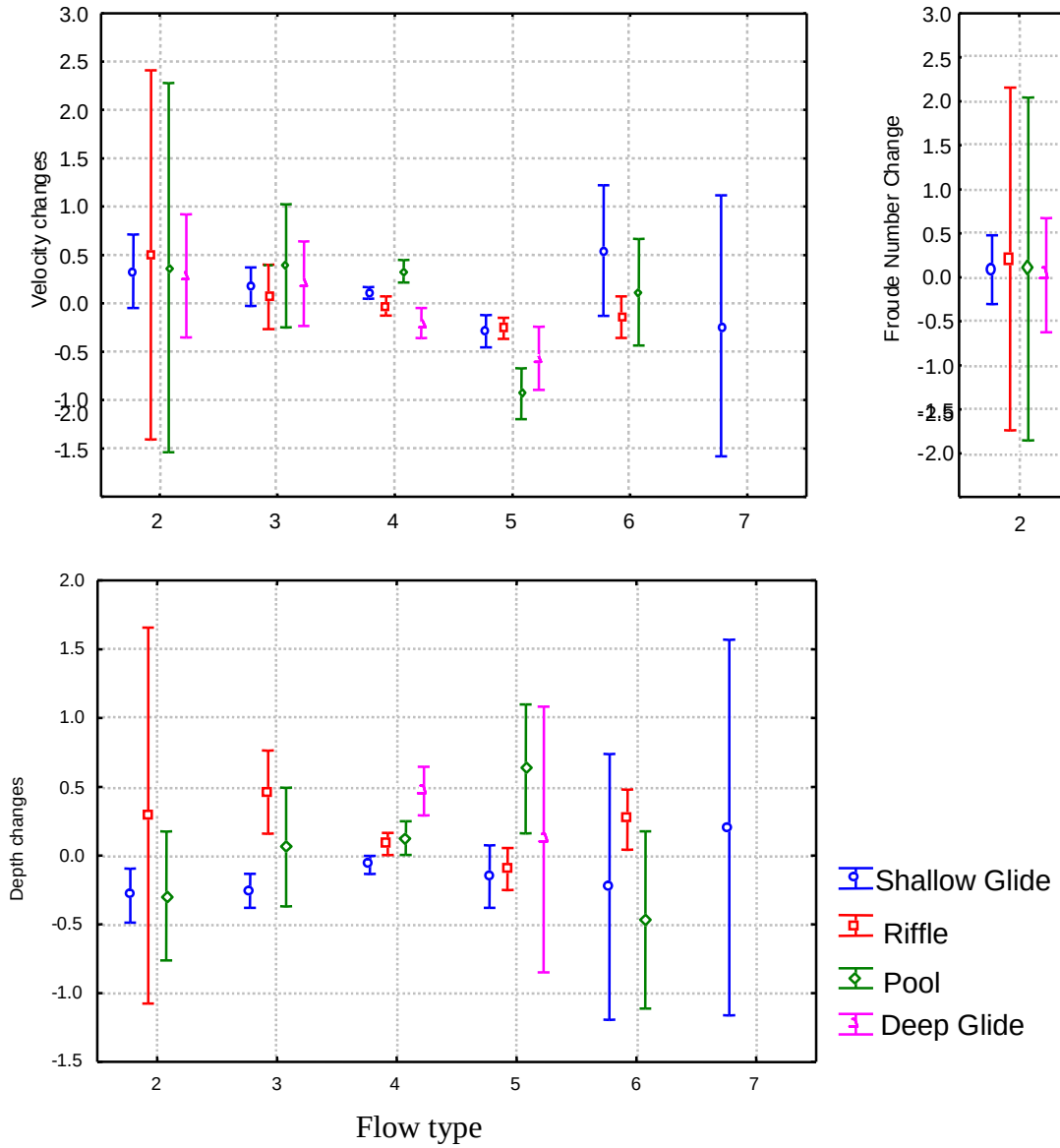

Figure 8.7: Mean plot of factorial general linear model analysis for the continuous standardised parameters vs. the combination of mesohabitat x flow type. Vertical bars denote 95% confidence interval. Codes for flow type are explained in Table 8.1. Classification of mesohabitat and flow types have been obtained according to Q_1=0.52m^{3}s^{-1} for velocity and Froude number changes and Q_2=0.34m^{3}s^{-1} for depth change.

(2) pools and (3) shallow glides. Rippled surfaces presented higher changes of velocity in pools and deep glides, the small changes being represented by riffles habitats. Unbroken standing waves showed two significantly different groups; (1) pools and (2) shallow glides & riffles. The amplitude of the confidence interval for deep glides did not allow this mesohabitat type to be included into any of the previous groups. Maximum velocity changes were presented in pools and deep glides.

Depth changes were different between mesohabitat types for smooth, rippled and unbroken standing waves. Smooth surfaces showed two significantly different groups; one made up of riffles and the other of shallow glides. Riffles showed higher depth changes than shallow glides and pools, the latter being the mesohabitat with smallest changes. Mesohabitat types in rippled surfaces were distributed in three groups: (1) deep glides, (2) pools & riffles and (3) shallow glides. The first mesohabitat type showed higher depth changes whilst shallow glides did not seem to be affected. Finally, unbroken standing waves showed two groups: (1) pools and (2) shallow glides & riffles, the first group being the one with higher depth changes.

Froude number changes were just identified for flow type 5 (unbroken standing waves). The parameters were distributed in two significantly different groups: (1) riffles and (2) pool & deep glides - the latter with higher Froude number changes.

General observation from the factorial analysis can be summarised in the following points:

- Just unbroken standing waves, smooth flow and rippled surfaces showed differences in the changes of the continuous parameters when grouping them by mesohabitat types. Habitats with these flow types showed the highest proportion of temporal change.

- Shallow and deep glides always presented opposite rates of changes when differences were detected and thus, they were always included in significantly different groups. However, they did not identify the extremes of the classification as in previous analysis.

2. Discriminant Analysis.

Table 8.8 shows the classification functions obtained for the discriminant analysis carried out with depth change and velocity change as independent variables and mesohabitat types at Q_2 as grouping variable. The classification function can be used to determine to which group a new observation will belong. In this case, for example, it would be possible to determine to which mesohabitat type the new observation belongs after considering the values of velocity and depth change. The classification scores are calculated for this purpose and are the result of applying the classification function to the values of depth and velocity change observed. Once the classification scores have been computed, the case (new observation) is classified as belonging to the group that presents higher classification score. Velocity and depth change showed similar values of coefficients in the classification function (except for shallow glides, where depth change presents a higher coefficient), which meant that both variables were equally relevant for the prediction of the mesohabitat type at which they belonged in Q_2. The percentage of points classified correctly when applying the classification function was equal to 96.4% for deep glides, 4.2% for riffles and 0% for shallow glides and pools.

Table 8.8: coefficients for the classification functions for mesohabitat types encountered at Q_2. Classification scores are = Depth Change coefficient *(depth change) + (velocity change coefficent *(velocity change) + constant.

Discriminant Groups / Coefficients	Shallow Glide p=0.50	Riffle p=0.32	Pool p=0.12	Deep Glide p=0.04
Depth Change	-0.131	0.088	0.108	0.478
Velocity Change	0.074	-0.095	0.106	-0.393
Constant	-0.702	-1.119	-2.115	-3.212

Table 8.9 shows the classification functions obtained for the discriminant analysis carried out with the flow types encountered at Q_2 as grouping variable and depth change and velocity change as independent terms. Results showed that the coefficients obtained for velocity changes for Unbroken standing Waves (UB) and Broken standing Waves (BW) were higher than those encountered for depth change. These results were consistent with those obtained for the General Linear Model analysis in section 8.4.1-2. Results obtained for the classification of new observations

need to be interpreted carefully for the flow type grouping criteria since the percentage of points correctly classified with the functions provided in Table 8.9 were 0% for all the flow types except for ripples (100%).

Table 8.9: coefficients for the classification functions for the mesohabitat types encountered at Q_2. Classification scores are = Depth Change coefficient *(depth change) + (velocity change coefficent * (velocity change) + constant. See Table 8.1 for flow type codes.

Coefficients \ Discriminant Groups	NPF p=0.045	SM p=0.12	RP p=0.70	UW p=0.09	BW p=0.03
Depth Change	-0.290	-0.143	0.0427	-0.059	0.164
Velocity Change	0.348	0.134	-0.0372	-0.124	0.193
Constant	-3.196	-2.151	-0.3557	-2.329	-3.371

Maps of rate of change were produced for the categorical values and compared with the spatial distribution of mesohabitat and flow type parameters (Figure 8.8 to Figure 8.11).

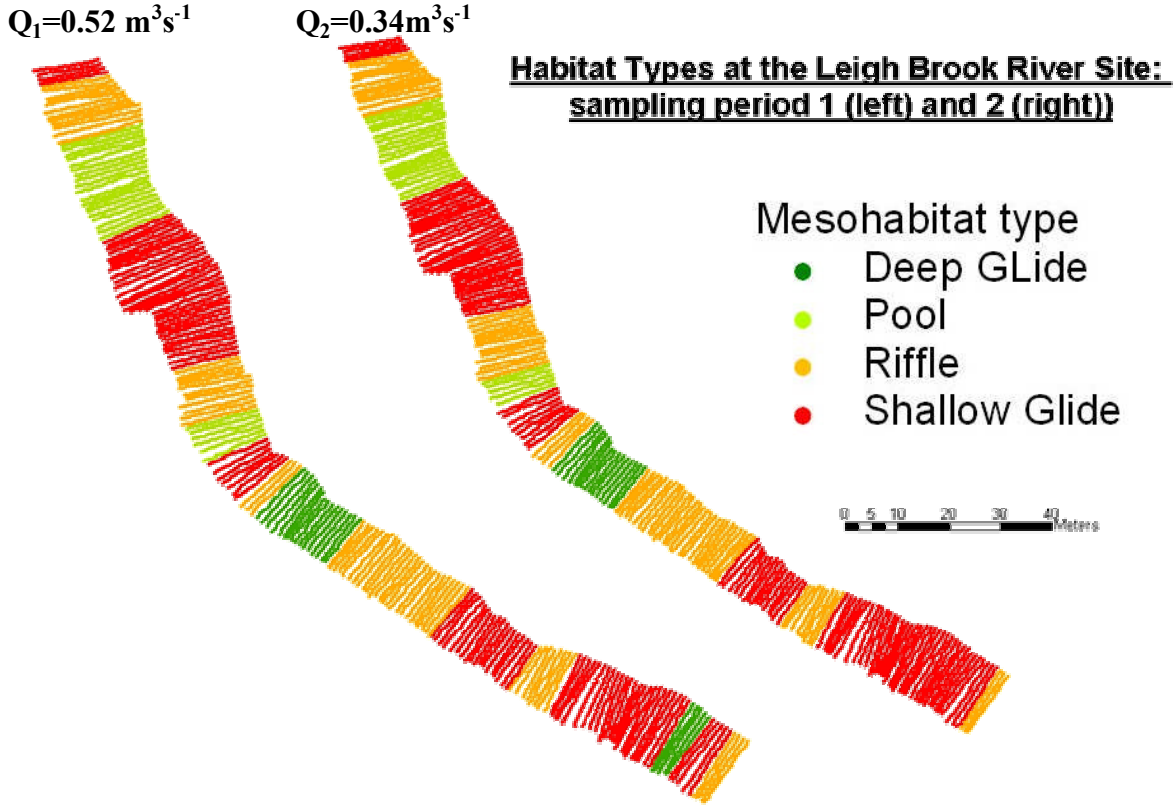

Figure 8.8: mesohabitat types identified at the two different flow rates, Leigh Brook.

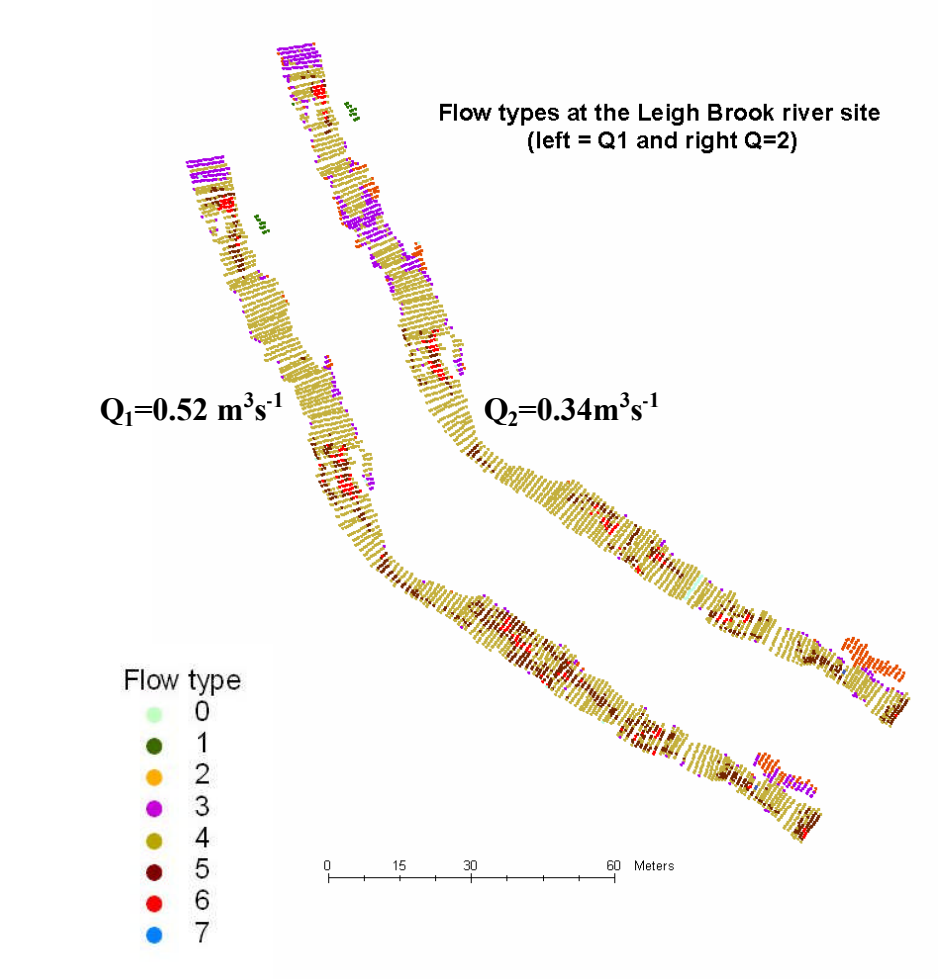

Figure 8.9: flow types identifies at the two different flow rates, Leigh Brook.

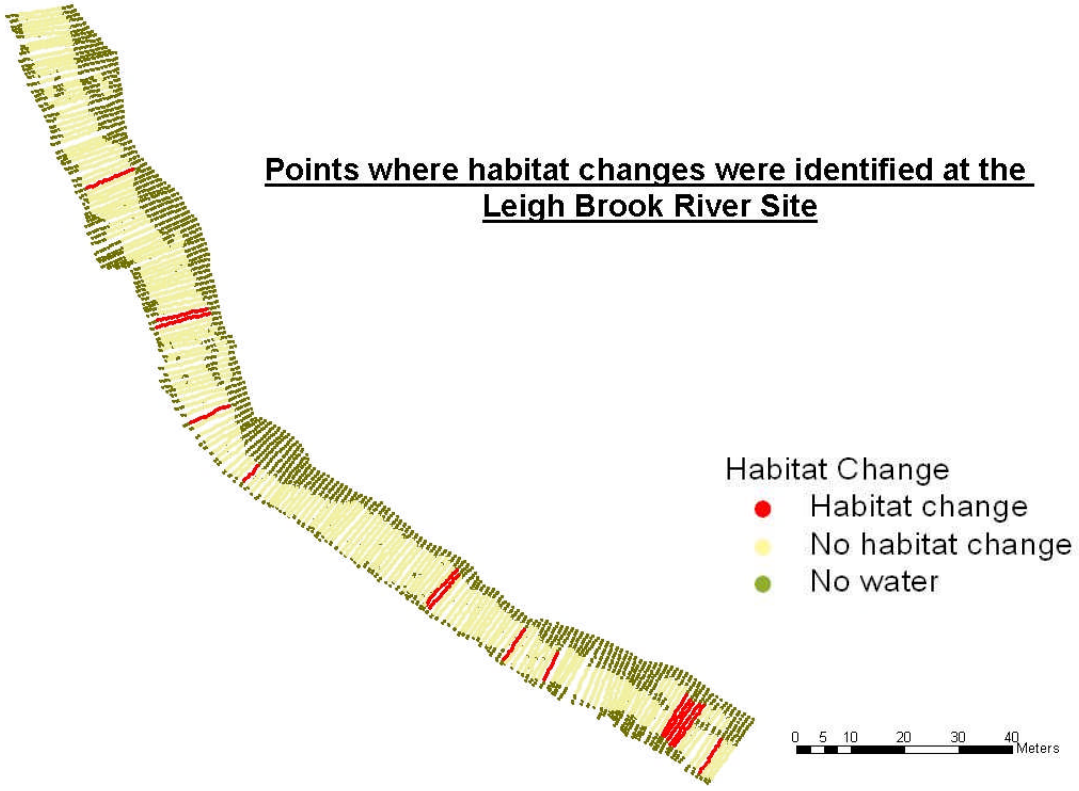

Figure 8.10: points where mesohabitat type changes where detected (red), Leigh Brook.

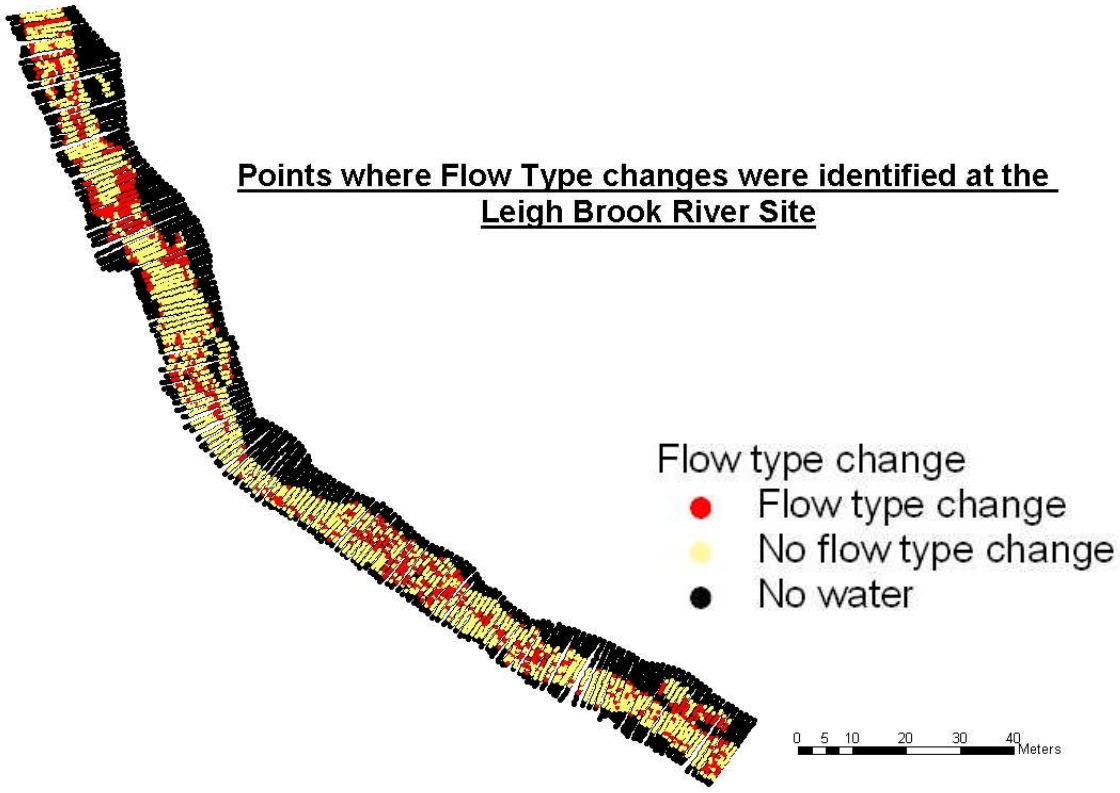

Figure 8.11: points where flow type changes where detected (red), Leigh Brook.

Analysis of dry points

A total of 175 points presented dry conditions during the second monitoring field work. Results presented in this section include only those points that became dry when decreasing the discharge (from Q_1 to Q_2).

Riffles were the most frequent mesohabitat type to become dry for both discharges, followed by pools and shallow glides. Figure 8.12 shows the histograms of the mesohabitat types encountered for each discharge. Riffles and Pools were the mesohabitat types that had their cross-section more affected by a decrease in the discharge. Only 11 points from the 175 analysed changed their mesohabitat characterisation when decreasing the discharge, all of them being transformed from pools to shallow glides. No other changes were identified.

The mean value of depth change (depth Q_2 – depth Q_1) was equal to -0.0023 m, with a variance of 0.00048, a maximum difference of 0.1 m and a minimum difference in depth equal to -0.06 m. The distribution of depth change was slightly skewed to the left (skewness coefficient = -0.8) and highly peaked (kurtosis = 28.74).

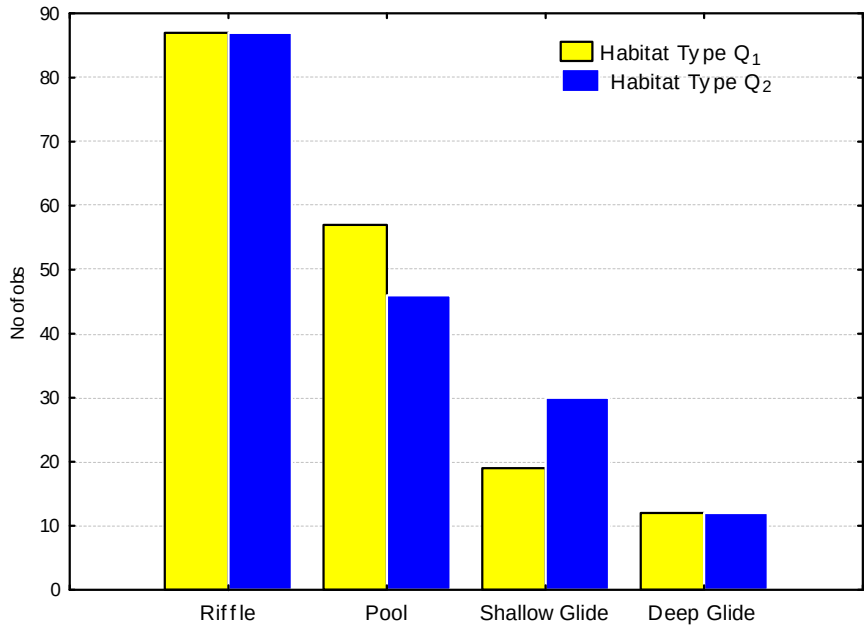

Figure 8.12: histogram of the mesohabitat types that become dry when decreasing the discharge (Habitat type 1) and histogram of the haitat types for the same points at the second discharge (Habitat type 2).

Figure 8.13 shows the histogram of the flow types encountered for the 175 points analysed. Rippled, Smooth and No Perceptible Flow were the flow types that were more likely to become dry for this decrease in discharge, becoming dry when this happened.

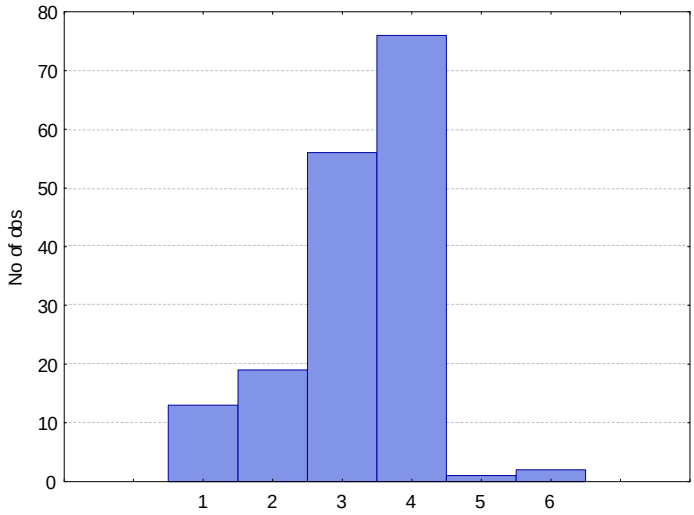

Figure 8.13: histograms of the flow types that become dry when decreasing the discharge. 1=No Flow, 2=No Perceptible Flow, 3=Smooth, 4=Rippled, 5=Unbroken Standing Waves and 6=Broken Standing Waves.

8.4.2. Hydromorphological changes due to variations in discharge for the Windrush river site.

1. Descriptive statistics

Results obtained for the Kolmogorov-Smirnov and Chi-square Normality tests showed that depth at discharge Q_1 = 1.4 m^3s^{-1}, depth at discharge Q_2 = 0.53 m^3s^{-1} and change of depth from Q_1 to Q_2 did not follow a Normal distribution (p-value<0.01). Values of skewness and kurtosis indicated that it could be accepted that the data followed a Normal distribution, except for the variable depth change, where the kurtosis exceeds 3 units. This means that the distribution had a distinct peak near the mean, had heavy tails and declined rather rapidly. The QQ-plots and histograms analysed indicated that the distribution for these data sets approximated to Normal but failed to pass the Chi-square and Kolmogorov-Smirnov test (see skewness and kurtosis values in Table 8.2 and compare them with those obtained in Table 8.10), even for the variable depth-change. No transformation was applied for the implementation of General Linear Models; it will be assumed that depth distribution is Normal.

Table 8.10 summarises the values of descriptive statistics obtained for the Windrush river site. The change of discharge produced a decrease in mean depth equal to 0.07 m. Maximum and minimum depth changes were equal to 0.73 m and -0.42 m, respectively.

Table 8.10: descriptive statistics for the continuous parameters measured at the Windrush river site. First flow corresponds to 1.4 m^3s^{-1} and second flow to 0.53 m^3s^{-1}.

Parameter	Mean	Median	Minimum	Maximum	Std.Dev.	Skewness	Kurtosis
Depth 2nd Flow (m)	0.39	0.29	0.00	1.40	0.32	0.93	0.06
Depth 1st Flow (m)	0.45	0.39	0.09	1.15	0.26	0.87	-0.07
Depth Change (m)	0.07	0.08	-0.42	0.73	0.13	-0.13	3.48

Figure 8.14 shows the histograms for each qualitative variable characterised at both discharges. Mesohabitat types encountered were mainly represented by shallow glides followed by deep glides for both discharges. Riffles only appeared for the first discharge whilst pools only appeared for the second discharge. Thus, the system was mainly dominated by a sequence of deep and shallow glides, with a few pools and riffles.

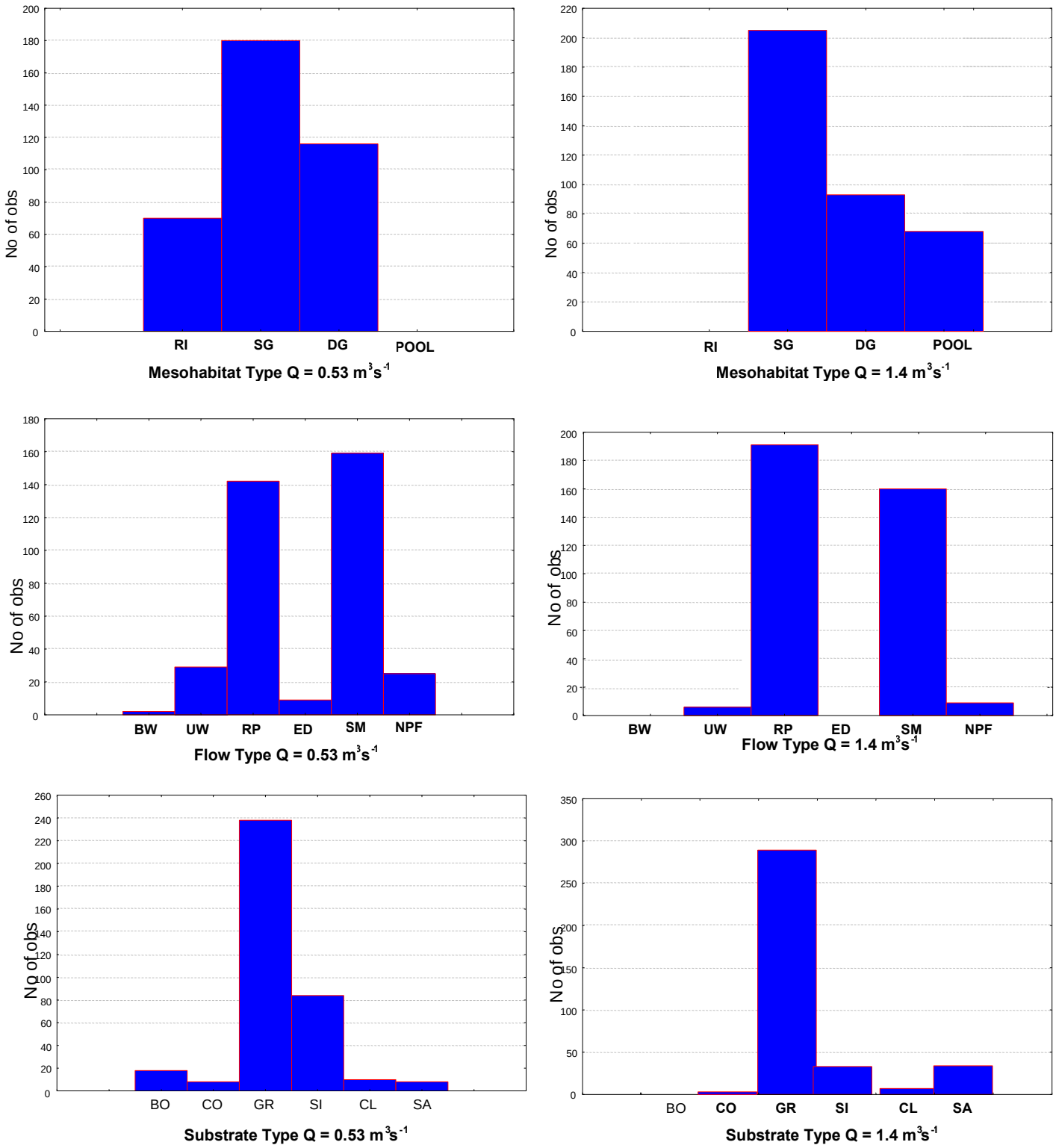

Figure 8.14: histograms obtained for the qualitative variables measured at the Windrush river site for both discharges Q_1=1.4 m^3s^{-1} and Q_2 = 0.53 m^3s^{-1}. The codes used are as follow: SG=Shallow Glide, DG=Deep Glide, RI=Riffle, BW=Broken standing waves, UW=unbroken standing waves, RP=rippled, ED=edge, SM=smooth NPF=no perceptible flow, BO=Boulder, CO=Cobble, GR=Gravel, SI=Silt, CL=Clay and SA=Sand.

165 points of 366 (45%) presented change of mesohabitat type between discharges. Table 8.11 and Table 8.12 show the percentage of points that changed from one class to another for both discharges. The mesohabitat types that showed the highest percentage of change were pools for a decrease in discharge (Table 8.11) and riffles for an increase in discharge (Table 8.12). This did not coincide with the results obtained for the Leigh Brook river site, where shallow and deep glides were the mesohabitat types showing highest percentage of change. A decrease in discharge (Table 8.11) transformed deep glides into shallow glides, pools into both, deep and shallow glides and shallow glides into riffles. An increase in discharge transformed deep glides into pools, riffles into shallow glides and shallow glides into deep glides or pools. Results suggested that the sequence of mesohabitat type changes went from pool to deep glide to shallow glide and to riffle when decreasing the flow and in the opposite direction when increasing the flow. The sequence was respected except for the relationship pool-shallow glide; some points collected in pools became shallow glides instead of deep glides when decreasing the flow and some shallow glides became pools when increasing the flow.

Table 8.11: percentage of points that change from the original situation mesohabitat (Q=1.4 m^3s^{-1}) to the mesohabitat at the final situation (Q=0.53m^3s^{-1}) for the Windrush river site.

		Original Situation Q=1.4 m^3s^{-1}		
		Deep Glide	Pool	Shallow Glide
Final Situation Q=0.53 m^3s^{-1}	Deep Glide	70	75	0
	Riffle	0	1	34
	Shallow glide	30	24	66
	Total Num. Points	93	68	205

Table 8.12: percentage of points that change from the original situation mesohabitat (Q=0.53m^3s^{-1}) to the mesohabitat at the final situation (Q=1.4 m^3s^{-1}) for the Windrush river site.

		Original Situation Q=0.53 m^3s^{-1}		
		Deep Glide	Riffle	Shallow Glide
Final Situation Q=1.4 m^3s^{-1}	Deep Glide	56	0	16
	Pool	44	1	8
	Shallow glide	0	99	76
	Total Number of points	116	70	180

Flow types (Figure 8.14) observed were mainly characterised by rippled and smooth areas. Broken standing Waves (BW) were the only flow type present only in one data set (second discharge). Unbroken Standing Waves (UW), Rippled (RP), Smooth (SM) and No Perceptible Flow (NPF) were present for both river discharges and did not

change their proportions considerably. Note that for the second discharge it was possible to observe Edge (ED) points (9 points) which were not present for the first discharge. The river width at the first discharge was higher than the river width for the second discharge and thus, there were not dry points for the second discharge. "Edge" points were not considered for the data analysis.

A total of 147 data points (40%) changed their flow type due to the changes in discharge. Table 8.13 and Table 8.14 show the percentage and total number of points that changed from one flow type to another when increasing and decreasing the discharge. Decrease in discharge generated a change of smooth flow type into rippled, no perceptible flow into rippled, rippled into smooth and unbroken standing waves into broken standing waves. Increase in discharge produced a change from no perceptible flow to rippled, smooth to rippled, rippled to smooth and unbroken standing waves to ripple. Broken standing waves were not analysed since there were just two points representing this flow type. The pattern identified for flow types was not as clear as that identified for mesohabitat types and thus, it was difficult to define a sequence of change for increase and decrease in discharge. This lack of pattern might be a result of the methodology applied to obtain information at the same locations for both discharges but since similar results were encountered for the previous analyses at the Leigh Brook river site, it can be concluded that mesohabitat types are a better tool to predict how a change in discharge is going to affect a river site and how the different hydromorphological features are going to be distributed.

Table 8.13: percentage of points that change from the original flow type (Q=1.4 m^3s^{-1}) to the flow type at the final situation (Q=0.53 m^3s^{-1}) for the Windrush river site.

		Original Situation Q=1.4 m^3s^{-1}			
		No perceptible flow (NPF)	Smooth (SM)	Rippled (RP)	Unbroken Standing (UW)
Final Situation Q=0.53 m^3s^{-1}	NPF	89	3	6	0
	SM	0	67	29	0
	RP	11	25	55	7
	UW	0	5	10	67
	BW	0	0	0	16
	Total Number of points	9	159	183	6

Table 8.14: percentage of points that change from the original flow type (Q= 0.53 m^3s^{-1}) to the flow type at the final situation (Q= 1.4 m^3s^{-1}) for the Windrush river site.

		Original Situation Q=0.53 $m^3 s^{-1}$				
		No perceptible flow (NPF)	Smooth (SM)	Rippled (RP)	Unbroken Standing (UW)	Broken Standing (BW)
Final Situation Q=1.4 m^3s^{-1}	NPF	32	0	0	0	0
	SM	24	67	27	26	0
	RP	44	33	73	59	50
	UW	0	0	0	15	50
	Total Number of points	25	159	142	29	2

Finally, substrate types showed the highest number of changes between discharges (Figure 8.14). Gravel (GR) remains the dominant substrate type at both discharges, followed by Silt (SI) at the second discharge and Sand –Silt at the first discharge. Boulders were only present for the second discharge. Only 33% (124 points) of the points showed a change in substrate type. The changes did not follow a clear pattern of numbers of points changing from one class to another. No conclusions could be drawn from the analysis of substrate types.

2. General Linear Models

Figure 8.15 shows the results (LS mean plots) for the categorical variables and the change of depth from Q_2 = 0.53 m^3s^{-1} to Q^1 = 1.4 m^3s^{-1}. Results for all the General Linear Models [Change in depth ~ mesohabitat type where mesohabitat type is coded as Deep Glide, Shallow Glide and Riffle], [Change in depth ~ flow type, where flow type is coded as Smooth, Ripple, No perceptible flow, unbroken standing waves and broken standing waves] and [Depth changes~ substrate type, where substrate is coded as gravel, silt, clay, cobble, sand and boulder] showed that there was evidence to reject the null hypothesis ($p<0.001$). The analysis was based on the qualitative variables characterised at the second discharge measured since these data included the real values obtained during the field data collection procedure.

Mesohabitat types showed differences in depth change for the three mesohabitat types analysed. Higher depth changes were observed in riffles, whilst deep glides show the smallest changes in water depth (Table 8.15). This behaviour did not coincide with the behaviour observed at the Leigh Brook river site for all points.

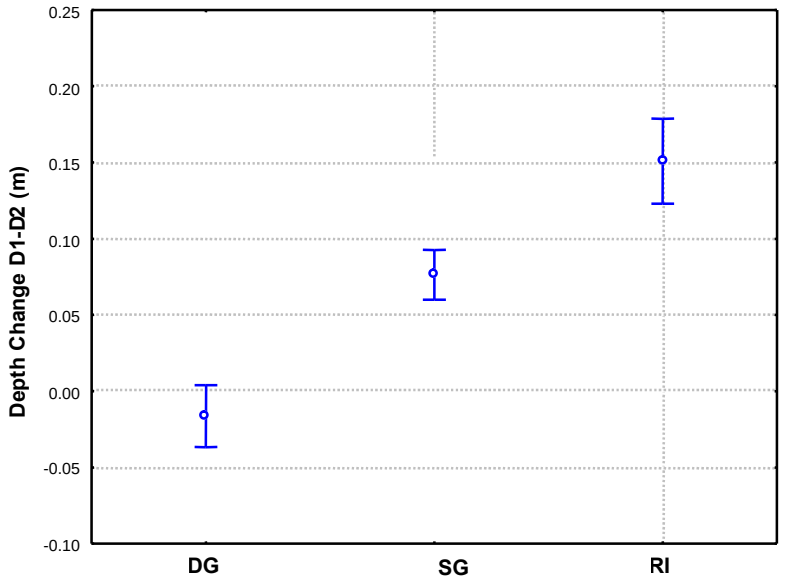

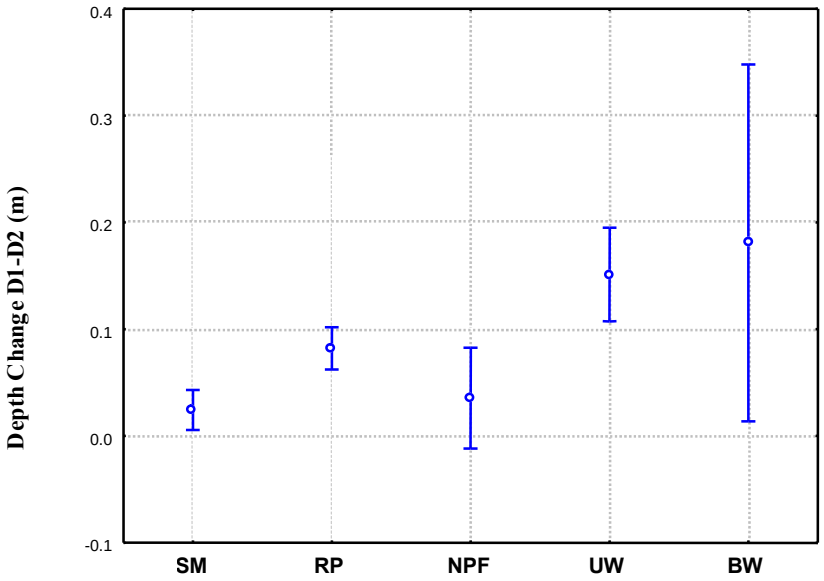

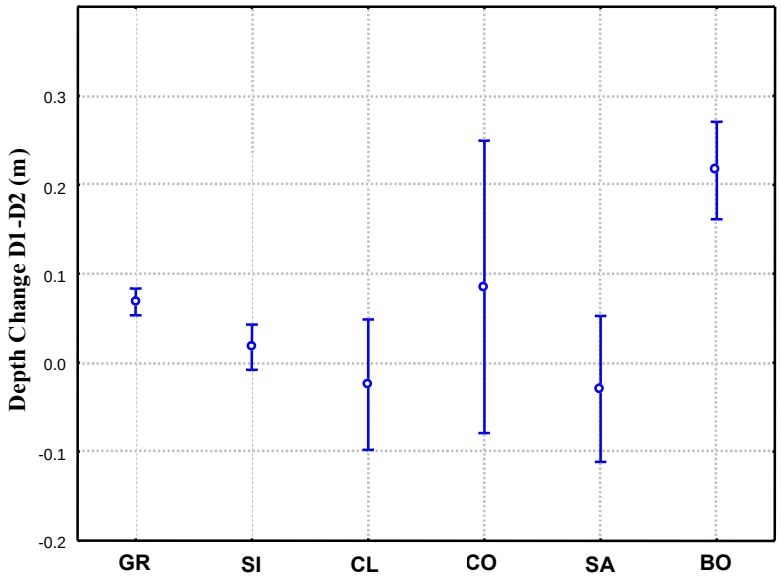

Figure 8.15: results obtained for the following GLM [Change in depth ~ mesohabitat type where mesohabitat type is coded as Deep Glide –DG-, Shallow Glide –SG- and Riffle –RI-], [Change in depth ~ flow type, where flow type is coded as Smooth –SM-, Ripple – RP-, No perceptible flow –NPF-, unbroken standing waves –UW- and broken standing waves-BW-] and [Depth changes~ substrate type, where substrate is coded as gravel –GR-, silt-SI-, clay-CL-, cobble-CO-, sand-SA- and boulder-BO-]. D1 corresponds to depth at discharge Q^1 = 1.4 m^3s^{-1} and D2 corresponds to discharge Q_2= 0.53 m^3s^{-1}.

Results for the flow types indicated that unbroken standing waves (UW) presented the highest change in depth when increasing the discharge and that smooth, rippled and no perceptible flow type did not significantly differ in the increase of water depth due to changes in discharge. Note that broken standing waves (BW) presented the widest confidence interval due to the few points that were identified for this flow type. Therefore no discussion on this flow type is included in this section.

Table 8.15: descriptive statistics for the different parameters of change grouped by mesohabitat types (Q= 0.53 m^3s^{-1}) for the Windrush river site. None standardised parameters.

	Descriptive Stat.	Shallow glide	Riffle	Deep glide
Depth Change (cm)	Mean	7.6	16.4	-1.6
	Minimum	-18.6	-17.2	-42.4
	Maximum	24.0	35.6	61.9
	Std. Dev.	5.8	11.5	16.11
Total number of points		180	70	116

Finally, the General Linear Model analysis for substrate types showed that boulders can be considered significantly different to the other substrates in terms of increase of depth when changing the discharge. Boulders were followed by Gravel substrate type in terms of increase of depth. Gravel is different to boulder, silt, clay and sand. Silt, clay, cobble and sand did not present significant differences between them in terms of depth change originated by changes in discharge.

8.4.3. The variogram as a tool to detect temporal changes

Figure 8.16 shows the values of range, sill and nugget obtained for each river site at the different discharges. The discharges at which data were collected were not coincident for all the river sites. This made comparison of the results between river sites difficult. The variograms were fitted with the spherical model, azimuth tolerance = 60, azimuth = 0 (along the river), maximum distance = 30 m and lag distances equal to 0.5 m and 1 m for wet points and wet & dry points, respectively. These values were selected according to the sensitivity analysis carried out in Chapter 5. Extreme values were found for some of the river sites and excluded from the analysis.

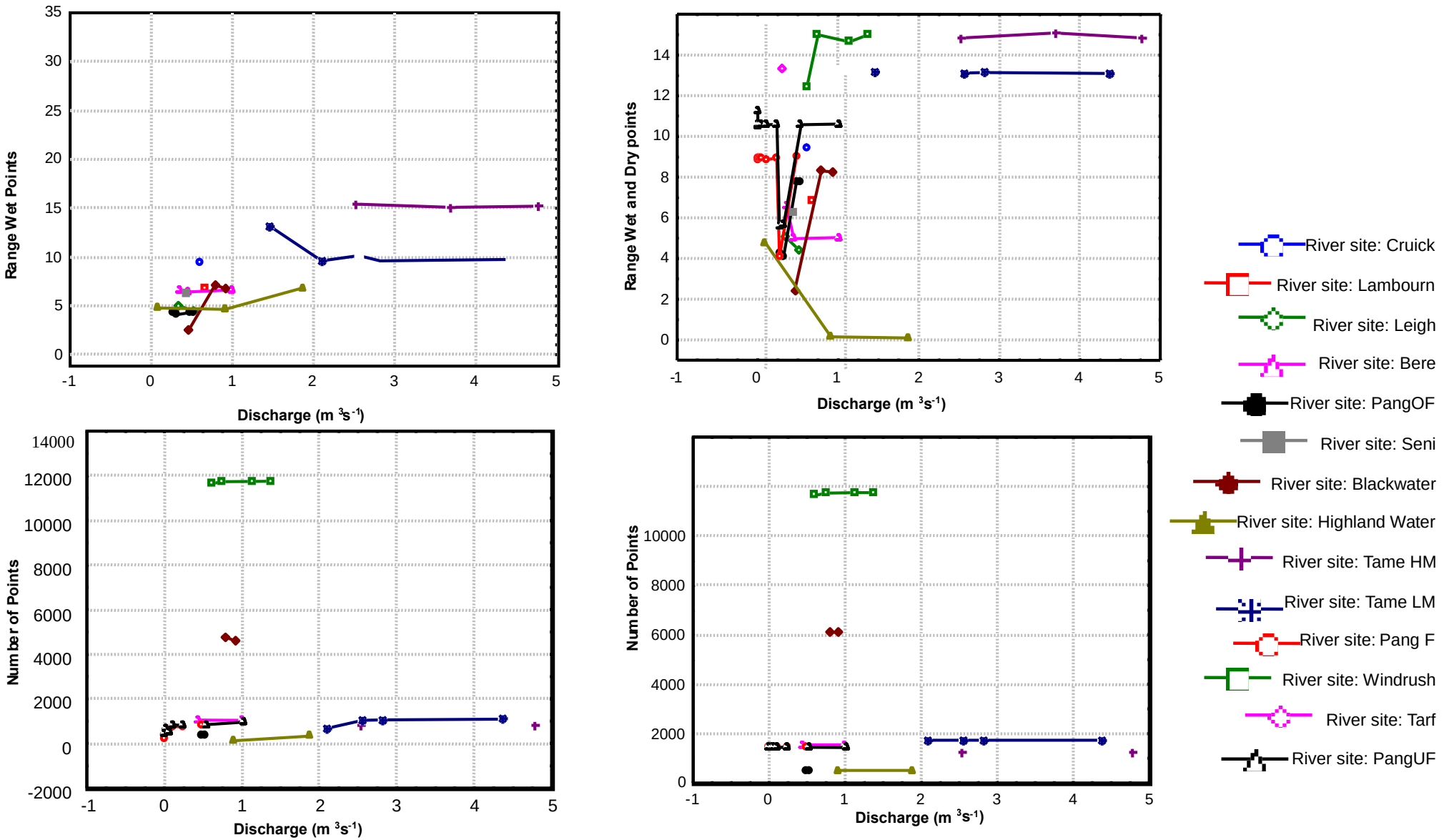

Figure 8.16: values of range obtained for the analysed river sites at different discharges. Left top – results for the wet points, where wet corresponds to positive depth. Right top – results for the dry + wet points, where dry and wet are negative and positive depths respectively. Images on the bottom show the number of points used for each variogram calculation.

Results for the analysis with only wet points indicated that for the majority of river sites, the range increased when decreasing the discharge. The variability of depth seemed to increase between points when decreasing the discharge. The Windrush and the Blackwater presented different behaviour: here range values decreased when decreasing the discharge.

Range values for the analysis with wet and dry points showed the same pattern as that observed for the wet points. Windrush and Blackwater, accompanied by Pang Old Fenced, followed the opposite pattern than that observed for the majority of the river sites. The fact that the patterns were respected for both analyses indicates that the changes detected by the variogram were a consequence of changes in depth variation encountered when changing the discharge and not a consequence of the sensitivity of the variogram to the number of points sampled.

For all of the analyses the pattern of change depended upon the river site being analysed. Modified river sites such as the Tame Highly Modified and the Tame Less Modified presented smaller variation of range, sill and nugget values. This was not associated with the number of points used for the data analysis.

No clear pattern was identified for the sill and nugget values for analyses of wet and dry points and only wet points. The variation between different discharges was not as significant as that encountered for the range parameter. No values of variation are provided since there were just few points represented for each river site.

Note that for this study, the channel bed was considered constant for all the discharges analysed. Thus, changes identified by the variogram only represented the variation introduced in the system by a decrease/ increase of water level as a consequence of the discharge, without considering the actual modification of the channel bed produced by this increase (e.g. erosion of the bank or bed channel, deposition of debris, vegetation growth, among others).

8.4.4. Analysis of river width

Figure 8.17 (top) shows the width from bank to bank obtained at each discharge for each of the cross sections considered for the Windrush. Results show that width did not change for the majority of cross-sections except for those located at distances downstream between 80 m to 120 m (Figure 8.17 bottom), where an island was located. Figure 8.18 shows the Windrush at two different sections of the sampled reach

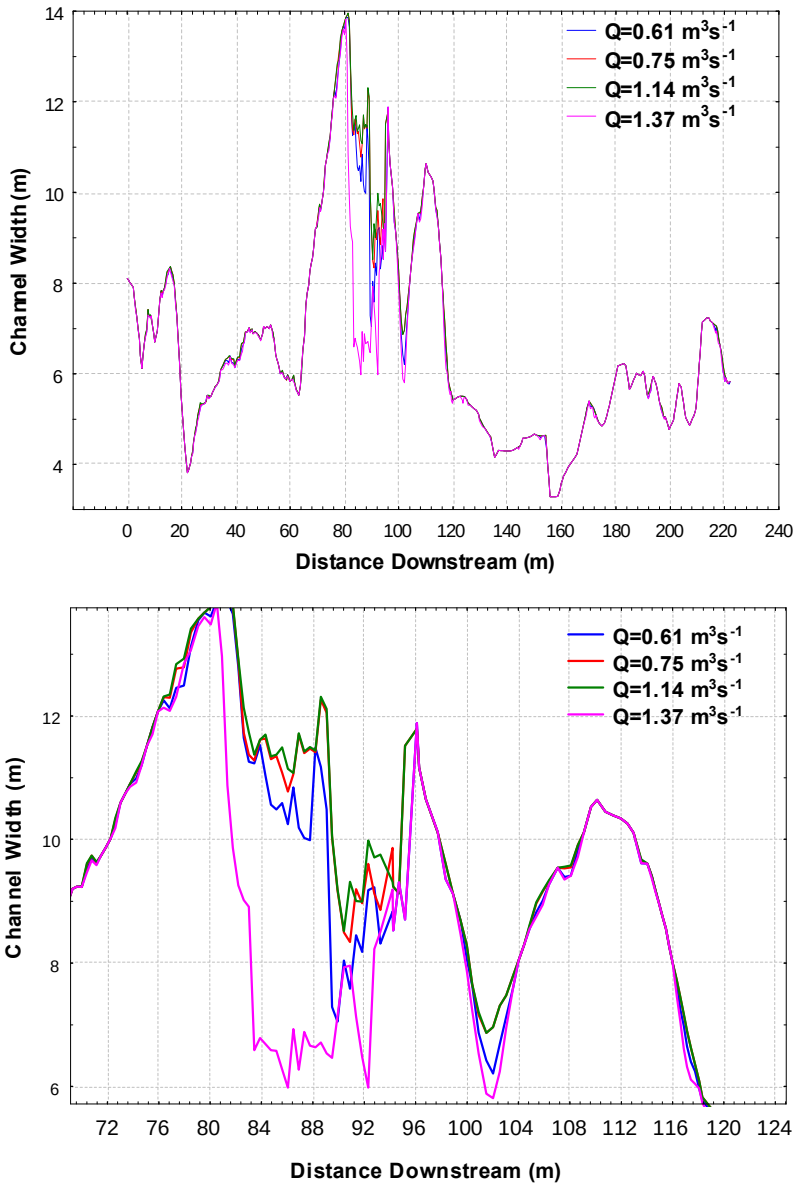

Figure 8.17: width obtained at each of the 586 cross-sections calculated (top) and a detail for those cross sections where the changes in width can be observed between discharges (bottom). Note that the x axis represents the distance downstream where the cross-section is located. Changes have been considered linear between two consecutive cross-sections.

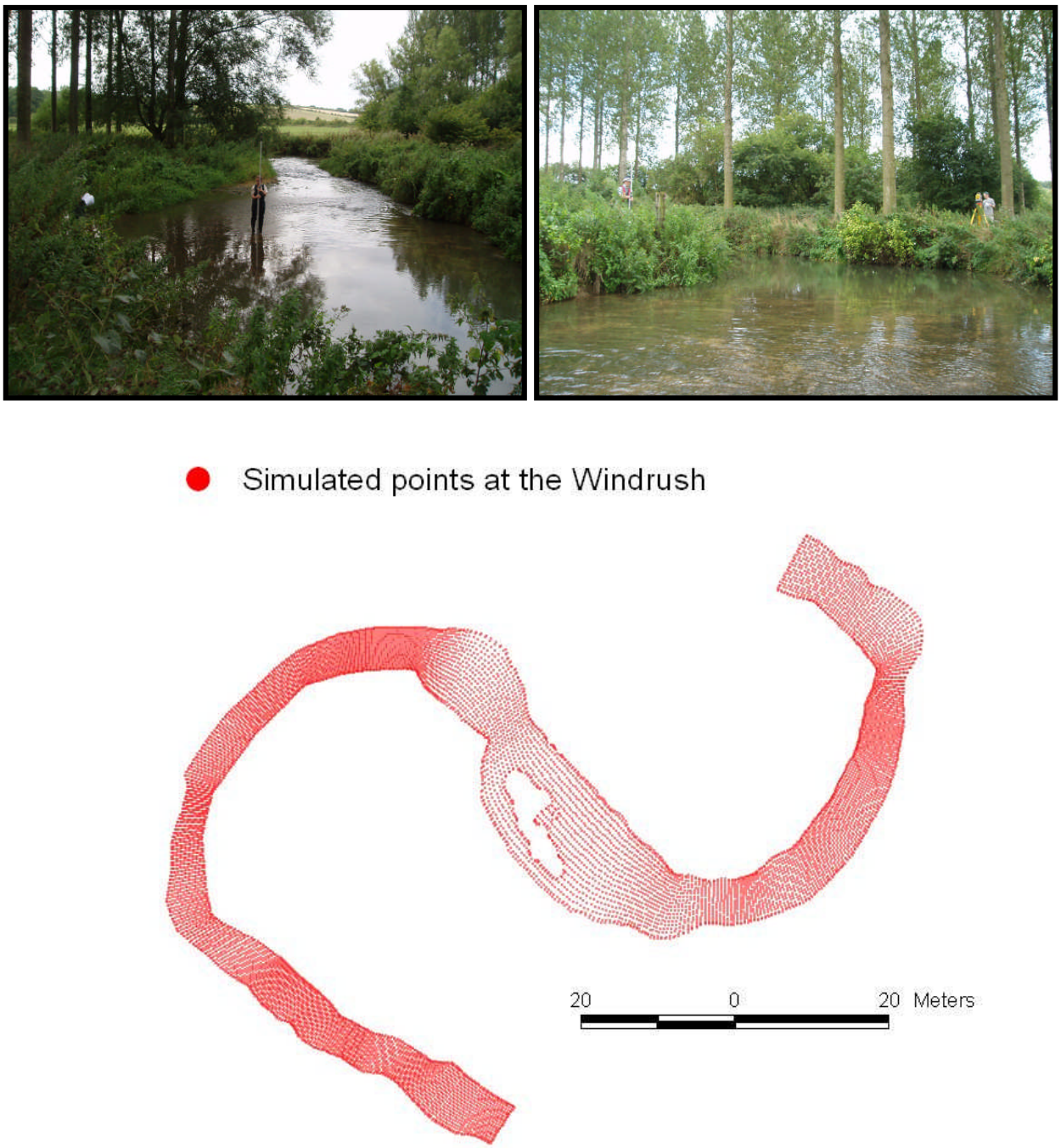

Figure 8.18: photograps taken at the Windrush river site at two different sections of the sampled reach (top) and map with the simulated data (bottom).

Table 8.16 summarises the changes in width obtained when comparing the width at discharge 0.61 m^3s^{-1} with the others (width at Qx - width at Q=0.61 m^3s^{-1}). Mean differences increased when increasing the discharge, except when considering widths at discharge 1.37 m^3s^{-1} where mean width increase was smaller than for discharge

1.14 m^3s^{-1}. The distribution of the width changes were not Normal when assessing the skewness and the kurtosis coefficients. The distributions were significantly peaked and shifted to the right. The mean width values for each discharge are presented in Figure 8.19.

Table 8.16: descriptive statistics width obtained for the difference between width measured at discharge 0.61 m^3s^{-1} and with at the specified discharge. Positive values indicate increase of width and negative values decrease in width.

Discharge compared	Mean (m)	Minimum (m)	Maximum (m)	Variance	Skewness	Kurtosis
0.75	0.15	-0.37	4.84	0.50	5.17	26.10
1.14	0.22	-0.18	5.60	0.75	4.76	22.31
1.37	0.21	-0.18	5.55	0.71	4.83	22.93

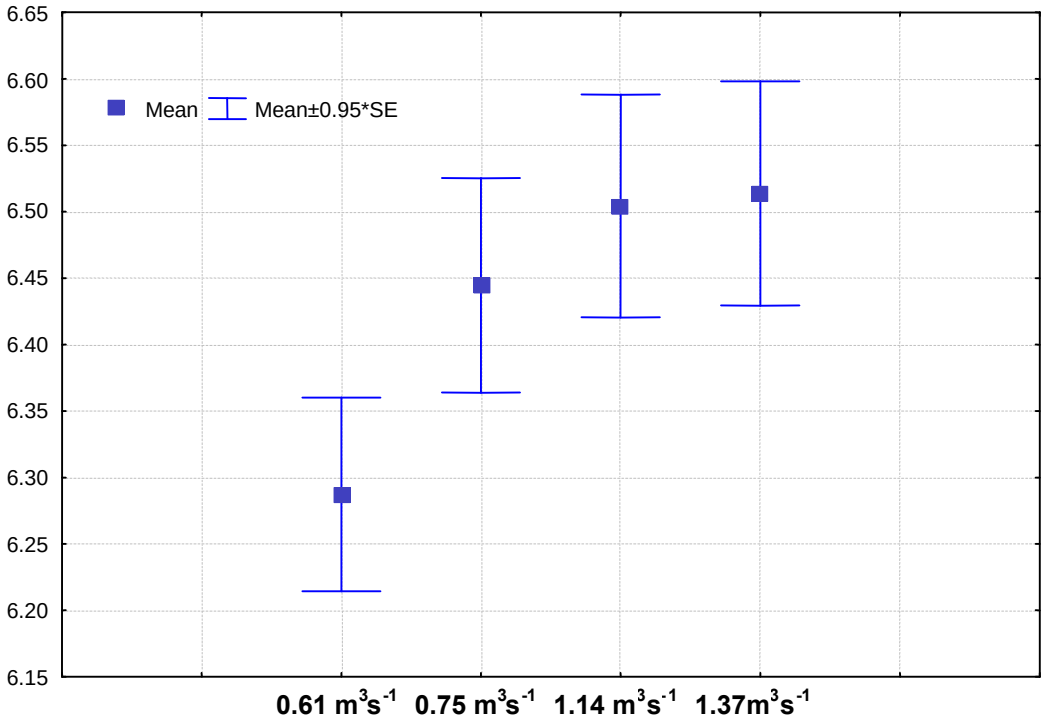

Figure 8.19: mean width obtained for each discharge considered. Vertical lines denote 0.95 times the Standard Error.

8.5. Discussion

8.5.1. Hydromorphological changes due to variations in discharge.

Two different river sites, the Leigh Brook and the Windrush, were analysed to determine how specific changes in discharge affected mesohabitat and flow types. The Leigh Brook river site was characterised by a sequence of shallow glides, deep glides, riffles and pools whilst the Windrush was mainly represented by a sequence of shallow glides and deep glides. Two different discharges were considered for each river site: 0.52 m^3s^{-1} and 0.34 m^3s^{-1} for the Leigh Brook and 1.4 m^3s^{-1} and 0.53 m^3s^{-1} for the Windrush.

Mesohabitat and flow types that were most affected by the change in discharge were not consistent for both river sites. Shallow and deep glides showed the most significant changes for the Leigh Brook river site, whilst riffles, deep glides and pools were the most affected for the Windrush river site for the discharges investigated. These differences might be related to the type of river analysed and the two discharges considered at each river site. The differences in sequences of mesohabitat types, the surface occupied by each mesohabitat type and the physical characteristics of each river site might explain the differences encountered between the rivers. Different typologies have identified the fact that changes in discharge have different effects according to the river type that is being analysed (Leopold, 1994, Brierley and Fryirs, 2000, Rosgen, 1994, Rosgen 1994, Brierley and Fryirs, 2005) Changes in discharge do not affect to the same extent all rivers (Leopold, 1994)); small rivers accommodate an increase in discharge by increasing both depth and velocity in nearly equal amounts whilst large rivers (e.g. the Amazon) show a clear increase in velocity only. However, for both river sites it was possible to identify the following sequence of changes: *pool – deep glide – shallow glide – riffle* that defined the changes that could be expected when increasing or decreasing the discharge. This is in agreement with the theory explained by Leopold (1994); at low flow the pool-riffle sequence is more evident and it is characterised by alternating flat reaches of low gradient and steeper reaches involving white water. When discharge increases the longitudinal profile of the water surface becomes less stepped and the riffle is "drowned out" changing to glide mesohabitat type.

The fact that pools changed to both deep and shallow glides when decreasing the discharge at the Windrush site might be explained by the quantity of change of discharge considered. The change in discharge at the Windrush was high enough to make some points located in the pools decrease two consecutive steps on the proposed sequence, down to shallow glides. This might indicate that thresholds of change between consecutive mesohabitat types depend on the mesohabitat type considered and the change in discharge.

In general, when discharge decreases, the deepest areas experience higher changes (in terms of depth) whilst when discharge increases, shallow areas were more affected. Increases in discharge transformed shallow areas into deeper and smoother (in terms of surface flow type) mesohabitat types whilst decrease of the discharge transformed deepest areas into shallower and less smooth mesohabitat types in terms of surface flow type.

The combined analysis of velocity and depth change results for the Leigh Brook river site indicated that shallow and deep glides were the mesohabitat types that present higher changes in depth and velocity, respectively. Changes in flow were dissipated through depth or velocity increments; those habitats that absorbed flow energy through depth (shallow glides) did not present velocity changes, whilst habitats that dissipate the energy through velocity changes (deep glides) did not show significant changes in depth. This is related to the fact that at low flow the gradient of the WSL is small over the pool and steeper over the riffle Leopold (1994). Increase in discharge causes a decrease in the slope of the riffle WSL whilst the gradient over the pool increases. This pattern continues until the discharge is high enough to straighten the water surface profile. The gradient of the WSL is a direct measure of the rate of loss of potential energy associated to the frictional resisting forces Leopold (1994).

Results obtained for surface flow types at both river sites did not show such a clear pattern as those identified for mesohabitat types. In general, flow type increases its intensity when increasing the discharge and decreases intensity with decrease in discharge. However, these relationships could not be identified as the general rule since the opposite pattern was also observed. This suggested that mesohabitat types

were a better tool to predict how a change in discharge is going to affect a river site and how the different hydromorphological features are going to be distributed.

Changes in qualitative classification of the substrate associated with changes in discharge do not present a clear pattern on the direction of change at the Windrush river site. Areas with coarser material (boulders and gravel) present the highest changes in depth. Substrate changes might be due to different causes such as substrate composition (interaction between heterogeneous substrate particles (Leopold, 1994)), channel structure, supply from upstream as well as discharge changes. Channel roughness decreases as discharge increases, which indicates that finer sediments should be encountered when increasing the discharge (Leopold, 1994). However, no pattern could be observed when analysing the changes in substrate. This might be associated with the extrapolation procedure used to assign the substrate type for the first discharge analysed at the Windrush site. Substrate presented more variability in space than depth and velocity. Therefore higher errors might be expected when obtaining the substrate classification for the first discharge as these values might not represent the true situation during the first discharge.

The analysis of dry points at the Leigh Brook river site showed that riffles and pools, followed by shallow glides, were the mesohabitat types that are more affected when decreasing discharge. The fact that pools were one of the mesohabitat types more affected was the most relevant since this mesohabitat type was not predominant at the Leigh Brook river site, which was characterised by a sequence of riffles and shallow glides. Flow types that were more affected when decreasing the discharge at the Leigh Brook river site are ripple, smooth and no perceptible flow.

8.5.2. The variogram as a tool to detect temporal changes.

Temporal variation in rivers could be caused by different factors: changes in the sediment regime, changes in the energy distribution, change in discharge or anthropogenic changes to channel structure, among others. The analysis carried out in this chapter to determine if the variogram was a useful tool to detect temporal changes only considered changes in the system due to variations in discharge. The bed channel was considered constant and invariable for all the discharges analysed at each river .

site. Results show that it was possible to observe changes between river sites and discharges in terms of variogram model parameters. However, the number of discharges considered was not enough to quantify the changes of the variogram for specific changes in discharge. It would be necessary to develop the study for a higher range of discharges that was comparable between river sites.

8.5.3. A brief analysis of river width.

Width analysis was carried out with data obtained from a hydraulic model for the Windrush. Results indicate that higher changes in river width were identified where the island was located. No conclusion could be established for this study since the data analysed were only from a short river reach.

8.6. Conclusions

Hydromorphological features such as mesohabitat and flow types respond to changes in discharge differently according to the characteristics of the river site and the increment of discharge being considered. A clear sequence of change was identified for mesohabitat types. This sequence steps from pool to riffle in the following order: pool – deep glide –shallow glide – riffle for decrease in discharge and vice versa for increase in discharge. The rate of change of discharge at which each mesohabitat type is transformed into a consecutive class depends on the mesohabitat type being considered. Further studies should be addressed to assess at which discharge increment/decrement the mesohabitat change is observed.

Riffles and pools are the mesohabitat types which present a higher number of dry points when discharge decreases. The monitoring of these mesohabitat types in terms of changes of the wetted perimeter or river width would be necessary if the sensitivity of river to water abstraction were to be assessed.

Flow type presents more spatial variation in space than mesohabitat types and thus, it is not possible to identify a clear sequence of change. The spatial variation of flow type is equal or even higher than the temporal variation. Mesohabitat types are a

better tool to assess how hydromorphological features are affected by changes in discharge (e.g. water abstraction). Further research is also needed to understand the hydraulic performance of mesohabitat and flow types.

The variogram could be a potential tool for the quantification of temporal changes in rivers. Further studies need to be developed for a more complete set of discharges.

9

Discussion and conclusions

This chapter discuss the outputs obtained from the research developed in this study focusing on the different sources of random error that can be encountered when characterising hydromorphological parameters. A set of guidelines are presented for the design of sampling strategies for depth, velocity and substrate. The scaling and temporal uncertainties are also discussed in this chapter. Further research ideas are proposed and conclusions drawn in the last section of this chapter.

9.1. Introduction

Collection of data on the physical habitat of rivers can be required for several purposes; for example the assessment of the ecological implications of water abstraction, historical habitat degradation or river restoration. Collection of such data can be costly and time consuming, so it is necessary to design effective and efficient sampling strategies, both in terms of spatial intensity and extent, and in terms of repetition of sampling (e.g. at different discharges).

This study has focused on the study of the uncertainties associated with the design of effective sampling strategies and monitoring programmes. Three main uncertainties were addressed in previous chapters: spatial, scale and temporal uncertainties. The spatial uncertainty refers to optimal sampling strategies in terms of trade-off between acceptable error and location and number of points. The scaling uncertainty focuses on assessing the river length that needs to be sampled to characterise spatial variability of a river site. The temporal problem examines how many times a river site needs to be sampled to characterise the temporal variability associated with changes in discharge.

The methodology applied to examine these uncertainties relies mainly on geostatistical theory (interpolation techniques). Interpolation techniques can be used

to predict values of the variables under study for non-measured locations or occasions. In this way, it may not be necessary to collect detailed data sets of information in time and/or space. This chapter discusses and summarises the output of this research. A set of guidelines for hydromorphological data collection are presented.

9.2. Discussion and recommendations for further research

9.2.1. Guidelines for hydromorphological data collection

Different sources of error or uncertainty are associated with the characterisation of hydromorphology in rivers as well as to the application of interpolation techniques (i.e. geostatistics). Table 9.1 summarises the sources of uncertainty that are associated with the different steps of measurement error when characterising hydromorphology. Measurement error is divided into systematic and random error. Systematic errors are biases in measurement which lead to measured values being systematically too high or too low whilst random error is present every time that a point is measured but varies unpredictably in size and direction (Muste, 2002). It is necessary to define and quantify these different sources of error/uncertainty to better interpret the data collected. This study has focused on the analysis of some components of the random error. The following sections discuss as a set of guidelines the uncertainty associated with (i) the equipment that is being used for depth data collection, (ii) the sampling strategy applied for the collection of data and (iii) the sampling density applied. Systematic error values can be obtained from the information on the equipment performance.

Table 9.1: components of measurement error associated to hydromorphological data collection.

Action	Measurement Error	Description
Depth -Velocity - Substrate measurement and mesohabitat - flow type identification.	Systematic Error	Equipment used
	Random Error	Equipment used Expertise of the surveyor River type Sampling conditions

a. Random error associated to the equipment type: Guidelines for the equipment to be used.

The first source of random error identified is that associated with the type of equipment that is being used. Only the analysis of the equipment available for depth data collection (i.e. total station and metric staff) was carried out. There was only one set of equipment available for the measurement of velocity and thus, the random error associated to this procedure could not be calculated. However, studies have already been developed on the performance of different set of equipment for velocity measurements. Results indicated that velocity data when measured by an Acoustic Doppler Current Profiler (ADCP) are inherently noisy because of the turbulence, instrument noise and variation in environmental factors such as water and scattered properties (Shields and Rigby, 2005). The different sources of noise associated to velocity data collection with ADCP are described by Muste et al (2004a, 2004b) and a set of guidelines provided for its quantification. River velocity profiles obtained from moving boats varied ±20% to those measurements obtained with the same set of equipment at a fixed location (Muste et al, 2004b in Shields and Rigby, 2005). Studies on the comparison of two different laser-based velocimeters have also been carried out (Muste et al, 1998).

Random error associated to the "equipment" or in this case, methodology, applied for the characterisation of mesohabitat and flow types was not analysed. Different methodologies are available for the characterisation of these qualitative variables as described in Chapter 2. Each methodology is based on different thresholds levels of velocity, depth and substrate for the establishment of mesohabitat and flow types. Moreover, different types are defined by each methodology. The typologies proposed are based on the visual observation of hydromorphological features and therefore a degree of subjectivity in the classification is expected. Thus, mesohabitat and flow type classifications depend upon (i) the methodology applied for the classification, (ii) the expertise of the surveyor (it varies between surveyors and even for the same surveyor – low reliability) and (iii) the variability, in terms of mesohabitat and flow types, encountered at the river site. A study (Maddock et al, 2006) is currently being developed in order to identify the differences encountered between four different mesohabitat mapping methodologies (Norwegian Mesohabitat Classification Method,

River Habitat Survey, Rapid Habitat Mapping and MesoCasimir), different surveyors (comparison of 2 surveyors) and to determine the reliability of each surveyor (two repetitions for each methodology). Results for the comparison between the Norwegian Mesohabitat Classification Method and River Habitat Survey are already available (Borsanyi et al, 2005).

The following paragraphs discuss and summarise the results obtained for the quantification of the random error associated with two different sets of equipment for the measurement of depth: the metric staff (MS) and the total station(TS). It also includes the random error associated with two different methodologies (i.e. sampling strategies) for data collection with the total station: heterotopic and isotopic (described in Chapter 3). The discussion presented in this section focuses on the reliability of depth data collection in rivers. Reliability refers to the reproducibility of a measurement and quantified by taking repetitions of the same measurement. In this study the reliability was analysed for the two different types of equipment and associated to the morphological characteristics (i.e. mesohabitat and flow types) of the measured site. Validity, which is the agreement between the value measured and its true value, could not be tested as it was not possible to determine the real value of depth at the sampled locations.

It is necessary to consider the reliability of depth measurement since this can have an effect on the objective for which data were collected. For example, it was found that differences between isotopic and heterotopic depth measurements can give results of channel volume that differ by more than ≈ 3 m^3 (volume varied between 89.1 m^3 to 86.3 m^3 depending on the sampling strategy for an area of 470 m^2).

Reliability of depth measurements according to the equipment and sampling strategy applied.

Table 9.2 summarises the differences encountered between (i) the two sets of equipment, (ii) heterotopic vs. isotopic data sets and (iii) observed Water Surface Level values vs. WSL values predicted with descriptive geometry. The values in Table 9.2 were calculated by averaging the results of all the river sites analysed. The differences encountered were assumed to be independent and therefore, a total value

was provided by adding up the differences encountered in each study. This value corresponds to the measurement/calculation of depth for heterotopic data sets. For isotopic data sets it is not necessary to consider the random error associated to WSL calculation.

Table 9.2: values of differences encountered between metric staff (MS) vs. total station (TS), and heterotopic vs. isotopic data sets. TS vs. MS shows the averaged difference between depth measured with TS and depth measured with MS for all the river sites analysed. Heterotopic vs. Isotopic shows the difference between depth collected following these two sampling strategies. Triangulation refers to the difference between observed and predicted WSL with descriptive geometry when locating the WSL 10 m apart from each other.

Parameter	TS vs. MS	Heterotopic vs. Isotopic	WSL calculation Triangulation	Total
Mean Error (cm)	2.25	3.3	4.29	9.84
Maximum absolute difference (cm)	6.20	12.36	16.03	34.6
Mean difference (cm)	2.00	1.08	3.40	6.48

Differences between the sets of equipment were not as large as those encountered between sampling strategies (Table 9.2). Isotopic data sets require a measurement of a WSL on the same vertical line as the topographical points measured. This makes the measurement of WSL more difficult than for heterotopic data sets since there is an added source of random error associated to the collection of WSL data. Sampling conditions (e.g. weather conditions), surveyor expertise (e.g. accuracy in the readings associated to the proper application of the equipment), surveyor physical characteristics (e.g. height and weight of the surveyor are associated to the ability to stay still at the site during the measurement and to the accuracy with which the measurement is being taken) and characteristics of the river type (e.g. substrate or discharge are important when locating the staff vertically for the measurement of the water surface level) make it difficult to locate the total station staff in the same vertical line as the measured topographical point. Isotopic data sets are difficult to collect and do not provide any advantage in relation to the heterotopic data sets; points are difficult to locate on the same vertical line and therefore, the same procedure and source of error as that associated with the heterotopic data sets is encountered. Heterotopic data sets are recommended for depth data collection since (i) the error introduced is not much larger than that obtained between sampling equipment (MS and TS) (ii) they are easier to collect and (iii) isotopic data sets have horizontal deviation between WSL and topographical (TO) points of about 10 cm.

Reliability of depth measurements depending on the mesohabitat and flow type at the sampled point

All natural rivers are characterised by unsteady (depth and velocity vary in time), nonuniform (depth and velocity vary along the reach) flow that present super-critical (high velocity and low depth, described as rapid or shooting) and sub-critical flow conditions (low velocity and high depth, described as calm and tranquil) (Mount, 1995 and Julien, 2002). When throwing a stick into flowing water at super-critical flow conditions, the ripples formed are swept in the downstream direction whilst in sub-critical flow conditions the ripples move upstream from the source of disturbances Pools and runs are characterised by sub-critical flow conditions whilst super-critical flow conditions are representative of riffles (occasionally) and chutes.

Rippled surfaces are encountered under turbulent, unsteady, non-uniform and generally supercritical flow which corresponds to situations such as hydraulic jump and flow separation processes. In the hydraulic jump situation, there is a change from supercritical to sub-critical conditions that transforms the kinetic energy (velocity) of the flow into gravitational energy (depth). This change from Froude number >1 to Froude Number <1 creates turbulence on the water surface (Mount, 1995). Flow separation processes occur when an obstacle is present on the channel bed. In the presence of an obstacle such as a boulder (i.e. increase of pressure), the friction of the system increases, decreasing the kinetic energy of the laminar layer. The laminar layer is characterised by low kinetic energy and a reduced depth. Thus, the fluid immediately upstream of the turbulent boundary layer collapses with the fluid on the laminar layer and it is displaced outwards (separation point), separating it from the bed. This fluid is reattached to the bed channel downstream (reattachment point). A separation bubble is created between the separation and the reattachment point. This separation bubble creates eddies, vortices and/or rollers on the surface as a consequence of the loss of direction in the separated flow (water detached from the bed enters the main current as a free shear stress layer with sub-critical turbulent flow conditions and this causes water to go in all directions (Mount, 1995)).

The rippled surfaces produced by the eddies, vortices and rollers make it difficult to (i) position the total station staff on the water surface level, (ii) vertically position the

total station staff on the channel bed for the topographical measurement and (iii) accurately obtain readings from the metric staff. In addition, deep areas present the difficulty of positioning the total station staff at high level which makes it difficult to hold the staff vertically for the reading.

Results obtained were consistent with the above explanations. The metric staff provided larger readings than the total station in shallow areas and lower readings in deep areas; measurements obtained with the total station could be up to 12 cm larger than those detected with the metric staff when collecting data in shallow areas and 10 cm lower when collecting data in deep areas (> 0.5 m). This is due to the difficulties identified when obtaining the readings with the metric staff in fast flow shallow areas and when positioning the total station staff in deep areas. Mesohabitat types characterised by fast flow (riffles and chutes) were the features with highest differences between equipment types (≈4 cm), whilst mesohabitat types characterised by slow flow and smooth flow type showed the lowest differences between equipment sets. This is explained by the eddies, vortices and rollers that are encountered in chute and riffle mesohabitat types. Similarly, flow types that characterise chutes and riffle mesohabitat types presented the highest differences (≈4 cm) between sets of equipment. Thus, it is suggested to take measurements with MS in deep areas (> 0.5. m) and measurements with TS in shallow points.

Reliability of depth measurements depending on the methodology applied for Water Surface Level interpolation.

The value of depth also varies according to the methodology that is used to represent the water surface level (WSL) along the reach analysed. The gradient of the water surface changes along the reach being sampled according to the diversity of hydromorphological features present at the site and the discharge during the data collection. At low flows, pools have a lower gradient than riffles. This gradient becomes more homogeneous as discharge increases (Leopold, 1994). Different methodologies to determine the WSL at non measured locations provide different levels of accuracy in determining the changes of WSL gradient. When comparing geostatistical interpolation with descriptive geometry it was possible to observe that mean absolute differences (ME) are ≈5 cm, with maximum absolute differences that

can be larger than 30 cm in depth. It was not possible to determine the validity of the measurements as no true value of the location of the water surface level and its steepness could be calculated.

When applying geostatistics (kriging) for the prediction of WSL, it was found that the gradient of the WSL could be ignored at the river sites analysed since WSL was highly spatially correlated (i.e. spatial correlation is high over long distances (more than 27 m)). These results were consistent with those obtained for the prediction of WSL with descriptive geometry; the further apart the points were located, the higher the accuracy in the predictions (maximum distance between points equal to 20 m). This may be explained by the fact that a higher number of points sampled along the reach defines a higher number of triangles for the calculation of the WSL. Three WSL sampled points create a triangle that defines a slope gradient on the WSL. Each triangle is associated to a source of random error and therefore, when considering the whole water surface level at the sampled reach, the WSL is defined by a set of triangles of different slope orientation that might not show any continuity between consecutive triangles. A smoother surface is defined when spacing the WSL sampled points further apart from each other. However, it is necessary to consider the different morphological features present in the reach that is going to be sampled when applying descriptive geometry for the calculation of the WSL; reaches where changes in WSL slope are present (e.g. chutes or cascades) would require a more intensive sampling strategy.

It is recommended to apply descriptive geometry (or any form of linear interpolation) for the prediction of WSL at non measured locations since (i) a smaller number of measurements is required and (ii) the difference between predictions obtained with geostatistical interpolation (kriging) and descriptive geometry have been quantified and show similar values to those differences obtained between total station and metric staff.

b. Random error associated to the sampling strategy: Guidelines for the design of a sampling strategy

Predictions of depth obtained with geostatistical interpolation techniques (kriging) depend upon different factors such as the position of the points along the sampled reach. The distribution of the sampled points determine the lag distance required for the variogram calculation, the goodness of fit of the variogram model as well as the distance of neighbourhood search required for the kriging procedure. This section summarises and discusses the results obtained for the comparison of different sampling strategies carried out in Chapter 4.

It is recommended that grid sampling strategies be applied when characterising the spatial pattern of depth, velocity and Froude number rather than applying any type of transect sampling strategy. Results obtained with regular or stratified transects have been shown to be highly sensitive to the number of points sampled, as well as to the location of these transects. In general, regular grids provided better results than random and stratified grid sampling strategies, the latter being the worst in the grid sampling range. The use of random grids should be preferred to the use of stratified and regular grids since (i) results obtained for random grids do not significantly differ from those obtained with regular grids and (ii) random sampling strategies (i.e. random walk) are less time consuming sampling strategies. Also, it should be noted that in many cases, stratified grids cannot be applied for velocity measurements as it is difficult to visually identify velocity changes at the river site. Instead, random grids are the preferred sampling strategy.

It is recommended that high resolution data sets be collected for velocity when trying to apply kriging interpolation techniques since (i) the spatial relationship between points is lost at very short distances (between 0.5 m to 5 m) and (ii) worse results are obtained for velocity than for depth when applying the same sampling strategy. Economic factors are the main restriction when proposing the sampling design to be carried out in a river reach and since velocity data collection is more costly and time consuming than any other hydromorphological variable, small sampling densities are usually applied for its characterisation. This makes it impossible to properly calculate the velocity variogram for application of kriging (geostatistics) where more than 50

measurements are required (Webster and Oliver, 2001). Thus, it is recommended that different extrapolation procedures be used for the prediction of velocity values at non measured locations when (i) low sampling densities are being applied and (ii) points are separated by more than $\cong 3$ m.

The use of two and three dimensional hydraulic models such as Depth Integrated Velocity and Solute Transport model (DIVAST) (Falconer et al, 1998) and the SSIIM Computational Fluid Dynamics model (Olsen, 1996, 2000 in Booker et al, 2004b and Wilson, C.A.M.E., 2000) for the prediction of velocity at non measured locations can overcome the above limitations. These models have already been successfully applied in ecohydraulics (Bockelmann et al, 2004 and Booker et al, 2004b) and although they have some limitations, they provide "acceptable" results for velocity and depth. For example, results for different applications of the SSIIM model showed that when testing predicted velocity against field observations the correlation value was R^2 = 0.688 (Booker et al, 2004) and R^2 = 0.77 (Nicholas and Sambrook, 1999).

The limitations encountered for the interpolation of velocity with geostatistical techniques can also be overcome with the application of the co-kriging of depth and velocity. Co-kriging is "a natural extension of kriging when a multivariate variogram or covariance model and multivariate data are available" (Wackernagel, 2003). This means that if there is a spatial relationship between the variables the measurement of the first variable (depth) can be used to improve the prediction of the second variable (velocity), which has been sampled at a lower density. Heterotopic or isotopic co-kriging are potential solutions since depth can be easily measured at those points where velocity has been sampled.

For Froude number characterisation it is recommended to space sampling points less than 9 m from each other as this is the point at which the spatial correlation between points is lost. Similarly to velocity, it would be possible to apply co-kriging to Froude number due to the relationship that exists between this variable and depth and velocity.

The differences that could be encountered between sampling strategies in terms of Mean Error between predicted and observed values are equal to 7.6 cm for depth (ME between 8.4 cm and 16 cm for the Austrian channel and between 1 cm to 6 cm for the Leigh Brook), 0.18 ms^{-1} for velocity (ME between 0.008 ms^{-1} and 0.19ms^{-1} for the Austrian channel and between 0.10 ms^{-1} and 0.17 ms^{-1} for the Leigh Brook) and 0.067 (ME oscillates from 0.083 to 0.15 for the Leigh Brook) for Froude Number. These ranges were calculated as the difference between the Mean Error for the best sampling strategy for this indicator and the Mean Error for the worst sampling strategy for the same indicator; only the highest difference of both river sites has been represented. These ranges of difference encountered between sampling strategies are just a guideline since the ranges proposed do not only show the differences between sampling strategies but also the random error associated with the mesohabitat types where the data was sampled, the sampling conditions or the river type analysed. It was not possible to separate these sources of error from the effect that the sampling strategy has on the predicted values.

The comparison of the results in Table 9.2 with the ranges obtained between sampling strategies indicate that differences associated to the type of equipment used for depth data collection, the type of sampling strategy (heterotopic or isotopic) applied for the characterisation of the WSL are less significant than the differences encountered between sampling strategies. No conclusions can be drawn from this comparison since the results obtained for the characterisation of the random error associated to the type of equipment, the sampling strategy for Water Surface Level and the interpolation procedure for WSL represent the situation encountered at two rivers with very different characteristics to those river sites used for the comparison of sampling strategies. Moreover, the equipment used for the measurement of depth and velocity were not the same in both studies. This makes it difficult to establish definitive conclusions regarding the relevance of the different sources of random error. Similar results should be obtained in order to determine the relation between velocity sampling equipment and sampling strategy.

The approach selected to determine the most efficient location of the sampled points consisted of the comparison of different sampling strategies such as regular transects and regular grids. Other potential methodologies for determining the best distribution

of sampled points for the application of geostatistics are available and research should be carried out to compare methodologies. For example, Russo (1984) studied the problem of the sampling network design for the variogram estimation of soil properties (i.e. how best to locate the sampling points in the field in order to obtain a minimum value of MSD (Mean Square Deviation) for the entire domain of lag classes). Bogaert and Russo (1999) expressed the covariance matrix of the parameter estimator as a function of the sampling design. An optimization algorithm was proposed so the way that variogram model parameters are influenced by the choice of a set of sampling locations can be analysed. The issue of defining an effective sampling design has been approached by many other authors as discussed in Chapter 2.

c. Guidelines for the design of a sampling density.

The different objectives for which hydromorphological sampling strategies are defined are diverse and include purposes such as river restoration or morphological quality assessment. Each objective for which hydromorphological data are being collected requires a specific level of accuracy in the representation of the "real environment". For example, for post-project appraisal of river restoration projects (Downs and Kondolf, 2002 in Legleiter and Roberts, 2005) and for morphological estimation of sediment transport (Ashmore and Church, 1998 and Gaeuman et al, 2003 in Legleiter and Roberts, 2005), accurate characterisation of channel topography is critical (Lane, 1998 in Legleiter and Roberts, 2005) whilst less accuracy is required for purposes such as river habitat mapping. Since the list of purposes for which data are collected is wide and the level of accuracy selected is still associated with subjective criteria, a more practical approach has been taken. A set of tables that relates the sampling density to the accuracy of the predicted values have been developed so the end user can relate the level of accuracy wanted with the sampling density required. This accuracy was measured with a series of quantitative indicators. A set of tables with rows describing sampling densities tested and columns describing the indicators analysed, has been provided for each river site (Appendix 4.2). A general table that informs on accuracy obtained for each indicator (e.g. maximum difference between predicted and observed values) and each sampling strategy is also included to summarise the results obtained for all the river sites.

The general pattern for the nine indicators analysed showed that the accuracy of the predictions decreases with sampling density. The point at which the value of a specific indicator starts changing with the sampling density applied differs according to the indicator considered. For the majority of indicators analysed, sampling densities smaller to 0.4 points/m^2 are not detailed enough to provide "real" representations of the river site. Different objectives for which hydromorphological data are collected require different accuracy in each of the nine indicators presented. Therefore, different sampling densities should be applied for different sampling objectives. A set of tables relating sampling density and confidence interval obtained for each indicator are presented in Appendix 4.3.

From the pattern observed it is possible to divide the indicators into two main categories; (i) indicators highly dependent on the sampling density and (ii) less dependent indicators. The indicators which are highly dependent on the sampling density are: maximum difference between predicted and observed values; minimum difference between predicted and observed values; mean difference between predicted and observed values; Maximum Squared Error; MSE; p-value; R-squared and objective function value.

It is necessary to consider that the values shown in Appendix 4.3 are the result of a single random selection of points for each sampling density. No repetitions of the random selection were carried out since results obtained in Chapter 4 indicated that the changes associated with the random selection process were not significant for the final value of the indicator. It was not possible, therefore, to plot the standard deviation associated with each sampling density, river site and indicator. A brief study is presented in Appendix 4.4 where it was possible to observe the reliability of the variogram when selecting different sets of random points for a given sampling density. Webster and Oliver (1992) developed a similar study for an isotropic normally distributed soil property. Results indicated that the variogram variation stabilised when calculating the variogram with more than 225 points. A higher number of points might be required for an adequate determination of the depth variogram since depth is a more variable parameter than soil properties. For example, similar results to those presented by Webster and Oliver (1992) were obtained for the Bere river site when analysing the stability of the range deviation which occurs at a

sampling density of 1.4 points/m^2 (249 points). However, a higher number of points were necessary to properly determine the variogram for the Tame Highly Modified (1618 points for a sampling density of 0.6 points/m^2). It is recommended that the analysis to be repeated in order to account for the reliability of the depth variogram at the highest sampling densities tested; the deviations (standard error) calculated for these sampling densities are not representative since the points selected in each repetition represented a high percentage of the original data set (4 points/m^2) making it impossible not to include the same sampled points in the majority of the repetitions.

Table 9.3 shows the equation that has been obtained to characterise the change in the indicator value in relation to the change in the sampling density. These equations provide a guideline to understand the behaviour of each indicator and they must not be interpreted as an exact relation or a method to generalise to other rivers. The equations obtained for each river site and indicator are presented in Appendix 4.4.

Appendix 4.3 summarises the values of mean difference and maximum difference between predicted and observed depth measurements for different confidence intervals and sampling densities. Even for the most restrictive Confidence Intervals considered (99.9%) and the smallest sampling densities tested (0.2 points/m^2) the confidence interval of *mean difference* of depth value (between predicted and observed values) is smaller (≤0.05 cm) than the random error associated to the type of equipment used, the sampling strategy for WSL (heterotopic or isotopic), the method for the interpolation of WSL or the sampling strategy applied. Nevertheless, when analysing the values of *maximum difference* between predicted and observed depth values it is possible to conclude that for the most restrictive confidence intervals analysed (≥97.5%) and the smallest sampling densities considered (≤1.4 points/m^2) , the confidence interval value is higher (≥ 4.3 cm) than the differences between sets of equipment used for depth characterisation. Therefore, it can be concluded that (i) it is extremely important to adequately select the equipment that is going to be used to obtain depth measurements, (ii) sampling densities need to be appropriately selected when trying to decrease the maximum error in the predictions and (iii) it is essential to consider the random error that this is going to introduce in the final depth measurements.

Table 9.3: equations obtained for those indicators that were highly dependent on the sampling density, where x is the sampling density applied in points per square metre and y is the value of the indicator.

Indicator	Model	Equation
Maximum Difference (m)	exponential	y=0.364*exp(-0.6684*x)
Minimum Difference (m)	exponential	y=0.3013*exp(-0.6465*x)
Mean Difference (m)	exponential	y=0.0379*exp(-3.2402*x)
Maximum Squared Error	exponential	y=0.1565*exp(-1.3306*x)
MSE	exponential	y=0.0046*exp(-1.8527*x)
P-value	polynomial	$-0.2033+0.6964*-0.044*x^2$
R-squared	logarithmic	Y=0.9125+0.1908*log10(x)
Objective function	exponential	Y=295.0299*exp(1.0559*x)

During the data collection procedure it is necessary to apply higher sampling densities in deep areas (deep glides and pools) of the reach when measuring depth. This is due to the fact that the variogram is not able to predict the extreme values of the depth frequency distribution. The measurement of deep areas in more detail will allow the identification of the peaks of variability in the semivariograms and so, higher levels of accuracy will be achieved when predicting hydromorphological parameters in these areas.

The variogram has been able to detect differences in the spatial structure of the river sites analysed. Different sampling densities should be applied at each site; river sites with a high degree of variation in space will need higher sampling densities in order to obtain the same level of accuracy as river sites with low spatial variation or in other words, the higher the hydromorphological uniformity and continuity of the river site, the lower the sampling density that needs to be applied.

It is necessary to take into account that the analysis of sampling densities did not consider sampling densities smaller than 0.2 points/m^2 and considered that sampling densities of 4 points/m^2 represented the "real" hydromorphological situation for the reach. Therefore, the Confidence Intervals obtained can only be applied when the objective for which data are being collected allows consideration of sampling densities of 4 points/m^2 detailed enough for the representation of the real situation. In those cases where more detailed information is required a further analysis and set of tables should be developed. Similarly, higher spatial scales than those considered in this study will require less degree of detail in the information collected. The general

scale sampled in this study corresponds to 200 m, which corresponds to mesoscale level. Therefore, further analysis should be developed to identify the adequate sampling density required at macroscale level.

d. Guidelines for the interpolation procedure.

The spatial structure up and down a river differs from that encountered for the cross-stream direction. Rivers present different characteristics in terms of shape, vegetation, location and form of bars for each cross-section being analysed (Leopold, 1994). The characterisation of the cross-sectional spatial pattern (i.e. anisotropy) is difficult unless intensive data sets are collected. Therefore, it is suggested to give priority to the longitudinal variogram when analysing the spatial structure of depth at a river site. The longitudinal variogram reduces the above limitations by considering all the information provided by points collected in both directions. Using an azimuth tolerance up to 60° is necessary to understand the differences in the spatial pattern across and along the river.

Results obtained showed that it is necessary to carry out a sensitivity analysis when fitting the variogram model (see Chapter 5). The sensitivity analysis has to focus on the study of the number of pairs of points available, the lag distance, the maximum distance, the azimuth tolerance and the azimuth.

The variogram cloud is able to detect differences between the spatial structure of the channel bed and the spatial structure of the river banks. This suggests that the variogram cloud could be used as a tool (i) to describe the hydromorphological characteristics (depth) of the channel and (ii) to detect the temporal changes of the hydromorphological characteristics of the river. The variogram cloud is more informative than the empirical variogram when trying to study the spatial structure of a site. The empirical variogram is an average of the values obtained in the variogram cloud. It is suggested to use the variogram cloud as a complementary tool to the empirical variogram.

e. Guidelines to determine the length of the reach to be sampled.

The maximum distance that can be considered for the variogram calculation is a limiting factor when determining the spatial structure. The maximum distance that can be considered is always smaller than the total distance sampled (from 1/2 to 1/3 of the total distance sampled). This means that the distance sampled needs to be longer (from two to three times longer) than the maximum distance that needs to be considered for the analysis of the spatial structure.

Spectral analysis has proved to be useful for detecting cyclical patterns in the longitudinal spatial dimension at the two U.S. river sites analysed. The spatial scales defined by each cyclical pattern differ between river sites. This suggests that spatial scales might not correspond to a fixed sampling distance and that they need to be defined according to the characteristics of each river site. Results obtained for the two rivers in Texas indicate that there are repetitions in the spatial characteristics of depth every 500 m, 350 m, 110 m and 60 m. Note that the cyclical patterns corresponding to distances equal to 500 m coincide with the sampling distance proposed for some methodologies, such as River Habitat Survey. This indicates that the selection of sites of length 500 m could be justified from a statistical point of view. The reaches sampled for the scale analysis correspond to river sites that are wider and longer than any of the UK rivers analysed in this study. If a distance equal to 500 m was enough to detect cyclical patterns at river sites of such magnitudes, it is logical to think that this same length would be sufficient to identify the cyclic patterns at UK river sites of smaller or similar dimensions.

Reach lengths equal to 60 m, 350 m and 500 m define variograms that better simulate the one obtained with the original data sets. This suggests that these distances are more adequate for the characterisation of depth spatial pattern at the studied river sites. To determine whether these distances can be associated to a repetition of patterns of hydromorphological features (e.g. mesohabitat and flow types), it is suggested to repeat the study and compare the results with aerial photographs taken during the data collection procedure. Previous work (Leopold et al, 1964, Leopold, 1994, Leopold and Maddock, 1953, Osterkamp et al, 1983, Milne, 1982, Milne 1983 and Hedman and Osterkamp, 1982) focused on the analysis of the hydraulic geometry

of stream channels. Results showed that it was possible to identify a cyclic pattern of deeps and shallows that corresponds to a repeating distance of 5 to 7 widths. The cyclic patterns identified for the Brazos reach with spectral analysis correspond to 5 and 7 times the mean river width determined (river width = 100 m; cyclic patterns at 500 m and 750 m). Thus, it can be concluded that it is possible to detect the sequences of deep-shallow areas (pools and riffles) with spectral analysis.

A close relationship is always present between the wavelength, channel width and radius of curvature (Leopold, 1994) of a river. This relationship is encountered in channels of all sizes. Since spectral analysis was able to identify the relationship between the repetition (cyclic pattern) of deep and shallow areas for the sampled length, there is no reason to think that the periodogram would not be able to detect deep-shallow patterns in rivers of smaller sizes (e.g. the Bere, Lambourn or Cruick) providing that an adequate distance is sampled.

Those cycles identified at distances that do not correspond to 5 to 7 times the reach width might be associated to the relation identified by Leopold (1994) for the angle of deviation of a meander at each point from the downstream direction, which varies following a sine-generated curve. When plotting the value of the deviation angle it is possible to observe that the apexes are located at one-quarter and two-thirds wavelength as corresponds to a sine function. If we consider that for the Brazos river site the cycle of 750 m identifies the wavelength (one cycle of deep and shallow areas) it is possible to observe that one-quarter of this length is 187 m and three-quarters corresponds to 562 m, which are consistent with the 170 m and 500 m cycles identified by the periodogram. The same relationship can be encountered for the Sulphur river site when considering the cycle at 350 m as representative of the deep-shallow pattern; one-quarter of the cycle corresponds to 87.5 m, which is consistent with the cycle identified by the periodogram at 87 m. In this case, the periodogram was not able to identify the three-quarters cycle.

The division of a river into consecutive sampled reaches that combine with non sampled reaches has a consequence in the variogram calculation; variance values calculated for lag distances around the sampled reach length break the continuity of the variogram model, providing extremely high values of variance and therefore,

misleading values of predicted depth. This is due to a decrease in the number of pairs of points available for these distance intervals. Thus, geostatistics is not a suitable tool for the "extrapolation" (interpolation between reaches separated by a distance equal to or higher than the sampled reach) of depth data in rivers since the spatial correlation of this parameter is lost for distances larger than 80 m, which determines the up-scaling distance for which predictions can be obtained. Other techniques such as conditional simulation may provide more suitable means for interpolation.

The scales identified in this analysis constitute the first step to determine the sampling density that is required at macroscale level. As described in previous sections, sampling densities considered in this study have focus on the study at mesoscale level. Further research should focus on the analysis of an efficient sampling density and strategy at the spatial scales identified with spectral analysis.

f. Guidelines for monitoring of hydromorphological parameters

The implications of the temporal change study in Chapter 8 for design of monitoring programmes for mesohabitat assessment and sensitivity of rivers to water abstraction is summarised in the following paragraphs.

Results obtained showed that changes in hydromorphological features, such as mesohabitat and flow types, differ depending on the river type that is being analysed (e.g. sequences of mesohabitat types, the surface occupied by each mesohabitat type and the physical characteristics of each river site) and the change in discharge that is considered. This is consistent with results obtained in previous studies (Leopold, 1994, Brierley and Fryirs, 2000, Rosgen, 1994, Rosgen 1994, Brierley and Fryirs, 2005) as described in Chapter 8. However, it is possible to identify the following sequence of changes: *pool – deep glide – shallow glide – riffle* that defined the changes that could be expected when increasing or decreasing the discharge. Leopold (1994) determined that at low flow the pool-riffle sequence is more evident and it is characterised by alternating flat reaches of low gradient and steeper reaches involving white water. When discharge increases, the longitudinal profile of the water surface becomes less stepped and the riffle is "drowned out" changing to glide mesohabitat type.

The threshold of change between consecutive mesohabitat types of the proposed sequence depend upon the mesohabitat type considered and the change in discharge. Therefore, the first step to understand the changes that occur at a river site due to changes in discharge is to determine the instream geomorphic units (i.e. mesohabitat and flow types) present at the river site and associate this to the percentage flow exceedance at which the characterisation is being carried out. Then, it is possible to identify the complexity of the spatial structure in terms of these variables and to determine the expected sequence in mesohabitat/flow types that can be expected when changing the discharge. For rivers with limited ranges of instream geomorphic units (e.g. laterally-unconfined low energy rivers (Brierley and Fryirs, 2005)) where pools, glides or runs are dominant, changes are expected to be more noticeable in the whole mesohabitat type. On the other hand, for more diverse rivers (in terms of geomorphic units) (e.g. laterally-unconfined medium energy rivers (Brierley and Fryirs, 2005)), changes are expected to occur in those mesohabitat types that link pool and riffle features. This simplification of the results obtained needs to be understood in the context of the discussion presented in Chapter 8.

Characterisation of mesohabitat and flow types is necessary since the changes observed for these variables were more significant than those observed for the river width. In this study river width does not change much as discharge increases (Leopold, 1994) and thus it was considered that it was not an indicative variable to assess the sensitivity of rivers to water abstraction.

9.2.2. Further research

a. ***The link between random error of depth measurement and hydraulic characteristics.***

This study analysed the relation between (i) the random error in depth measurement associated to two different set of equipment and (ii) the mesohabitat/flow type where data were being collected. However, this study failed to properly identify the relation between different hydraulic conditions and the random error encountered in depth

measurements according to the set of equipment that is being used. Further research should focus on determining the reliability and validity of depth measurement that could be encountered for a range of discharges at each of the following hydraulic conditions:

(i) hydraulic jump
   a. sub-critical turbulent flow
   b. super-critical turbulent flow
   c. eddies at the hydraulic jump

(ii) separation flow
   a. separation bubble
   b. attachment point
   c. separation point
   d. eddies at the separation point
   e. vortices and rollers

The relation between increase in discharge and decrease of reliability/validity of depth measurements could be established through regression analysis. The study should be carried out in a flume under controlled conditions. Results could be linked later on to morphological characteristics (e.g. mesohabitat and flow types) according to the hydraulic features that are more frequent in specific mesohabitat and flow types. A complementary study could be carried out at a natural river site to test whether the results obtained for the flume conditions are consistent with results obtained in a natural channel.

b. *Stochastic spatio-temporal modelling of hydromorphological parameters*

Rivers are never static (Brierley and Fryirs, 2005). Brierley and Fryirs (2005) identify different sources of temporal variation which can be classified into (i) reach behaviour, (ii) river change or (iii) natural capacity of adjustment. The likelihood that adjustment takes place depends upon the river type, which is the ultimate reflection of the degrees of freedom of the river (e.g. geomorphic units, bed characteristics).
Prediction of responses of fluvial geomorphology due to temporal changes can be carried out through hydraulic based models (Brierley and Fryirs, 2005) which assume

that equilibrium channel morphology is quickly achieved. These assumptions are not adequate for longer-term trends or changes. A more stochastic approach is required to represent complex-interactive systems that are subject to different sources of perturbations, which reflect the different sources of temporal variation (river behaviour, change and natural capacity of adjustment).

Landscape evolution (e.g. changes in river morphology) does not follow deterministic processes moving to an equilibrium (Brierley and Fryirs, 2005). Several degrees of freedom can be identified at each river site, defining a specific sequence of spatial and temporal changes. "Whilst simulation models may be used for predictive purposes, their ultimate value may be little more than their role as tools for probing the depths of uncertainty" (Lane and Richards, 1997).

Previous studies have demonstrated that stochastic processes are a way of supplementing the already existent deterministic hydrodynamics models (Clifford et al., 2005). Furthermore, it has also been suggested that stochastic processes are of particular relevance to eco-hydraulic applications (e.g. river habitat quantification), where some degree of spatial and temporal dynamism (or uncertainty) is a characteristic (Clifford et al., 2005).

Habitat quantification is generally carried out through deterministic habitat models such as PHABSIM (Waddle, 2001 and U.S. Geological Survey , 2004), RYHABSIM (Mosley & Jowett, 1985), MesoHABSIM (Parasiewicz & Dunbar, 2001), CASIMIR (Jorde et al., 2001), HAMOSOFT (Mader et al., 2005) and HYDROSIGNATURE (Scharl & Le Coarer, 2005 and Le Coarer, 2005), amongst others. Only methodologies like HAMOSOFT (Mader et al., 2005) consider the spatial variability of the system as a stochastic process but none has focused on the statistical analysis of the temporal variability and the statistical interactions between spatial and temporal dimension. Modellers in eco-hydraulic science are starting to introduce higher statistical rigour into their models for the characterisation of the spatial or temporal pattern. However, most work has concentrated on simple separable models; a limitation that is also encountered in a wider range of applications (e.g. Skoien and Bloschl (2006)). In PHABSIM for example, which has been used in the UK since the 1980s and is now being used by the Environment Agency to support water resource

decision making in England and Wales (Spence & Hickley, 2000), the suitability of the micro-habitat conditions for aquatic life is assessed through a one-dimensional hydraulic approach applied to consecutive measured cross-sections. The number of cross-sections at the river sites is determined according to habitat diversity, the extent of the study area and the resources available (U.S. Geological Survey , 2004) but there are no clear guidelines in the Instream Flow Incremental Methodology (IFIM) literature describing how many transects are necessary to produce a reliable flow-habitat relationship (Payne et al, 2003). Data are collected at three different flows in order to model the physical habitat "correctly". Results obtained in this study show that cross-sectional measurements do not account for the variability of the morphological features and that this has a significant effect on the assessment of the hydromorphological quality of a river site. Other studies have shown that the number of transects sampled significantly modifies the results obtained with PHABSIM (Gard, 2005 and Payne et al., 2004) A significant improvement in understanding of the variance in space and time is critical to determining the frequency at which sampling and monitoring are required.

There is a need to (i) apply the existing theory on spatio-temporal stochastic processes to hydromorphological parameters and (ii) assess the differences between the habitat quantification obtained through spatio-temporal modelling and deterministic habitat models. There are various approaches to solving spatio-temporal problems (Kyriakidis and Journel,1999) which are based on geostatistics and these have been extended using Bayesian inference to hierarchical modelling (Banerjee *et al*, 2004). The limitation of the application of spatio-temporal analysis is the data required to understand the temporal dimension. For example, more than 40 temporal representations of the system are needed to understand the temporal variation of any parameter (Webster & Oliver, 2001). The selection criteria for a methodology that integrates the spatio-temporal variation has focused on the number of samples required. A geostatistical framework for dealing with temporal change of spatially varying properties was proposed by Papritz and Fluhler (1994). They discussed two situations: one where a few sites are measured at frequent intervals of time, and the other where a set of spatial data is collected simultaneously at few sampling times (less than ten). In the second case, a multivariate spatial random process is a suitable simplification of the general space-time process. Papritz and Fluhler (1994) illustrate

their method by developing the kriging equations for linear estimation of the change in two sets of observations measured at two different times.

The methodology proposed by Papritz and Fluhler (1994) is based on the pseudo cross variogram calculation. The cross variogram is half the expectation of the product of the increment of two variables. In order to calculate the cross variogram, it needs to be assumed that the spatial distribution of a hydromorphological property at any one time is a realization of a separate random process. If this hydromorphological property cannot be measured at identical points on two or more occasions, the experimental cross variogram between times cannot be obtained. In this situation it is necessary to calculate the *pseudo* cross variogram for which the spatial distribution of each hydromorphological property needs to be assumed to be a realization of a second order stationary random process; this signifies that the mean of the hydromorphological property is a constant, independent of any time shift. The methodology was developed for soil properties but hydromorphological parameters are characterised by more rapid changes and the assumption of a constant mean is not realistic so a trend must also be included in the model (Snepvangers et al, 2003). This trend can be modelled as a linear trend function consisting of the sum of products of coordinates in space and time and some unknown coefficients (universal kriging).

The analysis carried out in this chapter to determine if the variogram was a useful tool to detect temporal changes only considered changes in the system due to variations in discharge. The channel bed was considered constant and invariable for all the discharges analysed at each river site. Further research should consider the possibility of quantifying the different sources of variability that constitute the river system by isolating one variable (degree of freedom) at a time and applying geostatistical analysis.

c. *Limitations of Habitat Simulation Models (PHABSIM): Incorporating geostatistics to habitat models*

The guidelines given in previous paragraphs should be considered when applying transect sampling strategies for physical habitat models such as PHABSIM. The traditional PHABSIM methodology requires the description of the river site through

the measurement of transects at the selected reach (Bovee, 1997). As described in previous sections, results obtained in this study show that the characterisation of a river site (at least the spatial characterisation) is not captured when collecting data following cross-sections. Information, which should contribute to the habitat characterisation of the river site, can be lost. In PHABSIM, the problem can only be solved by increasing the number of sampled cross-sections, which has a time/cost implication. The incorporation of geostatistical analysis and kriging interpolation to methodologies such as PHABSIM may help to characterise the variability of the physical habitat by obtaining a more realistic "picture" of the sampled river reach.

Another issue associated with the application of PHABSIM is the use of habitat suitability indices (HSIs). PHABSIM uses HSIs to determine suitable intervals of depth, velocity, (and potentially substrate) for specific developmental stages of target species. For example, consider the suitability range for the spawning rainbow trout (Raleigh, 1986), where intervals are: [0.3048 m to 2.438 m] for depth, and [0.3048 ms^{-1} to 0.9144 ms^{-1}] for velocity. With this information one can determine if areas of the river reach under study have suitable depths and velocities. Errors, in terms of SE, ME and MSE, are associated with the prediction of hydromorphological values at non measured locations: values of mean error encountered for the analysed river sites are [0.008 ms^{-1} to 0.19 ms^{-1}] for velocity, [1 cm to 14 cm] for depth and [0.083 to 0.15] for Froude number. This indicates that the errors encountered (ME), especially for the velocity variable, could be high compared with the suitability intervals identified, making it difficult to accurately define the status of the habitat at the sampled reach. It is necessary to account for the sources of random error described in this study; if the sources of random error for depth are considered independent, it is possible to add the errors associated to the type of equipment used, the methodology used for WSL calculation, the sampling strategy applied and the sampling density selected. This can be used as a tool to identify the uncertainty associated to the habitat suitability indices; if depth or velocity values are close to the limits of the suitability index, the value of random error calculated may change the final decision on whether a reach is suitable or not in terms of depth or velocity.

The procedure used for the characterisation of habitat through the application of PHABSIM is also associated to several other limitations; (i) The number of transects

sampled significantly modifies the results obtained with PHABSIM. The 95% confidence intervals for the predicted habitat can vary from 9% to 73% depending upon the species and the number of transects (Gard, 2005). (ii) The model does not take into account water quality, sediment transport, or other constraints on habitat suitability and population (Spence & Hickley, 2000). (iii) The use of a single preference curve across a range of discharges has also been discussed. Ideally, this preference curve should vary according to the discharge that is being considered. The model output is highly sensitive to changes in the preferences curves and therefore, it has been stated that large errors can be encountered when applying PHABSIM and other models that use similar principles (Holm et al., 2001). (iv) PHABSIM has focused upon prediction of available habitat for life stages of target fish species. It has been demonstrated that the single target-species approach is probably not appropriate to many temperate river and stream ecosystems that are species rich (Freeman 1998 and Leonard and Orth, 1988 in Gore et al., 2001). Moreover, benthic communities are considered as a surrogate of fish species (Gore et al., 2001). (v) The model is difficult to calibrate and cannot be applied to areas that are frequently uncovered during low-flow periods (Ghanem et al, 1996 in Merwade, 2004; Merwade, 2002). (vi) The river reach is divided into trapezoidal cells, which even though being convenient for conceptualization, is not accurate. A single measurement of depth and velocity is collected for each trapezoidal cell. The fact that depth and velocity do not remain constant over any distance from the vertical or along the stream has been widely discussed as a limitation (Kondolf et al, 2000 and Payne, T.R., unpublished). Velocity can fluctuate turbulently over short time frames (Bhowmik and Xia, 1994). (vii) Depth, velocity, substrate and temperature are not the only variables that control the distribution of specific species, populations or communities (Payne, T.R., unpublished) and (viii) There are three different methodologies for obtaining the Weighted Usable Area which produce different result of WUA (Gan and McMahon, 1990) but only one is in common practice due to tradition and simplicity.

The use of mean velocity as a measure of habitat suitability for fish has been questioned (Shirvell and Dungey, 1983 in Jowett, 2003 and Scott and Shirvell, 1987 in Jowett, 2003). The first phase of habitat modelling is the characterisation of the hydraulic environment through the application of hydraulic models. Depending upon the main variations in the flow, models are simplified by integrating over depth to give a two-dimensional model (Bockelmann et al, 2004). Two dimensional hydraulic

models fail to represent the refugia created at the laminar layer by microscale features; only refugia associated with big boulders are represented, overestimating their relevance for habitat creation (Lane et al., 2006 and Crowder & Diplas, 2000). In 2D models only two-dimensional velocity and bed shear stress fields are predicted and results of depth stage and velocity predictions depend upon how well the hydromorphological characteristics of the river site have been defined (Brierley & Fryirs, 2000; Brierley & Fryirs, 2005).

Three dimensional hydraulic models can help to overcome the problems above mentioned by providing a better representation of the river system. Previous sections have already discussed the application of models such as DIVAST and SSIIM to ecohydraulic science. Booker et al (2004b) applied the SSIIM model for the creation of a three dimensional hydraulic-bioenergetic model with 835 topography points (sampling density = 1points/0.32m^2 = 3.12 points/m^2) and obtained results of differences between predicted and observed water surface elevations <0.01 m, differences that are very small in comparison to measurement error (Booker et al, 2004b). It is always necessary for this purpose to apply an interpolation procedure in order to predict the bathymetry of the bed channel all along the reach that is going to be simulated. The results obtained in this study provide a set of guidelines for the interpolation of such bathymetry with geostatistical techniques. The main limitation of three dimensional models is the required data inputs. Although advances in technology make it easier to collect larger and more accurate data sets, the process is still time and cost consuming. Numerical modelling is being used to simulate the shape of the channel bed so less field data is required (Tsujimoto & Klaassen, 2006 personal comment). It is necessary to determine (i) whether it is necessary to use three dimensional hydraulic models for habitat modelling, (ii) what are the larger and smaller scales required to obtain ecologically meaningful information with three dimensional hydraulic models and (iii) how it is possible to better integrate biological and behavioural understanding into habitat models (Lane et al., 2006). Biological knowledge about river habitat species behaviour is still a limitation for the development of more accurate habitat models.

Habitat models in future need to take into account the effect that the vegetation has on the ecosystem in terms of habitat availability and hydraulic characteristics. Hydraulic

models that include the effect of the vegetation have been developed in laboratory flumes and therefore lack a component that explains the real distribution of the vegetation in nature. Generally, in hydraulic flume experiments vegetation is represented through a regular distribution of plants without considering different species and their interactions in space (e.g. processes of competence, temporal change in growth and death among others). These limitations can be assessed through the application of geostatistical theory. Geostatistics can be combined with general theory on plant ecology to quantify the spatial distribution of vegetation along a desired river site.

River habitat models generally do not consider the temporal morphological changes that occur in the system. Morphodynamic models are able to predict the change of the morphological characteristics of the system and they are starting to be combined with habitat models for the characterisation of the temporal variability of the system (Wieprecht et al., 2006). However, there is still a need to carry out a validation of the models so confidence intervals can be calculated.

Finally, recent work for the modelling of river habitat is based on the application of fuzzy logic (Lane et al., 2006). This methodology substitutes the preference curves applied in the Instream Flow Incremental Methodology (PHABSIM) for a set of rules defined through logistic regression that are based on deterministic equations. A more stochastic approach is necessary in order to include the natural variability of the river ecosystem.

d. ***Other research possibilities - limitations of this project that could be addressed in further projects***

- Zig-Zag sampling strategies can be compared with those already analysed in this study. Zig-Zag design is usually applied when collecting data with an acoustic beam from a boat.
- Further analysis could be carried out to accurately characterise the levels of anisotropy that could be encountered between the cross-sectional and the longitudinal direction.

- It is suggested to repeat the analysis developed for the scope of this study for river sites that represent a wider range of hydromorphological characteristics. Results currently obtained are mainly focused on lowland rivers. This makes it impossible to extrapolate the proposed guidelines to reaches with different characteristics.
- Geostatistical analysis (kriging) has been successfully applied in many environmental-ecology studies (Rossi et al, 1992) and ecological spatial dependence studies. It is suggested to apply geostatistical analysis to better understand the interaction between the physical habitat and the existent biology at a site (e.g. macroinvertebrates, fish population or vegetation).
- There is a need to determine the level of accuracy that associated with each objective for which hydromorphological characterisation is being carried out so recommendations on sampling density and strategy can be provided.
- The variogram or variogram cloud could be a useful tool to define the spatial or temporal variability that is expected for a specific river type. Therefore, it could be used as an indicator of specific reference conditions which degraded reaches should aim for.
- Further analysis should be carried out to determine the effect that changes on sampling density have on the final output of models that require hydromorphological input (e.g. hydraulic or habitat models).
- The Water Framework Directive requires the characterisation of the hydromorphology in freshwater ecosystems for the assessment of the ecological status. This characterisation is usually carried out through visual assessment (see Chapter 2). Results obtained in this study showed that hydromorphological characterisation is associated to several sources of uncertainty which have an effect on the final output of the characterisation procedure. Further research is required

to determine the effect of these uncertainties on the final output of the ecological assessment procedure.

9.3. Conclusions

The following paragraphs summarise the main conclusions obtained. The conclusions need to be understood in relation to the concepts explained in the discussion section of each chapter and in Chapter 9. The information is presented as a set of guidelines that can be used for the design of hydromorphological sampling schemes in rivers. It needs to be noted that these guidelines primarily refer to lowland river sites with characteristics that are similar to those rivers analysed for this study. The conclusions are summarised below.

Hydromorphological data collection is associated with different sources of random error. These sources of random error need to be quantified and considered in the final measurement obtained so the level of uncertainty of the measurement can be determined. Random error of the measurements depends upon the type of equipment used, the sampling strategy applied and the type of interpolation technique used to predict the Water Surface Level (WSL) at non measured locations. As general guidelines, it is recommended to (i) use heterotopic data sets of WSL and topographical information for the characterisation of depth, (ii) to take depth measurements with metric staff in deep areas (> 0.5 m) and total station in shallow points (< 0.5 m) and (iii) apply descriptive geometry for the prediction of WSL.

Interpolation techniques are a useful tool to predict hydromorphological variables at non measured locations. However, the error or accuracy associated with the predictions need to be taken into account when analysing the final values obtained. The sampling strategy selected for the data collection has an influence on the accuracy of the predictions. It is recommended that grid sampling strategies be applied when characterising the spatial pattern of depth, velocity and Froude number rather than applying transect sampling strategies. The use of random grids (random walk) are preferred to the use of stratified and regular grid sampling strategies.

The sampling density applied during the field data collection has an effect on the accuracy of the predicted values. Accuracy decreases when decreasing the sampling density applied. A set of tables that relates the sampling density to the accuracy of the depth predictions have been developed under the scope of this study. A complementary set of tables that that relates accuracy, sampling density and confidence interval for the predicted values has also been developed. Accuracy has been measured in term of nine different qualitative indicators.Values obtained have been related to the characteristics of the river site at macroscale and mesoscale level. The end user is therefore able

- to relate both accuracy and sampling density, and associate the confidence interval to the selection.
- to identify the objective for data collection and the variables of relevance (e.g. characterisation of the frequency distribution or characterisation of the mean depth).
- to use the data provided to identify the most similar river type.
- to use the guidelines for the identified river to determine the sampling density required for a specific level of accuracy on in indicator.

The accuracy in the predictions has a different behaviour according to the qualitative indicator that is being considered. The indicators that are highly dependent on the sampling density analysed are: maximum / minimum / mean difference between predicted and observed values, maximum squared error, MSE, p-value, R-squared and objective function value. Different objectives for which hydromorphological data are collected require different specification for the level of accuracy required for each indicator. Therefore, different sampling densities should be applied for different objectives. The set of tables developed under the scope of this study provide a framework to identify the level of accuracy that will be provided for a specific sampling strategy applied.

It was observed that the spatial correlation for velocity and Froude number is lost at distances larger than 3 m and 9 m, which is the recommended spacing distance between sampled points. Velocity presents higher variability than depth and Froude

number and thus, higher resolution data sets are required for its characterisation when applying interpolation techniques (geostatistics). It was also observed that the variogram is not able to predict the extreme values (i.e. deepest/shallowest areas) of the river sites. The measurement of deepest and shallowest areas in detail will allow the variogram to predict these areas with higher accuracy.

The analysis carried out for the different sampling densities is based at mesoscale level. Results presented need to be carefully interpreted when a detailed representation of the system is required (densities higher than 4 points/m^2 required) or spatial scales > 200 m need to be analysed.

When considering the values of mean error obtained for each study it is possible to observe that the differences associated with the type of equipment used during the data collection procedure are less significant than the differences encountered between sampling strategies used to collect topographical and water surface level data (heterotopic or isotopic). Similarly, the type of sampling strategy applied for the collection of topographical and WSL (heterotopic or isotopic) is less significant than the general sampling strategy applied for the data collection (e.g. regular grid or transect). Random errors associated with the sampling strategy and the type of equipment are higher than the confidence intervals associated with any of the sampling densities considered.

Several considerations need to be taken into account when calculating the variogram for depth interpolation. These considerations are associated to the parameters that define the variogram equation and can be summarised as follow: (i) it is recommended the longitudinal variogram is used for depth predictions, (ii) it is suggested that azimuth tolerances be ≈60°, (iii) a sensitivity analysis of the variogram parameters that define the variogram (i.e. azimuth, azimuth tolerance, lag distance, maximum distance and number of pairs of points) is recommended.

The accuracy of the predictions always decreases around the edges of the sampled area and therefore, it is necessary to monitor a greater length of river than that of concern (i.e. the reach of interest should be from 1/2 to 1/3 of the total distance

sampled). Spectral analysis is a useful tool to detect the cyclic patterns that occur in rivers. This methodology provides results that are consistent with the more traditional description of the morphological structure of rivers defined by previous authors. Results obtained suggested that reach lengths of 500 m appear to provide satisfactory data for the characterisation of spatial pattern (i.e. identification of the sequences of deep and shallow areas defined by the habitat features).

Interpolation through geostatistics has been proved to be useful to reduce the number of points that need to be collected during the field data collection. However, less successful results were obtained when analysing the ability of geostatistics to extrapolate (i.e. interpolation between sampled reaches) information from the sampled reaches to higher scale levels.

The calculation of the temporal variogram for the interpolation of hydromorphological variables over time is difficult since it requires the repeated sampling of the site that is being characterised. The analyses carried out in this study focus on the hydromorphological differences observed between two discharges at two different river sites. Results were related to the mesohabitat and flow types identified at the river site. A sequence of change for the mesohabitat types has been identified and is described as follows: pool – deep glides – shallow glides - riffles. The sensitivity of each mesohabitat to changes in discharges is not equal for the four types identified. Therefore, it is necessary to characterise the mesohabitat types and the change in discharge occurred to better predict temporal changes for rivers with a low variation in the mesohabitat types, hydromorphological changes occur at the same level at all the mesohabitat types. In contrast, rivers with a higher variety of mesohabitat types, present higher changes in those types that link pools and riffles. It is suggested these mesohabitat types be sampled with higher detail to better characterise the temporal changes.

The work developed for the scope of this study provides a set of findings for the characterisation of depth, velocity and substrate in lowland rivers. In order to confirm these findings more work is needed and a wider range of river types need to be sampled. Ideas for further research projects have been developed in the discussion section.

10

References

Alfredsen, K., Svelle, K., Baevre, I. & Halleraker, J.H. (2004) Altered habitat conditions caused by longterm changes in hydromorphology in a Norwegian regulated river. *In*: Diego Garcia de Jalon and Pilar Vizcaino Martinez, *Fifth International Symposium on Ecohydraulics: aquatic habitat analysis and restoration,* Madrid, Spain, IAHR, 262-267, Vol. I.

Ashmore, P.E. & Church, M.A. (1998) Sediment transport and river morphology: a paradigm for study. *In*: Klingeman, P.C., Beschta, R.L., Komar, P.D., & Bradley, J.B.*Gravel-Bed Rivers in the Environment*. Highlands Ranch, Colorado, USA: Water Resources Publications, LLC, Chapter 7, 115-148.

Ayres, F. (1958) *Schaum's outline of theory and problems of first year college mathematics.* Schaum's outline series. United States of America: McGraw-Hill Book Company.

Banerjee, S., Carlin, B.P., & Gelfand, A.E. (2004) *Hierarchical modelling and analysis for spatial data.* Monographs on statistics and applied probability 101. USA: Chapman and Hall/CRC: a CRC Press Company.

Bayliss, A. (1999) *Catchment descriptors. Flood Estimation Handbook: Procedures for Flood frequency estimation. Vol 5.* Institute of Hydrology, Wallingford, Oxfordshire, UK.

Bizjak, A. & Mikoš, M. (2004) Synthesis procedure of assessing the hydromorphological status of river corridors: the Dragonja river case study. *In*: Diego Garcia de Jalon and Pilar Vizcaino Martinez, *Fifth International Symposium on Ecohydraulics: aquatic habitat analysis and*

restoration, Madrid, Spain, IAHR. 325-330, Vol. I.

Bockelmann, B.N., Fenrich, E.K., Lin, B. & Falconer, R.A. (2004) Development of an ecohydraulics model for stream and river restoration. *Ecological Engineering,* 22 (4-5), 227-235.

Bogaert, P. & Russo, D. (1999) Optimal spatial sampling design for the estimation of the variogram based on a least squares approach. *Water Resources Research,* 35 (4), 1275-1289.

Booker, D.J. (2003) Hydraulic modelling of fish habitat in urban rivers during high flows. *Hydrological Processes,* 17, 577-599.

Booker, D.J., Dunbar, M.J., Acreman, M.C., Akande, K. & Declerck, C. (2004a) Habitat assessment at the catchment scale: application to the River Itchen, UK. *In*: British Hydrological Society International Conference: *Hydrology; Science & Practice for the 21st Century,* Imperial College London, 12th -16th July, Vol. I.

Booker, D.J., Dunbar, M.J. & Ibbotson, A. (2004b) Predicting juvenile salmonid drift-feeding habitat quality using a three-dimensional hydraulic-bioenergetic model. *Ecological Modelling,* 177 (1-2), 157-177.

Booker, D.J., Sear, D.A., & Payne, A.J. (2001) Modelling three-dimensional flow structures and patterns of boundary shear stress in a natural pool-riffle sequence. *Earth Surface Processes & Landforms,* 26, 553-576.

Borsanyi, P., Dunbar, M., Booker, D., Rivas Casado, M., & Alfredsen, K. (2005) The hydromorphological picture of meso-scale units of rivers. *In*: Harby, A., Baptist, M., Duel, H. et al., *Proceedings from the final meeting in Silkeborg, Denmark.,* Silkeborg, Denmark, National Enviromental Research Institute, 23-31.

Bovee, K.D. (1997) *Data collection procedures for the Physical Habitat Simulation system.* Fort Collins, CO: U.S. Geological Survey: 146 p.

Brierley, G.J. & Fryirs, K.A. (2000) River styles, a geomorphic approach to catchment characterisation: Implications for river rehabilitation in Bega catchment, New South Wales, Australia. *Environmental Management,* 25 (6), 661-679.

Brierley, G.J. & Fryirs, K.A. (2005) *Geomorphology and river management: applications of the River Styes Framework.* Oxford, UK.: Blackwell Publications. 398 pp.

Brunner, G.W. (2002) *Hec-Ras River Analysis System user's manual. Version 3.1.* Davis, USA.: US Army Corps of Engineers, CPD-68: Hydrologic Engineering Center. 420 p.

Buffagni, A. & Erba, S. (2002) *Guidance for the assessment of the Hydromorphological features of rivers within the STAR project. STAR project: Hydromorphological assessment.* CNR-IRSA

Water Research Institute, Italy.

Burgess, T.M. & Webster, R. (1980) Optimal interpolation and isarithmic mapping of soil properties: I) the semivariogram and punctual kriging, II) Block kriging. *Journal of Soils Science,* 31, 315-331.

Burgess, T.M. & Webster, R. (1984) Optimal sampling strategies for mapping soil types I. Risk distribution of boundary spacings. *Journal of Soil Science.,* 35, 641-654.

Burrough, P.A. & McDonnell, R.A. (1998) *Principles of geographical information systems. Spatial information systems and geostatistics.* 2nd ed. Oxford University Press.

Callan, R. (1999) *The essence of neural networks.* Essence of computing. Hemel Hempstead. London. UK: Prentice Hall Europe.

Carter, G.S. & Shankar, U. (1997) Creating rectangular bathymetry grids for environmental numerical modelling of gravel-bed rivers. *Applied Mathematical Modelling,* 21, 699-708.

Casado, M.R., White, S., Bellamy, P., Dunbar, M., Booker, M., & Maddock, I. (2006) Analysing the sensitivity of two variogram models for the characterisation of the spatial pattern of depth in rivers. *In*: Caetano, M. & Painho, M., *7th International Symposium on spatial accuracy assessment in natural resources and environmental sciences.,* Lisbon, Portugal, I. Instituto Geografico Portugues,

Chatfield, C. (1996) *The analysis of time series: an introduction. Texts in Statistical Science.* 5th ed. London: Chapman & Hall/CRC.

Chovanec, A., Jäger, P., Jungwirth, M., Koller-Kreimel, V., Moog, O., Muhar, S. & Schmutz, St. (2000) The Austrian way of assessing the ecological integrity of running waters: a contribution to the EU Water Framework Directive. *Hydrobiologia,* 422/423, 445-452.

Chow, V.T. (1964) *Handbook of Applied Hydrology*. New York: McGraw Hill.

Christakos, G. (2000) *Modern spatiotemporal geostatistics.* International association for mathematical geology. Studies in mathematical geology No. 6. Oxford University Press, New York.

Clifford, N.J., Soar, P.J., Harmar, O.P., Gurnell, A.M., Petts, G.E. & Emery, J.C. (2005) Assessment of Hydrodynamic Simulation Results for Eco-Hydraulic and Eco-Hydrological Applications: a Spatial Semivariance Approach. *Hydrological Processes,* 19 (18), 3631-3648.

Cressie, N. (1993) *Statistics for spatial data.* Revised ed. New York: Wiley.

Crowder, D.W. & Diplas, P. (2000) Using Two-Dimensional Hydrodynamic Models at Scales of Ecological Importance. *Journal of Hydrology,* 230 (3-4), 172-191.

Darby, S.E., Spyropoulus, M., Bressloff, N. & Rinaldi, M. (2004) Fluvial bank erosion in meanders: a CDF modelling approach. *In*: Diego Garcia de Jalon and Pilar Vizcaino Martinez, *Fifth International Symposium on Ecohydraulics: aquatic habitat analysis and restoration,* Madrid, Spain, IAHR. 268-273, Vol. I.

Directive 2000/60.EC. The Water Framework Directive: Directive 2000/60.EC of the European Parliament and the Council of 23 October 2000 establishing a framework for Community action in the field of water policy. Official Journal of the European Communities,)J L 327/1;22.12.2000. European parliament.

Downs, P.W. & Kondolf, G.M. (2002) Post-Project Appraisals in Adaptive Management of River Channel Restoration. *Environmental Management,* 29 (4), 477-496.

Emerson, C.W., Lam, N.S.N. & Quattrochi, D.A. (1999) Multiscale fractal analysis of image texture and pattern. *Photogrammetric Engineering and Remote Sensing.,* 65 (1), 51-61.

Emery, J.C., Gurnell, A.M., Clifford, N.J., Petts, G.E., Morrissey, I.P. & Soar, P.J. (2003) Classifying the hydraulic performance of riffle-pool bedforms for habitat assessment and river rehabilitation design. *River Research and Applications,* 19, 533-549.

Environment Agency (2003) *River habitat survey in Britain and Ireland: field survey guidance manual.* Environment Agency.

Falconer, R.A., Lin, B., Wu, Y., & Harris, E. (1998) *DIVAST user manual.* Environmental Water Management Research Centre.

Fox, P.J.A., Naura, M. & Scarlett, P. (1998) An account of derivation and testing of a standard field method, River Habitat Survey. *Aquatic Conservation: Marine and Freshwater Ecosystems,* 8, 455-475.

Frissell, C.A., Liss, W.J., Warren, C.E. & Hurley, M.D. (1986) A hierarchical framework for stream habitat classification: viewing streams in a watershed context. *Environmental management,* 10 (2), 199-214.

Gard, M.F. (2005) Variability in flow-habitat relationships as a function of transect number for Phabsim modelling. *River Research and Applications,* 21 (9), 1013-1019.

Gilvear, D.J. & Bryant. R.G. (2003) Analysis of aerial photography and other remotely sensed data. *In*: Kondolf, G.M. and Piégay H., *Tools in Fluvial Geomorphology.* Wiley, London: 134-168.

Gilvear, D.J., Waters, T.M. & Milner, A.M. (1998) Image analysis of aerial photography to quantify the effect of gold placer mining on channel morphology, Interior Alaska. *In*: Lane, S.N., Richards, K.S. and Chandler, J.H., eds. *Landform, monitoring, modelling and analysis.* Chichester: John Wiley and Sons

Habersack, H.M. (2000) The river-scaling concept (RSC): a basis for ecological assessment. *Hydrobiologia,* 422-423 (0), 49-60.

Harby, A., Baptist, M., Dunbar, M.J. & Schmutz, S. (2004) *State-of-the art in data sampling, modelling analysis and applications of river habitat modelling.* Cost Action 626.

Hardy, T.B. & Addley, R.C. (2003) Instream Flow Assessment Modelling: combining physical and behavioural-based approaches. *Canadian Water Resources Journal. Special issue: State-of-the-Art in Habitat Modelling and Conservation Flows,* 28 (2), 283-299.

Hauer, Ch., Habersack, H., Schmutz, St., Unfer, G., Maierhofer, K. & Novak, L. (2004) The effects of morphodynamic processes on the habitat quality of the Rheophilous Cyprinid Nase (Chondrostoma nasus) in a restored Austrian low-lan river. *In*: Diego Garcia de Jalon and Pilar Vizcaino Martinez, *Fifth International Symposium on Ecohydraulics: aquatic habitat analysis and restoration,* Madrid, Spain, IAHR. 798-802, Vol. II.

Hawkins, C.P., Kershner, J.L., Bisson, P.A. et al. (1993) A hierarchical approach to classifying stream habitat features. *Fisheries,* 18 (6), 3-12.

Hedman, E.R. & Osterkamp, W.R. (1982) *Streamflow characteristics related to channel geometry of streams in Western United States.* Geological Survey Professional Paper 2193, United States Government Printing Office. 17 p.

Hilderbrand, R.H., Lemly, A.D., Dennis, A., Dollof, A., & Andrew, C. (1999) Habitat sequencing and the importance of discharge in inferences. *North American Journal of Fisheries Management.,* 19, 198-202.

Howard, A.D. & Hemberger, A.T. (1991) Multivariate characterization of meandering. *Geomorphology,* 4, 161-186.

Johnson, R.K. (2000) *Defining reference condition and setting class boundaries in ecological monitoring assessment. Background document for the EU-funded REFCOND project.* Department of environmental assessment. Uppsala, Sweden.: Swedish university of agricultural science.

Johnston, K., Ver Hoef, J.M., Krivoruchko, K., & Lucas, N. (2001) *Using ArcGis geostatistical analysis. GIS by ESRI.* New York. United States of America: ESRI.

Jorde, K., Schneider, M., Peter, A. & Zoellner, F. (2001) Fuzzy based models for the evaluation of fish habitat quality and instream flow assessment. *In*: CD-ROM, *Proceedings of the 3rd International Symposium on Environmental Hydraulics.,* Tempe, Arizona,

Julien, P.Y. (2002) *River mechanics*. Cambridge: Cambridge University Press.

Kyriakidis, P.C. & Journel, A.G. (1999) Geostatistical Space-Time Models: a Review. *Mathematical Geology,* 31 (6), 651-684.

Lane, S.N. (1998) Hydraulic modelling in hydrology and geomorphology: a review of high resolution approaches. *Hydrological Processes,* 12 (8), 1131-1150.

Lane, S.N. & Richards, K.S. (1997) Linking river channel form and process: Time, space and causality revisited. *Earth Surface Processes and Landforms,* 22 (3), 249-260.

Lane, S.N., Mould, D.C., Carbonneau, P.E., Hardy, R.J. & Bergeron, N. (2006) Fuzzy modelling of habitat suitability using 2D and 3D hydrodynamic models: Biological challenges. *In*: Ferreira, R.M.L., Alves, E.C.T.L., Leal, J.G.A.B. and Cardoso, A.H., *River Flow 2006: Proceedings of the International Conference on Fluvial Hydraulics,* Lisbon, Portugal, Vol. 2. Taylor & Francis, London, 2043-2053.

Lark, R.M. (2002) Optimized spatial sampling of soil for estimation of the variogram by maximum likelihood. *Geoderma*, 105 (1-2), 49-80.

Lattin, J., Carroll, D., & Green, P.E. (2003) *Analyzing multivariate data.* Duxbury applied series. Canada: Thomson Brooks, ColeCurt Hinrichs.

Le Coarer, Y. (2005) *Hydrosignature*. Available at: http://hydrosignature.aix.cemagref.fr. Accessed 2005.

Le Coarer, Y. & Dumont, B. (1995) Modélisation de la morphodynaique fluviale pour la recherch des relations habitat/faune aquatique. *Coloque "Habitat-poissons" Bulletin Français de la Peçhe et de la Pisciculture.,* 337-339, 309-316.

Legleiter, C.J. & Kyriakidis, P.C. (2006) Forward and inverse transformations between cartesian and channel-fitted coordinate system for meandering rivers. *Mathematical Geology,* in press

Legleiter, C.J. & Roberts, D.A. (2005) Effects of Channel Morphology and Sensor Spatial Resolution on Image-Derived Depth Estimates. *Remote Sensing of Environment,* 95 (2), 231-247.

Leopold, L.B. (1994) *A view of the river*. London, England: Harvard University Press. 290 p.

Leopold, L.B. & Maddock, T. (1953) *The hydraulic geometry of stream channels and some physiographic implications*. Geological Survey Professional Paper 252, United States Government Printing Office.

Leopold, L.B., Wolman, M.G. & Miller, J.A. (1964) *Fluvial processes in geomorphology.* San Francisco: Freeman.

Lin, L.I.-K. (1989) A Concordance Correlation-Coefficient to Evaluate Reproducibility. *Biometrics,* 45 (1), 255-268.

Maddock, I. (1999) The Importance of Physical Habitat Assessment for Evaluating River Health. *Freshwater Biology,* 41 (2), 373-391.

Maddock, I., Bickerton, M.A., Spence, R. & Pickering, T. (2001) Reallocation of compensation releases to restore river flows and improve instream habitat availability in the Upper Derwent catcment, Derbyshire, UK. *Regulated Rivers: Research and Management,* 17, 417-441.

Maddock, I.P. & Bird, D. (1996) The application of habitat mapping to identify representative PHABSIM sites on the river Tavy, Devon, UK. *In*: Leclerc, M., Capra, H., Valentin, S., Boudreault, A. and Cote, Y., *Procedings of the 2nd International Symposium on Habitats and Hydraulics.* Quebec city, Canada. pp. 203-215., Vol. I.

Maddock, I., Hill, G., Dunbar, M., Acreman, M., Eastman, K., Mouton, A., Rivas-casado, M., & Smolar-Zvanut, N. (2006) Assessing rapid habitat mapping methods for observer variability. *In*: *International Conference on Riverine ecohydrology: advances in research and applications,* Stirling, 65-66.

Maddock, I.P. & Lander, K. (2002) Testing the effectiveness of rapid habitat mapping to describe instream hydraulics. *In*: Anon., *Proceedings of the Environmental Flows for River Systems Working Conference and Fourth International Ecohydraulics Symposium.,* Cape Town, South Africa, Vol. I.

Mader, H. & Laaha, G. (unpublished) Flow velocity measurements and analysis at low velocity habitats: accuracy considerations.

Mader, H., Meixner, H., & Tucket, P. (2005) Weighted Usable Volume Habitat Modeling - The real world calculation of livable space. *In*: Harby, A., Baptist, M., Duel, H. et al., *Proceedings from the final meeting in Silkeborg. Cost 626 European Aquatic Modelling Network.,* Silkeborg, Denmark, National Environmental Research Institute, 227//239.

Magdaleno, F., Olaya, V. & Merino, S. (2004) Interaction between environmental flow requirements and fluvial morphology analyzed trough remote sensing, GIS and DIP. *In*: Diego Garcia de Jalon and Pilar Vizcaino Martinez, *Fifth International Symposium on Ecohydraulics: aquatic habitat analysis and restoration,* Madrid, Spain, IAHR, 1211-1215, Vol. II.

McBratney, A.B. & Webster, R. (1983) How many observations are needed for regional estimation of soil properties. *Soil Science,* 135 (3), 177-183.

Meisel, J.E. & Turner, M.G. (1998) Scale detection in real and artificial landscapes using semivariance analysis. *Landscape ecology,* 13, 347-362.

Merwade, V. (2002) *Development of a methodology for accurate representation of rivers in two and three dimensions.* PhD thesis, Faculty of the Graduate School of the University of Texas at Austin.

Merwade,V. *Geospatial representation of river channels*. Available at: www.crwr.utexas.edu/gis/gishydro03/channels/channels.htm. Accessed 2004 .

Milne, J.A. (1982) Bed Forms and Bend-Arc Spacings of Some Coarse-Bedload Channels in Upland Britain. *Earth Surface Processes and Landforms,* 7 (3), 227-240.

Milne, J.A. (1983) Variation in Cross-Sectional Asymmetry of Coarse Bedload River Channels. *Earth Surface Processes and Landforms,* 8 (5), 503-511.

Mosley, M.P. & Jowett, I.G. (1985) Fish habitat analysis using river flow simulation. *New Zealand Journal of Marine and Fresh Water Research.,* 19, 293-309.

Mount, J.F. (1995) *California rivers and streams: The conflict between fluvial processes and land use.* Berkeley, University of California Press, 359 pp.

Muhar, S. (1996) Habitat improvement of Austrian rivers with regard to different scales. *Regulated Rivers: Research and Management,* 12, 471-482.

Muhar, S., Unfer, G., Schmutz, S., Jungwirth, M., Egger, G. & Angermann, K. (2004) Assessing river restoration programmes: habitat conditions, fish fauna and vegetation as indicators for the possibilities and constrains of river restoration. *In*: Diego Garcia de Jalon and Pilar Vizcaino Martinez, *Fifth International Symposium on Ecohydraulics: aquatic habitat analysis and restoration,* Madrid, Spain, IAHR, 300 - 305, Vol. I.

Muller, W.G. & Zimmerman, D.L. (1999) Optimal designs for variogram estimation. *Environmetrics,* 10, 23-37.

Muste, M. (2002) Sources of bias errors in flume experiments on suspended-sediment transport. *Journal of Hydraulic Research,* 40 (6), 695-708.

Muste, M., Fujita, I. & Kruger, A. (1998) Experimental Comparison of Two Laser-Based Velocimeters for Flows With Alluvial Sand. *Experiments in Fluids,* 24 (4), 273-284.

Muste, M., Yu, K., Pratt, T., & Abraham, D. (2004a) Practical Aspects of ADCP Data Use for Quantification of Mean River Flow Characteristics; Part II: Fixed-Vessel Measurements. *Flow Measurement and Instrumentation,* 15 (1), 17-28 .

Muste, M., Yu, K. & Spasojevic, M. (2004b) Practical Aspects of ADCP Data Use for Quantification of Mean River Flow Characteristics; Part I: Moving-Vessel Measurements. *Flow Measurement and Instrumentation,* 15 (1), 1-16.

Nestler, J. & Sutton, V.K. (2000) Describing scales of features in river channels using fractal geometry concepts. *Regulated Rivers: Research and Management,* 16, 1-22.

Nicholas, A.P. & Smith, G.H.S. (1999) Numerical Simulation of Three-Dimensional Flow Hydraulics in a Braided Channel. *Hydrological Processes,* 13 (6), 913-929.

Nickerson, C.A.E. (1997) A Note on "a Concordance Correlation Coefficient to Evaluate Reproducibility". *Biometrics,* 53 (4), 1503-1507.

Nielsen, D.R. & Wendroth, O. (2003) *Spatial and temporal statistics: sampling field soils and their vegetation.* Catena Verlag, Reiskirchen, Germany: GeoEcology textbook. 397 p.

Nikora, V.I., Sapozhnikov, V.B. & Noever, D.A. (1993) Fractal geometry of individual river channels and its computer simulation. *Water resources research,* 29 (10), 3561-3568.

Nixon, S. (2002) *Working Group 3.1: Development of a Geographical Information System. Task 5: Exploring potential links to EEA's. EUROWATERNET/WATERBASE*.

Olsen, N.R.B. (1996) *A three-dimensional numerical model for simulation of sediment movements in water intakes with multi-block option. SSIIM users manual Version 1.4.*

Olsen, N.R.B. (2000) *A three-dimensional numerical model for simulation of sediment movements in water intakes with multi-block option. SSIIM users manual Version 1.1 and 2.0 for OS/2 and windows.*

Olsen, N.R.B. & Stokseth, S. (1995) Three-dimensional numerical modelling of water flow in a river with large bed roughness. *Journal of Hydraulic Research,* 33, 571-581.

Osterkamp, W.R., Lane, L.J., & Foster, G.R. (1983) *An analytical treatment of channel-morphology relations*. Geological Survey Professional Paper 1288, United States Government Printing Office.

Osting, T.D. (2004) *An improved anisotropic scheme for interpolating scattered bathymetric data points in sinuous river channels.* CRWR Online Report 04-01. Centre for Research in Water Resources. Bureau of Engineering Research, The University of Texas at Austin.

Owen, R., Duncan, W., & Pollard, P. (2001) *Definition and establishment of reference conditions.* Aberdeen, Scotland: Scottish environment protection agency.

Papritz, A. & Fluhler, H. (1994) Temporal change of spatially autocorrelated soil properties: optimal estimation by cokriging. *Geoderma ,* 62, 29-43.

Parasiewicz, P. (1996) Estimation of physical habitat characteristics using automation and geodesic-based sampling. *Regulated Rivers: Research and Management,* 12, 575-583.

Parasiewicz, P. (2001) MesoHabsim: a concept for application of instream flow models in river restoration planning. *Fisheries,* 26 (9), 6-13.

Parasiewicz, P. (2003) Upscaling: integrating habitat model into river management. *Canadian Water Resources Journal. Special issue: State-of-the-Art in Habitat Modelling and Conservation Flows,* 28 (2), 283-299.

Parasiewicz, P. & Dunbar, M.J. (2001) Physical habitat modelling for fish - a developing approach. *Large Rivers,* 12 (2/4), 239-268.

Payne, T.R., Eggers, S.D., & Parkinson, D.B. (2004) The number of transects required to compute a robust PHABSIM Habitat Index. *Hydroecology Applique,* 14 - 1, 27-53.

Petts, G.E. & Amoros, C. (1996) *Fluvial Hydrosystems*. London: Chapman & Hall.

Raleigh, R.F., Zuckerman, L.D., & Nelson, P.C. (1986) *Habitat suitability index models and instream flow suitability curves: Brown Trout.* National Ecology Center. Division of Wildlife and Contaminant Research. Research and Development.: US Fish and Wildlife Service. U.S. Department of the Interior. Washington.

Raven, P.J., Holmes, N.T.H., Charrier, P., Dawson, F.H., Naura, M. & Boon, P.J. (2002) Towards a harmonized approach for hydromorphological assessment of rivers in Europe: a qualitative comparison of three survey methods. *Aquatic Conservation: Marine and Freshwater Ecosystems,* 12, 405-424.

Raven, P.J., Holmes, N.T.H., Dawson, F.H. & Everard, M. (1998) Quality assessment using River Habitat Survey data. *Aquatic Conservation Marine and Freshwater Ecosystems.,* 8, 477-499.

REFCOND (2001) *Detailed work program. EU Water Framework Directive project: development of a protocol for identification of reference conditions, and boundaries between, high, good and moderate status in lakes and watercourses.* CIS working group 2/3.

REFCOND (2003) *Final guidance on establishing reference conditions and ecological status class boundaries for inland surface waters*. CIS working group 2/3.

Rigol, J.P., Jarvis, C.H. & Stuart, N. (2001) Artificial neural networks as a toll for spatial interpolation. *International Journal of Geographical Information Science.,* 15 (4), 323-343.

Rivas Casado, M., Bellamy, P., White, S., Dunbar, M. & Booker, D. (2004) Defining hydromorphological sampling strategies for ecological assessment. *In*: Diego Garcia de Jalon and Pilar Vizcaino Martinez, *Fifth International Symposium on Ecohydraulics: aquatic habitat analysis and restoration,* Madrid, Spain, IAHR., 407-414, Vol. I.

Rodriguez-Iturbe, I. & Rinaldo, A. (2001) *Fractal river basins: chance and self-organisation.* USA: Cambridge University Press.

Rosgen, D.L. (1994a) *Applied river morphology*. Colorado: Widland Hydrology, Pagosa Springs, Colorado.

Rosgen, D.L. (1994b) A classification of natural rivers. *Catena,* 22, 169-199.

Rossi, R.E., Mulla, D.J., Journel, A.G. & Franz, E.H. (1992) Geostatistical tools for modelling and interpreting ecological spatial dependence. *Ecological monographs,* 62 (2), 277-314.

Rowntree, K. & Wadeson, R. (1998) A geomorphological framework for the assessment of instream flow requirements. *Aquatic Ecosystem Health and Management,* 1, 125-141.

Russell, S. & Norvig, P. (2003) *Artificial intelligence: a modern approach.* 2nd ed. Prentice Hall Series in Artificial Intelligence. London: Stuart Russell and Peter Norvig, Editors.

Russo, D. (1984) Design of an optimal sampling network for estimating the variogram. *Soil Science,* 48, 708-716.

San Martín, D., Rodríguez, E., Ayesa, E., Martín, C., Sancho, L., Salterain, A. & Unzue, J.A. (2004) Development and verification of an Ebro river water quality model for its course through Zaragoza, Calhidra. *In*: Diego Garcia de Jalon and Pilar Vizcaino Martinez, *Fifth International Symposium on Ecohydraulics: aquatic habitat analysis and restoration,* Madrid, Spain, IAHR, 182-186, Vol. I.

Sanz-Ronda, F.J., Martinez de Azagra, A. & Arenal-Gutierrez, E. (2003) Evaluation of different sampling strategies to quantify stream habitat (preliminary results). *In*: U.S. Geological Service. USGS. U.S. Department of the Interior. *International IFIM Users' Workshop.,* Fort Collins, Colorado., Vol. I.

Scharl, A. & Le Coarer, Y. (2005) Morphohydraulic quantification of non spatialized datasets with the "Hydrosignature" software. *In*: Harby, A., Baptist, M., Duel, H. et al., *Proceedings from the final meeting in Silkeborg. Cost 626 European Aquatic Modelling Network.,* Silkeborg, Denmark, National Environmental Research Institute, 313-326.

Scruton, D.A., Heggenes, J., Valentin, S., Harby, A. & Bakken, T.H. (1998) Field sampling design and spatial scale in habitat-hydraulic modelling: comparison of three models. *Fisheries Management and Ecology.,* 5, 225-240.

Shields, F.D. & Rigby, J.R. (2005) River Habitat Quality From River Velocities Measured Using Acoustic Doppler Current Profiler. *Environmental Management,* 36 (4), 565-575.

Skoien, J. & Bloschl, G. (2006) Spatio-temporal geostatistical analysis of runoff and precipitation.

Hydrology and Earth System Sciences Discussions, 3, 941-985.

Skoien, J.O. & Bloschl, G. (2003) Characteristic space-time scales in hydrology. *Water Resources Research,* 39 (10)

Snepvangers, J.J.J.C., Heuvelink, G.B.M. & Huisman, J.A. (2003) Soil Water Content Interpolation Using Spatio-Temporal Kriging With External Drift. *Geoderma,* 112 (3-4), 253-271. Special Issue: Sp. Iss. Si.

Spence, R. & Hickley, P. (2000) The Use of Phabsim in the Management of Water Resources and Fisheries in England and Wales. *Ecological Engineering,* 16 (1), 153-158.

Statzner, B. & Higler, B. (1985) Questions and comments on the River Continuum Concept. *Canadian Journal of Fisheries and Aquatic Sciences,* 42, 1038-1044.

Thomas, J.A. & Bovee, K.D. (1993) Application and Testing of a Procedure to Evaluate Transferability of Habitat Suitability Criteria. *Regulated Rivers-Research & Management,* 8 (3), 285-294.

Thomson, J.R., Taylor, M.P., Fryirs, K.A. & Brierley, G.J. (2001) A geomorphological framework for river characterization and habitat assessment. *Aquatic Conservation: Marine and Freshwater Ecosystems,* 11, 373-389.

Thomson, J.R., Taylor, M.P., Fryirs, K.A. & Brierley, G.J. (2003) Are River Styles ecologically meaningfull? A test of the ecological significance of geomorphic river characterisation scheme. *Aquatic Conservation: Marine and Freshwater Ecosystems,* in press

U.S. Geological Survey (2004) *Introduction to the Physical Habitat Simulation System (PHABSIM).* Accessed 2004.

Vannote, R.L., Minshall, G.W., Cummins, K.W., Sedell, J.R. & Cushing, C.E. (1980) The River Continuum Concept. *Canadian Journal of Fisheries and Aquatic Science ,* (37), 130-137.

Wackernagel, H. (1998) *Multivariate geostatitics: an introduction with applications*. Second completely revised edition. Ecole de Mines de Paris. France ed. New York: Springer.

Waddle, T.J. (2001) *PHABSIM for Windows: user's manual and exercises.* Fort Collins, CO: U.S. Geological Survey. USGS.

Wadeson, R.A. & Rowentree, K.M. (1998) Application of the hydraulic biotope concept to the classification of instream habitats. *Aquatic Ecosystem Health and Management,* 1, 143-157.

Wadzuk, B.H.B. (2001) Model bathymetry for sinuous dendritic reservoirs. *In*: Casamitjana, X., University of Girona, Catalonia, Spain., Proceedings of the 6th International Workshop on Physical Processes in Natural Waters.:

Webster, R. & Oliver, M.A. (1992) Sample adequately to estimate variograms of soil properties. *Journal of Soil Science,* 43, 177-192.

Webster, R. & Oliver, M.A. (2001) *Geostatistics for environmental scientists.* Statistics in practice. Victor Barnett. West Sussex, England: John Wiley & Sons, Ltd.

Wieprecht, S., Eisner, A. & Noack, M. (2006) Modeling approach to simulate habitat dynamics. *In*: Ferreira, R.M.L., Alves, E.C.T.L., Leal, J.G.A.B. and Cardoso, A.H., *River Flow 2006: Proceedings of the International Conference on Fluvial Hydraulics,* Lisbon, Portugal, Vol. 2. Taylor & Francis, London, 2053-2063.

Wilson, C.A.M.E. (2000) SSIIM: Sediment Simulation in Intakes With Multiblock Option. A Model for Free Surface Flows a D-3 Model for the Prediction of Hydraulic and Water Quality Parameters in Free Surface Flows. *Hydrological Processes,* 14 (14), 2619-2622.

Winterbottom, S.J. & Gilvear, D.J. (1997) Quantification of channel bed morphology in gravel bed rivers using airborne multispectral imagery and aerial photography. *Regulated rivers: research and management.,* 13, 489-499.

Woo, H., Rhee, D.S., Ahn, H.K. & Oh, J.M. (2004) Effect of river-channel meander and degradation on hydro-geomorpho-logically induced vegetation expansion on sandbars. *In*: Diego Garcia de Jalon and Pilar Vizcaino Martinez, *Fifth International Symposium on Ecohydraulics: aquatic habitat analysis and restoration,* Madrid, Spain, IAHR, 312-317, Vol. I.

Working Group 2.7 (2003) *Water Framework Directive: Common Implementation Strategy. Working Group 2.7 Monitoring.* Guidance on Monitoring for the Water Framework Directive. Final Version.,

Appendix 1

Description of the river sites analysed.

The following appendix gives a brief description of the characteristics at each river site. A total of sixteen rivers (Austrian Channel, Bere, Blackwater, Brazos, Cruick, Highland Water, Lambourn, Leigh Brook, Pang, Peris, Seiont, Senni, Sulphur, Tame, Tarf and Windrush) have been described. Multiple reaches were analysed in some of the rivers and thus, the number of river sites to be analysed is nineteen.

Artificial channel in Austria

The data obtained for the laboratory channel (Figure A 1.1) have been provided by the Department of Water Management at University of Agricultural Sciences, Vienna (Hydrology and Hydraulic Engineering; BOKU). The channel was created in order to reproduce a natural straight stream and thus, woody debris were included along the stream. The simulated channel is 17 m long, 2.5 to 4m width, has a 5% of slope and includes two different mesohabitats classified as riffle and pool.

The topography was measured in a regular grid of dimension 5cm x 5cm. The woody debris were also measured, with special effort being invested in the definition of the border. A total of 17 cross sections were identified along the reach in order to obtain detailed topography and velocity values. The number of topographical measurements taken is equal to 13809 points, of which 116 defined the debris.

The discharge was maintained constant (210 ls^{-1}) in steady hydraulic conditions and was regulated by a weir located at the channel end. The water levels were measured at the left (17 points) and right (17 points) side of the creek. Several velocity measurements were obtained at each cross section as a result of the mean 1-minute reading (25Hz). Velocity was measured at different levels up to 7 cm below surface water level. Problems arise when trying to obtain velocities above this point, and so there are no velocity values belonging to this depth range. The velocity measurements were applied every 20 cm at each cross section and a reading was taken every 5 cm depth at each selected point. A total of 1238 velocity measurements were obtained for the channel

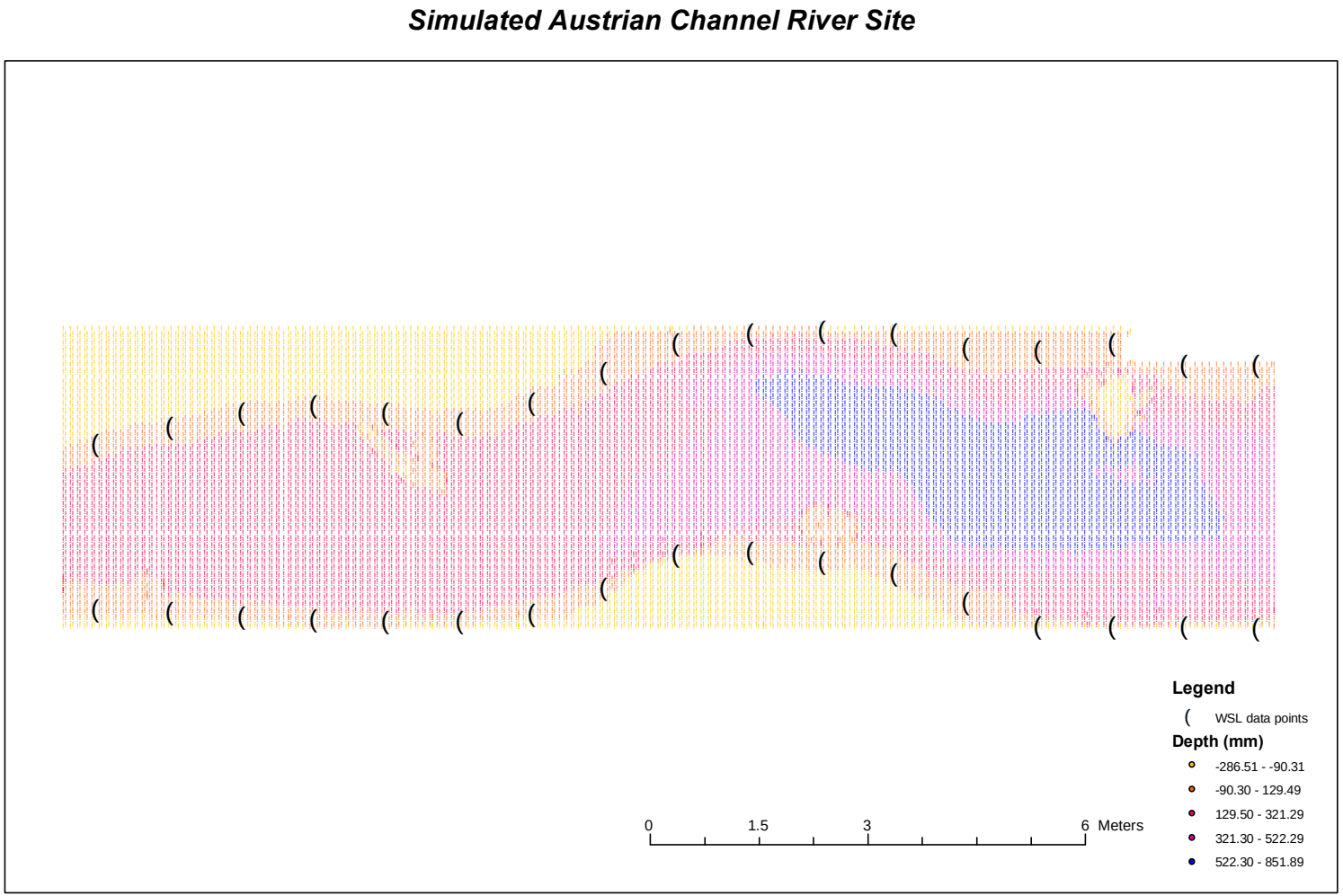

Figure Appendix 1.1: Data sets collected at Simulated Austrian channel River Site. Depth values have been represented in mm.

Bere stream

The Bere stream is one of the main tributaries of the Piddle catchment in Dorset. The Piddle catchment has an extension of approximately 190 km^2, of which 48 km^2 contribute to the Bere stream at the river site. The water quality of the rivers in the Piddle catchment is very good due to the character of the catchment which is mainly rural, with very little industrial development. In addition to this, the flood plain areas have been managed to maintain suitable water levels in riparian meadows and wetland areas. Thus, the rivers have remained clean enough to support thriving populations of brown trout and salmon, yet have the habitat characteristics in their lowland reaches to also sustain a healthy population of coarse fish. Currently, the status of the rivers is moving towards a trophic threshold due to several changes in the catchment area and this could significantly change the ecology in future.

The geology of the catchment is composed of Jurassic limestone, Upper Greensand, Chalk, sands of the Tertiary deposits, superficial sands or gravels, which provide the likelihood of large groundwater storage, and clay with flints. The dominant substrate at the Bere stream is a combination of sands, gravels and clay. The proximity of the Piddle catchment to the Frome and the chalk character of the geology point towards the possibility of groundwater interchange between these two areas. In addition, the chalk aquifer presents extensive karst development that contribute to the water interchange. The existence of faults provides constraints on groundwater and influences the contributions to outflows. Mean annual rainfall in the Bere area is around 800 mm.

The water quality information has been obtained from the station located at the confluence between the Bere at Chamberlaynes. The water quality has been classified (GQA classification) as grade A for Biological Oxygen Demand, ammonia and dissolved oxygen content. The nitrate content was considered grade 5 whilst the phosphate content was 3. These results indicate that the river has a very good water quality and that the main problems are due to high nutrient levels. The water quality indicates that water abstraction is possible for all uses and that salmonid and cyprinid fisheries could be supported in this area. The biology has been classified as grade A and thus, it can be considered as similar to that expected for an unpolluted river.

Bere River Site

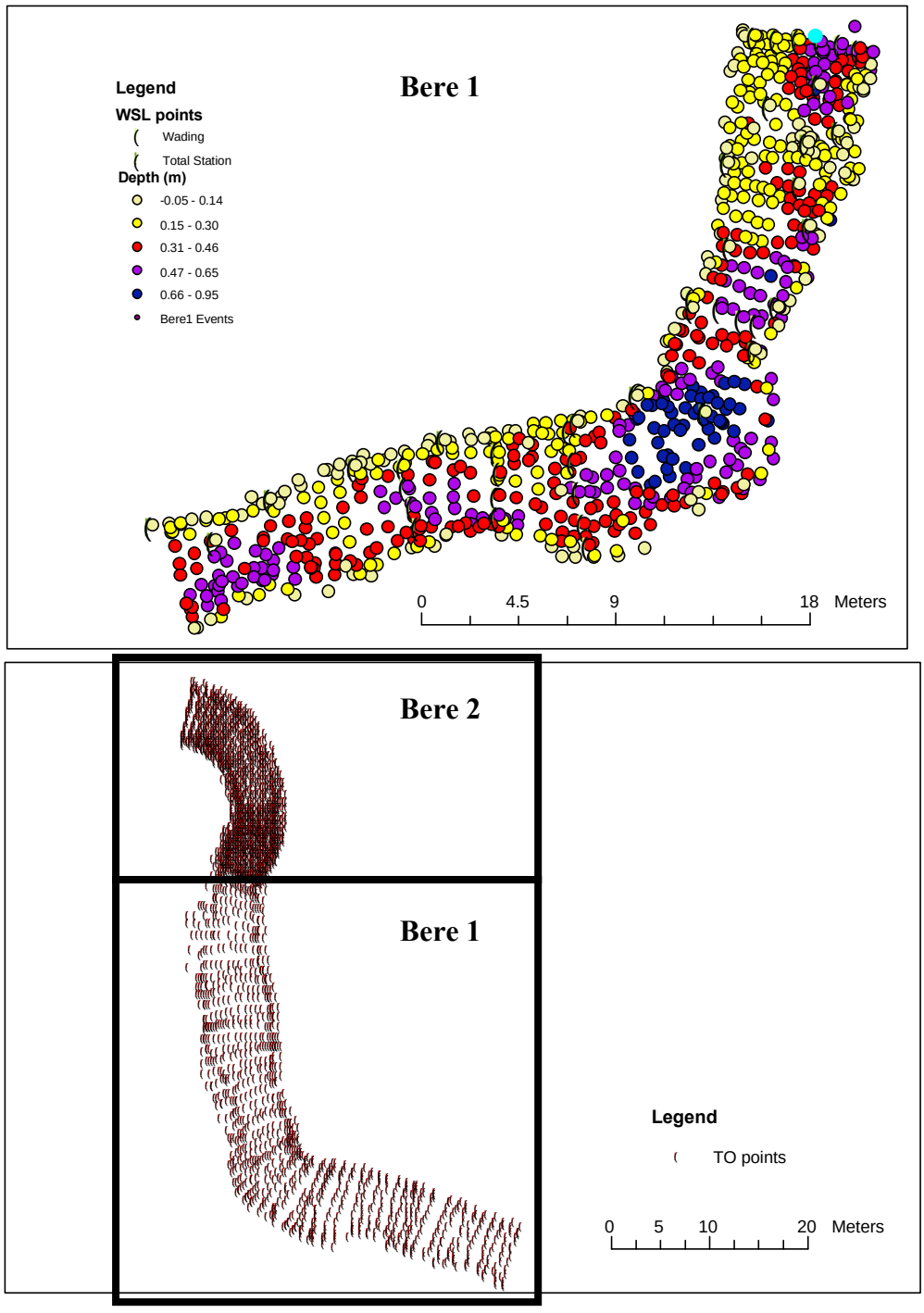

Figure A1.2: Data sets collected at Bere 1 (top and bottom) and Bere 2 (bottom) River Sites..

The Bere river site (Figure A1.2) is located at coordinates 385900E, 92015N. Data from the river section should be straightened for further data analysis due to the fact that it does not present a straight shape. The topographical data collected at the Bere stream was measured in September of 1998 (Q=0.365 m^3s^{-1}), January of 2000 and July of 2000 (Q=0.45 m^3s^{-1}). The data sets measured in September 1998 and January 2000 correspond to a different location to the data set measured in July 2000. The total number of points measured for the first location (Bere 1) in September and January is 2759 over a total river length of 80m, whilst 794 points were measured over a distance of 45m in the second location (Bere 2) in July. The mean width of these river sites is ≅ 5.8 m. The water surface level was only measured in the second location and so no depth measurement can be obtained for the first location. Two different methods where applied for the WSL measurement; a total station and wading rod. A total of 43 points were collected for the water surface level representation; 20 randomly located points with a total station and 23 points with the wading rod method, describing 5 complete cross sections.

Blackwater

The Blackwater river rises in Rowhill Nature Reserve, which is on the Surrey and Hampshire border between Aldershot and Farnham. The Blackwater river is the centre piece of the Blackwater Valley. The main tributaries are Cove Brook and the Whitewater.

The geology of the valley is defined at the southern end by the Hogs Back, a ridge of chalk that forms the southern limit of the London Basin. Tertiary deposits of London Clays, Bagshot formation, Bracklesham Beds and Barton Beds are found in the surrounding valley. The current land uses for the catchment area include gravel and sand extraction and urban expansion.

The water quality values for the Blackwater river site have been obtained from the station located at Aldershot. The GQA classifies the BOD as grade B, ammonia as grade A, DO as grade C, nitrate and phosphate as grade 3 and biology as C. These results indicate that advanced treatment is required if the water is used for potable supply and that the biology is worse than that expected for unpolluted rivers. The closest gauging station to the river site is located at Farnborough (39123). The station

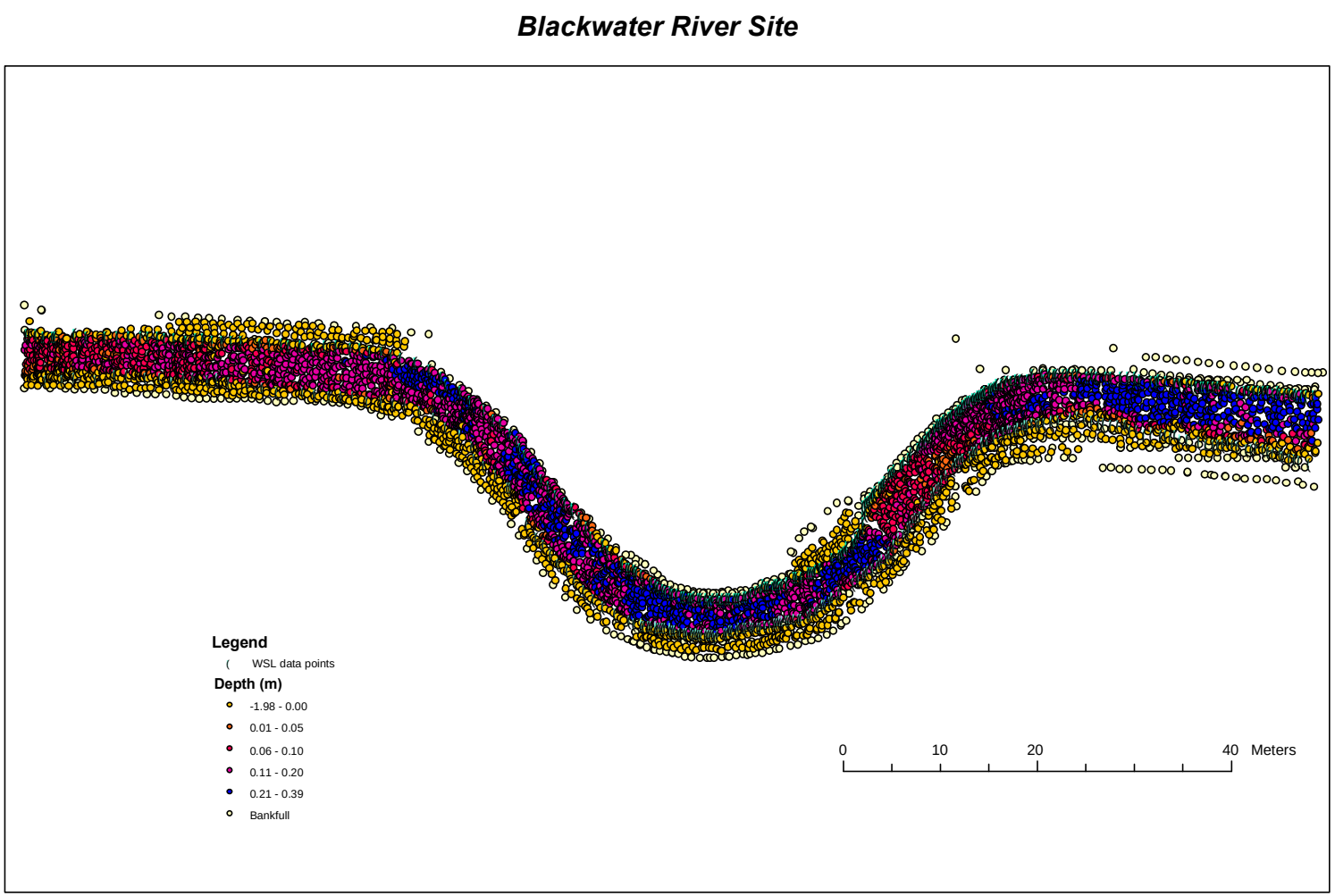

Figure A1.3: Data sets collected at Blackwater River Site. Depth values have been represented in metres.

defines a catchment area of 35.5 km^2, defining a mean, Q_{10} and Q_{95} flows equal to 0.51 m^3s^{-1}, 0.926 m^3s^{-1} and 0.144 m^3s^{-1}.

The river site (Figure A1.3) is located at coordinates 488390E, 150725N, with a length of 155 m and an averaged width of 5.8 m. The data set available is constituted of two topographical files of 4876 and 886 points. The first one defines the topography of the channel bed (4876 points) whilst the second defines the bankfull shape. The Water Surface Level has been described through a data set of 476 points, collected following the wetted edge of the river bed. Data were collected at three different discharges: Q=0.46 m^3s^{-1}, Q=0.79 m^3s^{-1} and Q=0.92 m^3s^{-1}.

Brazos

The Brazos River (Rio Brazos de Dios) is a 2060 km river. Its catchment area is equal to116,000 km^2. The Brazos is the longest length of river stretching through Texas. Amongst the tributaries of the Brazos we can encounter the Clear Fork of the Brazos, Bosque River; Little River; Yegua Creek; and Navasota River. The Brazzos passes through Dallas-Fort Worth, Waco, Bryan-College Station, Sugar Land, and the Gulf of Mexico where its mouth is located. There are three dams and nineteen major reservoirs along the Brazos. The Brazos is primarily important today as a source of water for power and irrigation. The water is administered by the Brazos River Authority. The geology of the Brazos is formed by Permian strata which is characterised by a high content of thick salt bed that dissolve into waters increasing the salinity.

The data set for the Brazos site (Figure A1.4) included 37288 topographical data points collected along a 7.5 km reach. Maximum depth at the Brazos site is equal to 12.95 m, with a mean depth of 2.57 m and a variance equal to 1.83. Mean width is equal to 100 m which provides a depth-width ratio of 0.025. The sinuosity index is equal to 3.2. Data were collected using a single beam depth sounder for both river sites. The site is characteristics of a lowland meandering river.

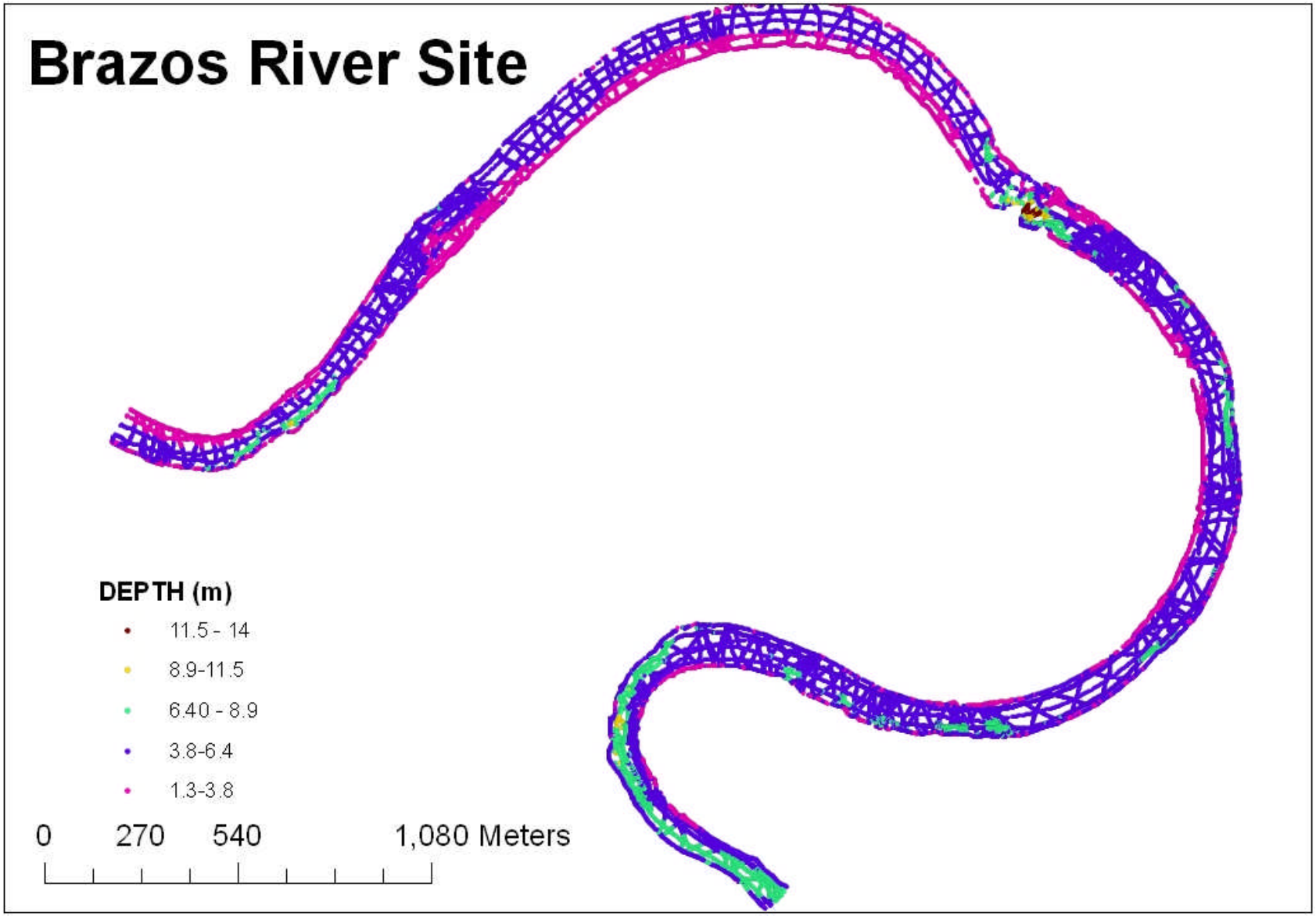

Figure A1.4: Data sets collected at Brazos River Site.

The Cruick

The Cruick Water is located in Angus (Scotland) and is a tributary of the North Esk river. It rises on Mowat's Seat in the Braes of Angus and flows south into the valley of Strathmore and then east to join the river North Esk. The total length of the river is 26 km.

The geology at the Cruick is mainly composed of a combination of highly permeable aquifer at the surface (with areas overlayed by a clay layer of unknown thickness) and weakly permeable rocks. Thick beds of marine and estuarine clay overlie Devonian sandstone and form an effective barrier between the aquifer and the surface activities. The Lower Devonian sandstone aquifer forms part of an elongate structural feature in which the strata have been extensively folded. Mudstones and igneous rocks can be found between the sandstone layers.

The land use in the catchment is mainly agricultural which depends on irrigation for successful crop production. The Cruick Water catchment area is considered to be at high risk due to the combination of a high permeable aquifer system and a high level of water abstraction.

The Cruick river site (Figure A1.5) is located at coordinates 418745E, 215725N. The sampled stream is 230 m long and approximately 5m wide, with a strong curvature that justifies the application of straightening techniques before further data analysis. Both, topographic and WSL data sets, were collected in August 2002 ($Q = 0.61\ m^3s^{-1}$). A total of 2432 points were collected for the topographical data set, whilst only 83 were measured for the WSL. Irregular grids were applied in both data sets.

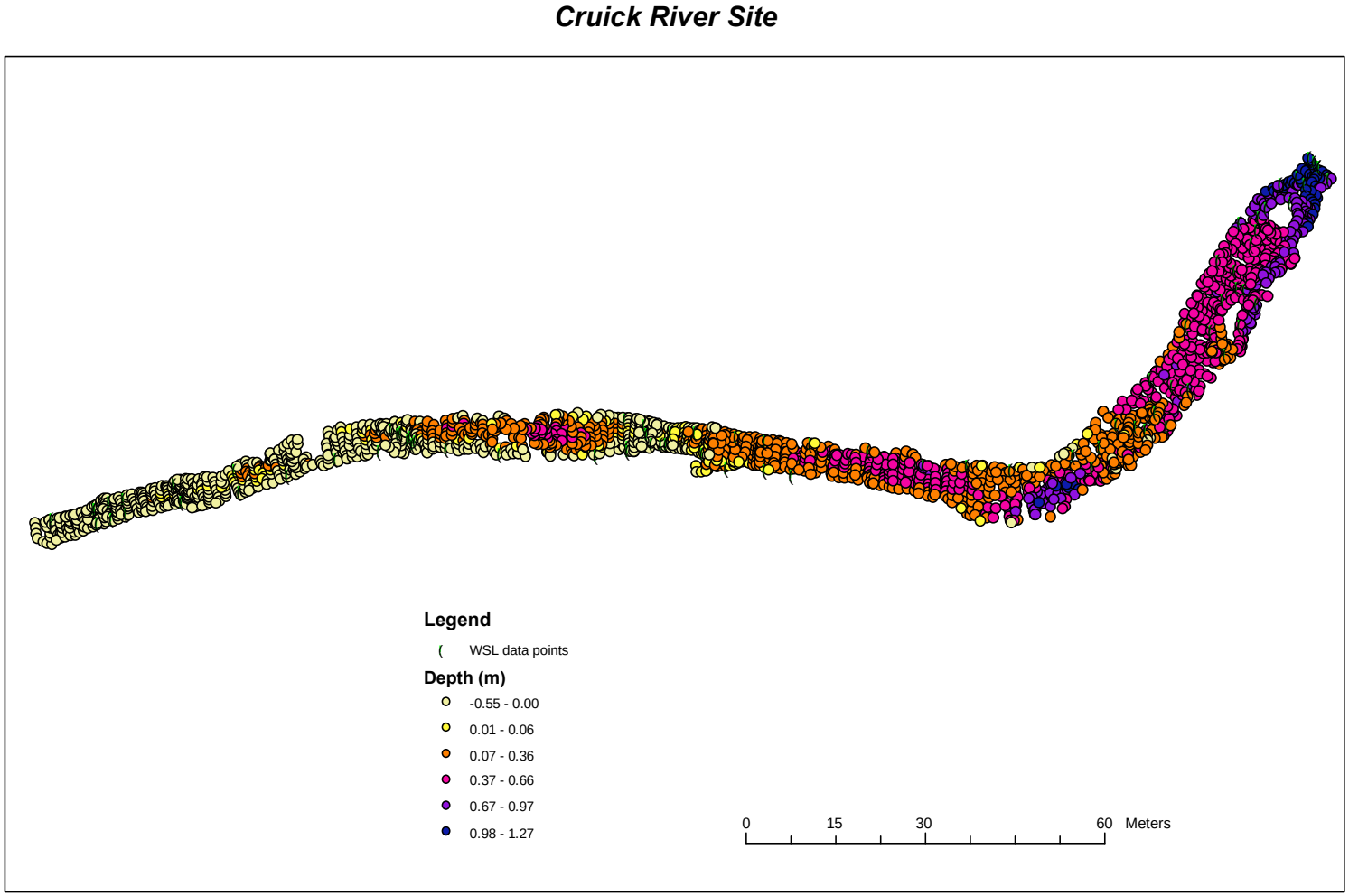

Figure A1.5: Data sets collected at Cruick River Site. Depth values have been represented in metres.

Highland Water

The Highland Water is located in the New Forest catchment in Hampshire and is a meandering gravel-bed river with an active bedload of fine-coarse gravels, and a suspended load of silts and clays. The Highland Water has two main tributaries; the Long Brook and the Bagshot Gutter.

The river is characterised by a large number of organic debris dams and a damp riparian forest floodplain that regulate the equilibrium between sedimentation and erosion, storing bedload upstream and forcing water and suspended sediments downstream (floodplain).

The water quality of the Highland Water river obtained at the Bank stream station (Environment Agency, 2002) defines the contents of ammonia and BOD as grade A, the dissolved oxygen content as grade C, the nitrates as grade 2, the phosphates as grade 5 and the biology as B. According to the values obtained for the Environment Agency classification, the water from Higland Water river site can be used as potable supply after advanced treatment and is good for cyprinid fisheries. Additionally, the content of nitrates is very low, the content of phosphates is very high and the biology is a little short of that expected for an unpolluted river.

The extension of the New Forest catchment area is $12km^2$ approximately and is located to the Northwest of the town of Lyndhurst. The geology is composed of an underlying Eocene Barton group (marine clays and sands) capped by older River Gravels. In the valley floor, the deposits bordering the channels are dominated by sands and gravels laid down as alluvium, that sometimes are overlain by peat. The characteristic types of soils are podsols for the older river gravel geological areas and peat soils at some points of the valley floor.

The climate for the Highland Water river site is oceanic, characterised by mild wet winters and wet warm summers. Rainfall is around 750mm per year and temperature oscillates between 2 degrees Celsius in winter to 21 degrees Celsius in summer. The small catchment area and the geology result in a very flashy regime for the Highland Water. The flow regime is temperate oceanic, with a maximum in January and a minimum in August. No gauging stations are available from the National Water

Archive. However, there is a gauging station at Millyford (SU 268077) which records values of mean daily flow equal to 0.12m^3s^{-1}.

The Highland Water river site is located at coordinates 426500E, 107500N, at 30 m AOD and 6.5 km from the river origin, with a length of 50 m and mean width of approximately 6.5 m. The nearest villages to the river site are Millyford, Bank, Emery Down and Lyndhurst. The selected stream presents a smooth curvature along the river and hence, it would be convenient to straighten it in order to apply further data analysis. The data set collected at the Highland Water river site in July of 1999 is constituted of two topographical and three different water surface level data sets. The topographical data sets represent the bed channel topography (392 points) and the river bank (117 points). The water surface level data sets have been collected for three different flows; 0.09 m^3s-1, 1.88 m^3s-1 and 0.91 m^3s-1 in March and April of 1999 with 16, 17 and 24 points respectively. The points have been collected in the central area of the river for the first and third WSL data set, and at the river edge for the second one (Figure A1.6).

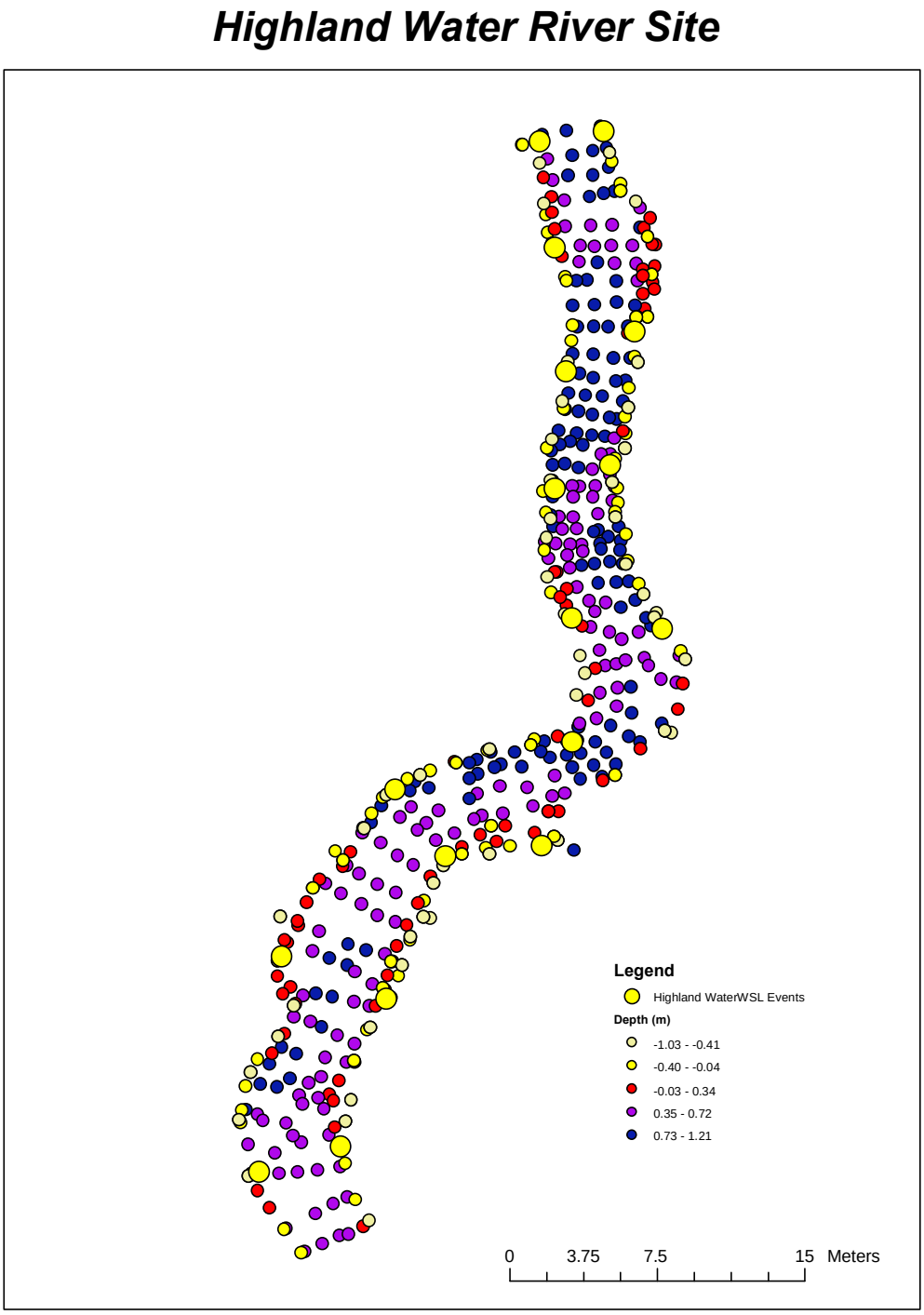

Figure A1.6: Data sets collected at Highland Water River Site.

Lambourn

The river Lambourn is located in the Thames Region and it rises near the village of Lambourn, in the chalk of the Berkshire Downs at an altitude of about 152m. Three stations (CEH Wallingford, 2000) are located in the Lambourn at; East Shefford, Welford and Shaw. The two first stations are located upstream of the studied river site whilst the last one is located downstream. The river altitude at East Shefford is 101.9m and 75.6m at Shaw. The mean flow of the Lambourn at East Shefford is 0.76 m^3s^{-1} and 1.76 m^3s^{-1} at Shaw with Q_{95} equal to 0.113 m^3s^{-1} and 0.762 m^3s^{-1}, respectively. Q_{10} is equal to 1.57 m^3s^{-1} at East Shefford and 2.92 m^3s^{-1} at Shaw. The catchment area at the river site is approximately 185 km^2, with 154km^2 at East Shefford and 234 km^2 at Shaw.

The Lambourn flows through the Kennet Valley in a south-easterly direction to Newbury, with a total length of 26 km. Bagnor, Boxford, Speen and Newbury are the closest urban areas to the selected river site. The river joins the Kennet at an altitude of 85 m. The Winterbourne stream is the most important tributary of the Lambourn. This tributary flows into the Lambourn from the north-east (upstream of Newbury). The catchment is mainly rural characterised by farming activities, with deciduous woods along the catchment boundary. The river Lambourn is considered to have one of the least modified catchments in southern England, with one of the lowest rates of abstraction.

Water quality, water quantity and habitat quality are all considered high according to the Natura 2000 data form for the selection of Special Protection Areas (SPA), Sites of Community Importance (SCI) and Special Areas of Conservation (SAC). The river is classified as General Quality Assessment (GQA) biological class “B” and chemical class “A” at the Boxford station. Water abstractions are possible for any use according to the chemical quality level and the water quality is excellent for salmonid and cyprinid fisheries. The main problems identified in the river are localised higher nutrient levels and siltation due to the presence of sewage treatment works.

Most of the river has been designated a Site of Special Scientific Interest (SSSI) and Special Area of Conservation (SAC). The extension of the protected site is 27.27 ha, characterised by alluvial soils, basic geology, lowland geomorphology and valley

landscape. The catchment area has been included in the Atlantic biogeographic region. The habitats considered as a primary reason for the selection of the site are water courses of plain to montane levels with *Ranunculion fluitantis* and *Callitricho-Batrachion* vegetation. The species that is a primary reason for selection of this site as a SSSI is *Cotus gobio* (Bullhead). The *Lampetra planeri* (Brook Lamprey) is also present as a qualifying feature for the SSSI selection but it is not considered as a primary reason. The Bullhead is a small-bottom living fish that appears to favour fast-flowing, clear shallow water, with a hard substrate (gravel/cobble/pebble). It is frequently found in upland streams. The Brook Lamprey is a non-migratory freshwater species, found in streams with clean gravel beds for spawning and soft marginal silt or sand for the ammocoete larvae.

The coordinates for the Lambourn river site (Figure A1.7) are 444565E, 169280N. The selected site is a straight short stream (46 m) with a mean width of 7.5 m, located at 90 m AOD and 19 km from the river origin. The stream is characterised by a gentle slope of approximately 0.4% and a mean depth around 30 cm. The river topography has been described (July 2002; Q = 0.67 m^3s^{-1}) through two different sets of topographical data with 1916 and 289 points, respectively. The first set corresponds to topographical points measured in non vegetated areas whilst the second one has been collected in vegetated areas. Both data sets are distributed irregularly along the river. The water surface level data set for this river site consists of 4 points measured in the central area of the river.

Lambourn River Site

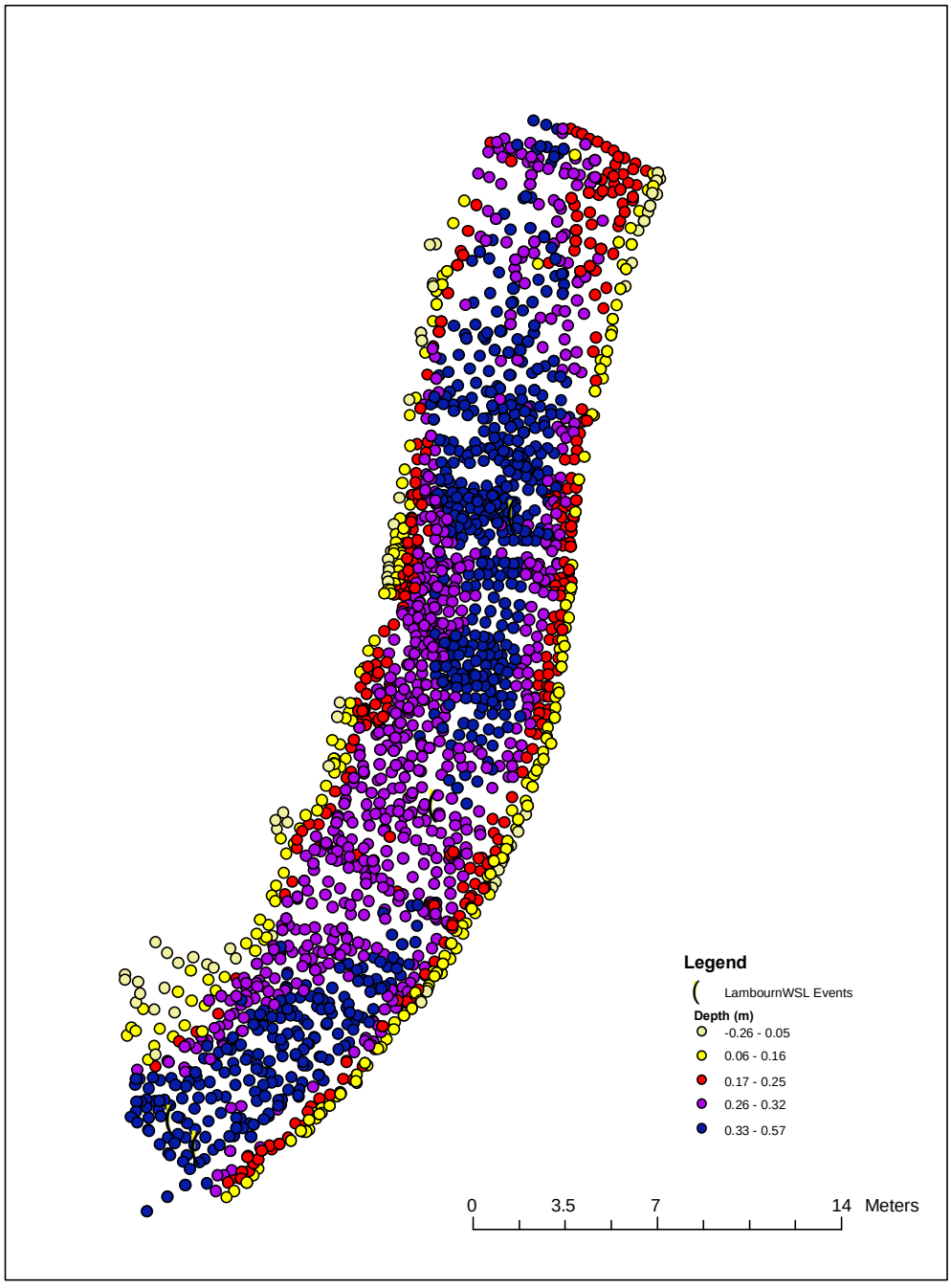

Figure A1.7: Data sets collected at the Lambourn River Site.

Leigh Brook

The Leigh Brook is a tributary of the river Teme and rises on the Malvern Hills in Worcestershire. Data was collected in a 198 m reach (Figure A1.8) within the Knapp and Papermill Nature reserve, which is managed by the Worcestershire Wildlife Trust. The reach is 10 m to 15 m wide and 2 m to 3 m deep from streambed to bankfull. The catchment area upstream the selected reach is approximately 80 km^2.

Data was collected by the Department of Applied Sciences, Geography and Archeology at University College Worcester (Worcester, UK). The variables characterised at the 5429 georeferenced points collected are quantitative (i.e. Froud Number, Velocity, Depth) and qualitative (i.e. Habitat Type and Flow Type). Data was collected for two different flow rates for a period of three days following dry weather and steady flow conditions. The first survey occurred at a flow of 0.517 m^3s^{-1} (Q82), whilst the second was carried out under a discharge of 0.344 m^3s^{-1} (Q93) (Maddock & Lander, 2002).

The measured points were distributed following 200 cross-sections located at 1 m interval. Points were distributed across each cross-section by a 0.5 m interval. The topographical survey was carried out with a Nikon NPL-820 Reflectorless total station. Average water velocities were recorded at 0.6 x depth at those points located inside the wetted width of each transect.

Habitat types were defined for each point following the typology developed by Maddock & Bird (Maddock & Bird, 1996). The categorisation of the habitat types was obtained by association of the dominant type of each cross section to the points measured. Flow types were assigned according to the typology used within the River Habitat Survey (Environment Agency, 2003).

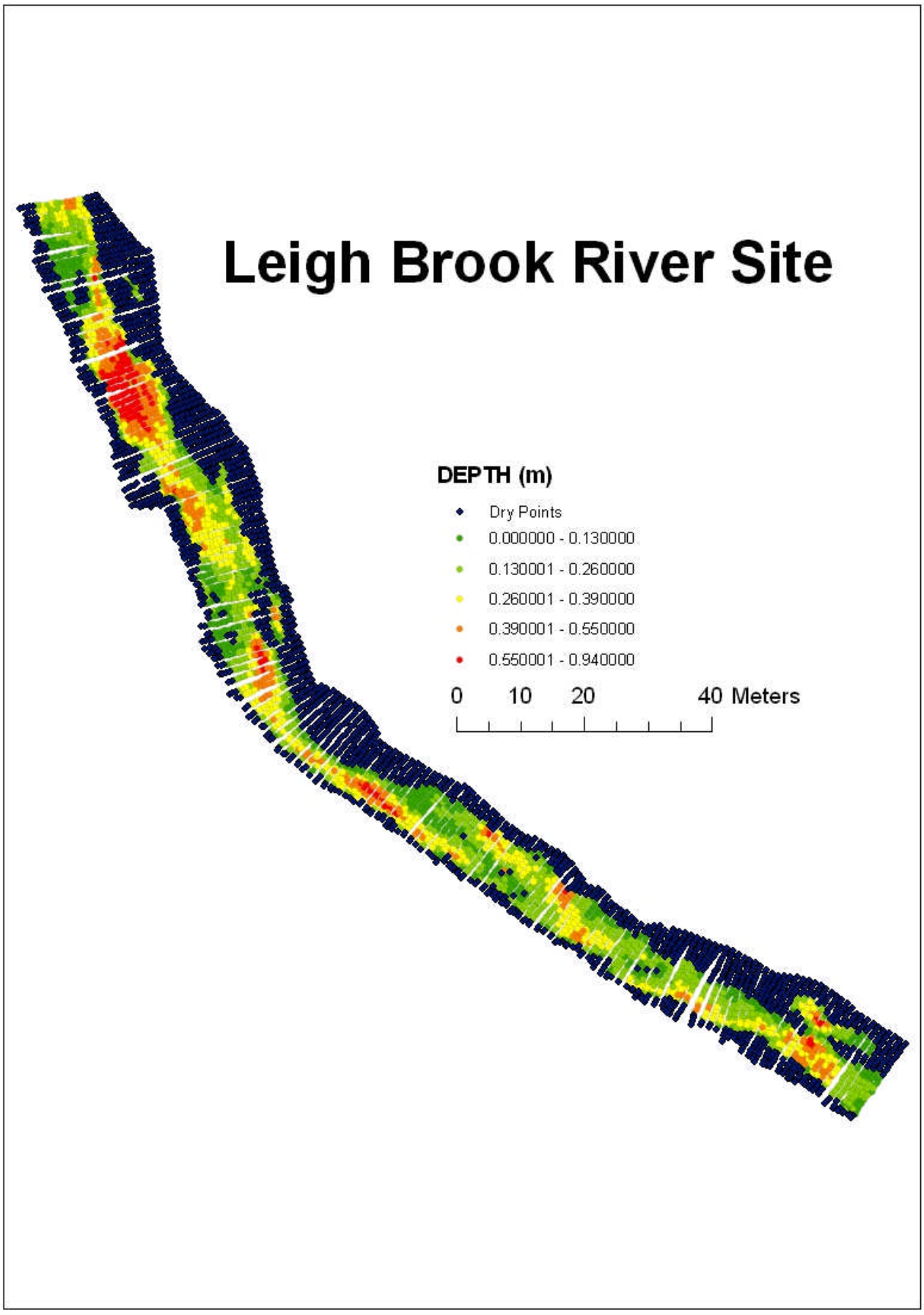

Figure A1.8: Data sets collected at the Leigh Brook River Site.

The Pang Old-fenced, The Pang Unfenced and The Pang Fenced.

The Pang, which drains 170 km^2, is a small tributary of the Thames and rises south of Compton. The catchment is located in central southern England and is characterised by a gentle slope and a maximum height of 186m (Lowbury Hill). The Pang flows in a southerly direction in the upper parts and then north easterly before joining the Thames.

The geology of the area is predominantly chalk which facilitates groundwater interchange between the Pang and the adjacent Lambourn catchment.. The higher land is formed of the Upper Chalk, which contains layers of flint nodules and patches of clay with flints in the surface that influence recharge on hill tops. In contrast, the floodplain is characterised by clays and sands of the Reading Beds.

The Pang has its origins in the Chalk aquifer of the West Berkshire Downs and thus, the river presents the characteristics of a chalk groundwater dominated river system, with slow, damped responses to rainfall and 'bourne' behaviour of headwater reaches when the water table is low.

The land use in the Pang catchment is mainly agricultural (farming and Christmas tree growing). Water pumping for water supply has been one of the main activities in the catchment and this dried the upper reaches of the Pang in the mid-1960s. The pumping also affected the lower reaches which became shallow and sluggish. However, recent changes in the abstraction regime have reduced groundwater losses, improving the river flows.

The closest monitoring stations to the selected river site are located at Bucklebury (39115), Frilsham (39114) and Pangbourne (39027), defining catchment areas of 109 km^2, 89.8 km^2 and 170.9 km^2, respectively. There is no gauging data available for these stations but the record of mean flow, Q_{10} and Q_{95} gives results equal to 0.27 m^3s^{-1}, 0.64 m^3s^{-1} and 0.001 m^3s^{-1} for the Bucklebury station, 0.23 m^3s^{-1}, 0.552 m^3s^{-1} and 0 m^3s^{-1} for the Frilsham station and 0.65 m^3s^{-1}, 1.17 m^3s^{-1} and 0.19 m^3s^{-1} for Pangbourne. The annual rainfall for the Pang area is close to 700 mm.

The Pang Fenced river site (Figure A.1.9) can be located by the coordinates 453625E, 175250N. The length of the stream is 155m, with a channel width of approximately 10.5 m. The curvature present in the selected stream indicates that straightening processes will be necessary before any further data analysis. Three different topographical data sets are available for the description of the bed channel at the Pang Fenced river site. Two topographical data sets were collected in January 2003 whilst the last one was collected in February of the same year. The January monitoring was used to obtain a detailed irregular data set of the area (1587 points), as well as a detailed cross section (148 points). The data set collected in February describes 9 different cross-sections and is composed of a total of 1225 points. The cross section measured in January was sampled again as one of the 9 sections measured in February.

The WSL is described through three different data sets collected in January, March and April 2003 with 37, 19 and 24 points, respectively. The flows for the two last data sets, whose points were distributed irregularly along the river, were 0.47688 m^3s^{-1} and 0.404 m^3s^{-1}. No gauging data are available for the first WSL data set whose points were distributed following a hypothetic axis along the river. The extent of this data set falls outside the limits of the topographical data set.

The coordinates for the Pang Old-fenced river site (Figure A1.10) are 453790E, 174635N. The selected stream is 31 m long, with a channel width of 7.5 m and it is characterised by a straight shape. Two different topographical data sets were collected for the Pang Old-fenced river site on the same day in February 2003 (Q = 0.48 m^3s^{-1}). The first one with 474 points was distributed following an irregular grid whilst the second, with 279 points, defines 4 detailed cross-sections of the river site. The three WSL data sets were collected in two different periods: February 2003 (on the same day as the topography data set Q = 0.48 m^3s^{-1}) and May 2003 (Q = 0.32 m^3s^{-1} and Q = 0.27 m^3s^{-1}) The data set collected in February 2003 is composed of 13 points located at the edge of the channel WSL. The data sets collected in May are composed of 7 and 9 points distributed along the central area of the river channel.

The Pang Unfenced river site (Figure A.1.11) is 107m long and 7.5 m wide. The river site is located at coordinates 453690E, 174550N and is characterised by a meandering shape that indicates that the data sets need to be straightened before further data

analysis. The topography of the river bed in the Pang Unfenced stretch is described by two data sets collected in February 2003 (Q = 1.02 m^3s^{-1}). The first one is formed by 1971 points distributed following an irregular grid along the river site. The second data set, which has a total of 1068 points, describes 9 detailed cross-sections spaced irregularly along the river site. The WSL has been monitored through out the three different data sets: two of them collected in February 2003 (Q = 1.02 m^3s^{-1}) and the last collected in May 2003 (Q = 1.020.32 m^3s^{-1}). The points collected in February, 23 and 25 for each data set were located at both edges of the WSL, whilst the data set collected in May was distributed randomly along the river.

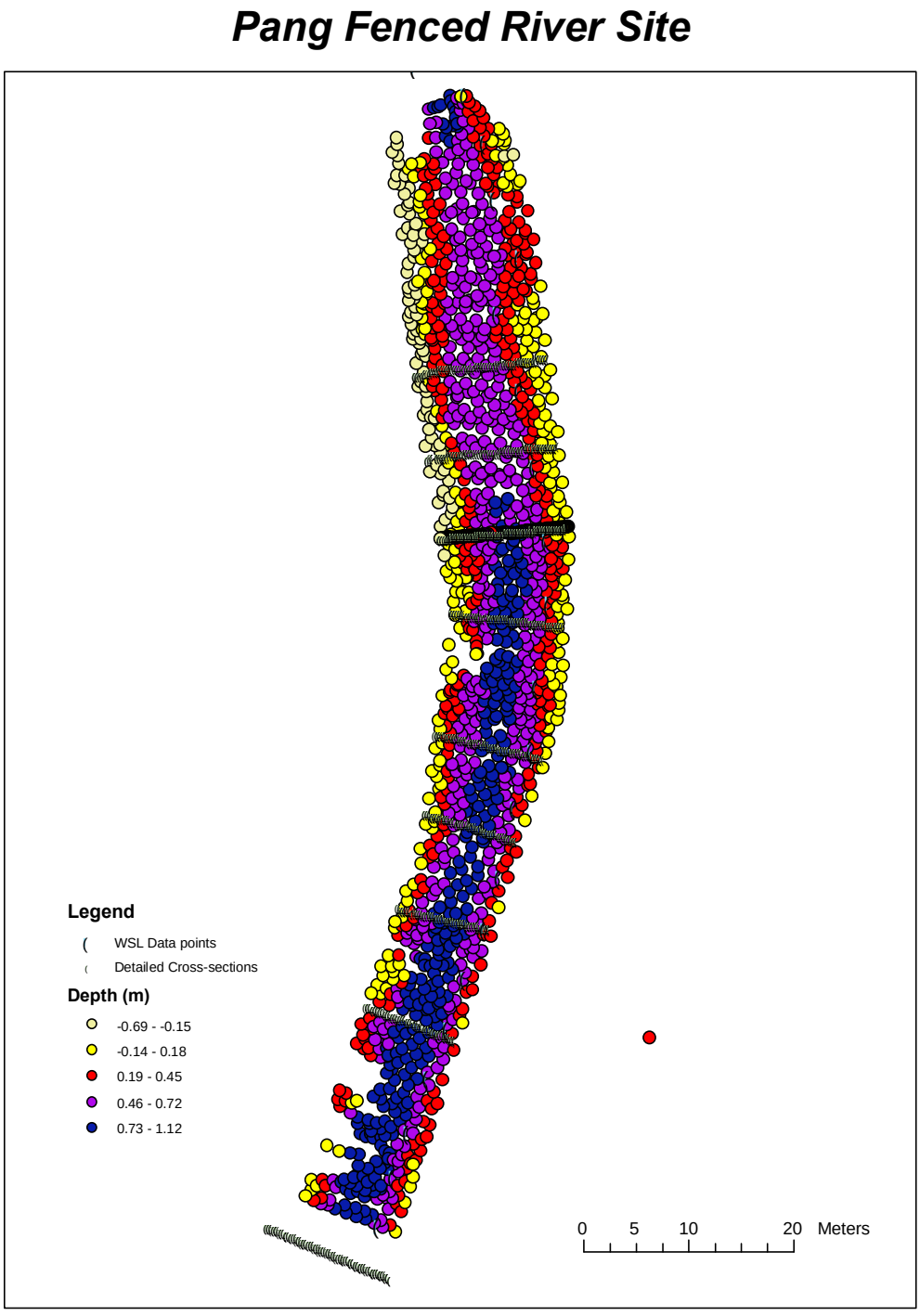

Figure A1.9: Data sets collected at Pang Fenced River Site.

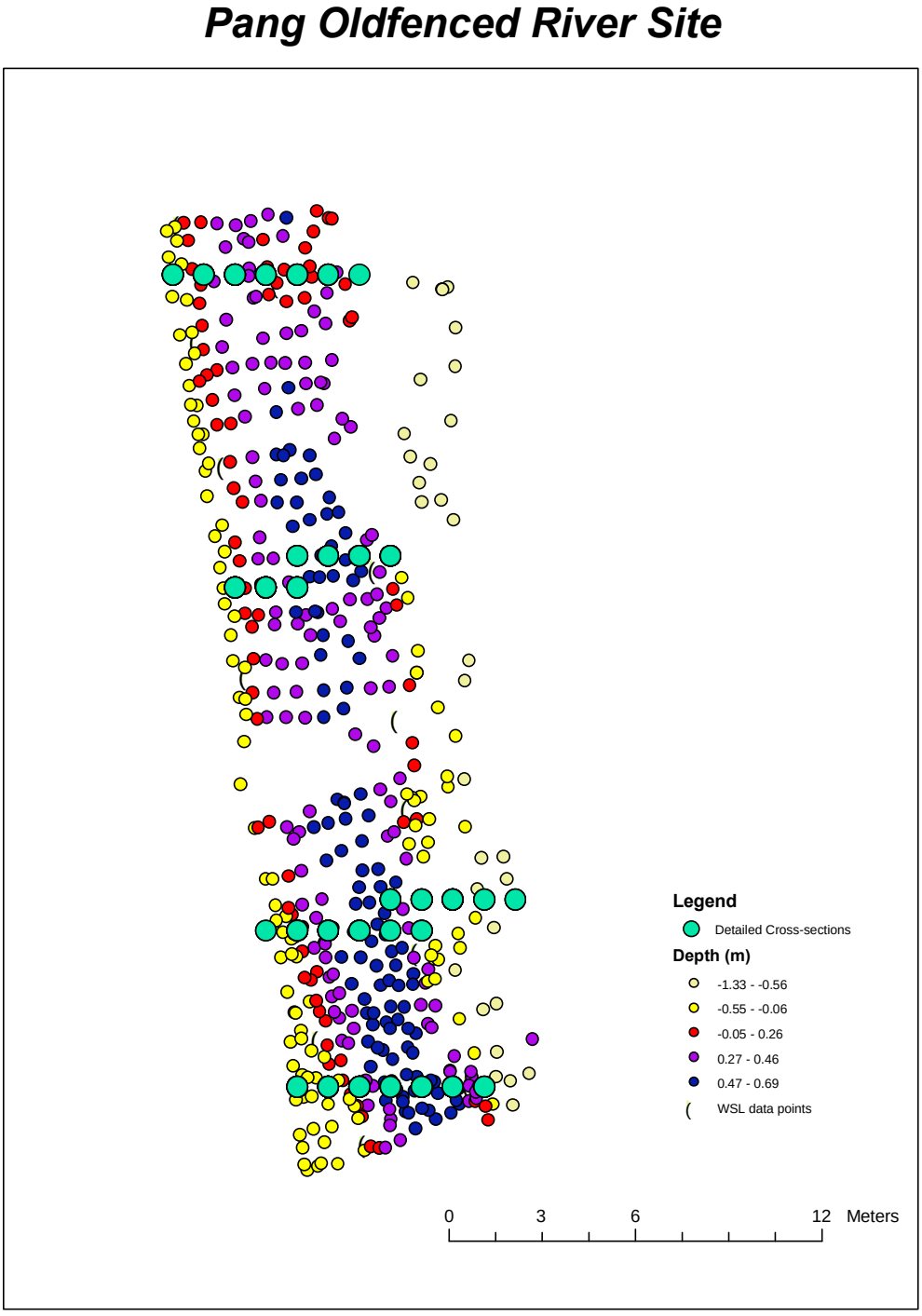

Figure A1.10: Data sets collected at Pang Old-fenced River Site.

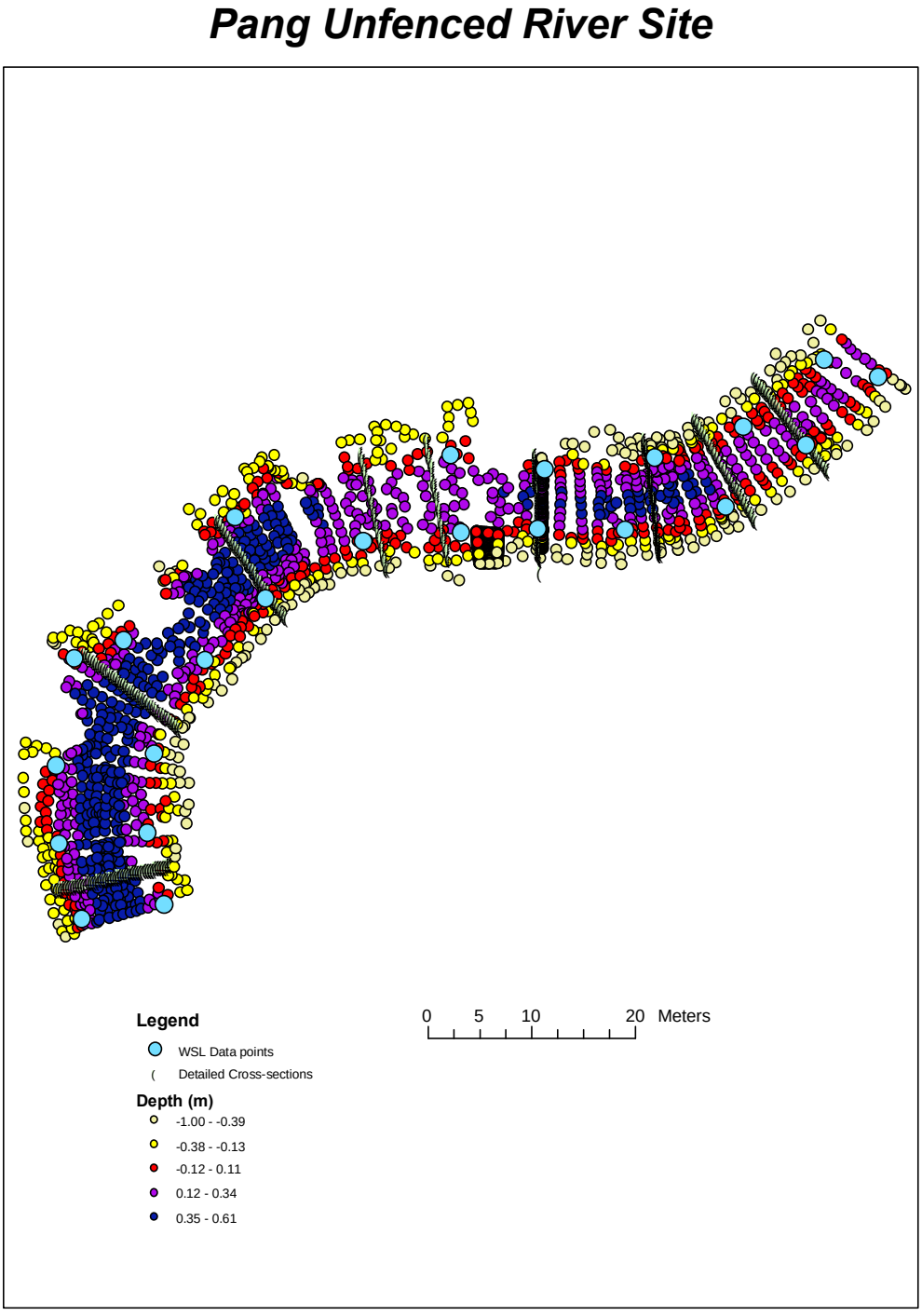

Figure A.1.11: Data sets collected at Pang Unfenced River Site.

Peris and Seiont

The rivers Seiont and Peris belong to the same catchment area, which is located in North Wales, Snowdonia. Afon Seiont or river Seiont is a tidal river that flows for 20km from Llyn Padarn to the menai straits at Caernarfon. The site was classified Site of Special Scientific Interest in 2003. The Peris is a small tributary of the river Seiont, characterised by a stepper gradient and coarser material than the Seiont. (Figure A.1.12)

The isotopic data set collected at the Seiont river site is constituted of 106 topographical points and 106 water surface level points. Depth was measured at each topographical point with the total station and the metric staff to allow the comparison of both sets of equipment. The data set collected at the Peris river site has 449 topographical points and 376 water surface level, from which 183 TO and 183 WSL points have been collected following an isotopic sampling strategy. Depth was measured with both, a metric staff and a total station, at 58 TO points of the Peris river sites respectively. The rest of the sampled points were measured with the total station following a heterotopic sampling strategy.

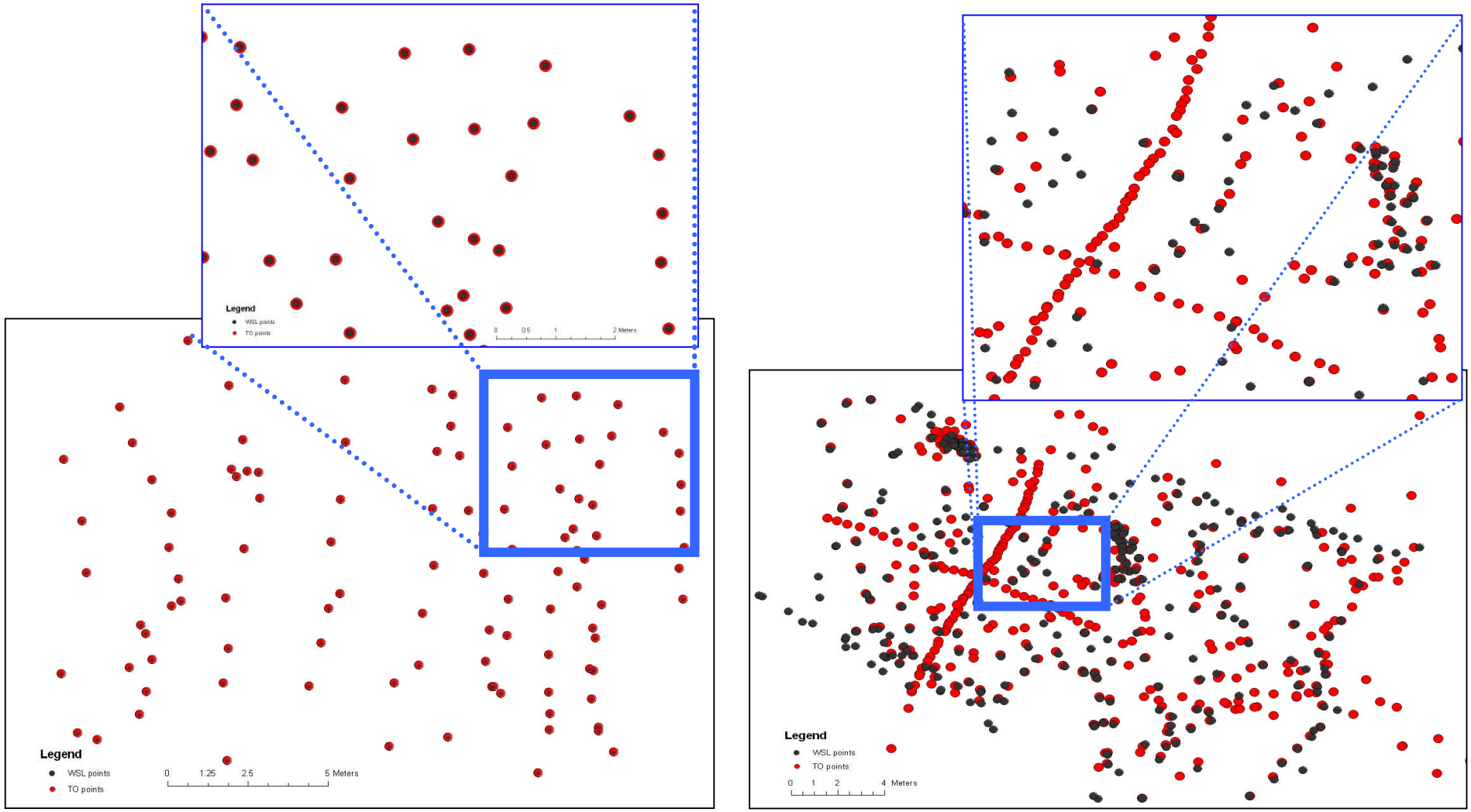

Figure A.1.12: topographical and water surface points measured at the Seiont (left) and Peris (right) river sites. Blue boxes show a detail of the sampling strategy applied, which is isotopic for the Peris and isotopic & heterotopic for the Seiont

The Senni

The Senni is a small tributary of the river Usk which is located in Wales, has a catchment area of 1007 km^2 and has been declared a Special Area of Conservation. The habitats present as a qualifying feature are the watercourses of plain to montane levels with *Ranunculion fluitantis* and *Callitricho-Batrachion* vegetation. In addition, the species that are a primary reason for the selection of this site are: Sea Lamprey (*Petromyzon marinus)*, Brook Lamprey (*Lampetra planeri),* River Lamprey (*Lampetra fluviatilis)*, Twaite Shad *(Alosa fallax)*, Atlantic Salmonid *(Salmo salar)*, Bullhead *(Cottus gobio)* and Otter *(Lutra lutra).*

The Senni catchment is fully contained in the Brecon Beacons National Park, which covers an area of 1347 km^2. The geology of the Senni catchment is composed of Old Red Sandstone. The uses of the land are mainly restricted to livestock farming, with approximately 5% of the surface occupied by forest. The dominant soils in the area are peat and the bed channel is composed of a combination of gravel-pebble-cobble with marginal areas composed of sand and silt.

The flow regime at the Senni site can be characterised using data from the station located at Pot Hen Hafod (56007). There are no flow series available at this station throughout the National River Flow Archive but values of mean flow, Q_{10} and Q_{95}, which respective values are 1.03 m^3s^{-1}, 2.37 m^3s^{-1} and 0.104 m^3s^{-1}, have been registered. The station is located upstream of the selected river site and includes a 20 km^2 catchment area. The water quality for the Senni river has been classified (GQA) as grade A for BOD, DO and ammonia, grade 1 for nitrate and phosphate and grade B for biological parameters. Thus, the system allows water abstraction for all uses and gives the possibility to support salmonid and cyprinid fisheries.

The coordinates for the Senni river site are 292980E, 226940N. The river site (Figure A.1.13) is 40m long, 8.8 m wide, defines a 28 km^2 catchment area and is characterised by a smooth curvature at the centre of its length. However, due to the shortness of the river site, straightening has not been considered necessary for the data analysis. A total of 895 topographical points were measured for this river site following an irregular sampling strategy. Five consecutive cross sections were surveyed in detail.

The WSL data set was measured in October 2000 with a flow of 0.44 m^3s^{-1}. The 24 points measured were located randomly along the river site.

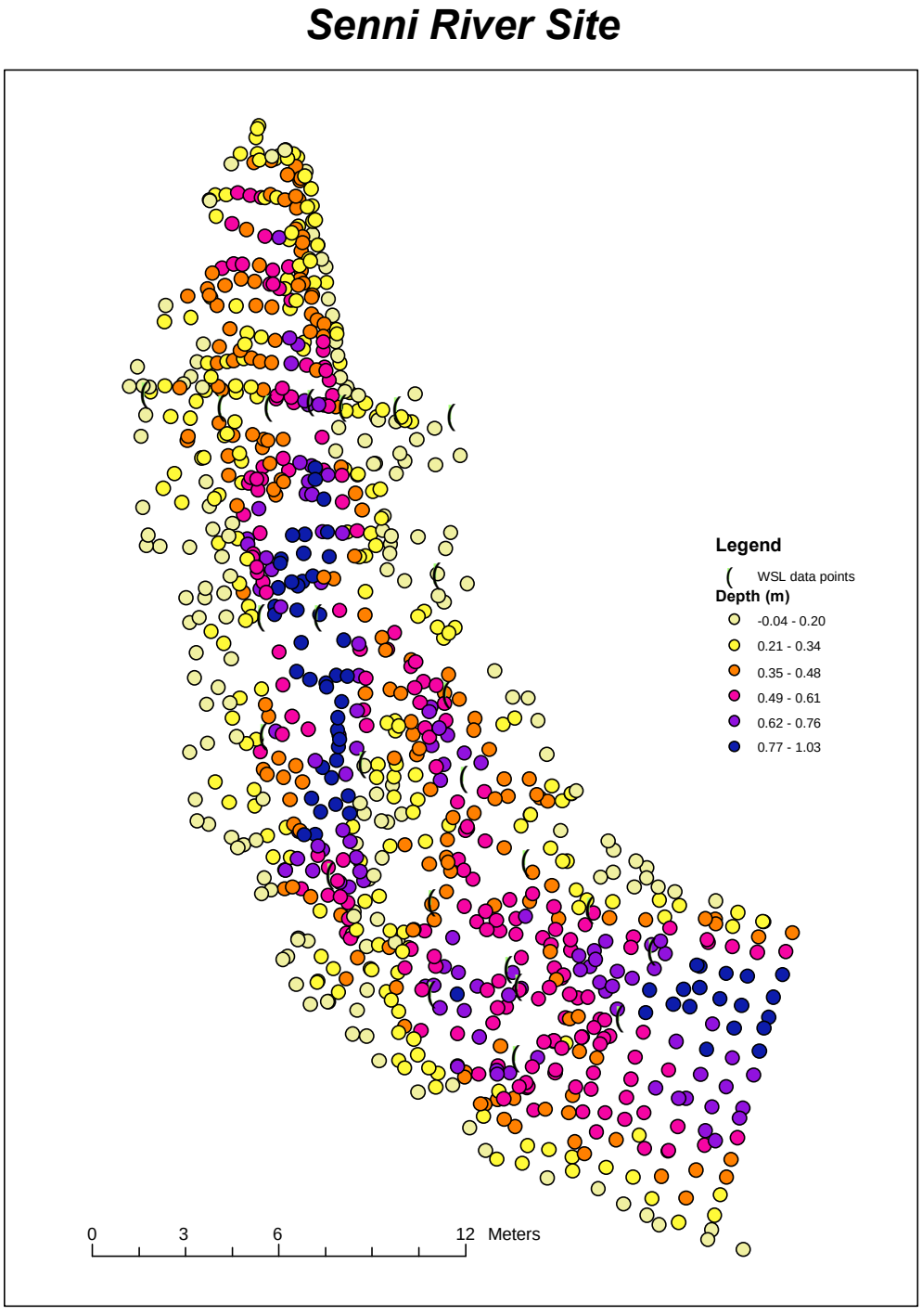

Figure A.1.13: Data sets collected at the Senni River site.

Sulphur

The Sulphur River is created in eastern Delta County (Texas) The river provides most of the water for Wright Patman Lake. The river flows through Miller County for 15 miles (24 km) until it joins with the Red River

The Sulphur data set (Figure A.1.14) had 8490 topographical data points collected along a 1.5 km reach. The maximum and mean depth at the Sulphur site is equal to 22.8 m and 12.86 m, respectively, with a variance is equal to 22.13. Mean width is equal to 35 m, which provides width – depth ratio equal to 0.36. The sinuosity index is equal to 1.81. Data were collected using a single beam depth sounder for both river sites.

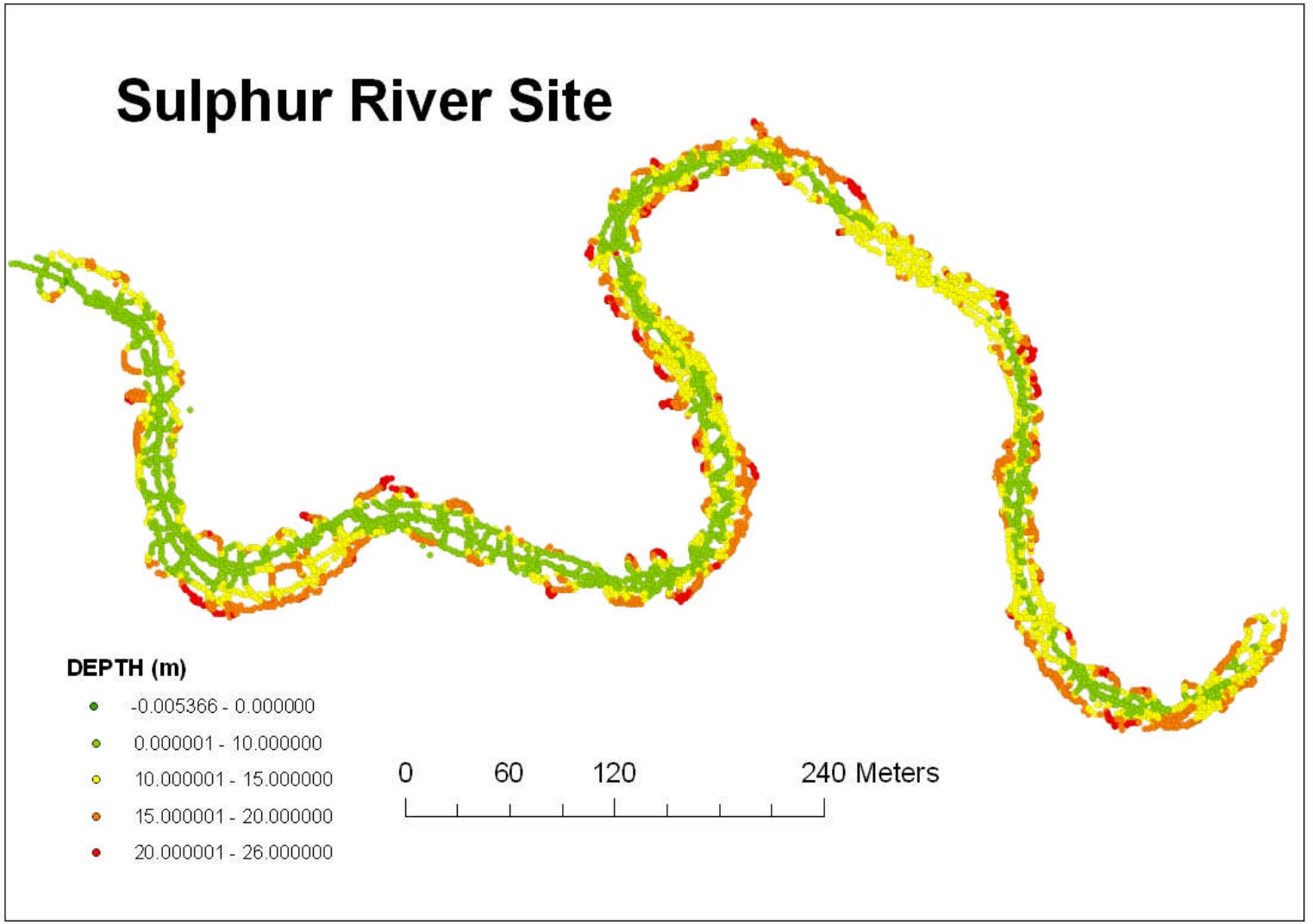

Figure A.1.13: Data sets collected at the Sulphur River site.

Tame HM and Tame LM

The river Tame catchment covers an area of 1490 km^2 at its confluence with the Trent river, with a catchment area of 183 km^2 and 188 km^2 at the Tame HM and Tame LM river sites, respectively. The length of the river is 285 km, with the highest point at 270m (Brecon Hill) and a lowest point at 50m (Chetwynd Bridge), rising at 150m AOD. The main tributaries are Oldbury Arm, Hockley Brook, Cole, Blythe and Black/Bourne Brook.

The geology of the Tame catchments is composed of Lower, Middle and Upper Carboniferous Coal Measures (between Dudley and Wolverhampton) in the upper area of the catchment. Triassic Mercia Mudstones and Triassic Sherwood Sandstones are also present in lower down the Tame catchment. The substrate for the majority of the river Tame is composed of a gravel-pebble combination, with limited presence of vegetation in the banks and channel.

The geology has promoted the abstraction of coal and clay in the past, which played a major role in the modification of the structure of the river Tame. Currently, the land use is divided between agricultural (55%), urban (41%) and woodland and rough grass (4%). The straightening of several parts of the river, pollution of running waters, flow alteration and the separation of the floodplain from the river are consequences of the activities in the Tame catchment over time. Thus, several research projects are being developed in the catchment area, such as LOCAR (Environment Agency, 2002), to study key water resource issues.

The mean annual rainfall in the Tame catchment is 740 mm of which approximately 450 mm constitutes runoff. The catchment is characterised by a flashy response to rainfall events due to the geology, the amount of water imported from outside the catchment (Wales) and the presence of several navigable waterways. Four gauging stations are located in the Tame river at Portwood (69027), Broomstair Bridge (69041), Bescot (28081) and Water Orton (28003). Bescot station is the closest to the selected river site, with a catchment area of 169 km^2 and mean flow, Q_{10} and Q_{95} equal to 2.37 m^3s^{-1}, 4.1 m^3s^{-1} and 0.92 m^3s^{-1}, respectively. The stations located upstream of the selected river sites in the Tame are Broomstair Bridge and Portwood with catchment areas of 113 km^2 and 150 km^2, respectively. The mean annual flow is

between 4.10 m^3s^{-1} and 3.55 m^3s^{-1} whilst Q_{95} is between 1.09 m^3s^{-1} at Broomstair and 1.31 m^3s^{-1} at Portwood. The Q_{10} values are 7.78 m^3s^{-1} at Portwood and 6.82 m^3s^{-1} at Broomstair. Water Orton station is located downstream of the monitoring sites, with a catchment area of 408 km^2 and mean flow, Q_{10} and Q_{95} equal to 5.62 m^3s^{-1}, 9.85 m^3s^{-1} and 2.45 m^3s^{-1}, respectively.

The water quality at the Tame HM and Tame LM river sites has been determined from data obtained from the station at the junction of arms-Bescot to Sandwell PK (Tame river). The GQA classifies the BOD and DO content as grade D, the ammonia as grade C, nitrate content as grade 5 and phosphate content as grade 6. The values indicate that the Tame river has nutrient problems due to the high and excessively high contents of nitrate and phosphate, respectively. In addition to this, the values indicate that the water could be abstracted for water supply after advanced treatment and that cyprinid fisheries could be supported in the area. The biological water quality has been classified as E and this indicates that the biology is restricted to pollution tolerant species.

The Tame HM river site (Figure A.1.15) is located at 402935E, 292890N coordinates. Tame HM is composed of one topographical set with 1206 points that were collected approximately following cross sections at the river site. The length of the selected river site is 112m, with a mean cross section width of approximately 13m, with a total of nearly 60 cross sections measured. The water surface level data set were collected for 4 different flows; 2.526 m^3s^{-1}, 3.693 m^3s^{-1}, 4.78 m^3s^{-1} and 4.25 m^3s^{-1} between November of 1999, July of 1999, and May 2001. The eight points measured in each WSL data set were located at the same coordinates on the edge of the river. The exception to this is the last WSL data set, where only four of these eight points were measured.

The Tame LM (Figure A.1.16) river site is located at coordinates 403020E, 292395N. The selected stream is 140m long, 13 m wide and is characterised by a straight shape. The topographical data set for this site consists of 1726 points collected following approximated cross sections. The WSL data were collected for six different flows between September of 1999 and November of 2000. The flows measured for the different WSL data sets are 2.559 m^3s^{-1}, 2.096 m^3s^{-1}, 2.559 m^3s^{-1}, 2.838 m^3s^{-1}, 1.4569

m^3s^{-1} and 4.372 m^3s^{-1}, each of them with 5 points located at the centre of the river channel, which were collected at the same coordinates in the different campaigns.

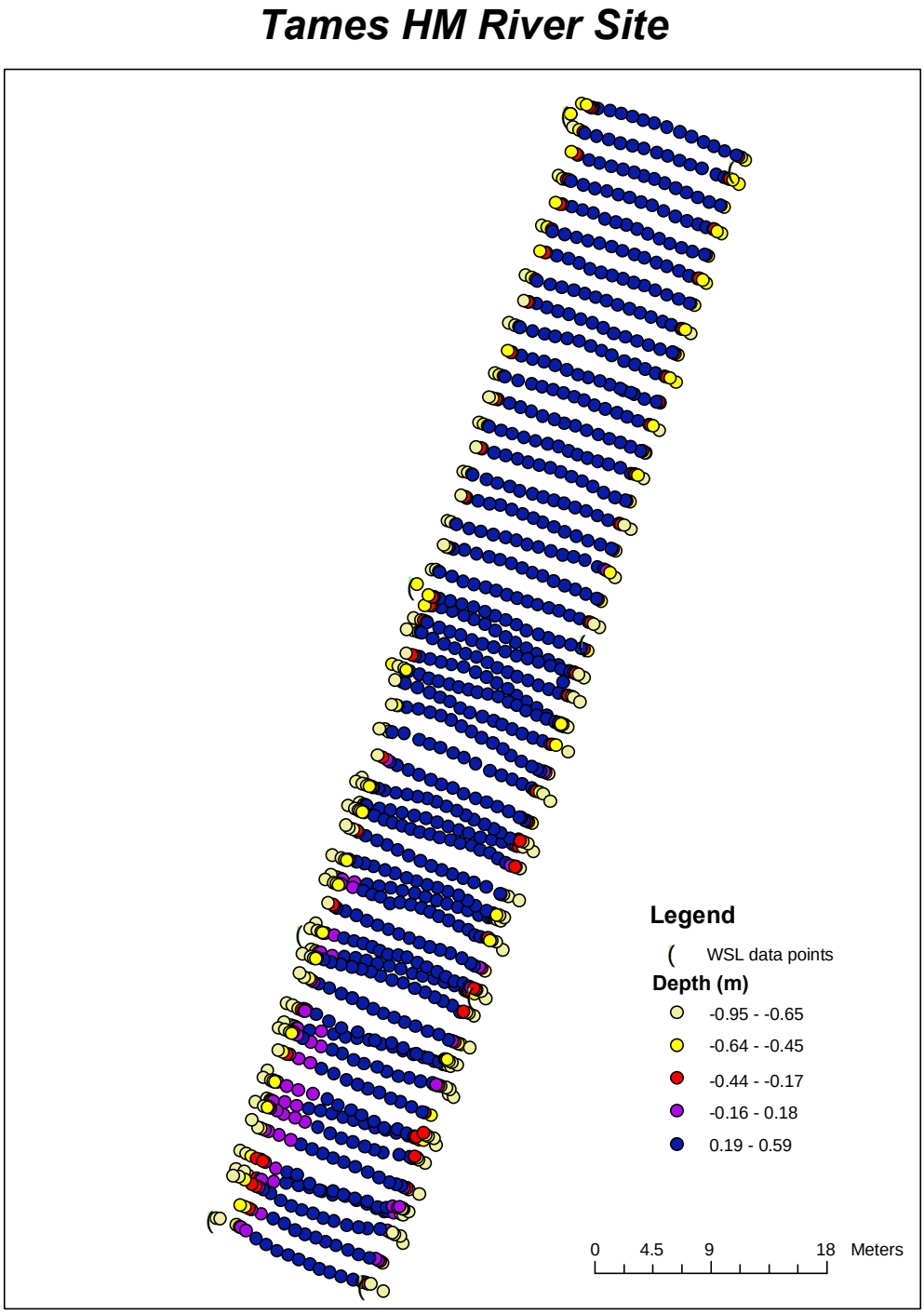

Figure A.1.15: Data sets collected at Tame HM River Site.

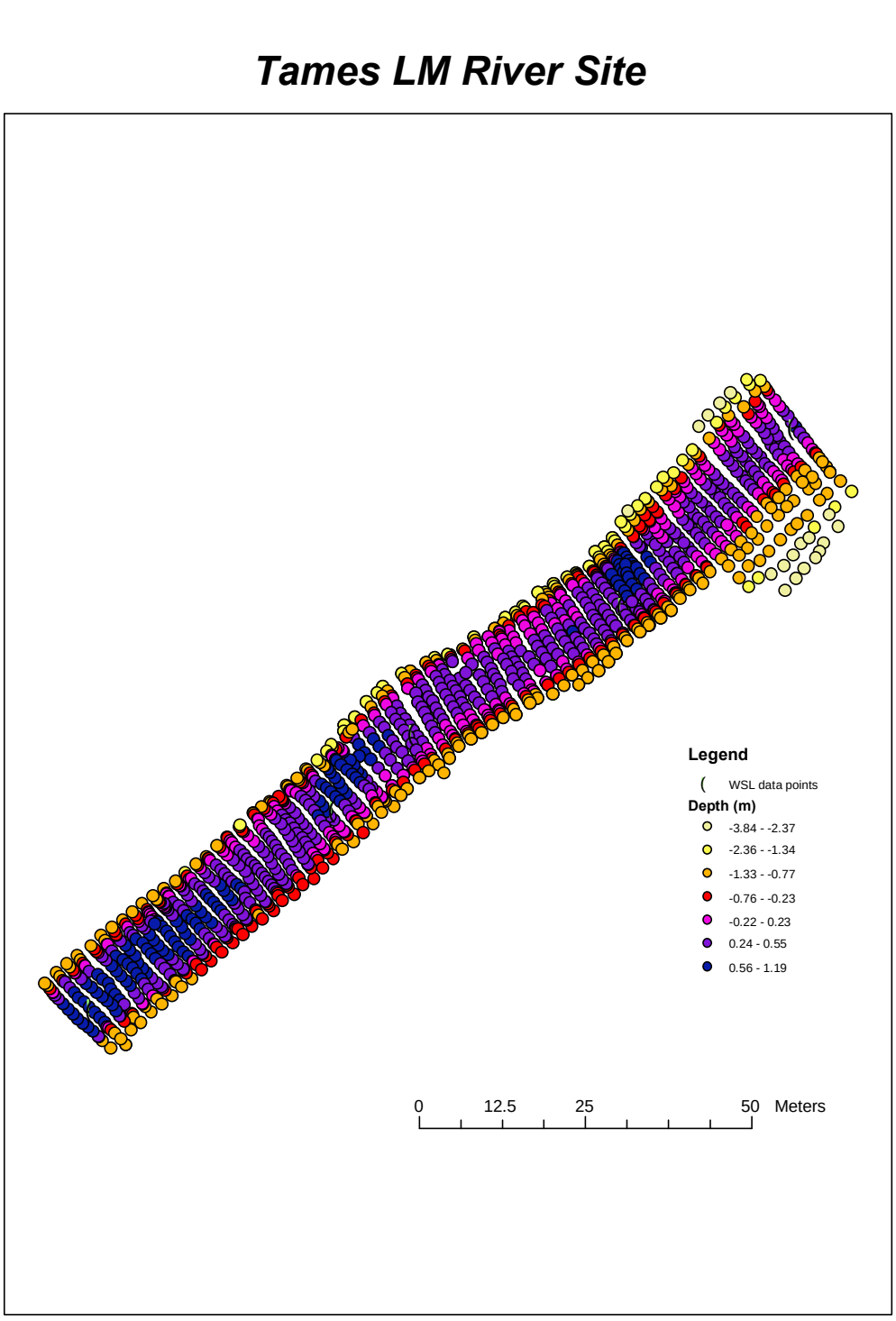

Figure A.1.16: Data sets collected at Tame LM River Site.

The Tarf

The site at the Tarf river is currently being studied by CEH Banchory as part of a project comparing Salmon productivity in upland and lowland rivers. It is located upstream of Tarfside and has a catchment area of approximately 15km^2 and lies at around 248 m above sea level. It is a tributary of the North Esk, which is on the northern edge of the Tayside region of Scotland. The geology is intrusive igneous, although the river runs over metamorphic rocks and old red sandstone in the lower reaches. There are no artificial influences to the flow regime. The area is all part of a large estate and is relatively isolated; access being up the North Esk valley. The main land uses in the catchment area are rough grazing with little tree cover.

The Tarf river site is considered to be a good status water body according to the study by the Scottish Protection Environment Agency (SEPA) (SEPA, 2003) although the site is influenced by human activities such as livestock agriculture, arable cropping, hill land and forestry. The water quality has been considered to have an overall classification of level B (2003) (fair) and a biological level A2 (Good).

The Tarf river site is located at coordinates 348765E, 782375N, at an altitude of 240m. The length of river surveyed is 212 m with a mean width equal to approximately 5.5 m. The catchment area at the river site, which is located 7 km from the original source, is 22 km^2. The data set collected at the Tarf river site (FigureA.1.17) has a total of 4937 topographical points and 252 water surface level points. The curvature of the river at the river site complicates the data analysis and thus, data sets require straightening. WSL and topographical points where measured during three consecutive days of field work, which had similar weather conditions. Hence, WSL data collected can be considered at “the same reference water level” during the complete survey and no adjustment needs to be done. WSL points were collected following an irregular grid, trying to sample the water level as many times as possible at both sides of the river banks.

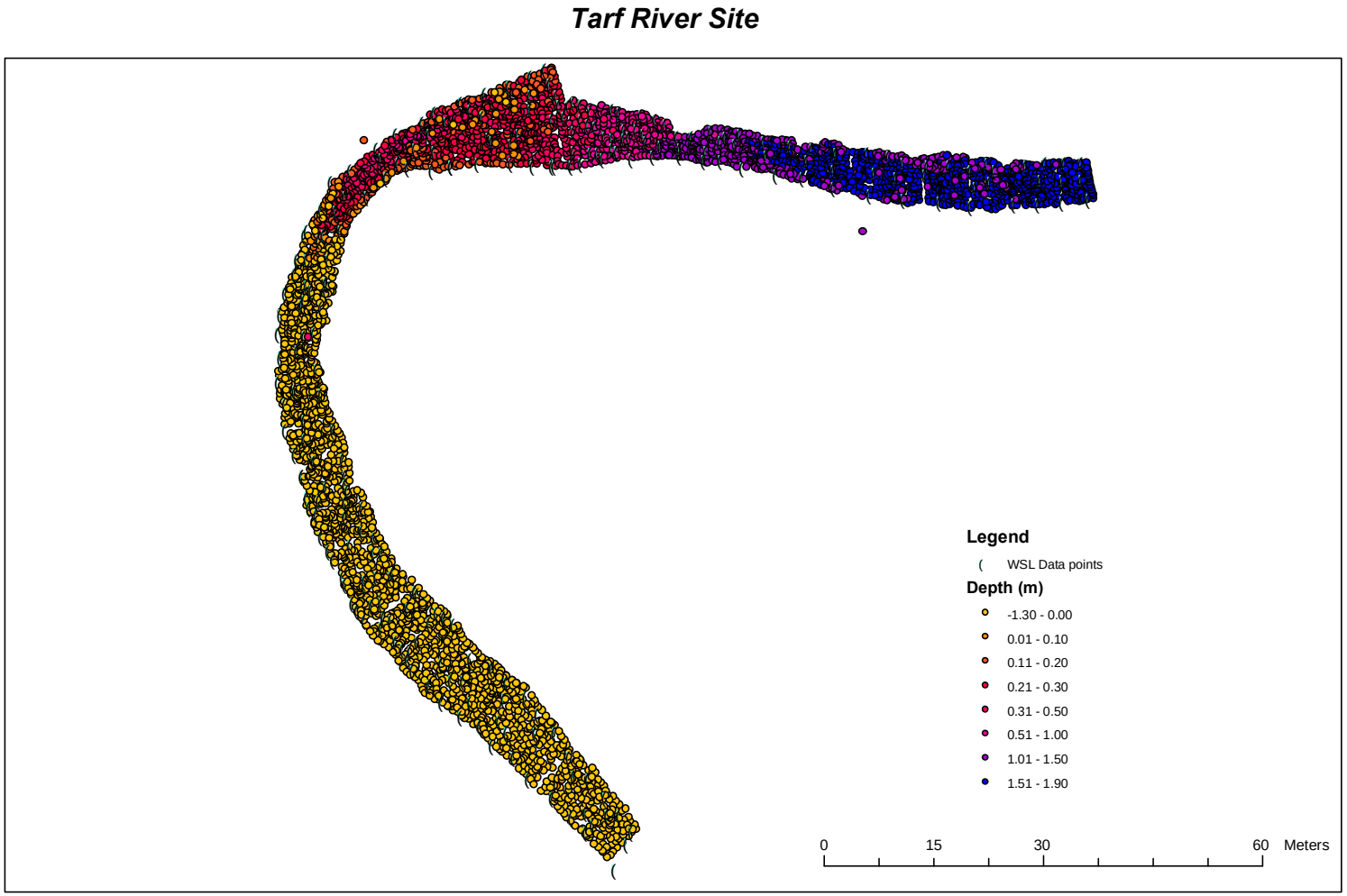

Figure A.1.17: Data sets collected at the Tarf River Site. Depth values have been represented in metres.

The Windrush

The river Windrush is a meandering river whose source is the Cotswold limestone. It originates approximately 4 km from Temple Guiting and is joined by a number of small tributaries (notably the River Dikler at Bourton-on-the-Water and the Sherborne Brook at Little Barrington). At the study area in Sherborne Park Estate, between Bourton-on the Water and Burford in Gloucestershire, the river flows through a water meadow system, belonging to the National Trust.

Land uses in the catchment area include mineral abstraction, especially for the Lower Windrush. Water abstraction is a major issue; water is abstracted from the river Windrush at Worsham and studies (Environment Agency, 2001) have been carried out to investigate the low flow problems on the Windrush.

At the Sherborne Brook station, according to the GQA classification, the water quality and biology are excellent (grade A) except for the nitrate content that is very high (grade 6). Thus, the Windrush river site is a natural ecosystem with particular nutrient problems which presents biology similar to that expected for an unpolluted river and excellent conditions for all kind of water supply uses and support of fisheries (salmonids or cyprinids).

The closest gauging station to the river site is the Windrush at Worsham (39076), which defines a catchment area of 296.0 km^2. The data registered by the NRFA at this location indicates that mean, Q_{10} and Q_{95} flows are equal to 2.17 m^3s^{-1}, 0.647 m^3s^{-1} and 4.28 m^3s^{-1}, respectively.

The Windrush river site (Figure A.1.18) data set is composed of 2259 topographical points and 380 water surface level points. The river site is located in an area of meandering 18 km from the river source. The river site defines a catchment area of 17 km^2 and is located at an altitude of 250 m. The length of river surveyed is 212 m, with a mean width of 9.7 m.

The meander area is characterised by pools which are deep enough to make the measurement of the water surface level impossible with the total station. Hence, WSL

values have been recorded with two different techniques; the total station (320 points) and immersion (60 points). WSL points recorded by immersion were collected during a different field monitoring exercise than those recorded with the total station. djustments need to be made in order to adapt both water surface level data sets to the same reference level. Note the detailed WSL and topographical data sets available for the upstream area of the river site. The meandering character of the river at the selected river sites complicates the application of geostatistical techniques. Straightening procedures therefore have to be applied in order to decrease the error in the data analysis.

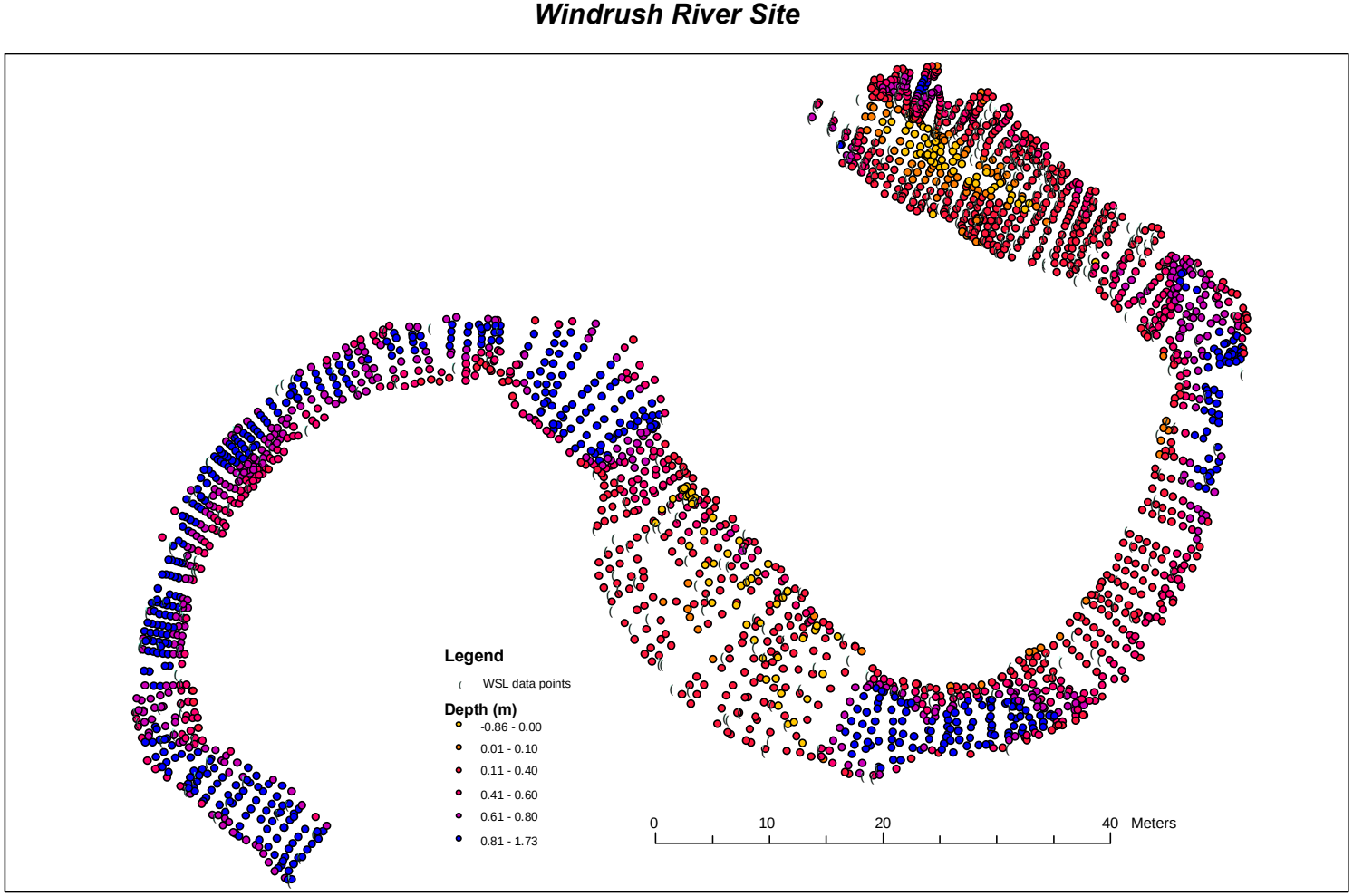

Figure A.1.18: Data sets collected at the Windrush River Site.

Appendix 2

Results obtained for the analysis in Chapter 4

This Appendix includes some of the graphical outputs obtained when analysing the differences between the sampling strategies considered in Chapter 4. Only those results not included in the text of Chapter 4 have been copied in this Appendix.

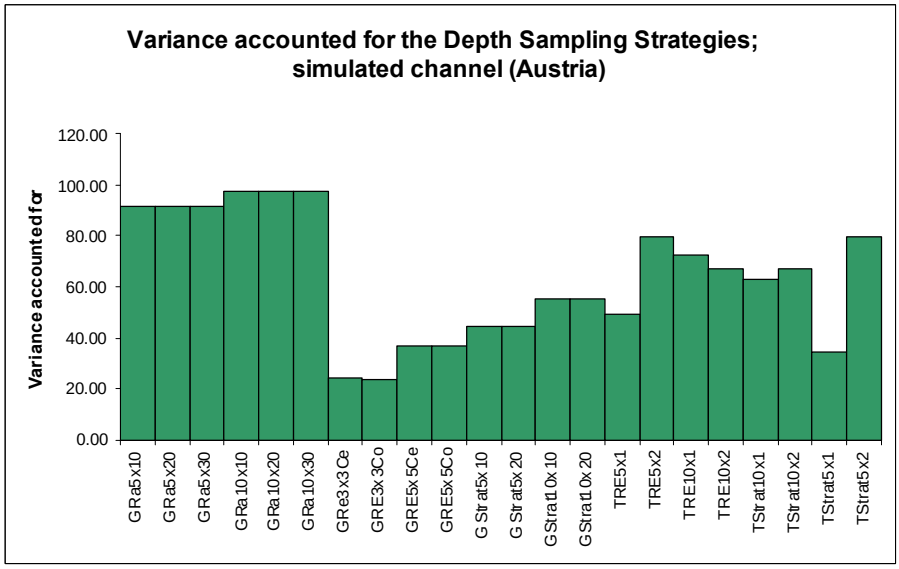

Figure Appendix 2.1: variance accounted for by the selected variograms for the artificial Austrian channel.

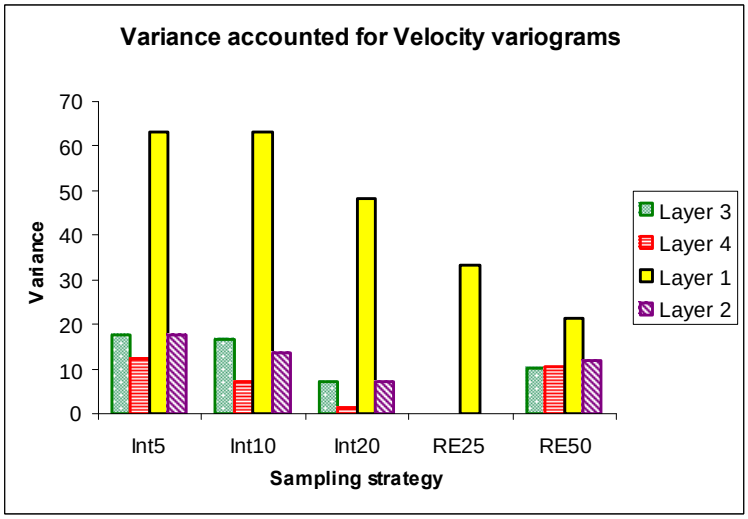

Figure Appendix 2.2: variance accounted by the selected variograms for the artificial Austrian channel velocity data set.

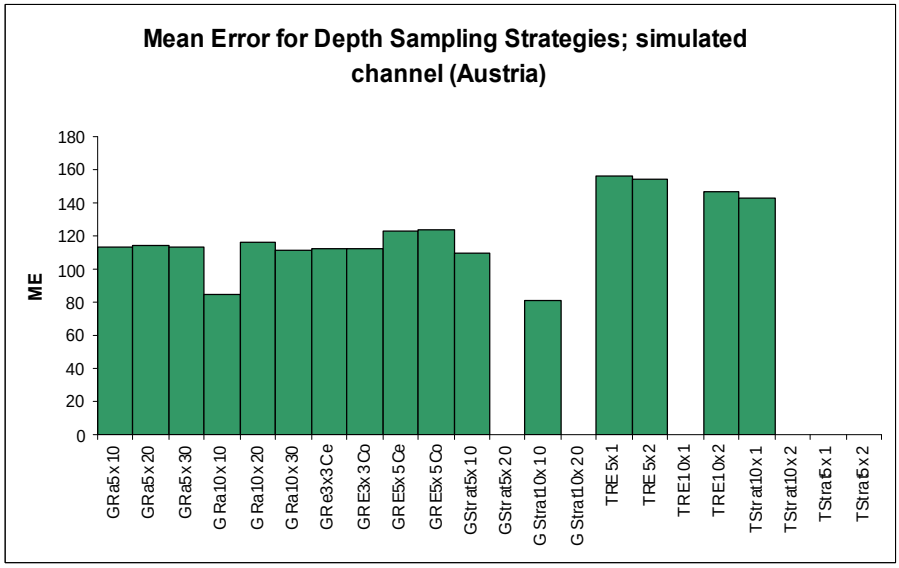

Figure Appendix 2.3: ME values obtained for the depth sampling strategies analysed at he artificial Austrian channel (Depth in mm).

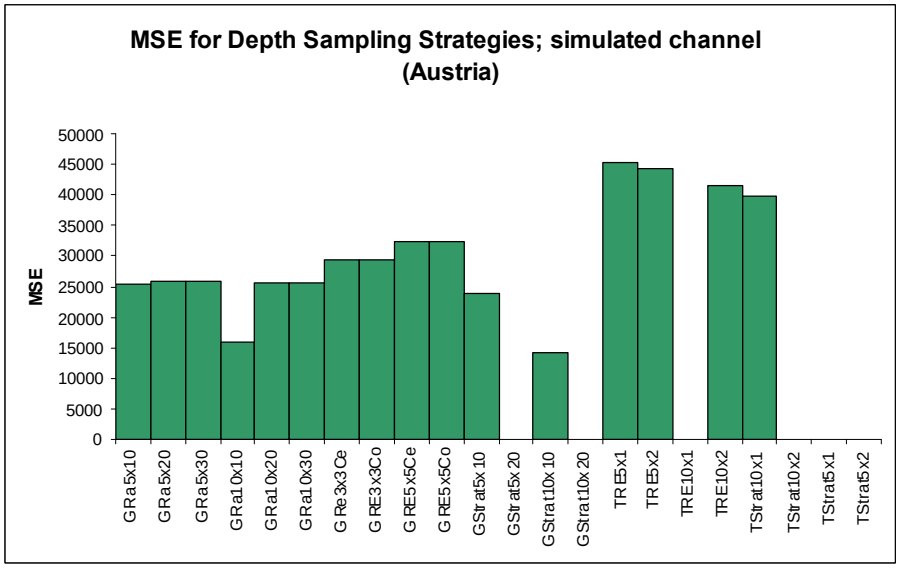

Figure Appendix 2.4: MSE obtained for the depth sampling strategies considered for the artificial Austrian channel. 0 value indicates that the predictions could not be calculated due to the structure of the data (Depth in mm).

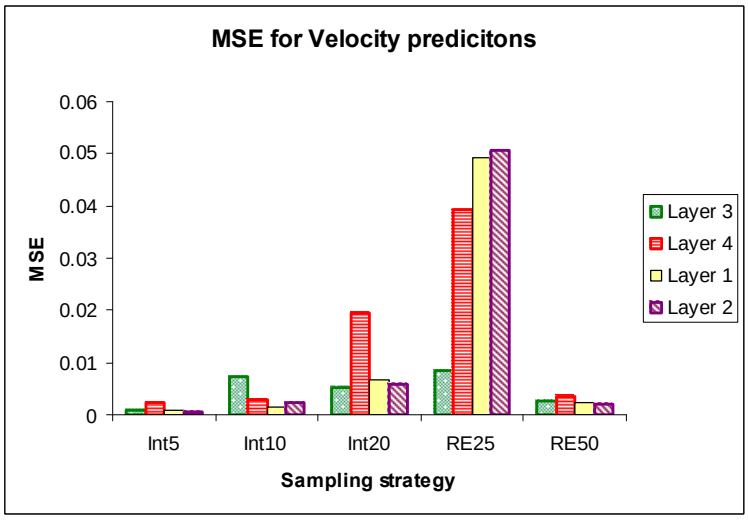

Figure Appendix 2.5: MSE for the different layers analysed of the artificial Austrian channel.

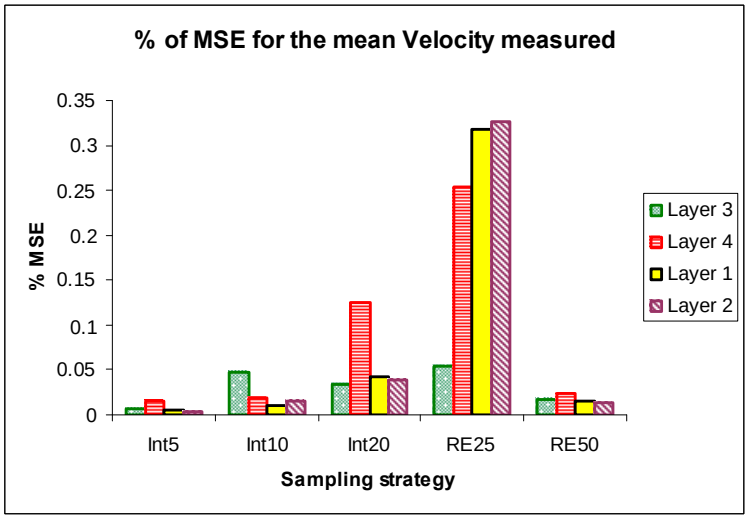

Figure Appendix 2.6: percentage of MSE in relation to the mean velocity value of the different layers in the artificial Austrian channel.

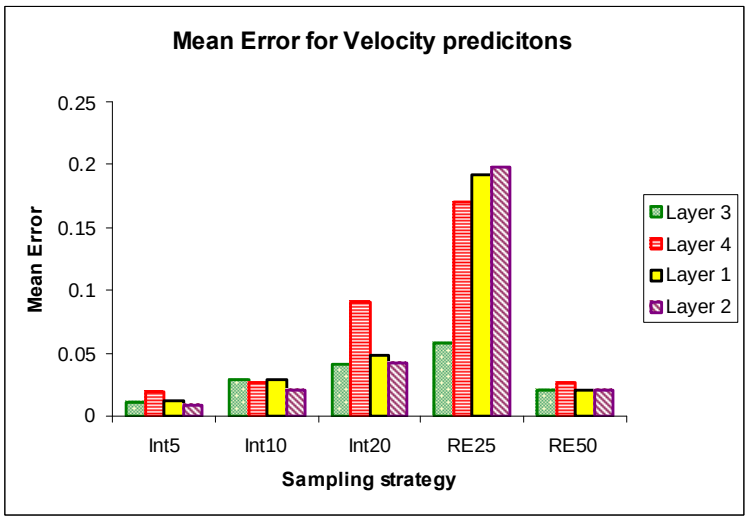

Figure Appendix 2.7: Mean Error obtained for the velocity predictions of the artificial Austrian channel.

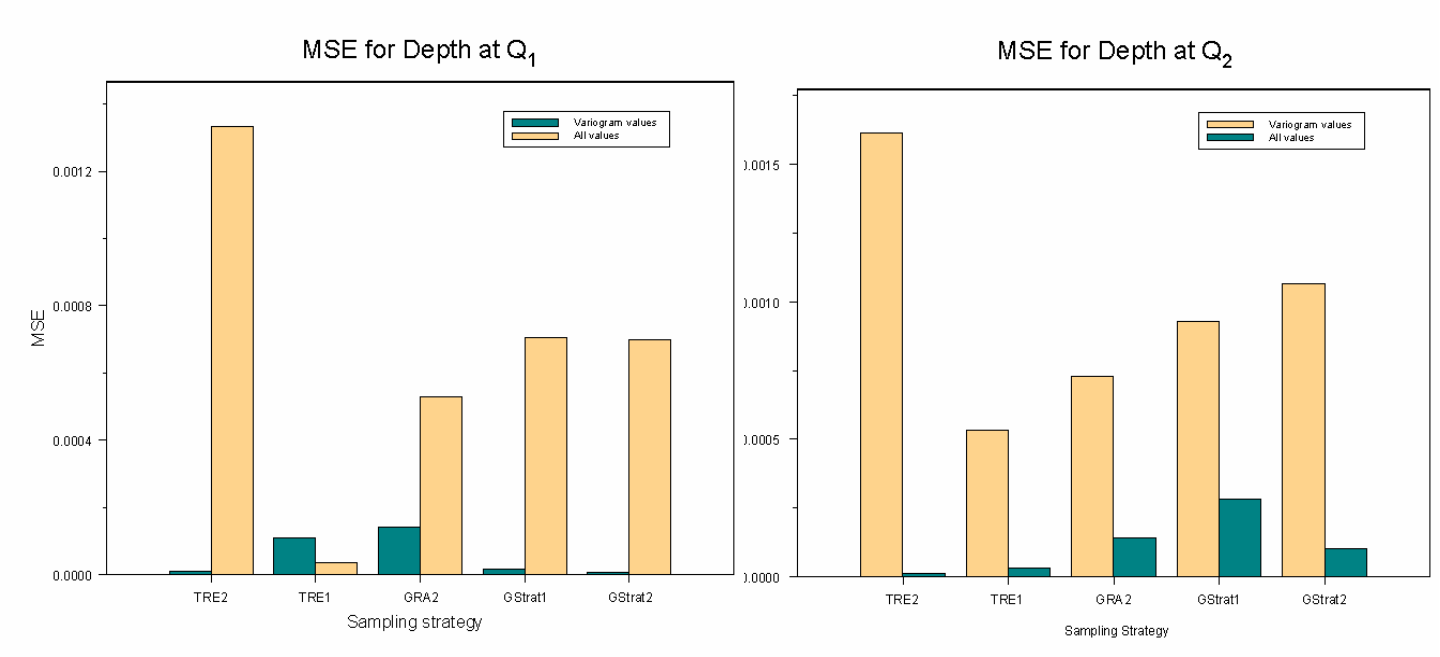

Figure Appendix 2.8: MSE per sampling strategy and flow analysed for depth measurements at the Leigh Brook river site. Green columns represent the MSE encountered when predicting depth at all the points included in the variogram calculation. Orange columns show the MSE encountered for the rest predicted points.

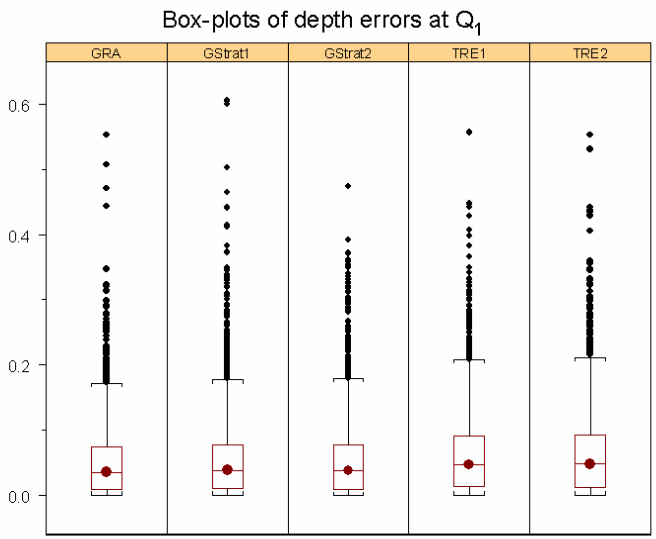

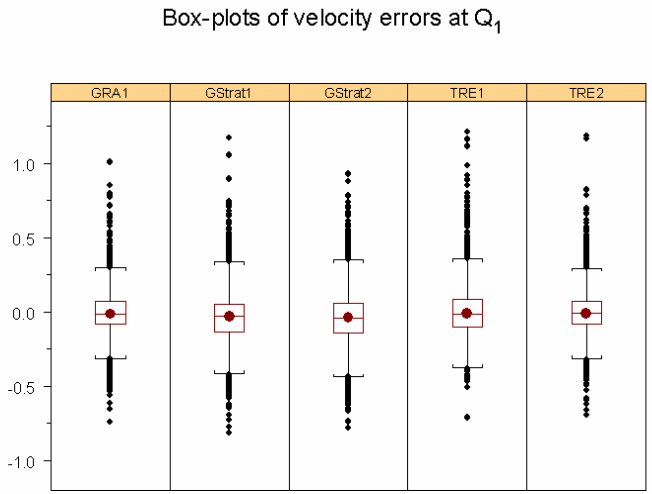

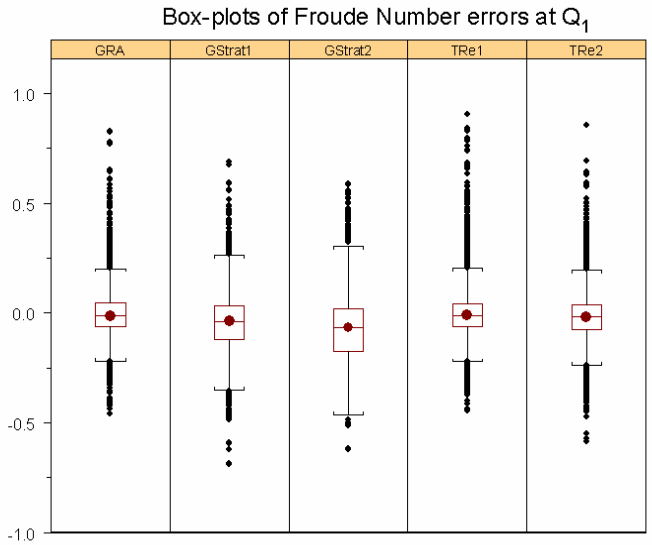

Figure Appendix 2.9: box-plots for the depth, velocity and Froude number difference between observed and predicted values obtained at Q_1. Results obtained for the Leigh Brook river site.

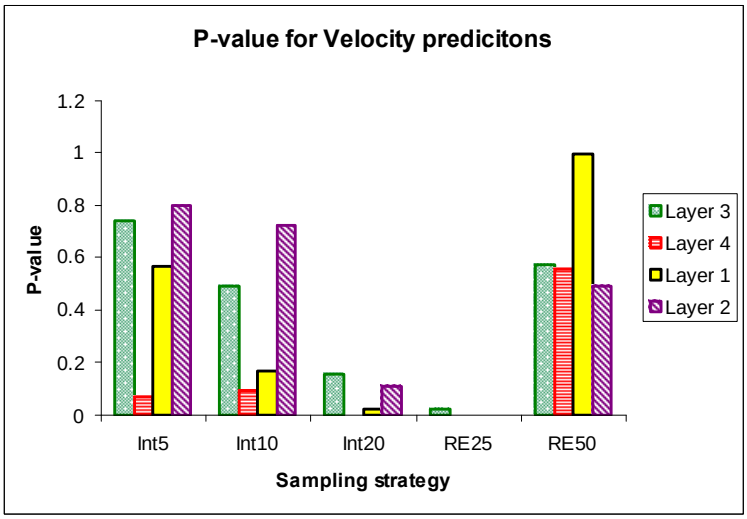

Figure Appendix 2.10: p-value for different layers and sampling strategies in the artificial Austrian channel.

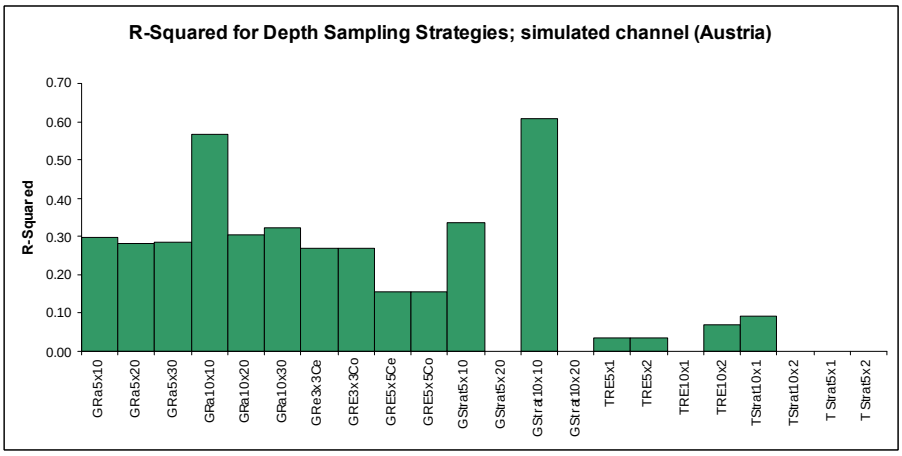

Figure Appendix 2.11: R-squared obtained for the different depth sampling strategies at the artificial Austrian channel. The higher the R-squared value, the more accurate the predictions are.

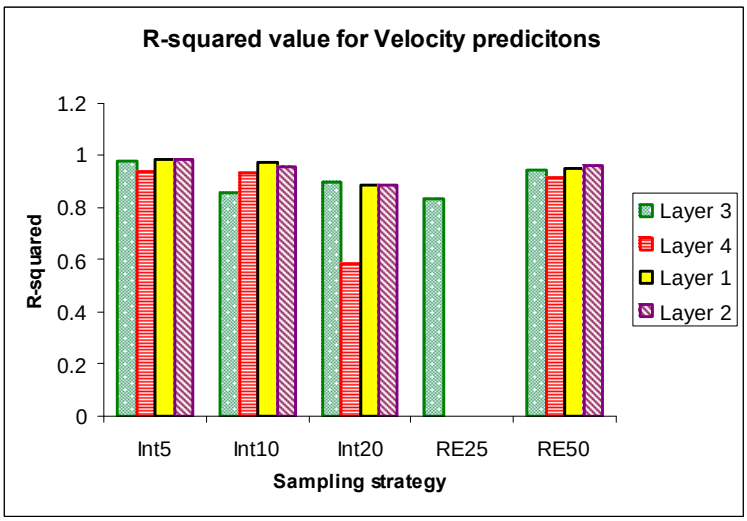

Figure Appendix 2.12: R-squared for different layers and sampling strategies in the artificial Austrian simulated channel.

Appendix 3.1

Results obtained for the analysis in Chapter 5 –descriptive statistics

This appendix includes all the graphical outputs obtained for the analysis in Chapter 5 section 5.4.2. Only few examples where included in the explanation given in Chapter 5 in order to reduce the length of the document. The structure of this Appendix follows this developed in Chapter 5. Plots have been collated in this document without either giving any explanation regarding the methodology used for the analysis nor the headings for the Figures. A full explanation is given in the correspondent section of Chapter 5.

Box Plots Dry & Wet Points

Depth Bere Q79 Boxplot for Depth (m)

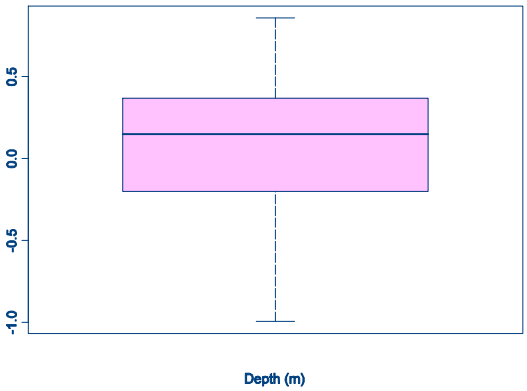

Depth Cruick Q51 Boxplot for Depth (m)

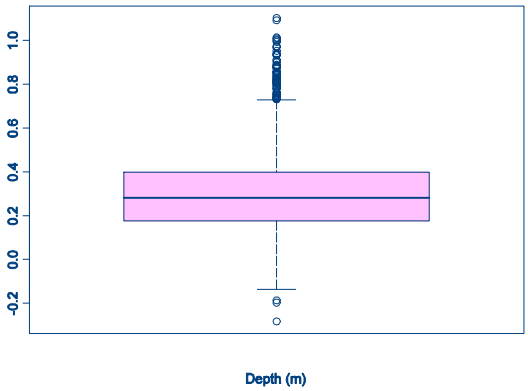

Depth Blackwater Q33 Boxplot for Depth (m)

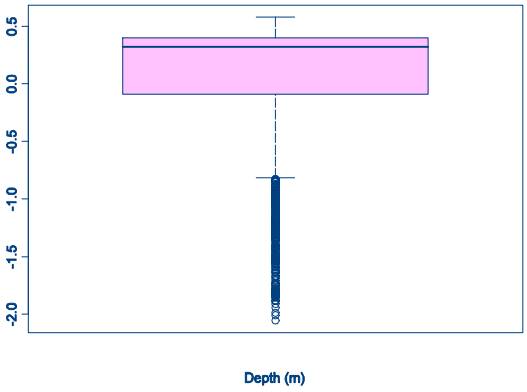

Depth HighlandWater Q43 Boxplot for Depth (m)

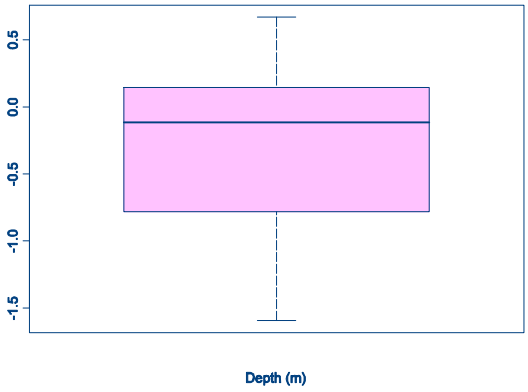

Depth Lambourn Q92 Boxplot for Depth (m)

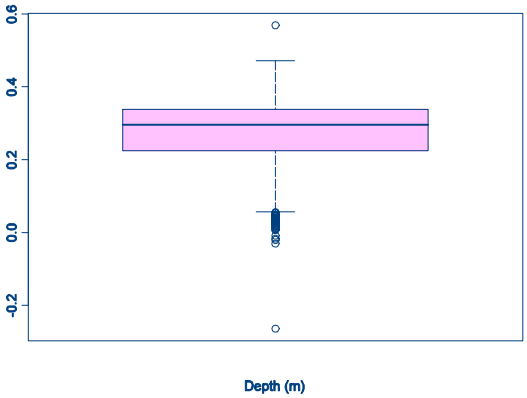

Depth Pang Old Fenced Q80 Boxplot for Depth (m)

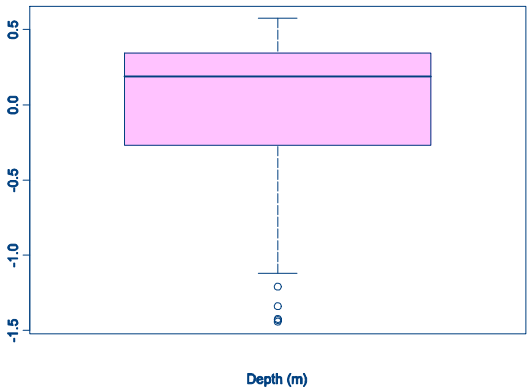

Depth Pang Fenced Q91 Boxplot for Depth (m)

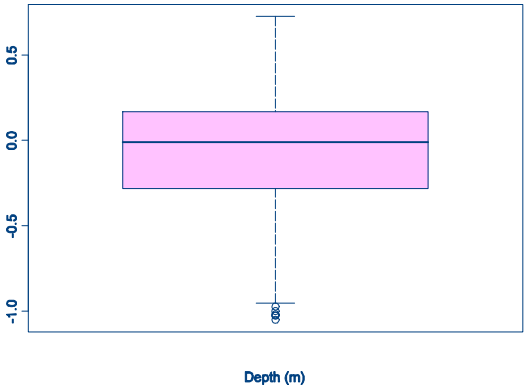

Depth Pang Old Fenced Q90 Boxplot for Depth (m)

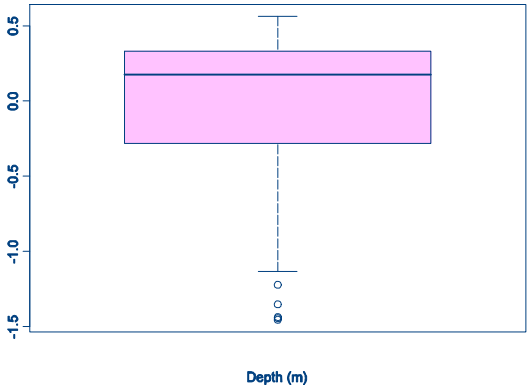

Depth Pang Unfenced Q80 Boxplot for Depth (m)

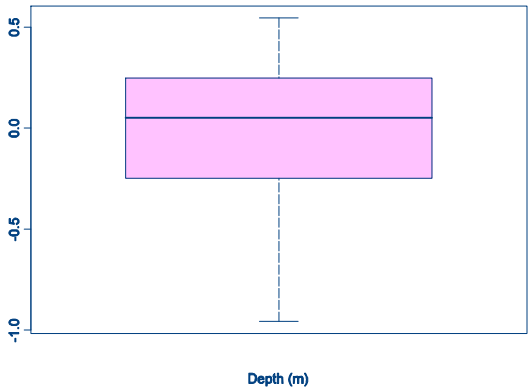

Depth Senni Q78 Boxplot for Depth (m)

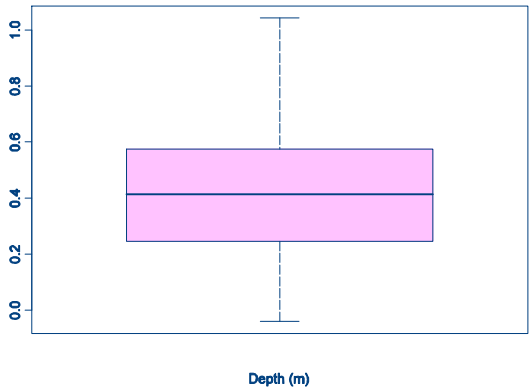

Depth Pang Unfenced Q90 Boxplot for Depth (m)

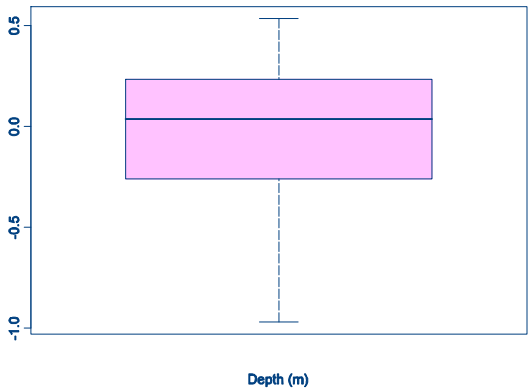

Depth Tames HM Q20 Boxplot for Depth (m)

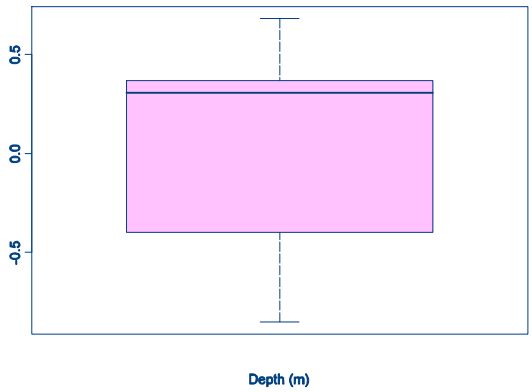

Depth TamesLM Q43 Boxplot for Depth (m)

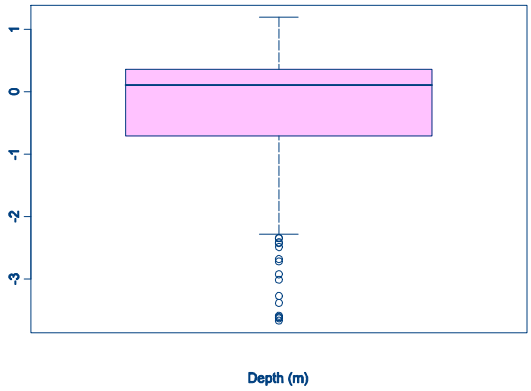

Depth Windrush Q? Boxplot for Depth (m)

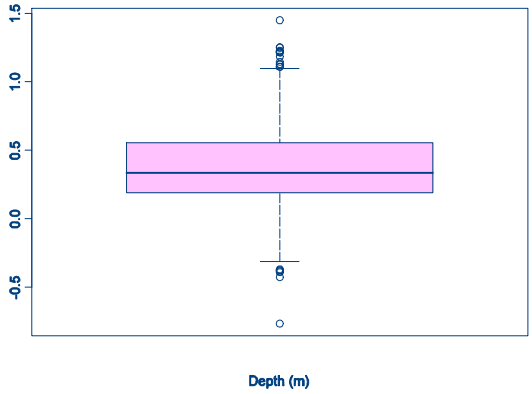

Depth Tarf Q51 Boxplot for Depth (m)

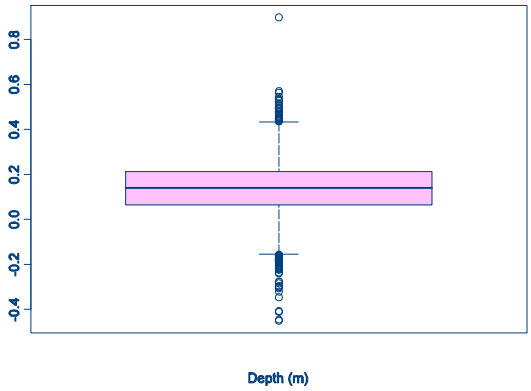

Box Plots Wet Points

wet Boxplot for Depth (m)

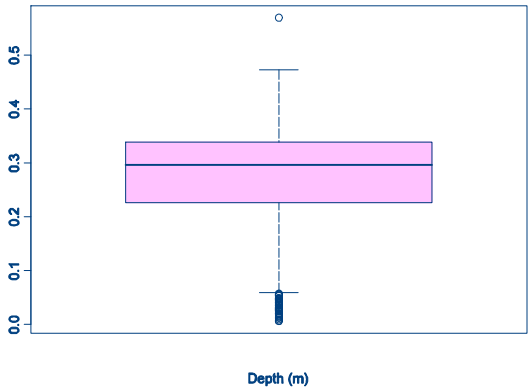

wet Points Pang Unfenced Q80 Boxplot for Depth (m)

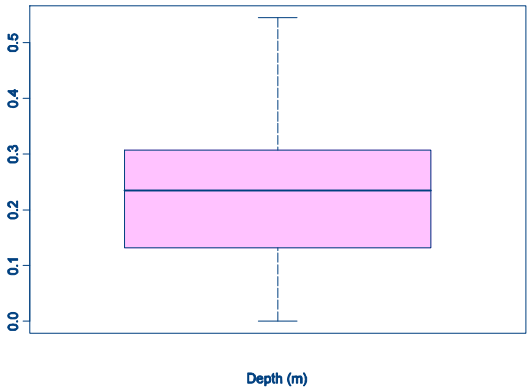

wet Pang Old Fenced Q80 Boxplot for Depth (m)

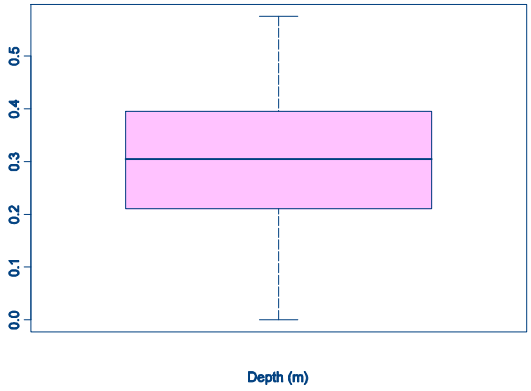

wet points Bere Q79 Boxplot for Depth (m)

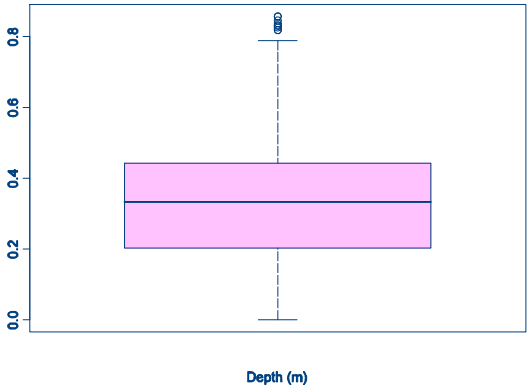

wet points Blackwater Q33 Boxplot for Depth (m)

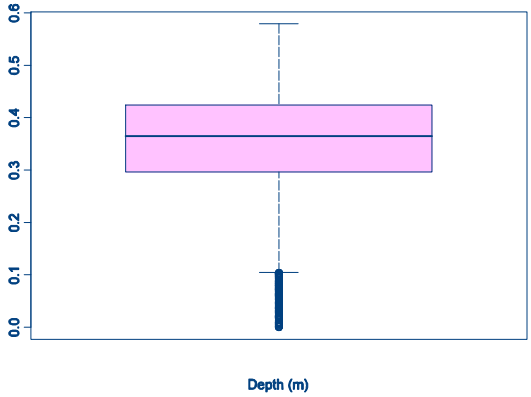

wet points HighlandWater Q43 Boxplot for Depth (m)

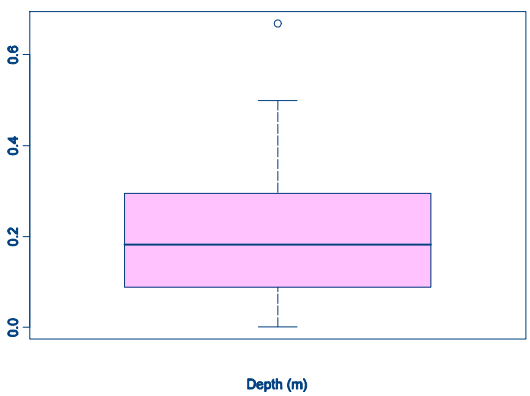

wet points Cruick Q51 Boxplot for Depth (m)

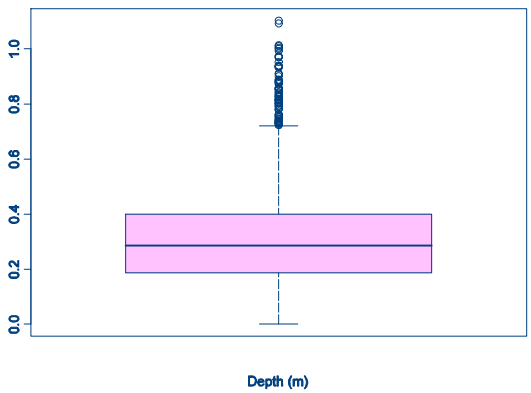

wet points Lambourn Q92 Boxplot for Depth (m)

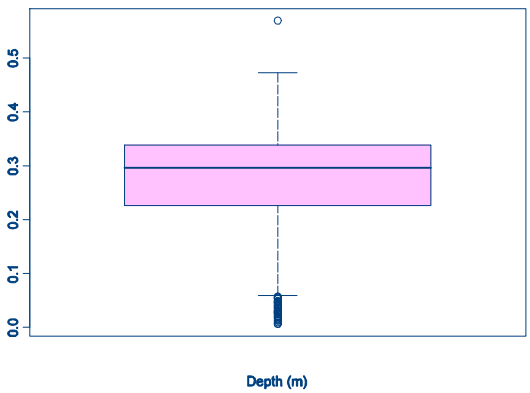

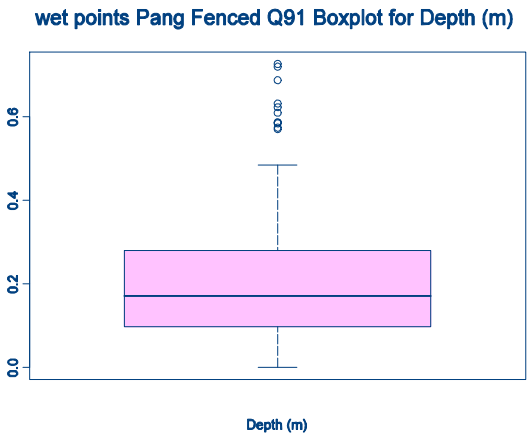
wet points Pang Fenced Q91 Boxplot for Depth (m)
0.0
0.2
0.4
0.6
Depth (m)

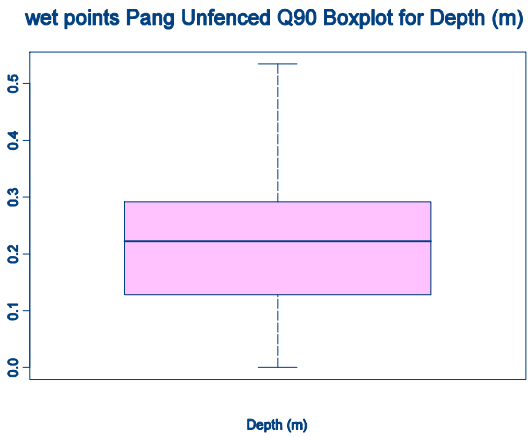
wet points Pang Unfenced Q90 Boxplot for Depth (m)
0.0
0.1
0.2
0.3
0.4
0.5
Depth (m)

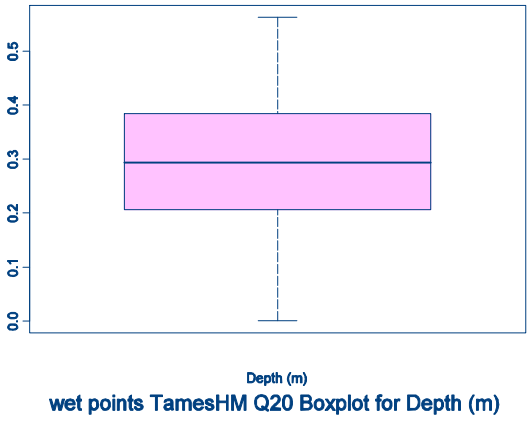
wet points Pang Old Fenced Q90 Boxplot for Depth (m)
0.0
0.1
0.2
0.3
0.4
0.5
Depth (m)

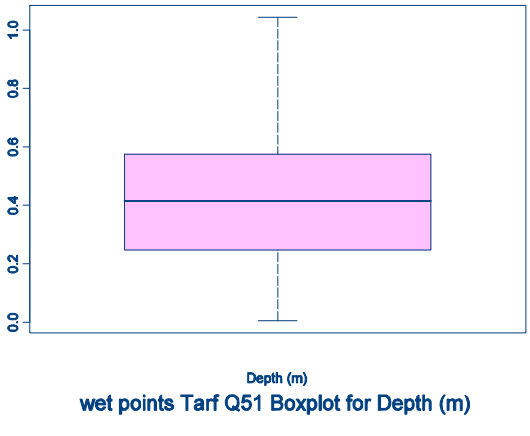
wet points Senni Q78 Boxplot for Depth (m)
0.0
0.2
0.4
0.6
0.8
1.0
Depth (m)

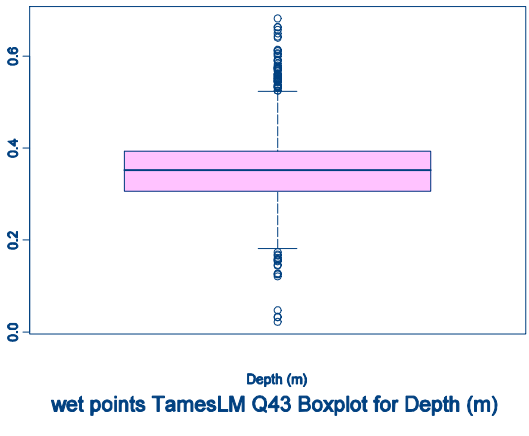
wet points TamesHM Q20 Boxplot for Depth (m)
0.0
0.2
0.4
0.6
Depth (m)

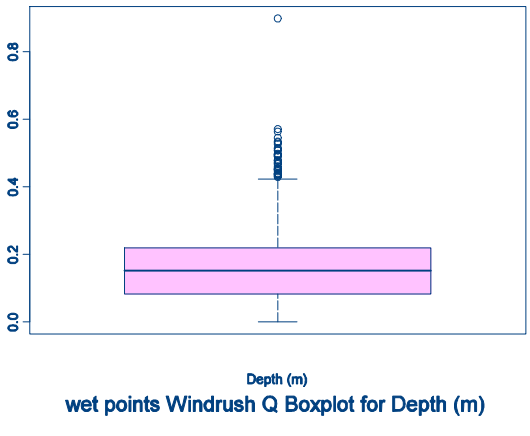
wet points Tarf Q51 Boxplot for Depth (m)
0.0
0.2
0.4
0.6
0.8
Depth (m)

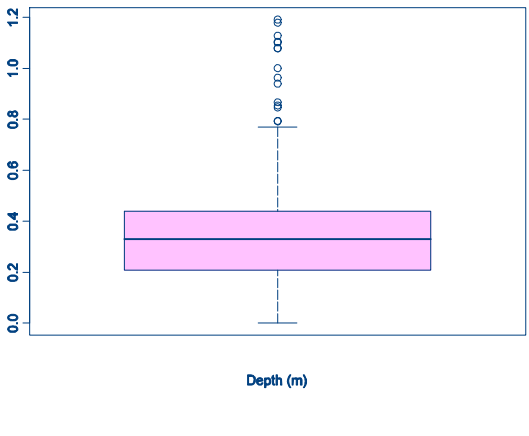
wet points TamesLM Q43 Boxplot for Depth (m)
0.0
0.2
0.4
0.6
0.8
1.0
1.2
Depth (m)

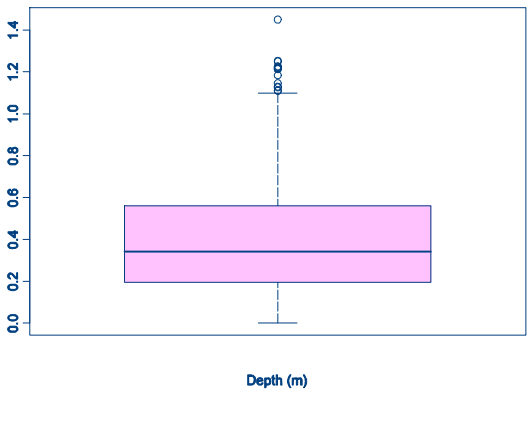
wet points Windrush Q Boxplot for Depth (m)
0.0
0.2
0.4
0.6
0.8
1.0
1.2
1.4
Depth (m)

QQplots Dry & Wet points

Depth Bere Q79 QQplot for Depth (m)

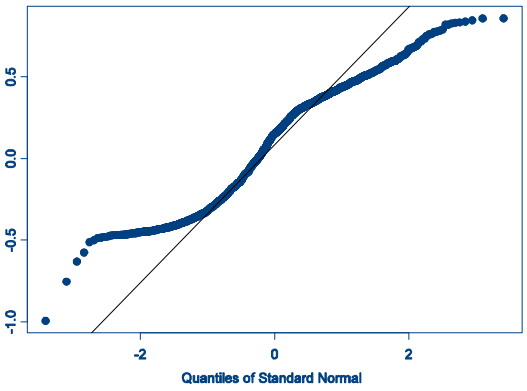

Depth Cruick Q51 QQplot for Depth (m)

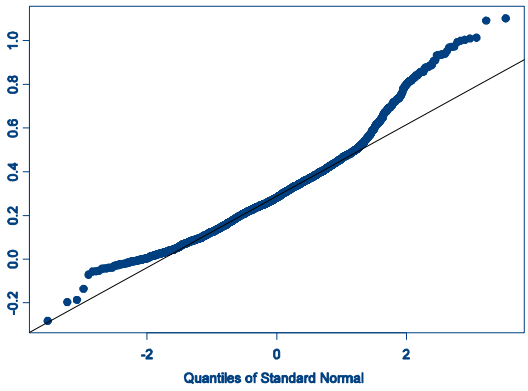

Depth Pang Fenced Q91 QQplot for Depth (m)

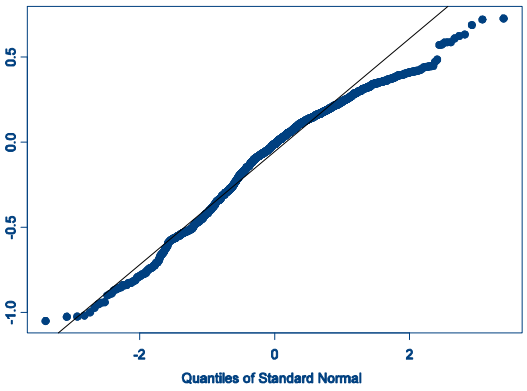

Depth HighlandWater Q43 QQplot for Depth (m)

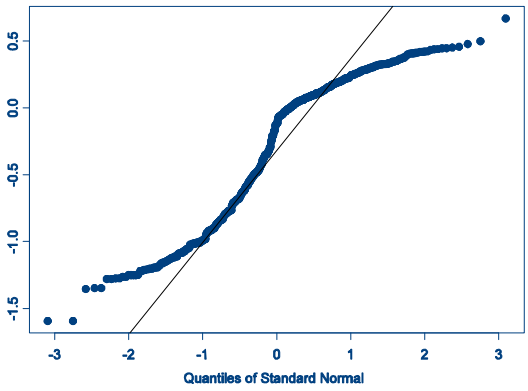

Depth Lambourn Q92 QQplot for Depth (m)

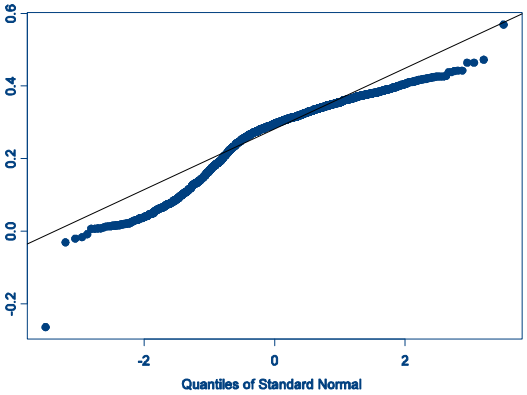

Depth Pang Old Fenced Q80 QQplot for Depth (m)

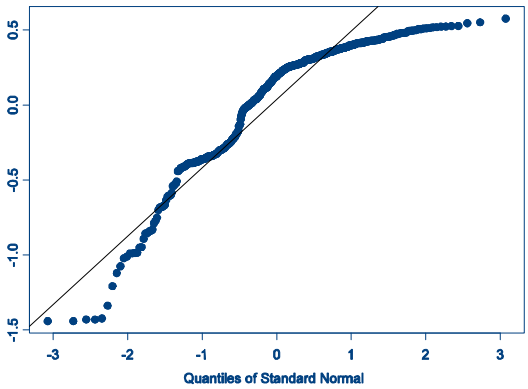

Depth Blackwater Q33 QQplot for Depth (m)

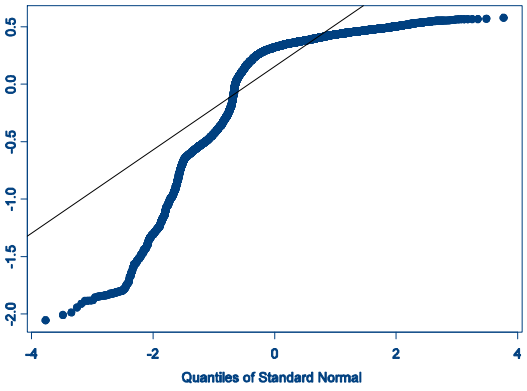

Depth Pang Old Fenced Q90 QQplot for Depth (m)

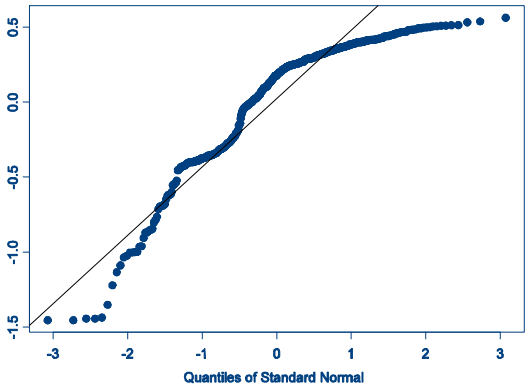

Depth Pang Unfenced Q80 QQplot for Depth (m)

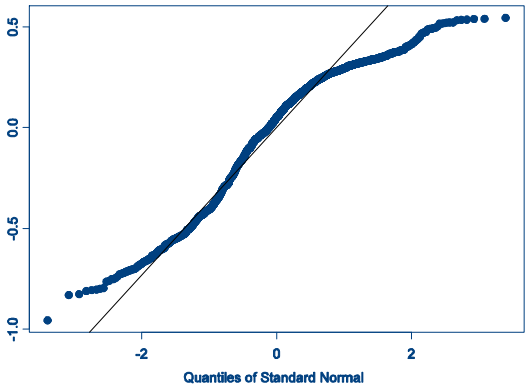

Depth Senni Q78 QQplot for Depth (m)

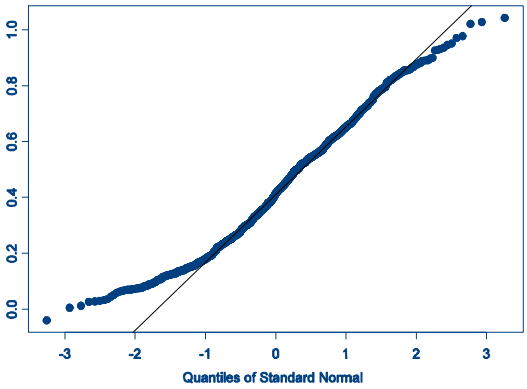

Depth Pang Unfenced Q90 QQplot for Depth (m)

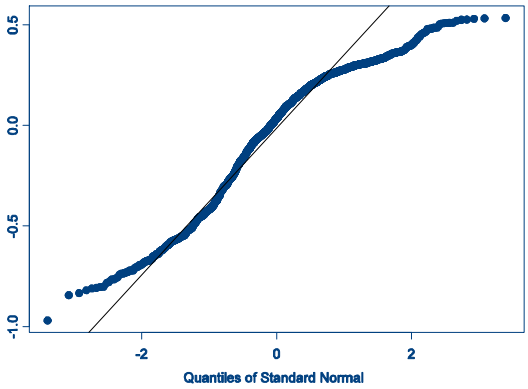

Depth Tames HM Q20 QQplot for Depth (m)

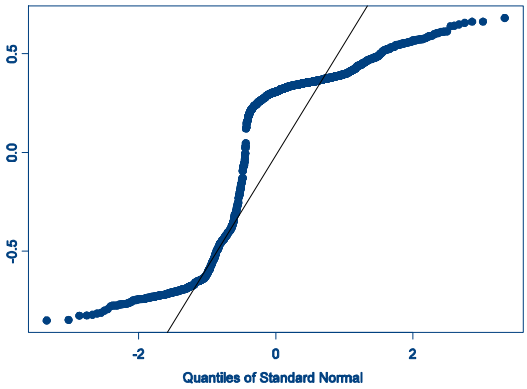

Depth TamesLM Q43 QQplot for Depth (m)

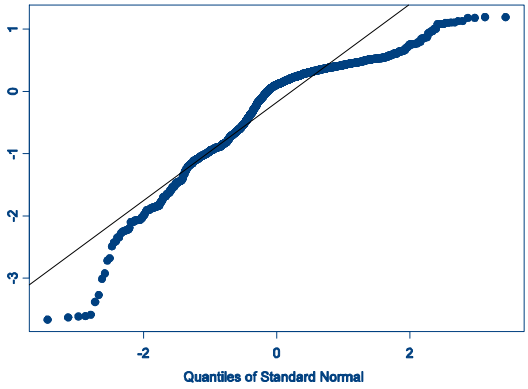

Depth Tarf Q51 QQplot for Depth (m)

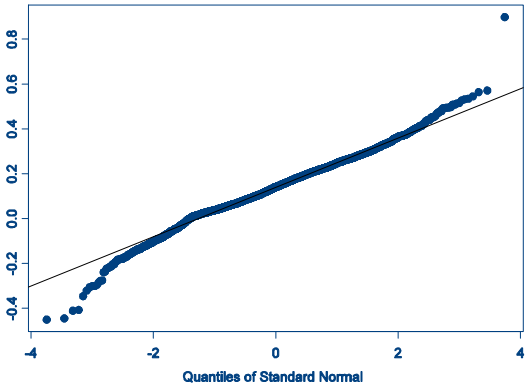

Depth Windrush Q? QQplot for Depth (m)

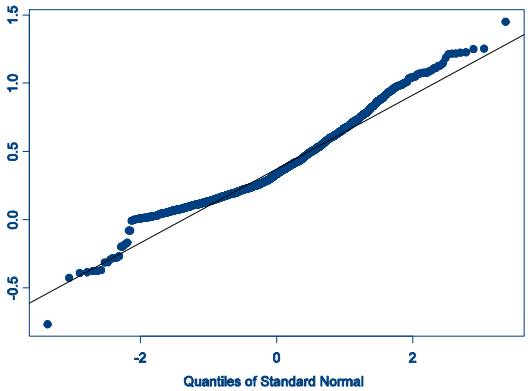

QQplots Wet Points

wet QQplot for Depth (m)

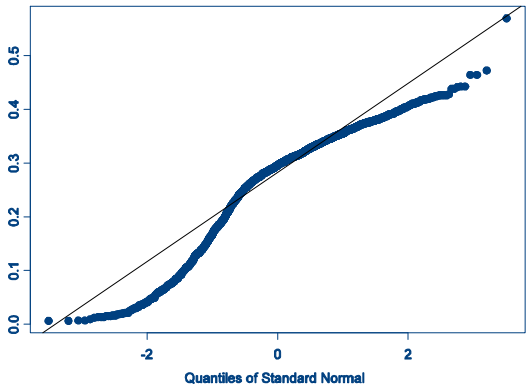

wet Pang Old Fenced Q80 QQplot for Depth (m)

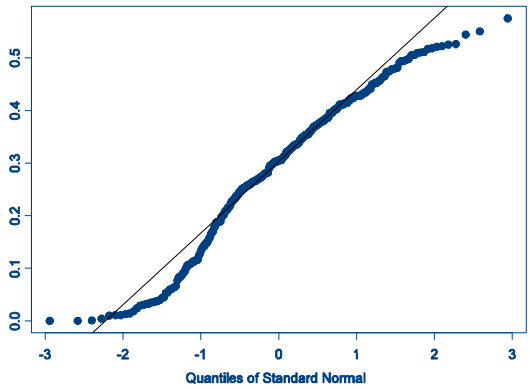

wet Points Pang Unfenced Q80 QQplot for Depth (m)

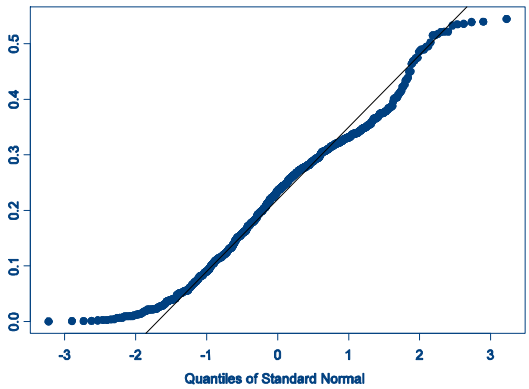

wet points Cruick Q51 QQplot for Depth (m)

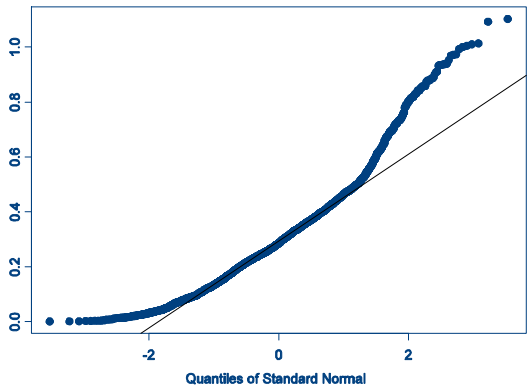

wet points Bere Q79 QQplot for Depth (m)

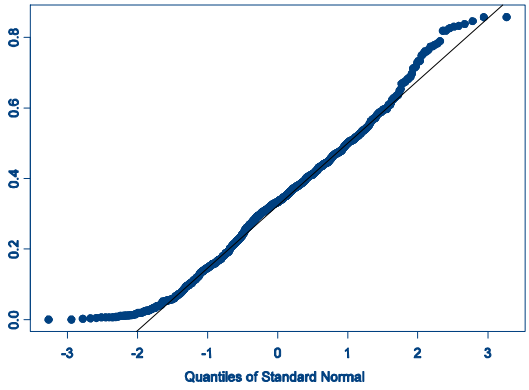

wet points HighlandWater Q43 QQplot for Depth (m)

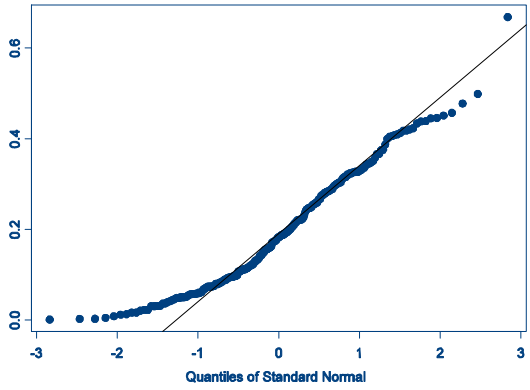

wet points Blackwater Q33 QQplot for Depth (m)

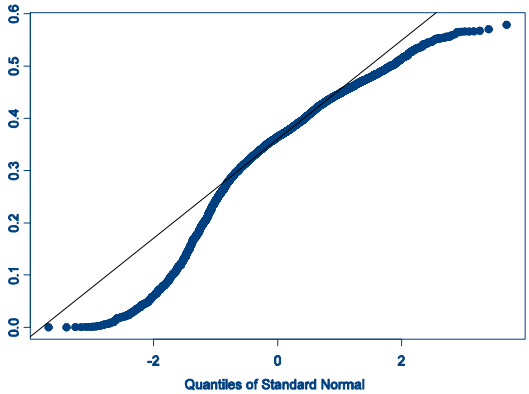

wet points Lambourn Q92 QQplot for Depth (m)

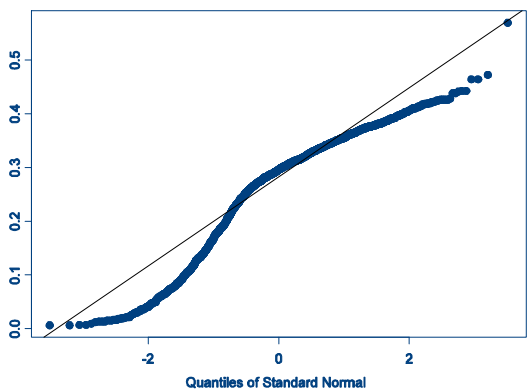

wet points Pang Fenced Q91 QQplot for Depth (m)

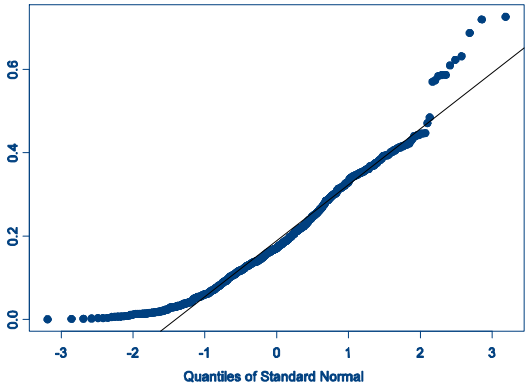

wet points Pang Unfenced Q90 QQplot for Depth (m)

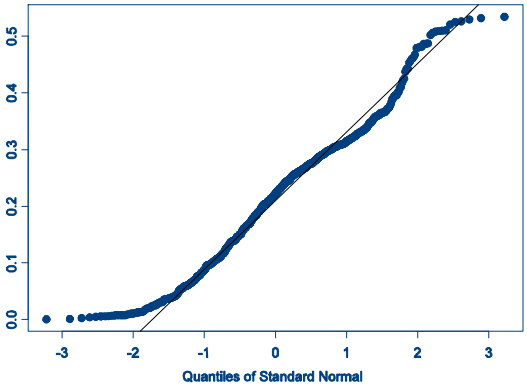

wet points Pang Old Fenced Q90 QQplot for Depth (m)

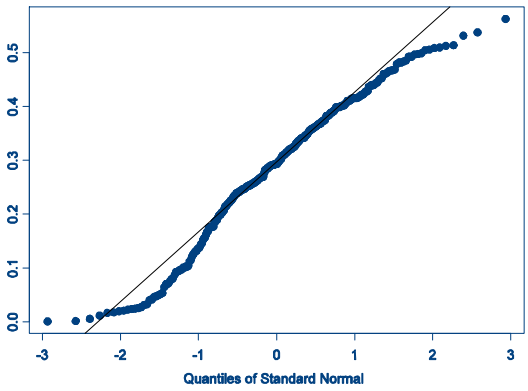

wet points Senni Q78 QQplot for Depth (m)

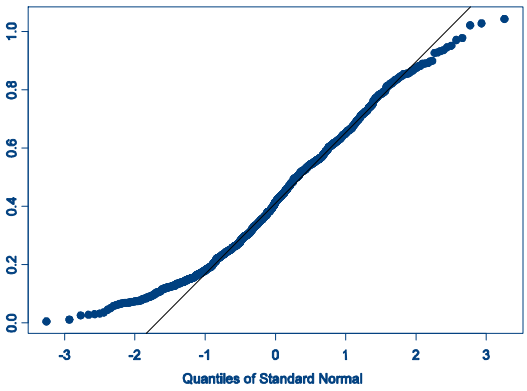

wet points TamesHM Q20 QQplot for Depth (m)

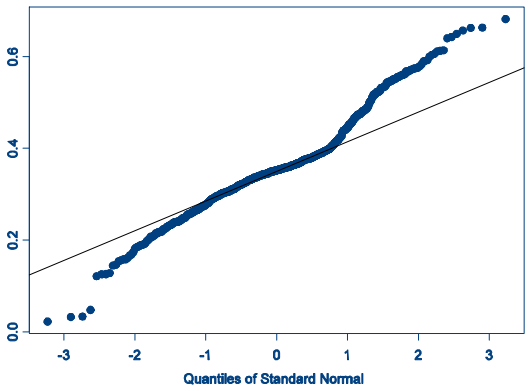

wet points Tarf Q51 QQplot for Depth (m)

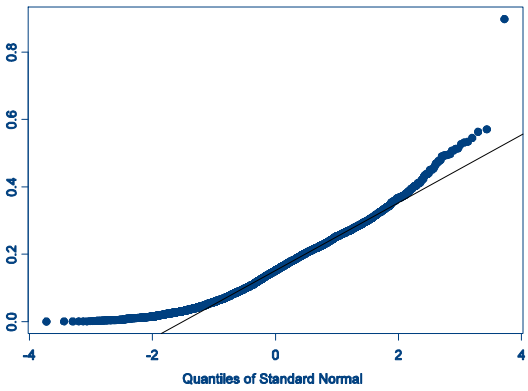

wet points TamesLM Q43 QQplot for Depth (m)

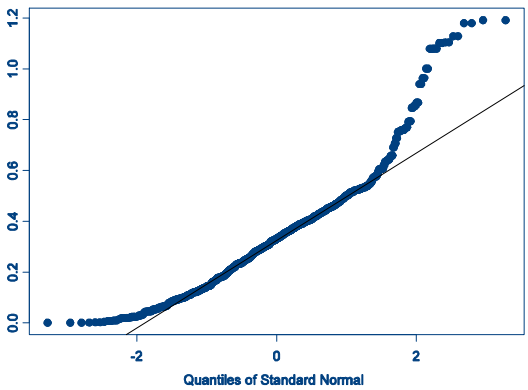

wet points Windrush Q QQplot for Depth (m)

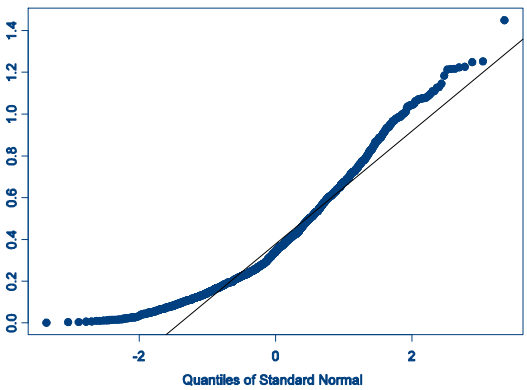

Histograms Dry & Wet points

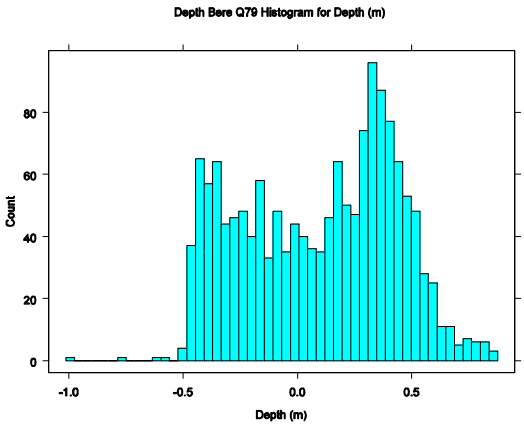

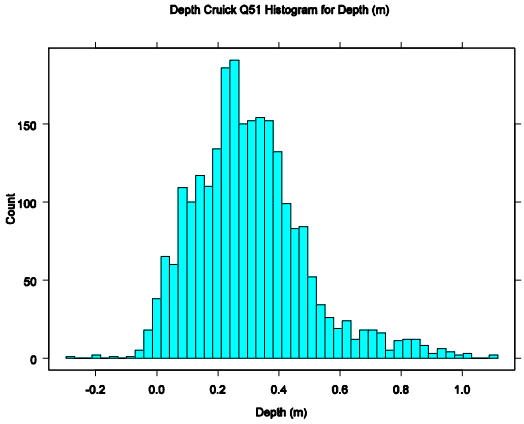

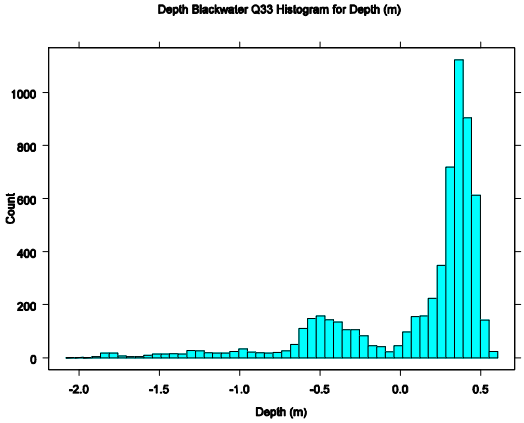

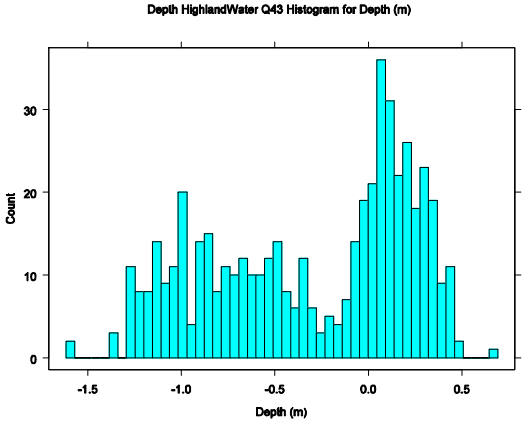

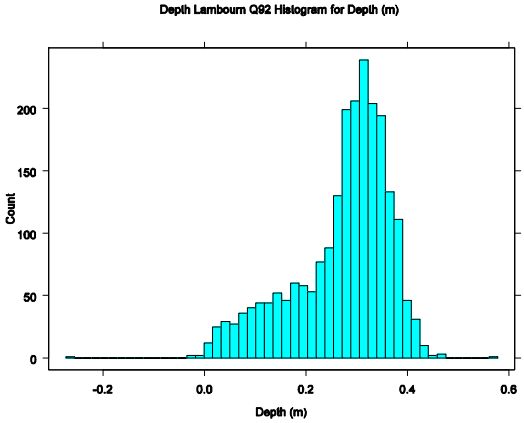

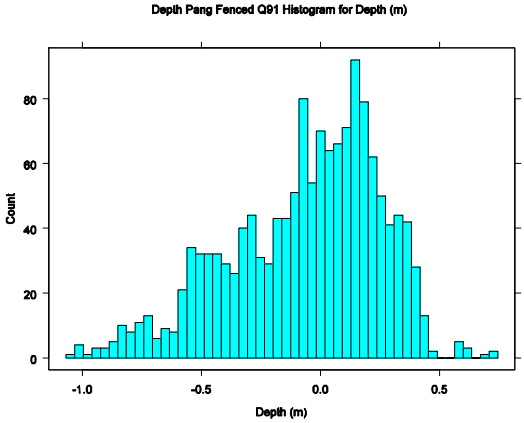

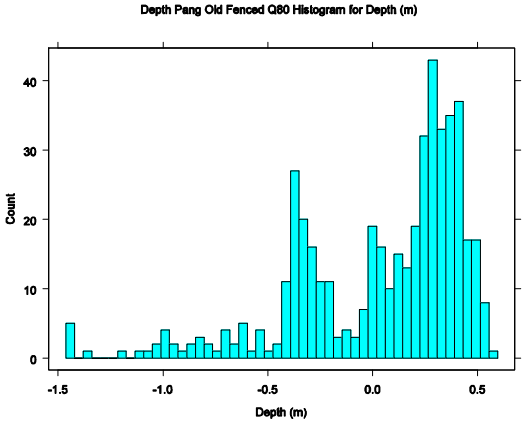

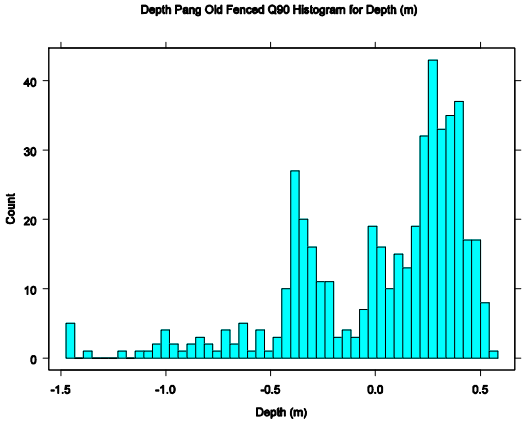

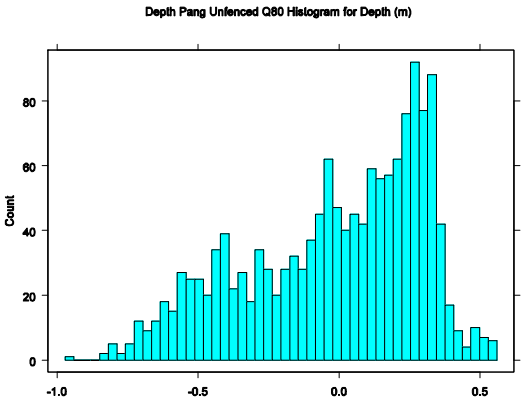
Depth Pang Unfenced Q80 Histogram for Depth (m)
Count
0
20
40
60
80
-1.0
-0.5
0.0
0.5

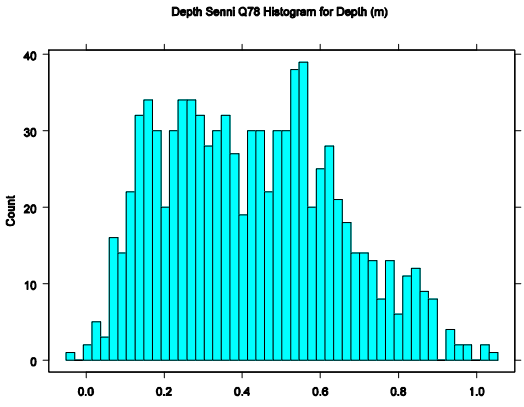
Depth Senni Q78 Histogram for Depth (m)
Count
0
10
20
30
40
0.0
0.2
0.4
0.6
0.8
1.0

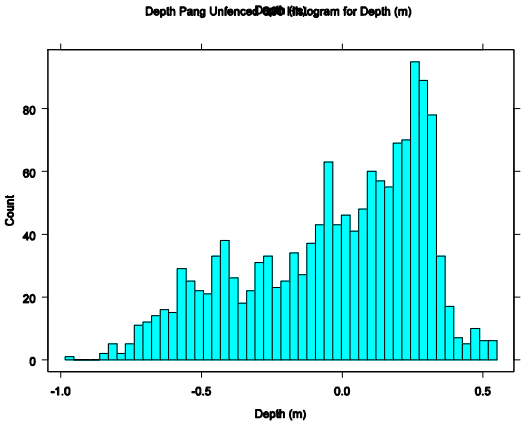
Count
0
20
40
60
80
-1.0
-0.5
0.0
0.5
Depth (m)

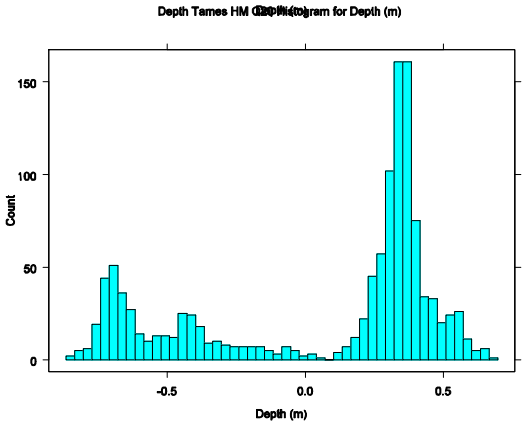
Count
0
50
100
150
-0.5
0.0
0.5
Depth (m)

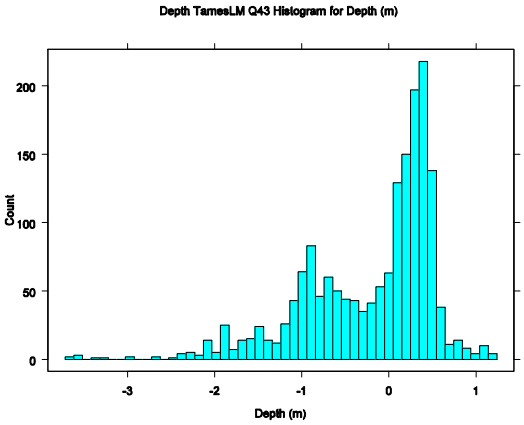
Depth TamesLM Q43 Histogram for Depth (m)
Count
0
50
100
150
200
-3
-2
-1
0
1
Depth (m)

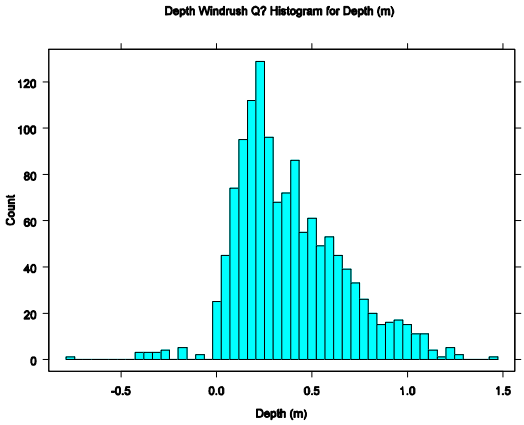
Depth Windrush Q? Histogram for Depth (m)
Count
0
20
40
60
80
100
120
-0.5
0.0
0.5
1.0
1.5
Depth (m)

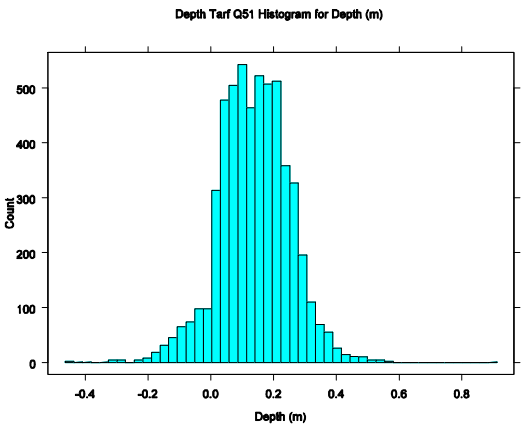
Depth Tarf Q51 Histogram for Depth (m)
Count
0
100
200
300
400
500
-0.4
-0.2
0.0
0.2
0.4
0.6
0.8
Depth (m)

Histogram Wet points

wet points Pang Unfenced Q90 Histogram for Depth (m)

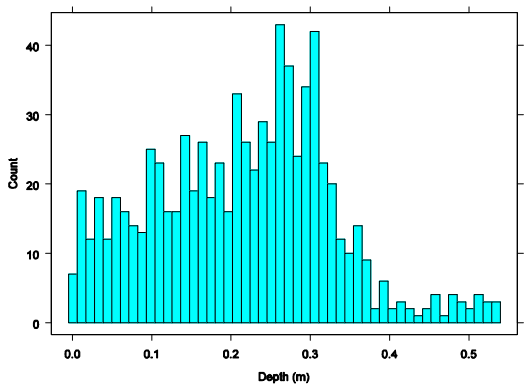

wet points Pang Old Fenced Q90 Histogram for Depth (m)

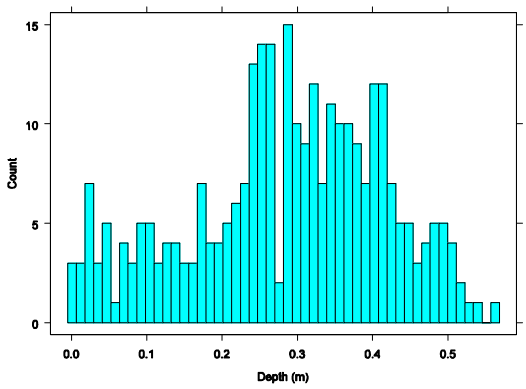

wet points Pang Fenced Q91 Histogram for Depth (m)

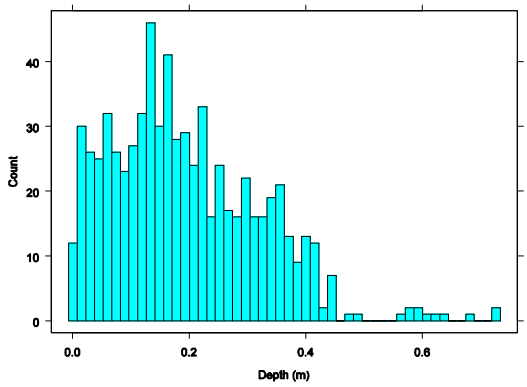

wet points TarnesLM Q43 Histogram for Depth (m)

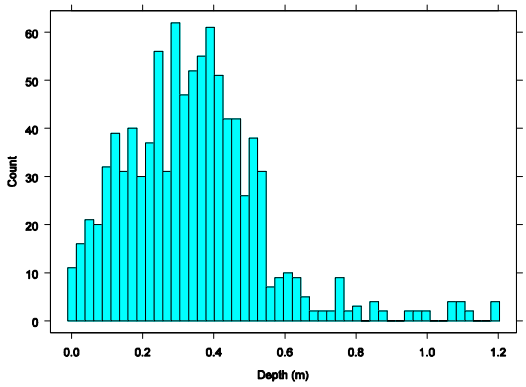

wet points TarnesHM Q20 Histogram for Depth (m)

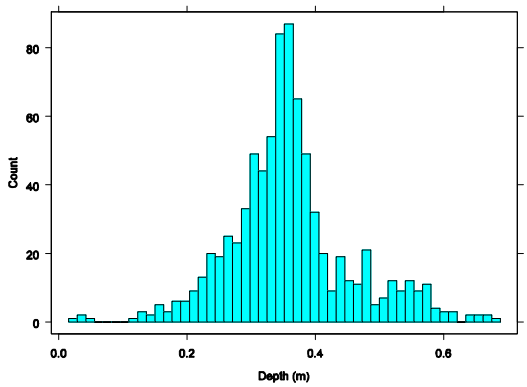

wet points Senni Q78 Histogram for Depth (m)

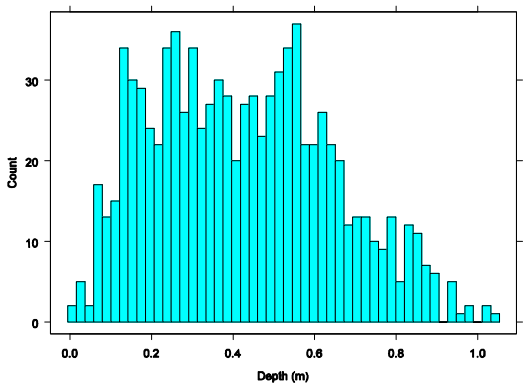

wet points Windrush Q Histogram for Depth (m)

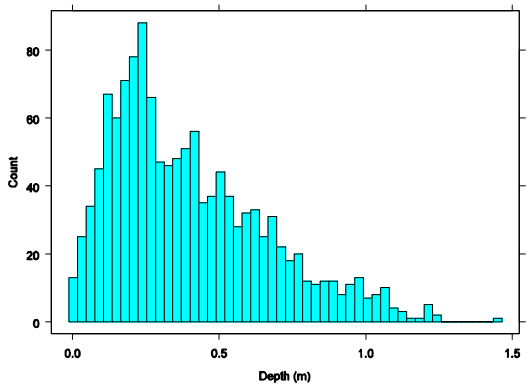

wet points Tarf Q51 Histogram for Depth (m)

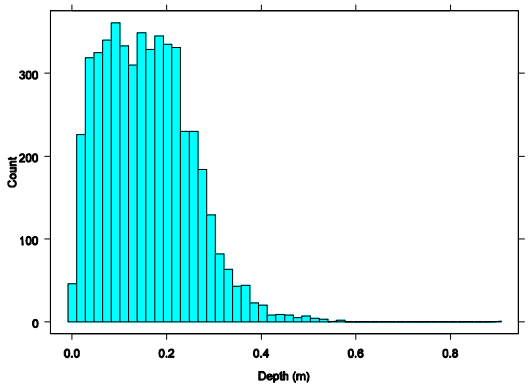

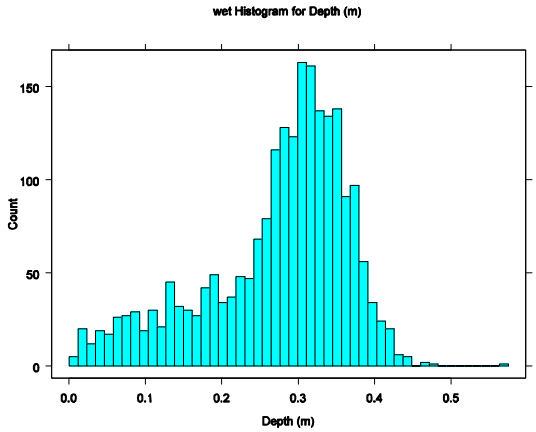
wet Histogram for Depth (m)
Count
Depth (m)

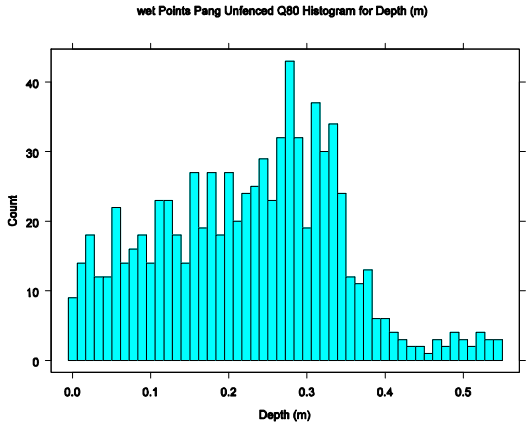
wet Points Pang Unfenced Q80 Histogram for Depth (m)
Count
Depth (m)

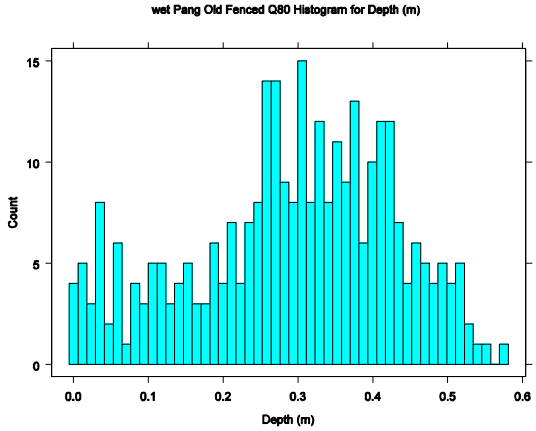
wet Pang Old Fenced Q80 Histogram for Depth (m)
Count
Depth (m)

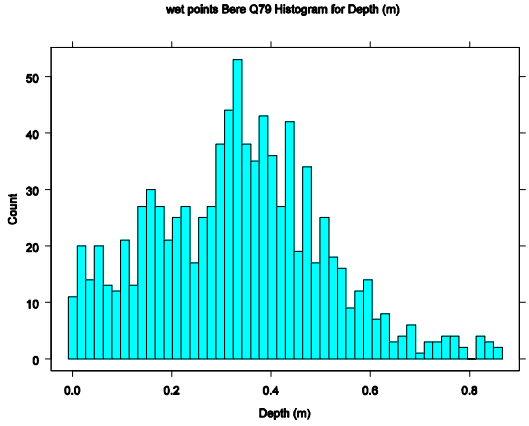
wet points Bere Q79 Histogram for Depth (m)
Count
Depth (m)

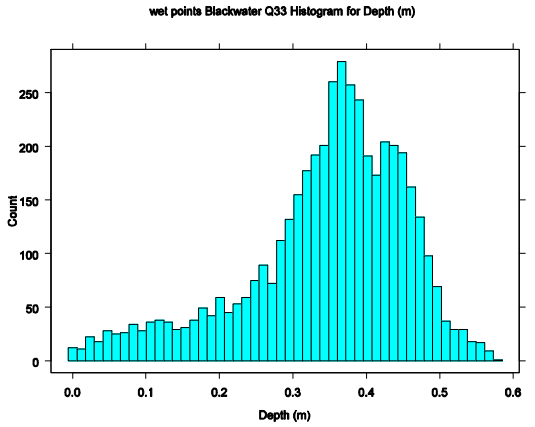
wet points Blackwater Q33 Histogram for Depth (m)
Count
Depth (m)

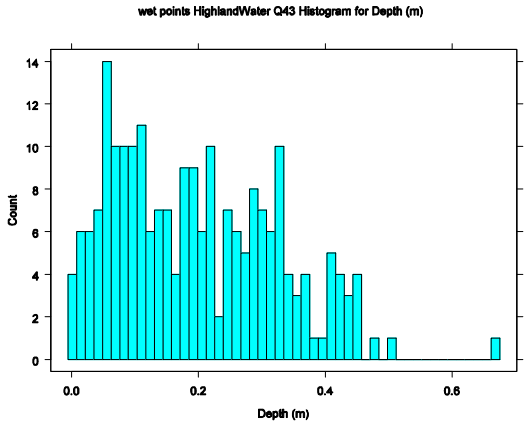
wet points HighlandWater Q43 Histogram for Depth (m)
Count
Depth (m)

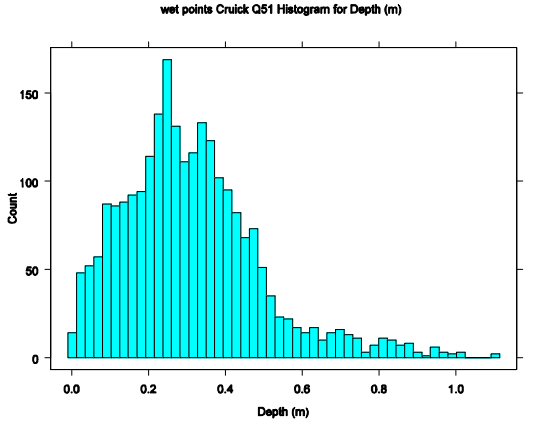
wet points Cruick Q51 Histogram for Depth (m)
Count
Depth (m)

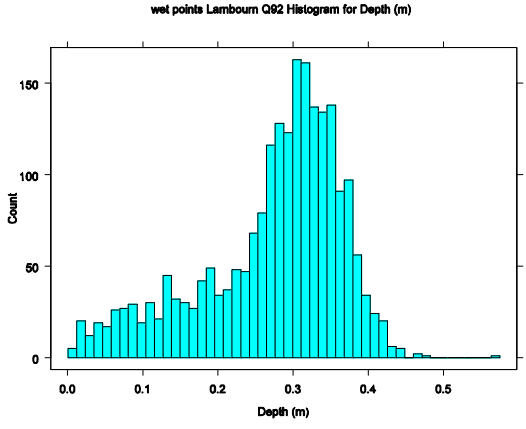
wet points Lambourn Q92 Histogram for Depth (m)
Count
Depth (m)

Table Appendix 3.1.1: descriptive statistics for depth at the studied river sites. Data sets include dry and wet points.

Site	% Flow Exceedance (Low Flows 2000)	Group	Num. Points	Min Depth	Max. Depth	Interval max-min	Median	Mean	1st Quartile	3rd Quartile	Std. Dev
Pang Old fenced	90	**1**	474	-1.45	0.56	2.01	0.176	0.025	-0.281	0.331	0.407
Pang fenced	91	**1**	1438	-1.05	0.726	-1.77	-0.011	-0.06	-0.28	0.16	0.314
Pang Unfenced	90	**1**	1468	-0.96	0.53	1.50	0.035	-0.030	-0.259	0.232	0.311
Lambourn	92	**1**	2205	-0.26	0.56	0.82	0.29	0.27	0.22	0.33	0.951
Leigh Brook	93	**1**	2983	0.00	0.85	0.85	0.18	0.20	0.09	0.30	0.148
Bere 2000	79	**2**	1546	-0.99	0.857	-1.85	0.149	0.094	-0.20	0.36	0.332
Pang Old fenced	80	**2**	474	-1.44	0.575	2.01	0.189	0.0378	-0.269	0.344	0.407
Pang Unfenced	80	**2**	1468	-0.95	0.544	4.45	0.050	-0.016	-0.28	0.24	0.311
Leigh Brook	82	**2**	2983	0.00	0.94	0.94	0.21	0.24	0.13	0.34	0.154
Senni	78	**2**	895	-0.04	1.04	1.08	0.41	0.42	0.24	0.57	0.219
Highland Water	43	**3**	501	-1.59	0.66	2.25	-0.11	-0.30	-0.78	0.14	0.531
Cruick	51	**3**	2431	-0.28	1.10	1.38	0.28	0.30	0.17	0.39	0.184
Tarf	50	**3**									
	52	**3**	5486	-0.45	0.89	1.34	0.14	0.13	0.06	0.21	0.112
	54	**3**									
Blackwater	33	**3**	6100	-2.05	0.578	2.64	0.321	0.099	-0.09	0.39	0.475
Tame LM	43	**3**	1726	-3.66	1.19	4.86	0.104	-0.19	-0.71	0.352	0.742
Windrush	?	**?**	1302	-0.76	1.44	2.20	0.33	0.38	0.18	0.55	0.277
TamesHM	20	**0**	1206	-0.85	0.68	1.53	0.306	0.066	-0.397	0.367	0.441

Table Appendix 3.1.2: descriptive statistics for depth at the studied river sites. Data sets only include wet points.

Site	% Flow exceedance (Low Flows 2000)	Group	Num. Points	Max. Depth	Median	Mean	1st Quartile	3rd Quartile	Std. Dev
Pang Old fenced	90	**1**	299	0.562	0.293	0.286	0.209	0.384	0.129
Pang fenced	91	**1**	700	0.726	0.171	0.193	0.098	0.279	0.127
Pang Unfenced	90	**1**	784	0.534	0.222	0.213	0.128	0.291	0.112
Lambourn	92	**1**	2200	0.569	0.296	0.272	0.226	0.338	0.093
Leigh Brook	93	**1**	2983	0.85	0.18	0.20	0.09	0.30	0.148
Bere 2000	79	**2**	924	0.875	0.332	0.332	0.203	0.442	0.173
Pang Old fenced	80	**2**	306	0.575	0.304	0.292	0.211	0.395	0.135
Pang Unfenced	80	**2**	801	0.544	0.234	0.222	0.131	0.307	0.116
Leigh Brook	82	**2**	2983	0.94	0.21	0.24	0.13	0.34	0.154
Senni	78	**2**	894	1.042	0.414	0.424	0.246	0.574	0.218
Highland Water	43	**3**	219	0.668	0.182	0.196	0.088	0.291	0.128
Cruick	51	**3**	2382	1.102	0.286	0.309	0.186	0.400	0.179
Tarf	50	**3**							
	52	**3**	5045	0.897	0.151	0.158	0.083	0.219	0.093
	54	**3**							
Blackwater	33	**3**	4529	0.578	0.364	0.344	0.295	0.344	0.110
Tame LM	43	**3**	957	1.191	0.330	0.340	0.207	0.439	0.197
Windrush	?	**?**	1278	1.449	0.341	0.398	0.194	0.560	0.264
TamesHM	20	**0**	810	0.681	0.352	0.359	0.305	0.393	0.095

Appendix 3.2

Results obtained for the analysis in Chapter 5 –sensitivity analysis for the lag distance

This appendix shows the graphical outputs obtained for the sensitivity analysis of lag distance developed in section 5.4.3. Results are presented in two section; a first one summarising the results obtained for the data sets with wet and dry points and a second one including results obtained for data sets with only wet points. Each river site analysed presents two outputs: (i) the experimental variogram obtained for the different lag distances and (ii) a comparison of the relation between the number of pair of points obtained for each lag distance of the variogram for the all the lag distances tested.

Lag Distance Dry & Wet points

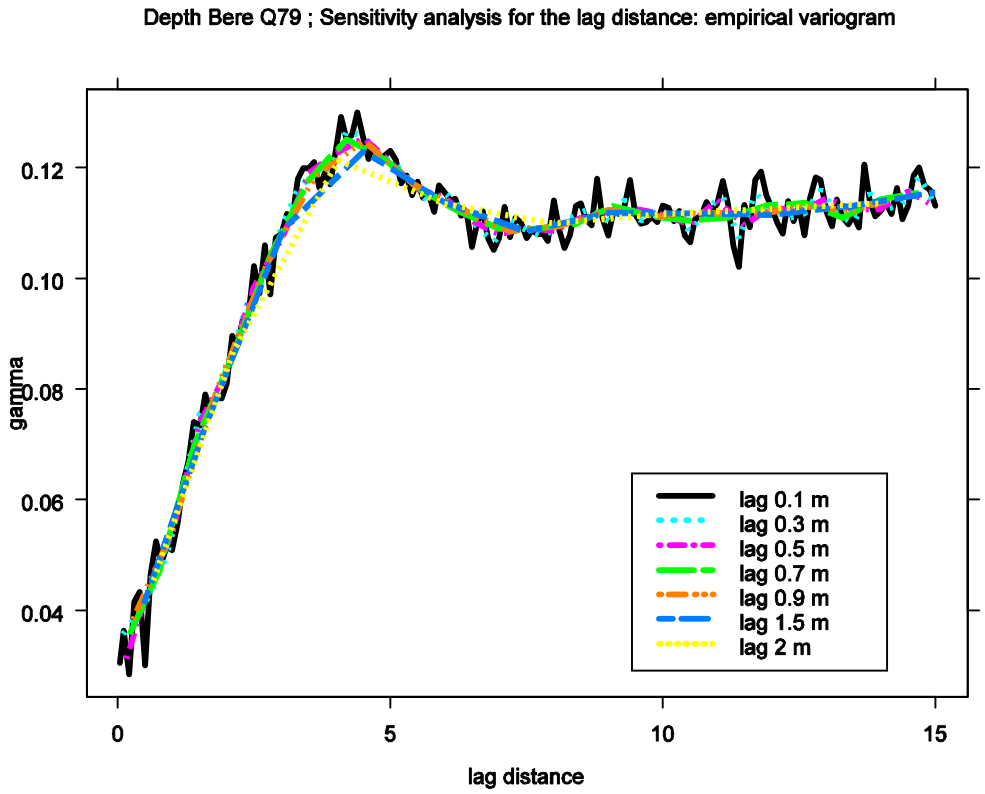

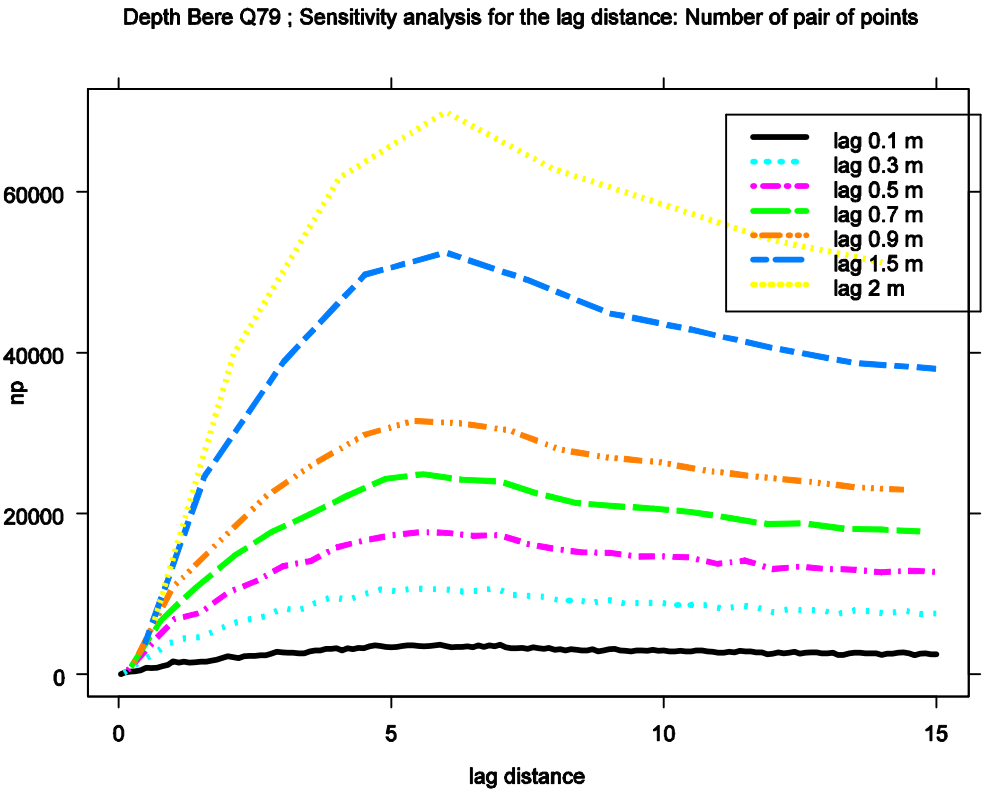

Depth Blackwater Q33 ; Sensitivity analysis for the lag distance: empirical variogram

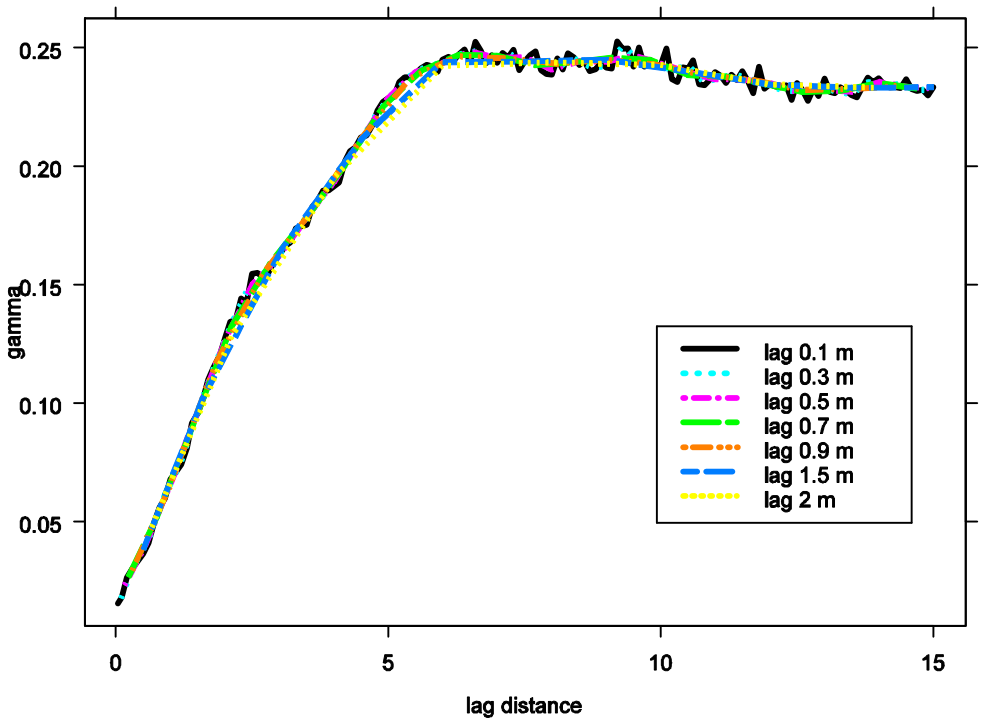

Depth Blackwater Q33 ; Sensitivity analysis for the lag distance: Number of pair of points

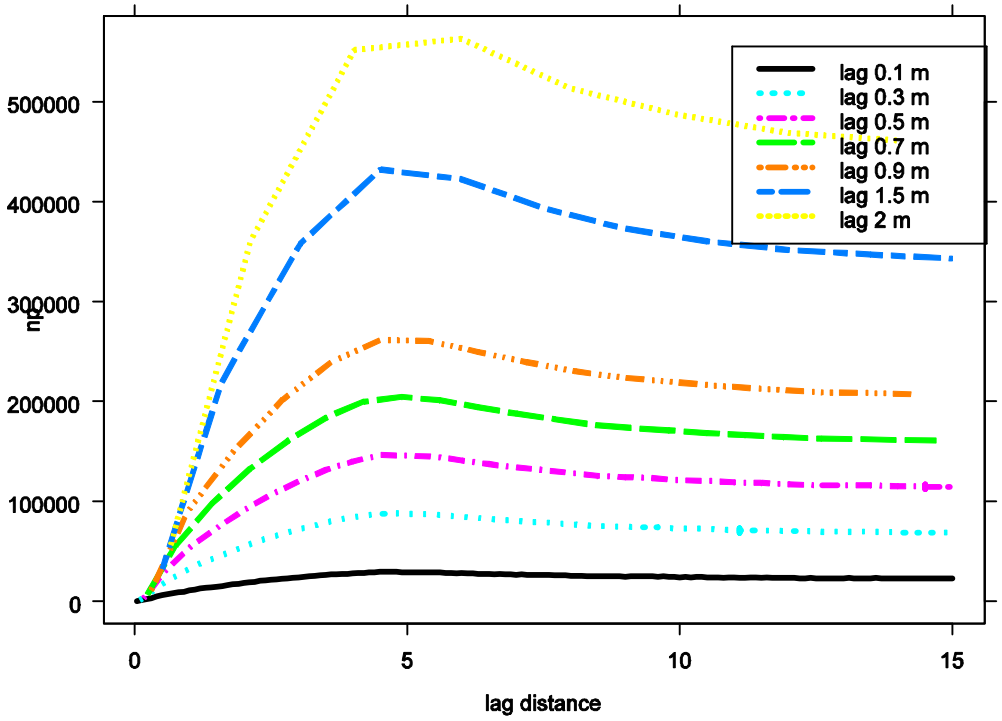

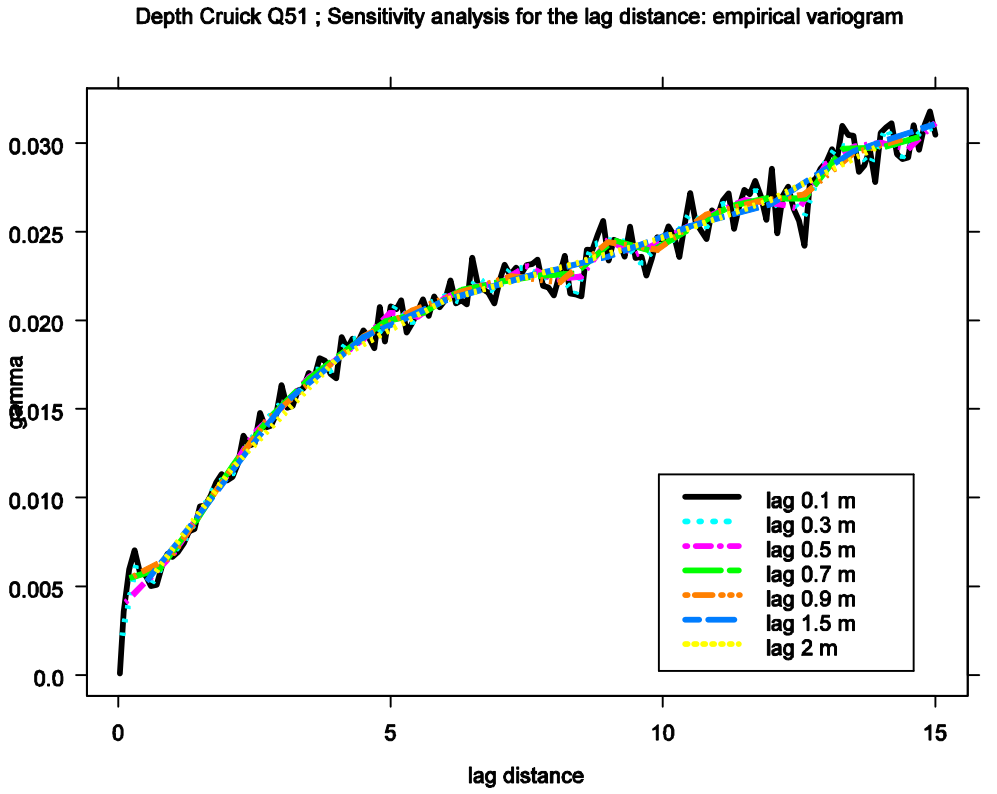
Depth Cruick Q51 ; Sensitivity analysis for the lag distance: empirical variogram
gamma
0.0
0.005
0.010
0.015
0.020
0.025
0.030
0
5
10
15
lag distance
lag 0.1 m
lag 0.3 m
lag 0.5 m
lag 0.7 m
lag 0.9 m
lag 1.5 m
lag 2 m

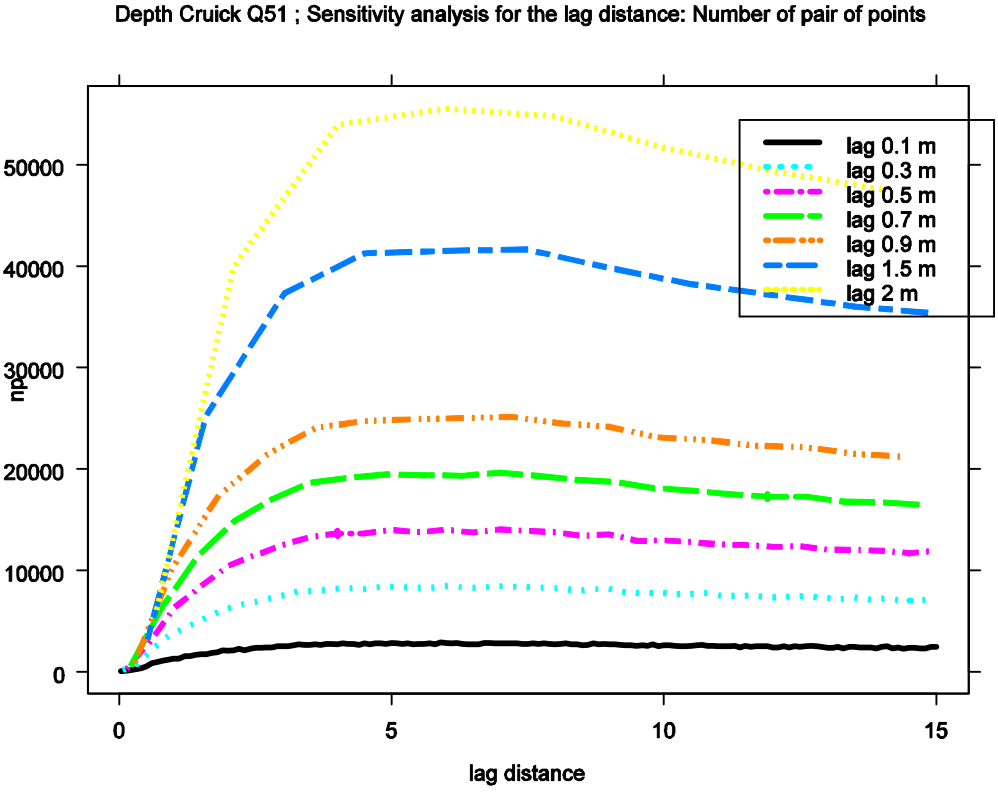
Depth Cruick Q51 ; Sensitivity analysis for the lag distance: Number of pair of points
np
0
10000
20000
30000
40000
50000
0
5
10
15
lag distance
lag 0.1 m
lag 0.3 m
lag 0.5 m
lag 0.7 m
lag 0.9 m
lag 1.5 m
lag 2 m

Depth HighlandWater Q43 ; Sensitivity analysis for the lag distance: empirical variogram

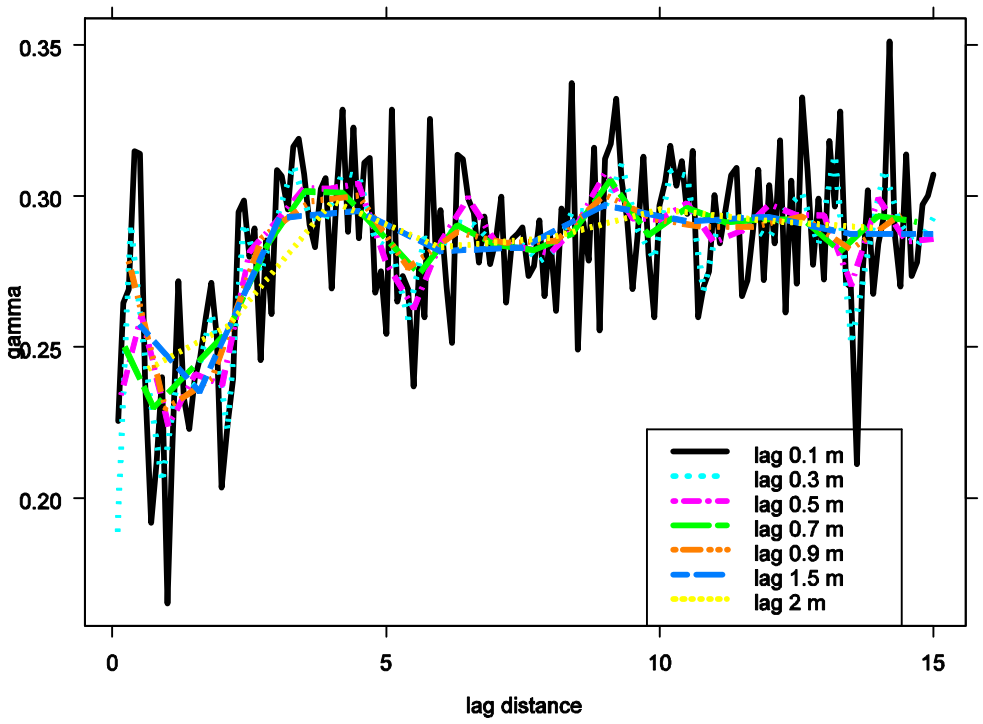

Depth HighlandWater Q43 ; Sensitivity analysis for the lag distance: Number of pair of points

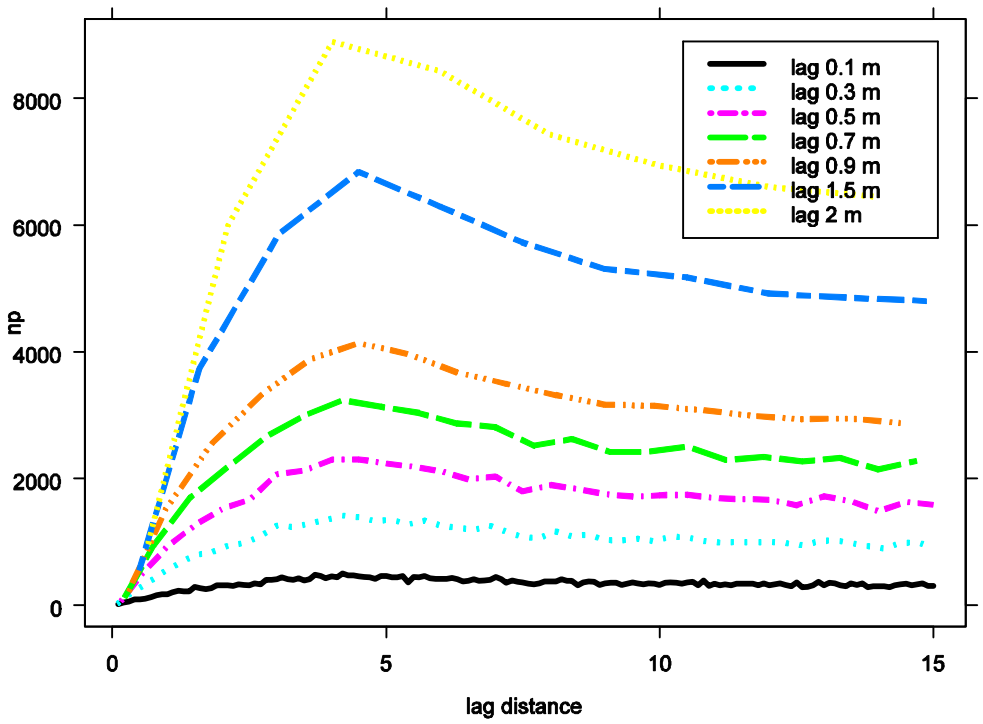

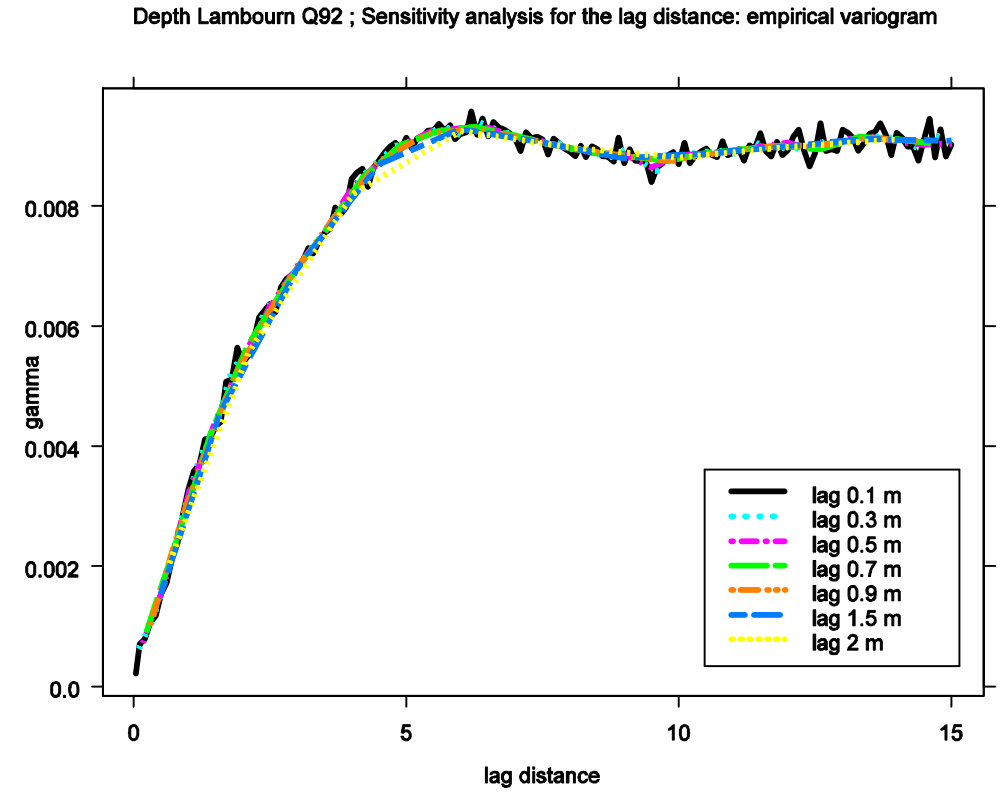
Depth Lambourn Q92 ; Sensitivity analysis for the lag distance: empirical variogram
gamma
0.0
0.002
0.004
0.006
0.008
0
5
10
15
lag distance
lag 0.1 m
lag 0.3 m
lag 0.5 m
lag 0.7 m
lag 0.9 m
lag 1.5 m
lag 2 m

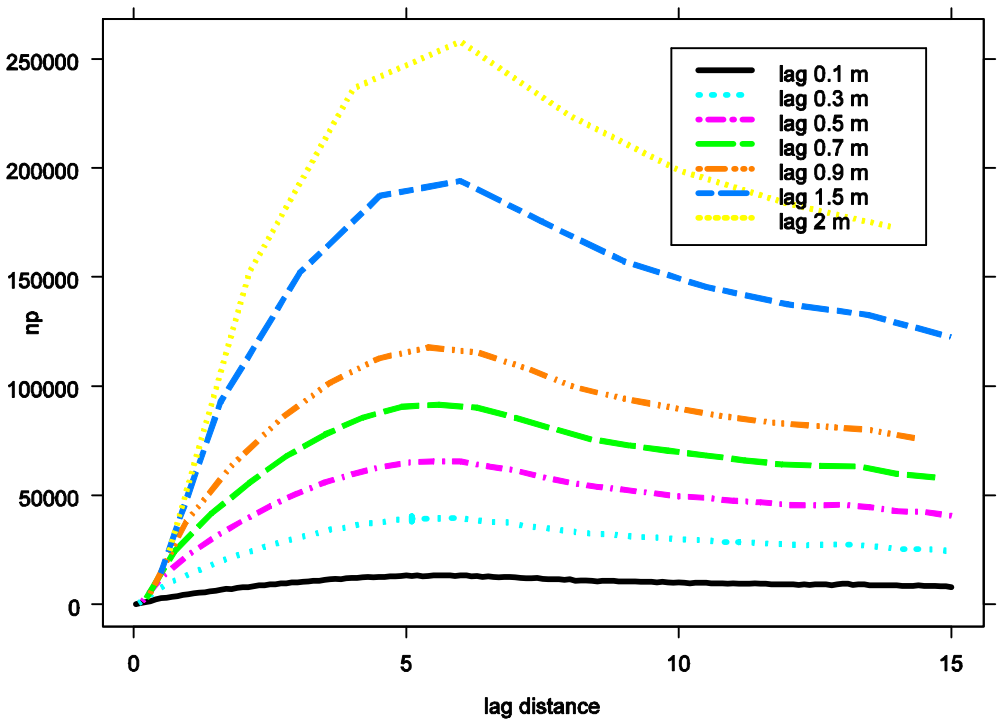
Depth Lambourn Q92 ; Sensitivity analysis for the lag distance: Number of pair of points
np
0
50000
100000
150000
200000
250000
0
5
10
15
lag distance
lag 0.1 m
lag 0.3 m
lag 0.5 m
lag 0.7 m
lag 0.9 m
lag 1.5 m
lag 2 m

Depth LeighBrook Q82 ; Sensitivity analysis for the lag distance: empirical variogram

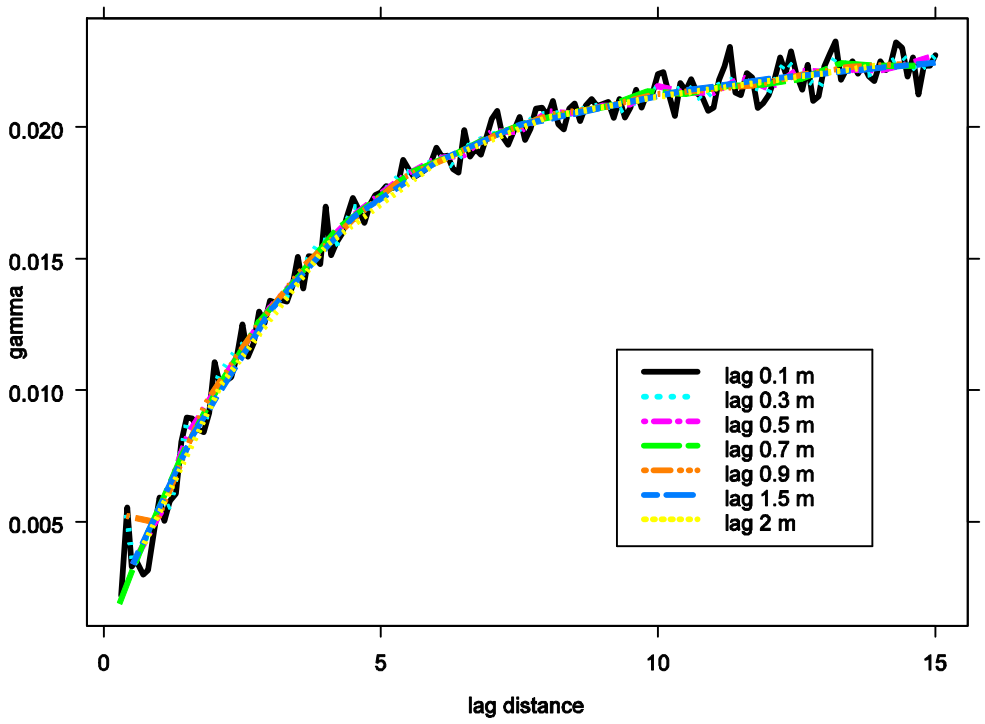

Depth LeighBrook Q82 ; Sensitivity analysis for the lag distance: Number of pair of points

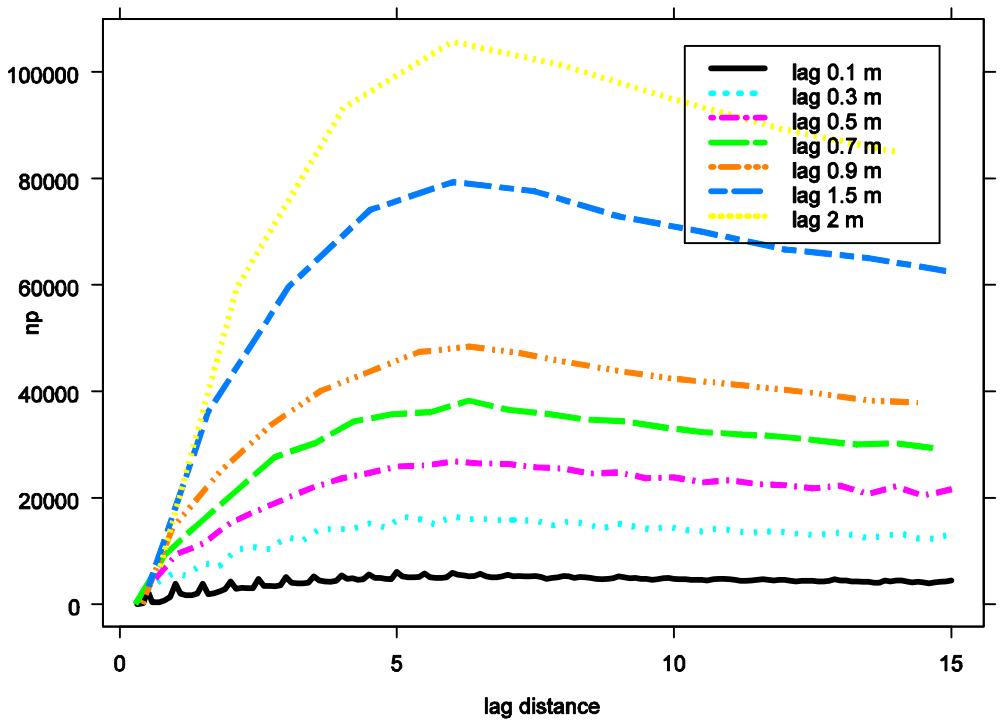

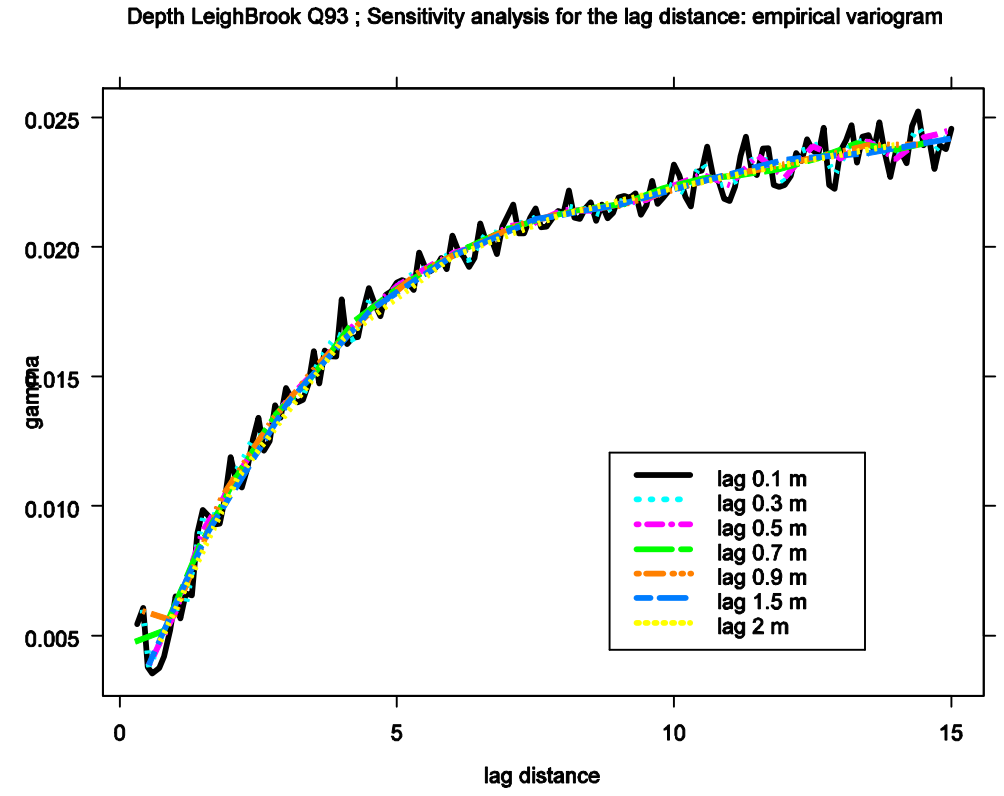
Depth LeighBrook Q93 ; Sensitivity analysis for the lag distance: empirical variogram
gamma
0.025
0.020
0.015
0.010
0.005
0
5
10
15
lag distance
lag 0.1 m
lag 0.3 m
lag 0.5 m
lag 0.7 m
lag 0.9 m
lag 1.5 m
lag 2 m

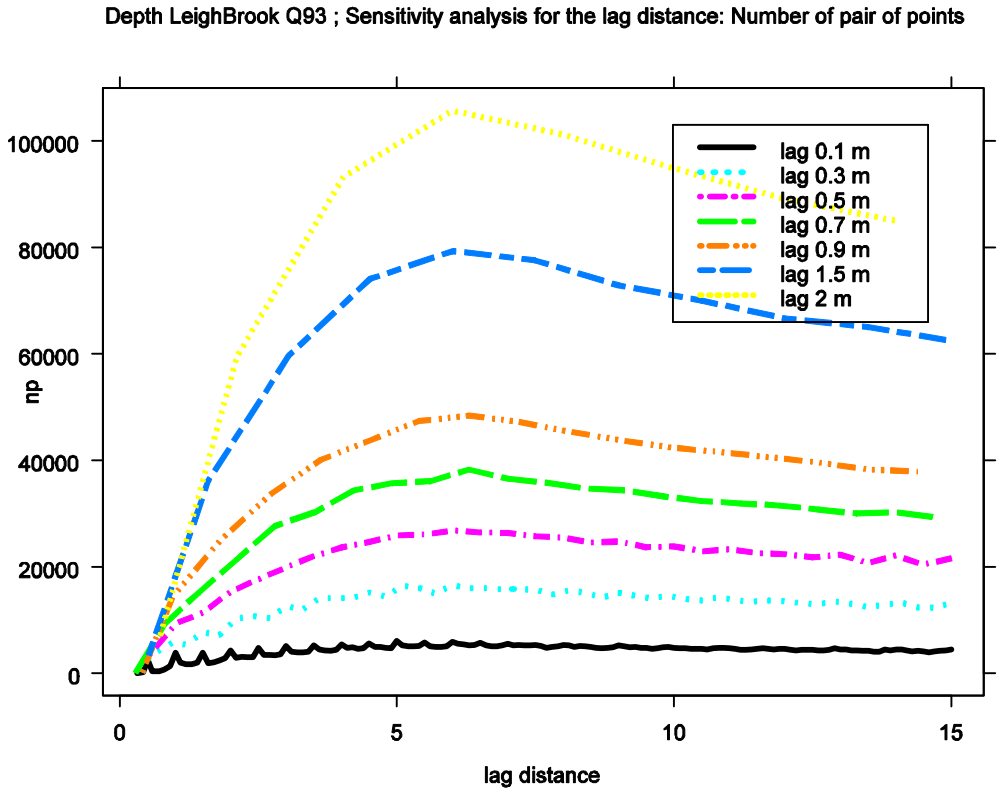
Depth LeighBrook Q93 ; Sensitivity analysis for the lag distance: Number of pair of points
np
100000
80000
60000
40000
20000
0
0
5
10
15
lag distance
lag 0.1 m
lag 0.3 m
lag 0.5 m
lag 0.7 m
lag 0.9 m
lag 1.5 m
lag 2 m

Depth Pang Fenced Q91 ; Sensitivity analysis for the lag distance: empirical variogram

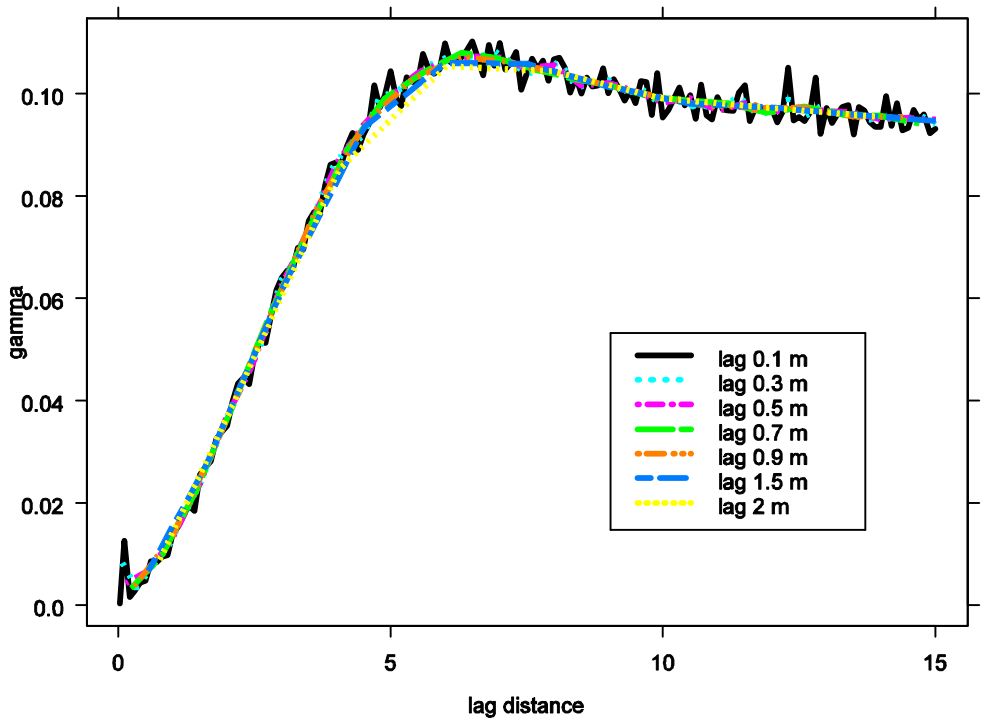

Depth Pang Fenced Q91 ; Sensitivity analysis for the lag distance: Number of pair of points

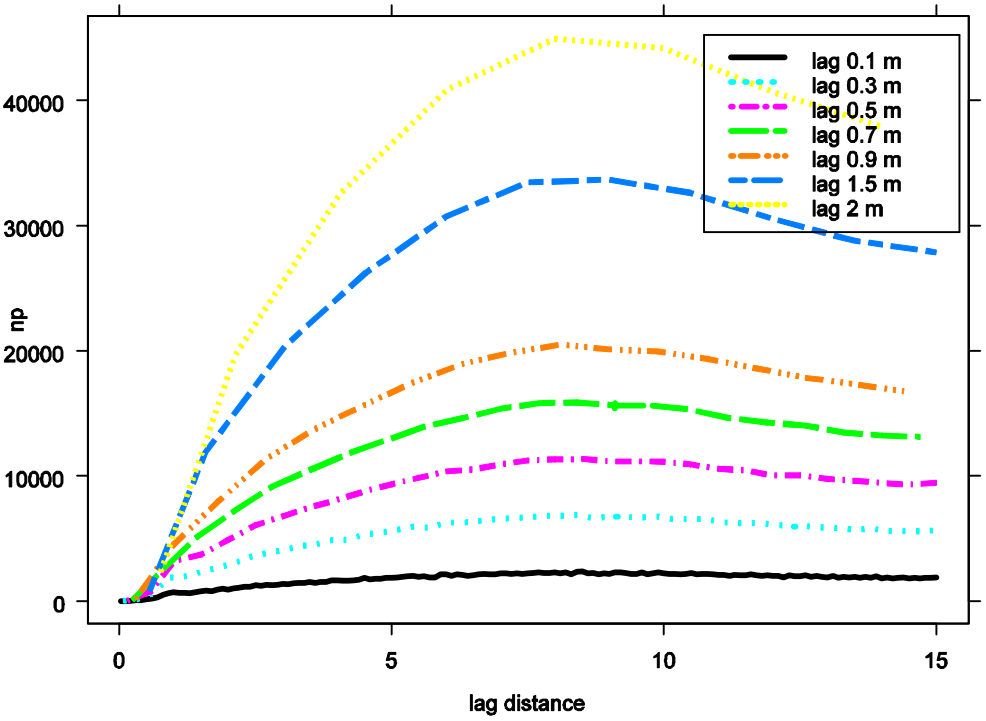

Depth Pang Old Fenced Q80 ; Sensitivity analysis for the lag distance: empirical variogram

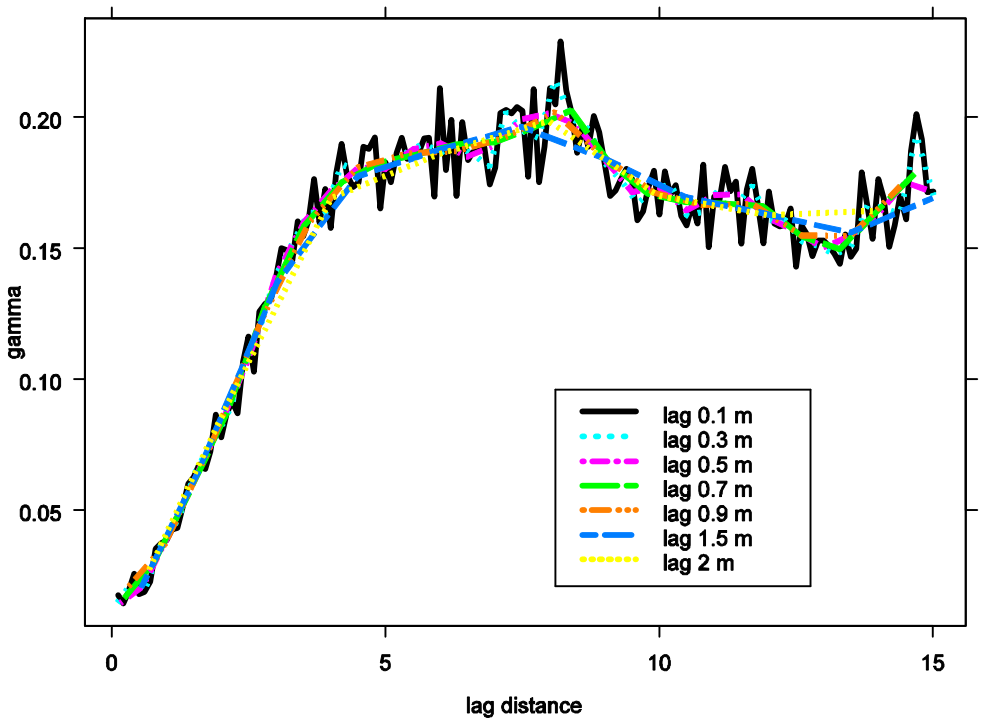

Depth Pang Old Fenced Q80 ; Sensitivity analysis for the lag distance: Number of pair of points

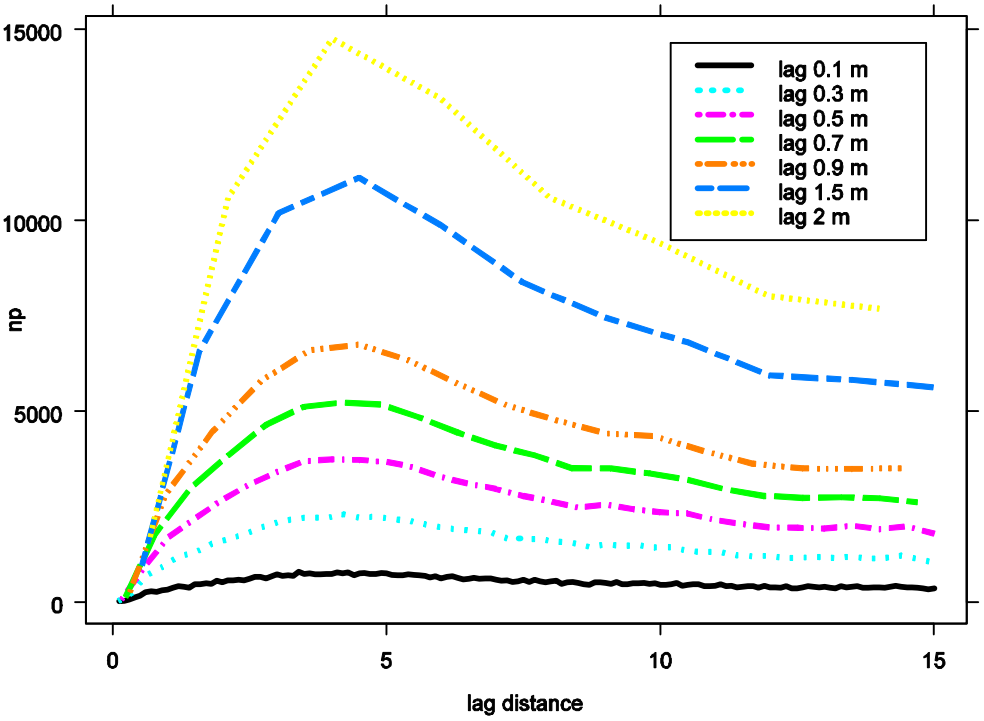

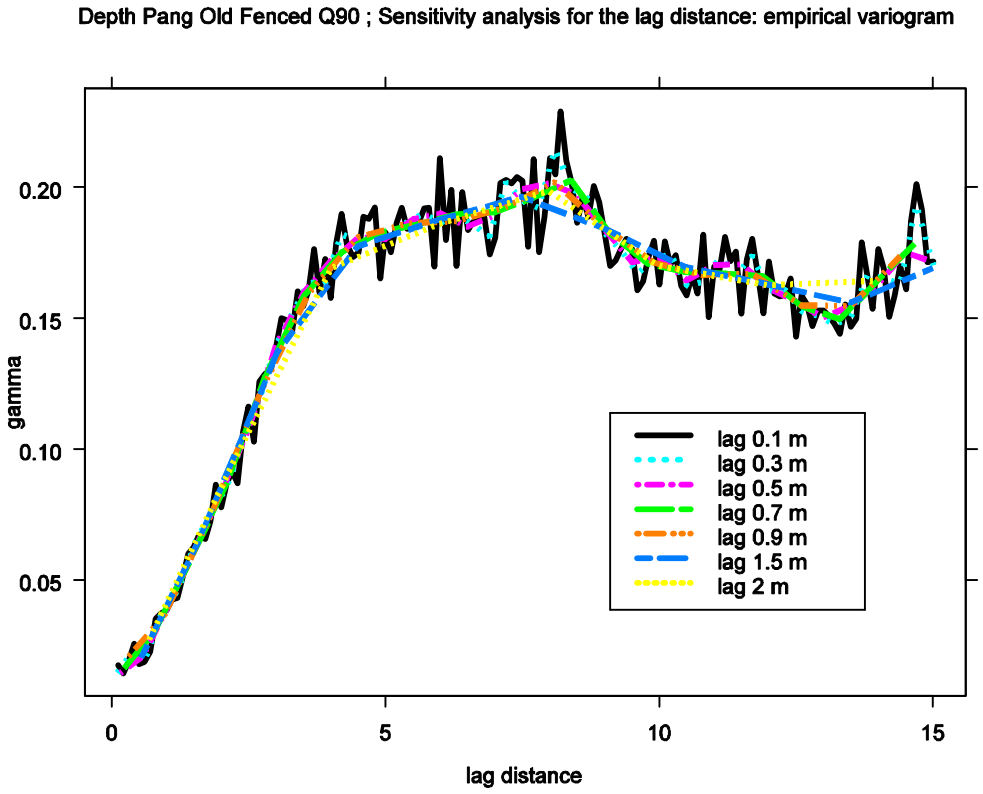
Depth Pang Old Fenced Q90 ; Sensitivity analysis for the lag distance: empirical variogram
gamma
0.05
0.10
0.15
0.20
0
5
10
15
lag distance
lag 0.1 m
lag 0.3 m
lag 0.5 m
lag 0.7 m
lag 0.9 m
lag 1.5 m
lag 2 m

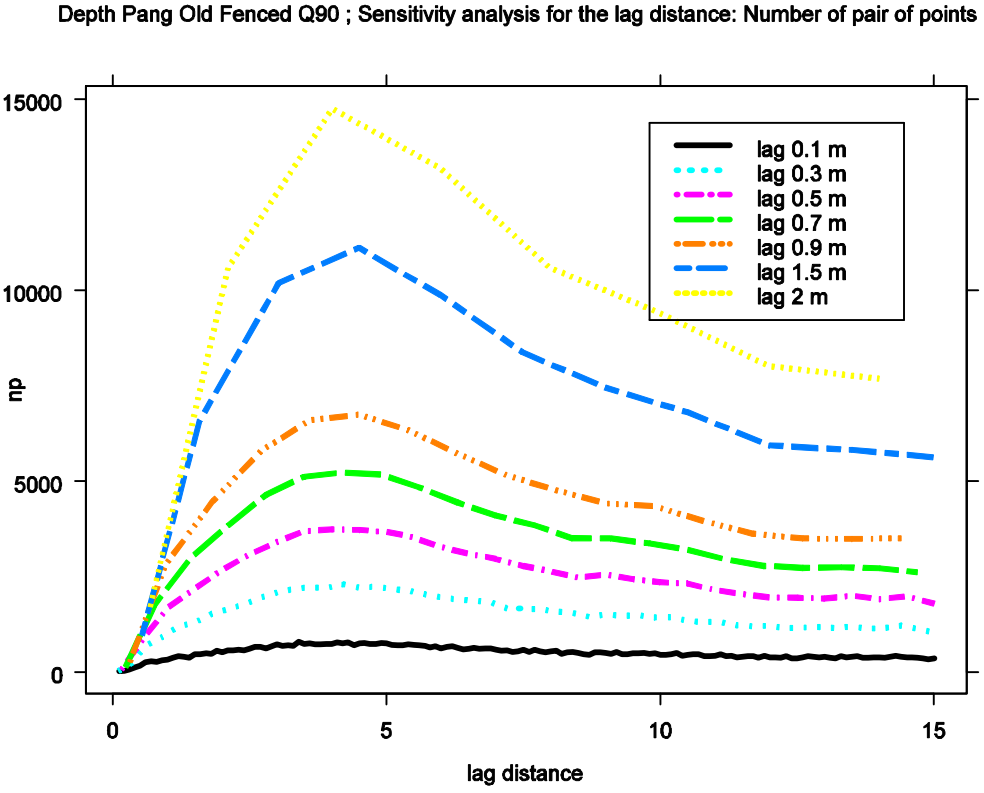
Depth Pang Old Fenced Q90 ; Sensitivity analysis for the lag distance: Number of pair of points
np
0
5000
10000
15000
0
5
10
15
lag distance
lag 0.1 m
lag 0.3 m
lag 0.5 m
lag 0.7 m
lag 0.9 m
lag 1.5 m
lag 2 m

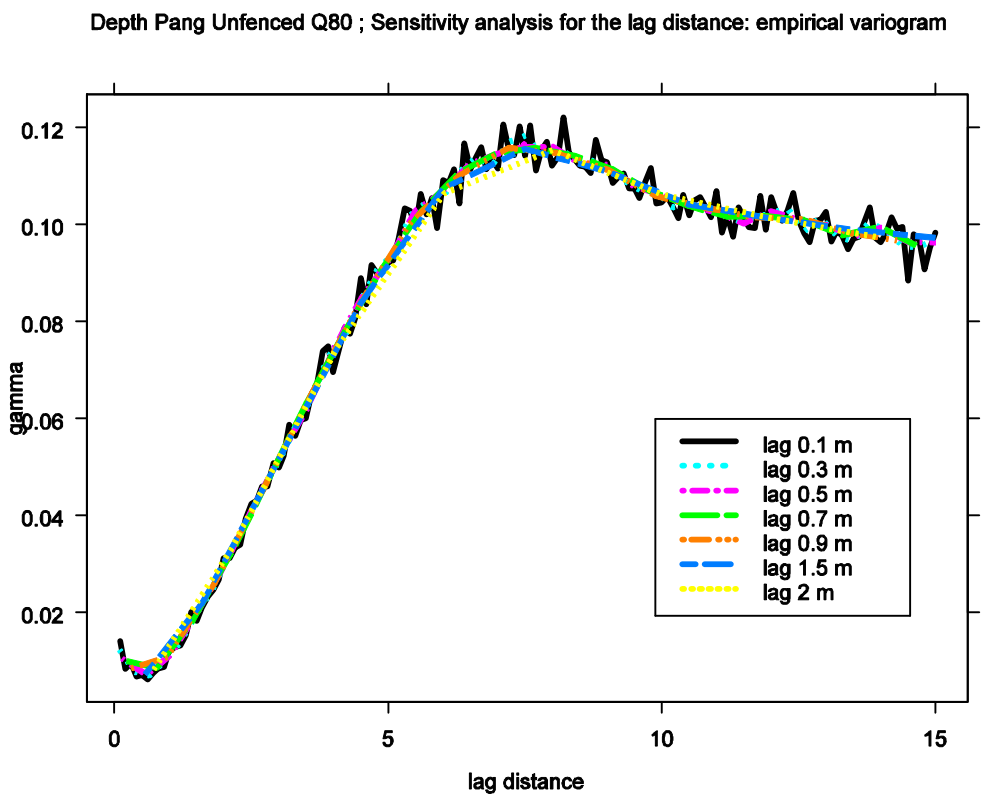
Depth Pang Unfenced Q80 ; Sensitivity analysis for the lag distance: empirical variogram
gamma
0.12
0.10
0.08
0.06
0.04
0.02
0
5
10
15
lag distance
lag 0.1 m
lag 0.3 m
lag 0.5 m
lag 0.7 m
lag 0.9 m
lag 1.5 m
lag 2 m

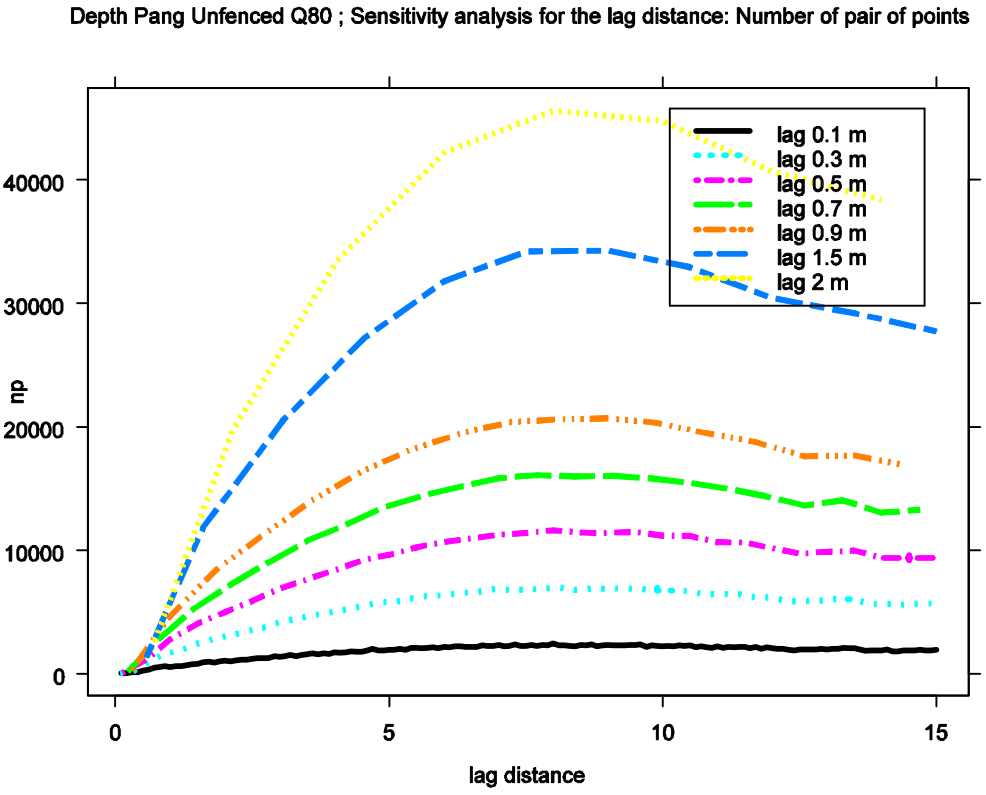
Depth Pang Unfenced Q80 ; Sensitivity analysis for the lag distance: Number of pair of points
np
40000
30000
20000
10000
0
0
5
10
15
lag distance
lag 0.1 m
lag 0.3 m
lag 0.5 m
lag 0.7 m
lag 0.9 m
lag 1.5 m
lag 2 m

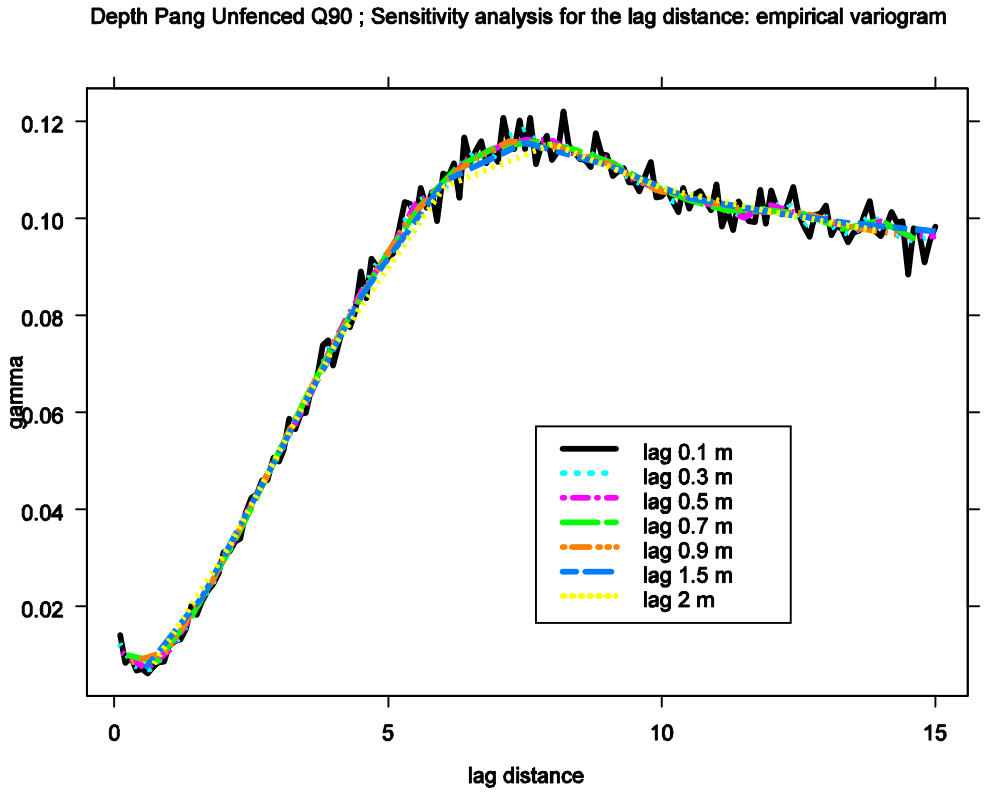
Depth Pang Unfenced Q90 ; Sensitivity analysis for the lag distance: empirical variogram
gamma
0.12
0.10
0.08
0.06
0.04
0.02
0
5
10
15
lag distance
lag 0.1 m
lag 0.3 m
lag 0.5 m
lag 0.7 m
lag 0.9 m
lag 1.5 m
lag 2 m

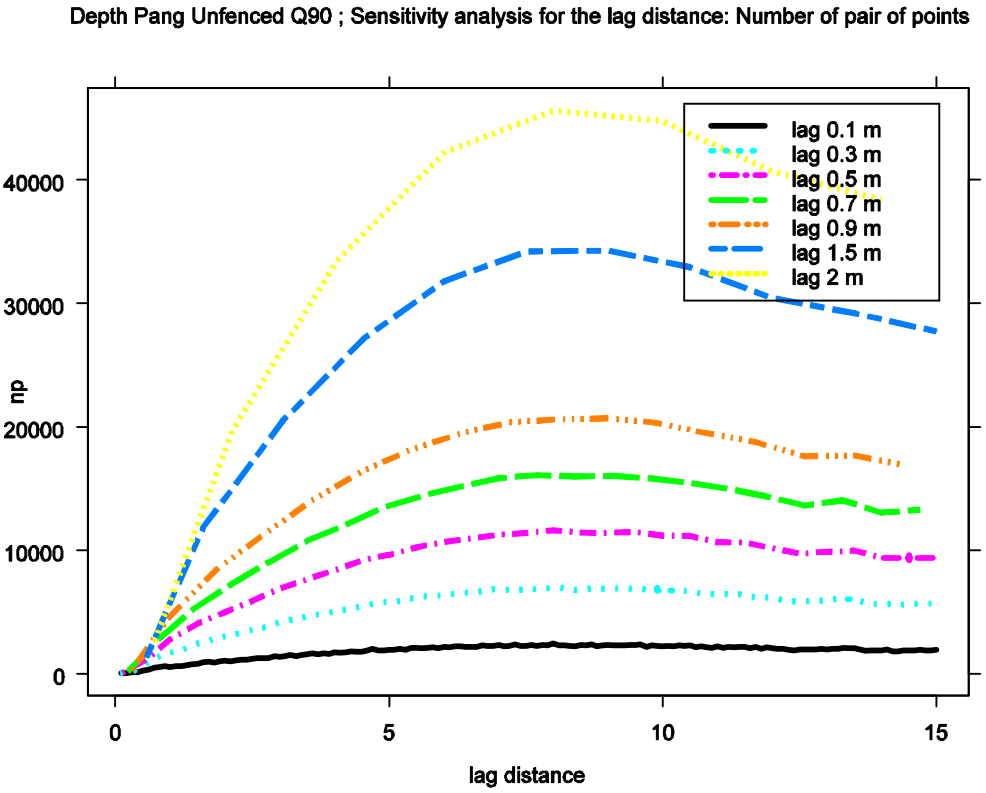
Depth Pang Unfenced Q90 ; Sensitivity analysis for the lag distance: Number of pair of points
np
40000
30000
20000
10000
0
0
5
10
15
lag distance
lag 0.1 m
lag 0.3 m
lag 0.5 m
lag 0.7 m
lag 0.9 m
lag 1.5 m
lag 2 m

Depth Senni Q78 ; Sensitivity analysis for the lag distance: empirical variogram

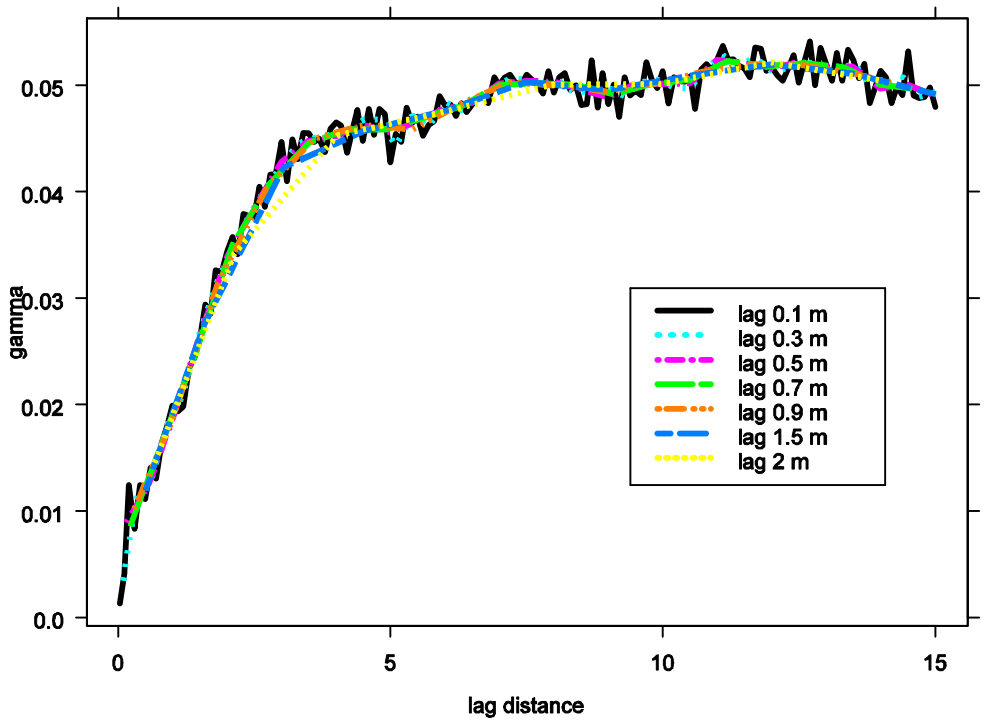

Depth Senni Q78 ; Sensitivity analysis for the lag distance: Number of pair of points

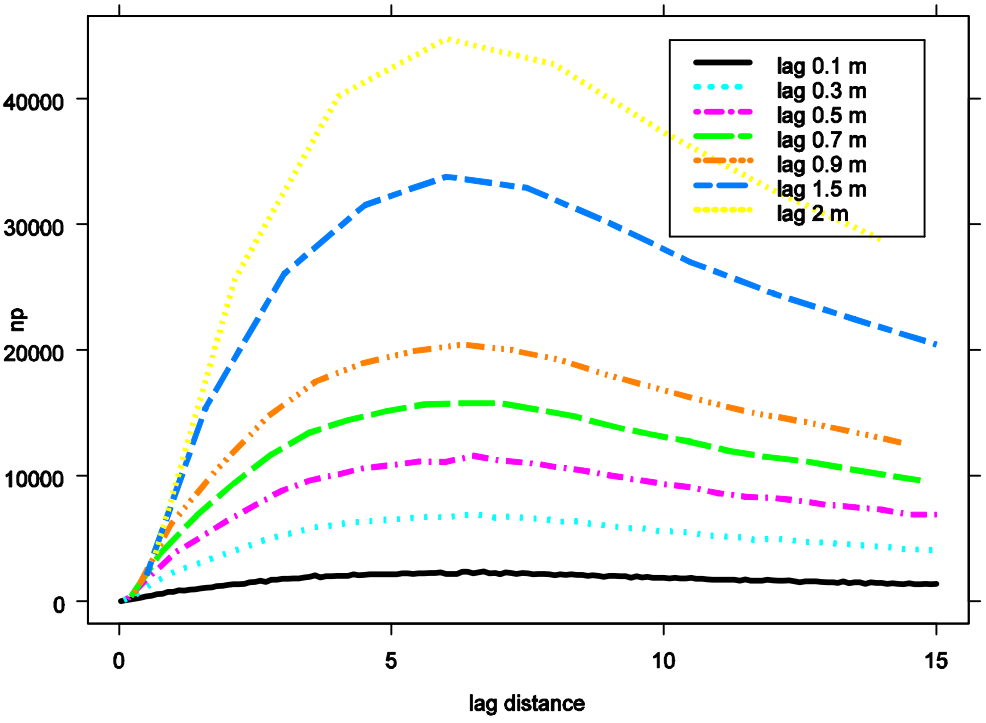

Depth Tames HM Q20 ; Sensitivity analysis for the lag distance: empirical variogram

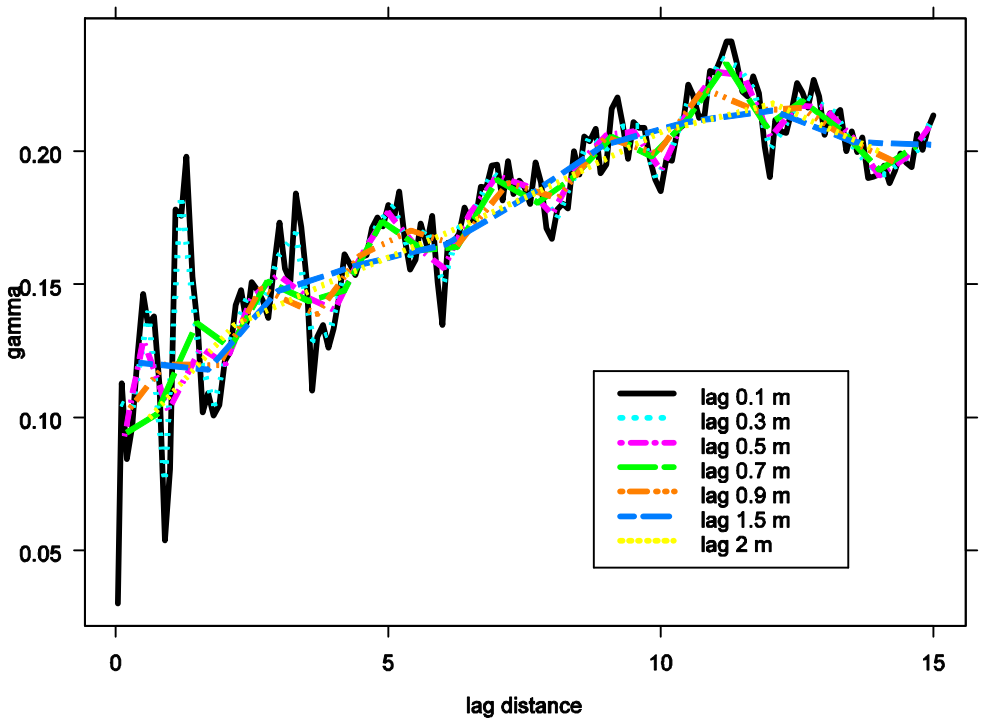

Depth Tames HM Q20 ; Sensitivity analysis for the lag distance: Number of pair of points

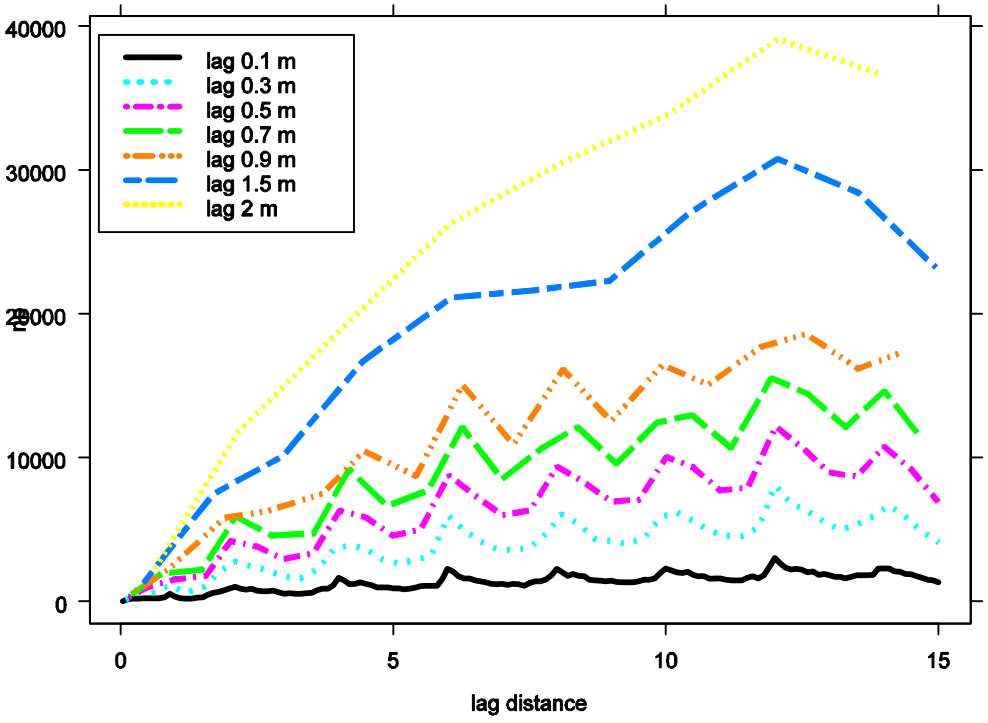

Depth TamesLM Q43 ; Sensitivity analysis for the lag distance: empirical variogram

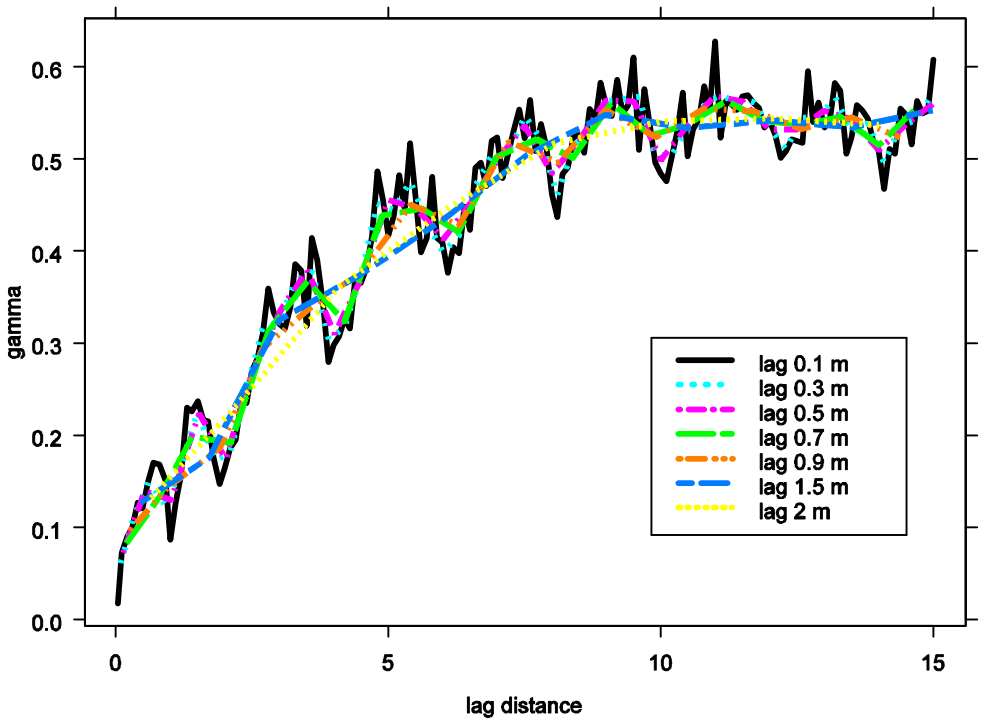

Depth TamesLM Q43 ; Sensitivity analysis for the lag distance: Number of pair of points

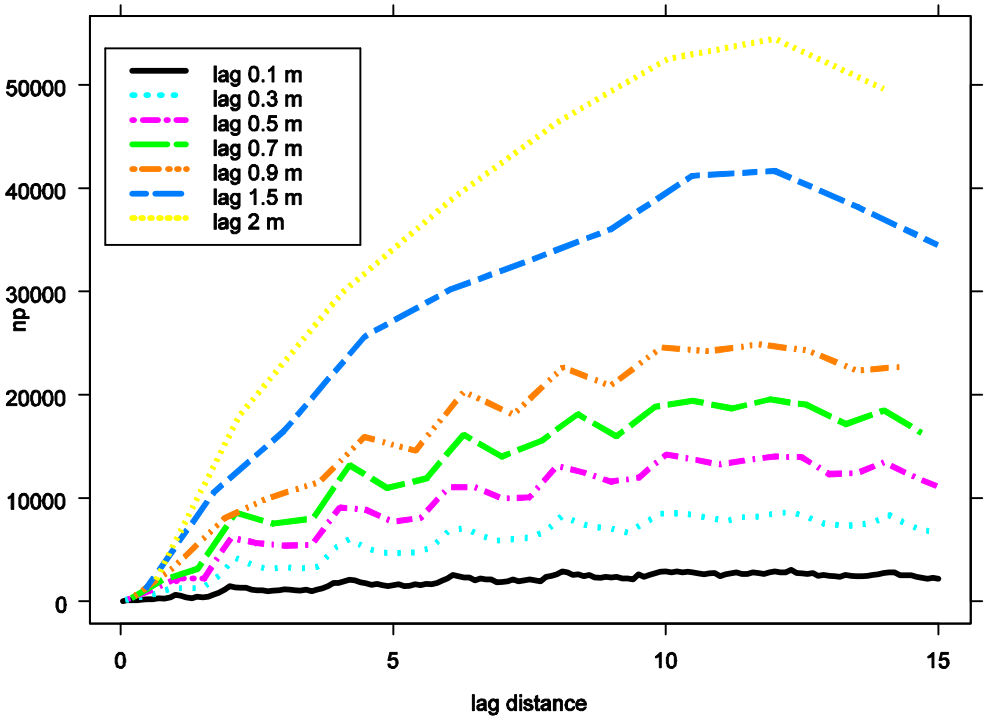

Depth Tarf Q51 ; Sensitivity analysis for the lag distance: empirical variogram

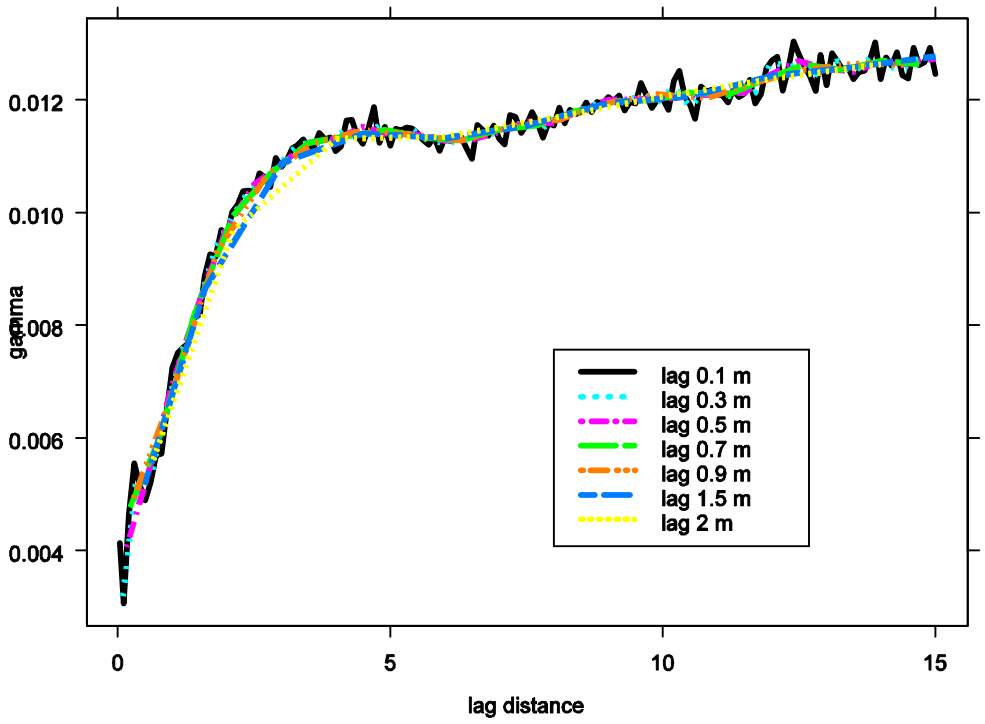

Depth Tarf Q51 ; Sensitivity analysis for the lag distance: Number of pair of points

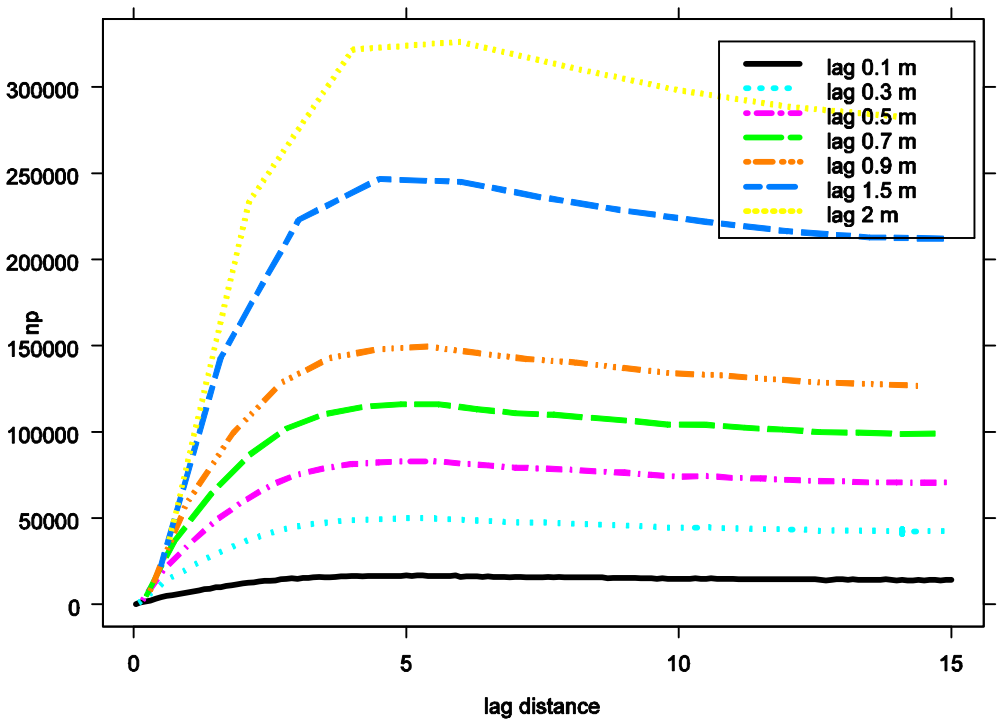

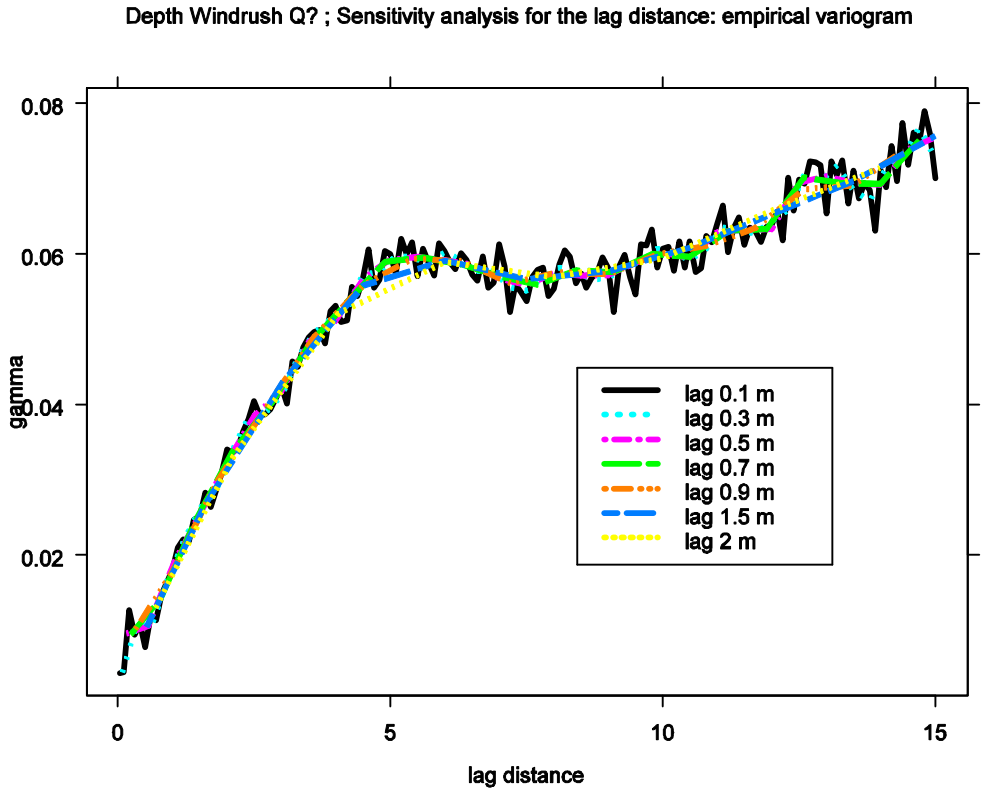
Depth Windrush Q? ; Sensitivity analysis for the lag distance: empirical variogram
gamma
0.08
0.06
0.04
0.02
0
5
10
15
lag distance
lag 0.1 m
lag 0.3 m
lag 0.5 m
lag 0.7 m
lag 0.9 m
lag 1.5 m
lag 2 m

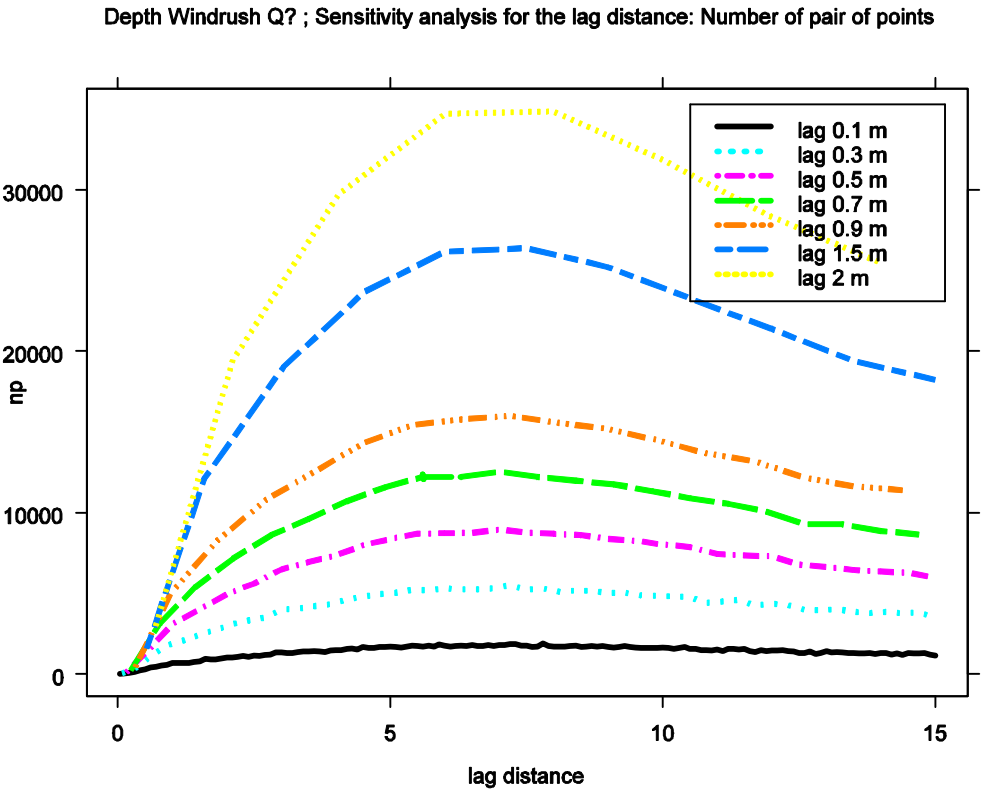
Depth Windrush Q? ; Sensitivity analysis for the lag distance: Number of pair of points
np
30000
20000
10000
0
0
5
10
15
lag distance
lag 0.1 m
lag 0.3 m
lag 0.5 m
lag 0.7 m
lag 0.9 m
lag 1.5 m
lag 2 m

Lag Distance – Wet points

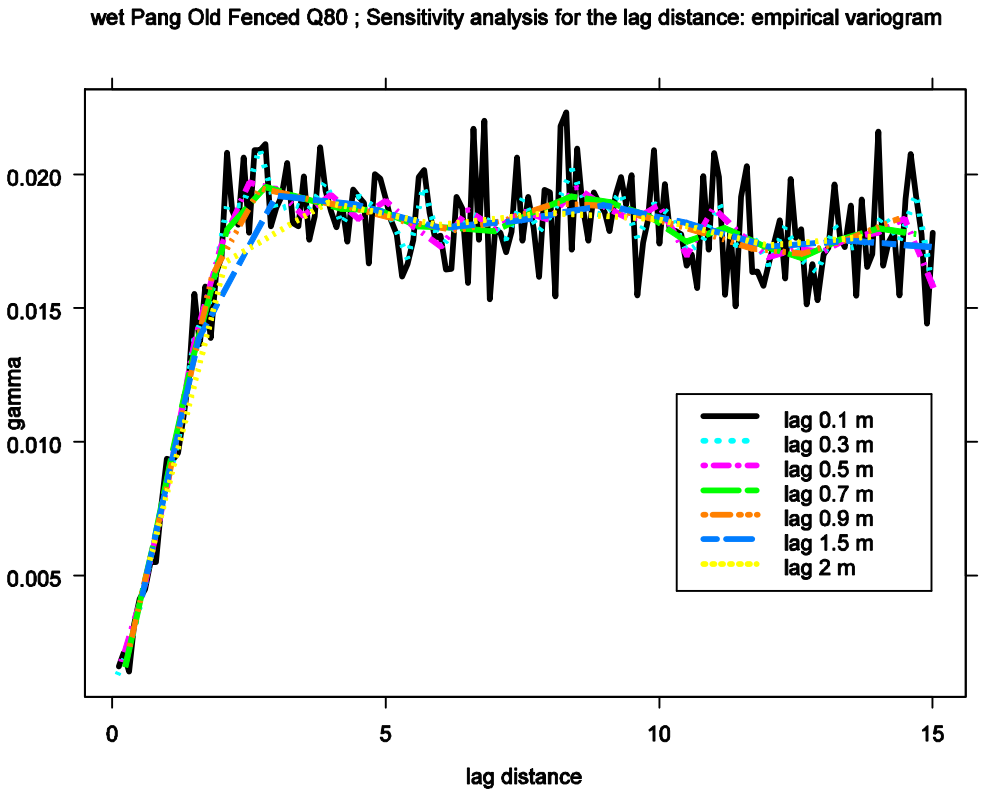

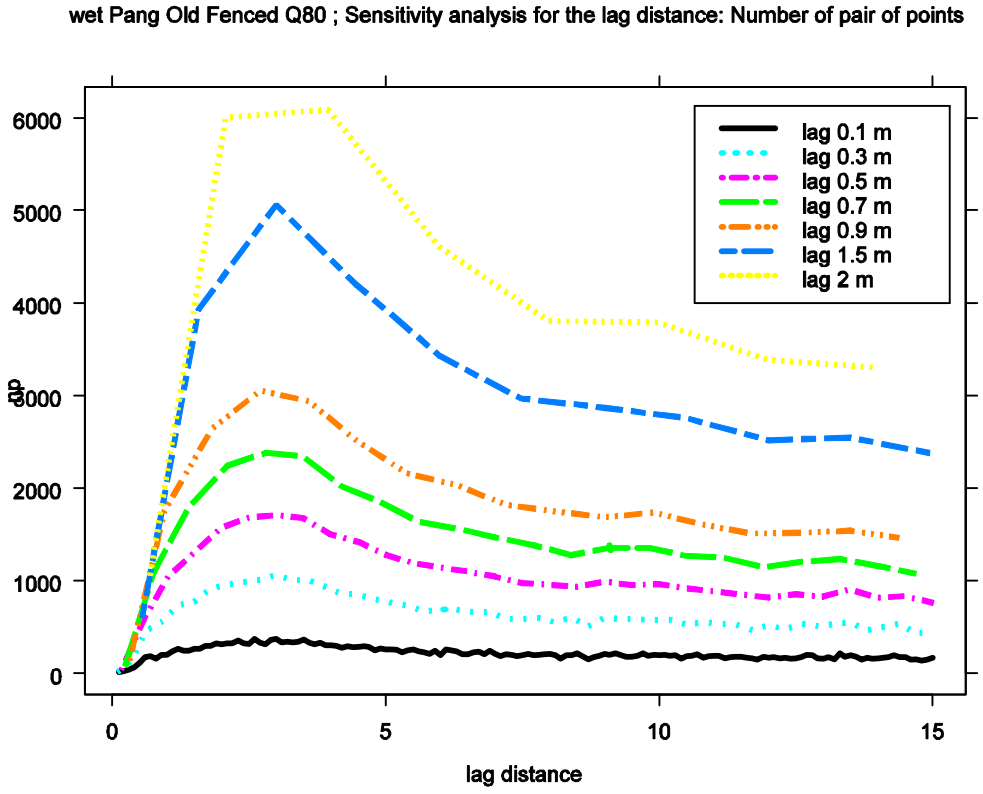

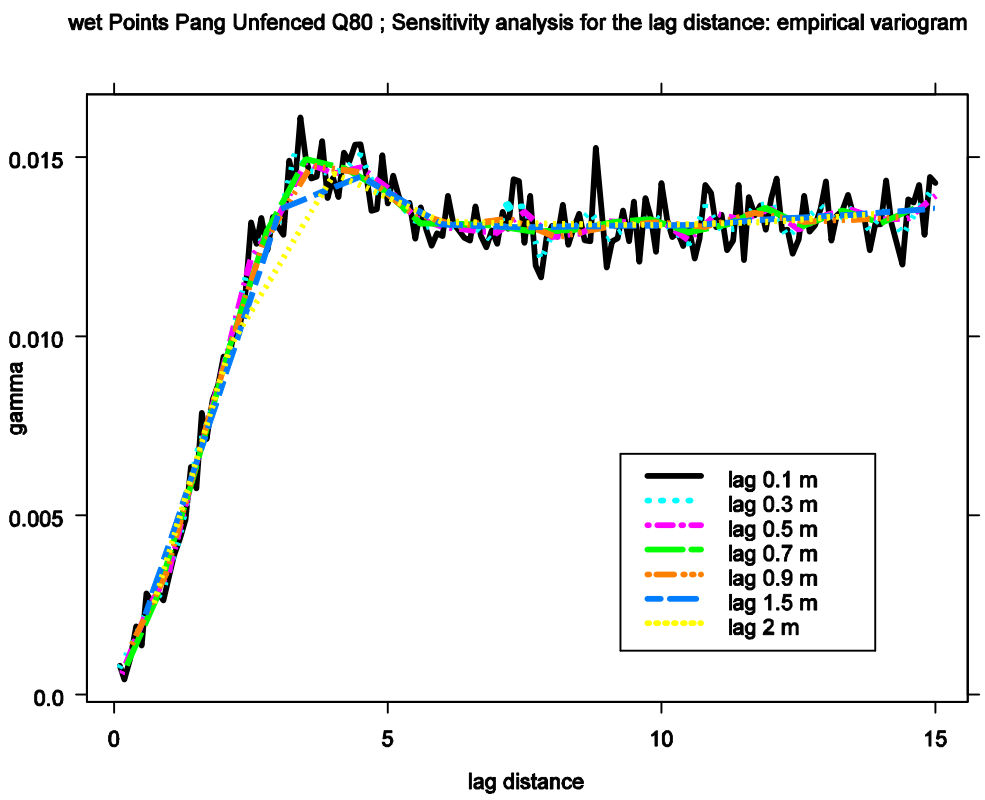
wet Points Pang Unfenced Q80 ; Sensitivity analysis for the lag distance: empirical variogram
gamma
0.0
0.005
0.010
0.015
0
5
10
15
lag distance
lag 0.1 m
lag 0.3 m
lag 0.5 m
lag 0.7 m
lag 0.9 m
lag 1.5 m
lag 2 m

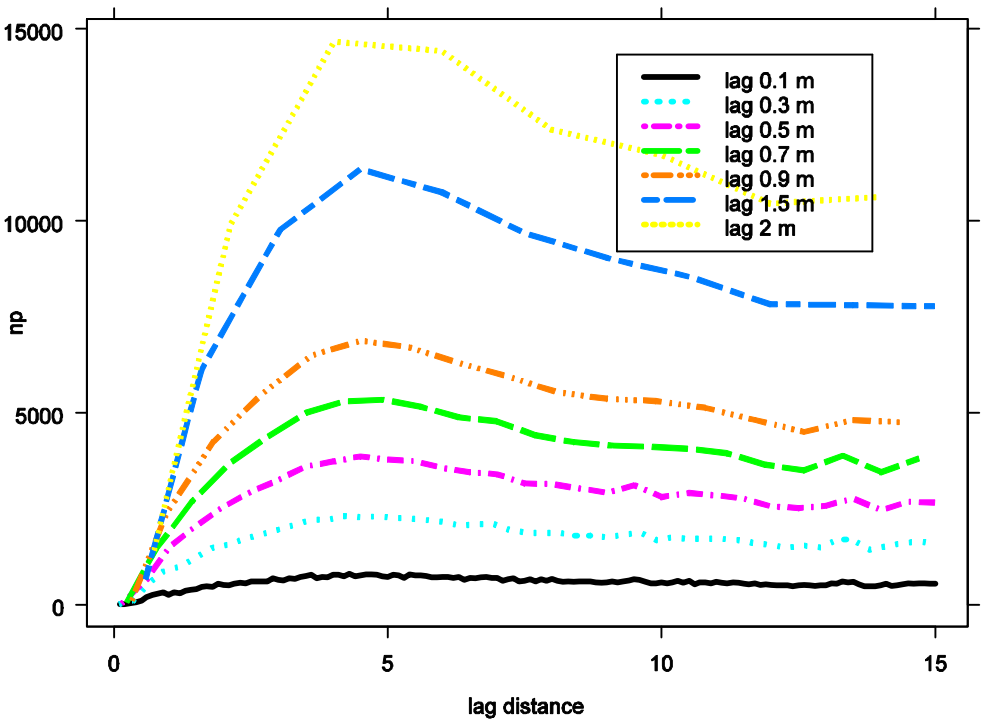
wet Points Pang Unfenced Q80 ; Sensitivity analysis for the lag distance: Number of pair of points
np
0
5000
10000
15000
0
5
10
15
lag distance
lag 0.1 m
lag 0.3 m
lag 0.5 m
lag 0.7 m
lag 0.9 m
lag 1.5 m
lag 2 m

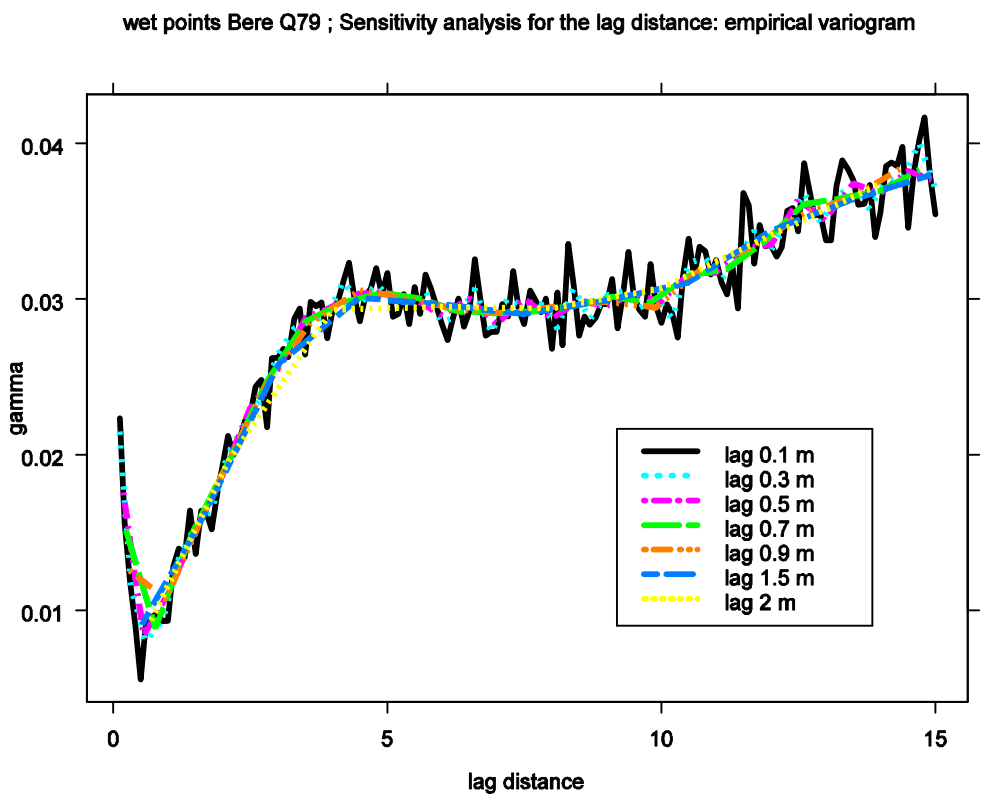
wet points Bere Q79 ; Sensitivity analysis for the lag distance: empirical variogram
gamma
0.04
0.03
0.02
0.01
0
5
10
15
lag distance
lag 0.1 m
lag 0.3 m
lag 0.5 m
lag 0.7 m
lag 0.9 m
lag 1.5 m
lag 2 m

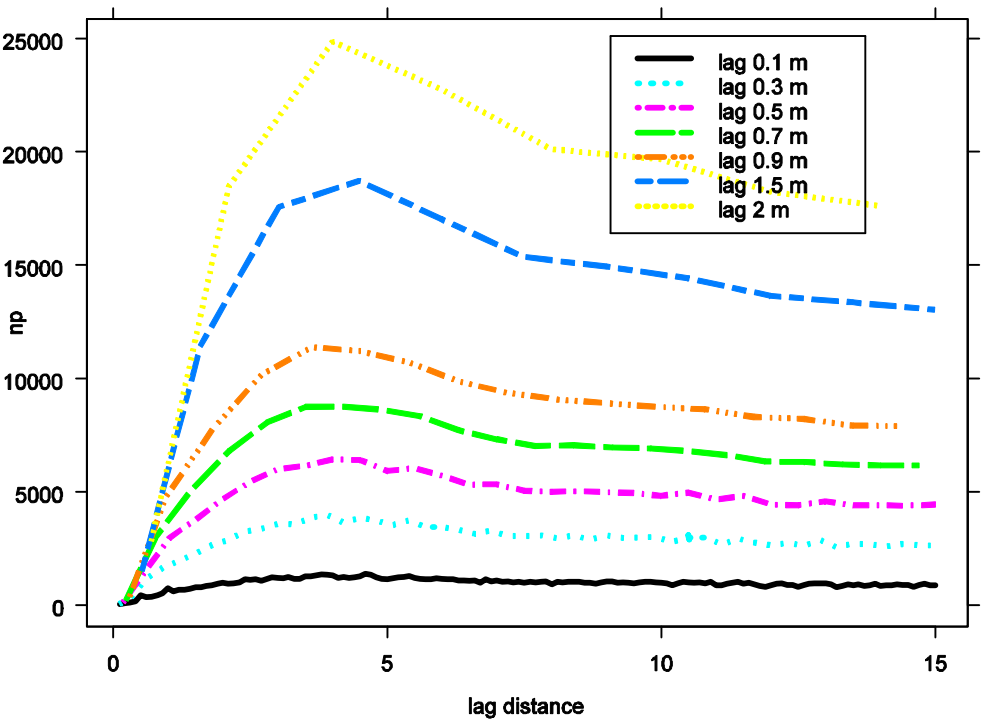
wet points Bere Q79 ; Sensitivity analysis for the lag distance: Number of pair of points
np
25000
20000
15000
10000
5000
0
0
5
10
15
lag distance
lag 0.1 m
lag 0.3 m
lag 0.5 m
lag 0.7 m
lag 0.9 m
lag 1.5 m
lag 2 m

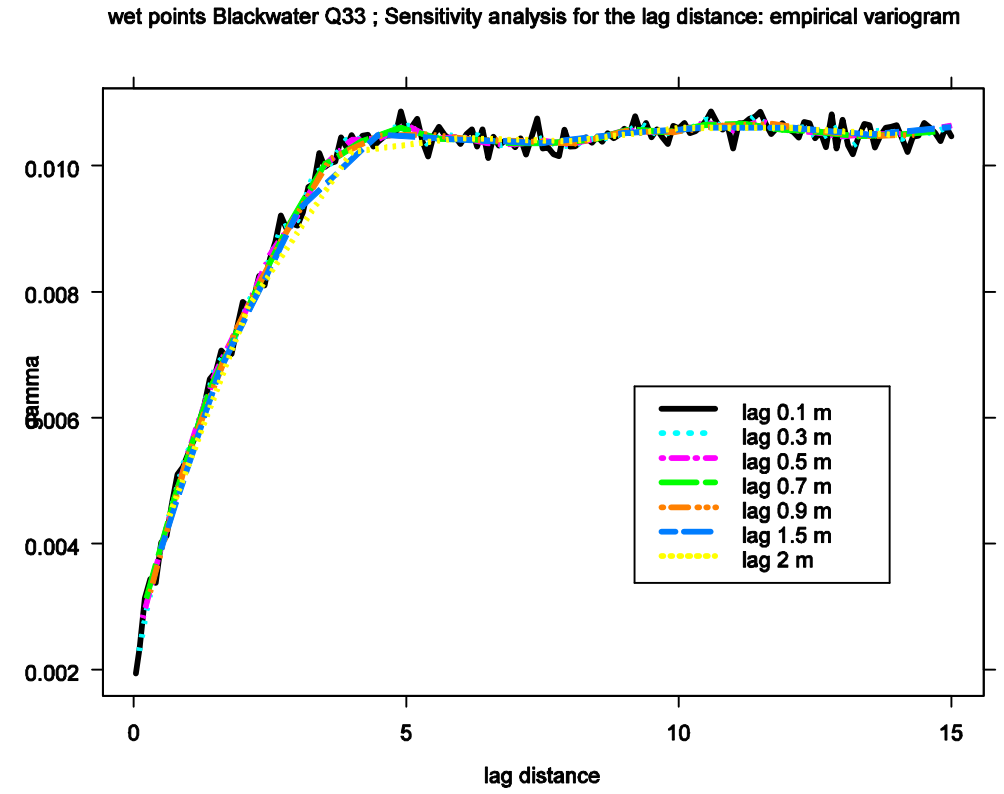
wet points Blackwater Q33 ; Sensitivity analysis for the lag distance: empirical variogram
gamma
0.002
0.004
0.006
0.008
0.010
0
5
10
15
lag distance
lag 0.1 m
lag 0.3 m
lag 0.5 m
lag 0.7 m
lag 0.9 m
lag 1.5 m
lag 2 m

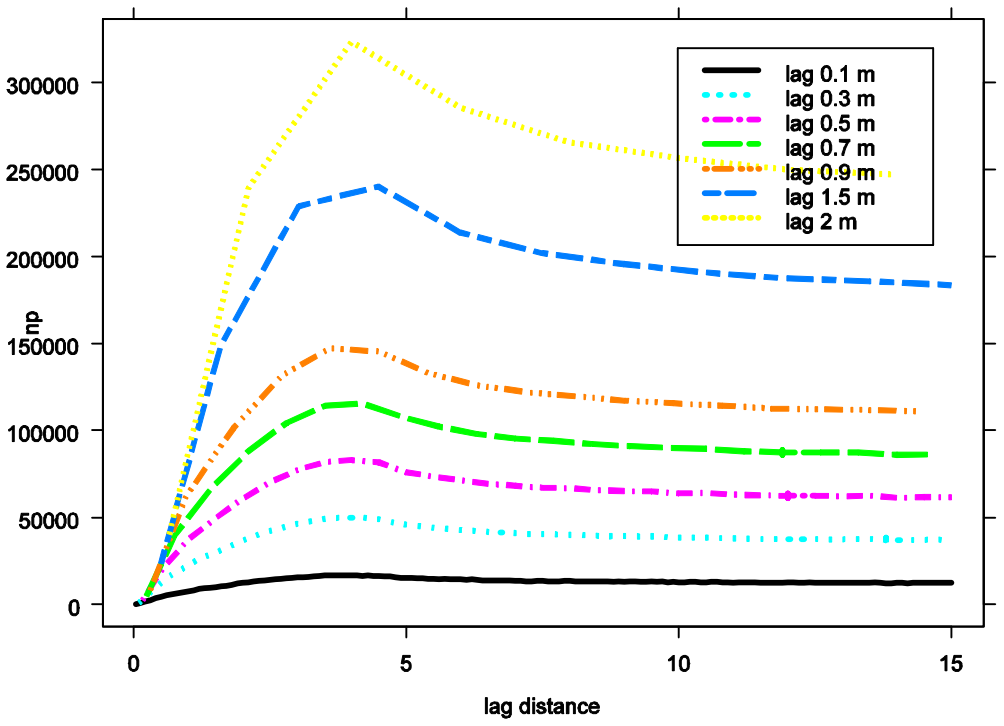
wet points Blackwater Q33 ; Sensitivity analysis for the lag distance: Number of pair of points
np
0
50000
100000
150000
200000
250000
300000
0
5
10
15
lag distance
lag 0.1 m
lag 0.3 m
lag 0.5 m
lag 0.7 m
lag 0.9 m
lag 1.5 m
lag 2 m

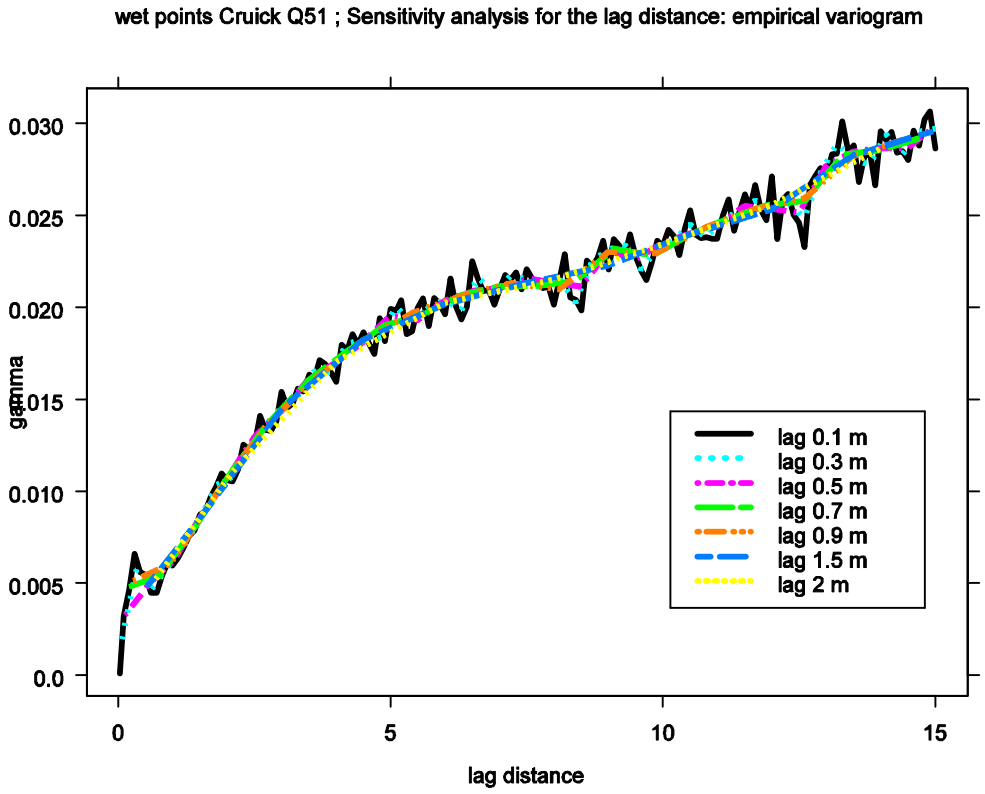
wet points Cruick Q51 ; Sensitivity analysis for the lag distance: empirical variogram
gamma
0.0
0.005
0.010
0.015
0.020
0.025
0.030
0
5
10
15
lag distance
lag 0.1 m
lag 0.3 m
lag 0.5 m
lag 0.7 m
lag 0.9 m
lag 1.5 m
lag 2 m

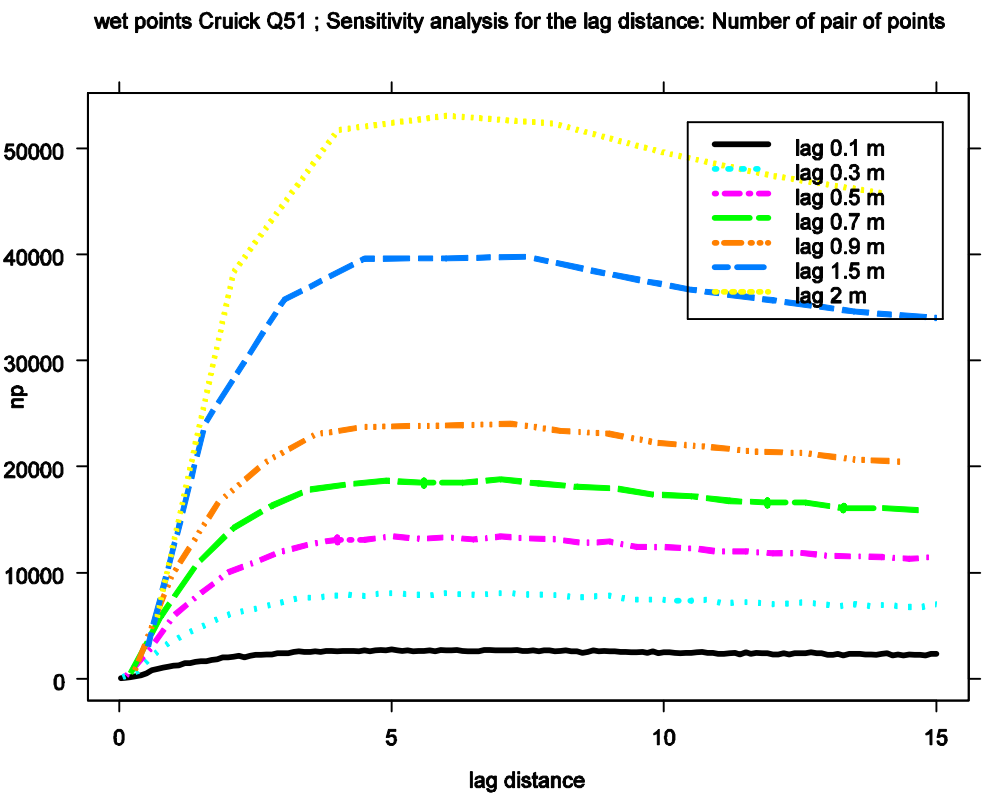
wet points Cruick Q51 ; Sensitivity analysis for the lag distance: Number of pair of points
np
0
10000
20000
30000
40000
50000
0
5
10
15
lag distance
lag 0.1 m
lag 0.3 m
lag 0.5 m
lag 0.7 m
lag 0.9 m
lag 1.5 m
lag 2 m

wet points HighlandWater Q43 ; Sensitivity analysis for the lag distance: empirical variogram

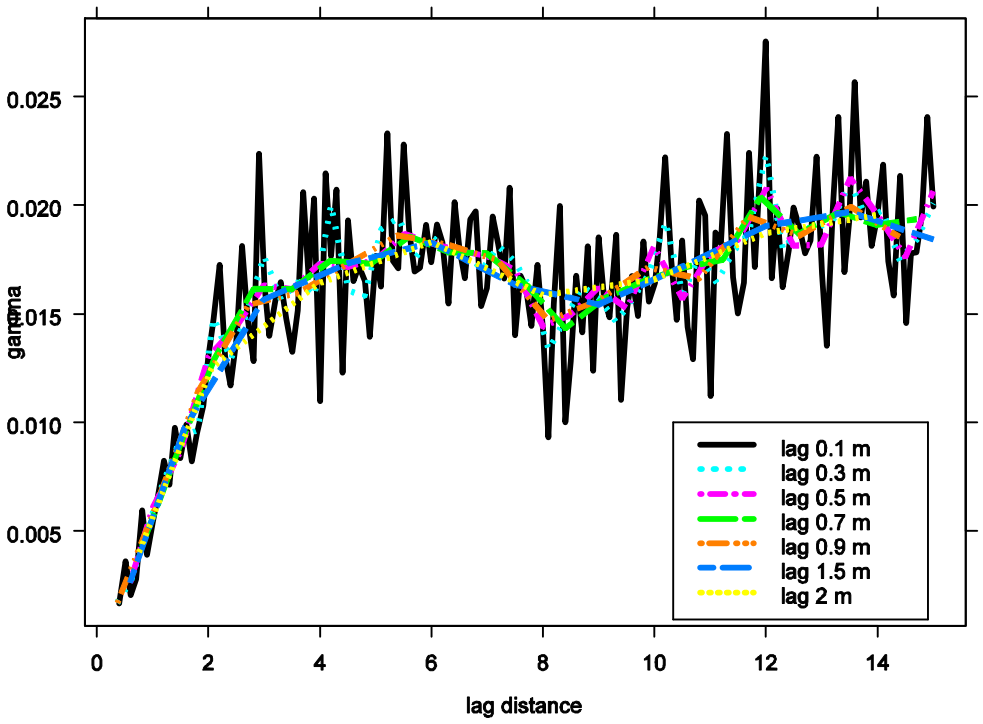

wet points HighlandWater Q43 ; Sensitivity analysis for the lag distance: Number of pair of points

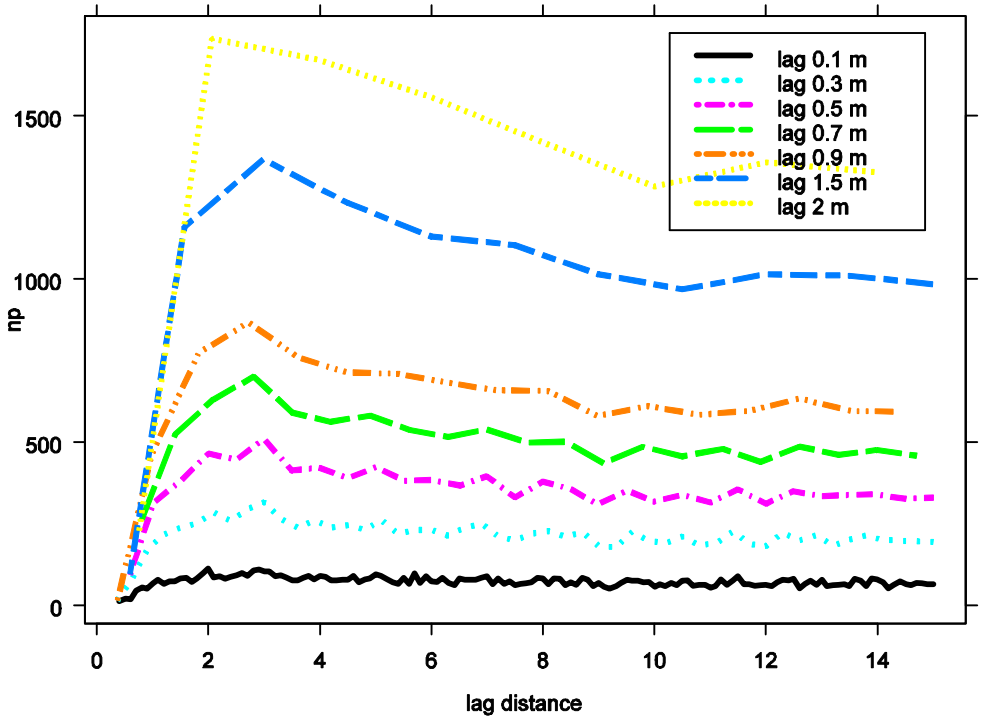

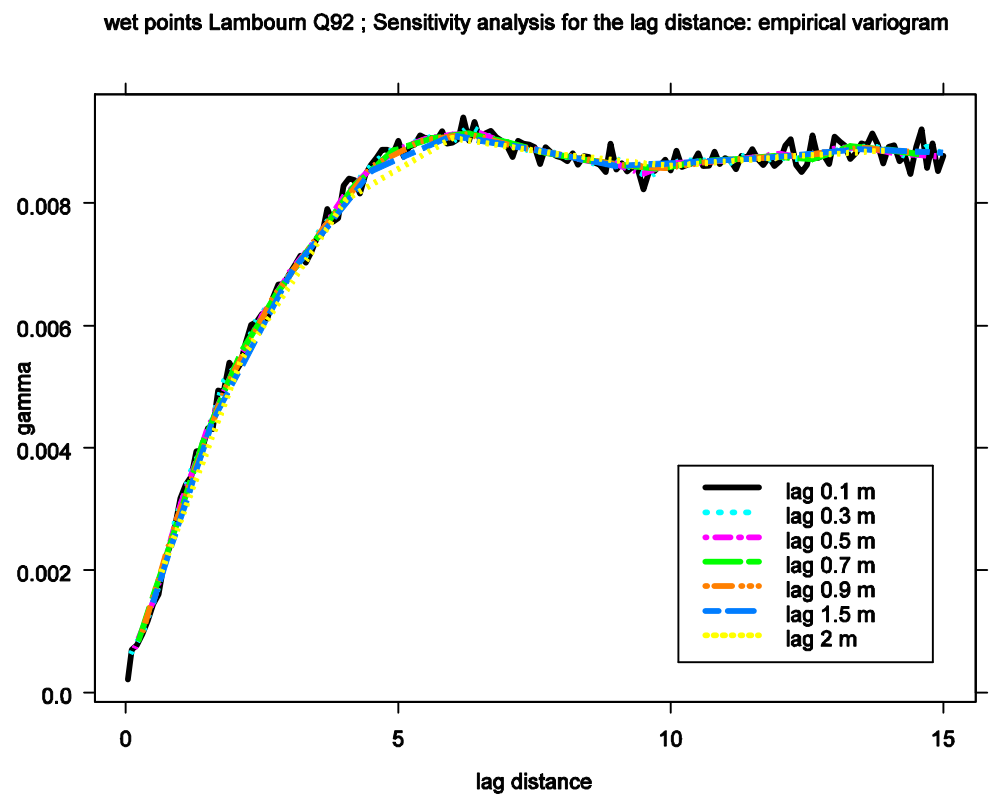
wet points Lambourn Q92 ; Sensitivity analysis for the lag distance: empirical variogram
gamma
0.0
0.002
0.004
0.006
0.008
0
5
10
15
lag distance
lag 0.1 m
lag 0.3 m
lag 0.5 m
lag 0.7 m
lag 0.9 m
lag 1.5 m
lag 2 m

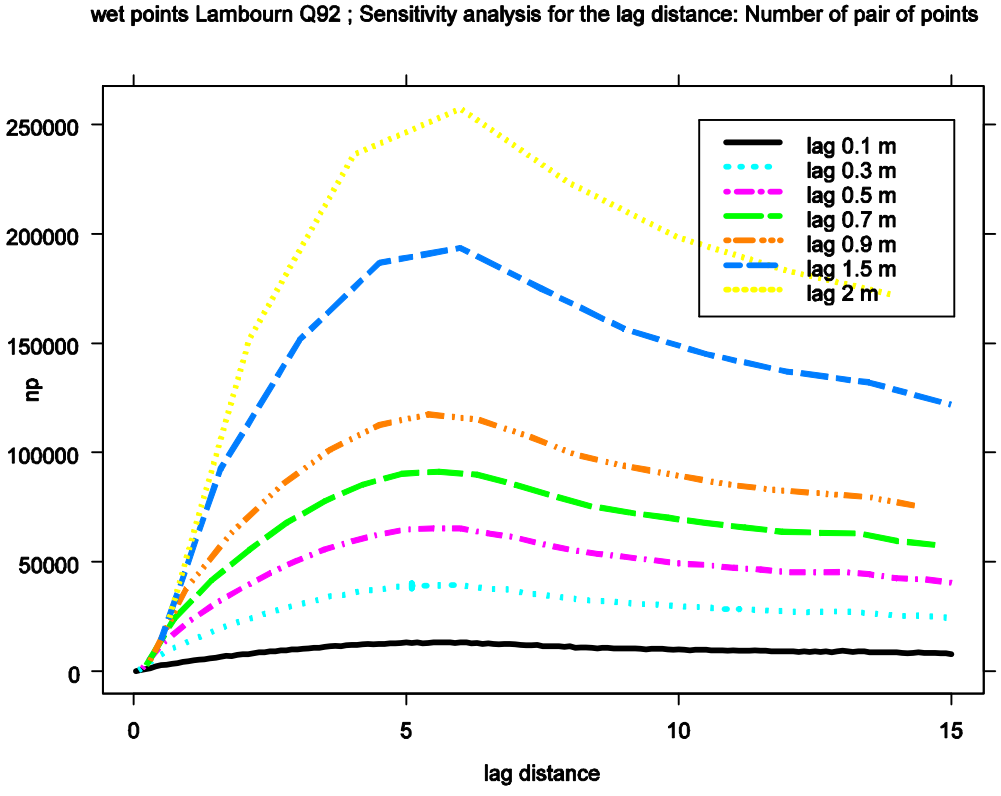
wet points Lambourn Q92 ; Sensitivity analysis for the lag distance: Number of pair of points
np
0
50000
100000
150000
200000
250000
0
5
10
15
lag distance
lag 0.1 m
lag 0.3 m
lag 0.5 m
lag 0.7 m
lag 0.9 m
lag 1.5 m
lag 2 m

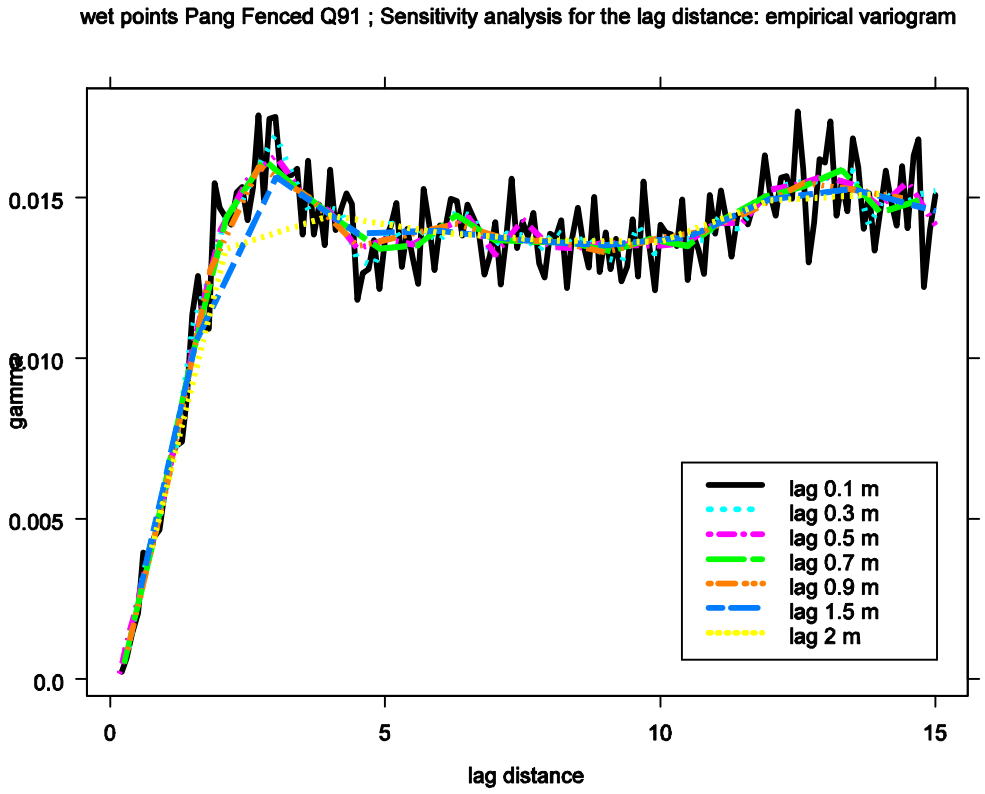
wet points Pang Fenced Q91 ; Sensitivity analysis for the lag distance: empirical variogram
gamma
0.0
0.005
0.010
0.015
0
5
10
15
lag distance
lag 0.1 m
lag 0.3 m
lag 0.5 m
lag 0.7 m
lag 0.9 m
lag 1.5 m
lag 2 m

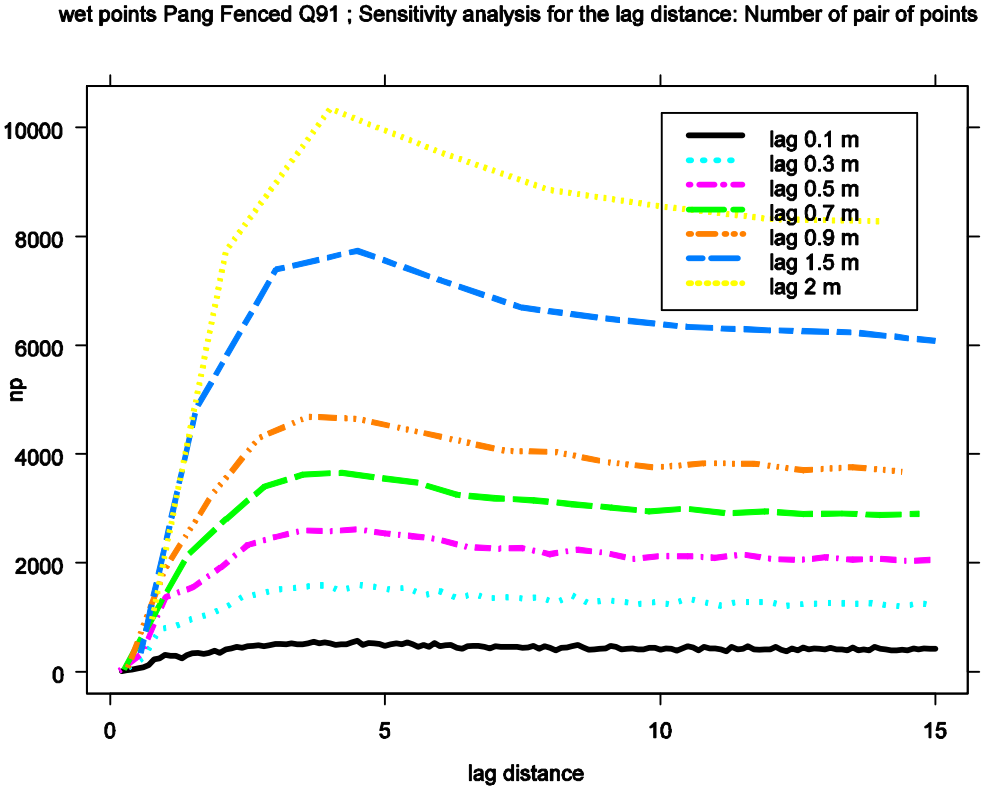
wet points Pang Fenced Q91 ; Sensitivity analysis for the lag distance: Number of pair of points
np
0
2000
4000
6000
8000
10000
0
5
10
15
lag distance
lag 0.1 m
lag 0.3 m
lag 0.5 m
lag 0.7 m
lag 0.9 m
lag 1.5 m
lag 2 m

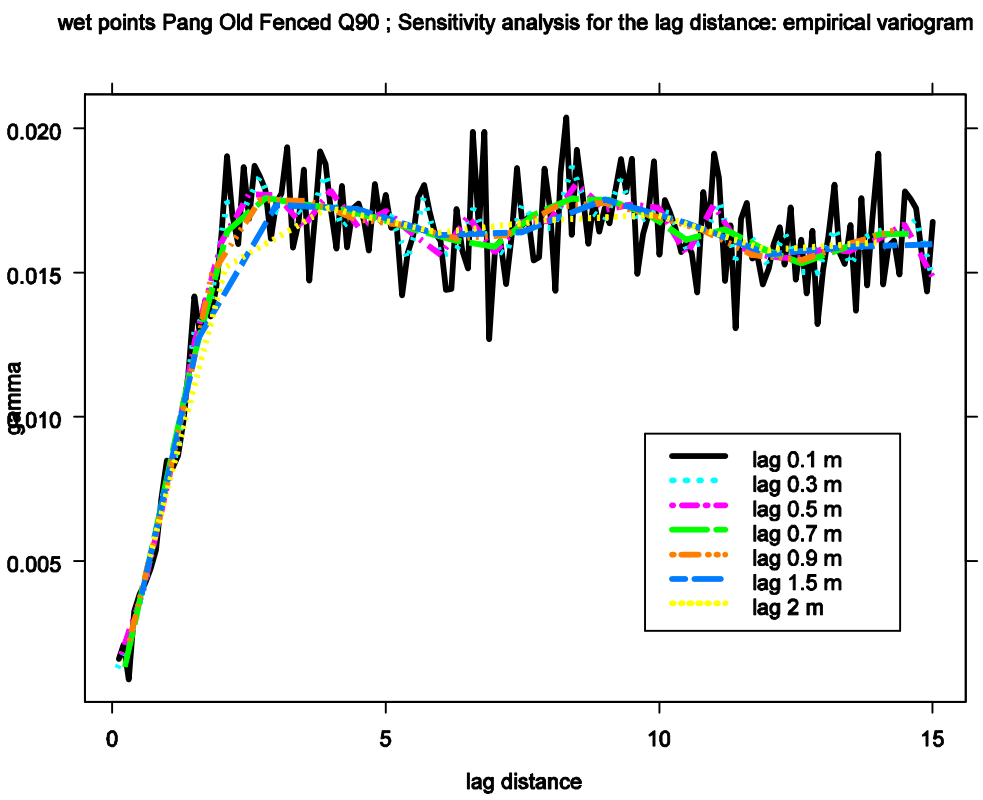
wet points Pang Old Fenced Q90 ; Sensitivity analysis for the lag distance: empirical variogram
gamma
0.020
0.015
0.010
0.005
0
5
10
15
lag distance
lag 0.1 m
lag 0.3 m
lag 0.5 m
lag 0.7 m
lag 0.9 m
lag 1.5 m
lag 2 m

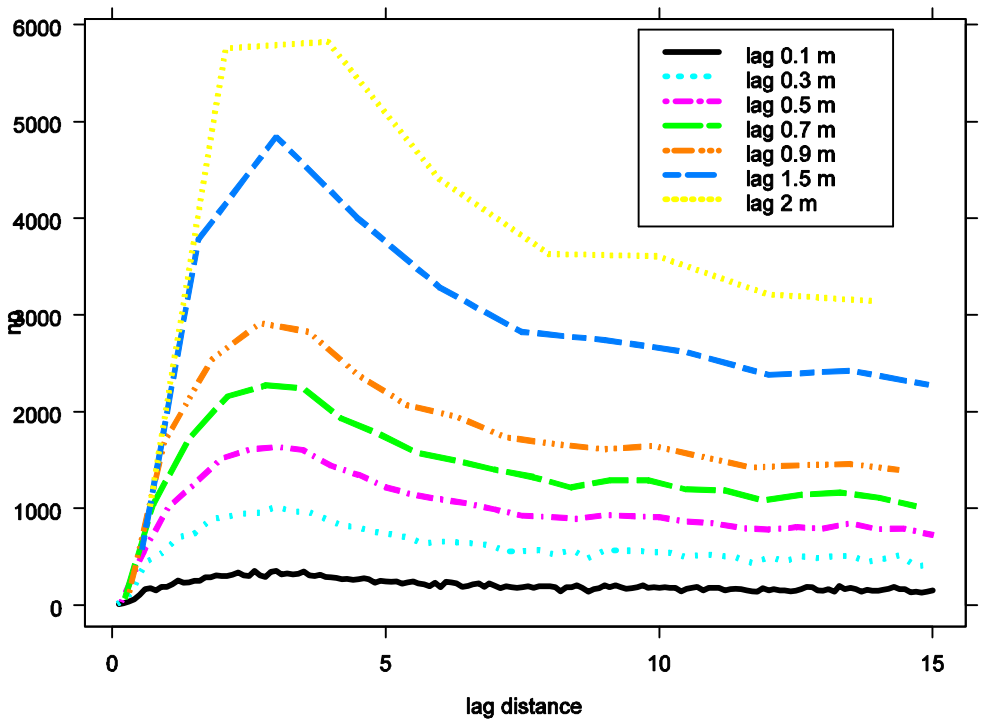
wet points Pang Old Fenced Q90 ; Sensitivity analysis for the lag distance: Number of pair of points
np
6000
5000
4000
3000
2000
1000
0
0
5
10
15
lag distance
lag 0.1 m
lag 0.3 m
lag 0.5 m
lag 0.7 m
lag 0.9 m
lag 1.5 m
lag 2 m

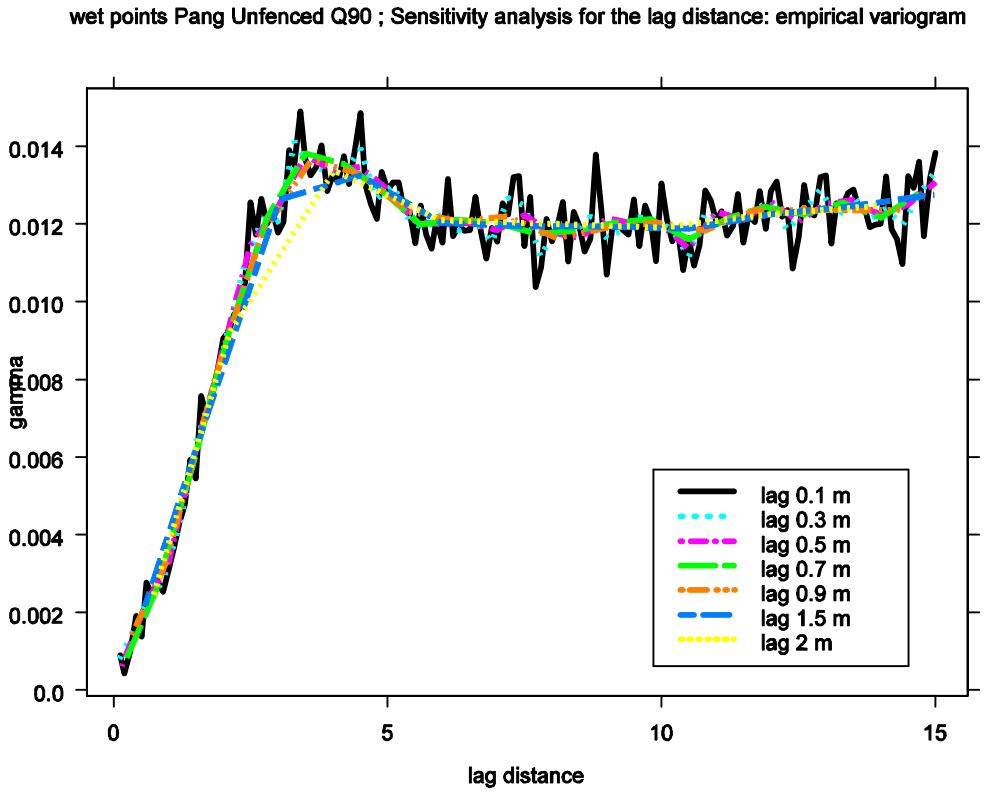
wet points Pang Unfenced Q90 ; Sensitivity analysis for the lag distance: empirical variogram
gamma
0.0
0.002
0.004
0.006
0.008
0.010
0.012
0.014
0
5
10
15
lag distance
lag 0.1 m
lag 0.3 m
lag 0.5 m
lag 0.7 m
lag 0.9 m
lag 1.5 m
lag 2 m

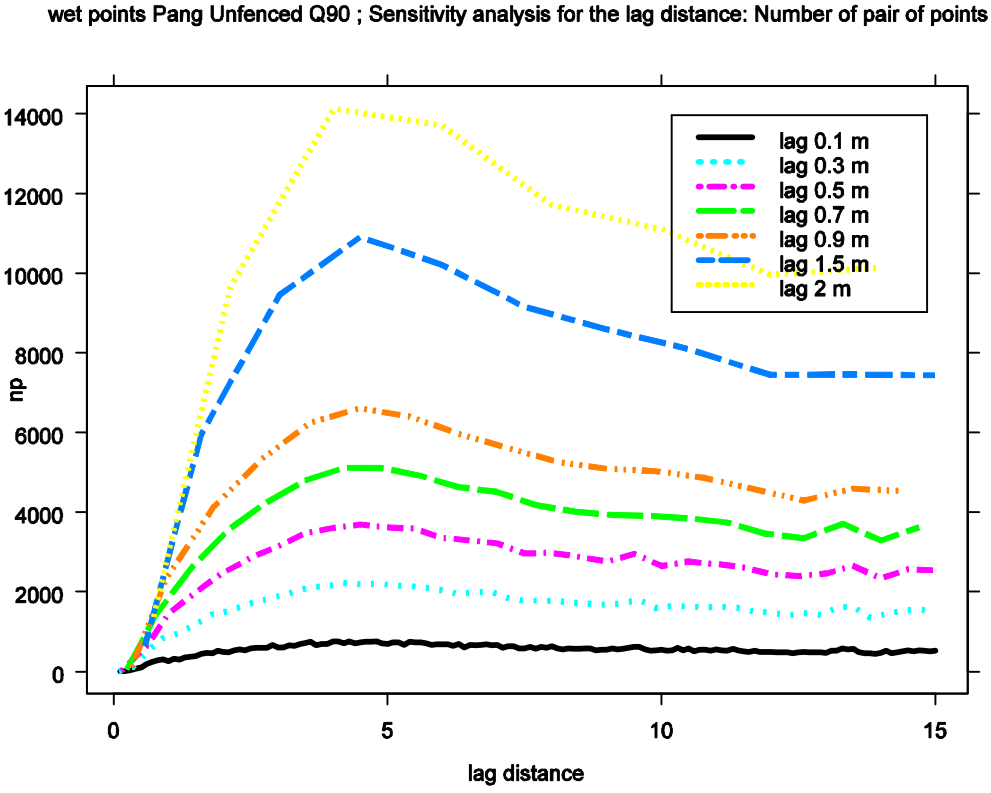
wet points Pang Unfenced Q90 ; Sensitivity analysis for the lag distance: Number of pair of points
np
0
2000
4000
6000
8000
10000
12000
14000
0
5
10
15
lag distance
lag 0.1 m
lag 0.3 m
lag 0.5 m
lag 0.7 m
lag 0.9 m
lag 1.5 m
lag 2 m

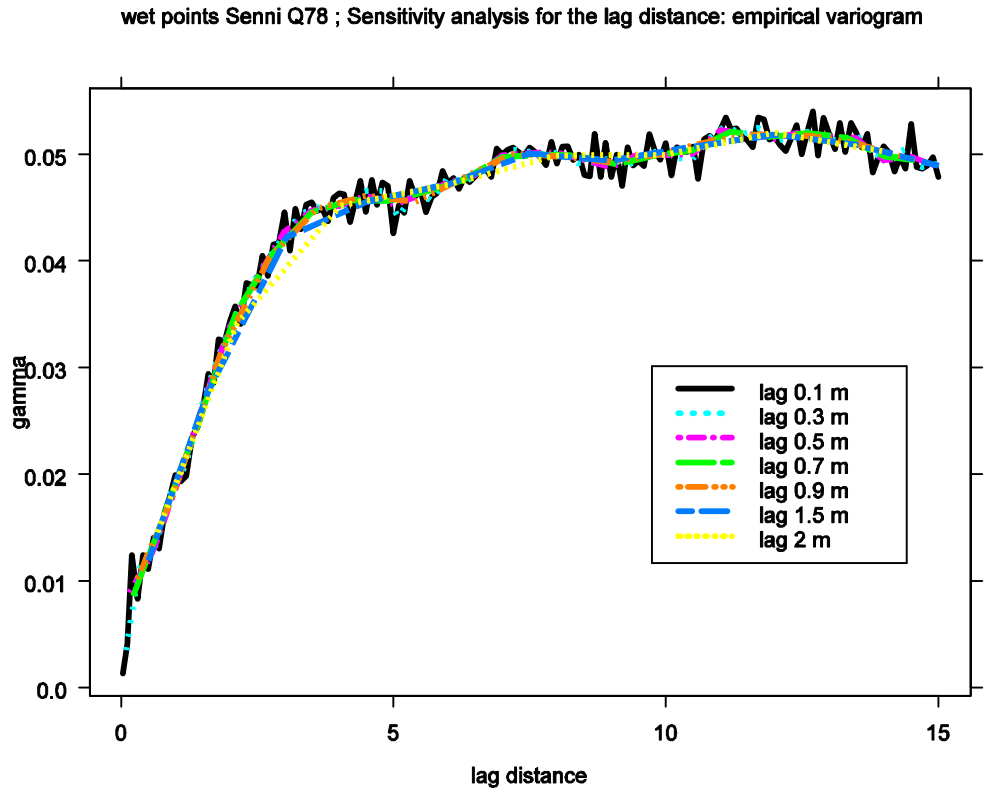
wet points Senni Q78 ; Sensitivity analysis for the lag distance: empirical variogram
gamma
0.0
0.01
0.02
0.03
0.04
0.05
0
5
10
15
lag distance
lag 0.1 m
lag 0.3 m
lag 0.5 m
lag 0.7 m
lag 0.9 m
lag 1.5 m
lag 2 m

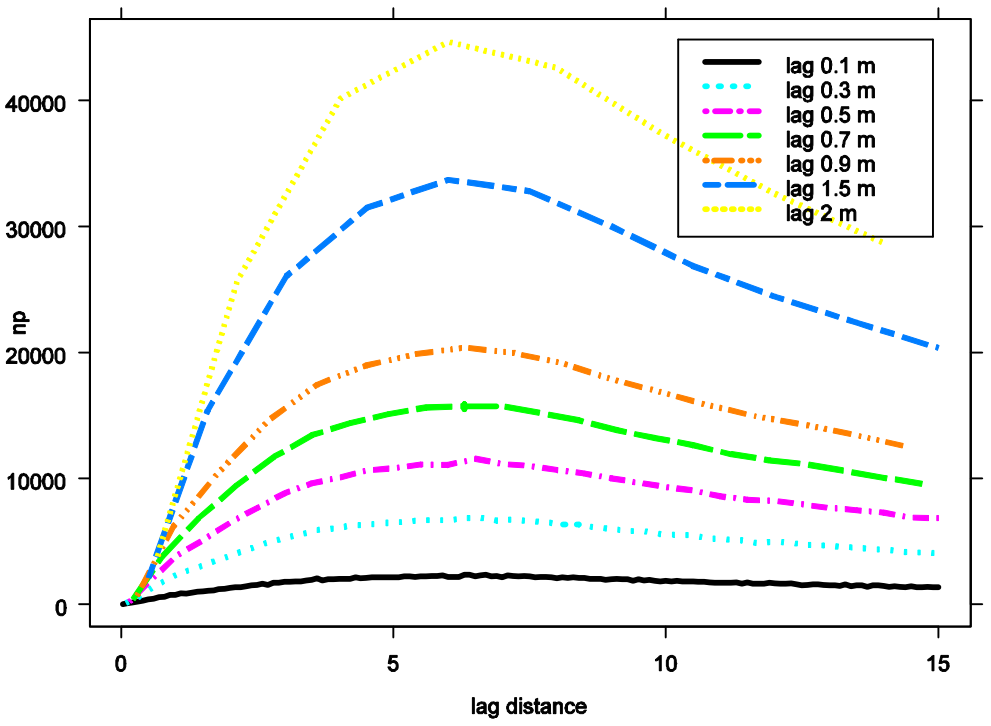
wet points Senni Q78 ; Sensitivity analysis for the lag distance: Number of pair of points
np
0
10000
20000
30000
40000
0
5
10
15
lag distance
lag 0.1 m
lag 0.3 m
lag 0.5 m
lag 0.7 m
lag 0.9 m
lag 1.5 m
lag 2 m

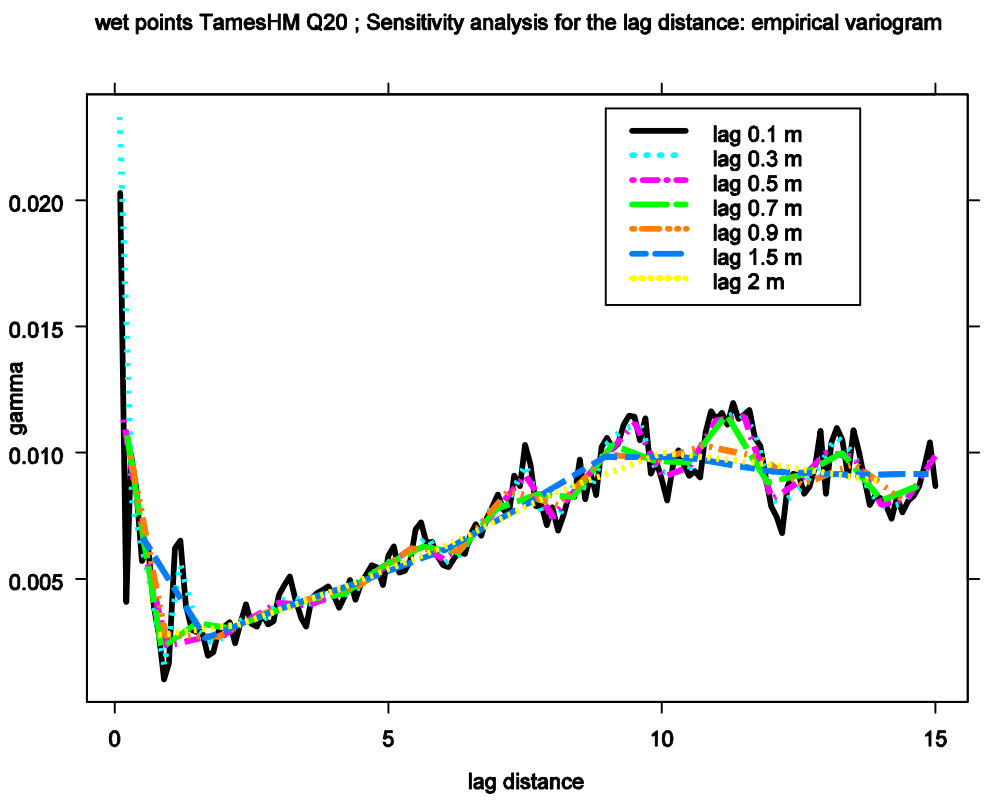
wet points TamesHM Q20 ; Sensitivity analysis for the lag distance: empirical variogram
lag 0.1 m
lag 0.3 m
lag 0.5 m
lag 0.7 m
lag 0.9 m
lag 1.5 m
lag 2 m
gamma
0.020
0.015
0.010
0.005
0
5
10
15
lag distance

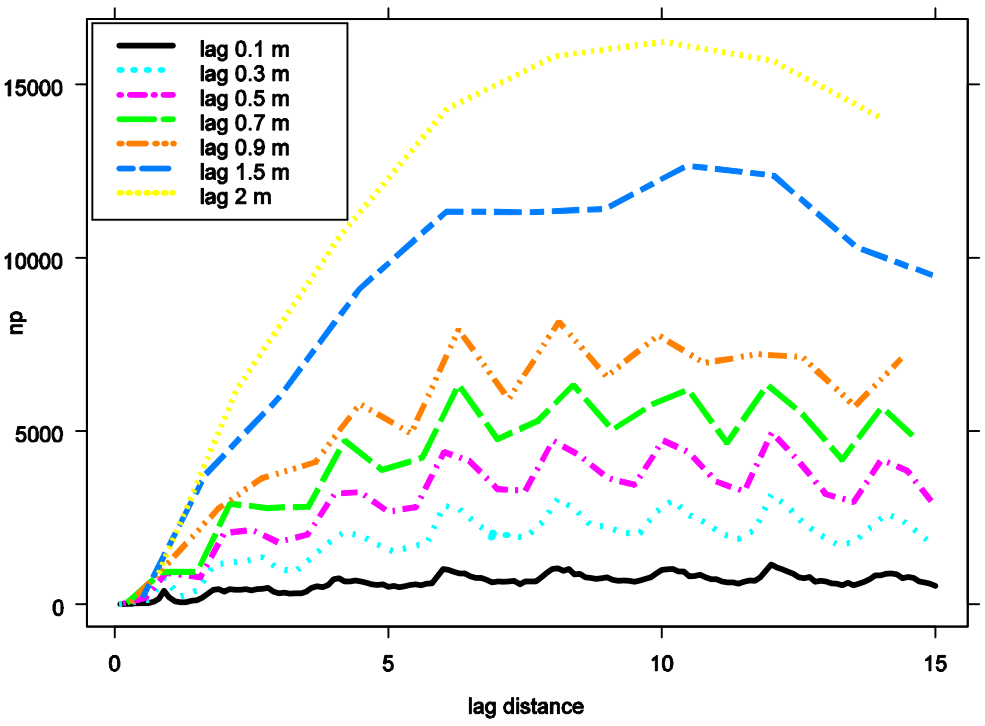
wet points TamesHM Q20 ; Sensitivity analysis for the lag distance: Number of pair of points
lag 0.1 m
lag 0.3 m
lag 0.5 m
lag 0.7 m
lag 0.9 m
lag 1.5 m
lag 2 m
np
15000
10000
5000
0
0
5
10
15
lag distance

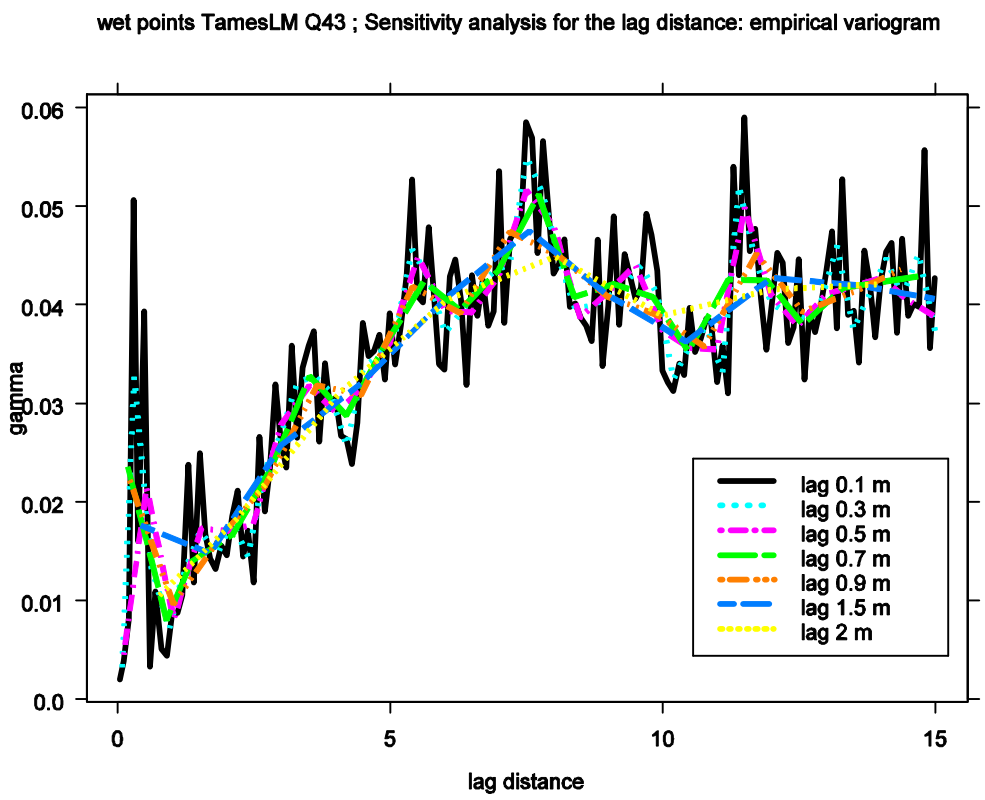
wet points TamesLM Q43 ; Sensitivity analysis for the lag distance: empirical variogram
gamma
0.0
0.01
0.02
0.03
0.04
0.05
0.06
0
5
10
15
lag distance
lag 0.1 m
lag 0.3 m
lag 0.5 m
lag 0.7 m
lag 0.9 m
lag 1.5 m
lag 2 m

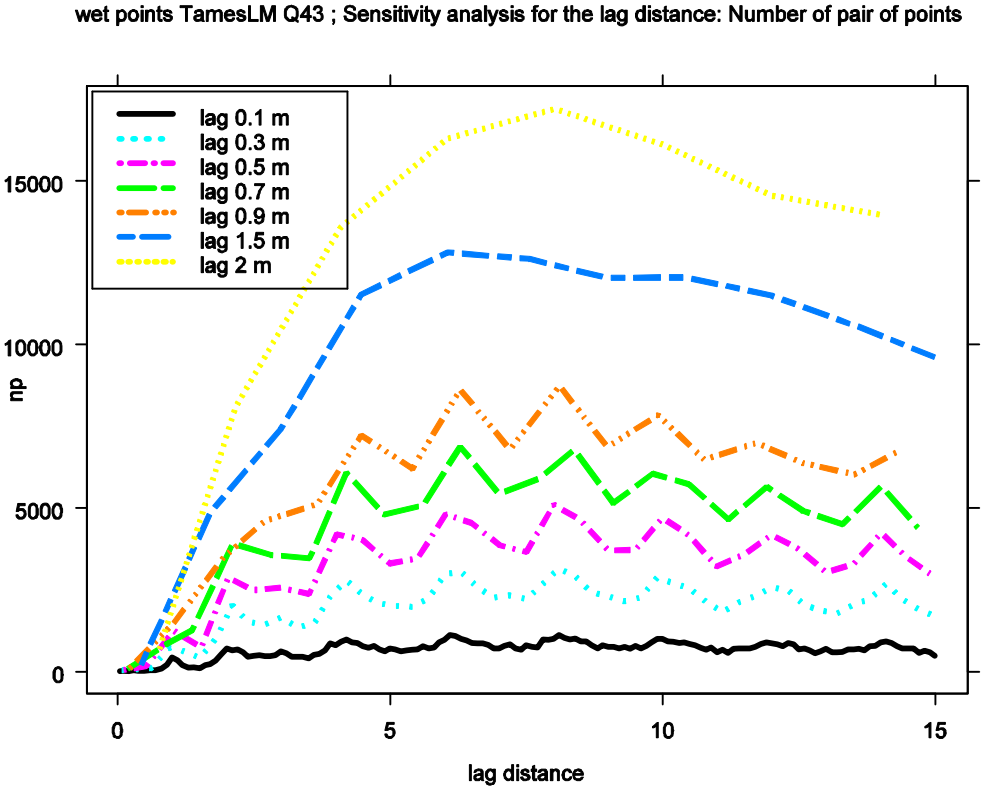
wet points TamesLM Q43 ; Sensitivity analysis for the lag distance: Number of pair of points
np
0
5000
10000
15000
0
5
10
15
lag distance
lag 0.1 m
lag 0.3 m
lag 0.5 m
lag 0.7 m
lag 0.9 m
lag 1.5 m
lag 2 m

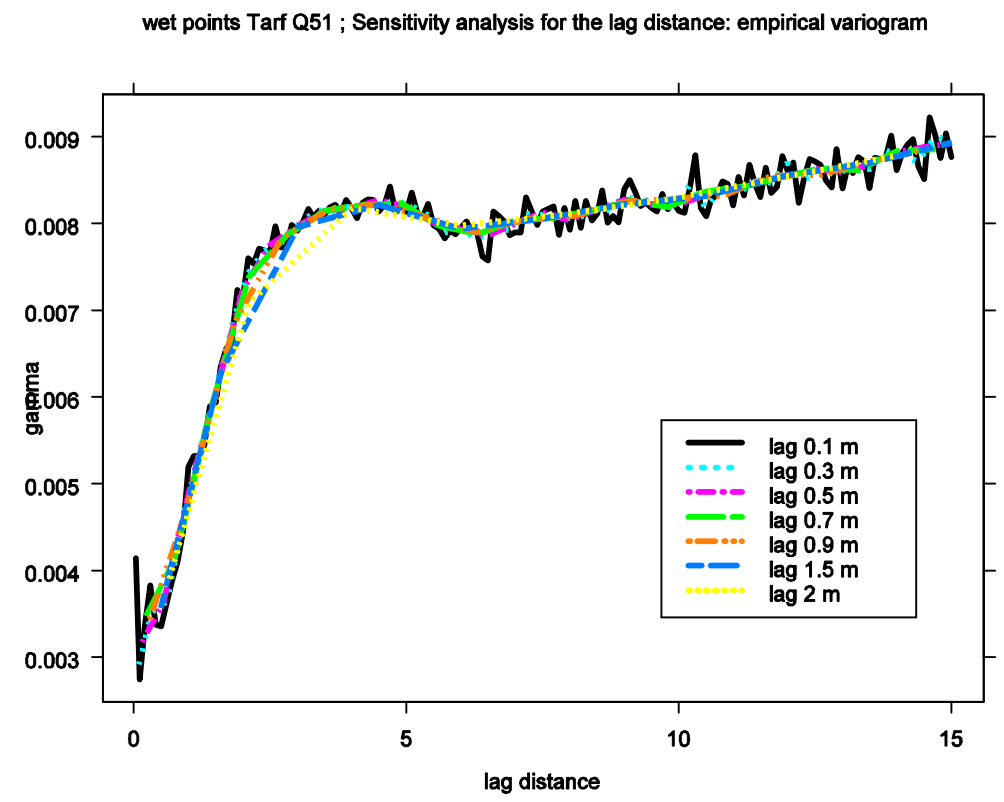
wet points Tarf Q51 ; Sensitivity analysis for the lag distance: empirical variogram
gamma
0.003
0.004
0.005
0.006
0.007
0.008
0.009
0
5
10
15
lag distance
lag 0.1 m
lag 0.3 m
lag 0.5 m
lag 0.7 m
lag 0.9 m
lag 1.5 m
lag 2 m

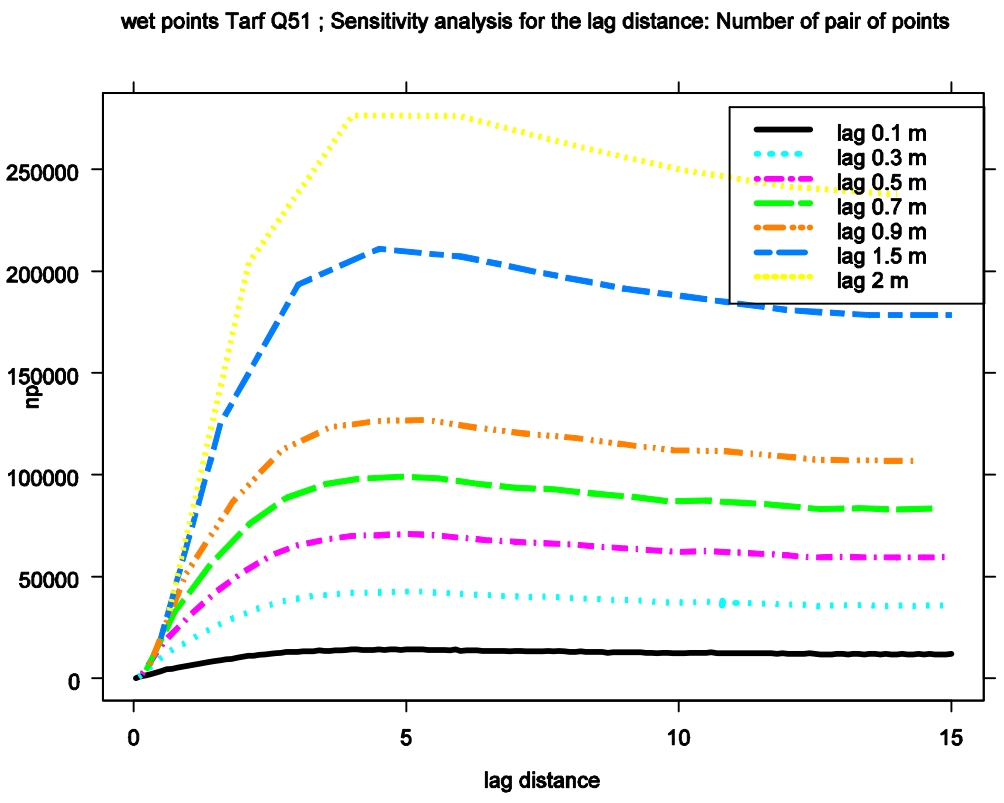
wet points Tarf Q51 ; Sensitivity analysis for the lag distance: Number of pair of points
npp
0
50000
100000
150000
200000
250000
0
5
10
15
lag distance
lag 0.1 m
lag 0.3 m
lag 0.5 m
lag 0.7 m
lag 0.9 m
lag 1.5 m
lag 2 m

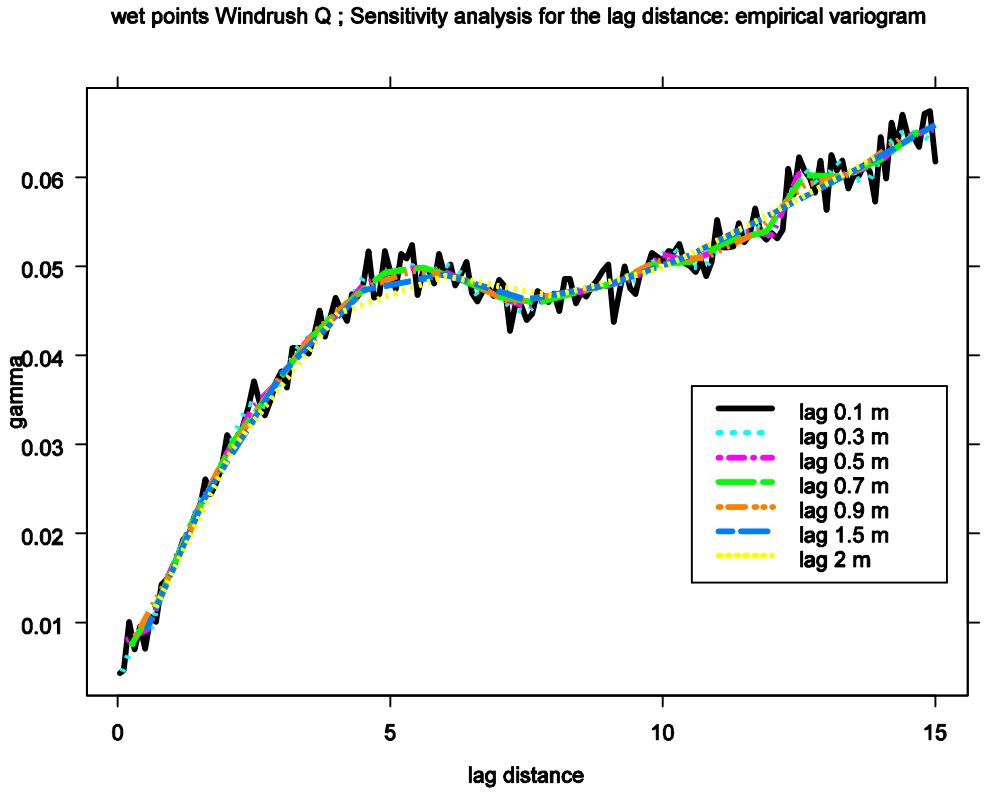
wet points Windrush Q ; Sensitivity analysis for the lag distance: empirical variogram
gamma
0.01
0.02
0.03
0.04
0.05
0.06
0
5
10
15
lag distance
lag 0.1 m
lag 0.3 m
lag 0.5 m
lag 0.7 m
lag 0.9 m
lag 1.5 m
lag 2 m

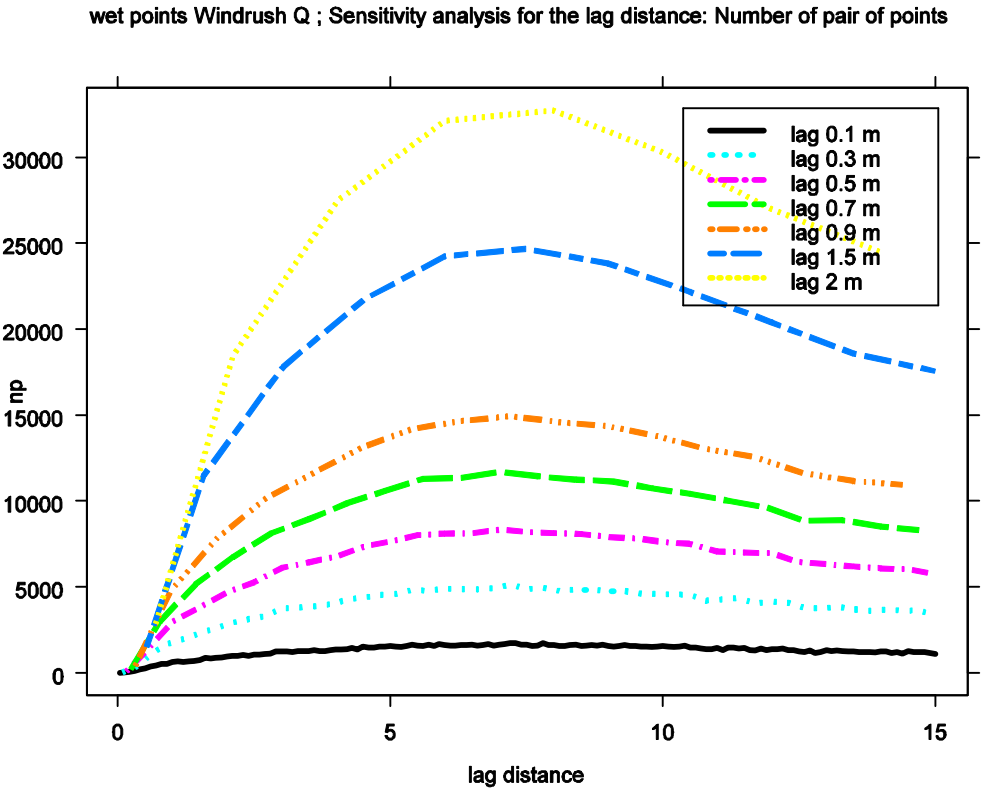
wet points Windrush Q ; Sensitivity analysis for the lag distance: Number of pair of points
np
0
5000
10000
15000
20000
25000
30000
0
5
10
15
lag distance
lag 0.1 m
lag 0.3 m
lag 0.5 m
lag 0.7 m
lag 0.9 m
lag 1.5 m
lag 2 m

Appendix 3.3

Results obtained for the analysis in Chapter 5 –sensitivity analysis for the azimuth tolerance

This Appendix includes all the graphical outputs obtained for the sensitivity analysis of the azimuth tolerance (section 5.4.3). Two main graphical outputs are shown in this appendix: (i) the first one identifying the relation between the number of points vs. lag distance and the variance between points and the lag distance (for two different azimuth directions; 0 and 90) for several azimuth tolerances and (ii) the second one plotting the differences between directional variogram 0 and directional variogram 90 for different azimuth tolerances. Each of these sections is divided in turn in two sub-sections; the first one including the results for the data sets with wet and dry points and the second one including results for the data sets with only wet points.

Azimuth tolerance Wet and dry points

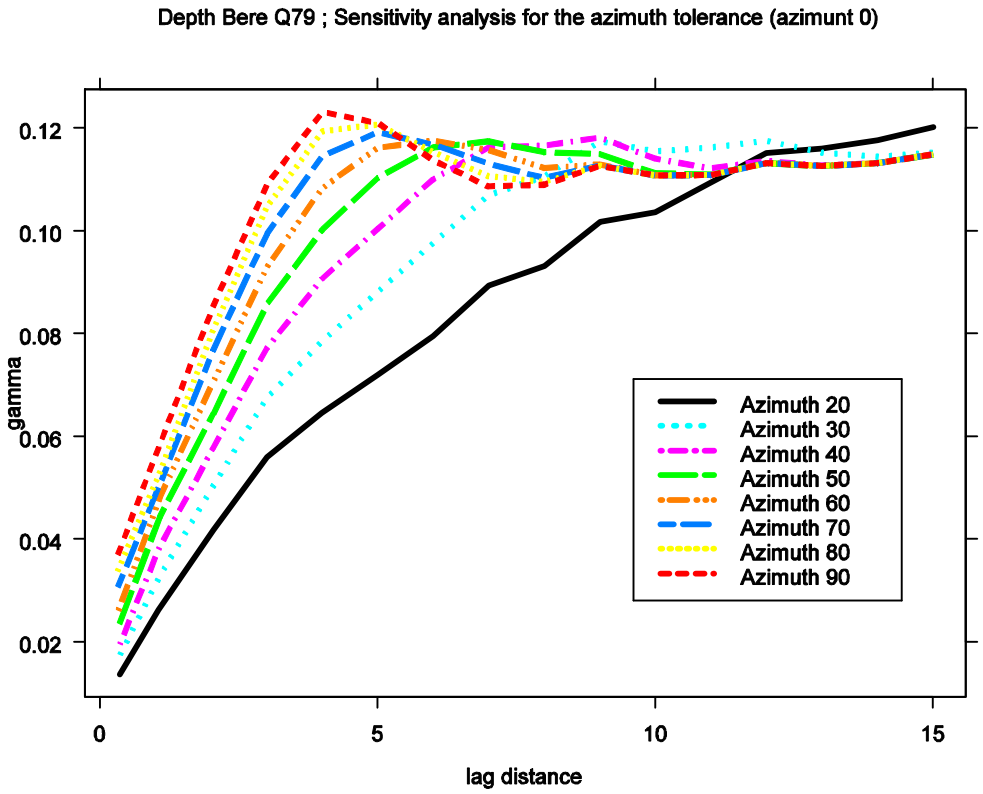

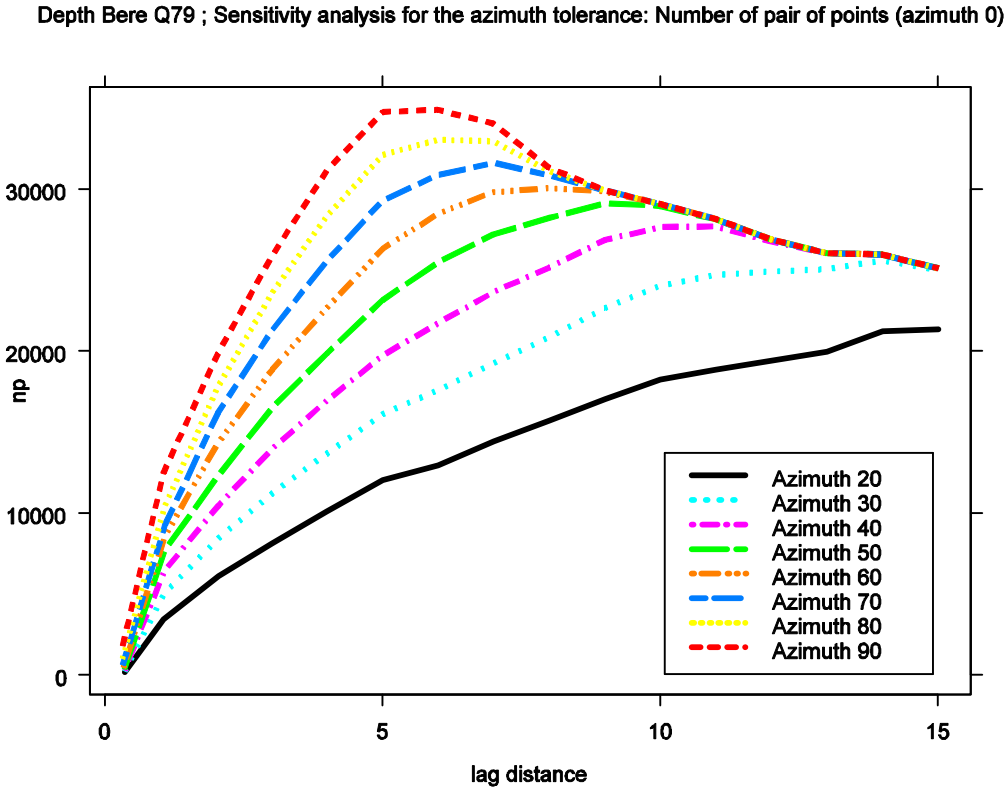

Depth Bere Q79 ; Sensitivity analysis for the azimuth tolerance (azimuth 90)

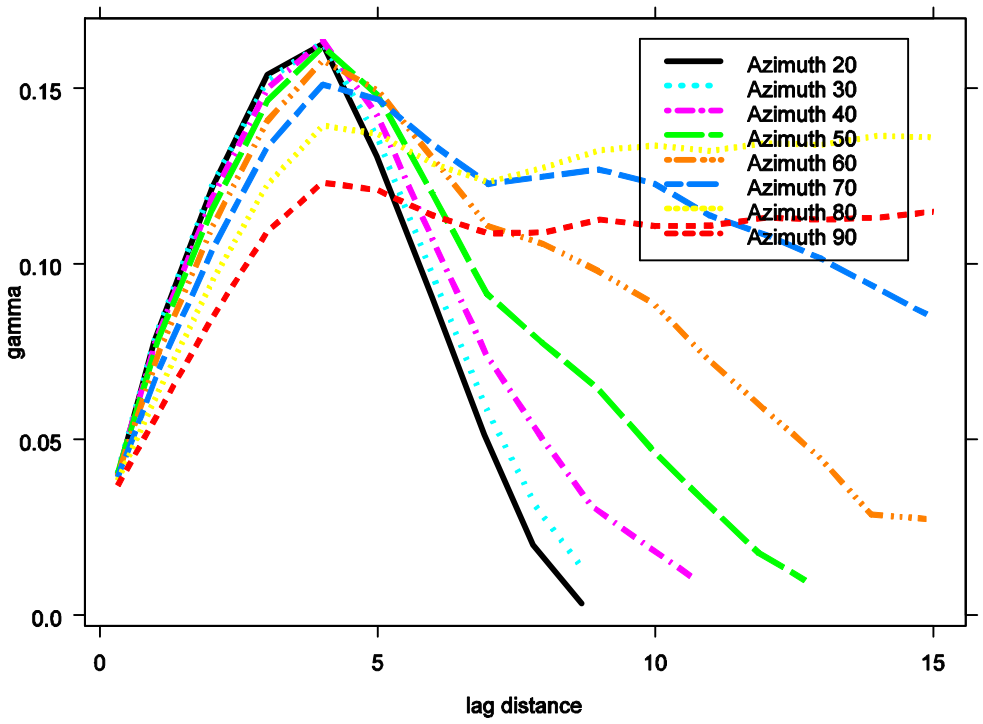

Depth Bere Q79 ; Sensitivity analysis for the azimuth tolerance: Number of pair of points (azimuth 90)

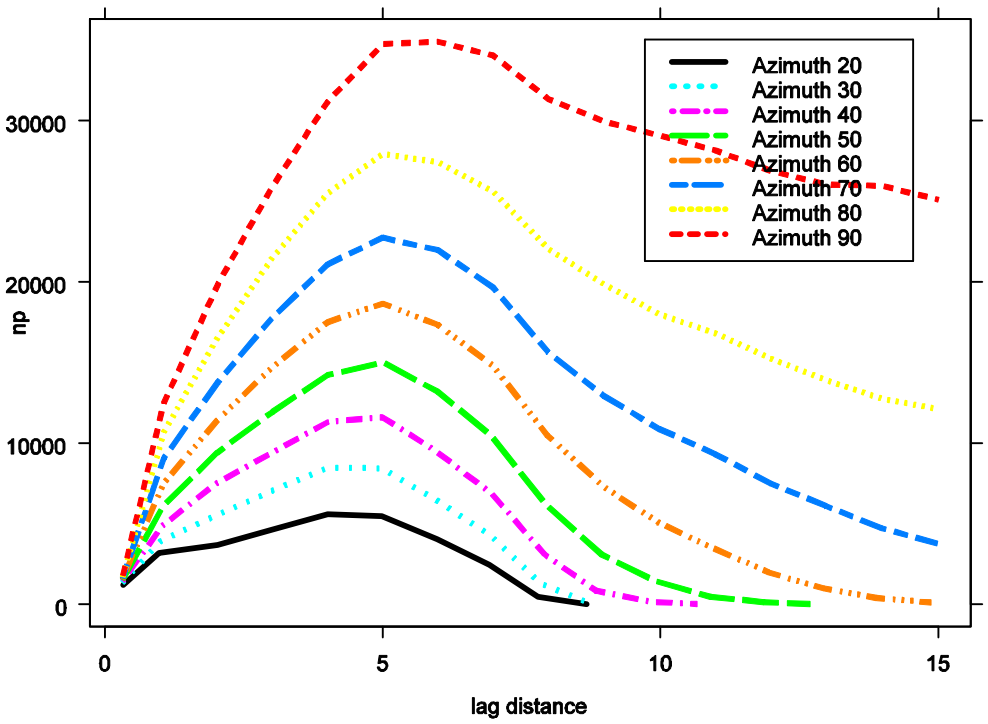

Depth Blackwater Q33 ; Sensitivity analysis for the azimuth tolerance (azimunt 0)

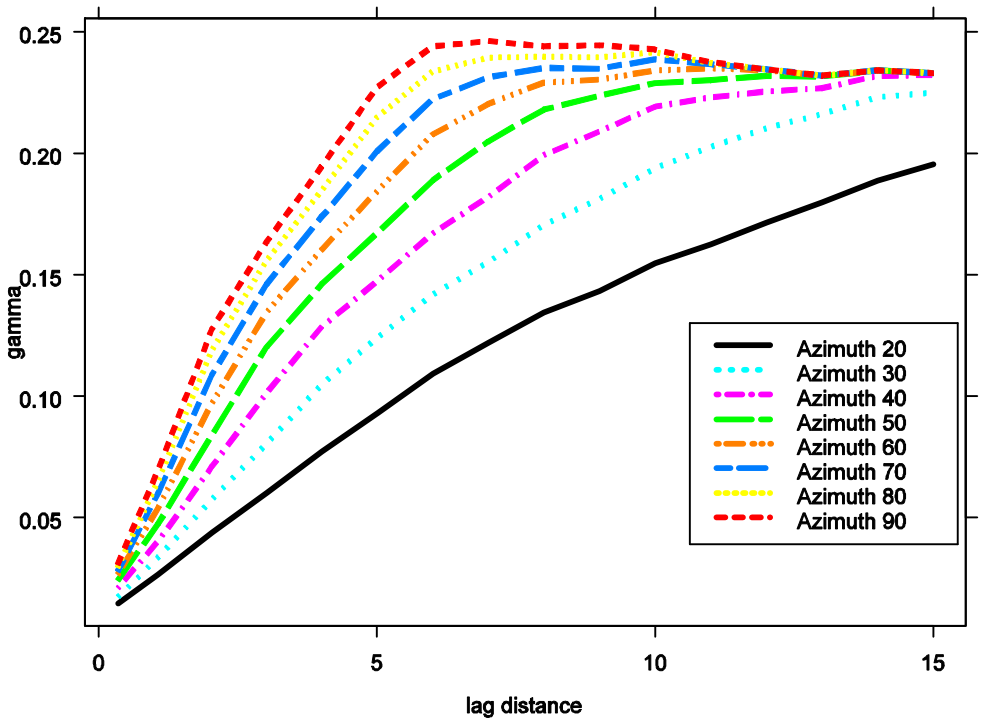

Depth Blackwater Q33 ; Sensitivity analysis for the azimuth tolerance: Number of pair of points (azimuth 0)

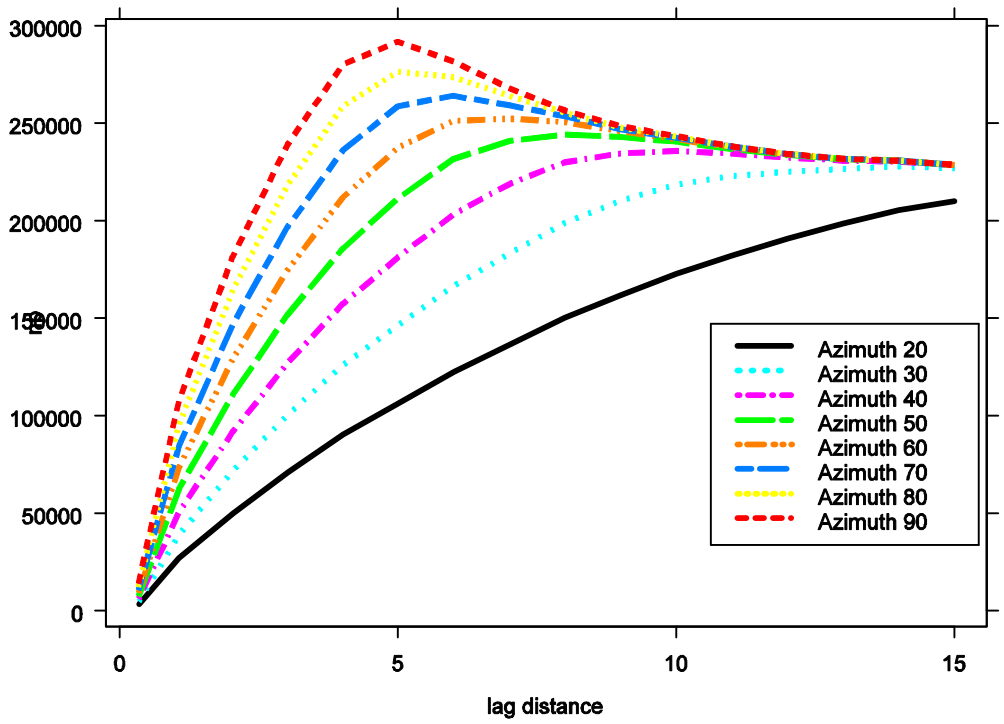

Depth Blackwater Q33 ; Sensitivity analysis for the azimuth tolerance (azimuth 90)

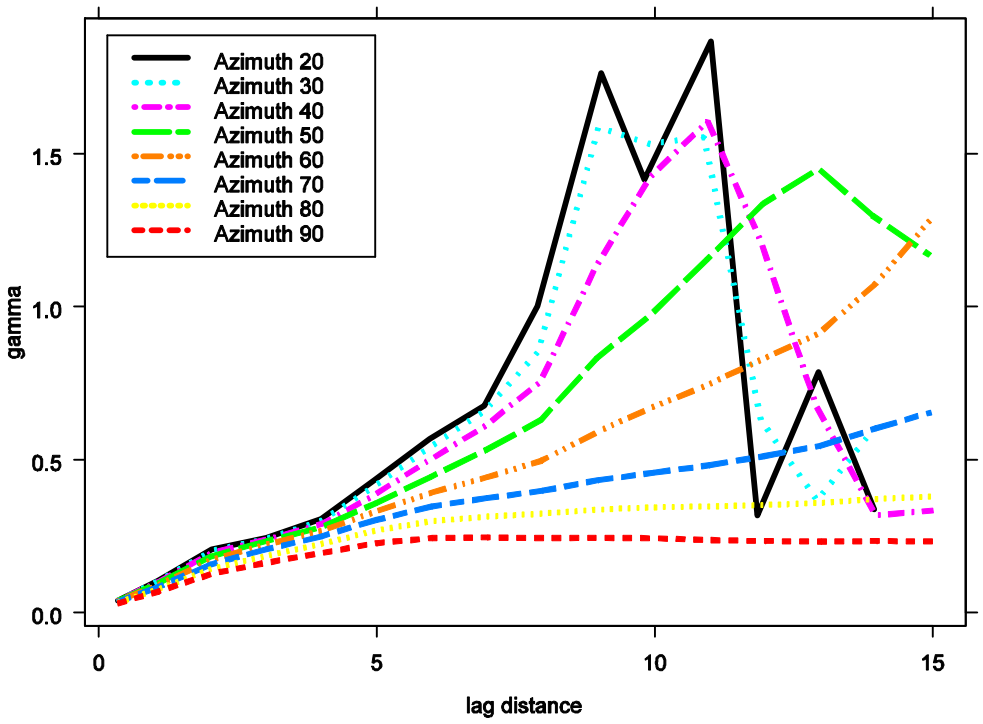

Depth Blackwater Q33 ; Sensitivity analysis for the azimuth tolerance: Number of pair of points (azimuth 90)

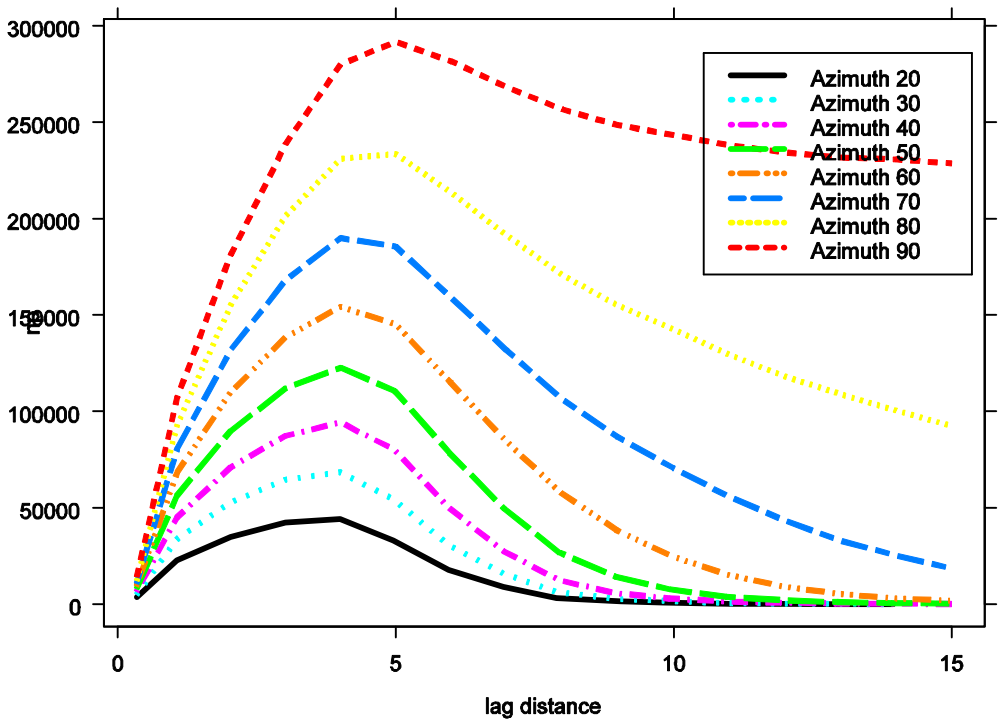

Depth Cruick Q51 ; Sensitivity analysis for the azimuth tolerance (azimunt 0)

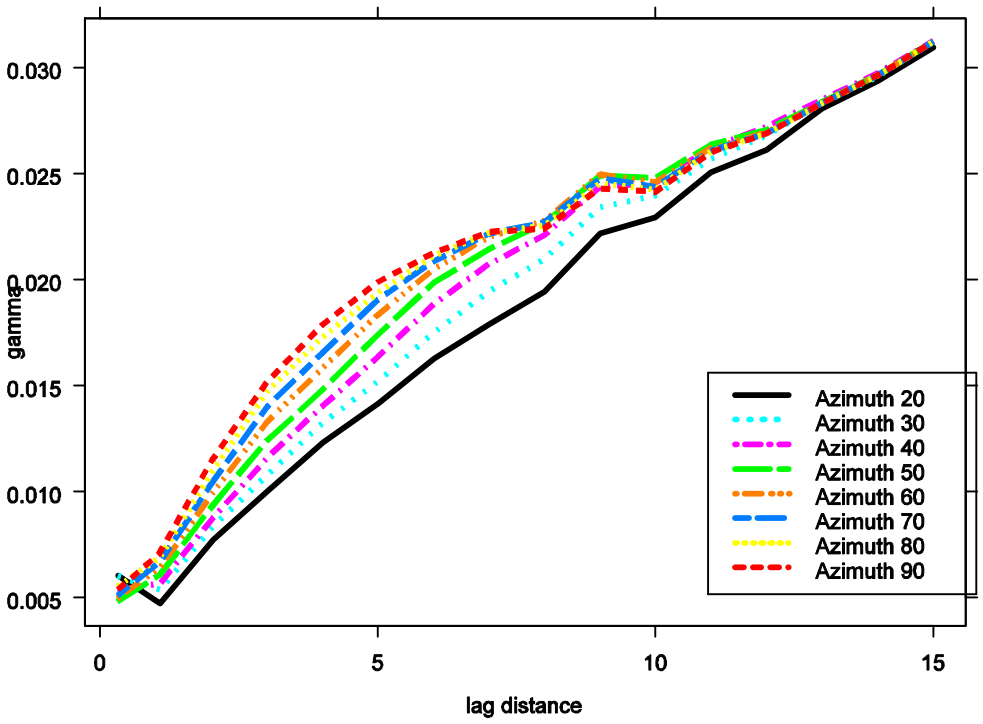

Depth Cruick Q51 ; Sensitivity analysis for the azimuth tolerance: Number of pair of points (azimuth 0)

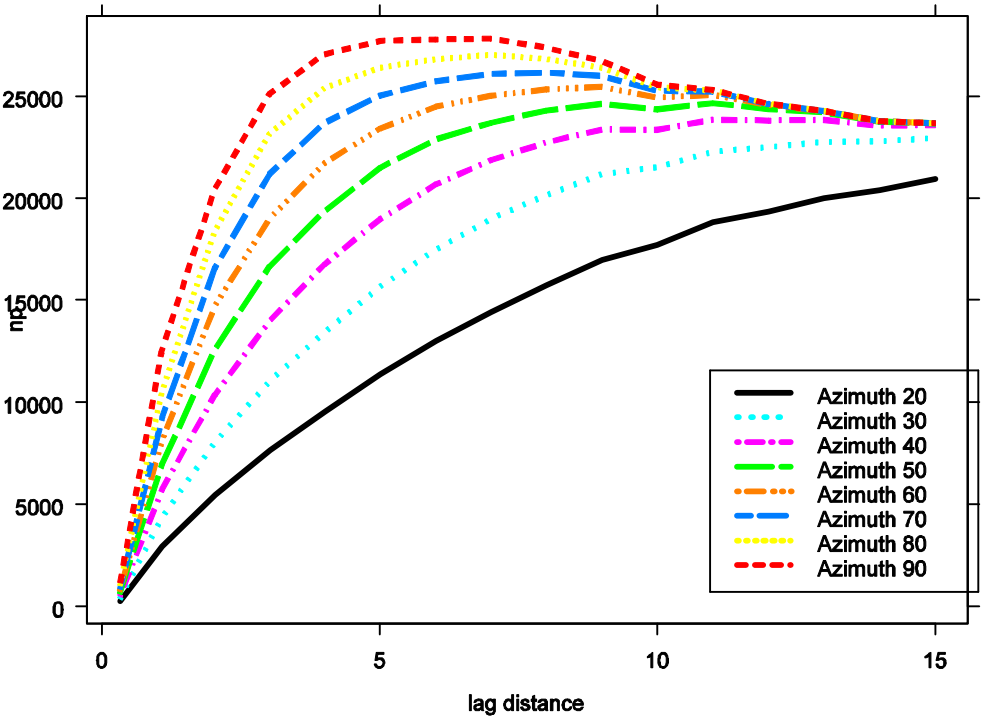

Depth Cruick Q51 ; Sensitivity analysis for the azimuth tolerance (azimuth 90)

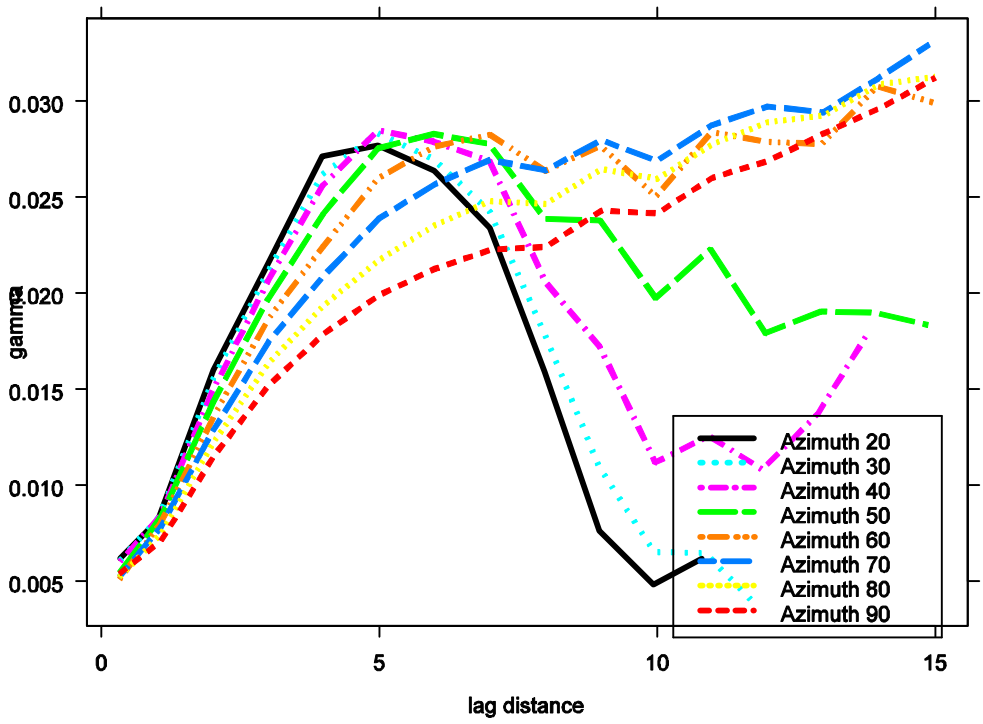

Depth Cruick Q51 ; Sensitivity analysis for the azimuth tolerance: Number of pair of points (azimuth 90)

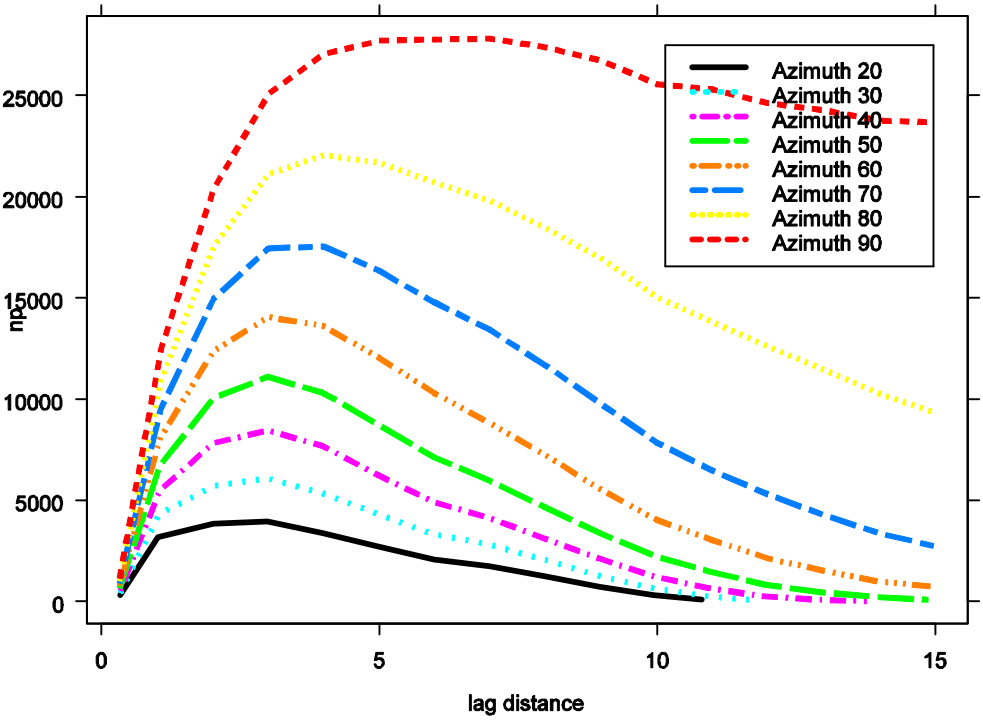

Depth HighlandWater Q43 ; Sensitivity analysis for the azimuth tolerance (azimunt 0)

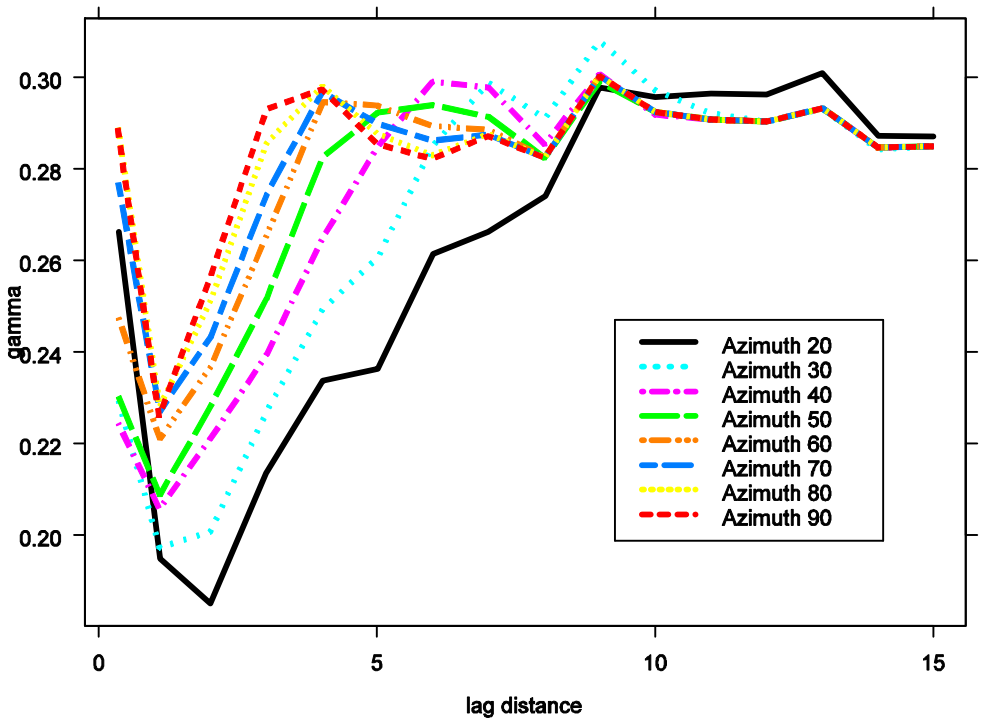

Depth HighlandWater Q43 ; Sensitivity analysis for the azimuth tolerance: Number of pair of points (azimuth 0)

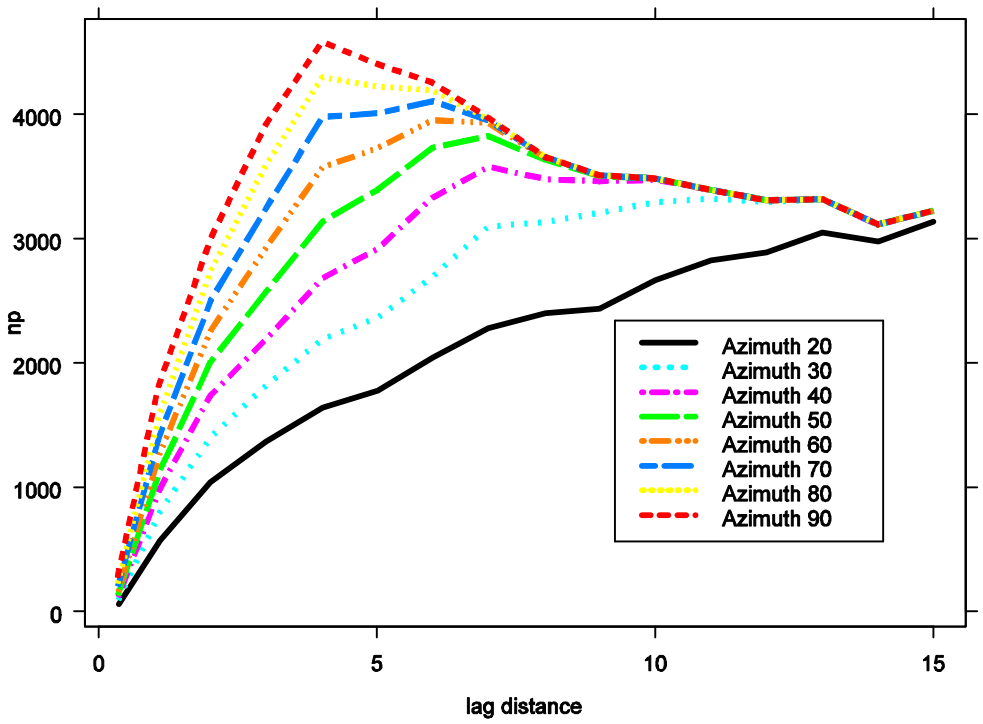

Depth HighlandWater Q43 ; Sensitivity analysis for the azimuth tolerance (azimuth 90)

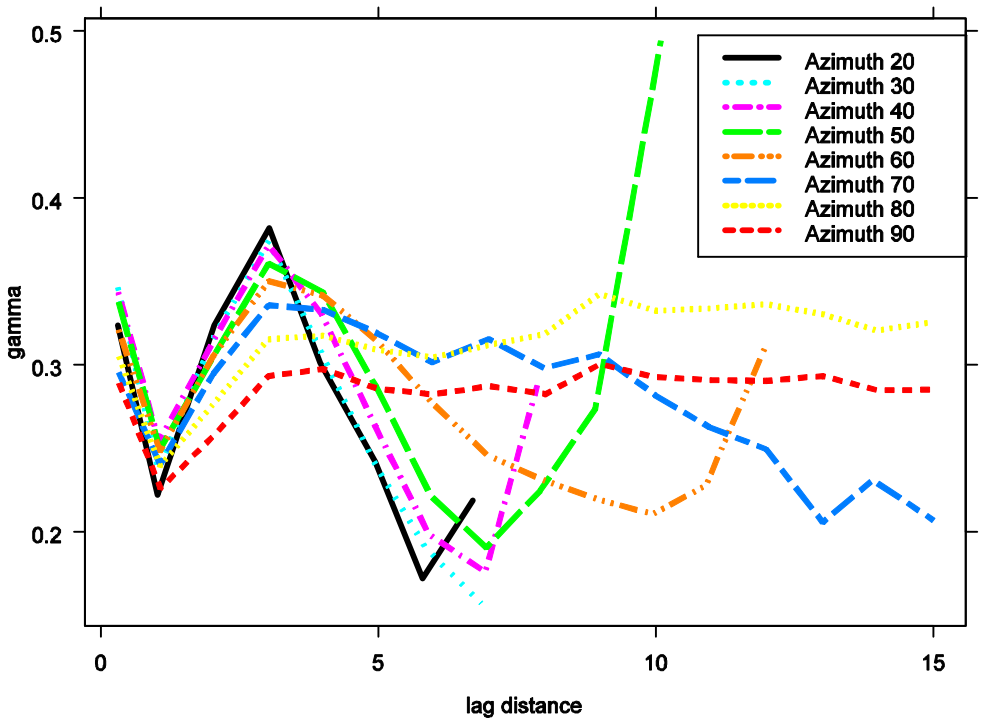

Depth HighlandWater Q43 ; Sensitivity analysis for the azimuth tolerance: Number of pair of points (azimuth 90)

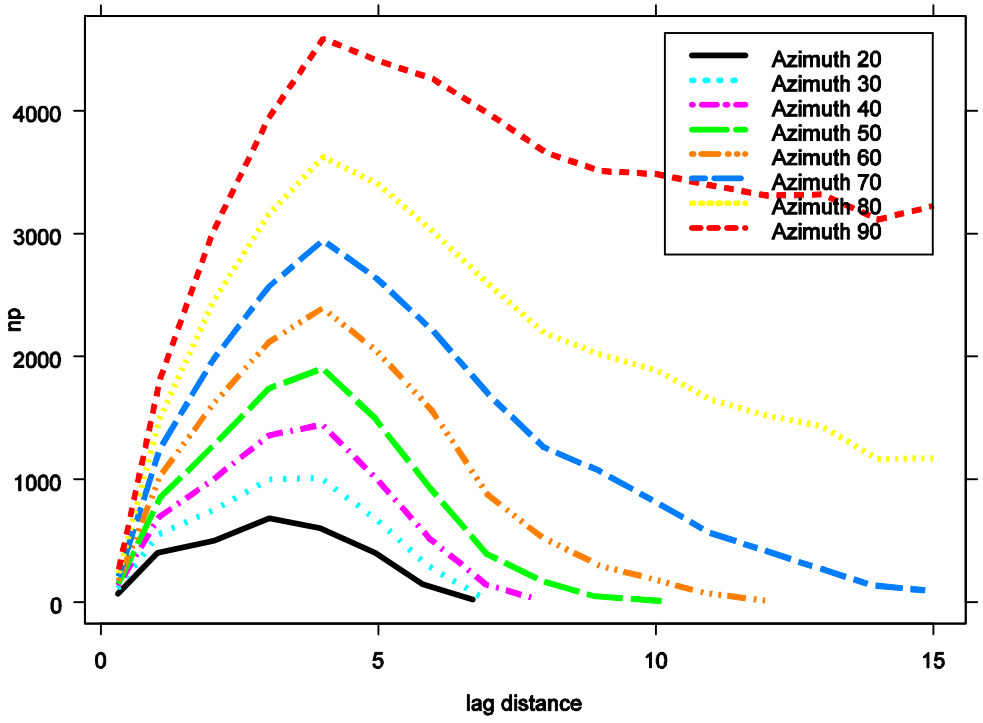

Depth Lambourn Q92 ; Sensitivity analysis for the azimuth tolerance (azimunt 0)

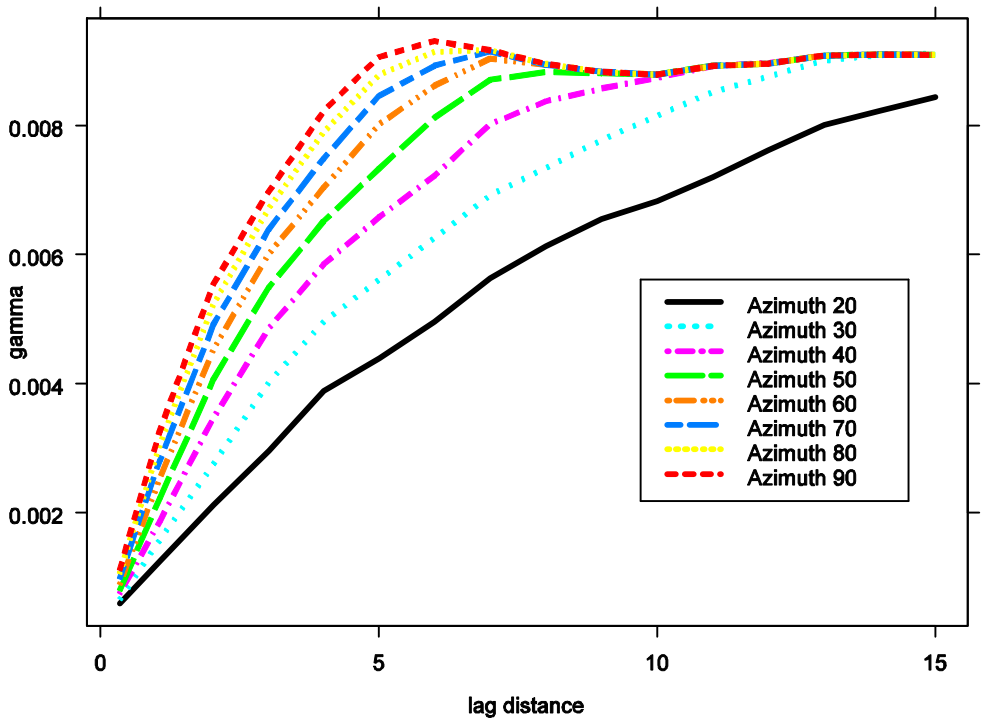

Depth Lambourn Q92 ; Sensitivity analysis for the azimuth tolerance: Number of pair of points (azimuth 0)

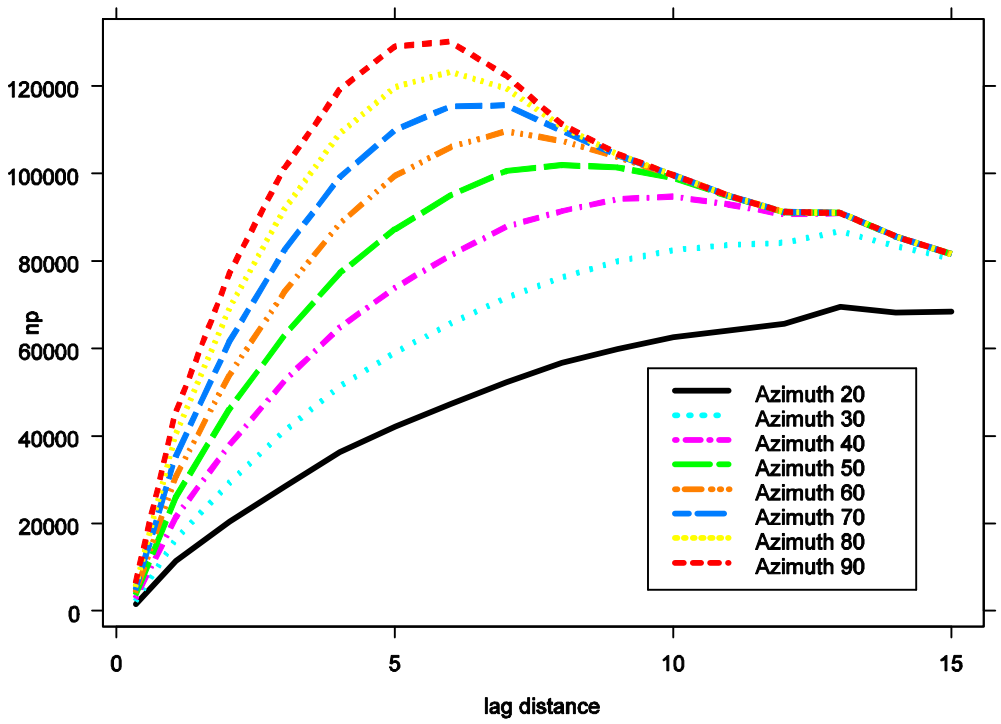

Depth Lambourn Q92 ; Sensitivity analysis for the azimuth tolerance (azimuth 90)

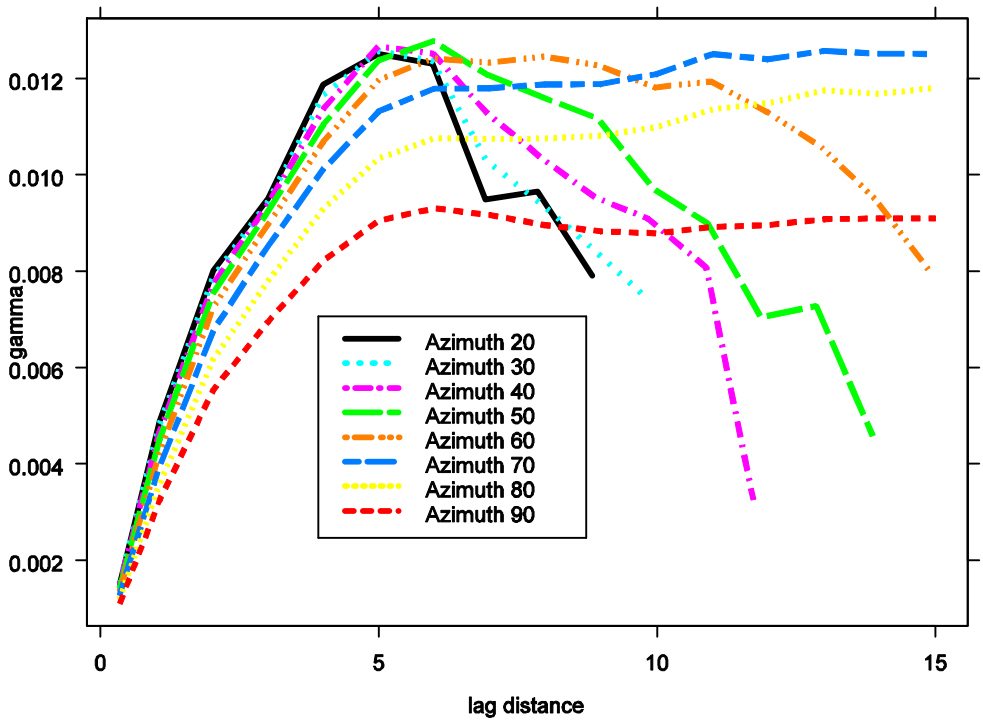

Depth Lambourn Q92 ; Sensitivity analysis for the azimuth tolerance: Number of pair of points (azimuth 90)

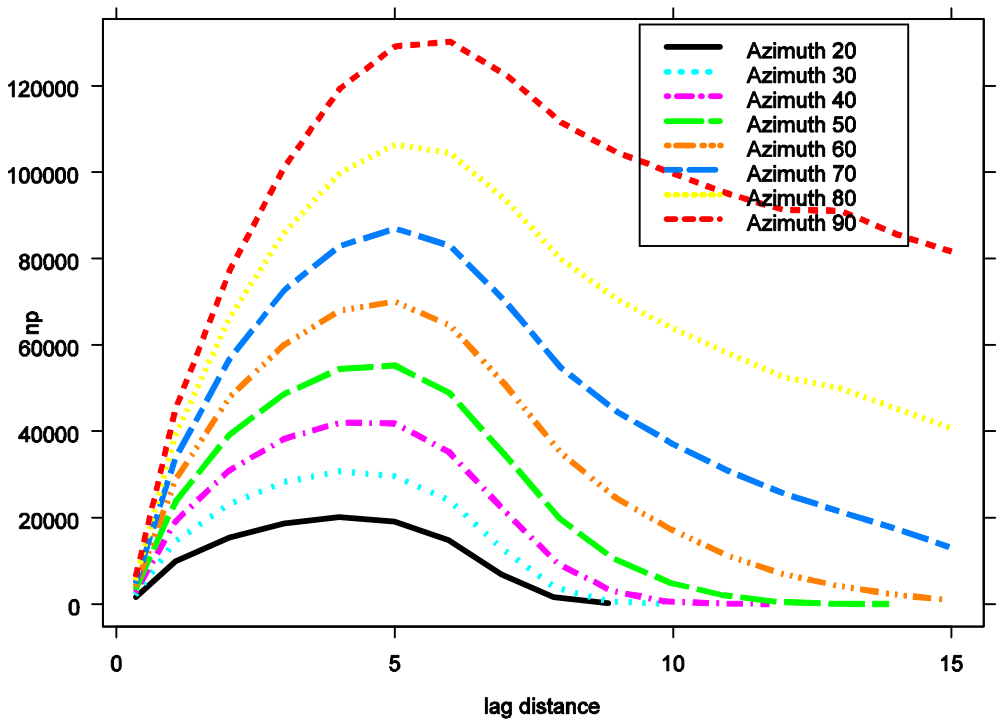

Depth LeighBrook Q82 ; Sensitivity analysis for the azimuth tolerance (azimunt 0)

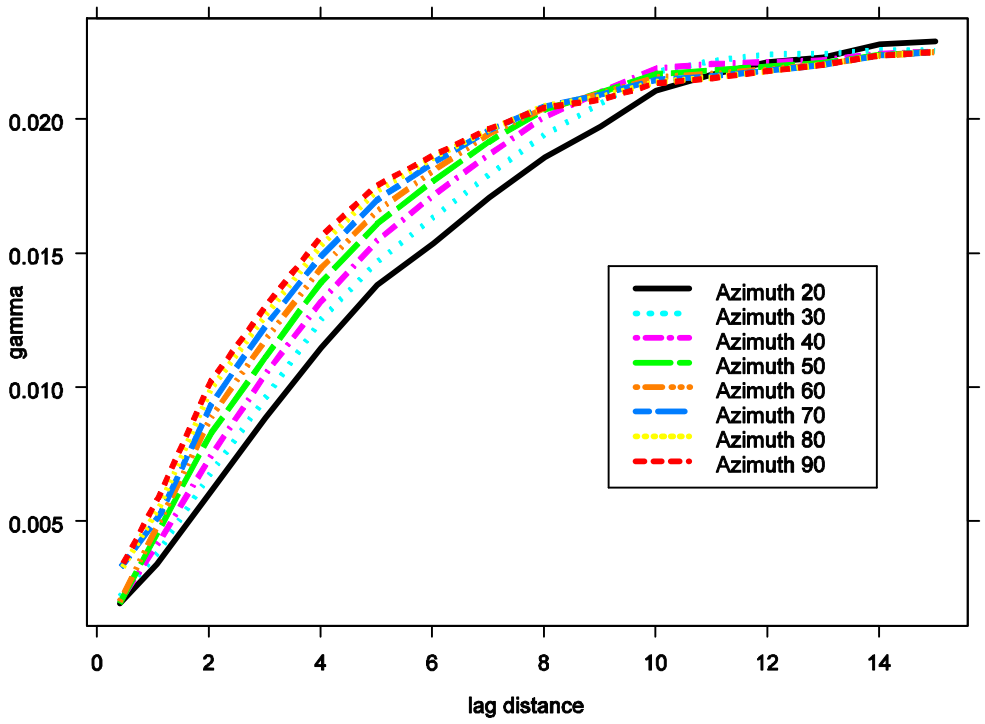

Depth LeighBrook Q82 ; Sensitivity analysis for the azimuth tolerance: Number of pair of points (azimuth 0)

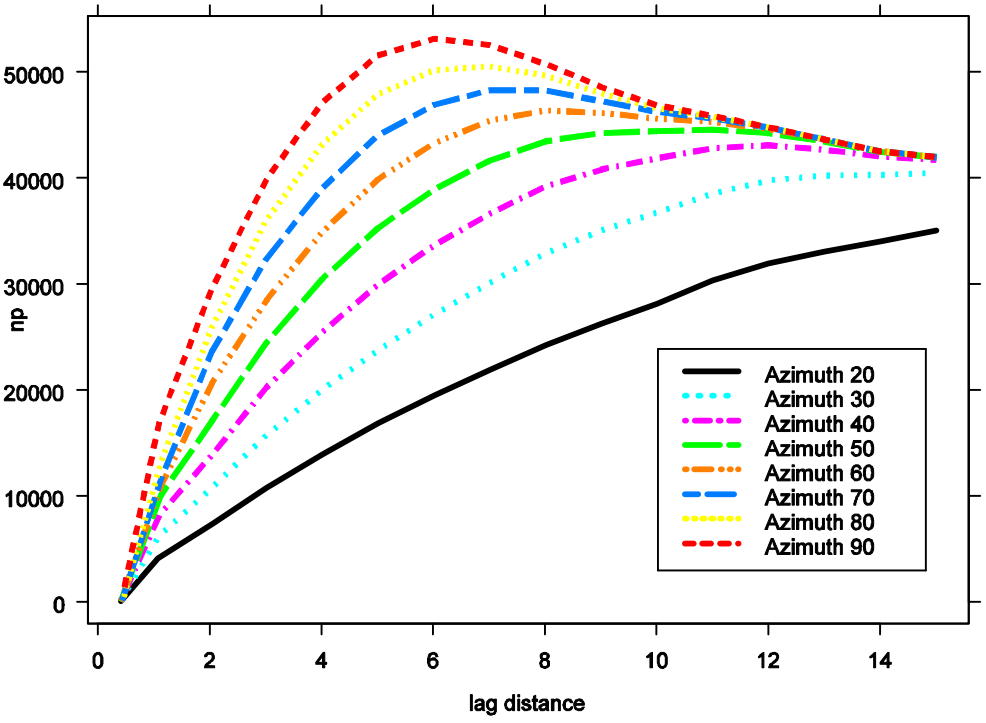

Depth LeighBrook Q82 ; Sensitivity analysis for the azimuth tolerance (azimuth 90)

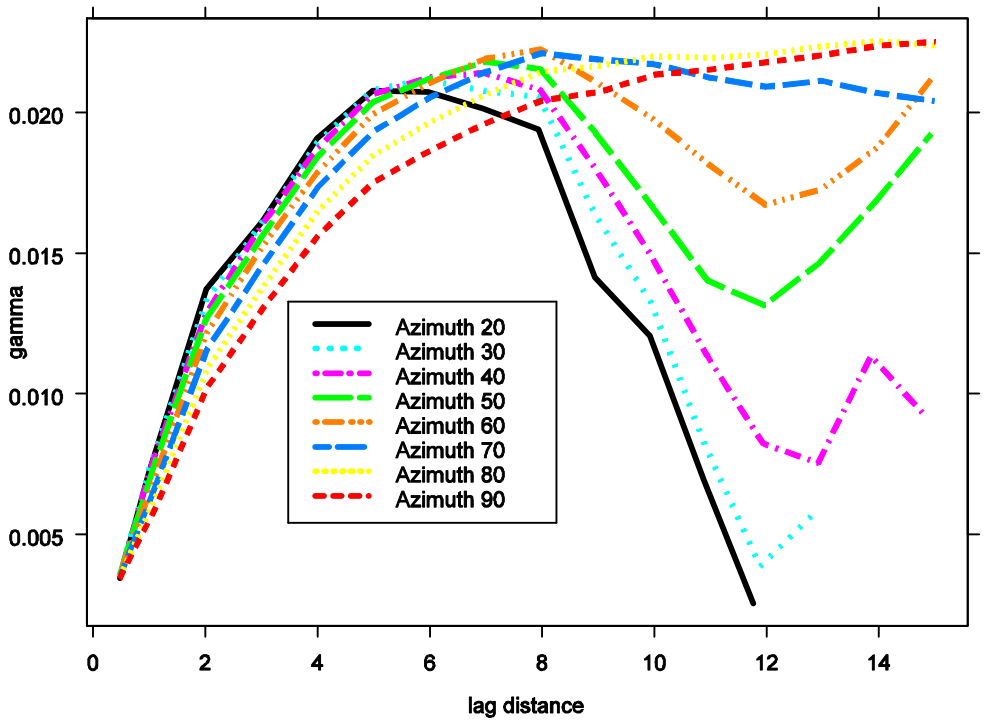

Depth LeighBrook Q82 ; Sensitivity analysis for the azimuth tolerance: Number of pair of points (azimuth 90)

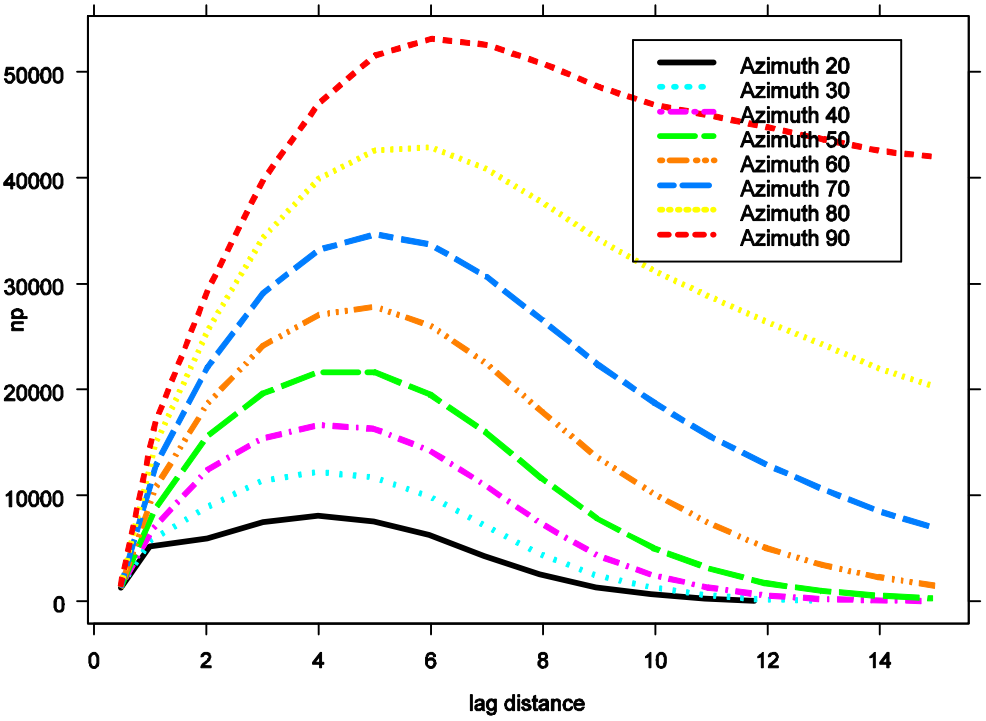

Depth LeighBrook Q93 ; Sensitivity analysis for the azimuth tolerance (azimunt 0)

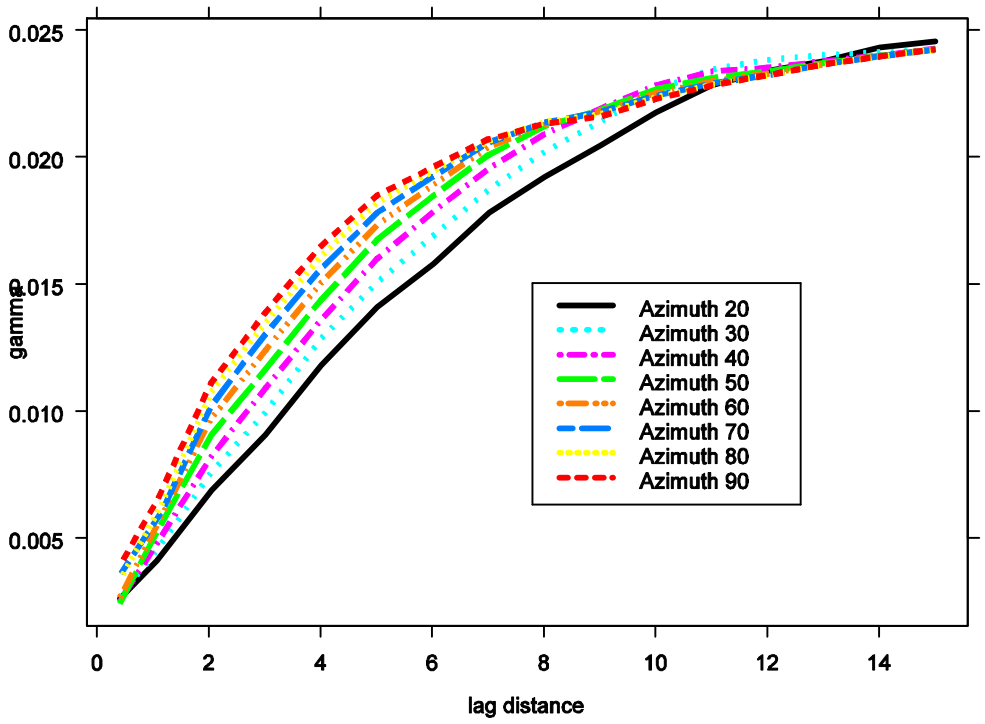

Depth LeighBrook Q93 ; Sensitivity analysis for the azimuth tolerance: Number of pair of points (azimuth 0)

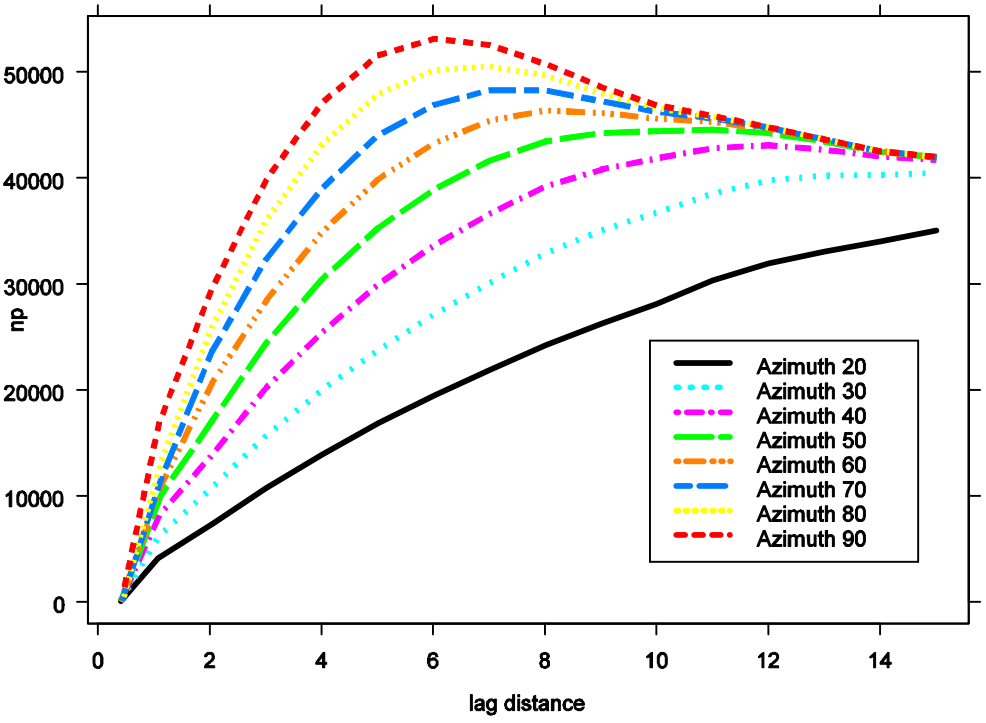

Depth LeighBrook Q93 ; Sensitivity analysis for the azimuth tolerance (azimuth 90)

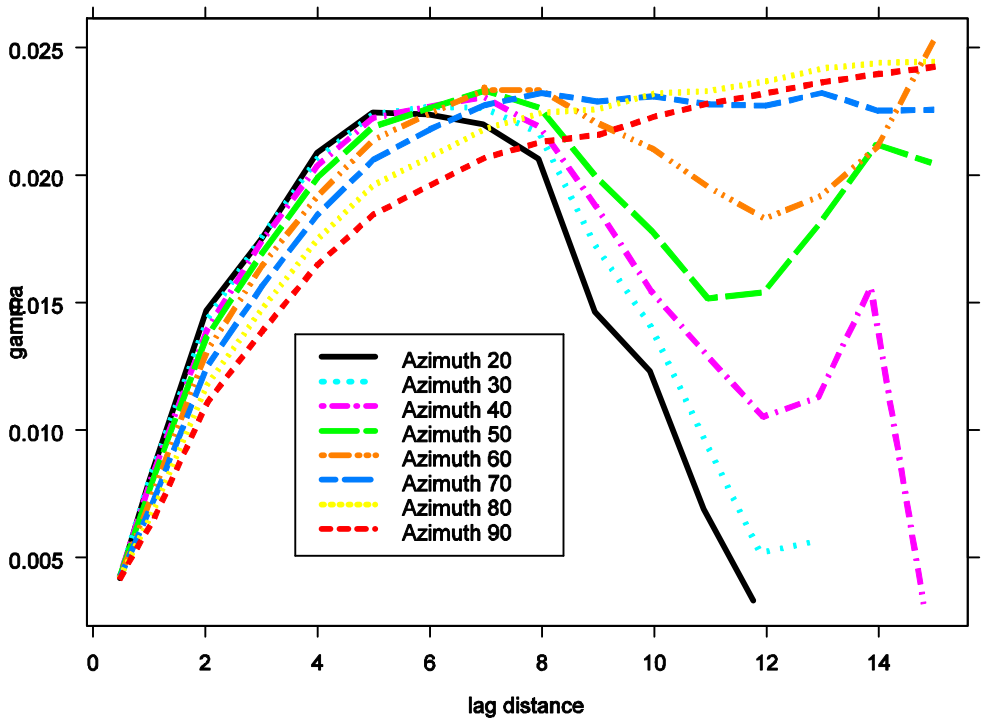

Depth LeighBrook Q93 ; Sensitivity analysis for the azimuth tolerance: Number of pair of points (azimuth 90)

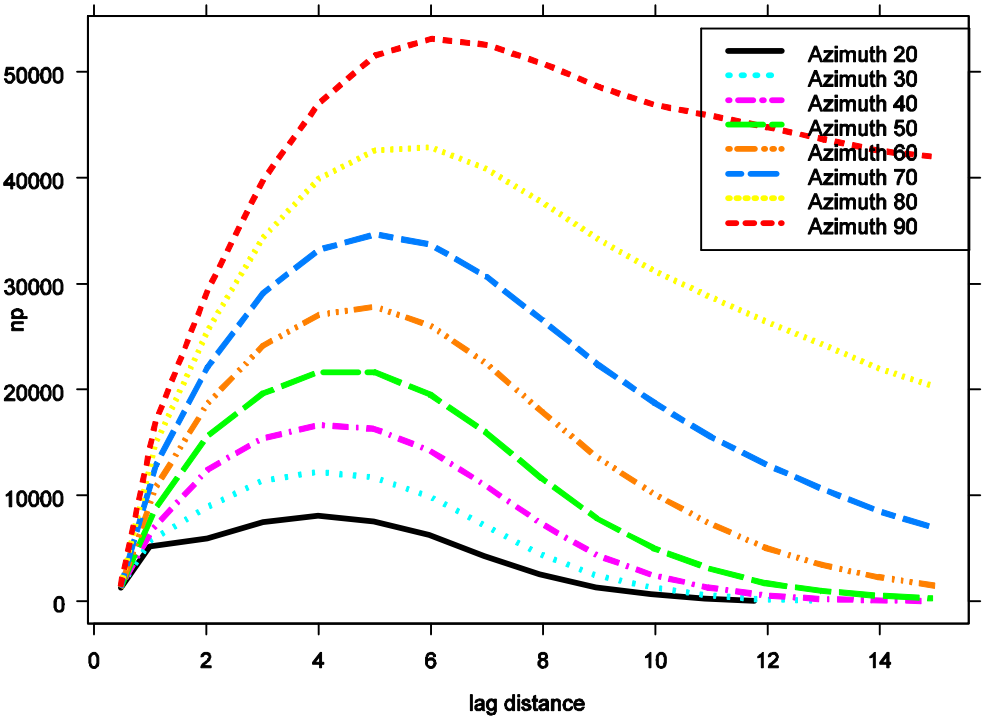

Depth Pang Fenced Q91 ; Sensitivity analysis for the azimuth tolerance (azimunt 0)

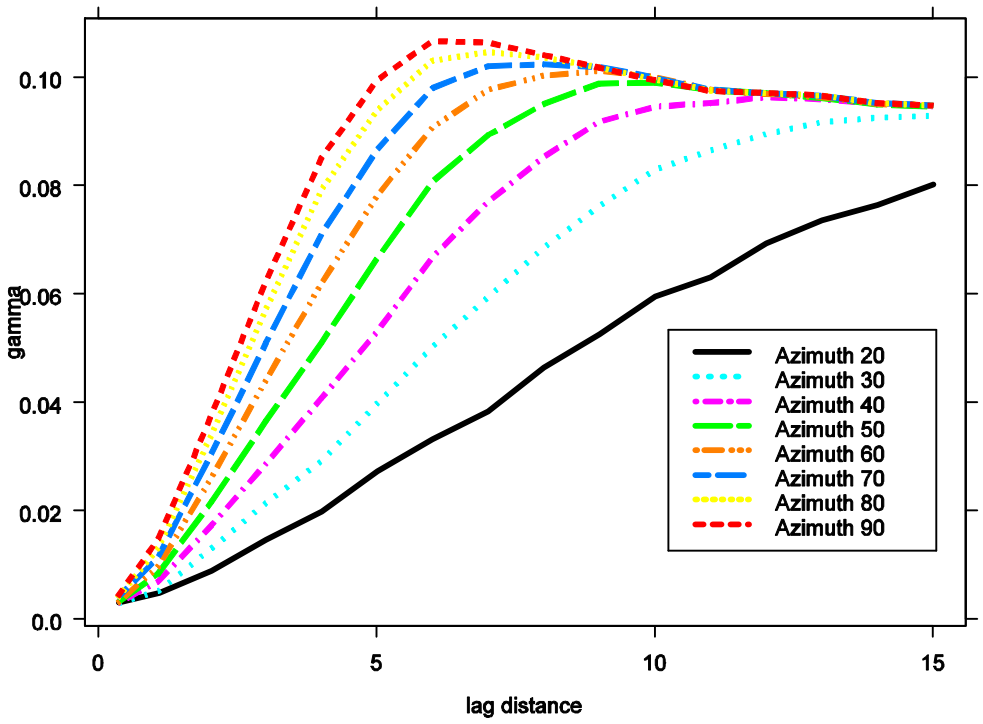

Depth Pang Fenced Q91 ; Sensitivity analysis for the azimuth tolerance: Number of pair of points (azimuth 0)

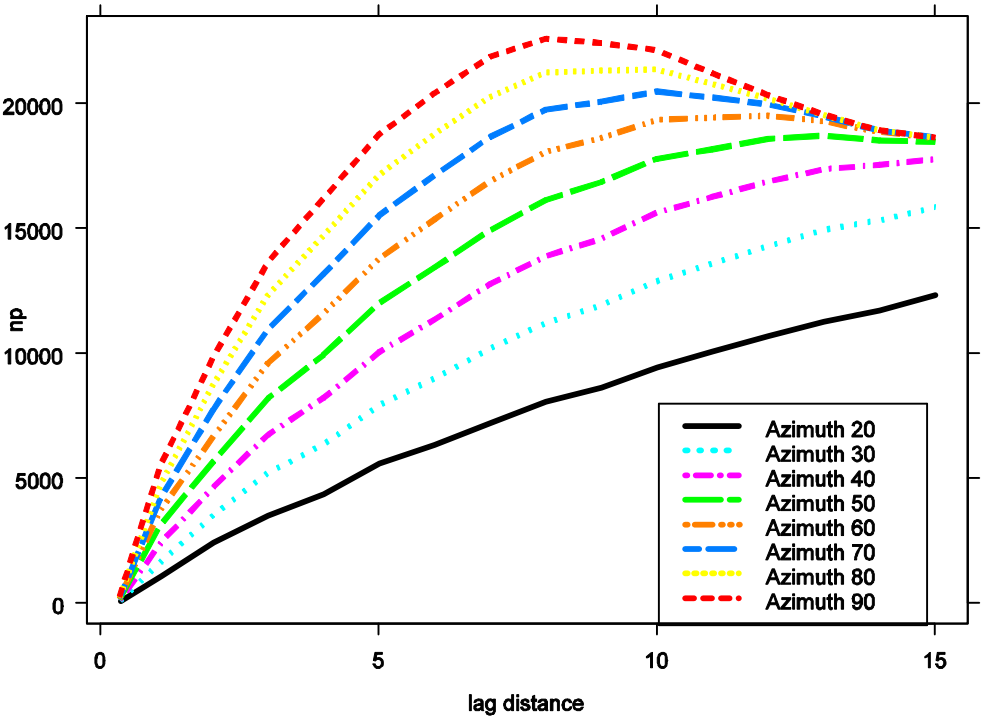

Depth Pang Fenced Q91 ; Sensitivity analysis for the azimuth tolerance (azimuth 90)

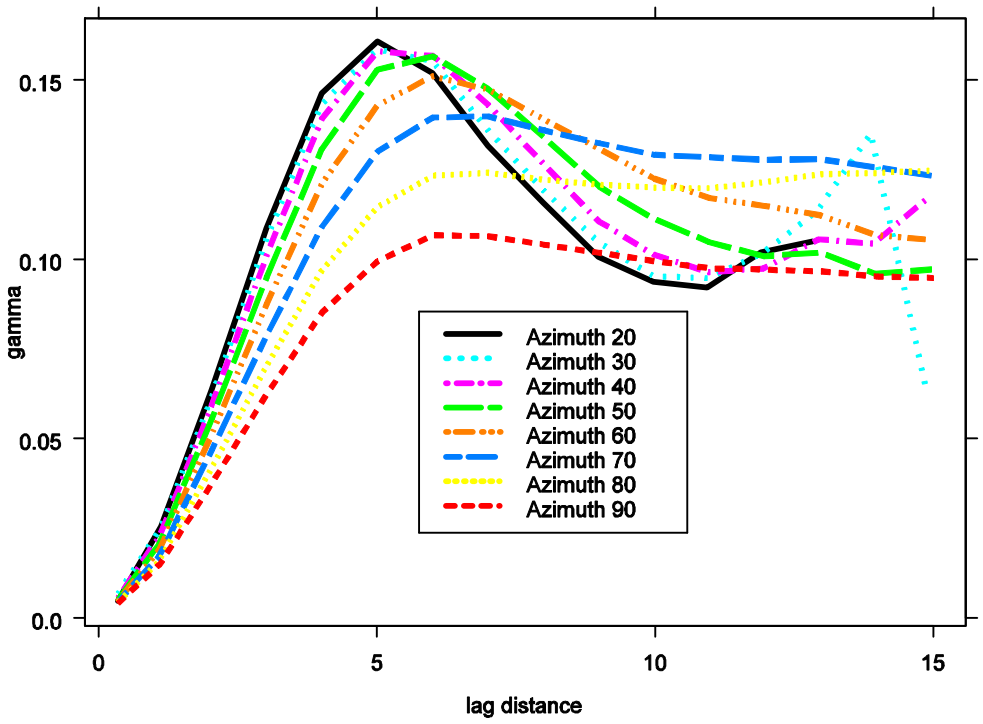

Depth Pang Fenced Q91 ; Sensitivity analysis for the azimuth tolerance: Number of pair of points (azimuth 90)

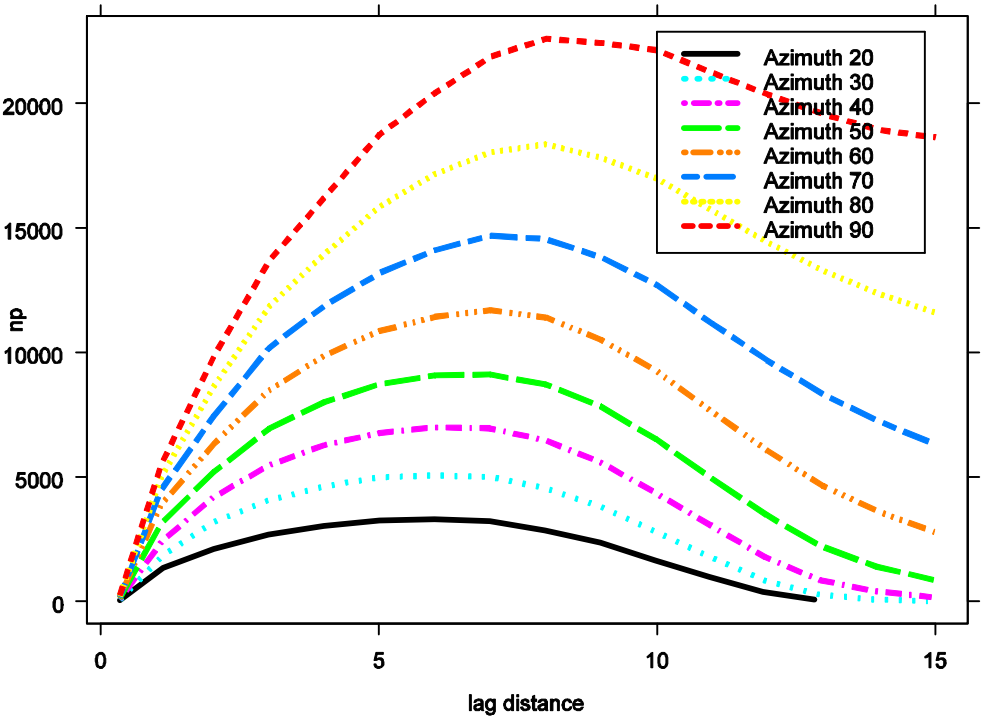

Depth Pang Old Fenced Q80 ; Sensitivity analysis for the azimuth tolerance (azimunt 0)

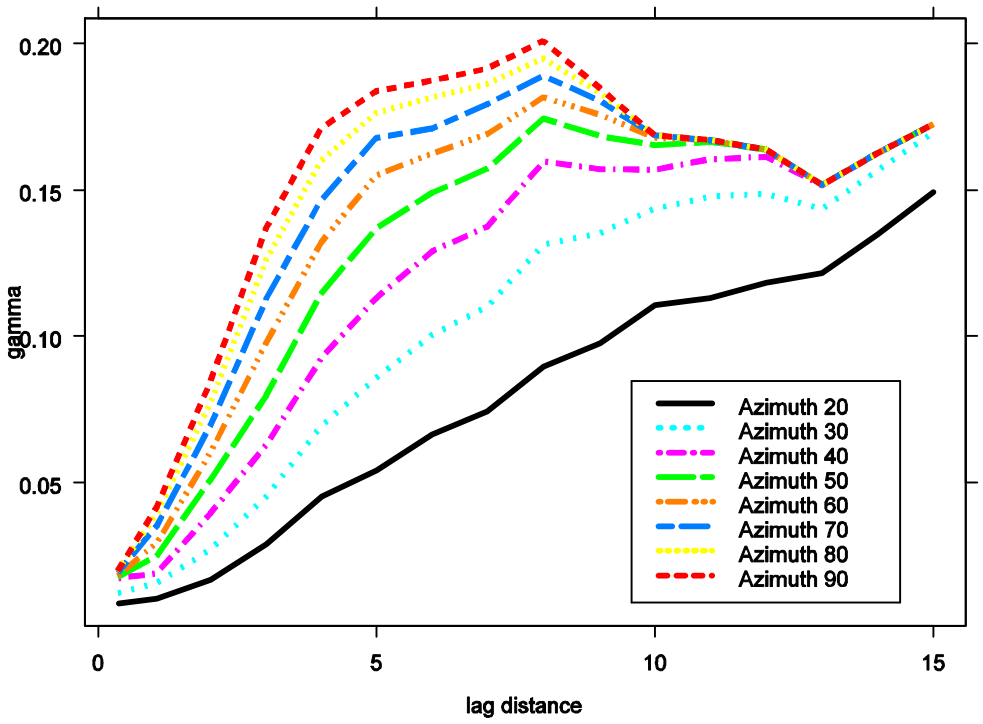

Depth Pang Old Fenced Q80 ; Sensitivity analysis for the azimuth tolerance: Number of pair of points (azimuth 0)

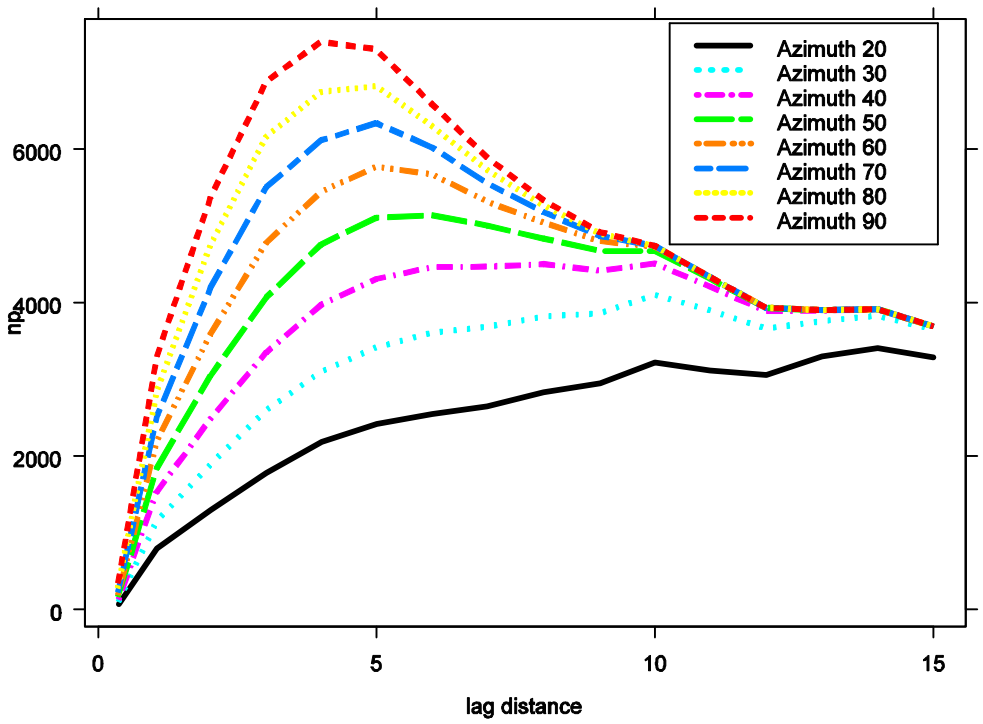

Depth Pang Old Fenced Q80 ; Sensitivity analysis for the azimuth tolerance (azimuth 90)

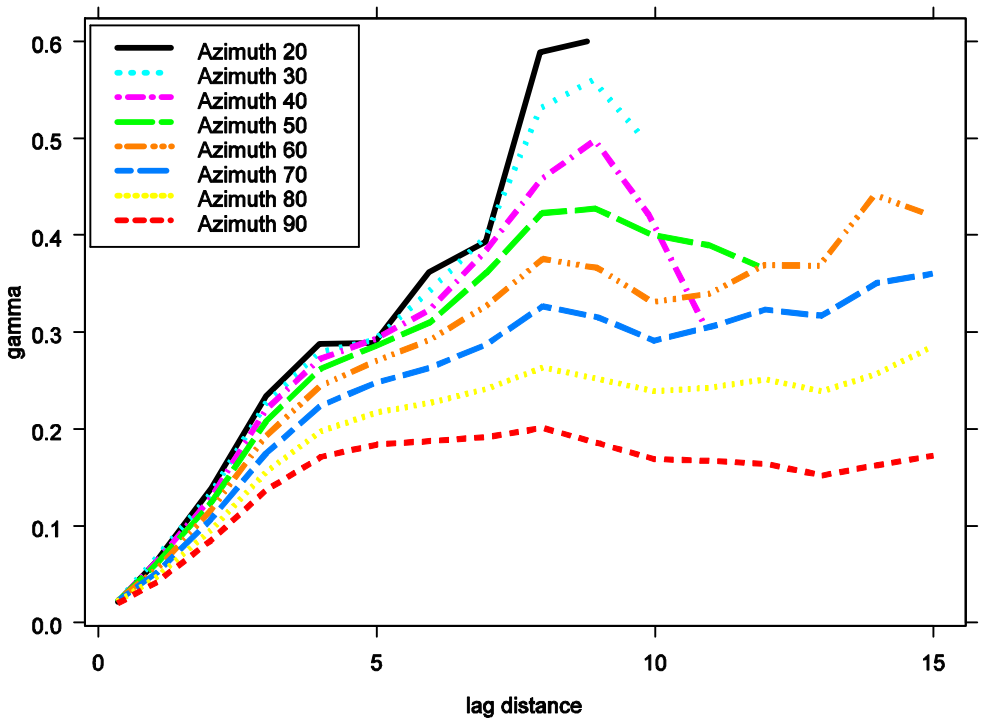

Depth Pang Old Fenced Q80 ; Sensitivity analysis for the azimuth tolerance: Number of pair of points (azimuth 90)

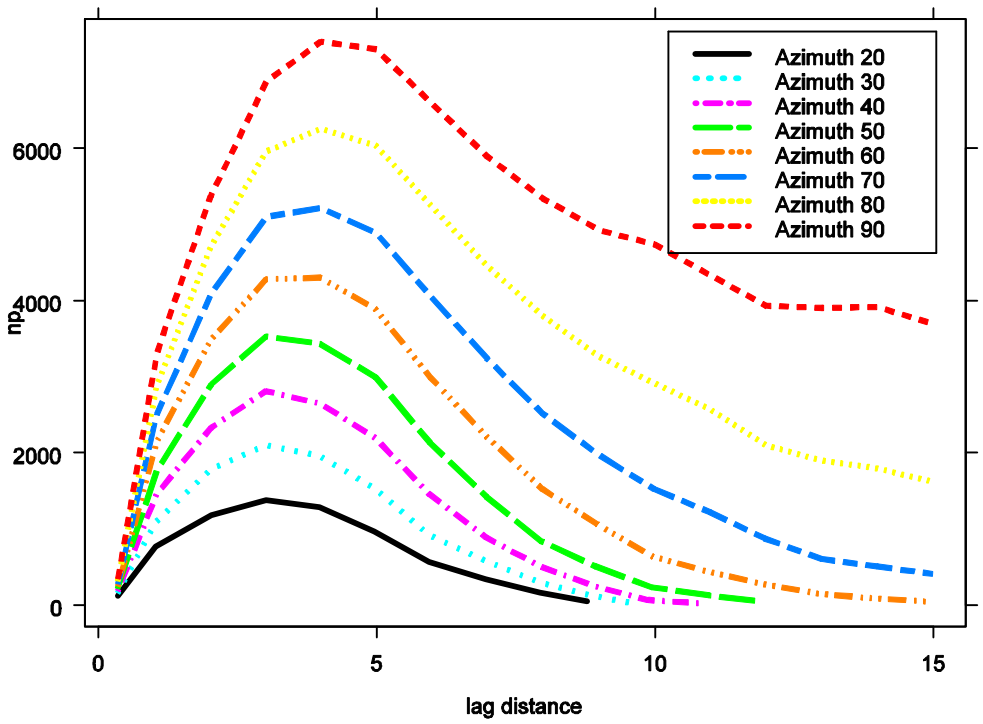

Depth Pang Old Fenced Q90 ; Sensitivity analysis for the azimuth tolerance (azimunt 0)

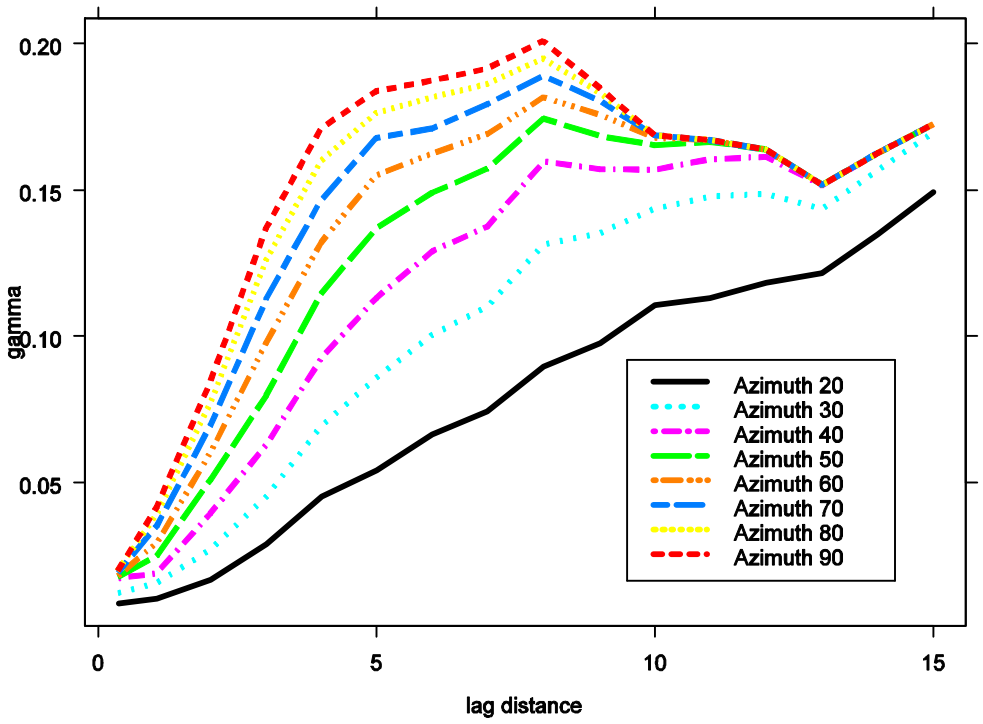

Depth Pang Old Fenced Q90 ; Sensitivity analysis for the azimuth tolerance: Number of pair of points (azimuth 0)

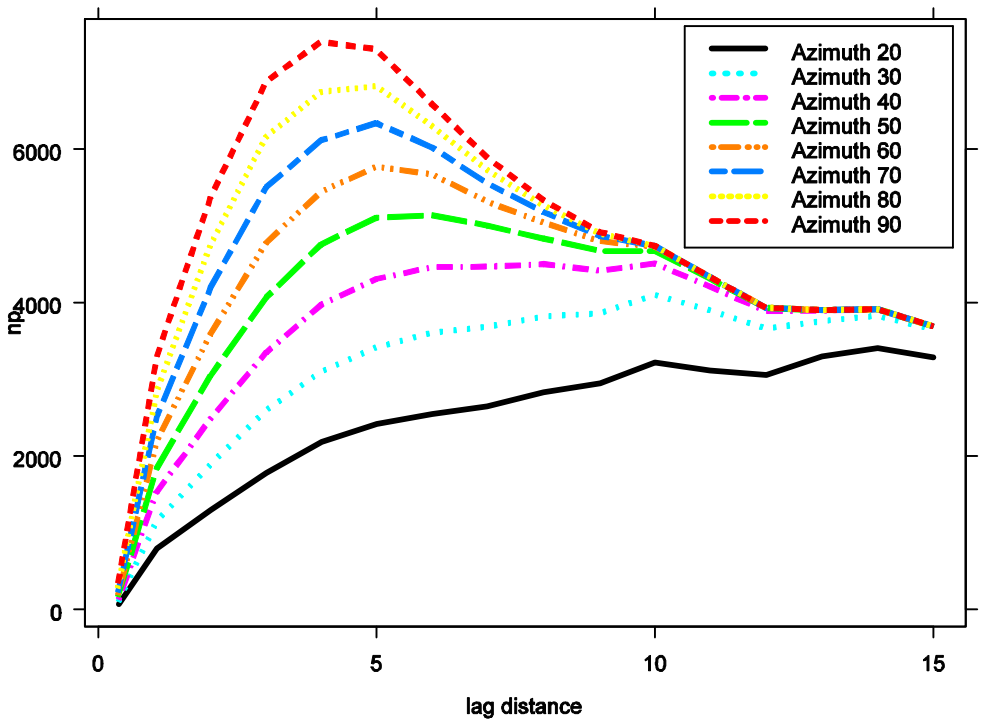

Depth Pang Old Fenced Q90 ; Sensitivity analysis for the azimuth tolerance (azimuth 90)

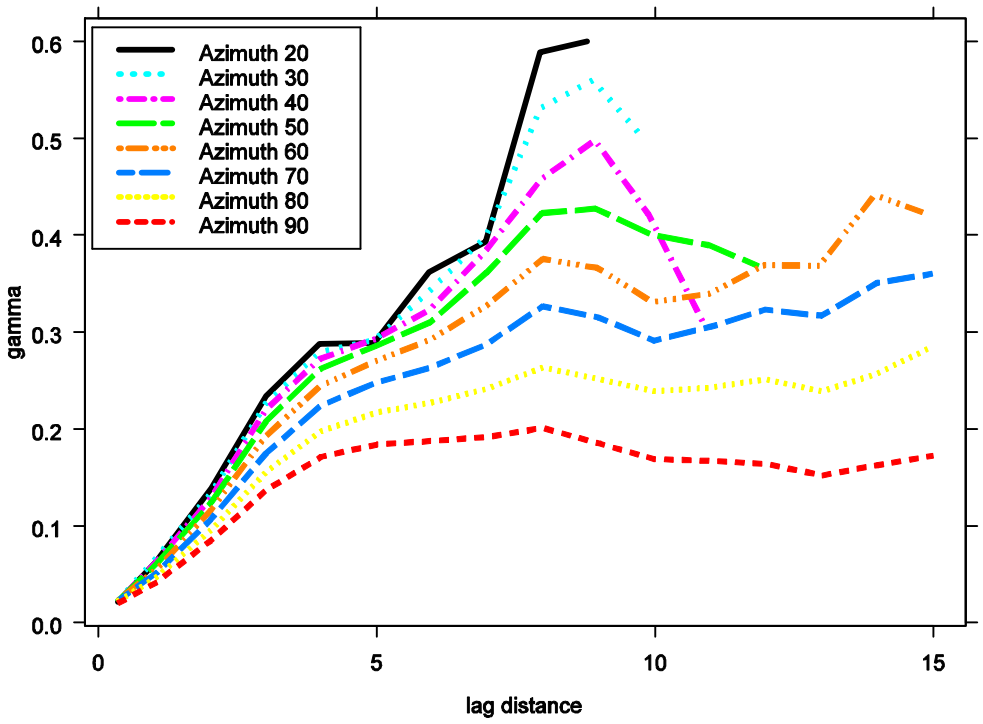

Depth Pang Old Fenced Q90 ; Sensitivity analysis for the azimuth tolerance: Number of pair of points (azimuth 90)

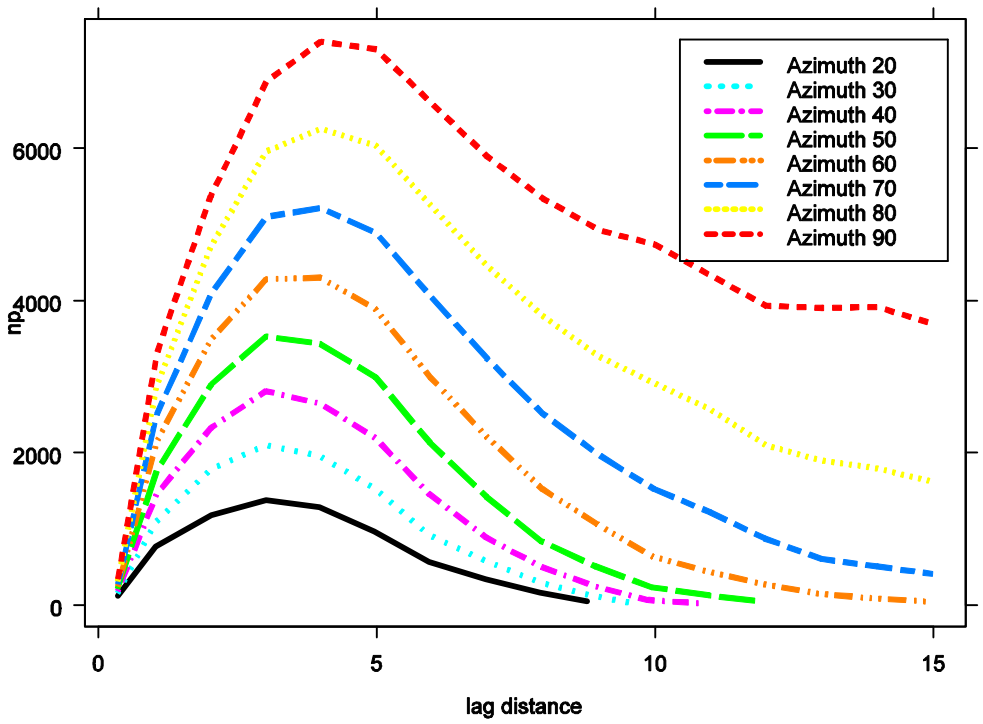

Depth Pang Unfenced Q80 ; Sensitivity analysis for the azimuth tolerance (azimunt 0)

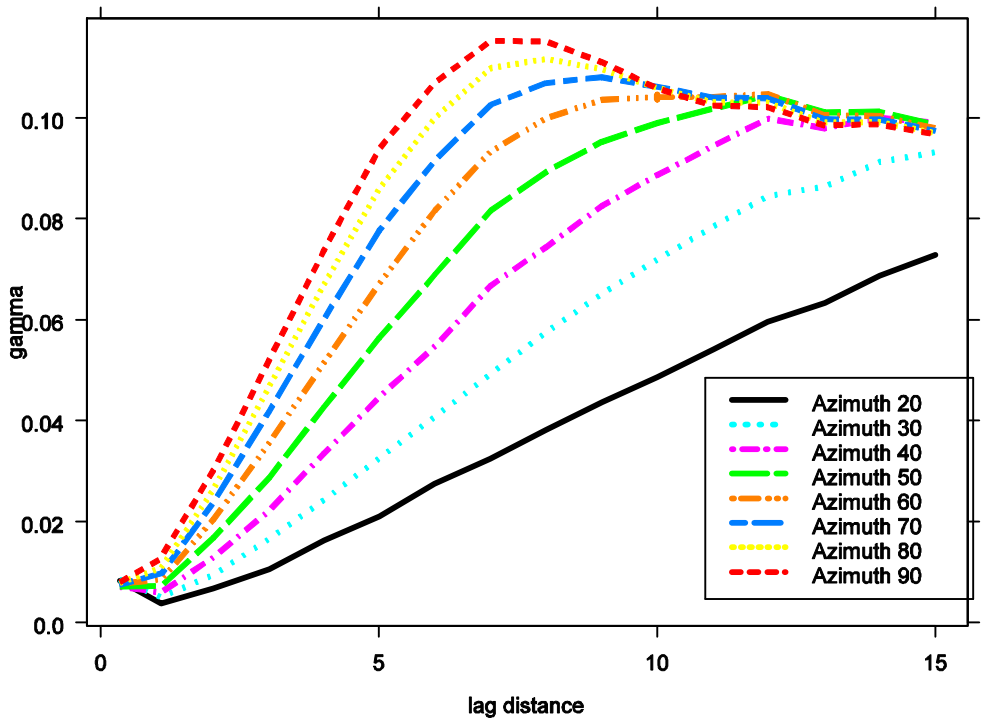

Depth Pang Unfenced Q80 ; Sensitivity analysis for the azimuth tolerance: Number of pair of points (azimuth 0)

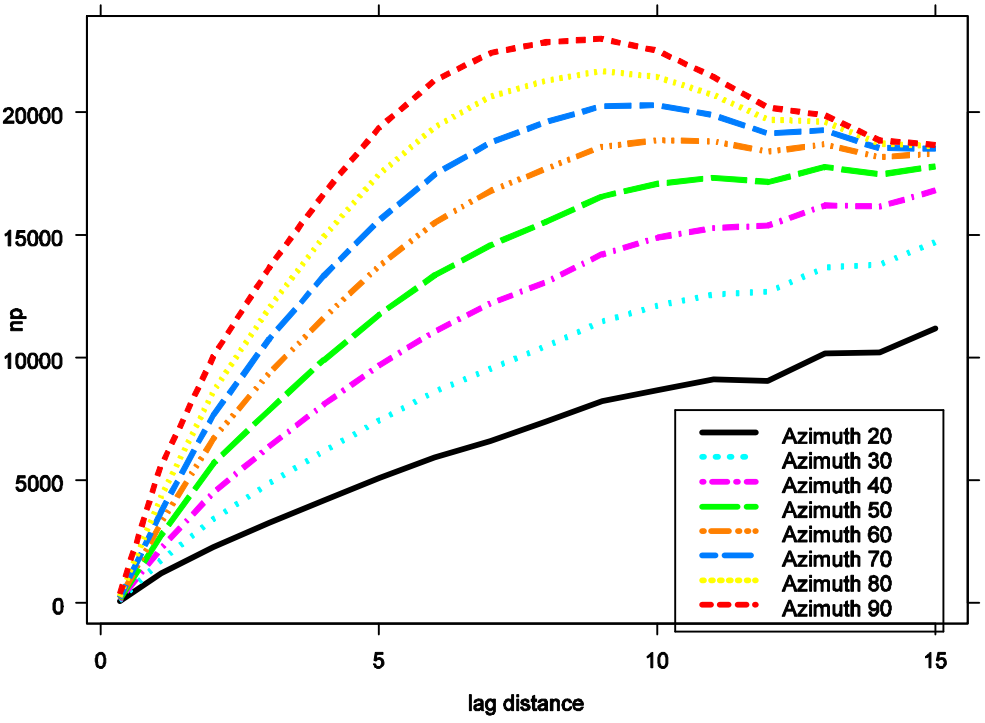

Depth Pang Unfenced Q80 ; Sensitivity analysis for the azimuth tolerance (azimuth 90)

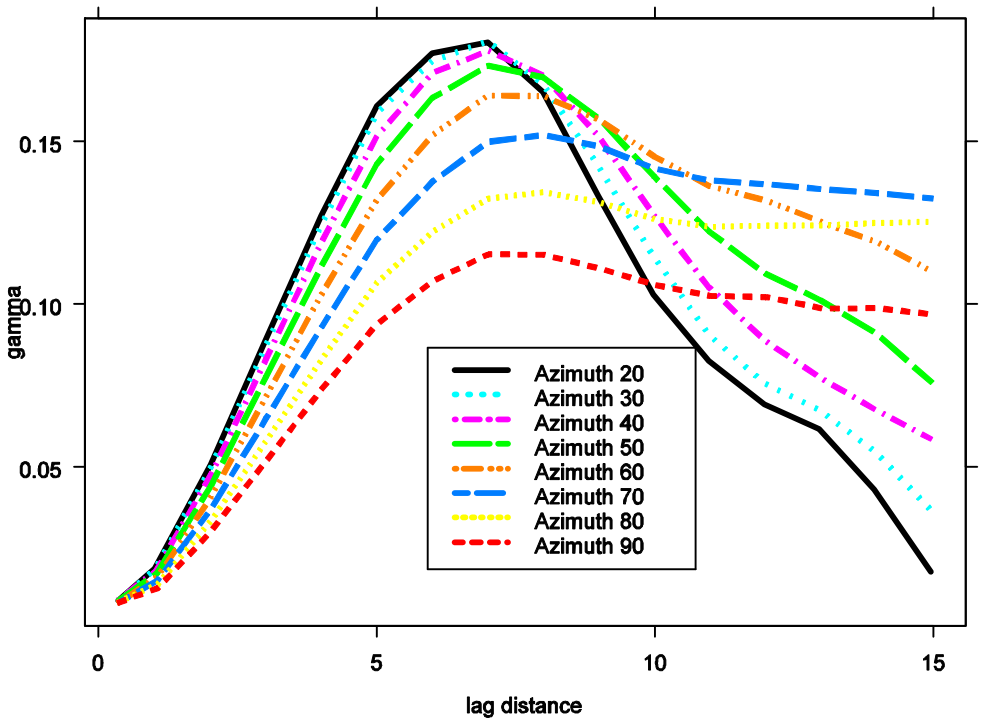

Depth Pang Unfenced Q80 ; Sensitivity analysis for the azimuth tolerance: Number of pair of points (azimuth 90)

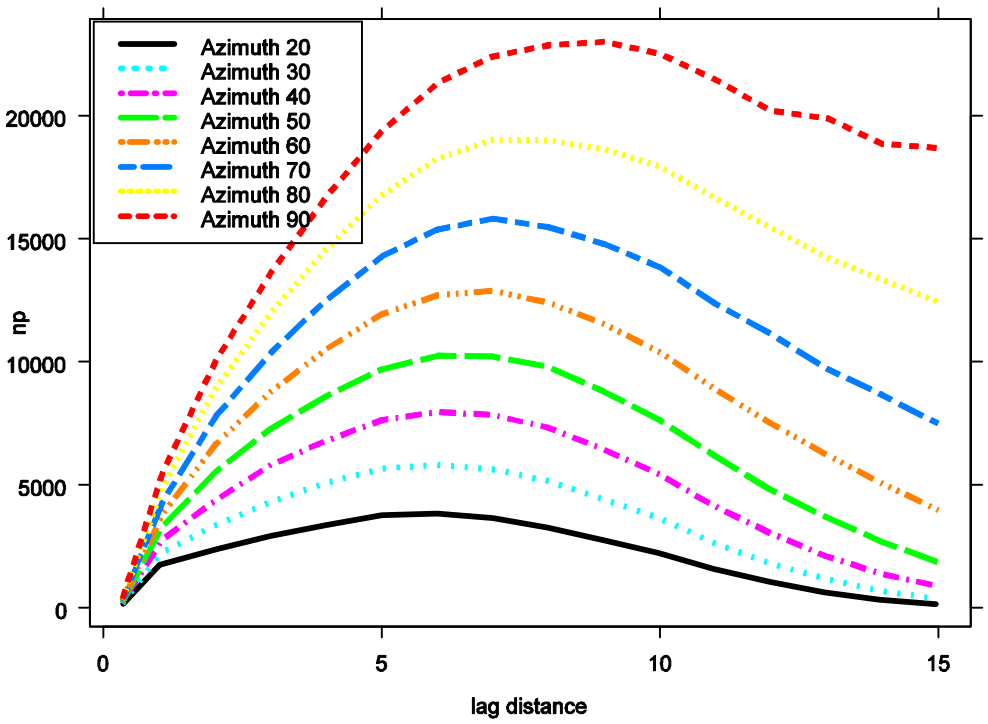

Depth Pang Unfenced Q90 ; Sensitivity analysis for the azimuth tolerance (azimunt 0)

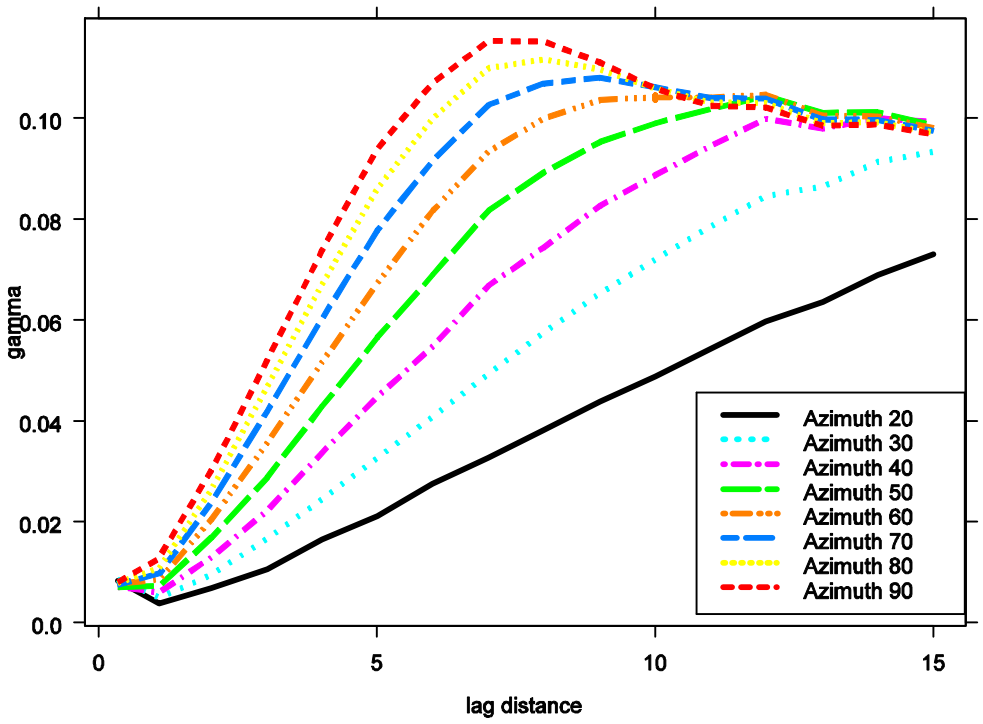

Depth Pang Unfenced Q90 ; Sensitivity analysis for the azimuth tolerance: Number of pair of points (azimuth 0)

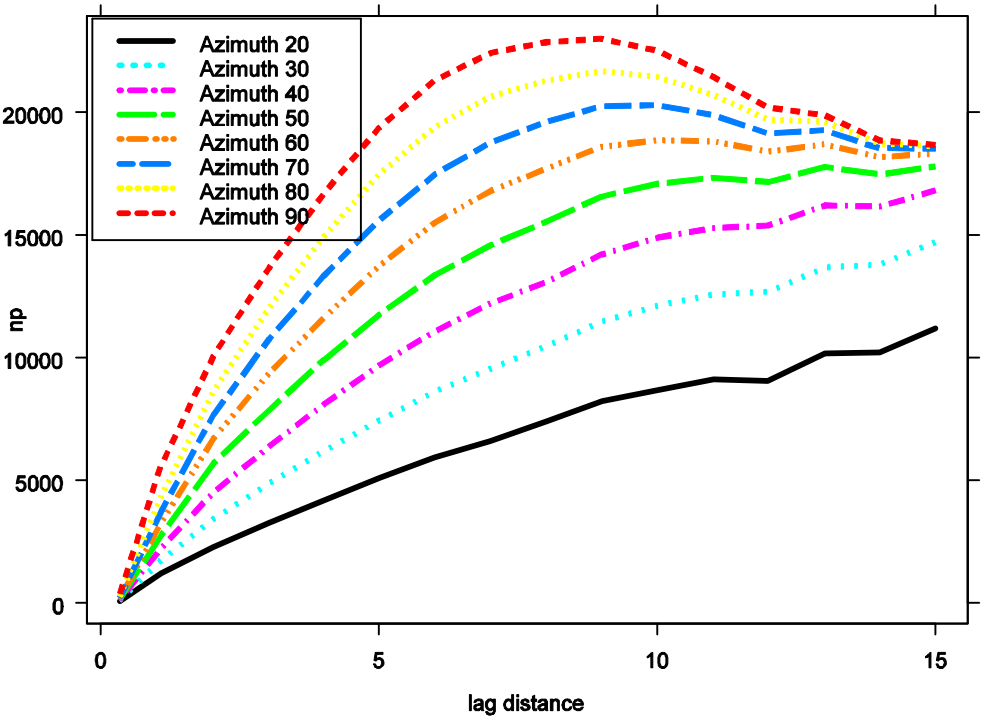

Depth Pang Unfenced Q90 ; Sensitivity analysis for the azimuth tolerance (azimuth 90)

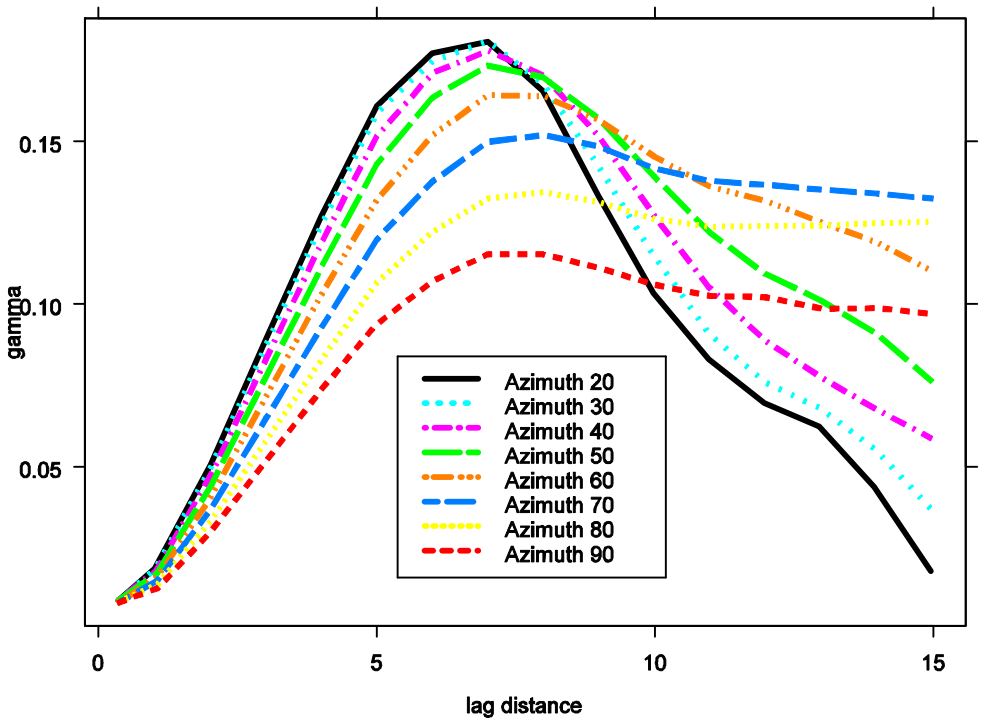

Depth Pang Unfenced Q90 ; Sensitivity analysis for the azimuth tolerance: Number of pair of points (azimuth 90)

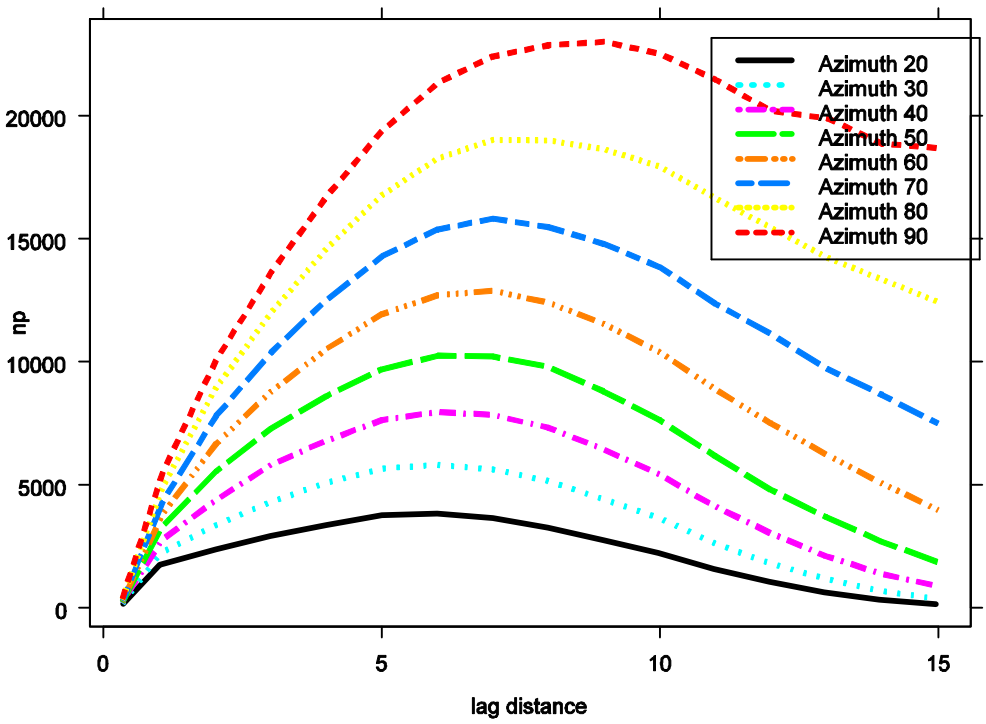

Depth Senni Q78 ; Sensitivity analysis for the azimuth tolerance (azimunt 0)

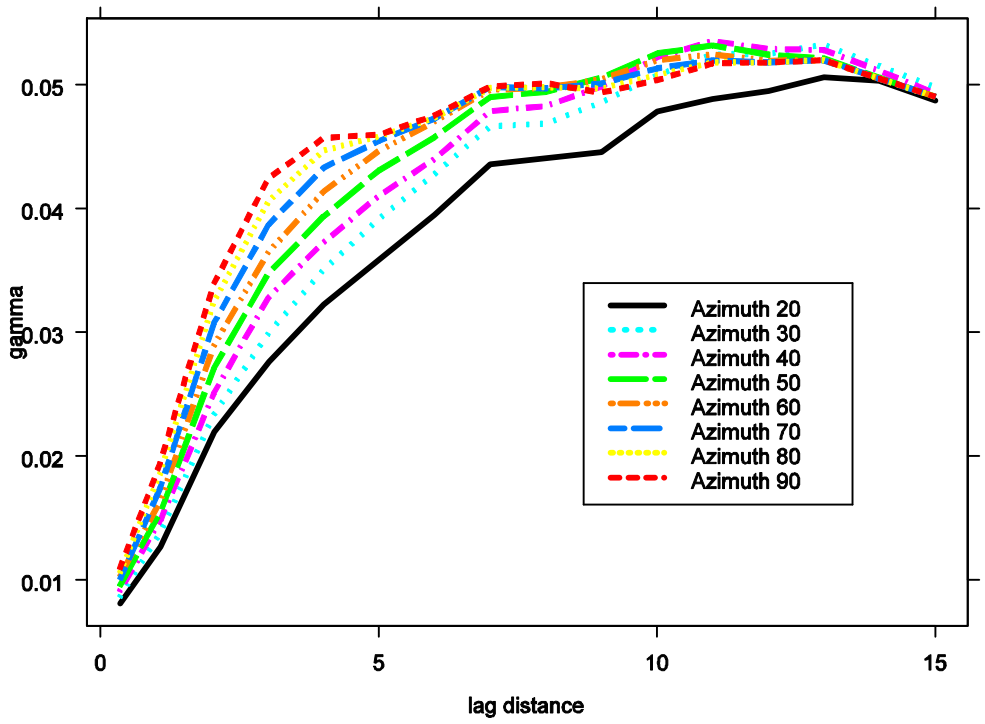

Depth Senni Q78 ; Sensitivity analysis for the azimuth tolerance: Number of pair of points (azimuth 0)

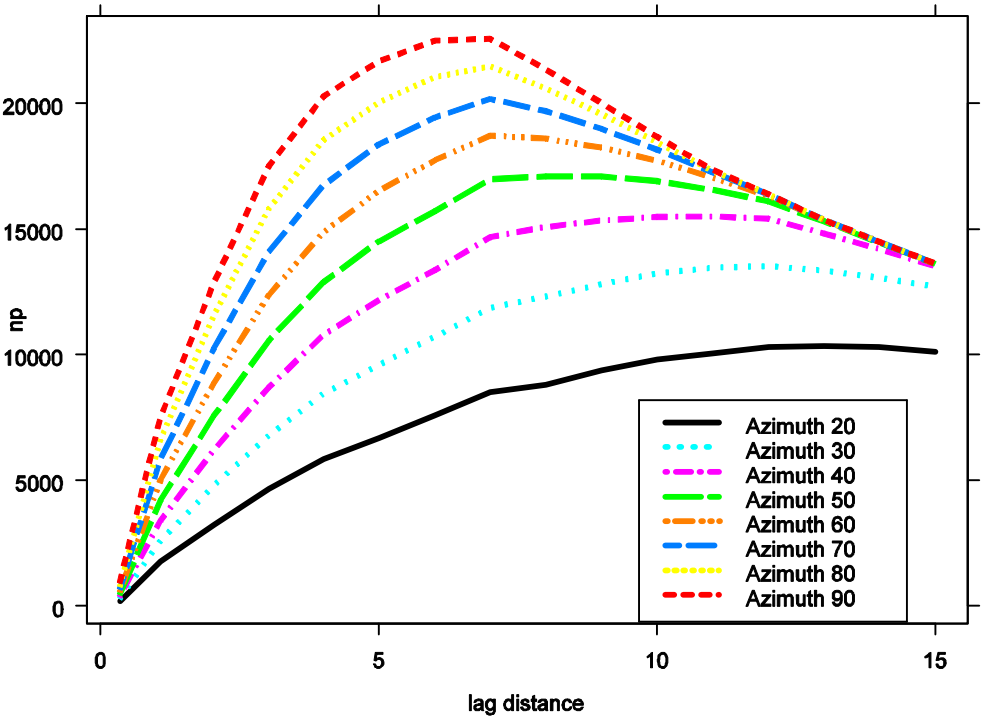

Depth Senni Q78 ; Sensitivity analysis for the azimuth tolerance (azimuth 90)

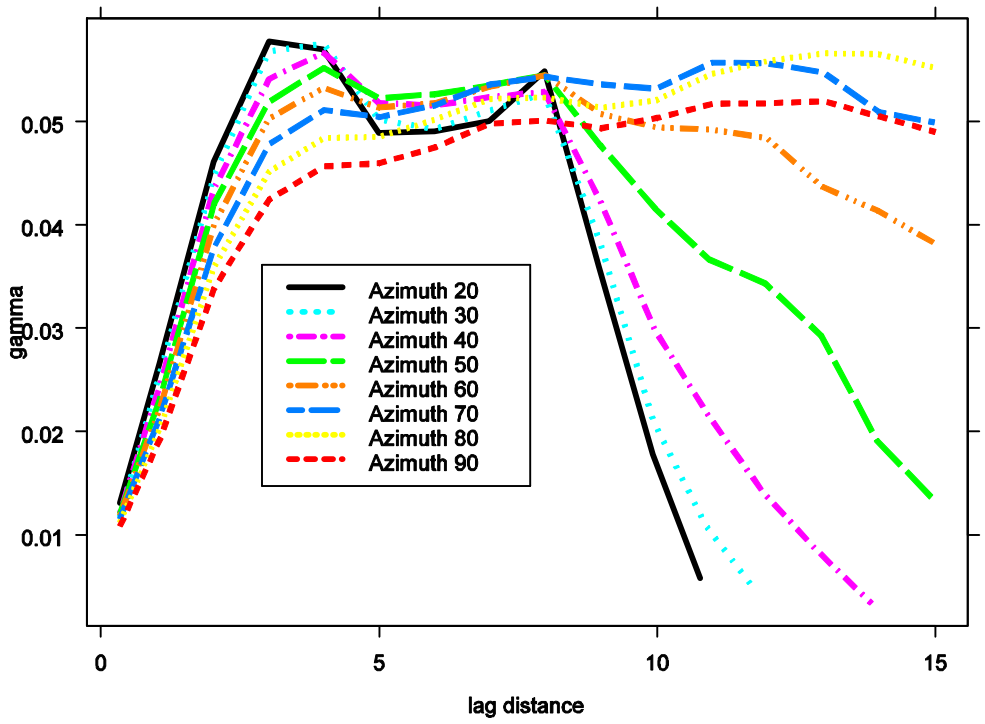

Depth Senni Q78 ; Sensitivity analysis for the azimuth tolerance: Number of pair of points (azimuth 90)

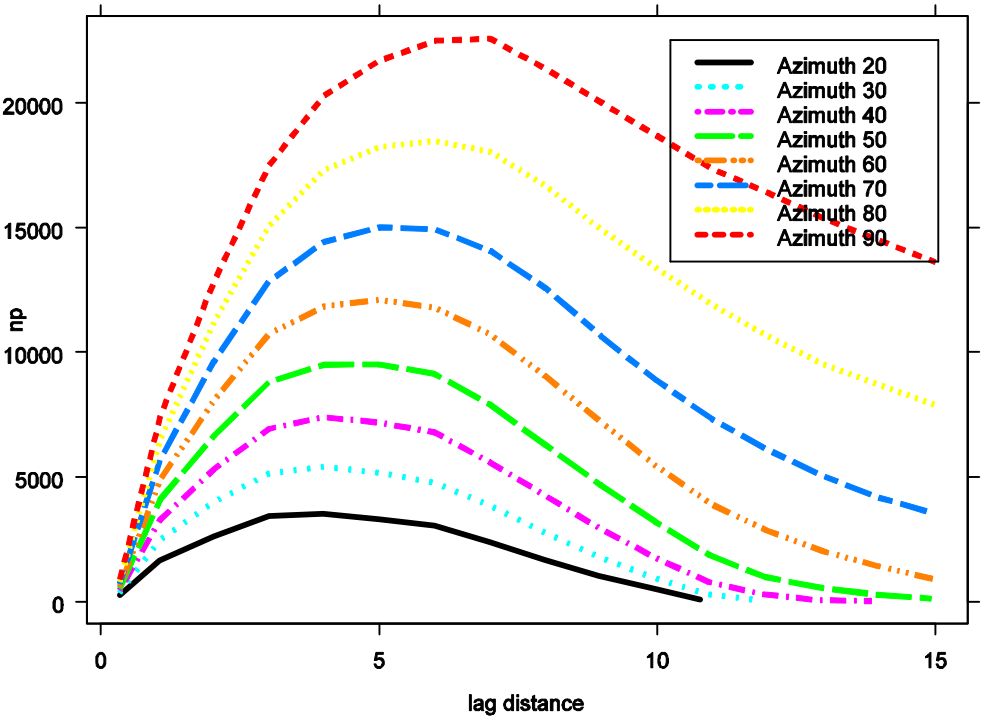

Depth Tames HM Q20 ; Sensitivity analysis for the azimuth tolerance (azimunt 0)

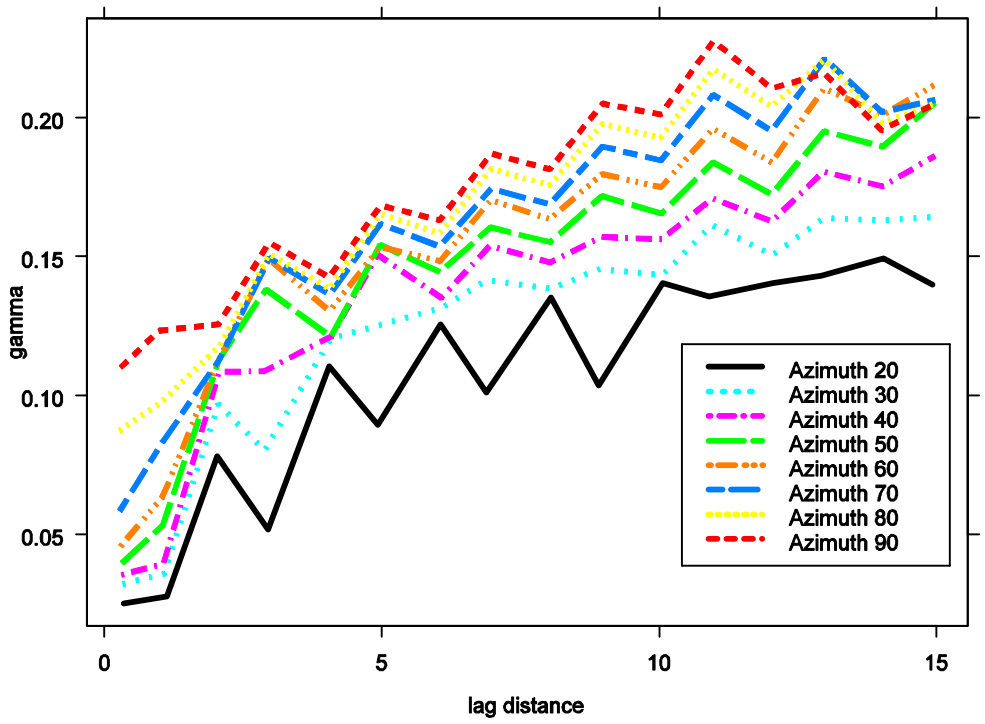

Depth Tames HM Q20 ; Sensitivity analysis for the azimuth tolerance: Number of pair of points (azimuth 0)

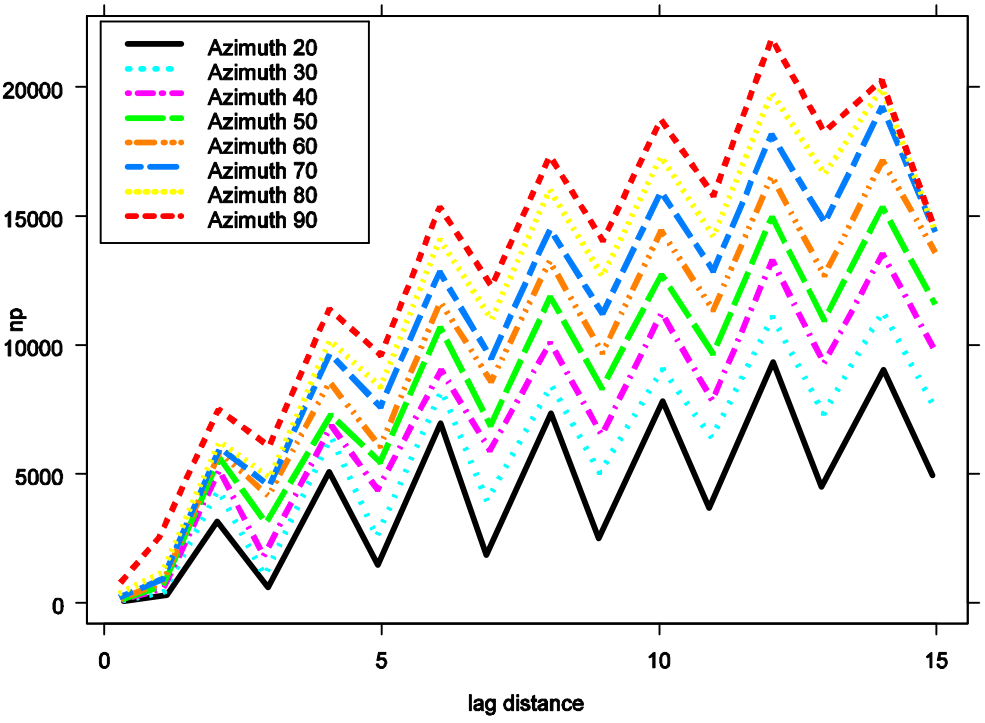

Depth Tames HM Q20 ; Sensitivity analysis for the azimuth tolerance (azimuth 90)

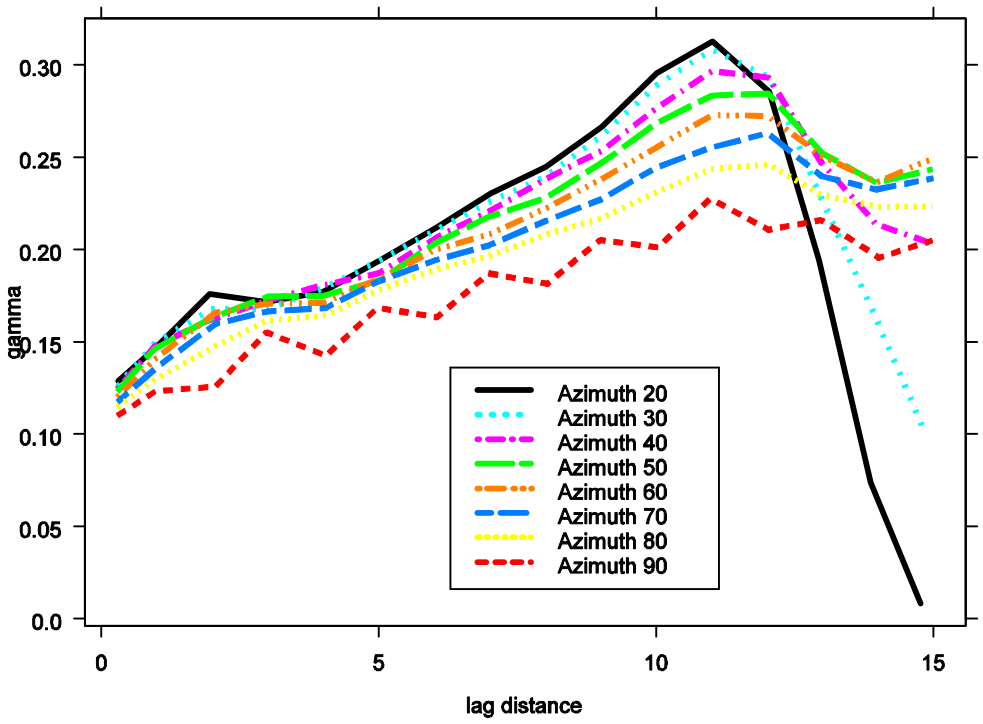

Depth Tames HM Q20 ; Sensitivity analysis for the azimuth tolerance: Number of pair of points (azimuth 90)

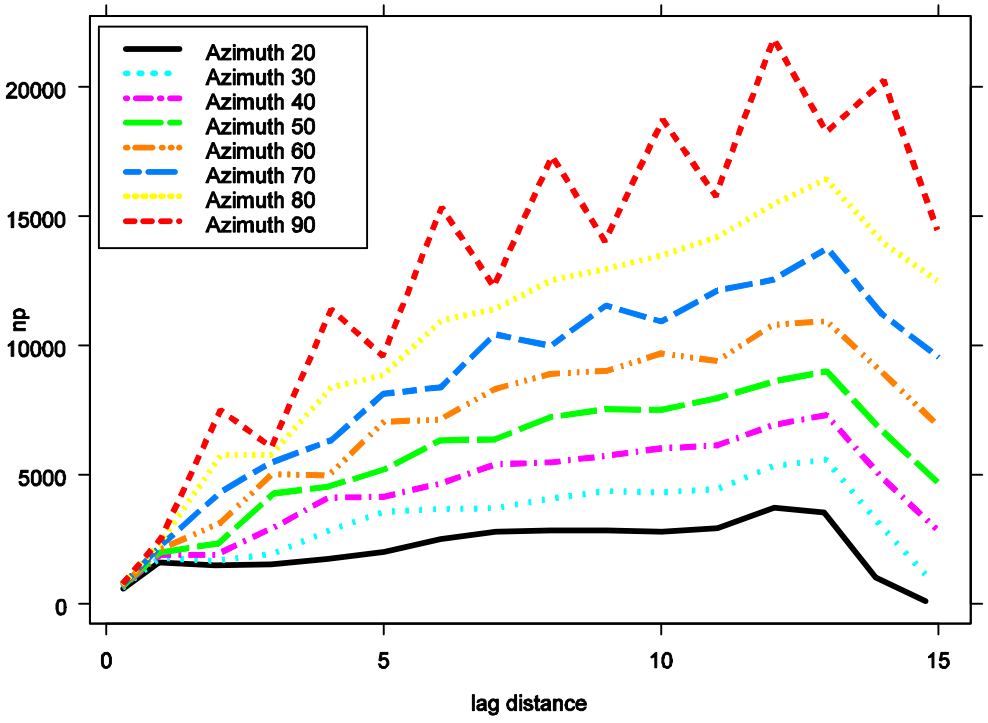

Depth TamesLM Q43 ; Sensitivity analysis for the azimuth tolerance (azimunt 0)

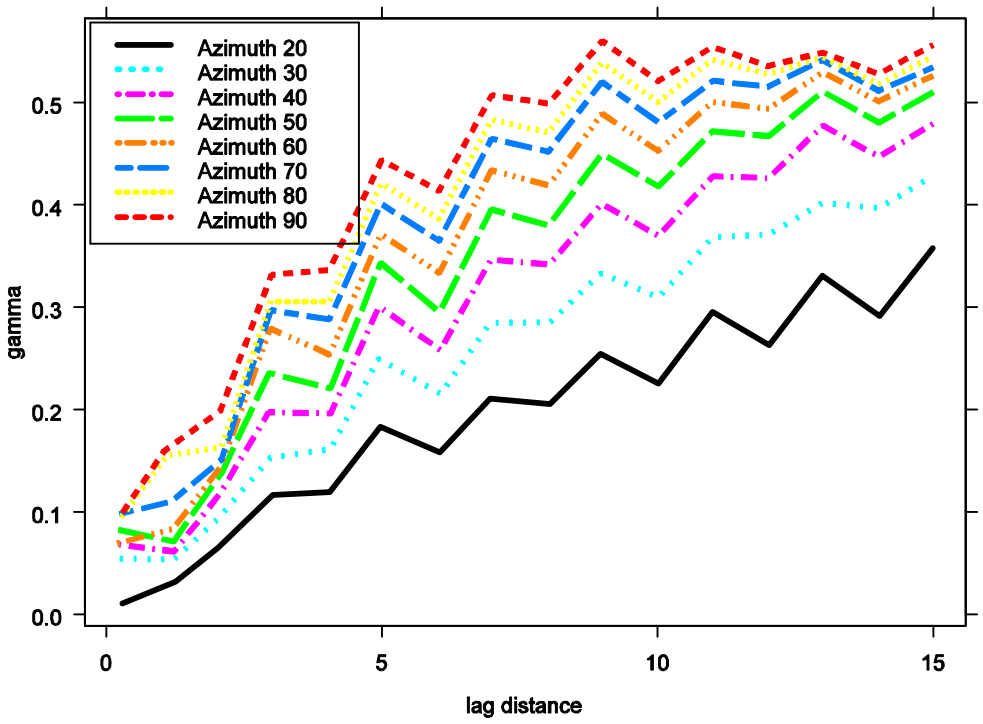

Depth TamesLM Q43 ; Sensitivity analysis for the azimuth tolerance: Number of pair of points (azimuth 0)

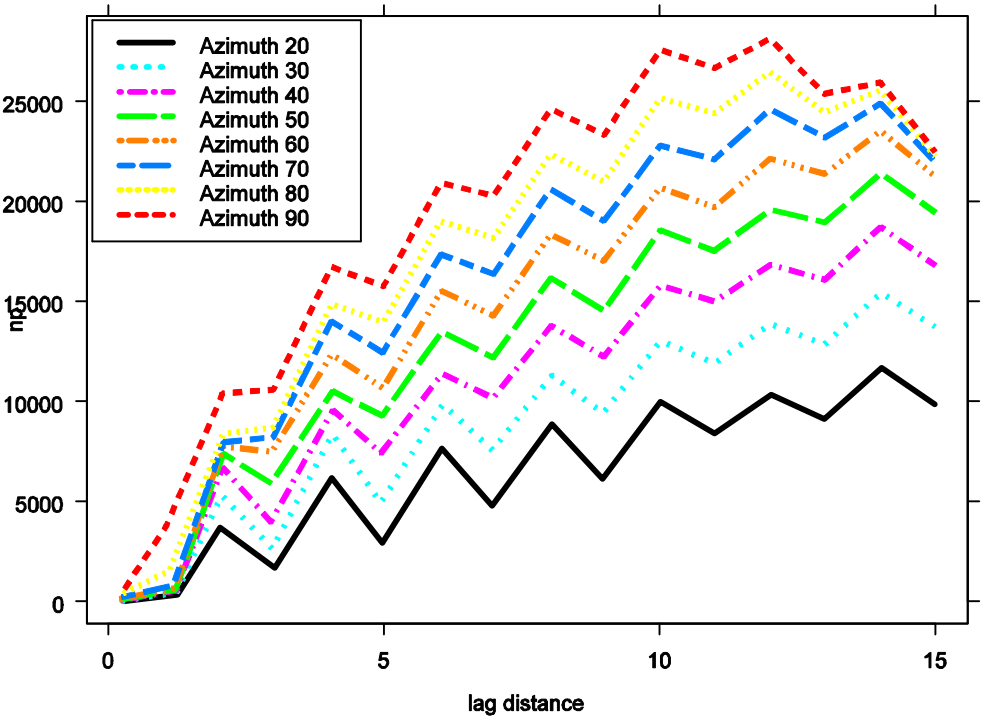

Depth TamesLM Q43 ; Sensitivity analysis for the azimuth tolerance (azimuth 90)

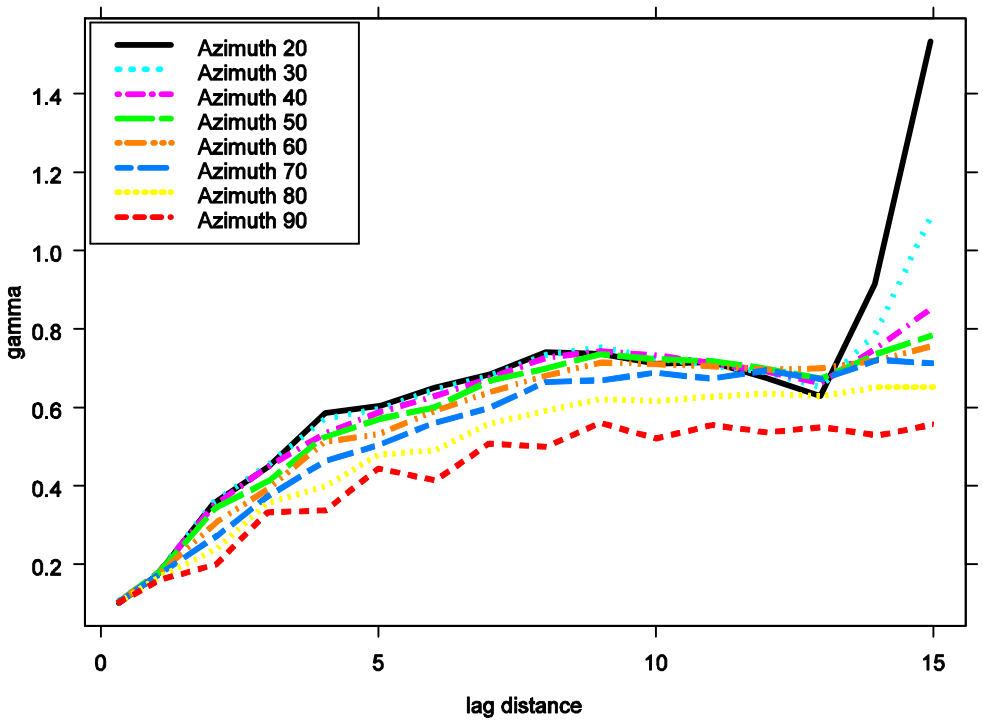

Depth TamesLM Q43 ; Sensitivity analysis for the azimuth tolerance: Number of pair of points (azimuth 90)

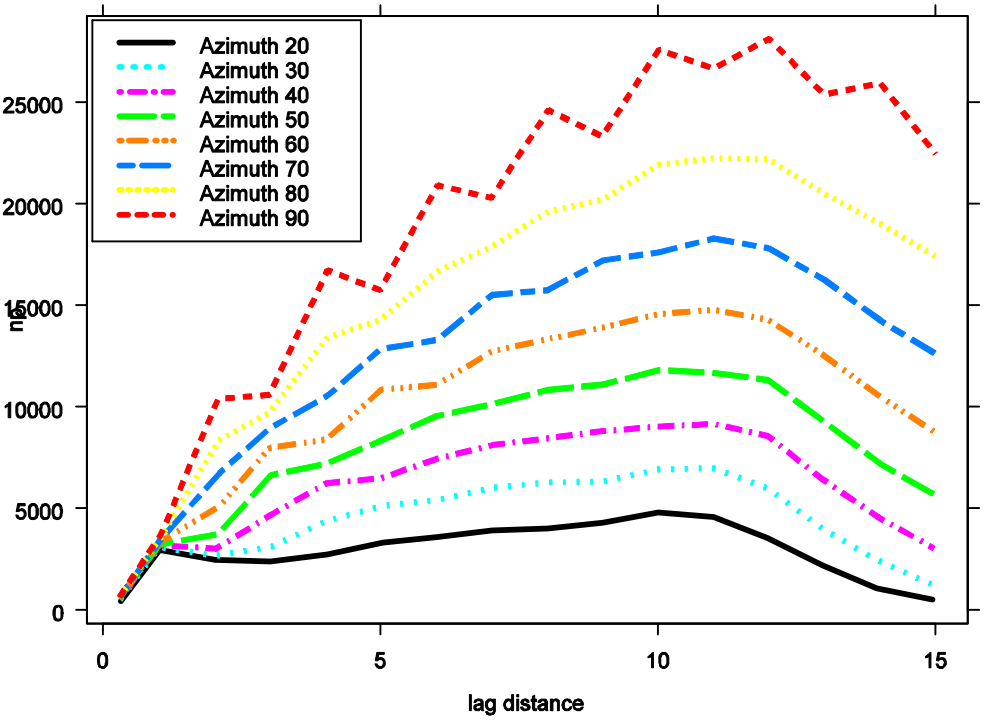

Depth Tarf Q51 ; Sensitivity analysis for the azimuth tolerance (azimunt 0)

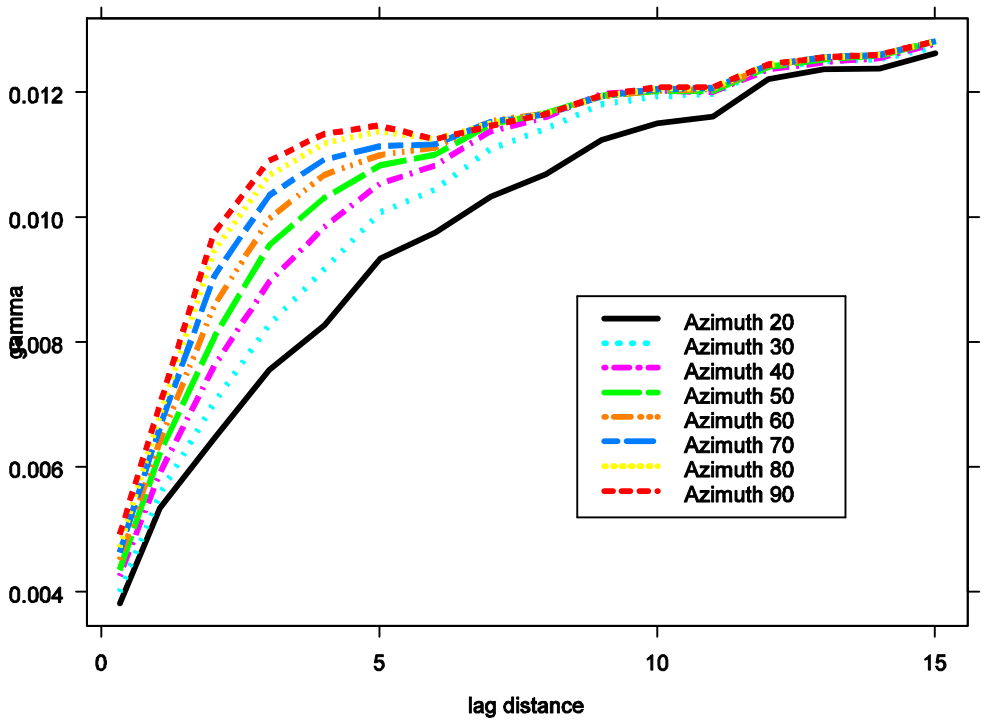

Depth Tarf Q51 ; Sensitivity analysis for the azimuth tolerance: Number of pair of points (azimuth 0)

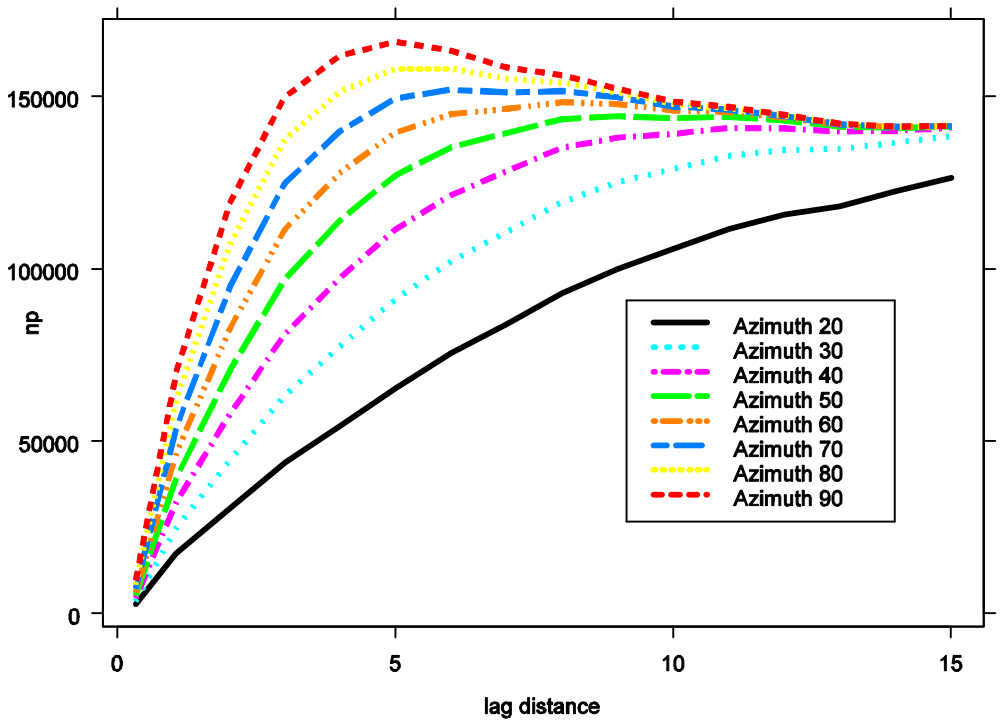

Depth Tarf Q51 ; Sensitivity analysis for the azimuth tolerance (azimuth 90)

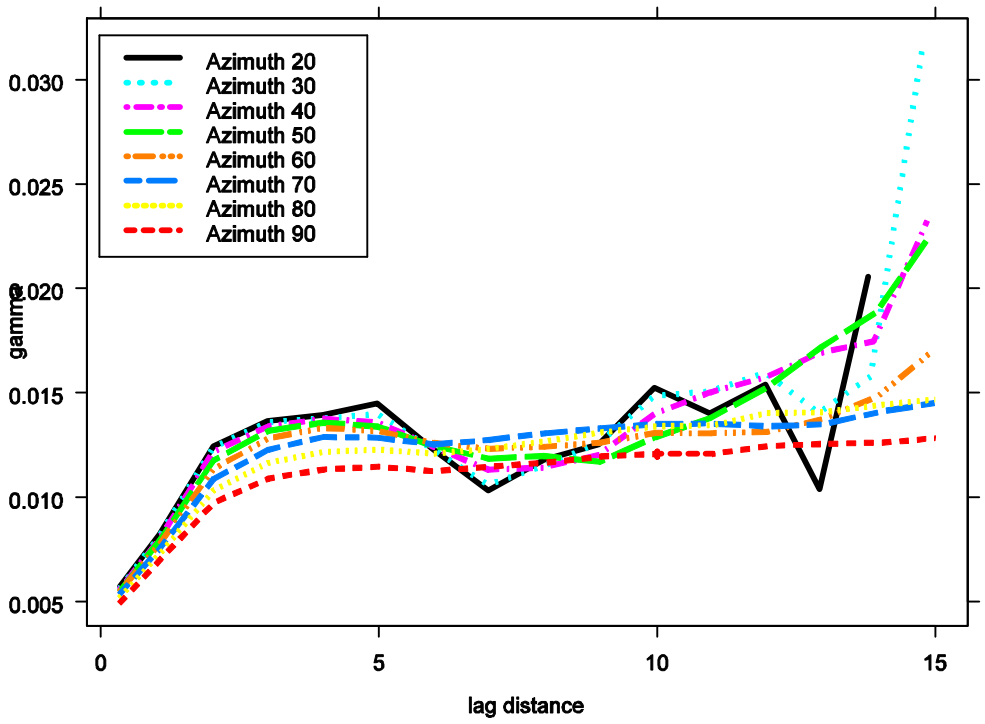

Depth Tarf Q51 ; Sensitivity analysis for the azimuth tolerance: Number of pair of points (azimuth 90)

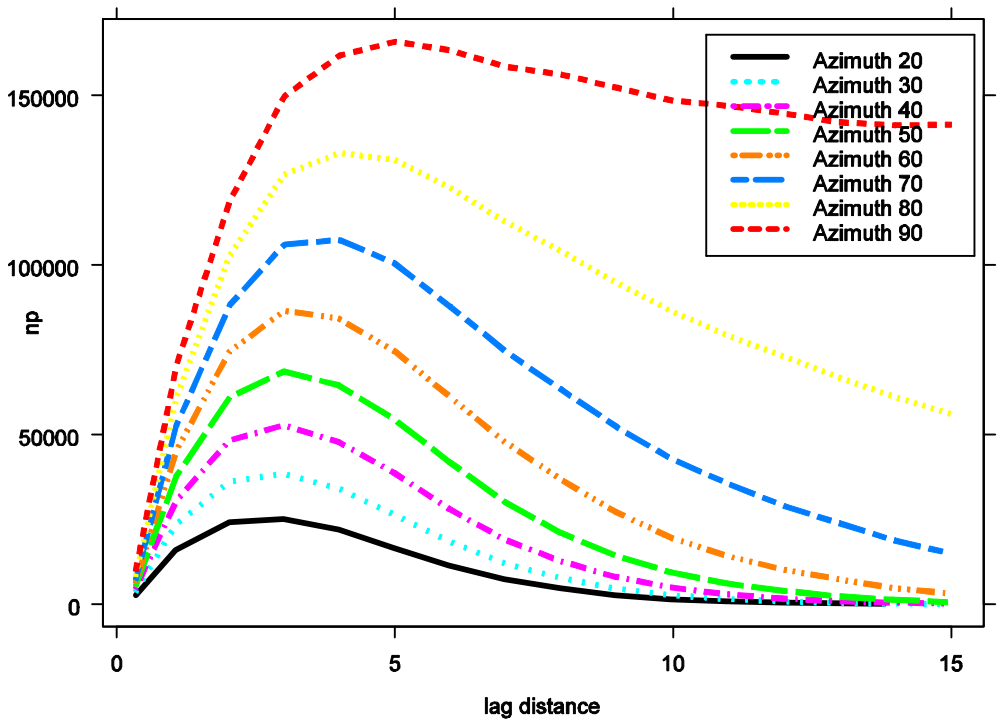

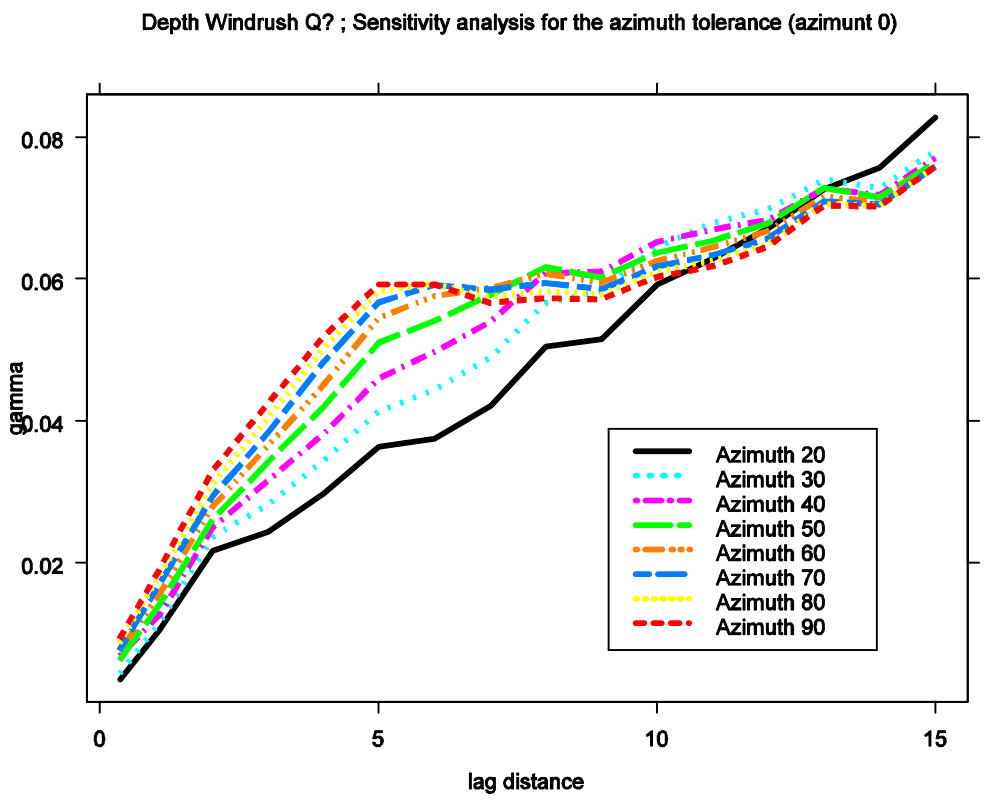
Depth Windrush Q? ; Sensitivity analysis for the azimuth tolerance (azimunt 0)
gamma
0.02
0.04
0.06
0.08
0
5
10
15
lag distance
Azimuth 20
Azimuth 30
Azimuth 40
Azimuth 50
Azimuth 60
Azimuth 70
Azimuth 80
Azimuth 90

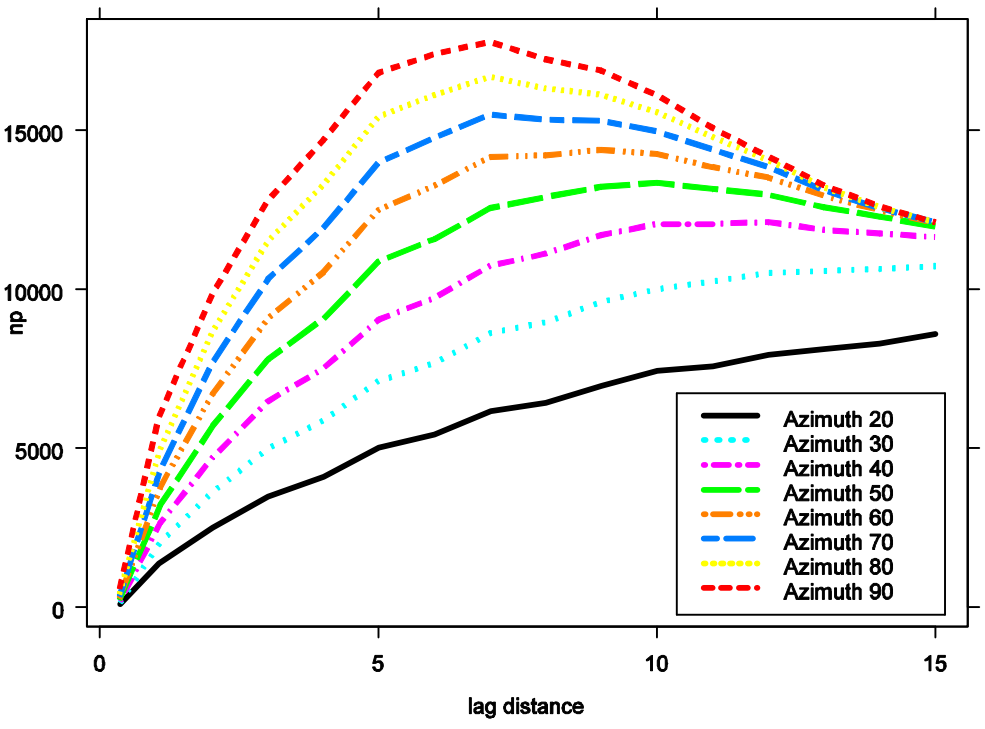
Depth Windrush Q? ; Sensitivity analysis for the azimuth tolerance: Number of pair of points (azimuth 0)
np
0
5000
10000
15000
0
5
10
15
lag distance
Azimuth 20
Azimuth 30
Azimuth 40
Azimuth 50
Azimuth 60
Azimuth 70
Azimuth 80
Azimuth 90

Depth Windrush Q? ; Sensitivity analysis for the azimuth tolerance (azimuth 90)

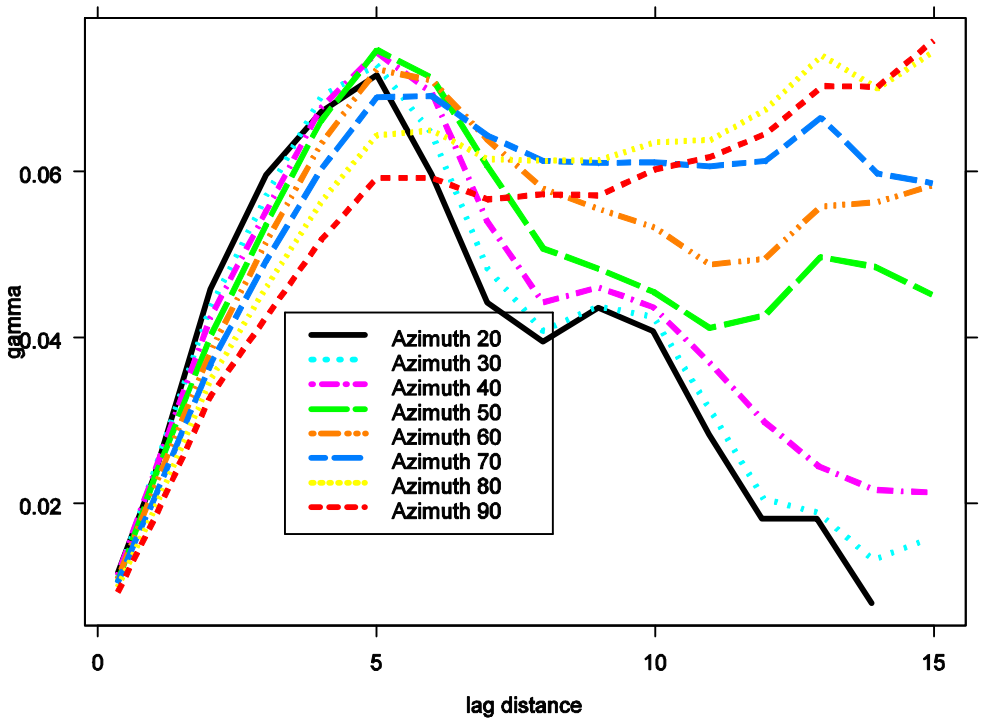

Depth Windrush Q? ; Sensitivity analysis for the azimuth tolerance: Number of pair of points (azimuth 90)

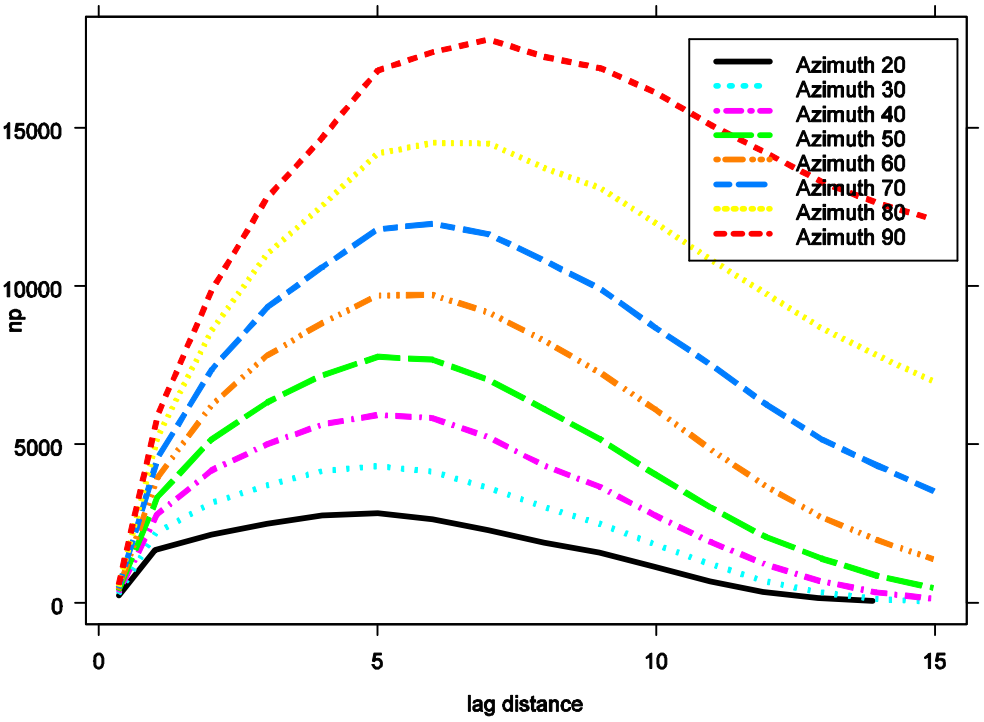

Azimuth tolerance Wet points

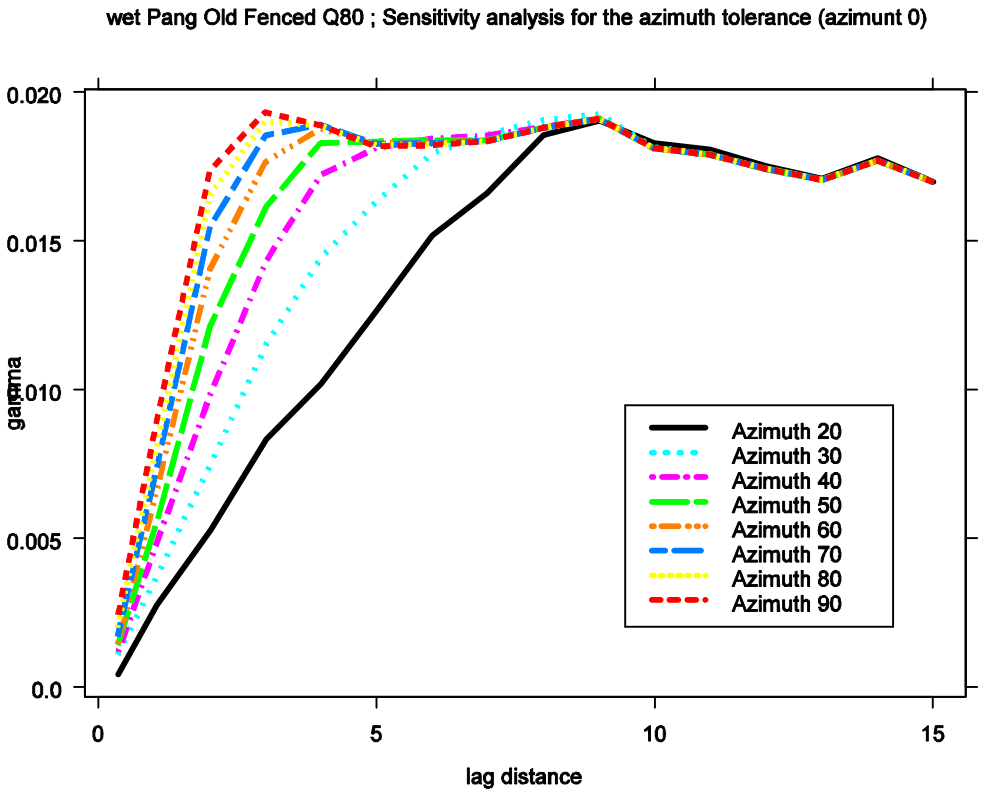

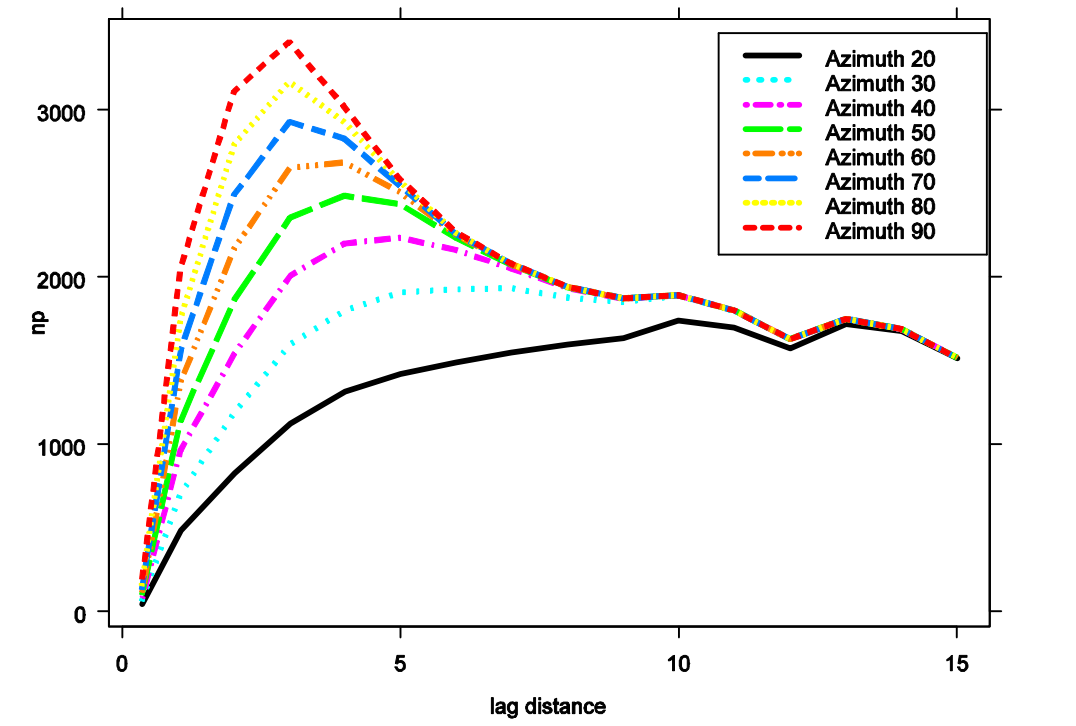

wet Pang Old Fenced Q80 ; Sensitivity analysis for the azimuth tolerance (azimuth 90)

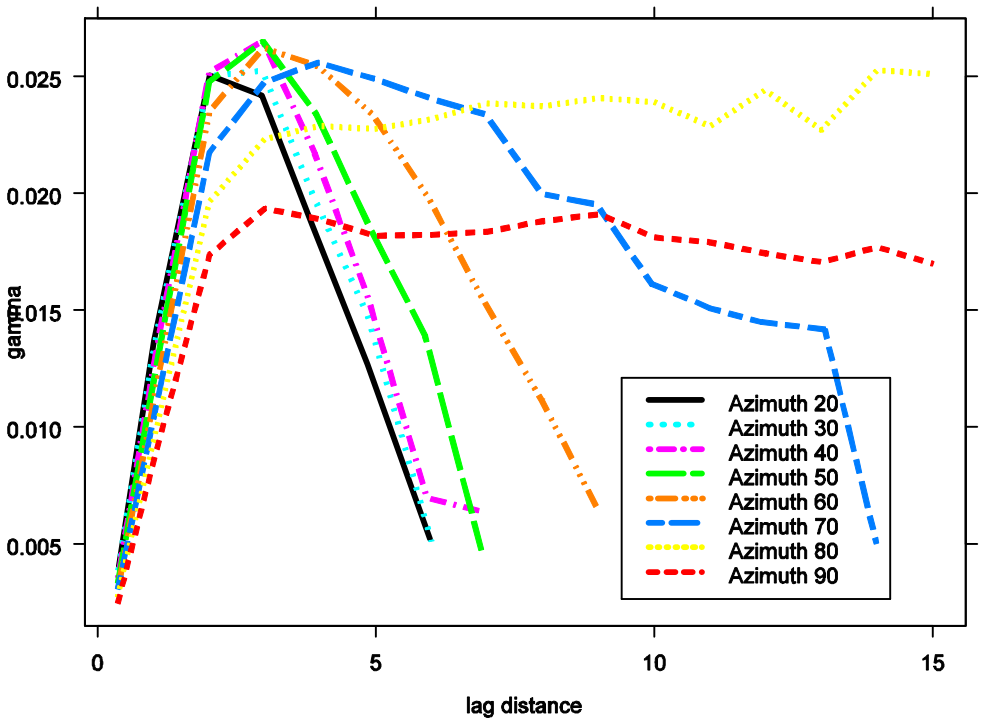

wet Pang Old Fenced Q80 ; Sensitivity analysis for the azimuth tolerance: Number of pair of points (azimuth 90)

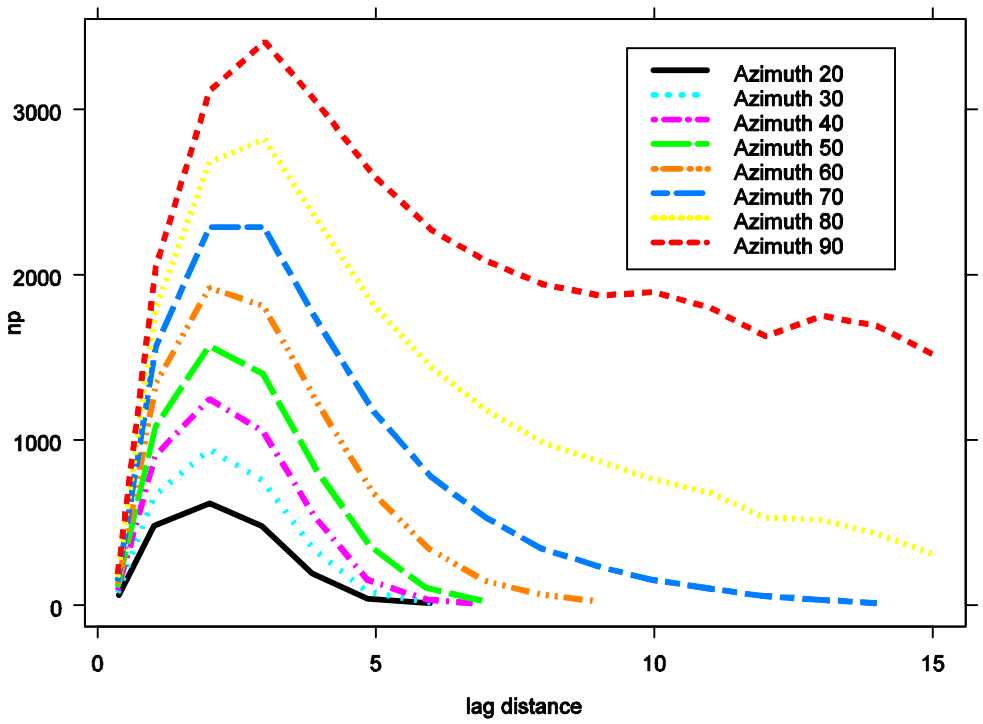

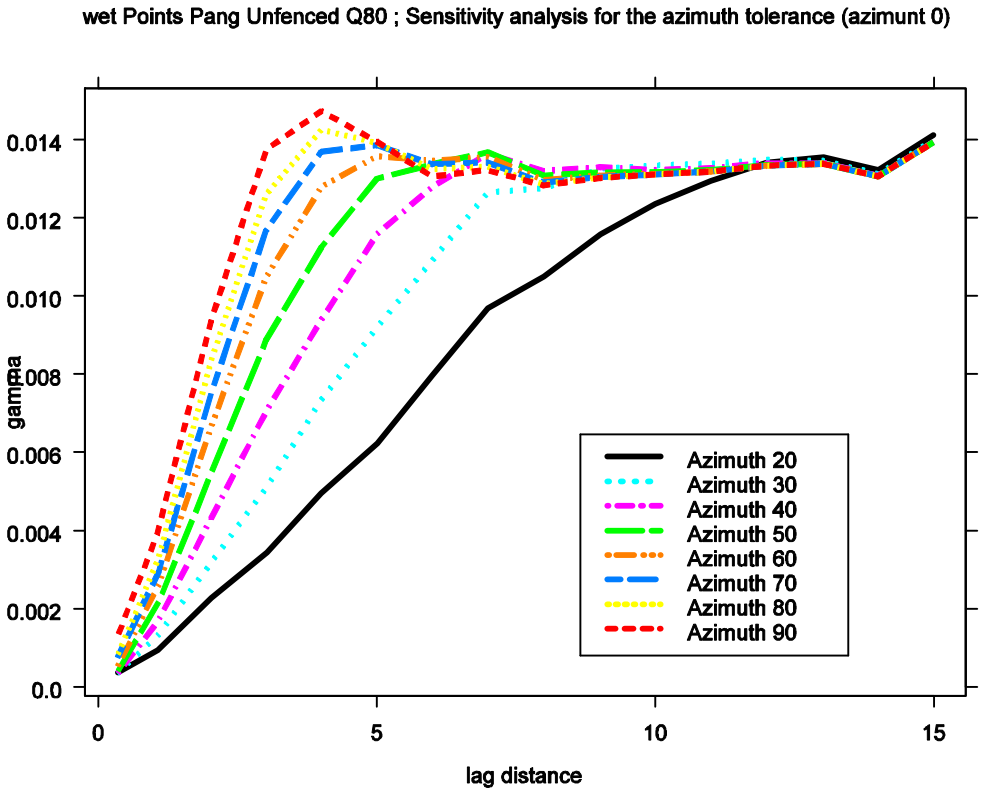
wet Points Pang Unfenced Q80 ; Sensitivity analysis for the azimuth tolerance (azimunt 0)
gamma
0.0
0.002
0.004
0.006
0.008
0.010
0.012
0.014
0
5
10
15
lag distance
Azimuth 20
Azimuth 30
Azimuth 40
Azimuth 50
Azimuth 60
Azimuth 70
Azimuth 80
Azimuth 90

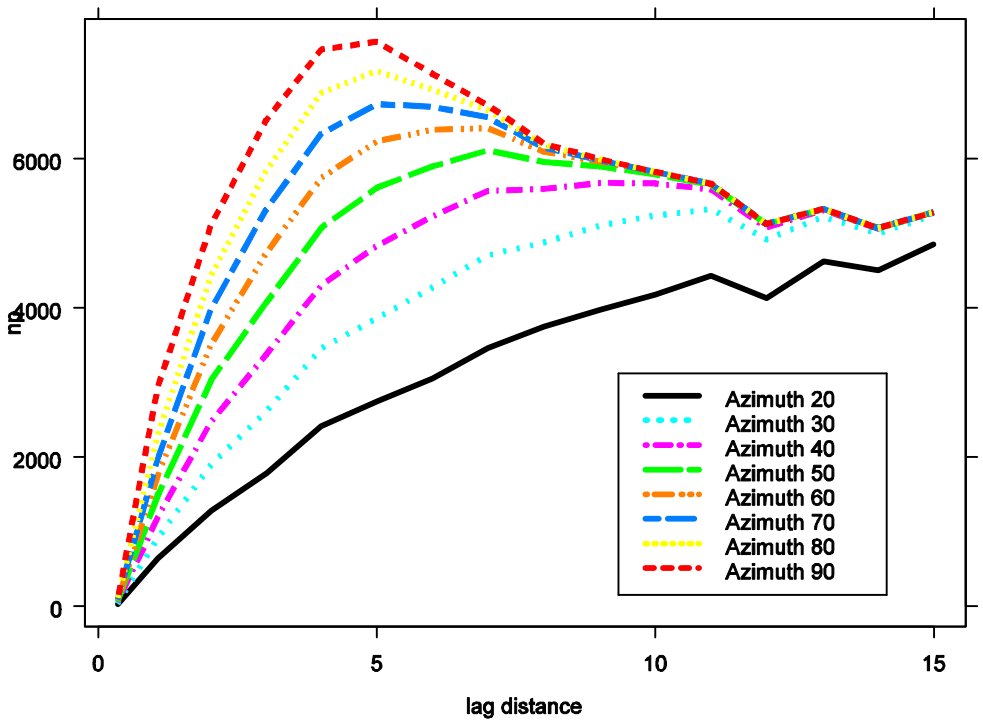
wet Points Pang Unfenced Q80 ; Sensitivity analysis for the azimuth tolerance: Number of pair of points (azimuth 0)
np
0
2000
4000
6000
0
5
10
15
lag distance
Azimuth 20
Azimuth 30
Azimuth 40
Azimuth 50
Azimuth 60
Azimuth 70
Azimuth 80
Azimuth 90

wet Points Pang Unfenced Q80 ; Sensitivity analysis for the azimuth tolerance (azimuth 90)

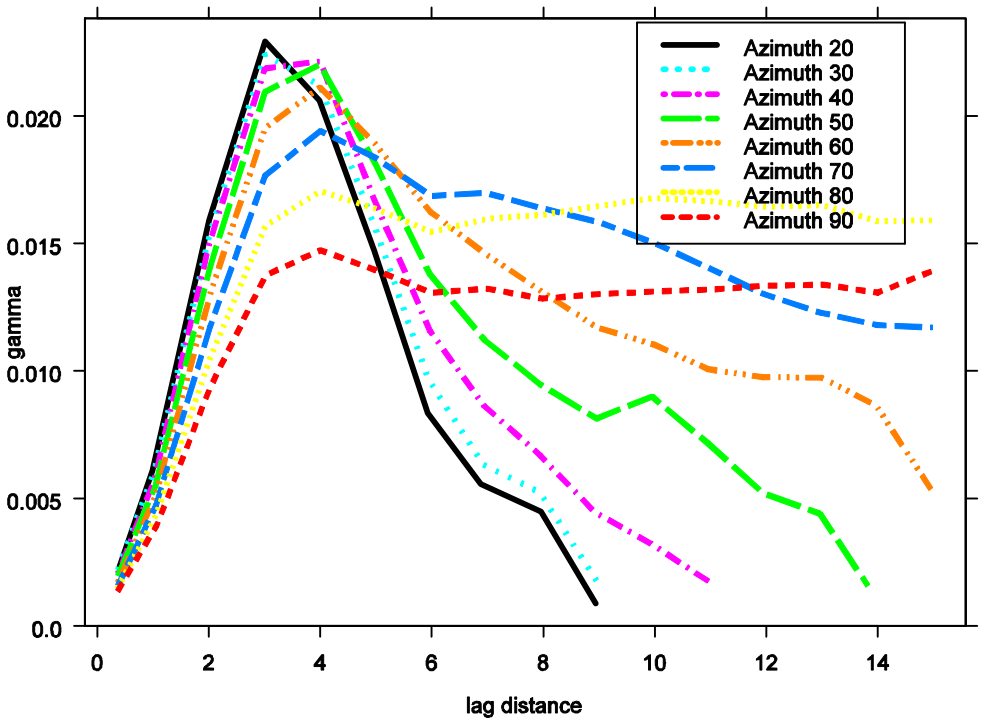

wet Points Pang Unfenced Q80 ; Sensitivity analysis for the azimuth tolerance: Number of pair of points (azimuth 90

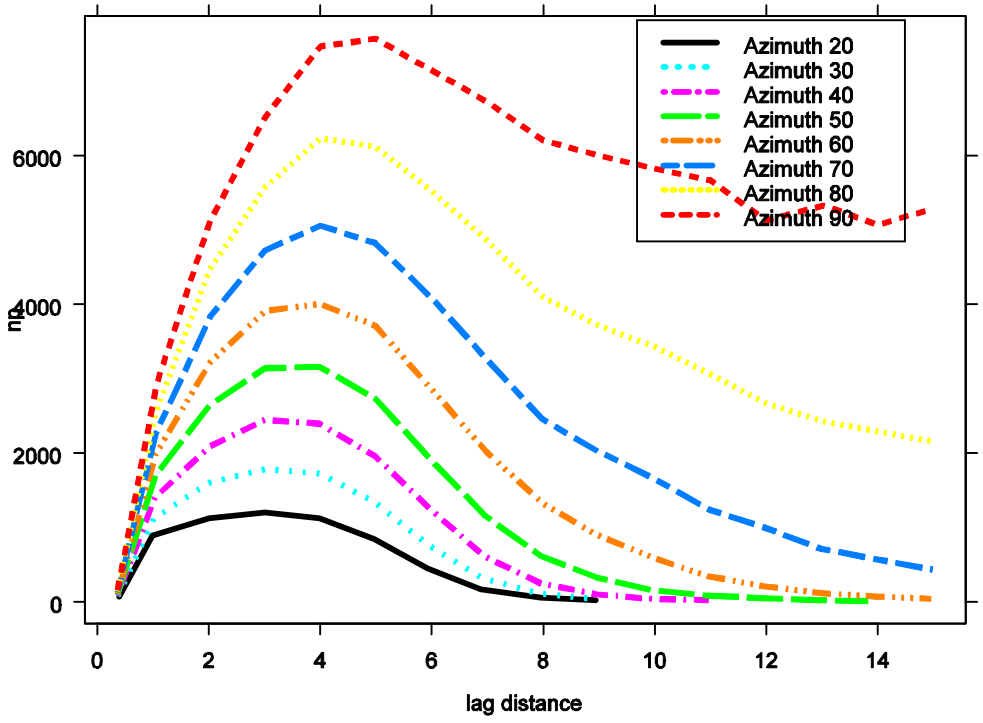

wet points Bere Q79 ; Sensitivity analysis for the azimuth tolerance (azimunt 0)

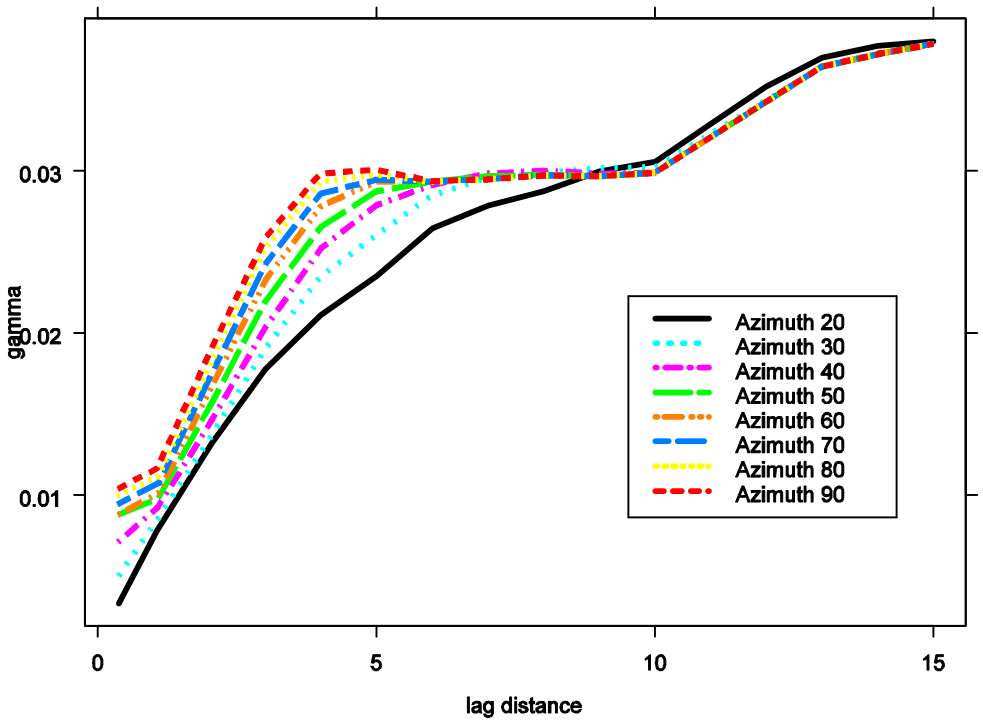

wet points Bere Q79 ; Sensitivity analysis for the azimuth tolerance: Number of pair of points (azimuth 0)

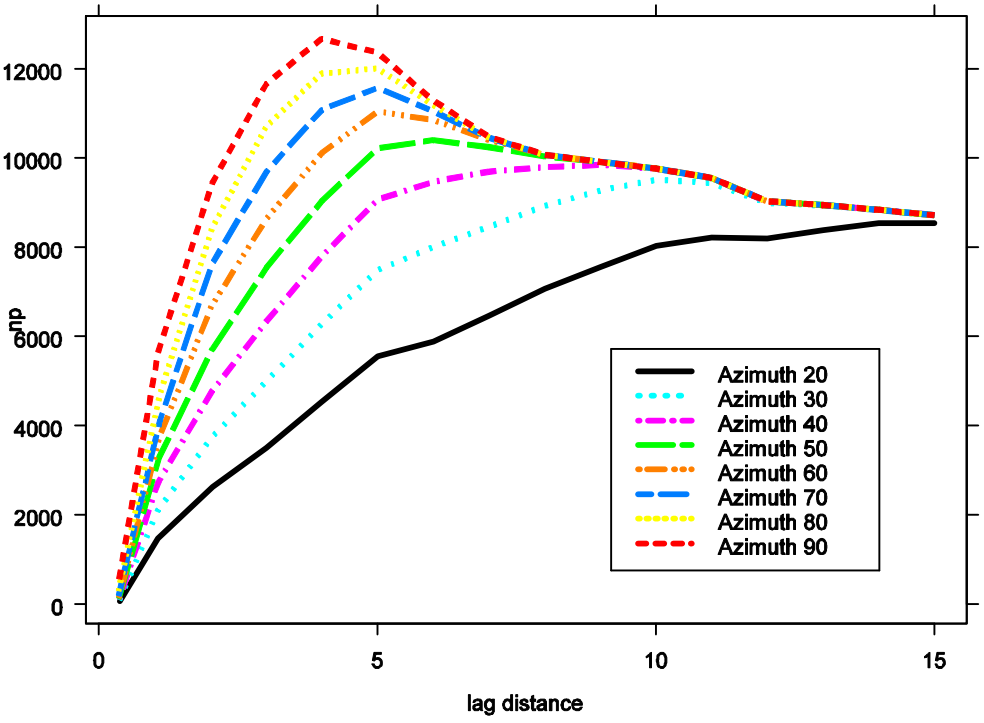

wet points Bere Q79 ; Sensitivity analysis for the azimuth tolerance (azimuth 90)

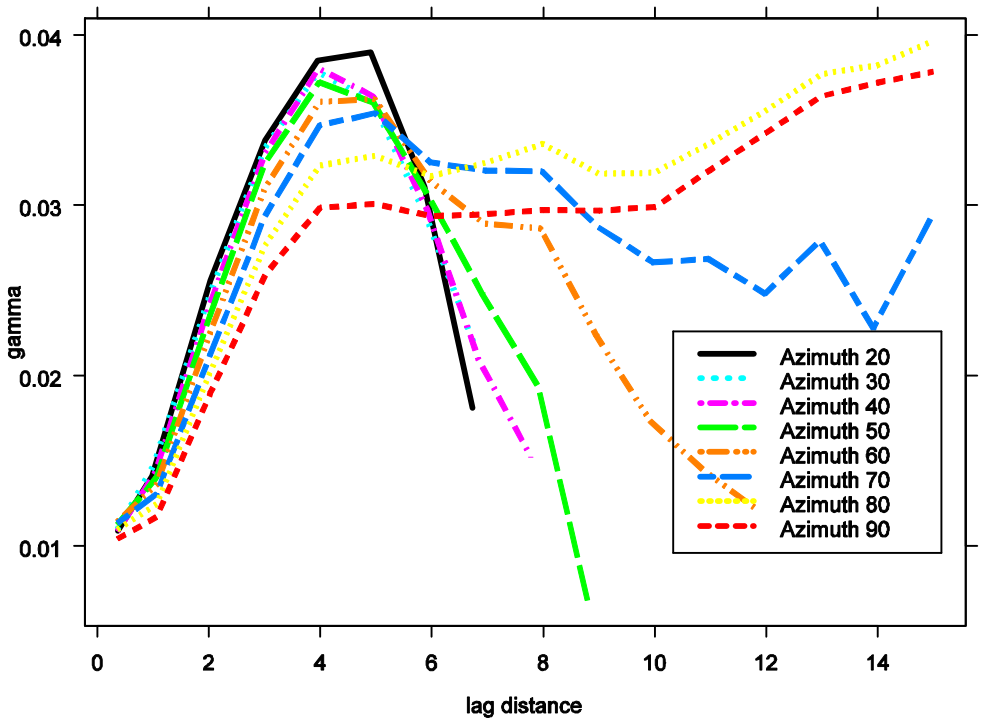

wet points Bere Q79 ; Sensitivity analysis for the azimuth tolerance: Number of pair of points (azimuth 90)

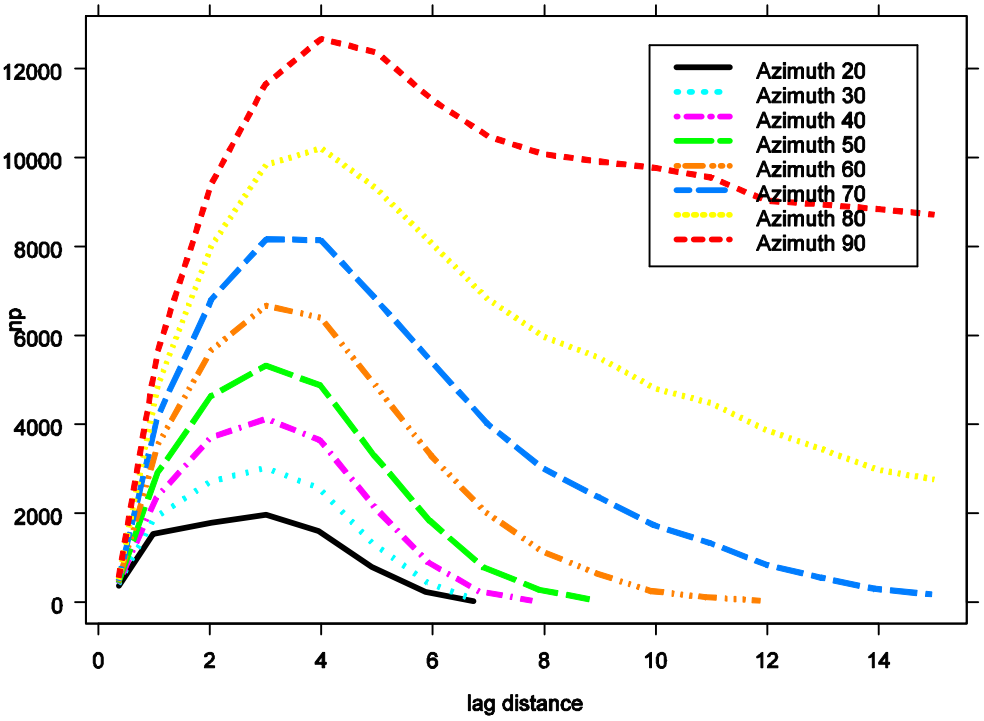

wet points Blackwater Q33 ; Sensitivity analysis for the azimuth tolerance (azimunt 0)

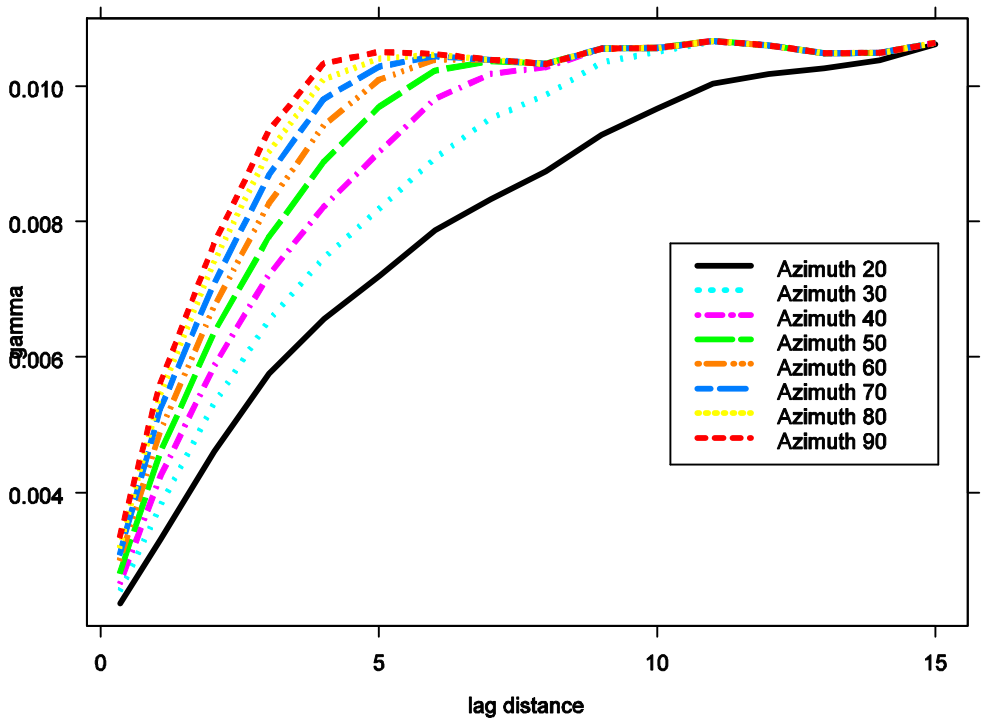

wet points Blackwater Q33 ; Sensitivity analysis for the azimuth tolerance: Number of pair of points (azimuth 0)

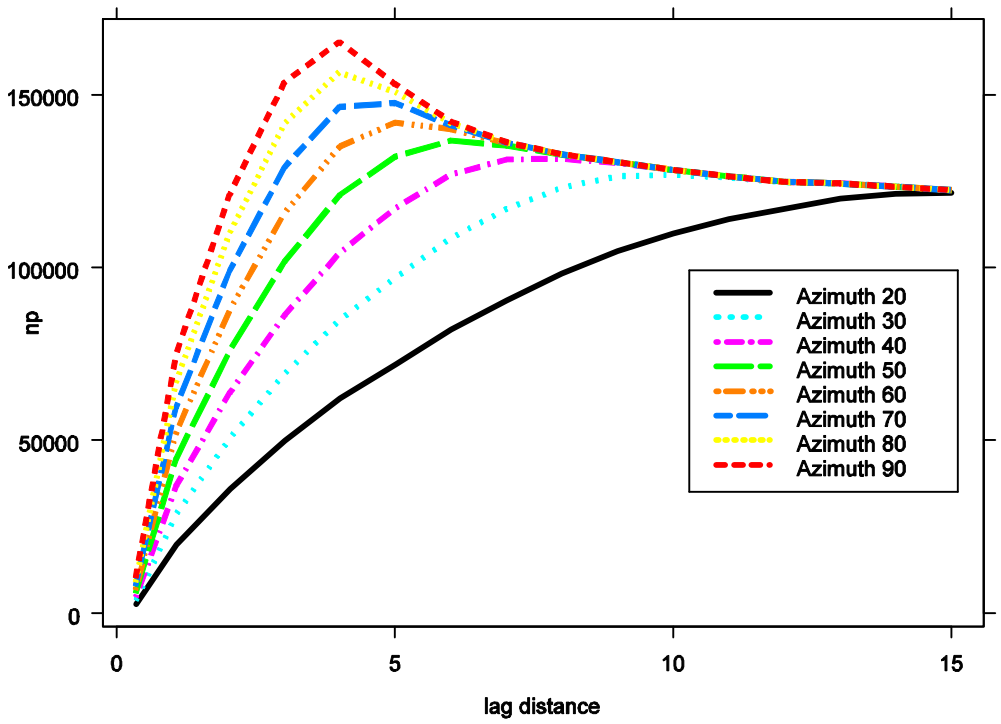

wet points Blackwater Q33 ; Sensitivity analysis for the azimuth tolerance (azimuth 90)

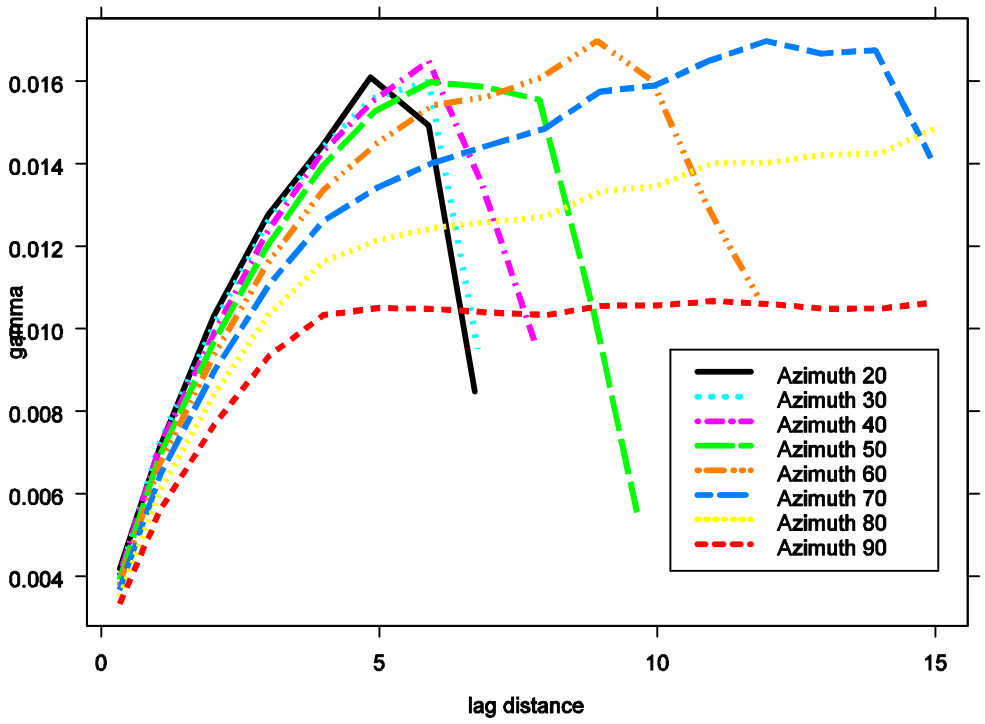

wet points Blackwater Q33 ; Sensitivity analysis for the azimuth tolerance: Number of pair of points (azimuth 90)

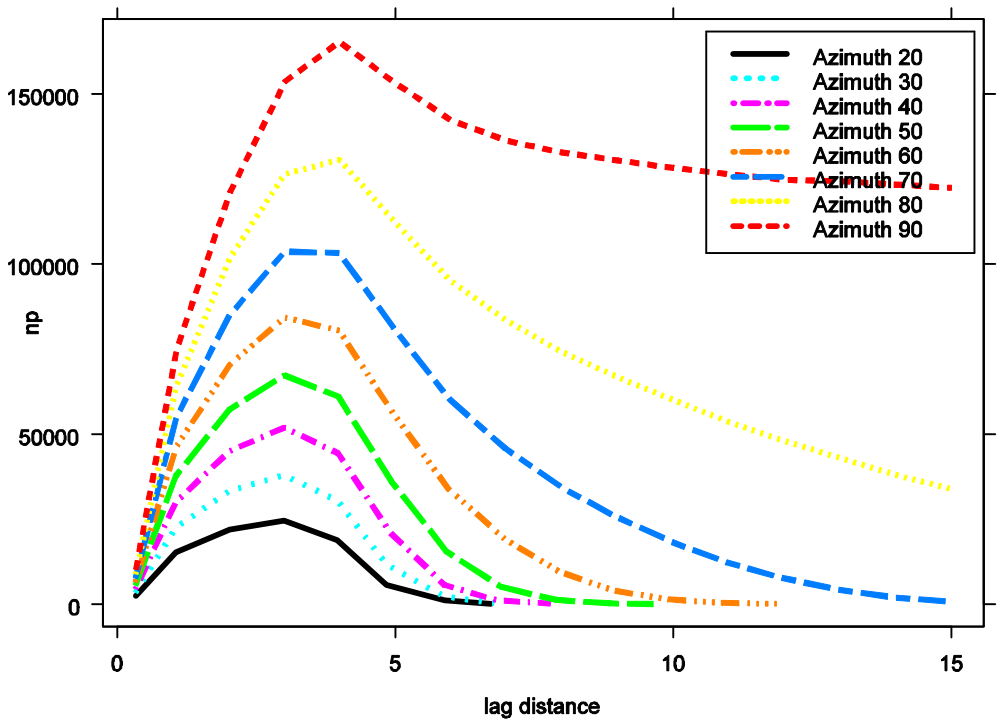

wet points Cruick Q51 ; Sensitivity analysis for the azimuth tolerance (azimunt 0)

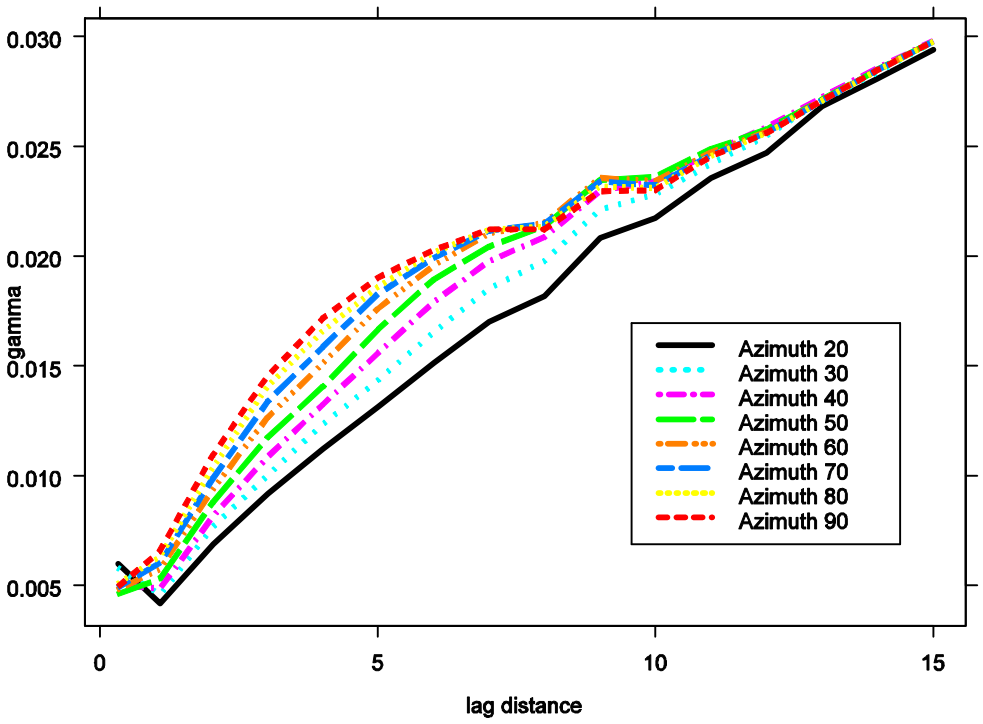

wet points Cruick Q51 ; Sensitivity analysis for the azimuth tolerance: Number of pair of points (azimuth 0)

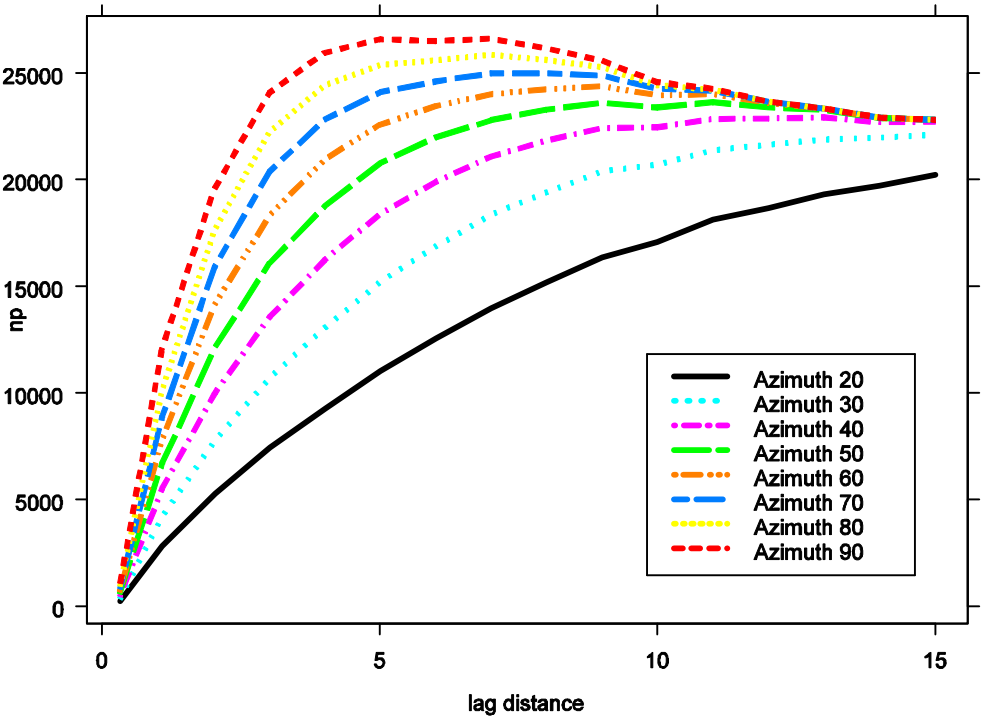

wet points Cruick Q51 ; Sensitivity analysis for the azimuth tolerance (azimuth 90)

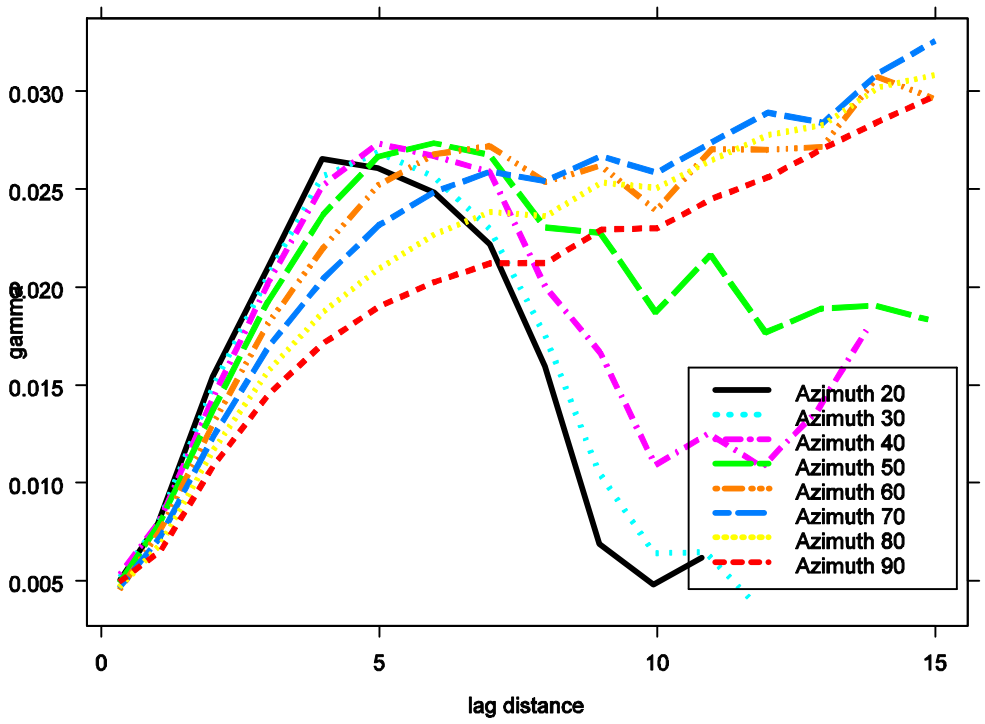

wet points Cruick Q51 ; Sensitivity analysis for the azimuth tolerance: Number of pair of points (azimuth 90)

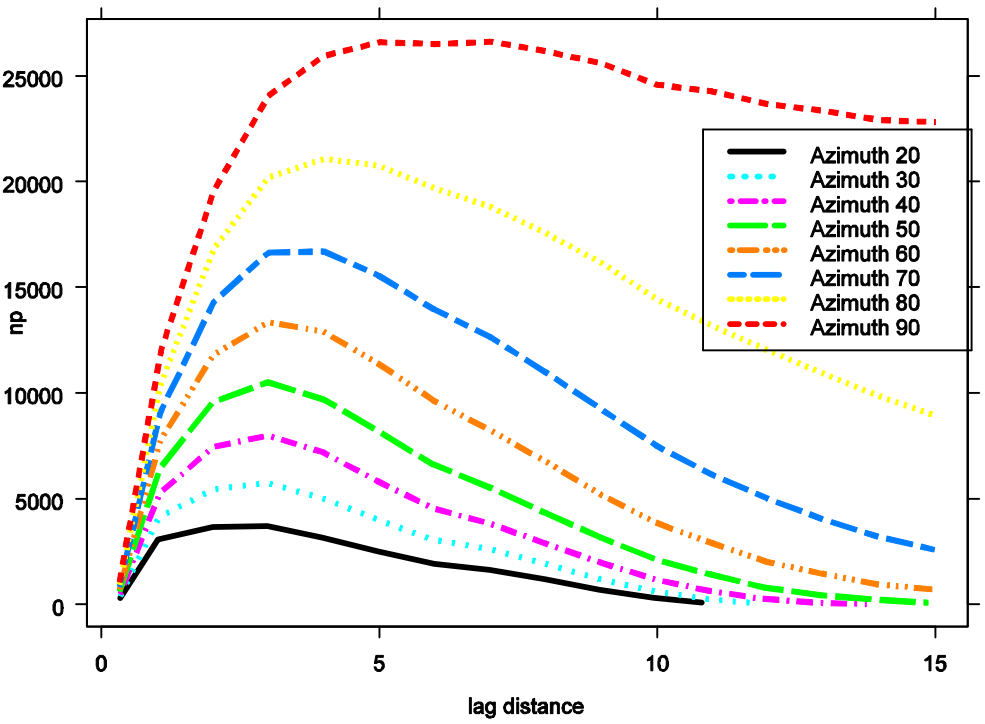

wet points HighlandWater Q43 ; Sensitivity analysis for the azimuth tolerance (azimunt 0)

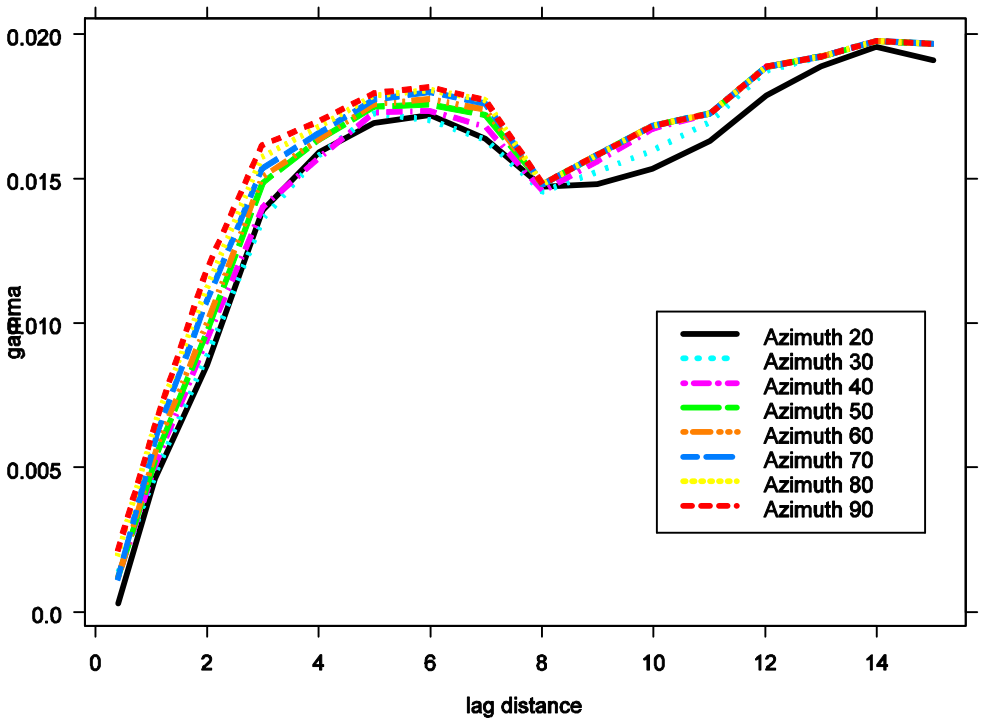

wet points HighlandWater Q43 ; Sensitivity analysis for the azimuth tolerance: Number of pair of points (azimuth 0)

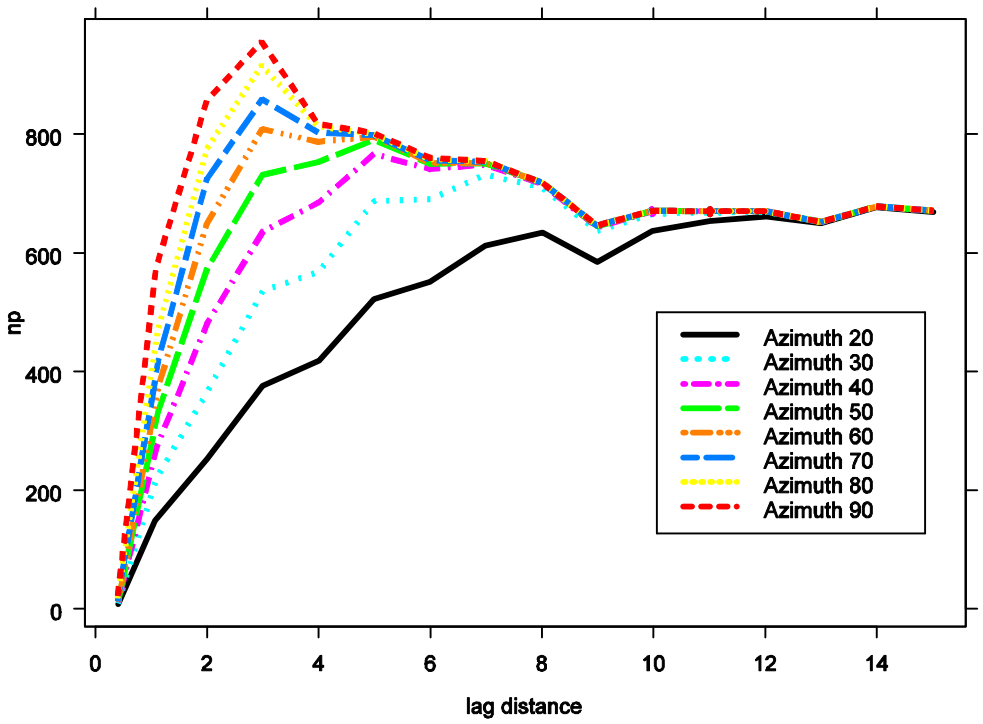

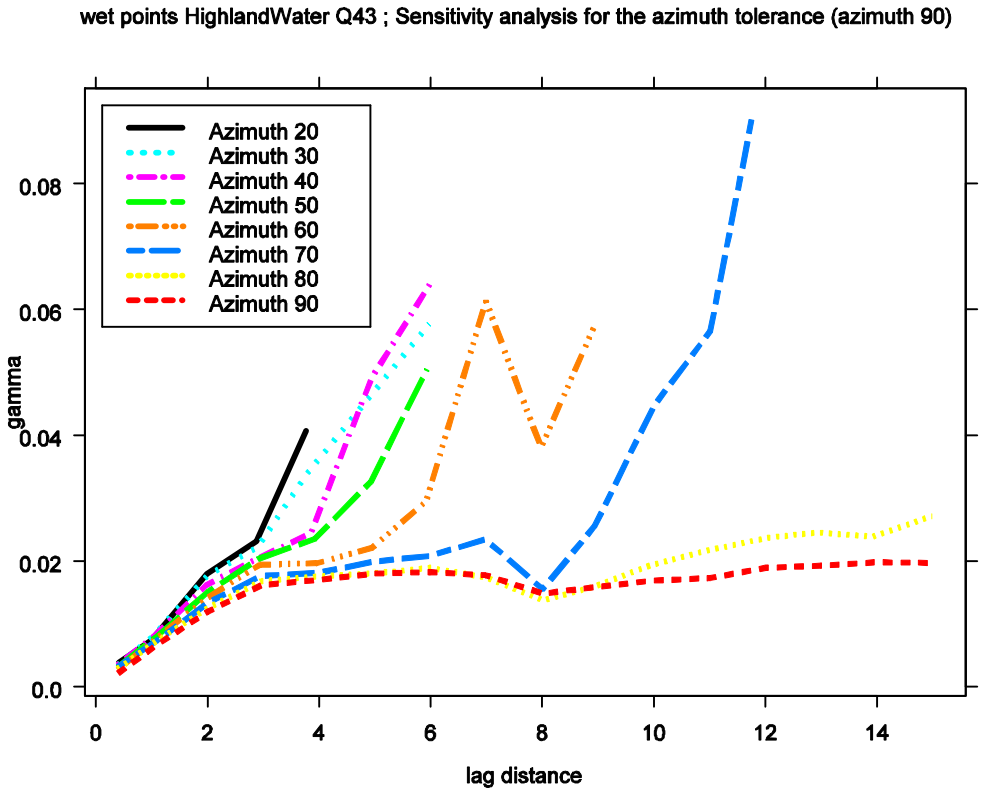
wet points HighlandWater Q43 ; Sensitivity analysis for the azimuth tolerance (azimuth 90)
Azimuth 20
Azimuth 30
Azimuth 40
Azimuth 50
Azimuth 60
Azimuth 70
Azimuth 80
Azimuth 90
gamma
0.0
0.02
0.04
0.06
0.08
0
2
4
6
8
10
12
14
lag distance

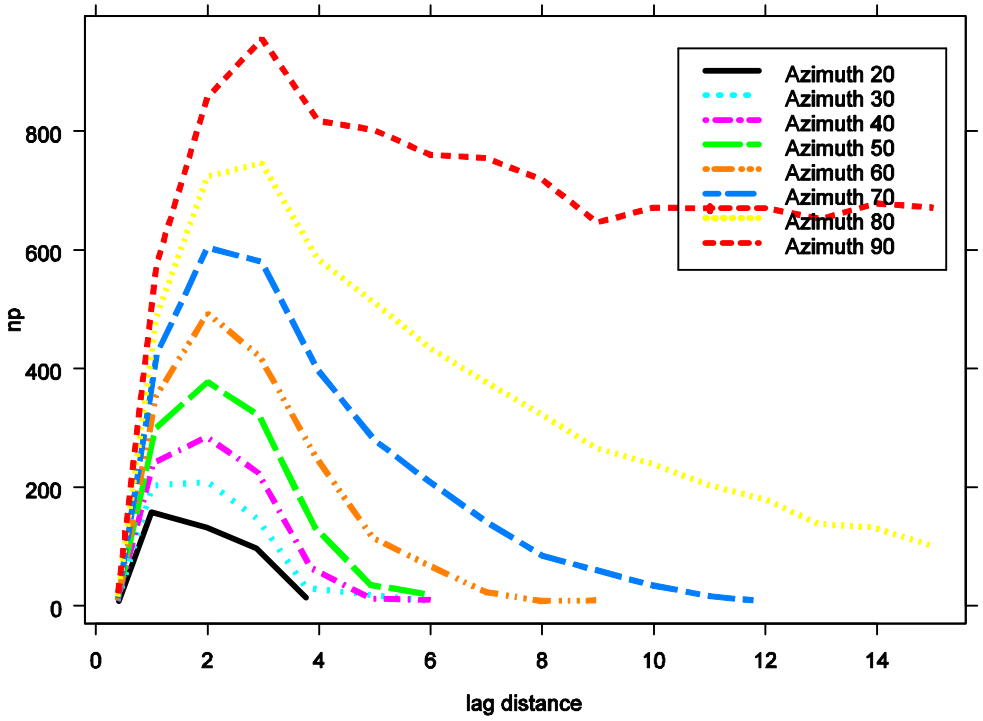
wet points HighlandWater Q43 ; Sensitivity analysis for the azimuth tolerance: Number of pair of points (azimuth 90)
Azimuth 20
Azimuth 30
Azimuth 40
Azimuth 50
Azimuth 60
Azimuth 70
Azimuth 80
Azimuth 90
np
0
200
400
600
800
0
2
4
6
8
10
12
14
lag distance

wet points Lambourn Q92 ; Sensitivity analysis for the azimuth tolerance (azimunt 0)

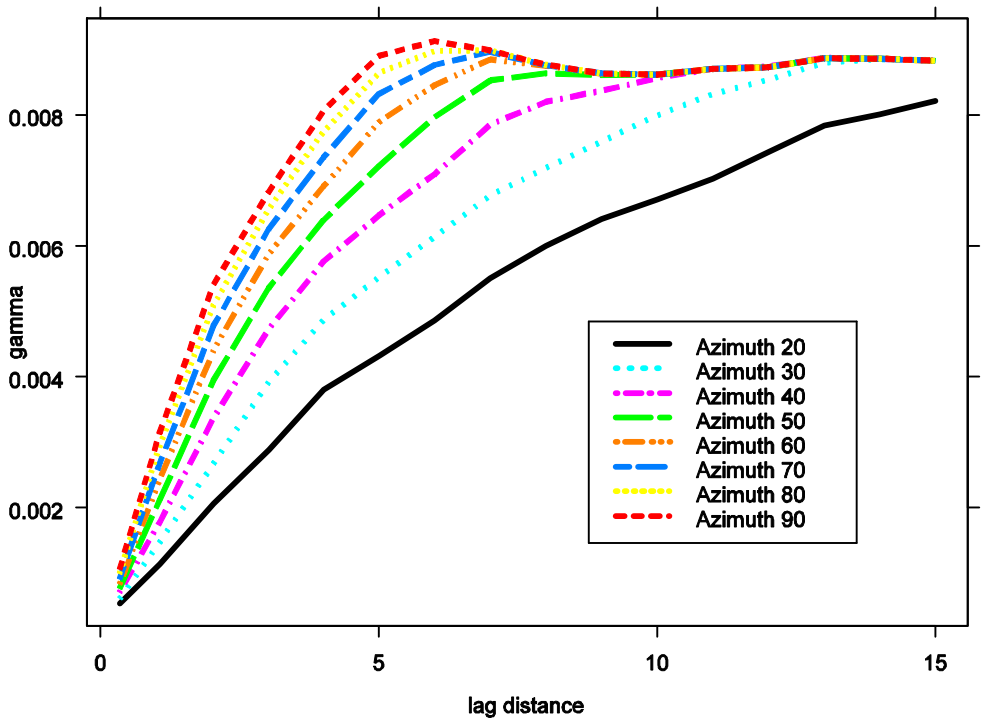

wet points Lambourn Q92 ; Sensitivity analysis for the azimuth tolerance: Number of pair of points (azimuth 0)

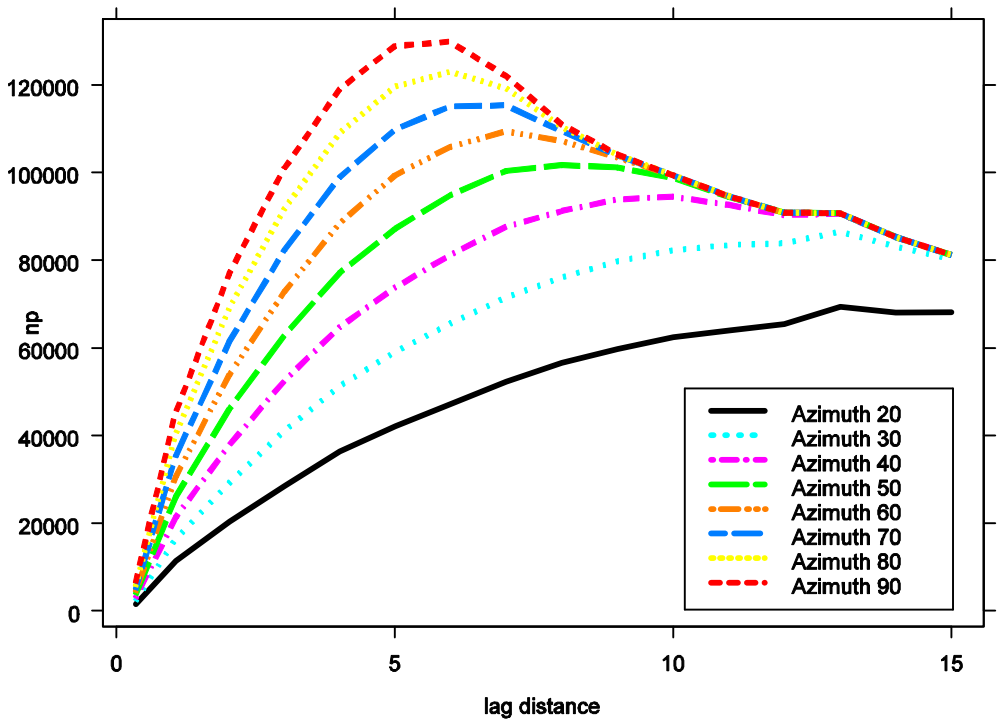

wet points Lambourn Q92 ; Sensitivity analysis for the azimuth tolerance (azimuth 90)

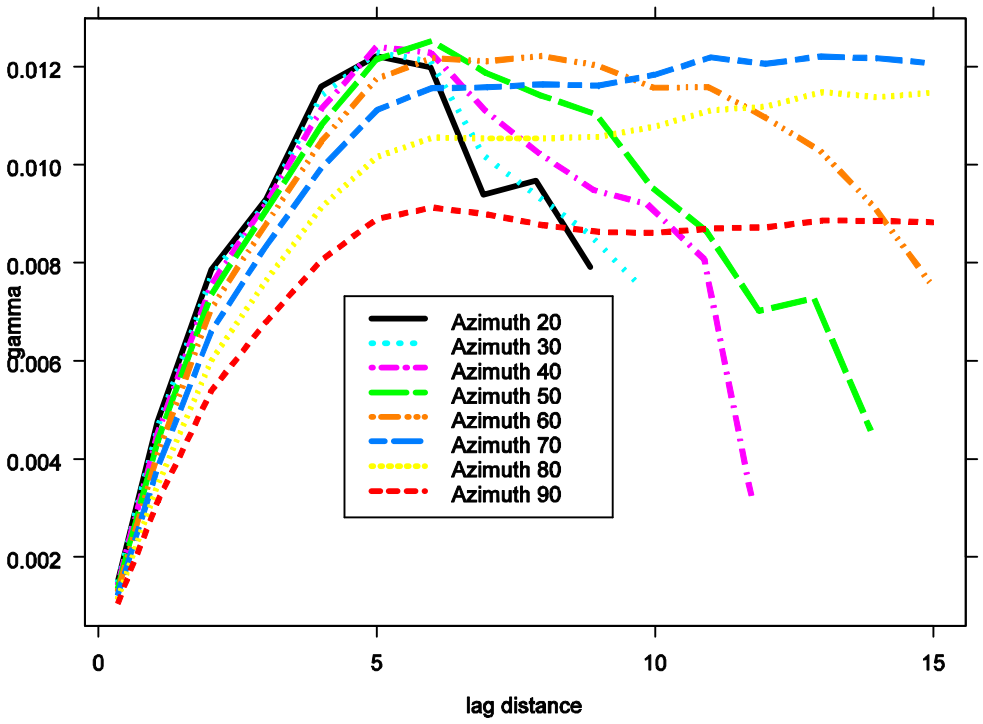

wet points Lambourn Q92 ; Sensitivity analysis for the azimuth tolerance: Number of pair of points (azimuth 90)

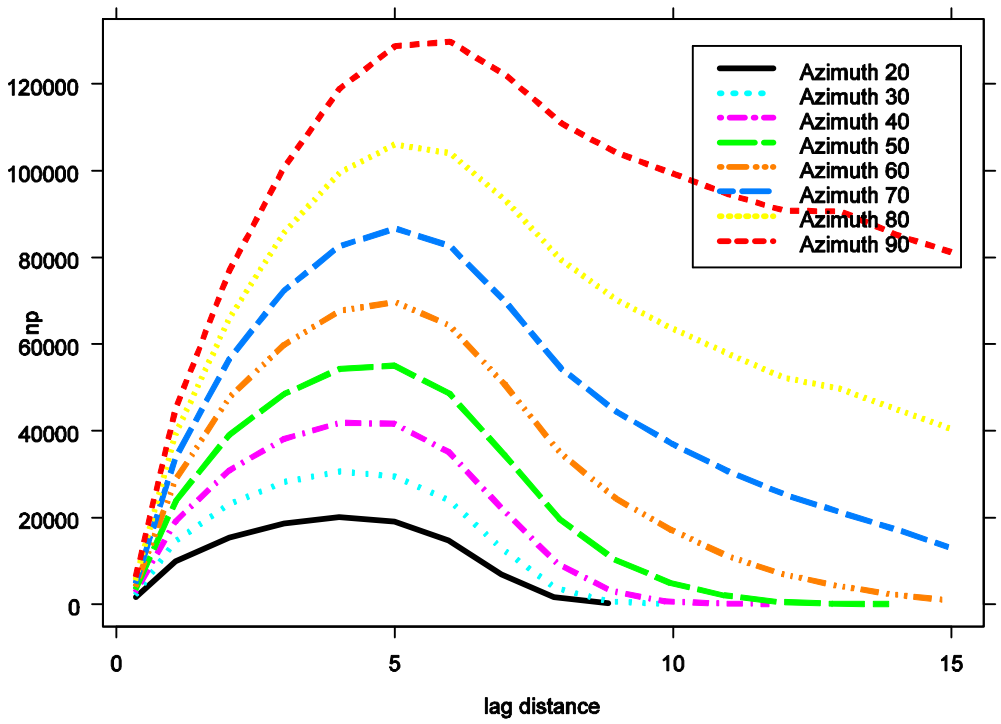

wet points Pang Fenced Q91 ; Sensitivity analysis for the azimuth tolerance (azimunt 0)

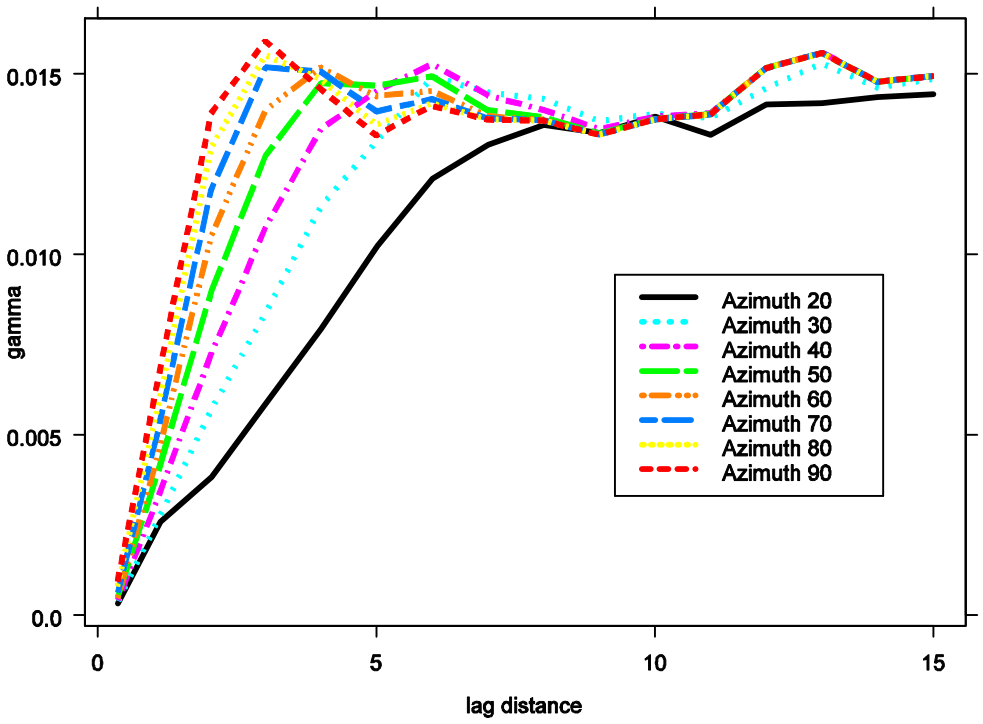

wet points Pang Fenced Q91 ; Sensitivity analysis for the azimuth tolerance: Number of pair of points (azimuth 0)

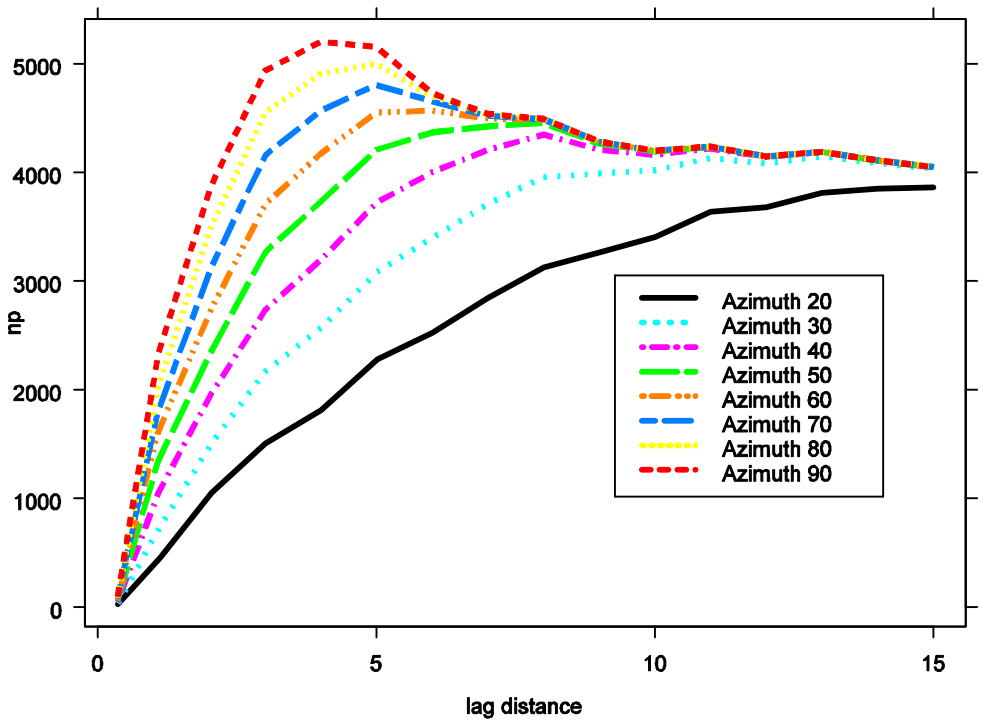

wet points Pang Fenced Q91 ; Sensitivity analysis for the azimuth tolerance (azimuth 90)

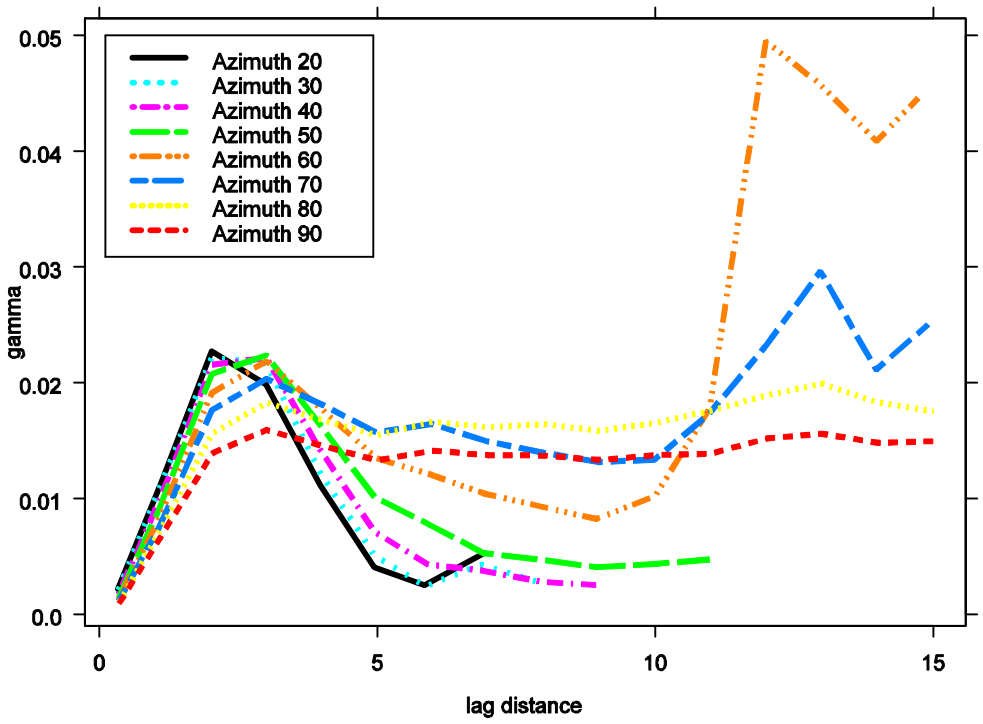

wet points Pang Fenced Q91 ; Sensitivity analysis for the azimuth tolerance: Number of pair of points (azimuth 90)

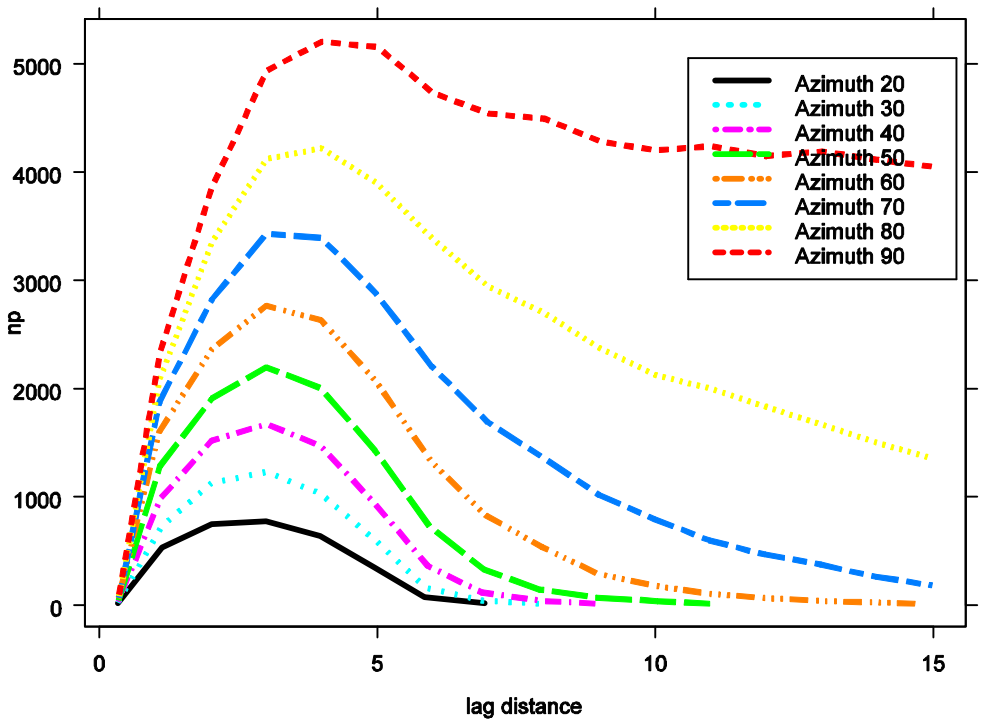

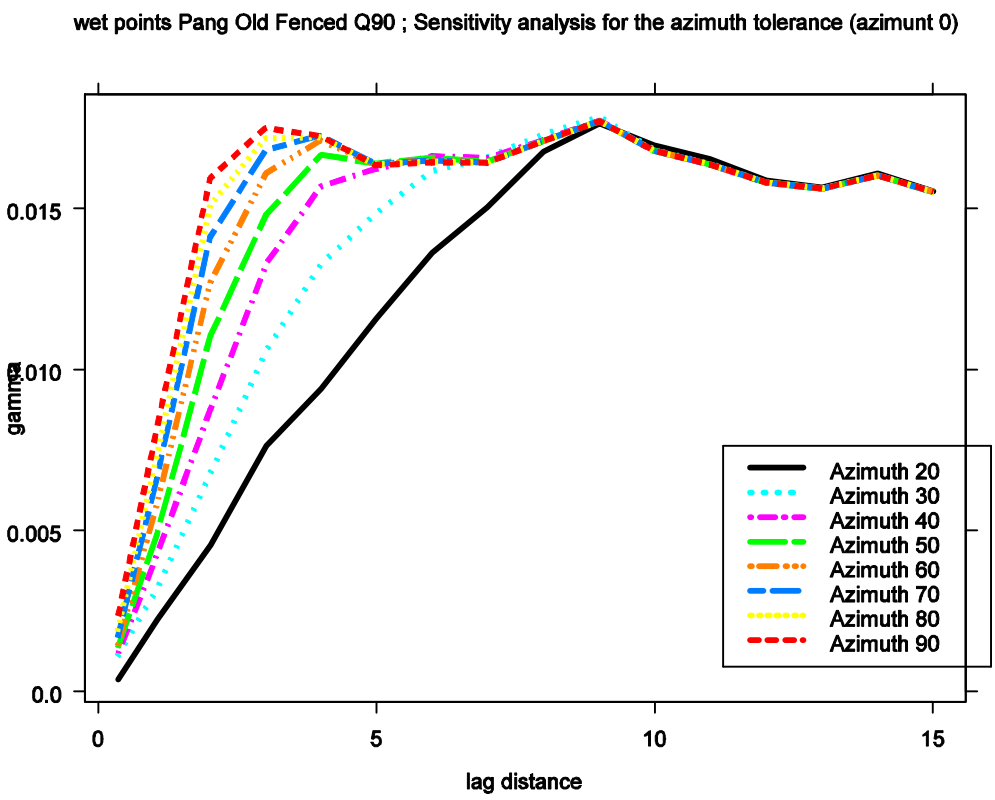
wet points Pang Old Fenced Q90 ; Sensitivity analysis for the azimuth tolerance (azimunt 0)
gamma
0.0
0.005
0.010
0.015
0
5
10
15
lag distance
Azimuth 20
Azimuth 30
Azimuth 40
Azimuth 50
Azimuth 60
Azimuth 70
Azimuth 80
Azimuth 90

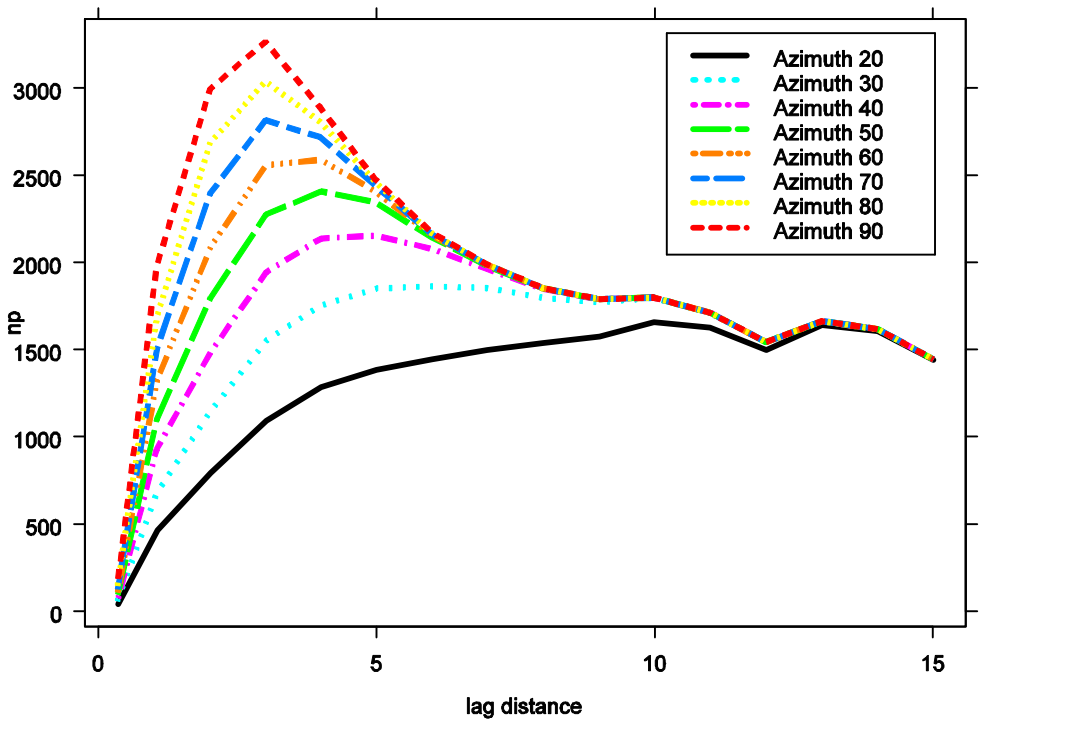
et points Pang Old Fenced Q90 ; Sensitivity analysis for the azimuth tolerance: Number of pair of points (azimuth
np
0
500
1000
1500
2000
2500
3000
0
5
10
15
lag distance
Azimuth 20
Azimuth 30
Azimuth 40
Azimuth 50
Azimuth 60
Azimuth 70
Azimuth 80
Azimuth 90

wet points Pang Old Fenced Q90 ; Sensitivity analysis for the azimuth tolerance (azimuth 90)

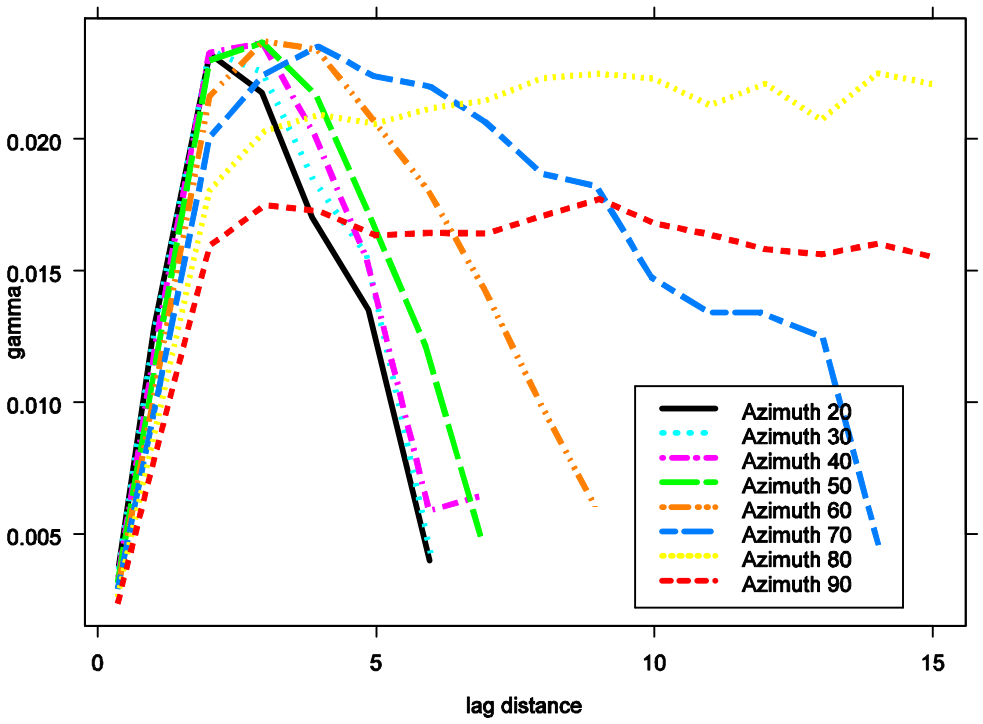

et points Pang Old Fenced Q90 ; Sensitivity analysis for the azimuth tolerance: Number of pair of points (azimuth 9

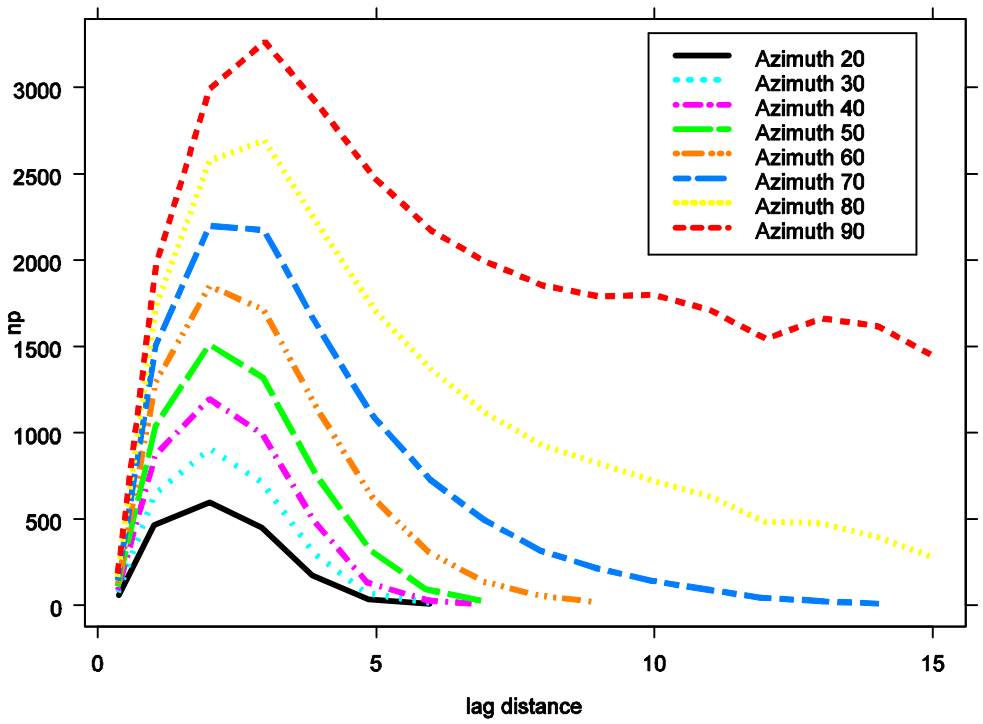

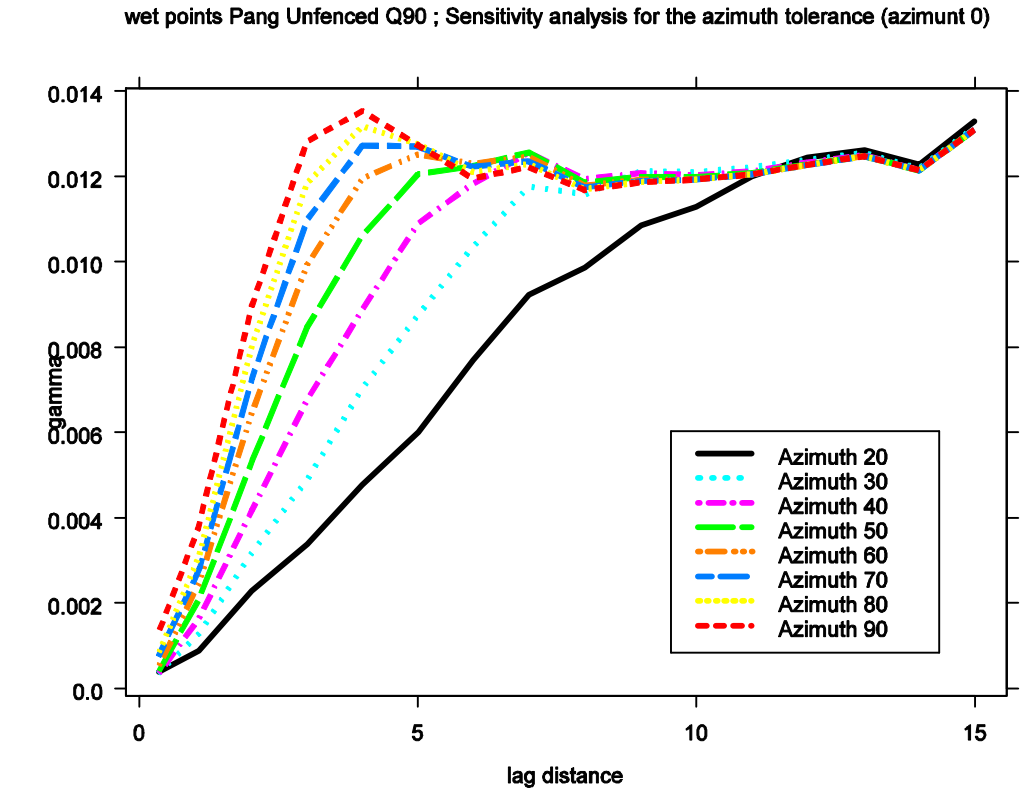
wet points Pang Unfenced Q90 ; Sensitivity analysis for the azimuth tolerance (azimunt 0)
gamma
lag distance
0.0
0.002
0.004
0.006
0.008
0.010
0.012
0.014
0
5
10
15
Azimuth 20
Azimuth 30
Azimuth 40
Azimuth 50
Azimuth 60
Azimuth 70
Azimuth 80
Azimuth 90

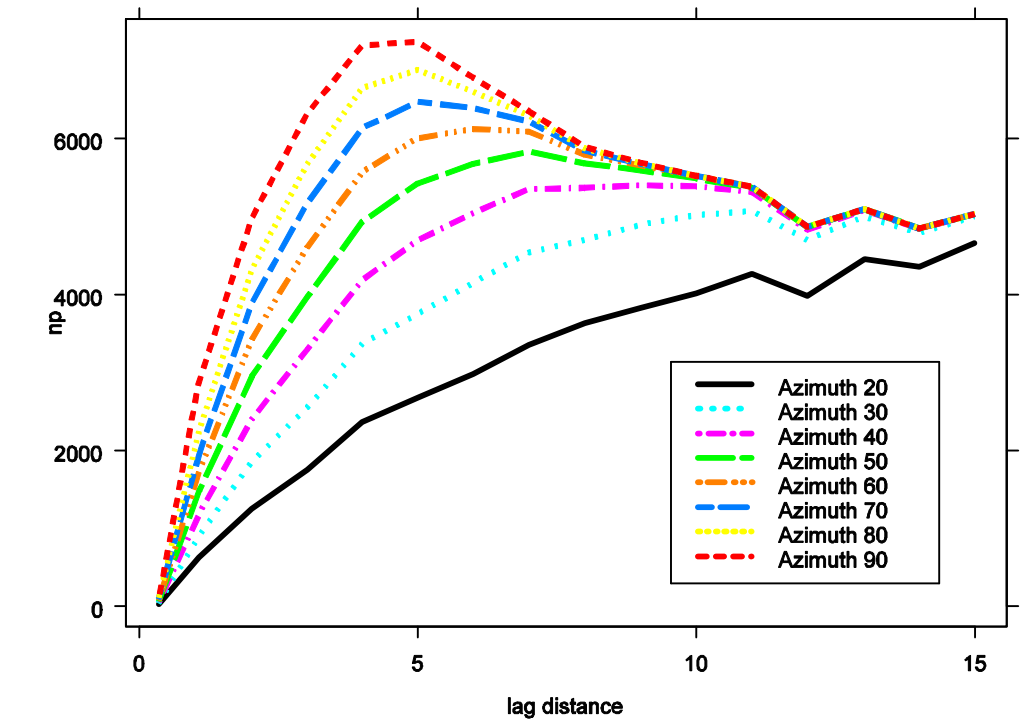
wet points Pang Unfenced Q90 ; Sensitivity analysis for the azimuth tolerance: Number of pair of points (azimuth 0)
np
lag distance
0
2000
4000
6000
0
5
10
15
Azimuth 20
Azimuth 30
Azimuth 40
Azimuth 50
Azimuth 60
Azimuth 70
Azimuth 80
Azimuth 90

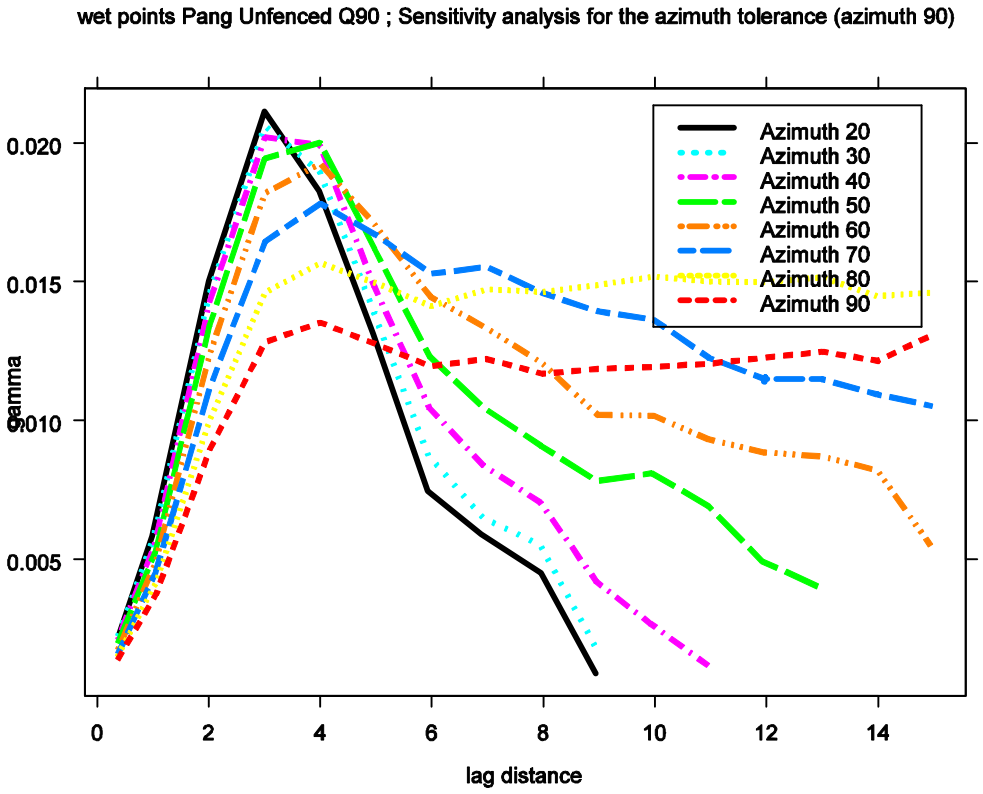
wet points Pang Unfenced Q90 ; Sensitivity analysis for the azimuth tolerance (azimuth 90)
Azimuth 20
Azimuth 30
Azimuth 40
Azimuth 50
Azimuth 60
Azimuth 70
Azimuth 80
Azimuth 90
0.020
0.015
0.010
0.005
gamma
0
2
4
6
8
10
12
14
lag distance

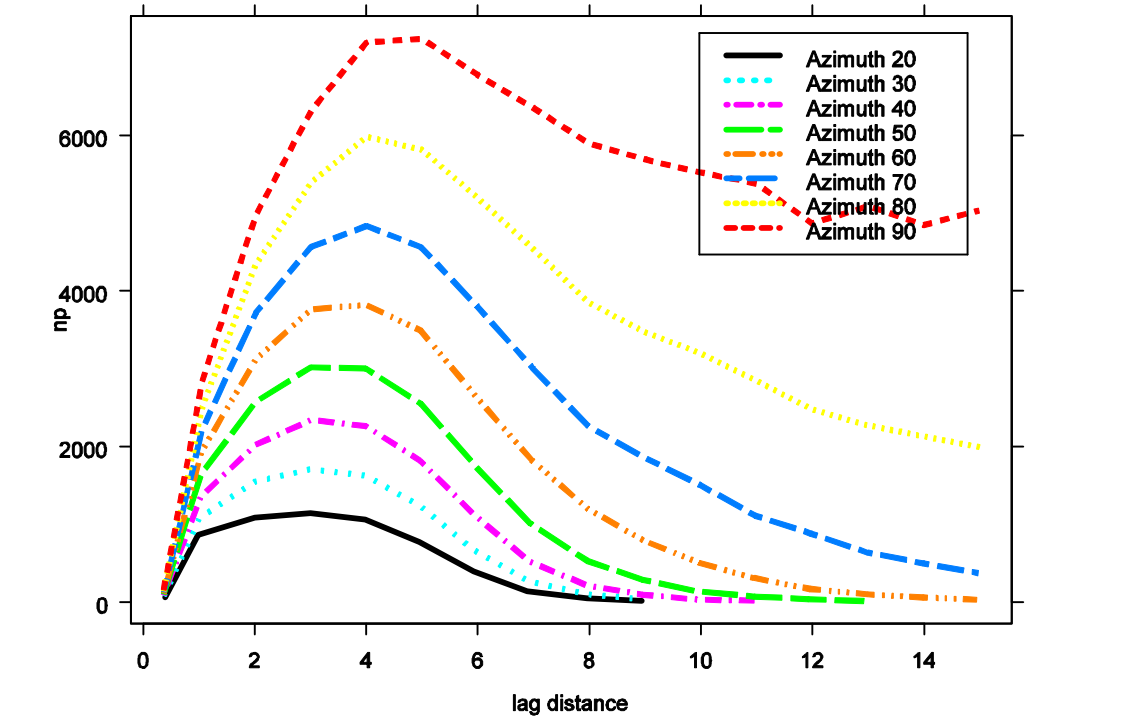
vet points Pang Unfenced Q90 ; Sensitivity analysis for the azimuth tolerance: Number of pair of points (azimuth 90
Azimuth 20
Azimuth 30
Azimuth 40
Azimuth 50
Azimuth 60
Azimuth 70
Azimuth 80
Azimuth 90
6000
4000
2000
0
np
0
2
4
6
8
10
12
14
lag distance

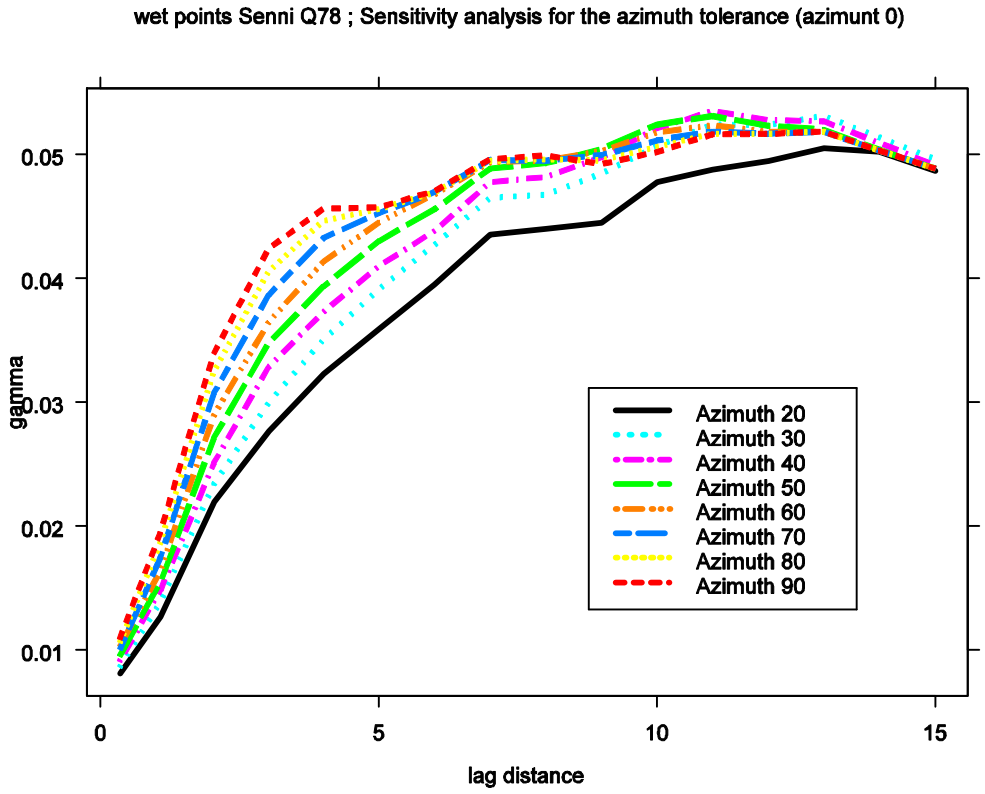
wet points Senni Q78 ; Sensitivity analysis for the azimuth tolerance (azimunt 0)
gamma
0.01
0.02
0.03
0.04
0.05
0
5
10
15
lag distance
Azimuth 20
Azimuth 30
Azimuth 40
Azimuth 50
Azimuth 60
Azimuth 70
Azimuth 80
Azimuth 90

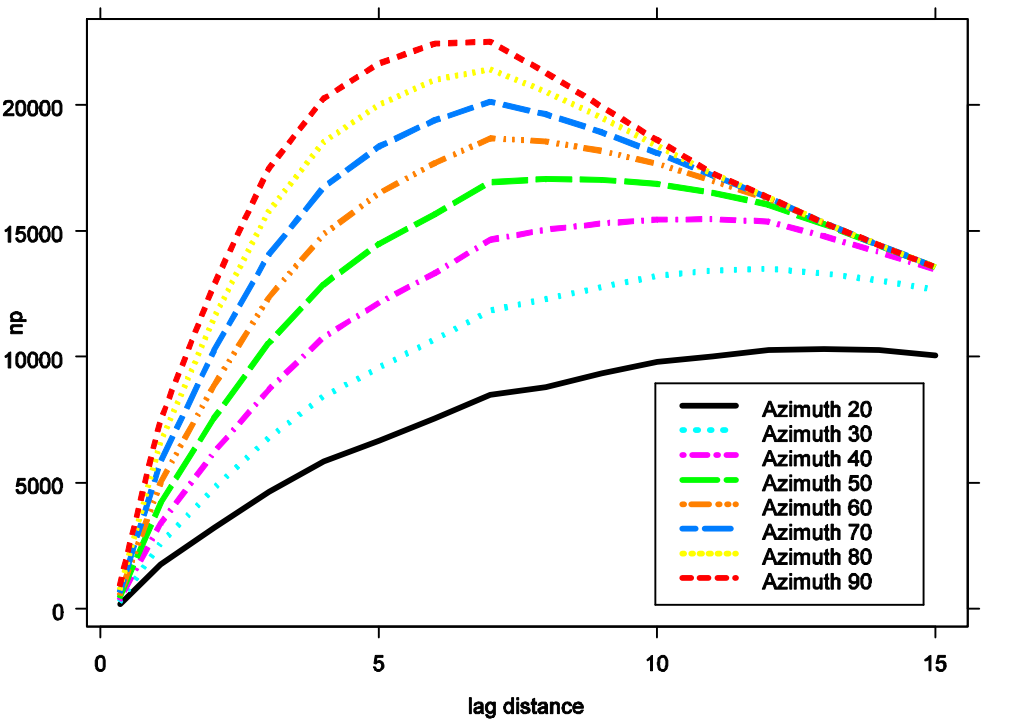
wet points Senni Q78 ; Sensitivity analysis for the azimuth tolerance: Number of pair of points (azimuth 0)
np
0
5000
10000
15000
20000
0
5
10
15
lag distance
Azimuth 20
Azimuth 30
Azimuth 40
Azimuth 50
Azimuth 60
Azimuth 70
Azimuth 80
Azimuth 90

wet points Senni Q78 ; Sensitivity analysis for the azimuth tolerance (azimuth 90)

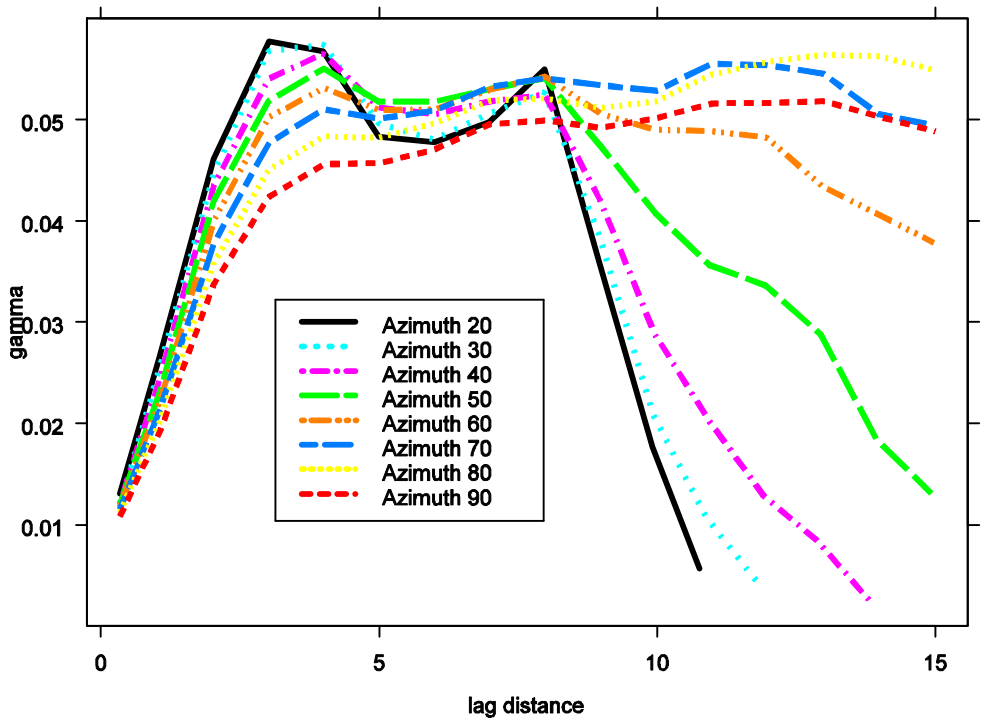

wet points Senni Q78 ; Sensitivity analysis for the azimuth tolerance: Number of pair of points (azimuth 90)

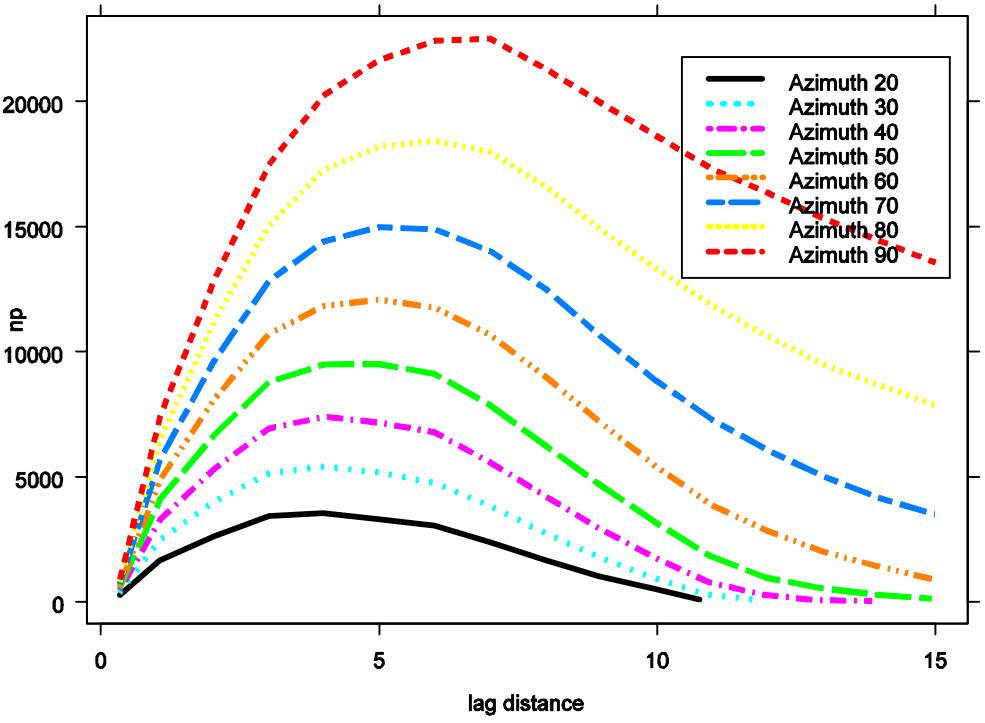

wet points TamesHM Q20 ; Sensitivity analysis for the azimuth tolerance (azimunt 0)

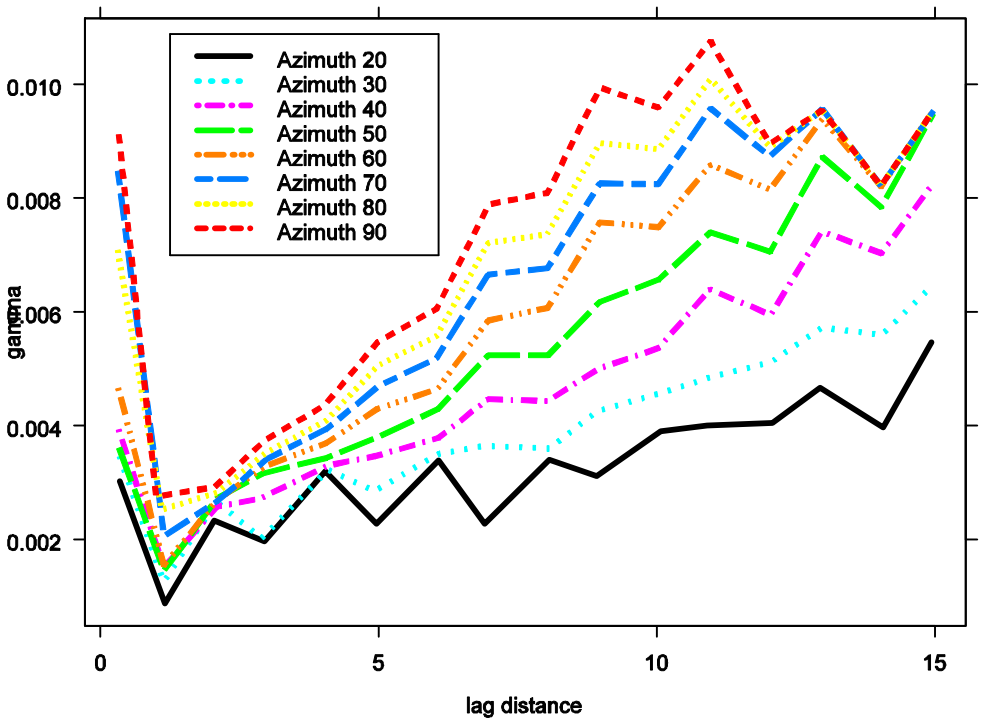

wet points TamesHM Q20 ; Sensitivity analysis for the azimuth tolerance: Number of pair of points (azimuth 0)

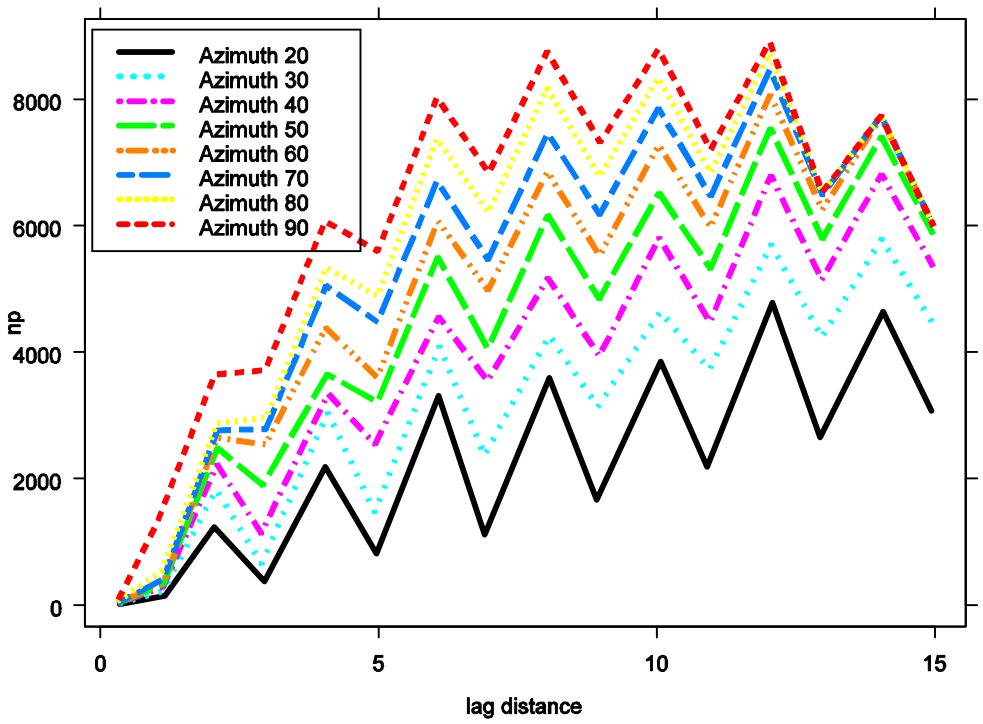

wet points TamesHM Q20 ; Sensitivity analysis for the azimuth tolerance (azimuth 90)

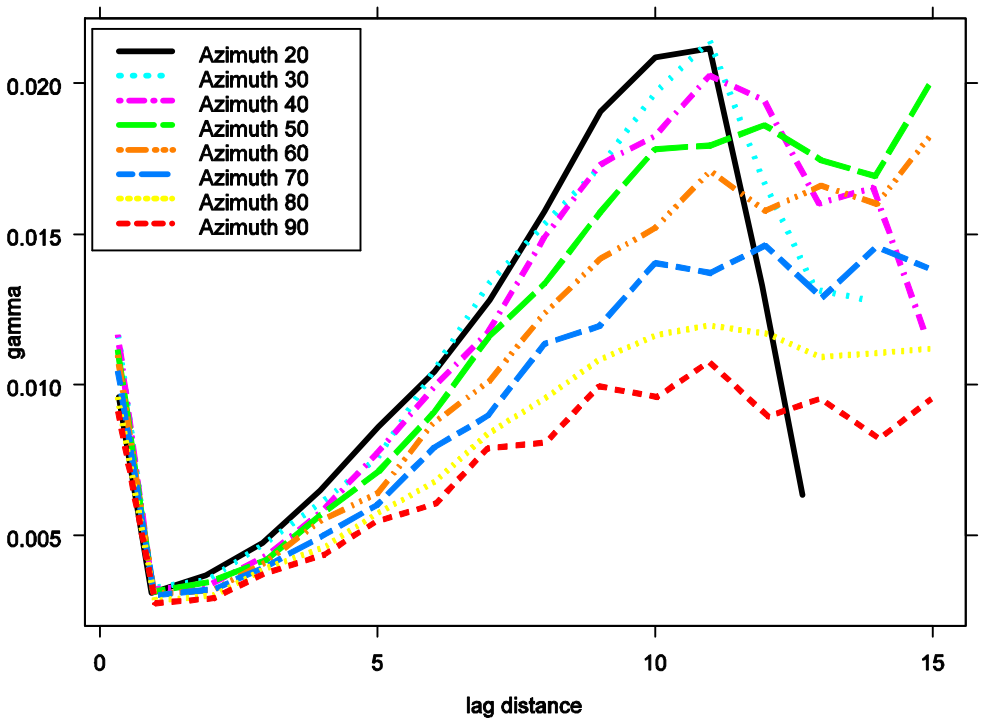

wet points TamesHM Q20 ; Sensitivity analysis for the azimuth tolerance: Number of pair of points (azimuth 90)

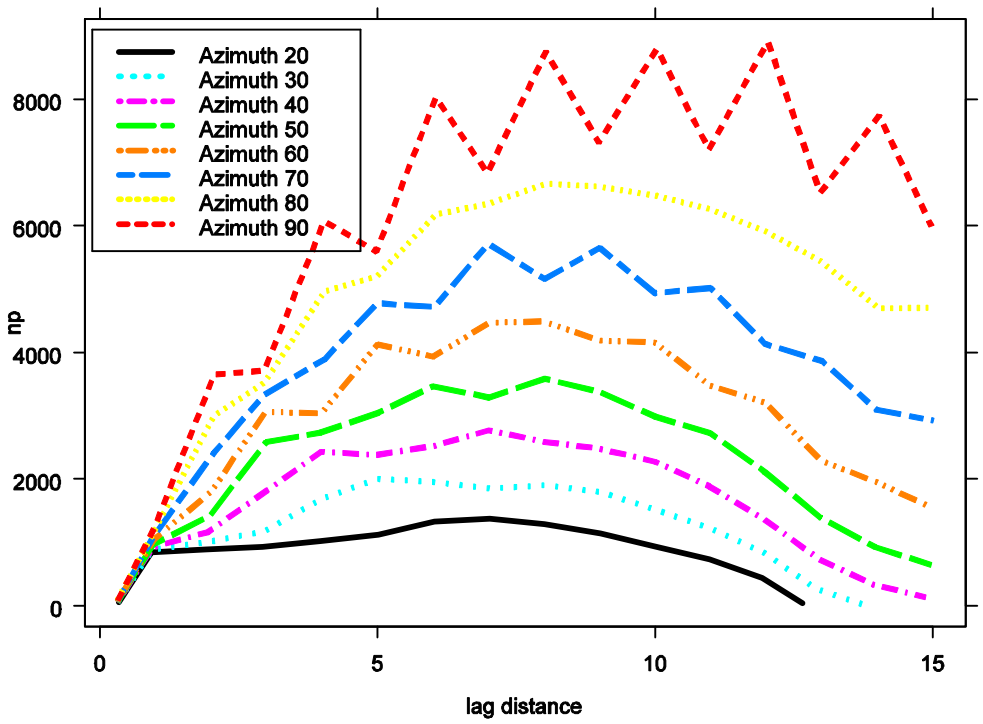

wet points TamesLM Q43 ; Sensitivity analysis for the azimuth tolerance (azimunt 0)

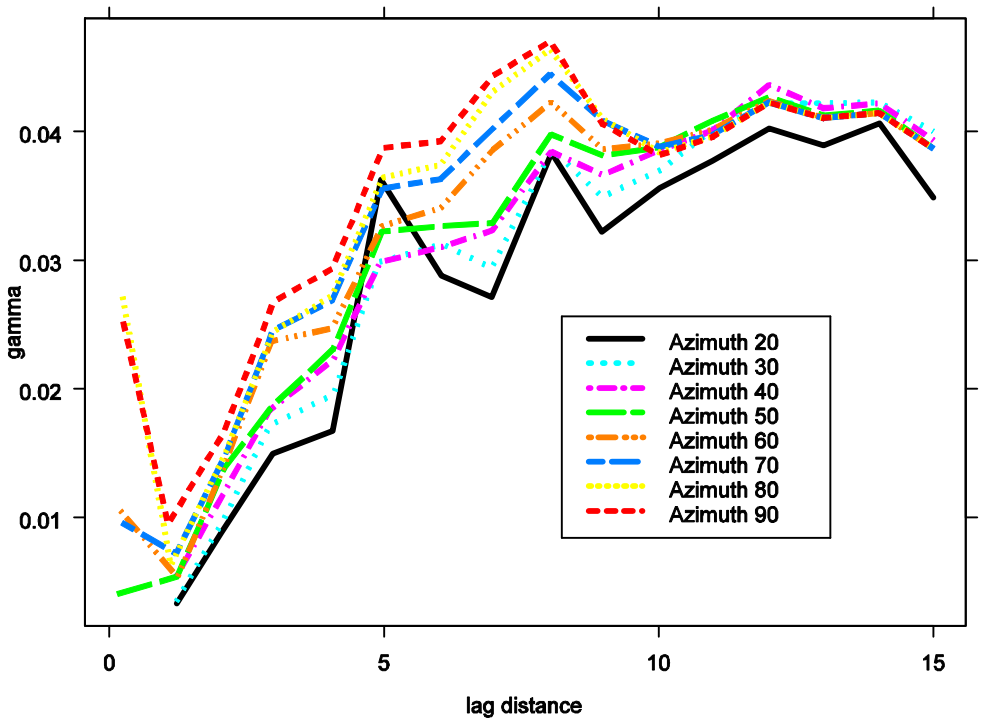

wet points TamesLM Q43 ; Sensitivity analysis for the azimuth tolerance: Number of pair of points (azimuth 0)

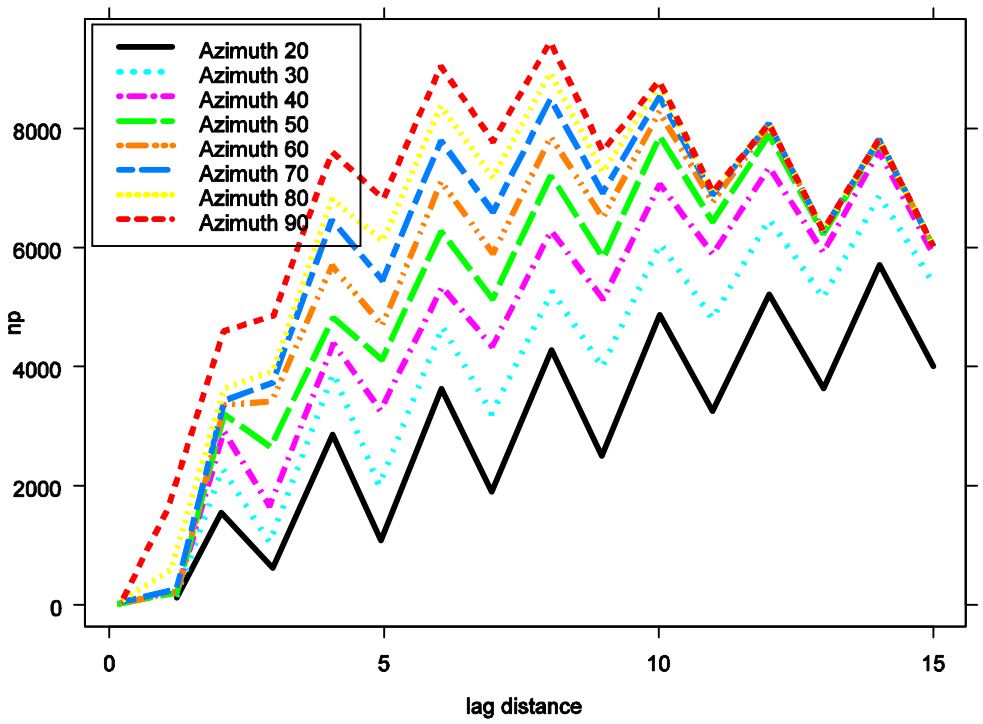

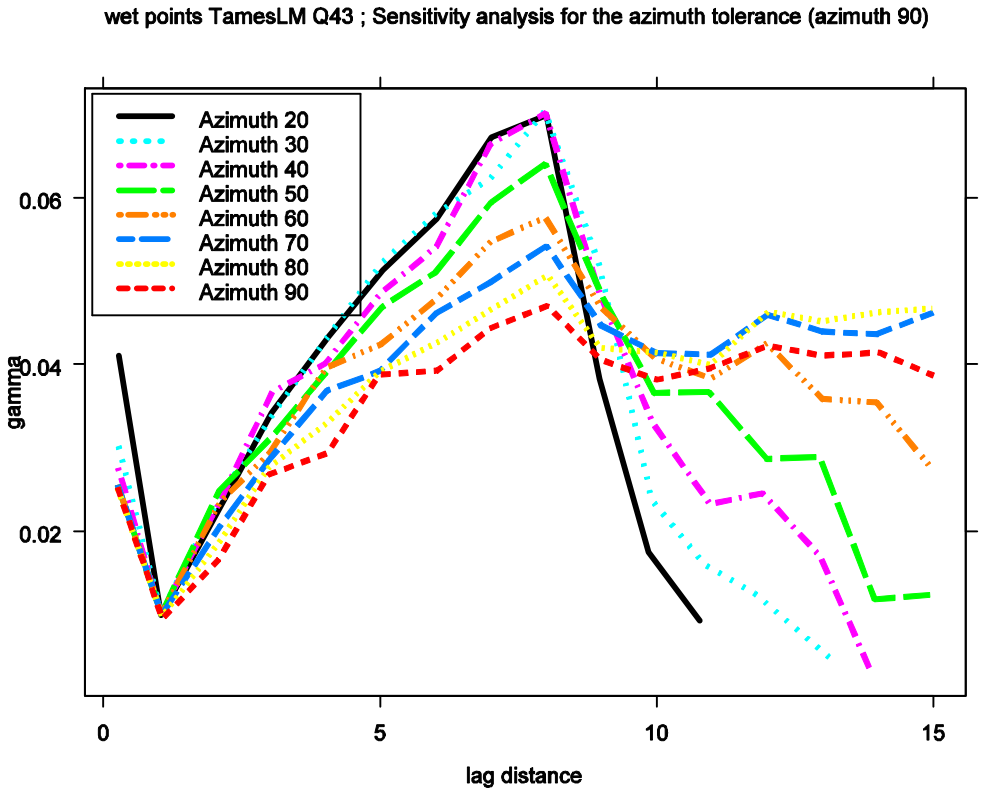
wet points TamesLM Q43 ; Sensitivity analysis for the azimuth tolerance (azimuth 90)
Azimuth 20
Azimuth 30
Azimuth 40
Azimuth 50
Azimuth 60
Azimuth 70
Azimuth 80
Azimuth 90
gamma
0.02
0.04
0.06
0
5
10
15
lag distance

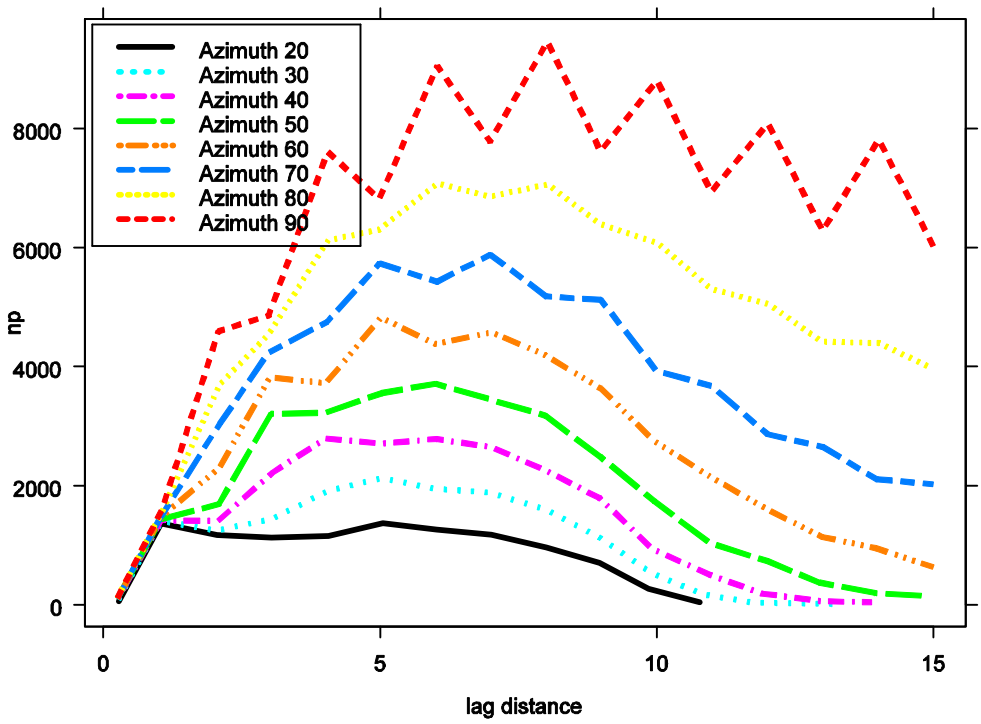
wet points TamesLM Q43 ; Sensitivity analysis for the azimuth tolerance: Number of pair of points (azimuth 90)
Azimuth 20
Azimuth 30
Azimuth 40
Azimuth 50
Azimuth 60
Azimuth 70
Azimuth 80
Azimuth 90
np
0
2000
4000
6000
8000
0
5
10
15
lag distance

wet points Tarf Q51 ; Sensitivity analysis for the azimuth tolerance (azimunt 0)

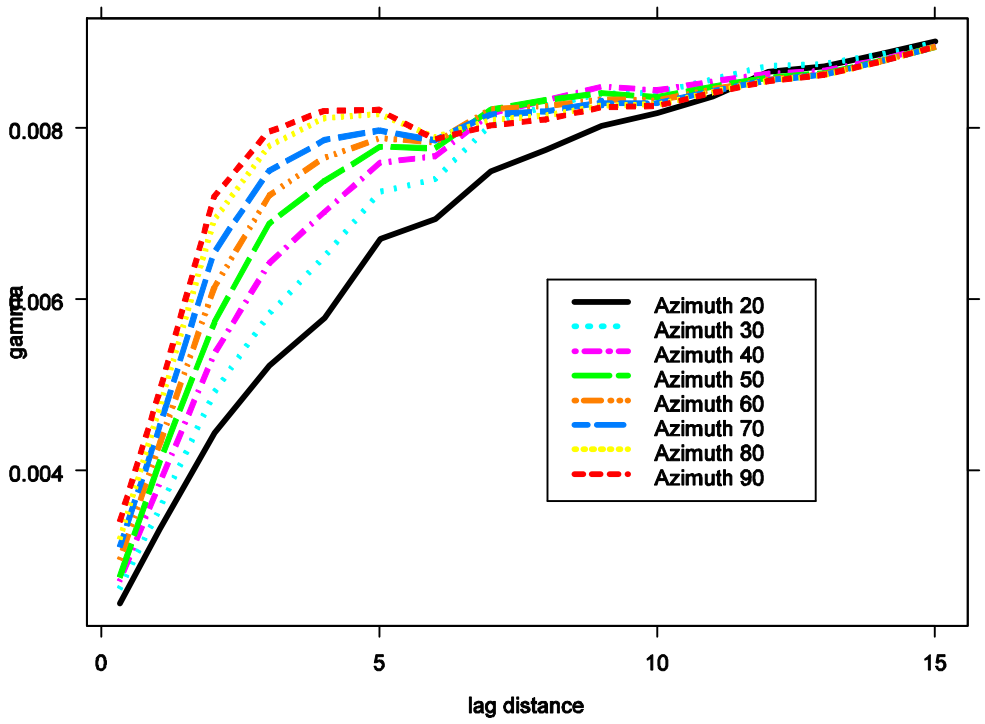

wet points Tarf Q51 ; Sensitivity analysis for the azimuth tolerance: Number of pair of points (azimuth 0)

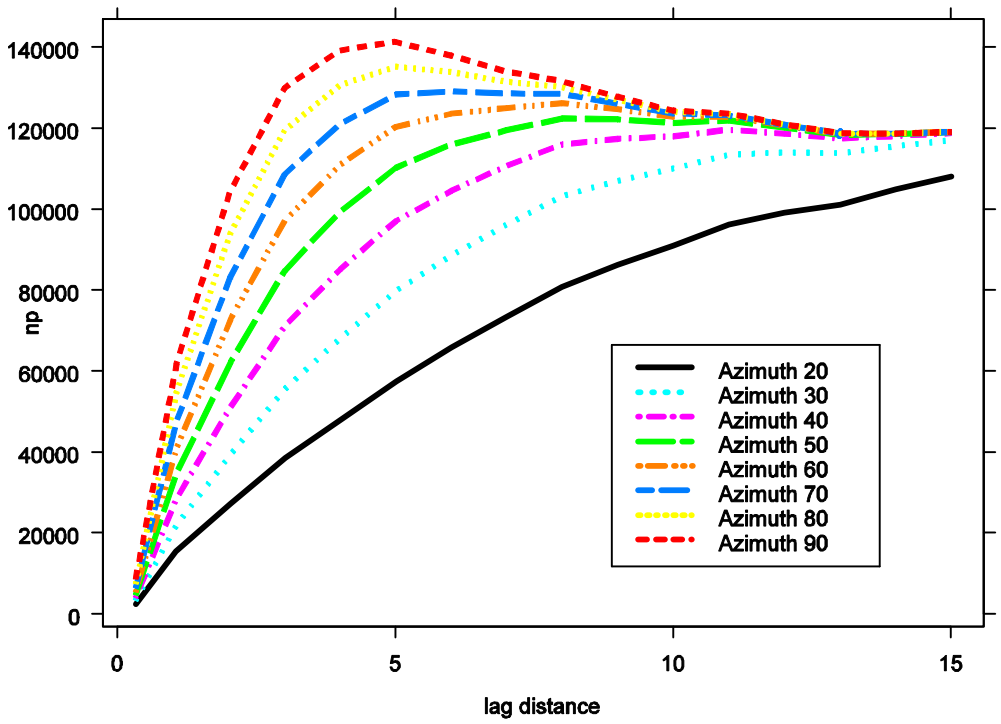

wet points Tarf Q51 ; Sensitivity analysis for the azimuth tolerance (azimuth 90)

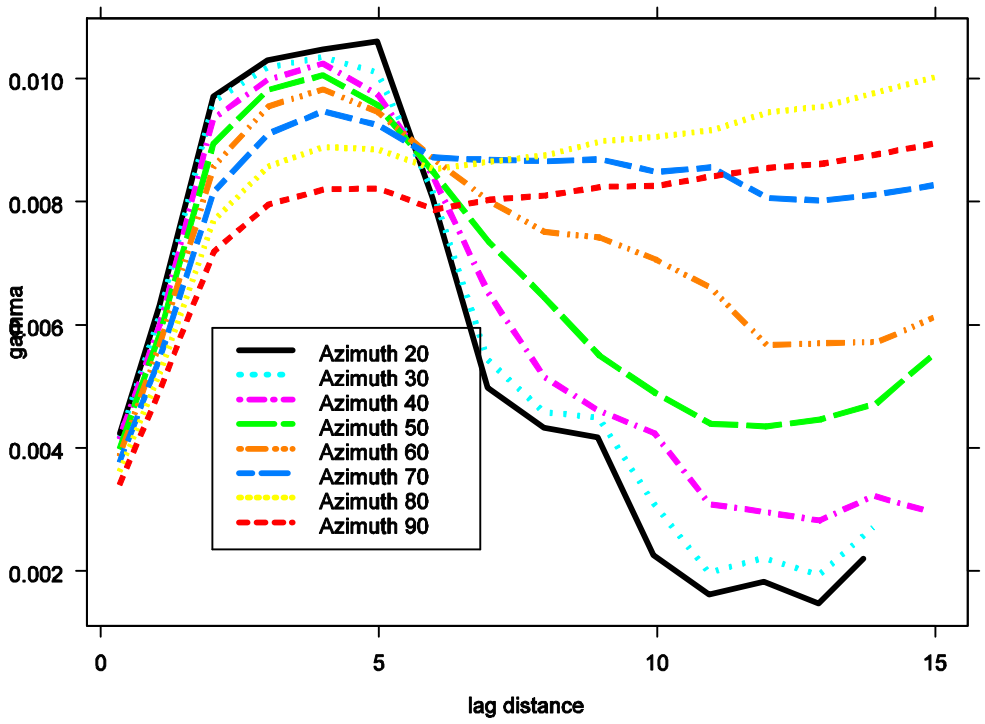

wet points Tarf Q51 ; Sensitivity analysis for the azimuth tolerance: Number of pair of points (azimuth 90)

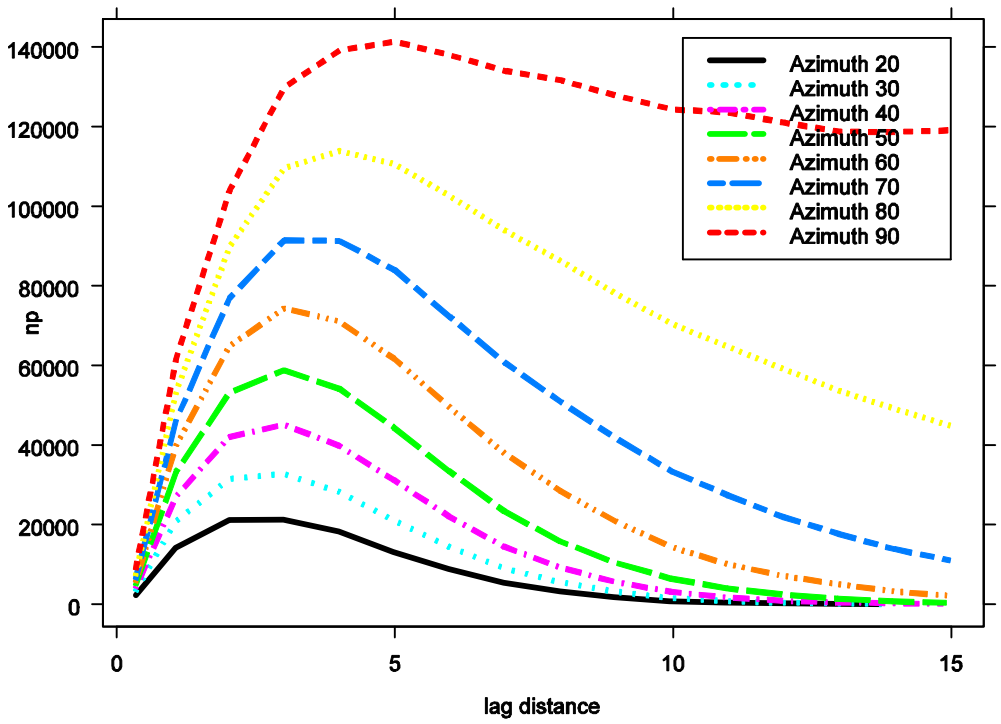

wet points Windrush Q ; Sensitivity analysis for the azimuth tolerance (azimunt 0)

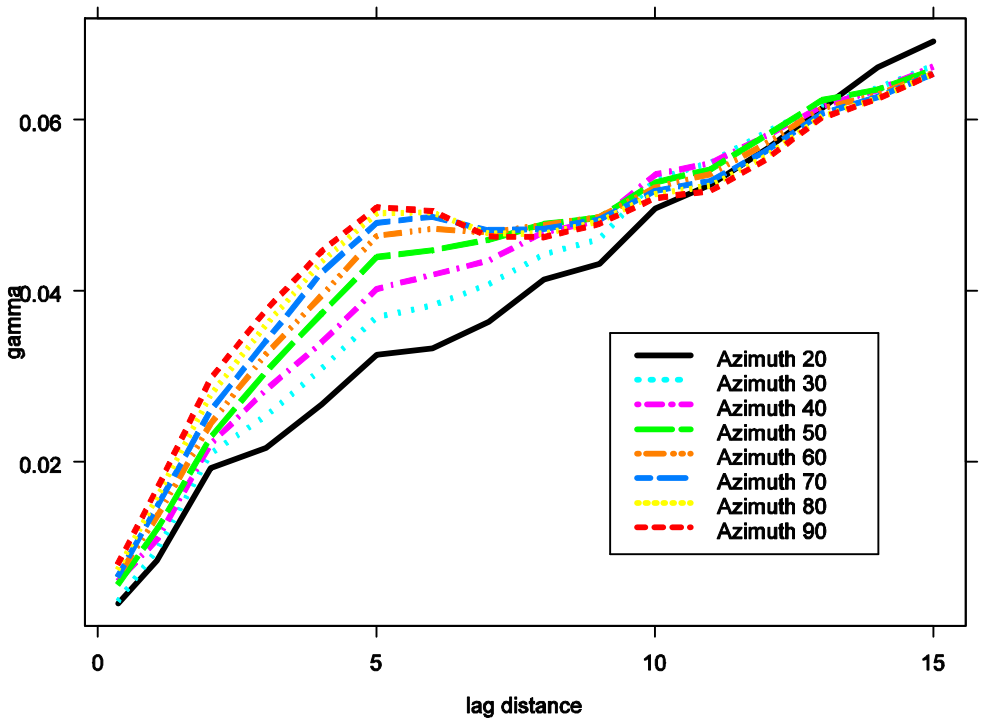

wet points Windrush Q ; Sensitivity analysis for the azimuth tolerance: Number of pair of points (azimuth 0)

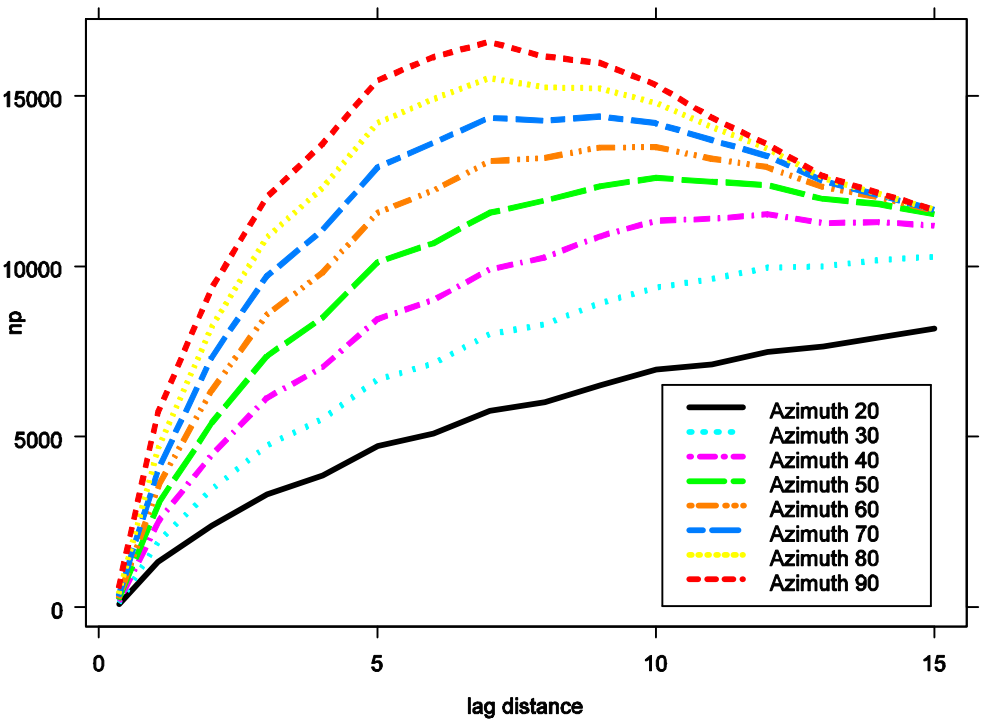

wet points Windrush Q ; Sensitivity analysis for the azimuth tolerance (azimuth 90)

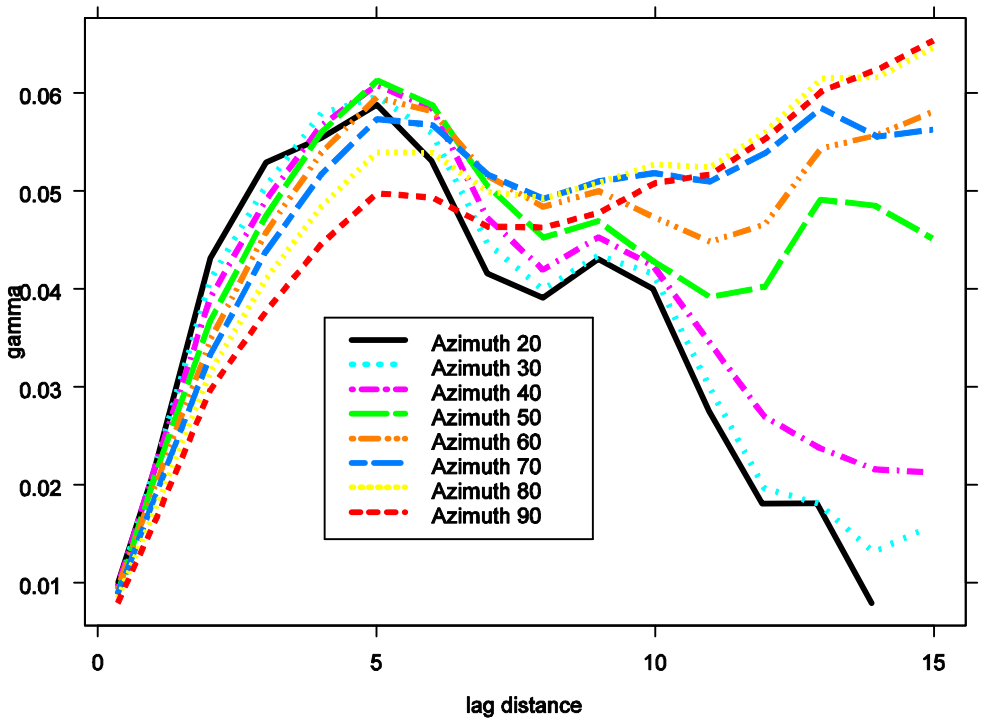

wet points Windrush Q ; Sensitivity analysis for the azimuth tolerance: Number of pair of points (azimuth 90)

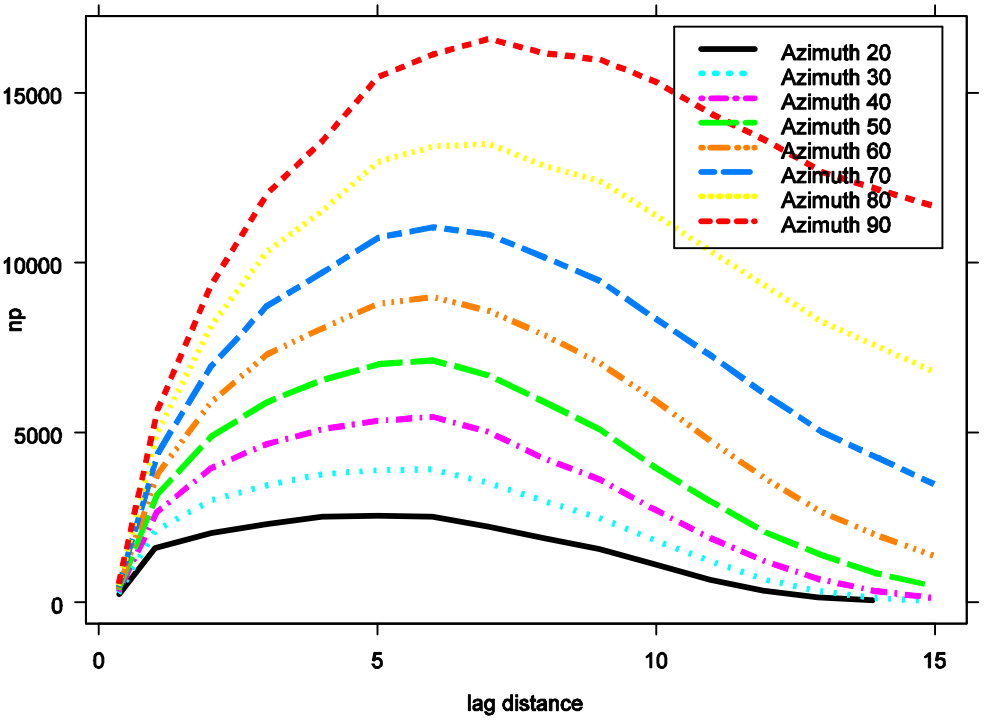

Azimuth tolerance wet & dry points

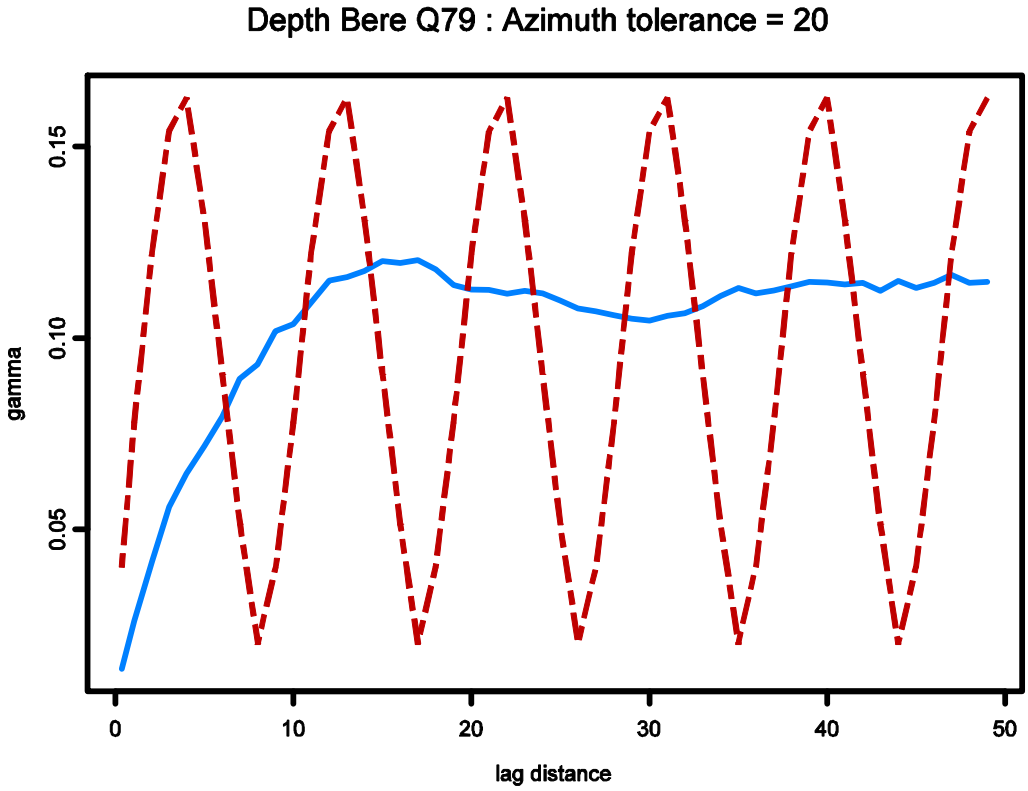

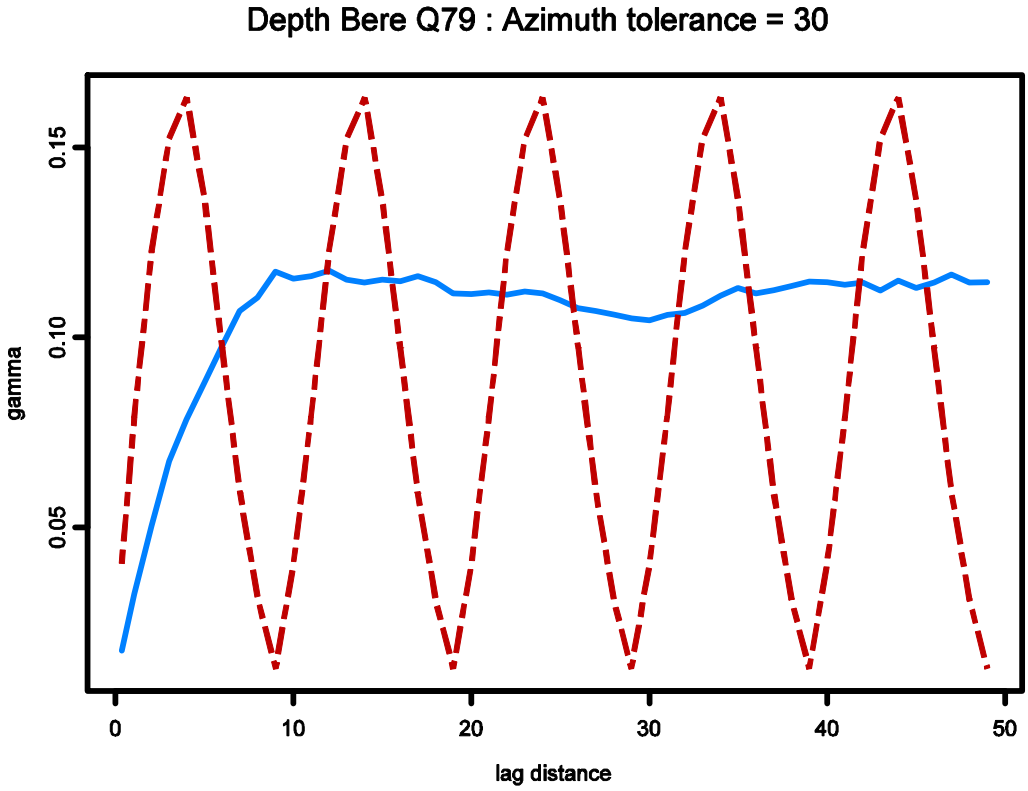

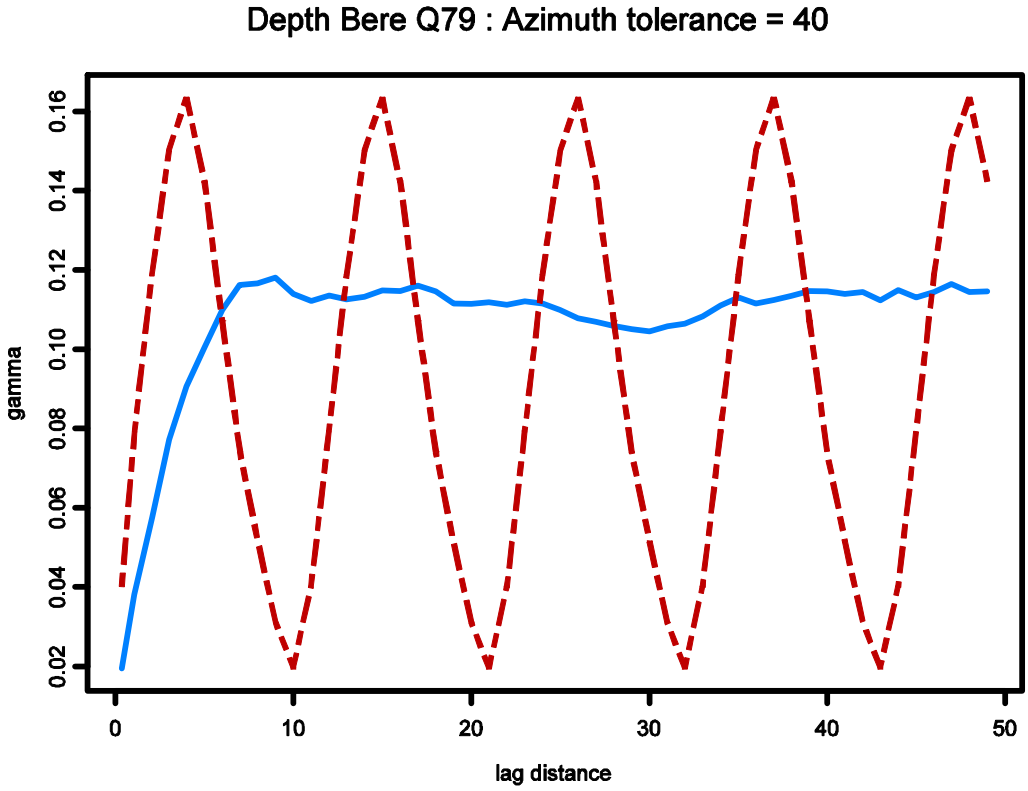
Depth Bere Q79 : Azimuth tolerance = 40
gamma
0.02
0.04
0.06
0.08
0.10
0.12
0.14
0.16
0
10
20
30
40
50
lag distance

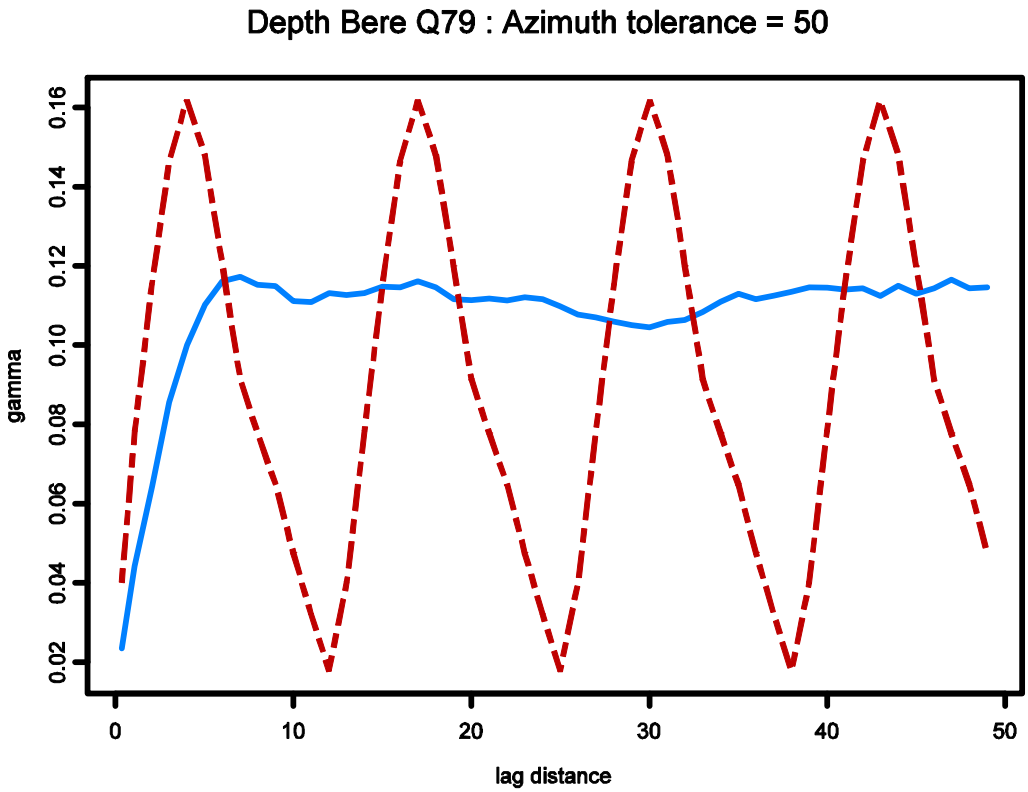
Depth Bere Q79 : Azimuth tolerance = 50
gamma
0.02
0.04
0.06
0.08
0.10
0.12
0.14
0.16
0
10
20
30
40
50
lag distance

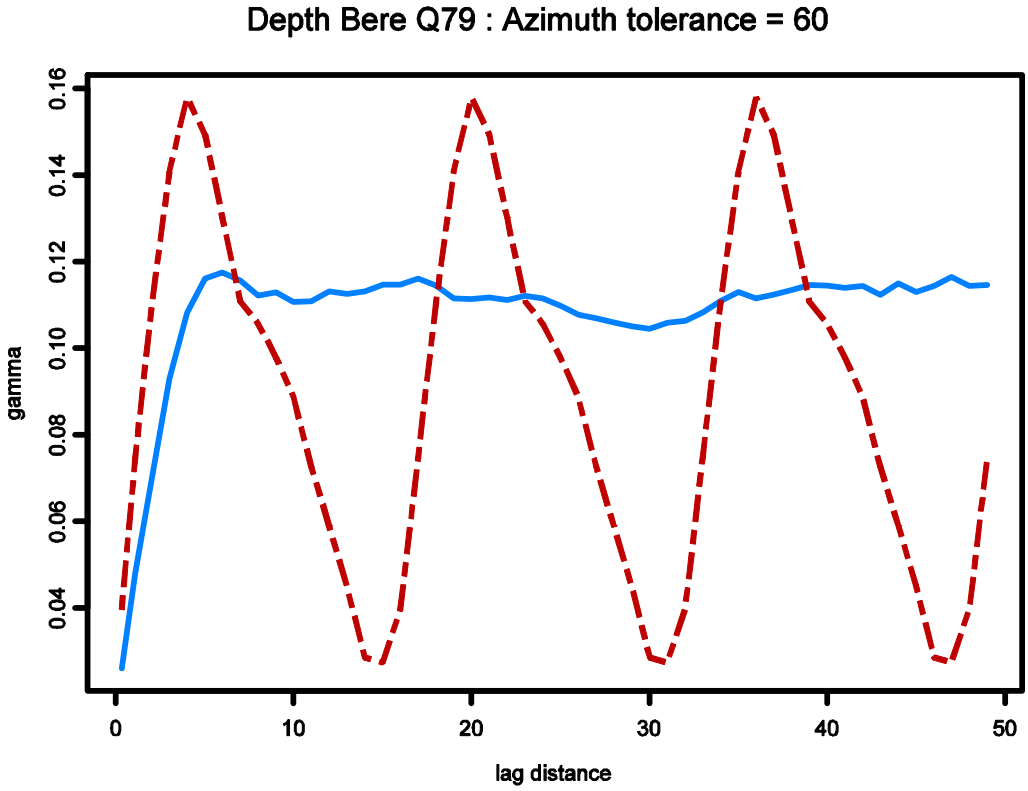
Depth Bere Q79 : Azimuth tolerance = 60
gamma
0.04
0.06
0.08
0.10
0.12
0.14
0.16
0
10
20
30
40
50
lag distance

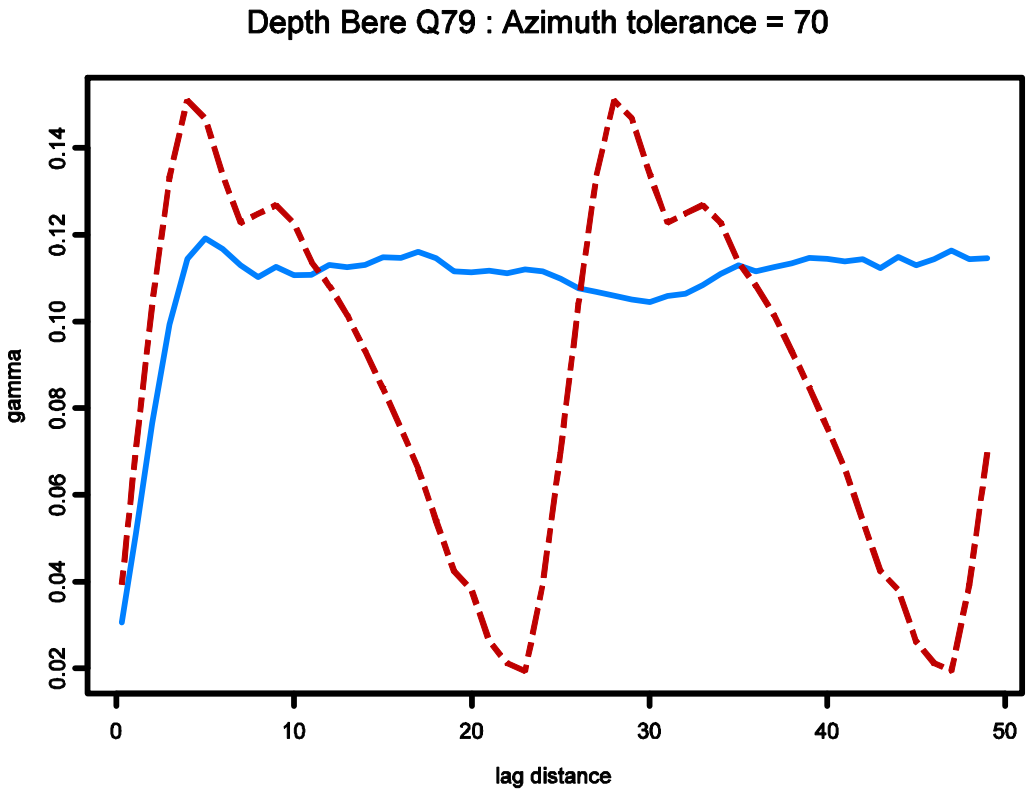
Depth Bere Q79 : Azimuth tolerance = 70
gamma
0.02
0.04
0.06
0.08
0.10
0.12
0.14
0
10
20
30
40
50
lag distance

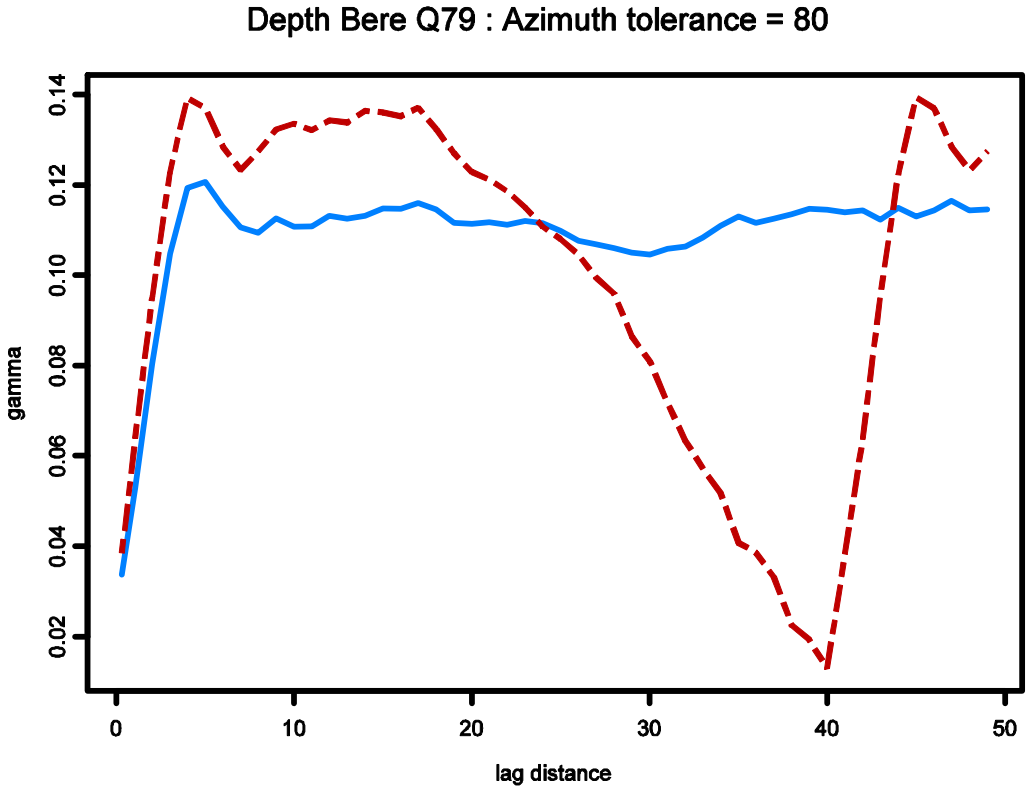
Depth Bere Q79 : Azimuth tolerance = 80
gamma
0.02
0.04
0.06
0.08
0.10
0.12
0.14
0
10
20
30
40
50
lag distance

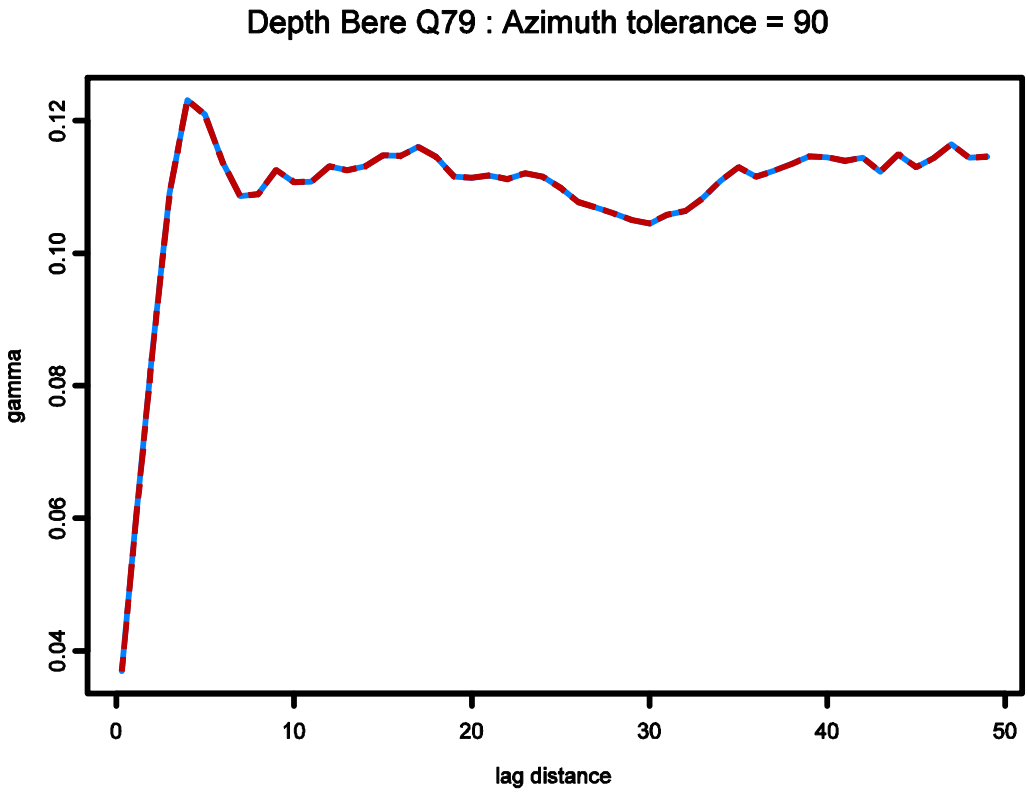
Depth Bere Q79 : Azimuth tolerance = 90
gamma
0.04
0.06
0.08
0.10
0.12
0
10
20
30
40
50
lag distance

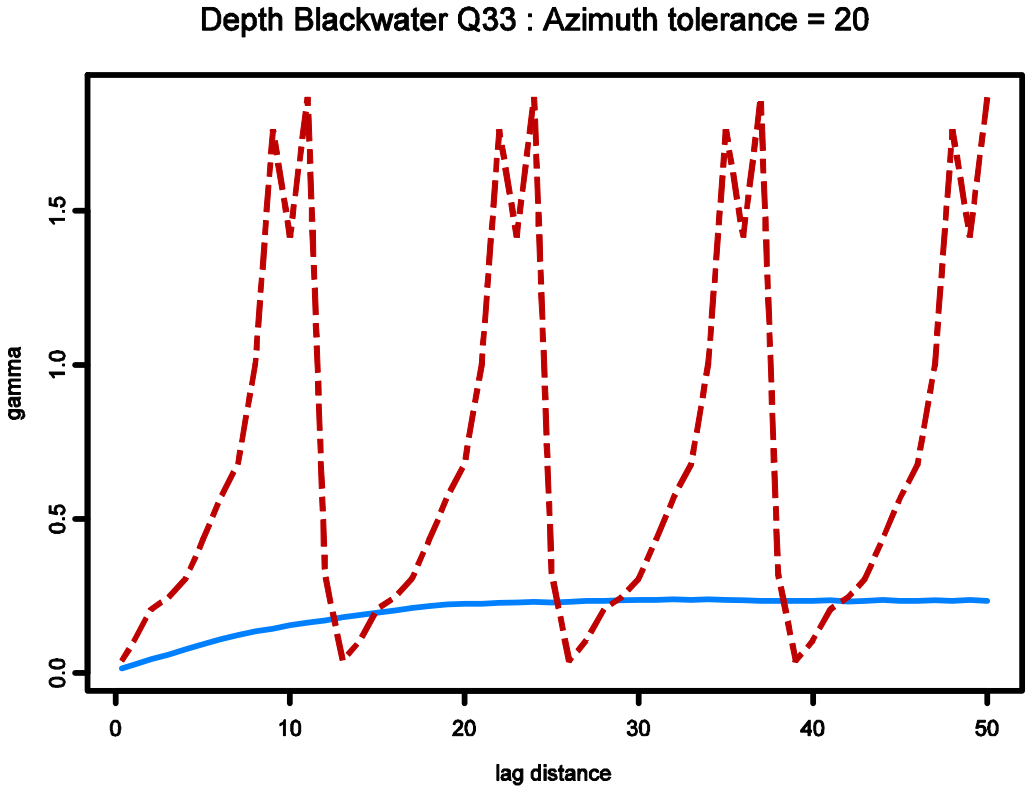
Depth Blackwater Q33 : Azimuth tolerance = 20
gamma
0.0
0.5
1.0
1.5
0
10
20
30
40
50
lag distance

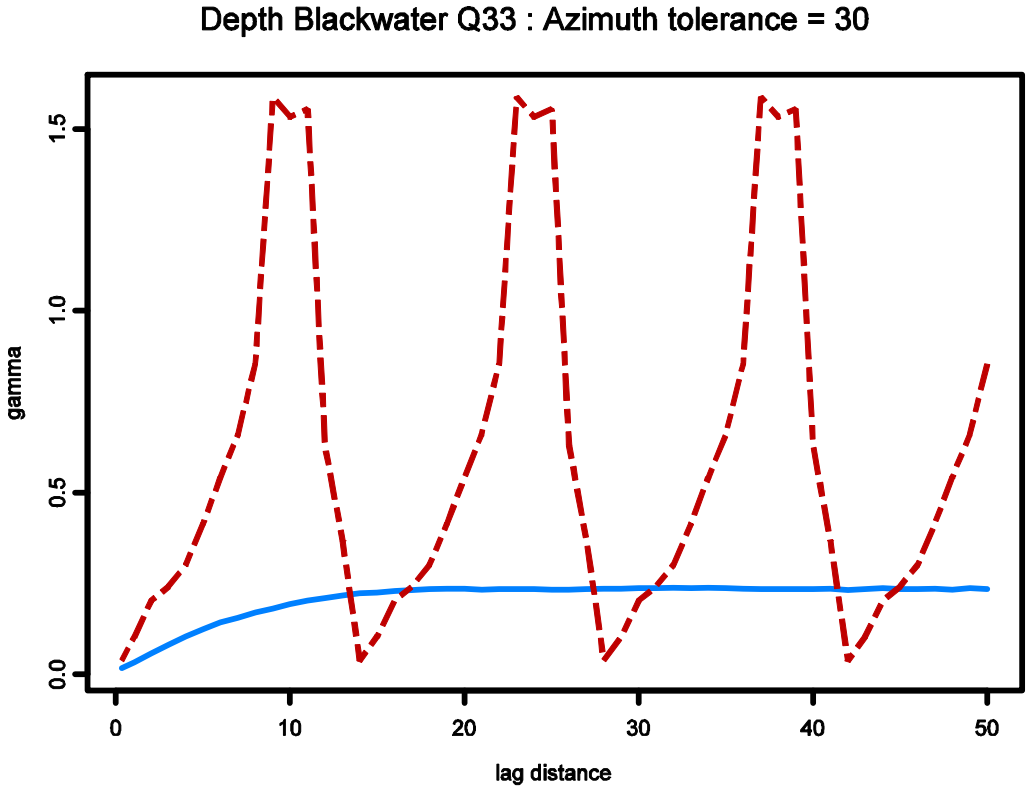
Depth Blackwater Q33 : Azimuth tolerance = 30
gamma
0.0
0.5
1.0
1.5
0
10
20
30
40
50
lag distance

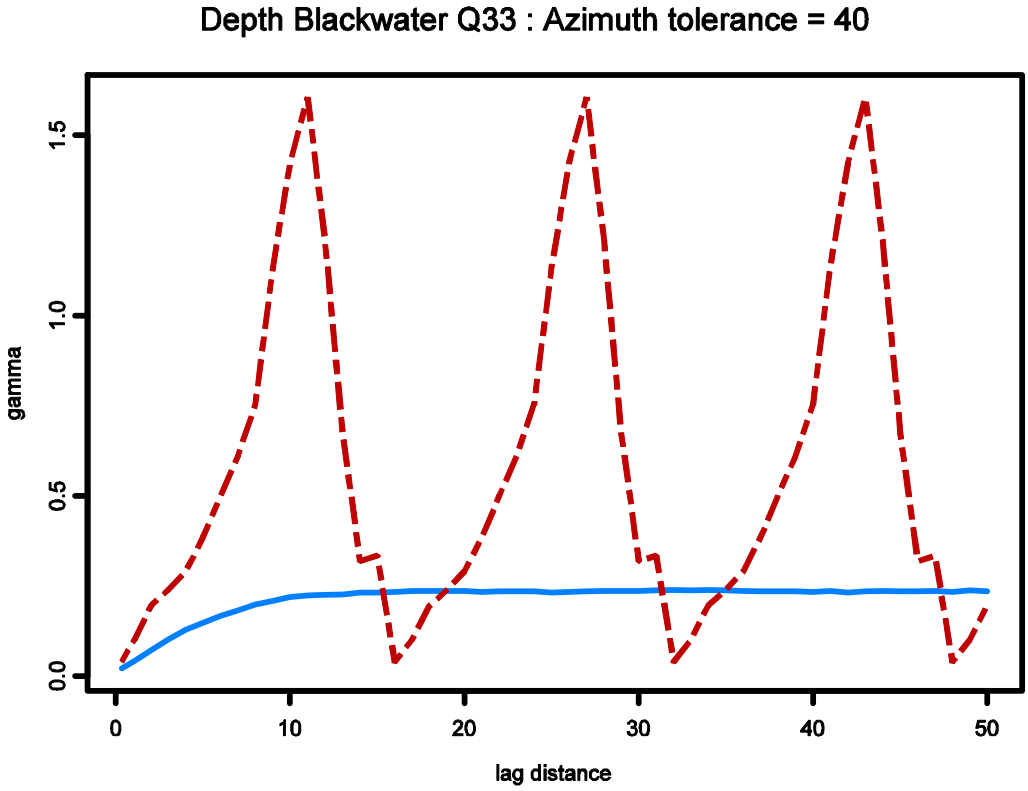
Depth Blackwater Q33 : Azimuth tolerance = 40
gamma
0.0
0.5
1.0
1.5
0
10
20
30
40
50
lag distance

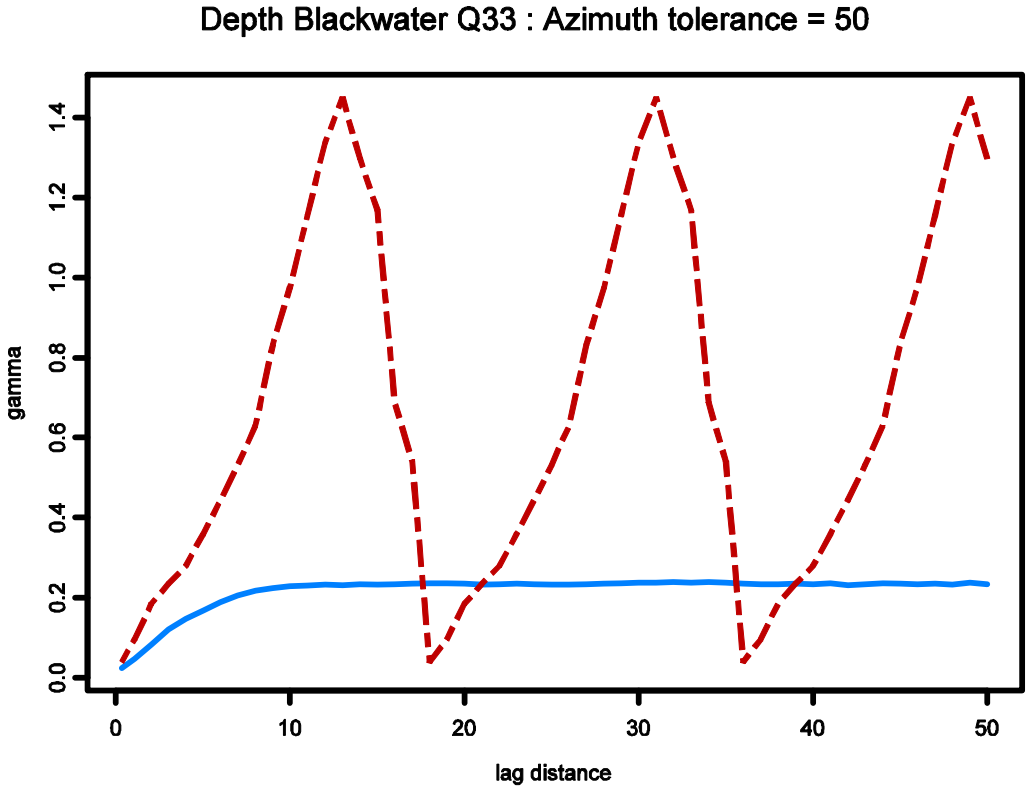
Depth Blackwater Q33 : Azimuth tolerance = 50
gamma
0.0
0.2
0.4
0.6
0.8
1.0
1.2
1.4
0
10
20
30
40
50
lag distance

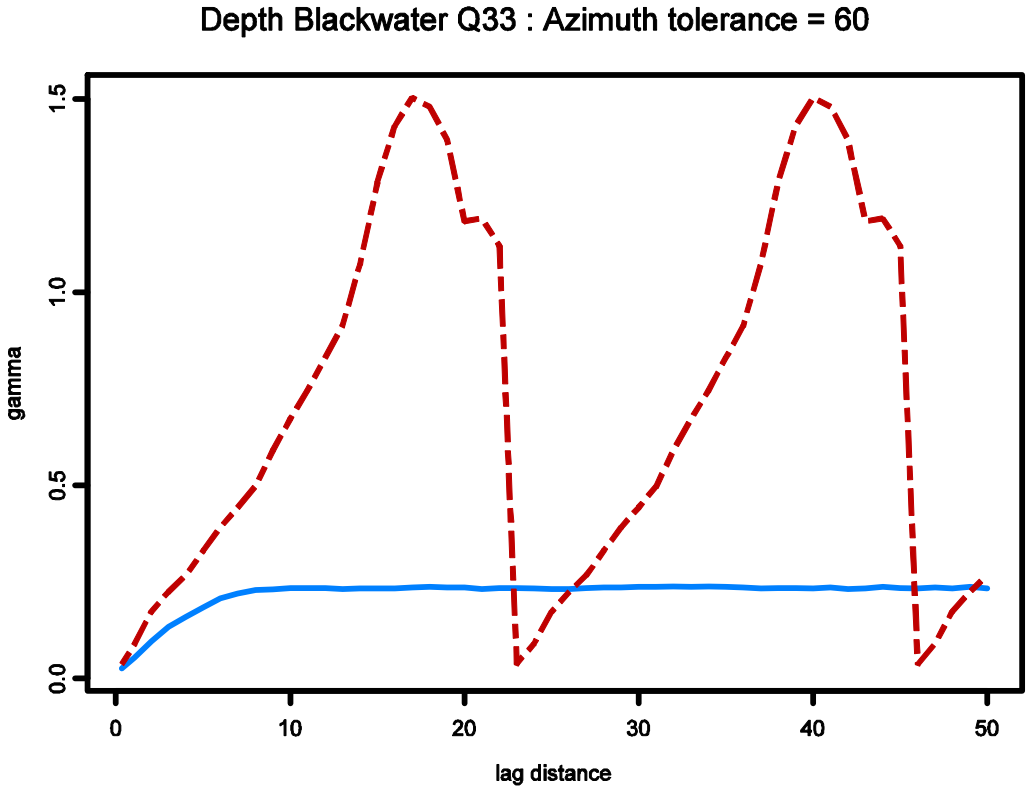
Depth Blackwater Q33 : Azimuth tolerance = 60
gamma
0.0
0.5
1.0
1.5
0
10
20
30
40
50
lag distance

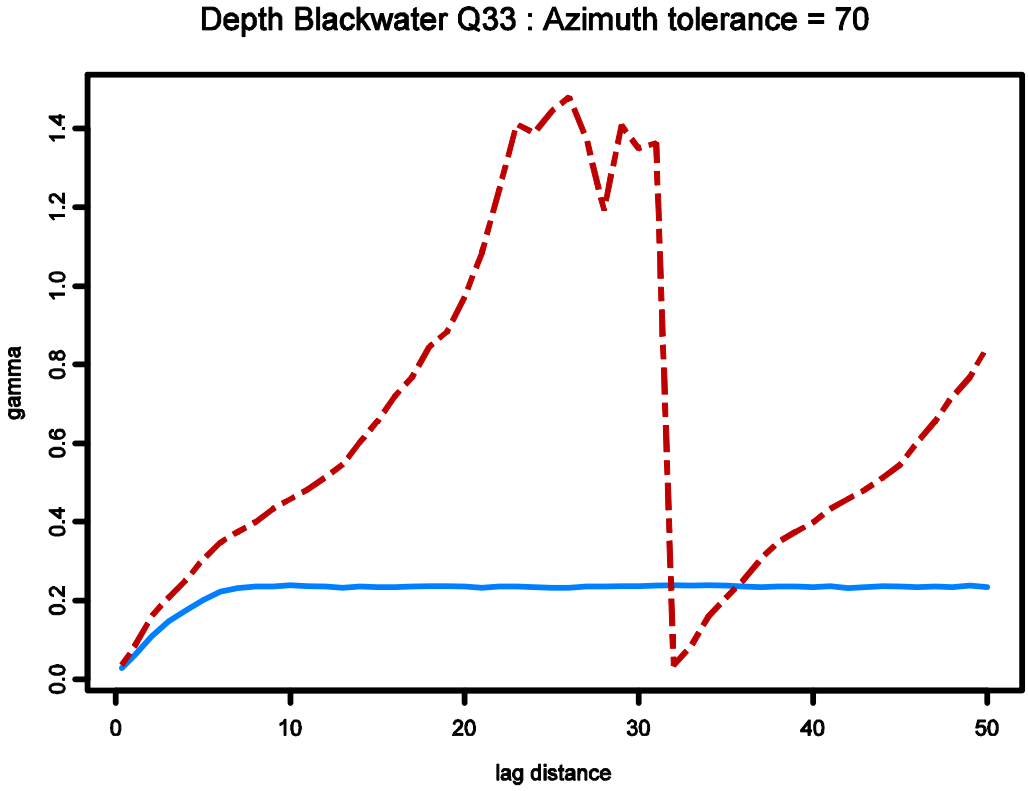
Depth Blackwater Q33 : Azimuth tolerance = 70
gamma
0.0
0.2
0.4
0.6
0.8
1.0
1.2
1.4
0
10
20
30
40
50
lag distance

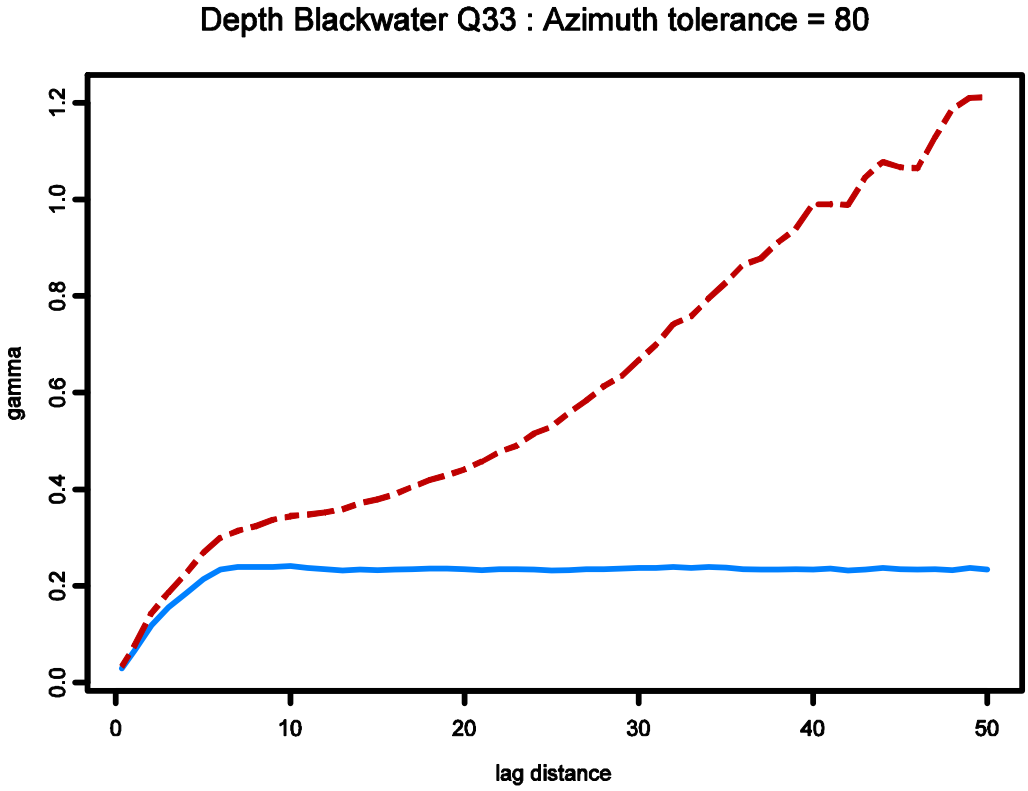
Depth Blackwater Q33 : Azimuth tolerance = 80
gamma
0.0
0.2
0.4
0.6
0.8
1.0
1.2
0
10
20
30
40
50
lag distance

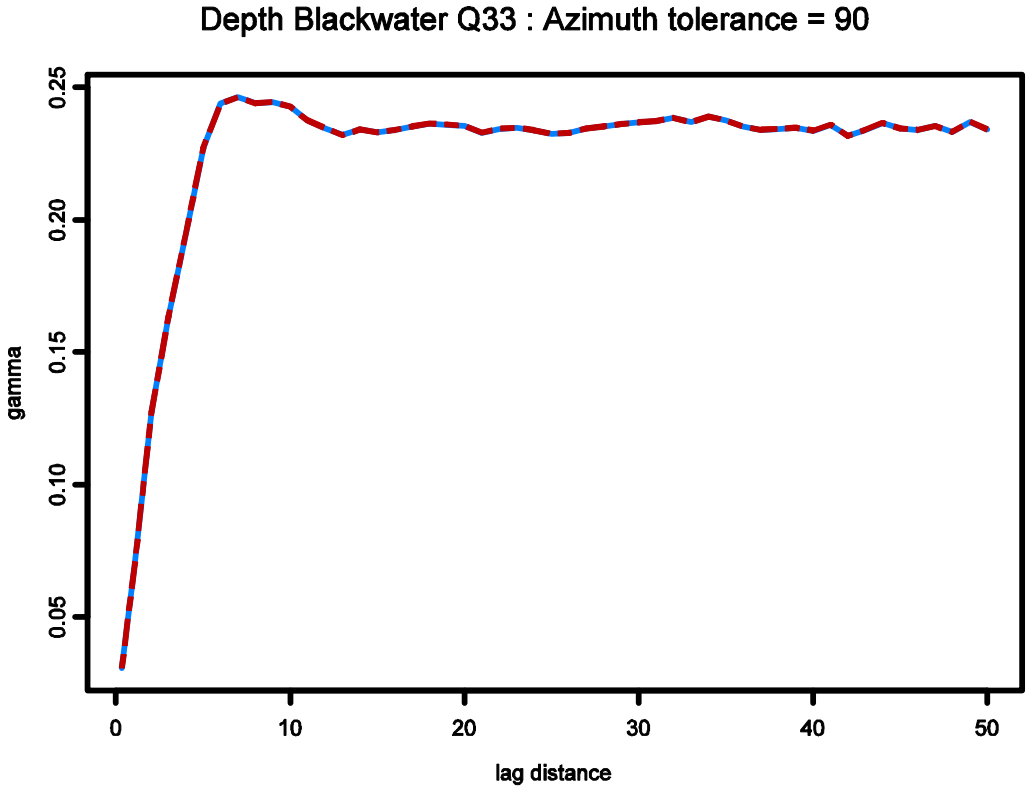
Depth Blackwater Q33 : Azimuth tolerance = 90
gamma
0.05
0.10
0.15
0.20
0.25
0
10
20
30
40
50
lag distance

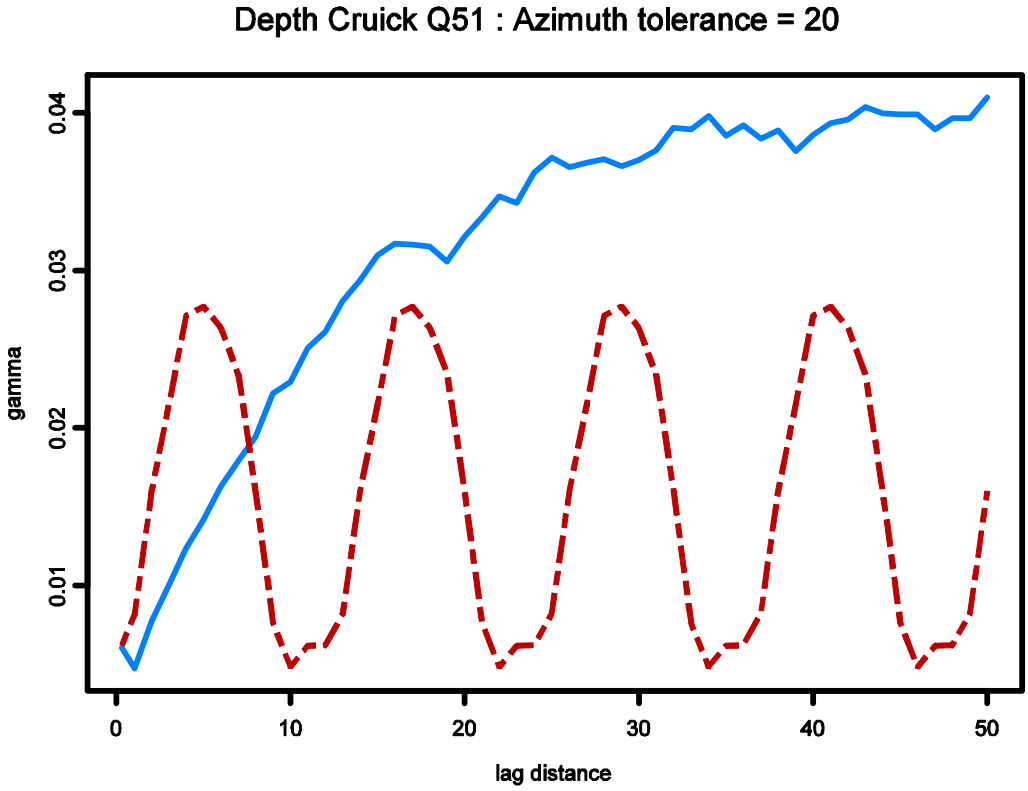
Depth Cruick Q51 : Azimuth tolerance = 20
gamma
0.01
0.02
0.03
0.04
0
10
20
30
40
50
lag distance

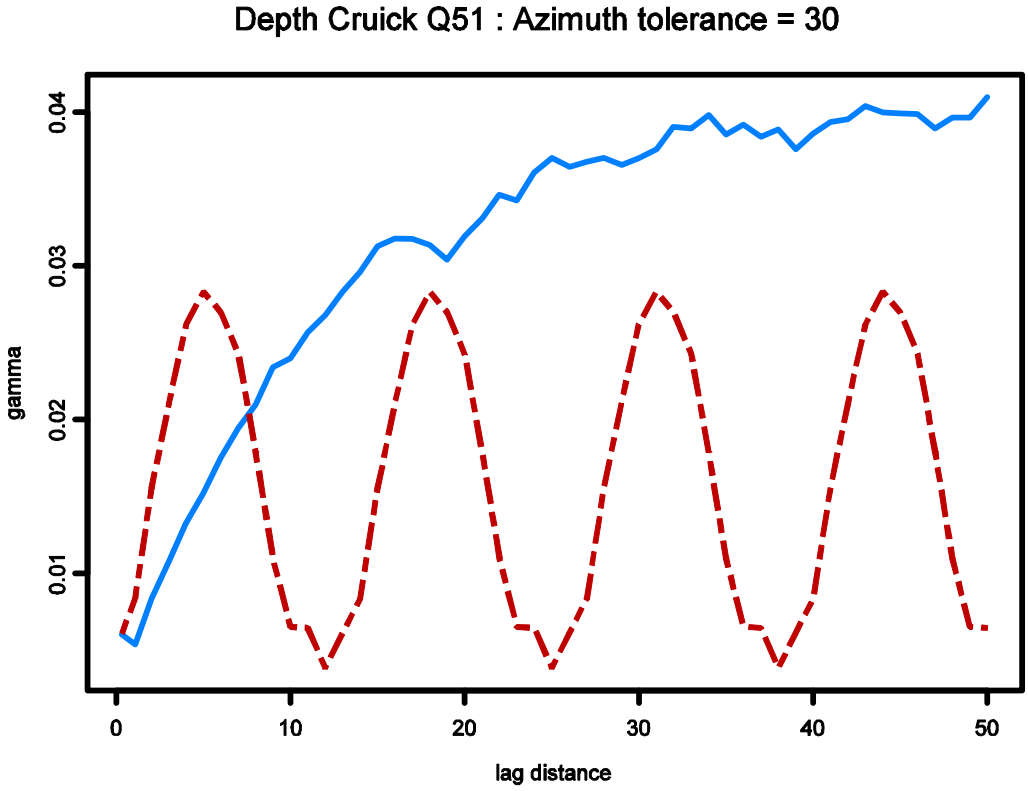
Depth Cruick Q51 : Azimuth tolerance = 30
gamma
0.01
0.02
0.03
0.04
0
10
20
30
40
50
lag distance

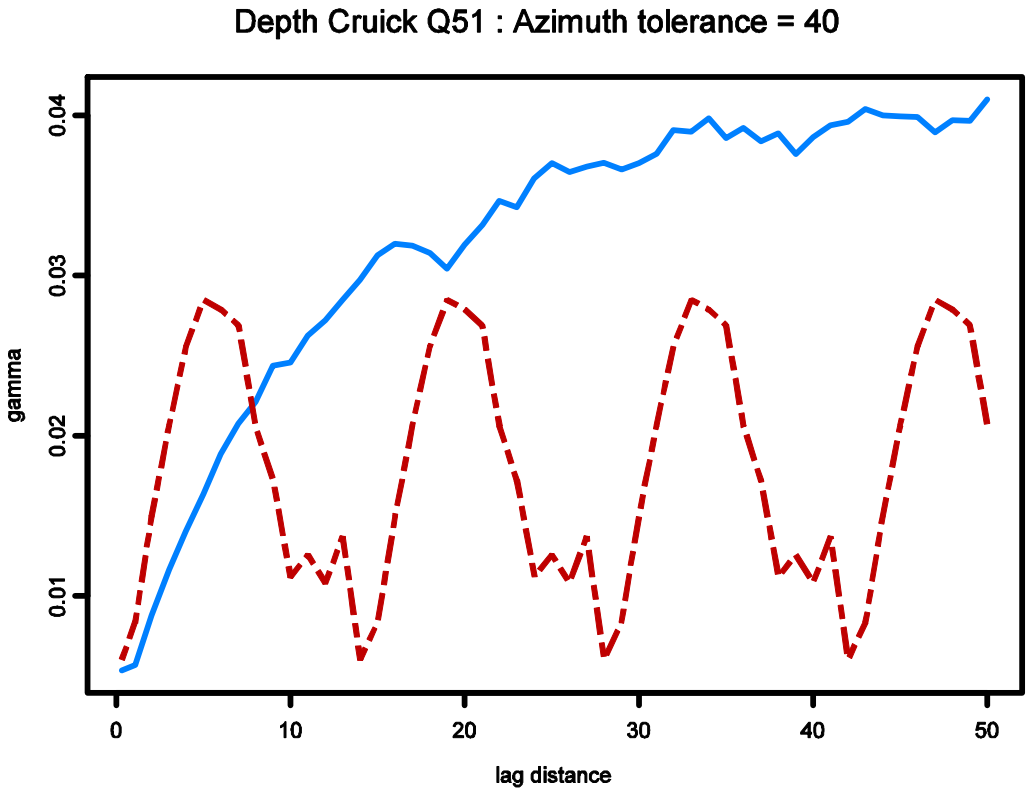
Depth Cruick Q51 : Azimuth tolerance = 40
gamma
0.01
0.02
0.03
0.04
0
10
20
30
40
50
lag distance

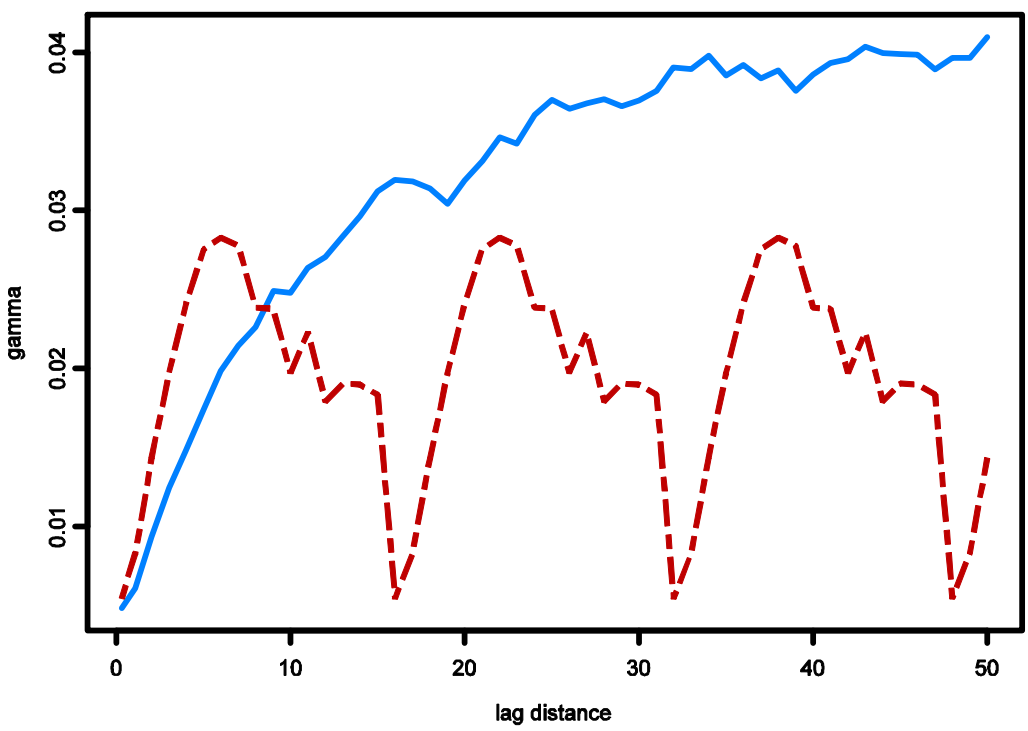
Depth Cruick Q51 : Azimuth tolerance = 50
gamma
0.01
0.02
0.03
0.04
0
10
20
30
40
50
lag distance

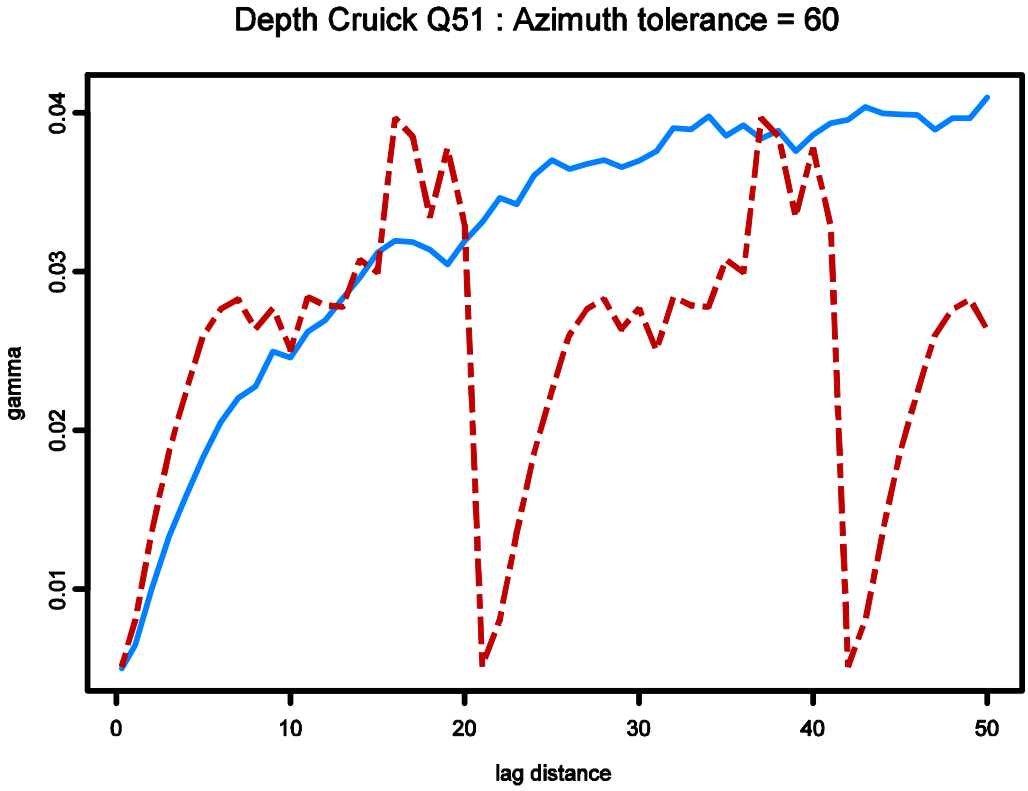
Depth Cruick Q51 : Azimuth tolerance = 60
gamma
0.01
0.02
0.03
0.04
0
10
20
30
40
50
lag distance

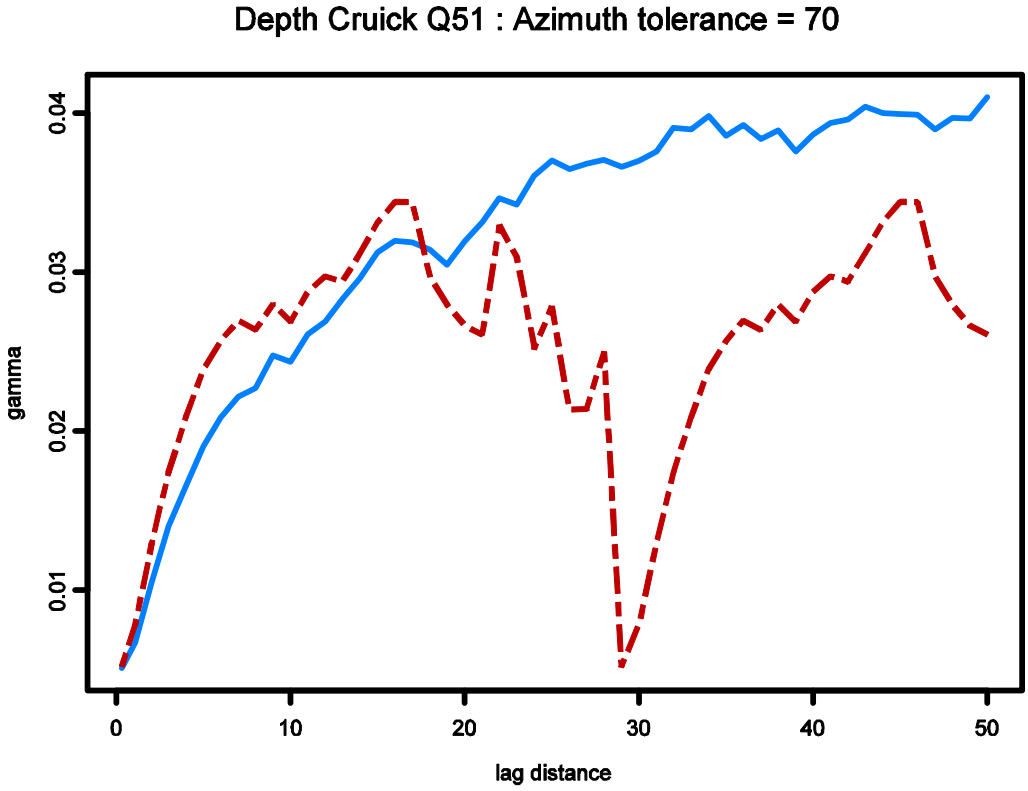
Depth Cruick Q51 : Azimuth tolerance = 70
gamma
0.01
0.02
0.03
0.04
0
10
20
30
40
50
lag distance

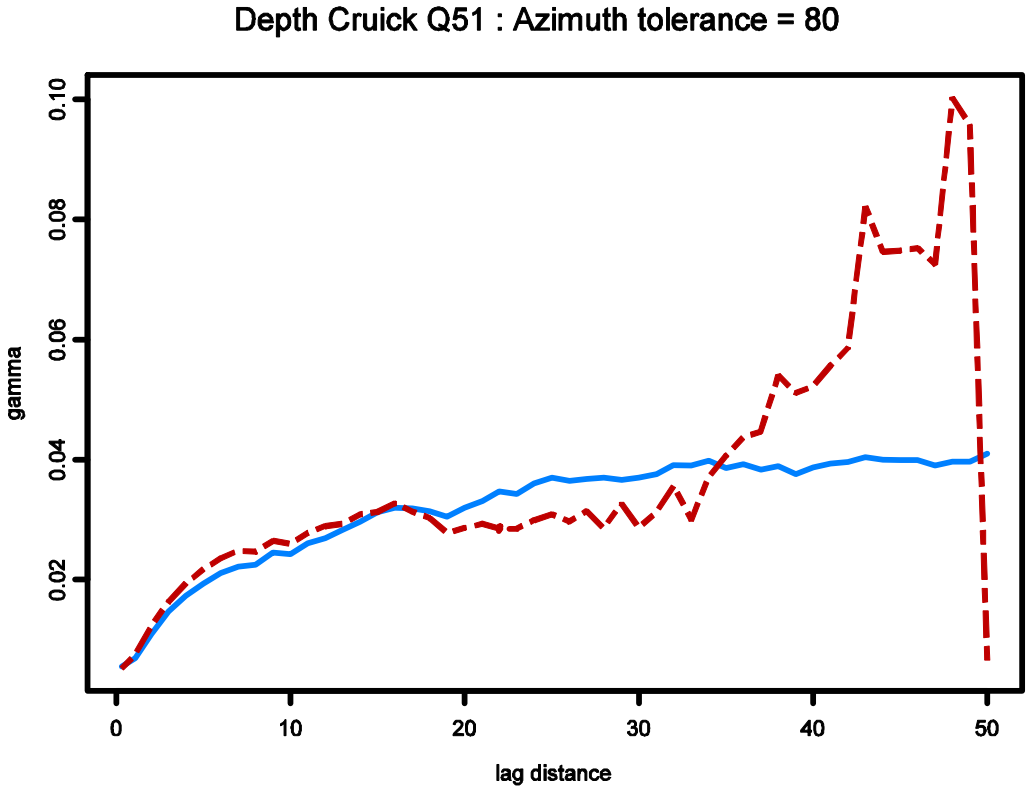
Depth Cruick Q51 : Azimuth tolerance = 80
gamma
0.02
0.04
0.06
0.08
0.10
0
10
20
30
40
50
lag distance

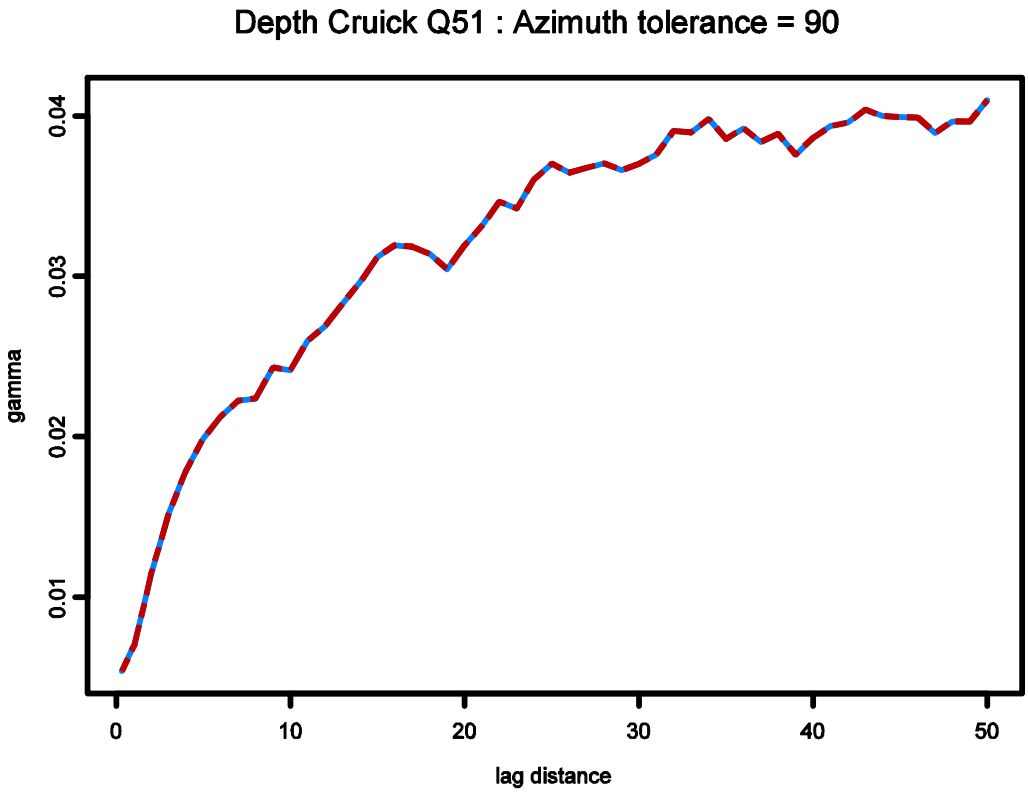
Depth Cruick Q51 : Azimuth tolerance = 90
gamma
0.01
0.02
0.03
0.04
0
10
20
30
40
50
lag distance

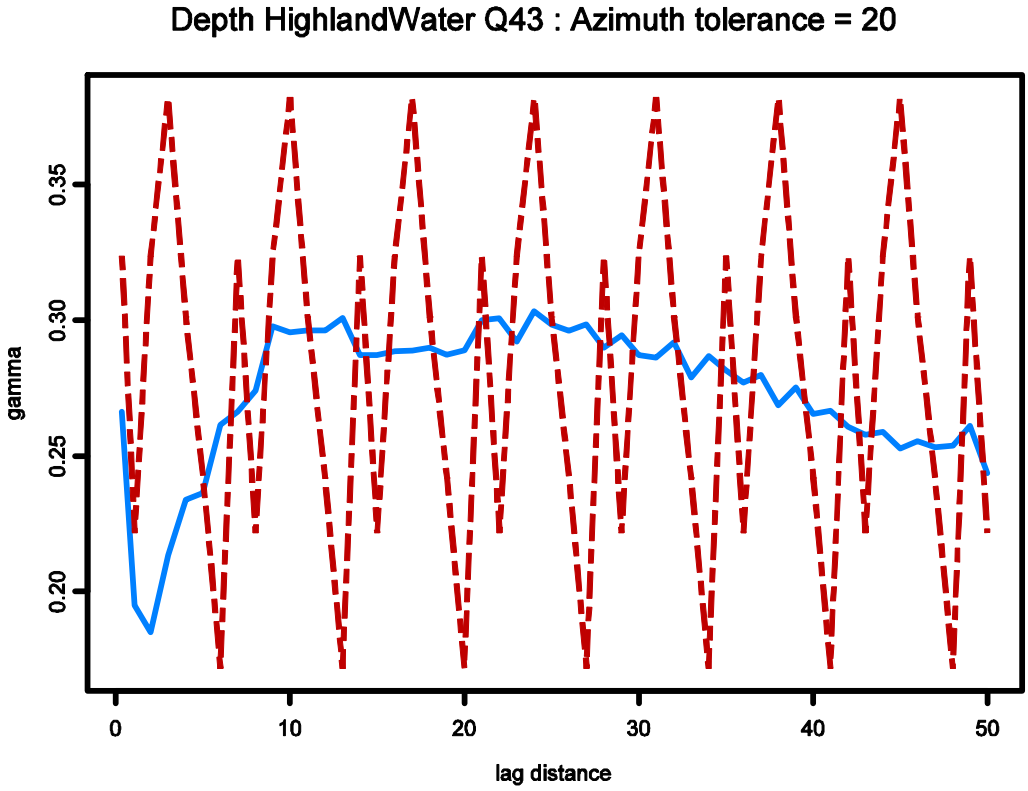
Depth HighlandWater Q43 : Azimuth tolerance = 20
gamma
0.20
0.25
0.30
0.35
0
10
20
30
40
50
lag distance

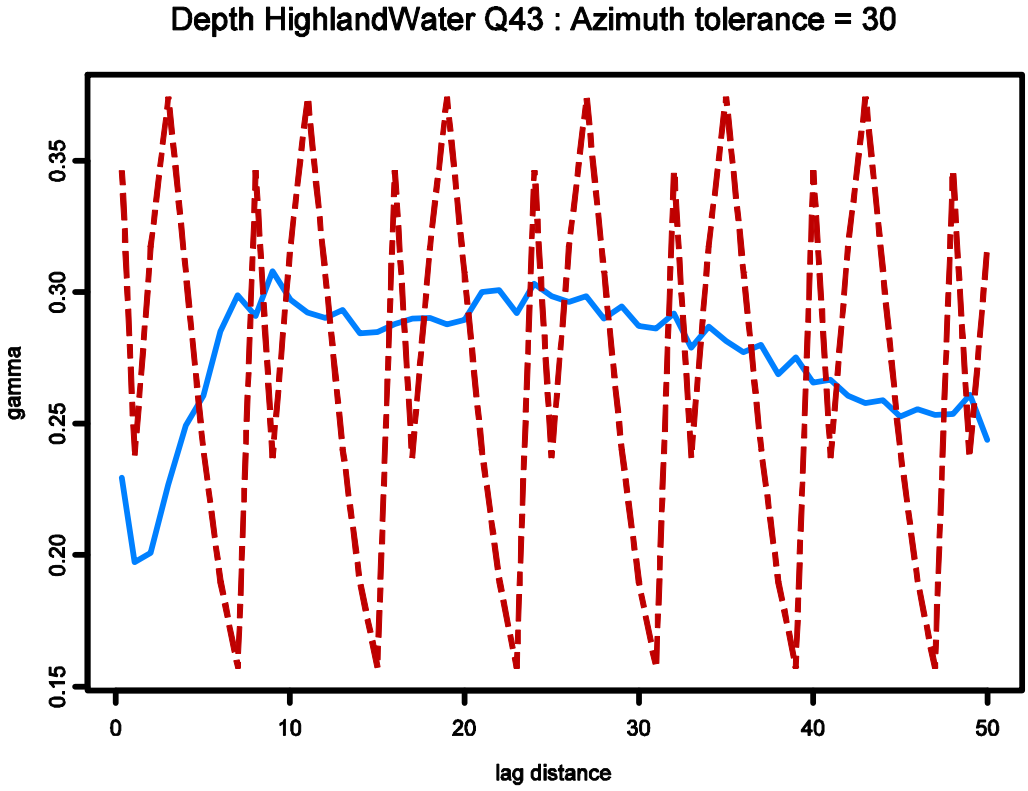
Depth HighlandWater Q43 : Azimuth tolerance = 30
gamma
0.15
0.20
0.25
0.30
0.35
0
10
20
30
40
50
lag distance

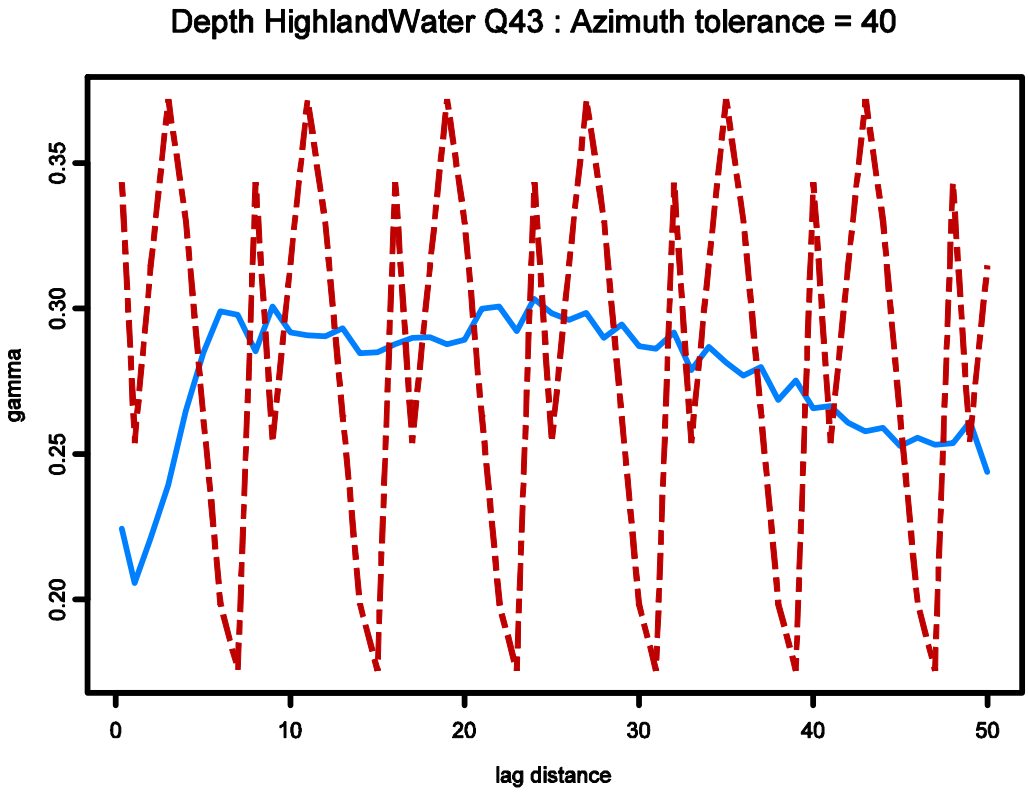
Depth HighlandWater Q43 : Azimuth tolerance = 40
gamma
0.20
0.25
0.30
0.35
0
10
20
30
40
50
lag distance

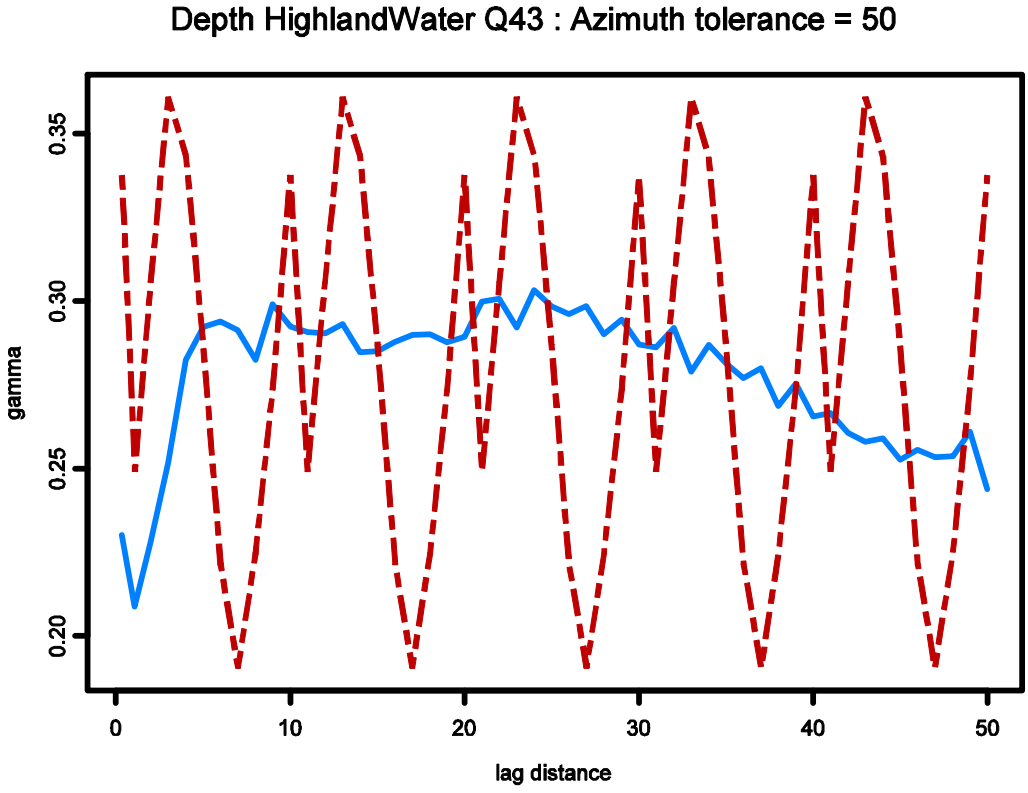
Depth HighlandWater Q43 : Azimuth tolerance = 50
gamma
0.20
0.25
0.30
0.35
0
10
20
30
40
50
lag distance

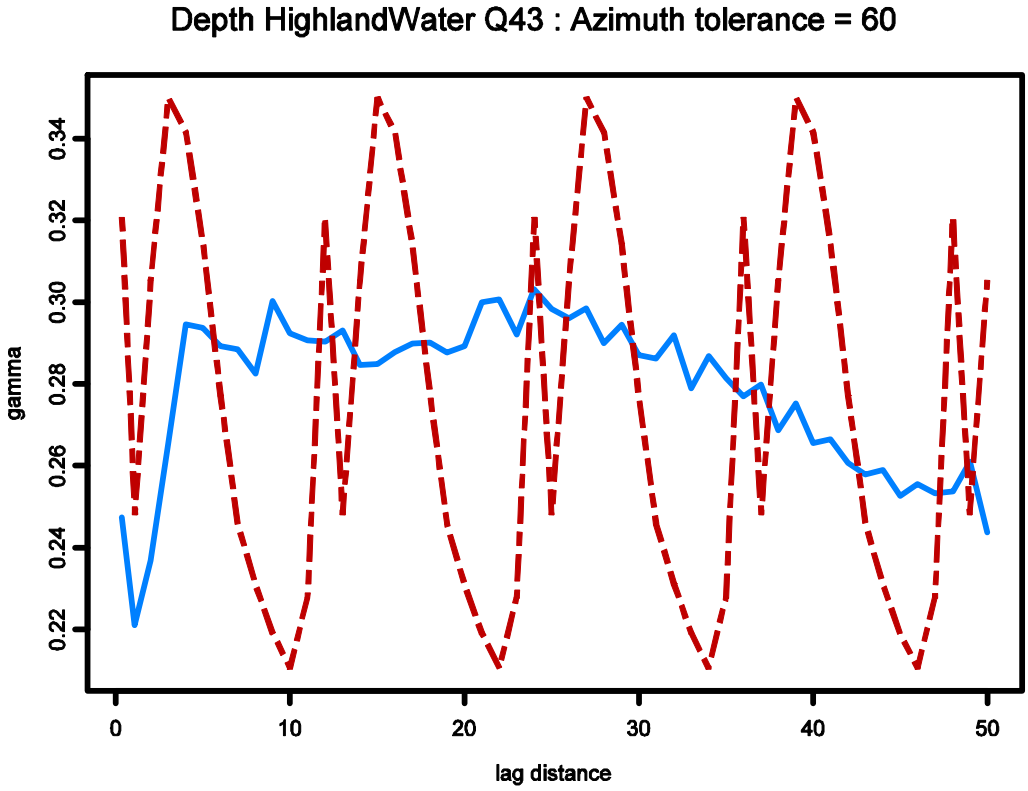
Depth HighlandWater Q43 : Azimuth tolerance = 60
gamma
0.22
0.24
0.26
0.28
0.30
0.32
0.34
0
10
20
30
40
50
lag distance

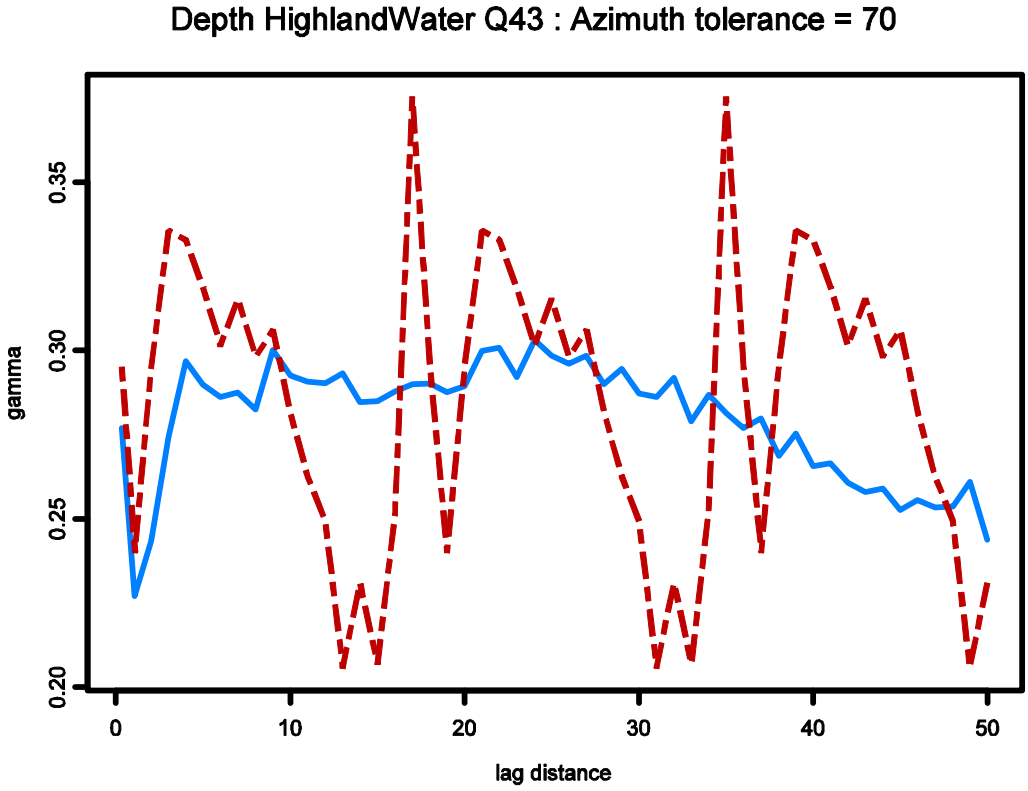
Depth HighlandWater Q43 : Azimuth tolerance = 70
gamma
0.20
0.25
0.30
0.35
0
10
20
30
40
50
lag distance

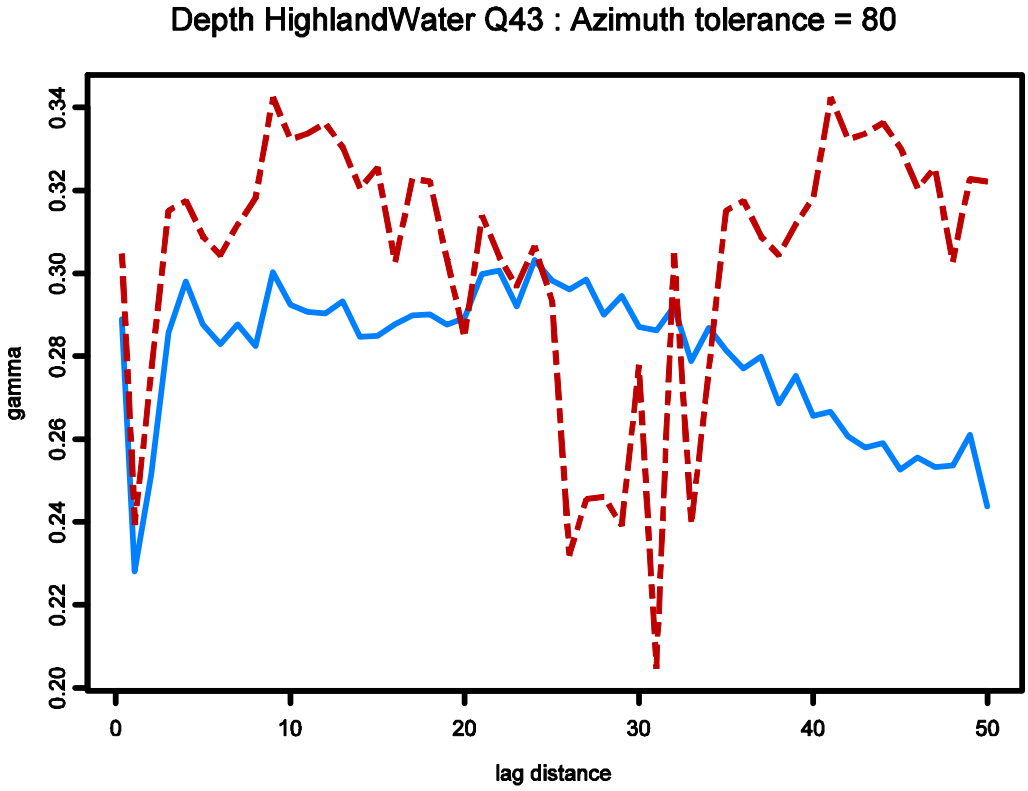
Depth HighlandWater Q43 : Azimuth tolerance = 80
gamma
0.20
0.22
0.24
0.26
0.28
0.30
0.32
0.34
0
10
20
30
40
50
lag distance

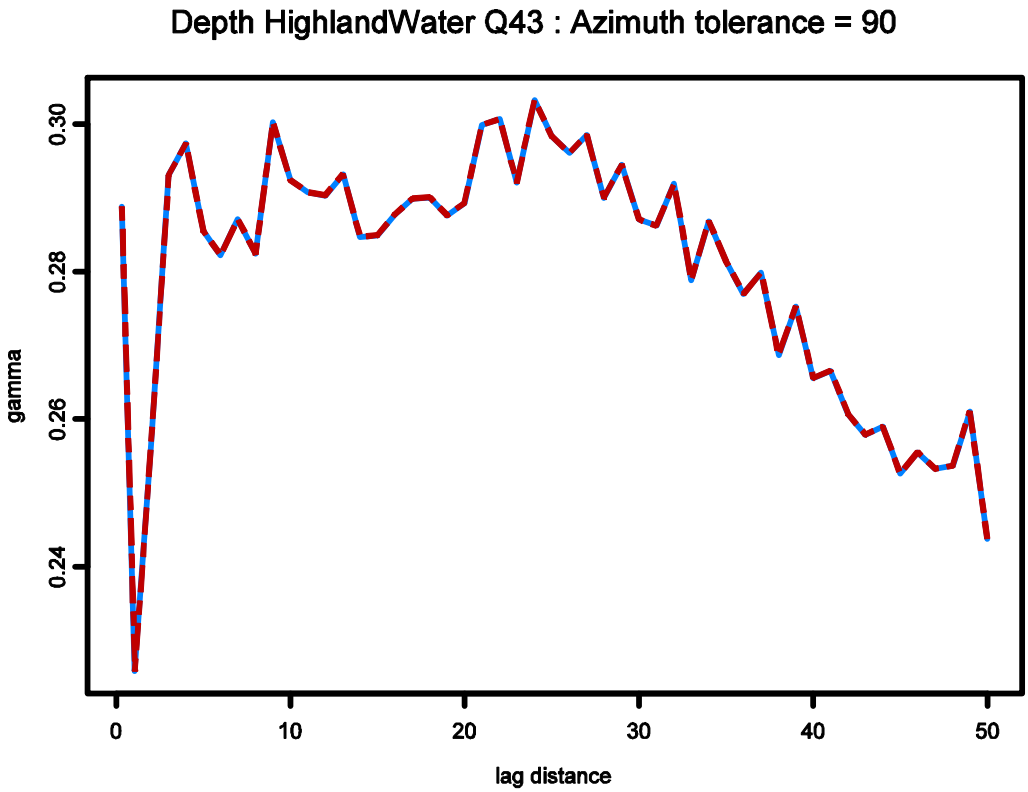
Depth HighlandWater Q43 : Azimuth tolerance = 90
gamma
0.24
0.26
0.28
0.30
0
10
20
30
40
50
lag distance

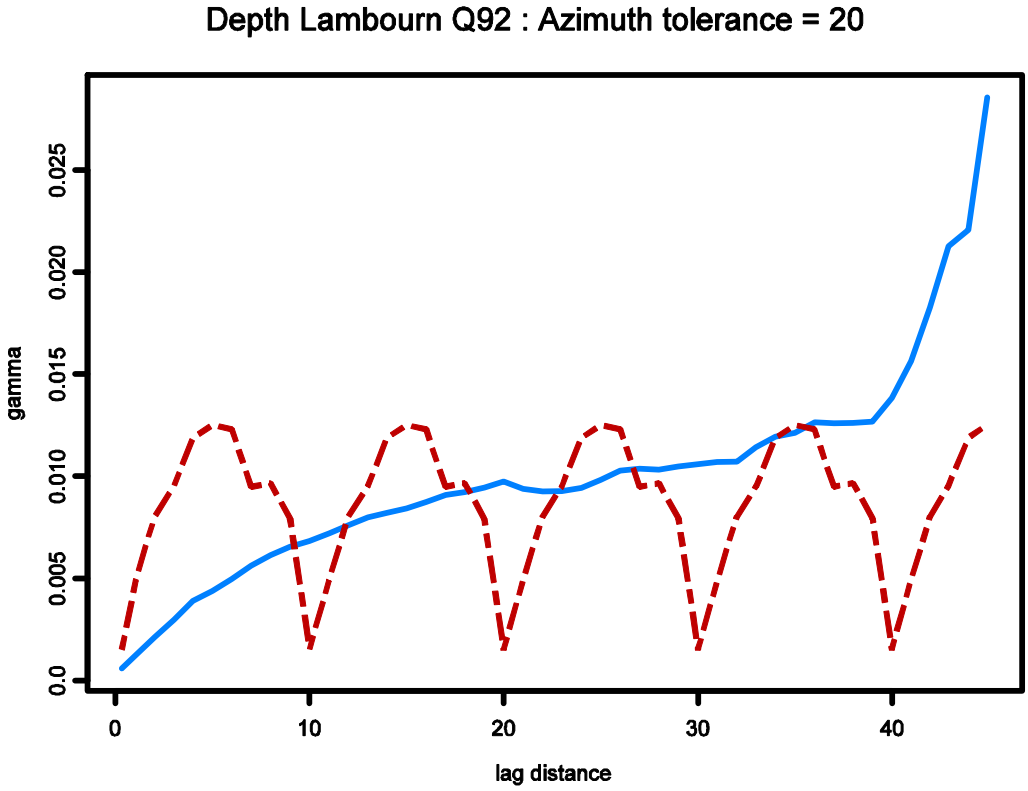
Depth Lambourn Q92 : Azimuth tolerance = 20
gamma
0.0
0.005
0.010
0.015
0.020
0.025
0
10
20
30
40
lag distance

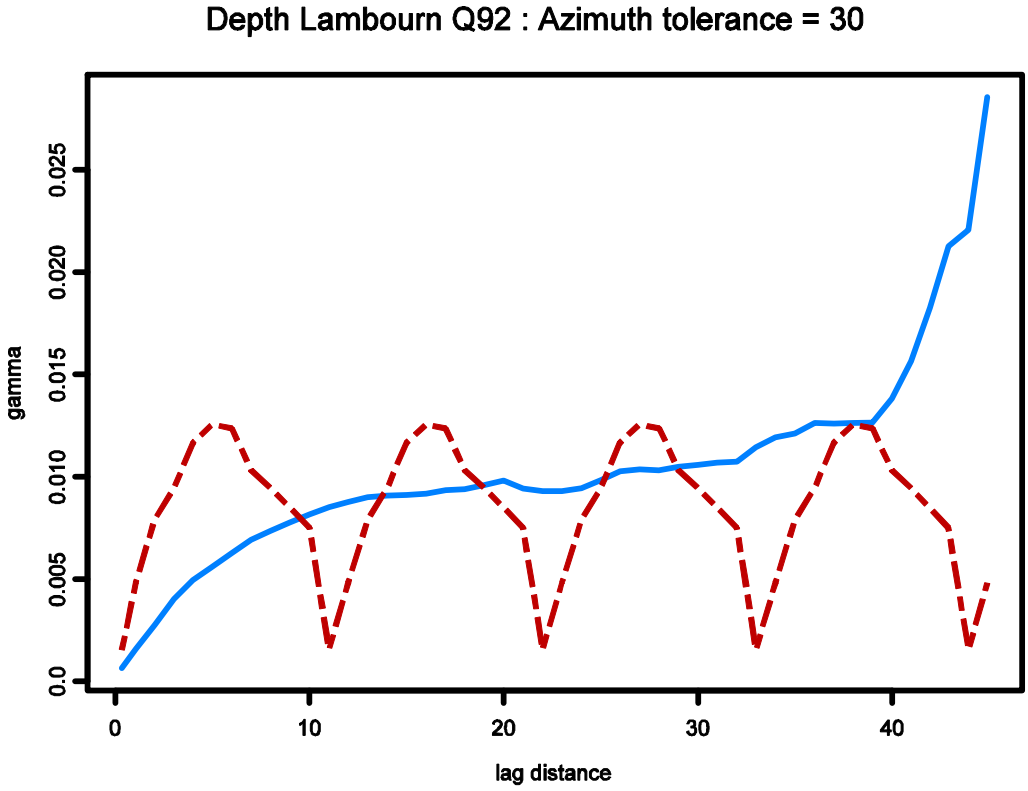
Depth Lambourn Q92 : Azimuth tolerance = 30
gamma
0.0
0.005
0.010
0.015
0.020
0.025
0
10
20
30
40
lag distance

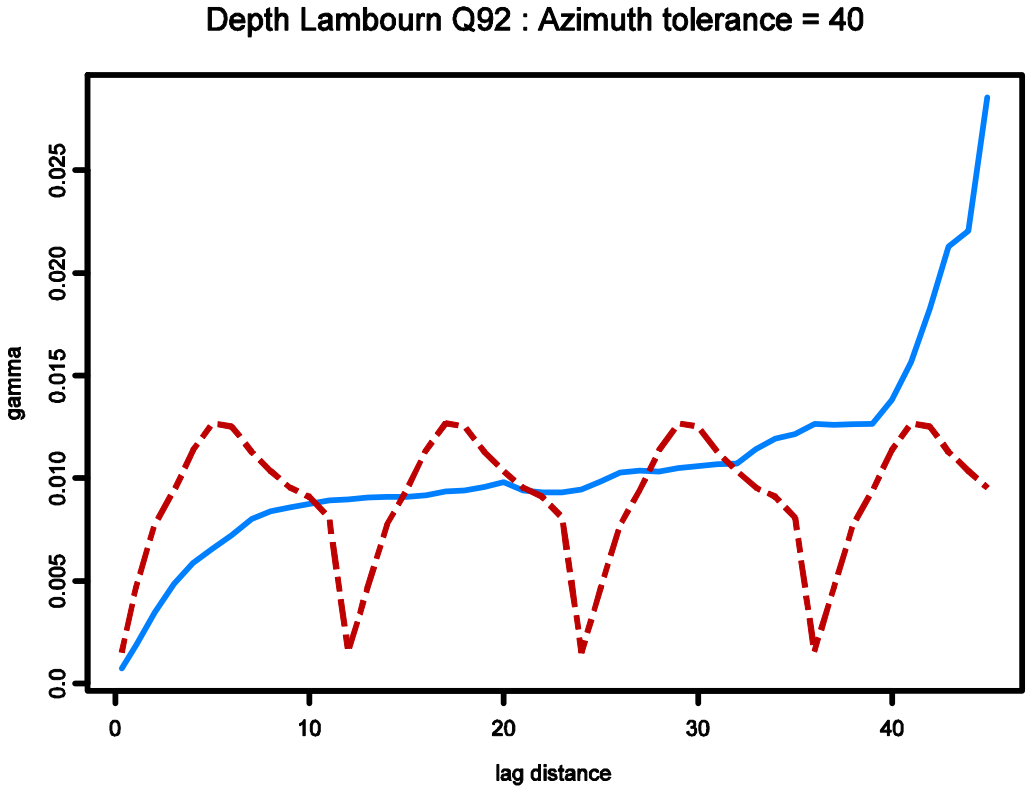
Depth Lambourn Q92 : Azimuth tolerance = 40
gamma
0.0
0.005
0.010
0.015
0.020
0.025
0
10
20
30
40
lag distance

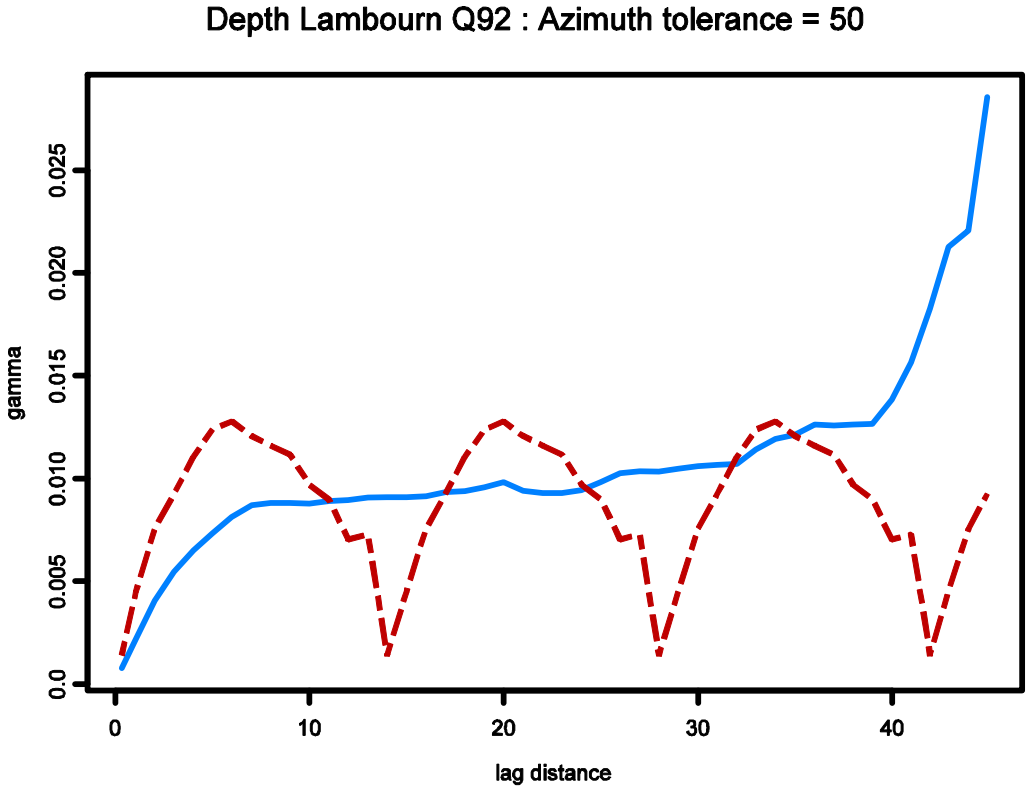
Depth Lambourn Q92 : Azimuth tolerance = 50
gamma
0.0
0.005
0.010
0.015
0.020
0.025
0
10
20
30
40
lag distance

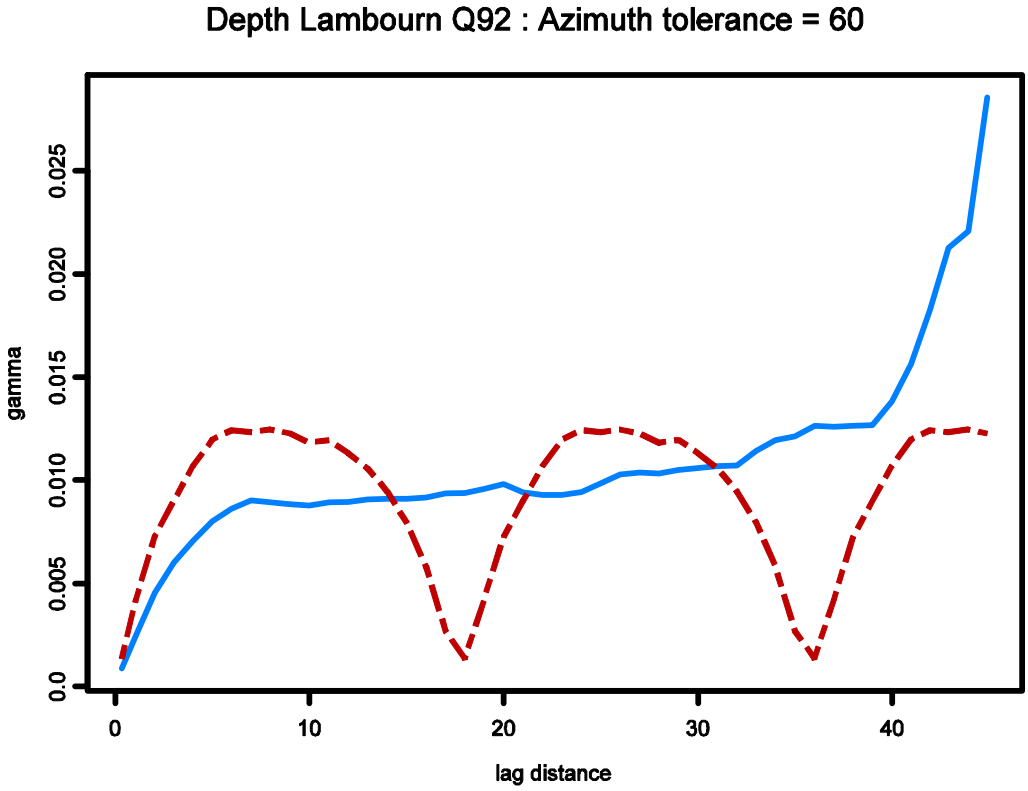
Depth Lambourn Q92 : Azimuth tolerance = 60
gamma
0.0
0.005
0.010
0.015
0.020
0.025
0
10
20
30
40
lag distance

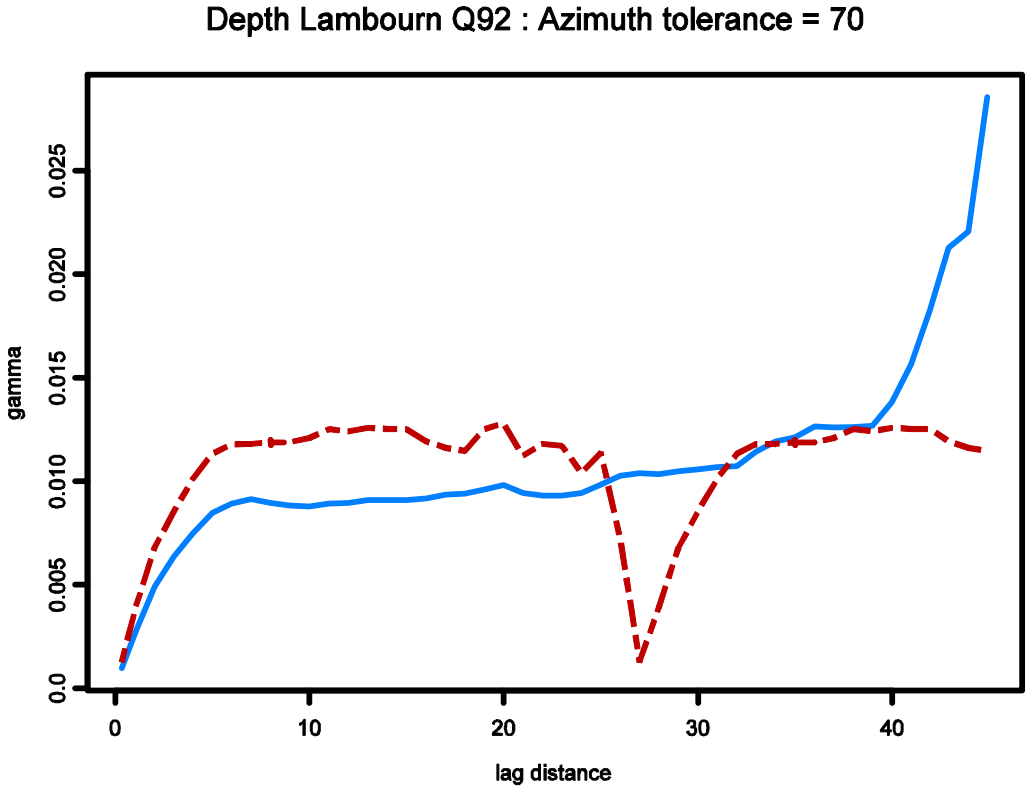
Depth Lambourn Q92 : Azimuth tolerance = 70
gamma
0.0
0.005
0.010
0.015
0.020
0.025
0
10
20
30
40
lag distance

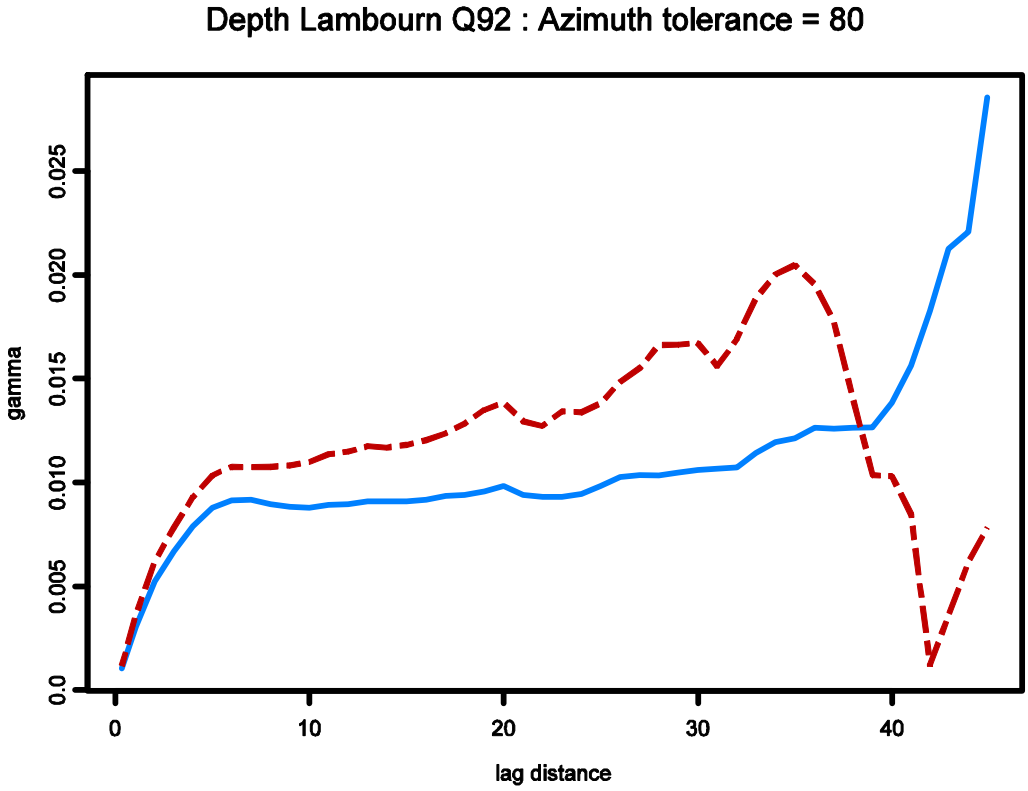
Depth Lambourn Q92 : Azimuth tolerance = 80
gamma
0.0
0.005
0.010
0.015
0.020
0.025
0
10
20
30
40
lag distance

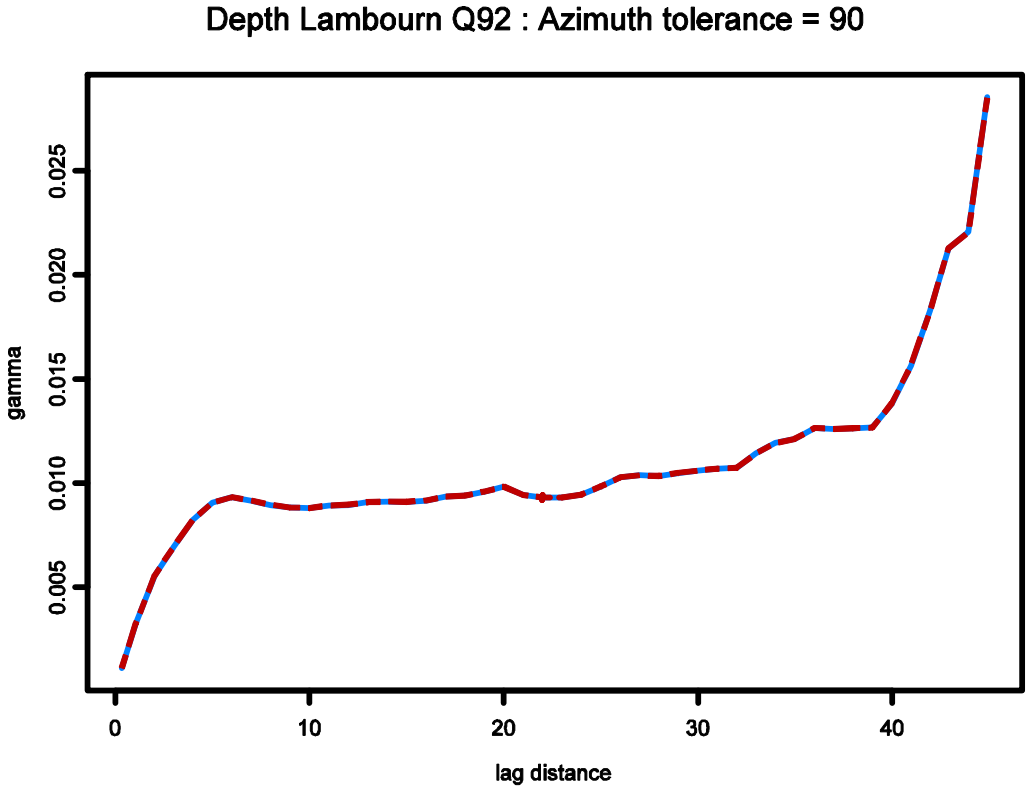
Depth Lambourn Q92 : Azimuth tolerance = 90
gamma
0.005
0.010
0.015
0.020
0.025
0
10
20
30
40
lag distance

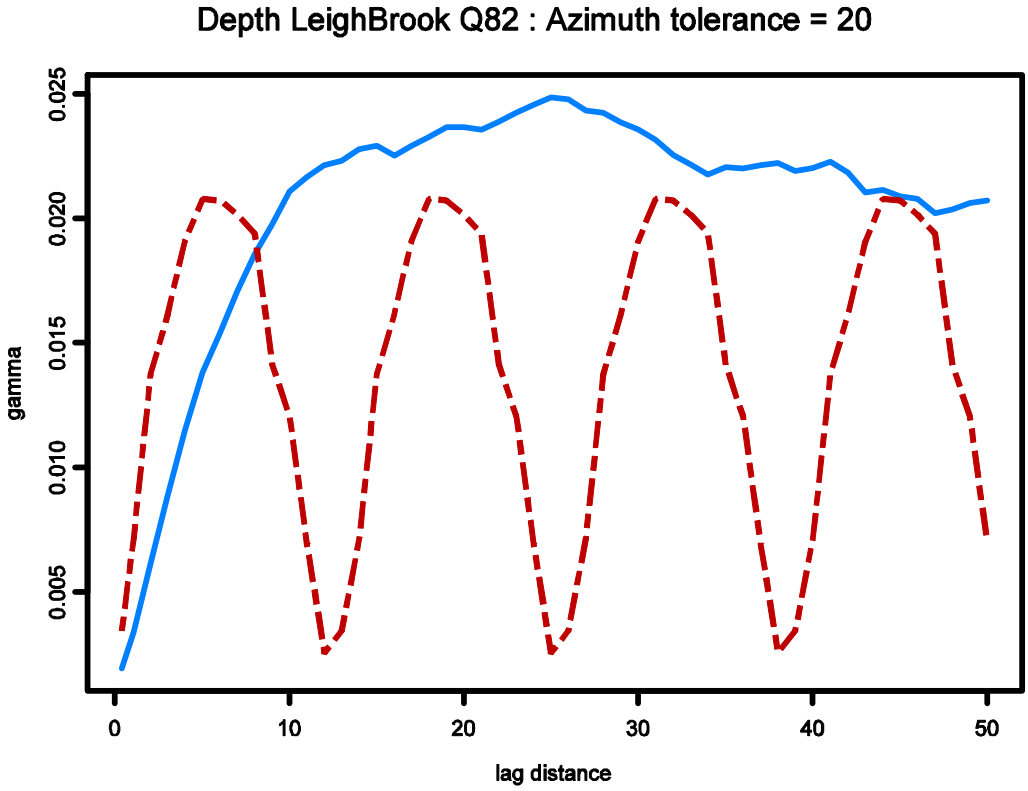
Depth LeighBrook Q82 : Azimuth tolerance = 20
gamma
0.005
0.010
0.015
0.020
0.025
0
10
20
30
40
50
lag distance

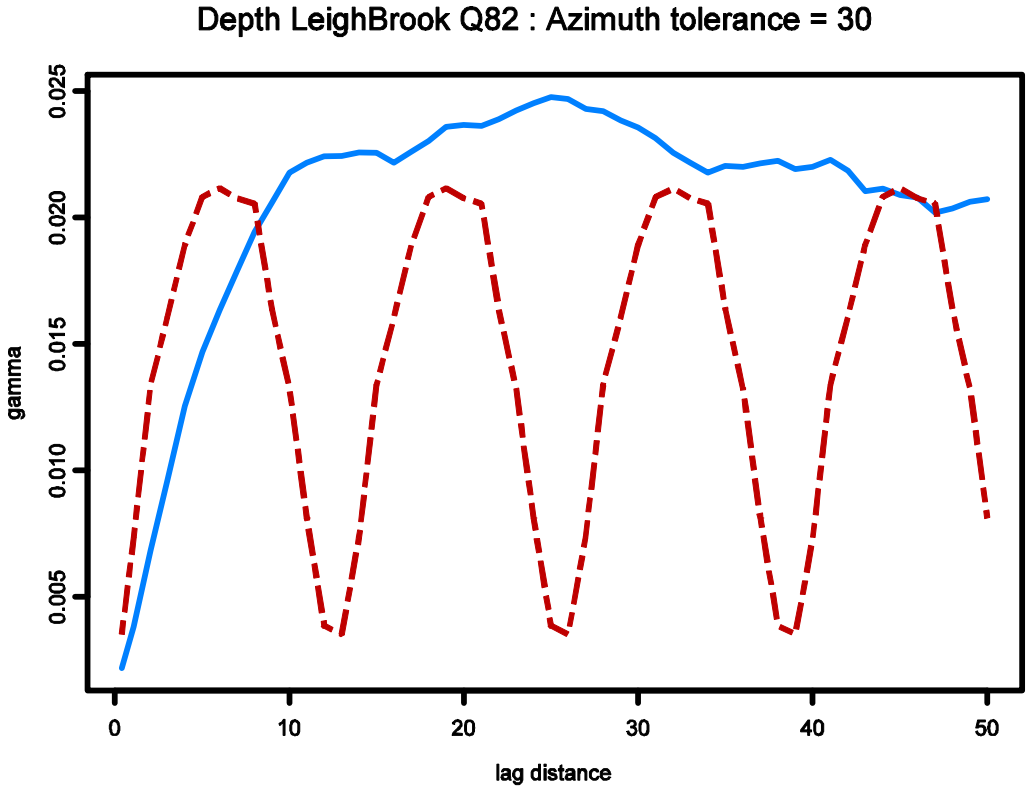
Depth LeighBrook Q82 : Azimuth tolerance = 30
gamma
0.005
0.010
0.015
0.020
0.025
0
10
20
30
40
50
lag distance

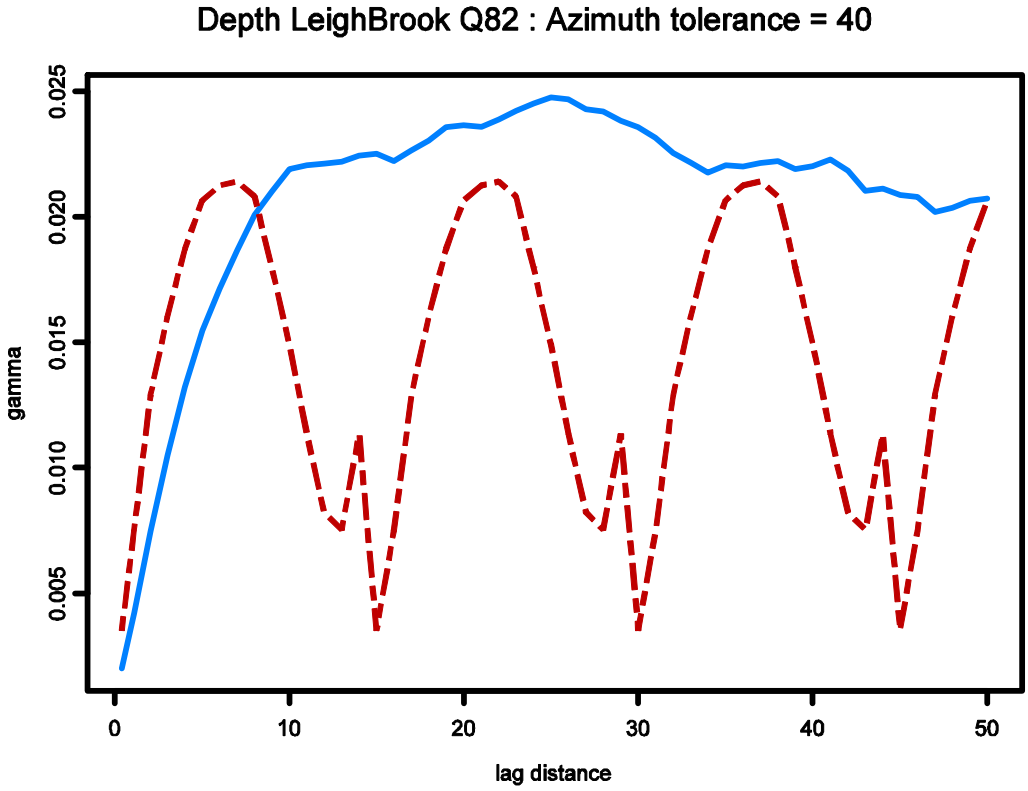
Depth LeighBrook Q82 : Azimuth tolerance = 40
gamma
0.005
0.010
0.015
0.020
0.025
0
10
20
30
40
50
lag distance

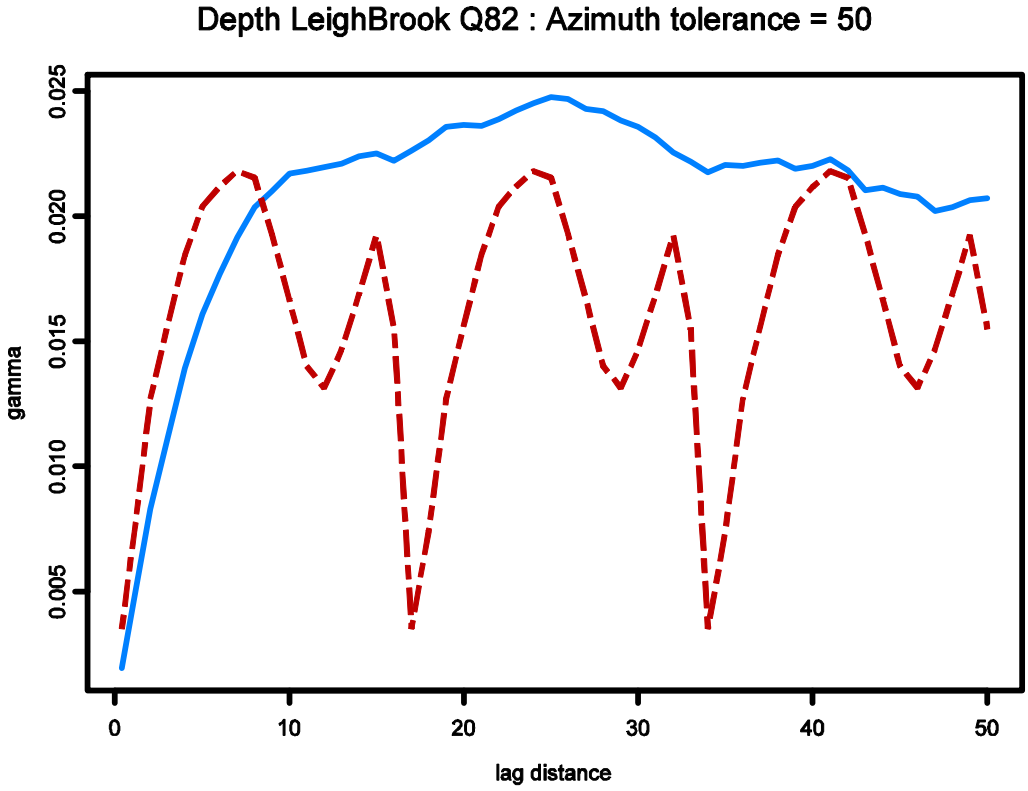
Depth LeighBrook Q82 : Azimuth tolerance = 50
gamma
0.005
0.010
0.015
0.020
0.025
0
10
20
30
40
50
lag distance

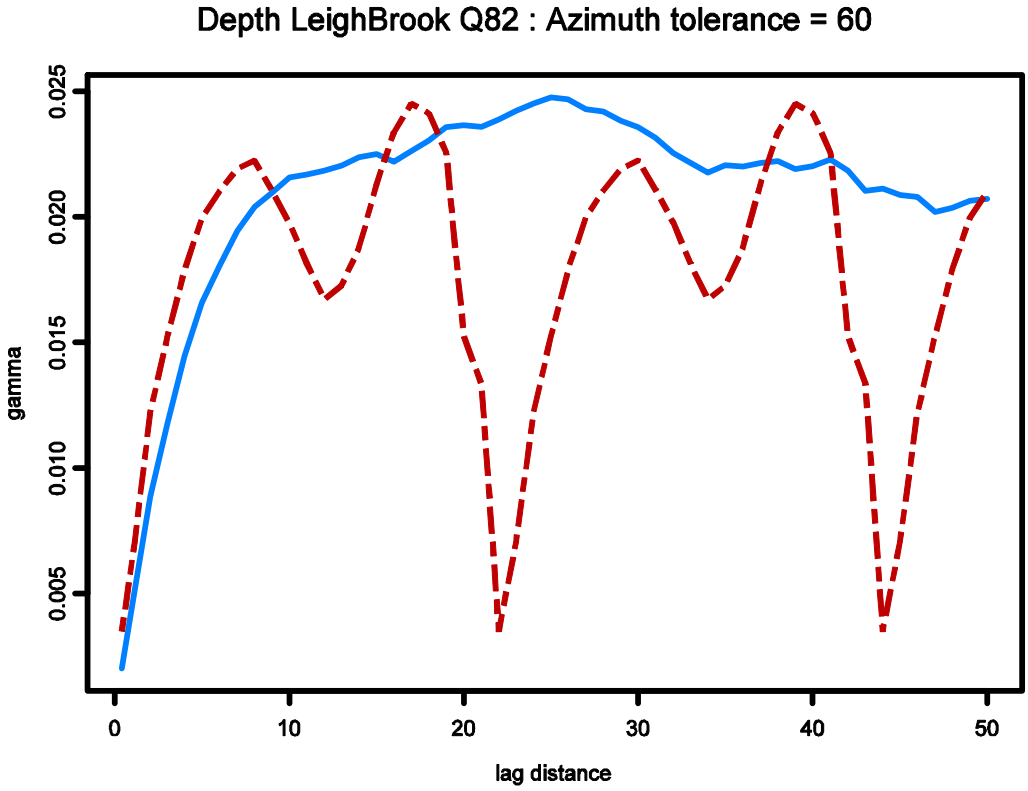
Depth LeighBrook Q82 : Azimuth tolerance = 60
gamma
0.005
0.010
0.015
0.020
0.025
0
10
20
30
40
50
lag distance

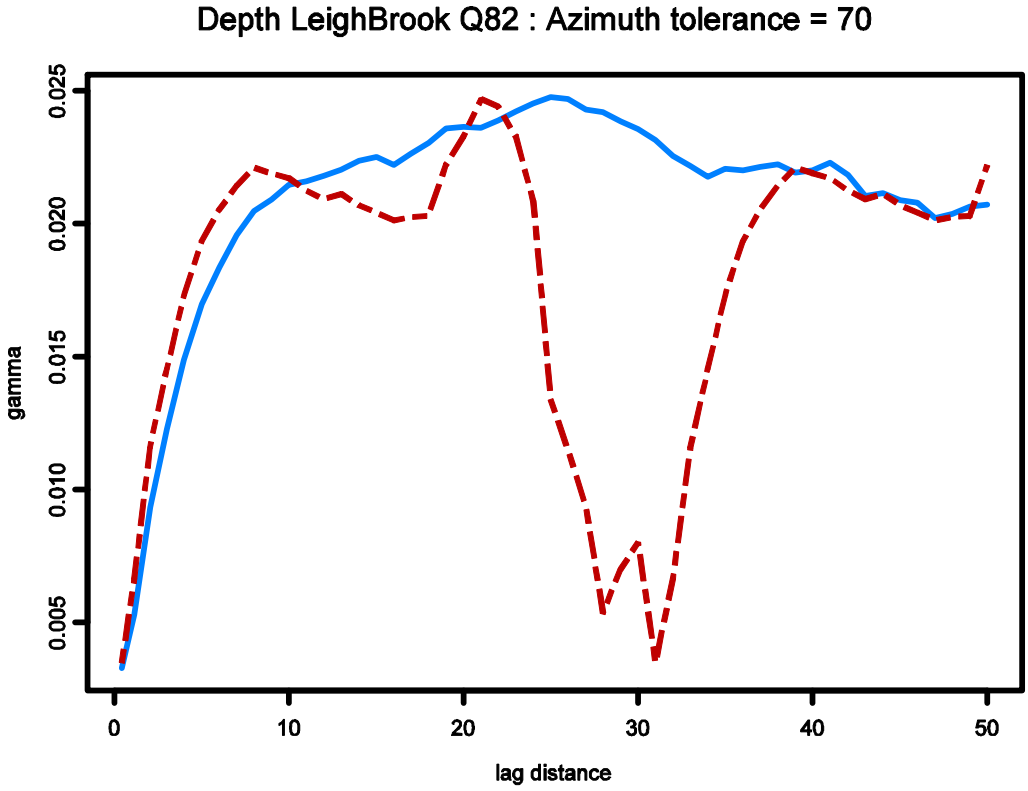
Depth LeighBrook Q82 : Azimuth tolerance = 70
gamma
0.005
0.010
0.015
0.020
0.025
0
10
20
30
40
50
lag distance

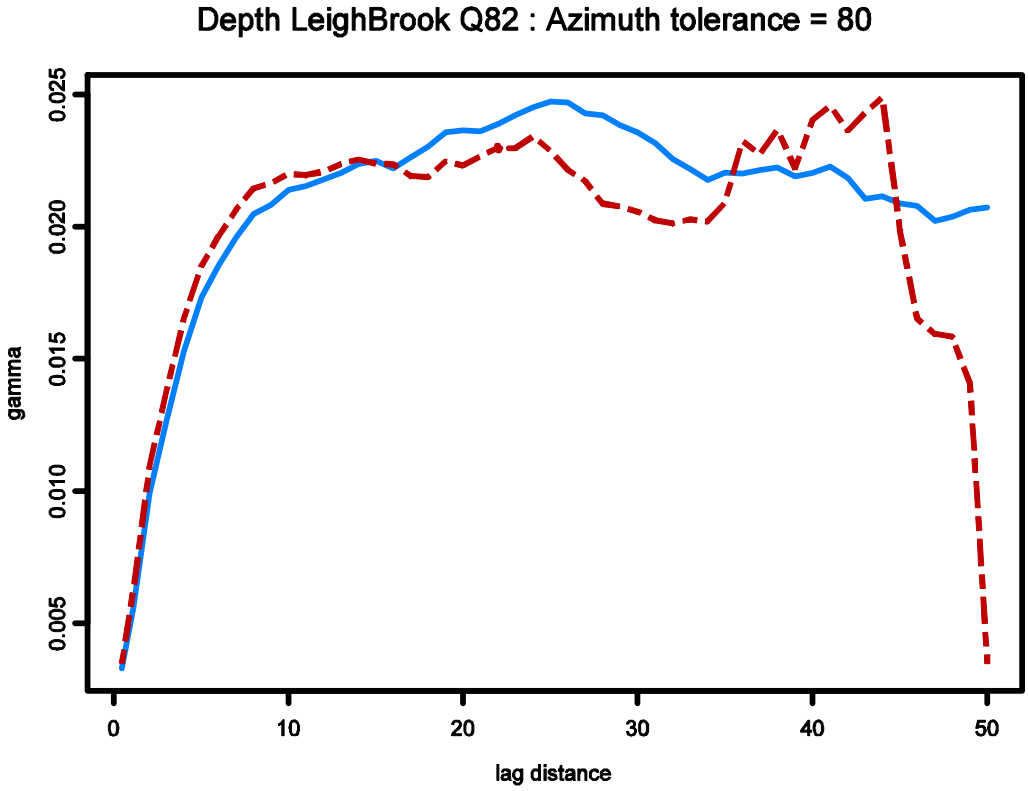
Depth LeighBrook Q82 : Azimuth tolerance = 80
gamma
0.005
0.010
0.015
0.020
0.025
0
10
20
30
40
50
lag distance

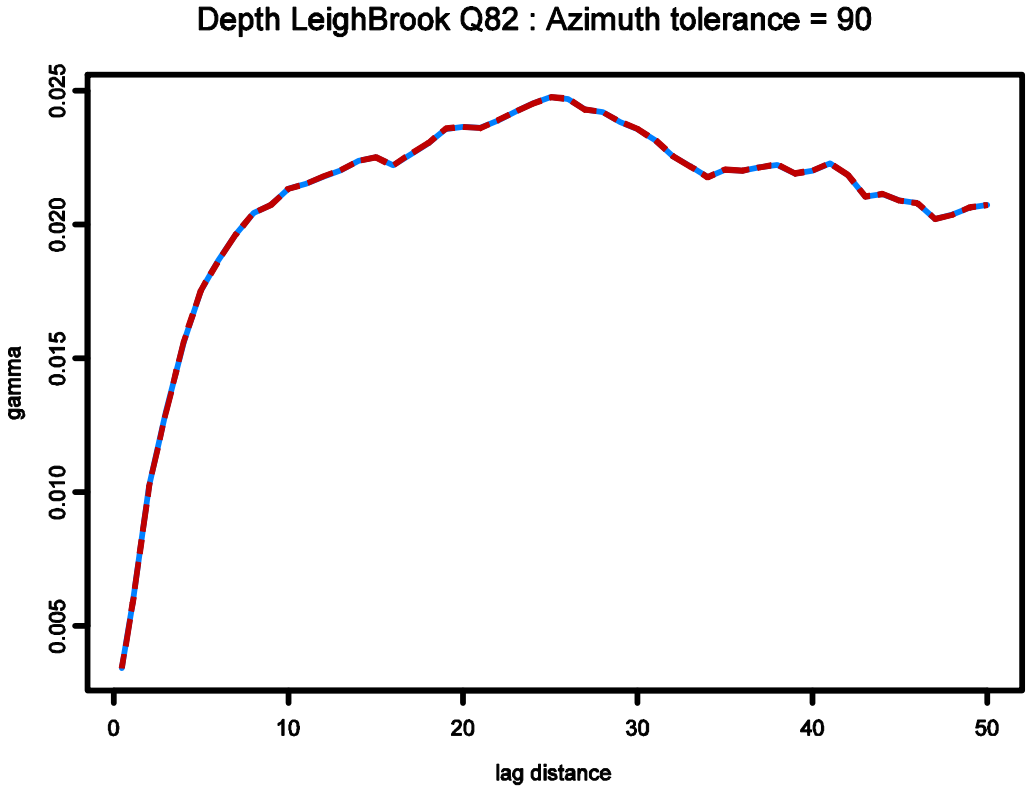
Depth LeighBrook Q82 : Azimuth tolerance = 90
gamma
0.005
0.010
0.015
0.020
0.025
0
10
20
30
40
50
lag distance

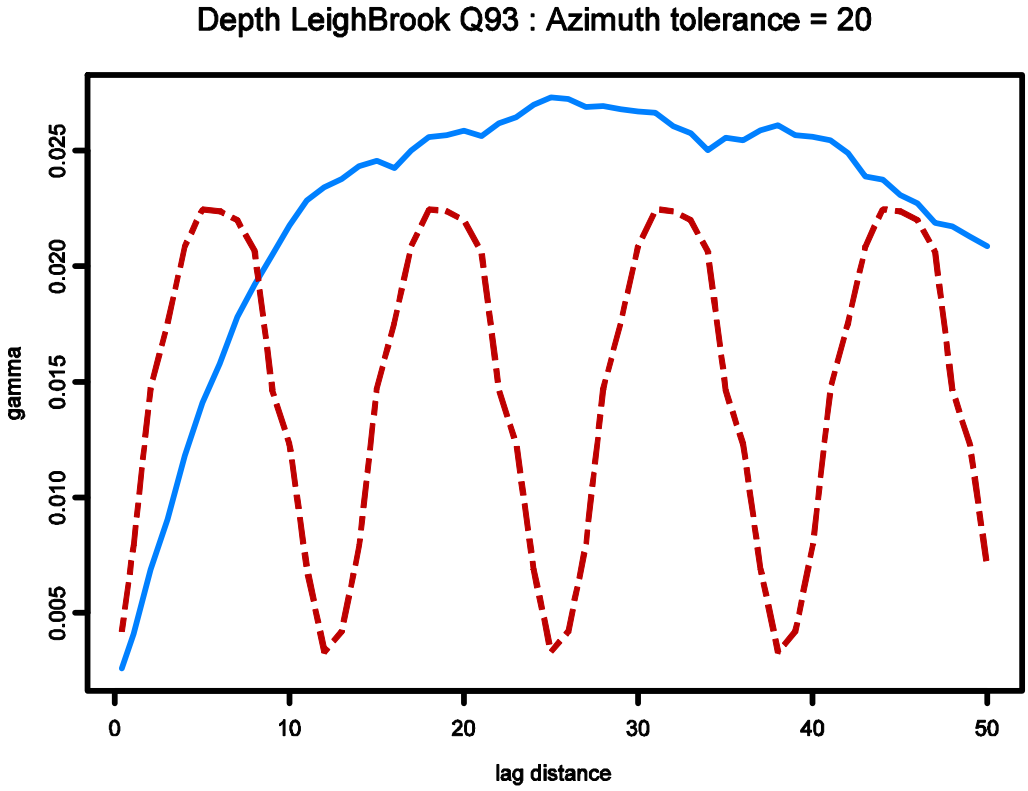
Depth LeighBrook Q93 : Azimuth tolerance = 20
gamma
0.005
0.010
0.015
0.020
0.025
0
10
20
30
40
50
lag distance

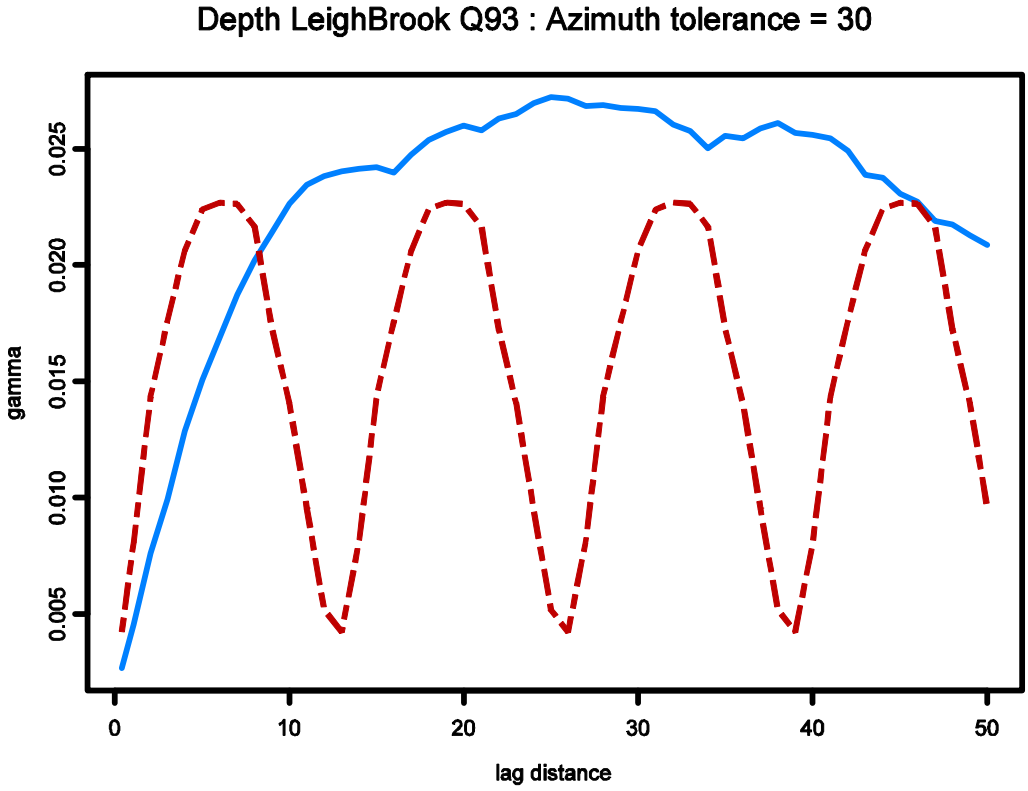
Depth LeighBrook Q93 : Azimuth tolerance = 30
gamma
0.005
0.010
0.015
0.020
0.025
0
10
20
30
40
50
lag distance

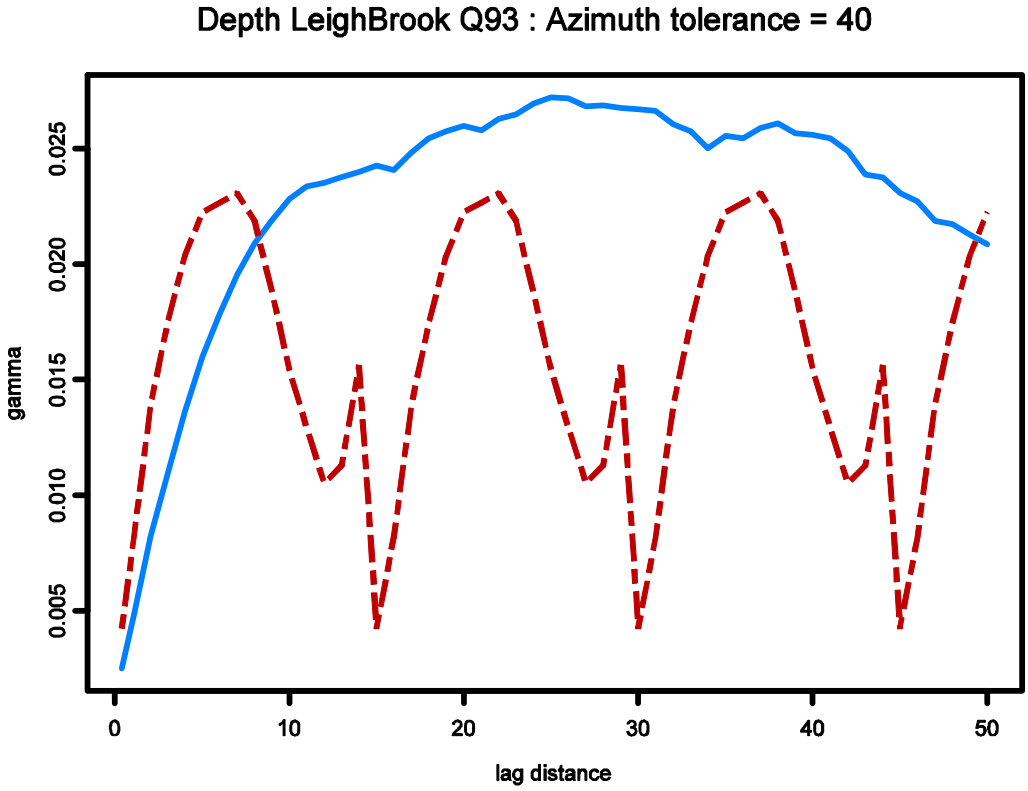
Depth LeighBrook Q93 : Azimuth tolerance = 40
gamma
0.005
0.010
0.015
0.020
0.025
0
10
20
30
40
50
lag distance

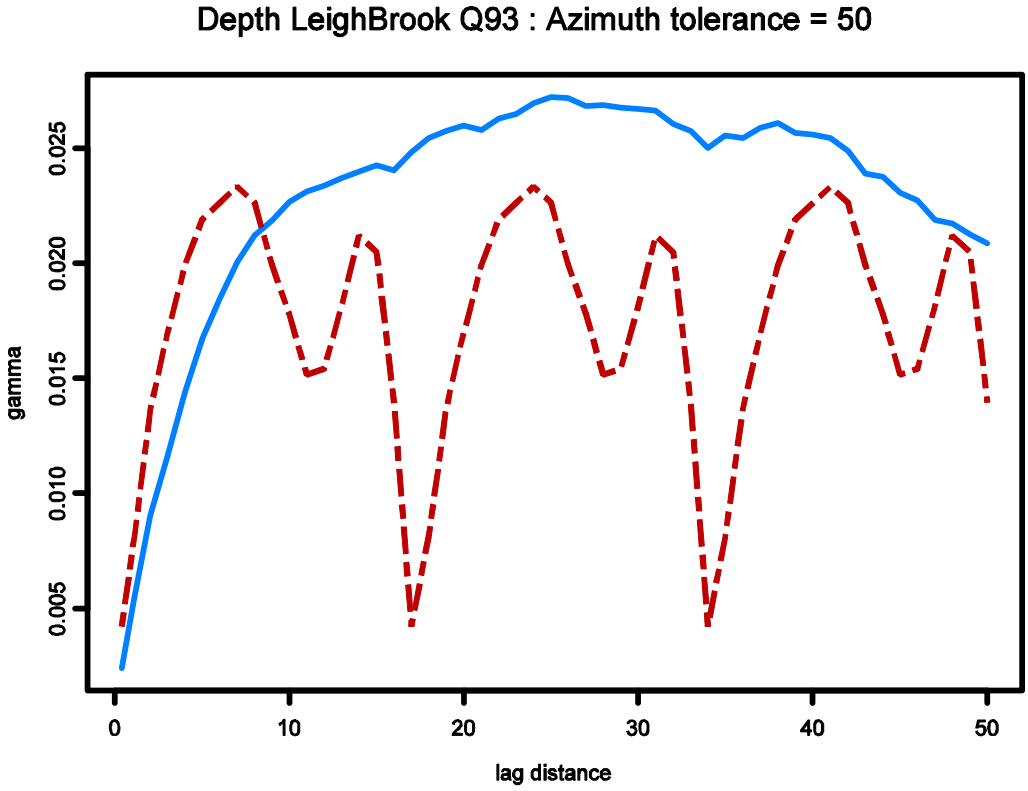
Depth LeighBrook Q93 : Azimuth tolerance = 50
gamma
0.005
0.010
0.015
0.020
0.025
0
10
20
30
40
50
lag distance

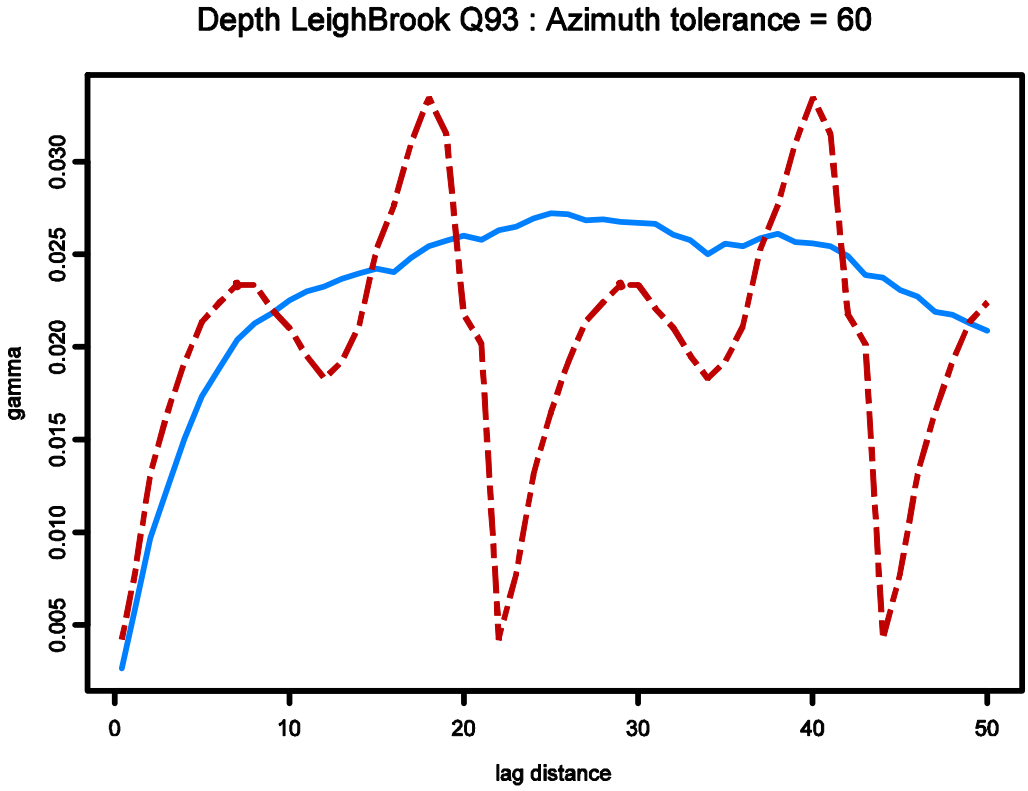
Depth LeighBrook Q93 : Azimuth tolerance = 60
gamma
0.005
0.010
0.015
0.020
0.025
0.030
0
10
20
30
40
50
lag distance

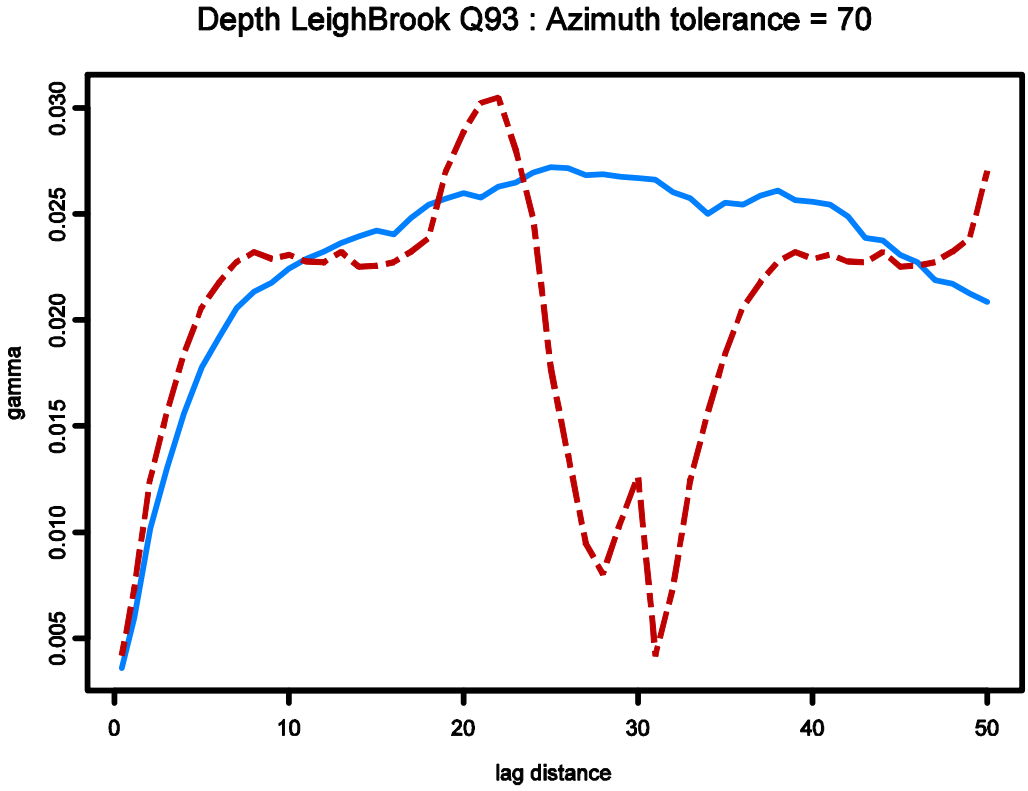
Depth LeighBrook Q93 : Azimuth tolerance = 70
gamma
0.005
0.010
0.015
0.020
0.025
0.030
0
10
20
30
40
50
lag distance

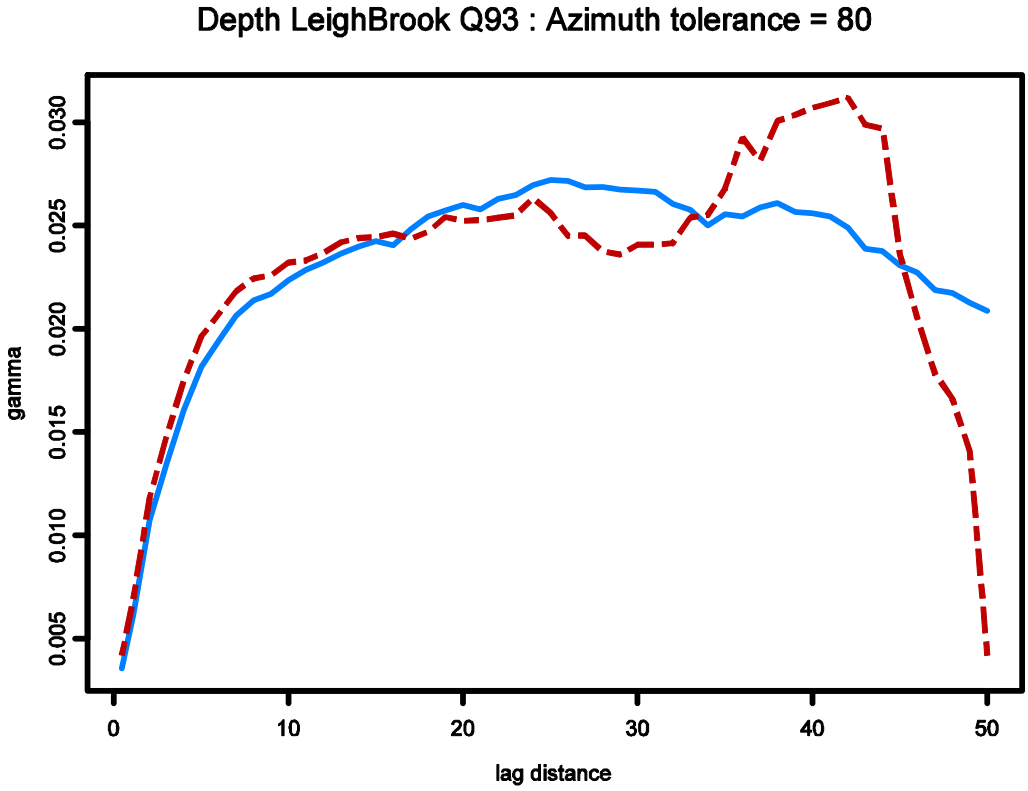
Depth LeighBrook Q93 : Azimuth tolerance = 80
gamma
0.005
0.010
0.015
0.020
0.025
0.030
0
10
20
30
40
50
lag distance

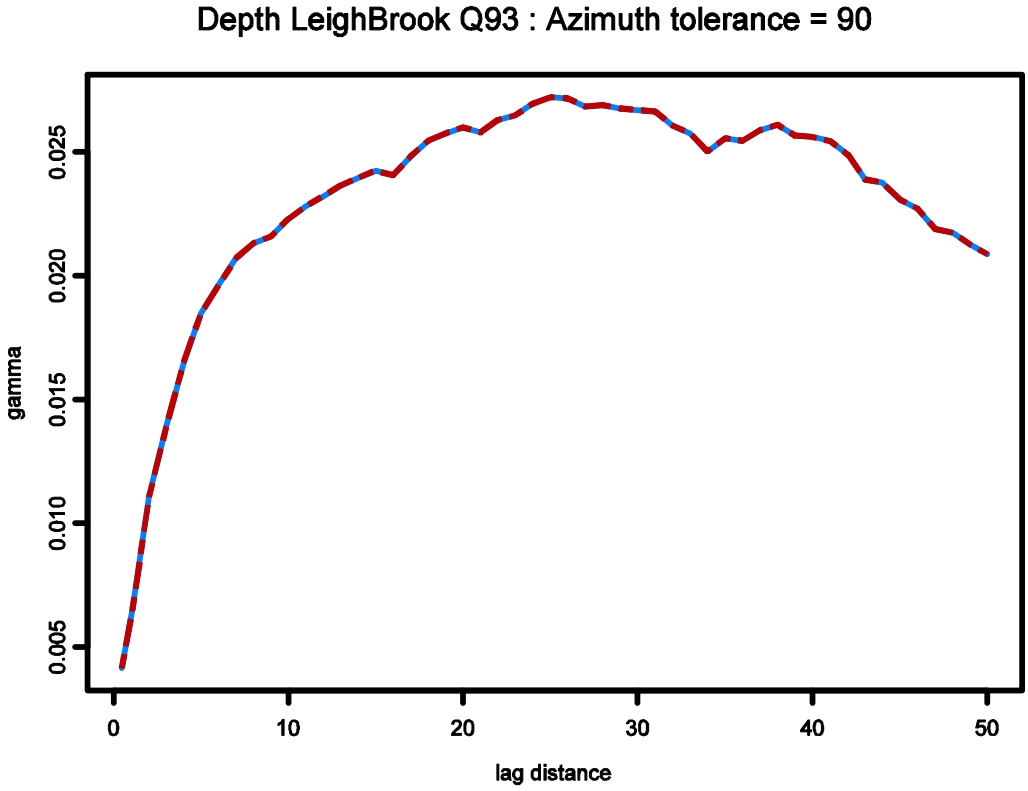
Depth LeighBrook Q93 : Azimuth tolerance = 90
gamma
0.005
0.010
0.015
0.020
0.025
0
10
20
30
40
50
lag distance

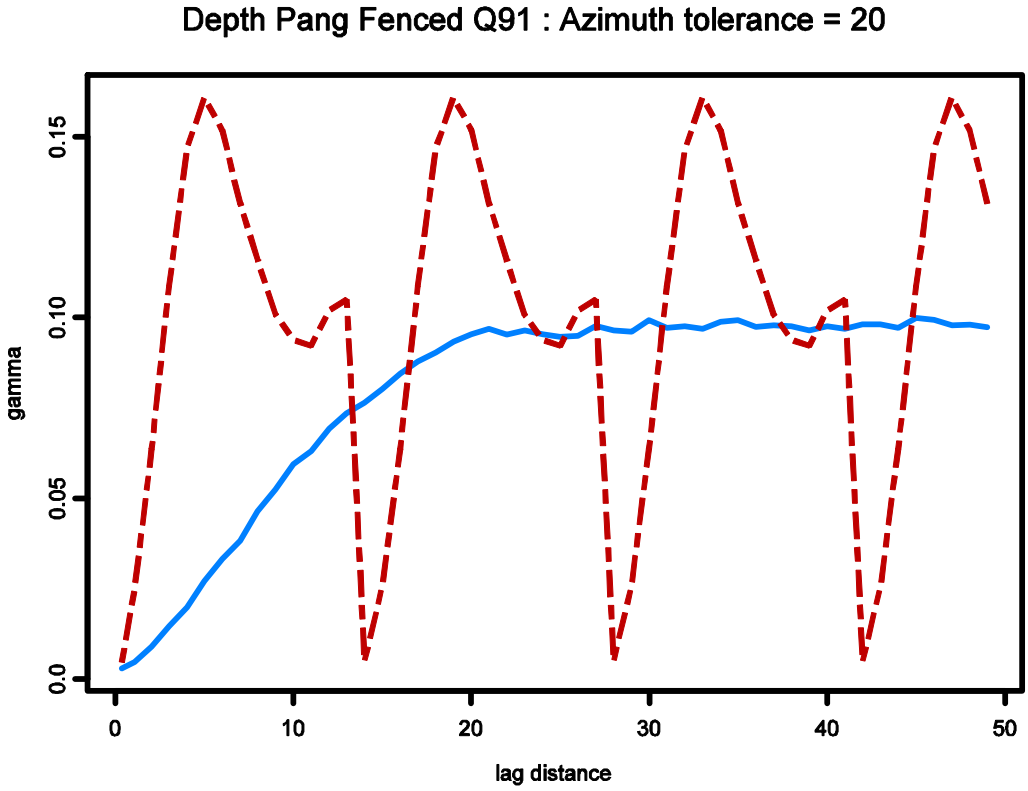
Depth Pang Fenced Q91 : Azimuth tolerance = 20
gamma
0.0
0.05
0.10
0.15
0
10
20
30
40
50
lag distance

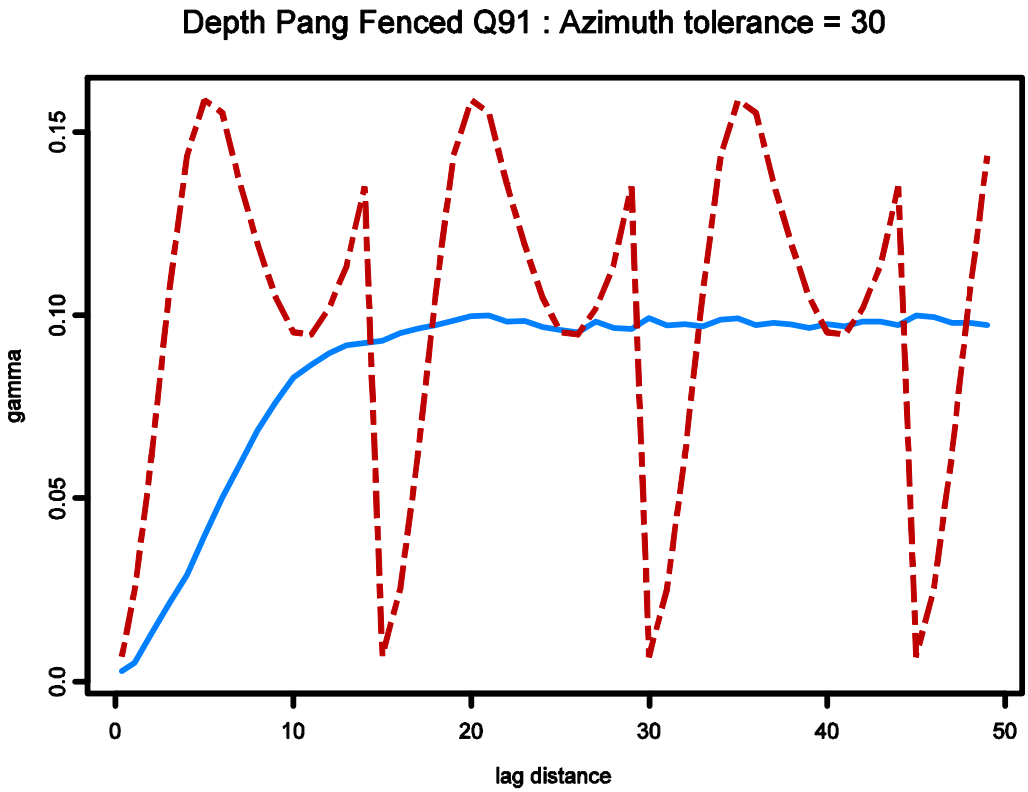
Depth Pang Fenced Q91 : Azimuth tolerance = 30
gamma
0.0
0.05
0.10
0.15
0
10
20
30
40
50
lag distance

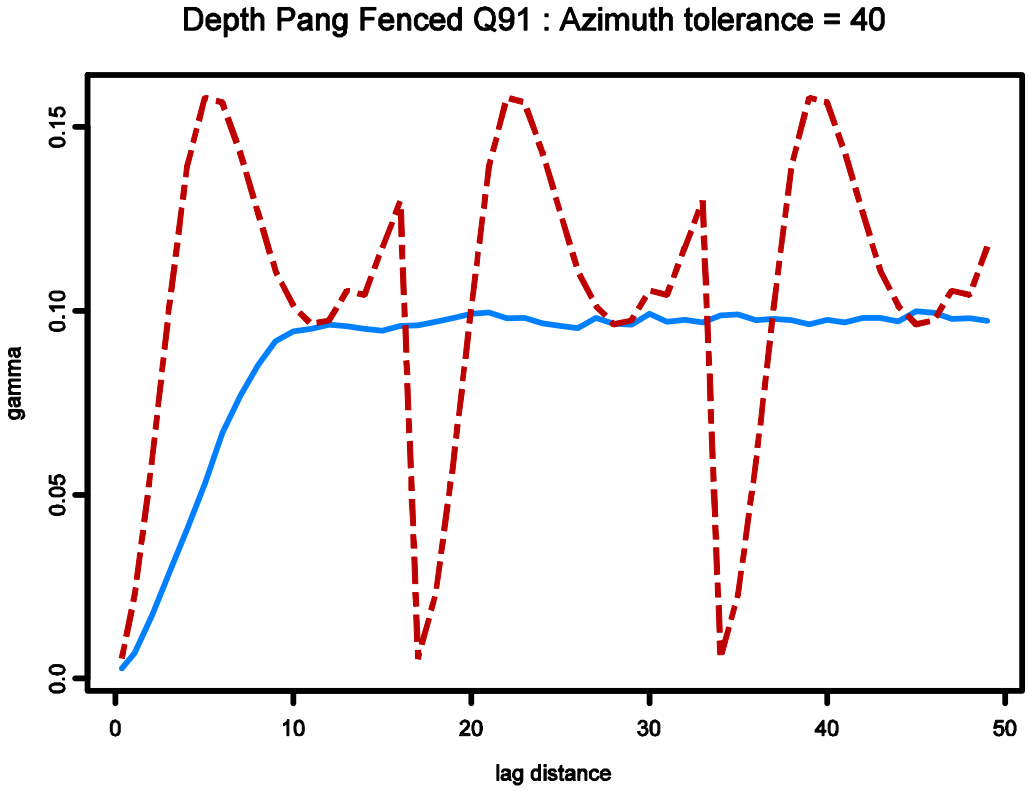
Depth Pang Fenced Q91 : Azimuth tolerance = 40
gamma
0.0
0.05
0.10
0.15
0
10
20
30
40
50
lag distance

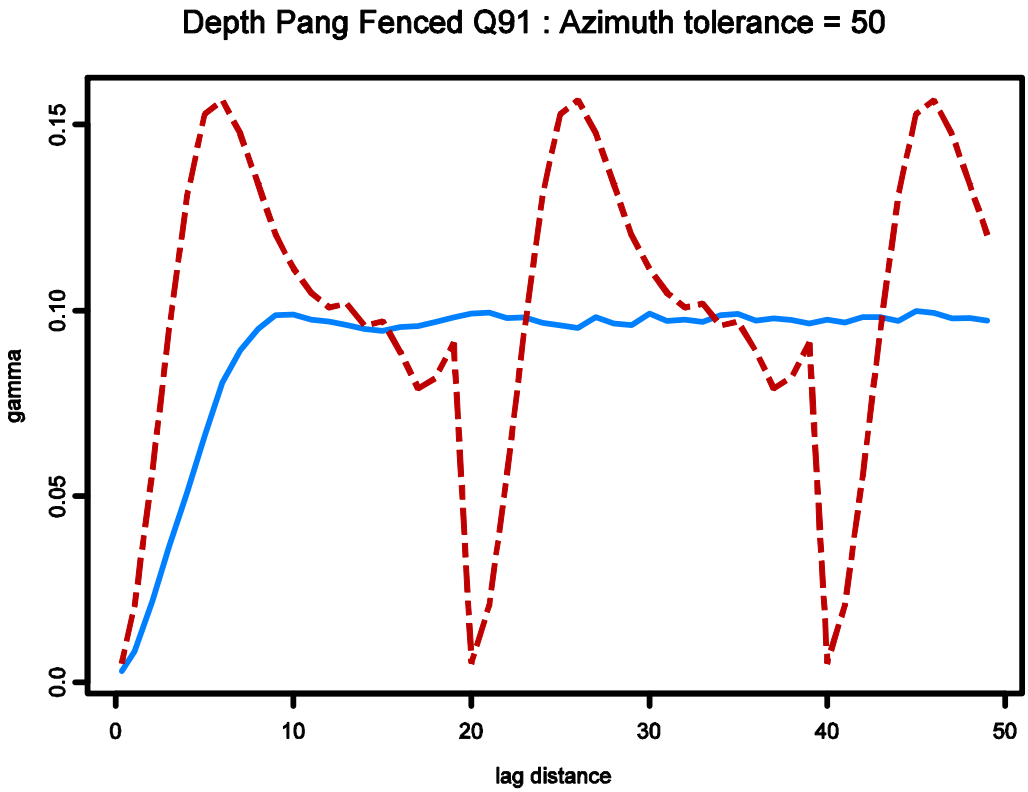
Depth Pang Fenced Q91 : Azimuth tolerance = 50
gamma
0.0
0.05
0.10
0.15
0
10
20
30
40
50
lag distance

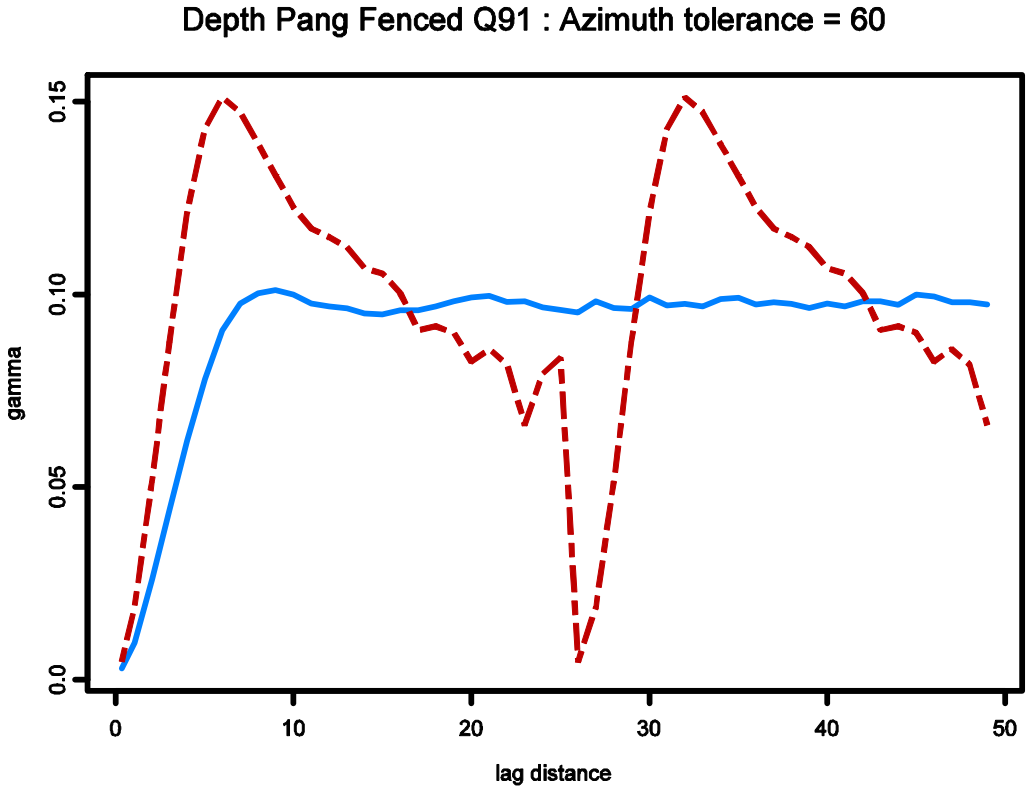
Depth Pang Fenced Q91 : Azimuth tolerance = 60
gamma
0.0
0.05
0.10
0.15
0
10
20
30
40
50
lag distance

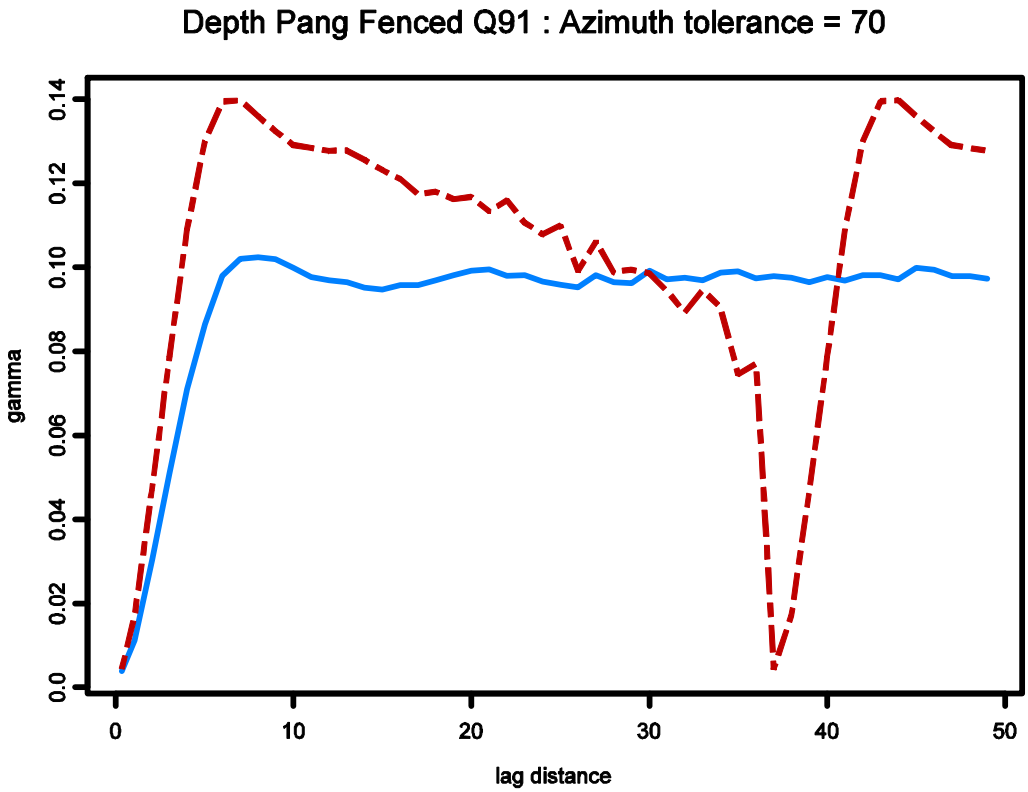
Depth Pang Fenced Q91 : Azimuth tolerance = 70
gamma
0.0
0.02
0.04
0.06
0.08
0.10
0.12
0.14
0
10
20
30
40
50
lag distance

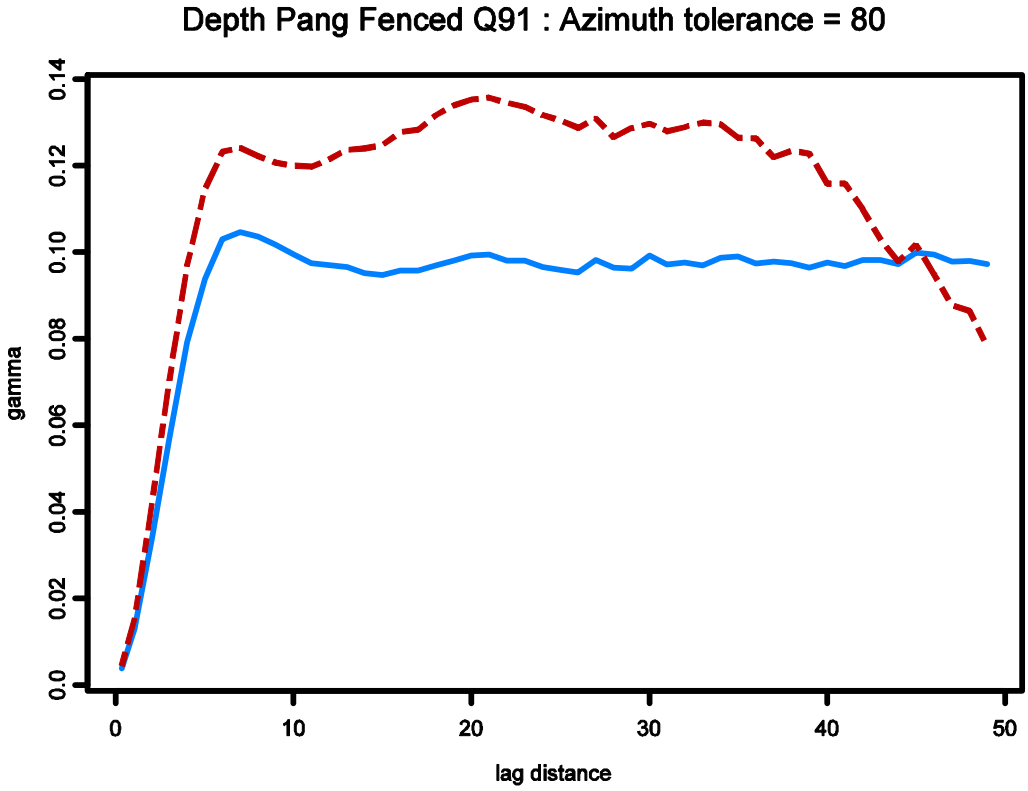
Depth Pang Fenced Q91 : Azimuth tolerance = 80
gamma
0.0
0.02
0.04
0.06
0.08
0.10
0.12
0.14
0
10
20
30
40
50
lag distance

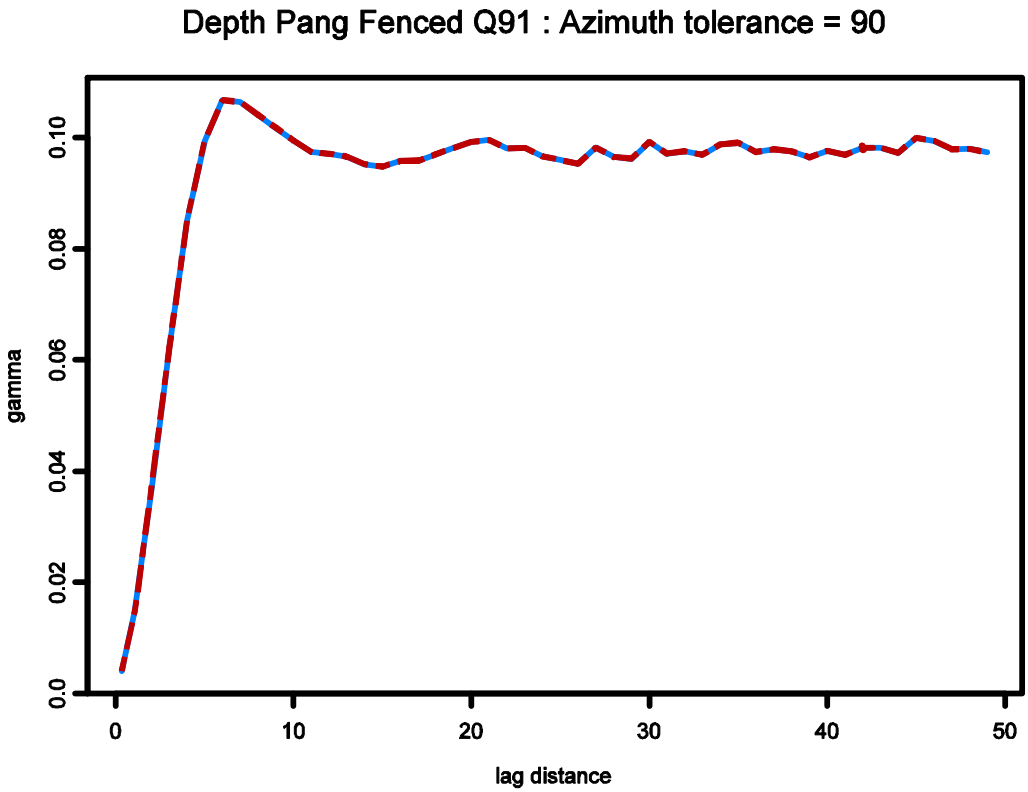
Depth Pang Fenced Q91 : Azimuth tolerance = 90
gamma
0.0
0.02
0.04
0.06
0.08
0.10
0
10
20
30
40
50
lag distance

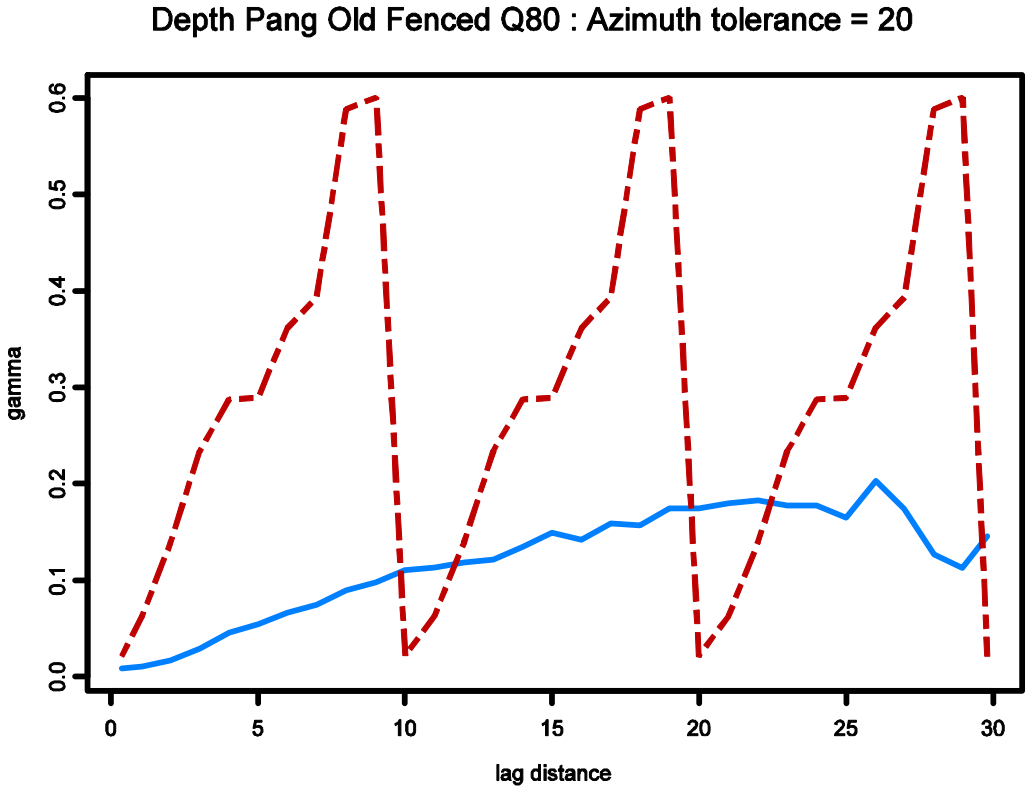
Depth Pang Old Fenced Q80 : Azimuth tolerance = 20
gamma
0.0
0.1
0.2
0.3
0.4
0.5
0.6
0
5
10
15
20
25
30
lag distance

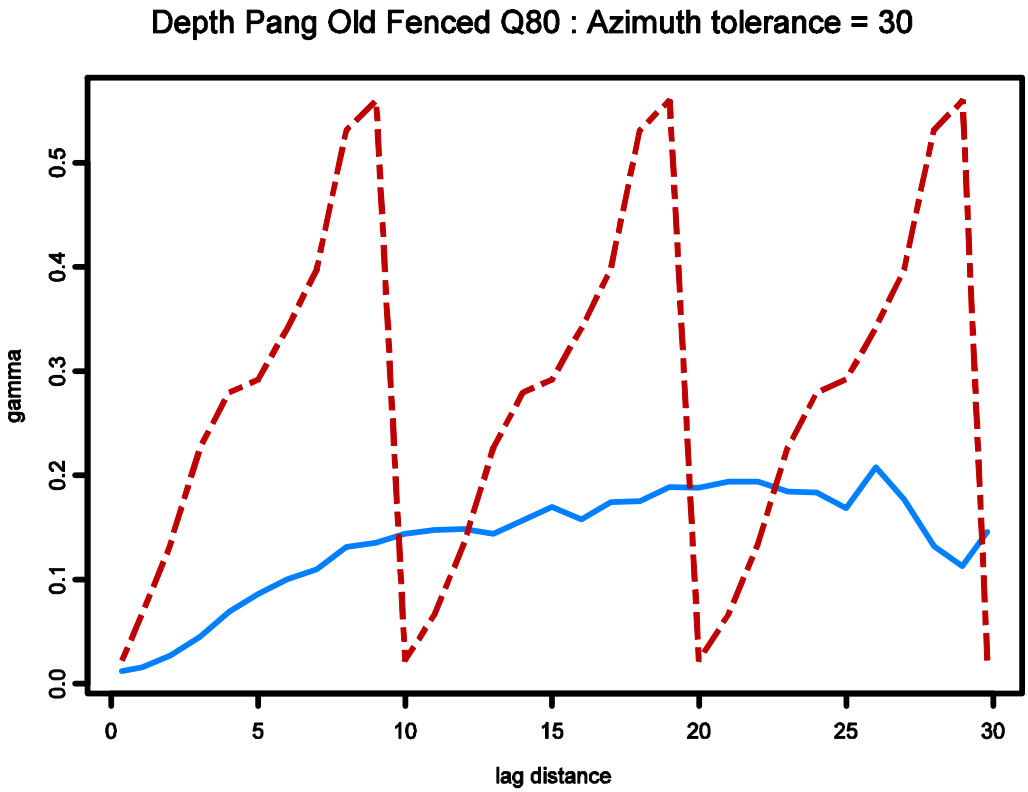
Depth Pang Old Fenced Q80 : Azimuth tolerance = 30
gamma
0.0
0.1
0.2
0.3
0.4
0.5
0
5
10
15
20
25
30
lag distance

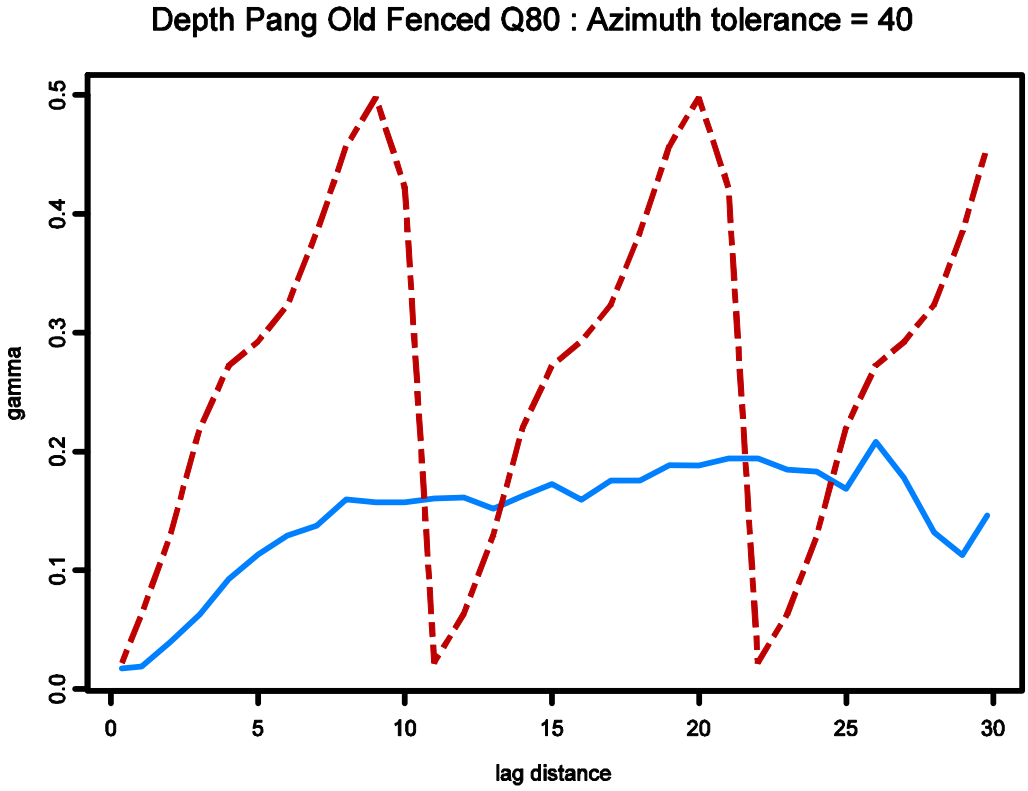
Depth Pang Old Fenced Q80 : Azimuth tolerance = 40
gamma
0.0
0.1
0.2
0.3
0.4
0.5
0
5
10
15
20
25
30
lag distance

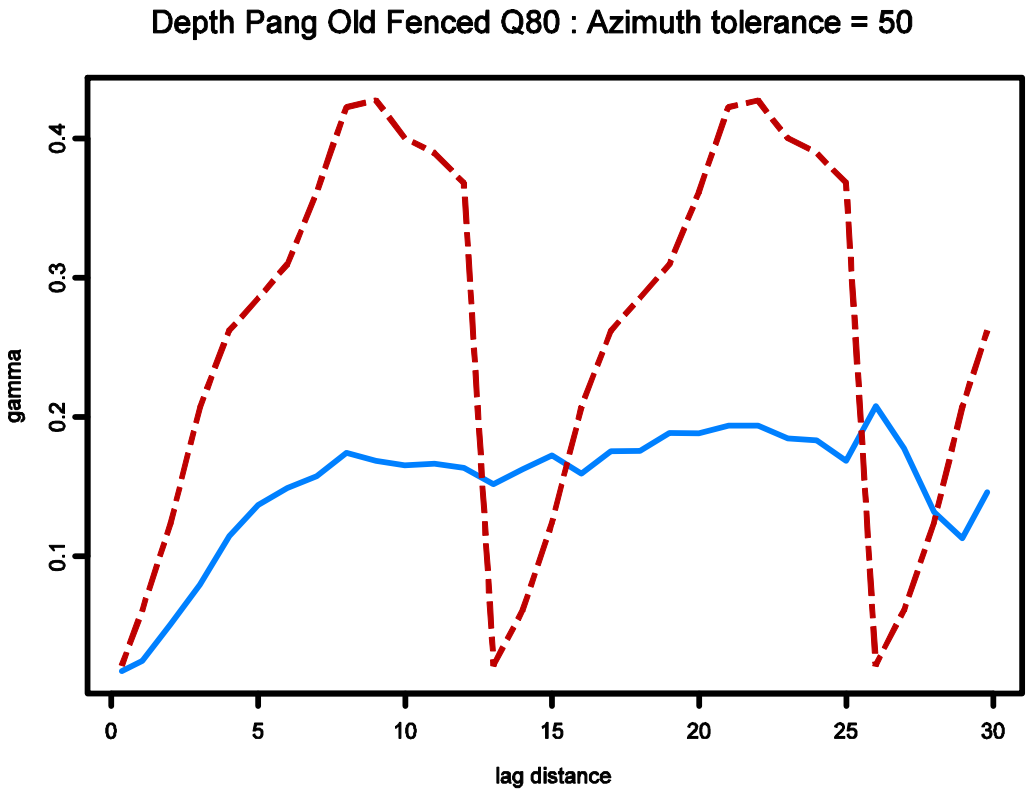
Depth Pang Old Fenced Q80 : Azimuth tolerance = 50
gamma
0.1
0.2
0.3
0.4
0
5
10
15
20
25
30
lag distance

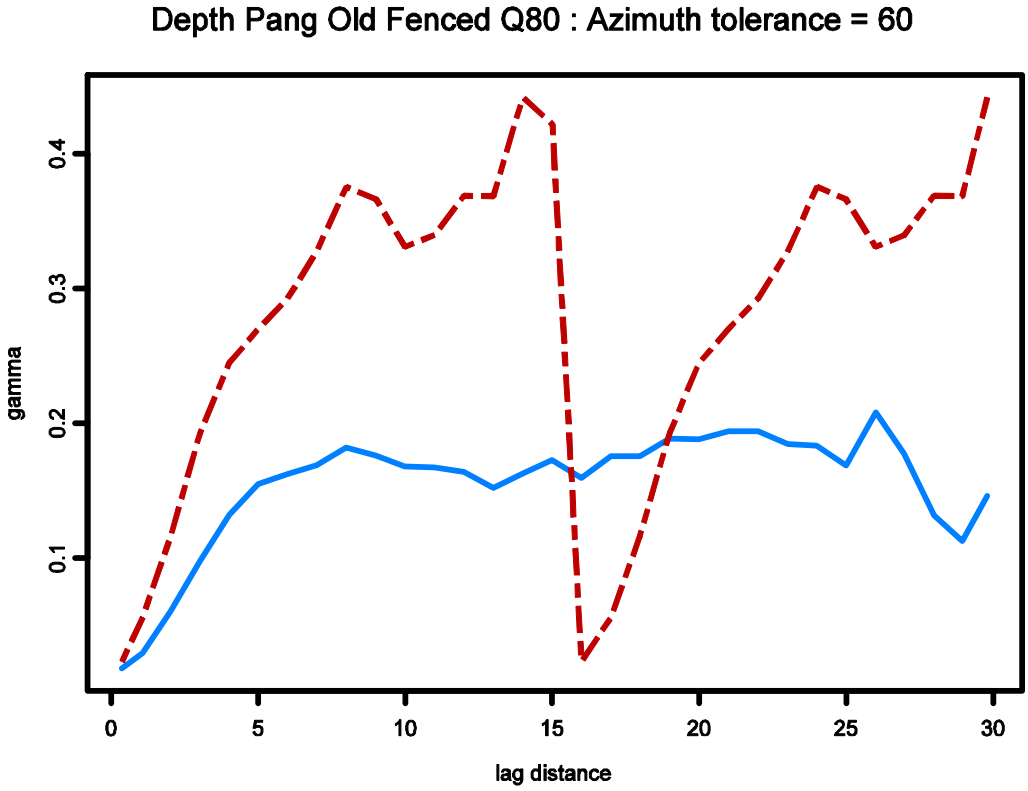
Depth Pang Old Fenced Q80 : Azimuth tolerance = 60
gamma
0.1
0.2
0.3
0.4
0
5
10
15
20
25
30
lag distance

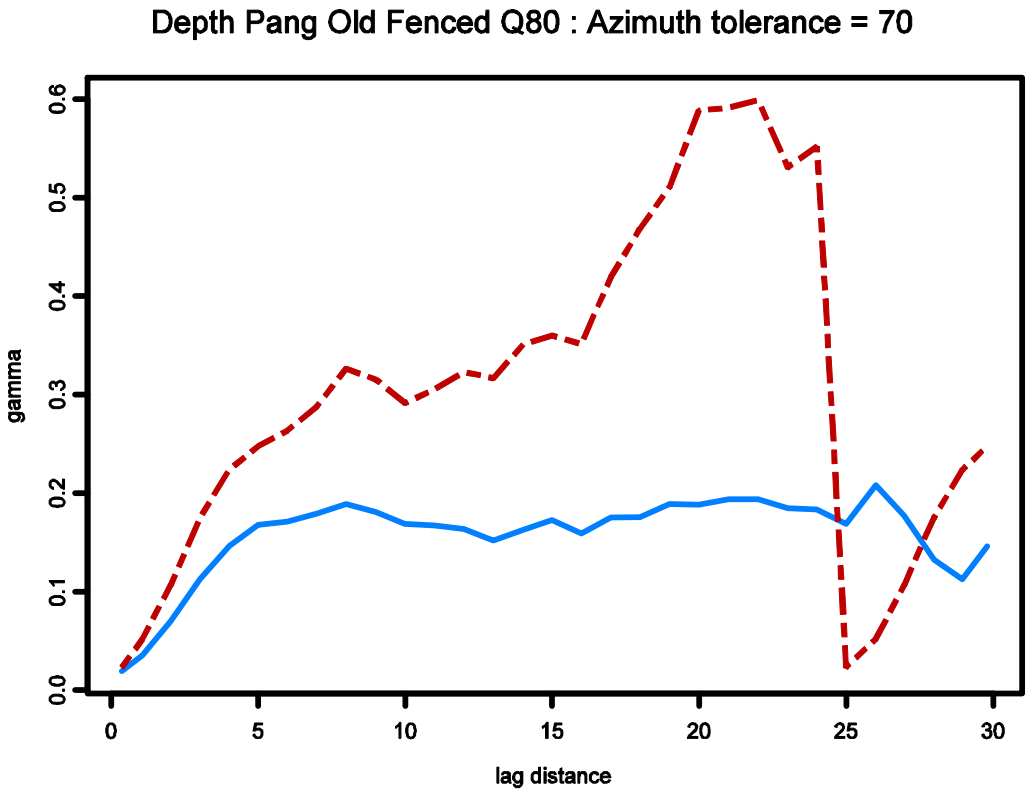
Depth Pang Old Fenced Q80 : Azimuth tolerance = 70
gamma
0.0
0.1
0.2
0.3
0.4
0.5
0.6
0
5
10
15
20
25
30
lag distance

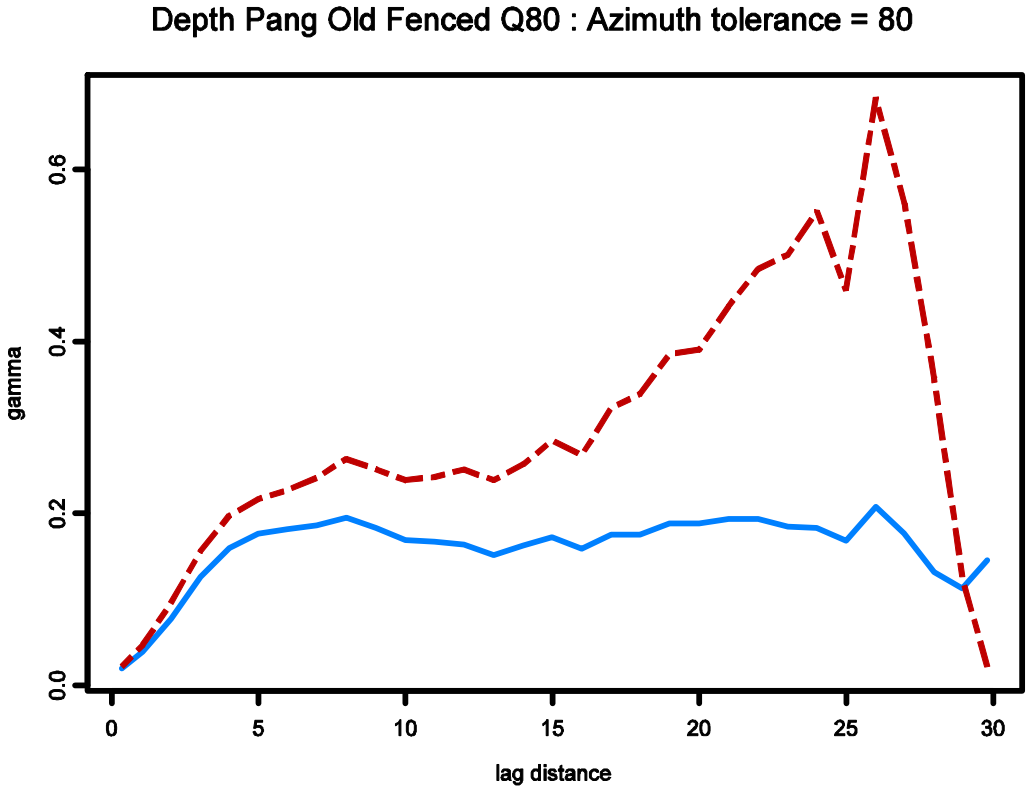
Depth Pang Old Fenced Q80 : Azimuth tolerance = 80
gamma
0.0
0.2
0.4
0.6
0
5
10
15
20
25
30
lag distance

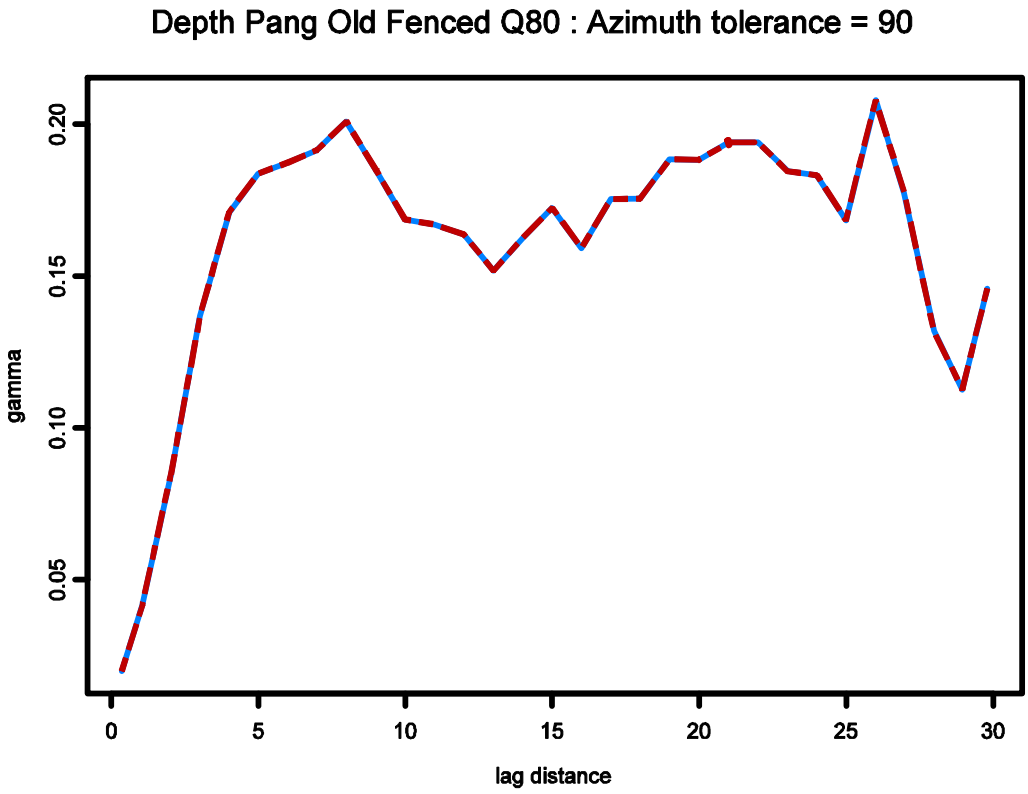
Depth Pang Old Fenced Q80 : Azimuth tolerance = 90
gamma
0.05
0.10
0.15
0.20
0
5
10
15
20
25
30
lag distance

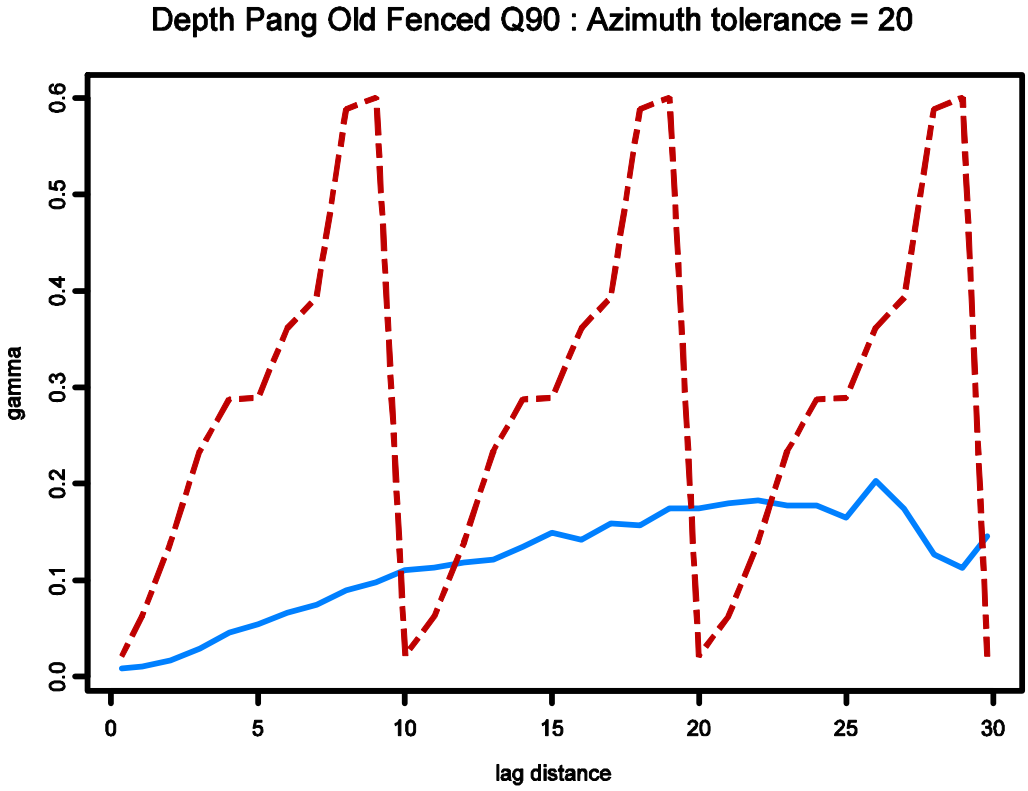
Depth Pang Old Fenced Q90 : Azimuth tolerance = 20
gamma
0.0
0.1
0.2
0.3
0.4
0.5
0.6
0
5
10
15
20
25
30
lag distance

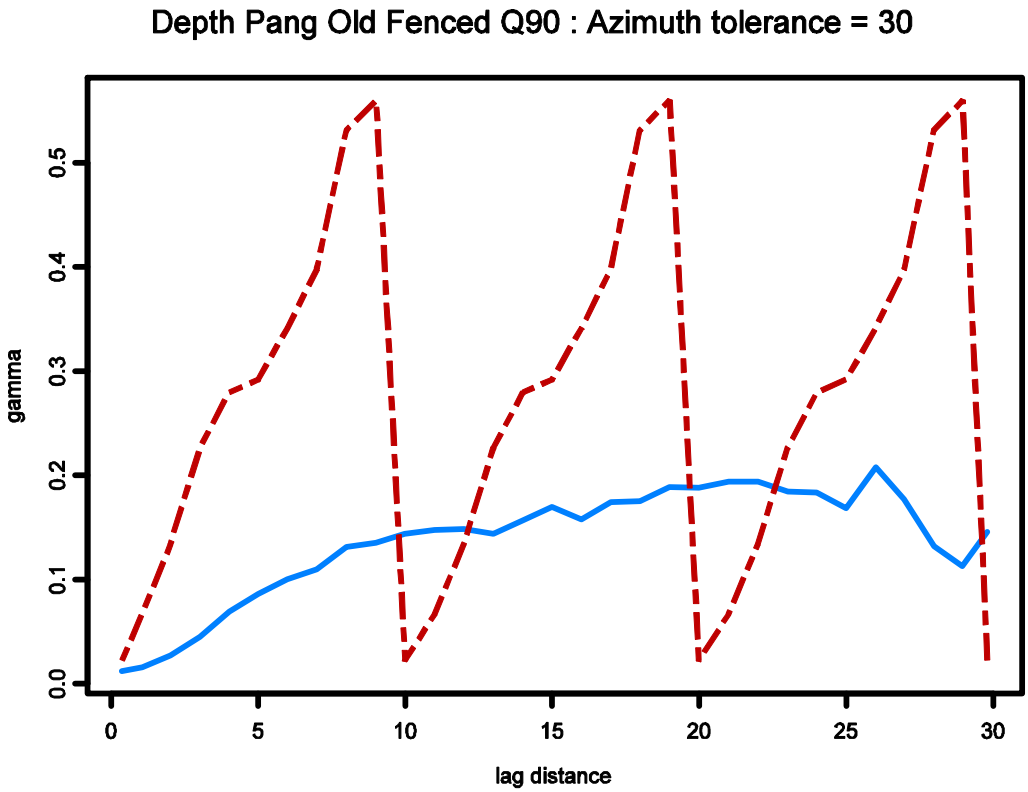
Depth Pang Old Fenced Q90 : Azimuth tolerance = 30
gamma
0.0
0.1
0.2
0.3
0.4
0.5
0
5
10
15
20
25
30
lag distance

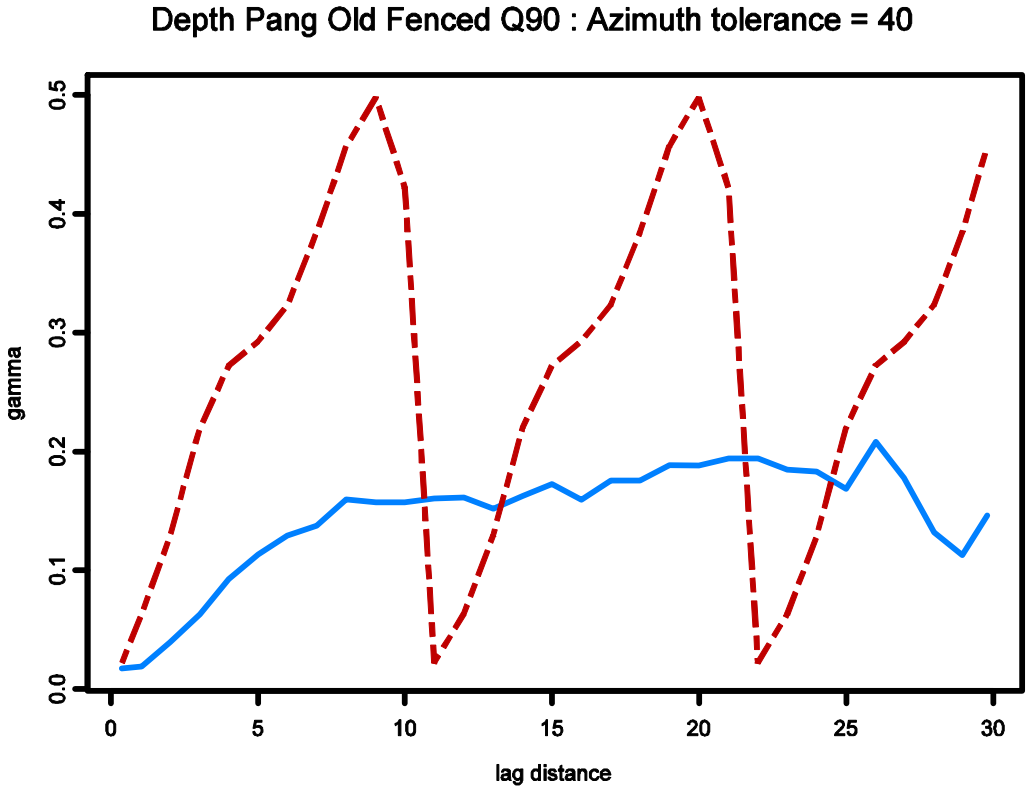
Depth Pang Old Fenced Q90 : Azimuth tolerance = 40
gamma
0.0
0.1
0.2
0.3
0.4
0.5
0
5
10
15
20
25
30
lag distance

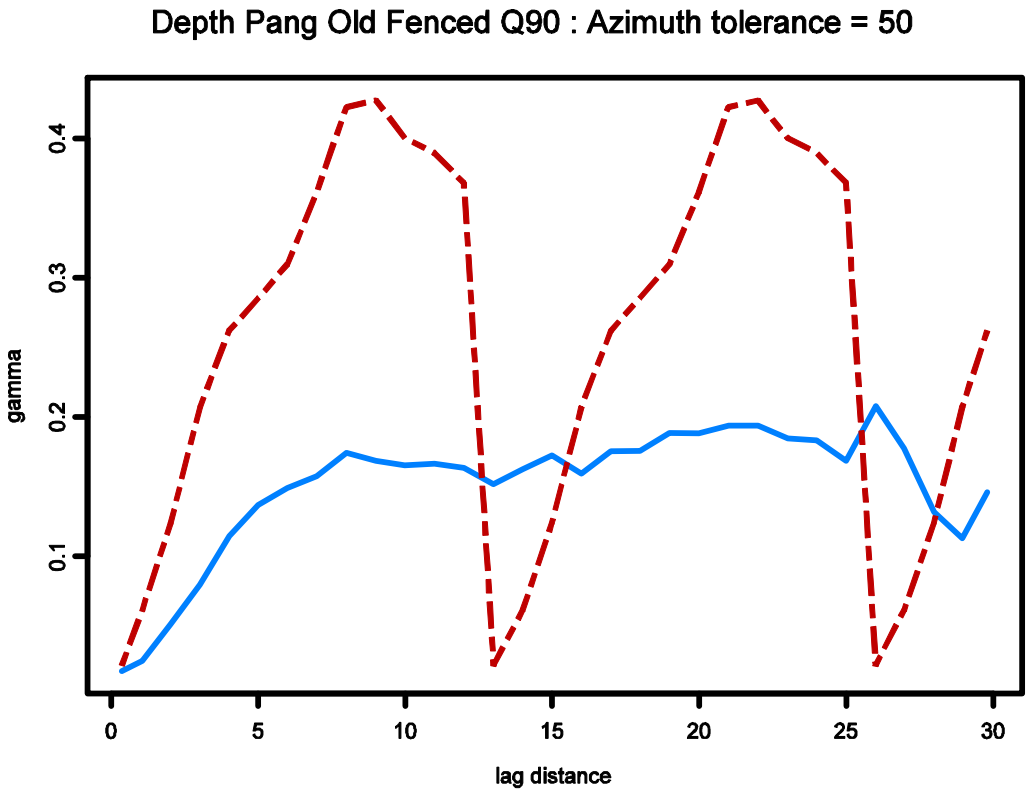
Depth Pang Old Fenced Q90 : Azimuth tolerance = 50
gamma
0.1
0.2
0.3
0.4
0
5
10
15
20
25
30
lag distance

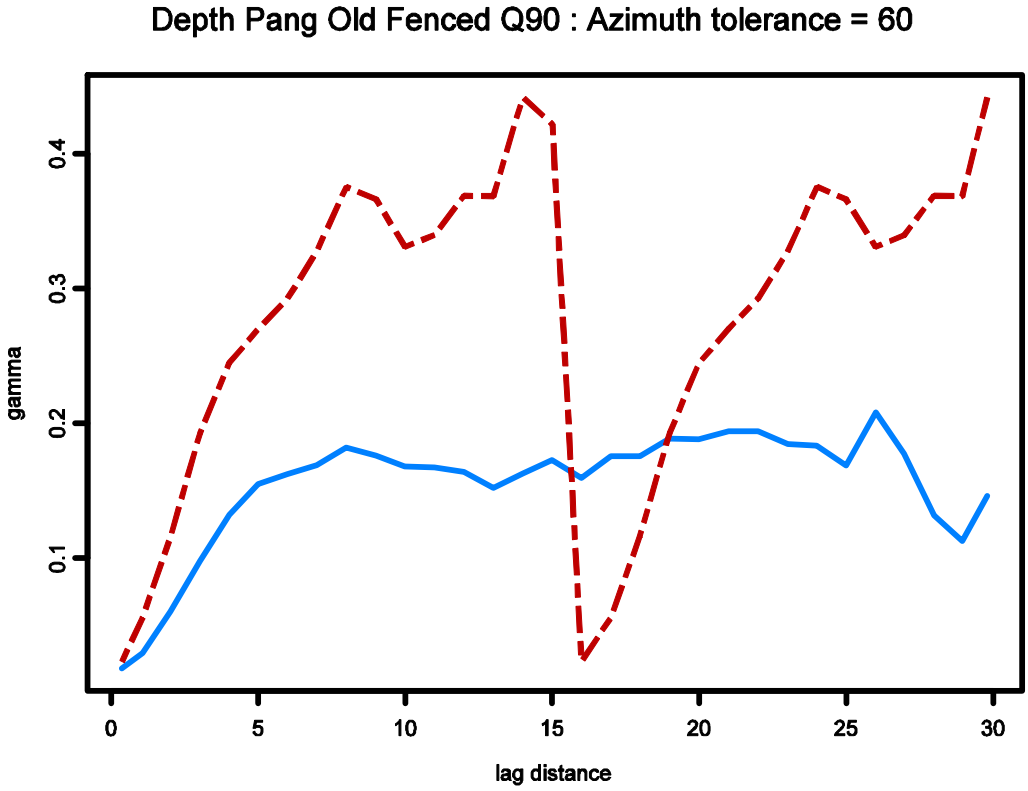
Depth Pang Old Fenced Q90 : Azimuth tolerance = 60
gamma
0.1
0.2
0.3
0.4
0
5
10
15
20
25
30
lag distance

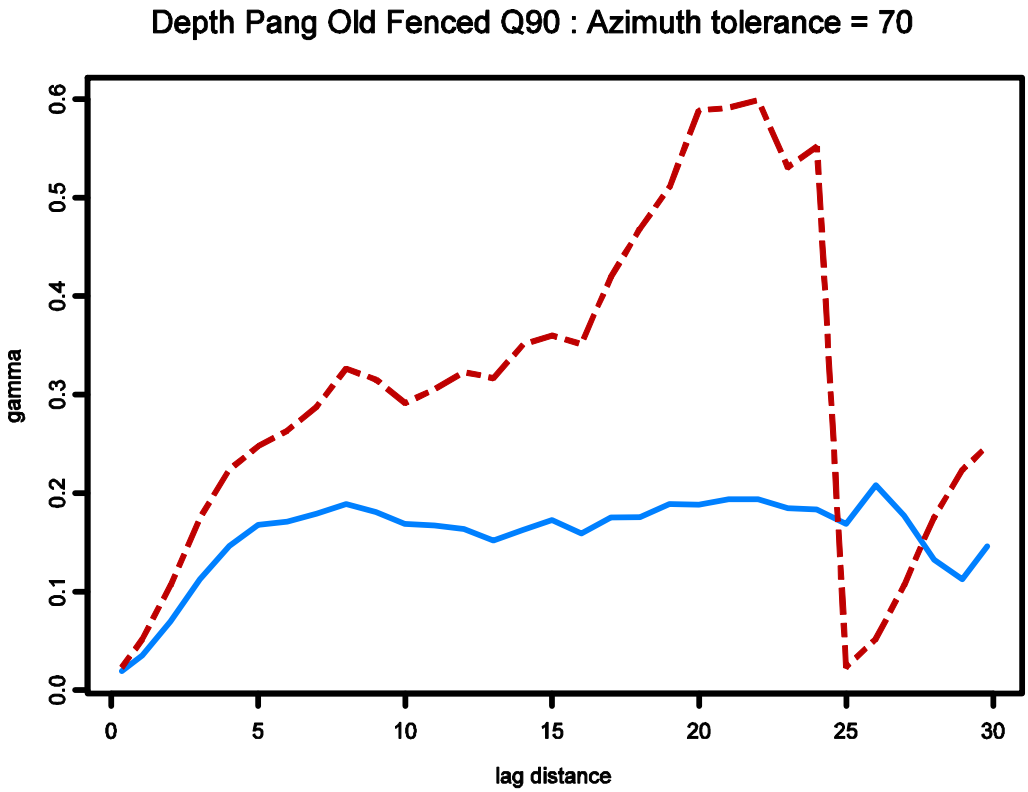
Depth Pang Old Fenced Q90 : Azimuth tolerance = 70
gamma
0.0
0.1
0.2
0.3
0.4
0.5
0.6
0
5
10
15
20
25
30
lag distance

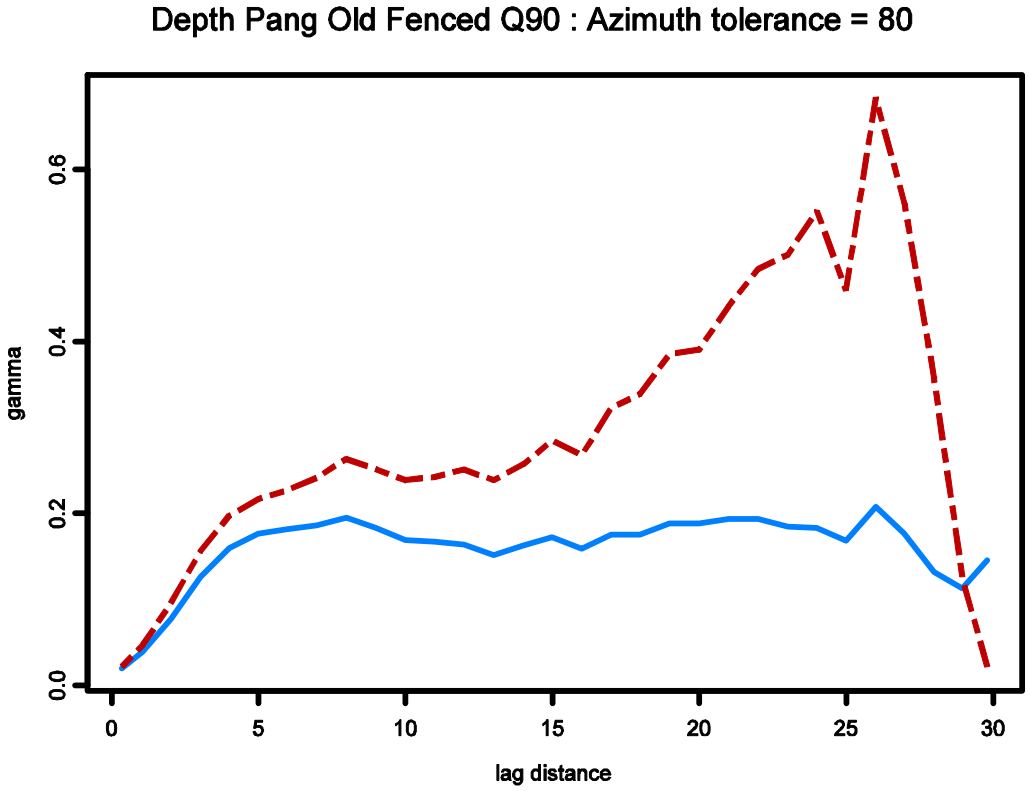
Depth Pang Old Fenced Q90 : Azimuth tolerance = 80
gamma
0.0
0.2
0.4
0.6
0
5
10
15
20
25
30
lag distance

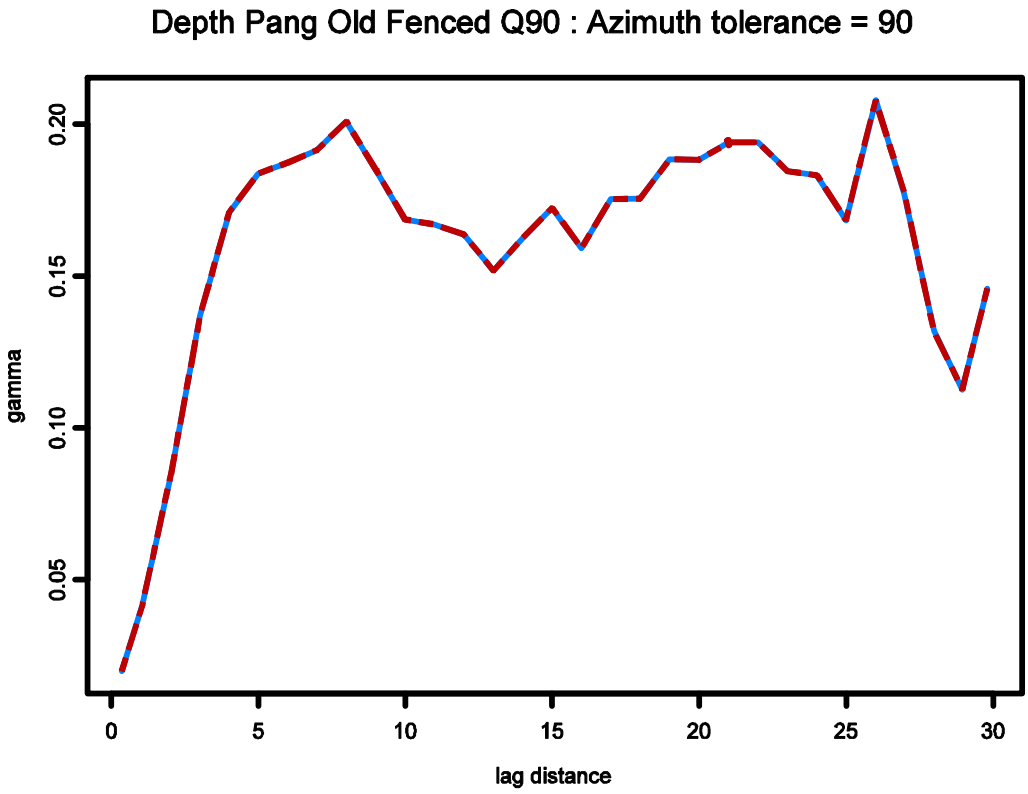
Depth Pang Old Fenced Q90 : Azimuth tolerance = 90
gamma
0.05
0.10
0.15
0.20
0
5
10
15
20
25
30
lag distance

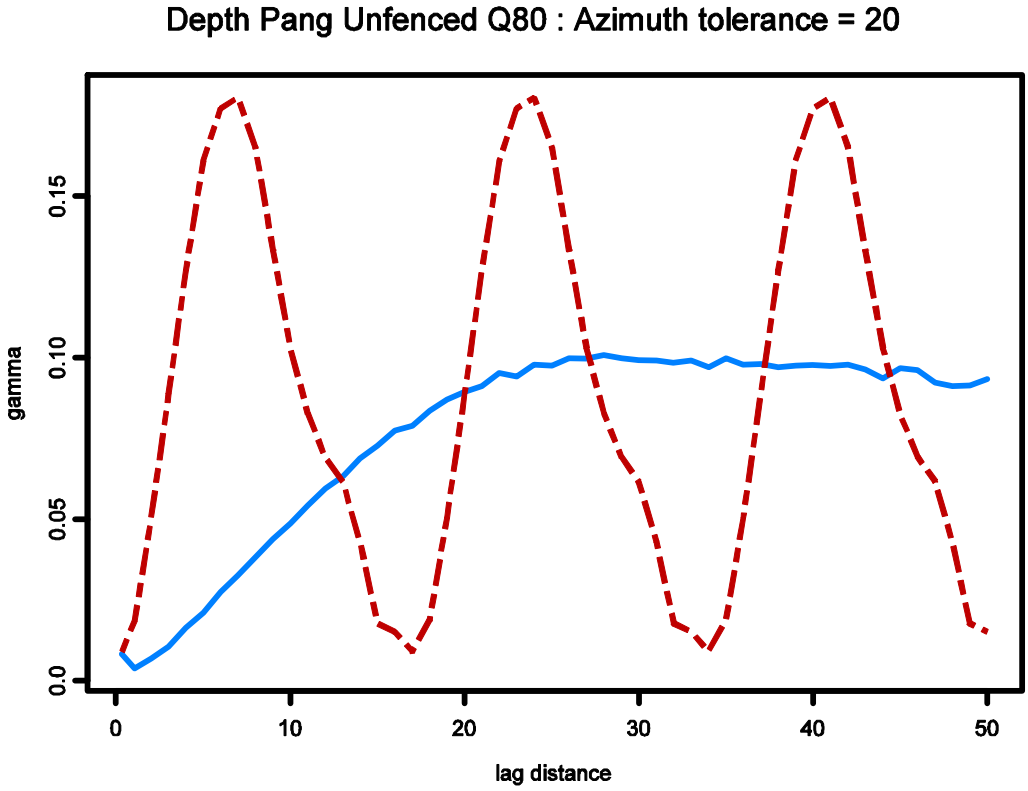
Depth Pang Unfenced Q80 : Azimuth tolerance = 20
gamma
0.0
0.05
0.10
0.15
0
10
20
30
40
50
lag distance

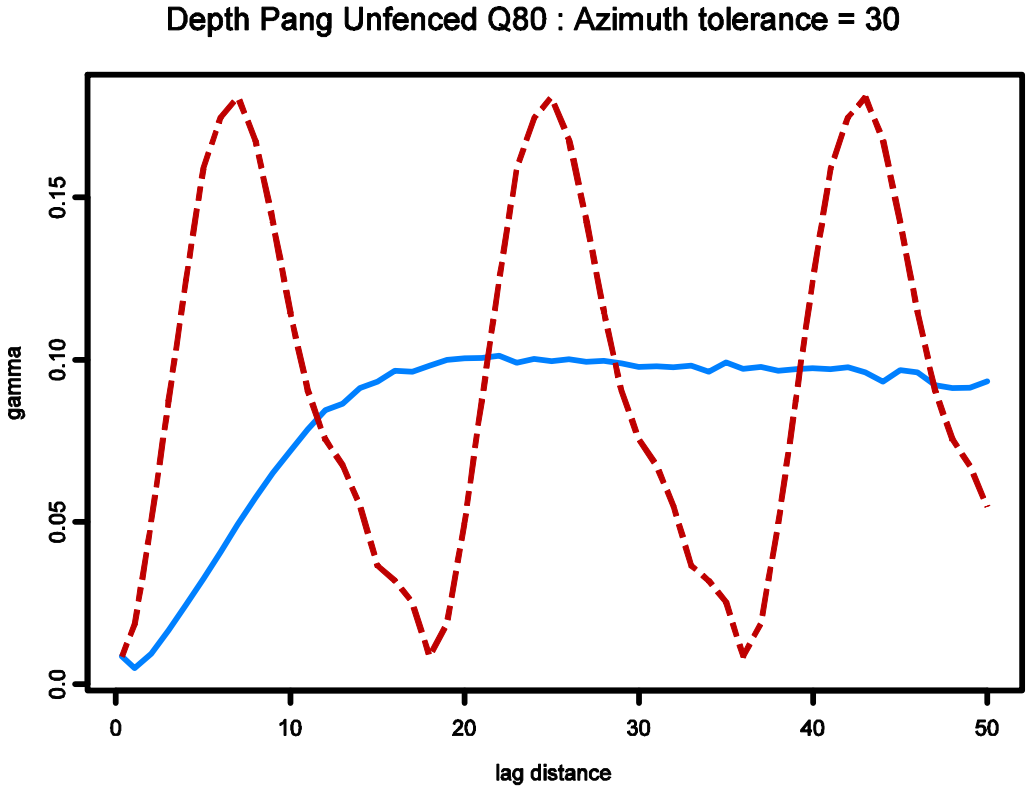
Depth Pang Unfenced Q80 : Azimuth tolerance = 30
gamma
0.0
0.05
0.10
0.15
0
10
20
30
40
50
lag distance

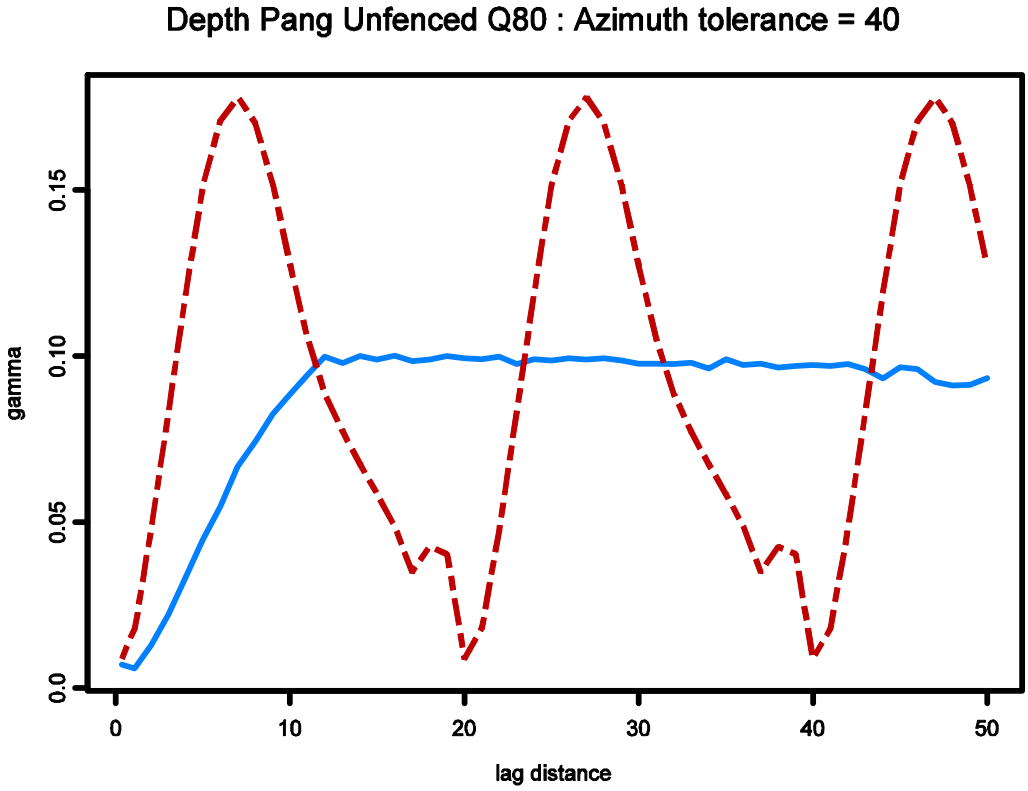
Depth Pang Unfenced Q80 : Azimuth tolerance = 40
gamma
0.0
0.05
0.10
0.15
0
10
20
30
40
50
lag distance

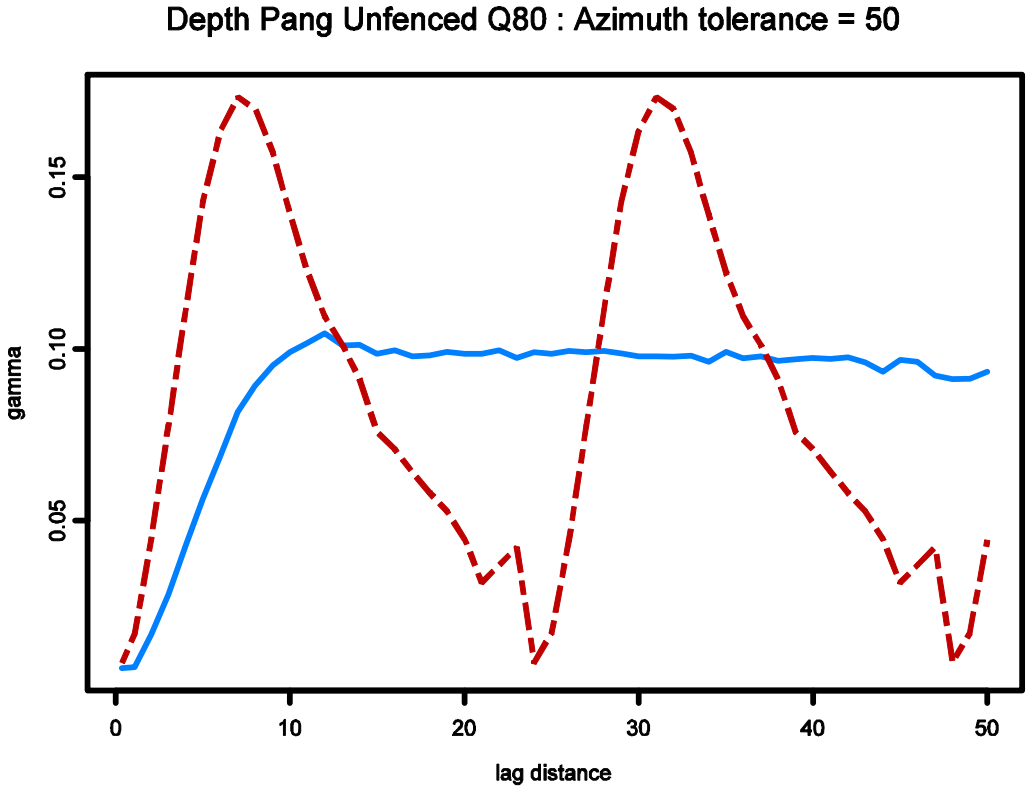
Depth Pang Unfenced Q80 : Azimuth tolerance = 50
gamma
0.05
0.10
0.15
0
10
20
30
40
50
lag distance

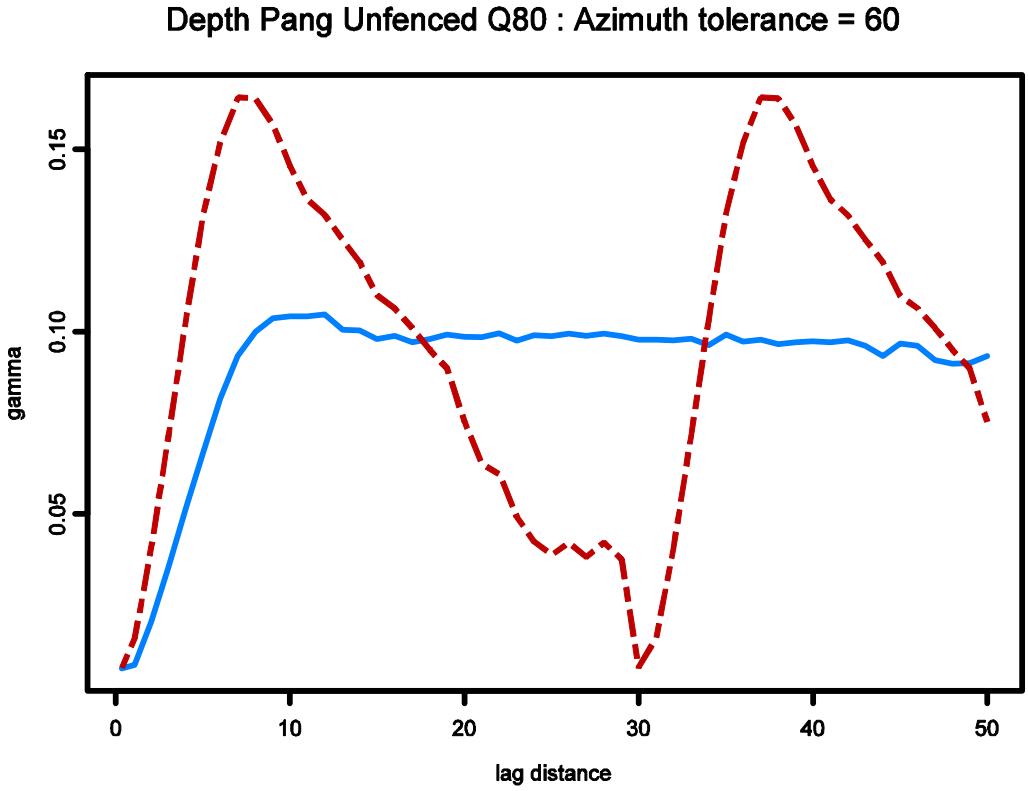
Depth Pang Unfenced Q80 : Azimuth tolerance = 60
gamma
0.05
0.10
0.15
0
10
20
30
40
50
lag distance

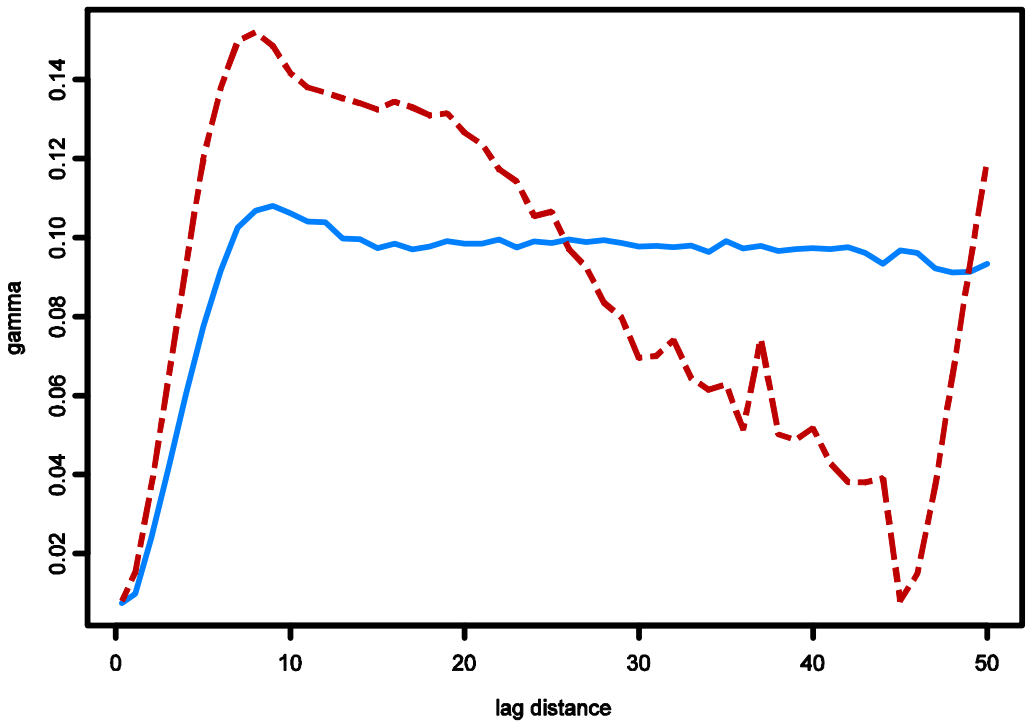
Depth Pang Unfenced Q80 : Azimuth tolerance = 70
gamma
0.02
0.04
0.06
0.08
0.10
0.12
0.14
0
10
20
30
40
50
lag distance

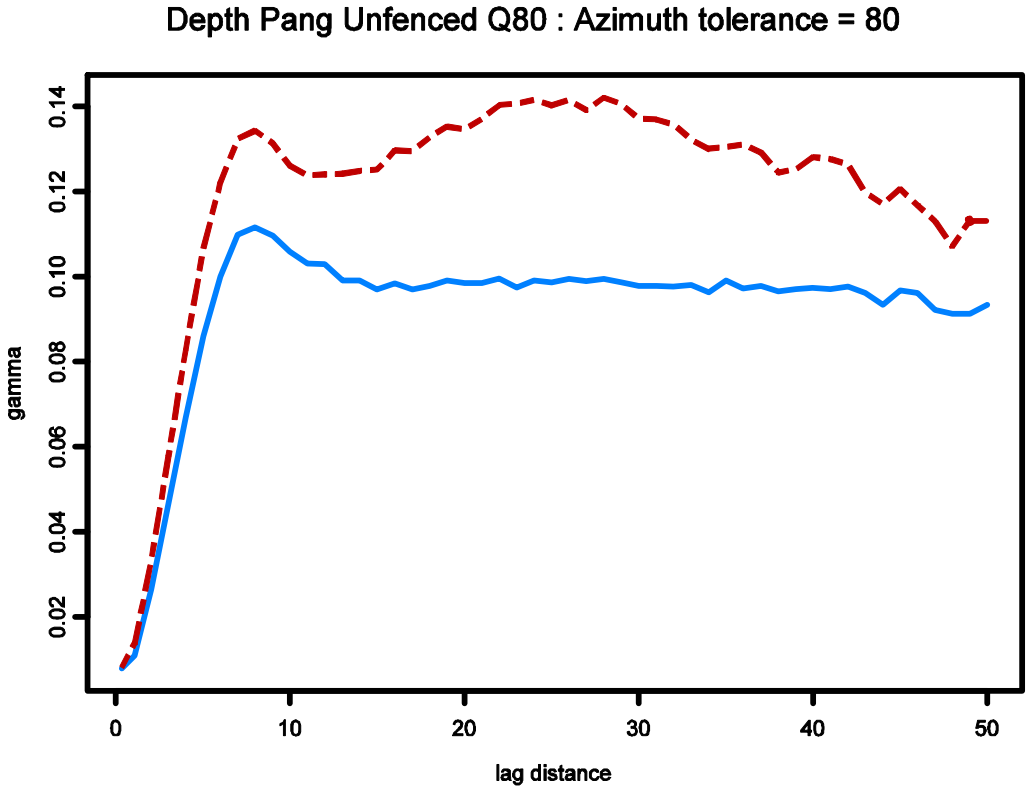
Depth Pang Unfenced Q80 : Azimuth tolerance = 80
gamma
0.02
0.04
0.06
0.08
0.10
0.12
0.14
0
10
20
30
40
50
lag distance

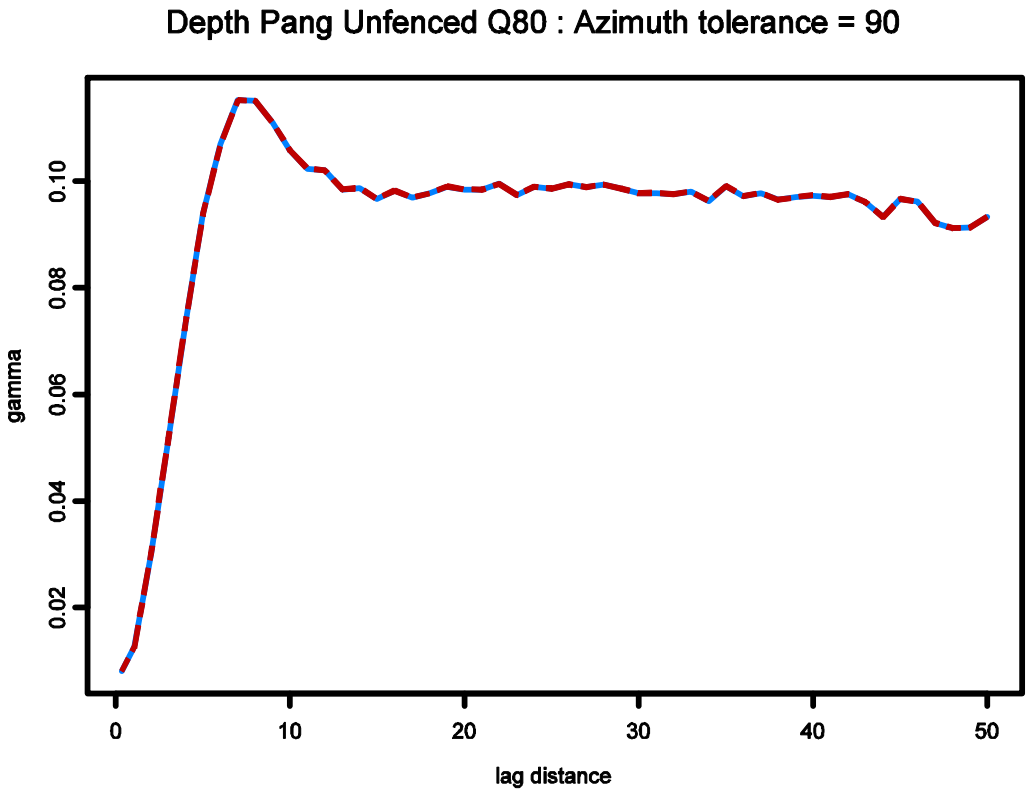
Depth Pang Unfenced Q80 : Azimuth tolerance = 90
gamma
0.02
0.04
0.06
0.08
0.10
0
10
20
30
40
50
lag distance

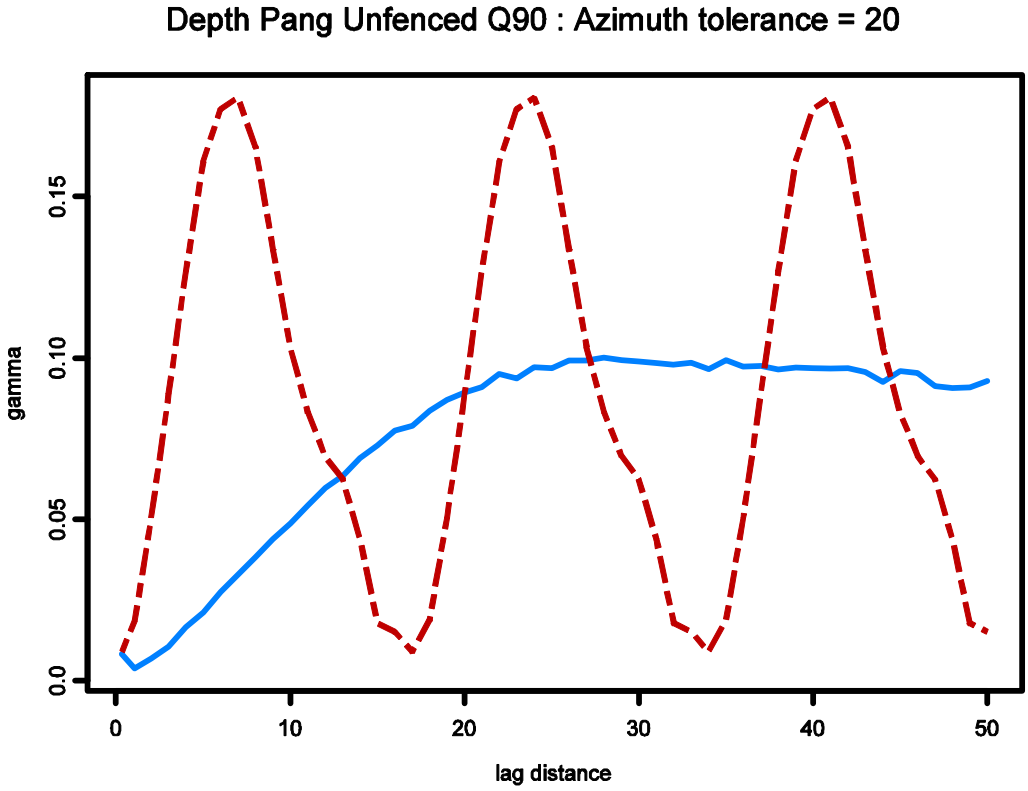
Depth Pang Unfenced Q90 : Azimuth tolerance = 20
gamma
0.0
0.05
0.10
0.15
0
10
20
30
40
50
lag distance

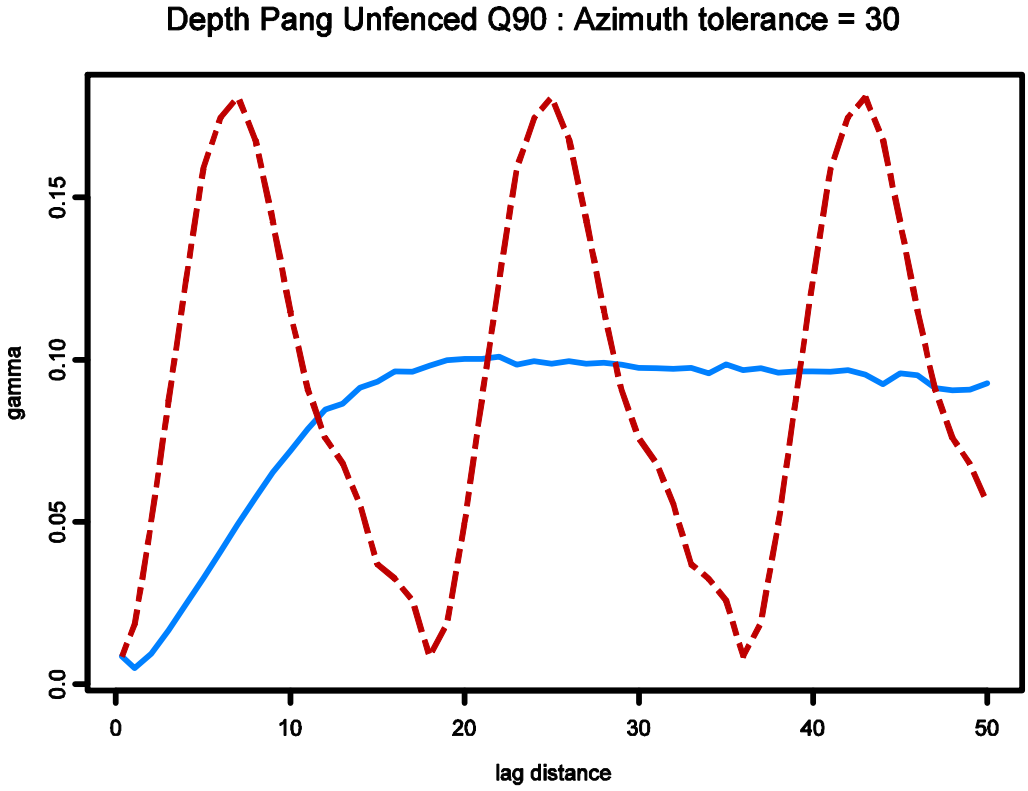
Depth Pang Unfenced Q90 : Azimuth tolerance = 30
gamma
0.0
0.05
0.10
0.15
0
10
20
30
40
50
lag distance

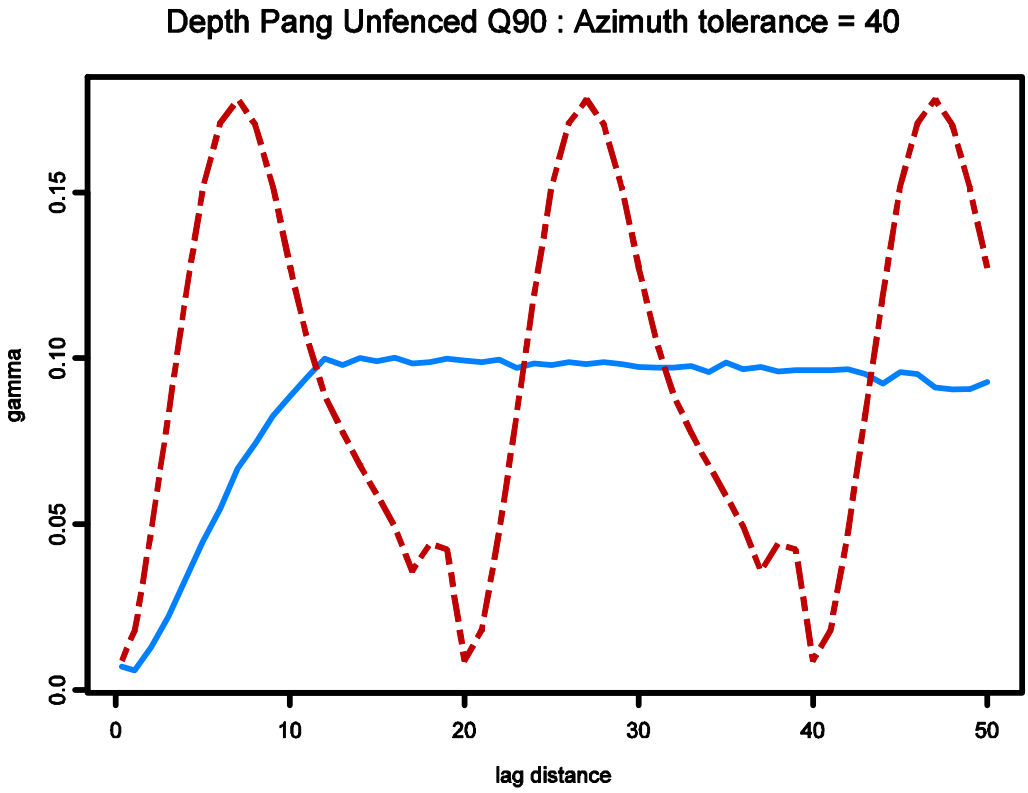
Depth Pang Unfenced Q90 : Azimuth tolerance = 40
gamma
0.0
0.05
0.10
0.15
0
10
20
30
40
50
lag distance

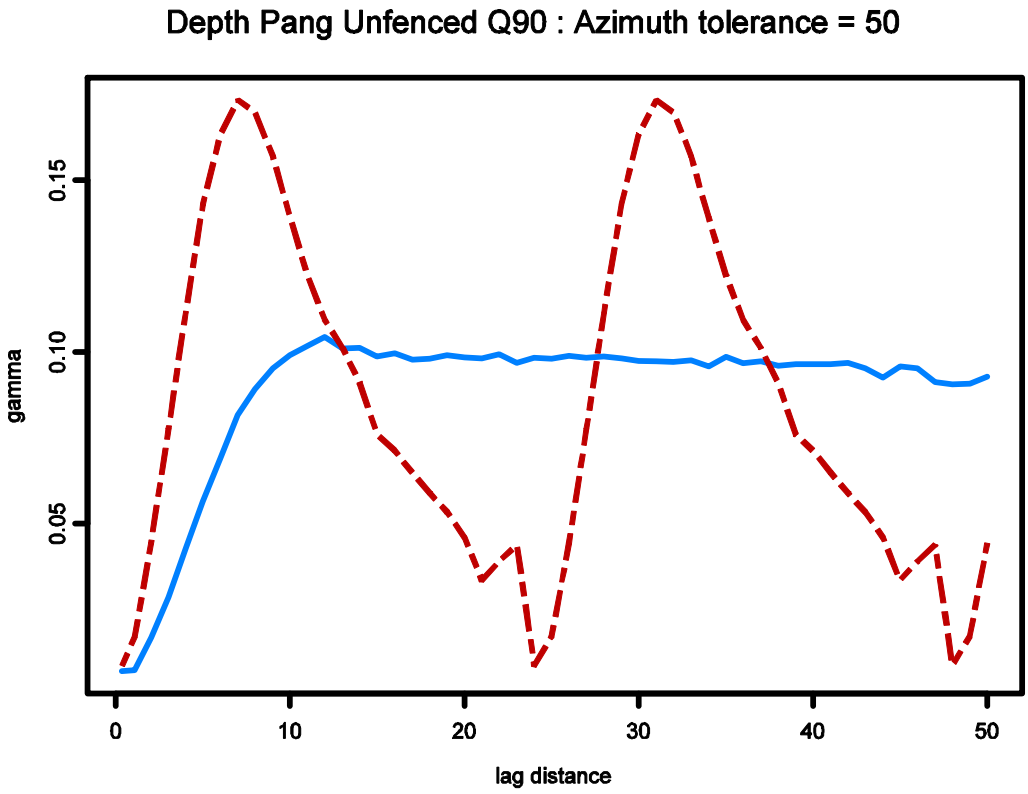
Depth Pang Unfenced Q90 : Azimuth tolerance = 50
gamma
0.05
0.10
0.15
0
10
20
30
40
50
lag distance

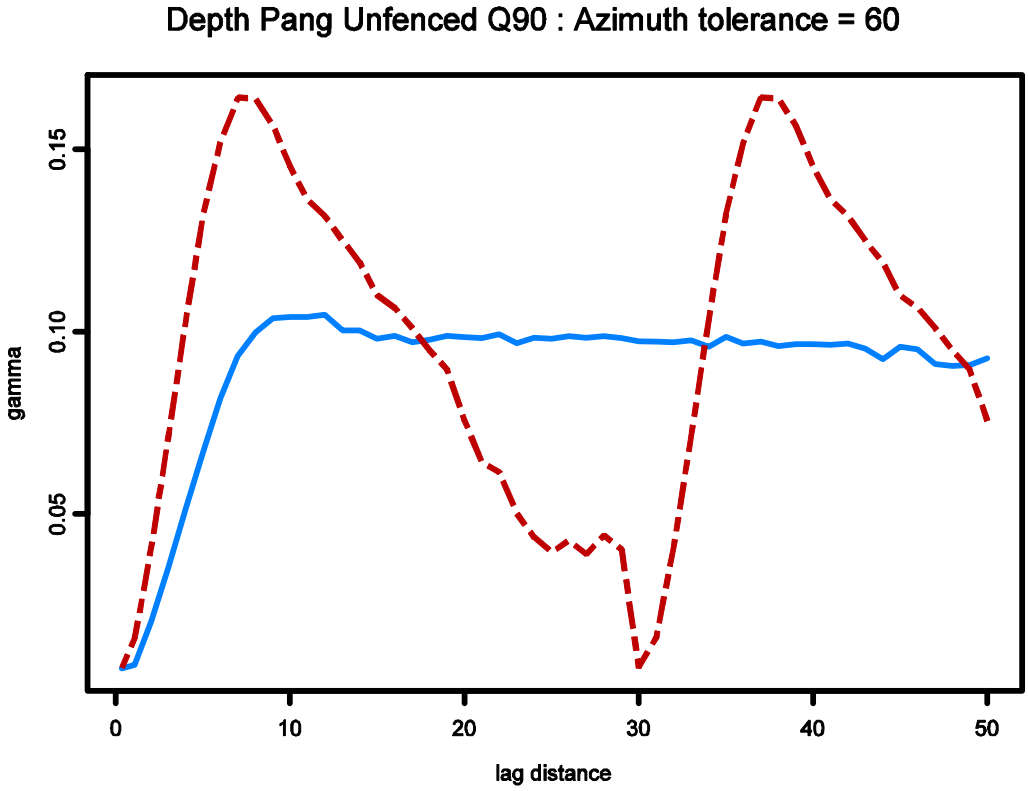
Depth Pang Unfenced Q90 : Azimuth tolerance = 60
gamma
0.05
0.10
0.15
0
10
20
30
40
50
lag distance

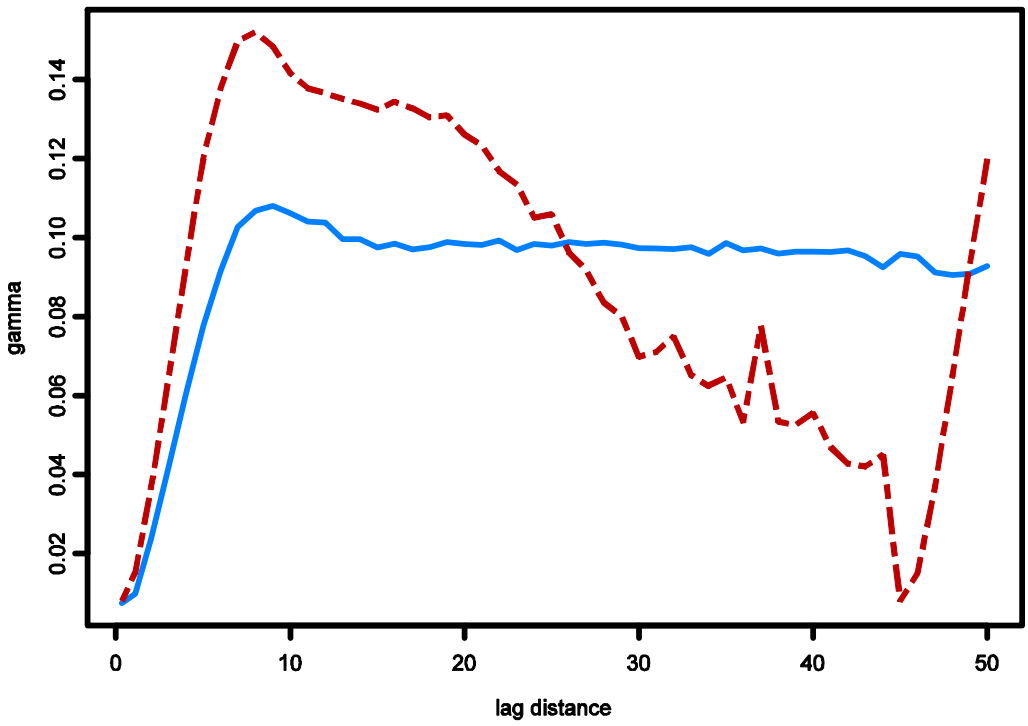
Depth Pang Unfenced Q90 : Azimuth tolerance = 70
gamma
0.02
0.04
0.06
0.08
0.10
0.12
0.14
0
10
20
30
40
50
lag distance

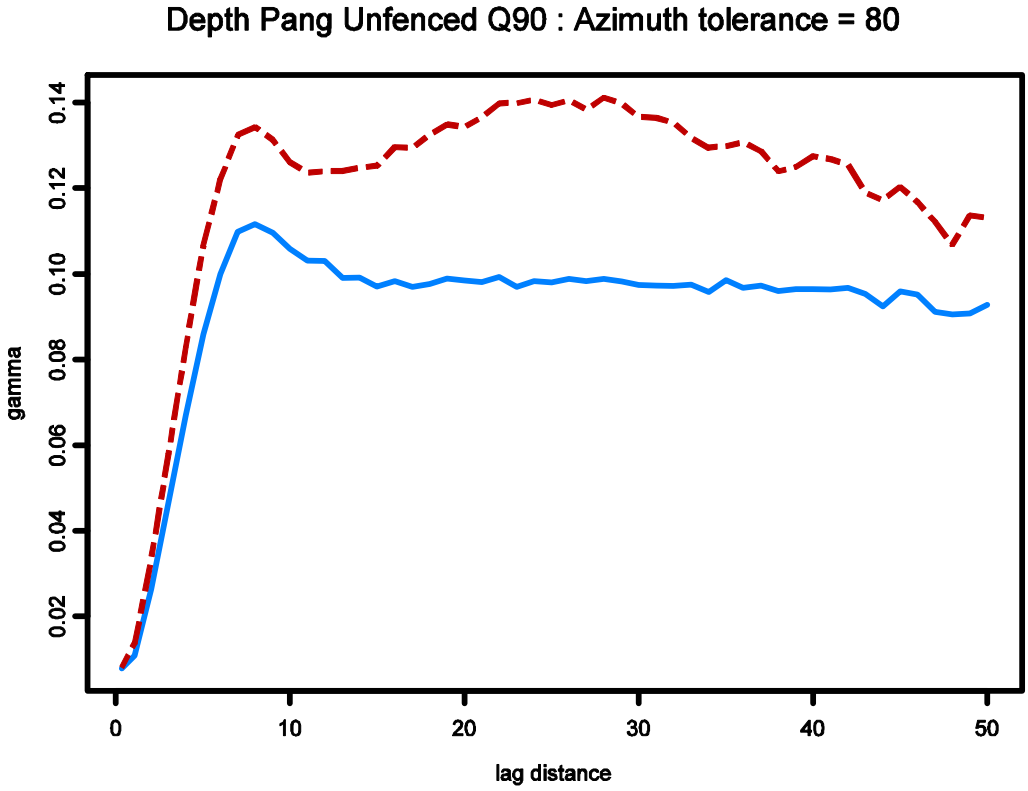
Depth Pang Unfenced Q90 : Azimuth tolerance = 80
gamma
0.02
0.04
0.06
0.08
0.10
0.12
0.14
0
10
20
30
40
50
lag distance

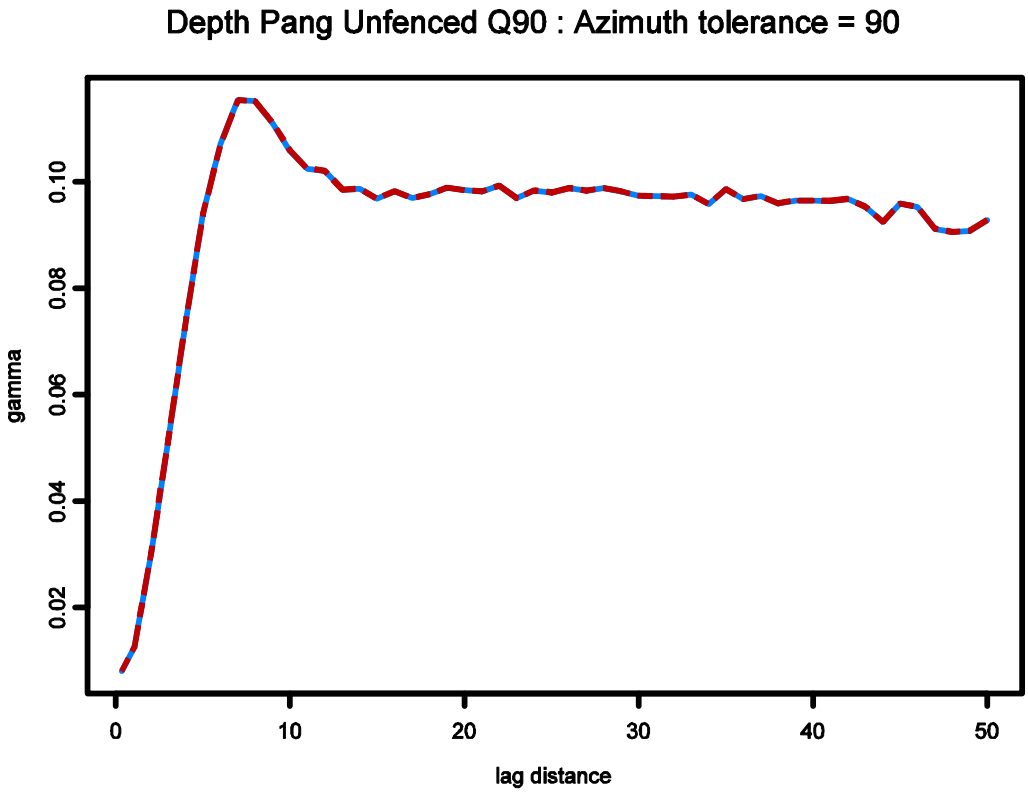
Depth Pang Unfenced Q90 : Azimuth tolerance = 90
gamma
0.02
0.04
0.06
0.08
0.10
0
10
20
30
40
50
lag distance

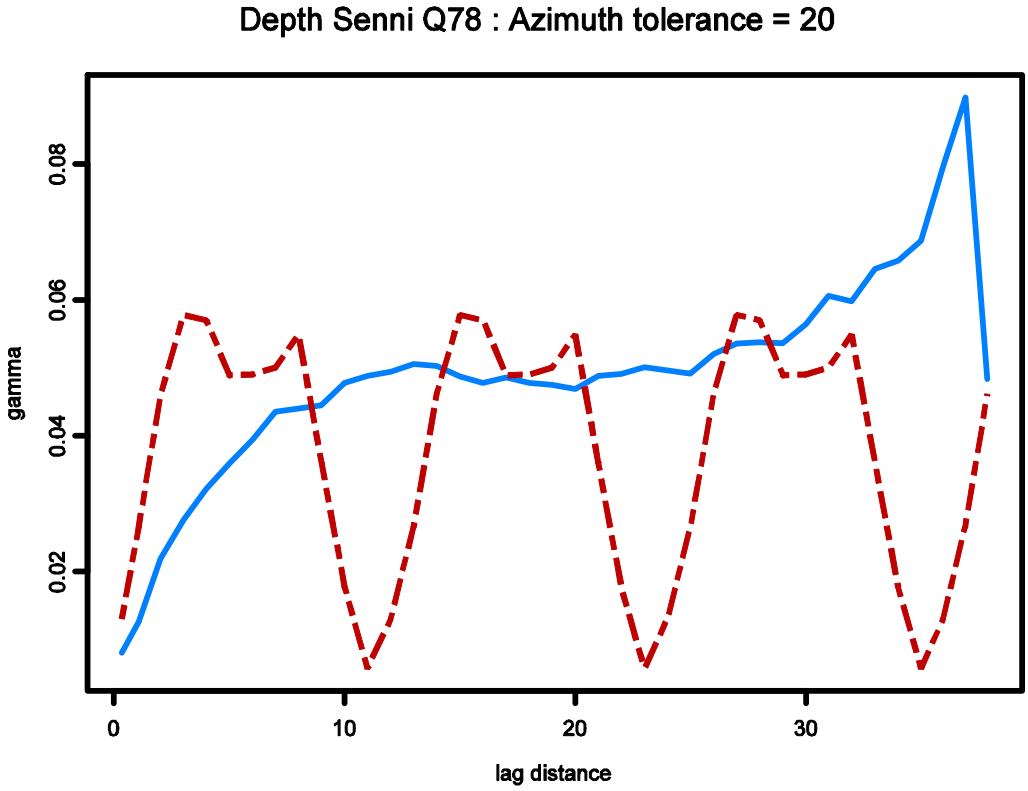
Depth Senni Q78 : Azimuth tolerance = 20
gamma
0.02
0.04
0.06
0.08
0
10
20
30
lag distance

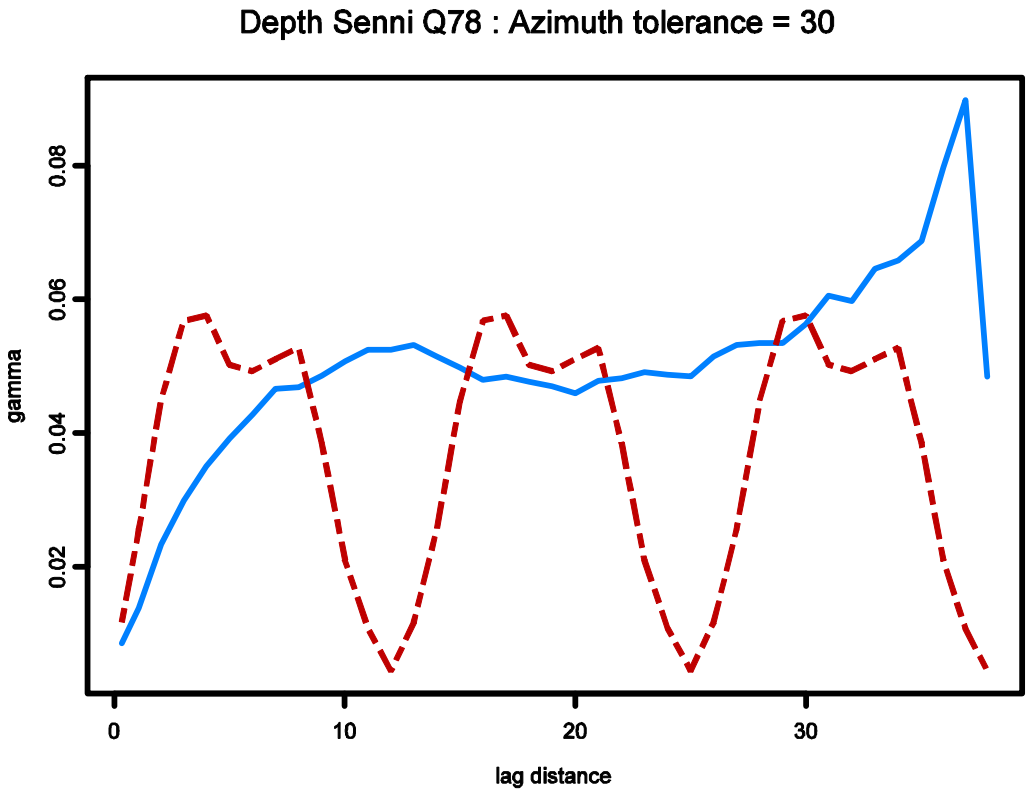
Depth Senni Q78 : Azimuth tolerance = 30
gamma
0.02
0.04
0.06
0.08
0
10
20
30
lag distance

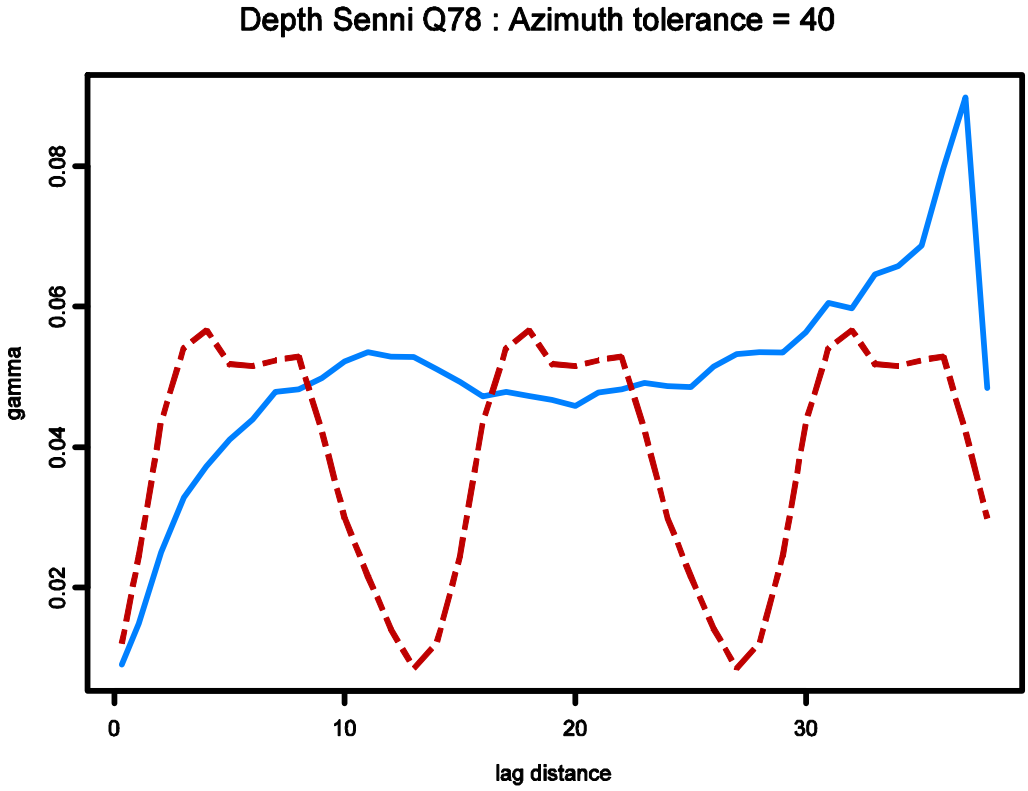
Depth Senni Q78 : Azimuth tolerance = 40
gamma
0.02
0.04
0.06
0.08
0
10
20
30
lag distance

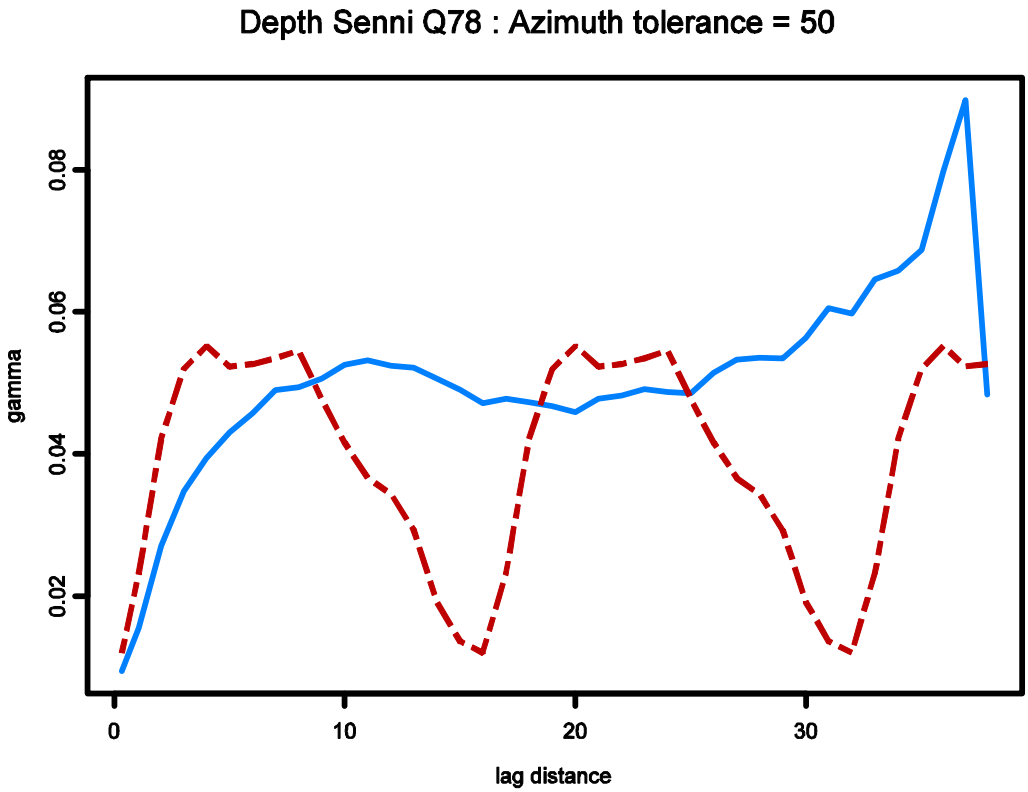
Depth Senni Q78 : Azimuth tolerance = 50
gamma
0.02
0.04
0.06
0.08
0
10
20
30
lag distance

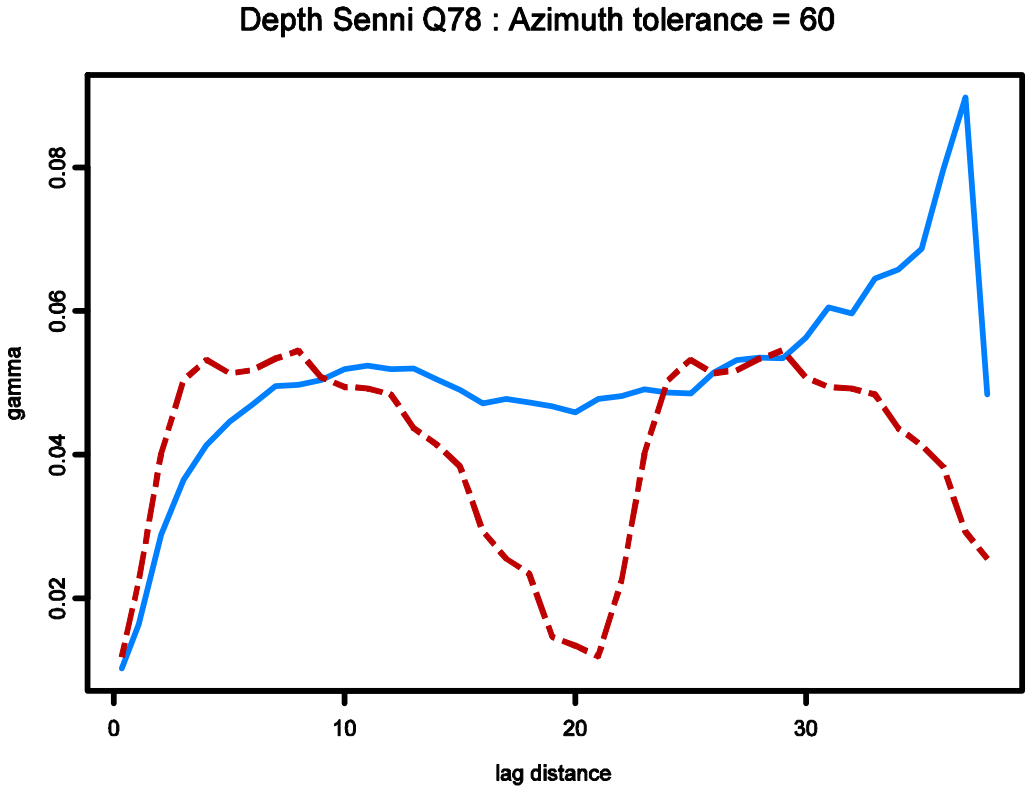
Depth Senni Q78 : Azimuth tolerance = 60
gamma
0.02
0.04
0.06
0.08
0
10
20
30
lag distance

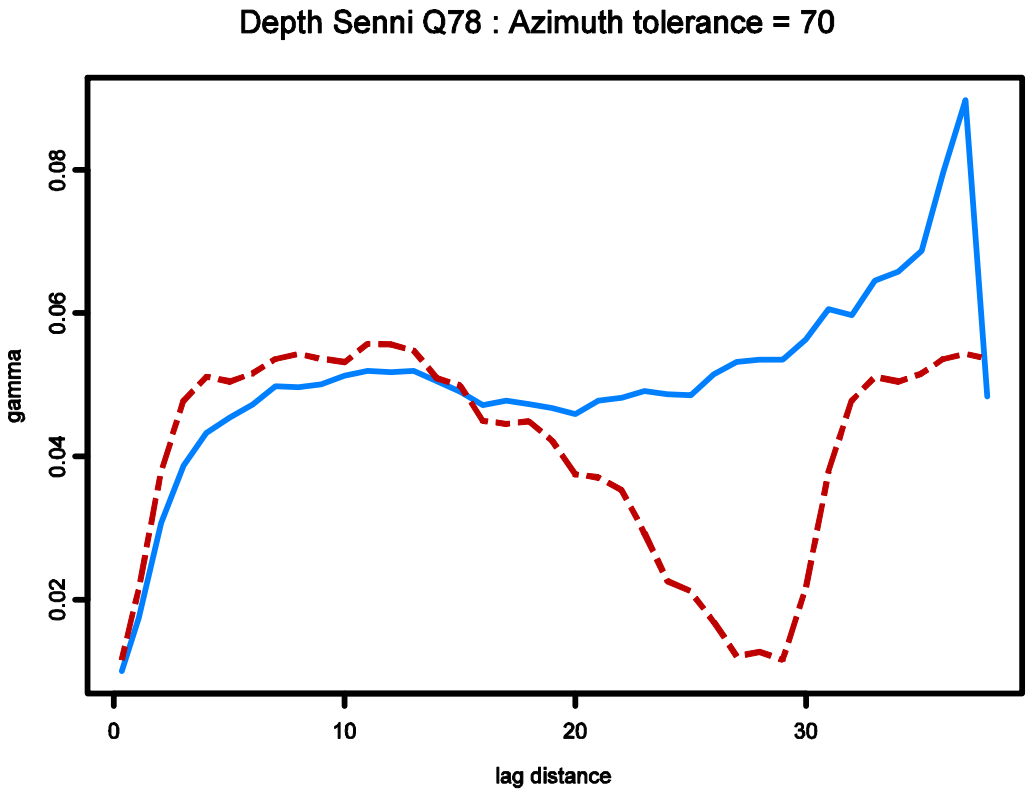
Depth Senni Q78 : Azimuth tolerance = 70
gamma
0.02
0.04
0.06
0.08
0
10
20
30
lag distance

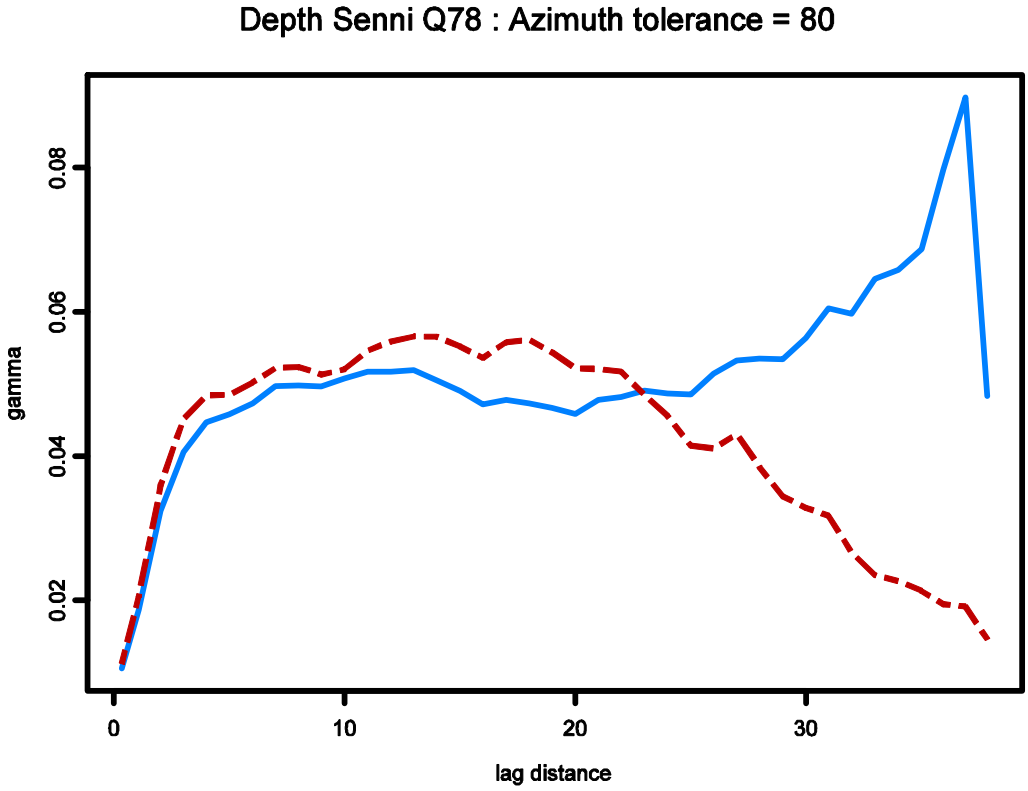
Depth Senni Q78 : Azimuth tolerance = 80
gamma
0.02
0.04
0.06
0.08
0
10
20
30
lag distance

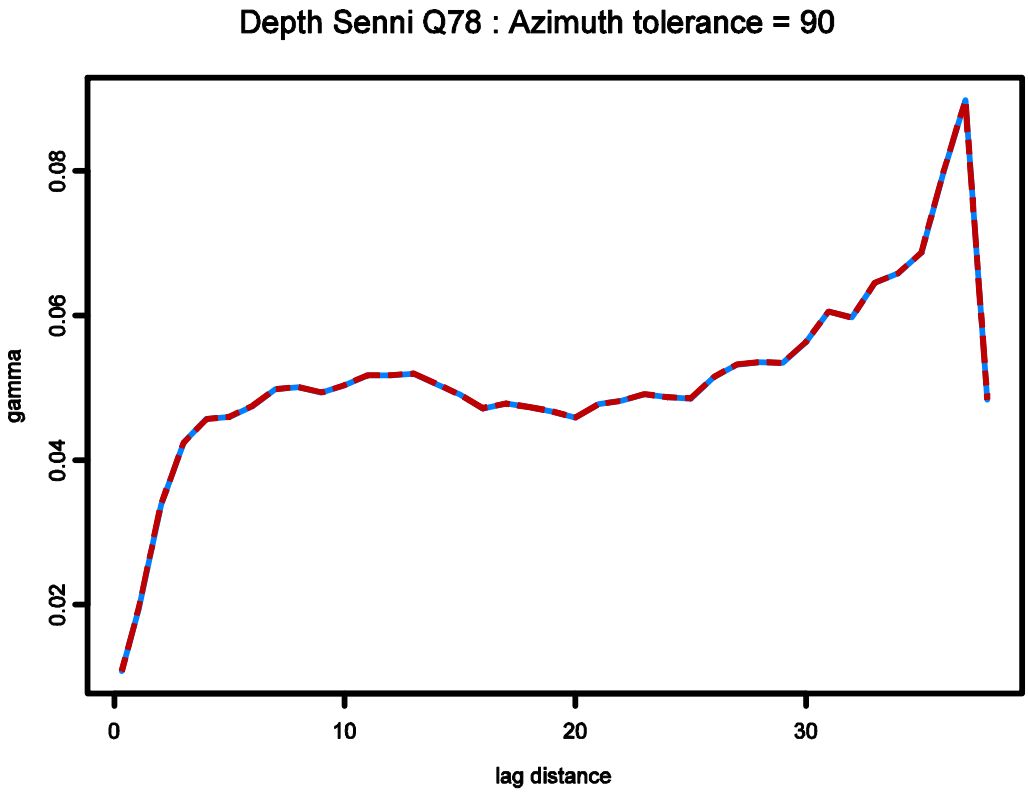
Depth Senni Q78 : Azimuth tolerance = 90
gamma
0.02
0.04
0.06
0.08
0
10
20
30
lag distance

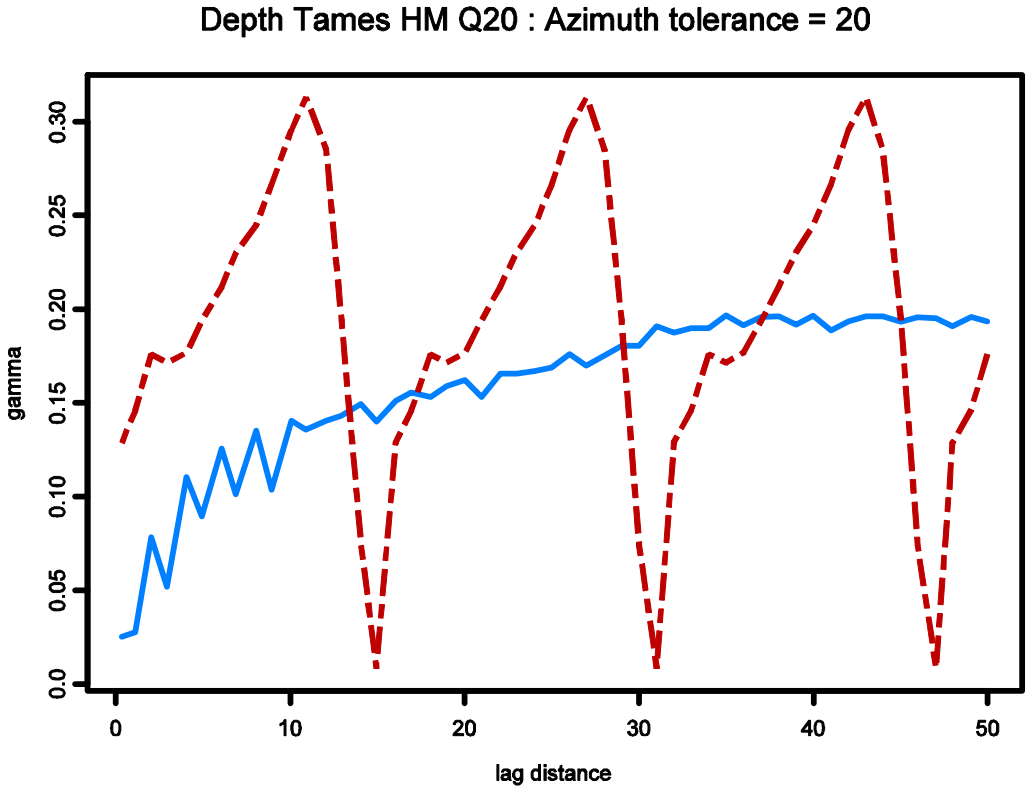
Depth Tames HM Q20 : Azimuth tolerance = 20
gamma
0.0
0.05
0.10
0.15
0.20
0.25
0.30
0
10
20
30
40
50
lag distance

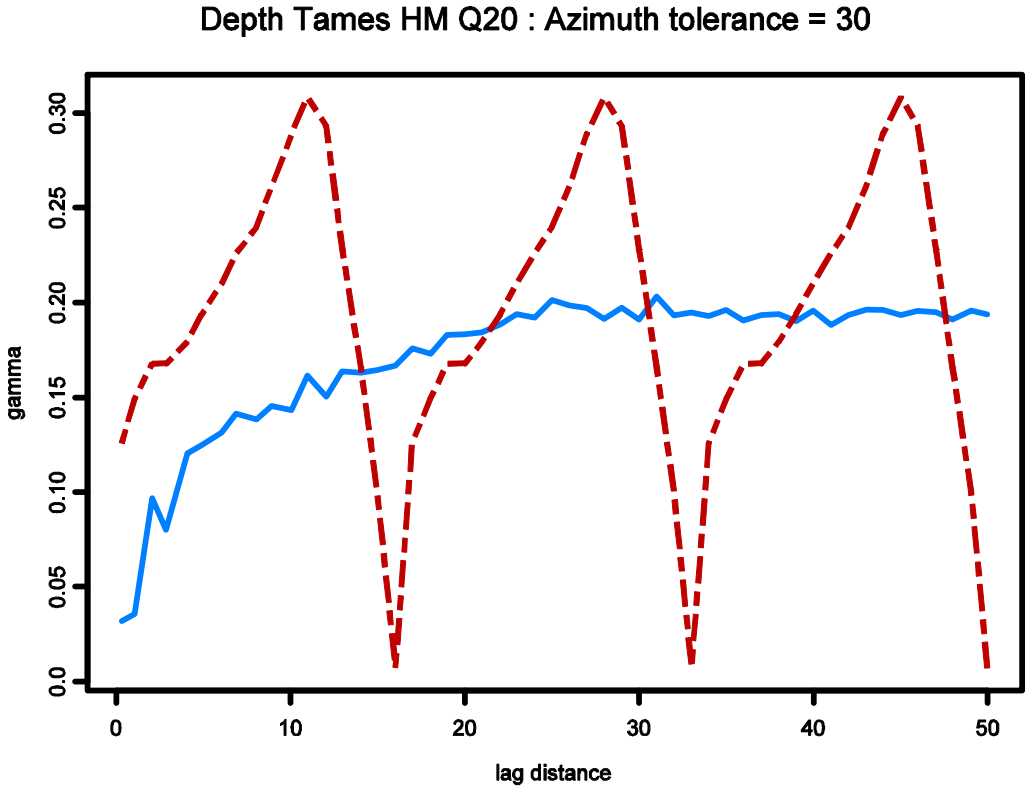
Depth Tames HM Q20 : Azimuth tolerance = 30
gamma
0.0
0.05
0.10
0.15
0.20
0.25
0.30
0
10
20
30
40
50
lag distance

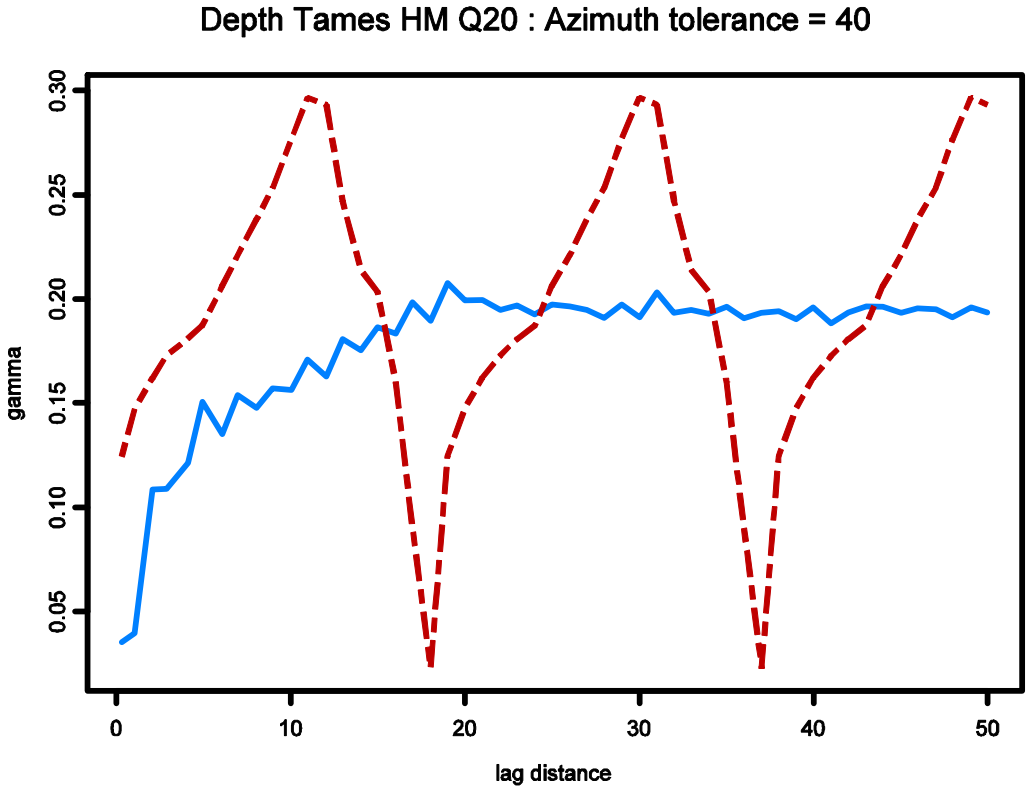
Depth Tames HM Q20 : Azimuth tolerance = 40
gamma
0.05
0.10
0.15
0.20
0.25
0.30
0
10
20
30
40
50
lag distance

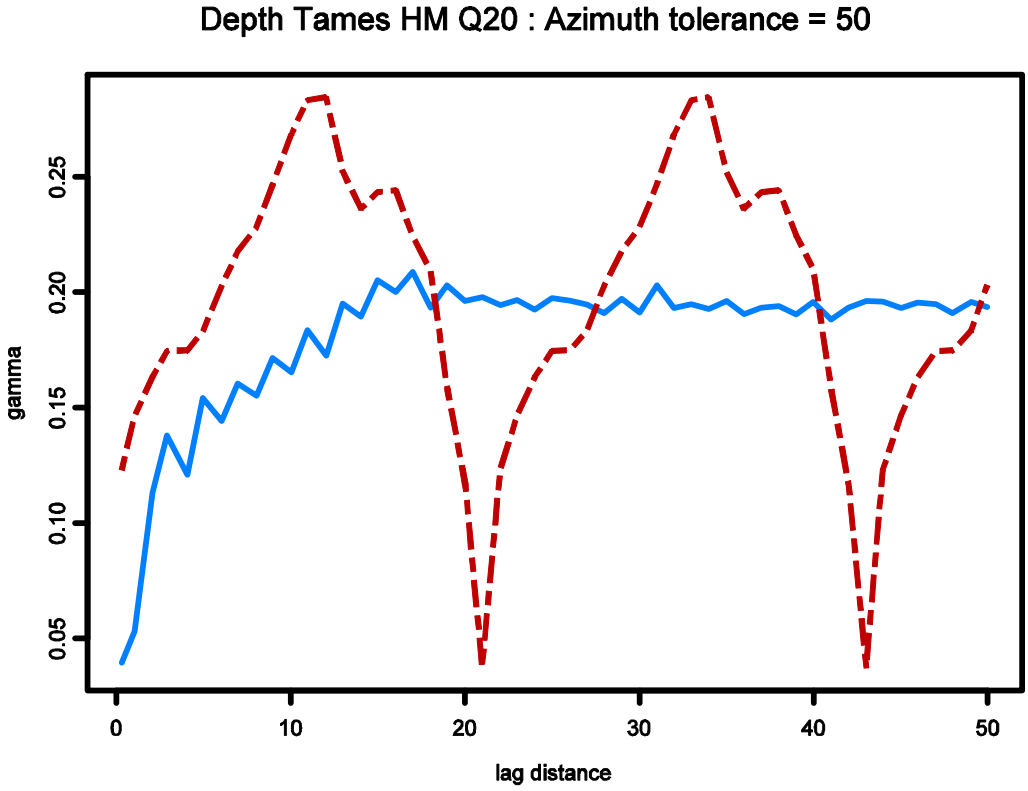
Depth Tames HM Q20 : Azimuth tolerance = 50
gamma
0.05
0.10
0.15
0.20
0.25
0
10
20
30
40
50
lag distance

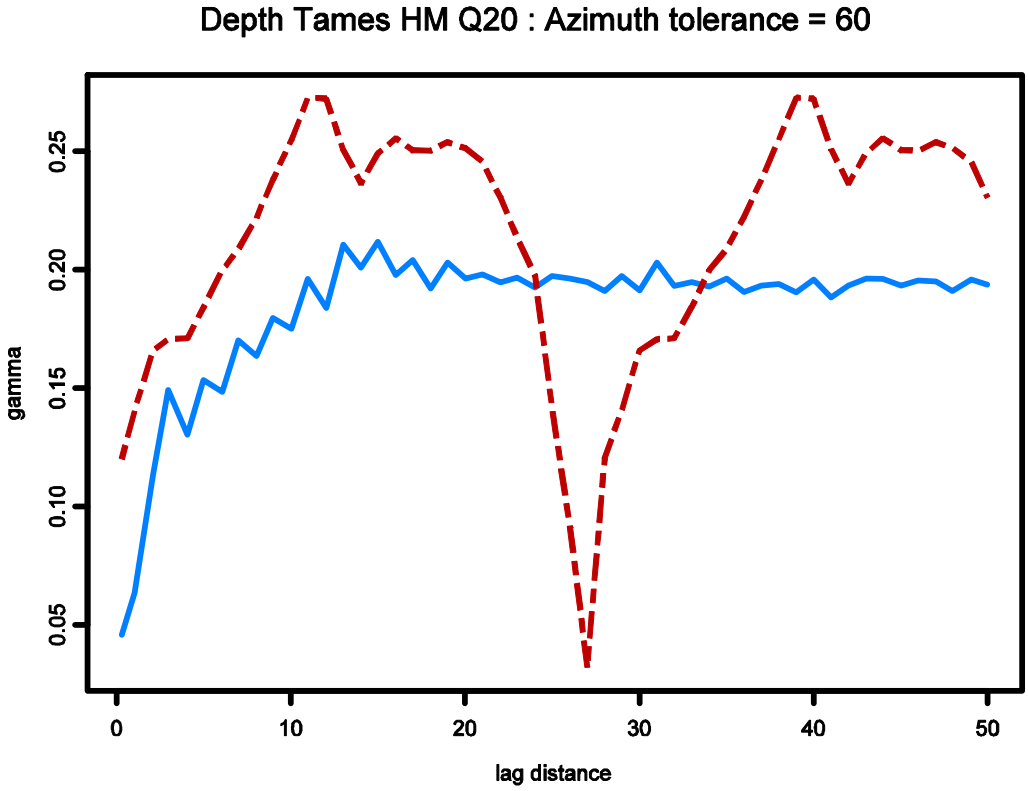
Depth Tames HM Q20 : Azimuth tolerance = 60
gamma
0.05
0.10
0.15
0.20
0.25
0
10
20
30
40
50
lag distance

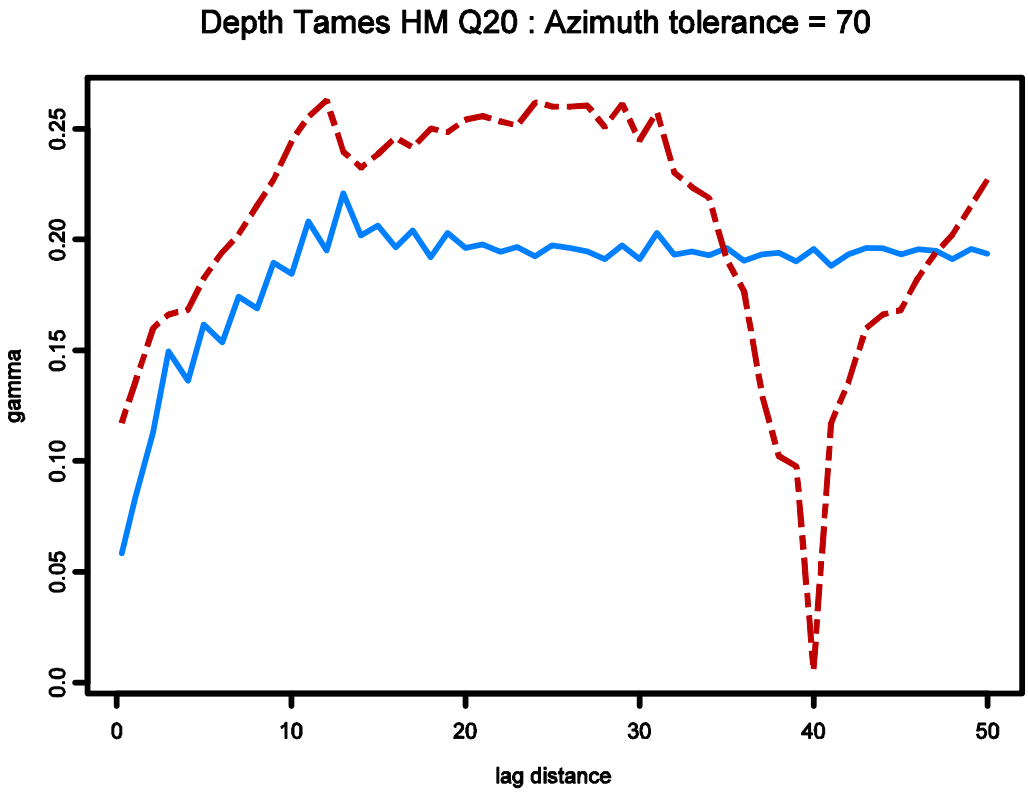
Depth Tames HM Q20 : Azimuth tolerance = 70
gamma
0.0
0.05
0.10
0.15
0.20
0.25
0
10
20
30
40
50
lag distance

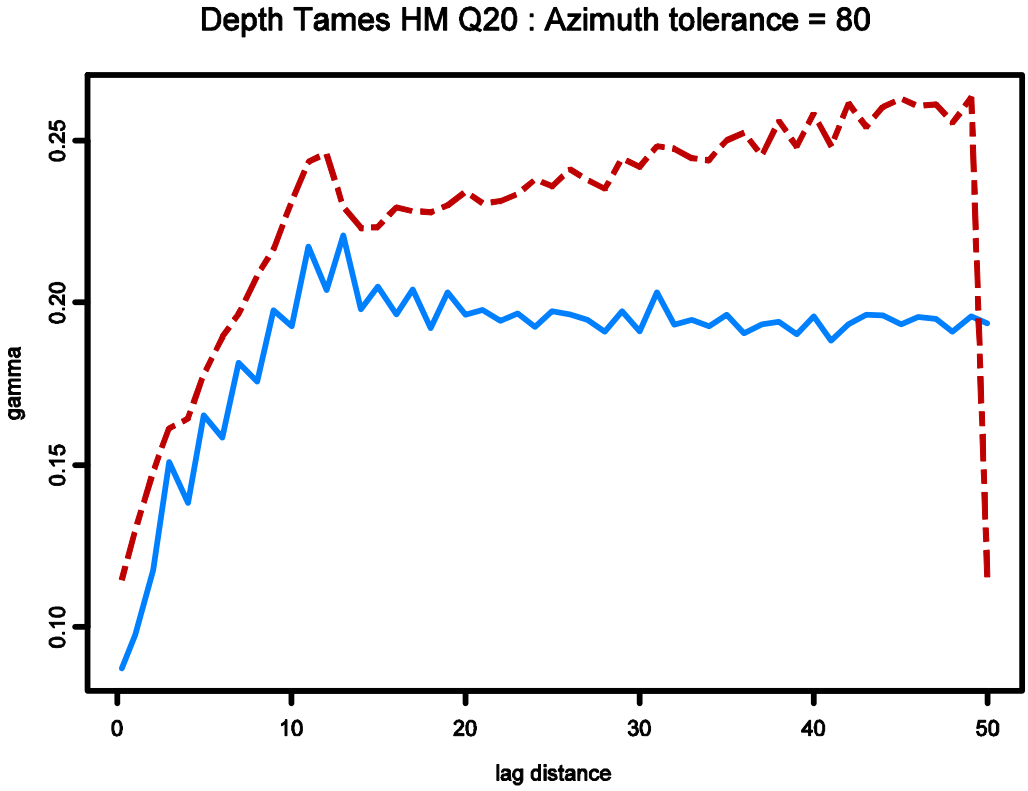
Depth Tames HM Q20 : Azimuth tolerance = 80
gamma
0.10
0.15
0.20
0.25
0
10
20
30
40
50
lag distance

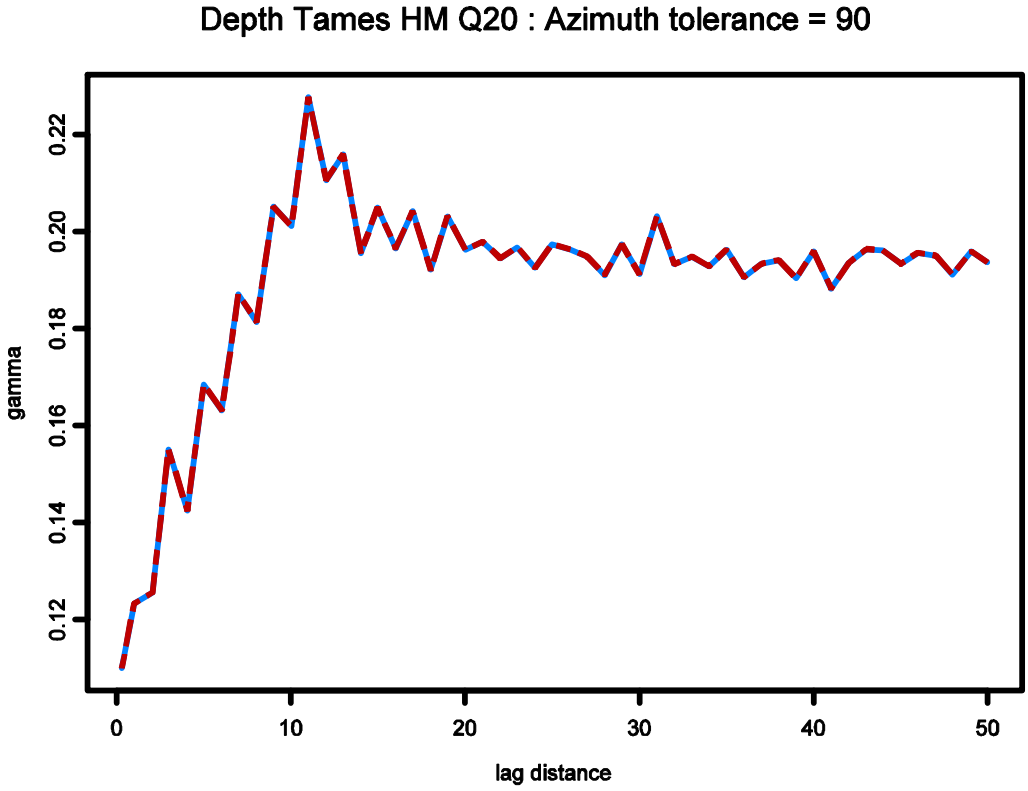
Depth Tames HM Q20 : Azimuth tolerance = 90
gamma
0.12
0.14
0.16
0.18
0.20
0.22
0
10
20
30
40
50
lag distance

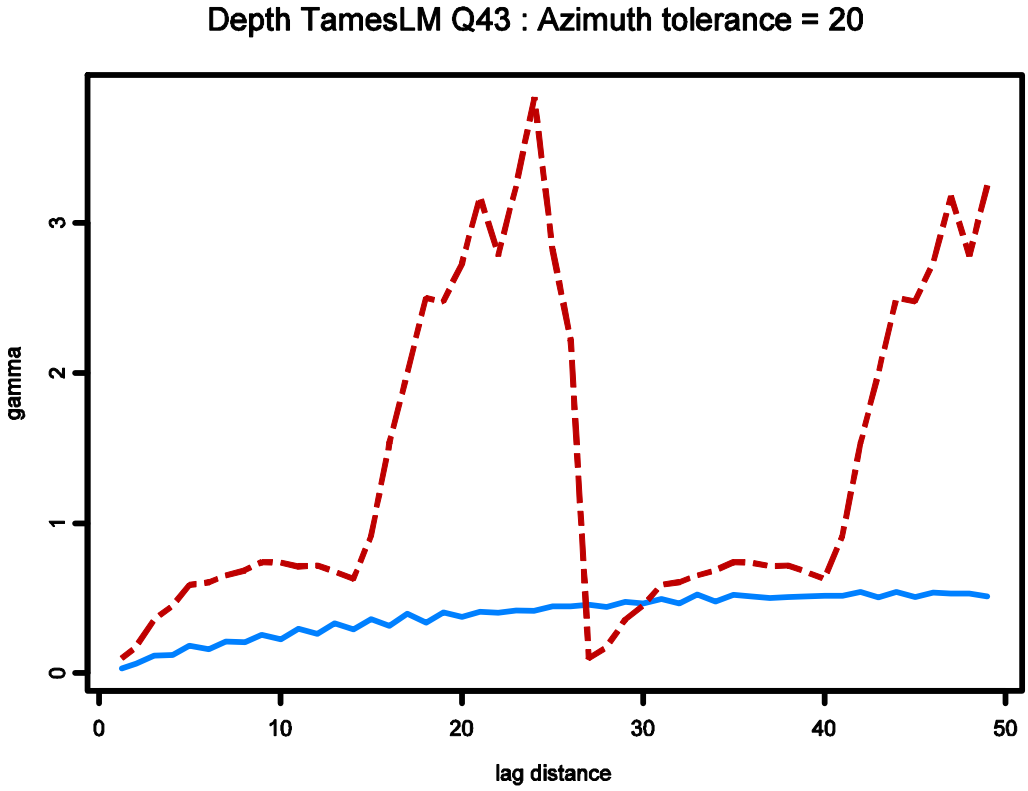
Depth TamesLM Q43 : Azimuth tolerance = 20
gamma
0
1
2
3
0
10
20
30
40
50
lag distance

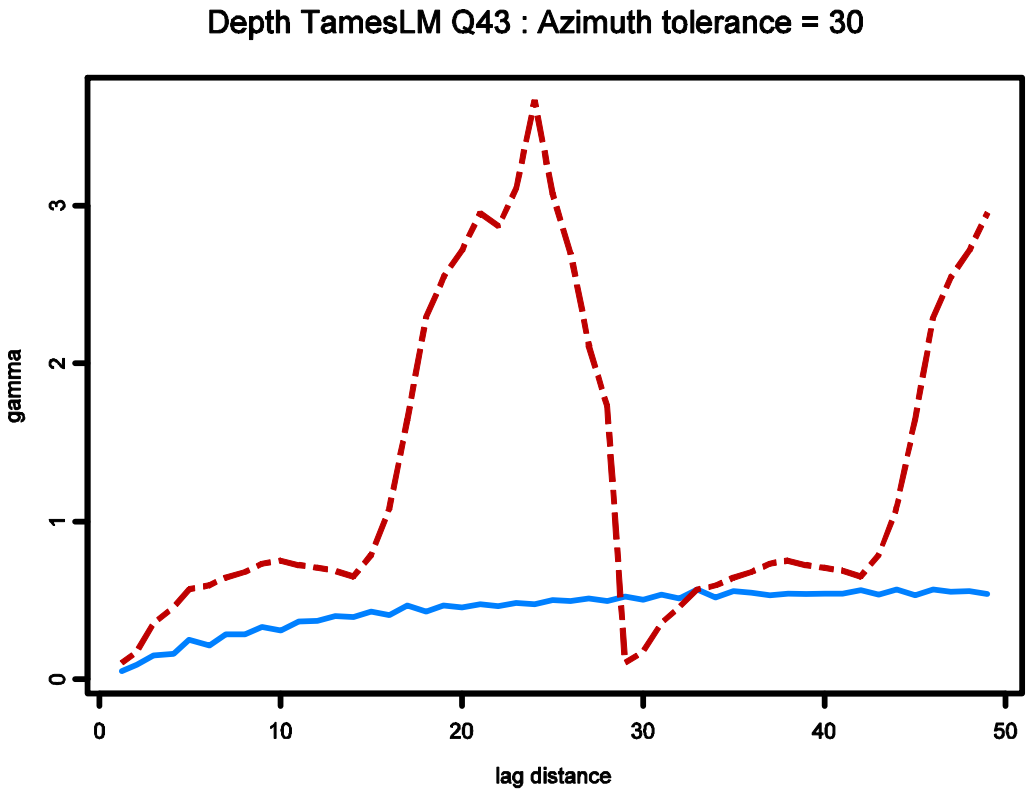
Depth TamesLM Q43 : Azimuth tolerance = 30
gamma
0
1
2
3
0
10
20
30
40
50
lag distance

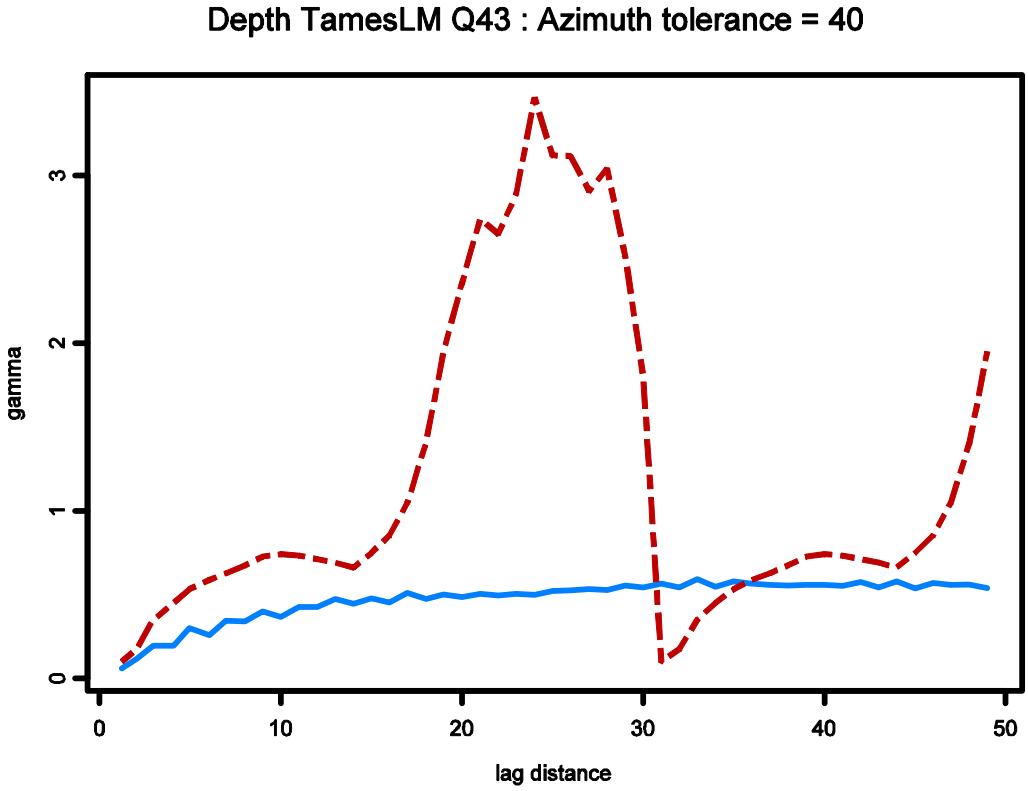
Depth TamesLM Q43 : Azimuth tolerance = 40
gamma
0
1
2
3
0
10
20
30
40
50
lag distance

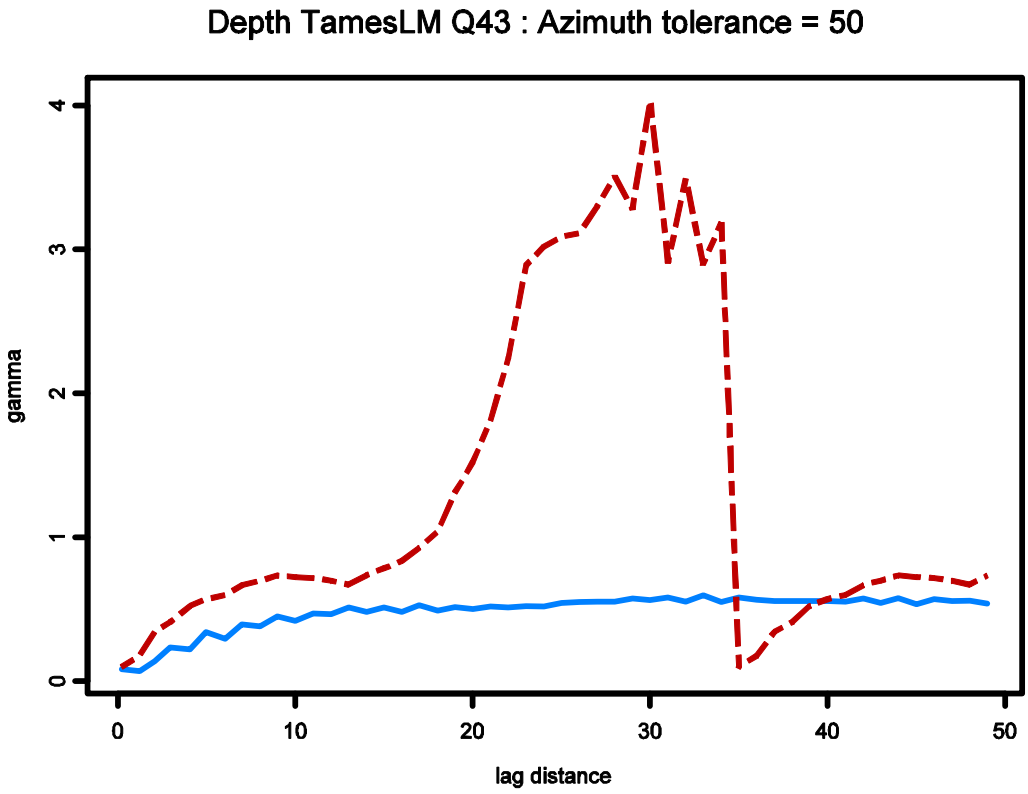
Depth TamesLM Q43 : Azimuth tolerance = 50
gamma
0
1
2
3
4
0
10
20
30
40
50
lag distance

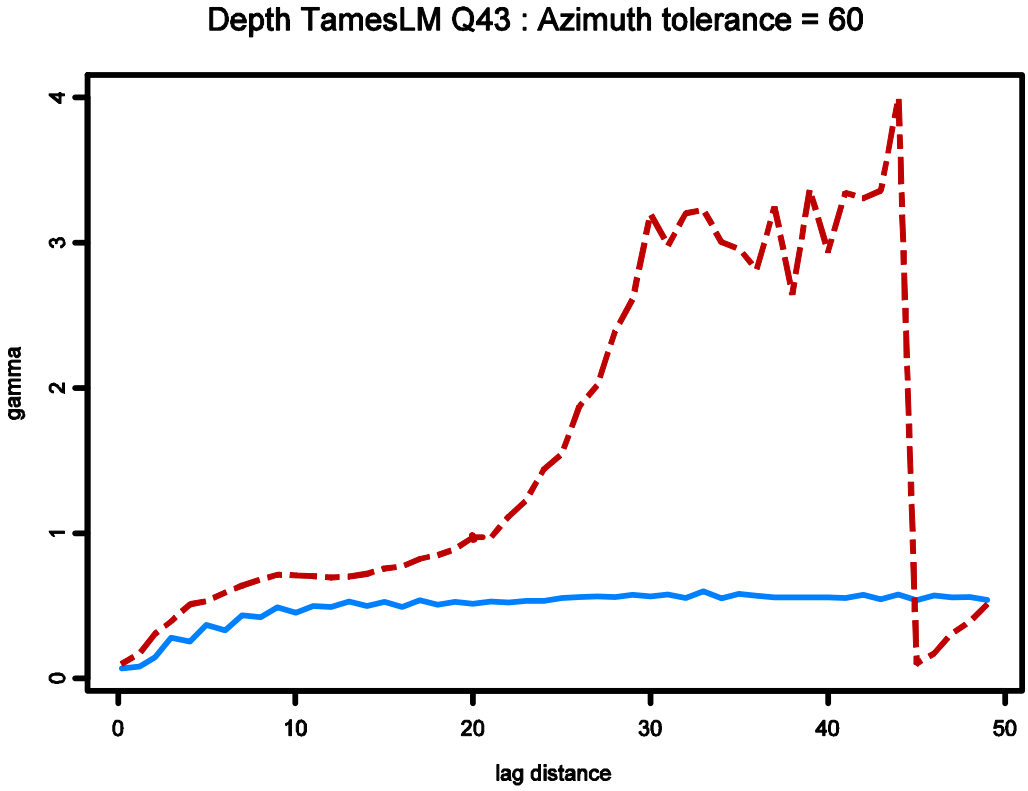
Depth TamesLM Q43 : Azimuth tolerance = 60
gamma
0
1
2
3
4
0
10
20
30
40
50
lag distance

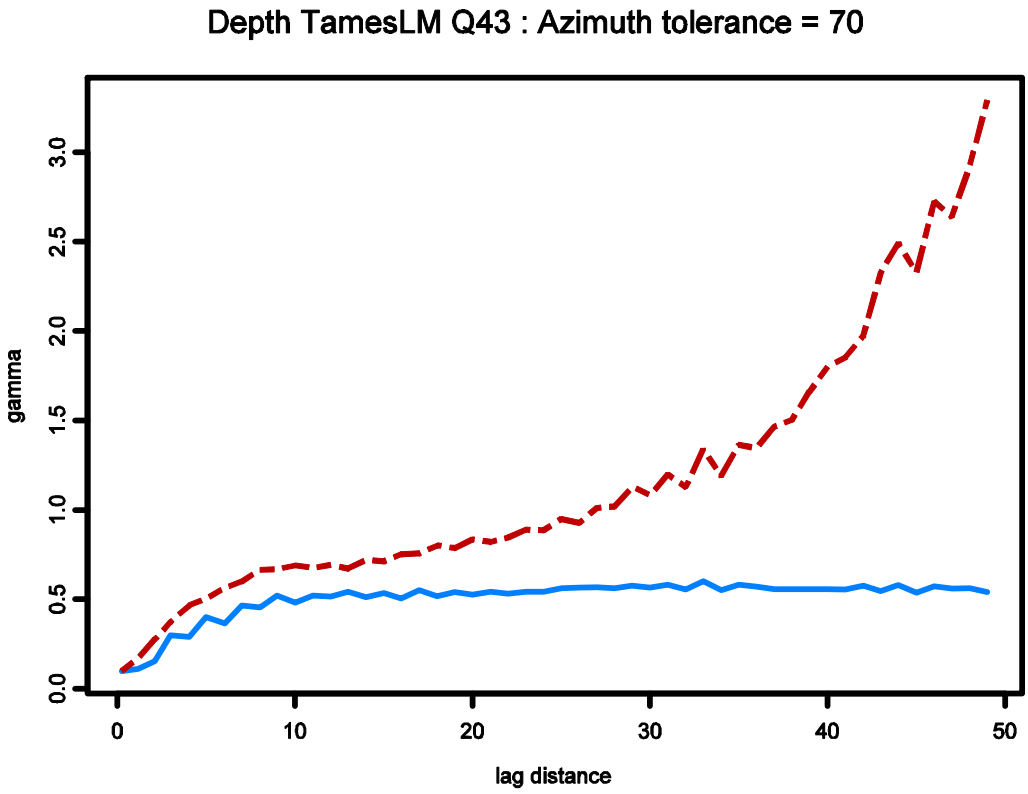
Depth TamesLM Q43 : Azimuth tolerance = 70
gamma
0.0
0.5
1.0
1.5
2.0
2.5
3.0
0
10
20
30
40
50
lag distance

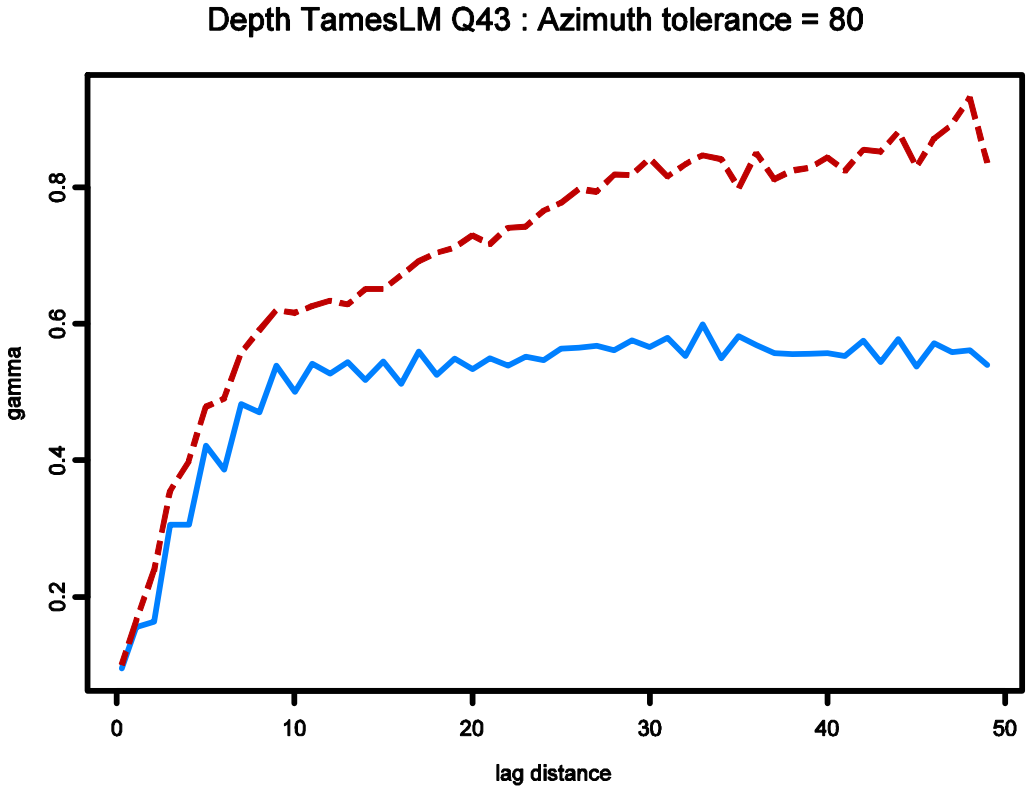
Depth TamesLM Q43 : Azimuth tolerance = 80
gamma
0.2
0.4
0.6
0.8
0
10
20
30
40
50
lag distance

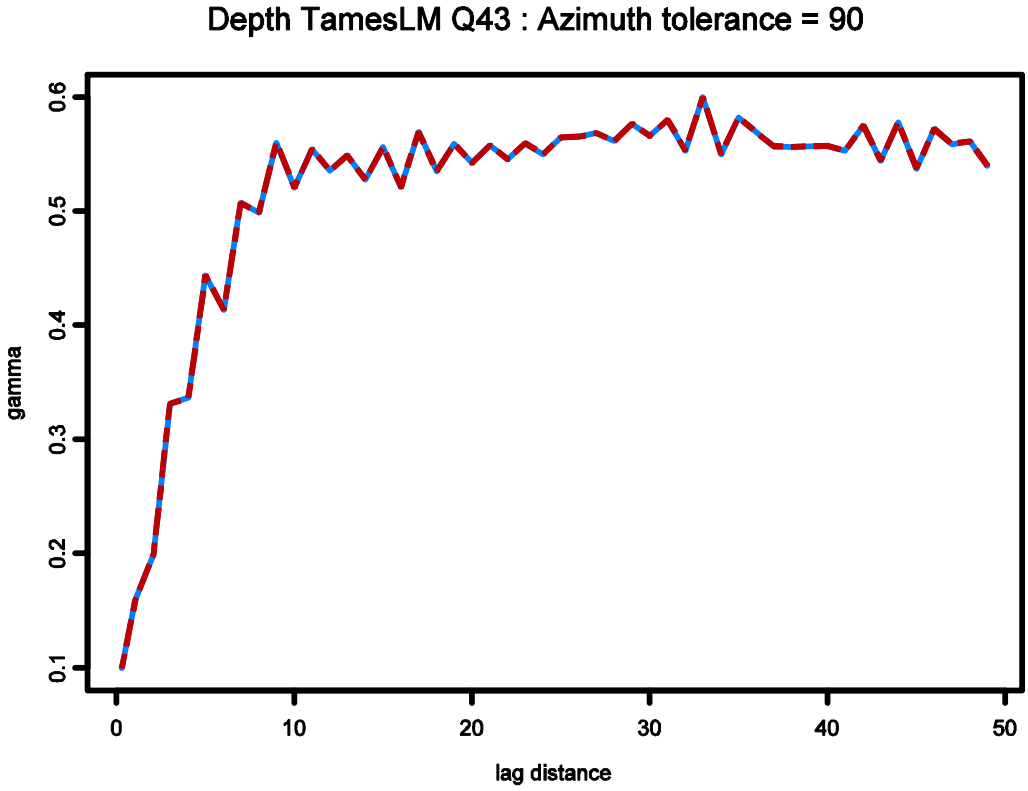
Depth TamesLM Q43 : Azimuth tolerance = 90
gamma
0.1
0.2
0.3
0.4
0.5
0.6
0
10
20
30
40
50
lag distance

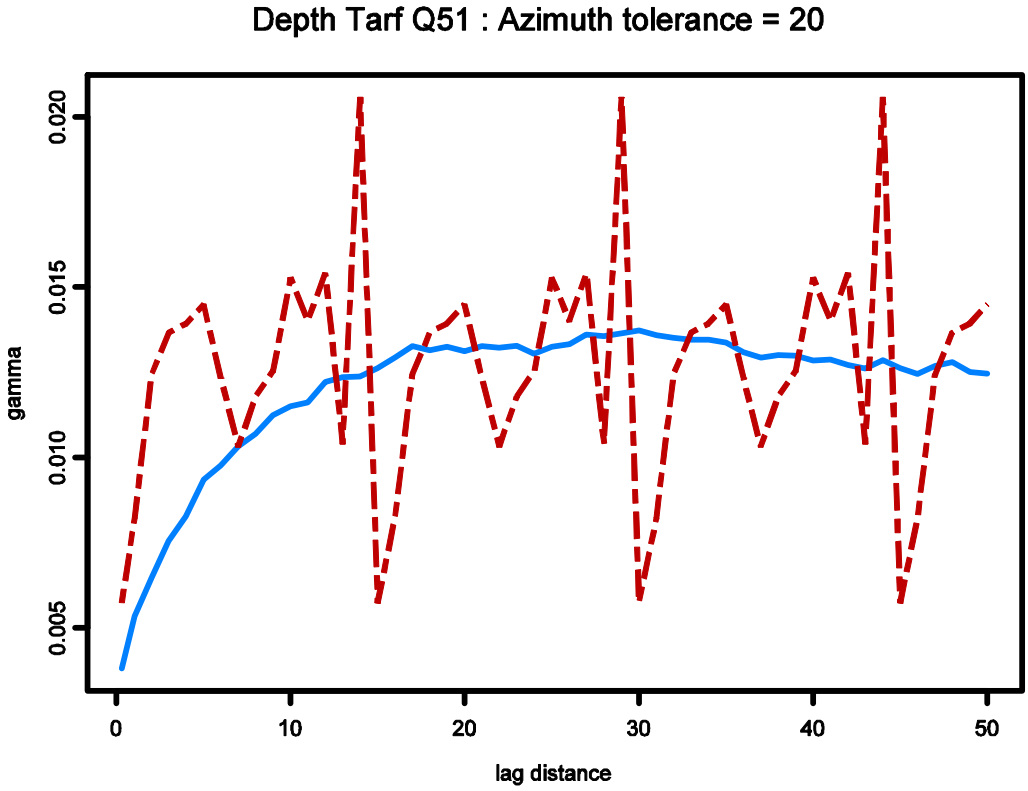
Depth Tarf Q51 : Azimuth tolerance = 20
gamma
0.005
0.010
0.015
0.020
0
10
20
30
40
50
lag distance

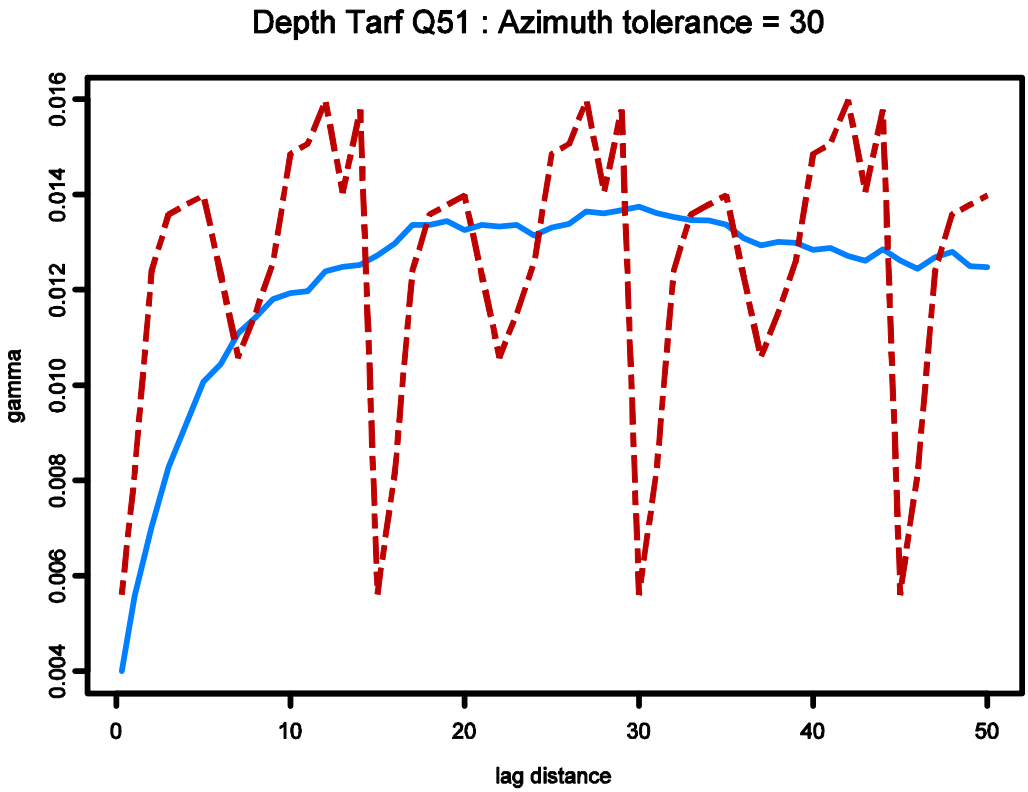
Depth Tarf Q51 : Azimuth tolerance = 30
gamma
0.004
0.006
0.008
0.010
0.012
0.014
0.016
0
10
20
30
40
50
lag distance

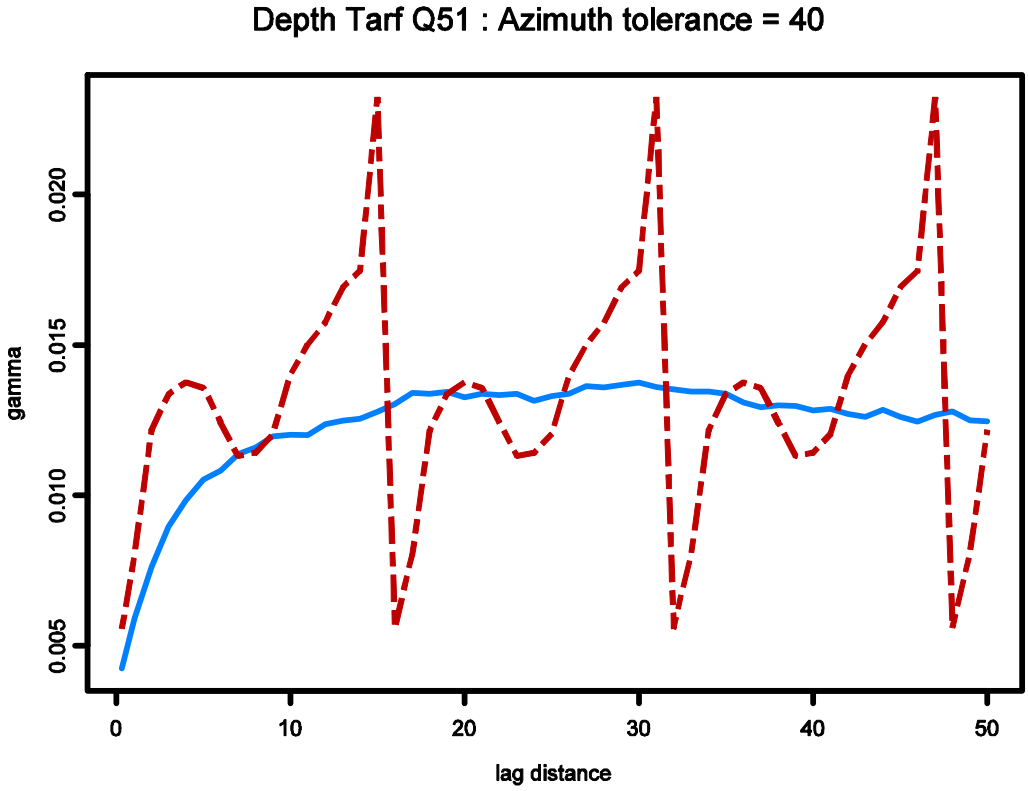
Depth Tarf Q51 : Azimuth tolerance = 40
gamma
0.005
0.010
0.015
0.020
0
10
20
30
40
50
lag distance

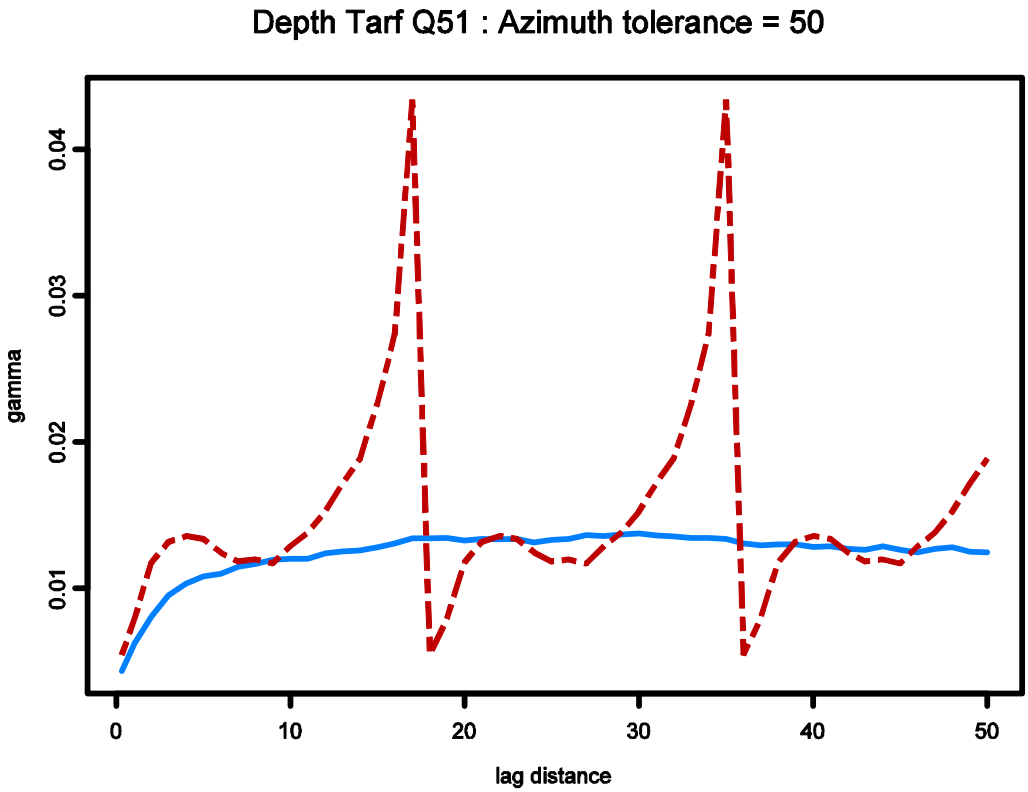
Depth Tarf Q51 : Azimuth tolerance = 50
gamma
0.01
0.02
0.03
0.04
0
10
20
30
40
50
lag distance

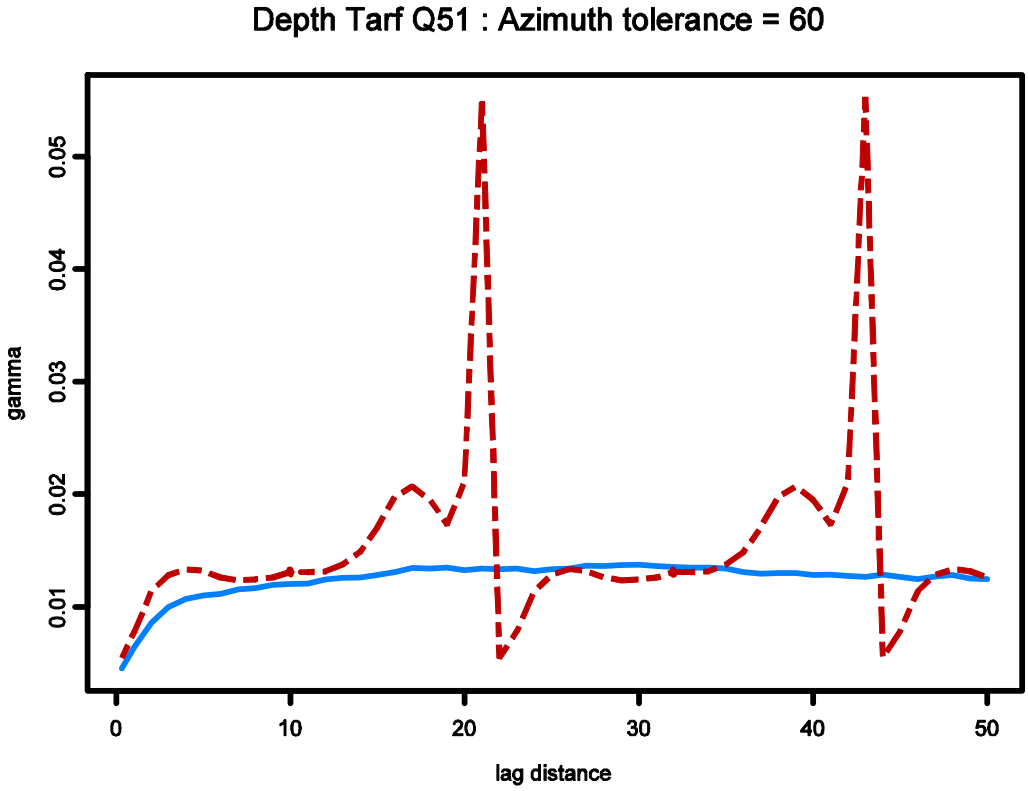
Depth Tarf Q51 : Azimuth tolerance = 60
gamma
0.01
0.02
0.03
0.04
0.05
0
10
20
30
40
50
lag distance

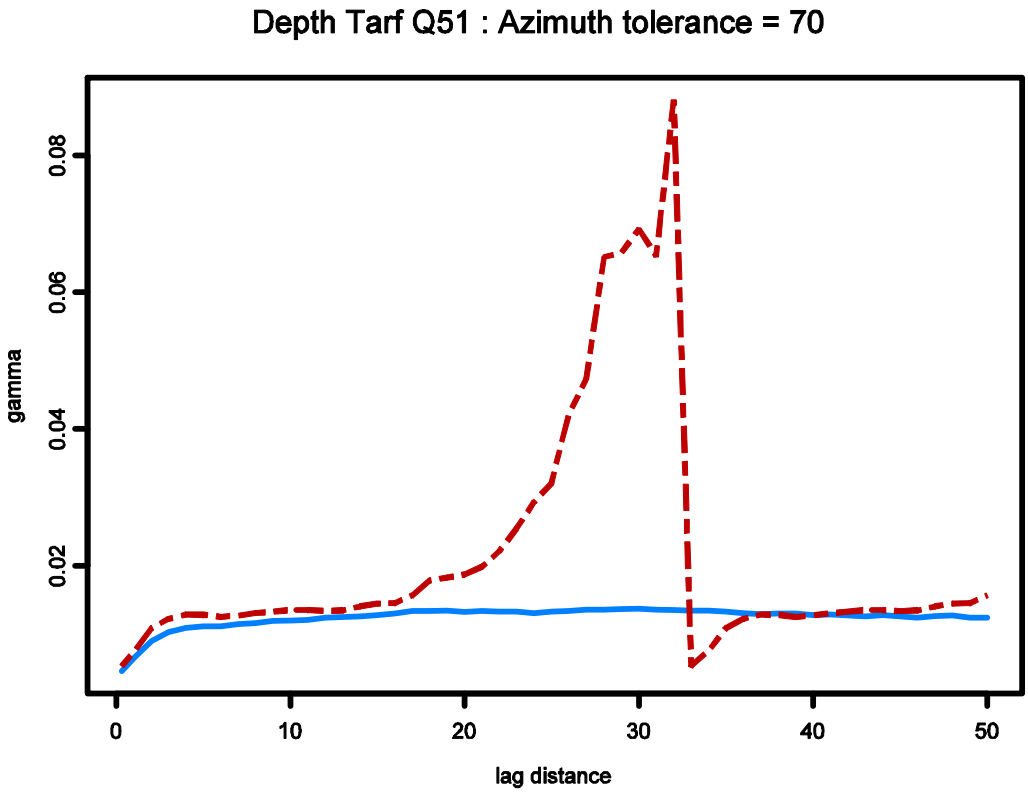
Depth Tarf Q51 : Azimuth tolerance = 70
gamma
0.02
0.04
0.06
0.08
0
10
20
30
40
50
lag distance

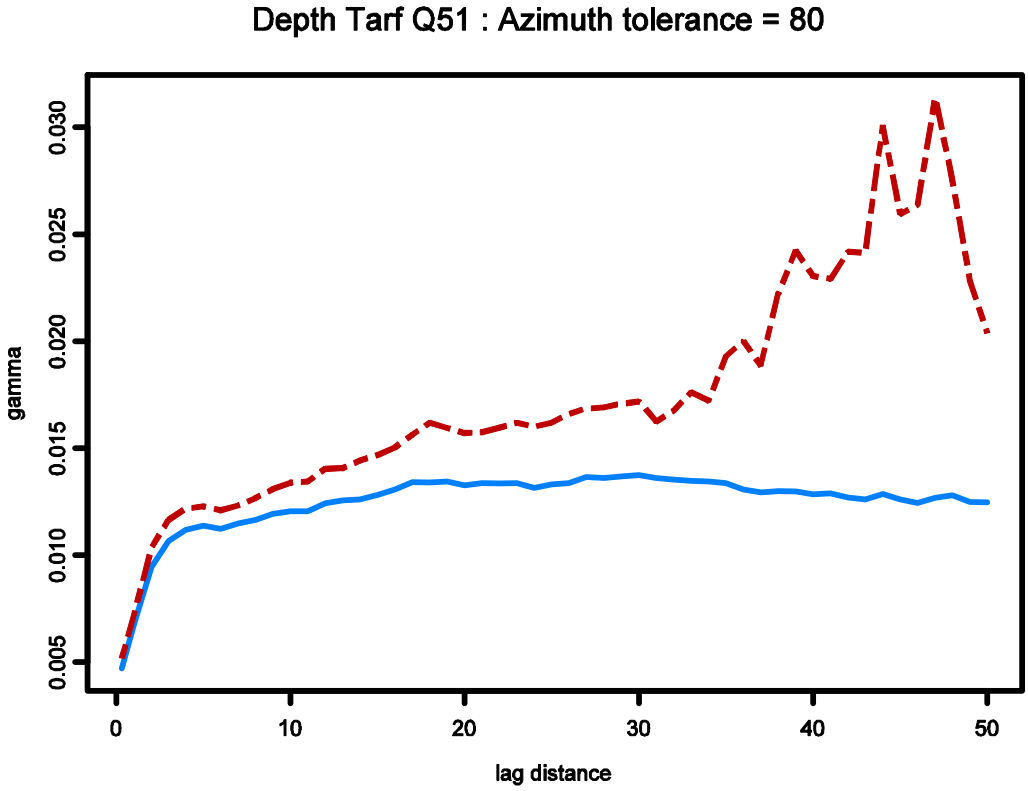
Depth Tarf Q51 : Azimuth tolerance = 80
gamma
0.005
0.010
0.015
0.020
0.025
0.030
0
10
20
30
40
50
lag distance

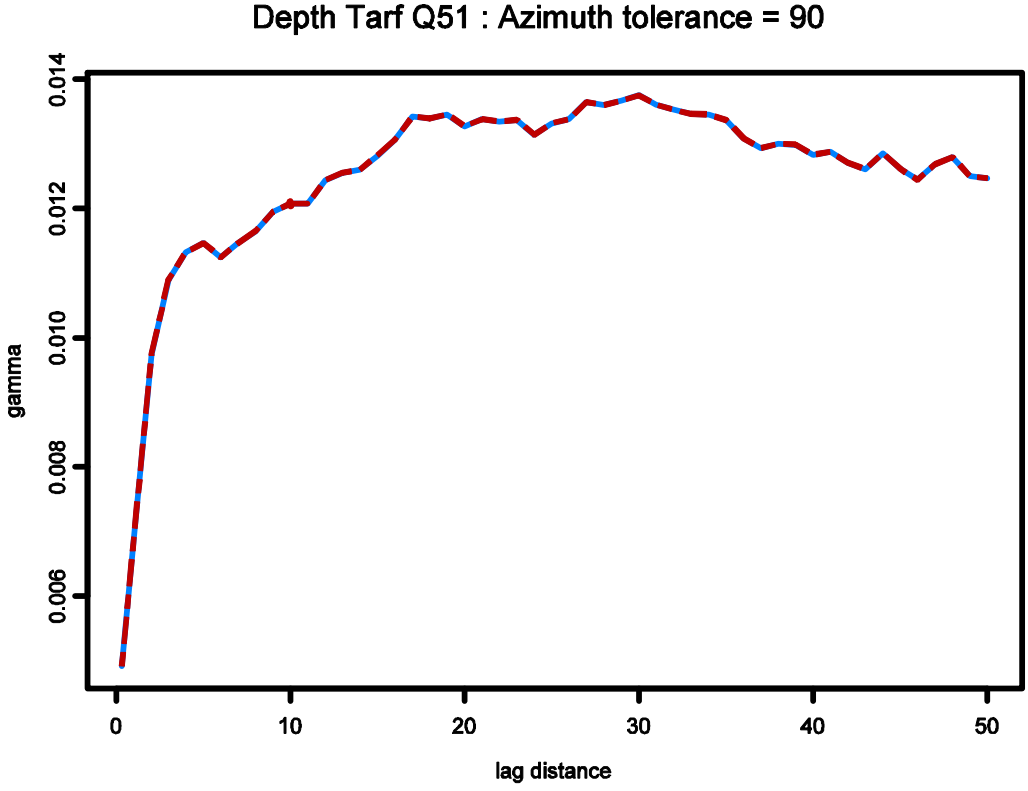
Depth Tarf Q51 : Azimuth tolerance = 90
gamma
0.006
0.008
0.010
0.012
0.014
0
10
20
30
40
50
lag distance

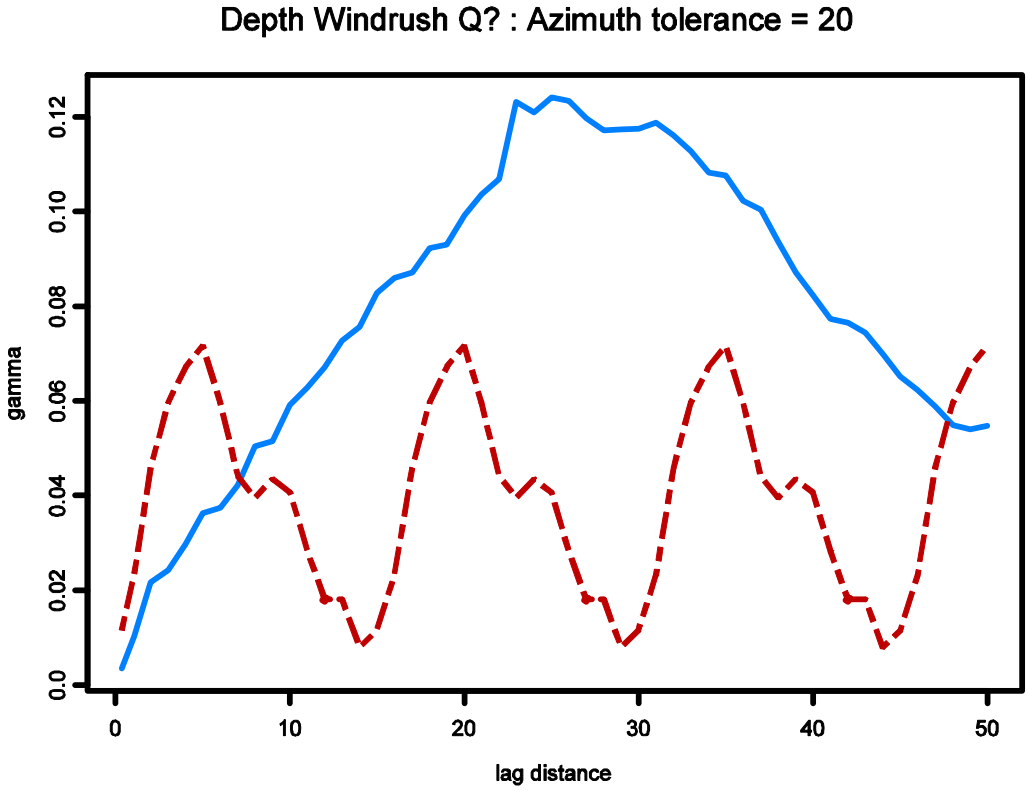
Depth Windrush Q? : Azimuth tolerance = 20
gamma
0.0
0.02
0.04
0.06
0.08
0.10
0.12
0
10
20
30
40
50
lag distance

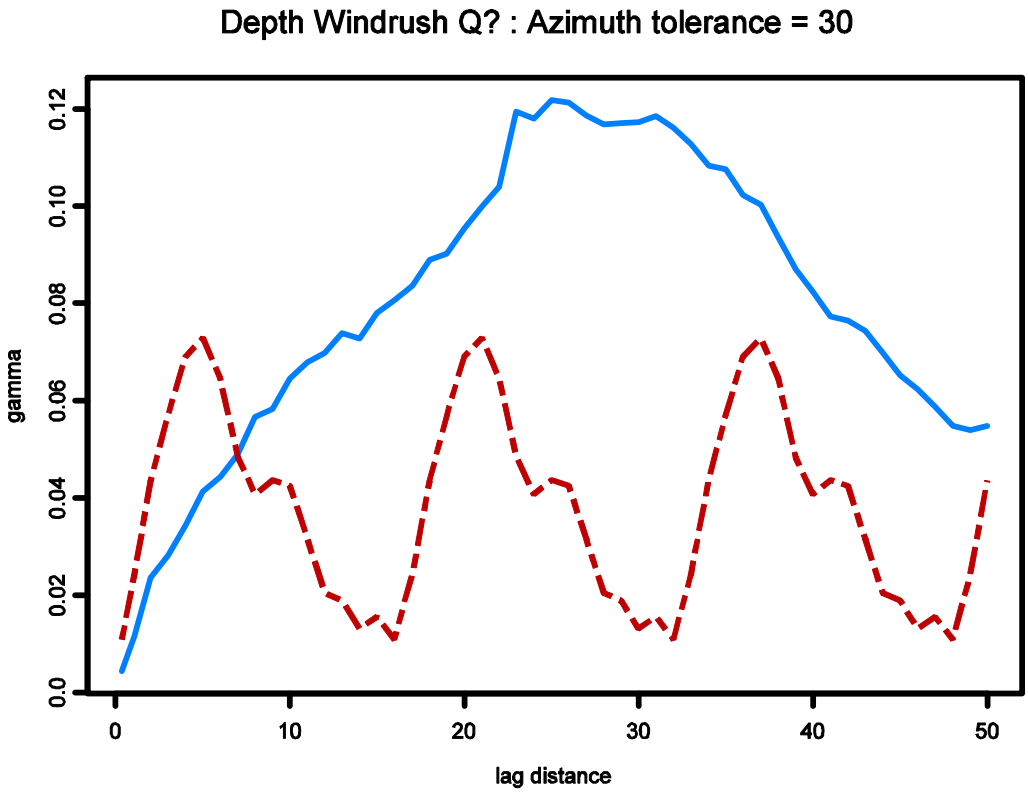
Depth Windrush Q? : Azimuth tolerance = 30
gamma
0.0
0.02
0.04
0.06
0.08
0.10
0.12
0
10
20
30
40
50
lag distance

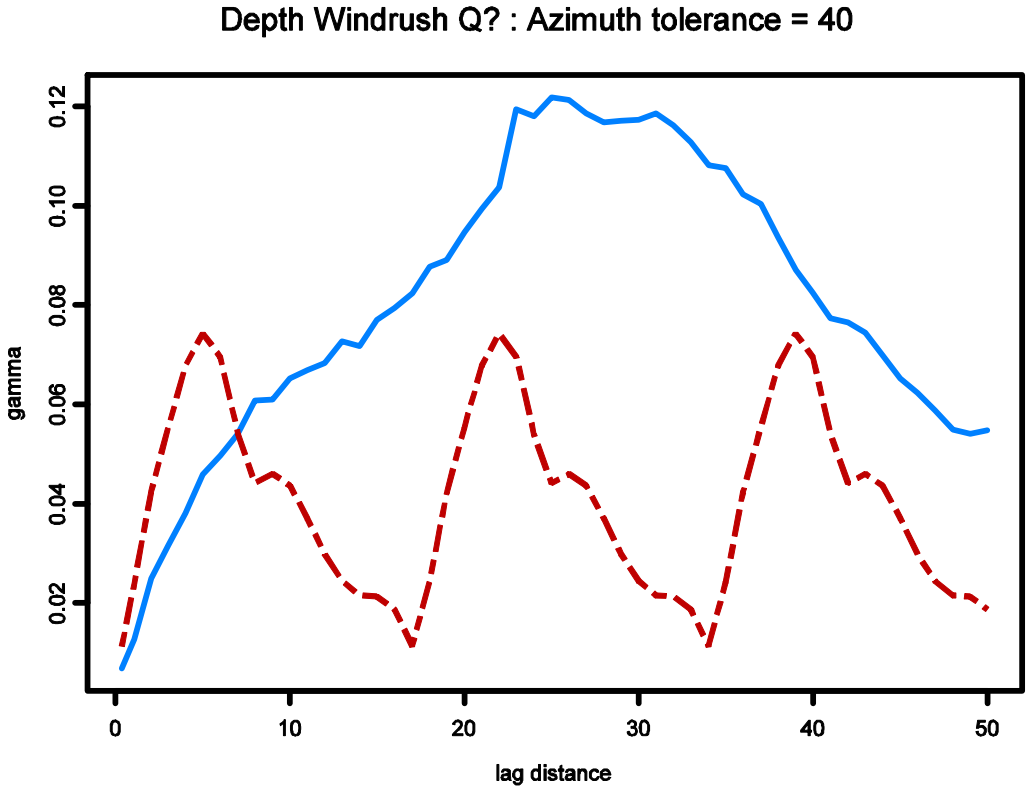
Depth Windrush Q? : Azimuth tolerance = 40
gamma
0.02
0.04
0.06
0.08
0.10
0.12
0
10
20
30
40
50
lag distance

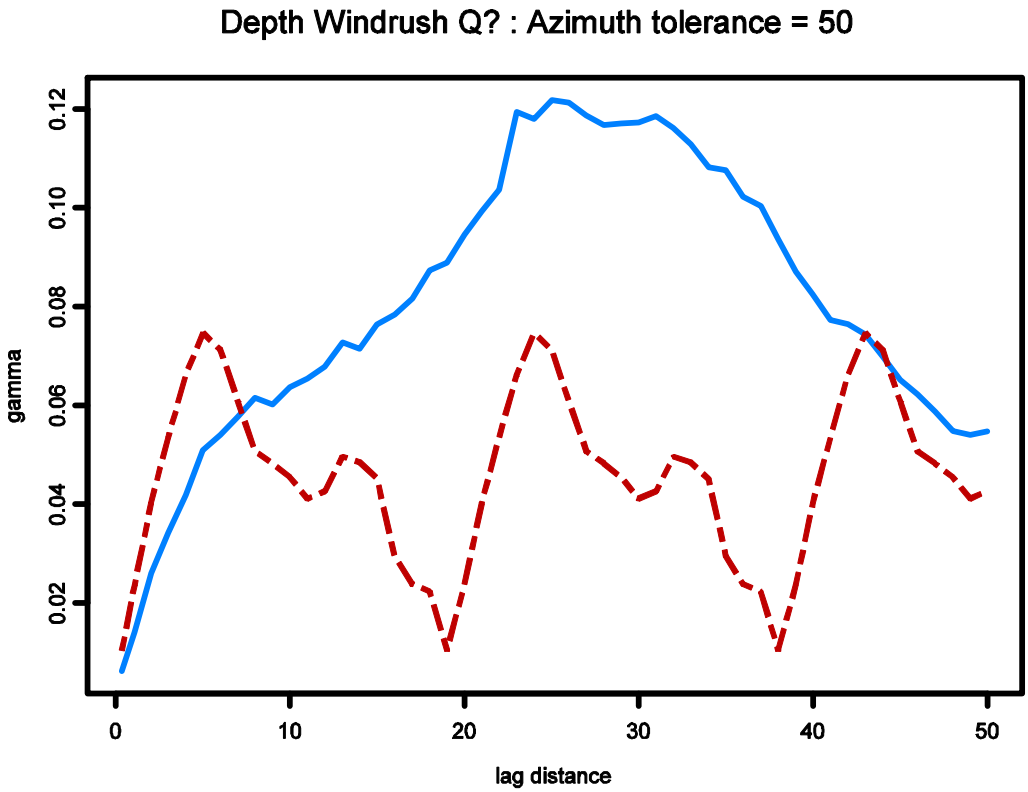
Depth Windrush Q? : Azimuth tolerance = 50
gamma
0.02
0.04
0.06
0.08
0.10
0.12
0
10
20
30
40
50
lag distance

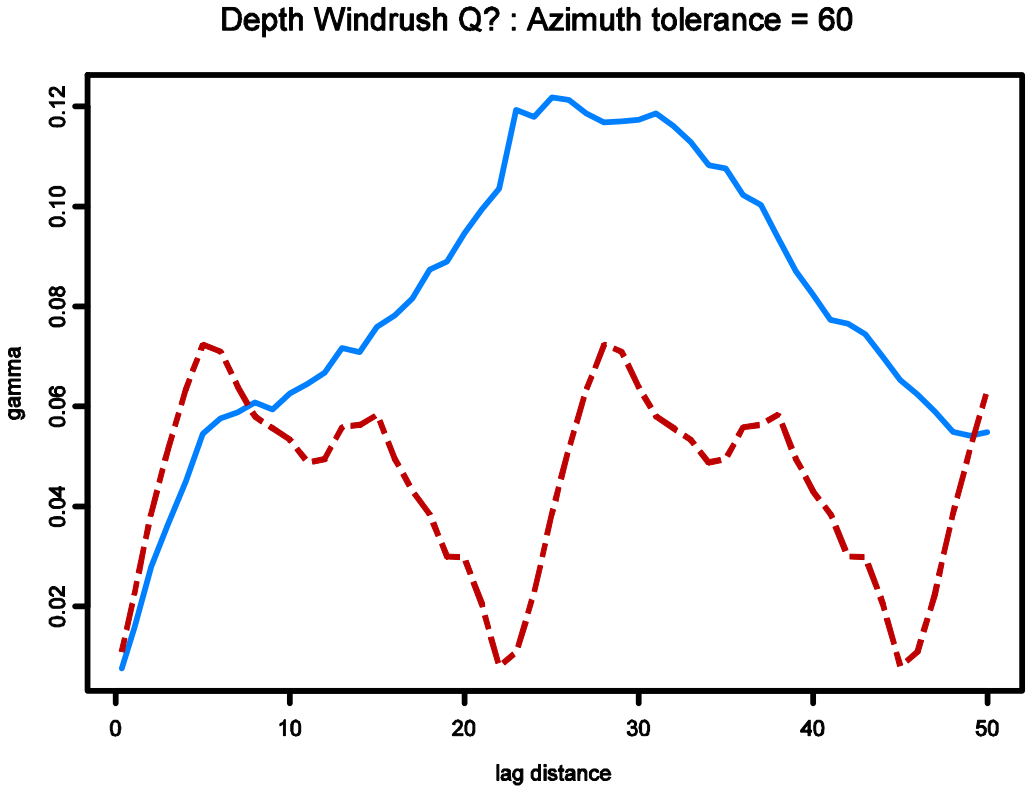
Depth Windrush Q? : Azimuth tolerance = 60
gamma
0.02
0.04
0.06
0.08
0.10
0.12
0
10
20
30
40
50
lag distance

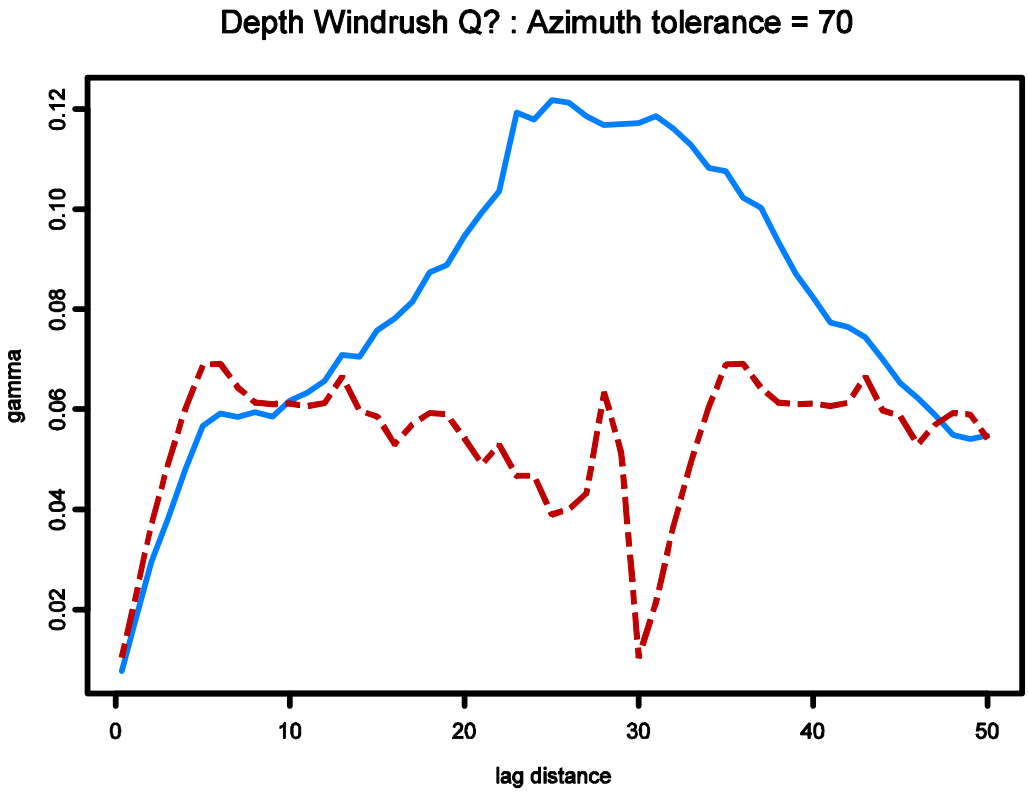
Depth Windrush Q? : Azimuth tolerance = 70
gamma
0.02
0.04
0.06
0.08
0.10
0.12
0
10
20
30
40
50
lag distance

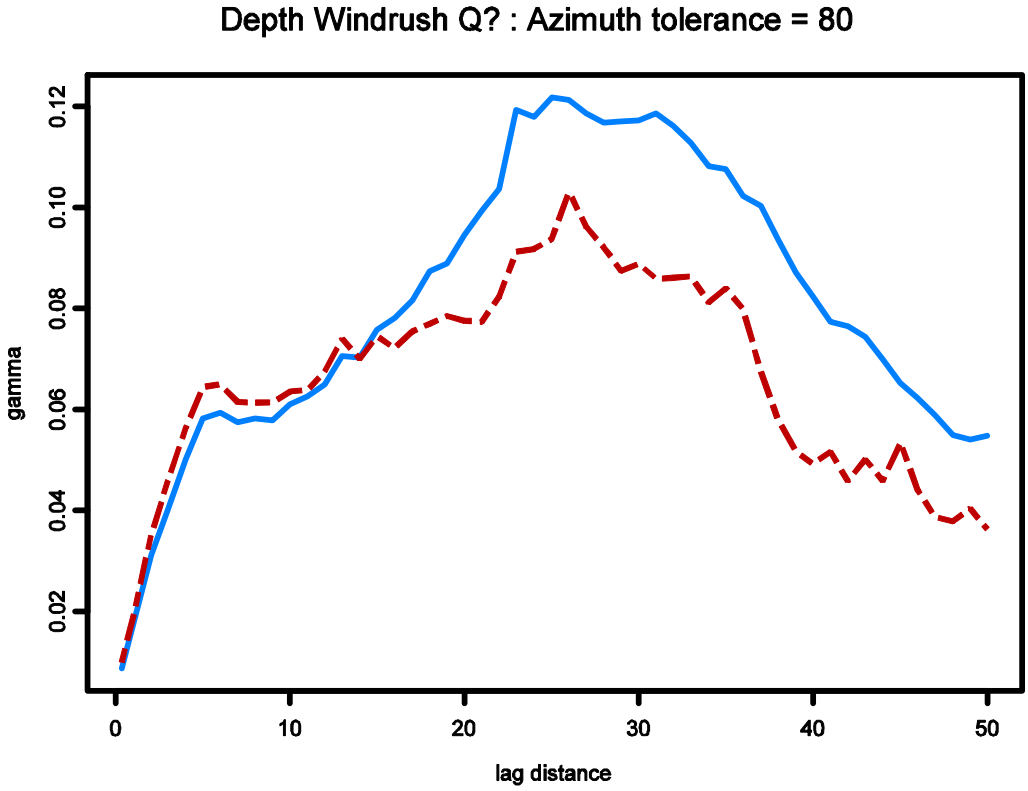
Depth Windrush Q? : Azimuth tolerance = 80
gamma
0.02
0.04
0.06
0.08
0.10
0.12
0
10
20
30
40
50
lag distance

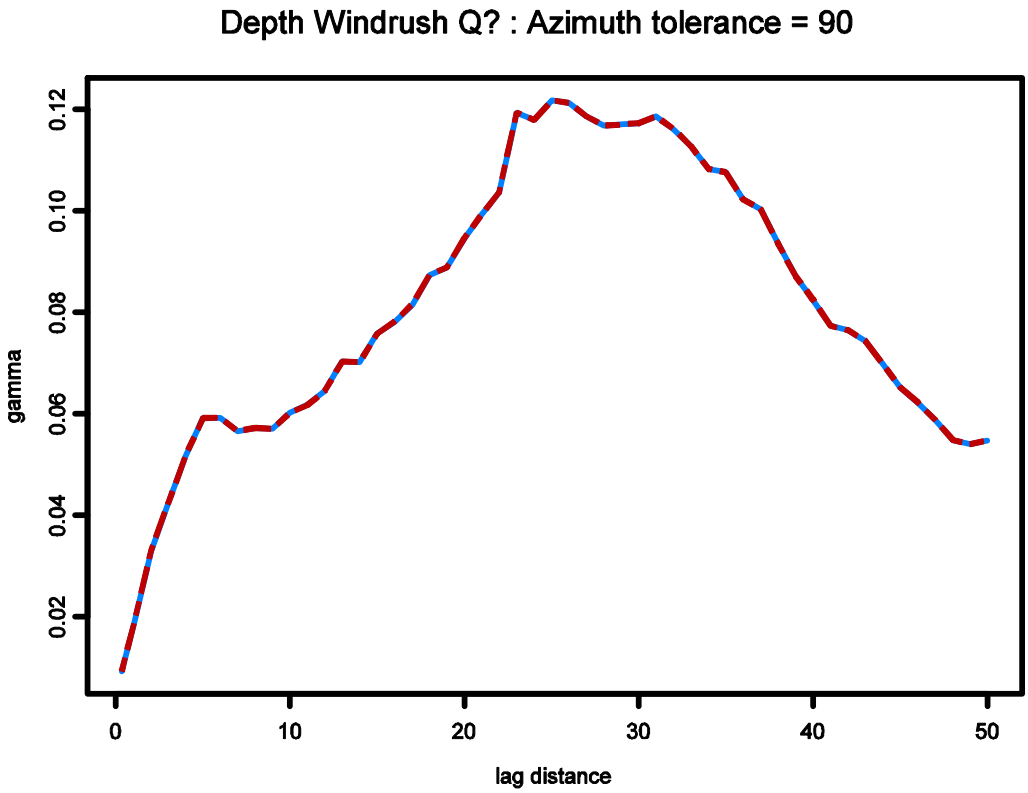
Depth Windrush Q? : Azimuth tolerance = 90
gamma
0.02
0.04
0.06
0.08
0.10
0.12
0
10
20
30
40
50
lag distance

Azimuth tolerance wet points

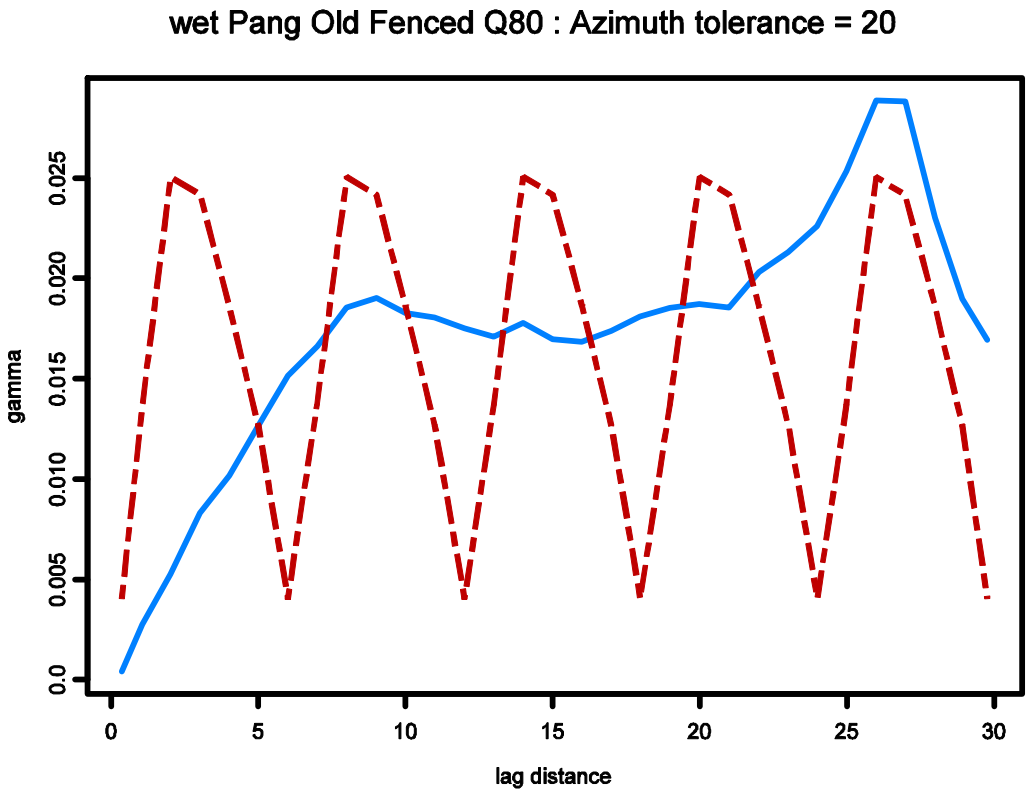

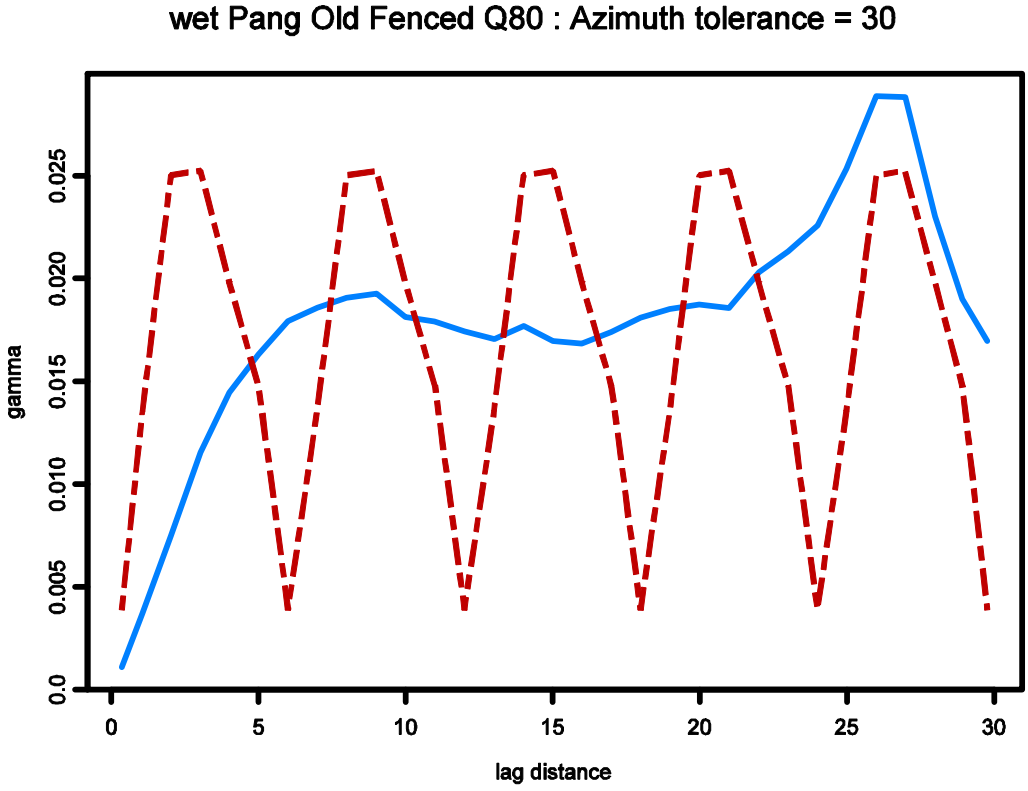

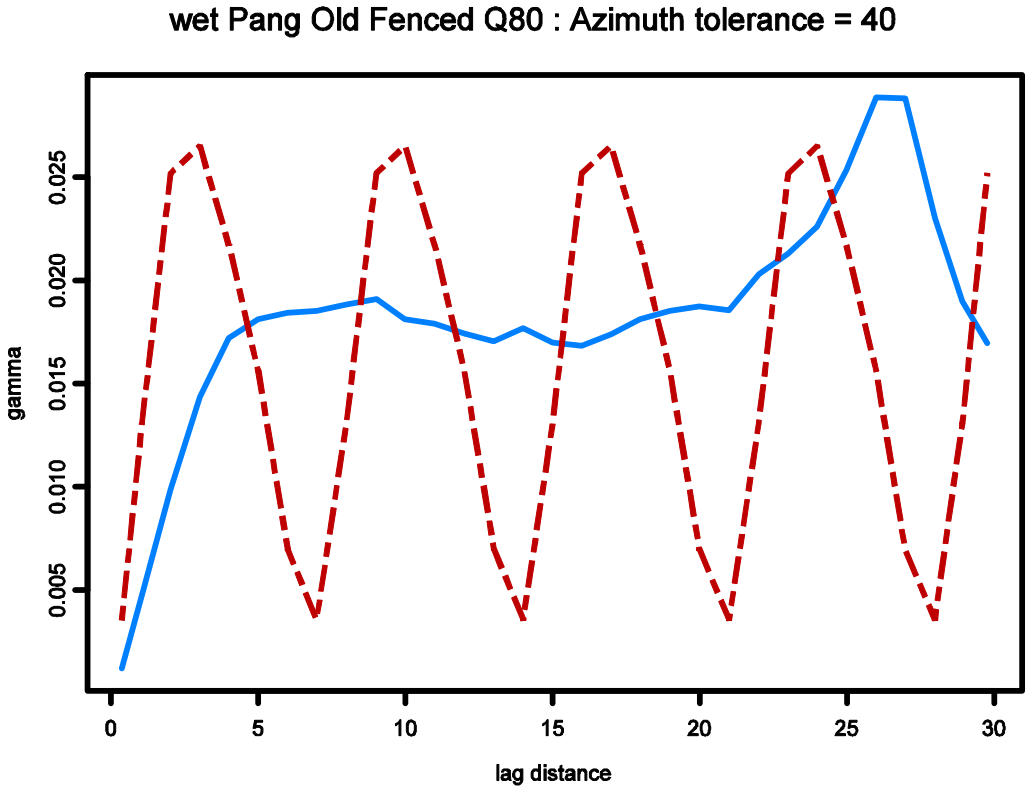
wet Pang Old Fenced Q80 : Azimuth tolerance = 40
gamma
0.005
0.010
0.015
0.020
0.025
0
5
10
15
20
25
30
lag distance

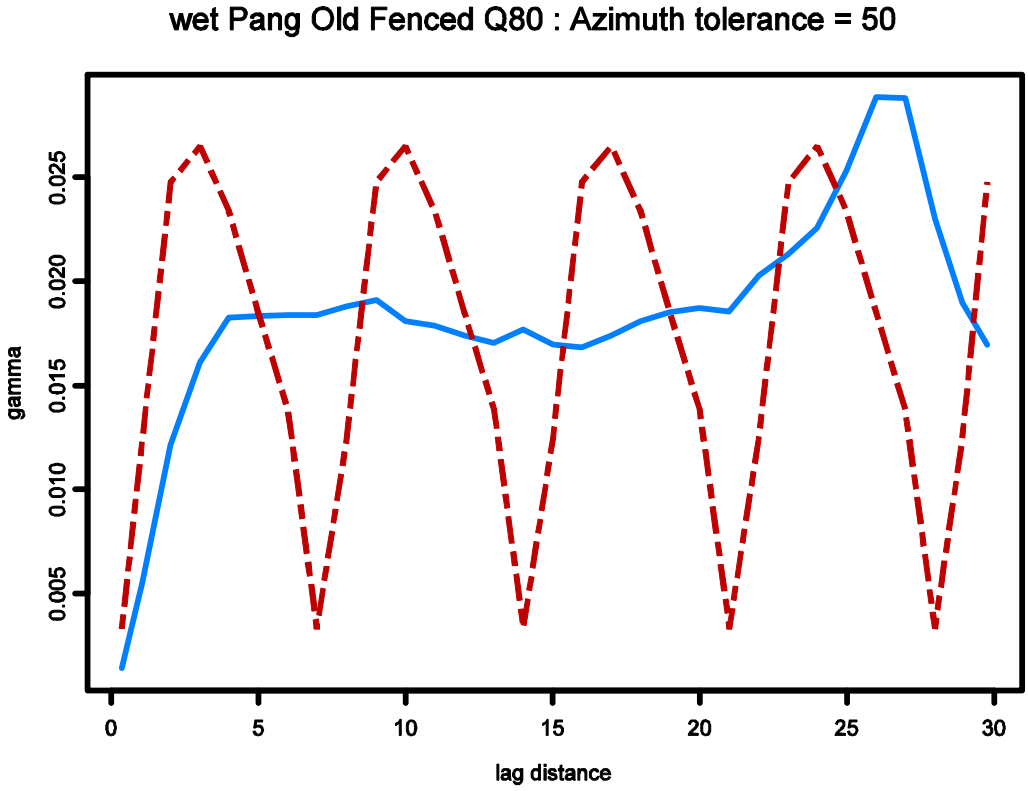
wet Pang Old Fenced Q80 : Azimuth tolerance = 50
gamma
0.005
0.010
0.015
0.020
0.025
0
5
10
15
20
25
30
lag distance

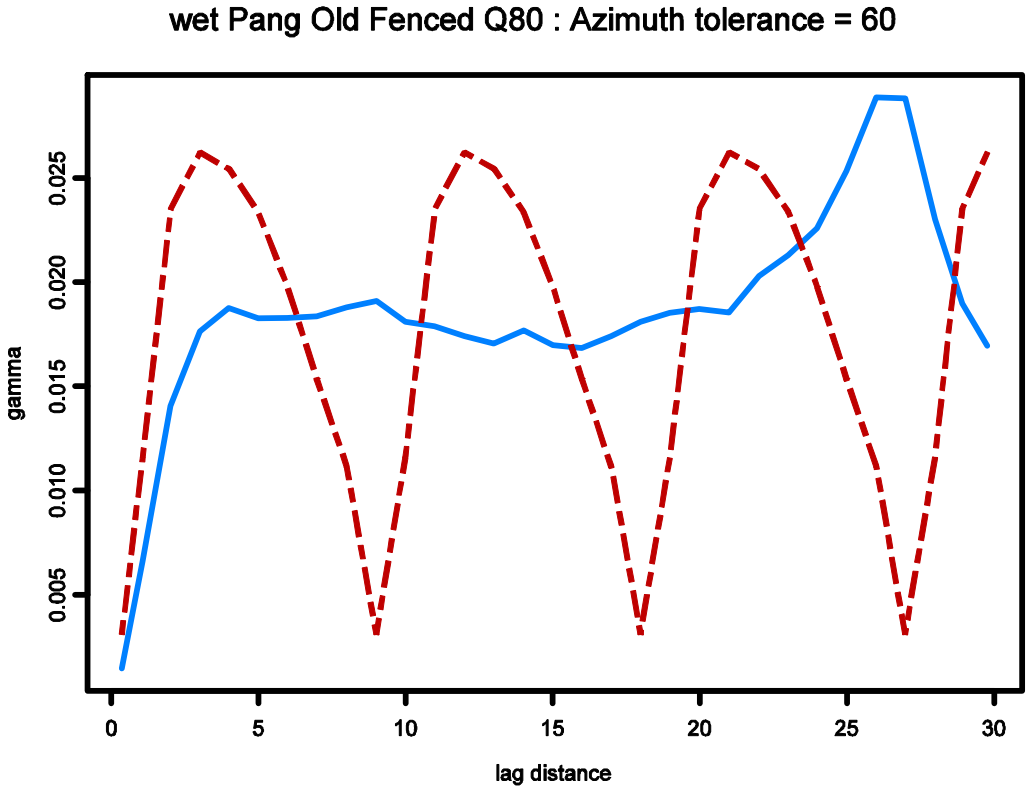
wet Pang Old Fenced Q80 : Azimuth tolerance = 60
gamma
0.005
0.010
0.015
0.020
0.025
0
5
10
15
20
25
30
lag distance

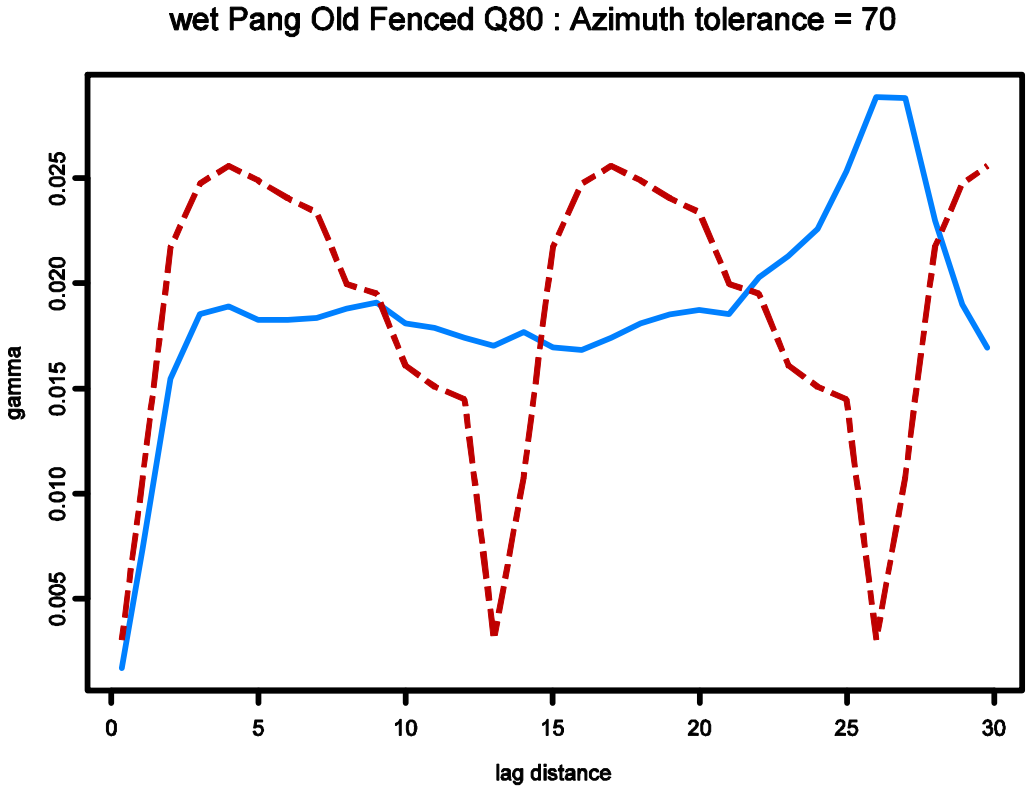
wet Pang Old Fenced Q80 : Azimuth tolerance = 70
gamma
0.005
0.010
0.015
0.020
0.025
0
5
10
15
20
25
30
lag distance

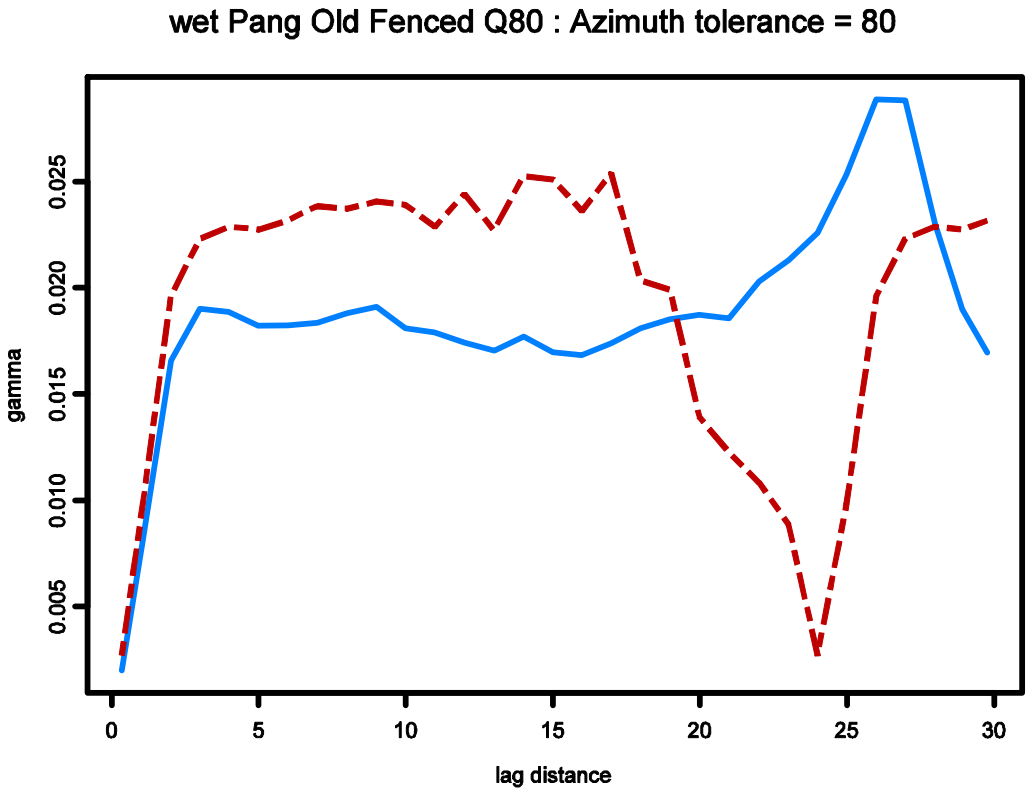
wet Pang Old Fenced Q80 : Azimuth tolerance = 80
gamma
0.005
0.010
0.015
0.020
0.025
0
5
10
15
20
25
30
lag distance

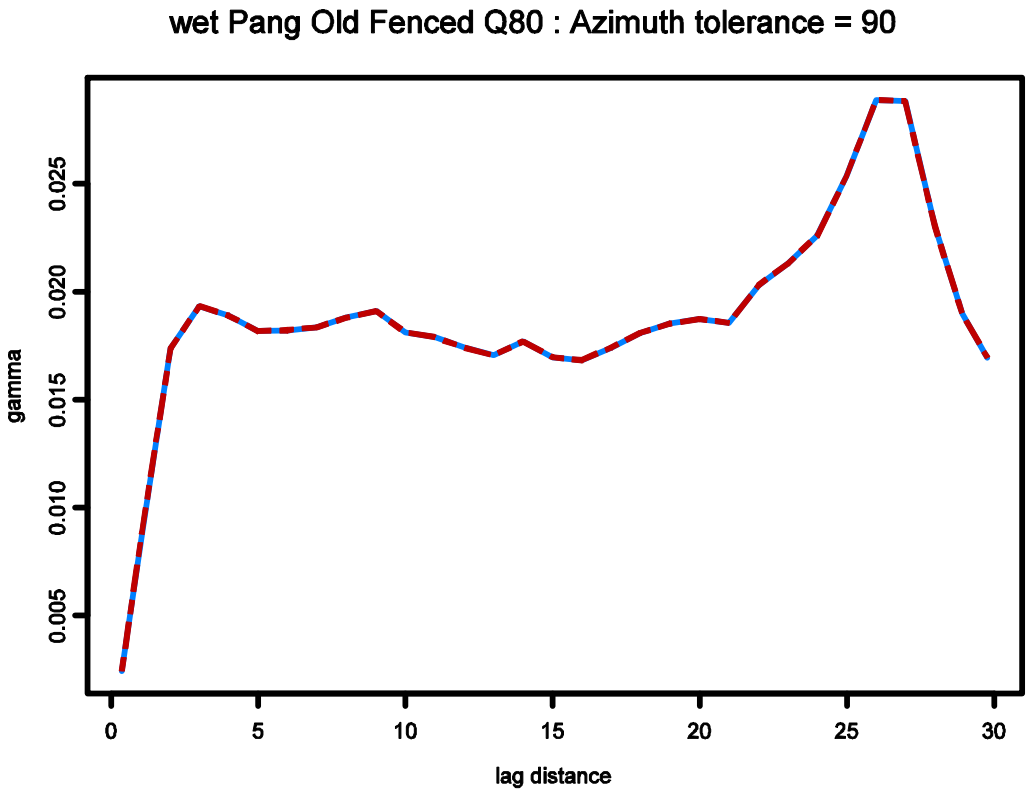
wet Pang Old Fenced Q80 : Azimuth tolerance = 90
gamma
0.005
0.010
0.015
0.020
0.025
0
5
10
15
20
25
30
lag distance

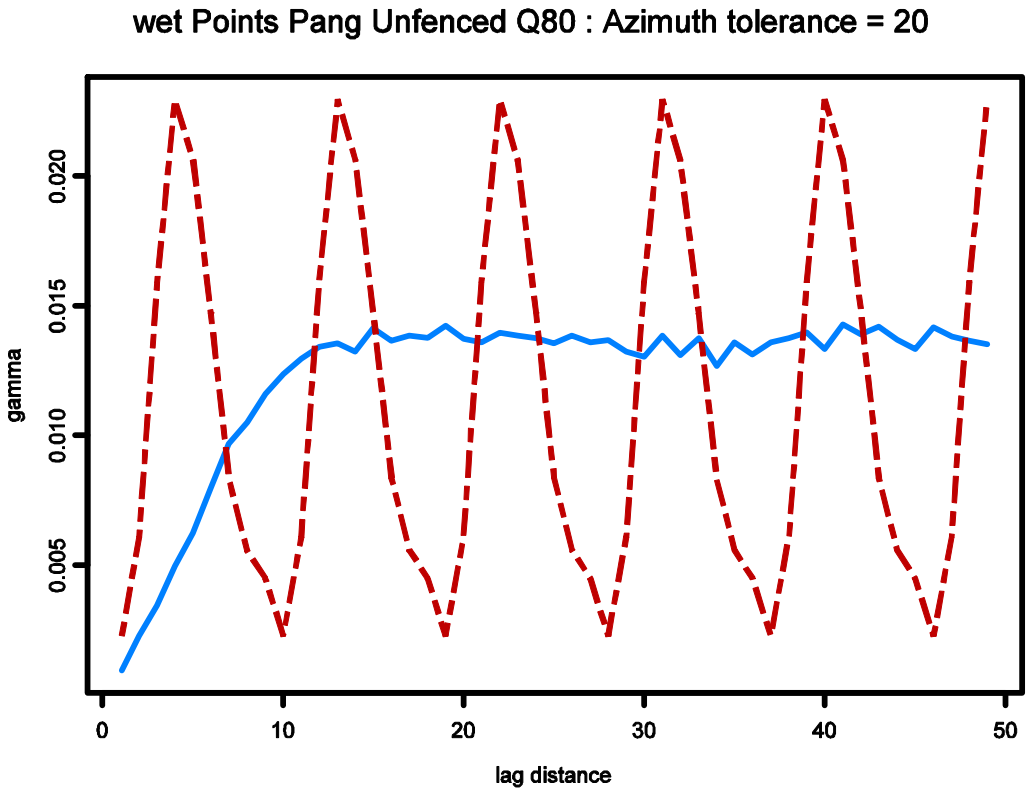
wet Points Pang Unfenced Q80 : Azimuth tolerance = 20
gamma
0.005
0.010
0.015
0.020
0
10
20
30
40
50
lag distance

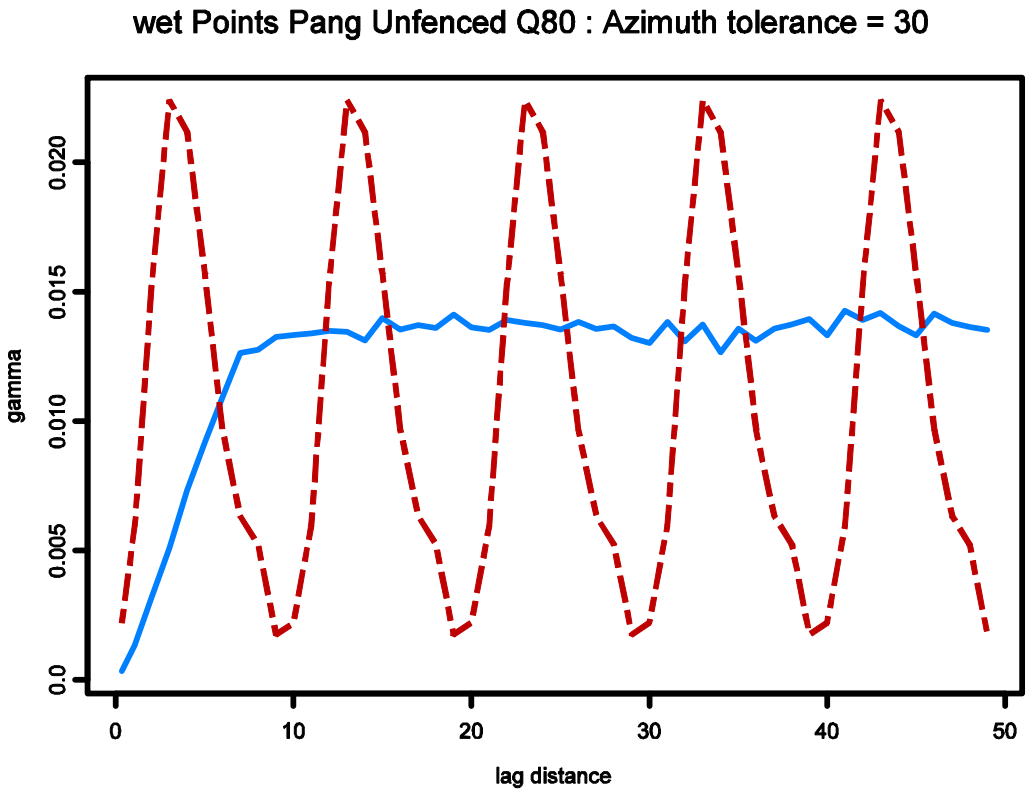
wet Points Pang Unfenced Q80 : Azimuth tolerance = 30
gamma
0.0
0.005
0.010
0.015
0.020
0
10
20
30
40
50
lag distance

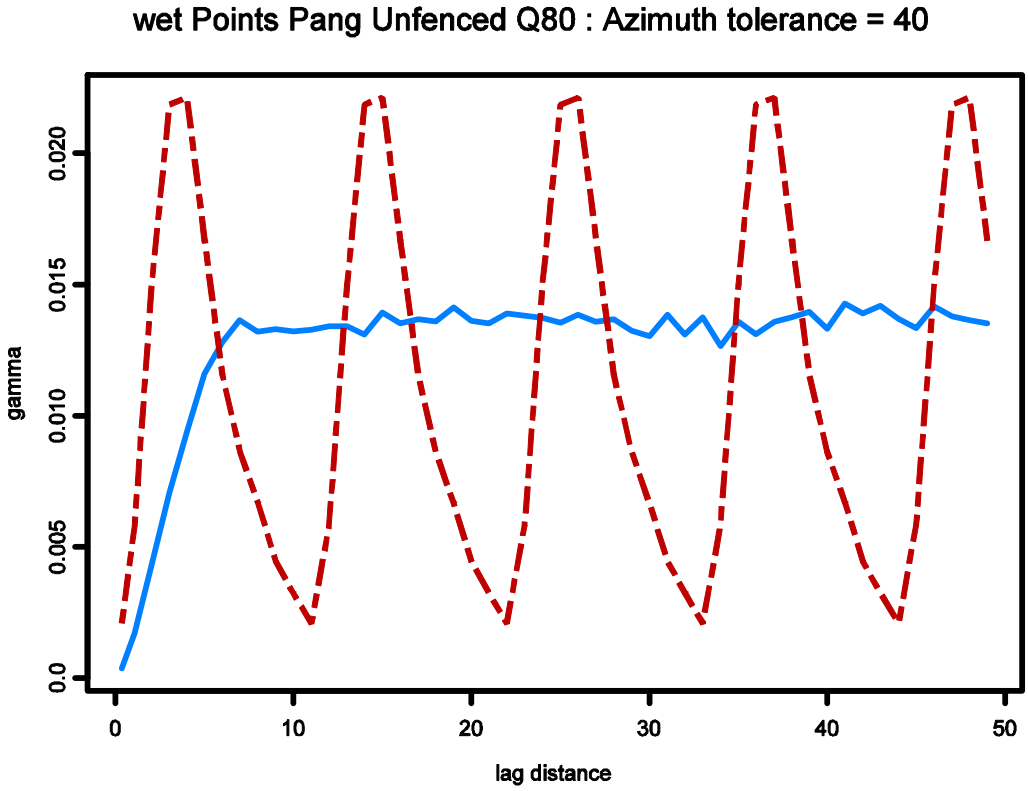
wet Points Pang Unfenced Q80 : Azimuth tolerance = 40
gamma
0.0
0.005
0.010
0.015
0.020
0
10
20
30
40
50
lag distance

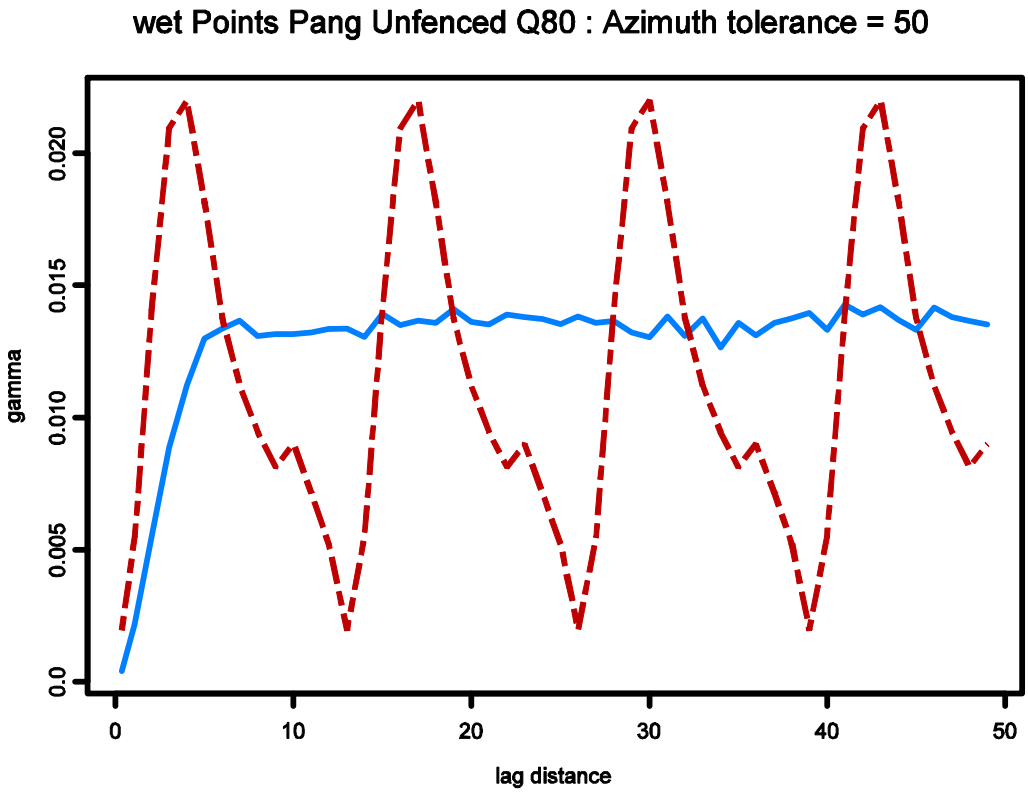
wet Points Pang Unfenced Q80 : Azimuth tolerance = 50
gamma
0.0
0.005
0.010
0.015
0.020
0
10
20
30
40
50
lag distance

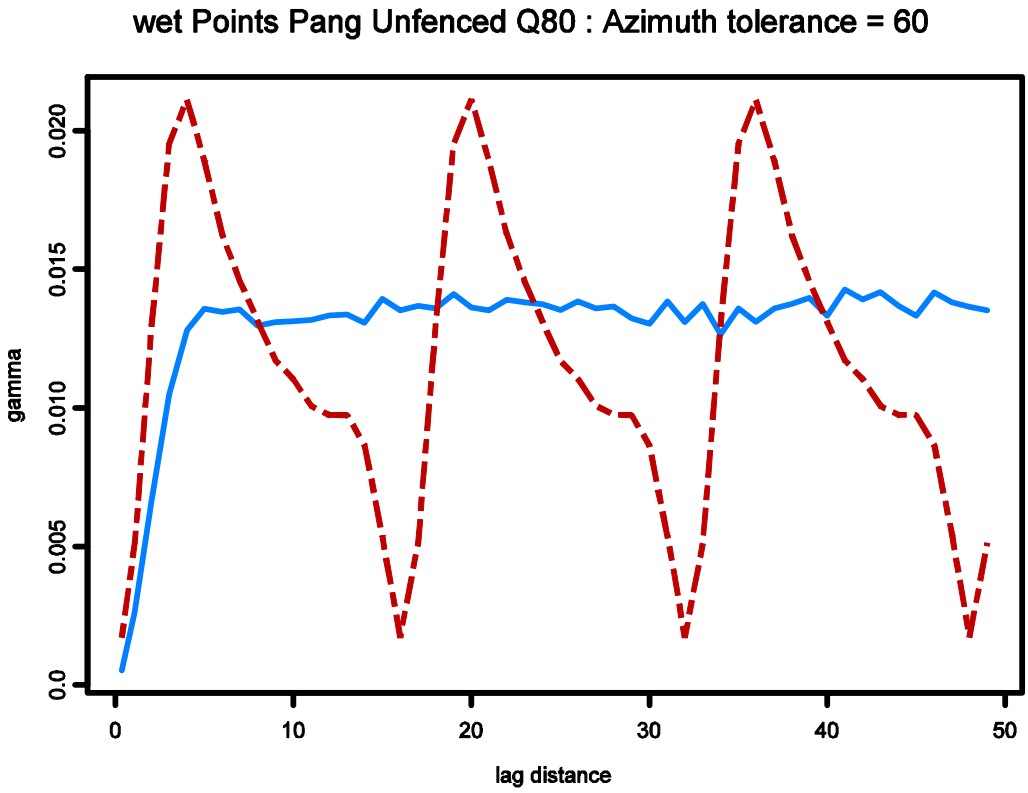
wet Points Pang Unfenced Q80 : Azimuth tolerance = 60
gamma
0.0
0.005
0.010
0.015
0.020
0
10
20
30
40
50
lag distance

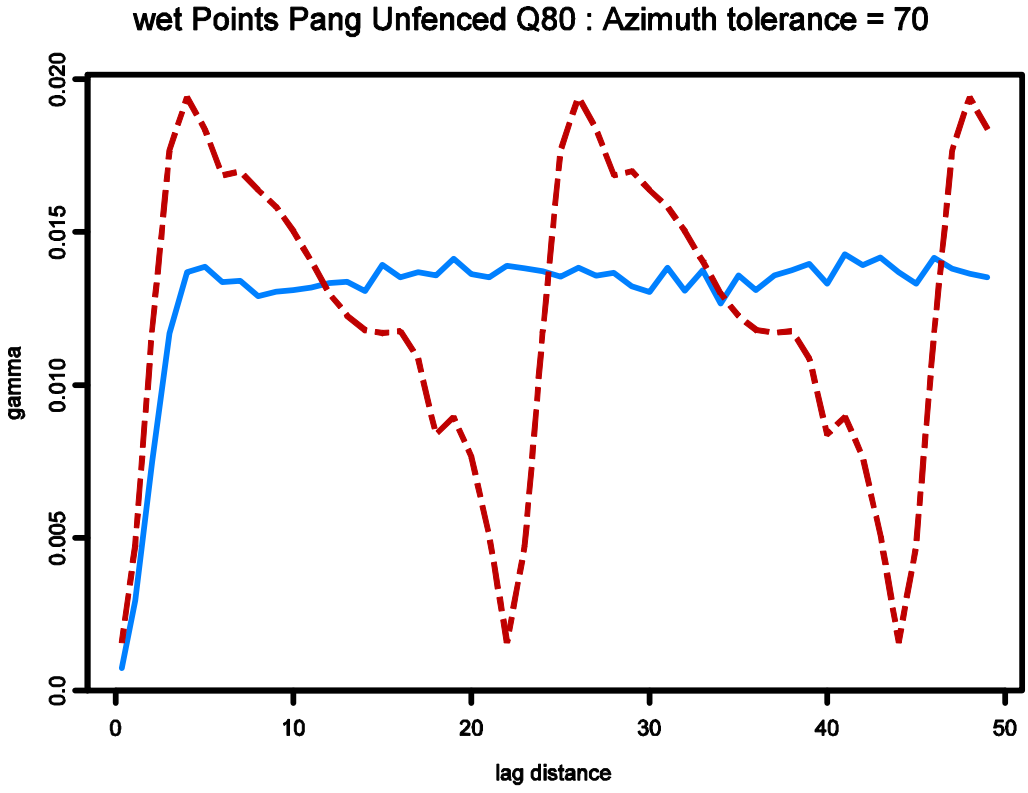
wet Points Pang Unfenced Q80 : Azimuth tolerance = 70
gamma
0.0
0.005
0.010
0.015
0.020
0
10
20
30
40
50
lag distance

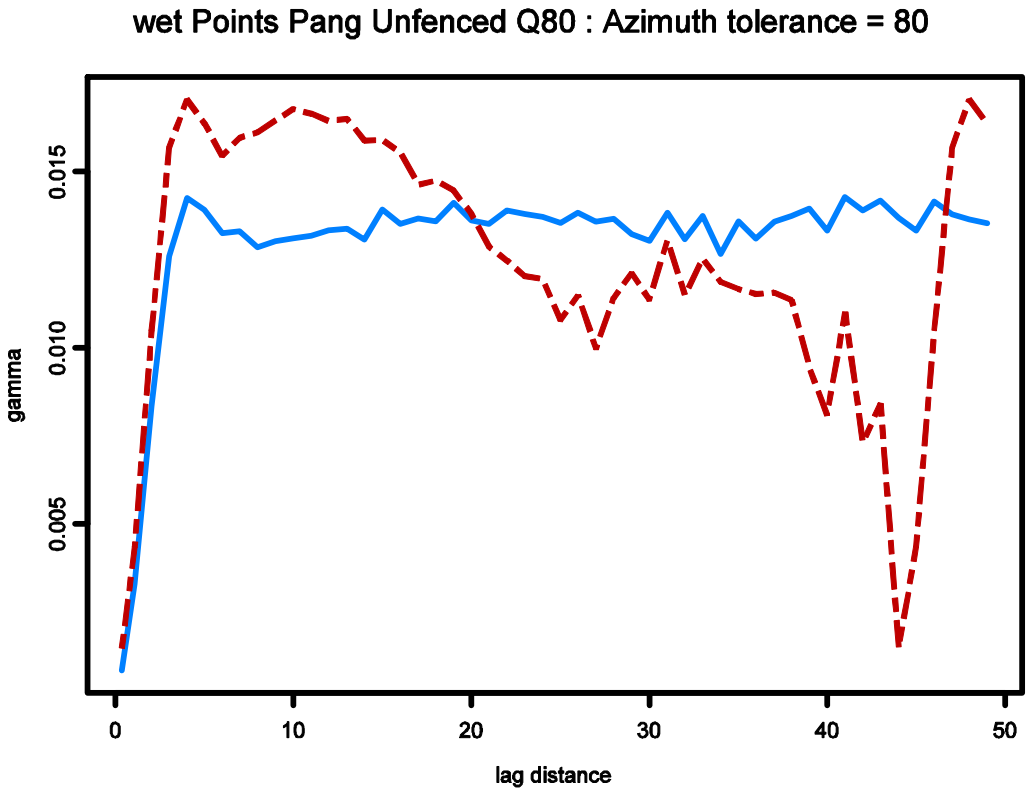
wet Points Pang Unfenced Q80 : Azimuth tolerance = 80
gamma
0.005
0.010
0.015
0
10
20
30
40
50
lag distance

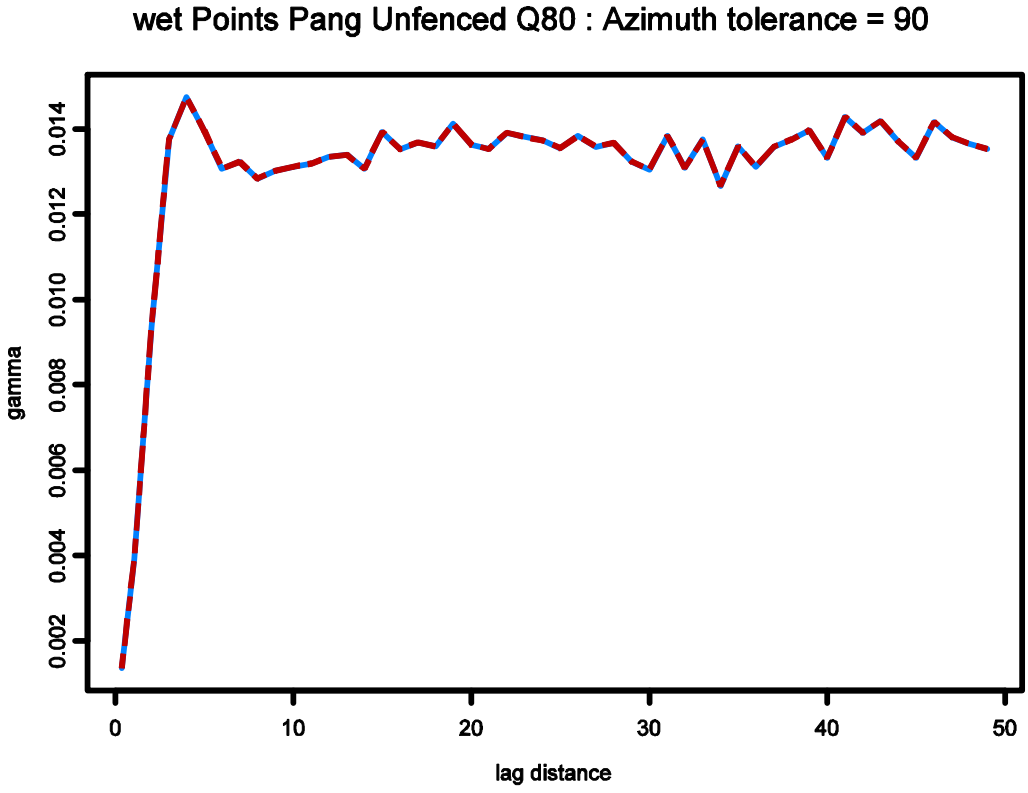
wet Points Pang Unfenced Q80 : Azimuth tolerance = 90
gamma
0.002
0.004
0.006
0.008
0.010
0.012
0.014
0
10
20
30
40
50
lag distance

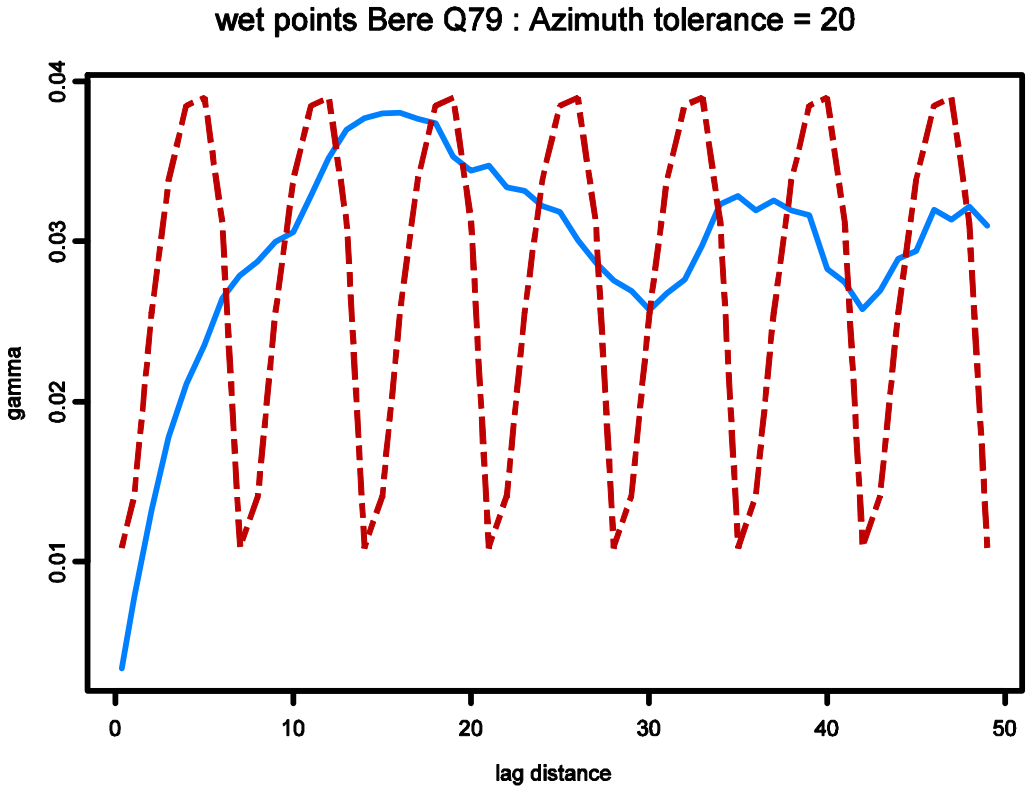
wet points Bere Q79 : Azimuth tolerance = 20
gamma
0.01
0.02
0.03
0.04
0
10
20
30
40
50
lag distance

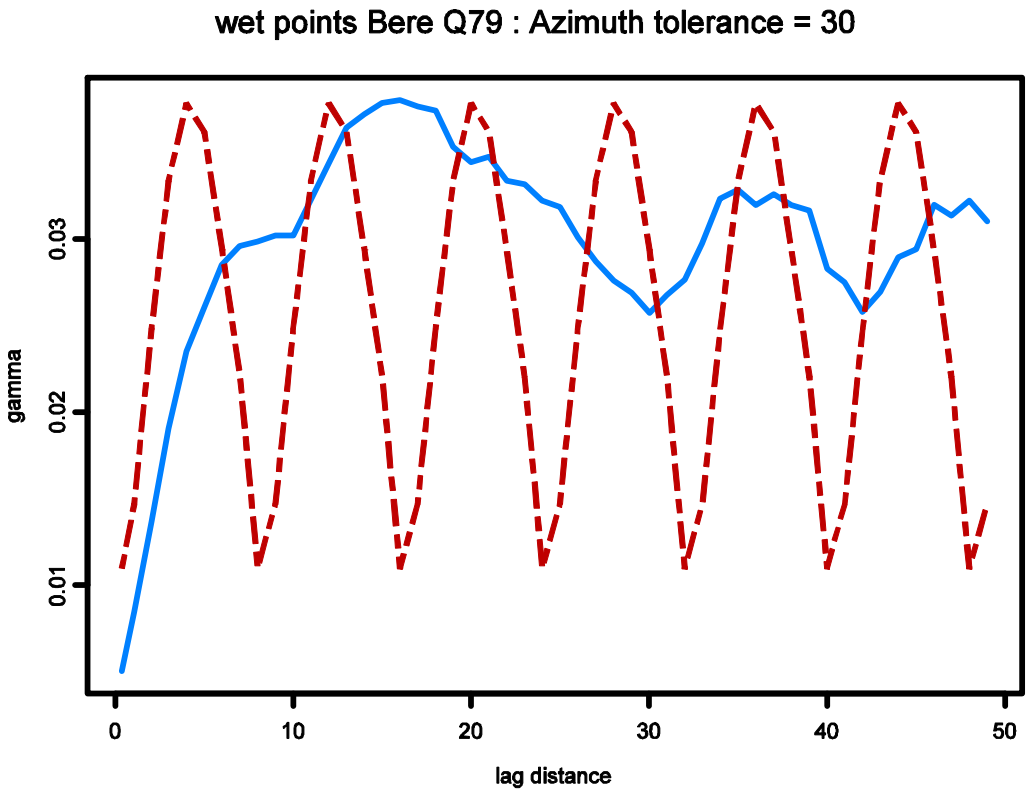
wet points Bere Q79 : Azimuth tolerance = 30
gamma
0.01
0.02
0.03
0
10
20
30
40
50
lag distance

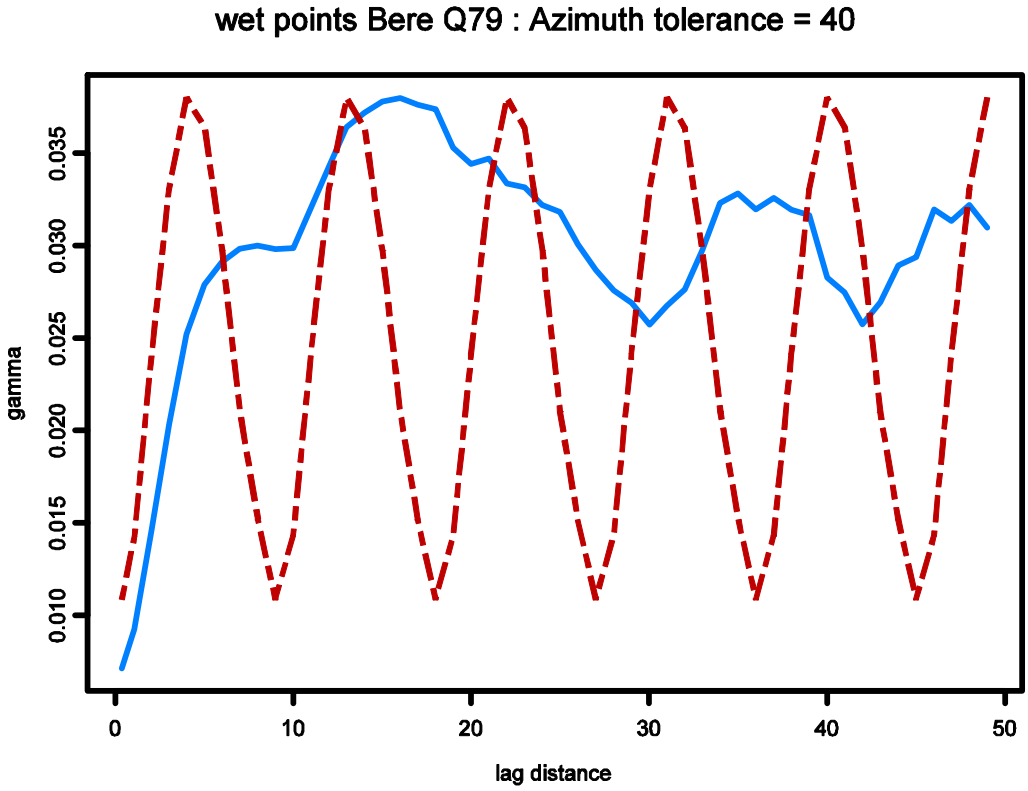
wet points Bere Q79 : Azimuth tolerance = 40
gamma
0.010
0.015
0.020
0.025
0.030
0.035
0
10
20
30
40
50
lag distance

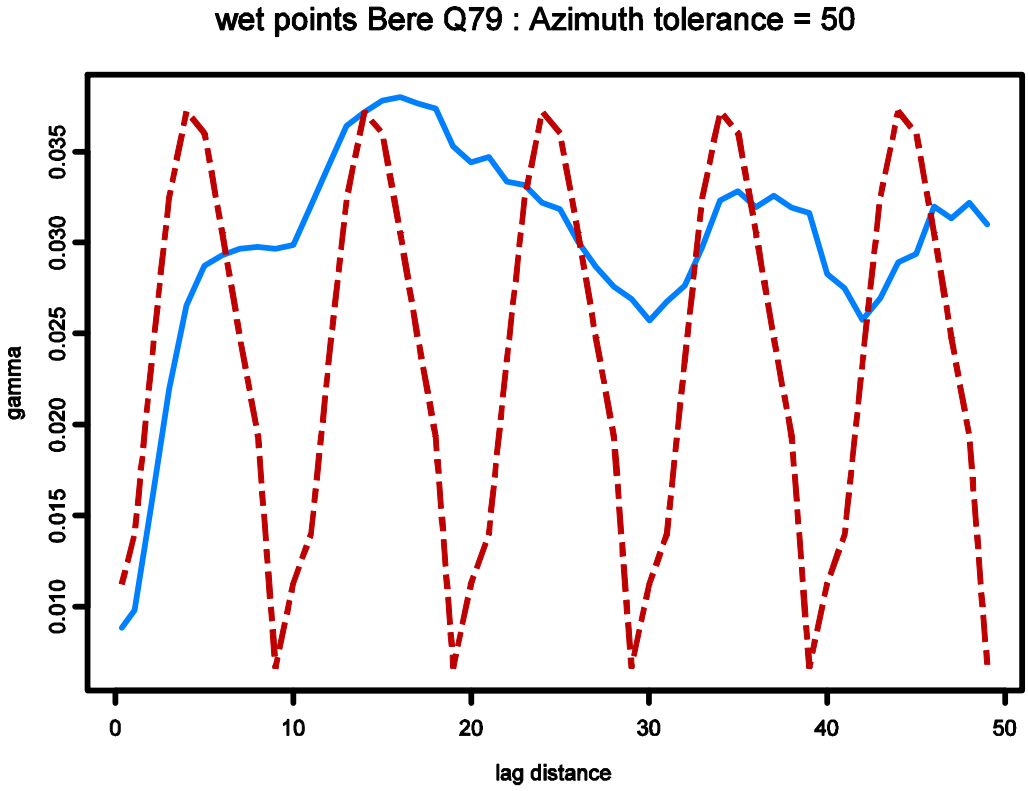
wet points Bere Q79 : Azimuth tolerance = 50
gamma
0.010
0.015
0.020
0.025
0.030
0.035
0
10
20
30
40
50
lag distance

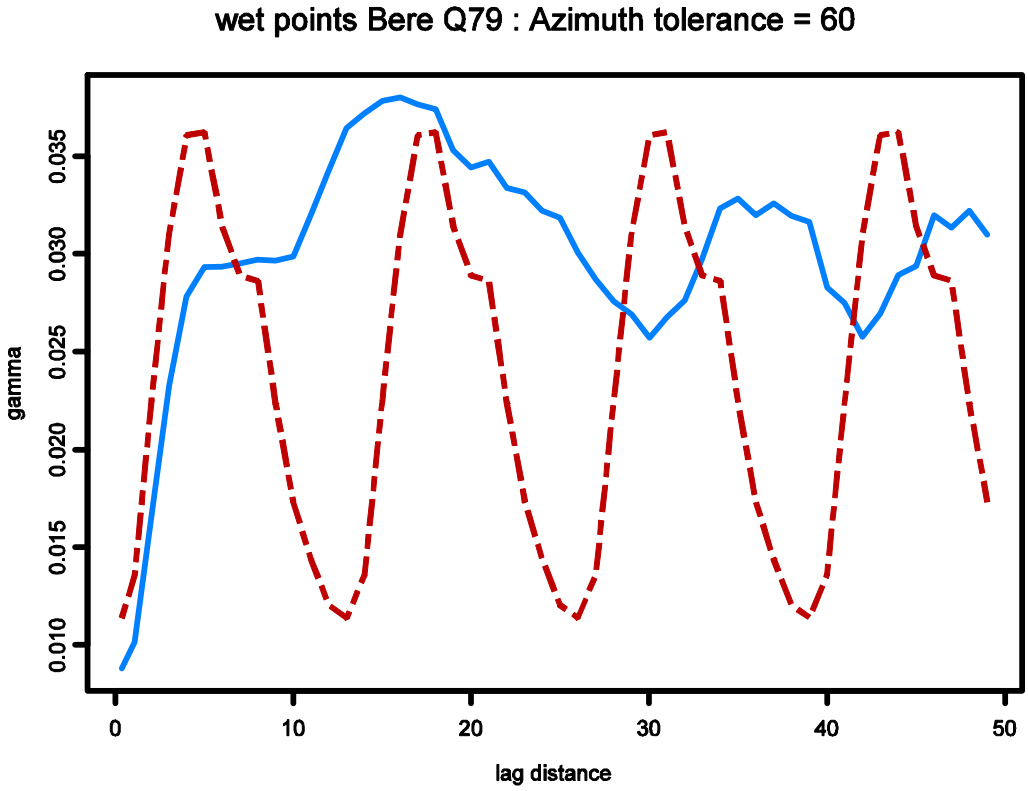
wet points Bere Q79 : Azimuth tolerance = 60
gamma
0.010
0.015
0.020
0.025
0.030
0.035
0
10
20
30
40
50
lag distance

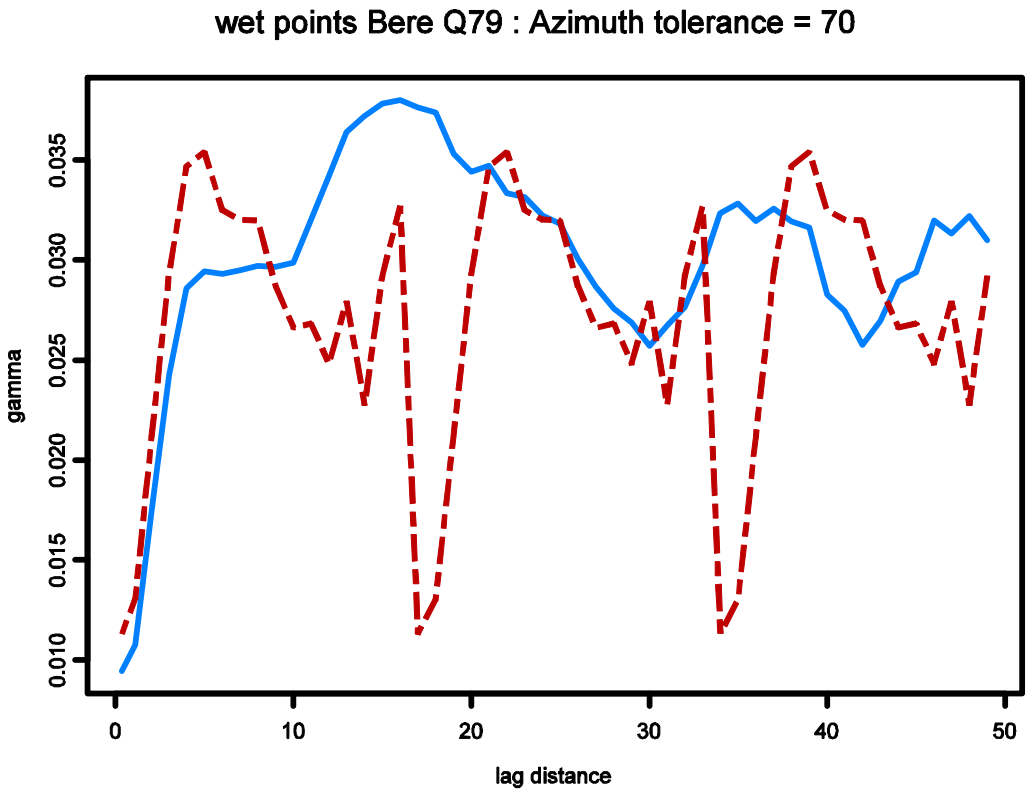
wet points Bere Q79 : Azimuth tolerance = 70
gamma
0.010
0.015
0.020
0.025
0.030
0.035
0
10
20
30
40
50
lag distance

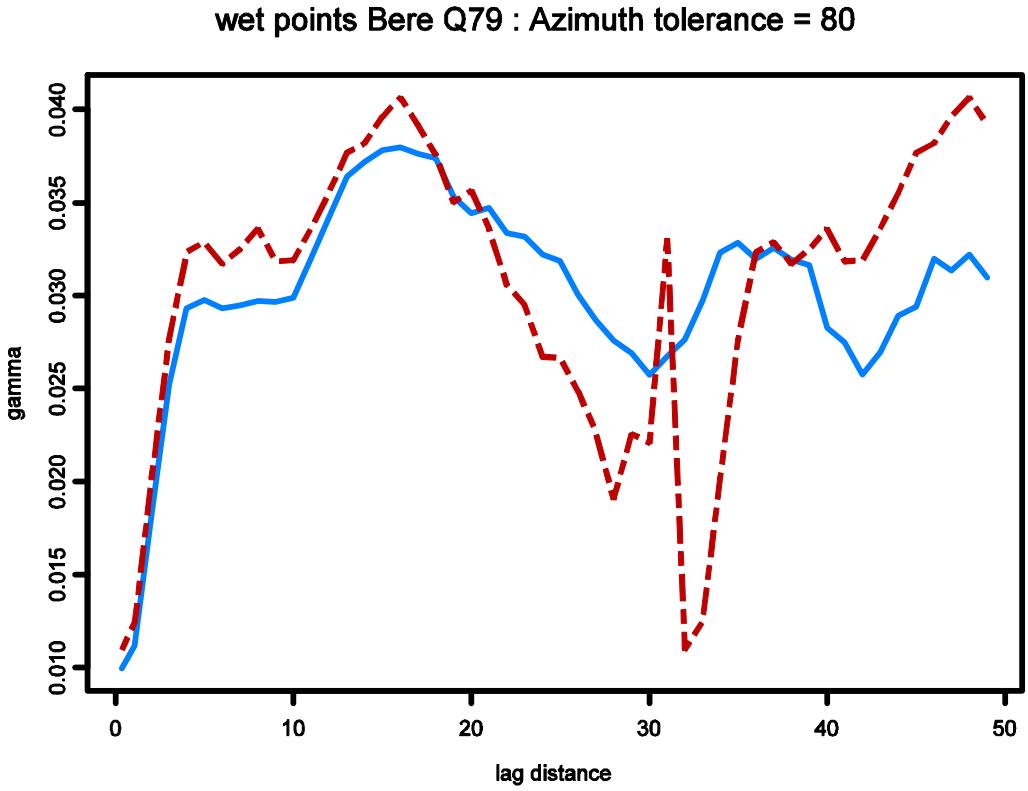
wet points Bere Q79 : Azimuth tolerance = 80
gamma
0.010
0.015
0.020
0.025
0.030
0.035
0.040
0
10
20
30
40
50
lag distance

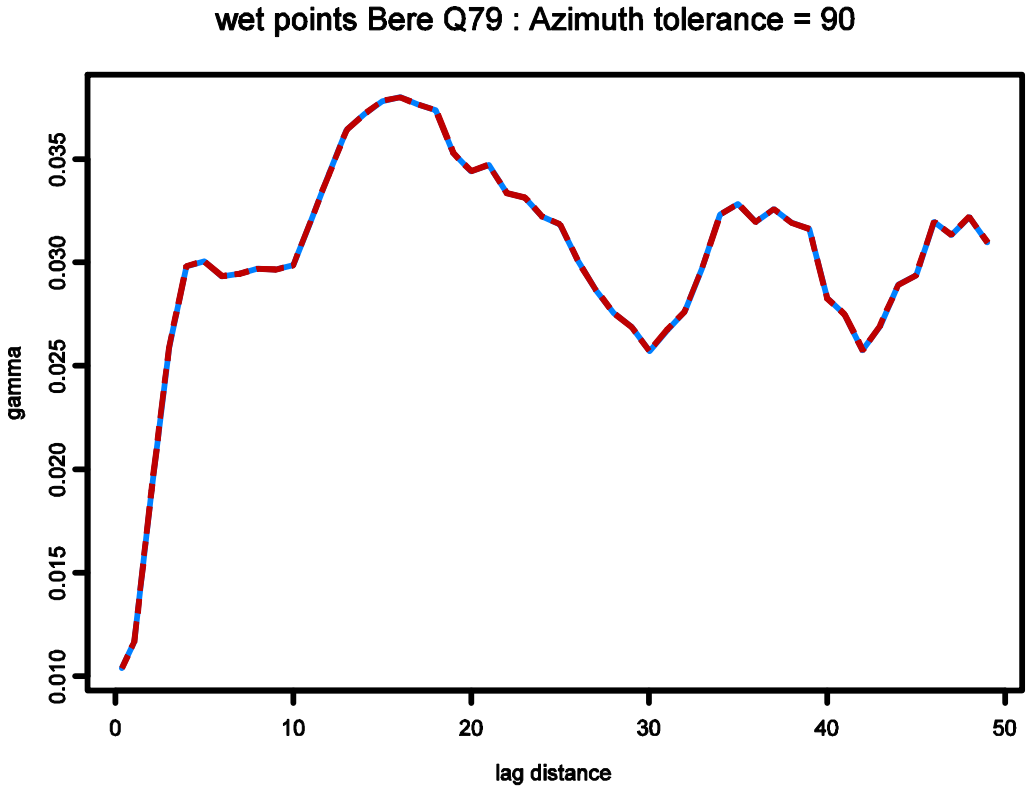
wet points Bere Q79 : Azimuth tolerance = 90
gamma
0.010
0.015
0.020
0.025
0.030
0.035
0
10
20
30
40
50
lag distance

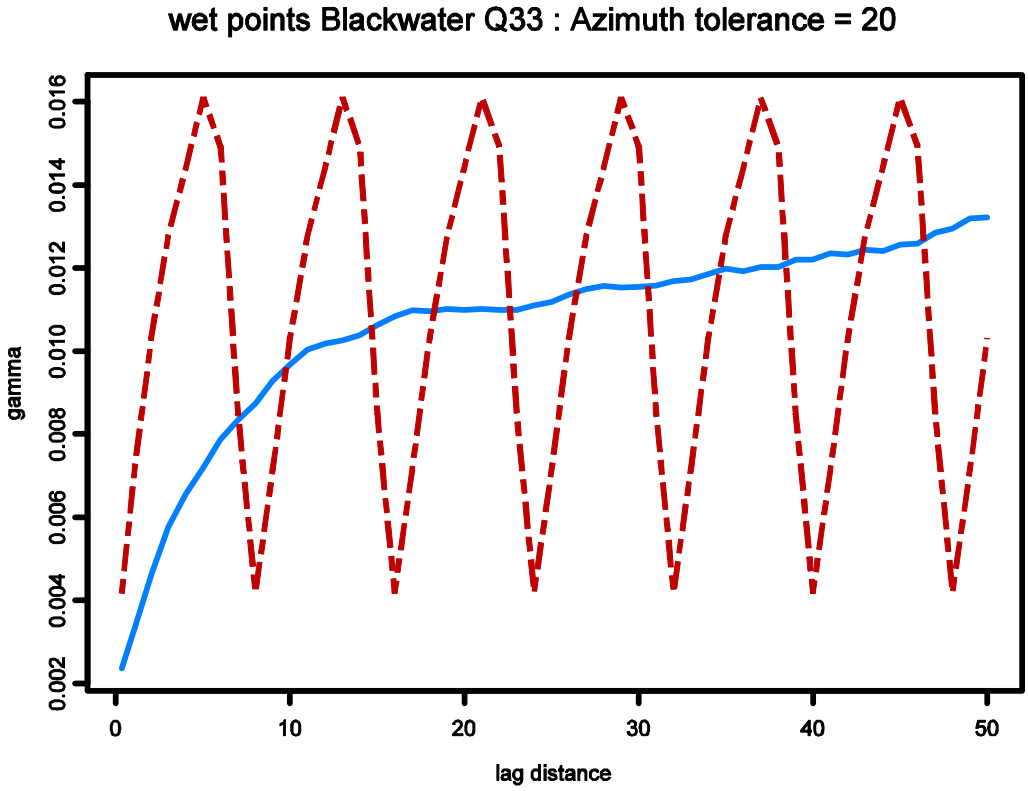
wet points Blackwater Q33 : Azimuth tolerance = 20
gamma
0.002
0.004
0.006
0.008
0.010
0.012
0.014
0.016
0
10
20
30
40
50
lag distance

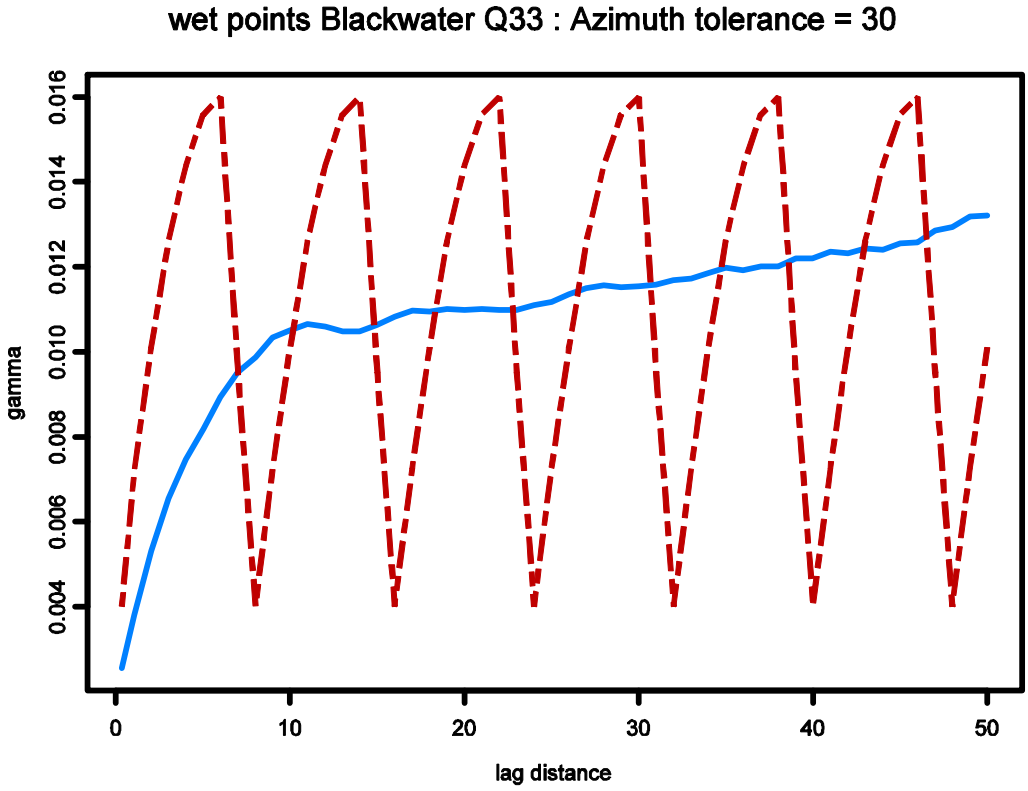
wet points Blackwater Q33 : Azimuth tolerance = 30
gamma
0.004
0.006
0.008
0.010
0.012
0.014
0.016
0
10
20
30
40
50
lag distance

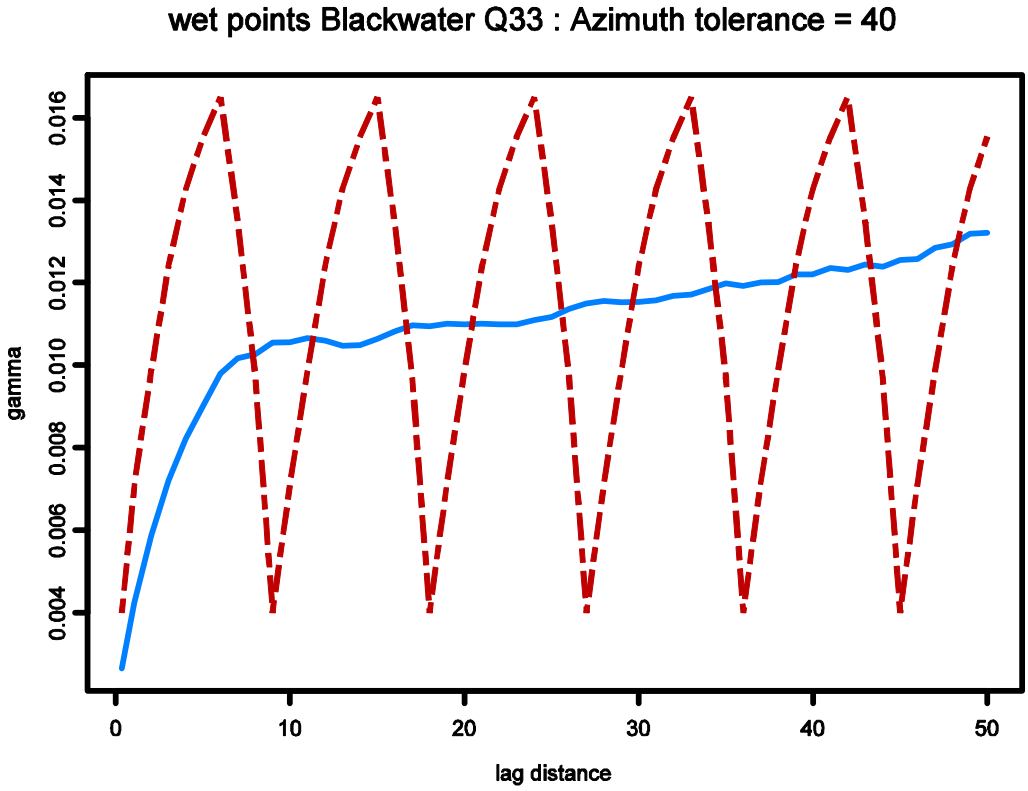
wet points Blackwater Q33 : Azimuth tolerance = 40
gamma
0.004
0.006
0.008
0.010
0.012
0.014
0.016
0
10
20
30
40
50
lag distance

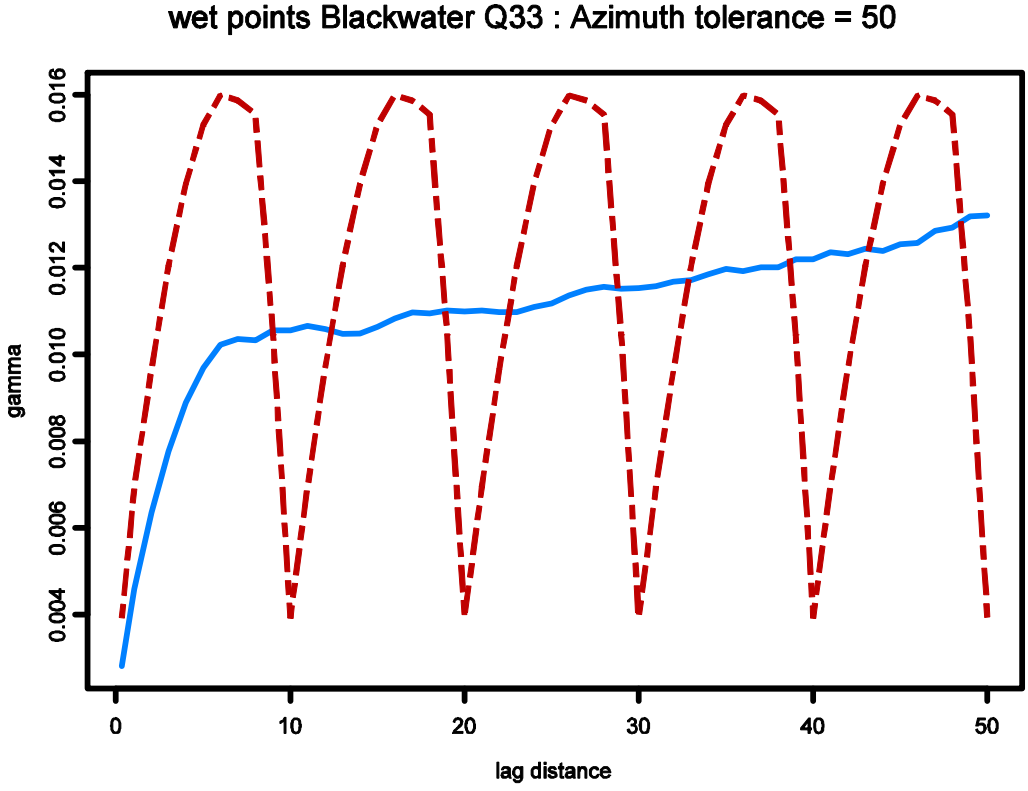
wet points Blackwater Q33 : Azimuth tolerance = 50
gamma
0.004
0.006
0.008
0.010
0.012
0.014
0.016
0
10
20
30
40
50
lag distance

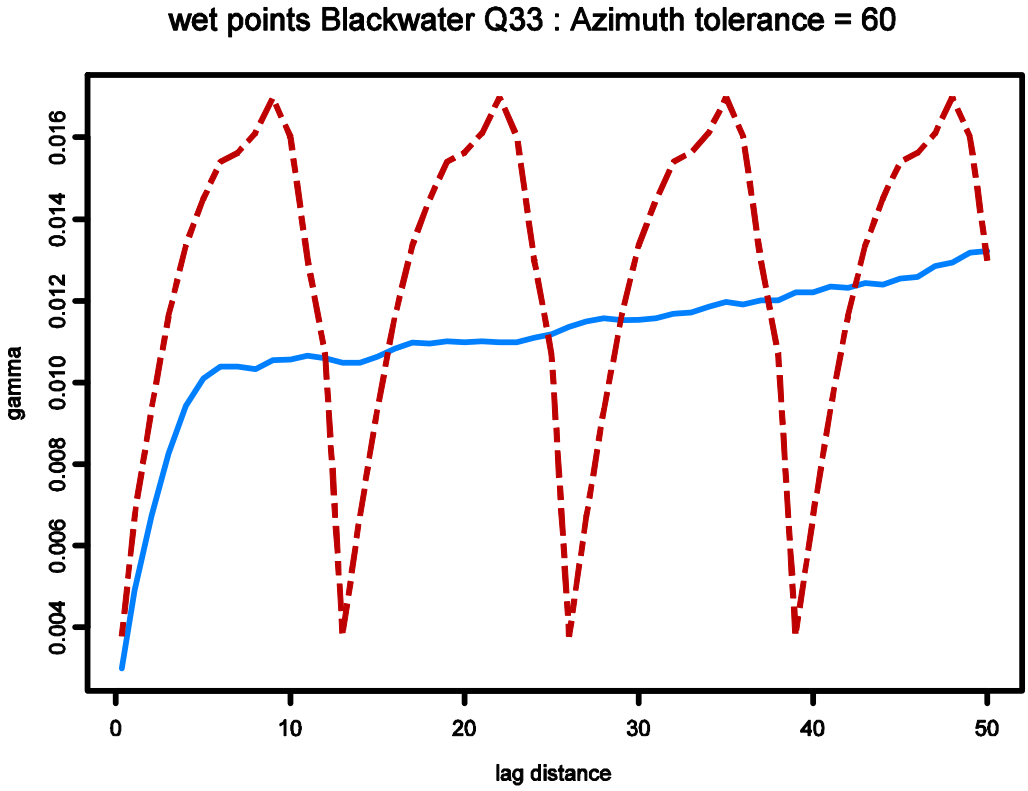
wet points Blackwater Q33 : Azimuth tolerance = 60
gamma
0.004
0.006
0.008
0.010
0.012
0.014
0.016
0
10
20
30
40
50
lag distance

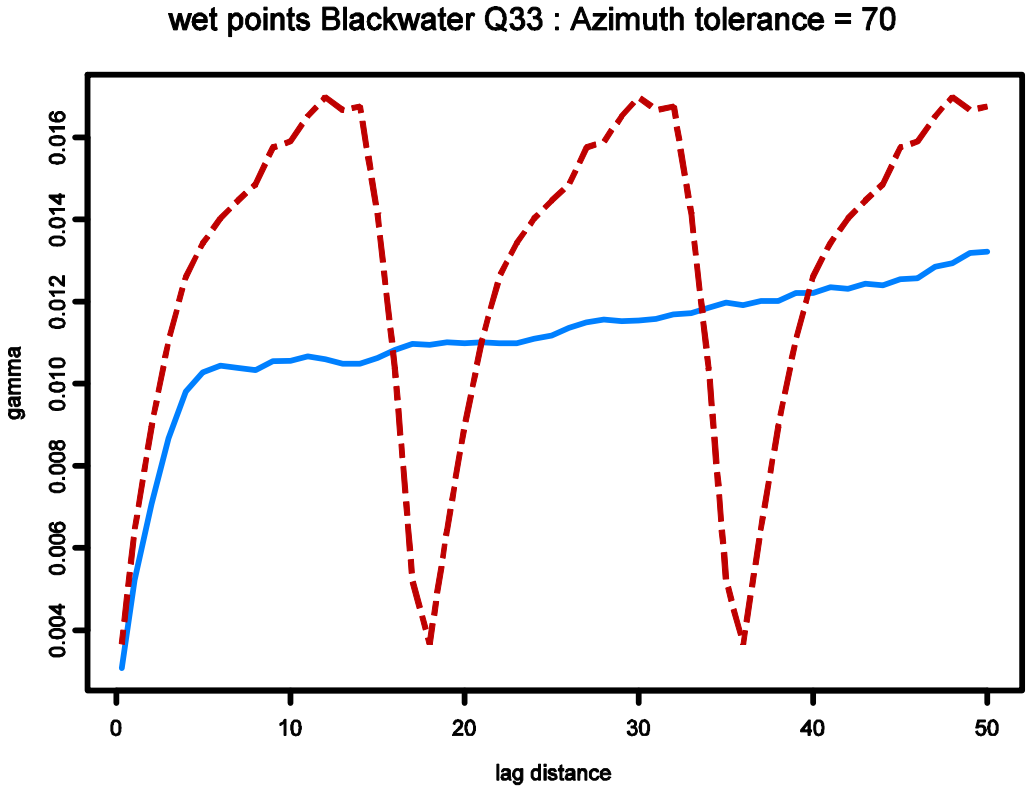
wet points Blackwater Q33 : Azimuth tolerance = 70
gamma
0.004
0.006
0.008
0.010
0.012
0.014
0.016
0
10
20
30
40
50
lag distance

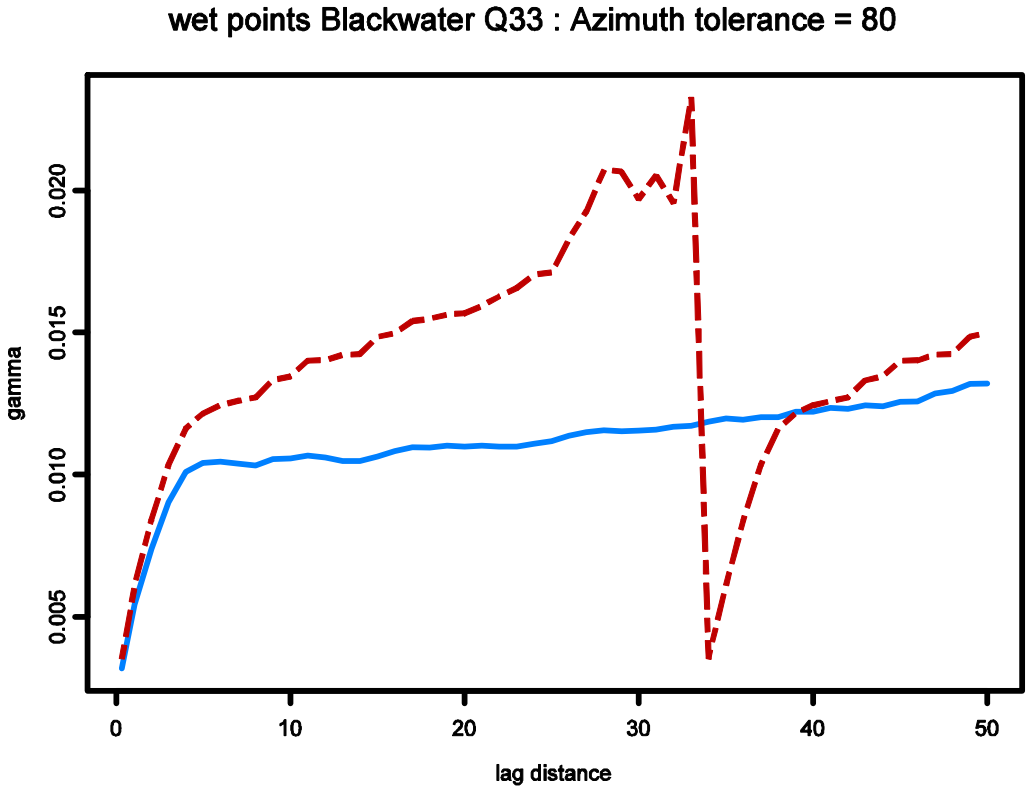
wet points Blackwater Q33 : Azimuth tolerance = 80
gamma
0.005
0.010
0.015
0.020
0
10
20
30
40
50
lag distance

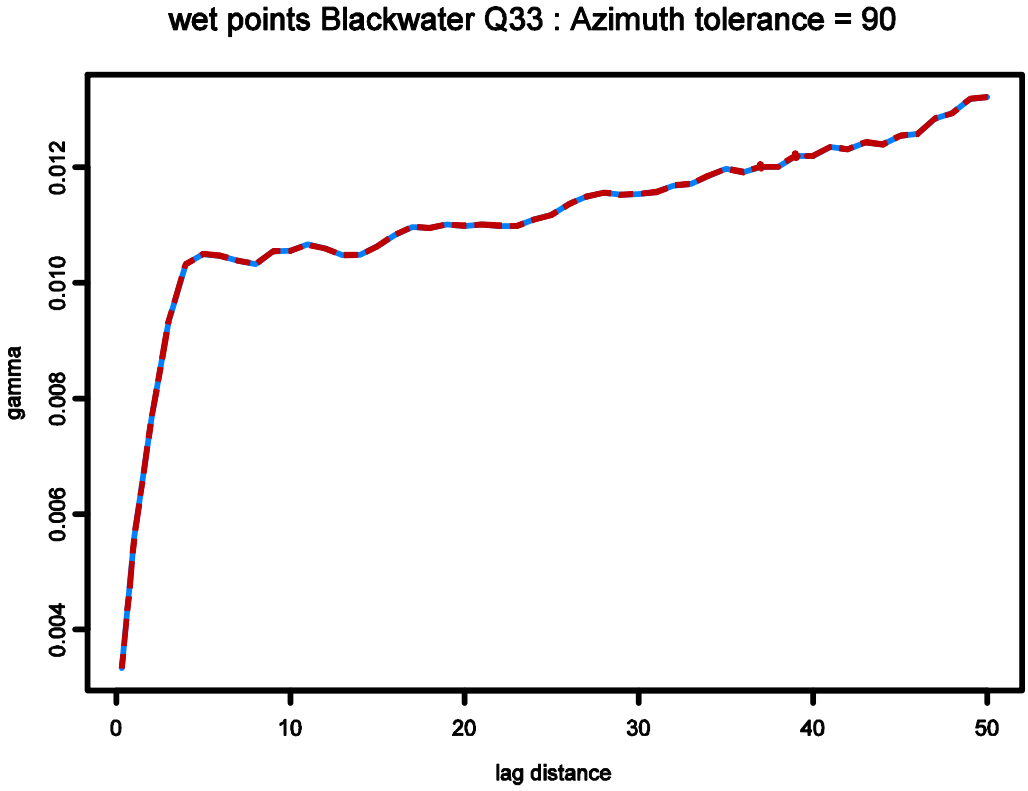
wet points Blackwater Q33 : Azimuth tolerance = 90
gamma
0.004
0.006
0.008
0.010
0.012
0
10
20
30
40
50
lag distance

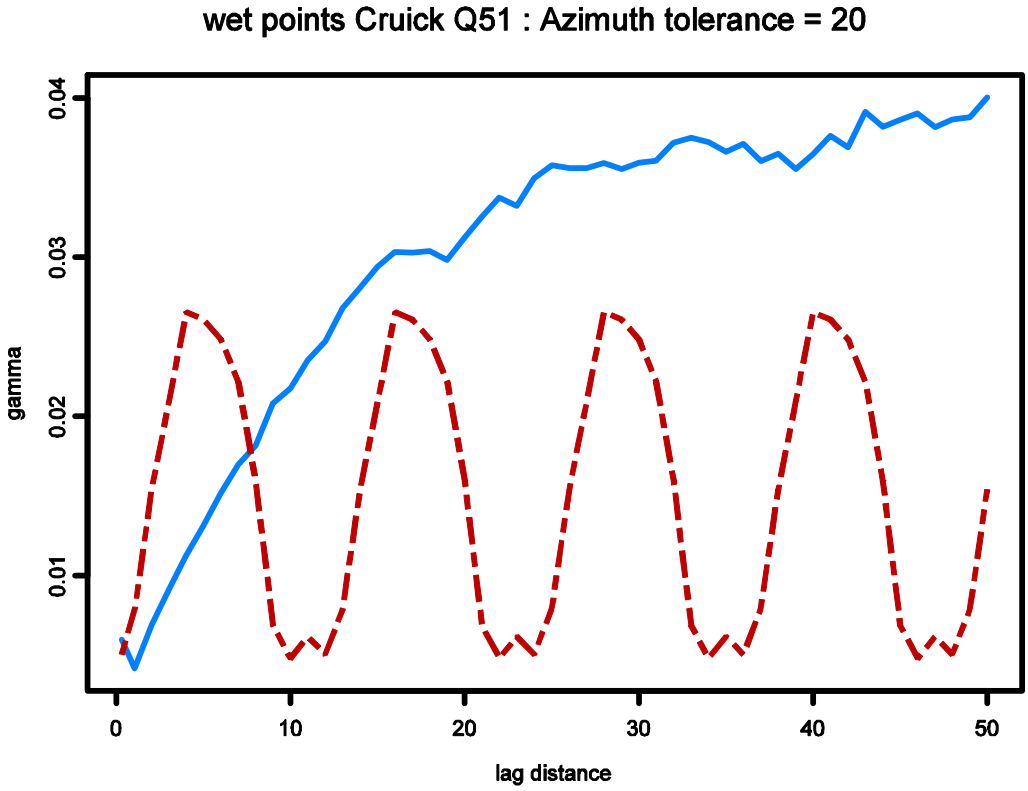
wet points Cruick Q51 : Azimuth tolerance = 20
gamma
0.01
0.02
0.03
0.04
0
10
20
30
40
50
lag distance

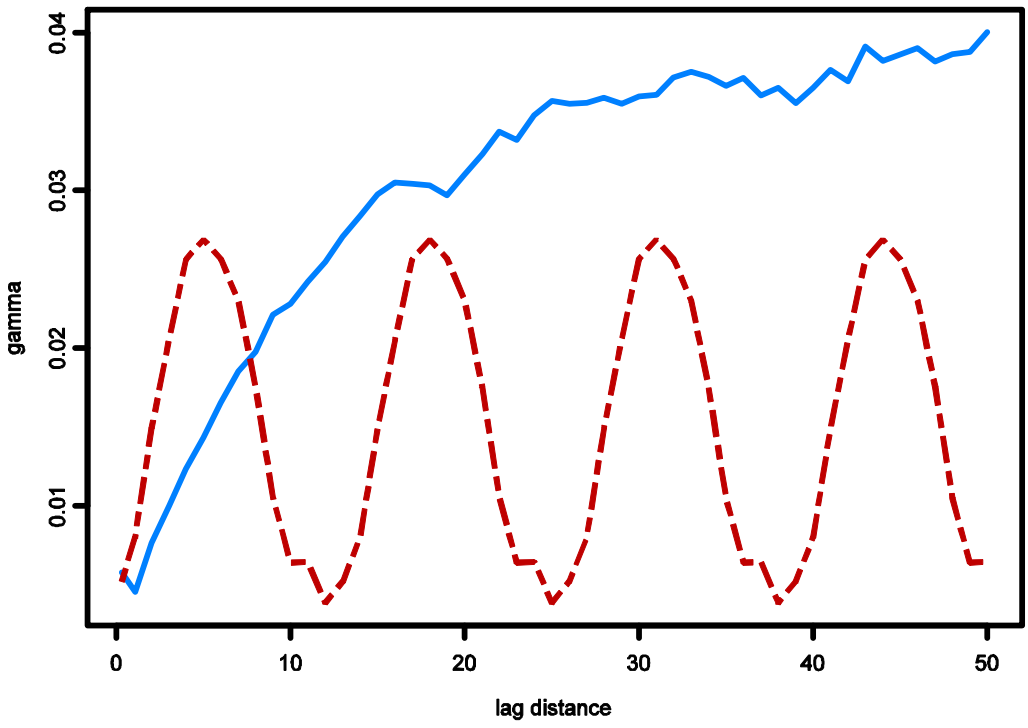
wet points Cruick Q51 : Azimuth tolerance = 30
gamma
0.01
0.02
0.03
0.04
0
10
20
30
40
50
lag distance

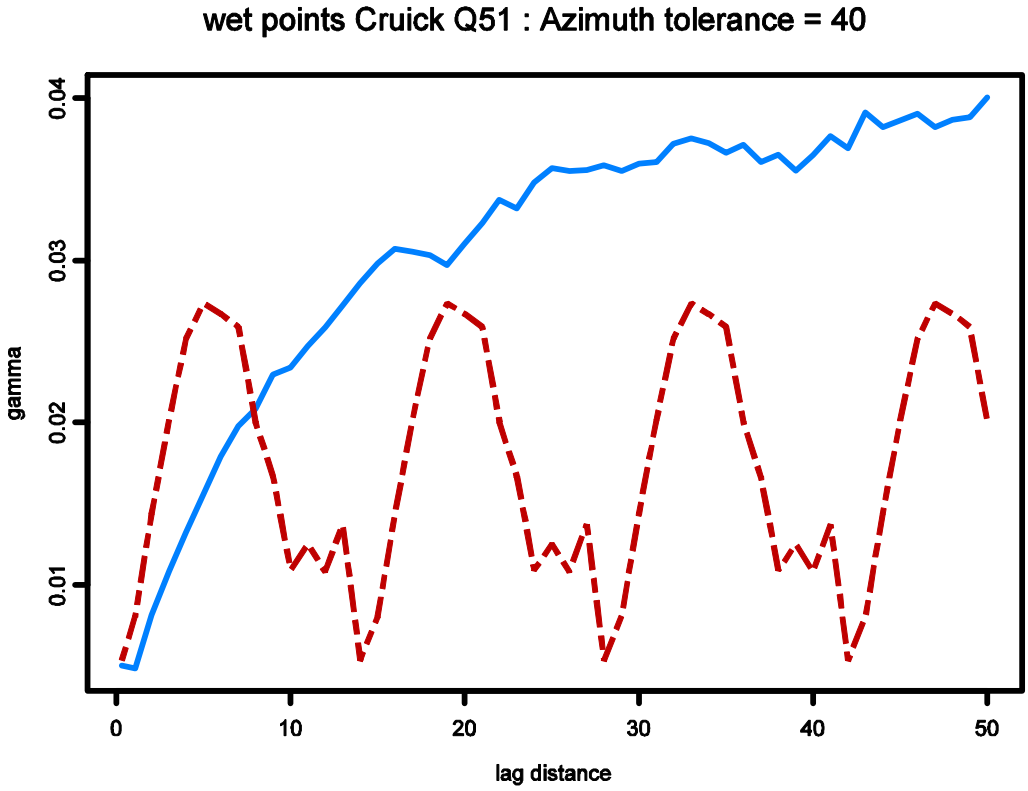
wet points Cruick Q51 : Azimuth tolerance = 40
gamma
0.01
0.02
0.03
0.04
0
10
20
30
40
50
lag distance

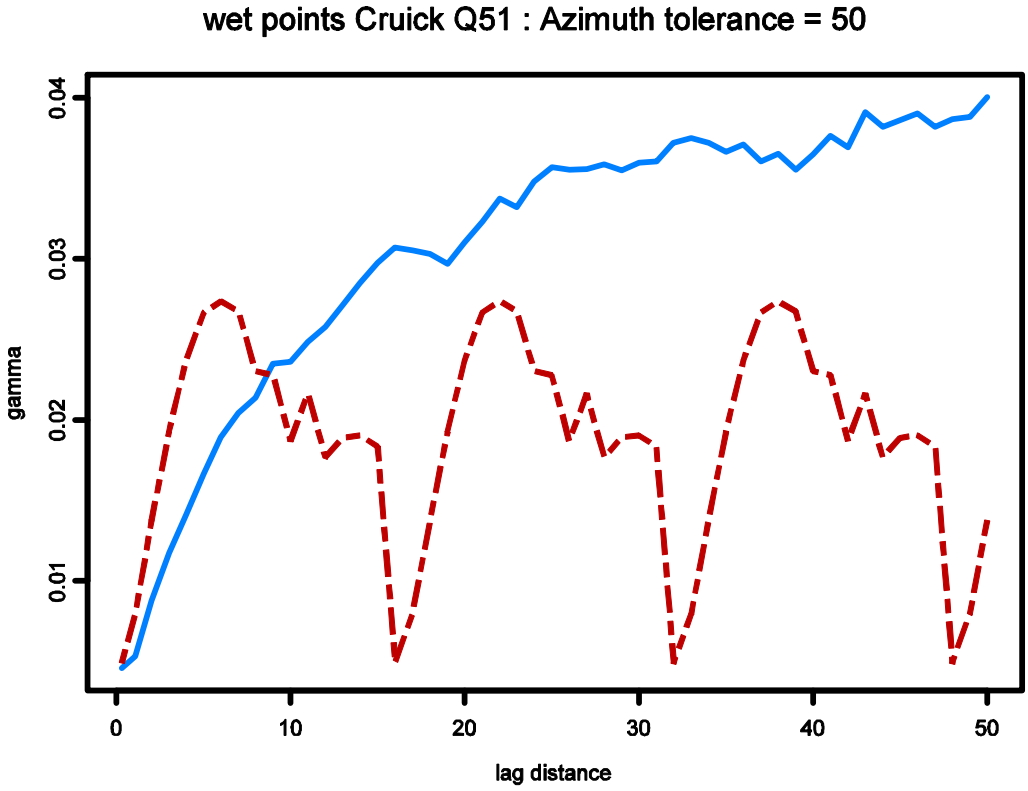
wet points Cruick Q51 : Azimuth tolerance = 50
gamma
0.01
0.02
0.03
0.04
0
10
20
30
40
50
lag distance

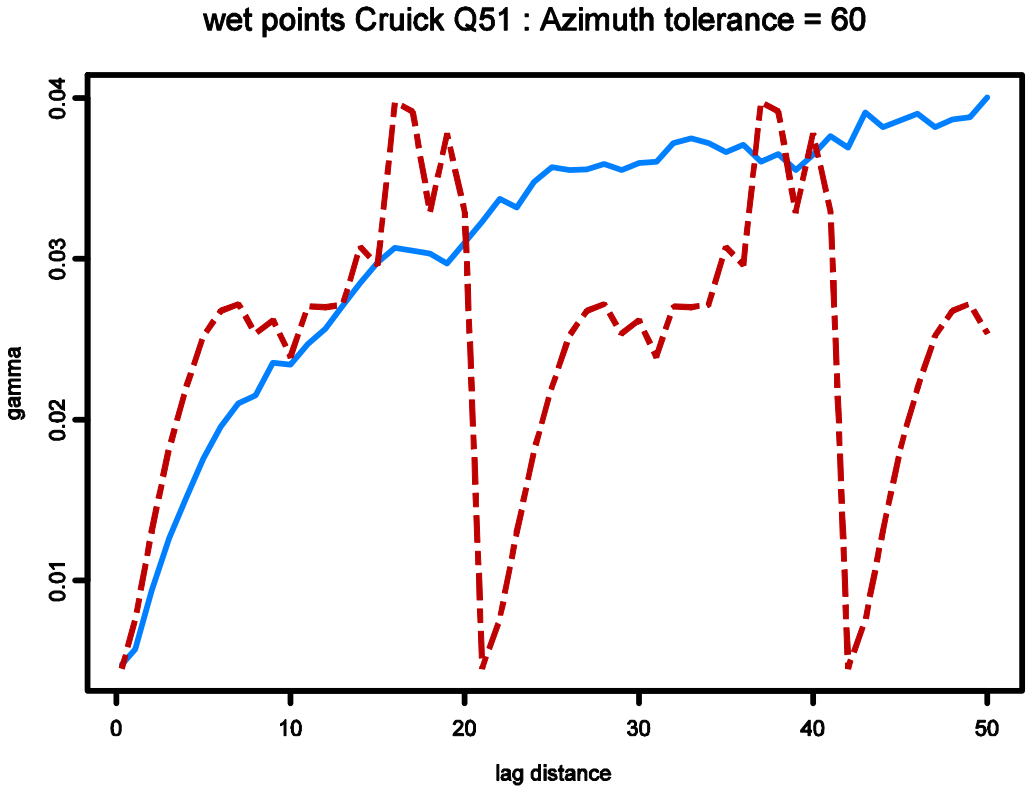
wet points Cruick Q51 : Azimuth tolerance = 60
gamma
0.01
0.02
0.03
0.04
0
10
20
30
40
50
lag distance

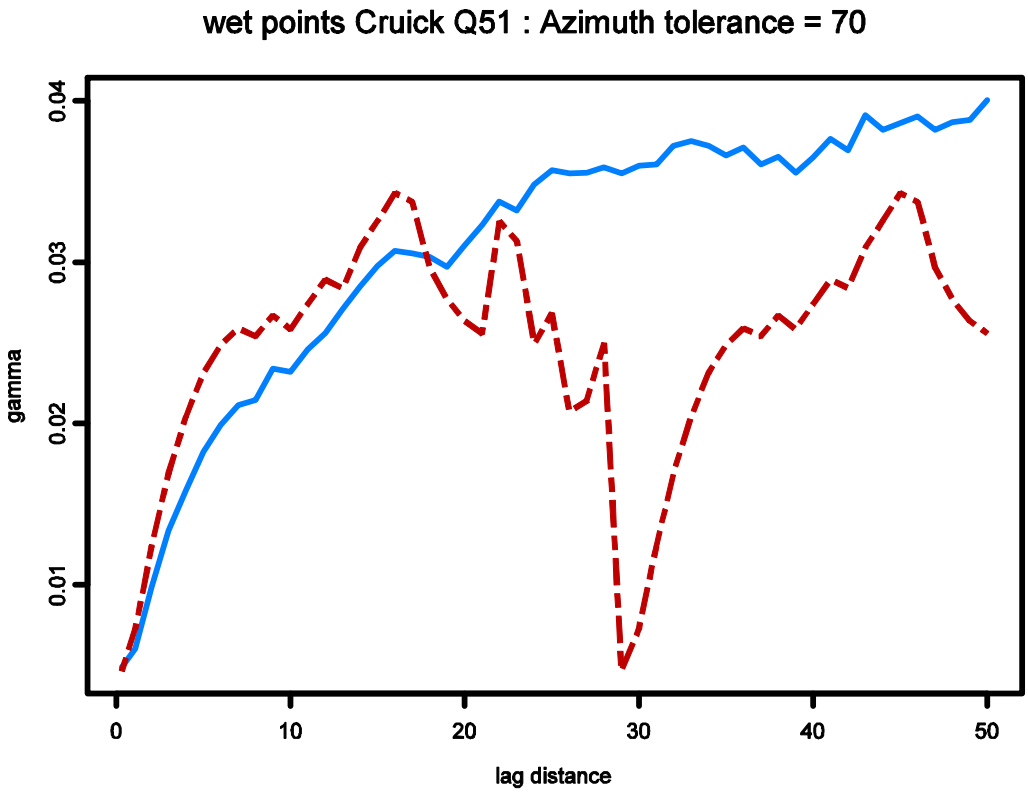
wet points Cruick Q51 : Azimuth tolerance = 70
gamma
0.01
0.02
0.03
0.04
0
10
20
30
40
50
lag distance

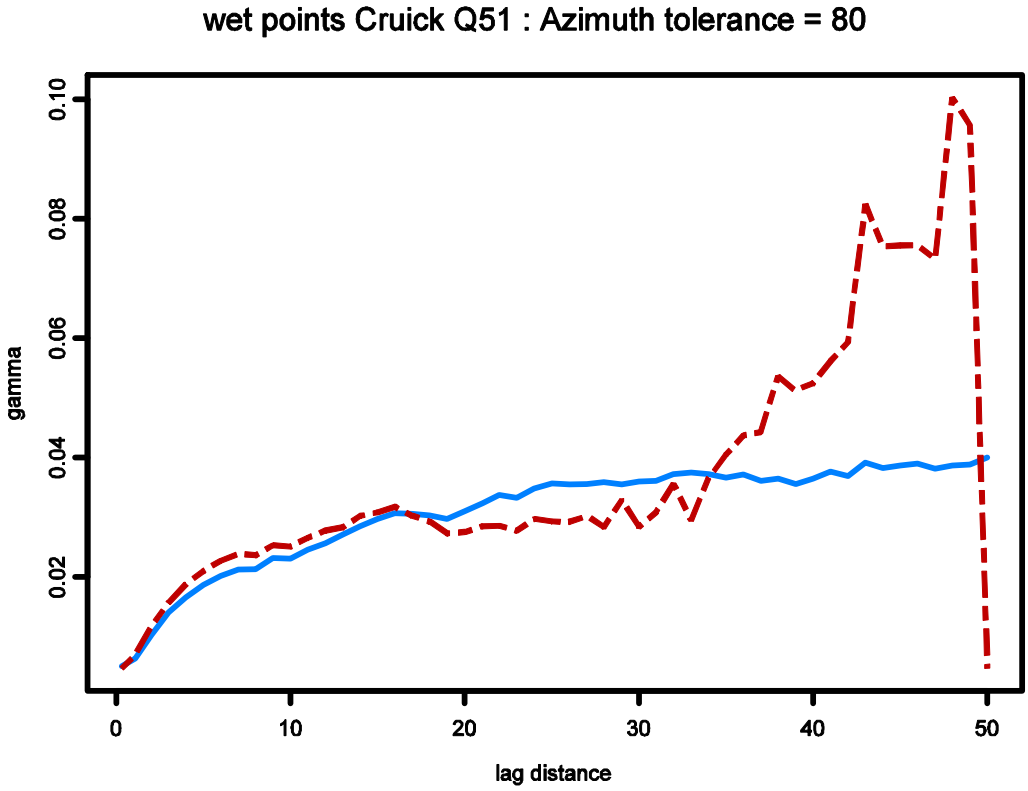
wet points Cruick Q51 : Azimuth tolerance = 80
gamma
0.02
0.04
0.06
0.08
0.10
0
10
20
30
40
50
lag distance

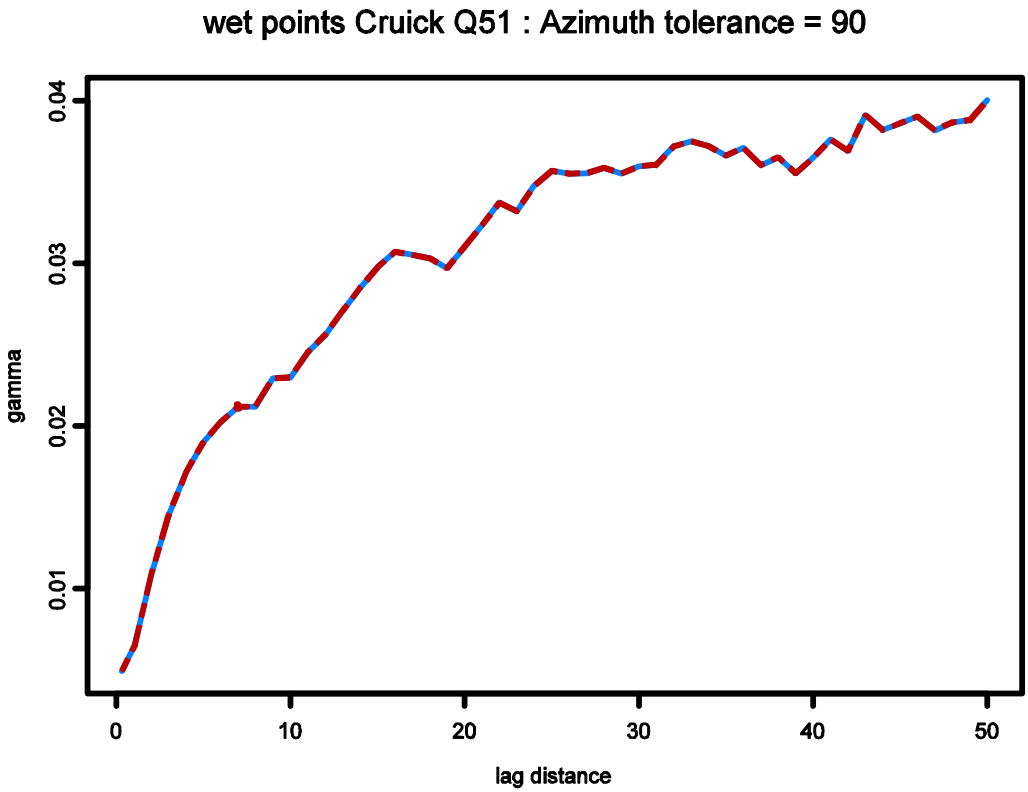
wet points Cruick Q51 : Azimuth tolerance = 90
gamma
0.01
0.02
0.03
0.04
0
10
20
30
40
50
lag distance

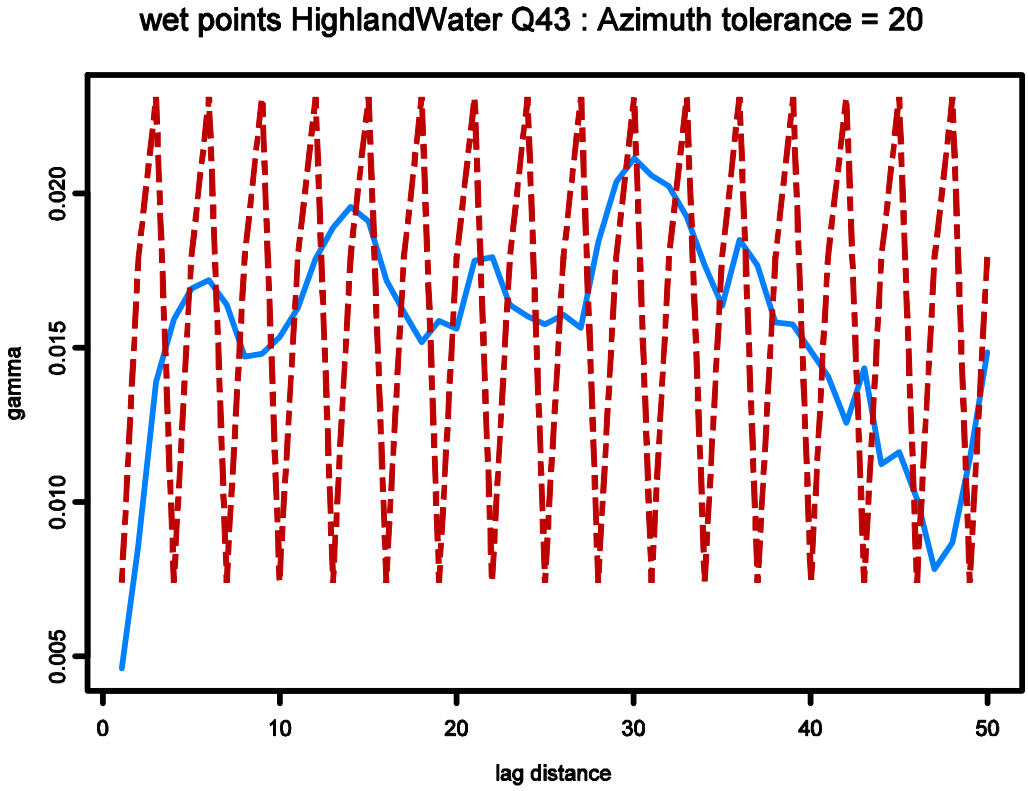
wet points HighlandWater Q43 : Azimuth tolerance = 20
gamma
0.005
0.010
0.015
0.020
0
10
20
30
40
50
lag distance

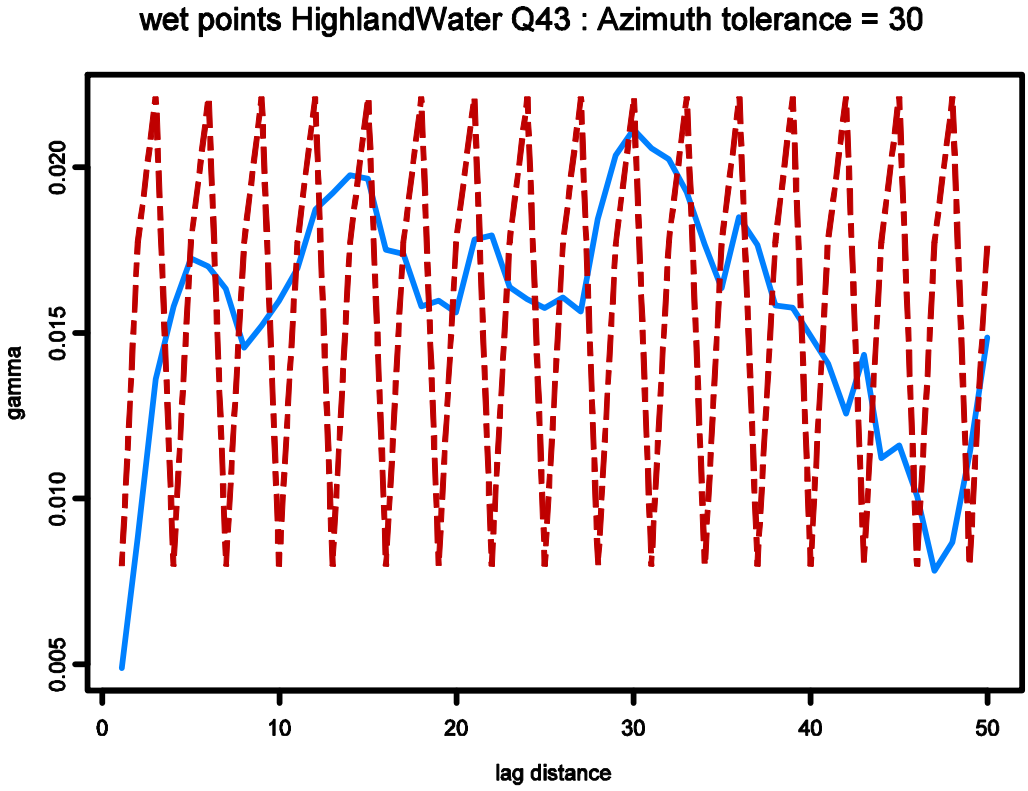
wet points HighlandWater Q43 : Azimuth tolerance = 30
gamma
0.005
0.010
0.015
0.020
0
10
20
30
40
50
lag distance

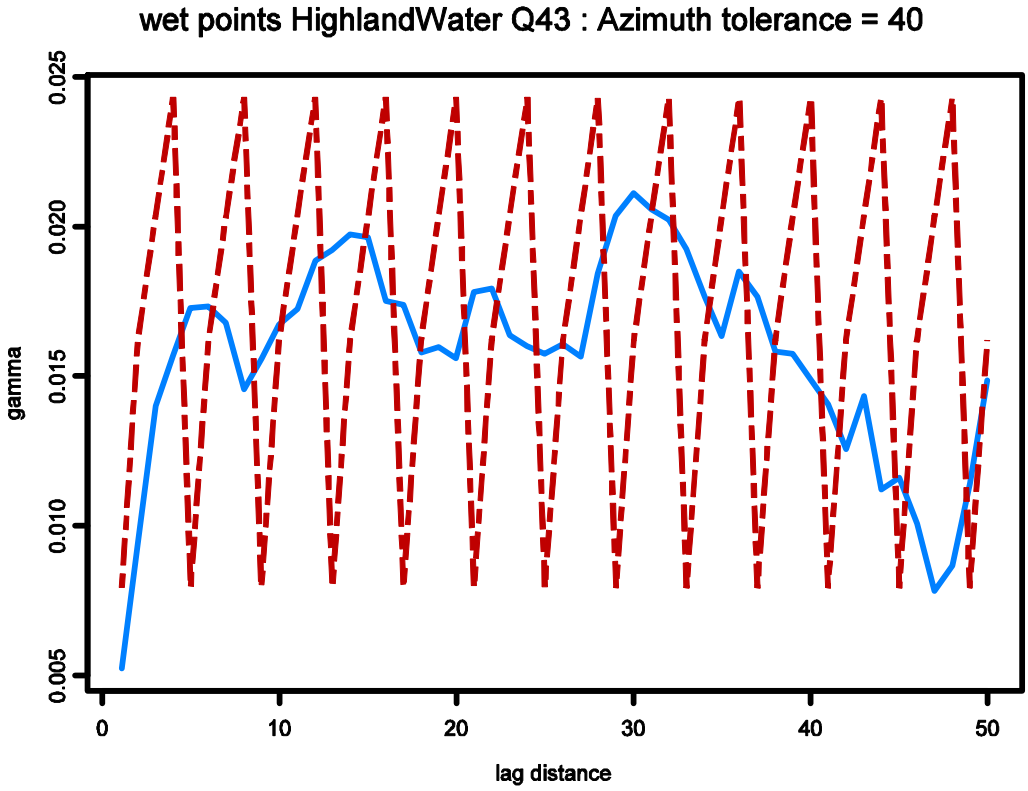
wet points HighlandWater Q43 : Azimuth tolerance = 40
gamma
0.005
0.010
0.015
0.020
0.025
0
10
20
30
40
50
lag distance

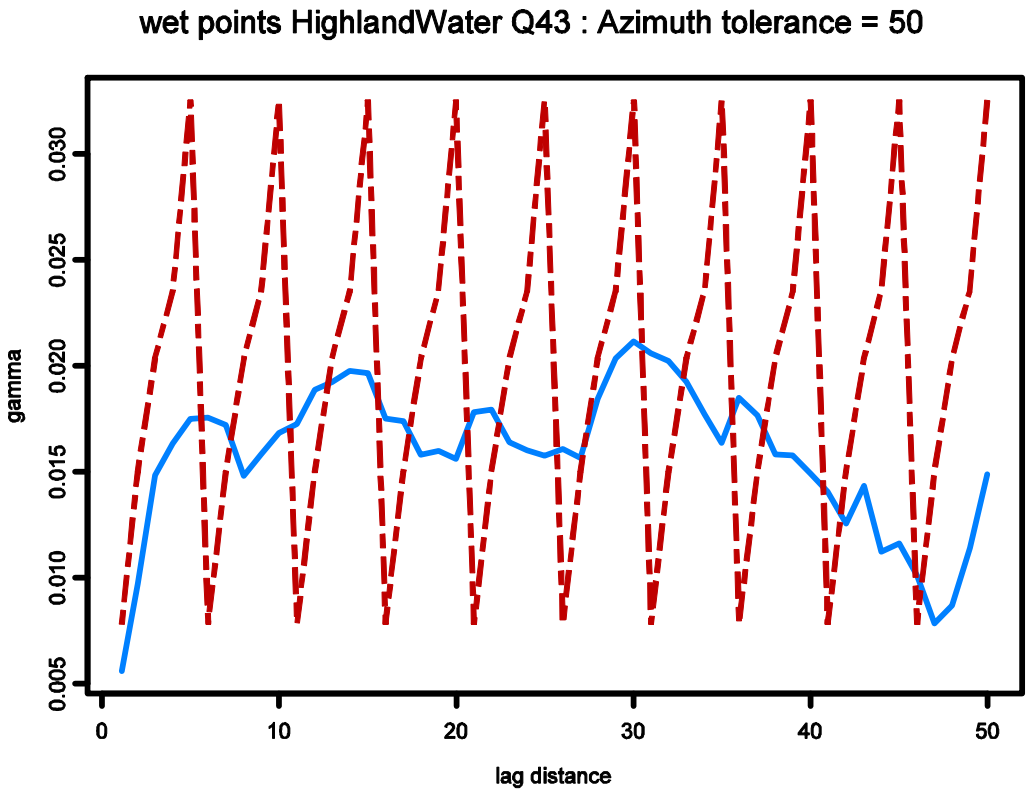
wet points HighlandWater Q43 : Azimuth tolerance = 50
gamma
0.005
0.010
0.015
0.020
0.025
0.030
0
10
20
30
40
50
lag distance

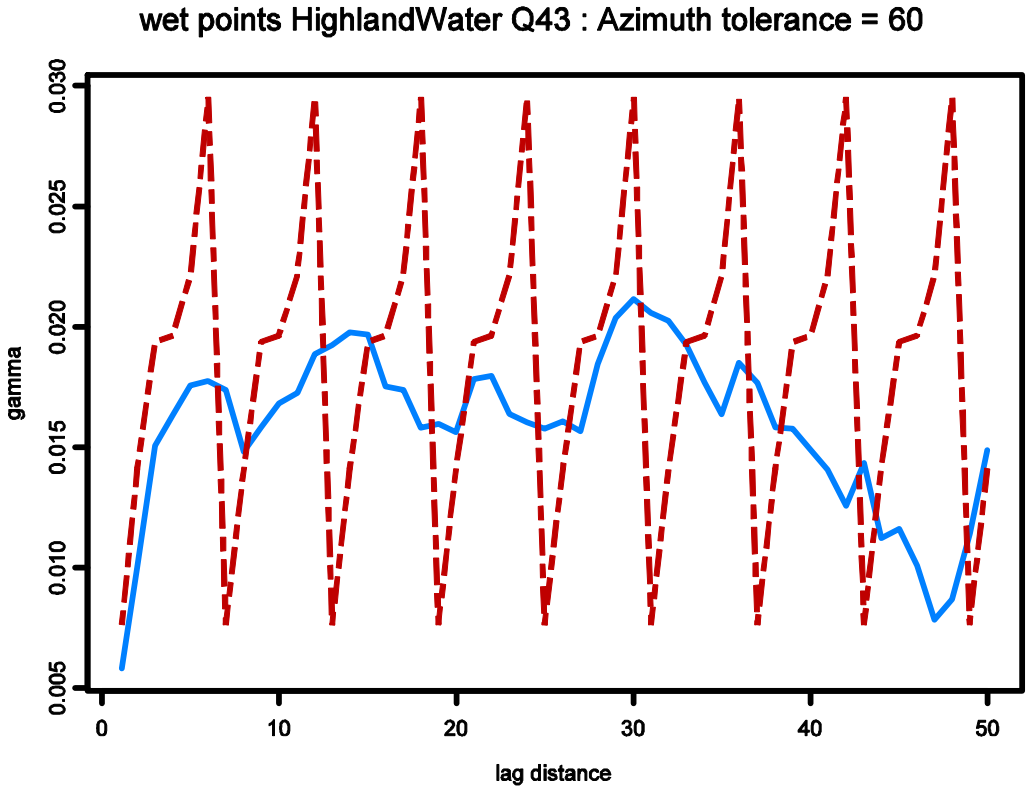
wet points HighlandWater Q43 : Azimuth tolerance = 60
gamma
0.005
0.010
0.015
0.020
0.025
0.030
0
10
20
30
40
50
lag distance

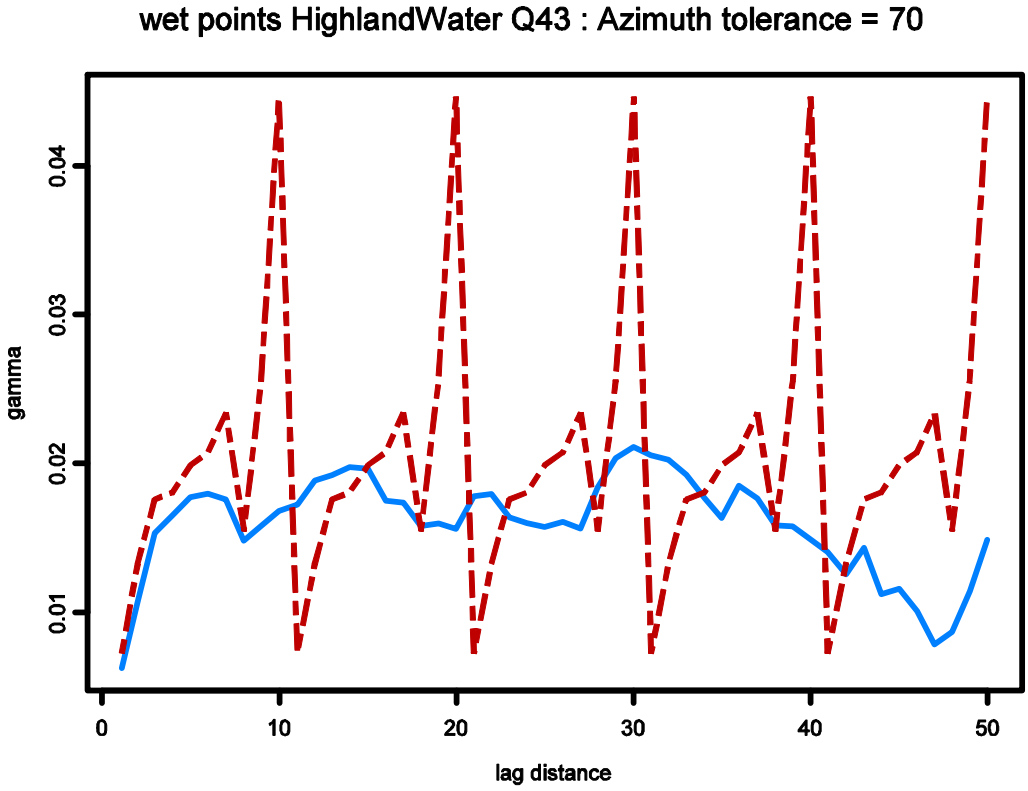
wet points HighlandWater Q43 : Azimuth tolerance = 70
gamma
0.01
0.02
0.03
0.04
0
10
20
30
40
50
lag distance

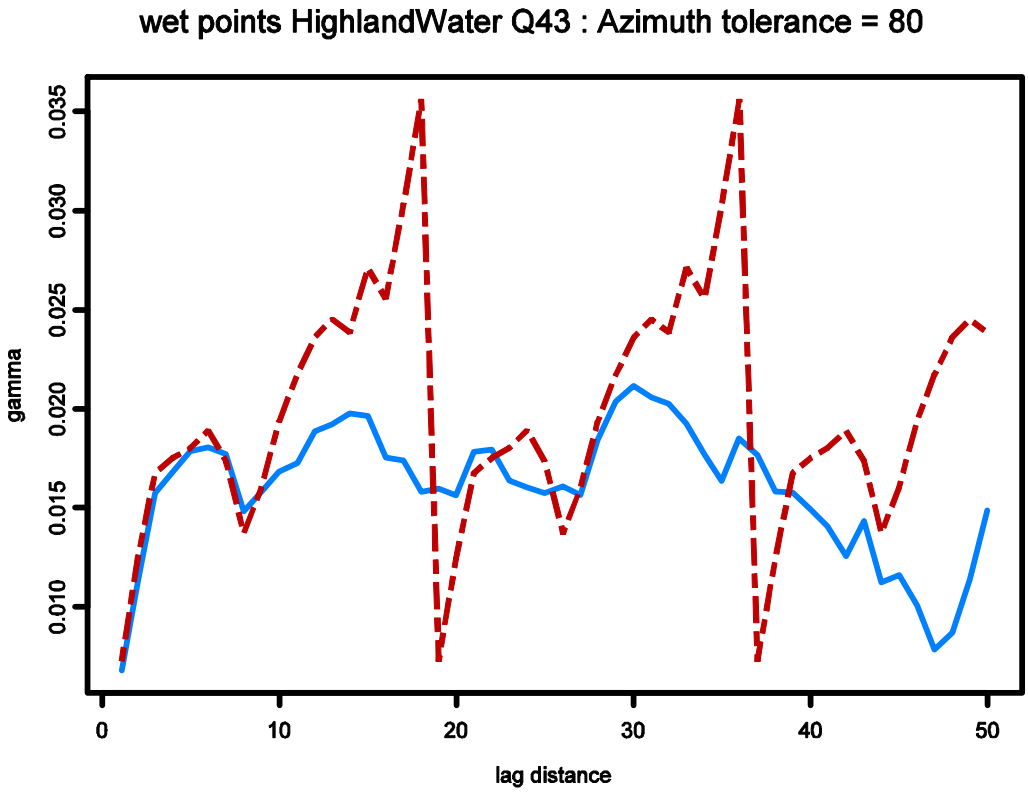
wet points HighlandWater Q43 : Azimuth tolerance = 80
gamma
0.010
0.015
0.020
0.025
0.030
0.035
0
10
20
30
40
50
lag distance

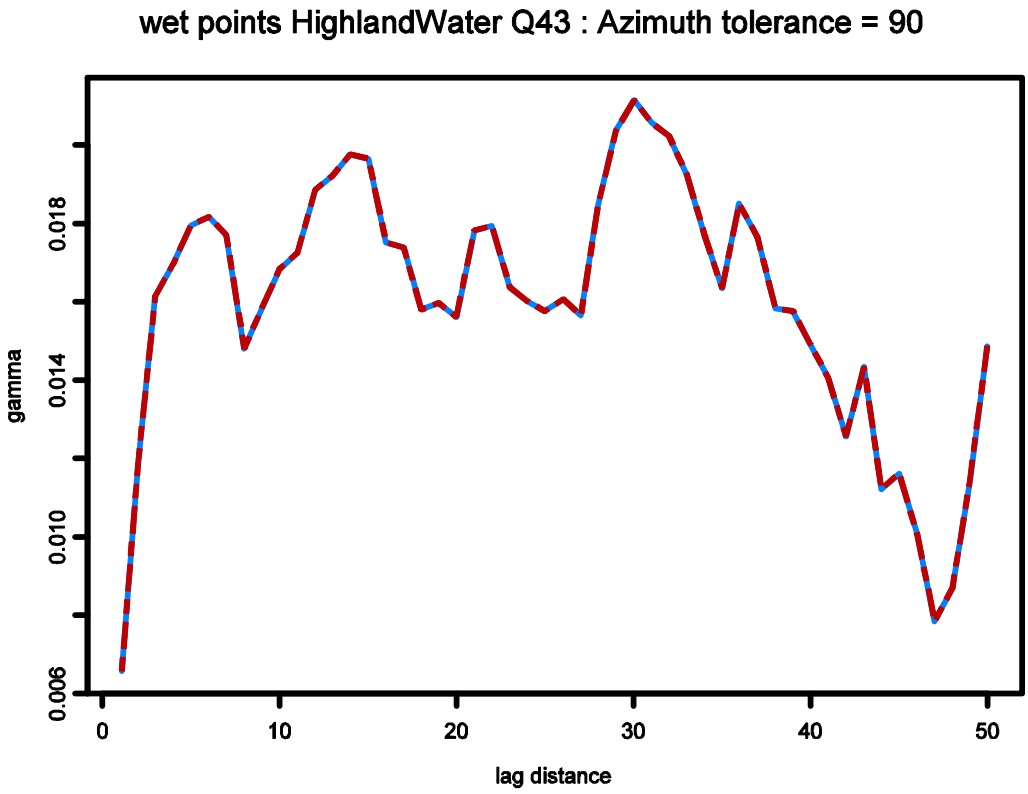
wet points HighlandWater Q43 : Azimuth tolerance = 90
gamma
0.006
0.010
0.014
0.018
0
10
20
30
40
50
lag distance

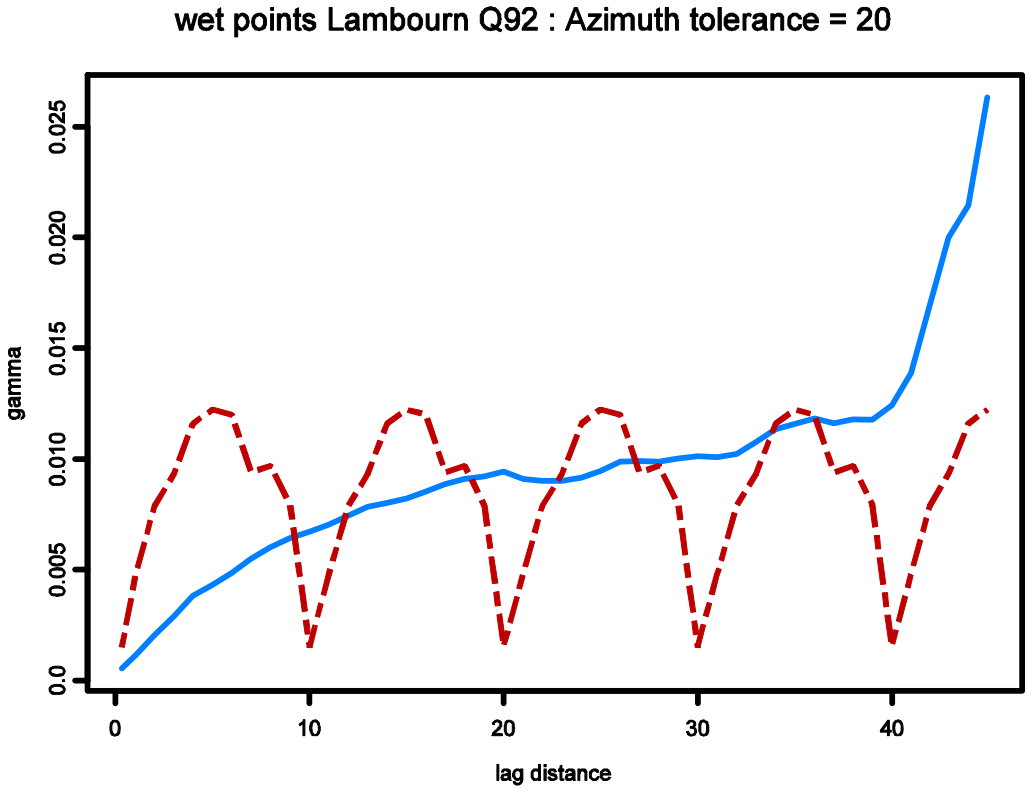
wet points Lambourn Q92 : Azimuth tolerance = 20
gamma
0.0
0.005
0.010
0.015
0.020
0.025
0
10
20
30
40
lag distance

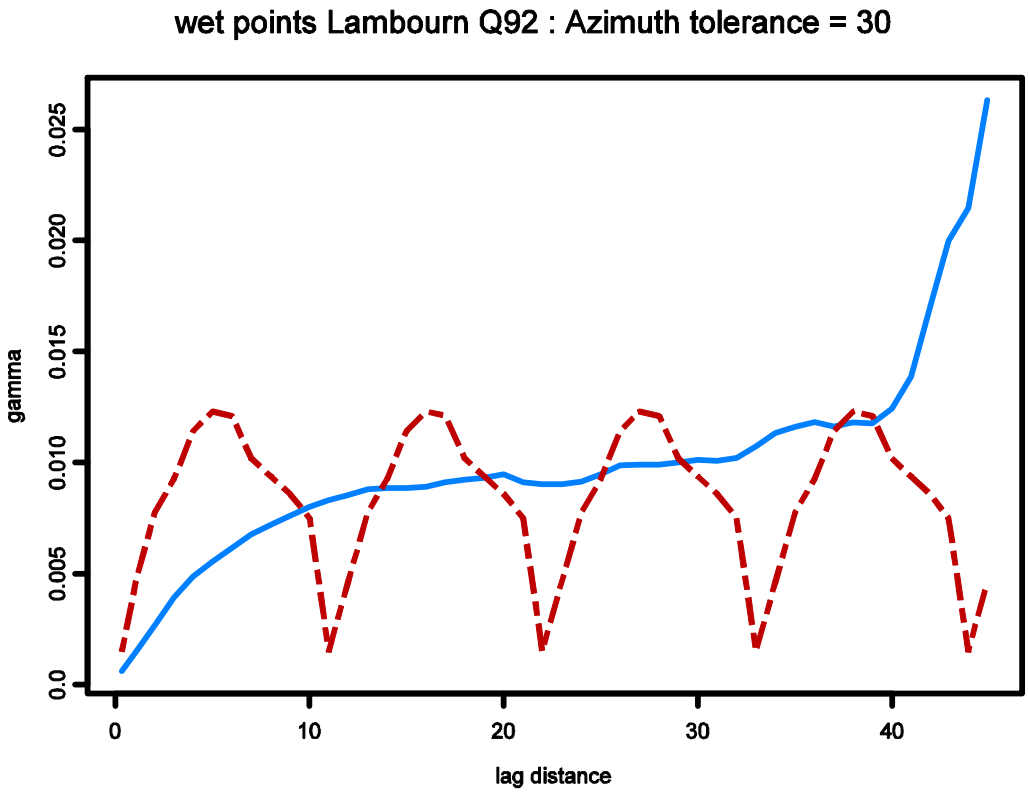
wet points Lambourn Q92 : Azimuth tolerance = 30
gamma
0.0
0.005
0.010
0.015
0.020
0.025
0
10
20
30
40
lag distance

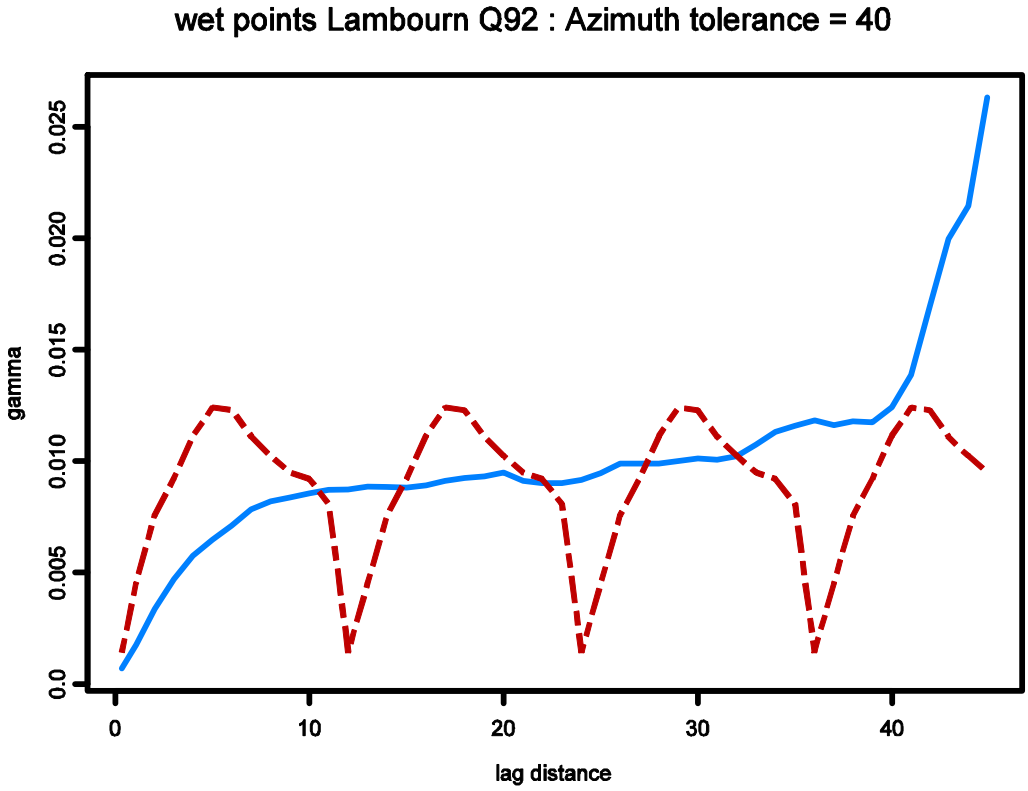
wet points Lambourn Q92 : Azimuth tolerance = 40
gamma
0.0
0.005
0.010
0.015
0.020
0.025
0
10
20
30
40
lag distance

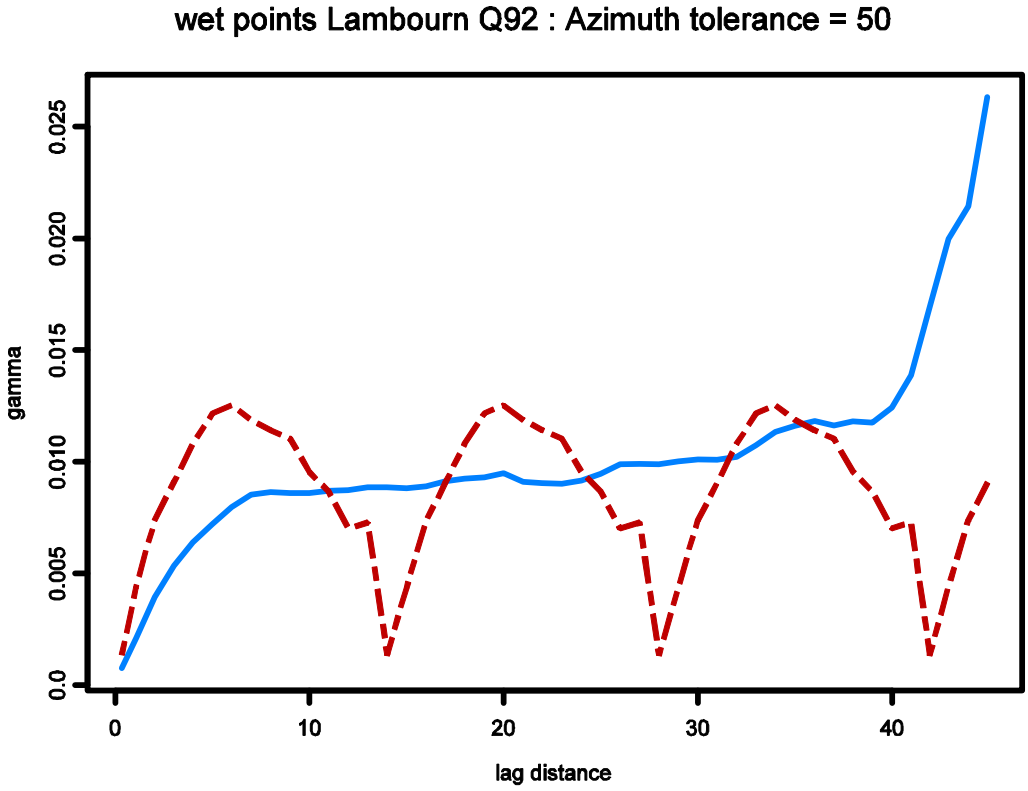
wet points Lambourn Q92 : Azimuth tolerance = 50
gamma
0.0
0.005
0.010
0.015
0.020
0.025
0
10
20
30
40
lag distance

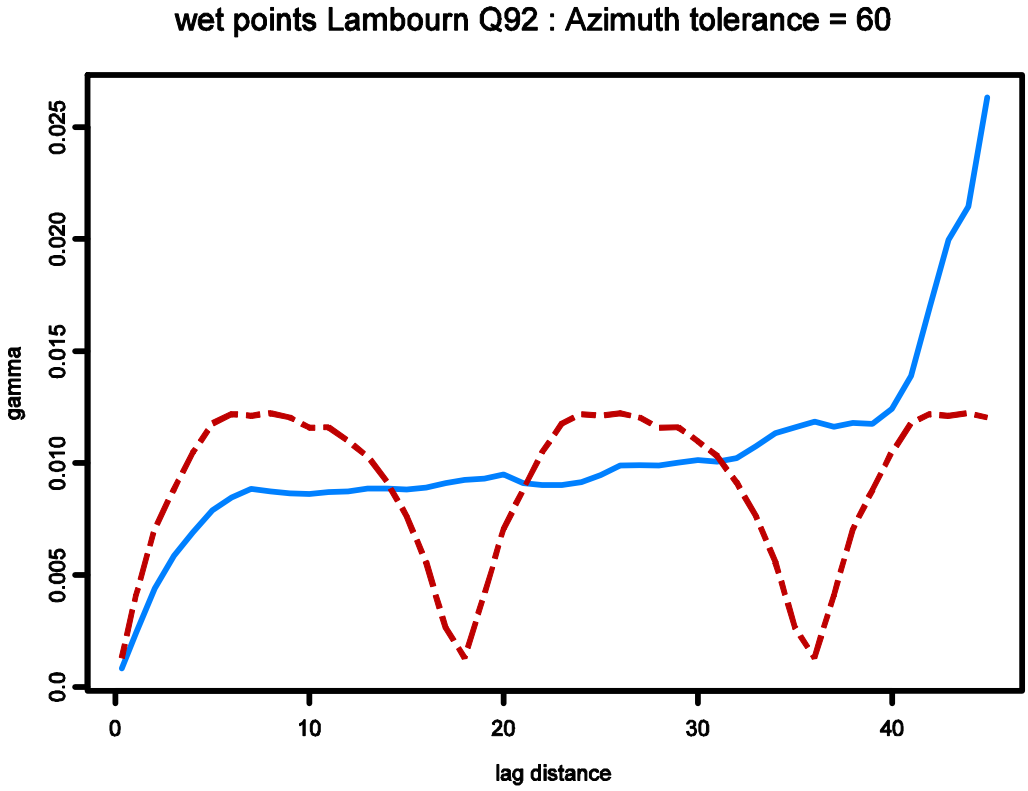
wet points Lambourn Q92 : Azimuth tolerance = 60
gamma
0.0
0.005
0.010
0.015
0.020
0.025
0
10
20
30
40
lag distance

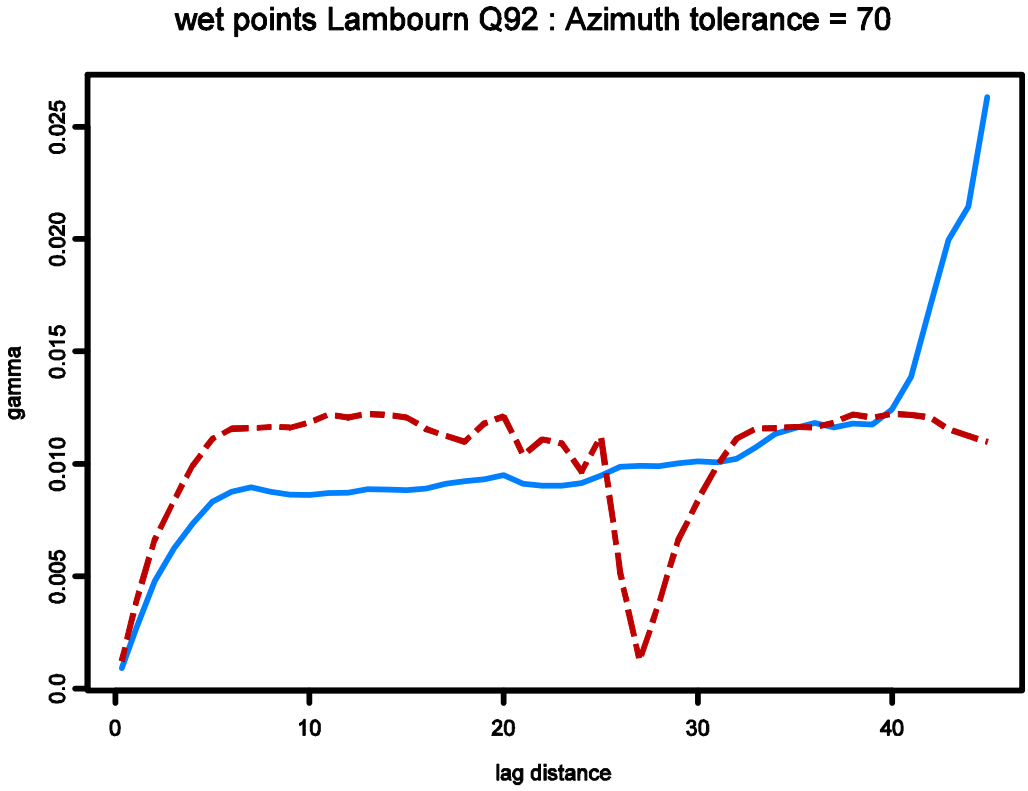
wet points Lambourn Q92 : Azimuth tolerance = 70
gamma
0.0
0.005
0.010
0.015
0.020
0.025
0
10
20
30
40
lag distance

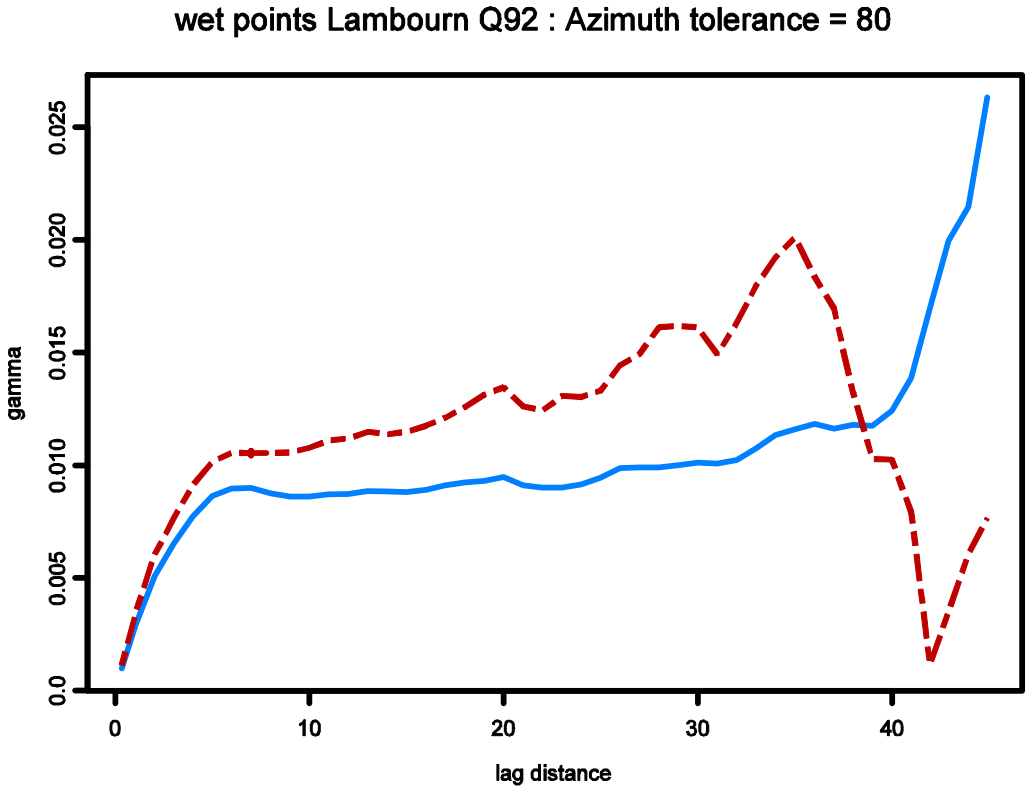
wet points Lambourn Q92 : Azimuth tolerance = 80
gamma
0.0
0.005
0.010
0.015
0.020
0.025
0
10
20
30
40
lag distance

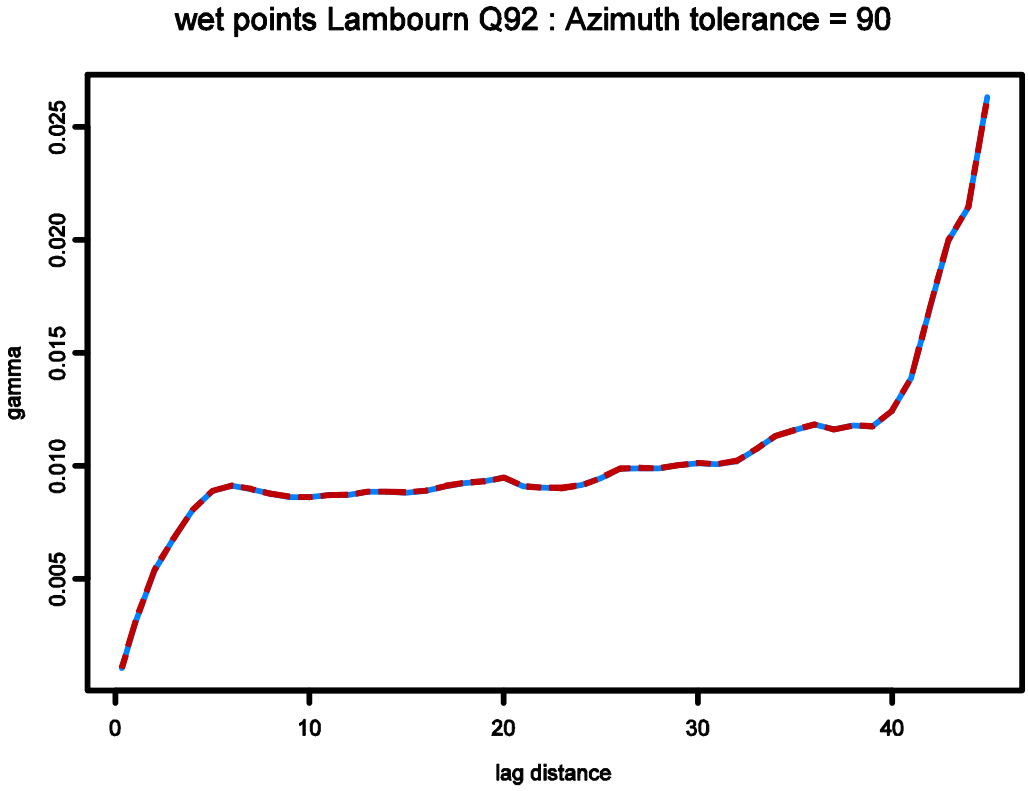
wet points Lambourn Q92 : Azimuth tolerance = 90
gamma
0.005
0.010
0.015
0.020
0.025
0
10
20
30
40
lag distance

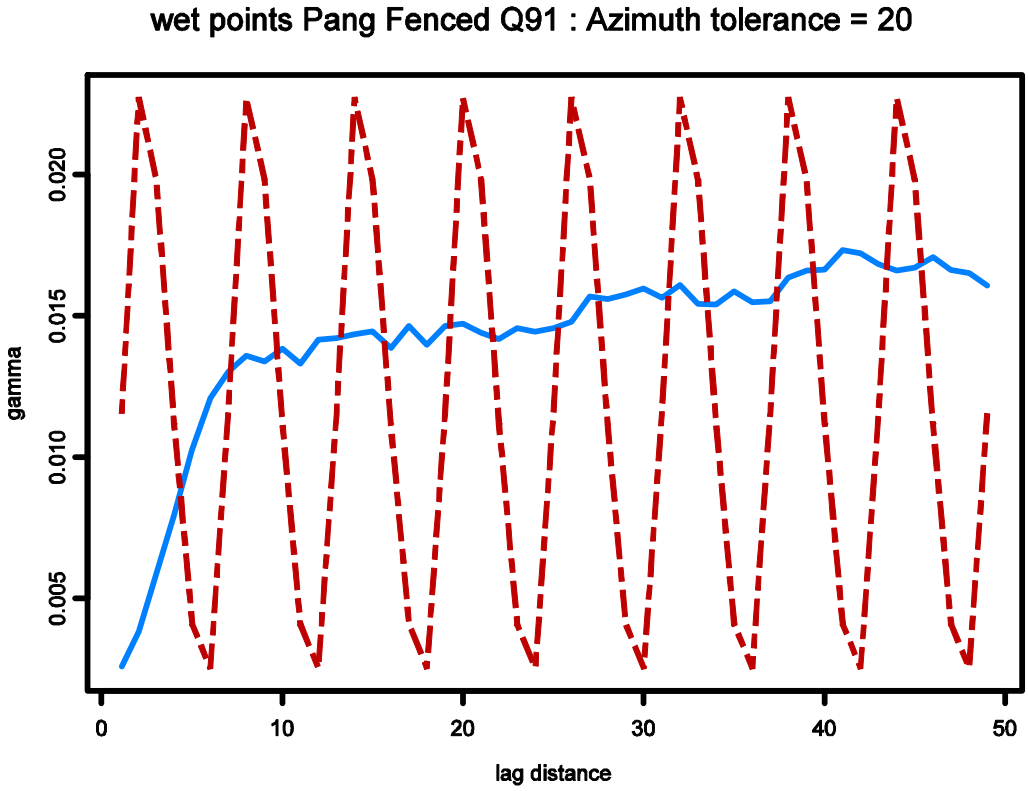
wet points Pang Fenced Q91 : Azimuth tolerance = 20
gamma
0.005
0.010
0.015
0.020
0
10
20
30
40
50
lag distance

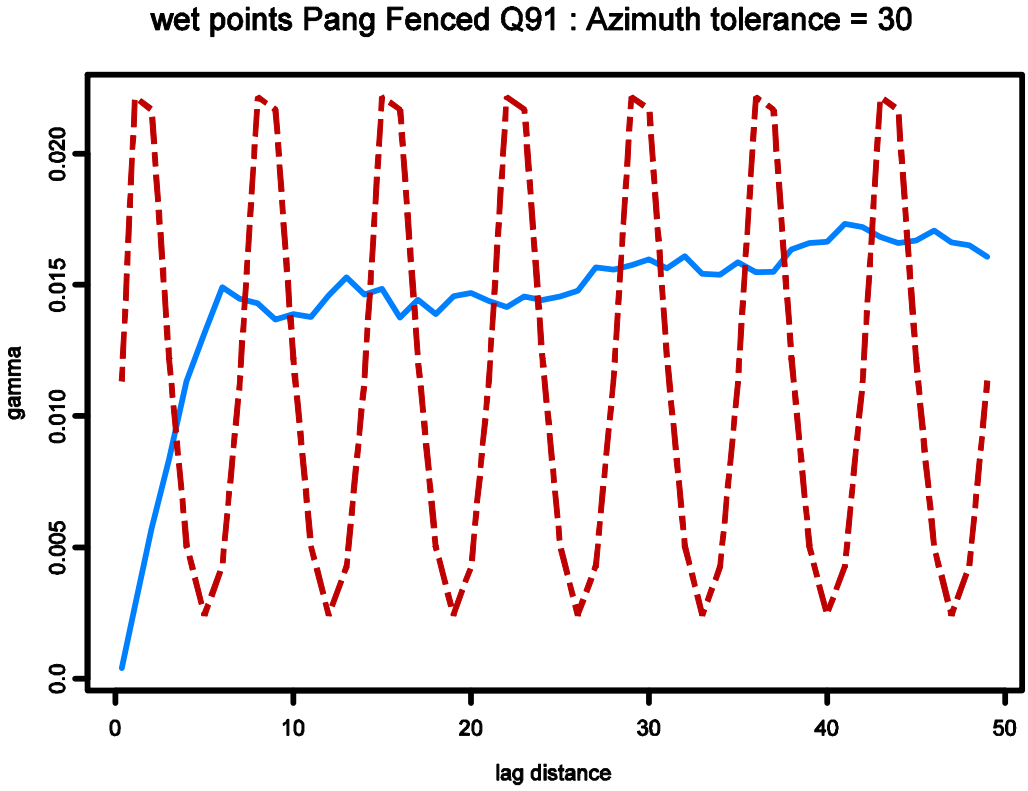
wet points Pang Fenced Q91 : Azimuth tolerance = 30
gamma
0.0
0.005
0.010
0.015
0.020
0
10
20
30
40
50
lag distance

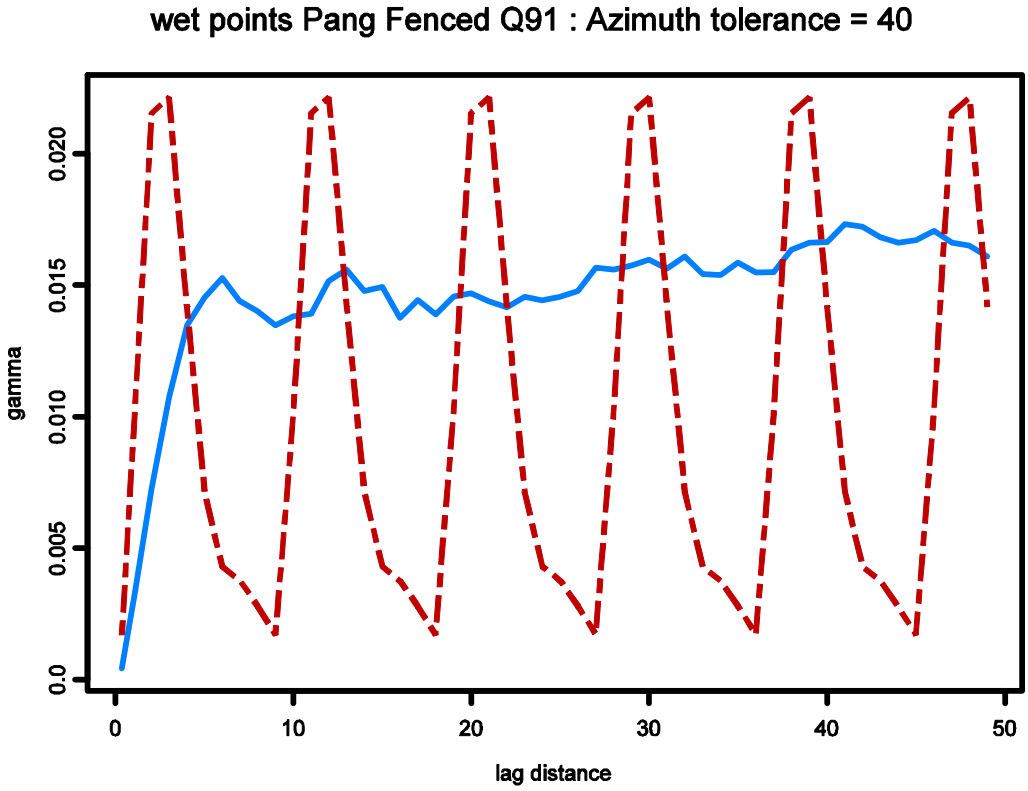
wet points Pang Fenced Q91 : Azimuth tolerance = 40
gamma
0.0
0.005
0.010
0.015
0.020
0
10
20
30
40
50
lag distance

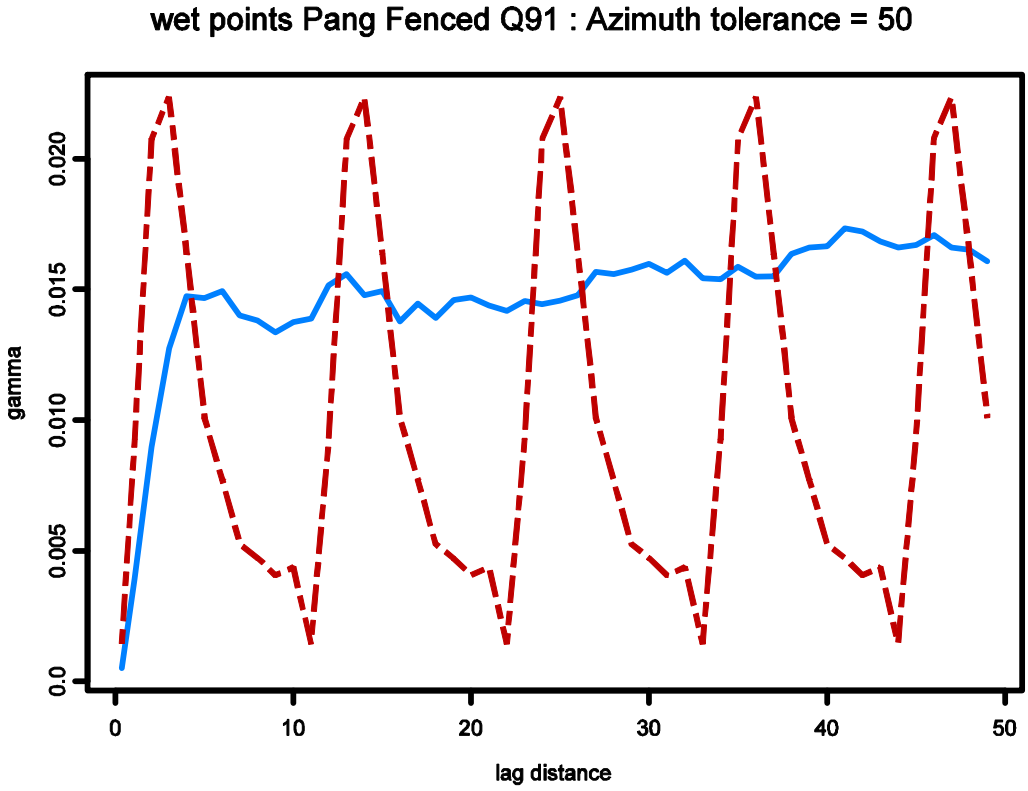
wet points Pang Fenced Q91 : Azimuth tolerance = 50
gamma
0.0
0.005
0.010
0.015
0.020
0
10
20
30
40
50
lag distance

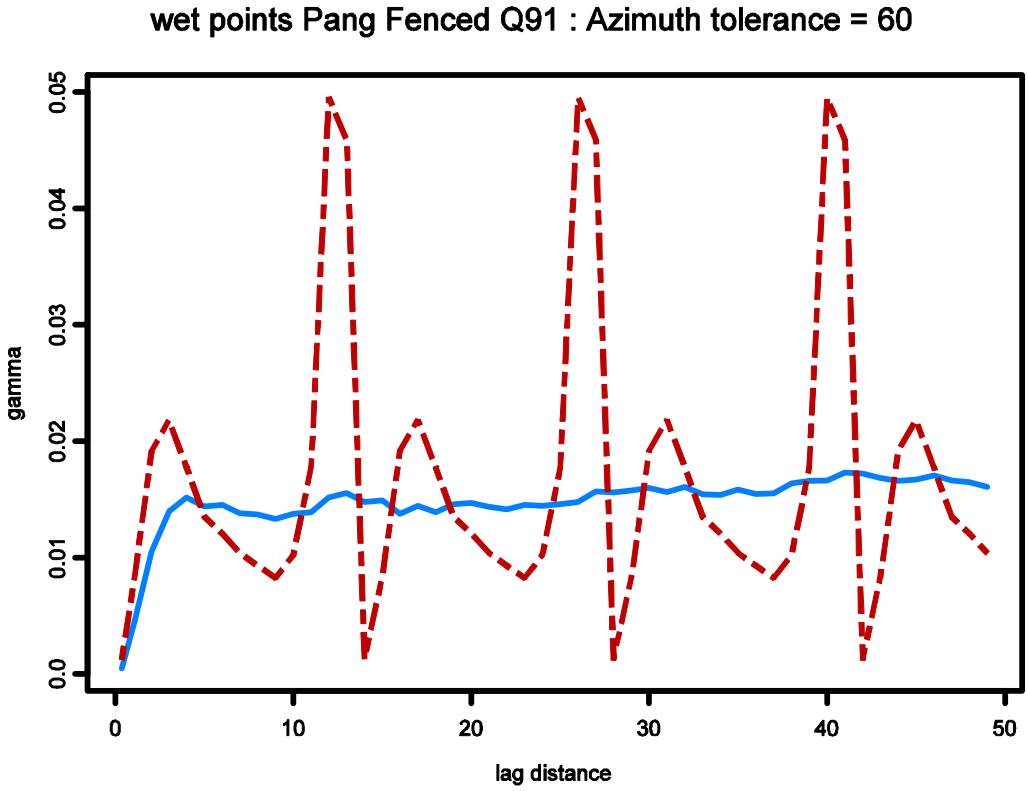
wet points Pang Fenced Q91 : Azimuth tolerance = 60
gamma
0.0
0.01
0.02
0.03
0.04
0.05
0
10
20
30
40
50
lag distance

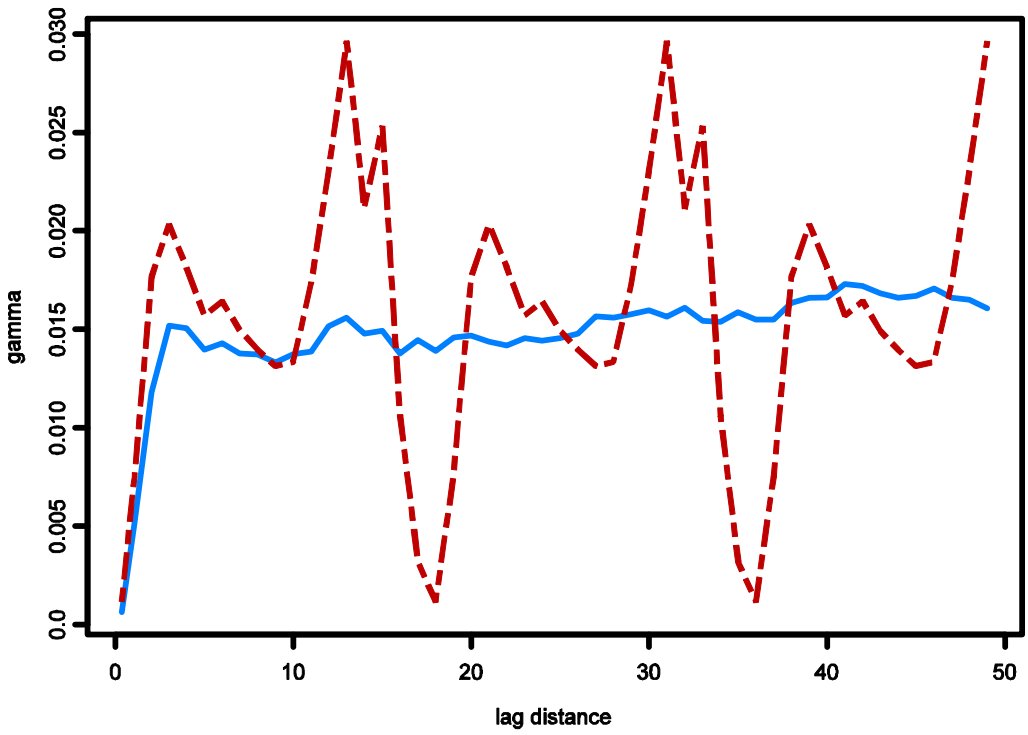
wet points Pang Fenced Q91 : Azimuth tolerance = 70
gamma
0.0
0.005
0.010
0.015
0.020
0.025
0.030
0
10
20
30
40
50
lag distance

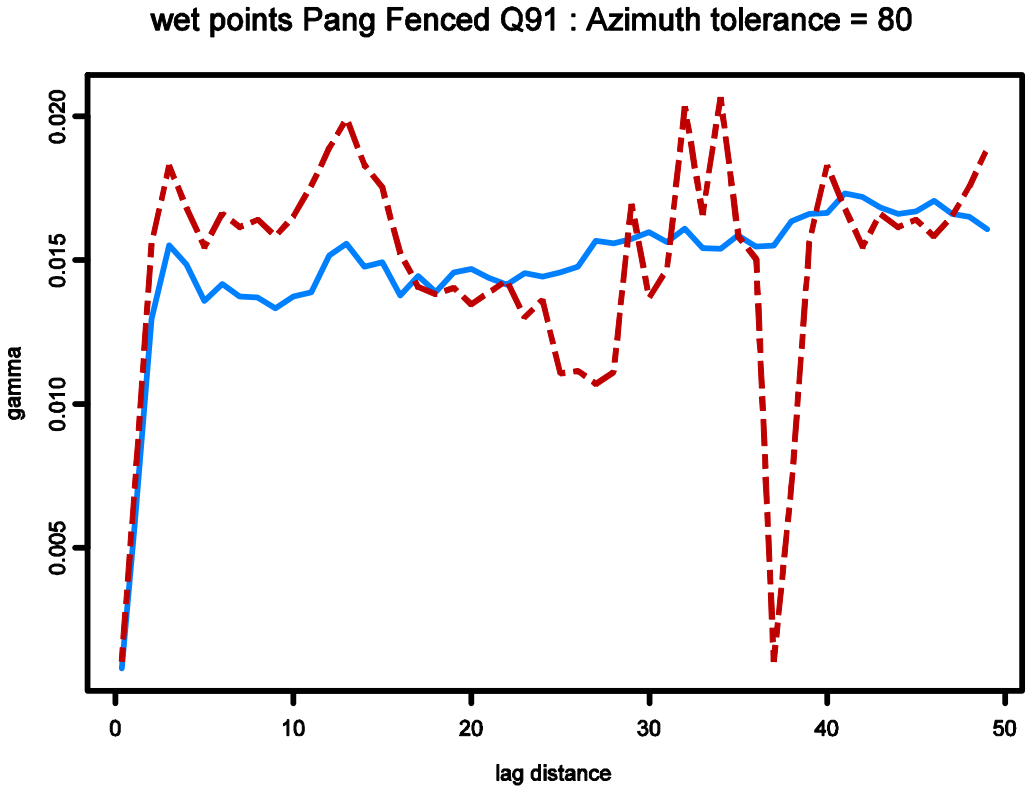
wet points Pang Fenced Q91 : Azimuth tolerance = 80
gamma
0.005
0.010
0.015
0.020
0
10
20
30
40
50
lag distance

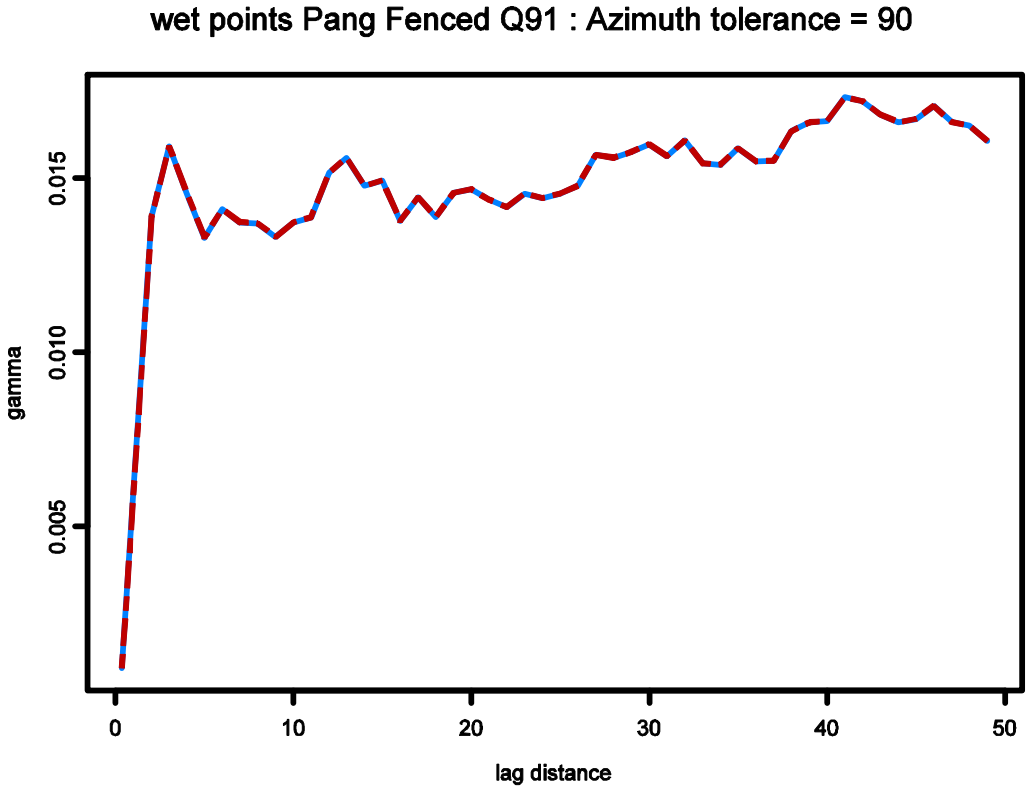
wet points Pang Fenced Q91 : Azimuth tolerance = 90
gamma
0.005
0.010
0.015
0
10
20
30
40
50
lag distance

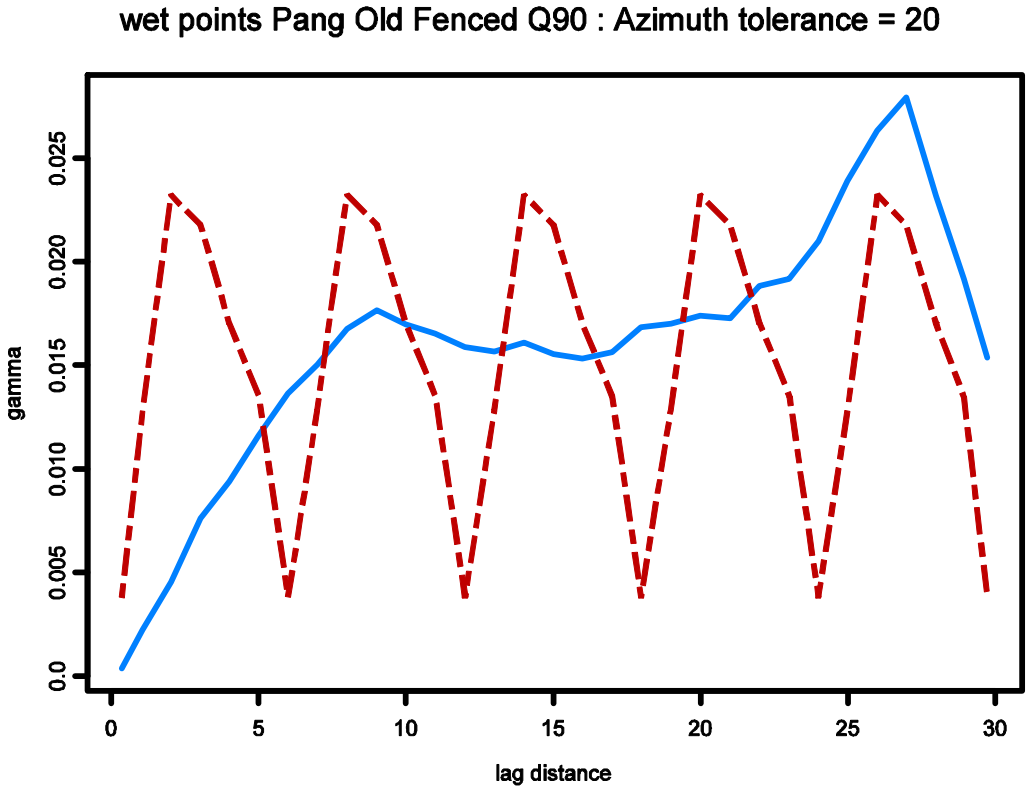
wet points Pang Old Fenced Q90 : Azimuth tolerance = 20
gamma
0.0
0.005
0.010
0.015
0.020
0.025
0
5
10
15
20
25
30
lag distance

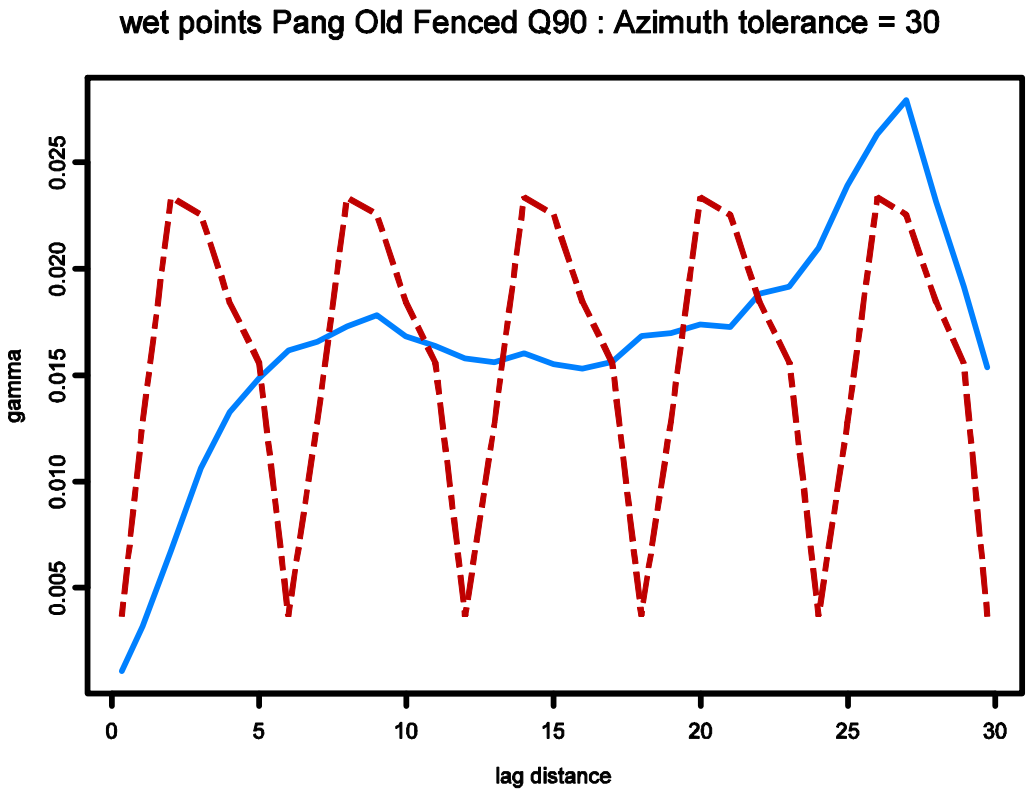
wet points Pang Old Fenced Q90 : Azimuth tolerance = 30
gamma
0.005
0.010
0.015
0.020
0.025
0
5
10
15
20
25
30
lag distance

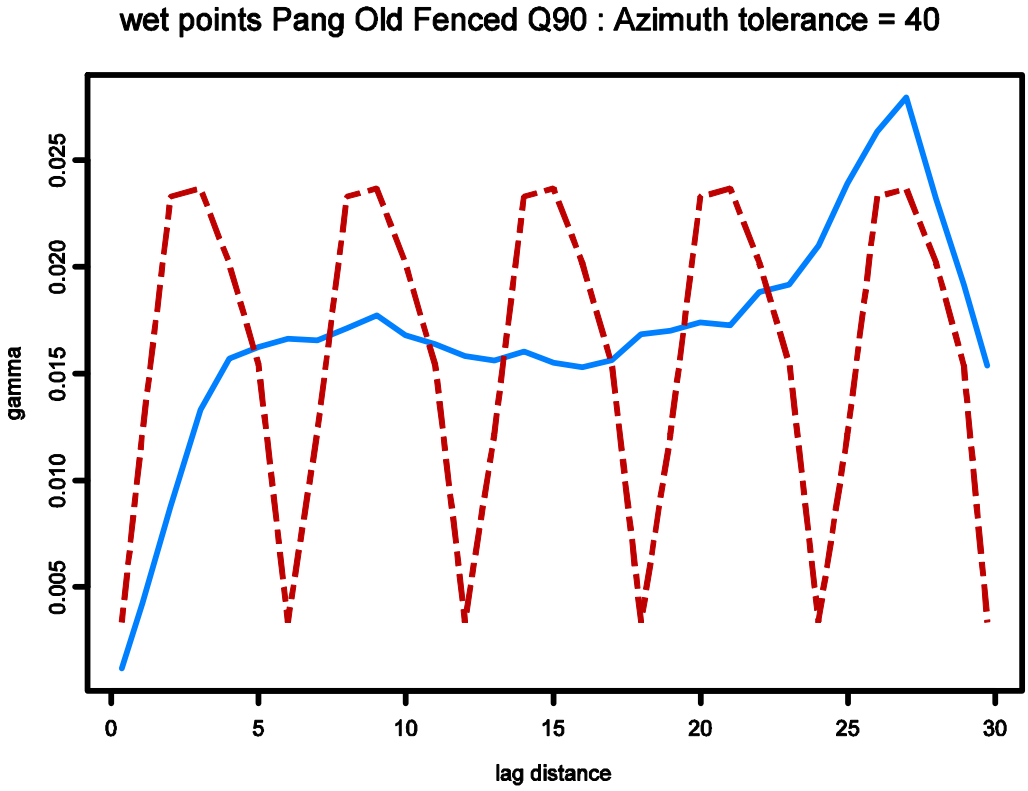
wet points Pang Old Fenced Q90 : Azimuth tolerance = 40
gamma
0.005
0.010
0.015
0.020
0.025
0
5
10
15
20
25
30
lag distance

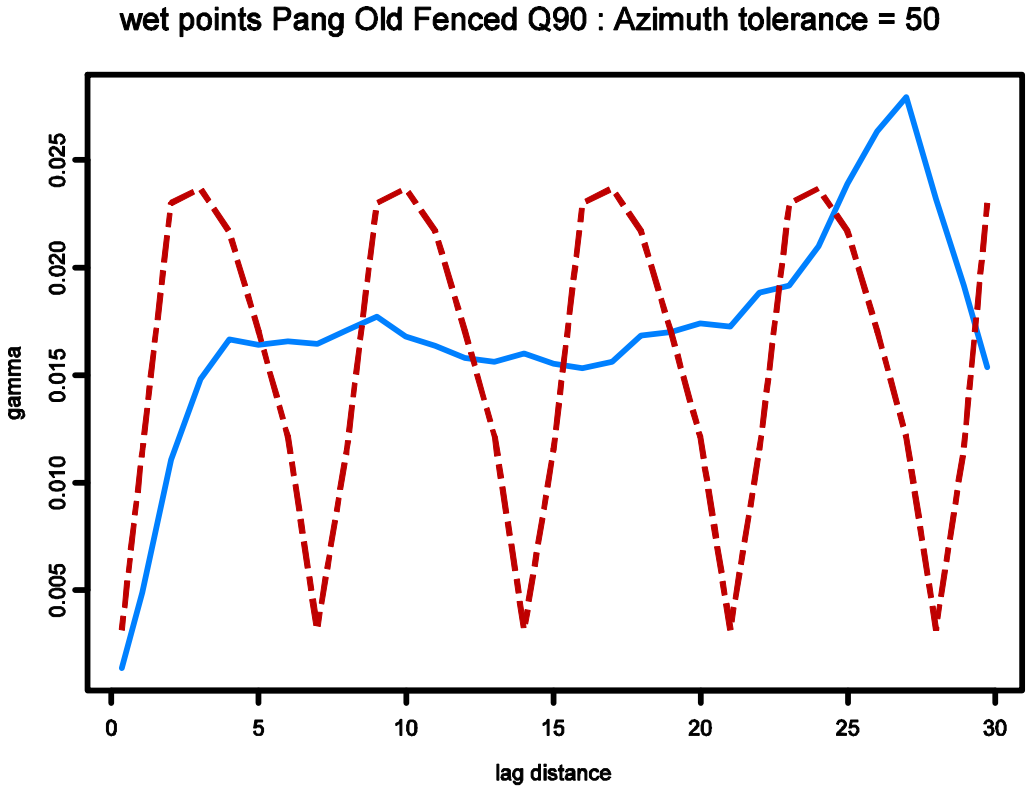
wet points Pang Old Fenced Q90 : Azimuth tolerance = 50
gamma
0.005
0.010
0.015
0.020
0.025
0
5
10
15
20
25
30
lag distance

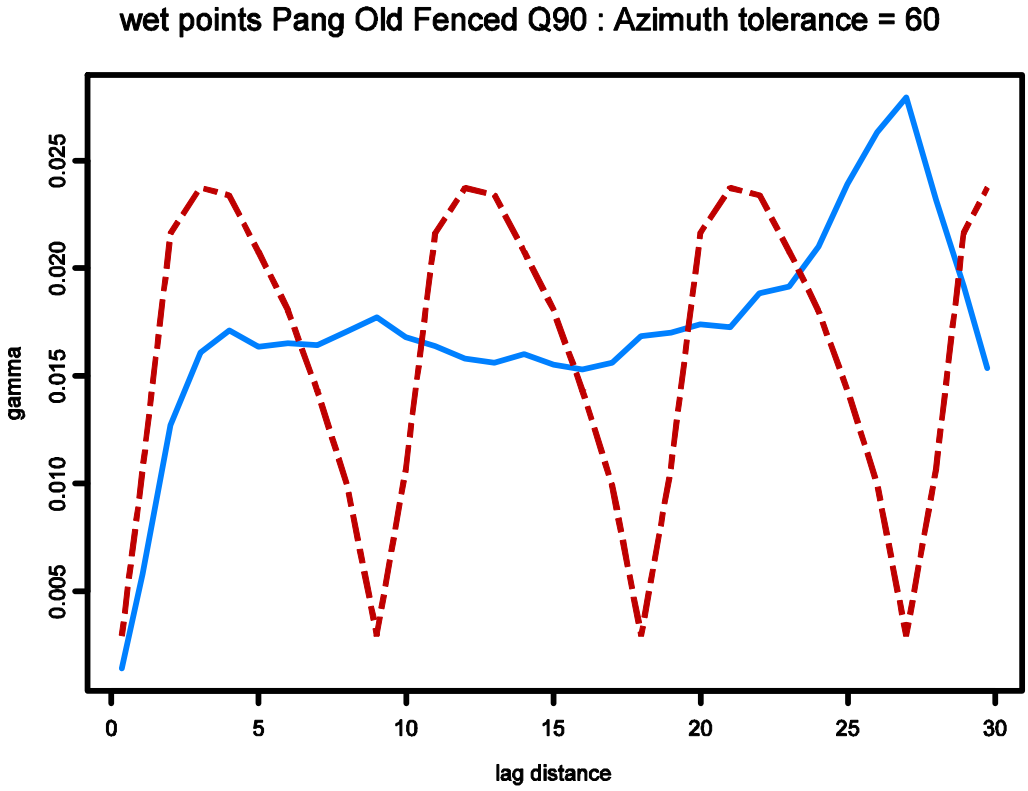
wet points Pang Old Fenced Q90 : Azimuth tolerance = 60
gamma
0.005
0.010
0.015
0.020
0.025
0
5
10
15
20
25
30
lag distance

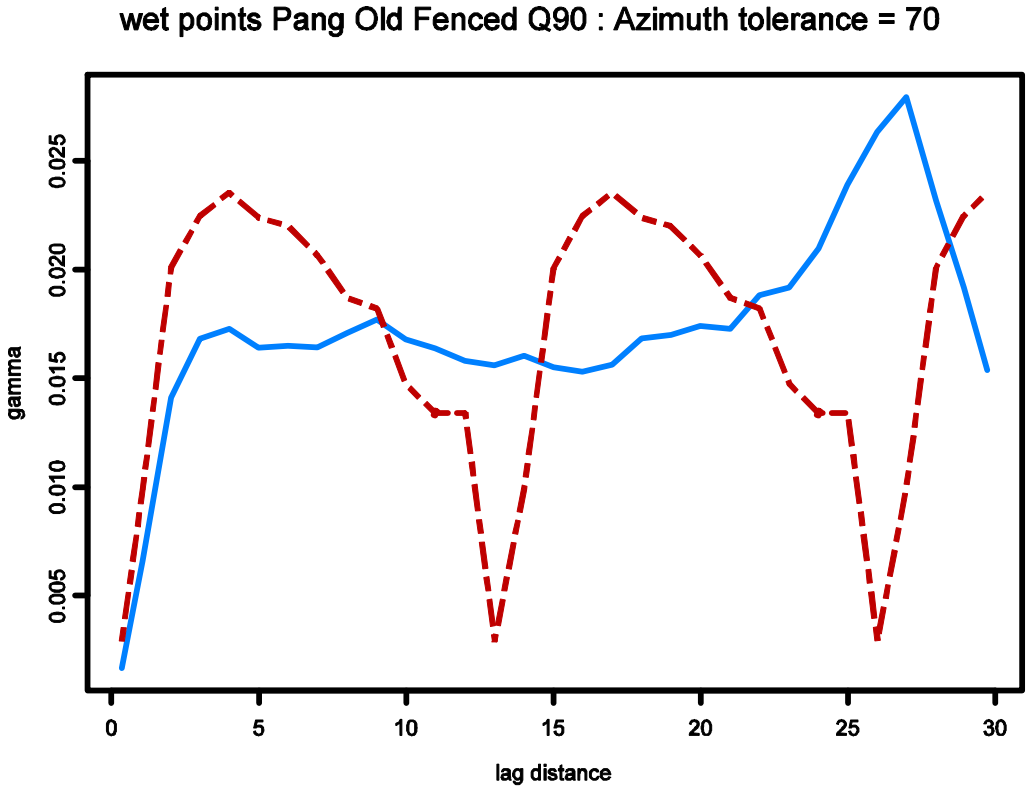
wet points Pang Old Fenced Q90 : Azimuth tolerance = 70
gamma
0.005
0.010
0.015
0.020
0.025
0
5
10
15
20
25
30
lag distance

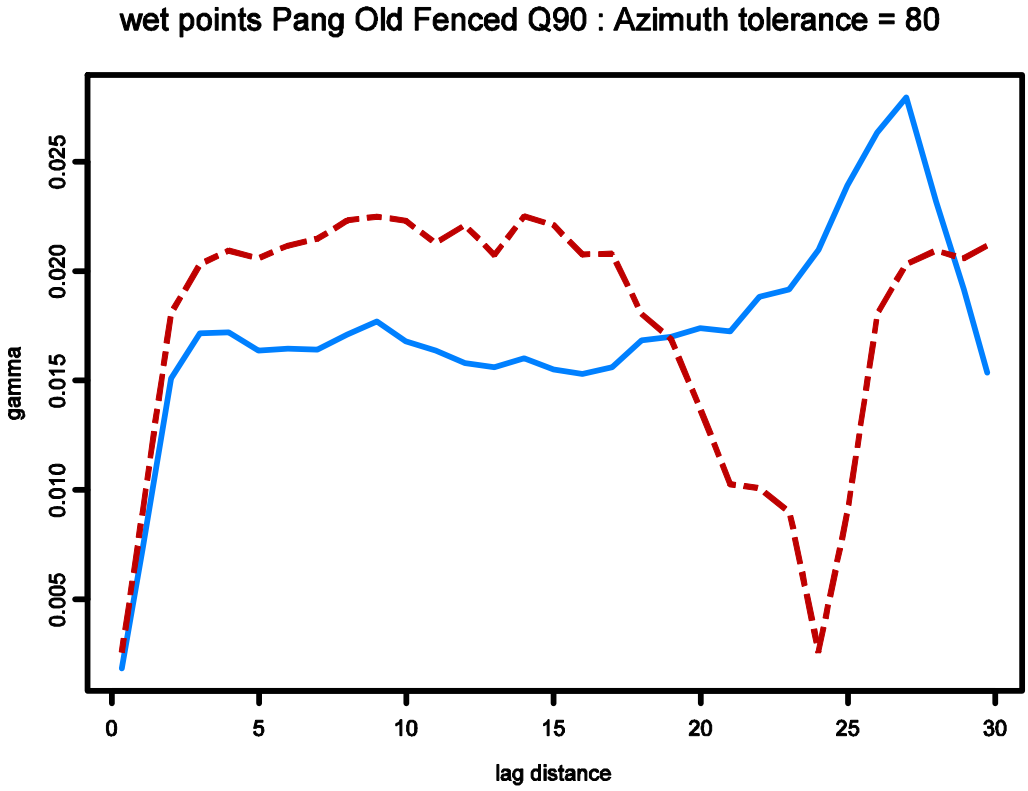
wet points Pang Old Fenced Q90 : Azimuth tolerance = 80
gamma
0.005
0.010
0.015
0.020
0.025
0
5
10
15
20
25
30
lag distance

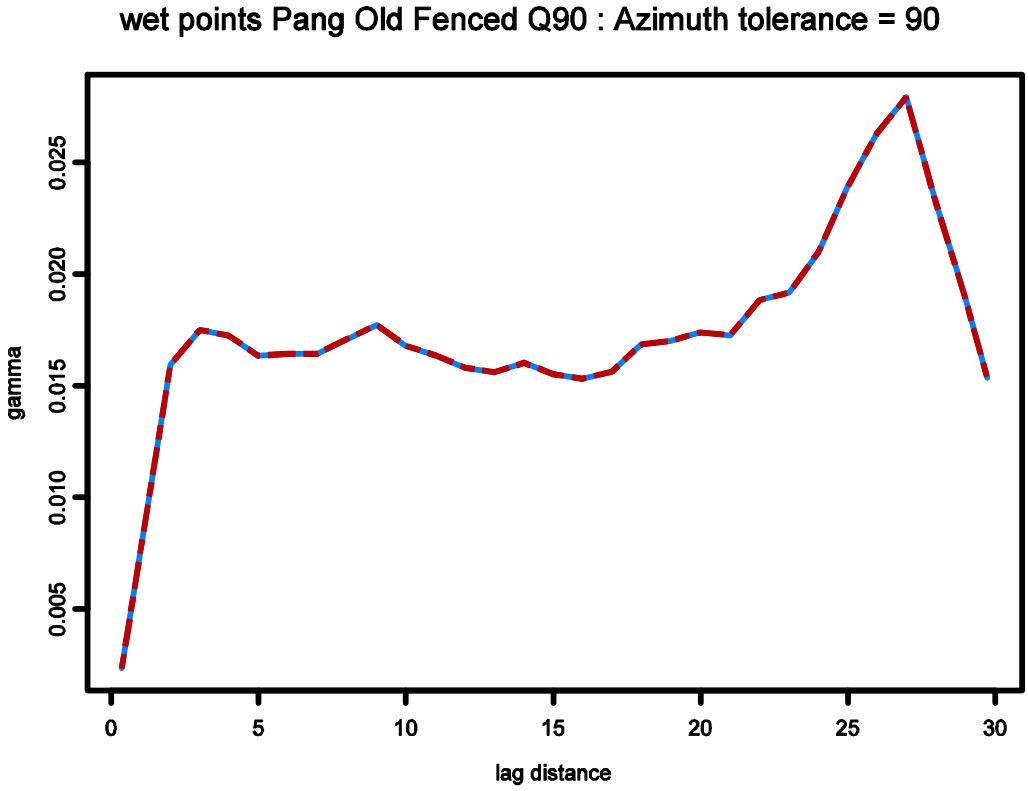
wet points Pang Old Fenced Q90 : Azimuth tolerance = 90
gamma
0.005
0.010
0.015
0.020
0.025
0
5
10
15
20
25
30
lag distance

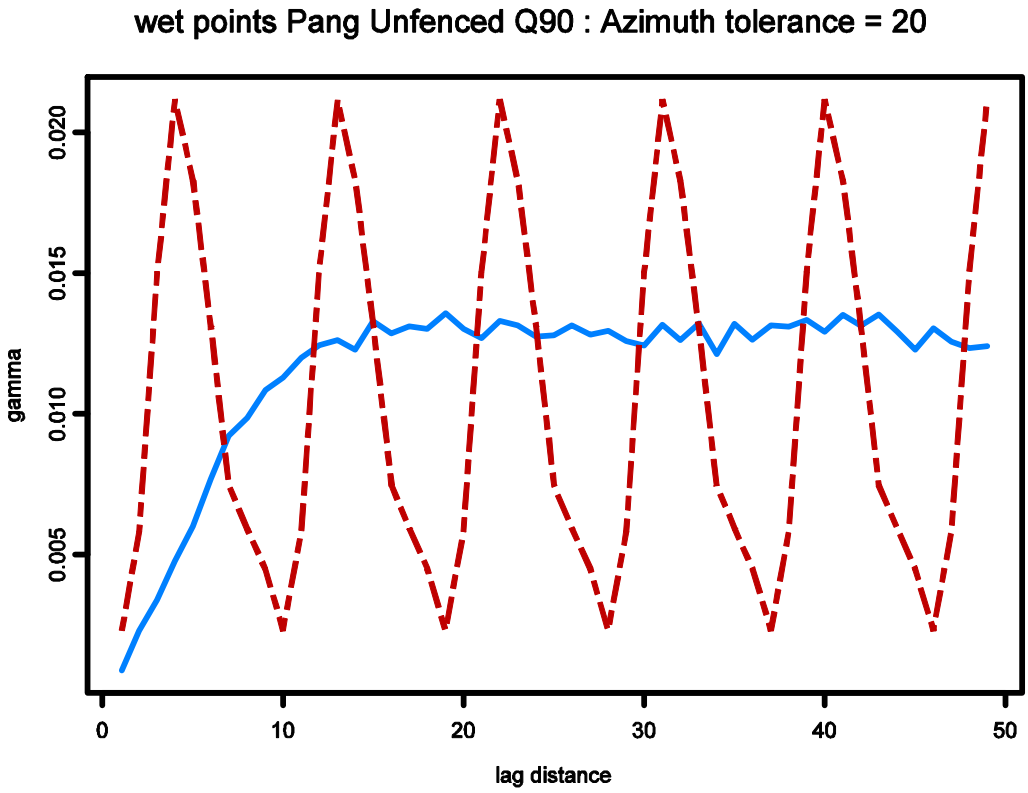
wet points Pang Unfenced Q90 : Azimuth tolerance = 20
gamma
0.005
0.010
0.015
0.020
0
10
20
30
40
50
lag distance

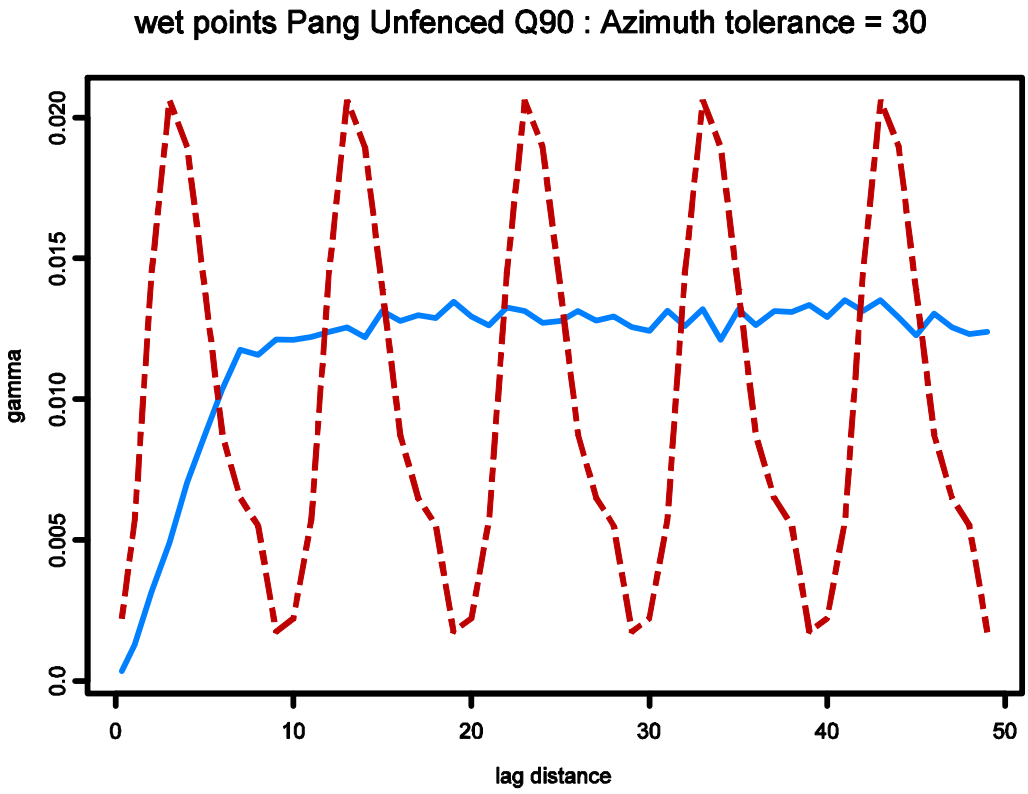
wet points Pang Unfenced Q90 : Azimuth tolerance = 30
gamma
0.0
0.005
0.010
0.015
0.020
0
10
20
30
40
50
lag distance

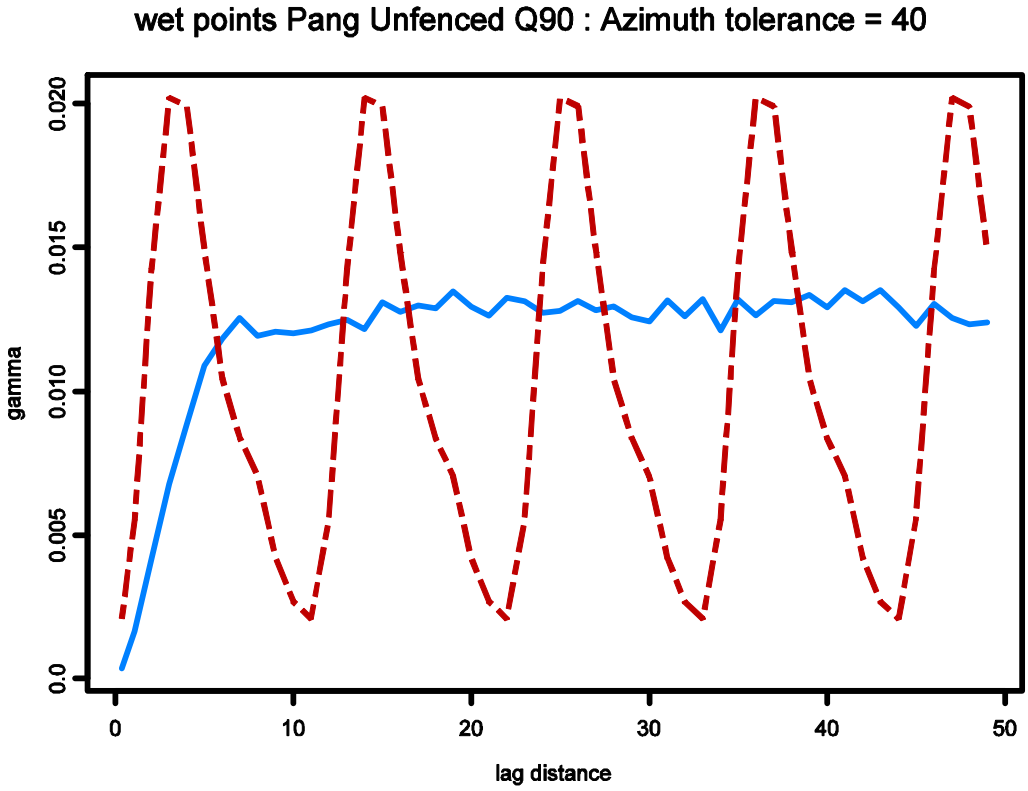
wet points Pang Unfenced Q90 : Azimuth tolerance = 40
gamma
0.0
0.005
0.010
0.015
0.020
0
10
20
30
40
50
lag distance

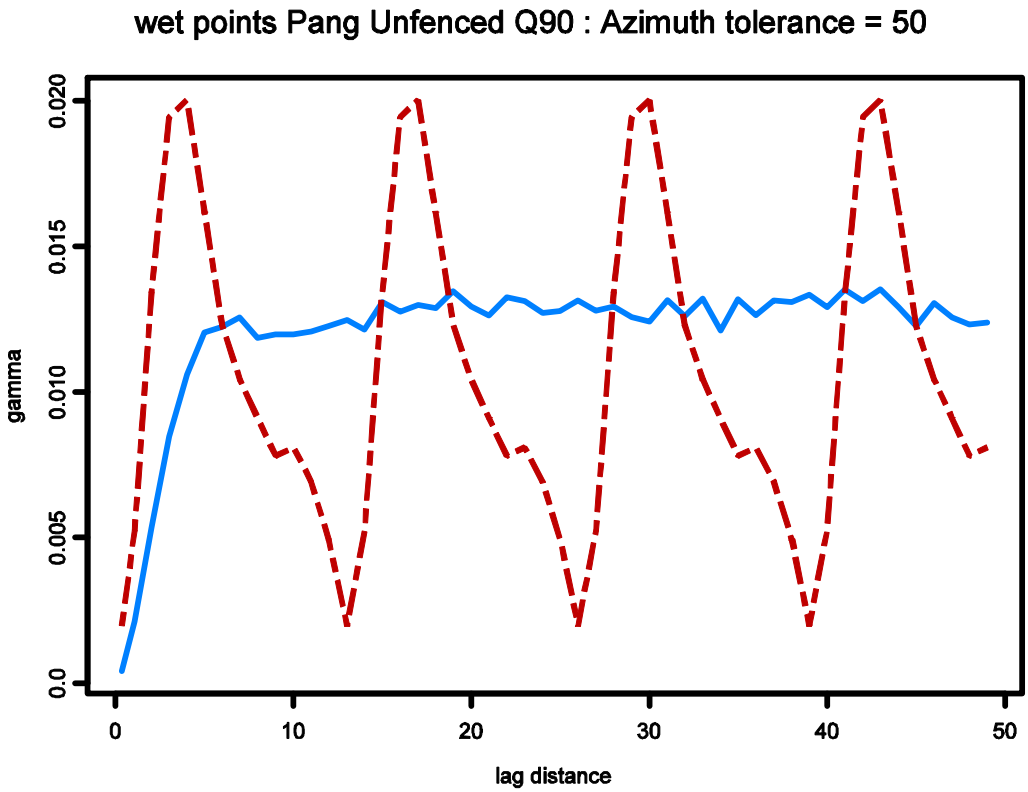
wet points Pang Unfenced Q90 : Azimuth tolerance = 50
gamma
0.0
0.005
0.010
0.015
0.020
0
10
20
30
40
50
lag distance

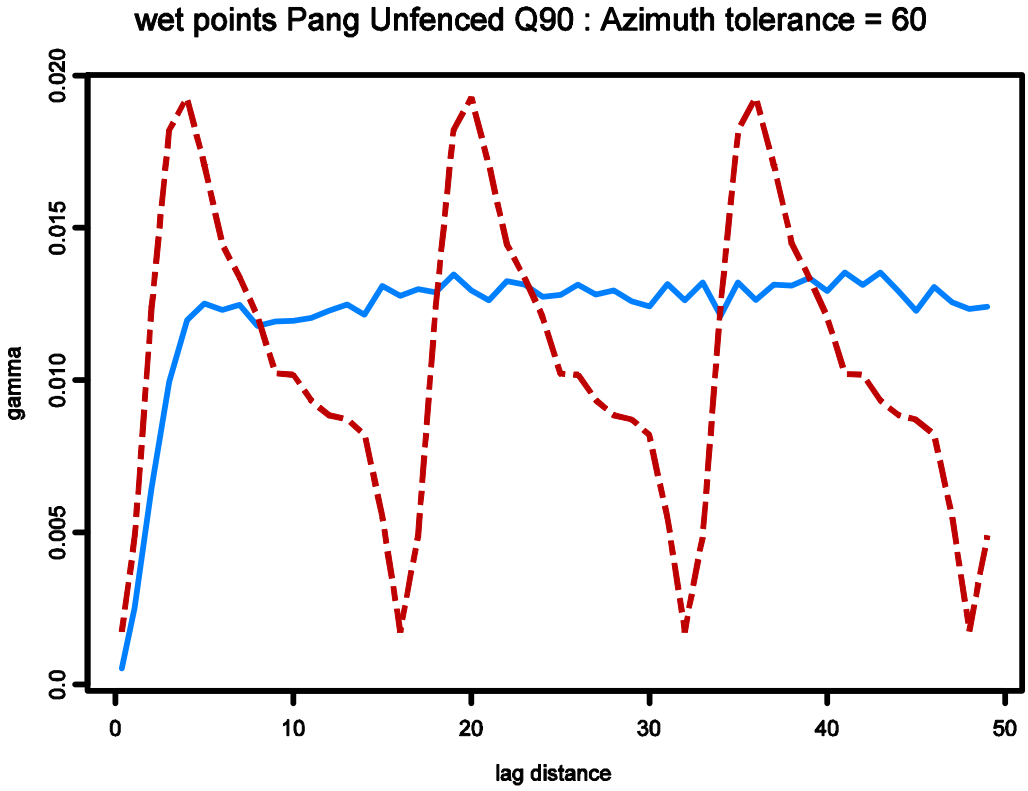
wet points Pang Unfenced Q90 : Azimuth tolerance = 60
gamma
0.0
0.005
0.010
0.015
0.020
0
10
20
30
40
50
lag distance

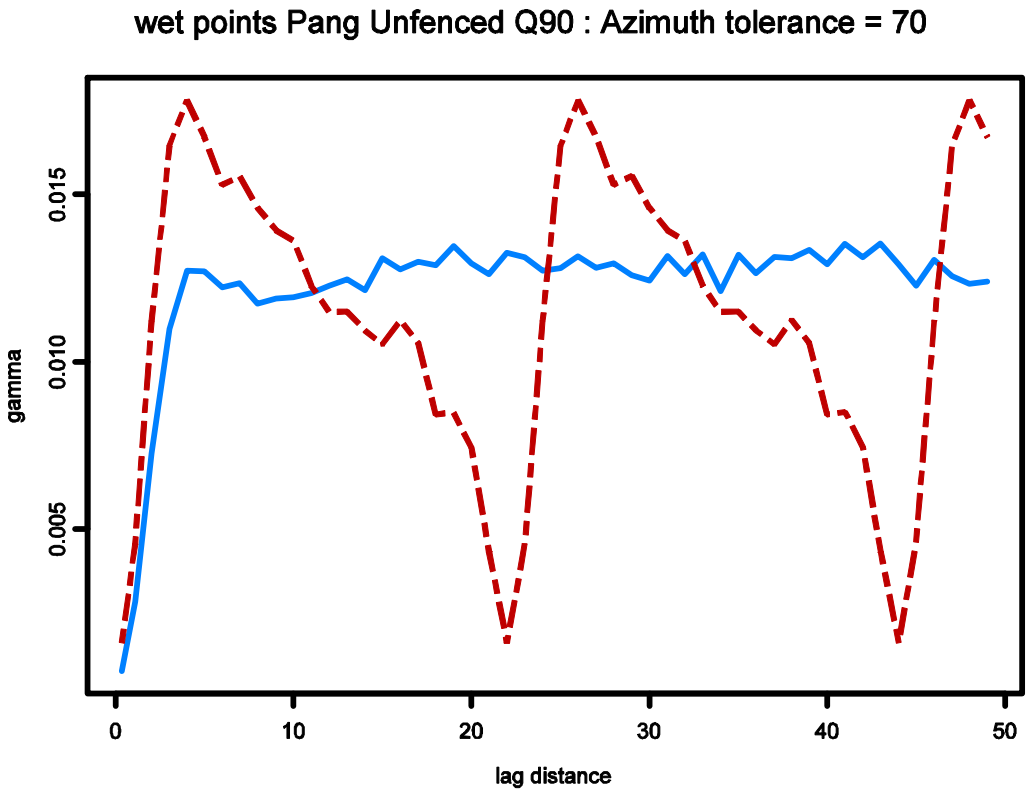
wet points Pang Unfenced Q90 : Azimuth tolerance = 70
gamma
0.005
0.010
0.015
0
10
20
30
40
50
lag distance

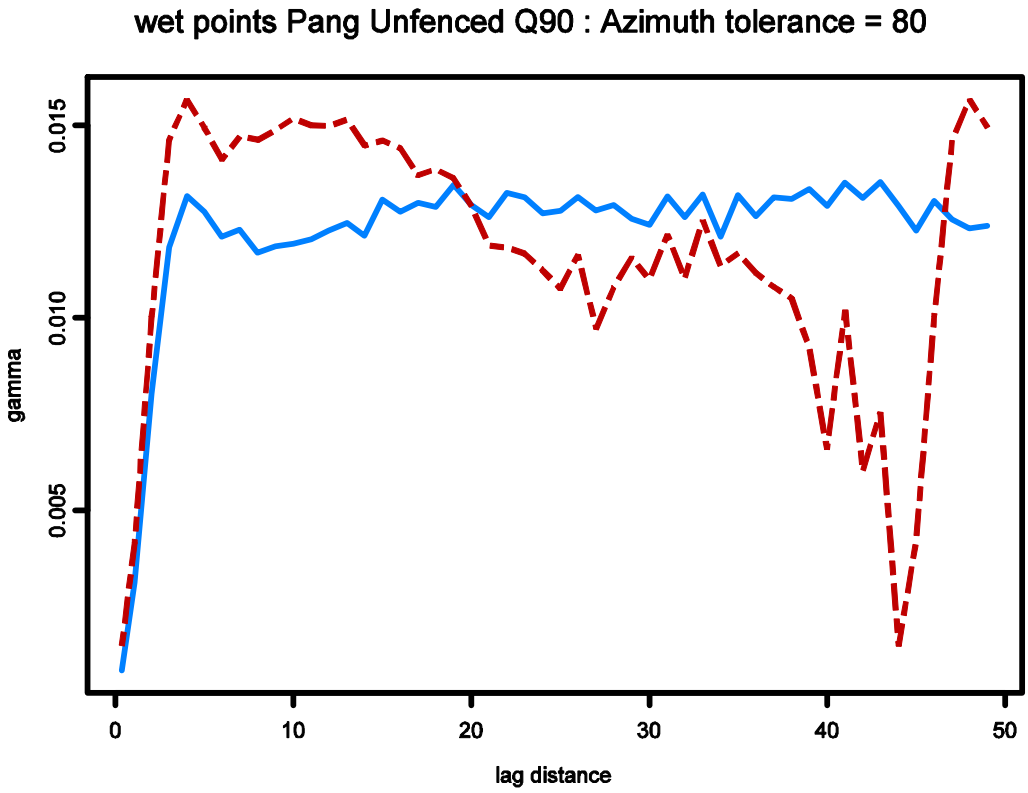
wet points Pang Unfenced Q90 : Azimuth tolerance = 80
gamma
0.005
0.010
0.015
0
10
20
30
40
50
lag distance

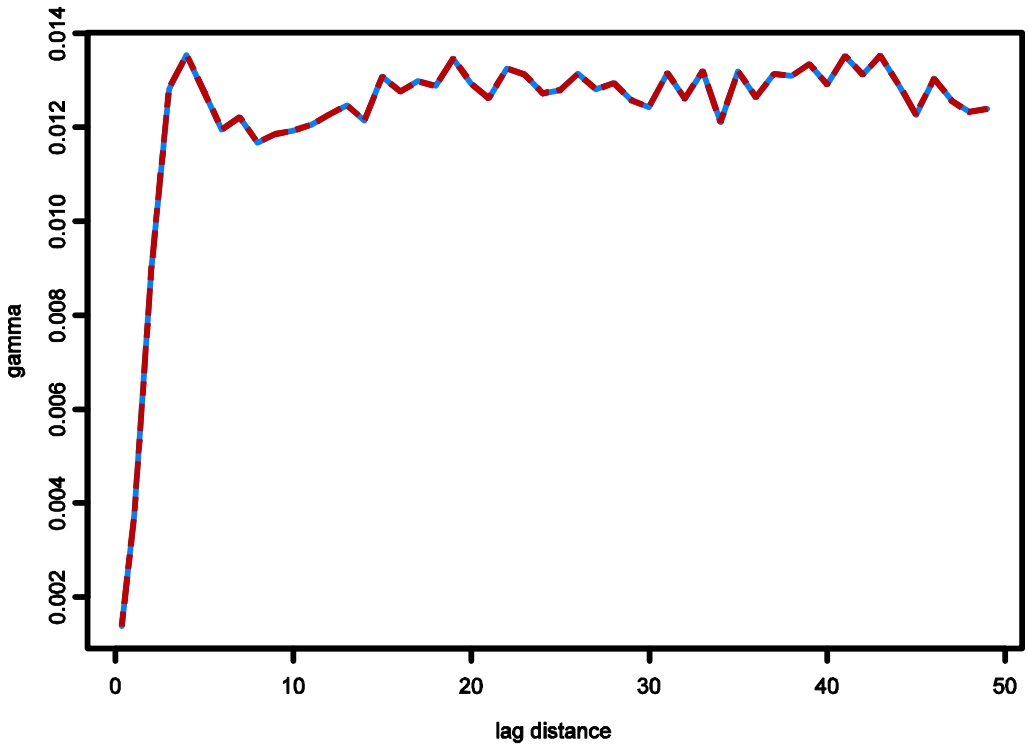
wet points Pang Unfenced Q90 : Azimuth tolerance = 90
gamma
0.002
0.004
0.006
0.008
0.010
0.012
0.014
0
10
20
30
40
50
lag distance

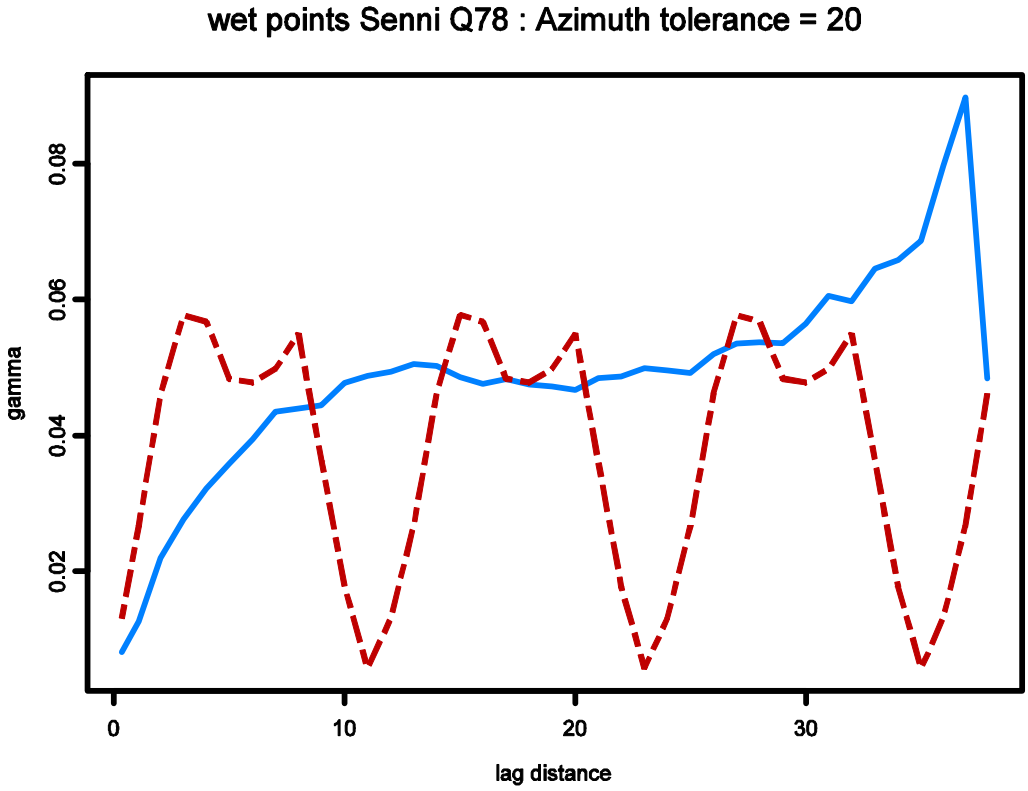
wet points Senni Q78 : Azimuth tolerance = 20
gamma
0.02
0.04
0.06
0.08
0
10
20
30
lag distance

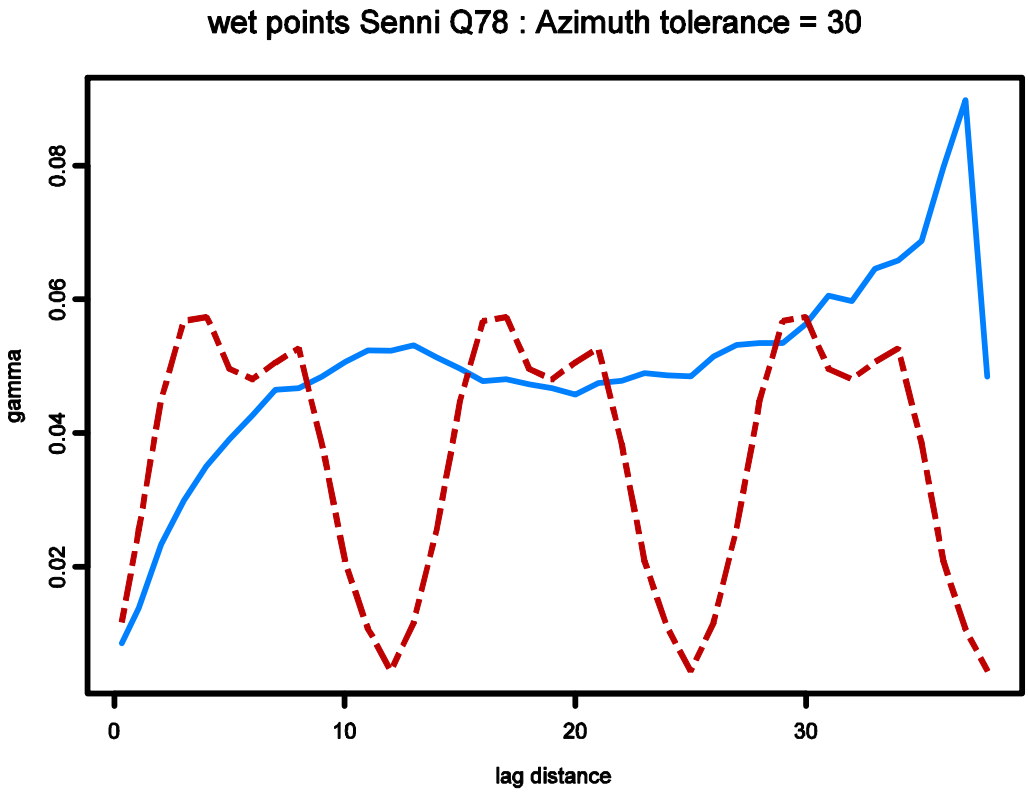
wet points Senni Q78 : Azimuth tolerance = 30
gamma
0.02
0.04
0.06
0.08
0
10
20
30
lag distance

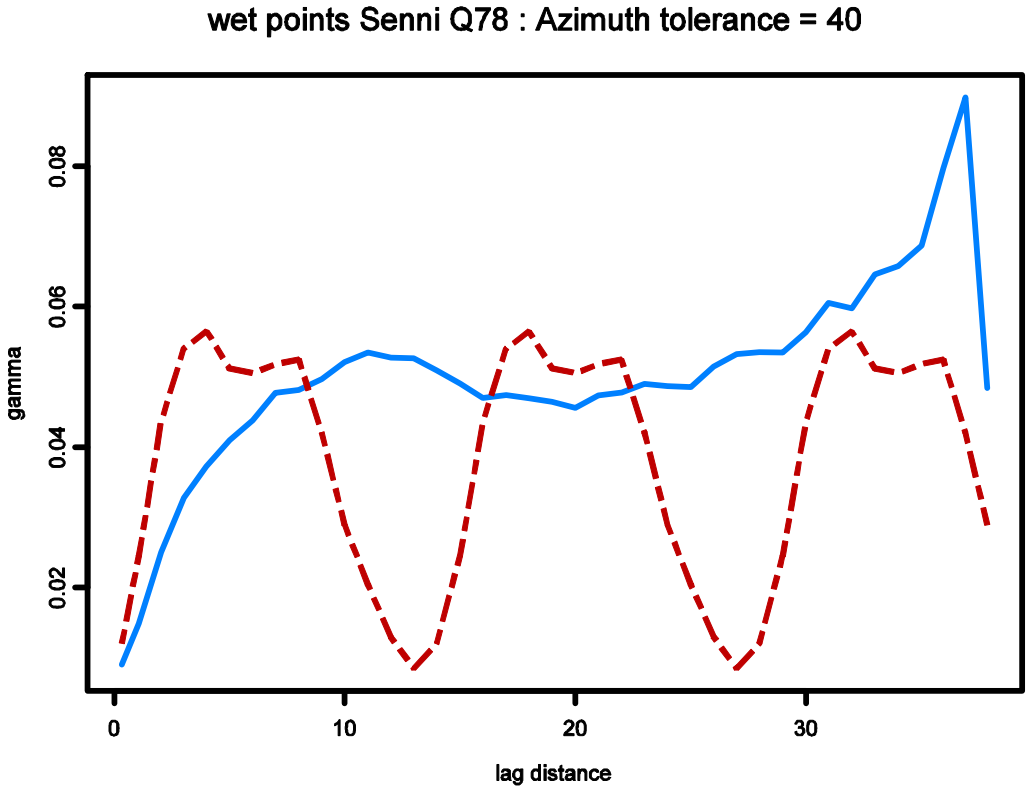
wet points Senni Q78 : Azimuth tolerance = 40
gamma
0.02
0.04
0.06
0.08
0
10
20
30
lag distance

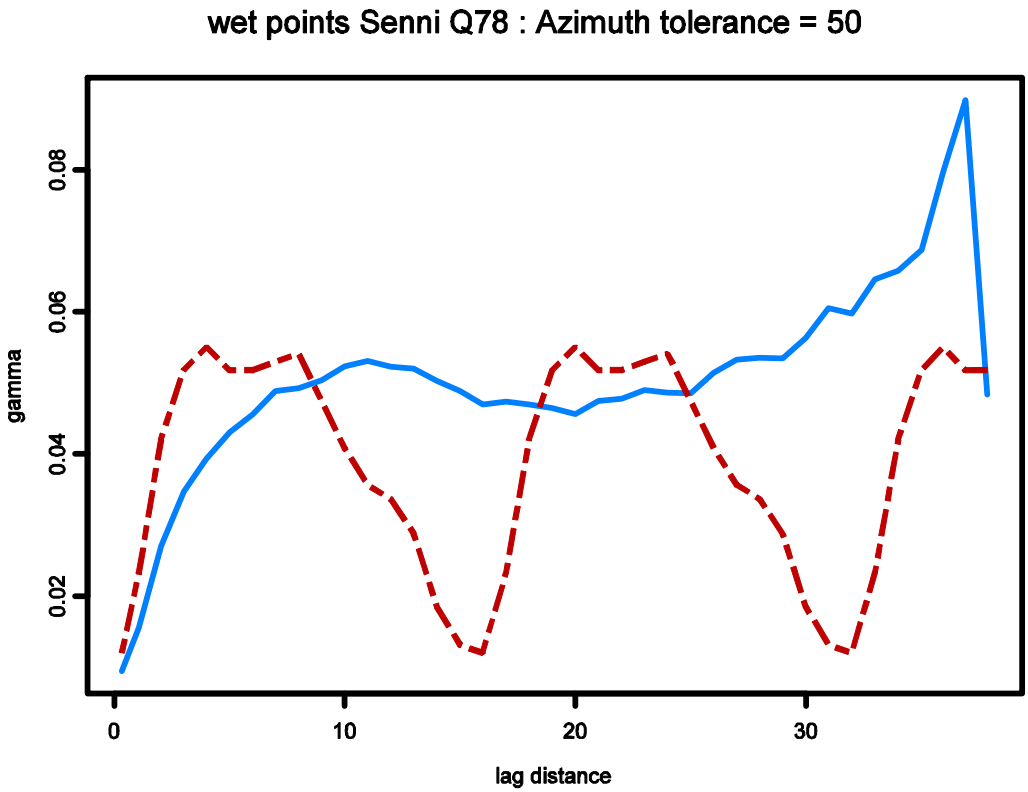
wet points Senni Q78 : Azimuth tolerance = 50
gamma
0.02
0.04
0.06
0.08
0
10
20
30
lag distance

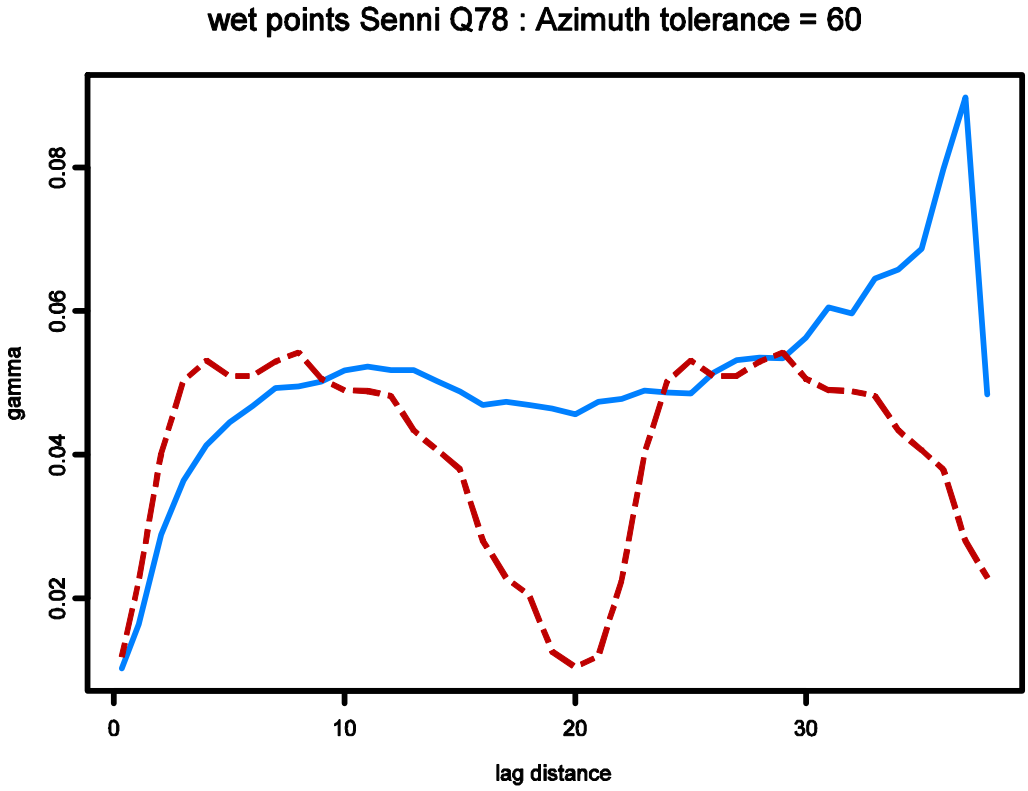
wet points Senni Q78 : Azimuth tolerance = 60
gamma
0.02
0.04
0.06
0.08
0
10
20
30
lag distance

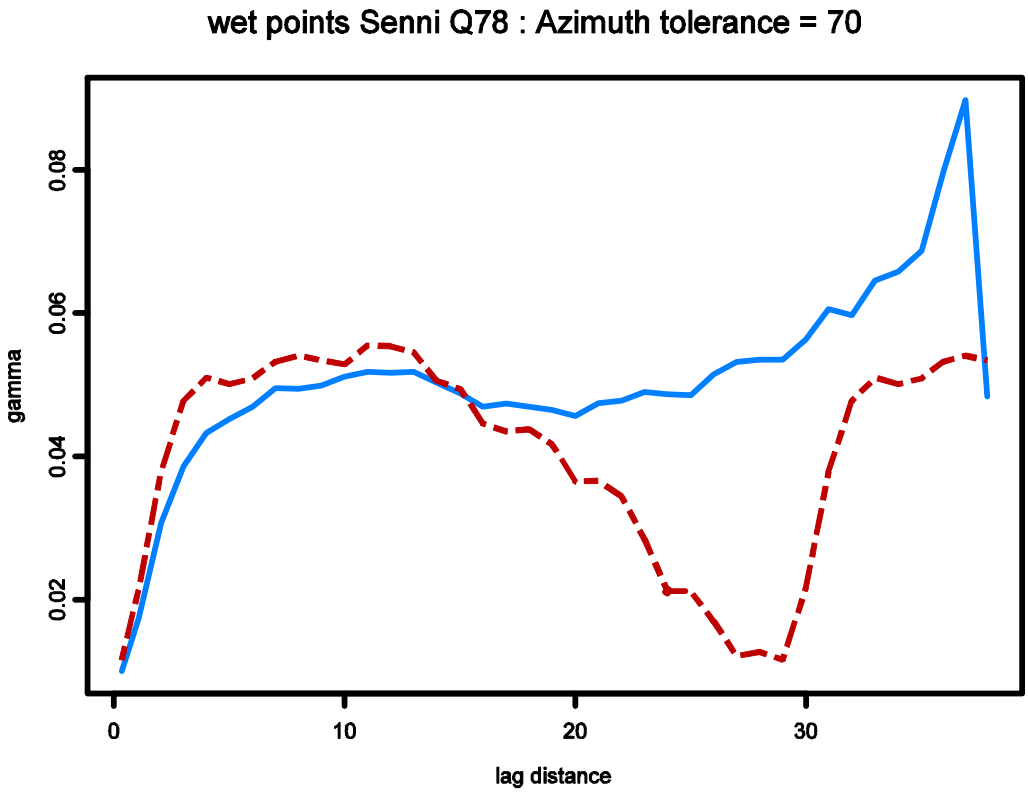
wet points Senni Q78 : Azimuth tolerance = 70
gamma
0.02
0.04
0.06
0.08
0
10
20
30
lag distance

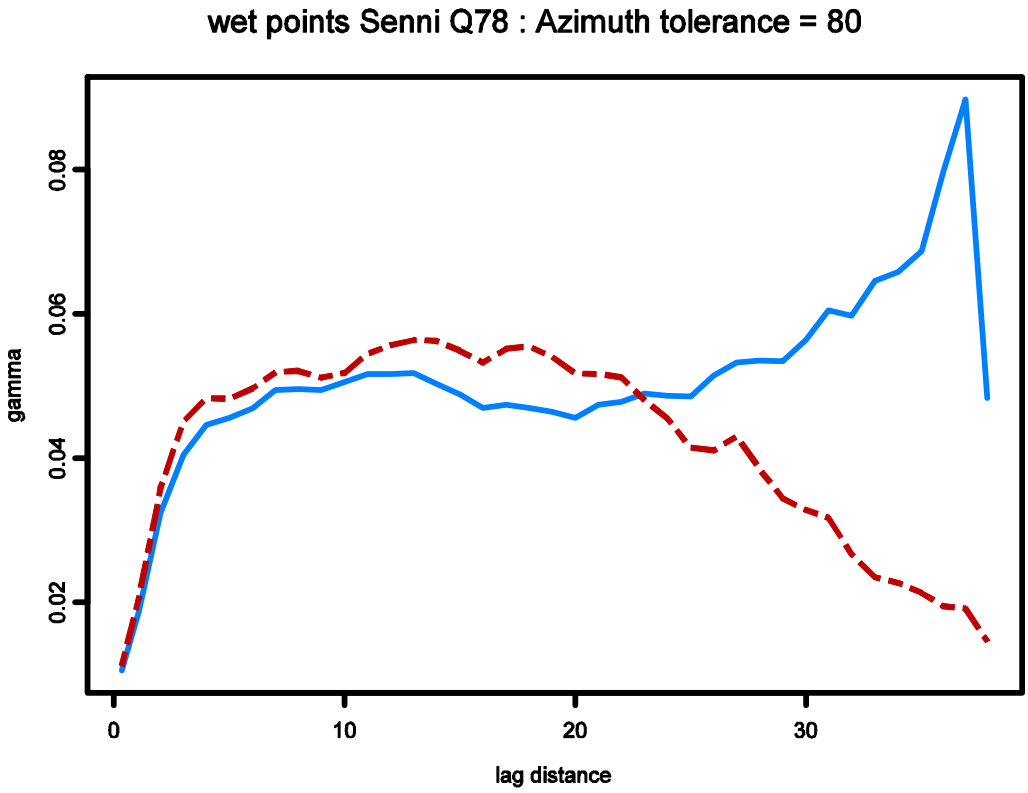
wet points Senni Q78 : Azimuth tolerance = 80
gamma
0.02
0.04
0.06
0.08
0
10
20
30
lag distance

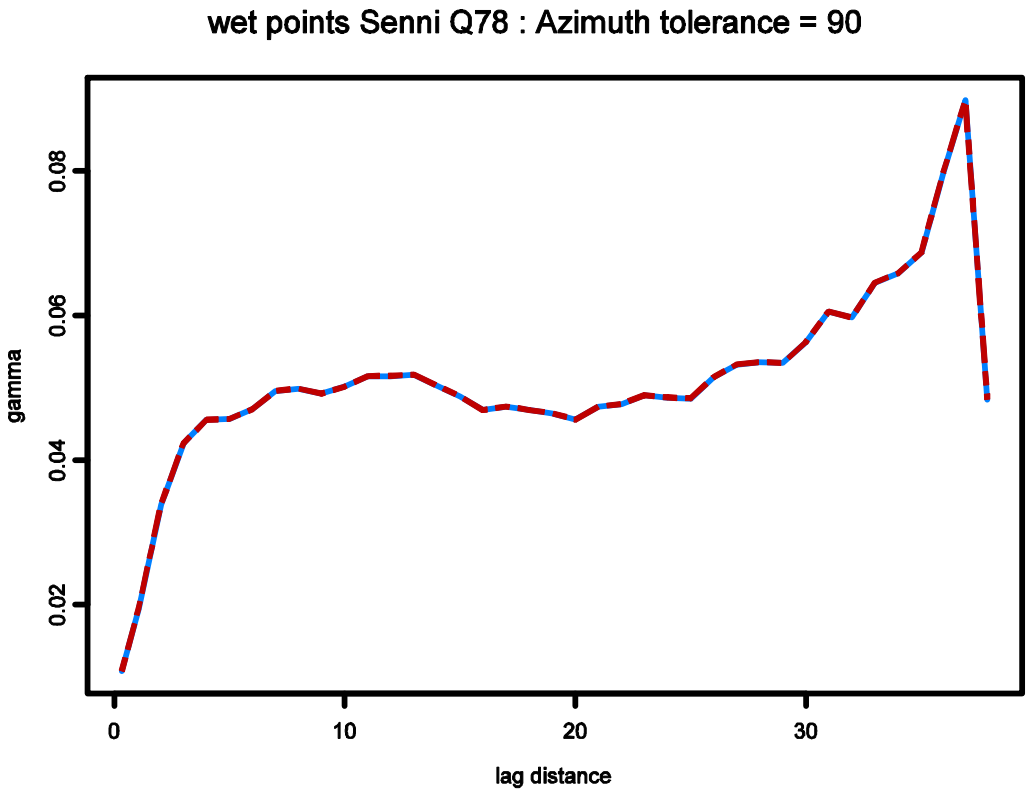
wet points Senni Q78 : Azimuth tolerance = 90
gamma
0.02
0.04
0.06
0.08
0
10
20
30
lag distance

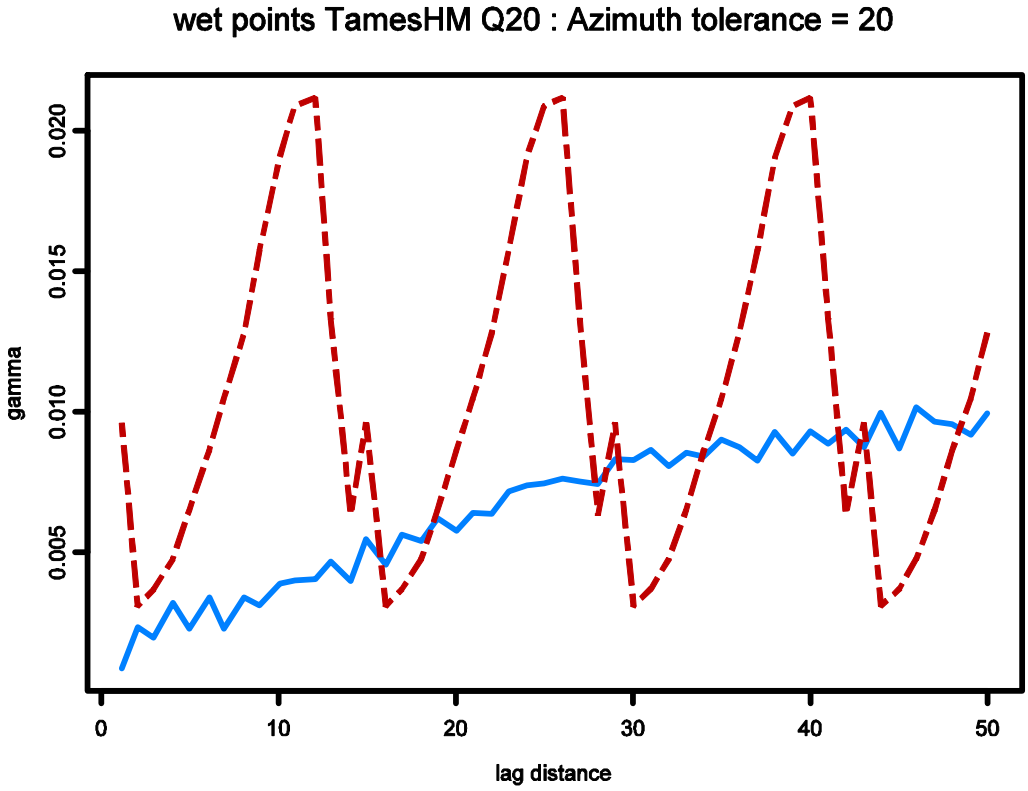
wet points TamesHM Q20 : Azimuth tolerance = 20
gamma
0.005
0.010
0.015
0.020
0
10
20
30
40
50
lag distance

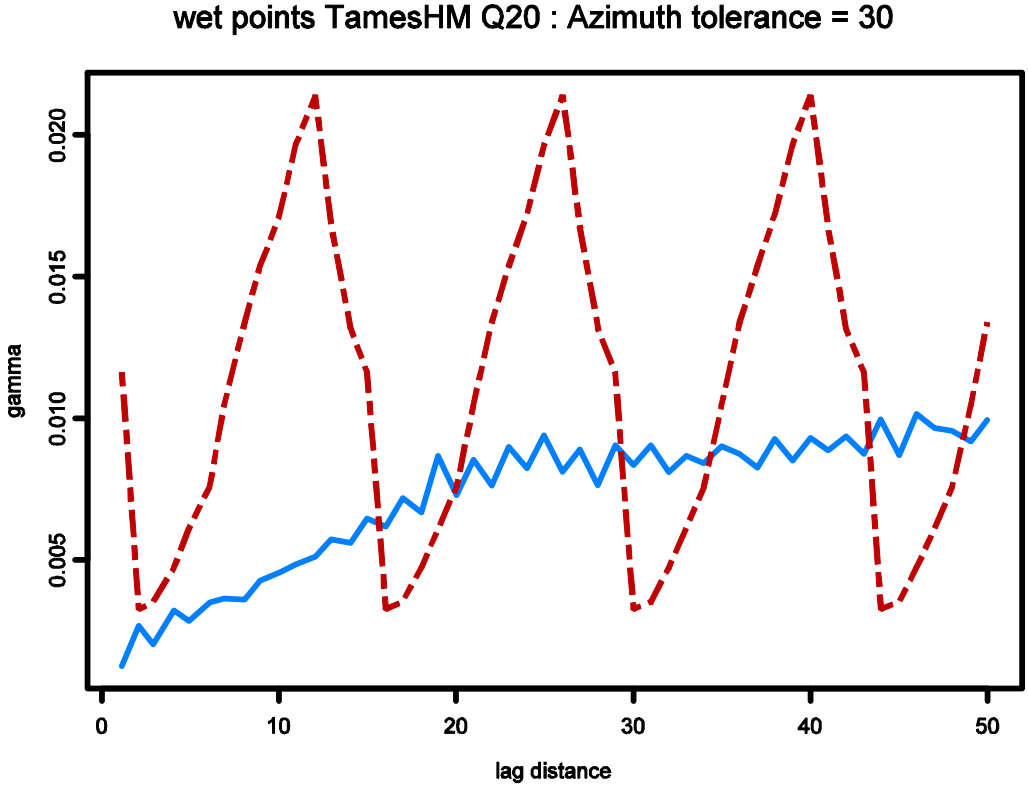
wet points TamesHM Q20 : Azimuth tolerance = 30
gamma
0.005
0.010
0.015
0.020
0
10
20
30
40
50
lag distance

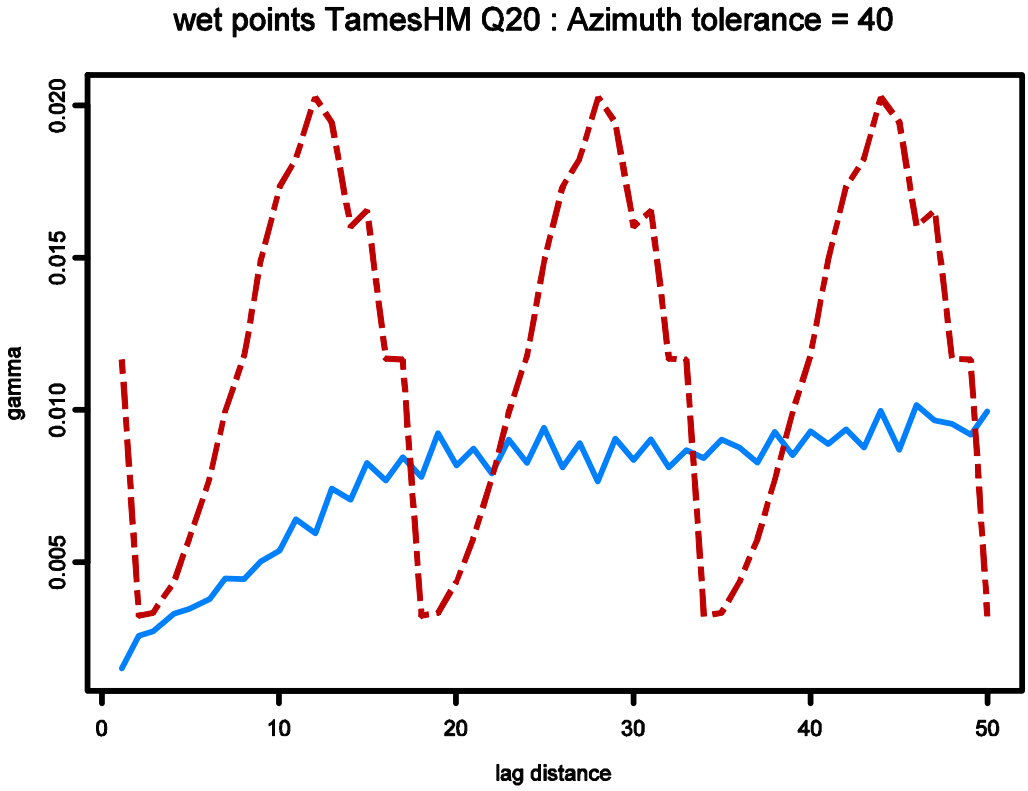
wet points TamesHM Q20 : Azimuth tolerance = 40
gamma
0.005
0.010
0.015
0.020
0
10
20
30
40
50
lag distance

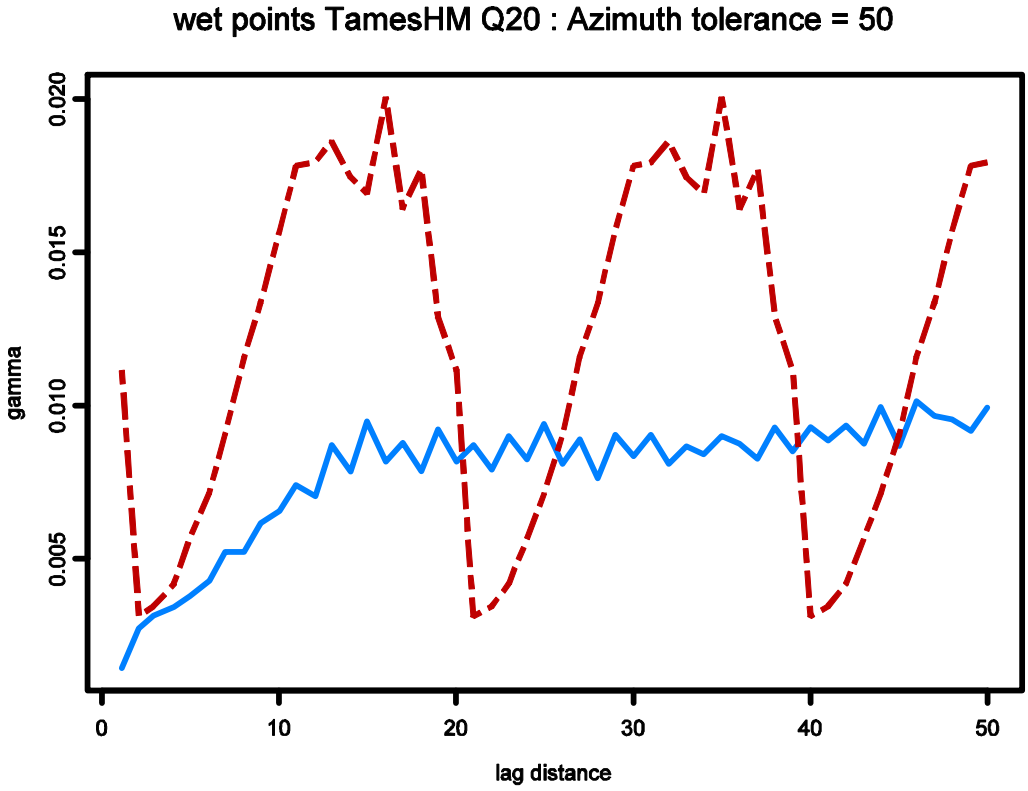
wet points TamesHM Q20 : Azimuth tolerance = 50
gamma
0.005
0.010
0.015
0.020
0
10
20
30
40
50
lag distance

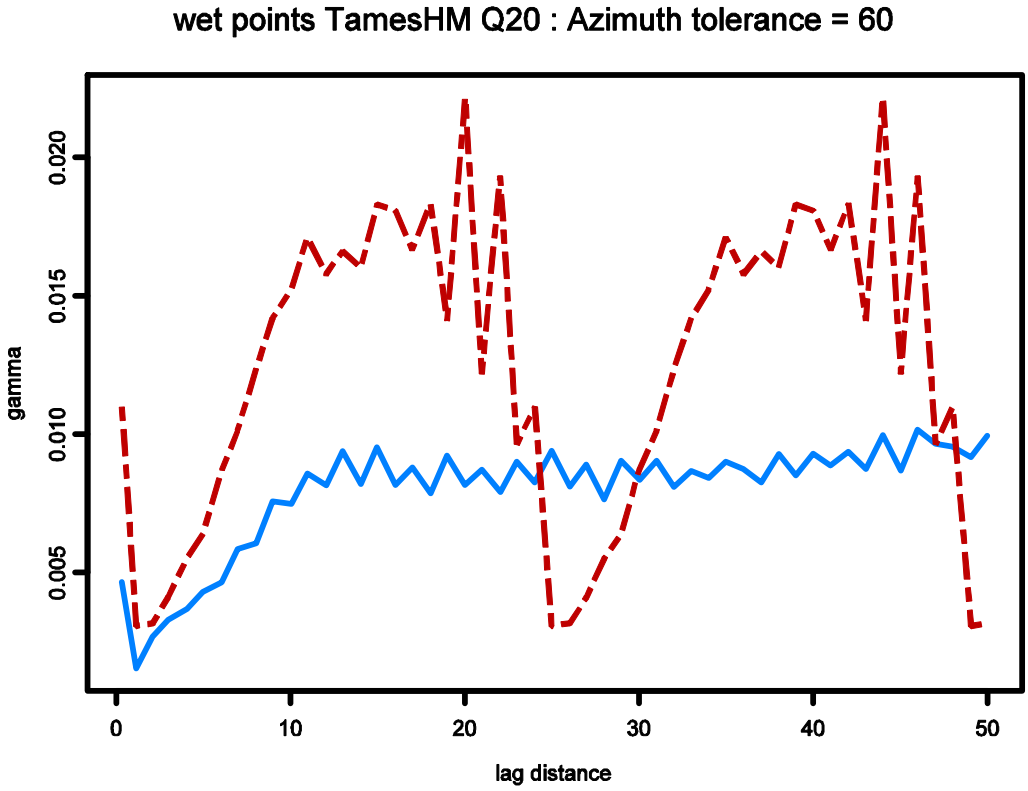
wet points TamesHM Q20 : Azimuth tolerance = 60
gamma
0.005
0.010
0.015
0.020
0
10
20
30
40
50
lag distance

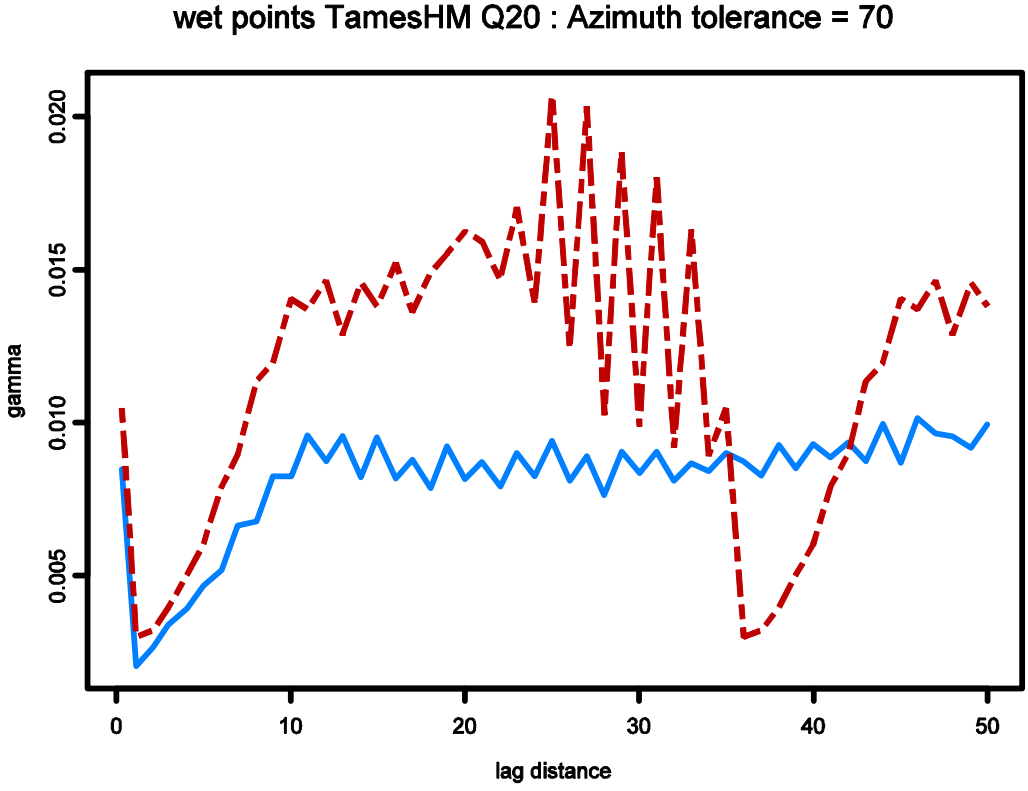
wet points TamesHM Q20 : Azimuth tolerance = 70
gamma
0.005
0.010
0.015
0.020
0
10
20
30
40
50
lag distance

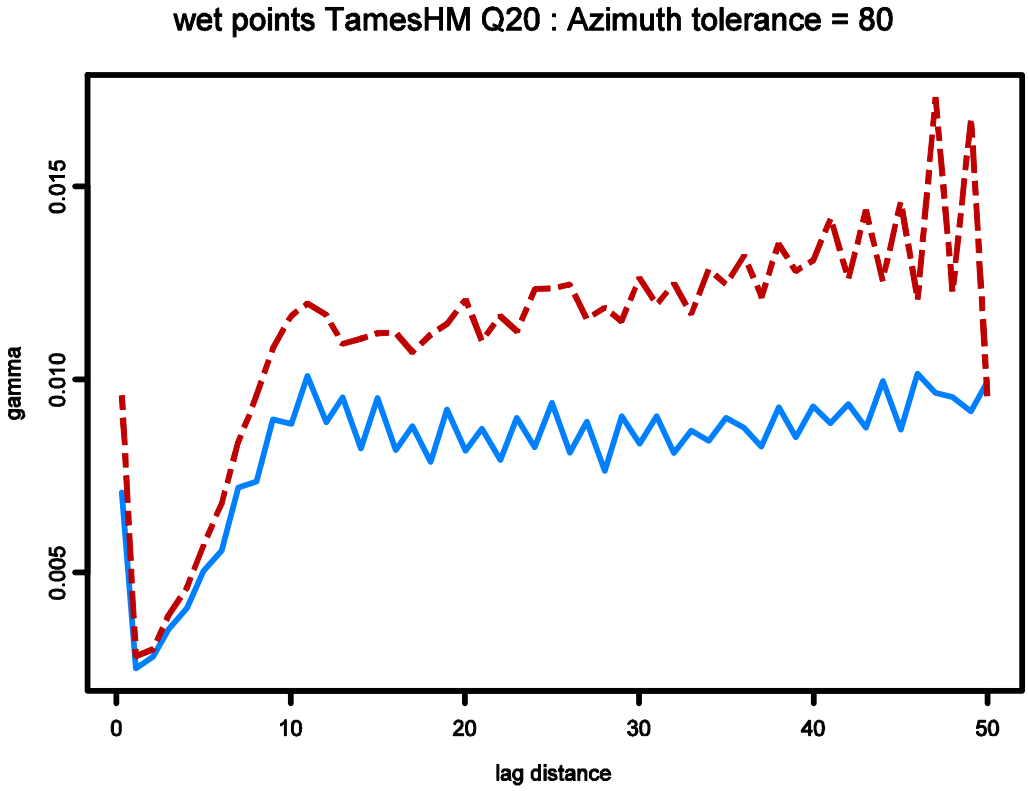
wet points TamesHM Q20 : Azimuth tolerance = 80
gamma
0.005
0.010
0.015
0
10
20
30
40
50
lag distance

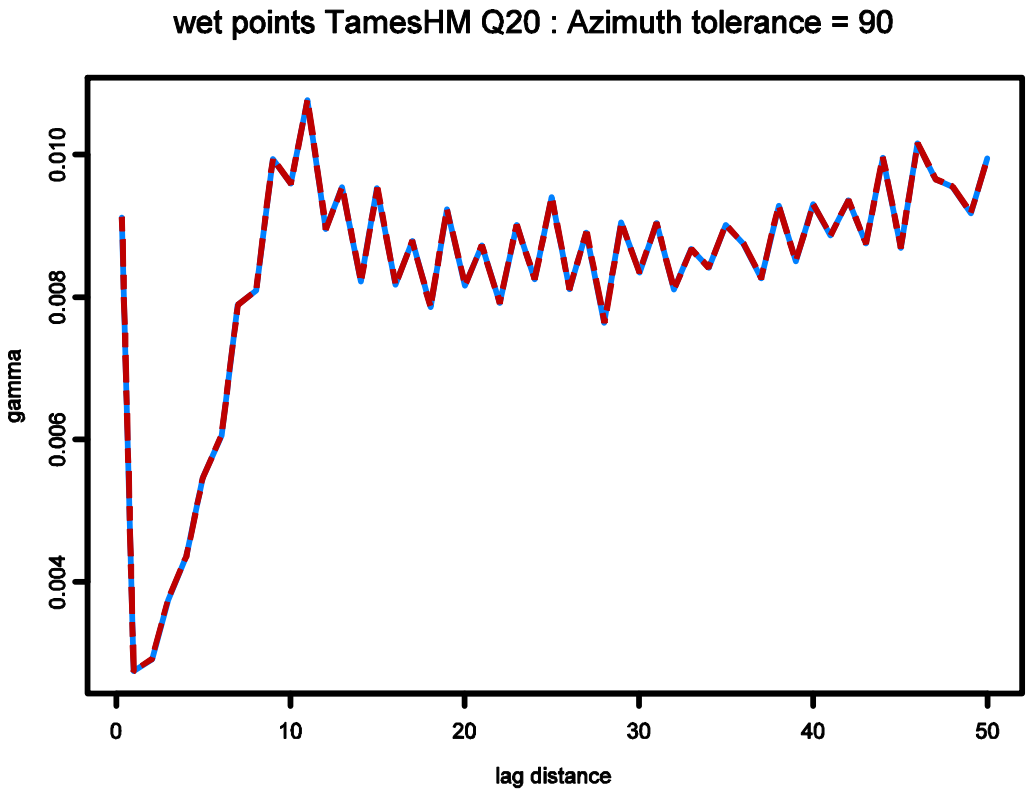
wet points TamesHM Q20 : Azimuth tolerance = 90
gamma
0.004
0.006
0.008
0.010
0
10
20
30
40
50
lag distance

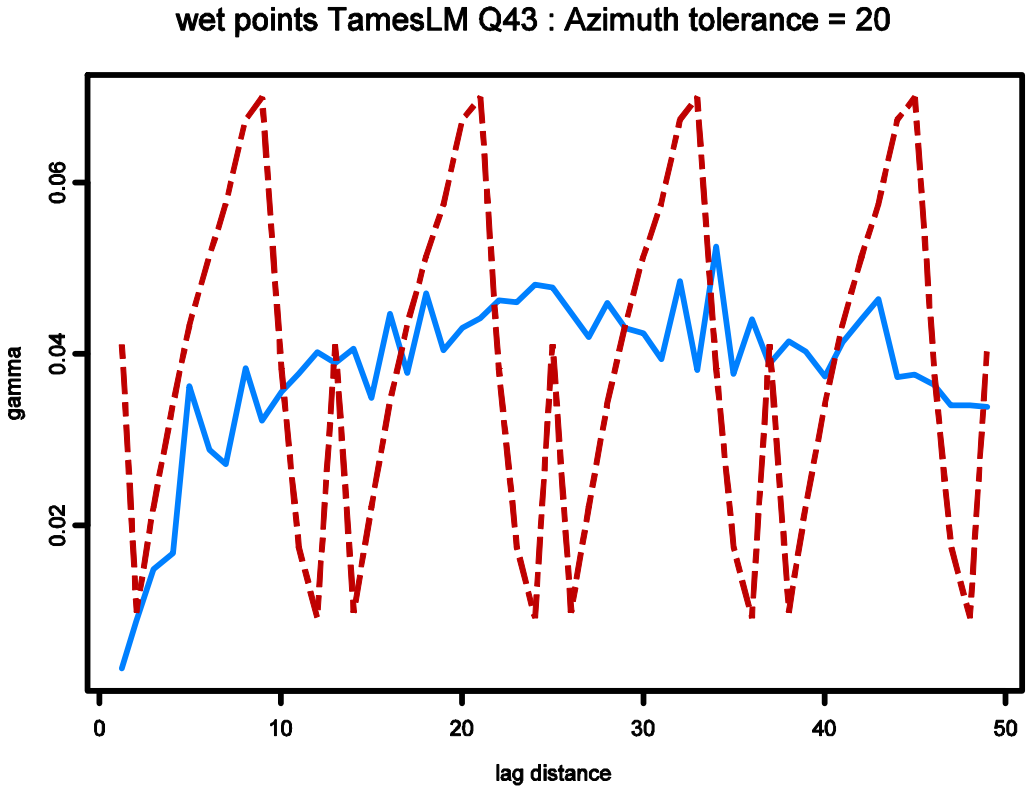
wet points TamesLM Q43 : Azimuth tolerance = 20
gamma
0.02
0.04
0.06
0
10
20
30
40
50
lag distance

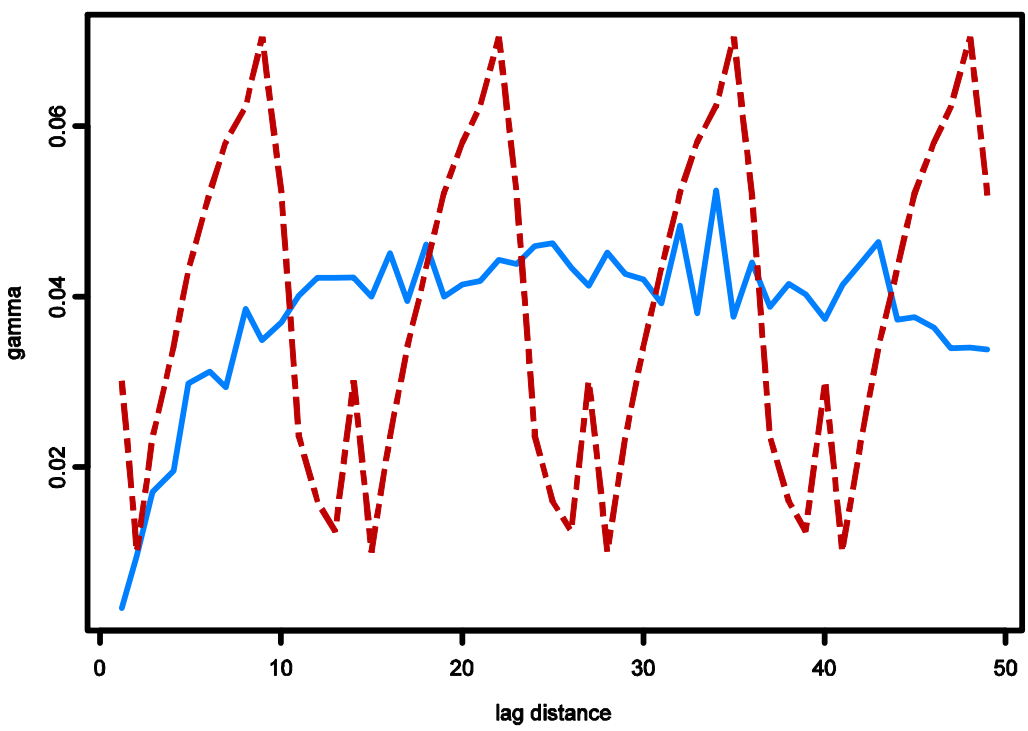
wet points TamesLM Q43 : Azimuth tolerance = 30
gamma
0.02
0.04
0.06
0
10
20
30
40
50
lag distance

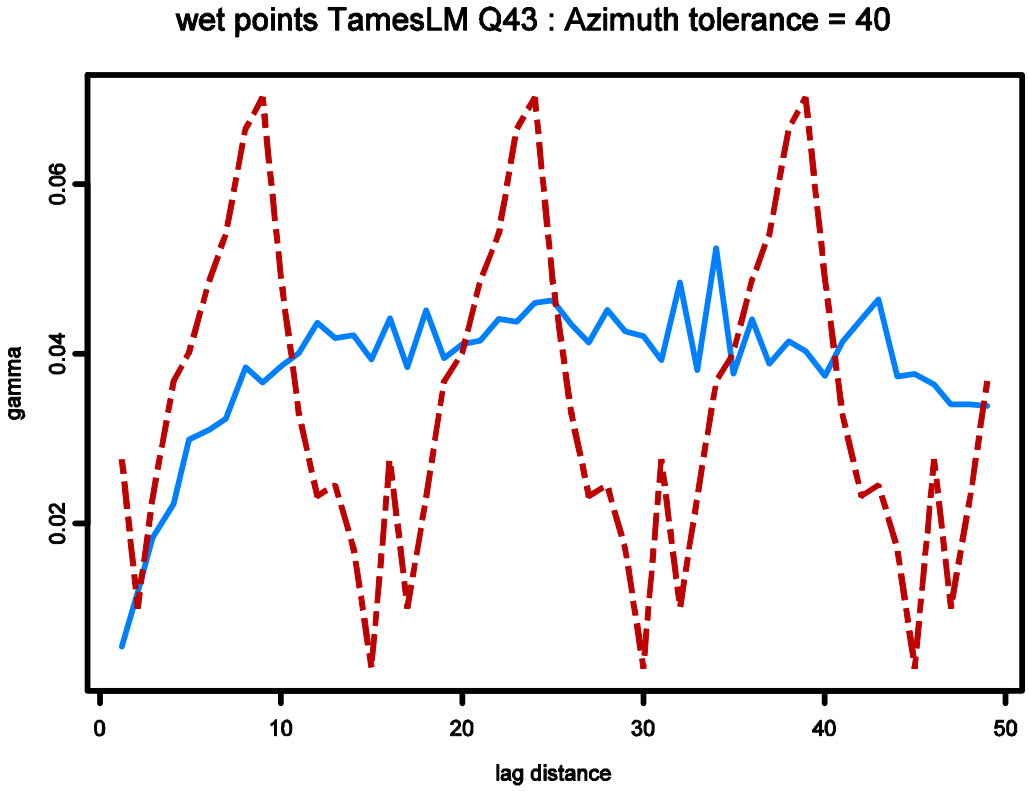
wet points TamesLM Q43 : Azimuth tolerance = 40
gamma
0.02
0.04
0.06
0
10
20
30
40
50
lag distance

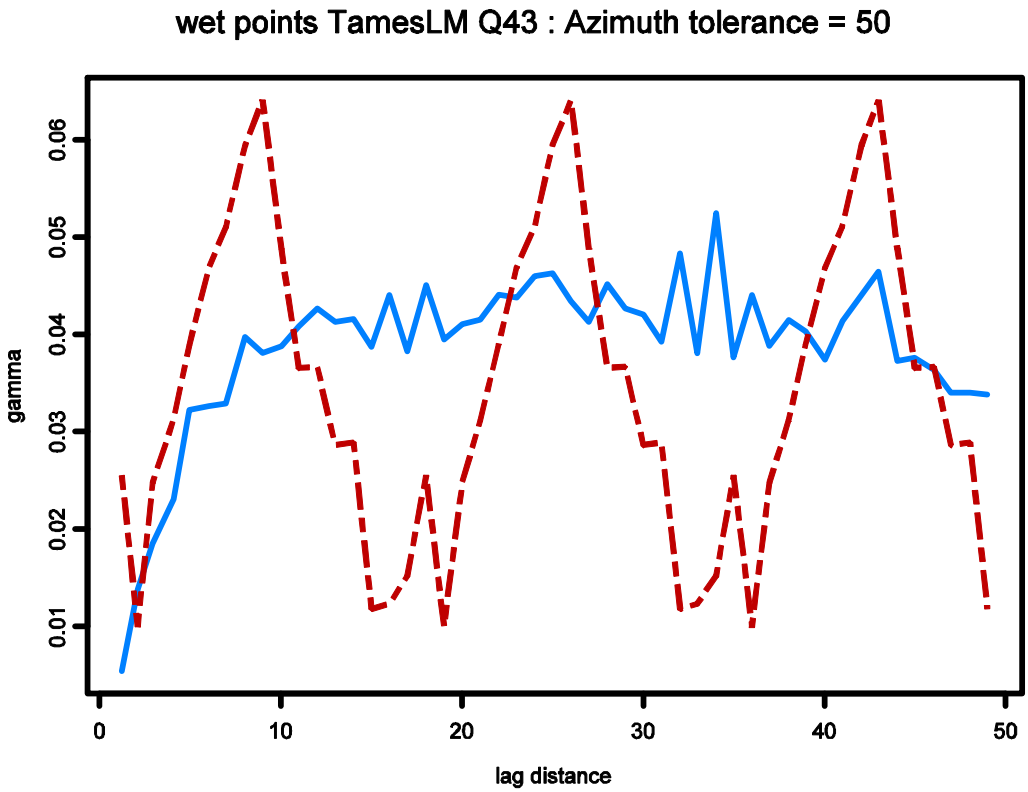
wet points TamesLM Q43 : Azimuth tolerance = 50
gamma
0.01
0.02
0.03
0.04
0.05
0.06
0
10
20
30
40
50
lag distance

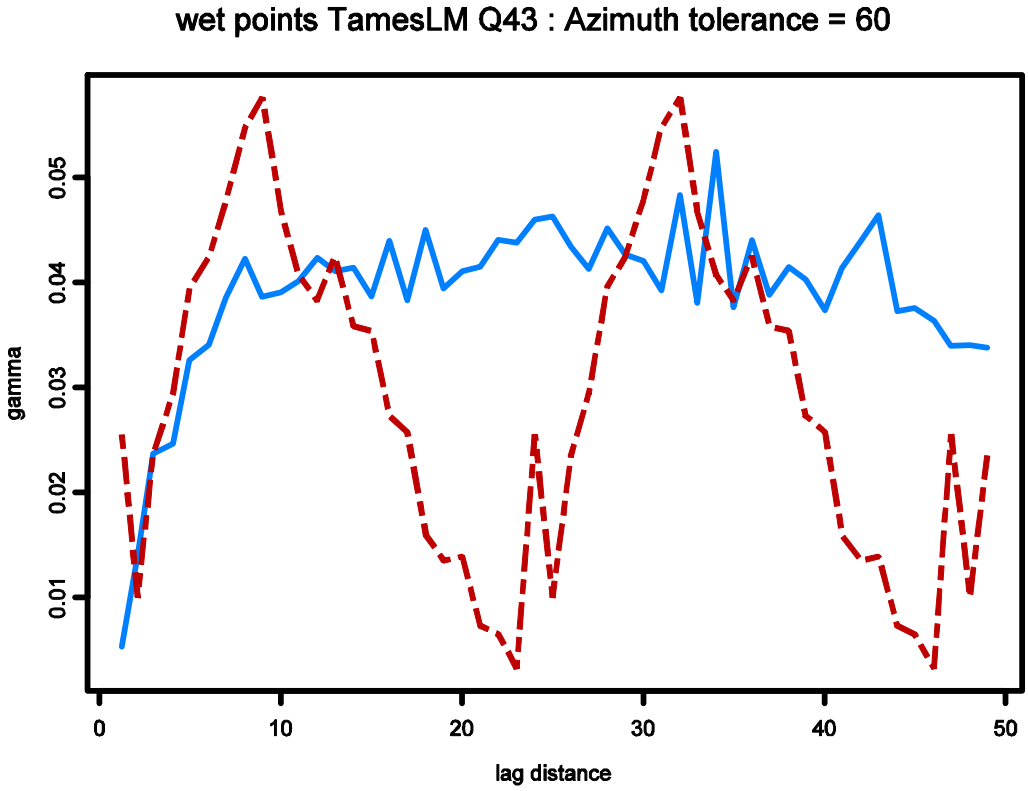
wet points TamesLM Q43 : Azimuth tolerance = 60
gamma
0.01
0.02
0.03
0.04
0.05
0
10
20
30
40
50
lag distance

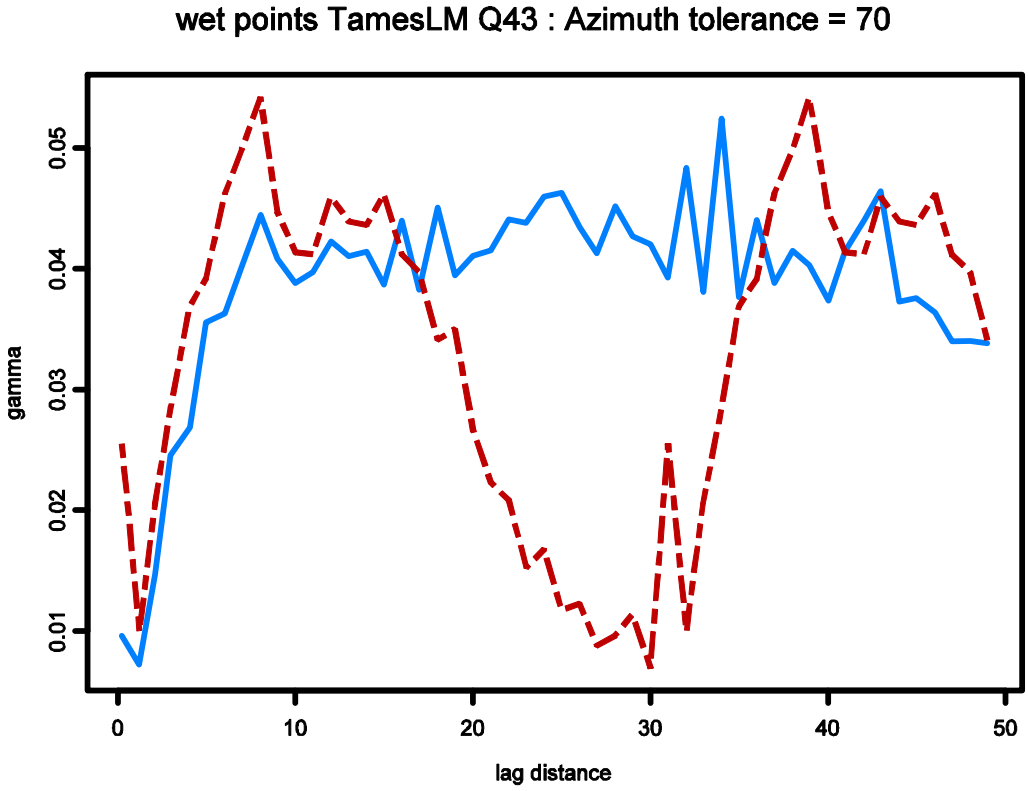
wet points TamesLM Q43 : Azimuth tolerance = 70
gamma
0.01
0.02
0.03
0.04
0.05
0
10
20
30
40
50
lag distance

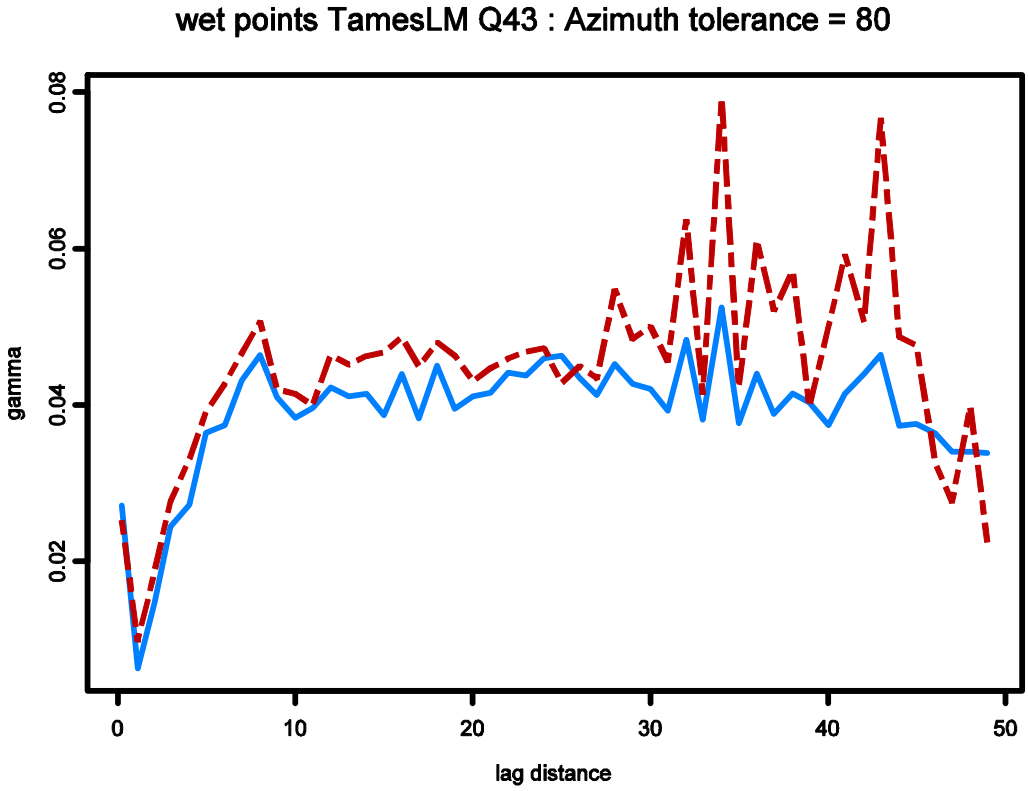
wet points TamesLM Q43 : Azimuth tolerance = 80
gamma
0.02
0.04
0.06
0.08
0
10
20
30
40
50
lag distance

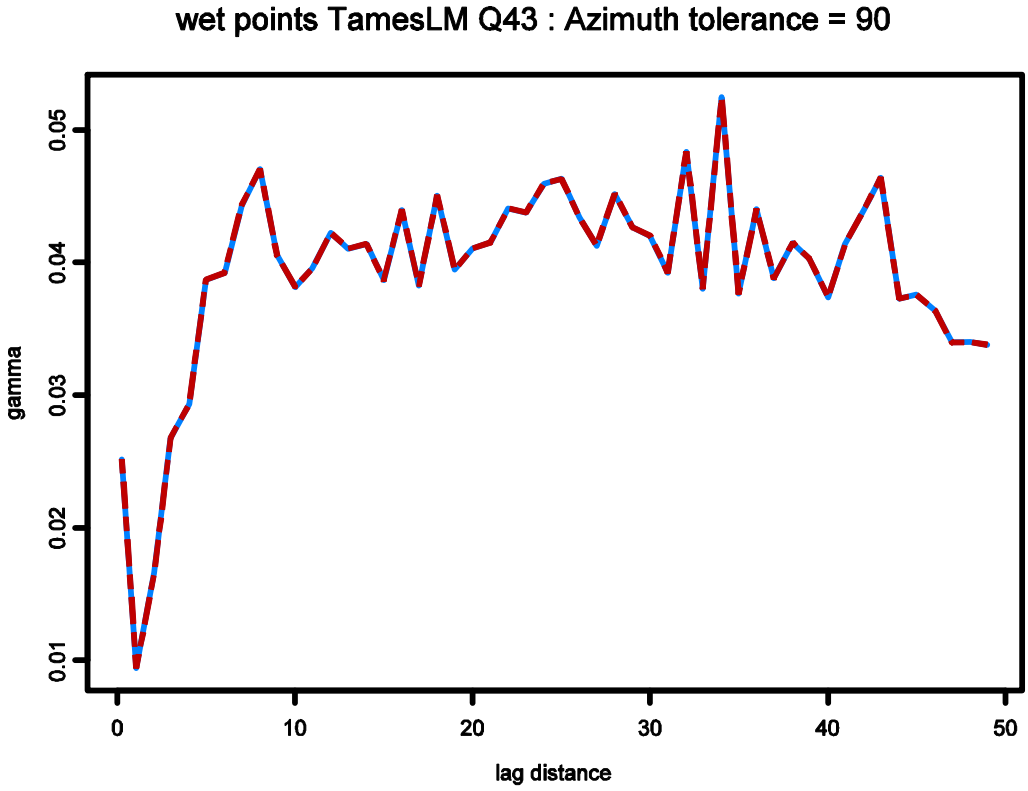
wet points TamesLM Q43 : Azimuth tolerance = 90
gamma
0.01
0.02
0.03
0.04
0.05
0
10
20
30
40
50
lag distance

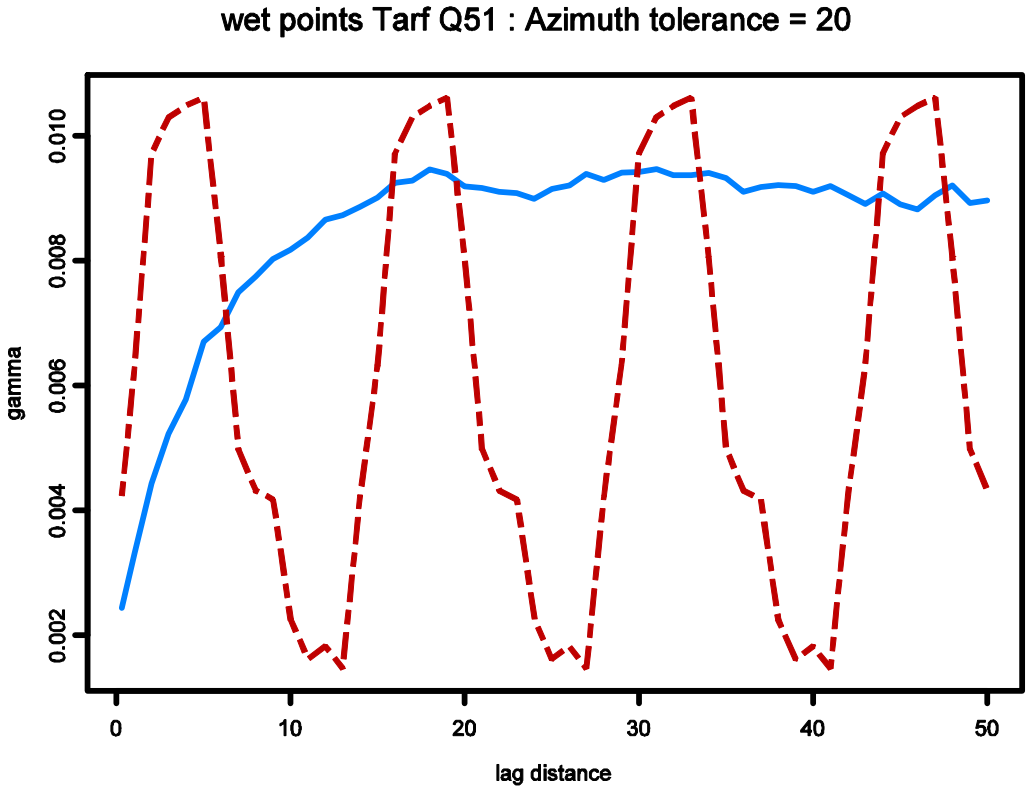
wet points Tarf Q51 : Azimuth tolerance = 20
gamma
0.002
0.004
0.006
0.008
0.010
0
10
20
30
40
50
lag distance

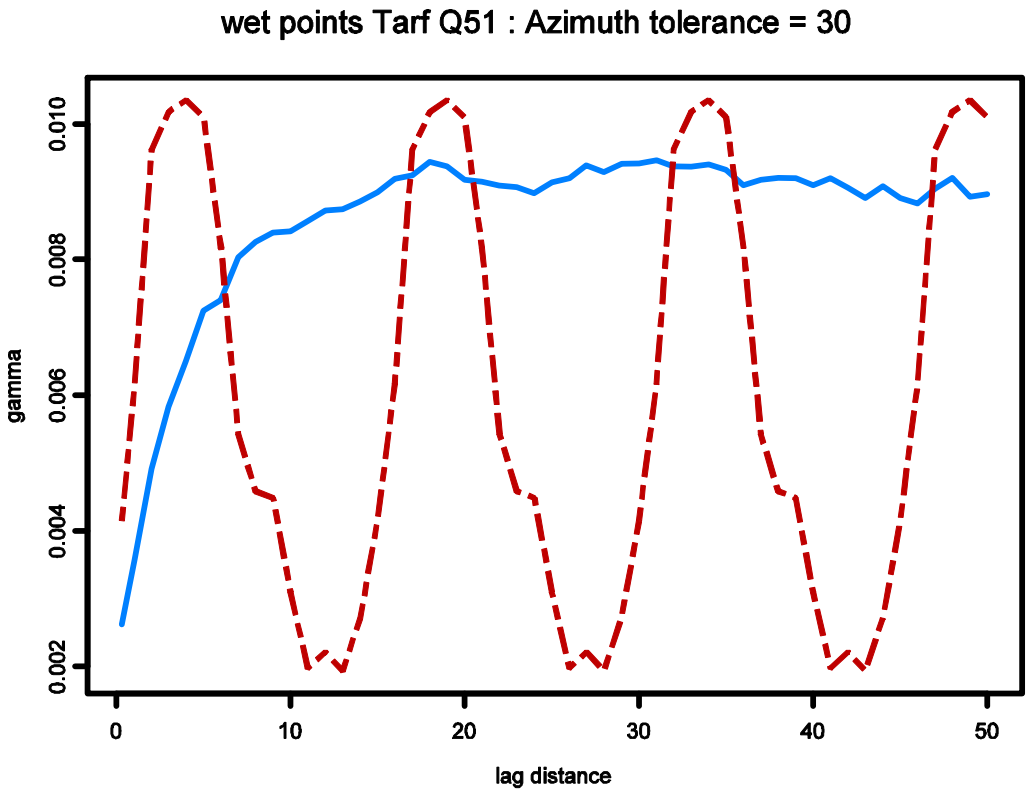
wet points Tarf Q51 : Azimuth tolerance = 30
gamma
0.002
0.004
0.006
0.008
0.010
0
10
20
30
40
50
lag distance

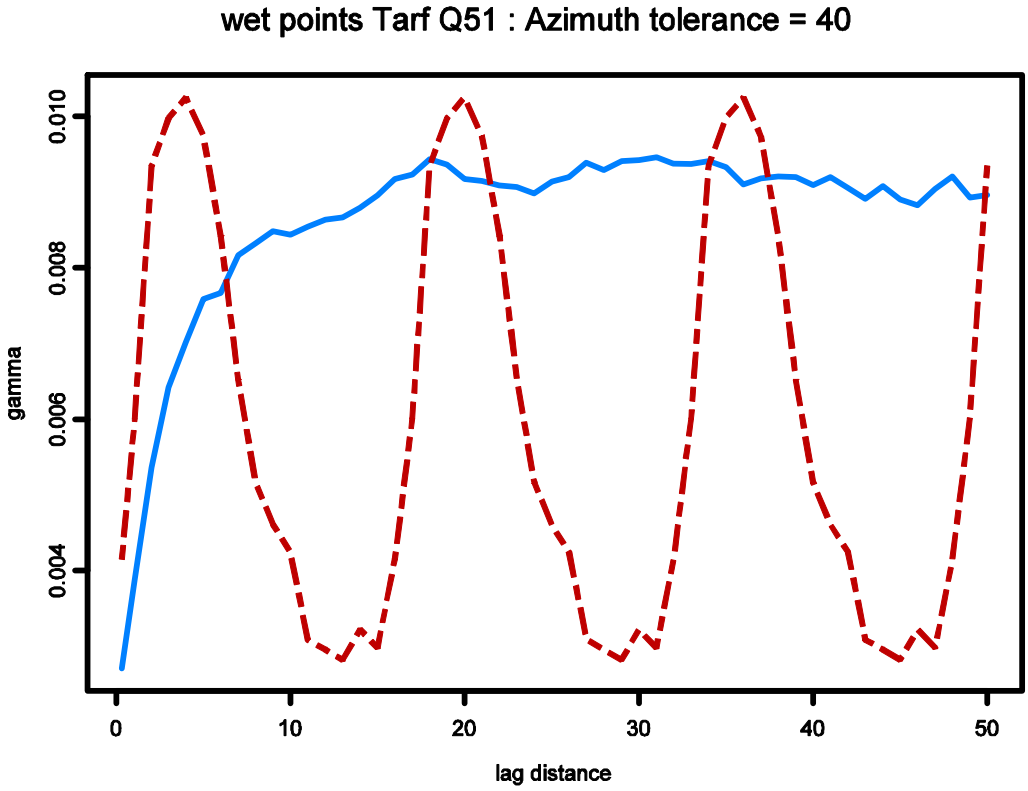
wet points Tarf Q51 : Azimuth tolerance = 40
gamma
0.004
0.006
0.008
0.010
0
10
20
30
40
50
lag distance

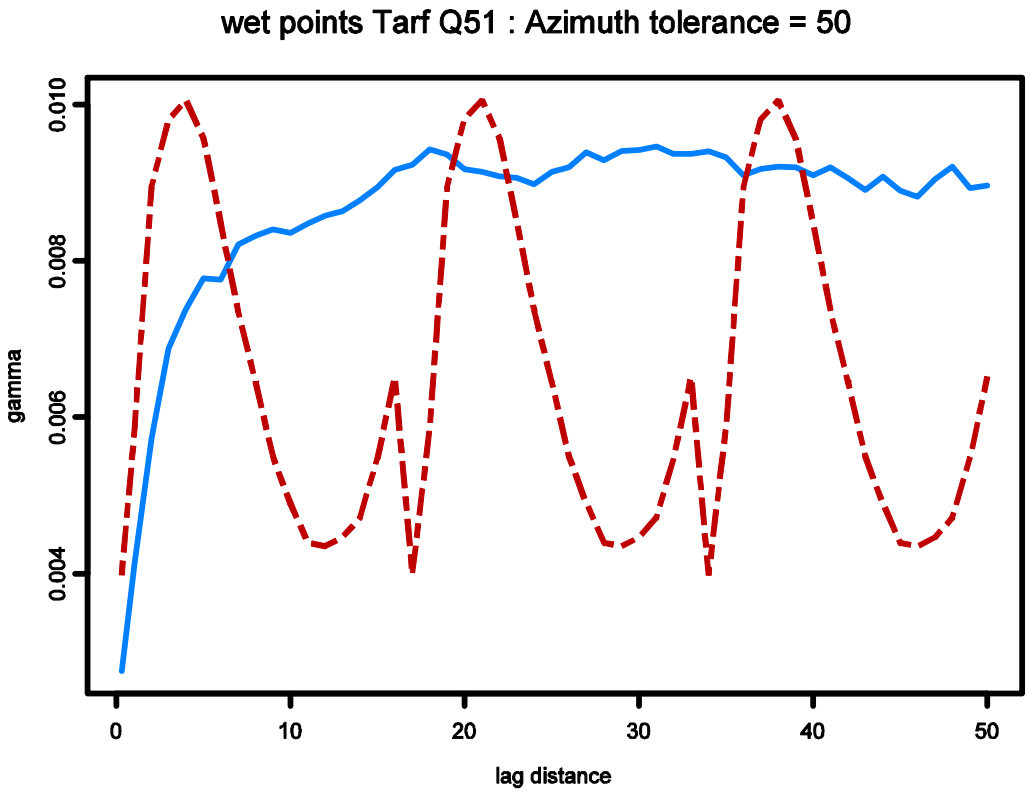
wet points Tarf Q51 : Azimuth tolerance = 50
gamma
0.004
0.006
0.008
0.010
0
10
20
30
40
50
lag distance

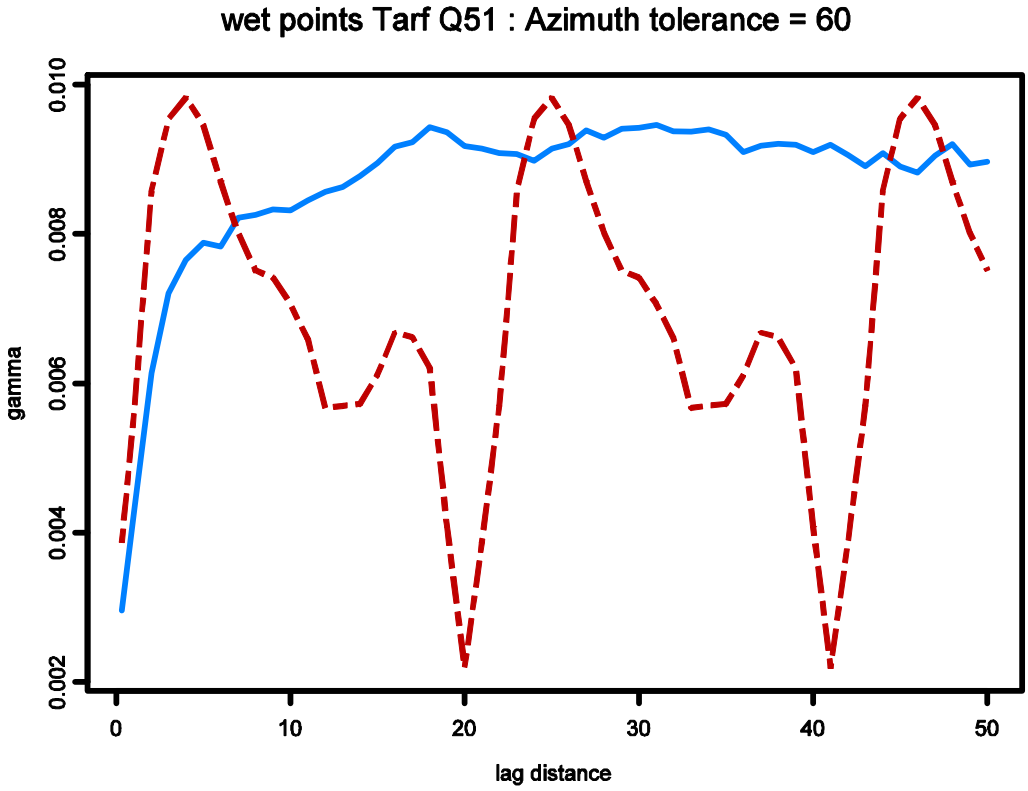
wet points Tarf Q51 : Azimuth tolerance = 60
gamma
0.002
0.004
0.006
0.008
0.010
0
10
20
30
40
50
lag distance

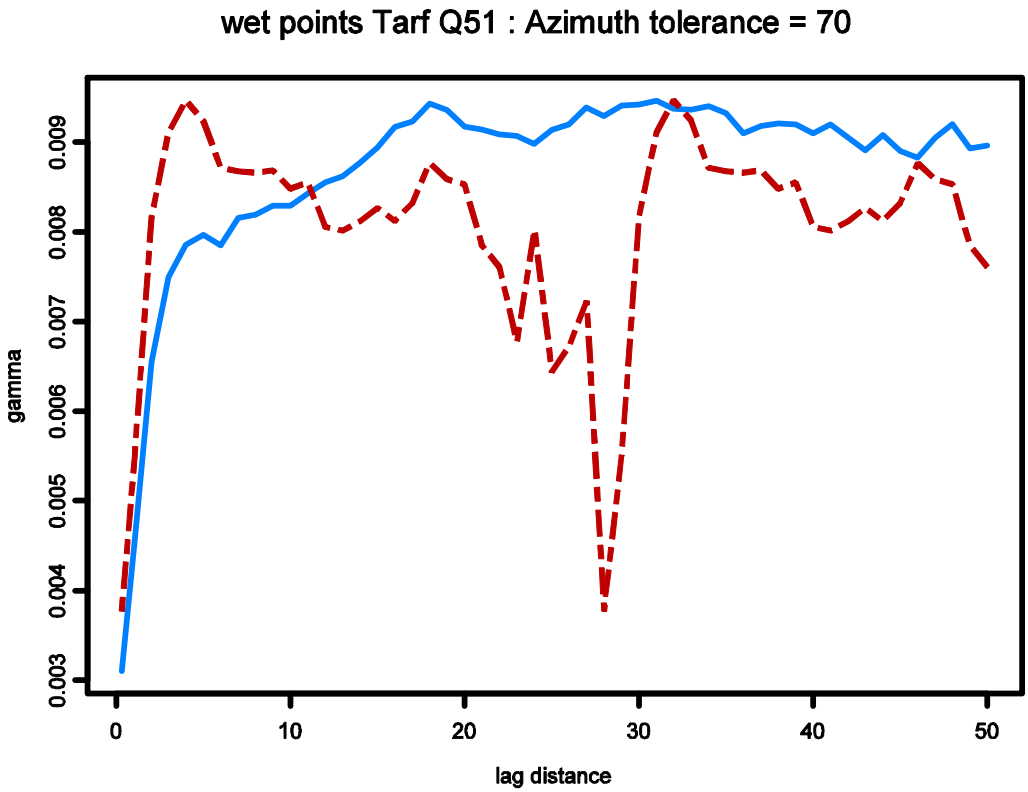
wet points Tarf Q51 : Azimuth tolerance = 70
gamma
0.003
0.004
0.005
0.006
0.007
0.008
0.009
0
10
20
30
40
50
lag distance

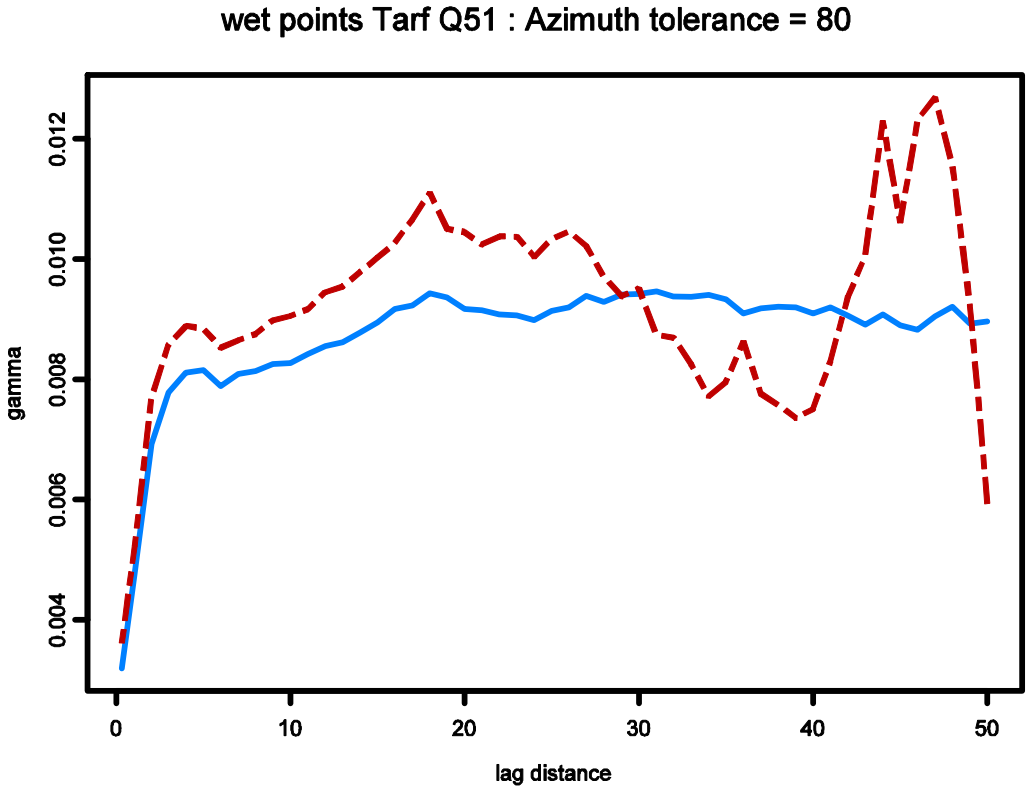
wet points Tarf Q51 : Azimuth tolerance = 80
gamma
0.004
0.006
0.008
0.010
0.012
0
10
20
30
40
50
lag distance

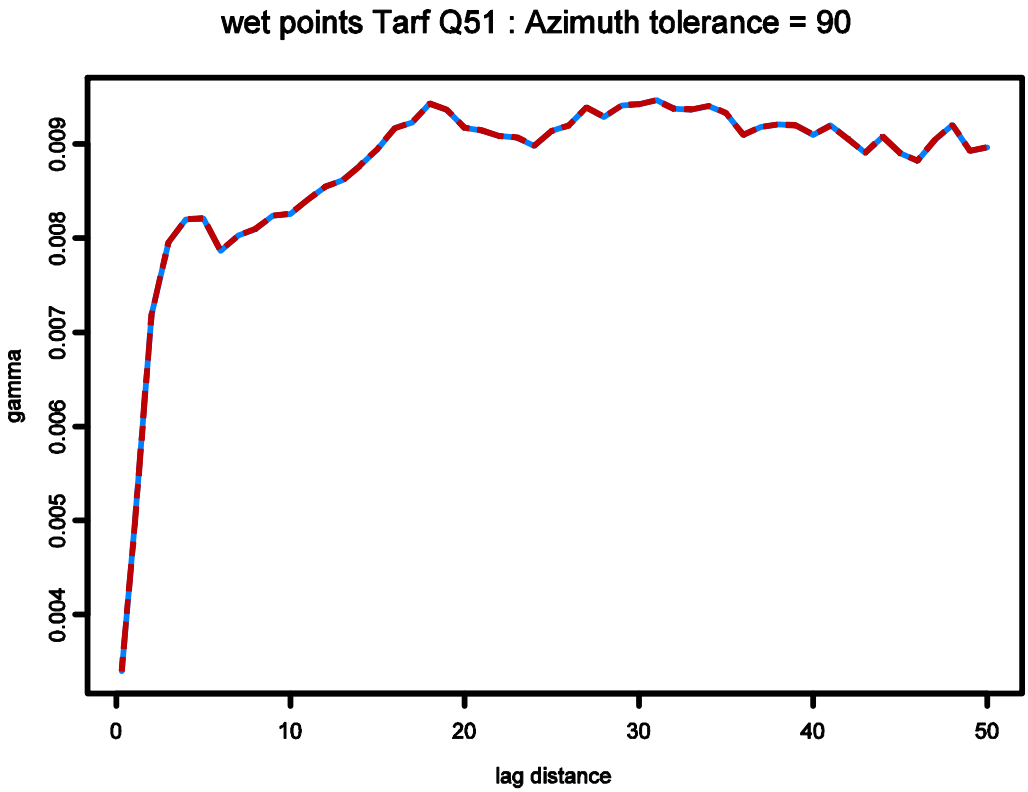
wet points Tarf Q51 : Azimuth tolerance = 90
gamma
0.004
0.005
0.006
0.007
0.008
0.009
0
10
20
30
40
50
lag distance

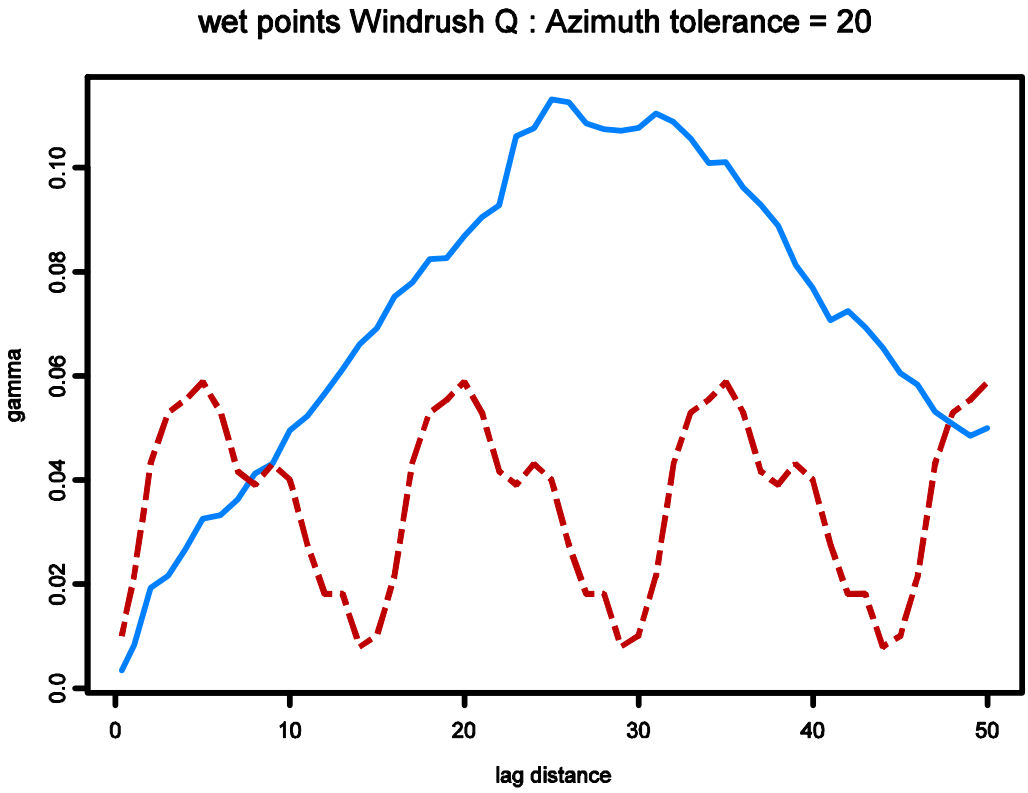
wet points Windrush Q : Azimuth tolerance = 20
gamma
0.0
0.02
0.04
0.06
0.08
0.10
0
10
20
30
40
50
lag distance

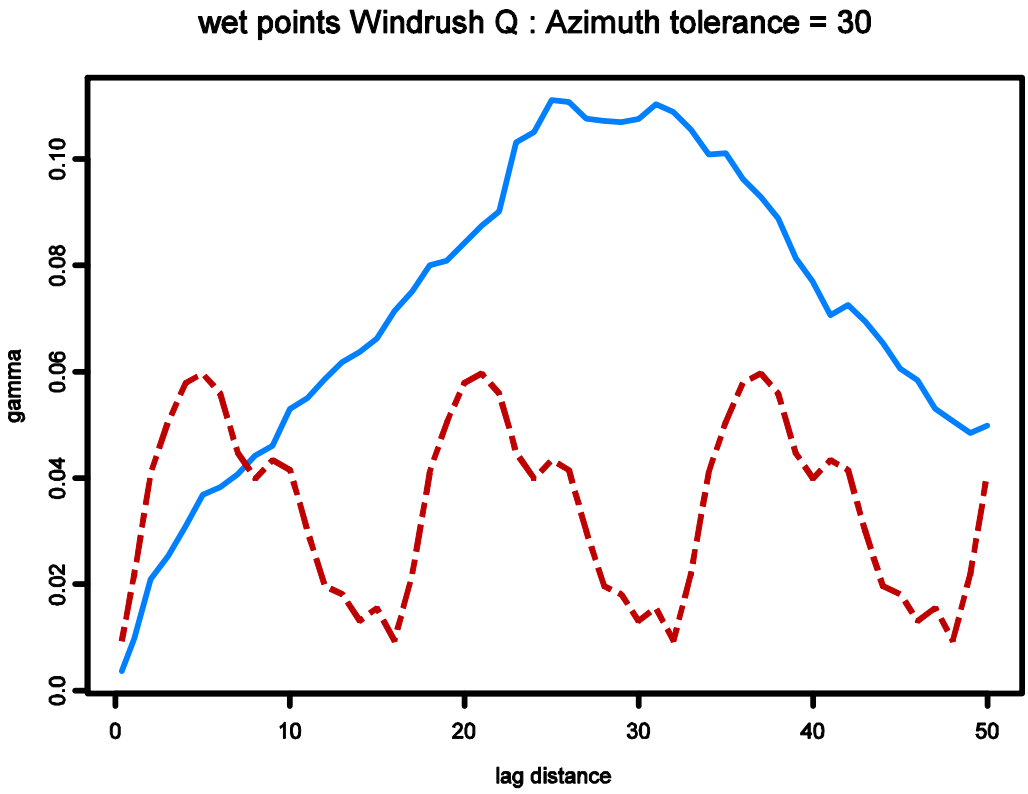
wet points Windrush Q : Azimuth tolerance = 30
gamma
0.0
0.02
0.04
0.06
0.08
0.10
0
10
20
30
40
50
lag distance

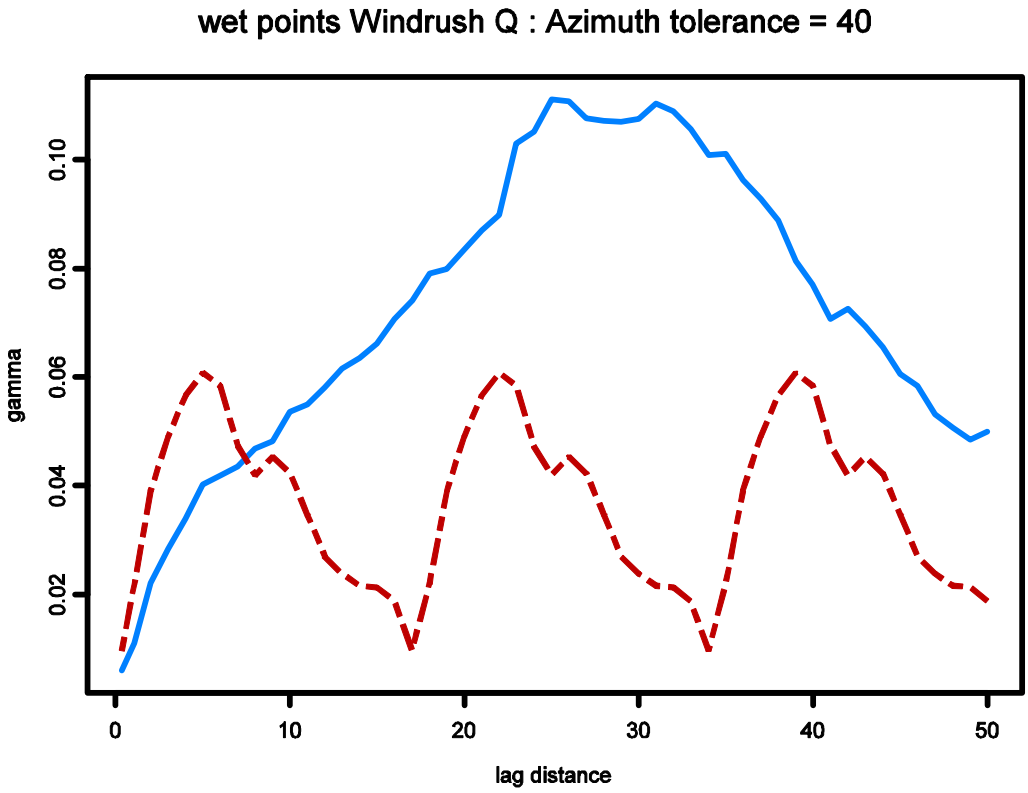
wet points Windrush Q : Azimuth tolerance = 40
gamma
0.02
0.04
0.06
0.08
0.10
0
10
20
30
40
50
lag distance

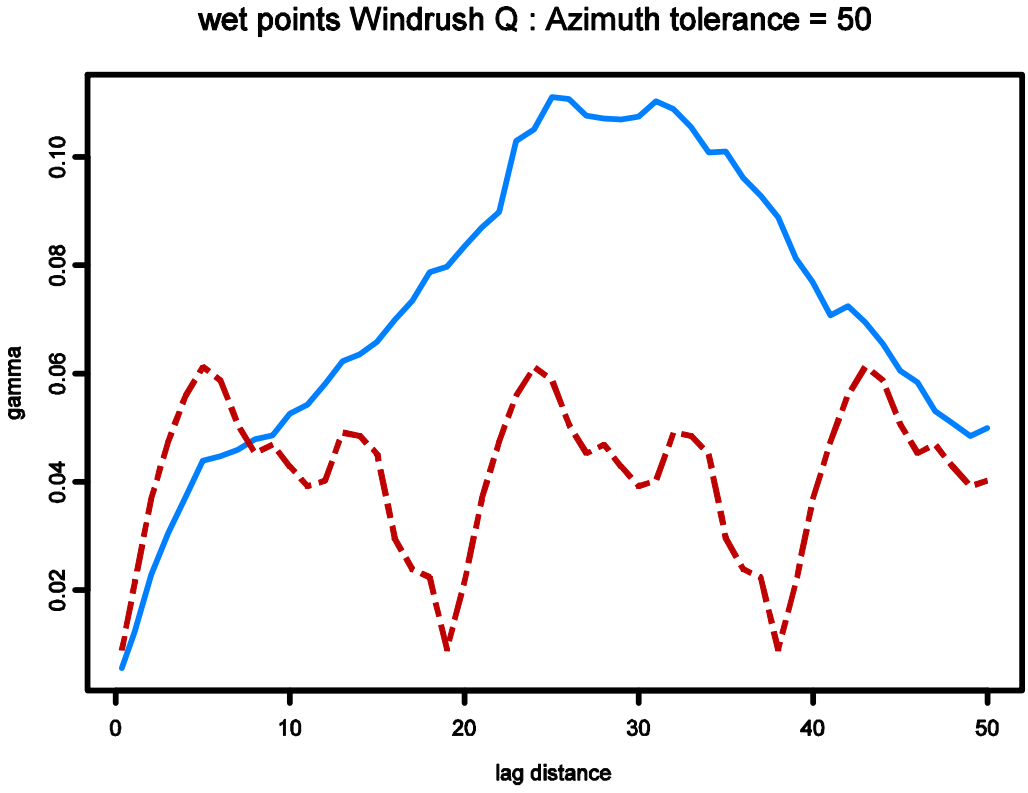
wet points Windrush Q : Azimuth tolerance = 50
gamma
0.02
0.04
0.06
0.08
0.10
0
10
20
30
40
50
lag distance

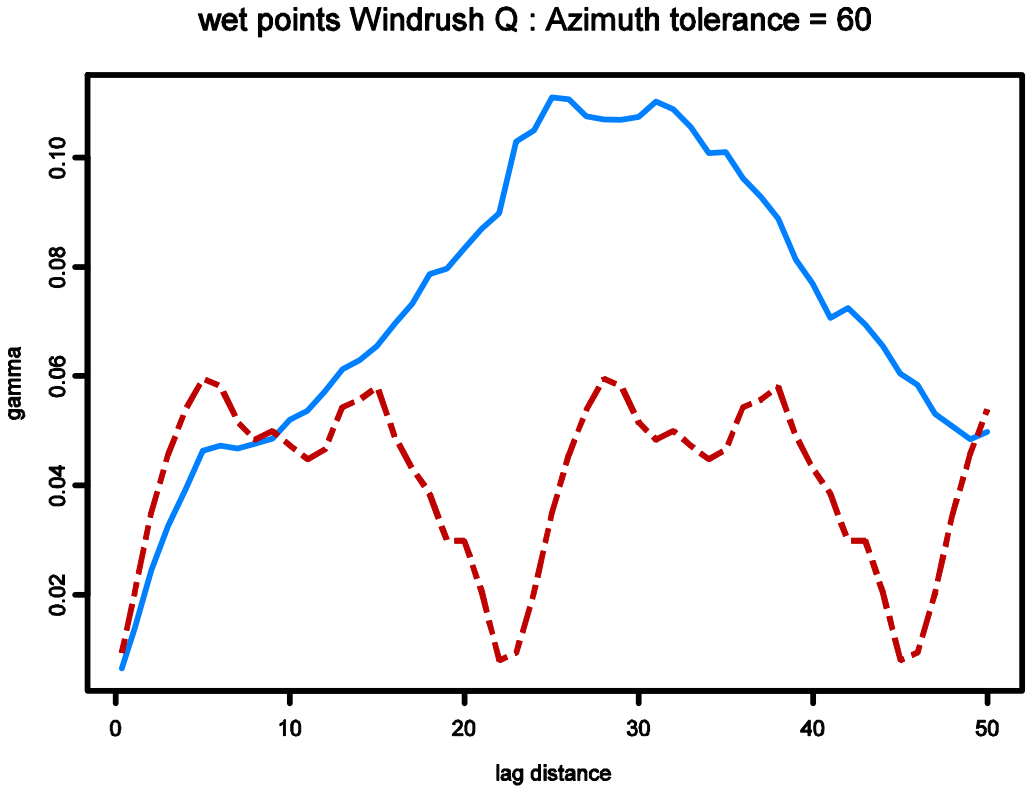
wet points Windrush Q : Azimuth tolerance = 60
gamma
0.02
0.04
0.06
0.08
0.10
0
10
20
30
40
50
lag distance

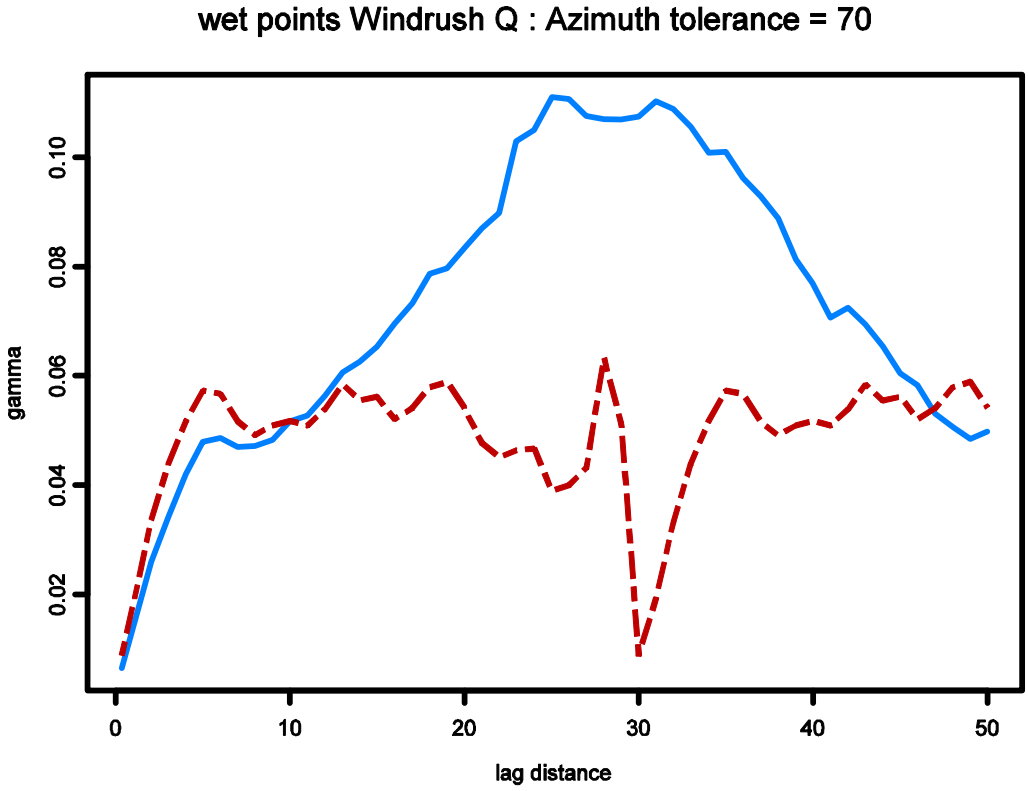
wet points Windrush Q : Azimuth tolerance = 70
gamma
0.02
0.04
0.06
0.08
0.10
0
10
20
30
40
50
lag distance

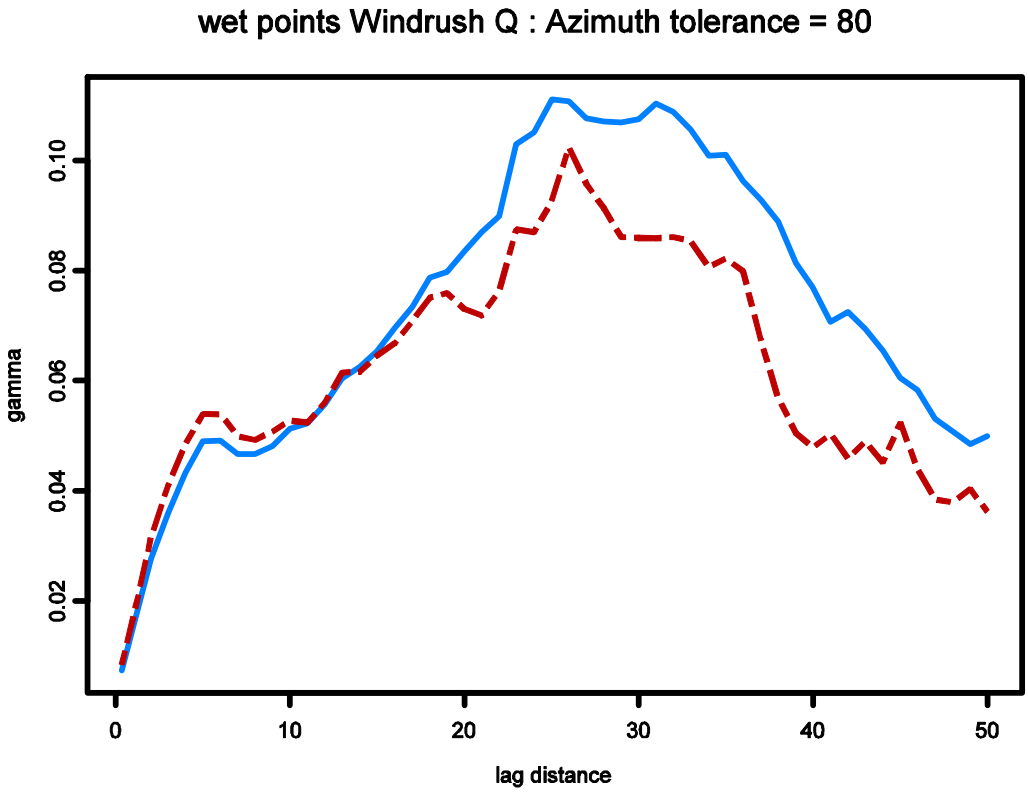
wet points Windrush Q : Azimuth tolerance = 80
gamma
0.02
0.04
0.06
0.08
0.10
0
10
20
30
40
50
lag distance

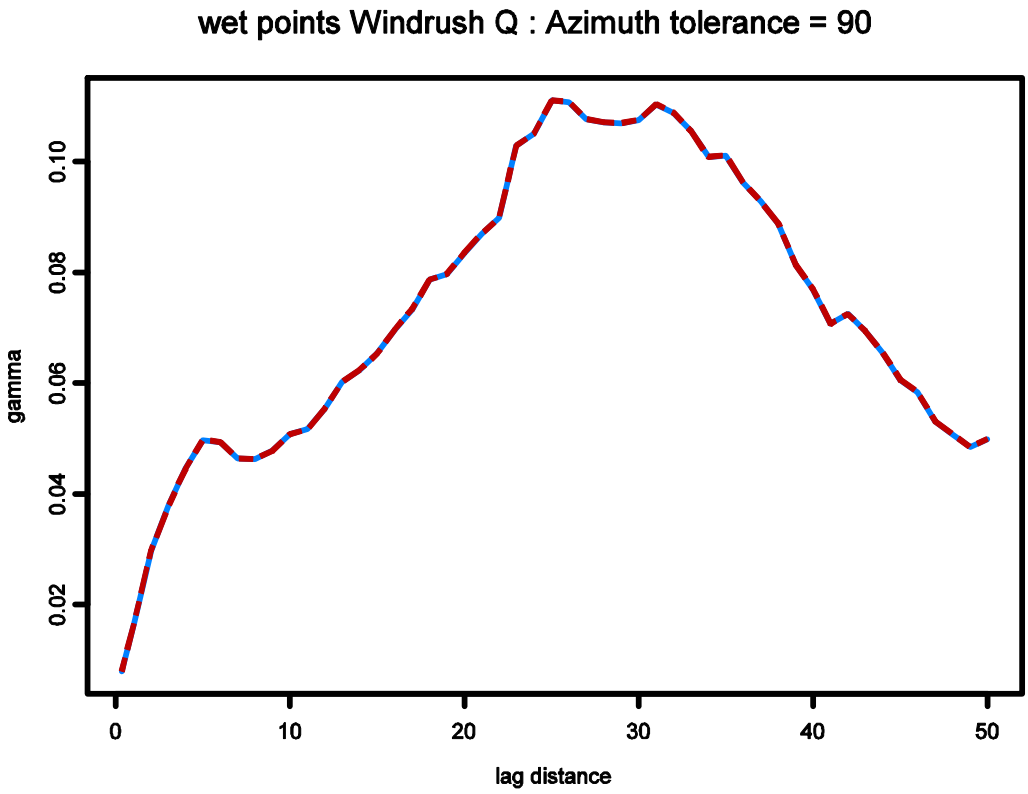
wet points Windrush Q : Azimuth tolerance = 90
gamma
0.02
0.04
0.06
0.08
0.10
0
10
20
30
40
50
lag distance

Appendix 3.4

Results obtained for the analysis in Chapter 5 –sensitivity analysis for the azimuth direction; anisotropy analysis

This appendix includes the graphical outputs obtained for the sensitivity analysis of the azimuth direction carried out in section 5.4.3. Results have been presented in two sections: the first one including the outputs for the data sets with dry and wet points and the second one showing the results obtained for the data sets with wet data points. Each data set analysed presents the following outputs: (i) a plot summarising four directional variograms calculated with azimuth tolerance equal to 60, maximum distance 30 m (although the plots shows up to maximum distance 50 m) and lag distance 0.5 m (for the data sets with dry and wet points) and 1 m (for the data sets with only wet points and (ii) a second plot showing the existent number of pair of points obtained for each variogram.

Anisotropy for the wet & dry points

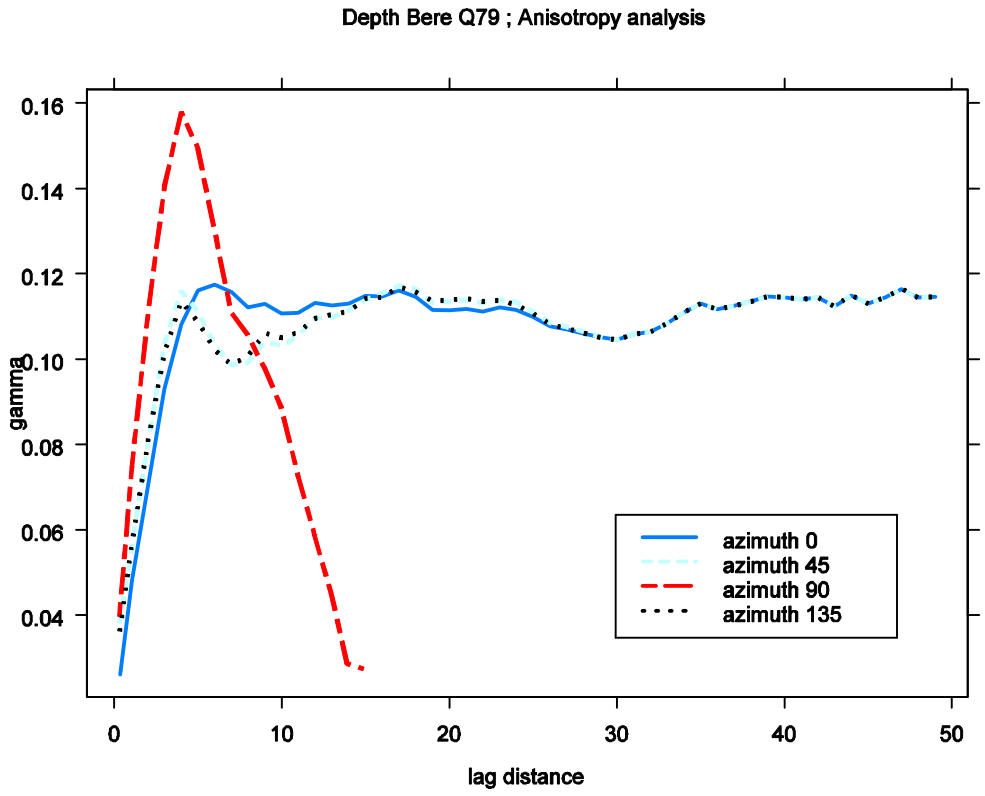

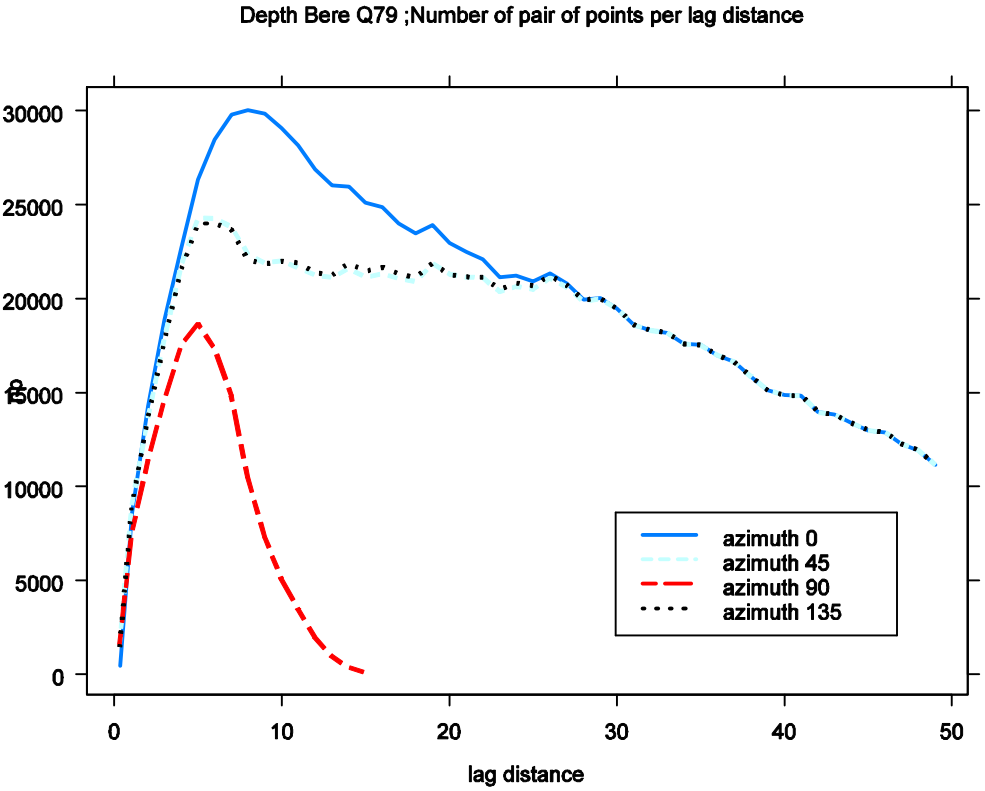

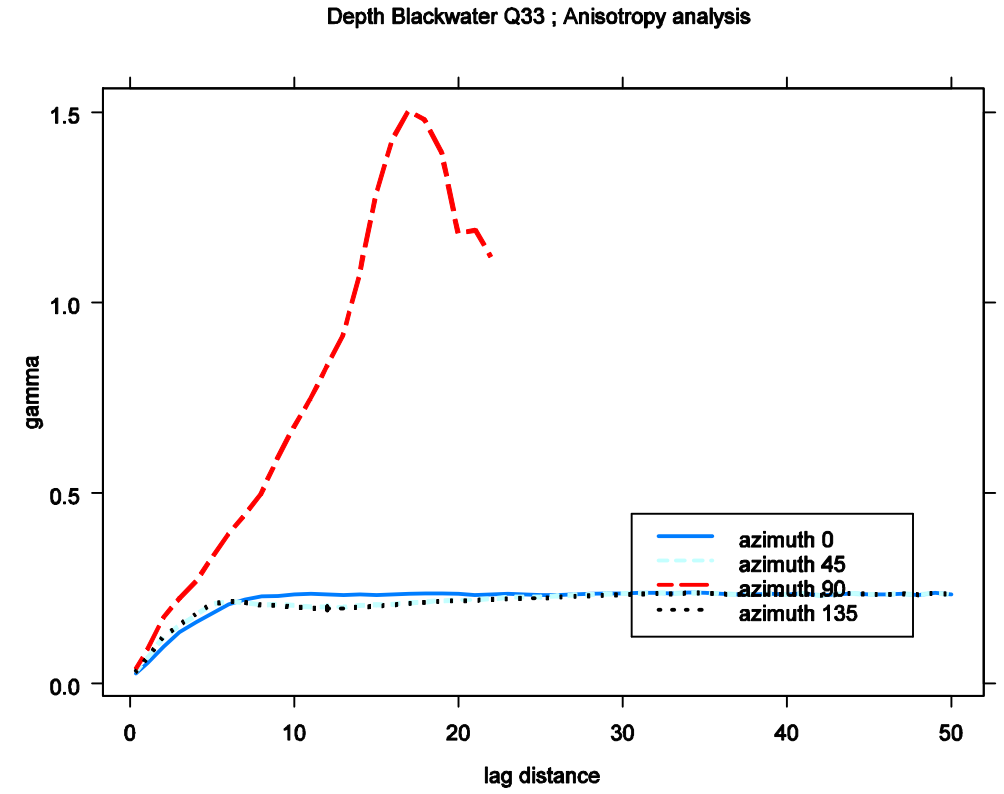
Depth Blackwater Q33 ; Anisotropy analysis
gamma
lag distance
azimuth 0
azimuth 45
azimuth 90
azimuth 135

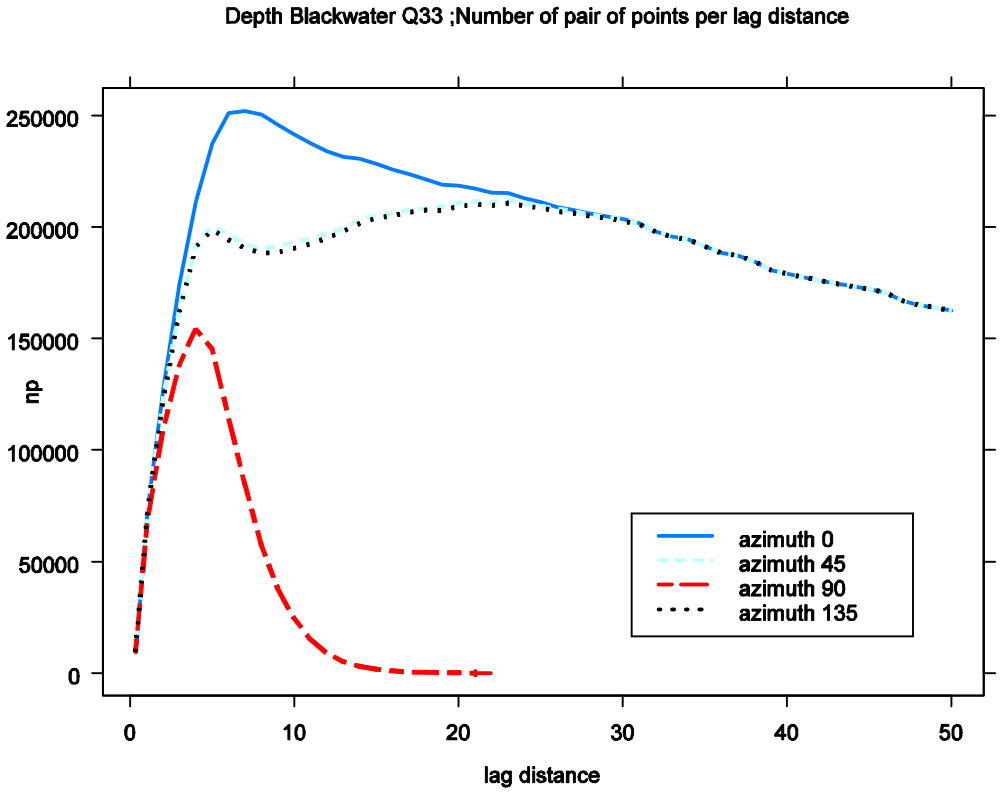
Depth Blackwater Q33 ;Number of pair of points per lag distance
np
lag distance
azimuth 0
azimuth 45
azimuth 90
azimuth 135

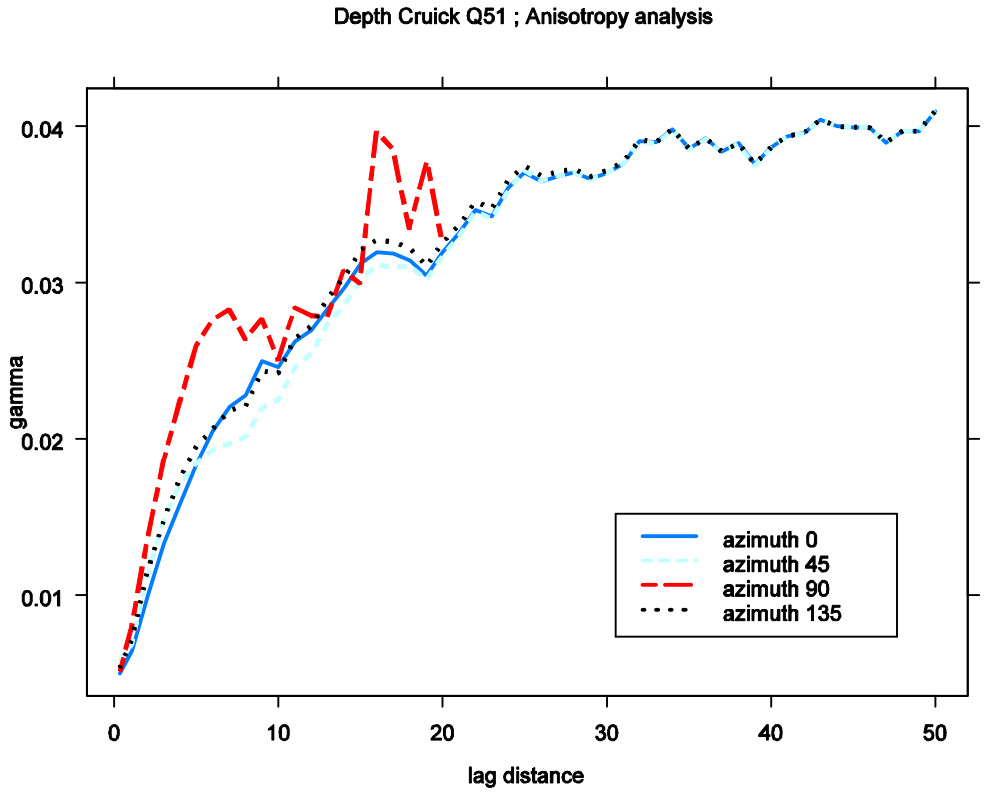
Depth Cruick Q51 ; Anisotropy analysis
gamma
0.04
0.03
0.02
0.01
0
10
20
30
40
50
lag distance
azimuth 0
azimuth 45
azimuth 90
azimuth 135

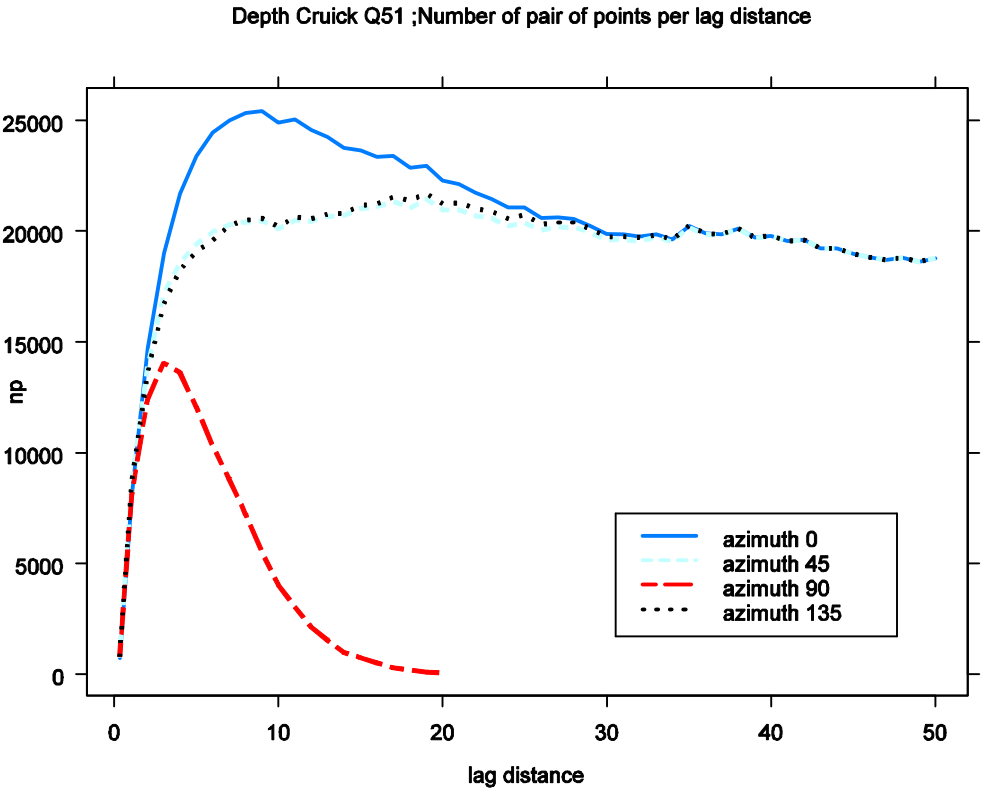
Depth Cruick Q51 ;Number of pair of points per lag distance
np
25000
20000
15000
10000
5000
0
0
10
20
30
40
50
lag distance
azimuth 0
azimuth 45
azimuth 90
azimuth 135

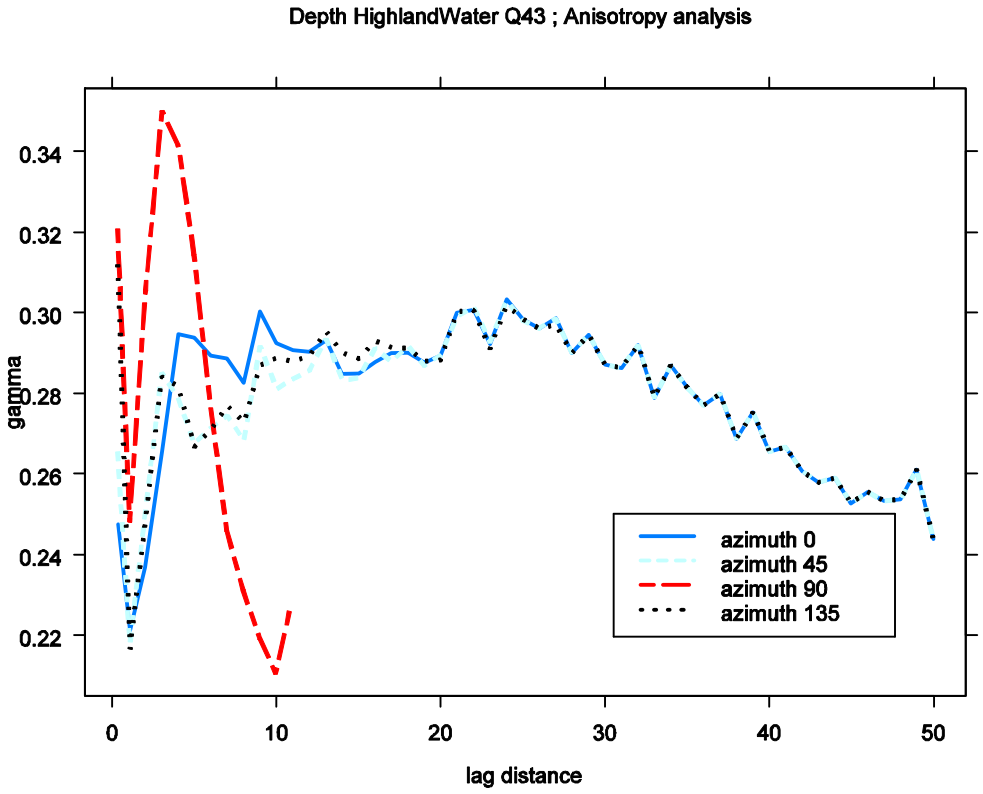
Depth HighlandWater Q43 ; Anisotropy analysis
gamma
0.34
0.32
0.30
0.28
0.26
0.24
0.22
0
10
20
30
40
50
lag distance
azimuth 0
azimuth 45
azimuth 90
azimuth 135

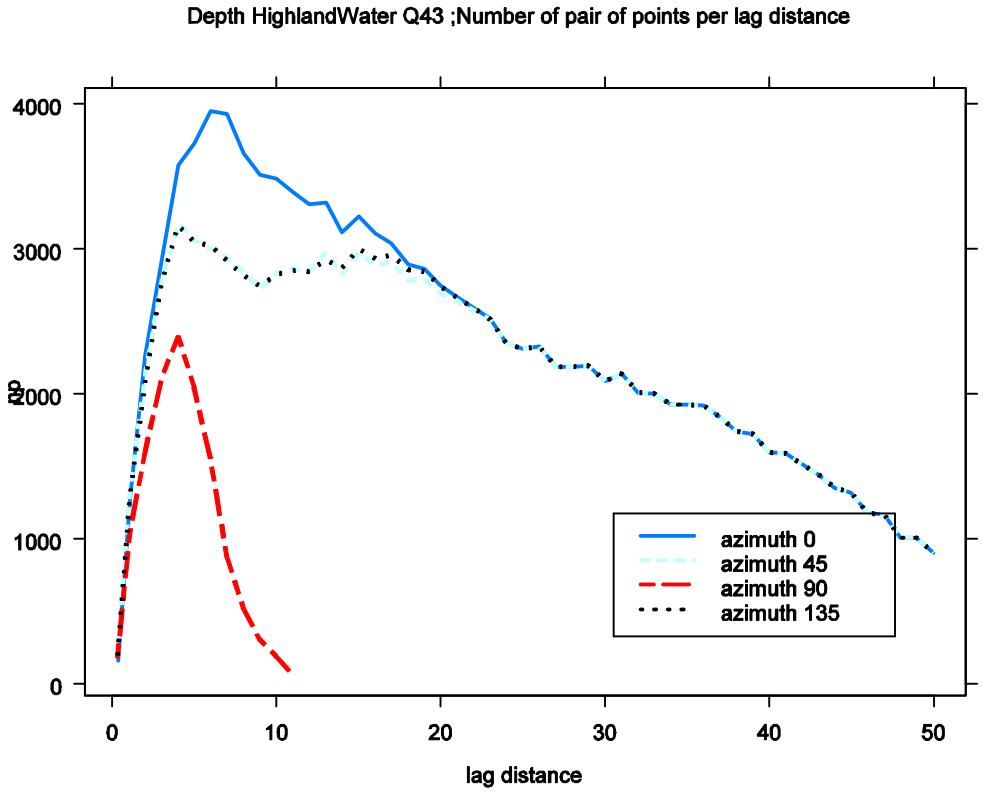
Depth HighlandWater Q43 ;Number of pair of points per lag distance
np
4000
3000
2000
1000
0
0
10
20
30
40
50
lag distance
azimuth 0
azimuth 45
azimuth 90
azimuth 135

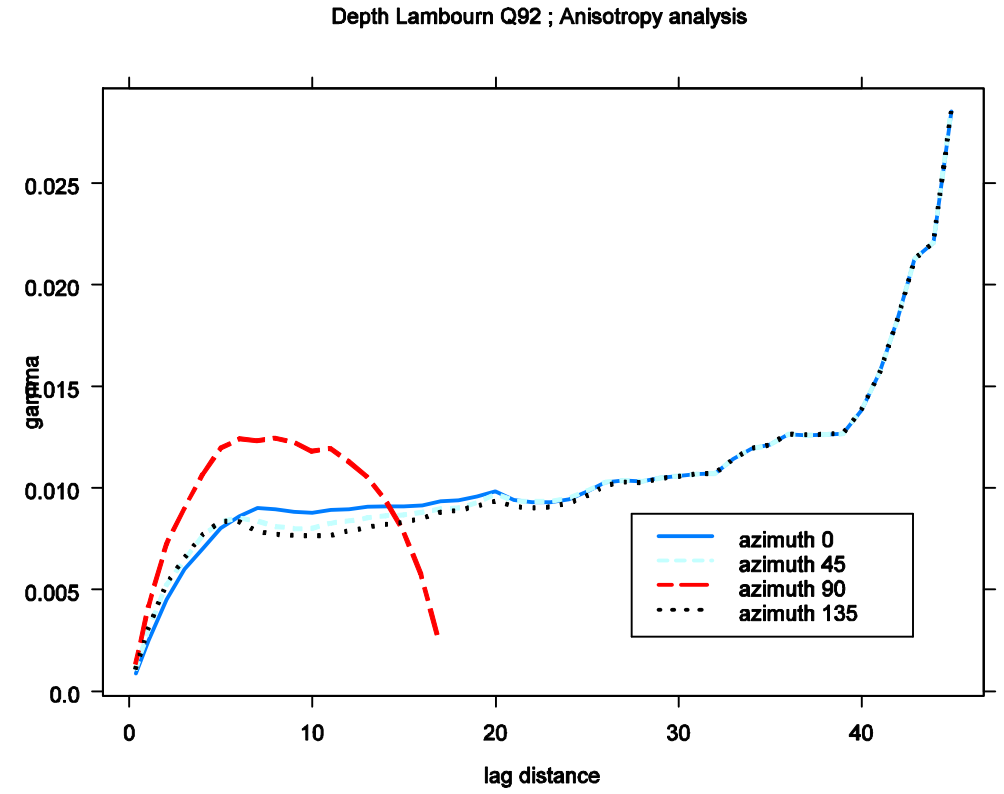
Depth Lambourn Q92 ; Anisotropy analysis
gamma
0.0
0.005
0.010
0.015
0.020
0.025
0
10
20
30
40
lag distance
azimuth 0
azimuth 45
azimuth 90
azimuth 135

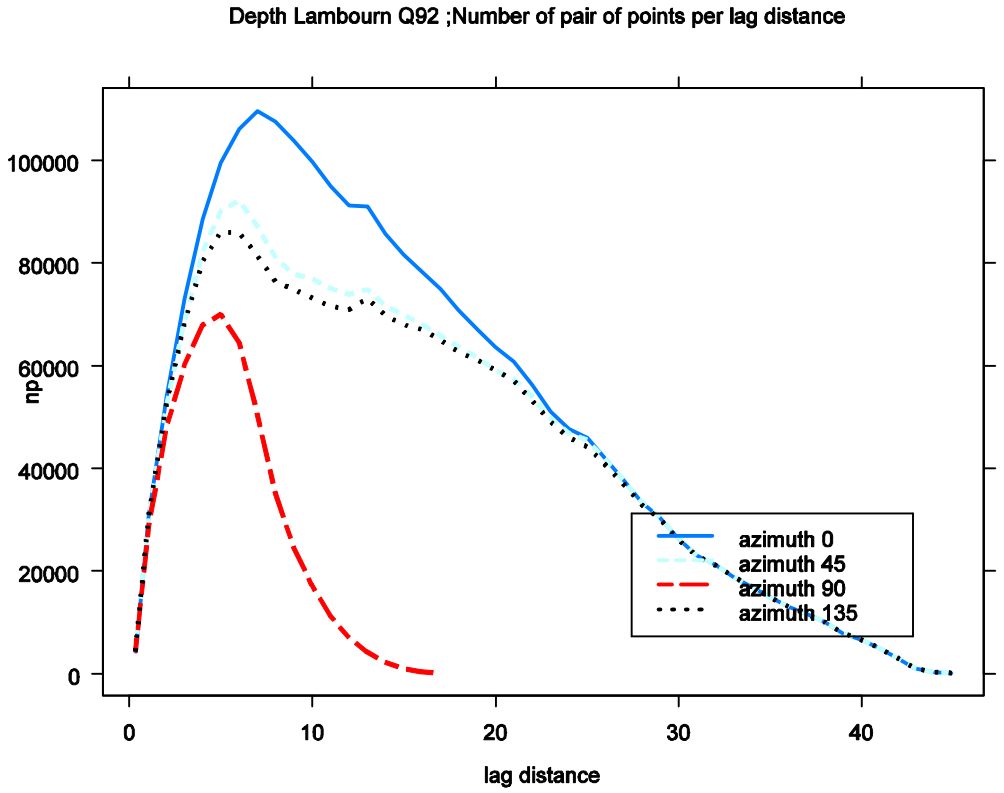
Depth Lambourn Q92 ;Number of pair of points per lag distance
np
0
20000
40000
60000
80000
100000
0
10
20
30
40
lag distance
azimuth 0
azimuth 45
azimuth 90
azimuth 135

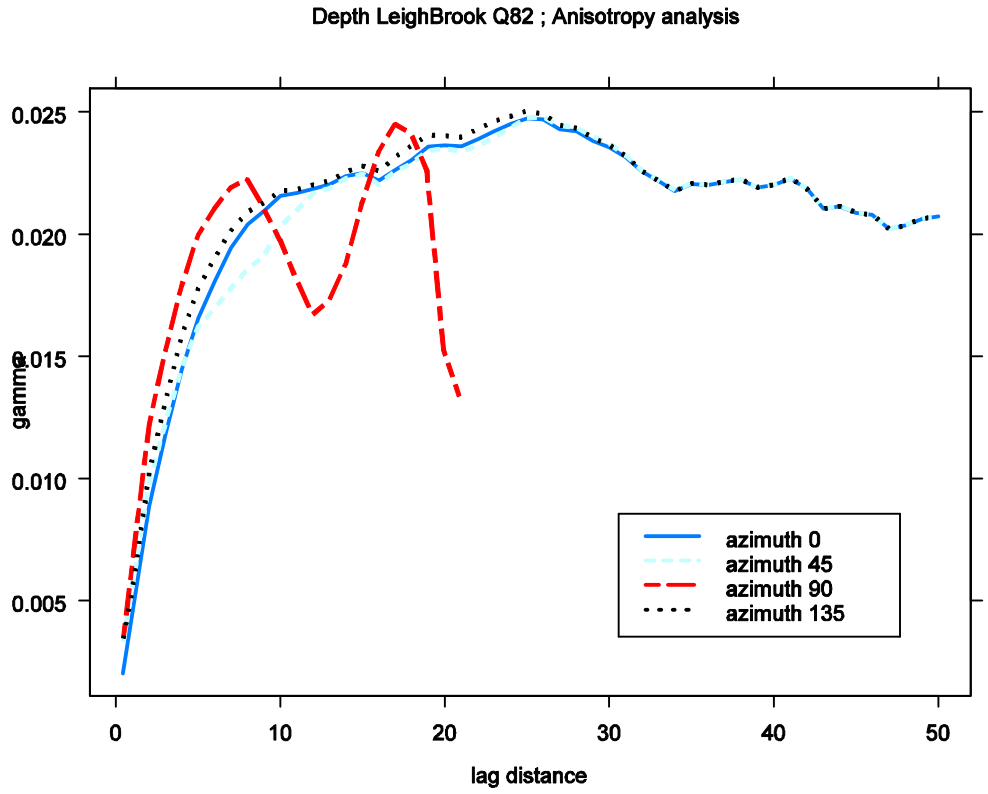
Depth LeighBrook Q82 ; Anisotropy analysis
0.025
0.020
0.015
0.010
0.005
gamma
0
10
20
30
40
50
lag distance
azimuth 0
azimuth 45
azimuth 90
azimuth 135

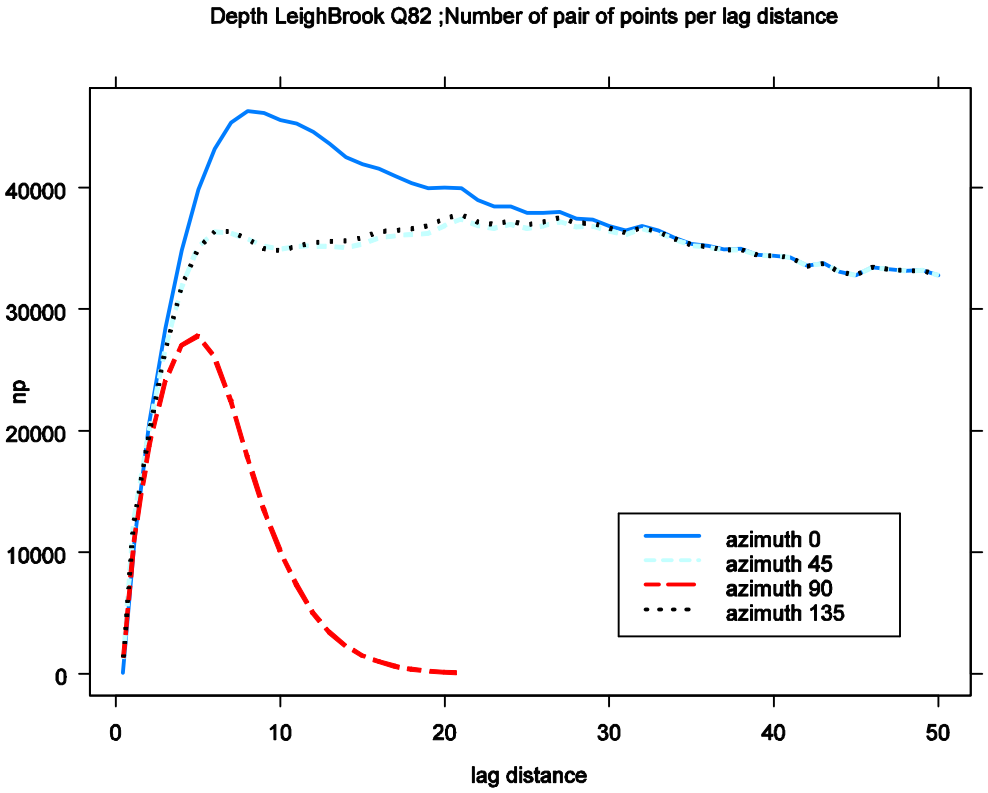
Depth LeighBrook Q82 ;Number of pair of points per lag distance
40000
30000
20000
10000
0
np
0
10
20
30
40
50
lag distance
azimuth 0
azimuth 45
azimuth 90
azimuth 135

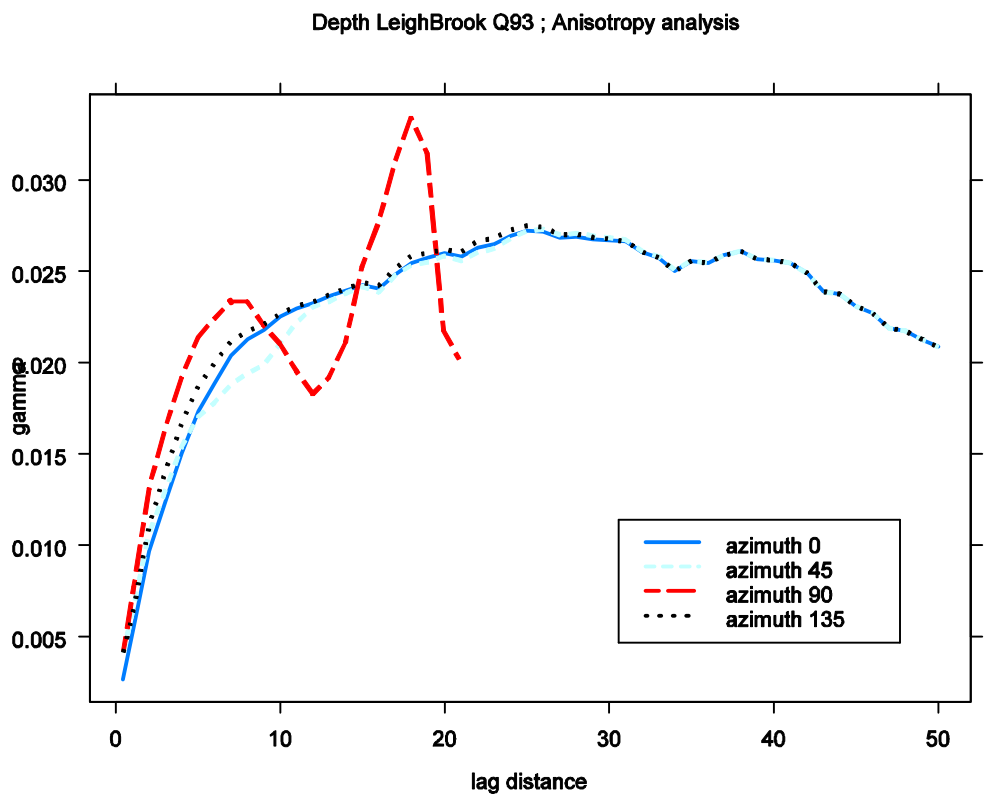
Depth LeighBrook Q93 ; Anisotropy analysis
gamma
0.030
0.025
0.020
0.015
0.010
0.005
0
10
20
30
40
50
lag distance
azimuth 0
azimuth 45
azimuth 90
azimuth 135

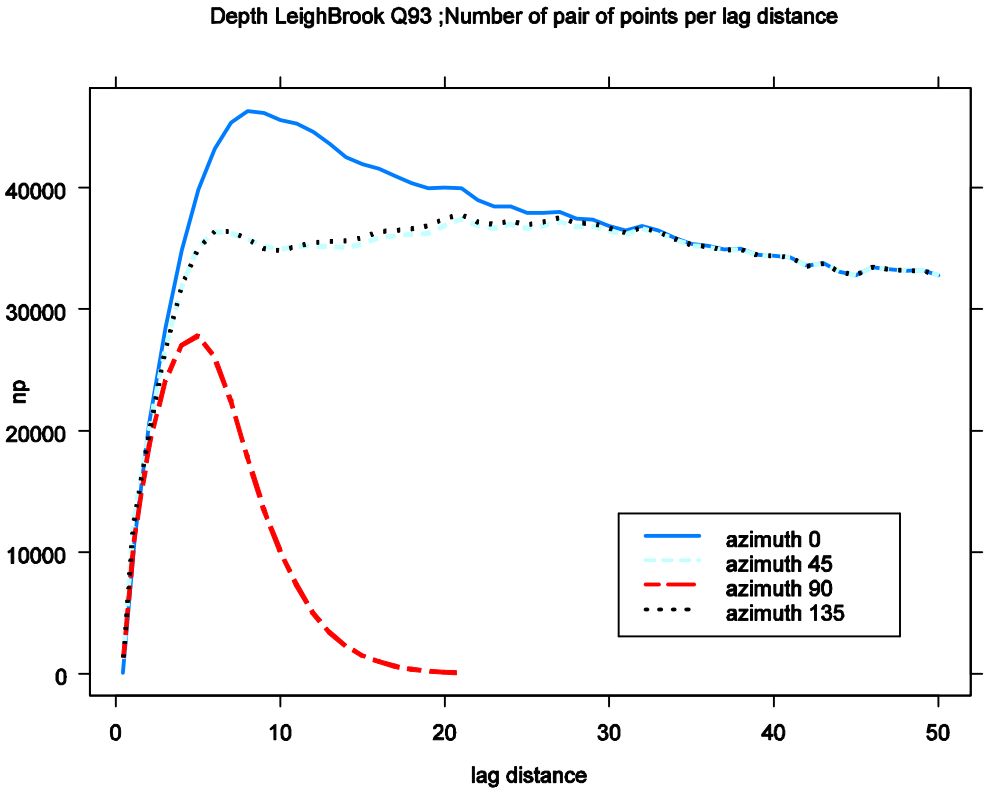
Depth LeighBrook Q93 ;Number of pair of points per lag distance
np
40000
30000
20000
10000
0
0
10
20
30
40
50
lag distance
azimuth 0
azimuth 45
azimuth 90
azimuth 135

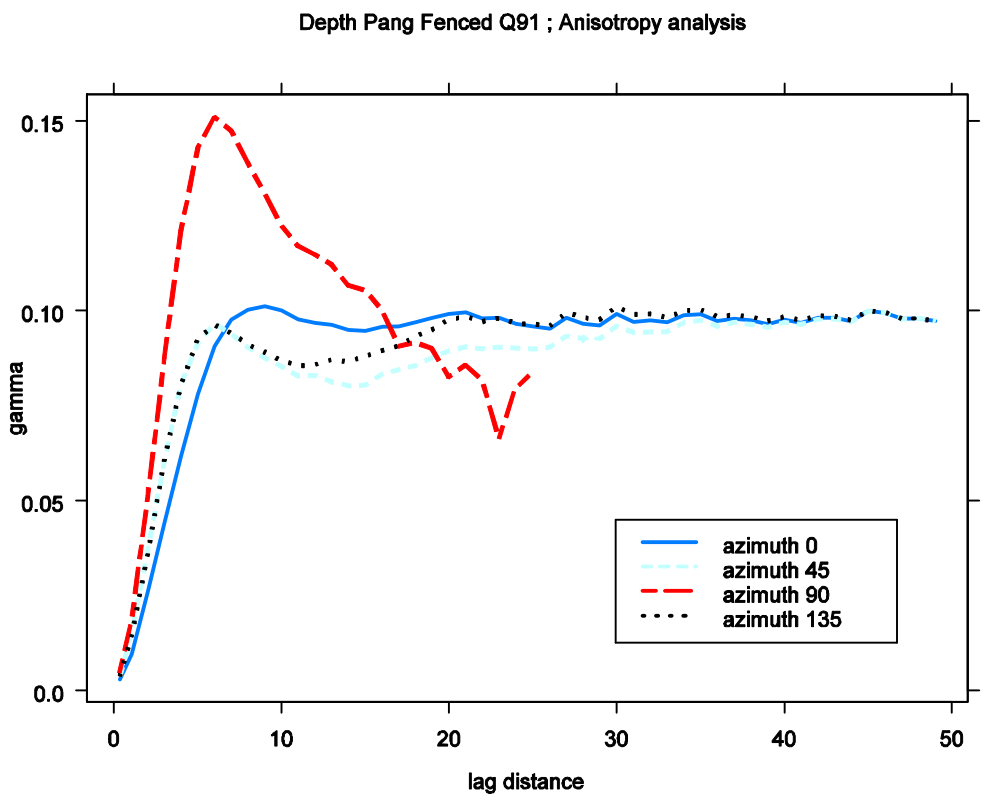
Depth Pang Fenced Q91 ; Anisotropy analysis
gamma
0.0
0.05
0.10
0.15
0
10
20
30
40
50
lag distance
azimuth 0
azimuth 45
azimuth 90
azimuth 135

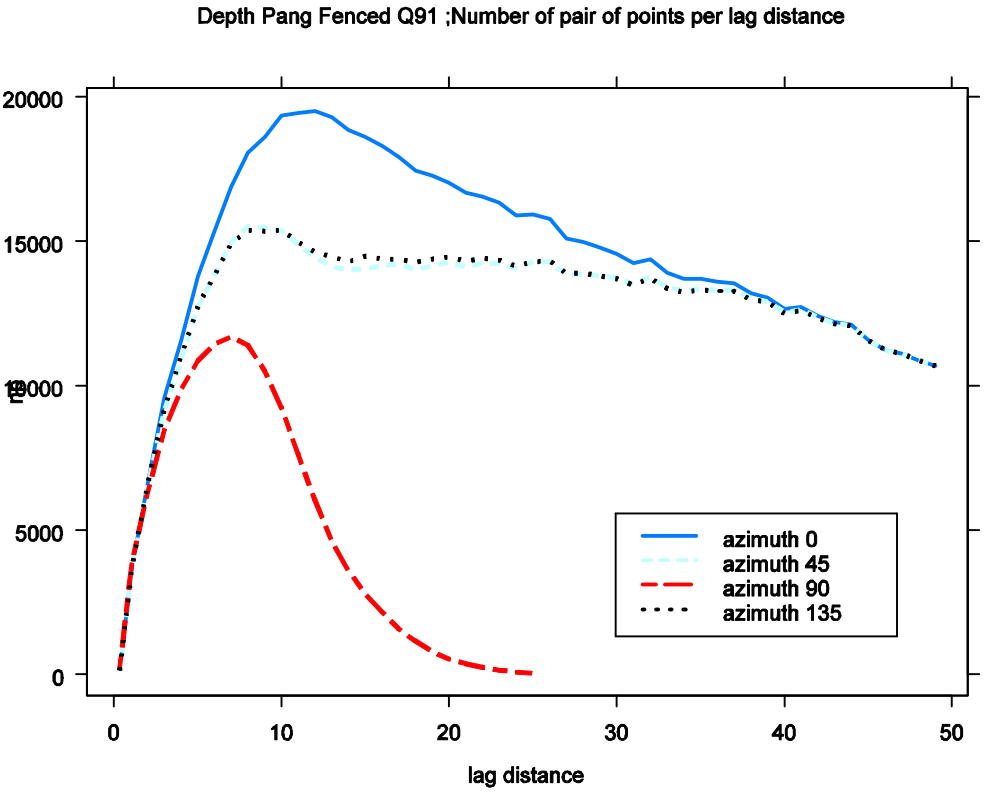
Depth Pang Fenced Q91 ;Number of pair of points per lag distance
0
5000
15000
20000
0
10
20
30
40
50
lag distance
azimuth 0
azimuth 45
azimuth 90
azimuth 135

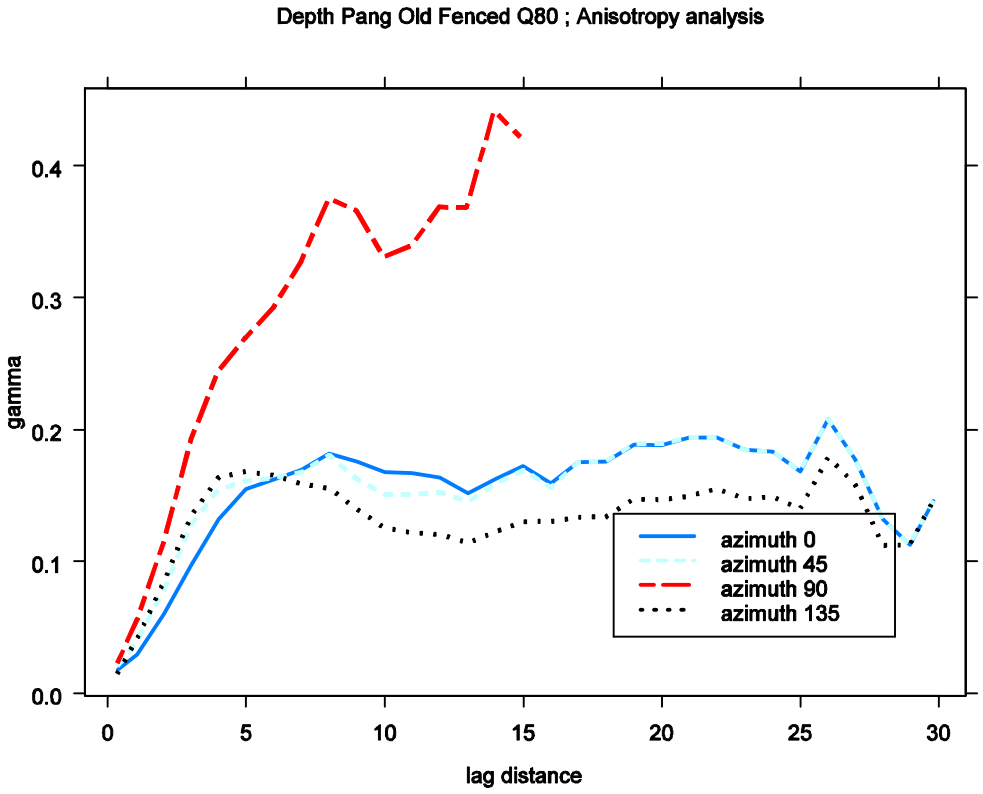
Depth Pang Old Fenced Q80 ; Anisotropy analysis
gamma
0.0
0.1
0.2
0.3
0.4
0
5
10
15
20
25
30
lag distance
azimuth 0
azimuth 45
azimuth 90
azimuth 135

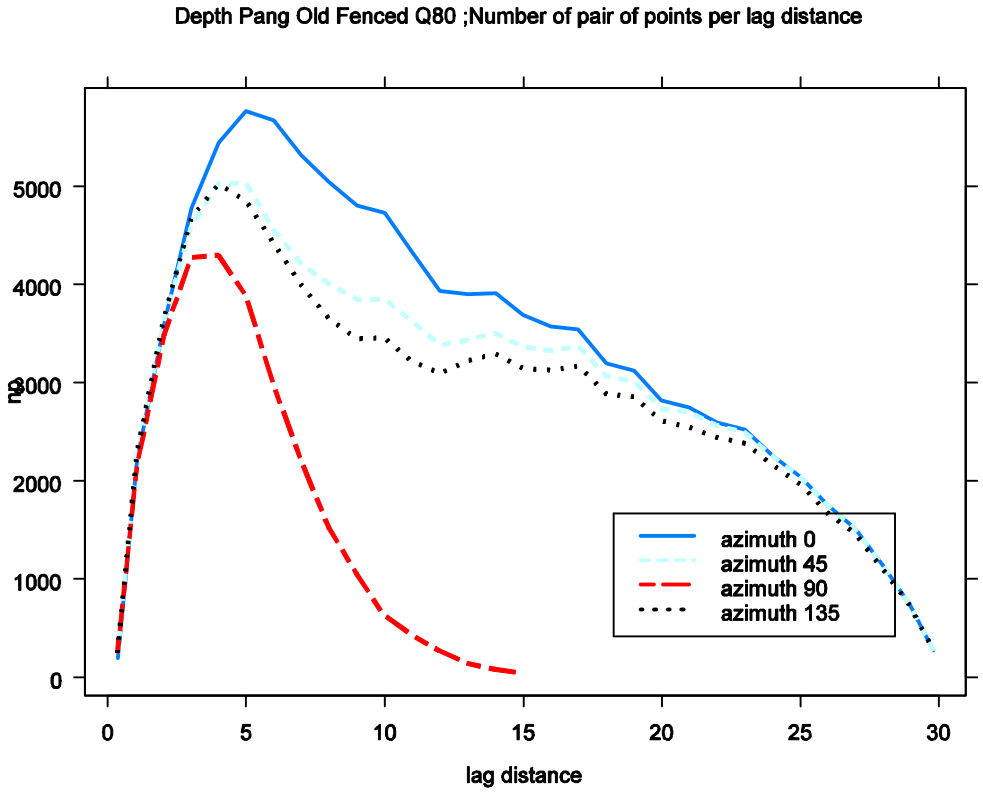
Depth Pang Old Fenced Q80 ;Number of pair of points per lag distance
np
0
1000
2000
3000
4000
5000
0
5
10
15
20
25
30
lag distance
azimuth 0
azimuth 45
azimuth 90
azimuth 135

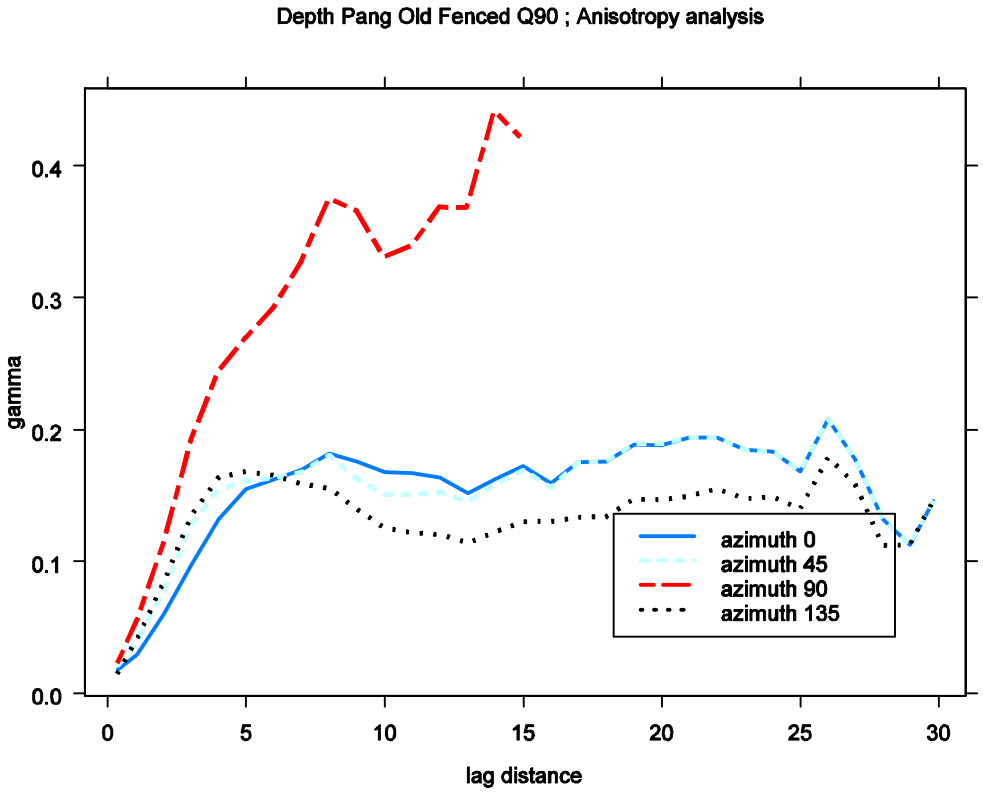
Depth Pang Old Fenced Q90 ; Anisotropy analysis
gamma
0.0
0.1
0.2
0.3
0.4
0
5
10
15
20
25
30
lag distance
azimuth 0
azimuth 45
azimuth 90
azimuth 135

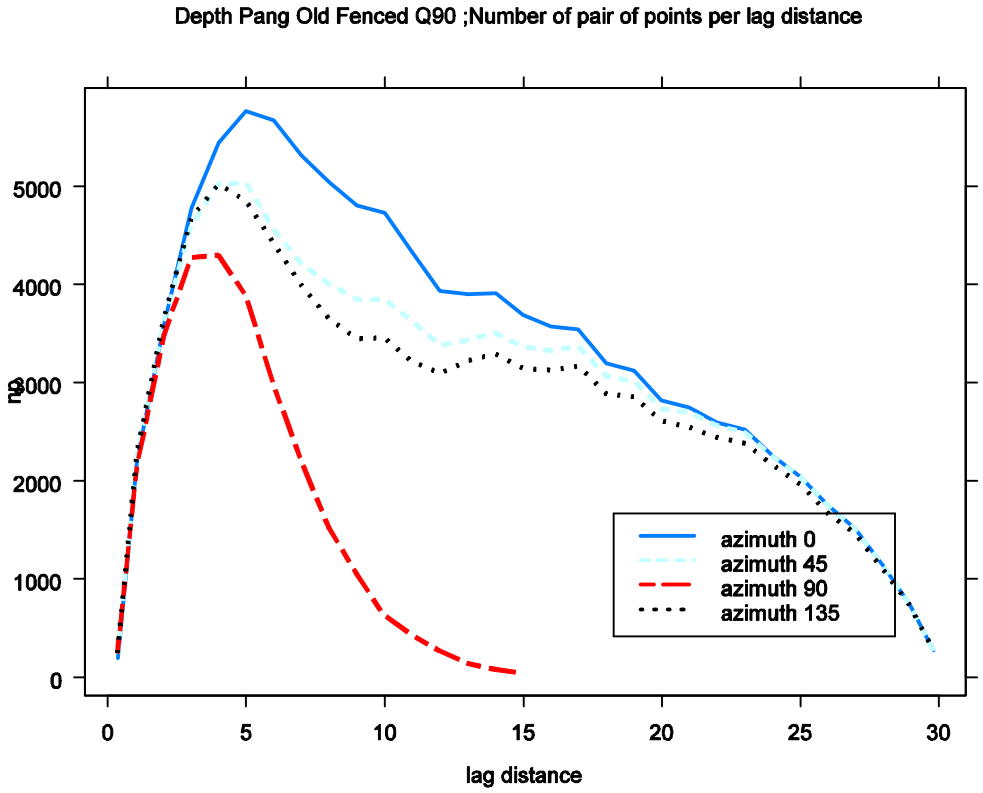
Depth Pang Old Fenced Q90 ;Number of pair of points per lag distance
np
0
1000
2000
3000
4000
5000
0
5
10
15
20
25
30
lag distance
azimuth 0
azimuth 45
azimuth 90
azimuth 135

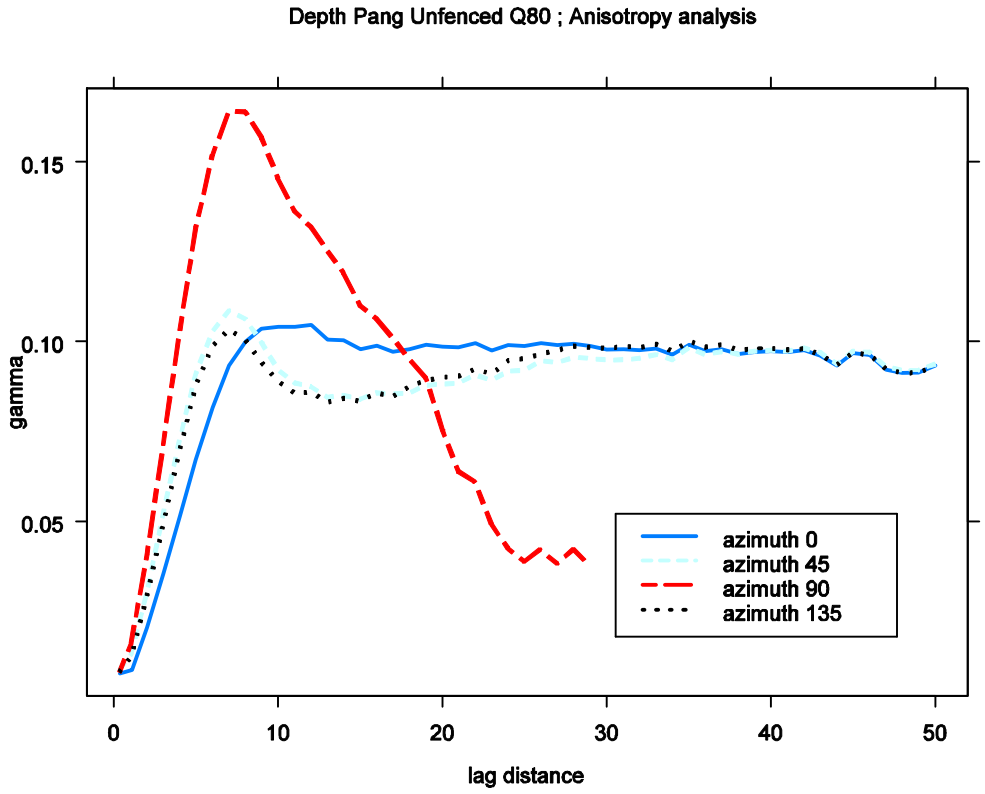
Depth Pang Unfenced Q80 ; Anisotropy analysis
gamma
0.15
0.10
0.05
0
10
20
30
40
50
lag distance
azimuth 0
azimuth 45
azimuth 90
azimuth 135

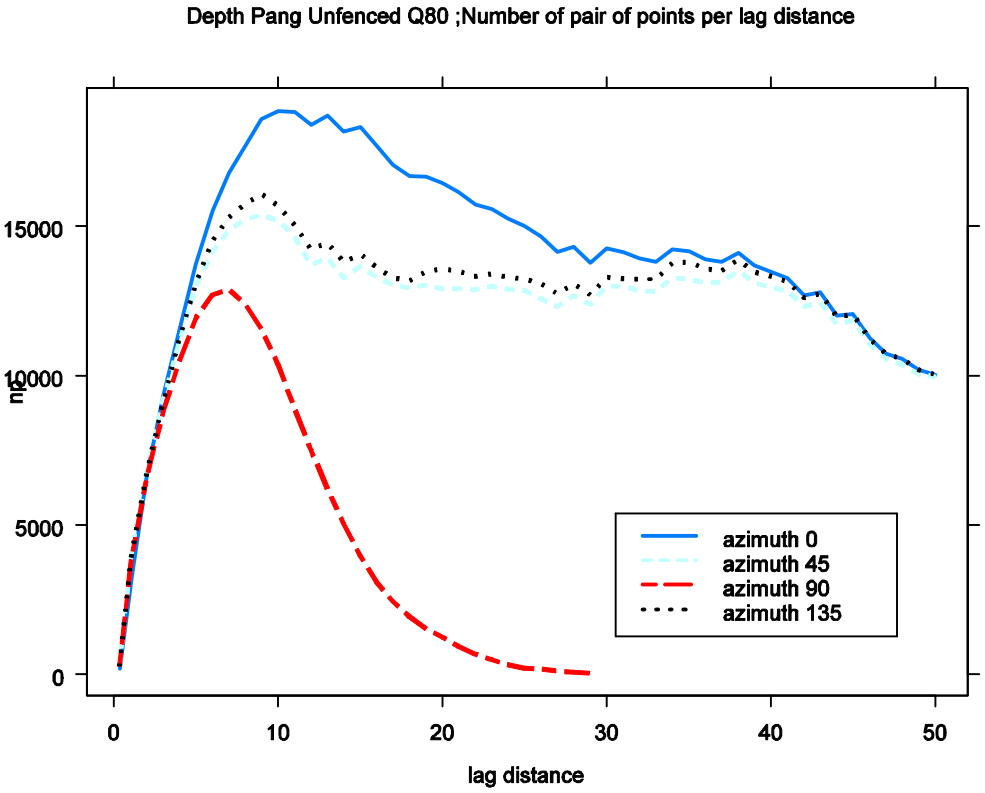
Depth Pang Unfenced Q80 ;Number of pair of points per lag distance
np
15000
10000
5000
0
0
10
20
30
40
50
lag distance
azimuth 0
azimuth 45
azimuth 90
azimuth 135

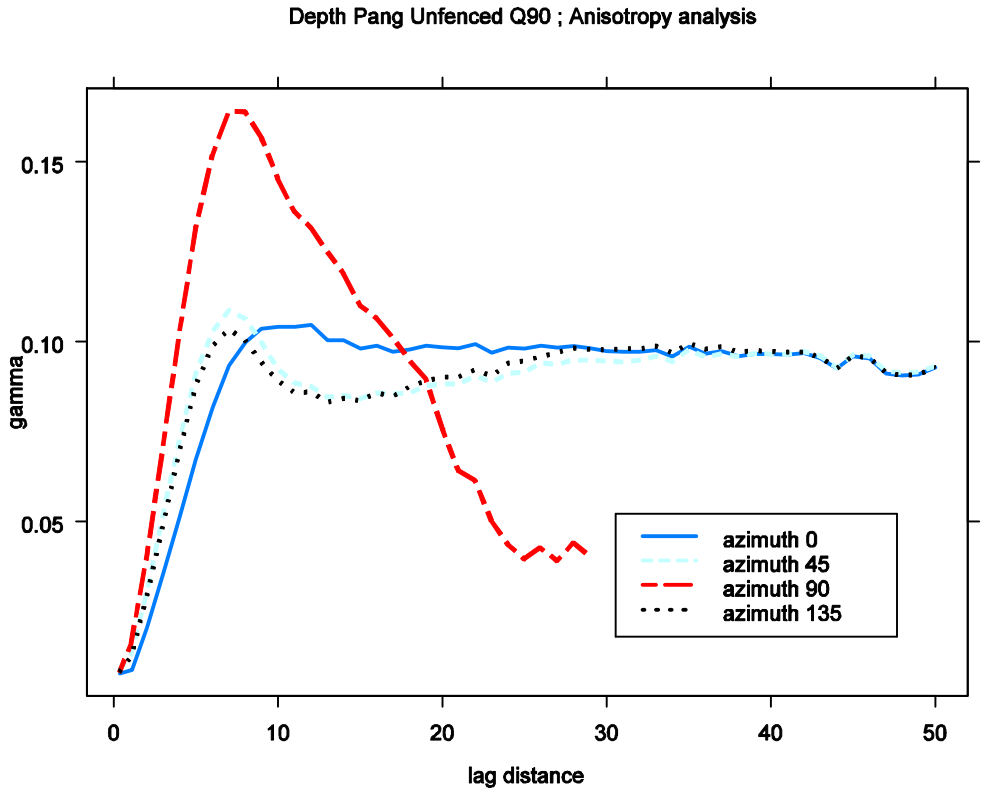
Depth Pang Unfenced Q90 ; Anisotropy analysis
gamma
0.15
0.10
0.05
0
10
20
30
40
50
lag distance
azimuth 0
azimuth 45
azimuth 90
azimuth 135

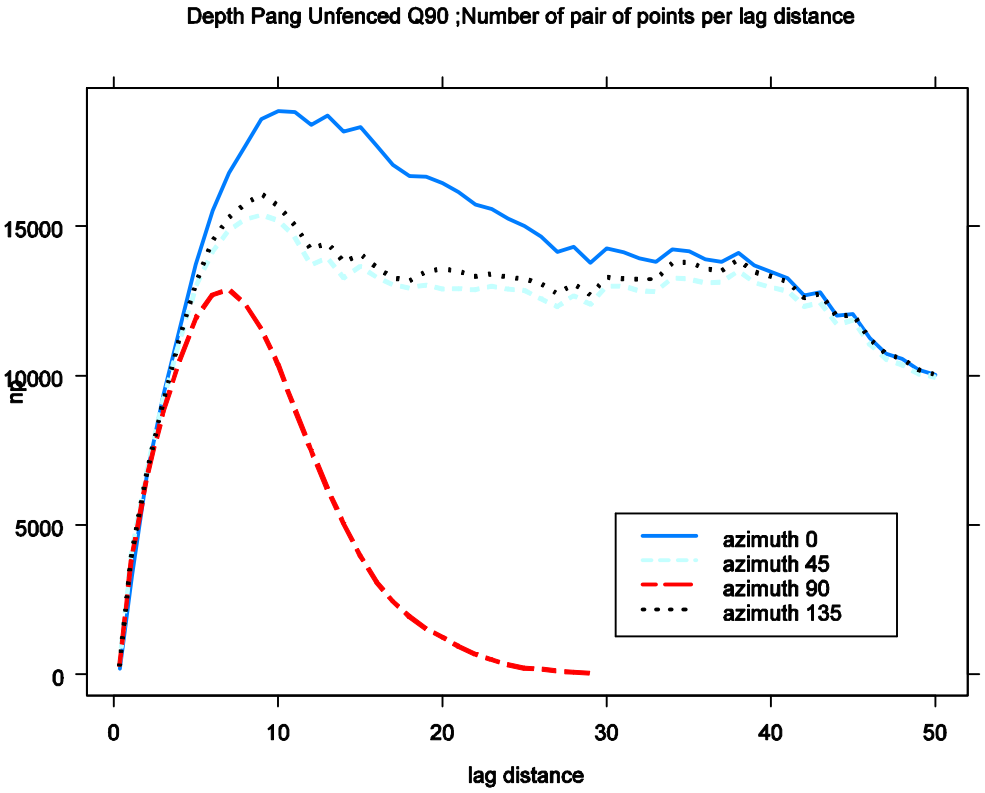
Depth Pang Unfenced Q90 ;Number of pair of points per lag distance
np
15000
10000
5000
0
0
10
20
30
40
50
lag distance
azimuth 0
azimuth 45
azimuth 90
azimuth 135

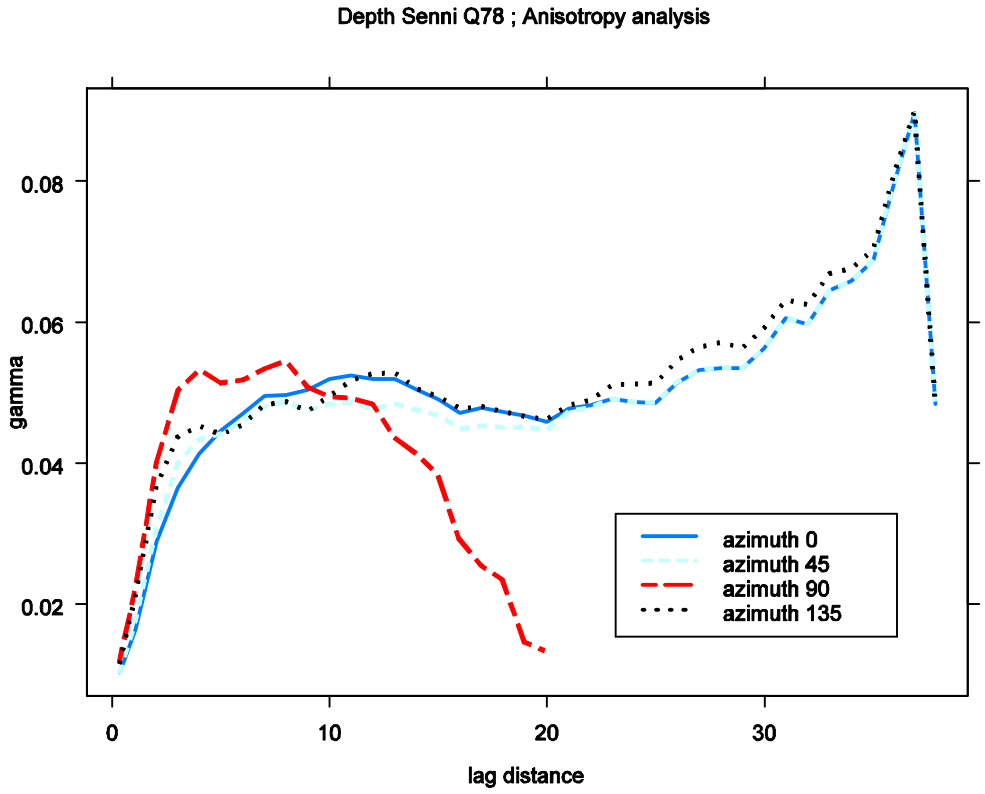
Depth Senni Q78 ; Anisotropy analysis
gamma
0.02
0.04
0.06
0.08
0
10
20
30
lag distance
azimuth 0
azimuth 45
azimuth 90
azimuth 135

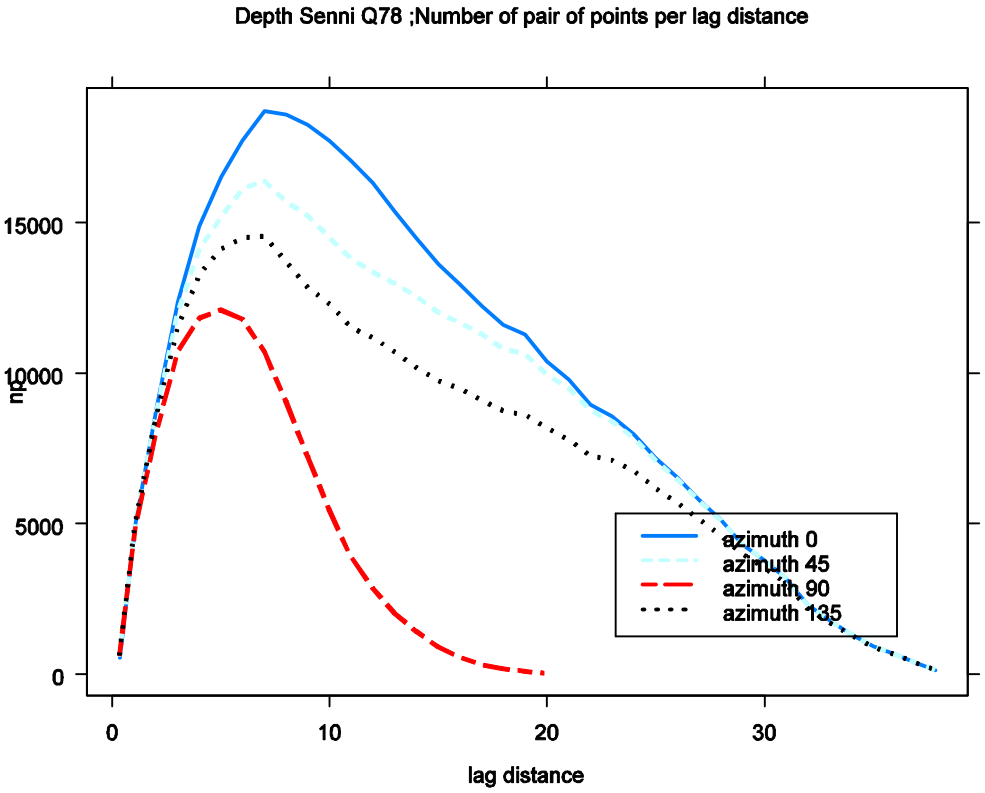
Depth Senni Q78 ;Number of pair of points per lag distance
np
0
5000
10000
15000
0
10
20
30
lag distance
azimuth 0
azimuth 45
azimuth 90
azimuth 135

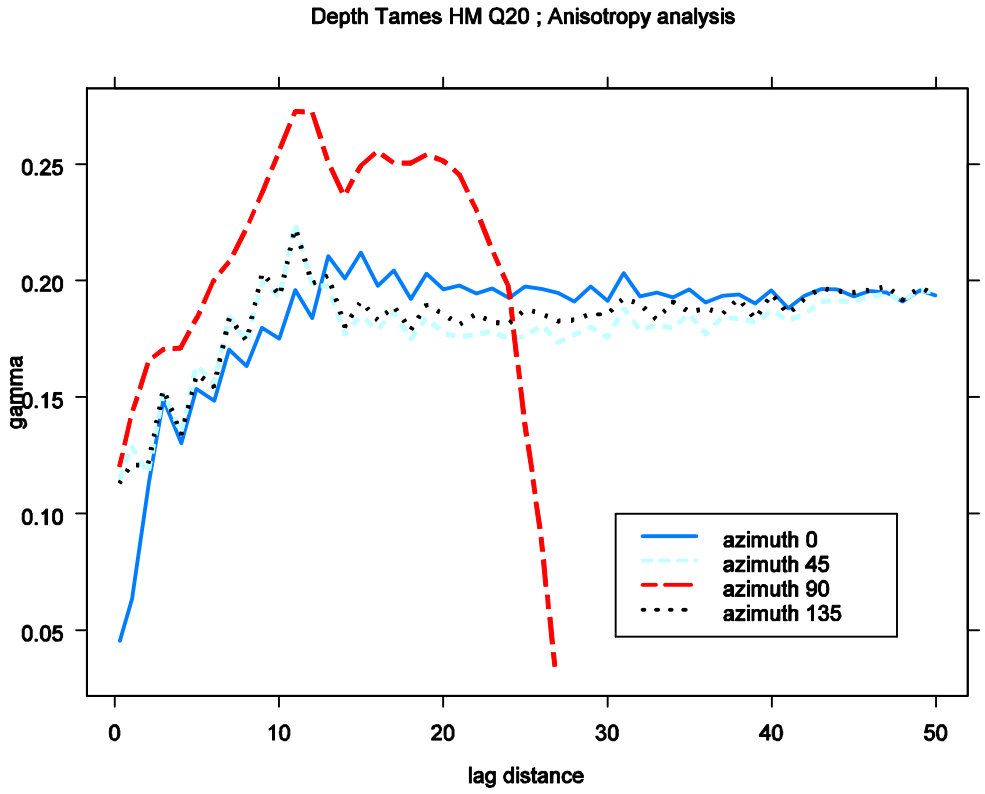
Depth Tames HM Q20 ; Anisotropy analysis
gamma
0.25
0.20
0.15
0.10
0.05
0
10
20
30
40
50
lag distance
azimuth 0
azimuth 45
azimuth 90
azimuth 135

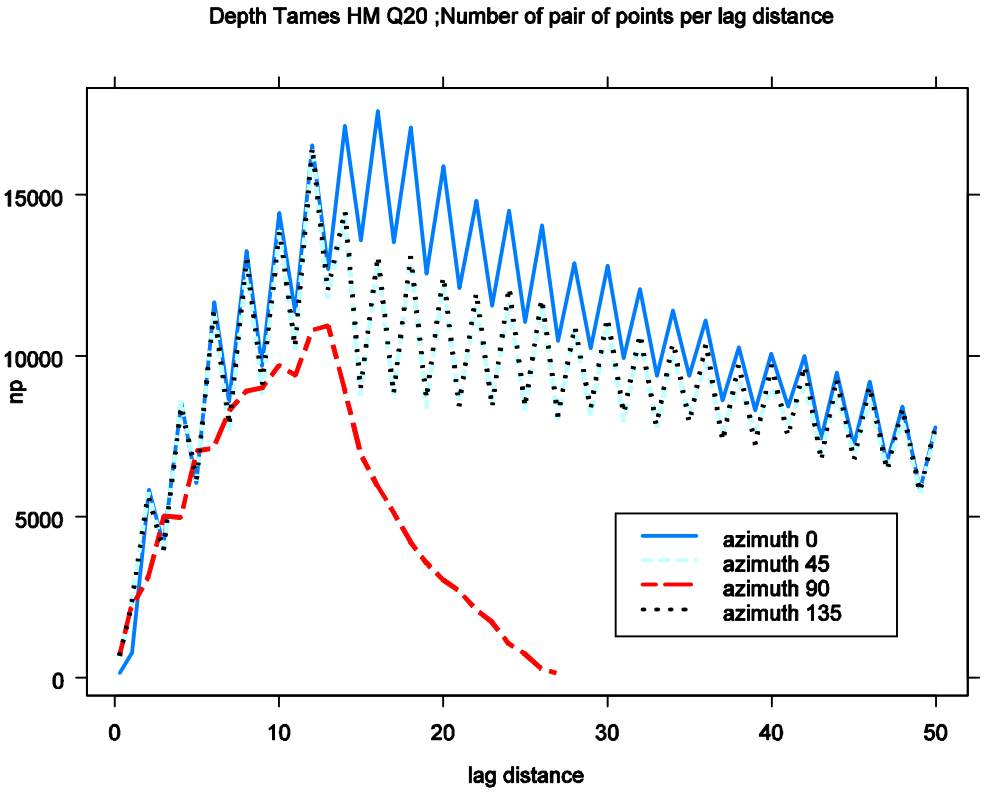
Depth Tames HM Q20 ;Number of pair of points per lag distance
np
15000
10000
5000
0
0
10
20
30
40
50
lag distance
azimuth 0
azimuth 45
azimuth 90
azimuth 135

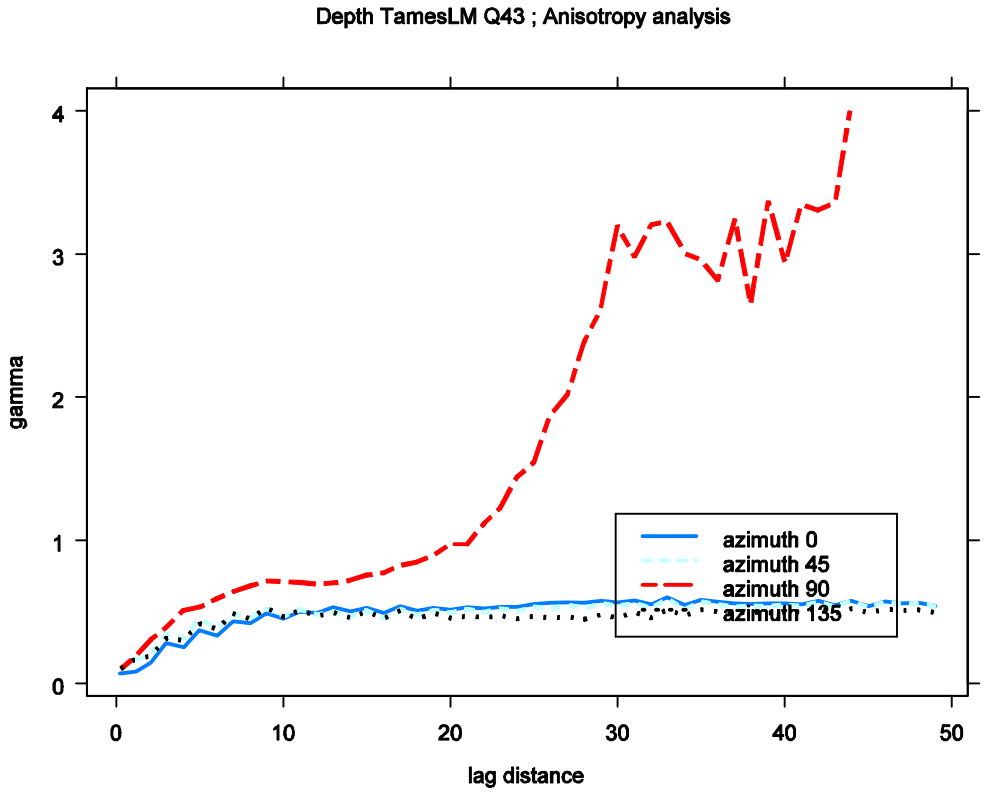
Depth TamesLM Q43 ; Anisotropy analysis
gamma
lag distance
azimuth 0
azimuth 45
azimuth 90
azimuth 135

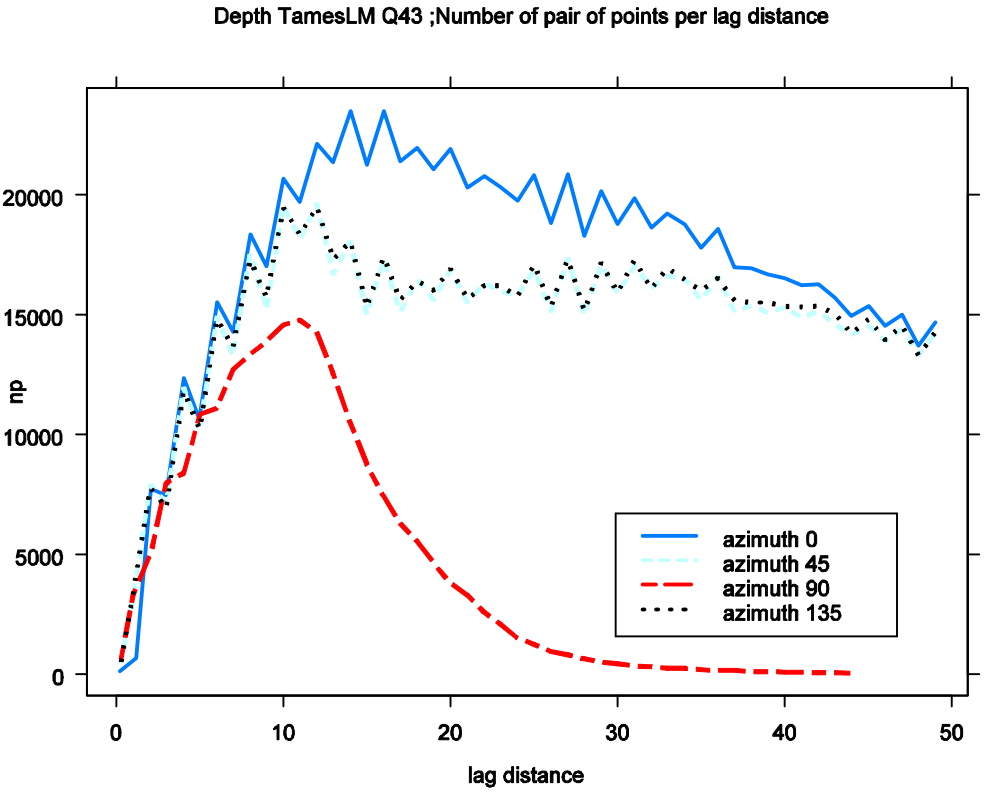
Depth TamesLM Q43 ;Number of pair of points per lag distance
np
lag distance
azimuth 0
azimuth 45
azimuth 90
azimuth 135

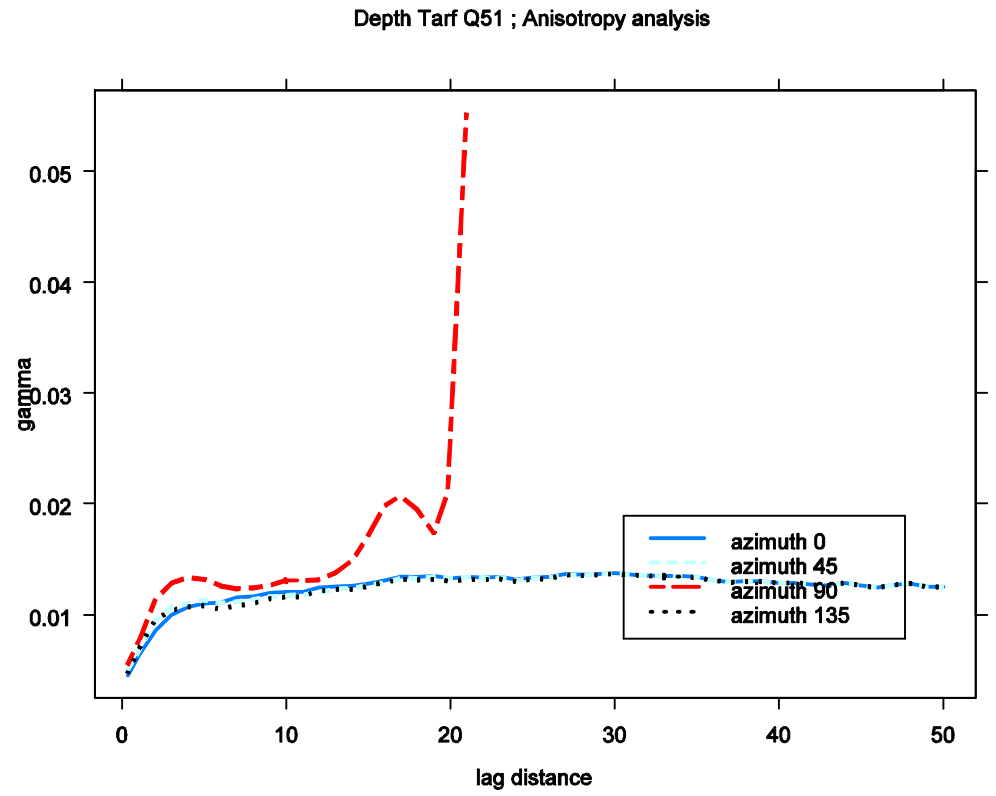
Depth Tarf Q51 ; Anisotropy analysis
gamma
0.05
0.04
0.03
0.02
0.01
0
10
20
30
40
50
lag distance
azimuth 0
azimuth 45
azimuth 90
azimuth 135

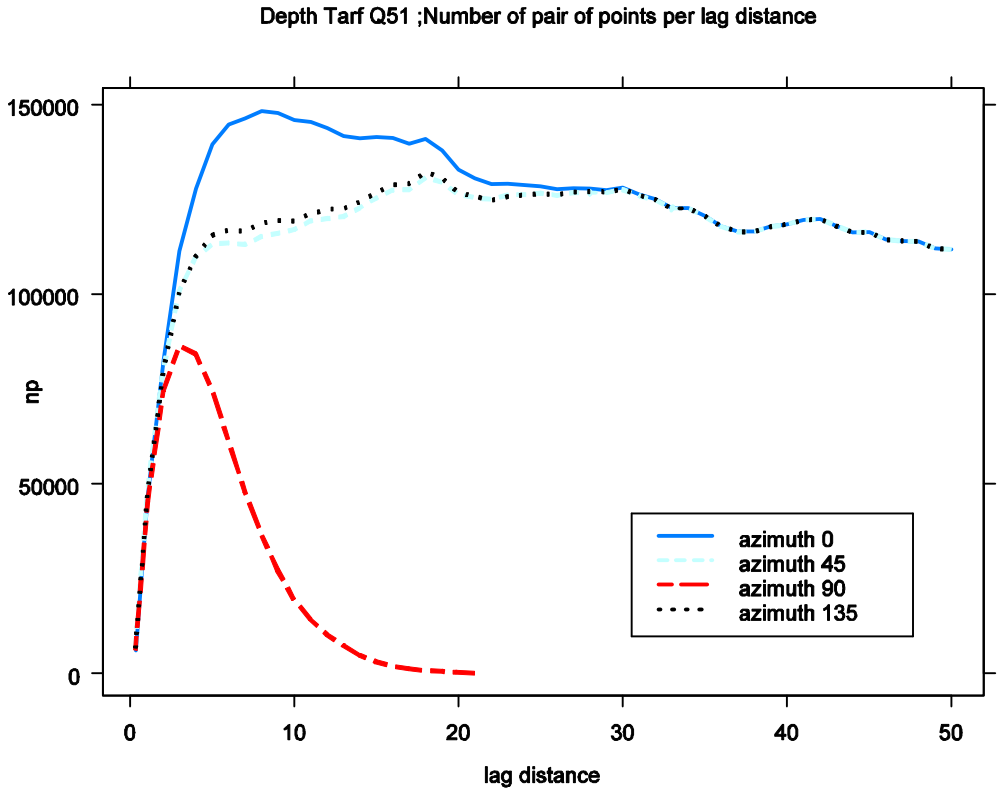
Depth Tarf Q51 ;Number of pair of points per lag distance
np
150000
100000
50000
0
0
10
20
30
40
50
lag distance
azimuth 0
azimuth 45
azimuth 90
azimuth 135

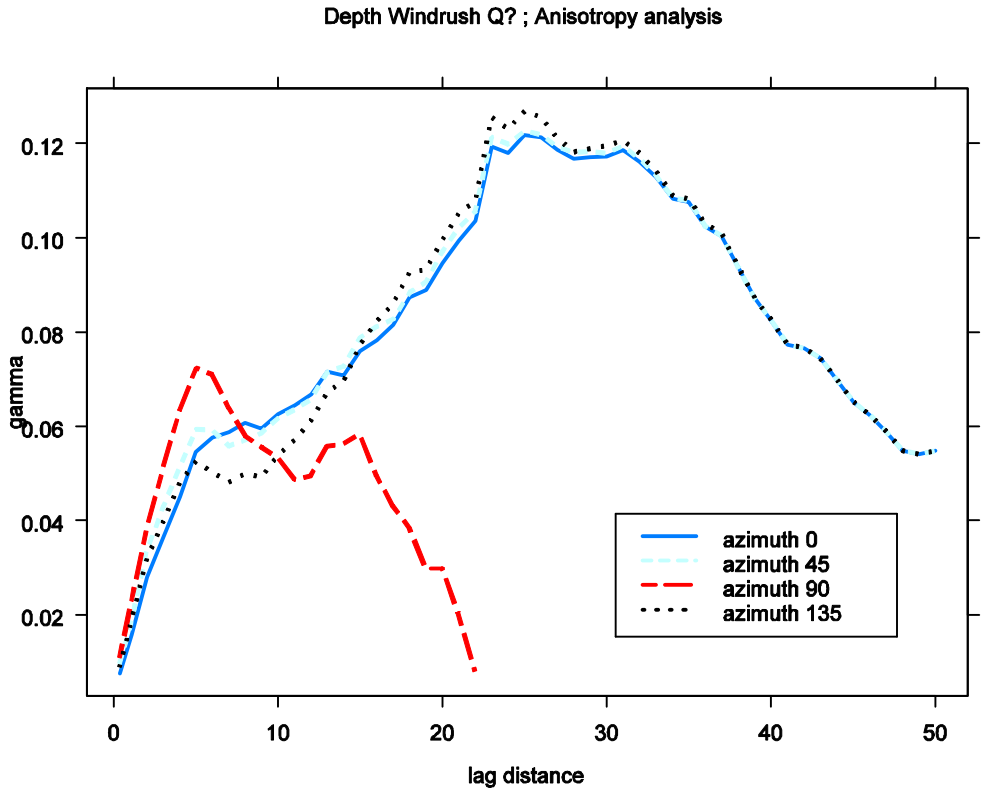
Depth Windrush Q? ; Anisotropy analysis
gamma
0.02
0.04
0.06
0.08
0.10
0.12
0
10
20
30
40
50
lag distance
azimuth 0
azimuth 45
azimuth 90
azimuth 135

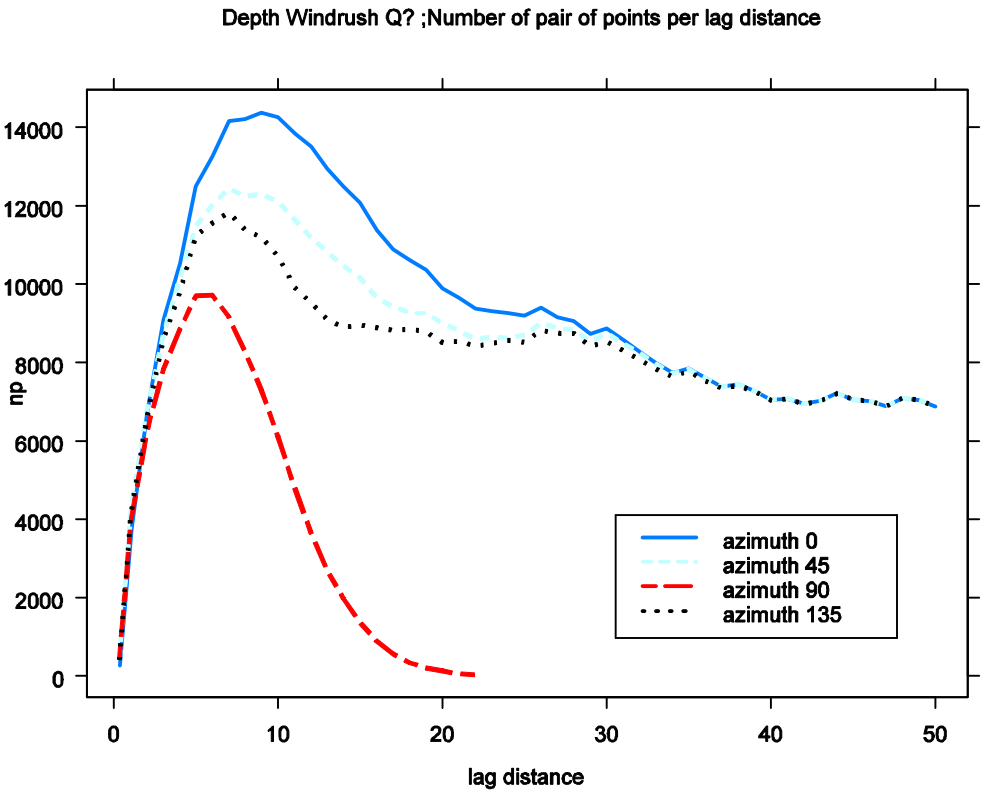
Depth Windrush Q? ;Number of pair of points per lag distance
np
0
2000
4000
6000
8000
10000
12000
14000
0
10
20
30
40
50
lag distance
azimuth 0
azimuth 45
azimuth 90
azimuth 135

Anisotropy analysis fir the wet points

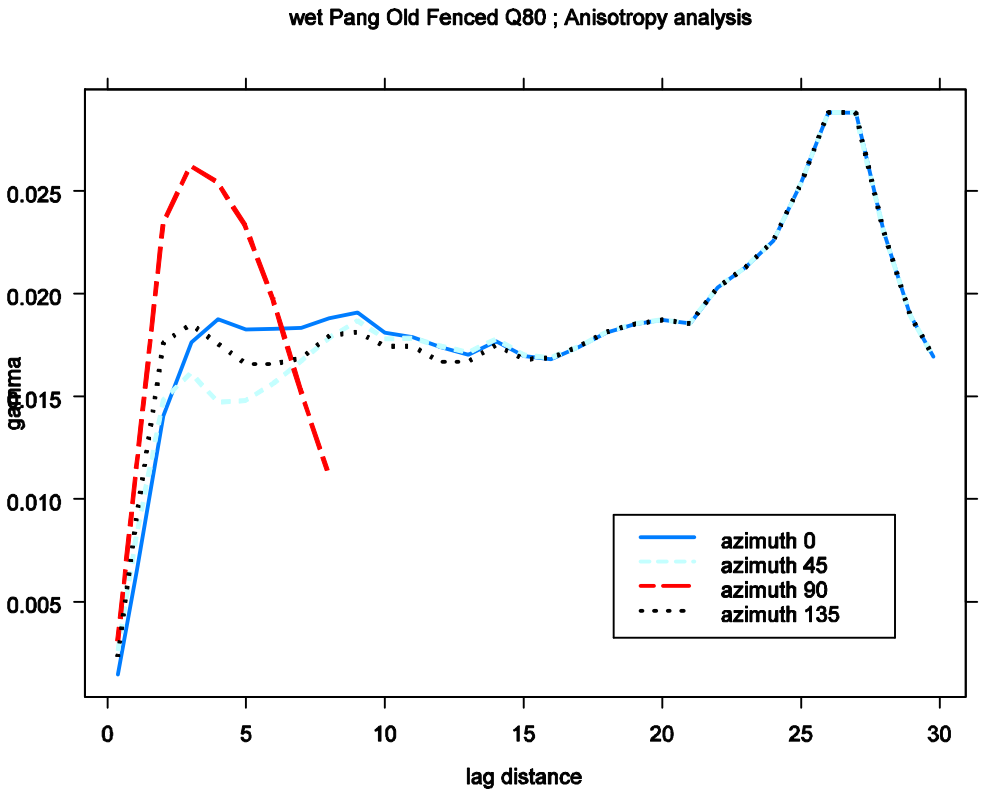

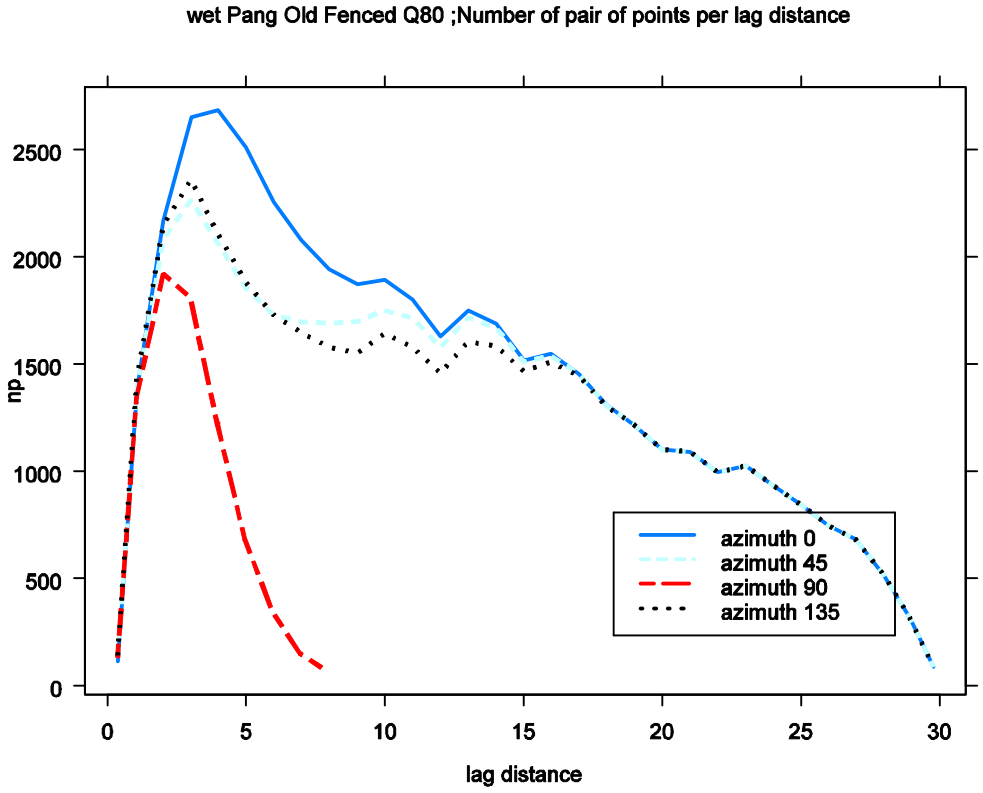

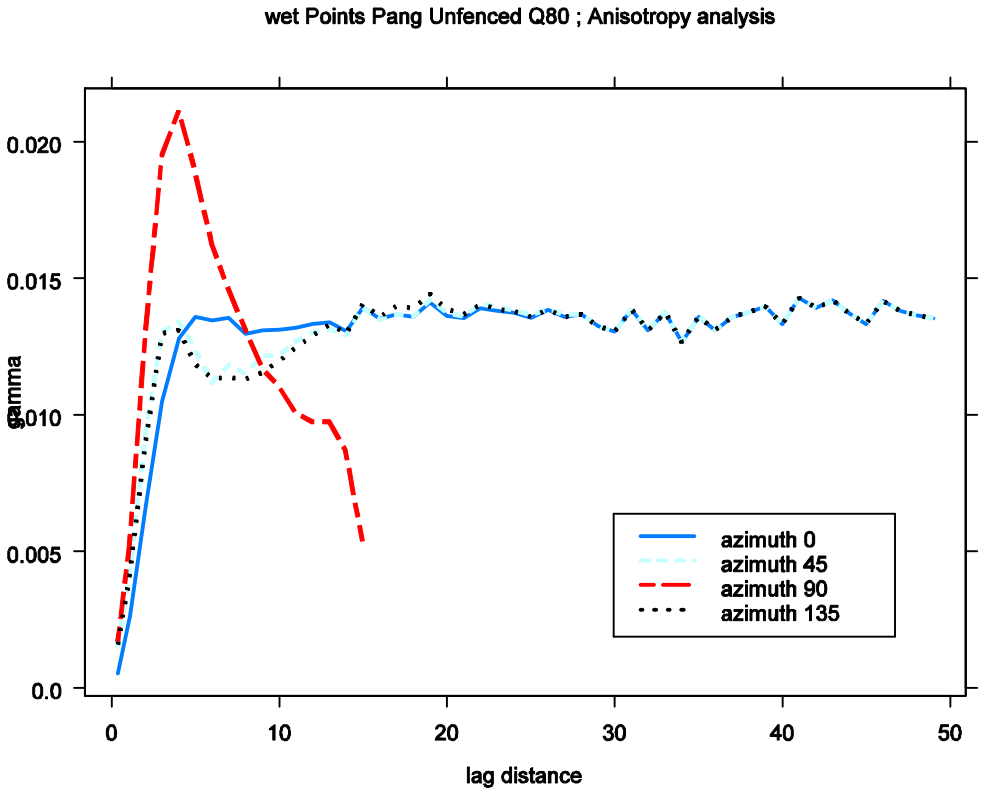
wet Points Pang Unfenced Q80 ; Anisotropy analysis
gamma
0.0
0.005
0.010
0.015
0.020
0
10
20
30
40
50
lag distance
azimuth 0
azimuth 45
azimuth 90
azimuth 135

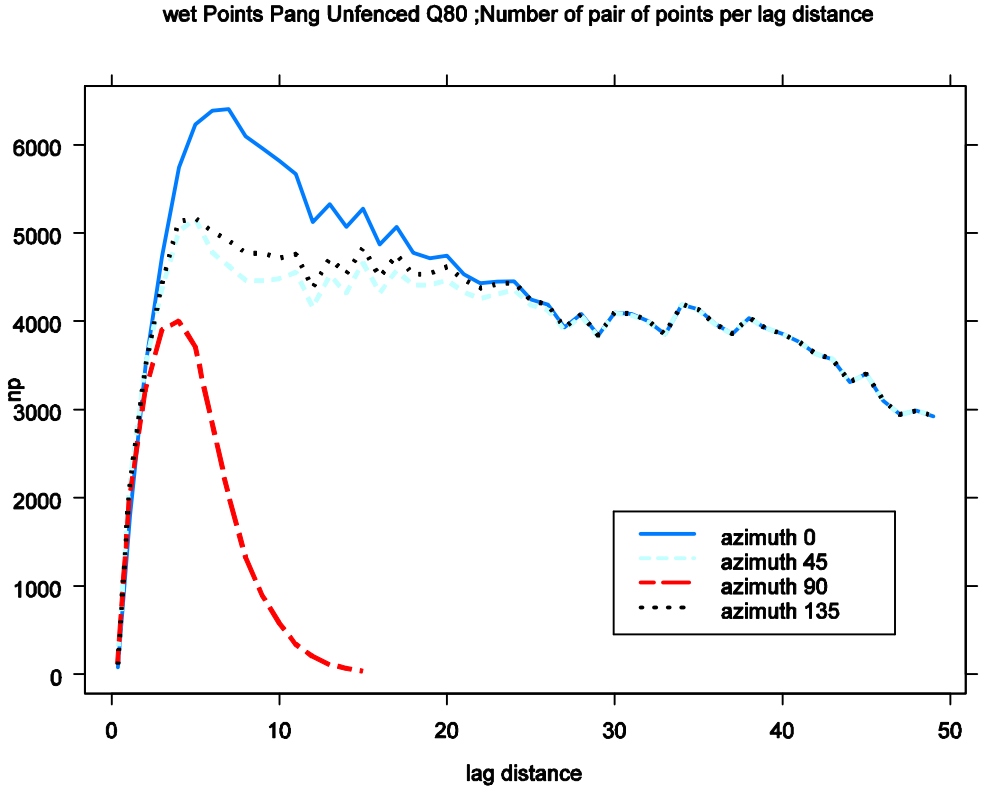
wet Points Pang Unfenced Q80 ;Number of pair of points per lag distance
np
0
1000
2000
3000
4000
5000
6000
0
10
20
30
40
50
lag distance
azimuth 0
azimuth 45
azimuth 90
azimuth 135

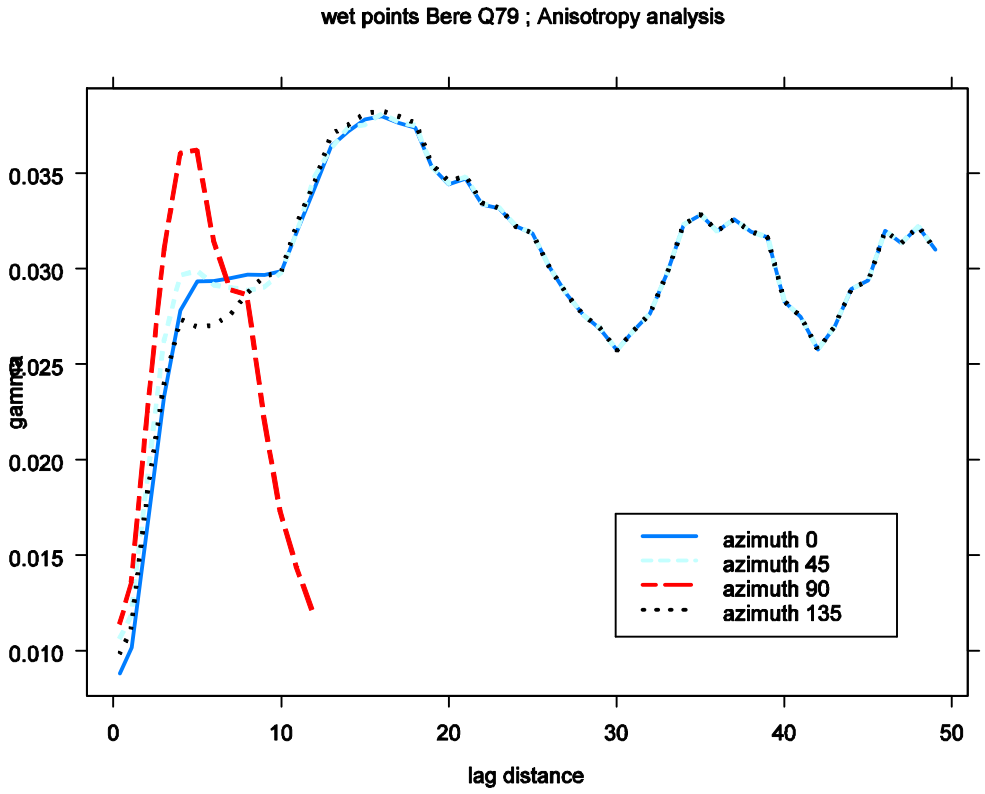
wet points Bere Q79 ; Anisotropy analysis
gamma
0.010
0.015
0.020
0.025
0.030
0.035
0
10
20
30
40
50
lag distance
azimuth 0
azimuth 45
azimuth 90
azimuth 135

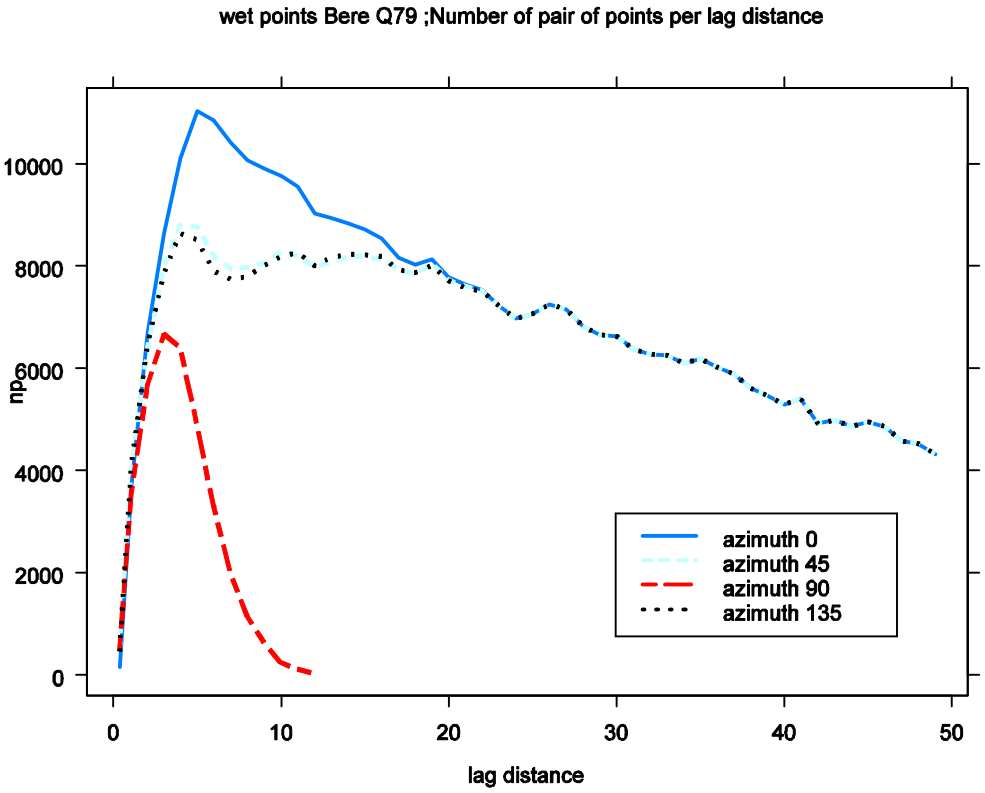
wet points Bere Q79 ;Number of pair of points per lag distance
np
0
2000
4000
6000
8000
10000
0
10
20
30
40
50
lag distance
azimuth 0
azimuth 45
azimuth 90
azimuth 135

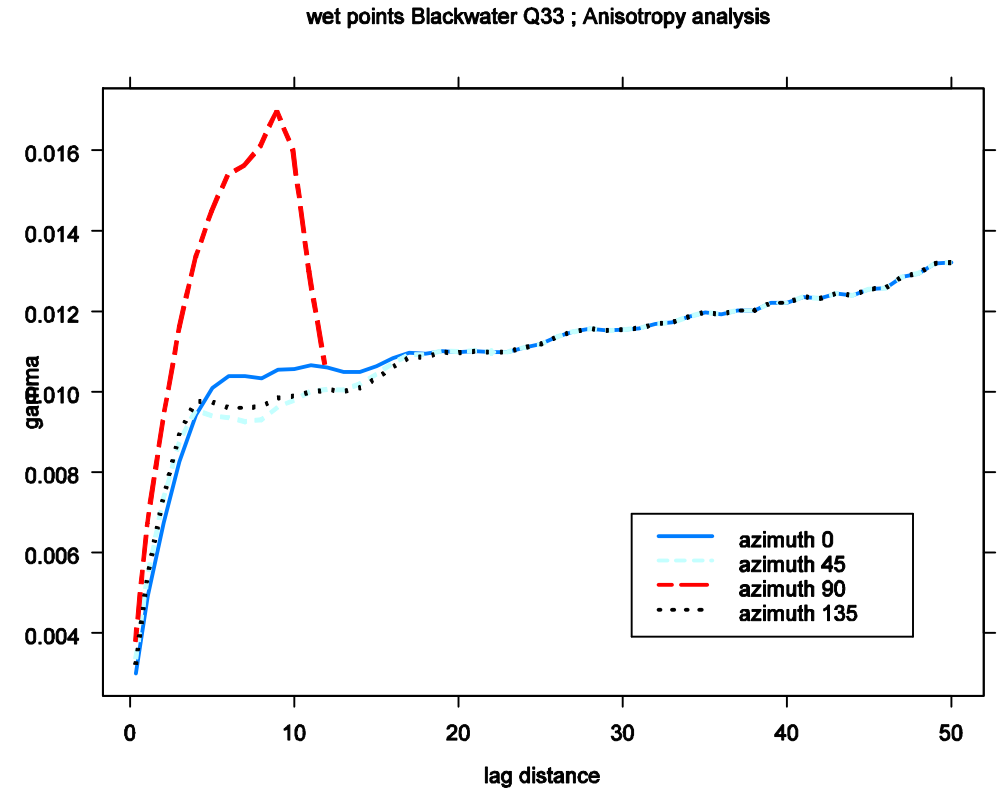
wet points Blackwater Q33 ; Anisotropy analysis
gamma
0.004
0.006
0.008
0.010
0.012
0.014
0.016
0
10
20
30
40
50
lag distance
azimuth 0
azimuth 45
azimuth 90
azimuth 135

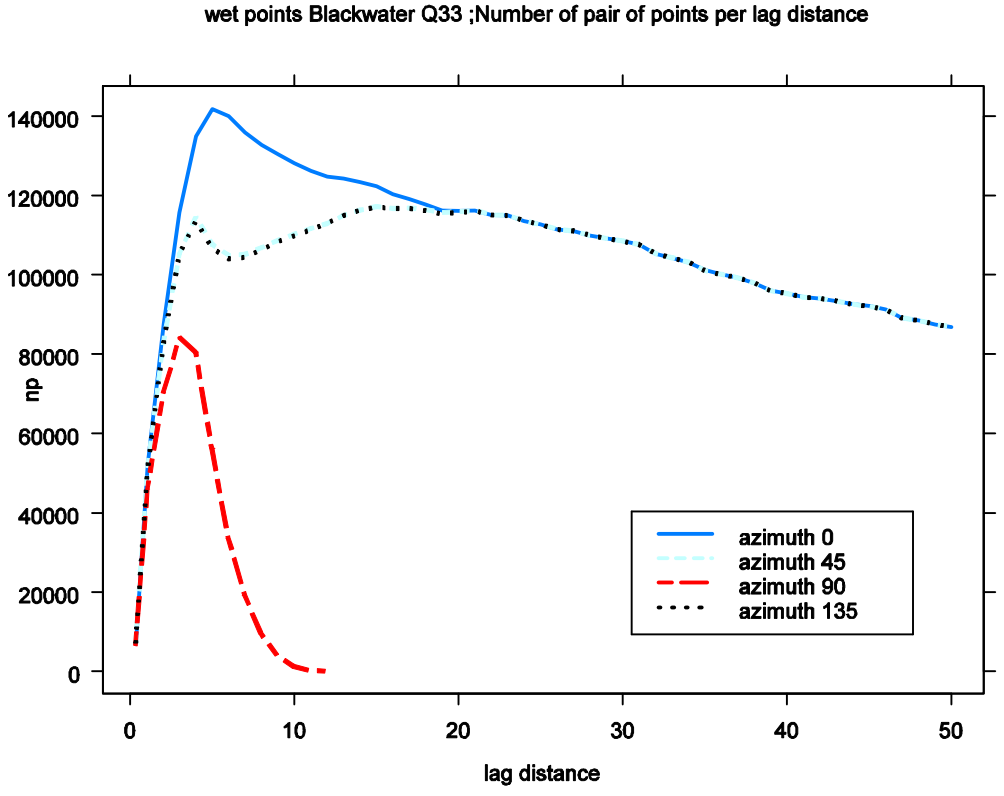
wet points Blackwater Q33 ;Number of pair of points per lag distance
np
0
20000
40000
60000
80000
100000
120000
140000
0
10
20
30
40
50
lag distance
azimuth 0
azimuth 45
azimuth 90
azimuth 135

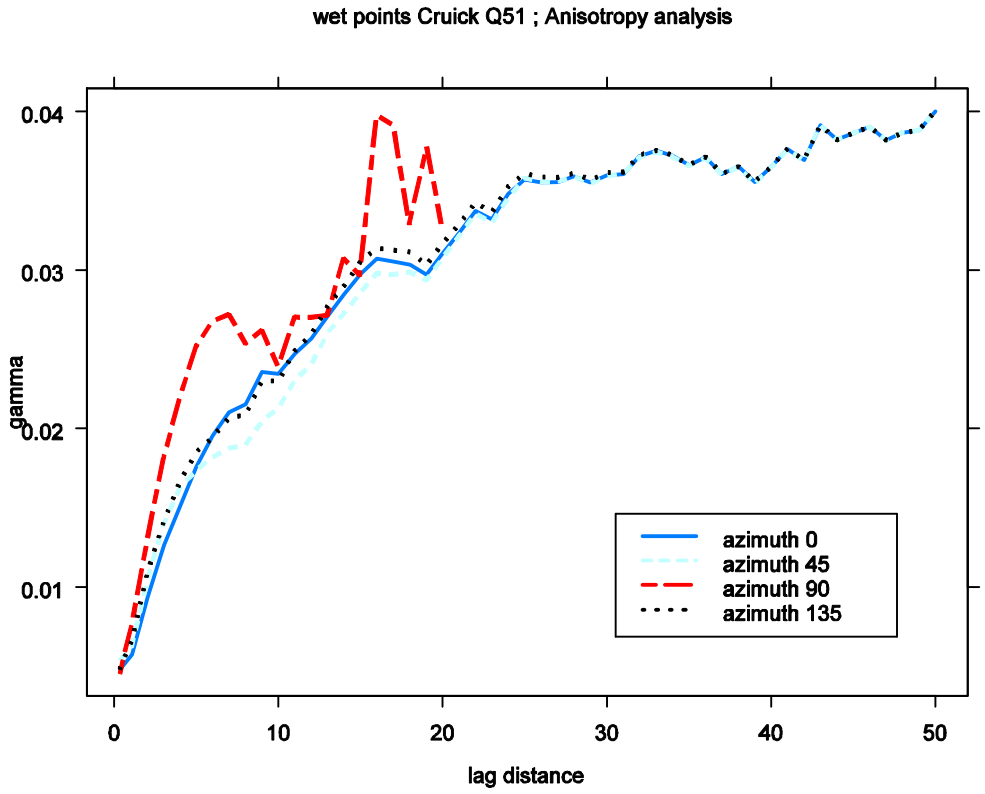
wet points Cruick Q51 ; Anisotropy analysis
gamma
0.04
0.03
0.02
0.01
0
10
20
30
40
50
lag distance
azimuth 0
azimuth 45
azimuth 90
azimuth 135

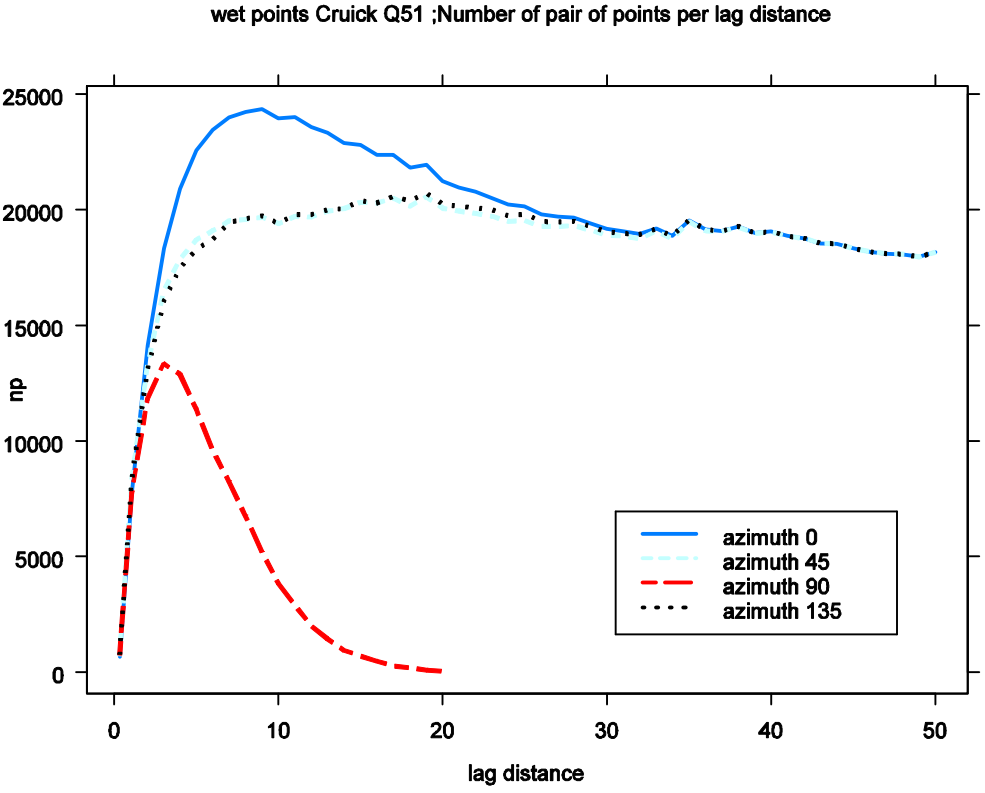
wet points Cruick Q51 ;Number of pair of points per lag distance
np
25000
20000
15000
10000
5000
0
0
10
20
30
40
50
lag distance
azimuth 0
azimuth 45
azimuth 90
azimuth 135

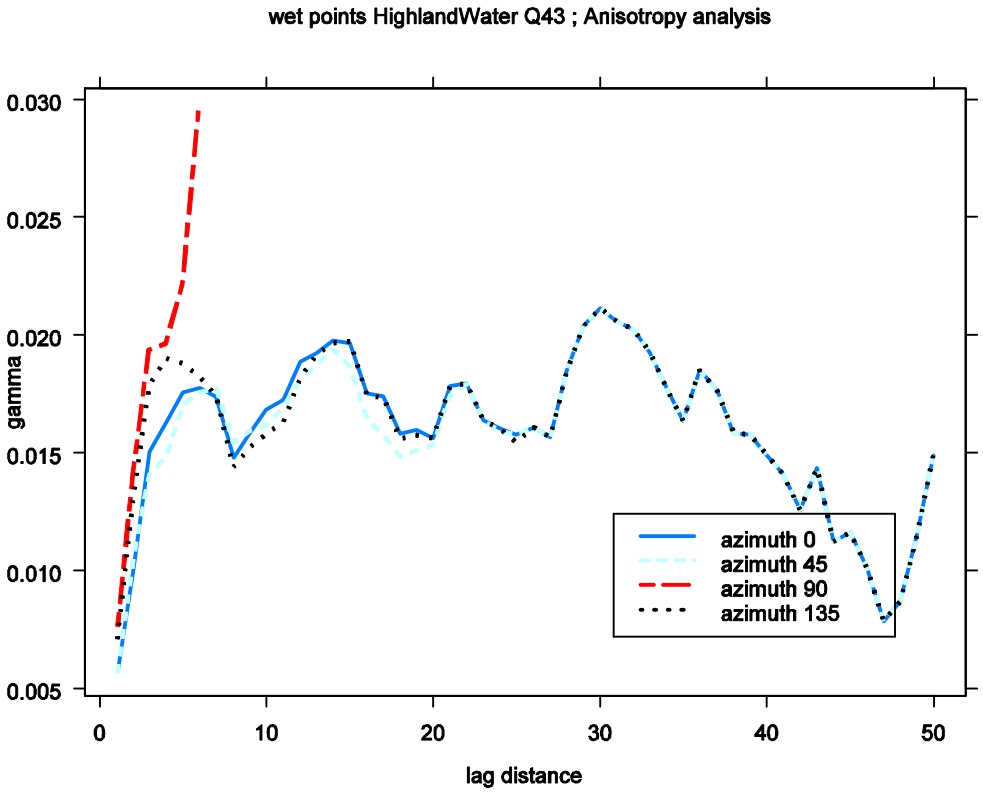
wet points HighlandWater Q43 ; Anisotropy analysis
gamma
lag distance
azimuth 0
azimuth 45
azimuth 90
azimuth 135

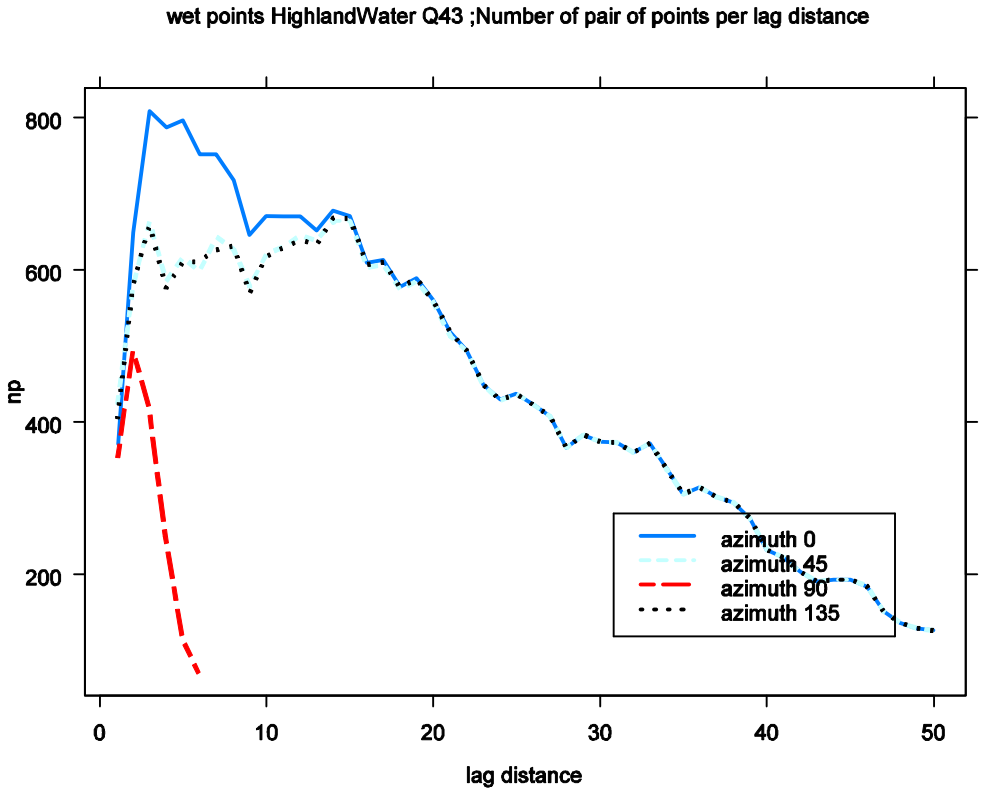
wet points HighlandWater Q43 ;Number of pair of points per lag distance
np
lag distance
azimuth 0
azimuth 45
azimuth 90
azimuth 135

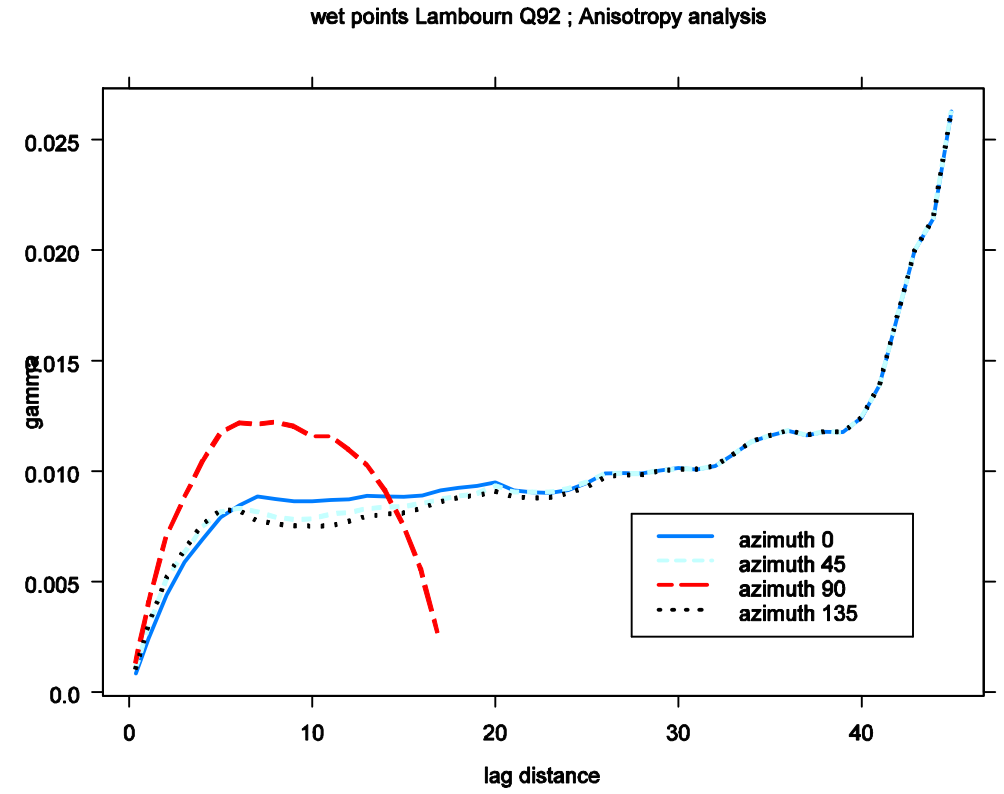
wet points Lambourn Q92 ; Anisotropy analysis
gamma
0.0
0.005
0.010
0.015
0.020
0.025
0
10
20
30
40
lag distance
azimuth 0
azimuth 45
azimuth 90
azimuth 135

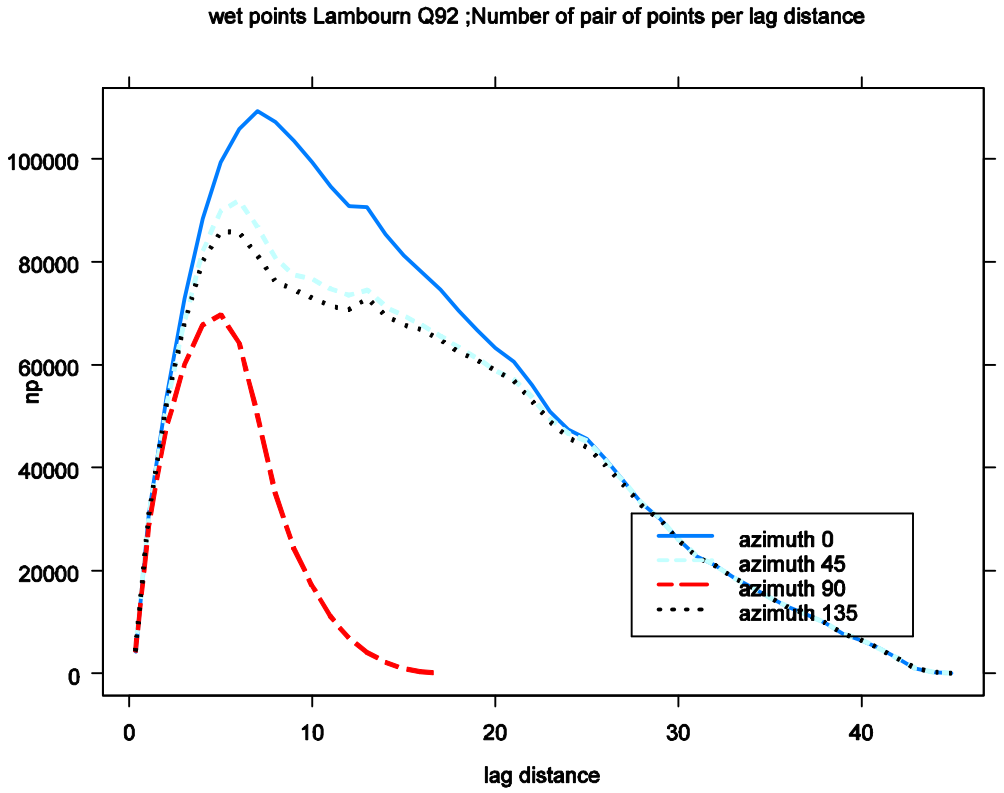
wet points Lambourn Q92 ;Number of pair of points per lag distance
np
0
20000
40000
60000
80000
100000
0
10
20
30
40
lag distance
azimuth 0
azimuth 45
azimuth 90
azimuth 135

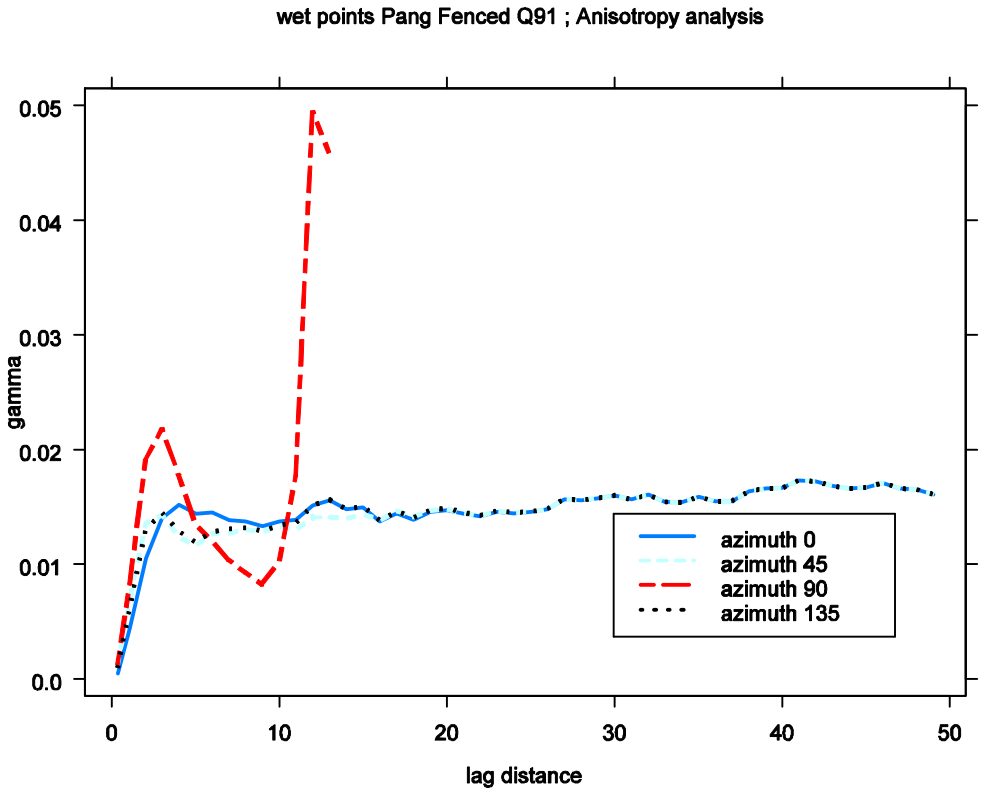
wet points Pang Fenced Q91 ; Anisotropy analysis
gamma
0.0
0.01
0.02
0.03
0.04
0.05
0
10
20
30
40
50
lag distance
azimuth 0
azimuth 45
azimuth 90
azimuth 135

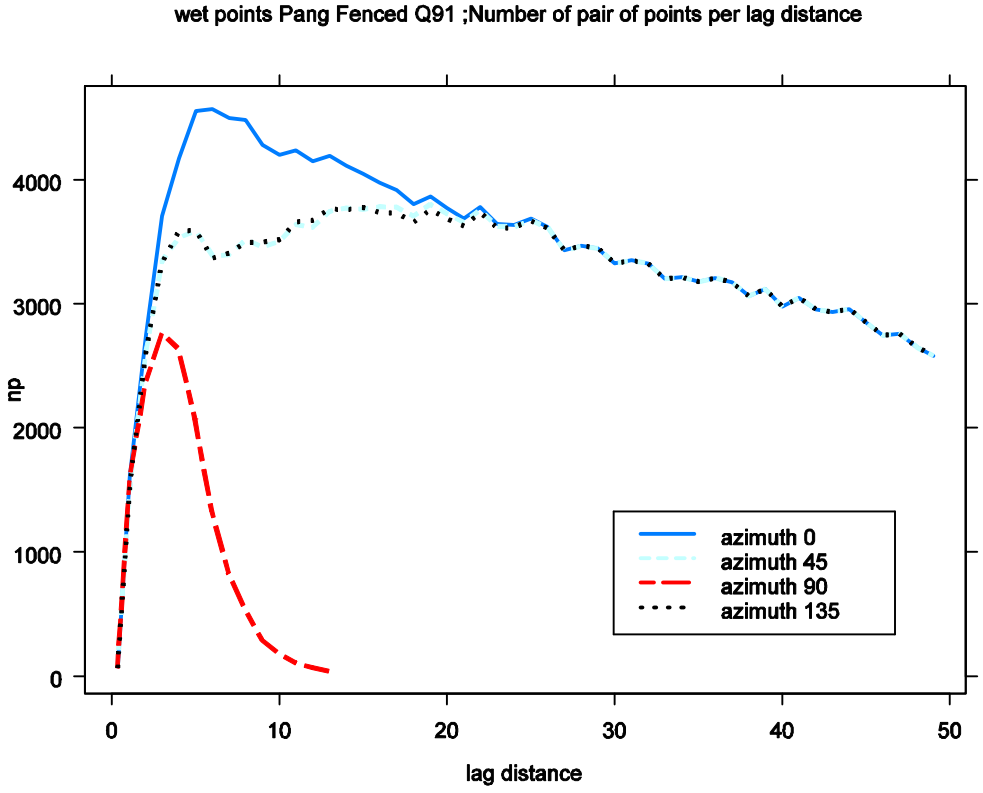
wet points Pang Fenced Q91 ;Number of pair of points per lag distance
np
0
1000
2000
3000
4000
0
10
20
30
40
50
lag distance
azimuth 0
azimuth 45
azimuth 90
azimuth 135

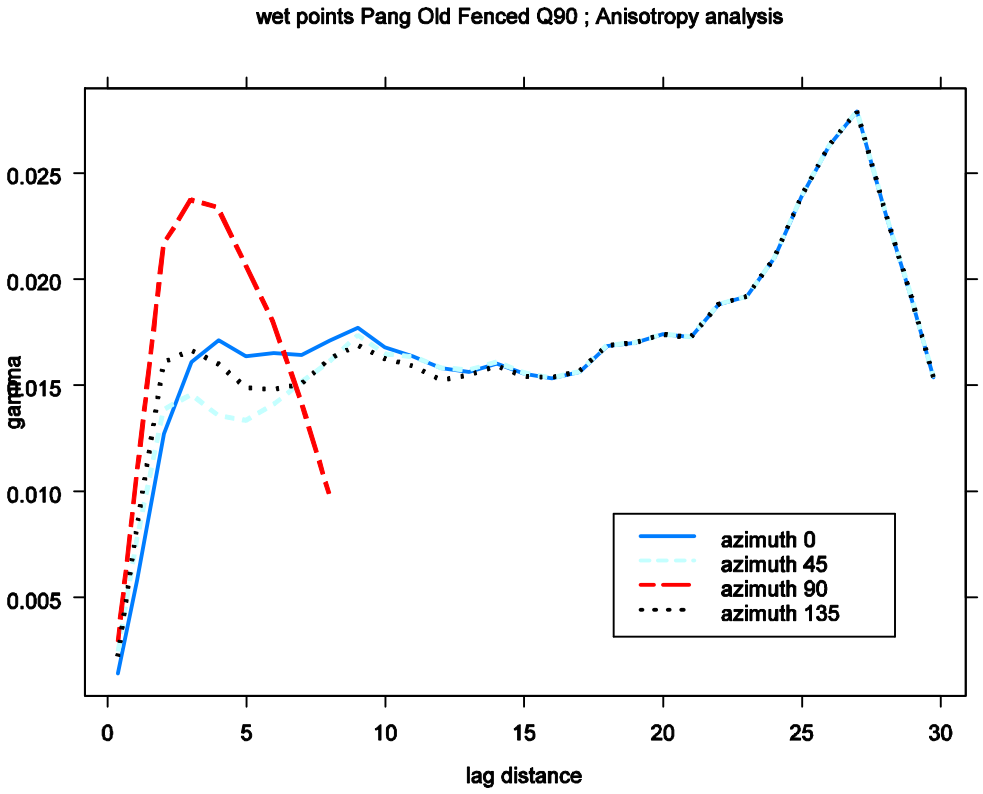
wet points Pang Old Fenced Q90 ; Anisotropy analysis
gamma
0.025
0.020
0.015
0.010
0.005
0
5
10
15
20
25
30
lag distance
azimuth 0
azimuth 45
azimuth 90
azimuth 135

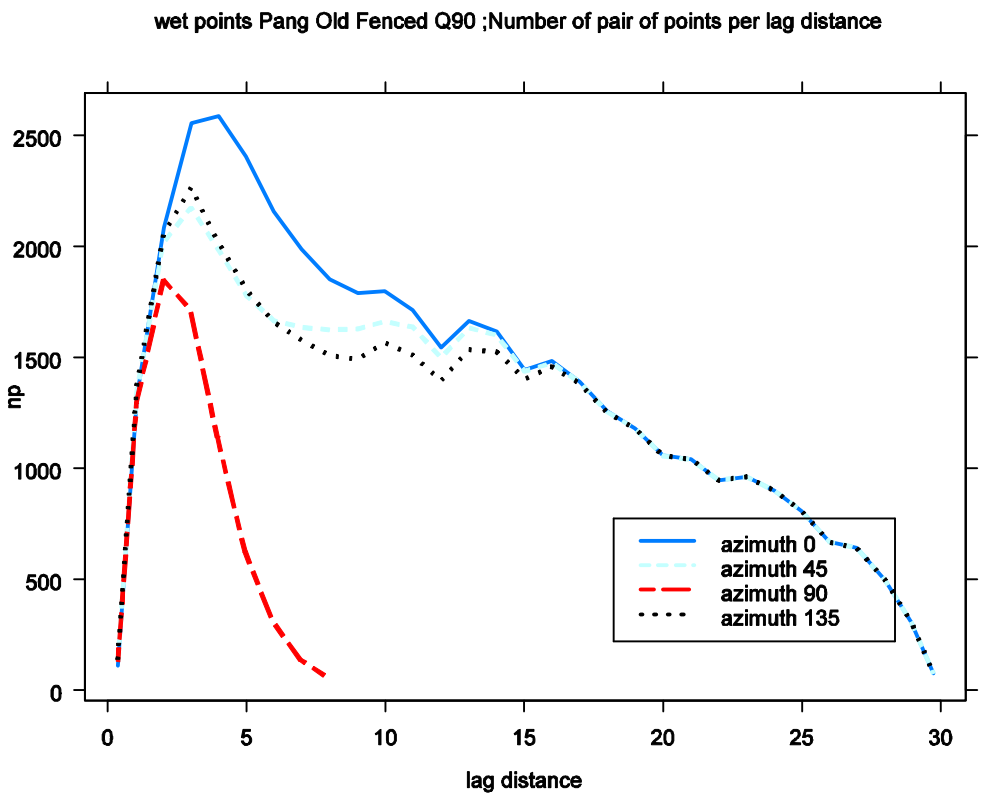
wet points Pang Old Fenced Q90 ;Number of pair of points per lag distance
np
2500
2000
1500
1000
500
0
0
5
10
15
20
25
30
lag distance
azimuth 0
azimuth 45
azimuth 90
azimuth 135

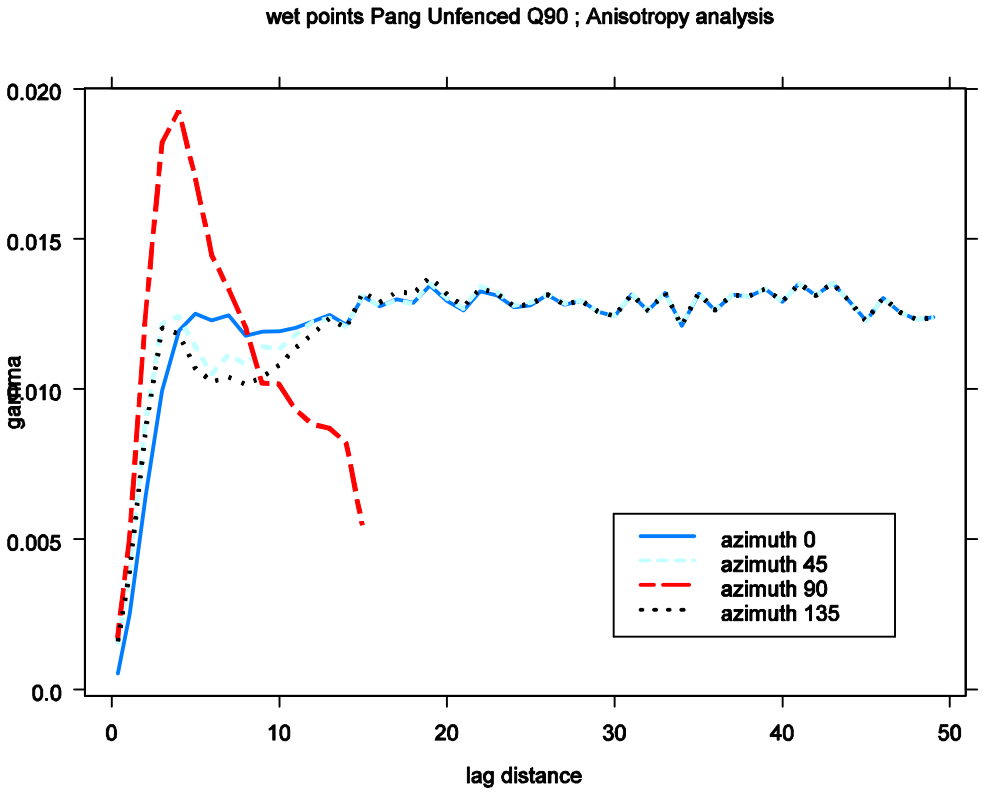
wet points Pang Unfenced Q90 ; Anisotropy analysis
0.020
0.015
0.010
0.005
0.0
gamma
0
10
20
30
40
50
lag distance
azimuth 0
azimuth 45
azimuth 90
azimuth 135

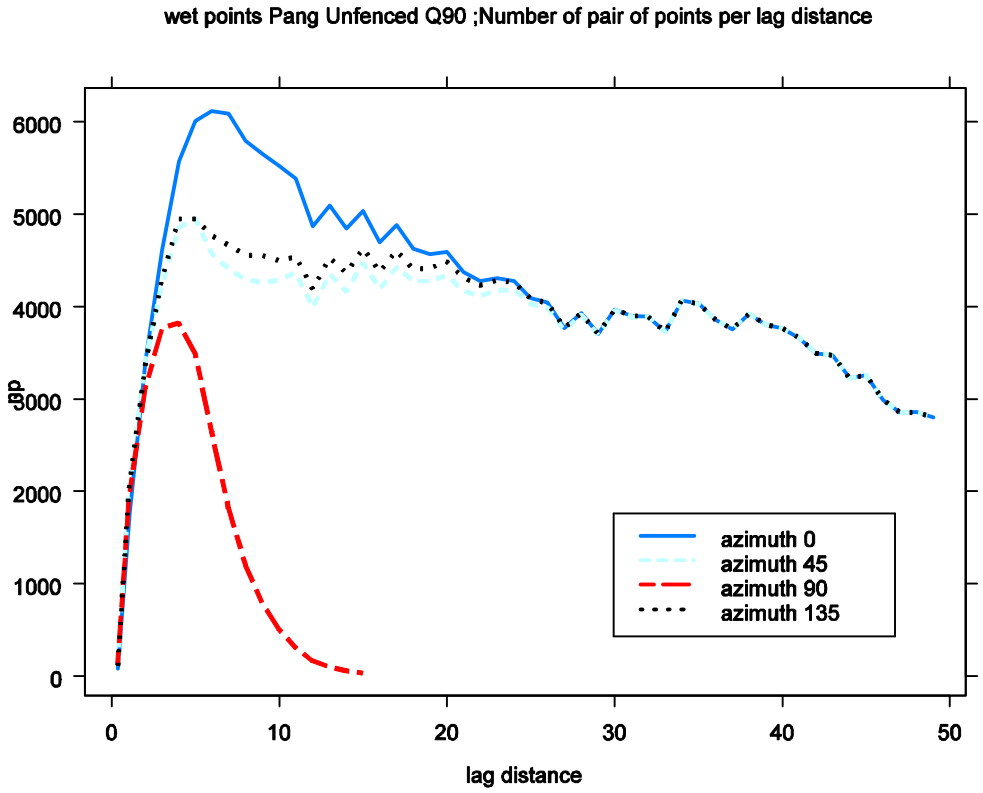
wet points Pang Unfenced Q90 ;Number of pair of points per lag distance
6000
5000
4000
3000
2000
1000
0
np
0
10
20
30
40
50
lag distance
azimuth 0
azimuth 45
azimuth 90
azimuth 135

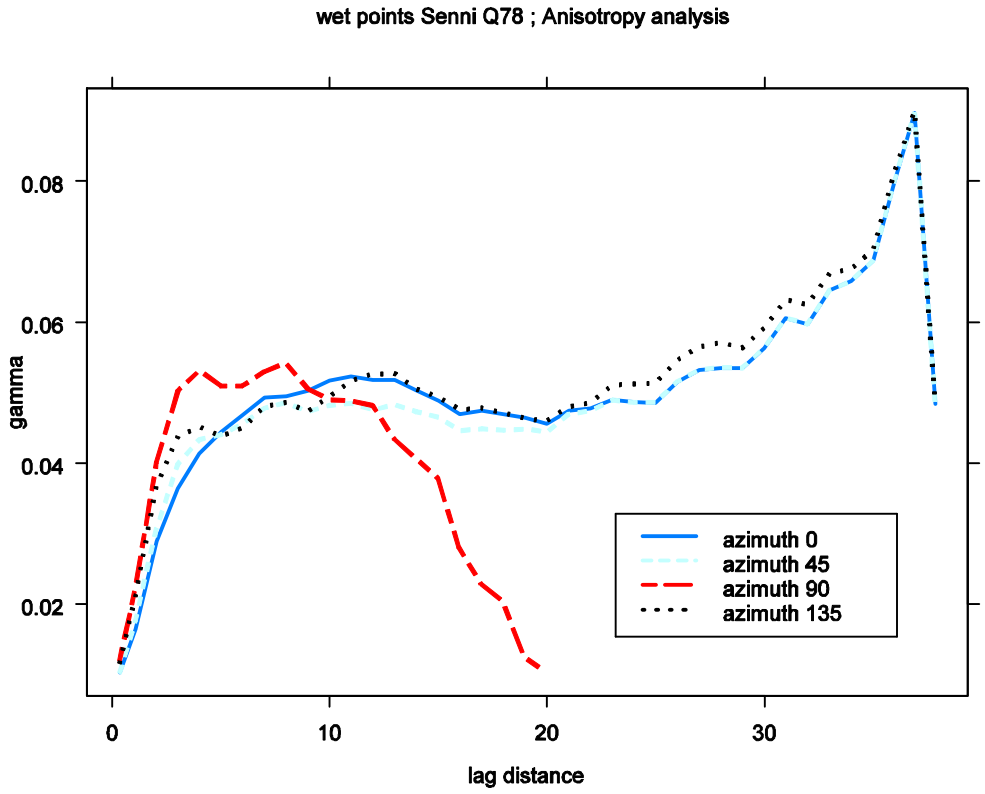
wet points Senni Q78 ; Anisotropy analysis
gamma
0.02
0.04
0.06
0.08
0
10
20
30
lag distance
azimuth 0
azimuth 45
azimuth 90
azimuth 135

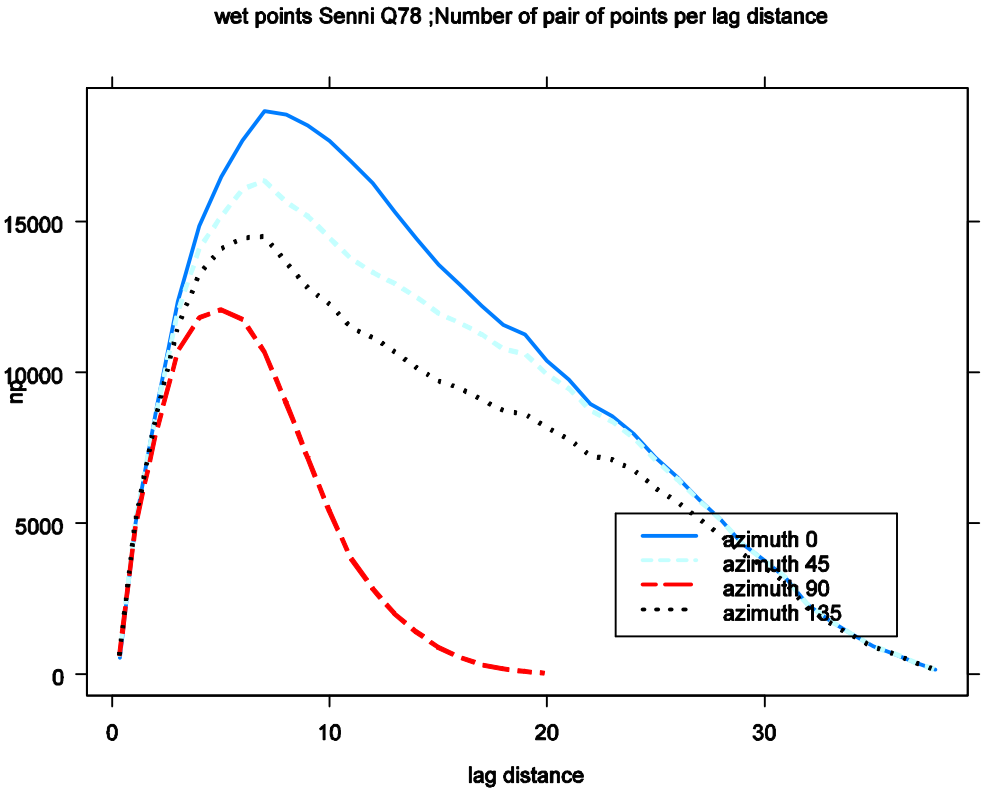
wet points Senni Q78 ;Number of pair of points per lag distance
np
0
5000
10000
15000
0
10
20
30
lag distance
azimuth 0
azimuth 45
azimuth 90
azimuth 135

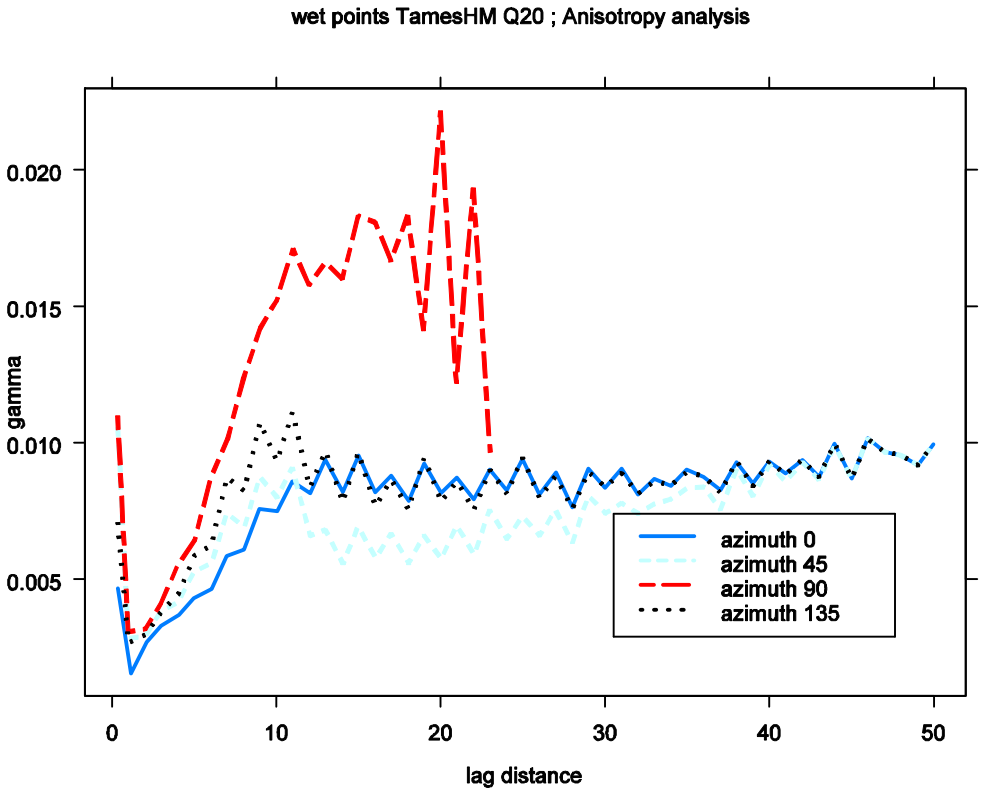
wet points TamesHM Q20 ; Anisotropy analysis
gamma
0.020
0.015
0.010
0.005
0
10
20
30
40
50
lag distance
azimuth 0
azimuth 45
azimuth 90
azimuth 135

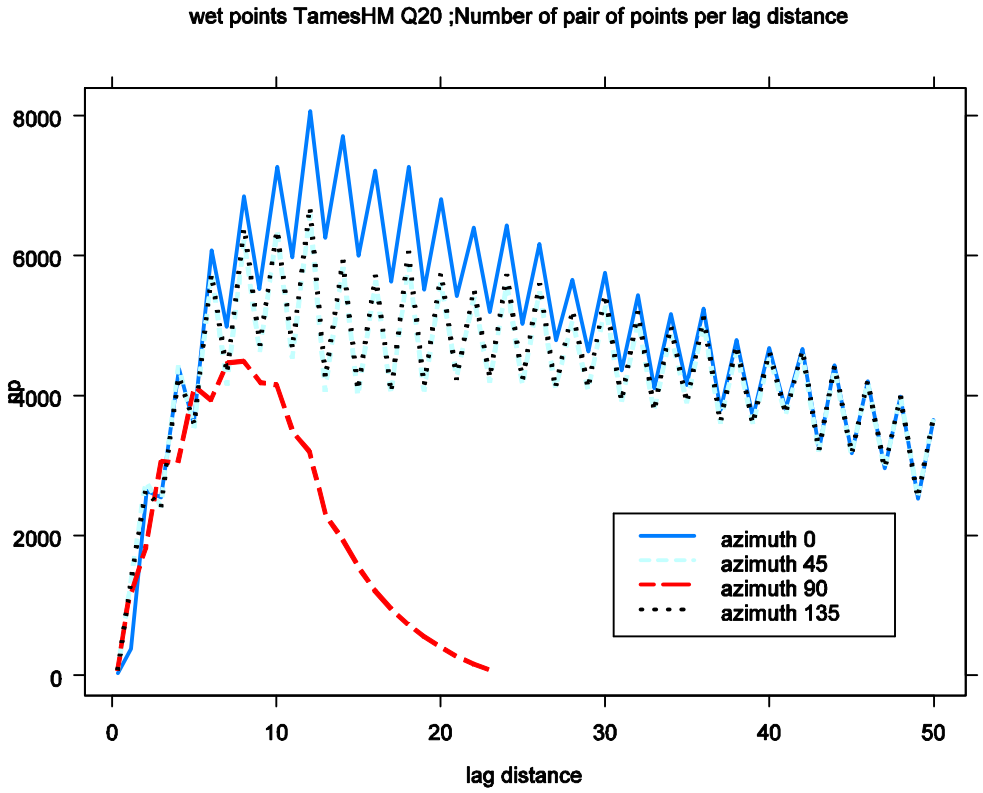
wet points TamesHM Q20 ;Number of pair of points per lag distance
np
8000
6000
4000
2000
0
0
10
20
30
40
50
lag distance
azimuth 0
azimuth 45
azimuth 90
azimuth 135

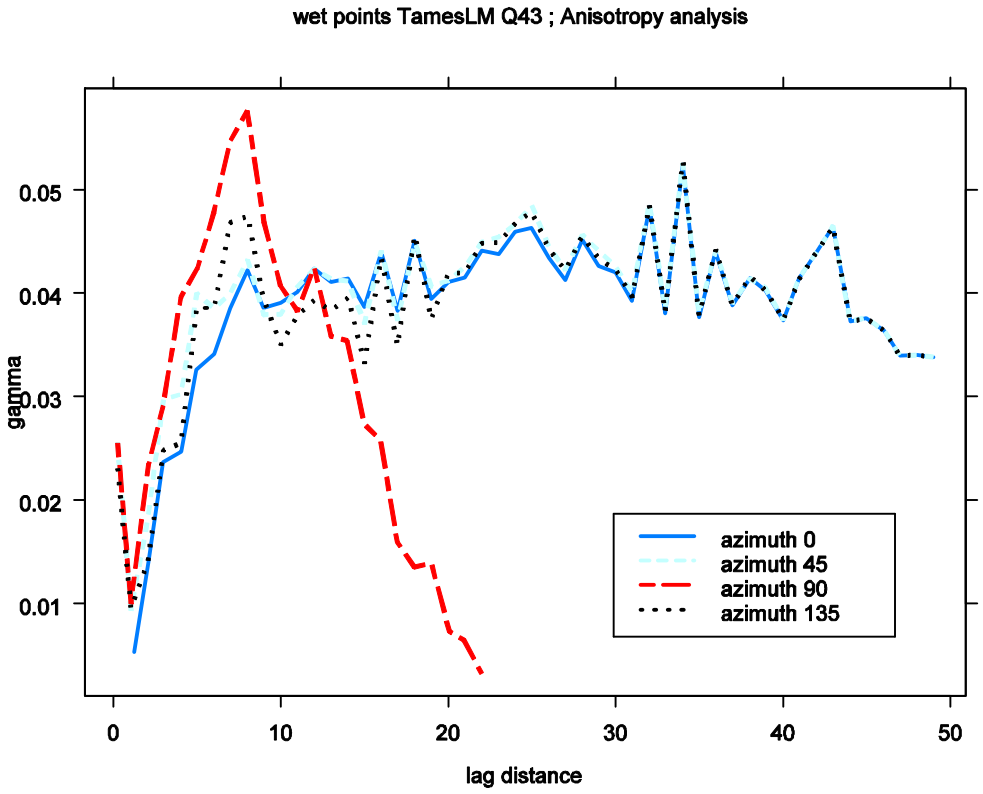
wet points TamesLM Q43 ; Anisotropy analysis
gamma
0.01
0.02
0.03
0.04
0.05
0
10
20
30
40
50
lag distance
azimuth 0
azimuth 45
azimuth 90
azimuth 135

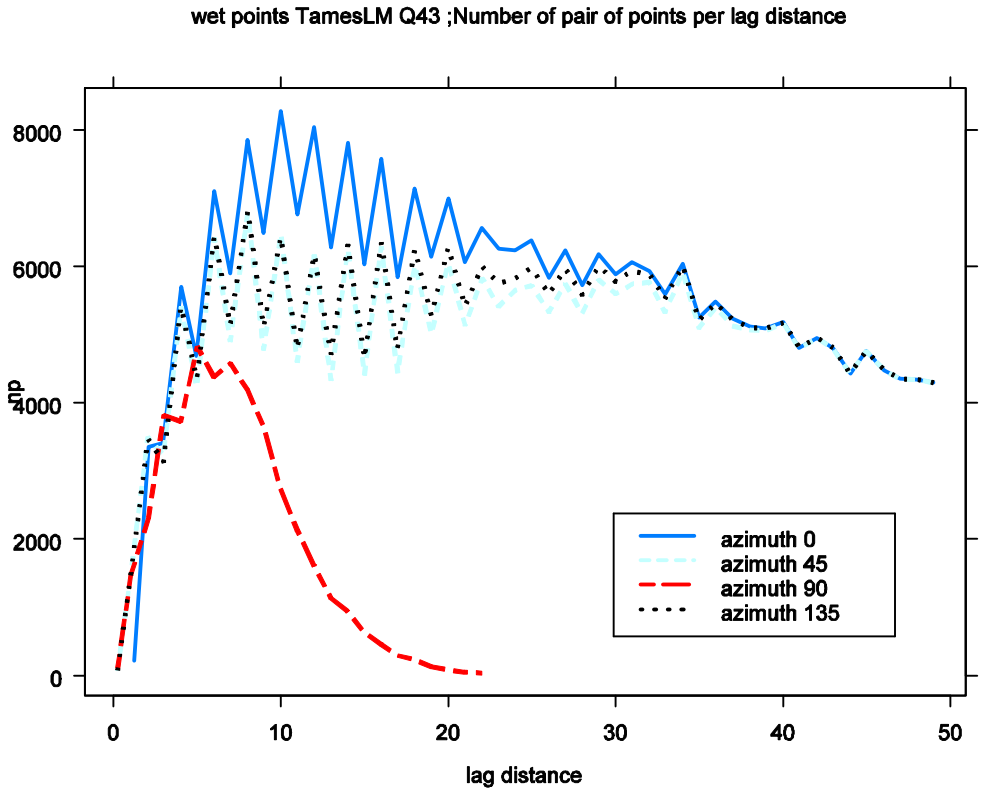
wet points TamesLM Q43 ;Number of pair of points per lag distance
np
0
2000
4000
6000
8000
0
10
20
30
40
50
lag distance
azimuth 0
azimuth 45
azimuth 90
azimuth 135

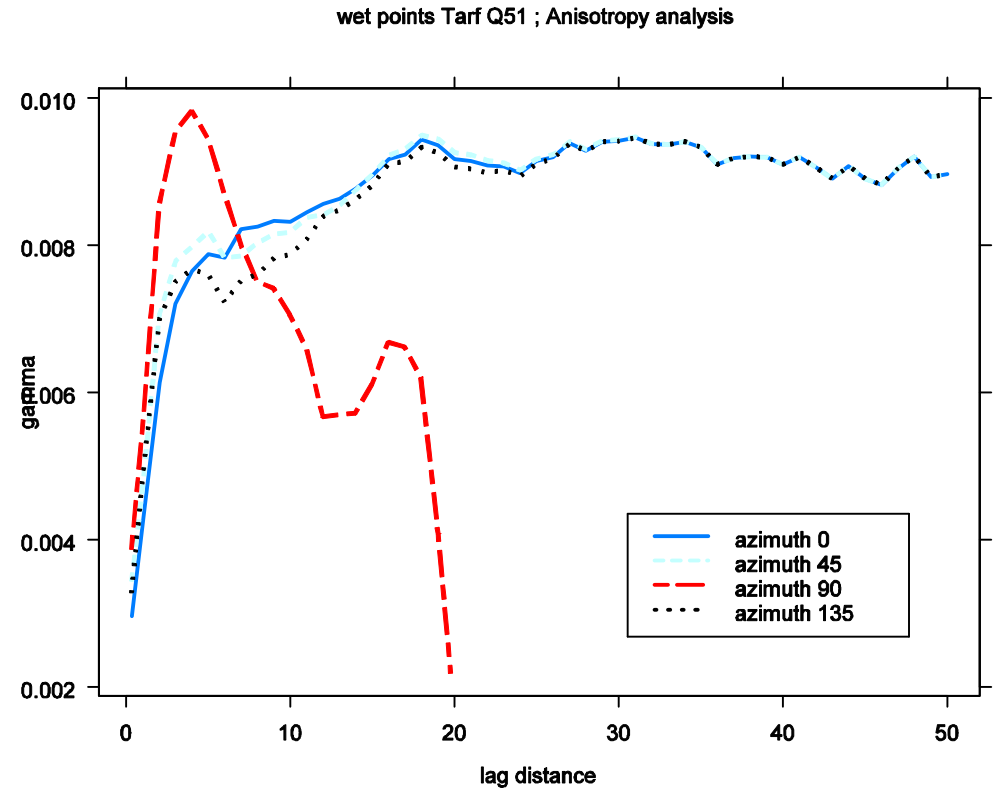
wet points Tarf Q51 ; Anisotropy analysis
gamma
0.010
0.008
0.006
0.004
0.002
0
10
20
30
40
50
lag distance
azimuth 0
azimuth 45
azimuth 90
azimuth 135

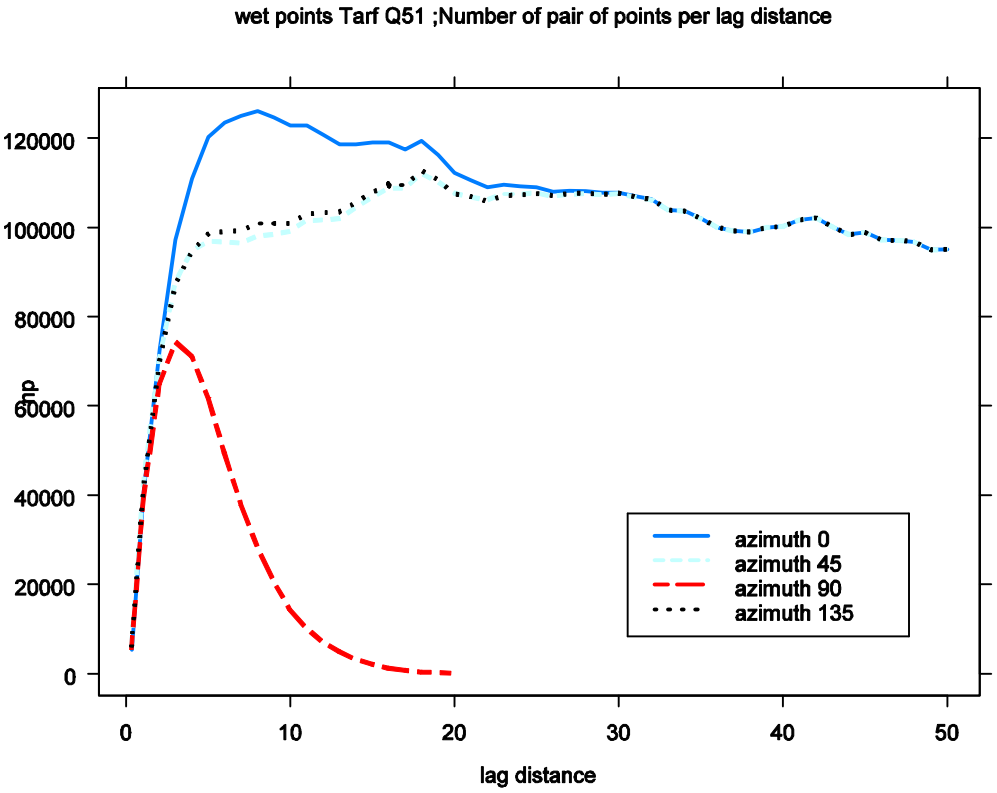
wet points Tarf Q51 ;Number of pair of points per lag distance
np
120000
100000
80000
60000
40000
20000
0
0
10
20
30
40
50
lag distance
azimuth 0
azimuth 45
azimuth 90
azimuth 135

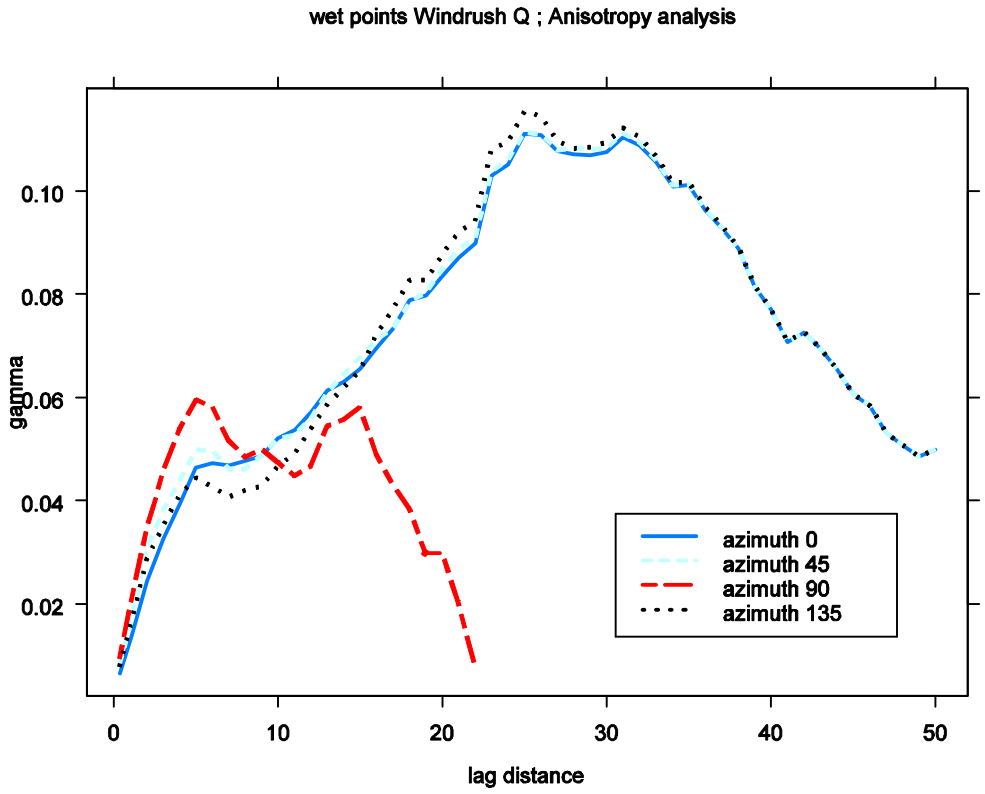
wet points Windrush Q ; Anisotropy analysis
gamma
0.10
0.08
0.06
0.04
0.02
0
10
20
30
40
50
lag distance
azimuth 0
azimuth 45
azimuth 90
azimuth 135

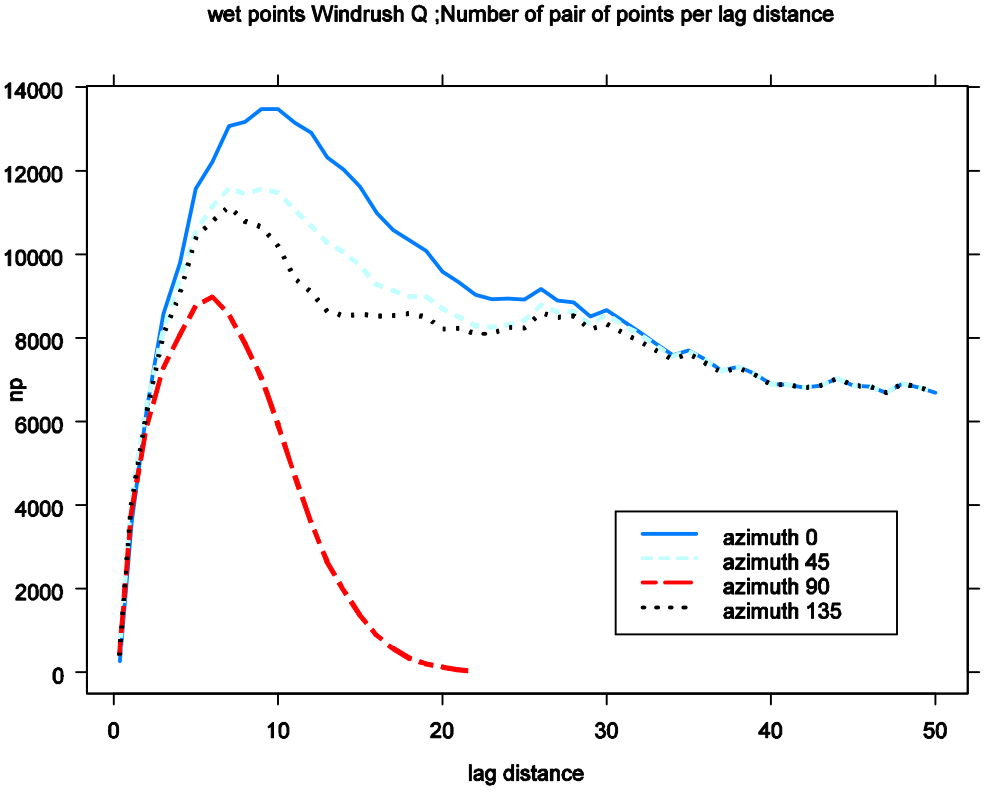
wet points Windrush Q ;Number of pair of points per lag distance
np
14000
12000
10000
8000
6000
4000
2000
0
0
10
20
30
40
50
lag distance
azimuth 0
azimuth 45
azimuth 90
azimuth 135

Appendix 3.5.1

Results obtained for the analysis in Chapter 5 –Sensitivity Analysis – Variogram values for combinations of lag and maximum distance considered: spherical variogram for dry and wet points.

This appendix summarises the results obtained for the sensitivity analysis developed in section 5.4.3. for the combination of lag distances and maximum distances selected. Results presented in this section only include the graphical output for the data sets analysed with dry and wet points. The variogram model analysed is the spherical one. Three different outputs, one for each variogram variable analysed (i.e. range, sill and nugget) are presented for each river site. Those river sites that had extreme variogram values are included twice: the graphical output is presented with two different axis scales so results can be better analysed.

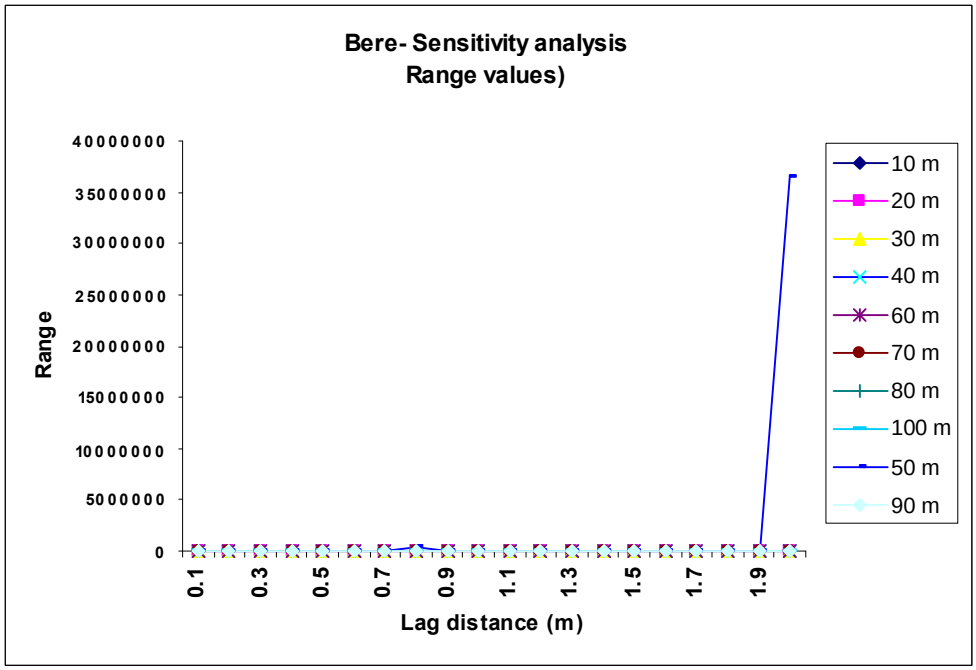
Bere- Sensitivity analysis
Range values)
Range
40000000
35000000
30000000
25000000
20000000
15000000
10000000
5000000
0
0.1
0.3
0.5
0.7
0.9
1.1
1.3
1.5
1.7
1.9
Lag distance (m)
10 m
20 m
30 m
40 m
60 m
70 m
80 m
100 m
50 m
90 m

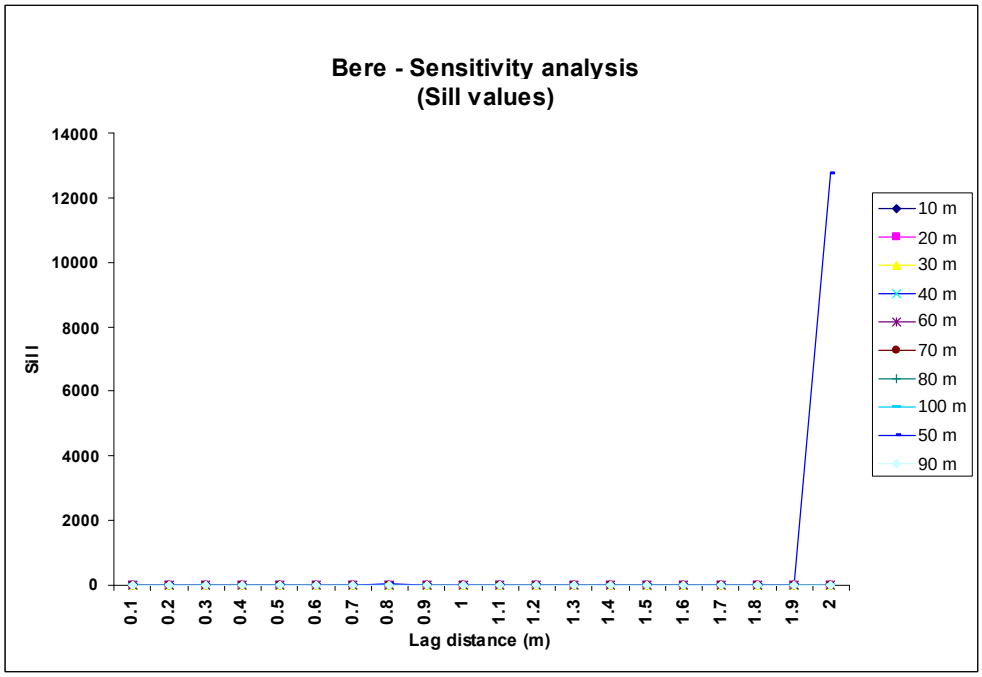
Bere - Sensitivity analysis
(Sill values)
Sill
14000
12000
10000
8000
6000
4000
2000
0
0.1
0.2
0.3
0.4
0.5
0.6
0.7
0.8
0.9
1
1.1
1.2
1.3
1.4
1.5
1.6
1.7
1.8
1.9
2
Lag distance (m)
10 m
20 m
30 m
40 m
60 m
70 m
80 m
100 m
50 m
90 m

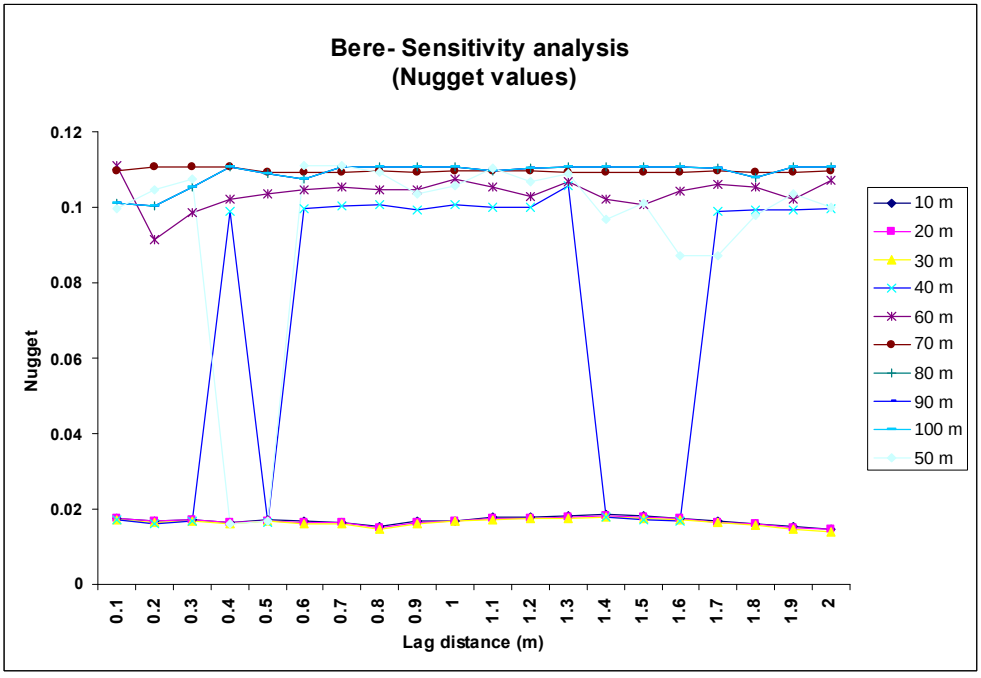
Bere- Sensitivity analysis
(Nugget values)
Nugget
0.12
0.1
0.08
0.06
0.04
0.02
0
0.1
0.2
0.3
0.4
0.5
0.6
0.7
0.8
0.9
1
1.1
1.2
1.3
1.4
1.5
1.6
1.7
1.8
1.9
2
Lag distance (m)
10 m
20 m
30 m
40 m
60 m
70 m
80 m
90 m
100 m
50 m

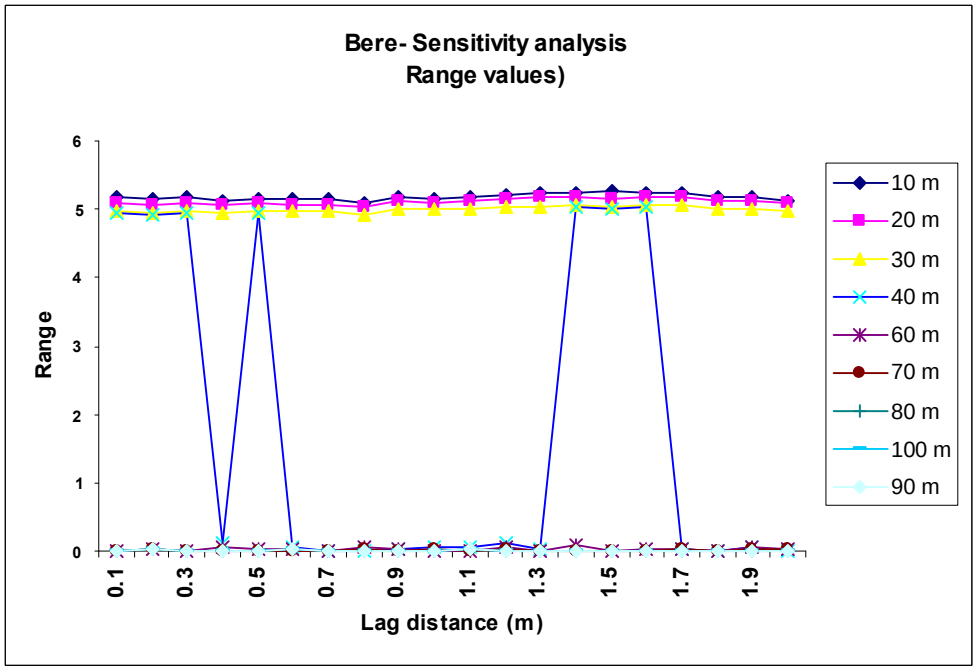
Bere- Sensitivity analysis
Range values)
Range
Lag distance (m)
10 m
20 m
30 m
40 m
60 m
70 m
80 m
100 m
90 m

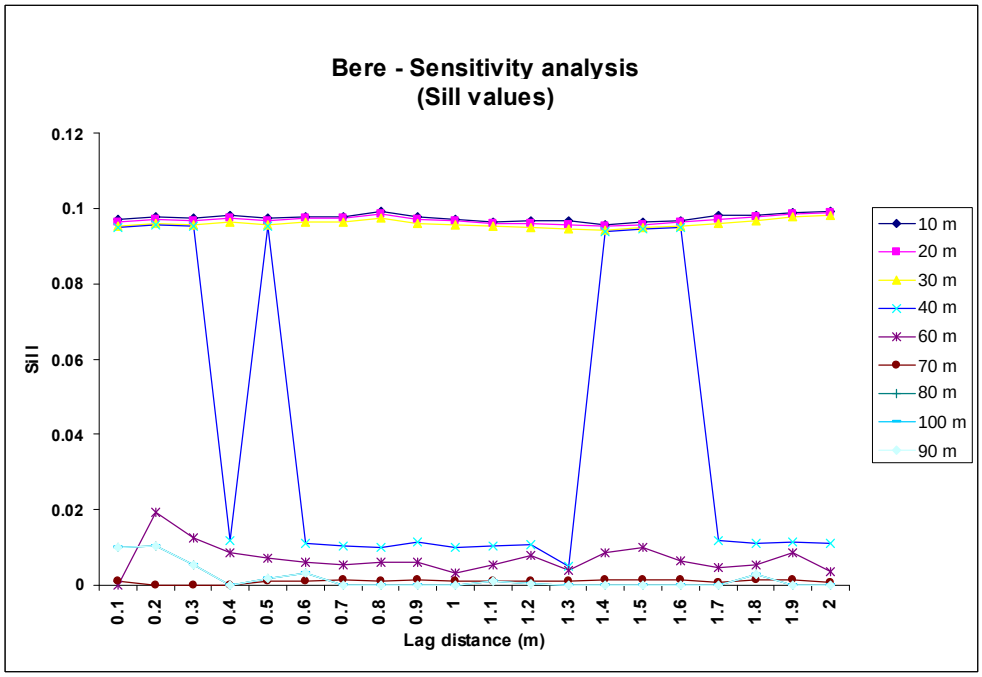
Bere - Sensitivity analysis
(Sill values)
Sill
Lag distance (m)
10 m
20 m
30 m
40 m
60 m
70 m
80 m
100 m
90 m

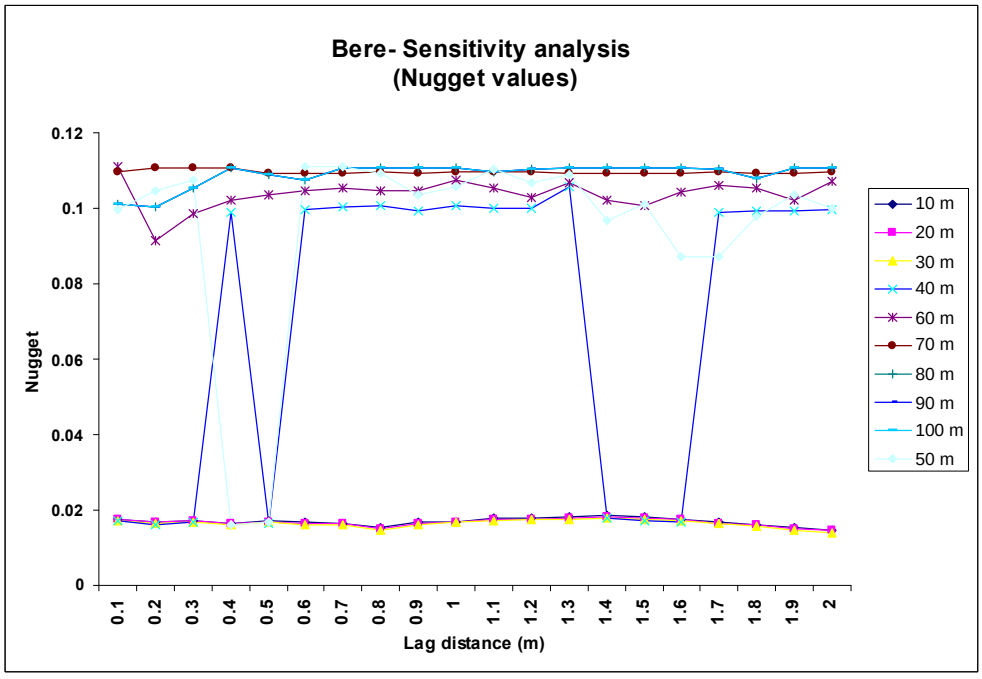
Bere- Sensitivity analysis
(Nugget values)
Nugget
Lag distance (m)
10 m
20 m
30 m
40 m
60 m
70 m
80 m
90 m
100 m
50 m

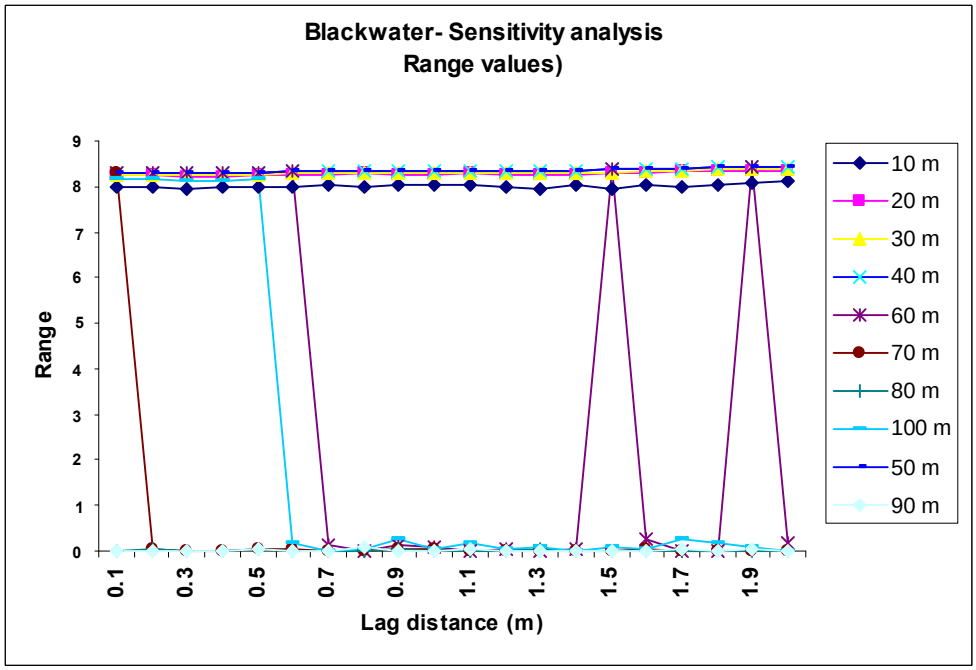
Blackwater- Sensitivity analysis
Range values)
Range
Lag distance (m)
10 m
20 m
30 m
40 m
60 m
70 m
80 m
100 m
50 m
90 m

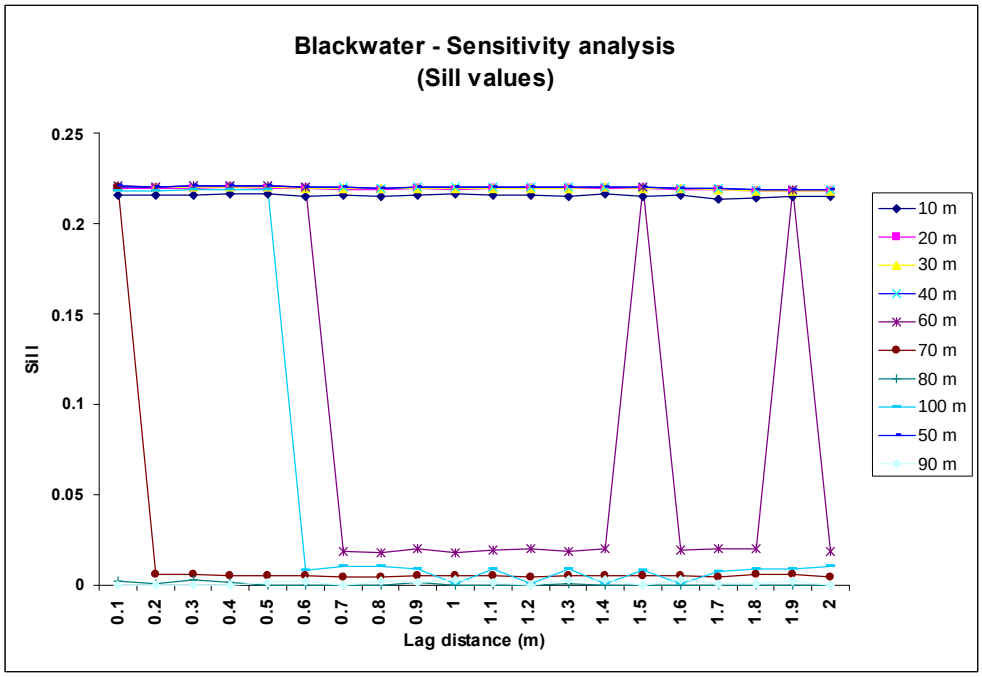
Blackwater - Sensitivity analysis
(Sill values)
Sill
Lag distance (m)
10 m
20 m
30 m
40 m
60 m
70 m
80 m
100 m
50 m
90 m

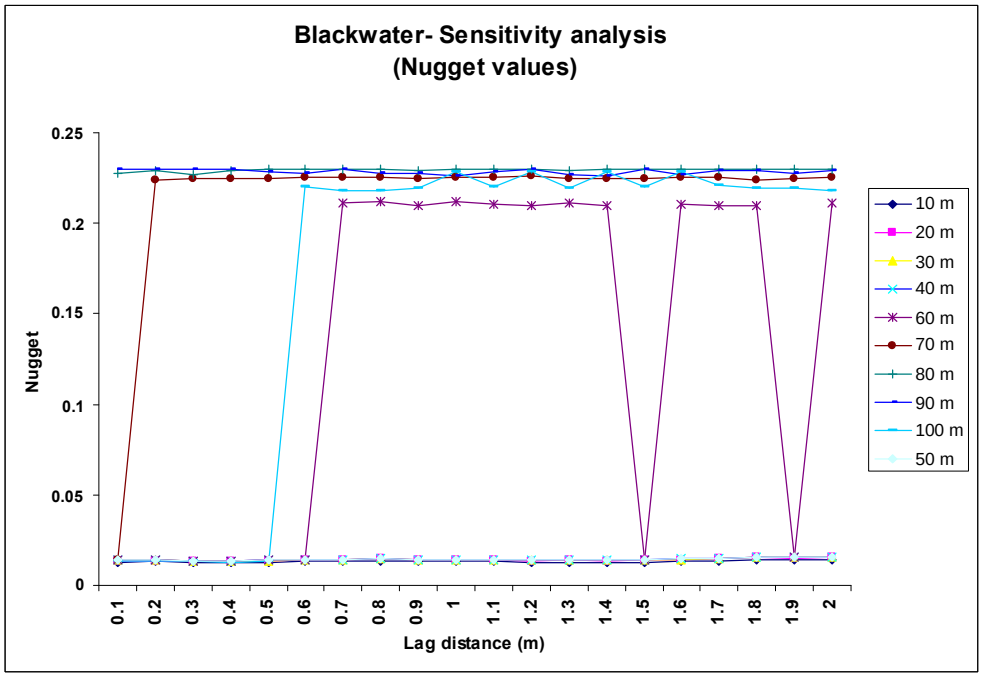
Blackwater- Sensitivity analysis
(Nugget values)
Nugget
Lag distance (m)
10 m
20 m
30 m
40 m
60 m
70 m
80 m
90 m
100 m
50 m

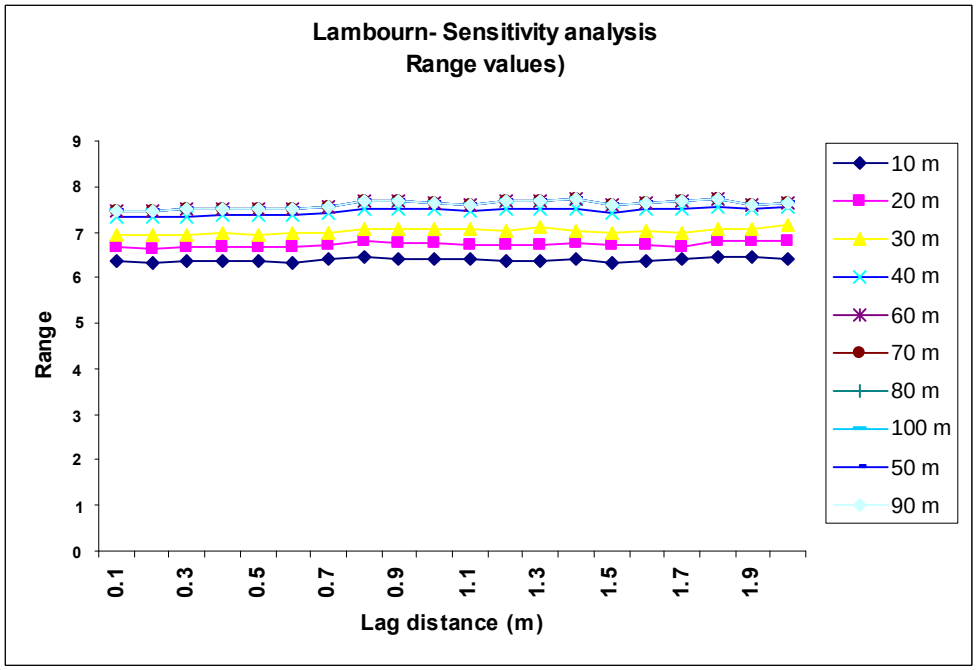
Lambourn- Sensitivity analysis
Range values)
Range
Lag distance (m)
10 m
20 m
30 m
40 m
60 m
70 m
80 m
100 m
50 m
90 m

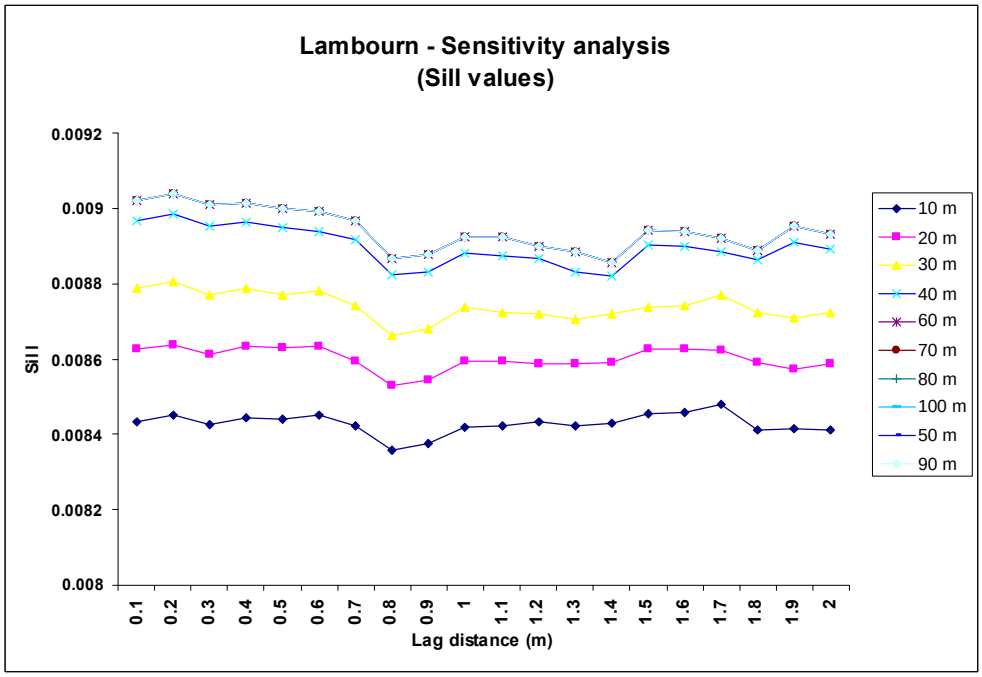
Lambourn - Sensitivity analysis
(Sill values)
Sill
Lag distance (m)
10 m
20 m
30 m
40 m
60 m
70 m
80 m
100 m
50 m
90 m

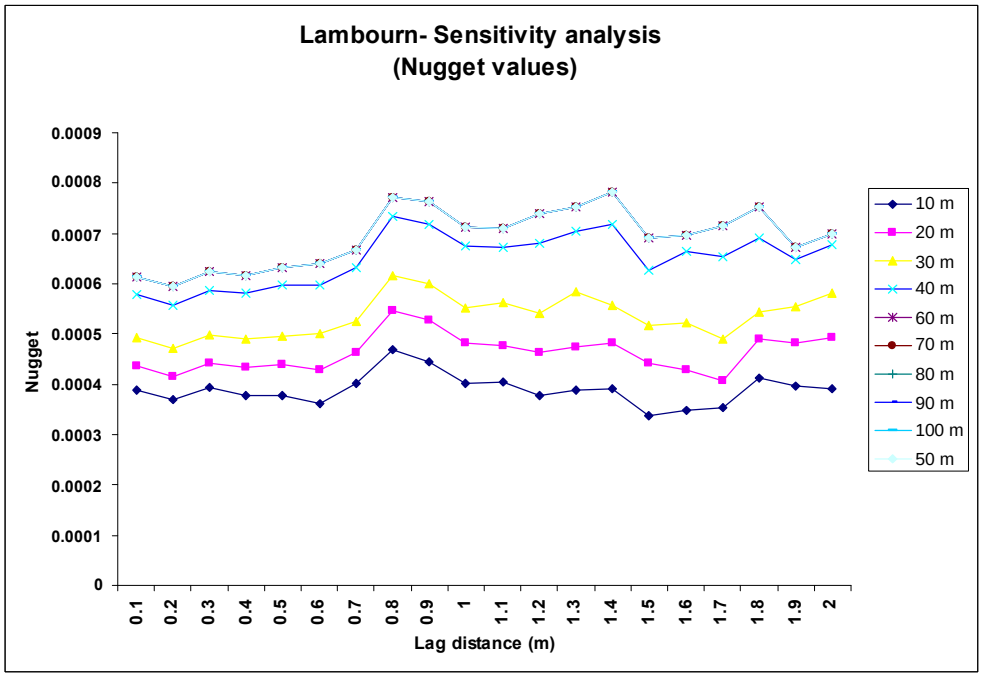
Lambourn- Sensitivity analysis
(Nugget values)
Nugget
Lag distance (m)
10 m
20 m
30 m
40 m
60 m
70 m
80 m
90 m
100 m
50 m

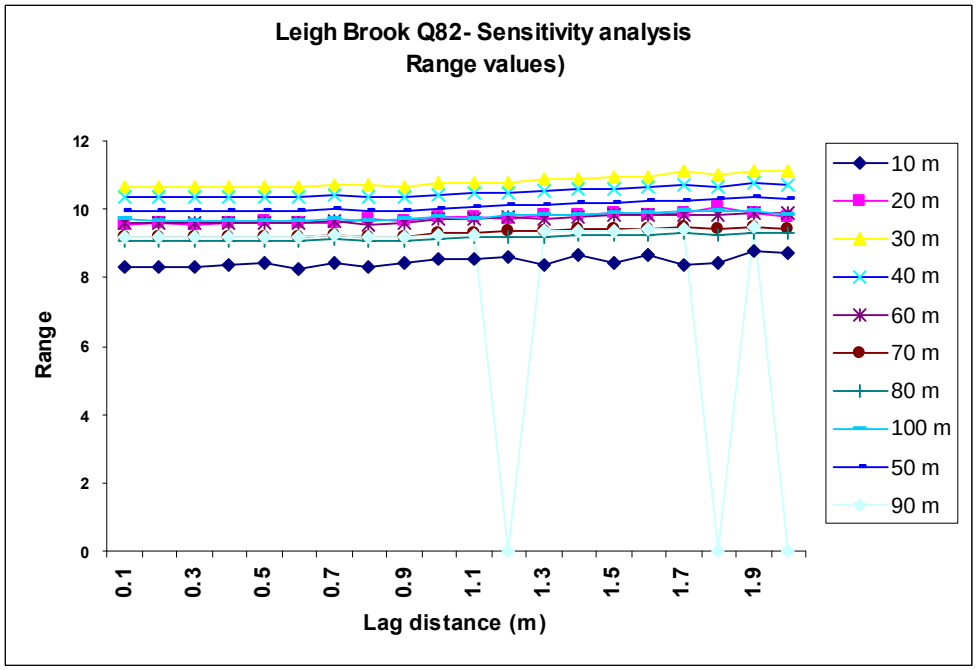
Leigh Brook Q82- Sensitivity analysis
Range values)
Range
Lag distance (m)
10 m
20 m
30 m
40 m
60 m
70 m
80 m
100 m
50 m
90 m

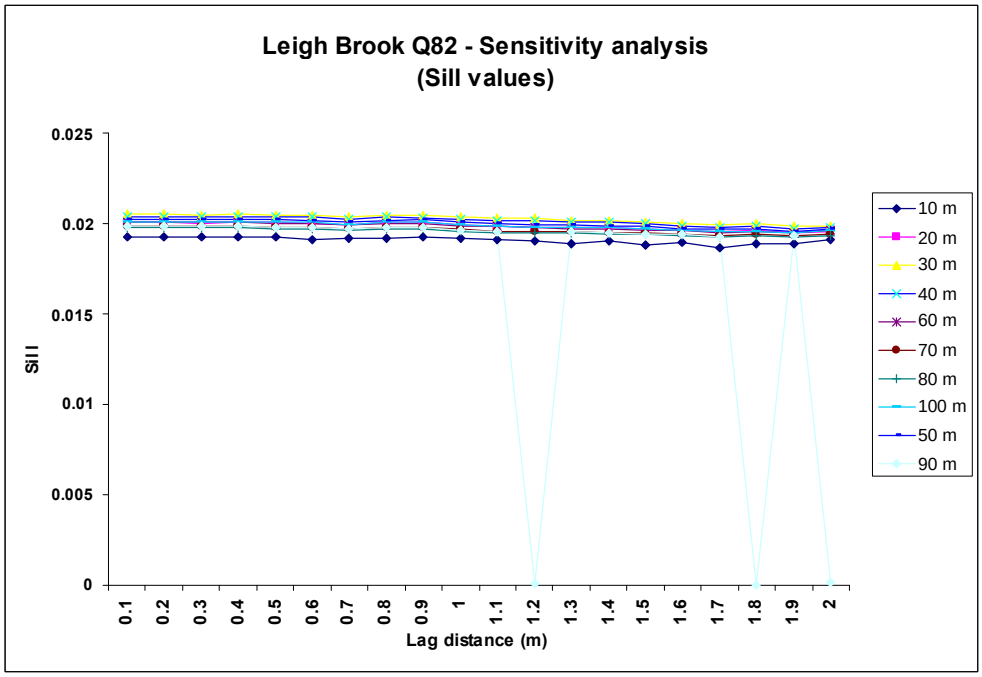
Leigh Brook Q82 - Sensitivity analysis
(Sill values)
Sill
Lag distance (m)
10 m
20 m
30 m
40 m
60 m
70 m
80 m
100 m
50 m
90 m

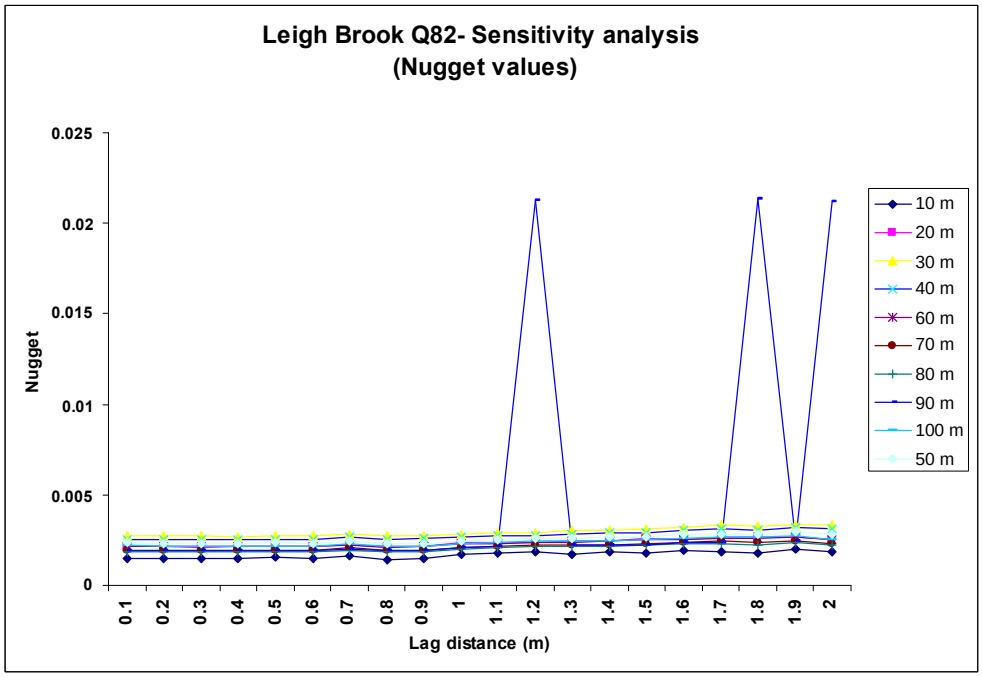
Leigh Brook Q82- Sensitivity analysis
(Nugget values)
Nugget
Lag distance (m)
10 m
20 m
30 m
40 m
60 m
70 m
80 m
90 m
100 m
50 m

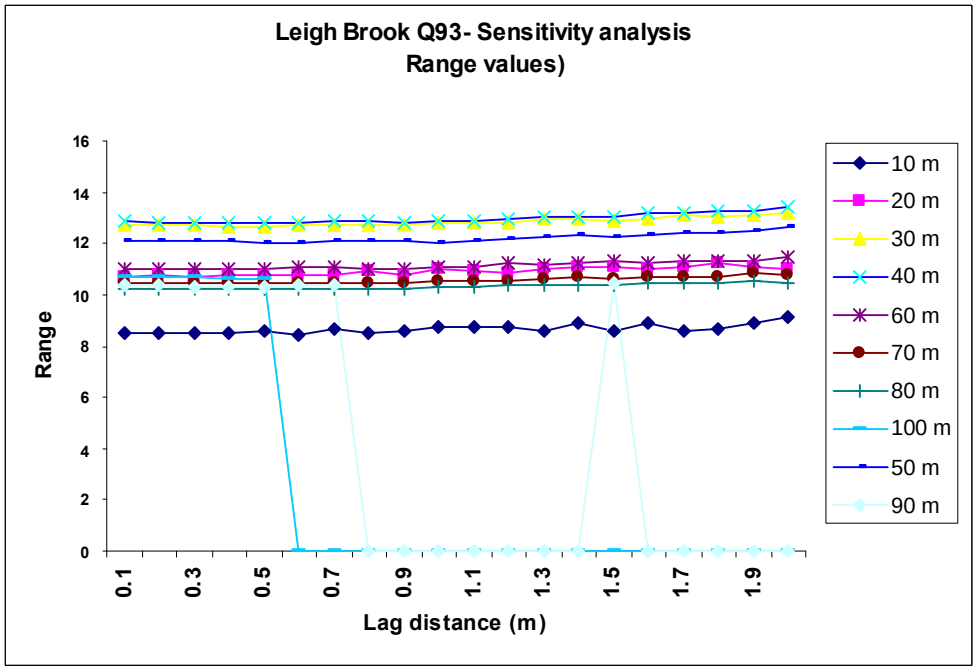
Leigh Brook Q93- Sensitivity analysis
Range values)
Range
Lag distance (m)
10 m
20 m
30 m
40 m
60 m
70 m
80 m
100 m
50 m
90 m

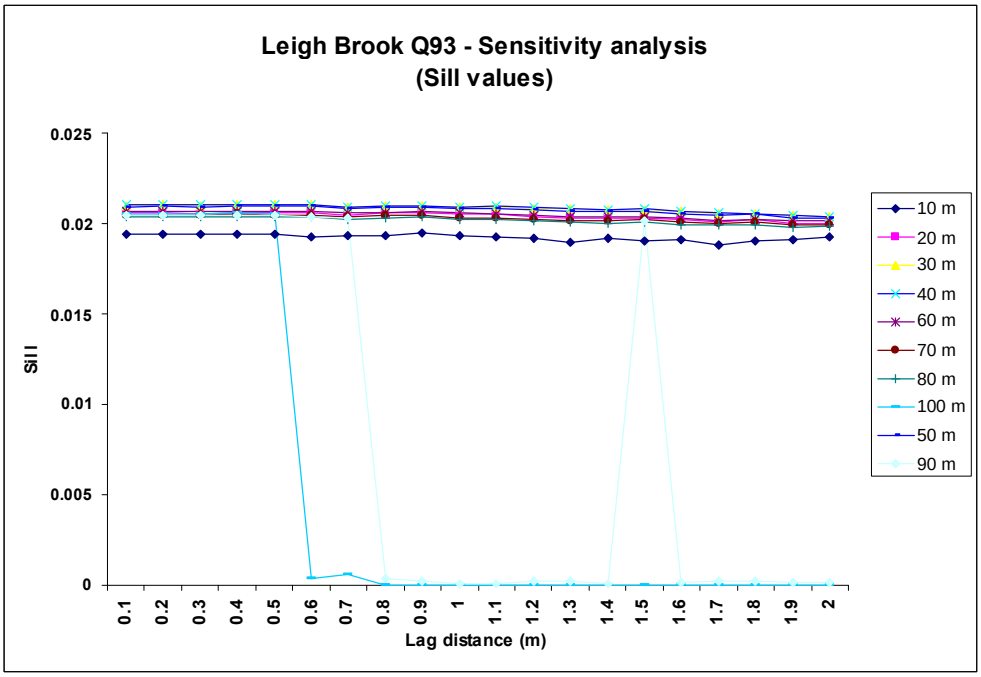
Leigh Brook Q93 - Sensitivity analysis
(Sill values)
Sill
Lag distance (m)
10 m
20 m
30 m
40 m
60 m
70 m
80 m
100 m
50 m
90 m

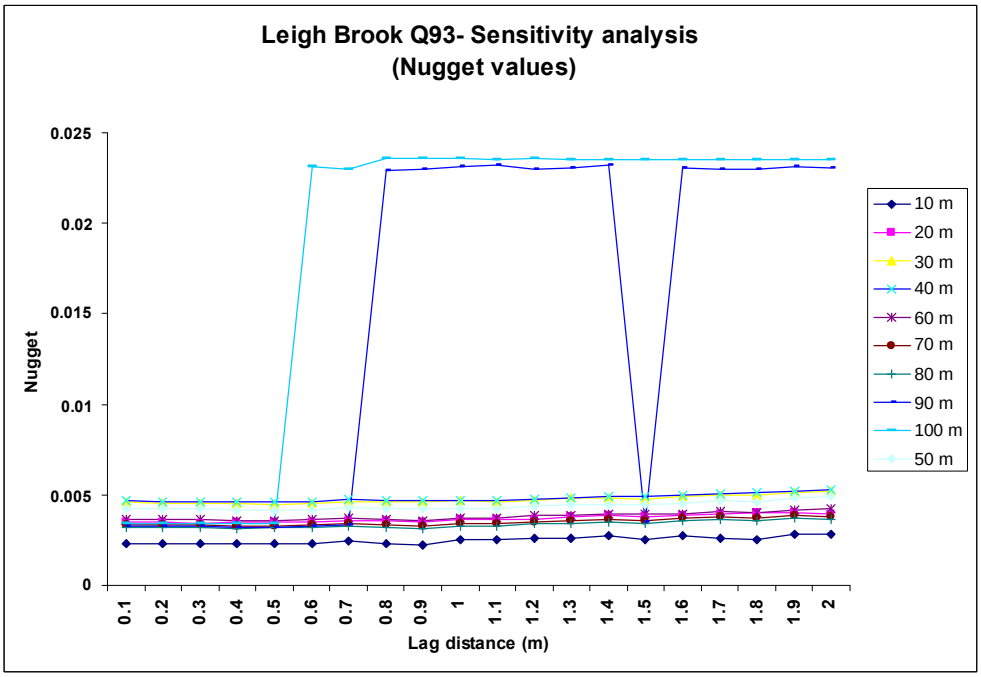
Leigh Brook Q93- Sensitivity analysis
(Nugget values)
Nugget
Lag distance (m)
10 m
20 m
30 m
40 m
60 m
70 m
80 m
90 m
100 m
50 m

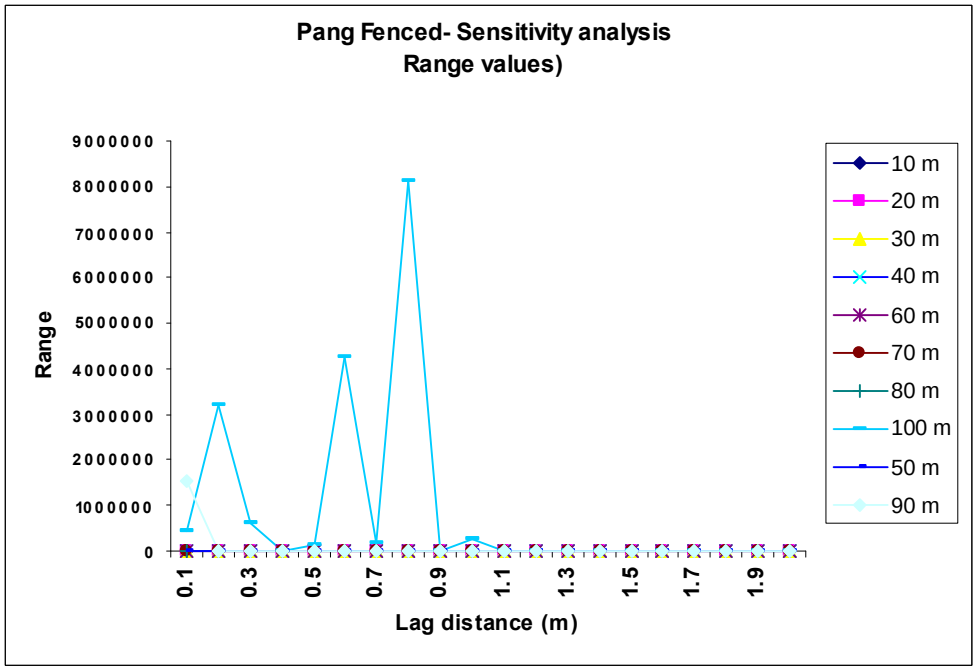
Pang Fenced- Sensitivity analysis
Range values)
Range
9000000
8000000
7000000
6000000
5000000
4000000
3000000
2000000
1000000
0
0.1
0.3
0.5
0.7
0.9
1.1
1.3
1.5
1.7
1.9
Lag distance (m)
10 m
20 m
30 m
40 m
60 m
70 m
80 m
100 m
50 m
90 m

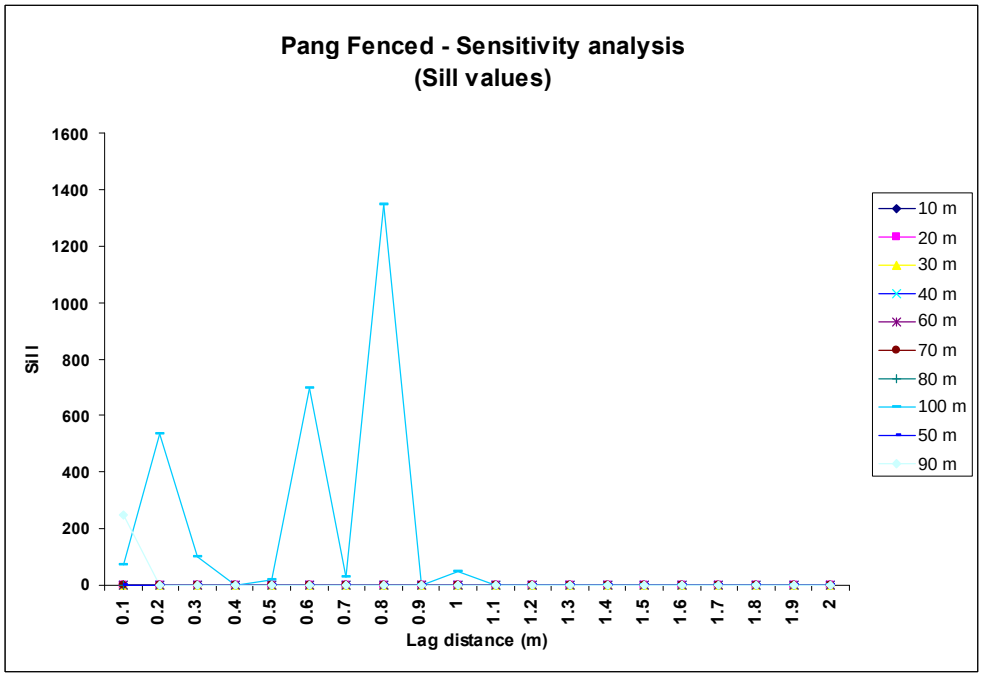
Pang Fenced - Sensitivity analysis
(Sill values)
Sill
1600
1400
1200
1000
800
600
400
200
0
0.1
0.2
0.3
0.4
0.5
0.6
0.7
0.8
0.9
1
1.1
1.2
1.3
1.4
1.5
1.6
1.7
1.8
1.9
2
Lag distance (m)
10 m
20 m
30 m
40 m
60 m
70 m
80 m
100 m
50 m
90 m

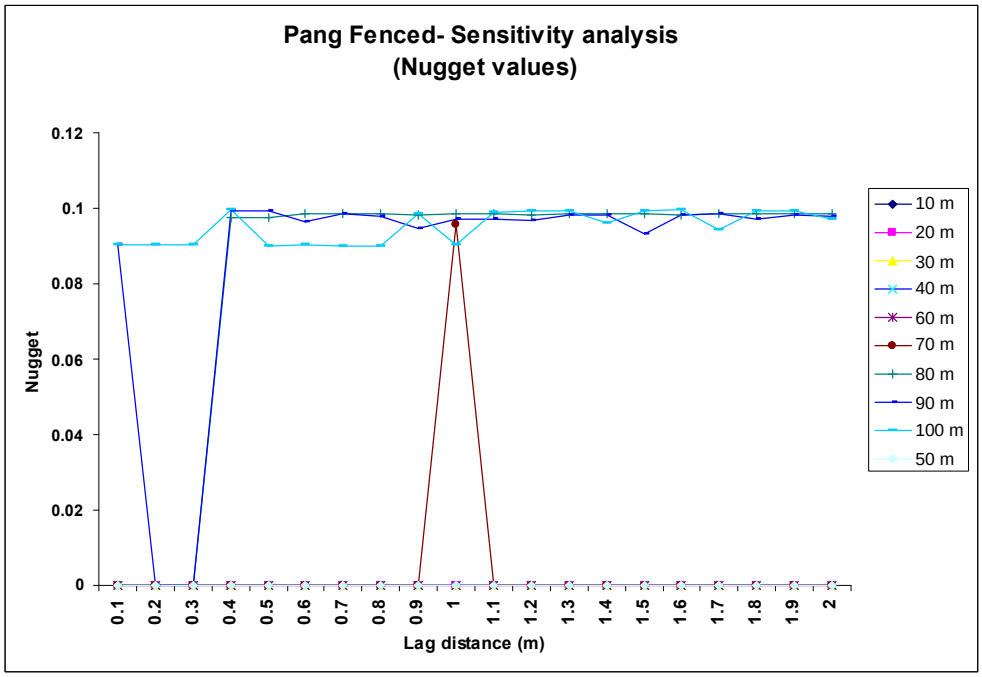
Pang Fenced- Sensitivity analysis
(Nugget values)
Nugget
0.12
0.1
0.08
0.06
0.04
0.02
0
0.1
0.2
0.3
0.4
0.5
0.6
0.7
0.8
0.9
1
1.1
1.2
1.3
1.4
1.5
1.6
1.7
1.8
1.9
2
Lag distance (m)
10 m
20 m
30 m
40 m
60 m
70 m
80 m
90 m
100 m
50 m

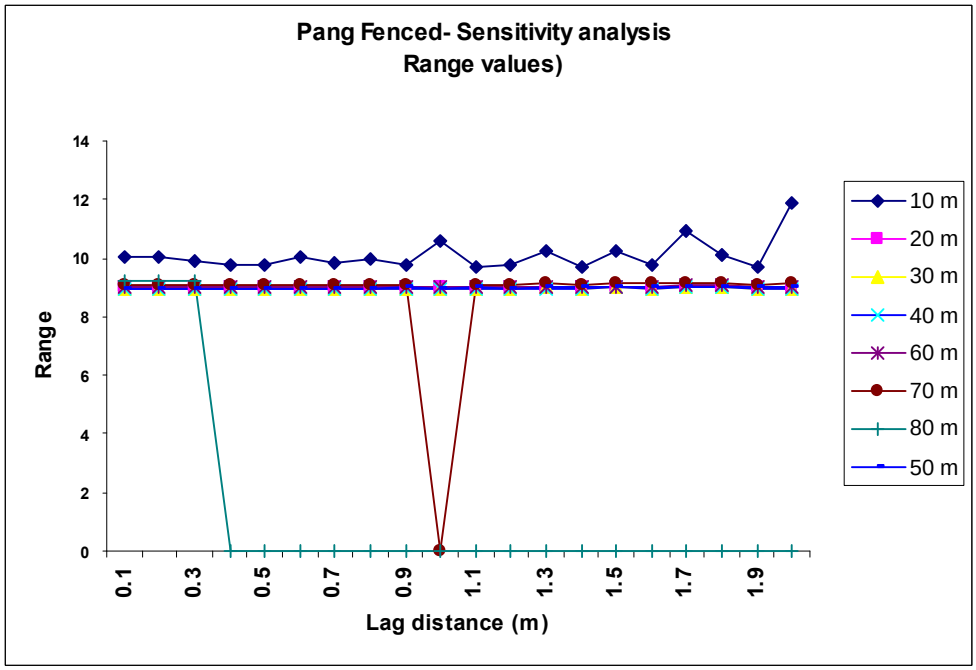
Pang Fenced- Sensitivity analysis
Range values)
Range
Lag distance (m)
10 m
20 m
30 m
40 m
60 m
70 m
80 m
50 m

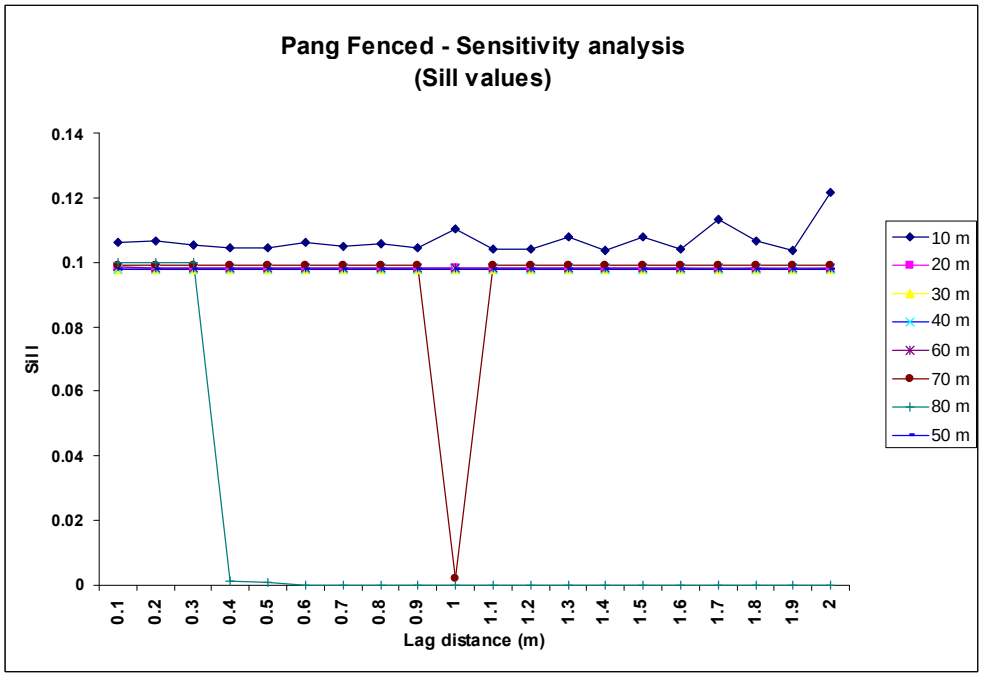
Pang Fenced - Sensitivity analysis
(Sill values)
Sill
Lag distance (m)
10 m
20 m
30 m
40 m
60 m
70 m
80 m
50 m

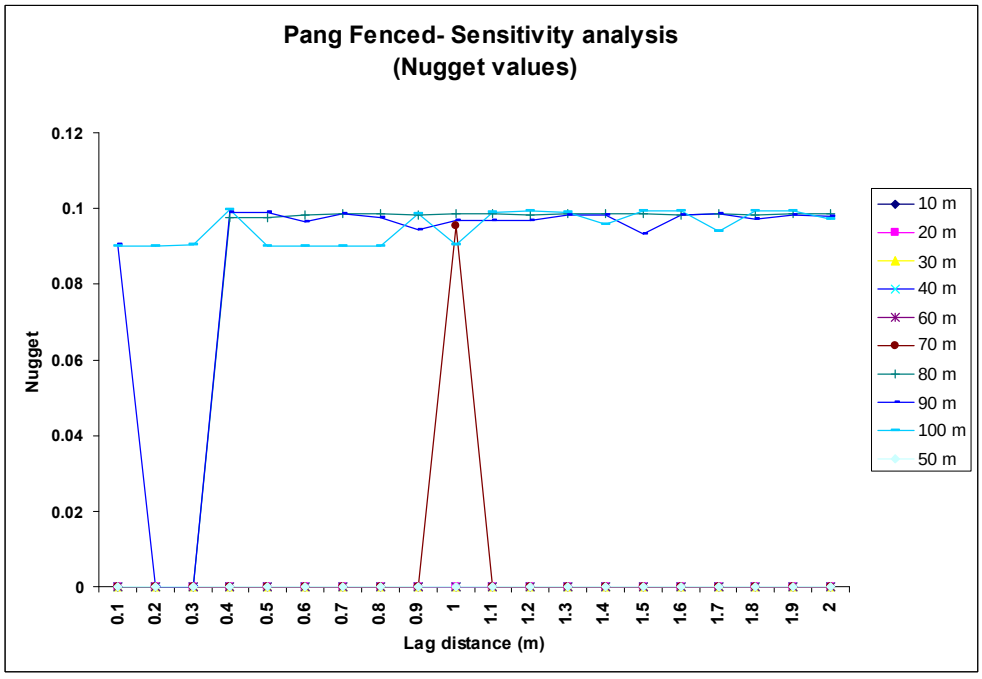
Pang Fenced- Sensitivity analysis
(Nugget values)
Nugget
Lag distance (m)
10 m
20 m
30 m
40 m
60 m
70 m
80 m
90 m
100 m
50 m

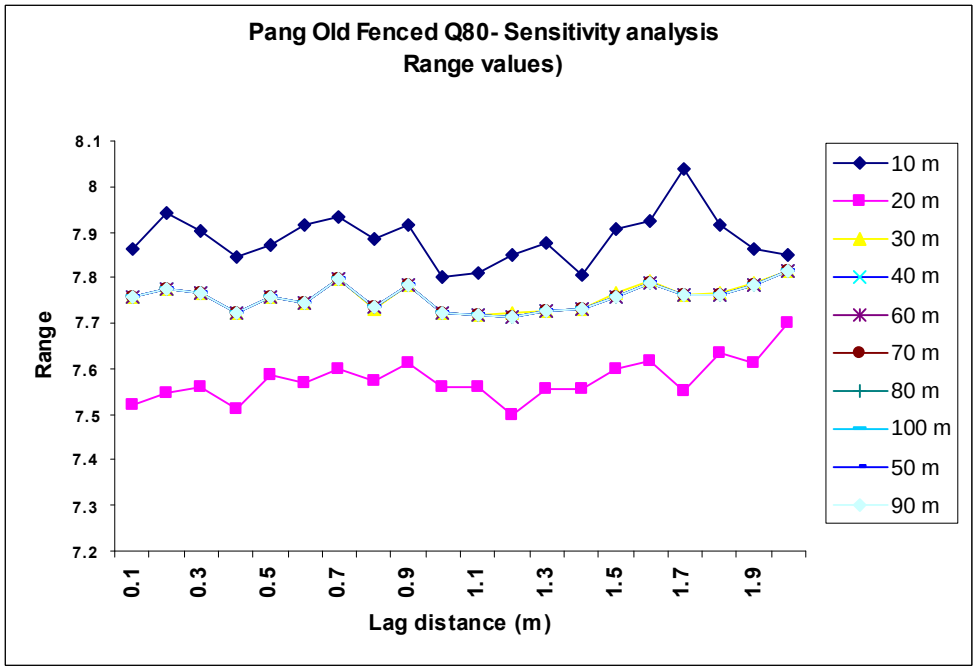
Pang Old Fenced Q80- Sensitivity analysis
Range values)
Range
8.1
8
7.9
7.8
7.7
7.6
7.5
7.4
7.3
7.2
0.1
0.3
0.5
0.7
0.9
1.1
1.3
1.5
1.7
1.9
Lag distance (m)
10 m
20 m
30 m
40 m
60 m
70 m
80 m
100 m
50 m
90 m

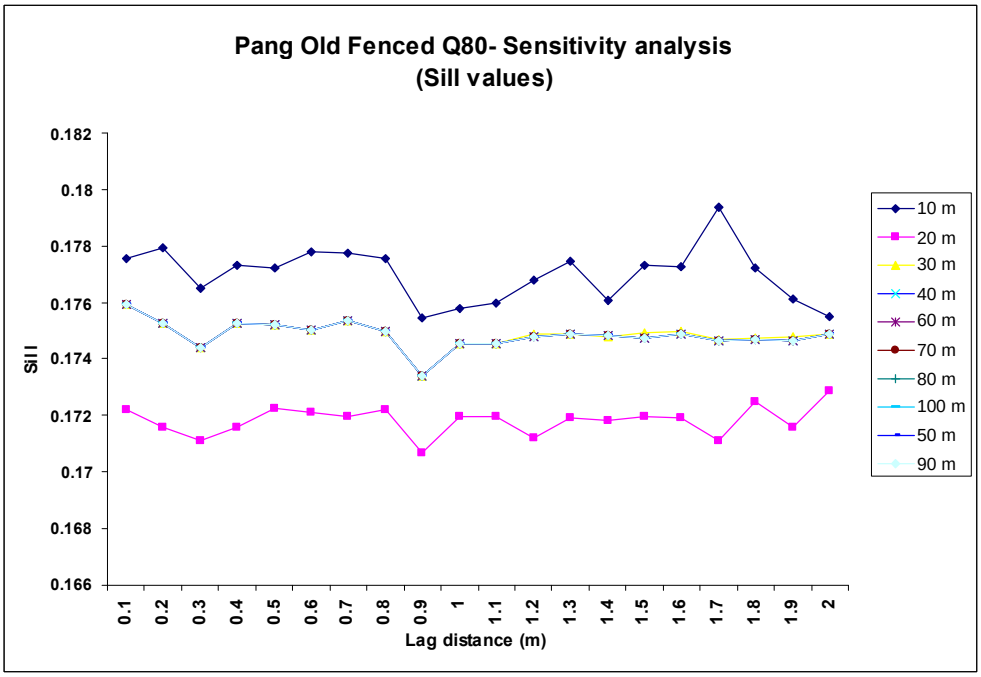
Pang Old Fenced Q80- Sensitivity analysis
(Sill values)
Sill
0.182
0.18
0.178
0.176
0.174
0.172
0.17
0.168
0.166
0.1
0.2
0.3
0.4
0.5
0.6
0.7
0.8
0.9
1
1.1
1.2
1.3
1.4
1.5
1.6
1.7
1.8
1.9
2
Lag distance (m)
10 m
20 m
30 m
40 m
60 m
70 m
80 m
100 m
50 m
90 m

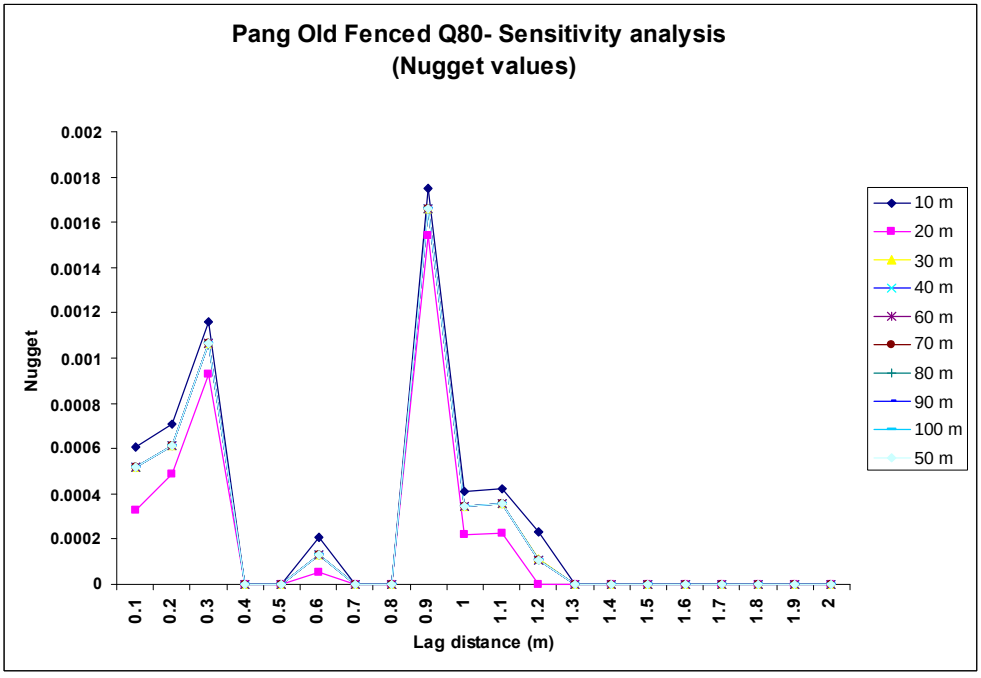
Pang Old Fenced Q80- Sensitivity analysis
(Nugget values)
Nugget
0.002
0.0018
0.0016
0.0014
0.0012
0.001
0.0008
0.0006
0.0004
0.0002
0
0.1
0.2
0.3
0.4
0.5
0.6
0.7
0.8
0.9
1
1.1
1.2
1.3
1.4
1.5
1.6
1.7
1.8
1.9
2
Lag distance (m)
10 m
20 m
30 m
40 m
60 m
70 m
80 m
90 m
100 m
50 m

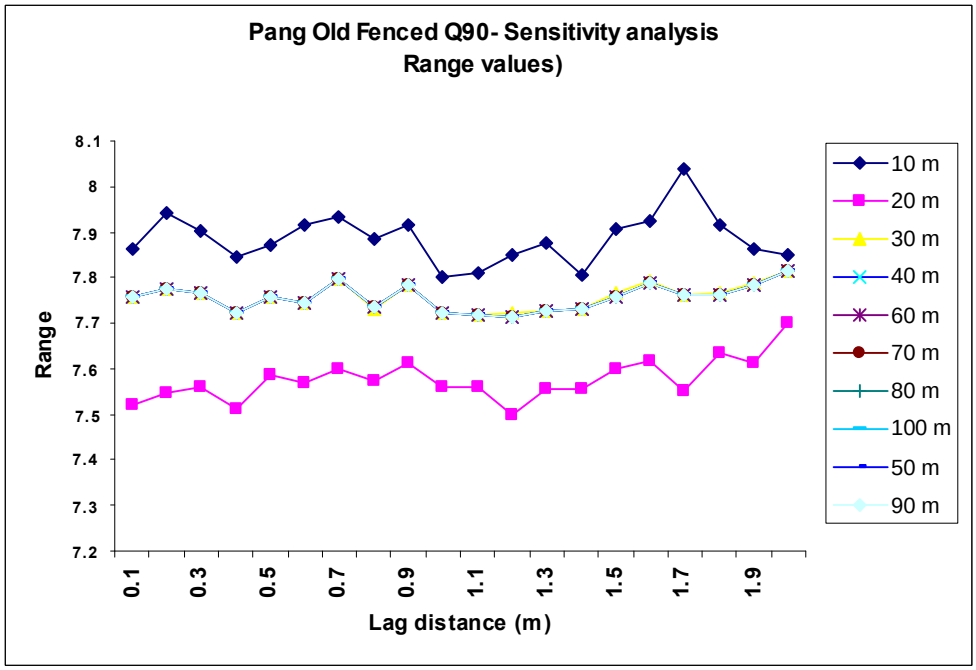
Pang Old Fenced Q90- Sensitivity analysis
Range values)
Range
8.1
8
7.9
7.8
7.7
7.6
7.5
7.4
7.3
7.2
0.1
0.3
0.5
0.7
0.9
1.1
1.3
1.5
1.7
1.9
Lag distance (m)
10 m
20 m
30 m
40 m
60 m
70 m
80 m
100 m
50 m
90 m

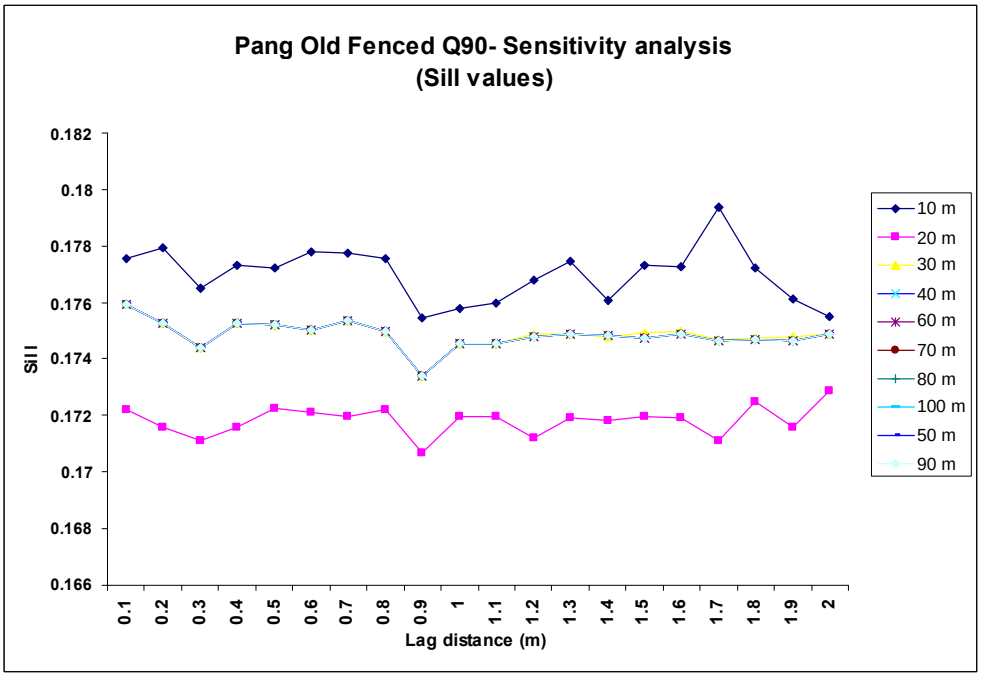
Pang Old Fenced Q90- Sensitivity analysis
(Sill values)
Sill
0.182
0.18
0.178
0.176
0.174
0.172
0.17
0.168
0.166
0.1
0.2
0.3
0.4
0.5
0.6
0.7
0.8
0.9
1
1.1
1.2
1.3
1.4
1.5
1.6
1.7
1.8
1.9
2
Lag distance (m)
10 m
20 m
30 m
40 m
60 m
70 m
80 m
100 m
50 m
90 m

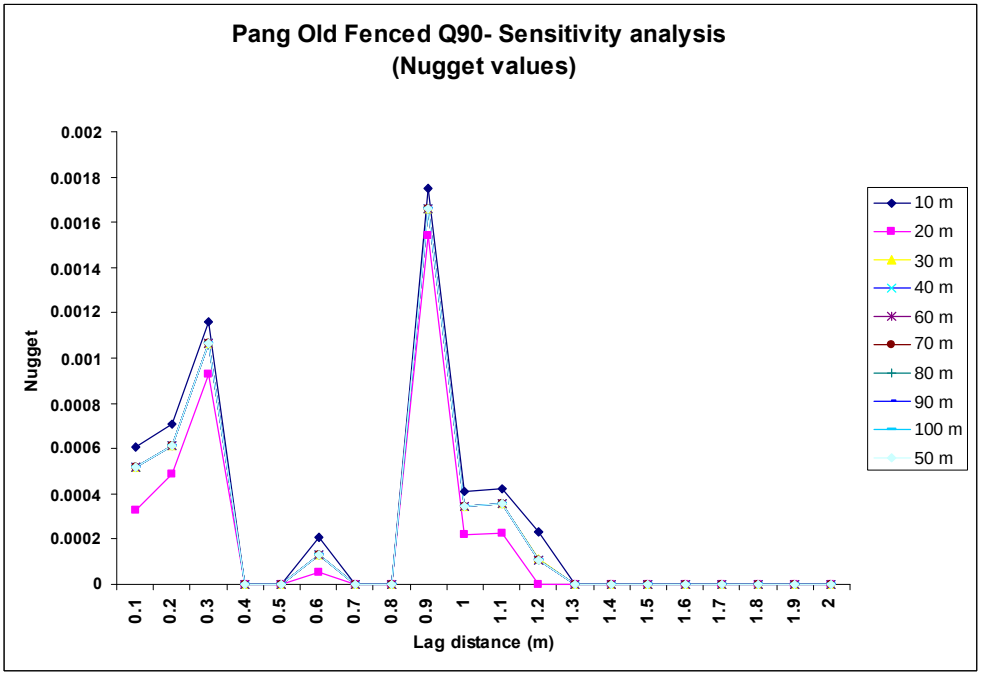
Pang Old Fenced Q90- Sensitivity analysis
(Nugget values)
Nugget
0.002
0.0018
0.0016
0.0014
0.0012
0.001
0.0008
0.0006
0.0004
0.0002
0
0.1
0.2
0.3
0.4
0.5
0.6
0.7
0.8
0.9
1
1.1
1.2
1.3
1.4
1.5
1.6
1.7
1.8
1.9
2
Lag distance (m)
10 m
20 m
30 m
40 m
60 m
70 m
80 m
90 m
100 m
50 m

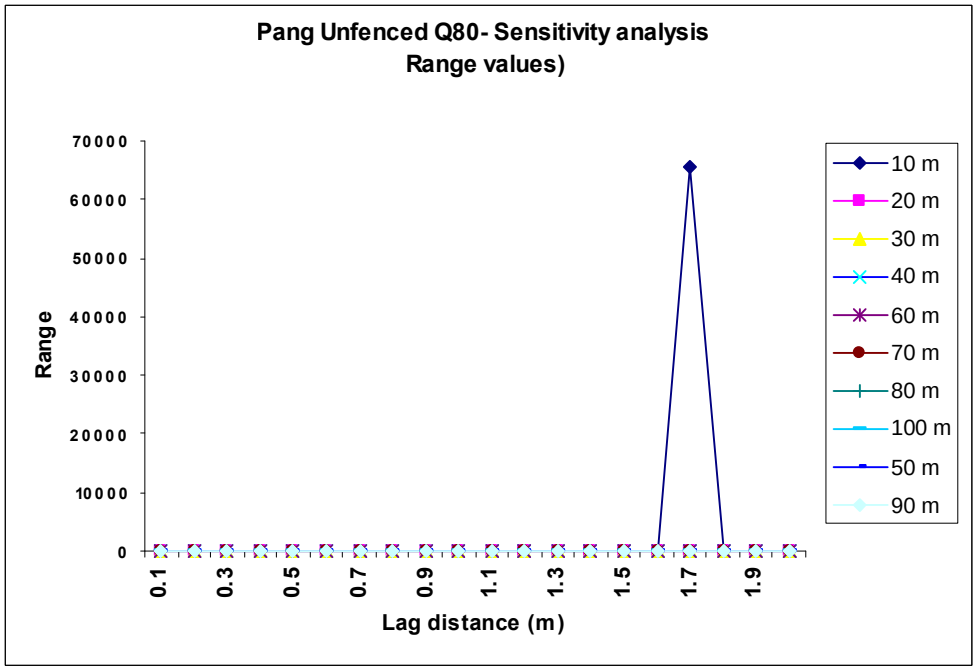
Pang Unfenced Q80- Sensitivity analysis
Range values)
Range
70000
60000
50000
40000
30000
20000
10000
0
0.1
0.3
0.5
0.7
0.9
1.1
1.3
1.5
1.7
1.9
Lag distance (m)
10 m
20 m
30 m
40 m
60 m
70 m
80 m
100 m
50 m
90 m

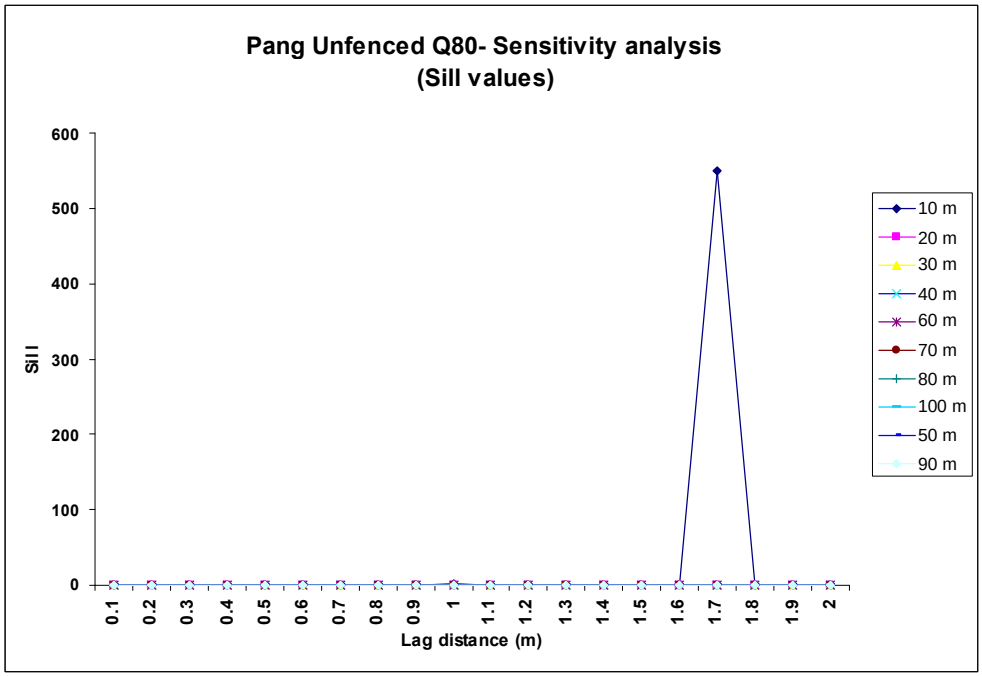
Pang Unfenced Q80- Sensitivity analysis
(Sill values)
Sill
600
500
400
300
200
100
0
0.1
0.2
0.3
0.4
0.5
0.6
0.7
0.8
0.9
1
1.1
1.2
1.3
1.4
1.5
1.6
1.7
1.8
1.9
2
Lag distance (m)
10 m
20 m
30 m
40 m
60 m
70 m
80 m
100 m
50 m
90 m

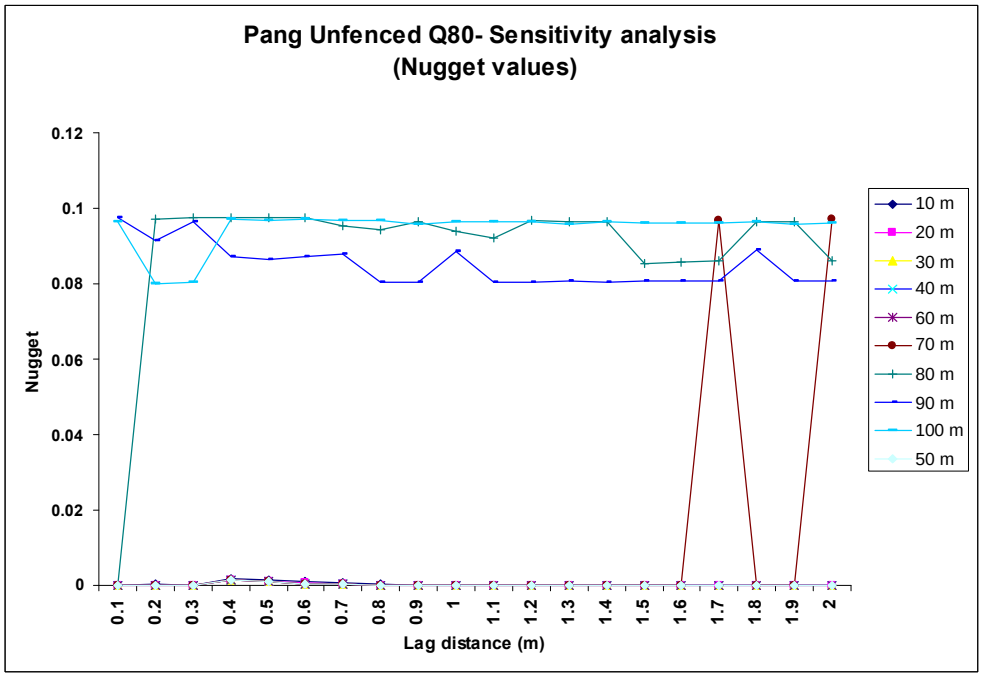
Pang Unfenced Q80- Sensitivity analysis
(Nugget values)
Nugget
0.12
0.1
0.08
0.06
0.04
0.02
0
0.1
0.2
0.3
0.4
0.5
0.6
0.7
0.8
0.9
1
1.1
1.2
1.3
1.4
1.5
1.6
1.7
1.8
1.9
2
Lag distance (m)
10 m
20 m
30 m
40 m
60 m
70 m
80 m
90 m
100 m
50 m

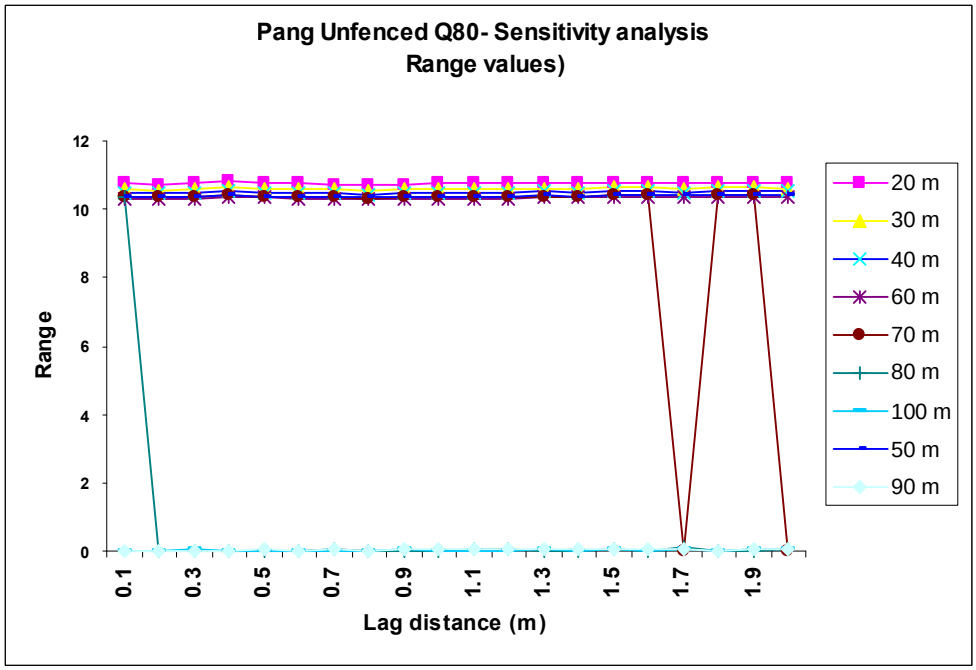
Pang Unfenced Q80- Sensitivity analysis
Range values)
Range
Lag distance (m)
20 m
30 m
40 m
60 m
70 m
80 m
100 m
50 m
90 m

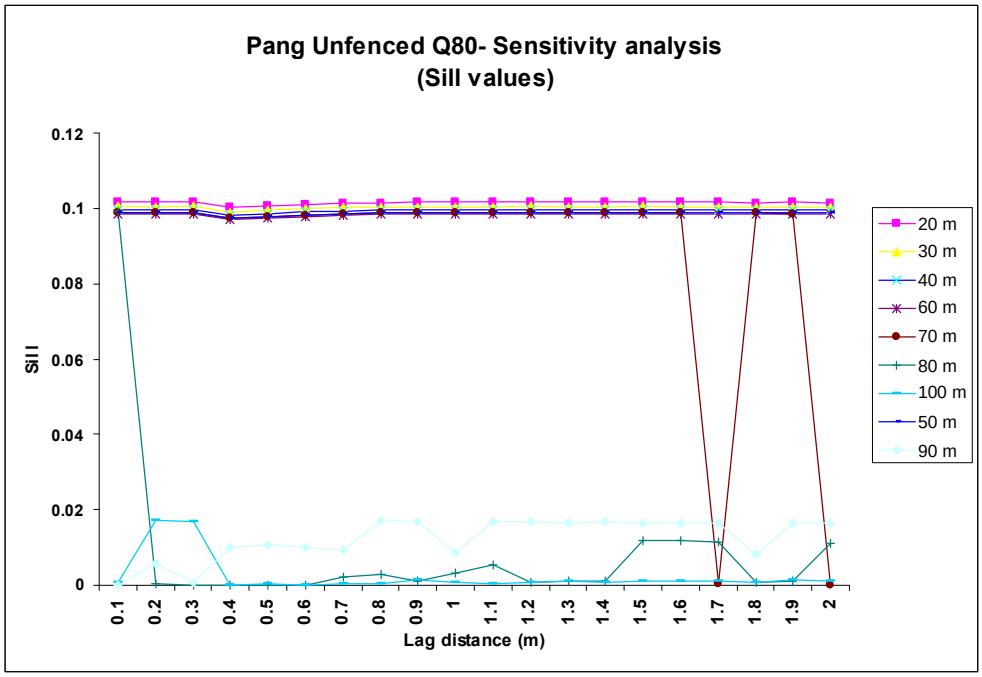
Pang Unfenced Q80- Sensitivity analysis
(Sill values)
Sill
Lag distance (m)
20 m
30 m
40 m
60 m
70 m
80 m
100 m
50 m
90 m

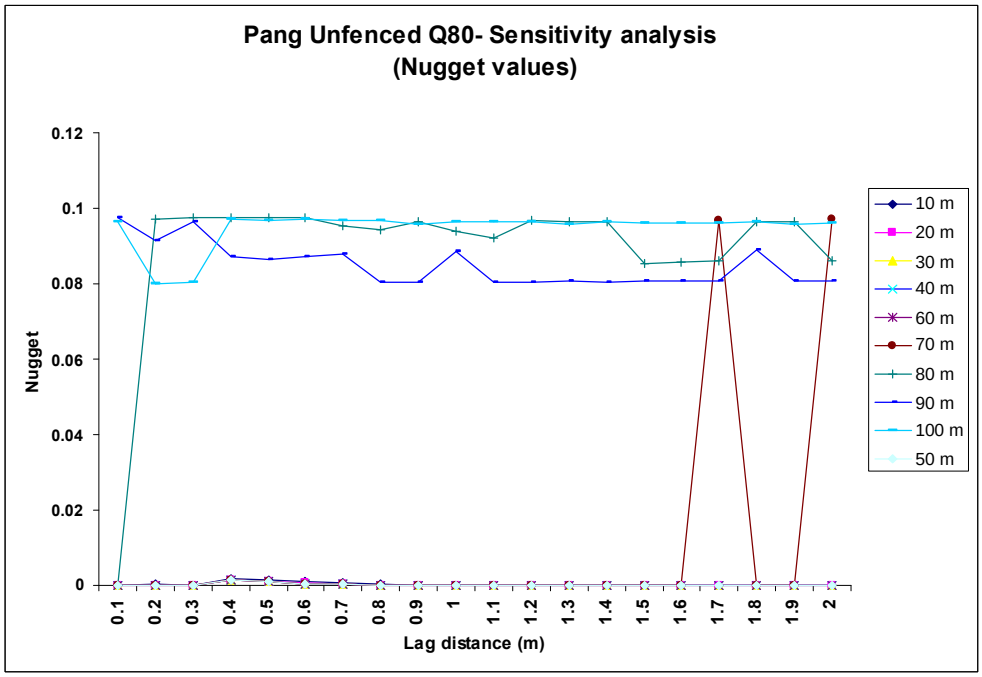
Pang Unfenced Q80- Sensitivity analysis
(Nugget values)
Nugget
Lag distance (m)
10 m
20 m
30 m
40 m
60 m
70 m
80 m
90 m
100 m
50 m

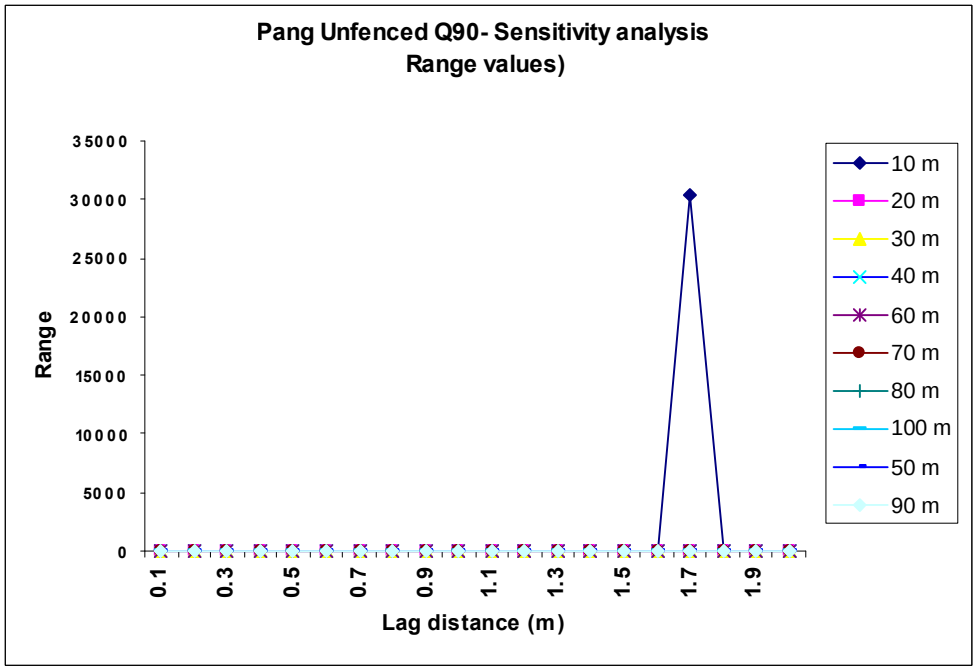
Pang Unfenced Q90- Sensitivity analysis
Range values)
Range
35000
30000
25000
20000
15000
10000
5000
0
0.1
0.3
0.5
0.7
0.9
1.1
1.3
1.5
1.7
1.9
Lag distance (m)
10 m
20 m
30 m
40 m
60 m
70 m
80 m
100 m
50 m
90 m

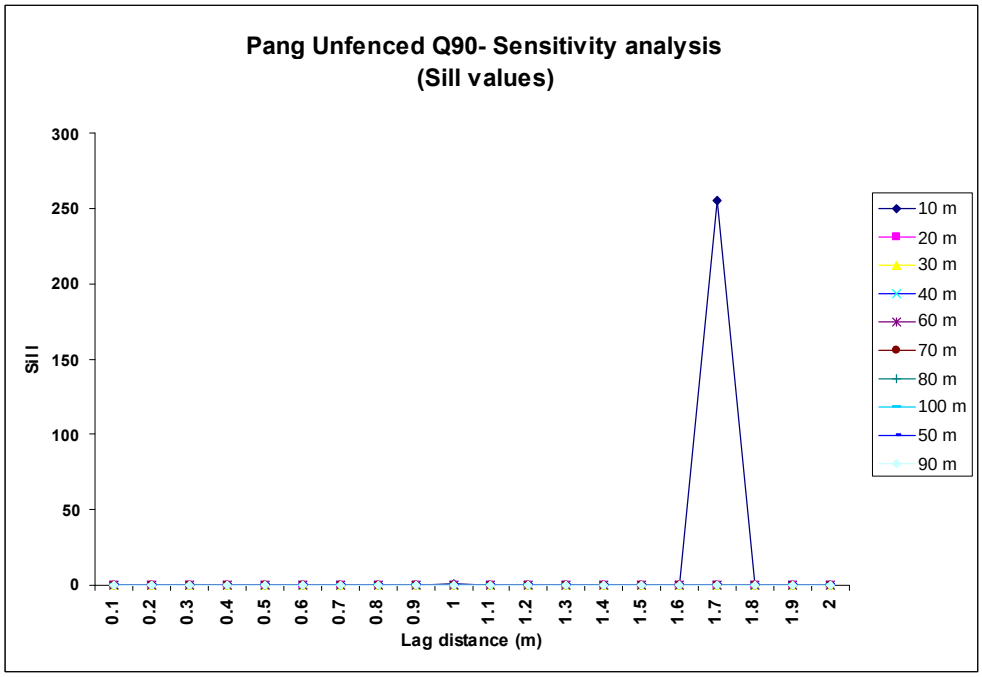
Pang Unfenced Q90- Sensitivity analysis
(Sill values)
Sill
300
250
200
150
100
50
0
0.1
0.2
0.3
0.4
0.5
0.6
0.7
0.8
0.9
1
1.1
1.2
1.3
1.4
1.5
1.6
1.7
1.8
1.9
2
Lag distance (m)
10 m
20 m
30 m
40 m
60 m
70 m
80 m
100 m
50 m
90 m

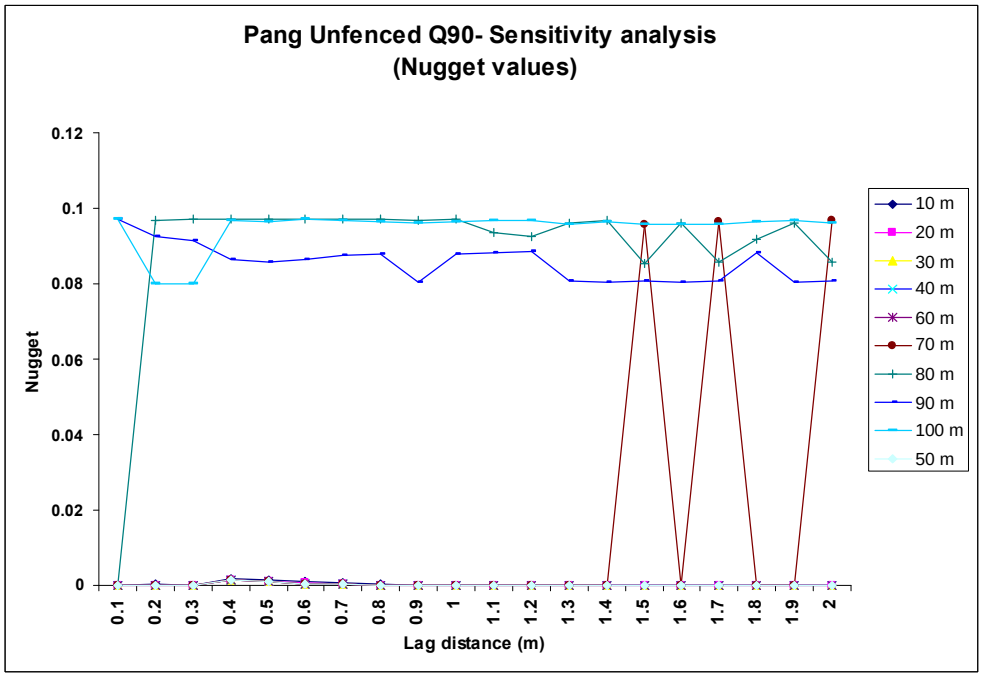
Pang Unfenced Q90- Sensitivity analysis
(Nugget values)
Nugget
0.12
0.1
0.08
0.06
0.04
0.02
0
0.1
0.2
0.3
0.4
0.5
0.6
0.7
0.8
0.9
1
1.1
1.2
1.3
1.4
1.5
1.6
1.7
1.8
1.9
2
Lag distance (m)
10 m
20 m
30 m
40 m
60 m
70 m
80 m
90 m
100 m
50 m

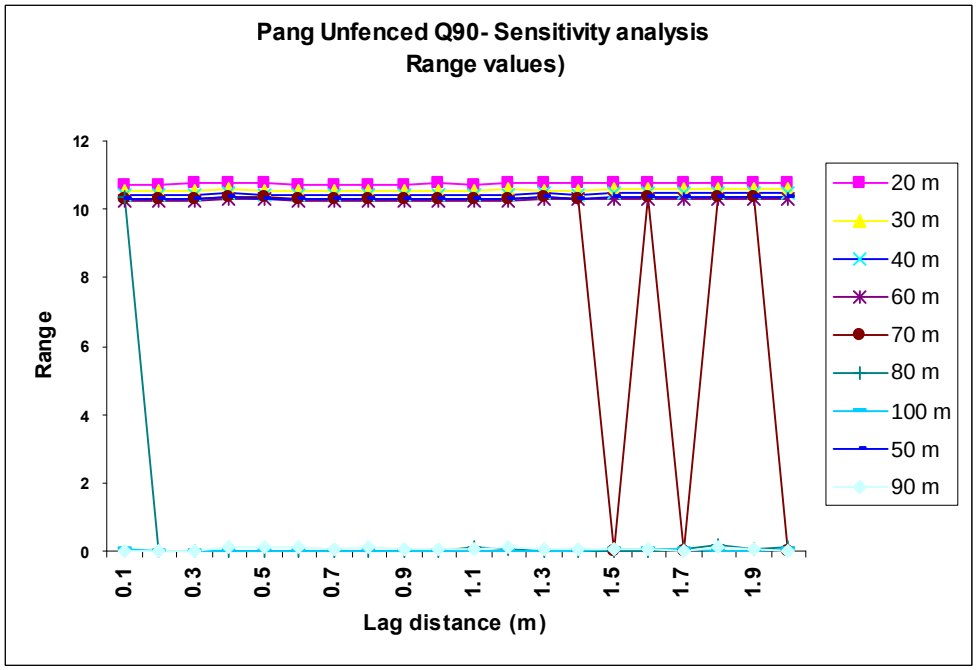
Pang Unfenced Q90- Sensitivity analysis
Range values)
Range
Lag distance (m)
20 m
30 m
40 m
60 m
70 m
80 m
100 m
50 m
90 m

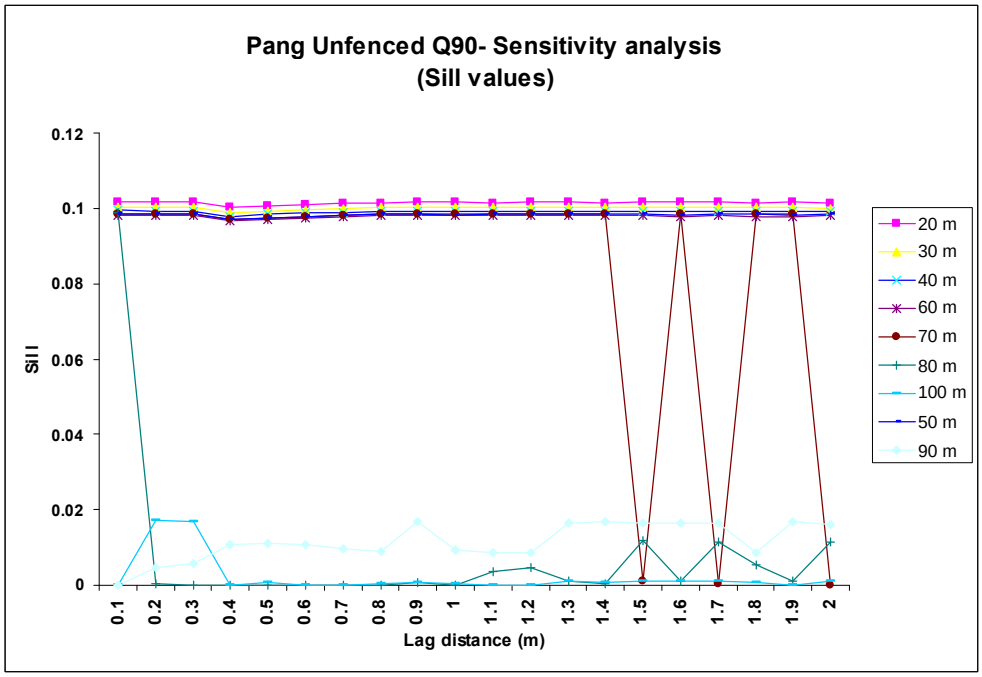
Pang Unfenced Q90- Sensitivity analysis
(Sill values)
Sill
Lag distance (m)
20 m
30 m
40 m
60 m
70 m
80 m
100 m
50 m
90 m

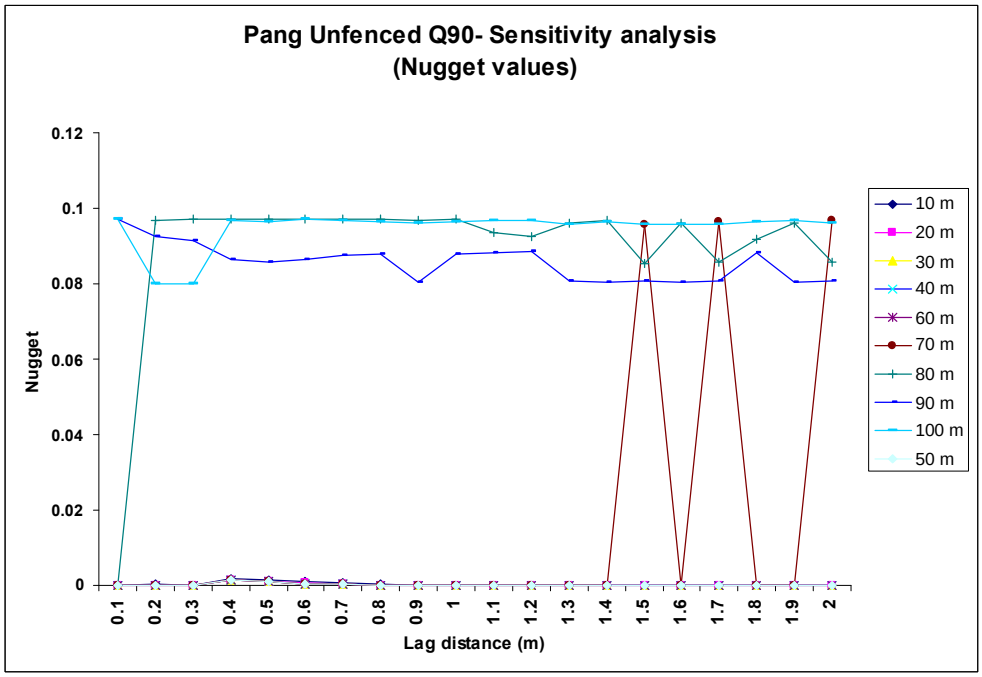
Pang Unfenced Q90- Sensitivity analysis
(Nugget values)
Nugget
Lag distance (m)
10 m
20 m
30 m
40 m
60 m
70 m
80 m
90 m
100 m
50 m

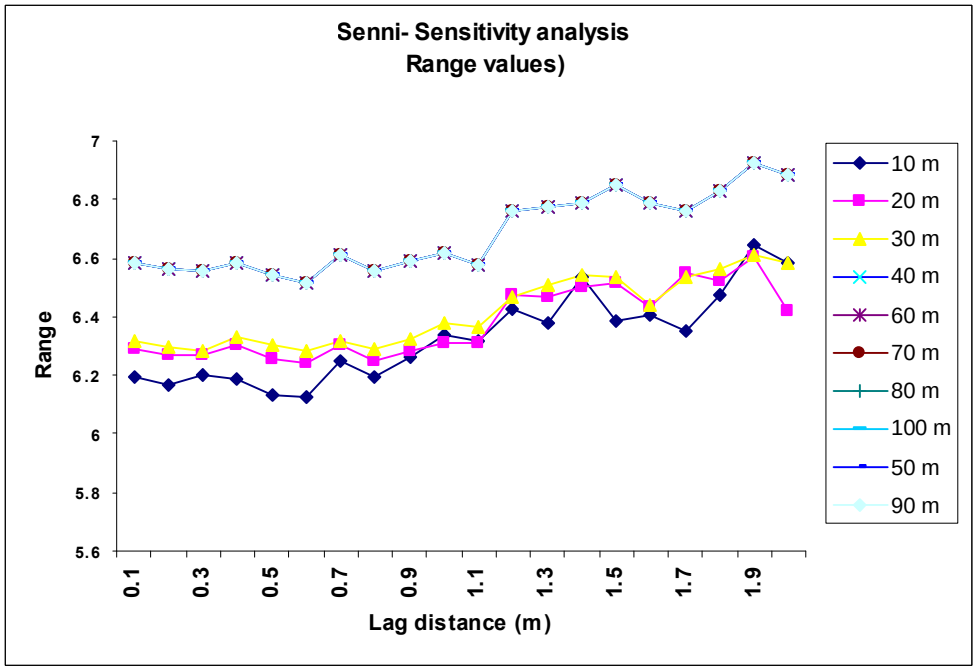
Senni- Sensitivity analysis
Range values)
Range
Lag distance (m)
10 m
20 m
30 m
40 m
60 m
70 m
80 m
100 m
50 m
90 m

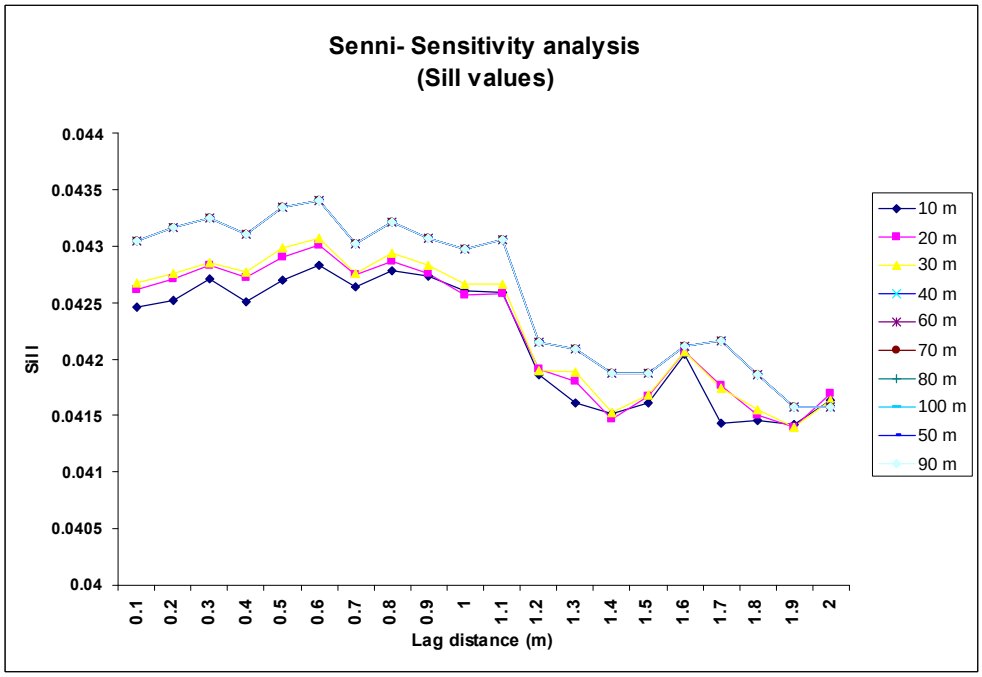
Senni- Sensitivity analysis
(Sill values)
Sill
Lag distance (m)
10 m
20 m
30 m
40 m
60 m
70 m
80 m
100 m
50 m
90 m

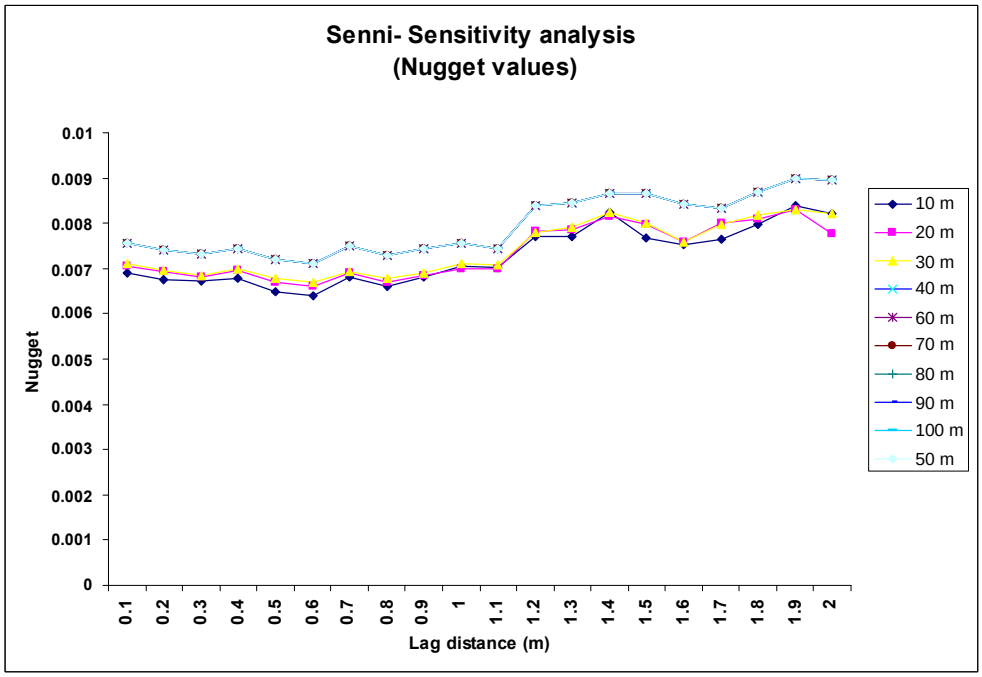
Senni- Sensitivity analysis
(Nugget values)
Nugget
Lag distance (m)
10 m
20 m
30 m
40 m
60 m
70 m
80 m
90 m
100 m
50 m

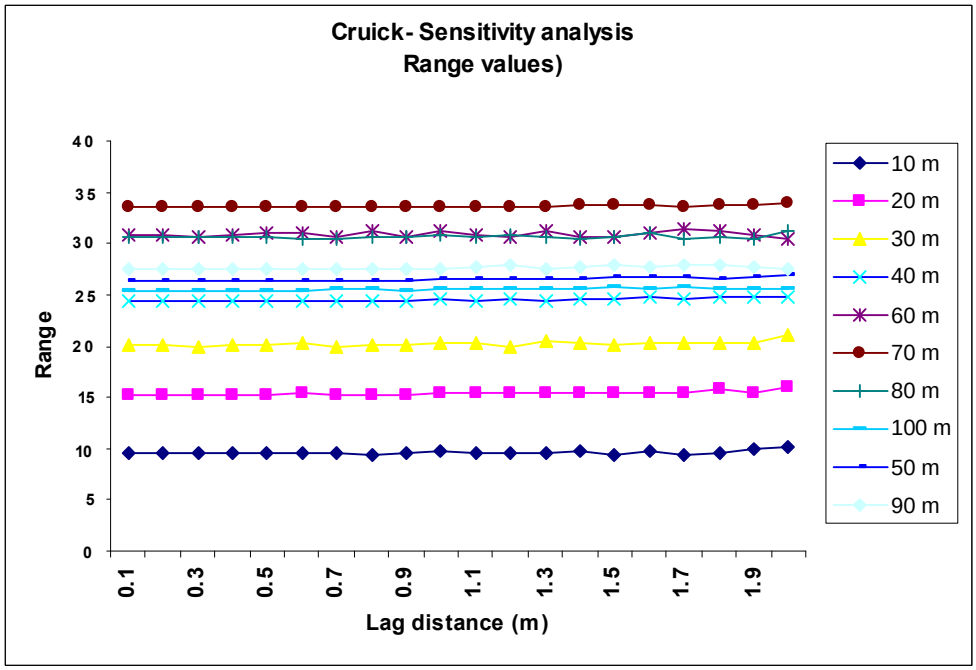
Cruick- Sensitivity analysis
Range values)
Range
Lag distance (m)
10 m
20 m
30 m
40 m
60 m
70 m
80 m
100 m
50 m
90 m

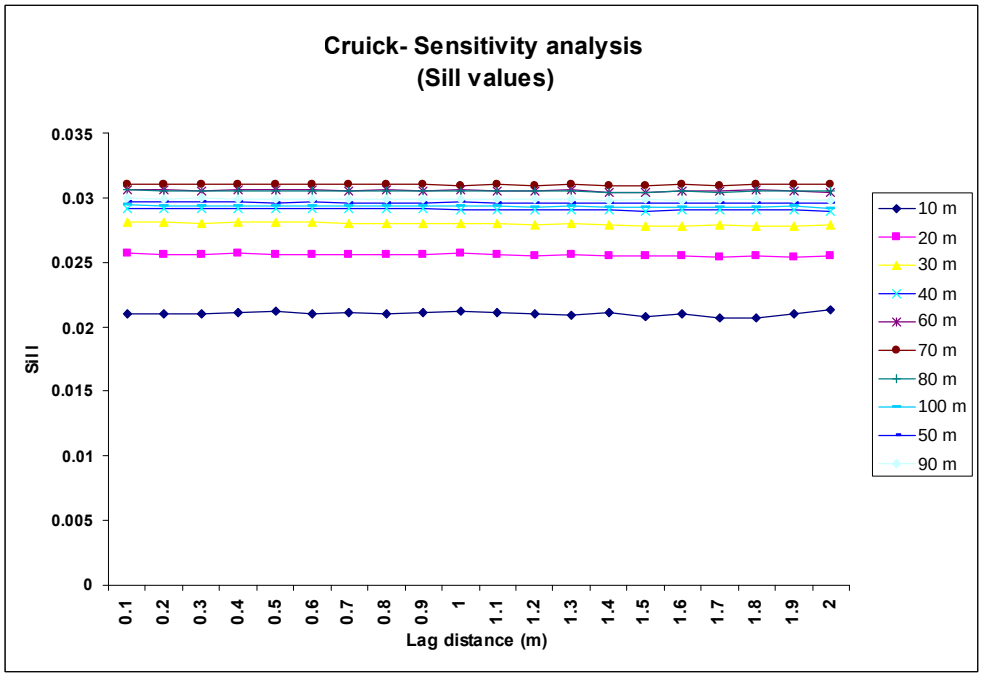
Cruick- Sensitivity analysis
(Sill values)
Sill
Lag distance (m)
10 m
20 m
30 m
40 m
60 m
70 m
80 m
100 m
50 m
90 m

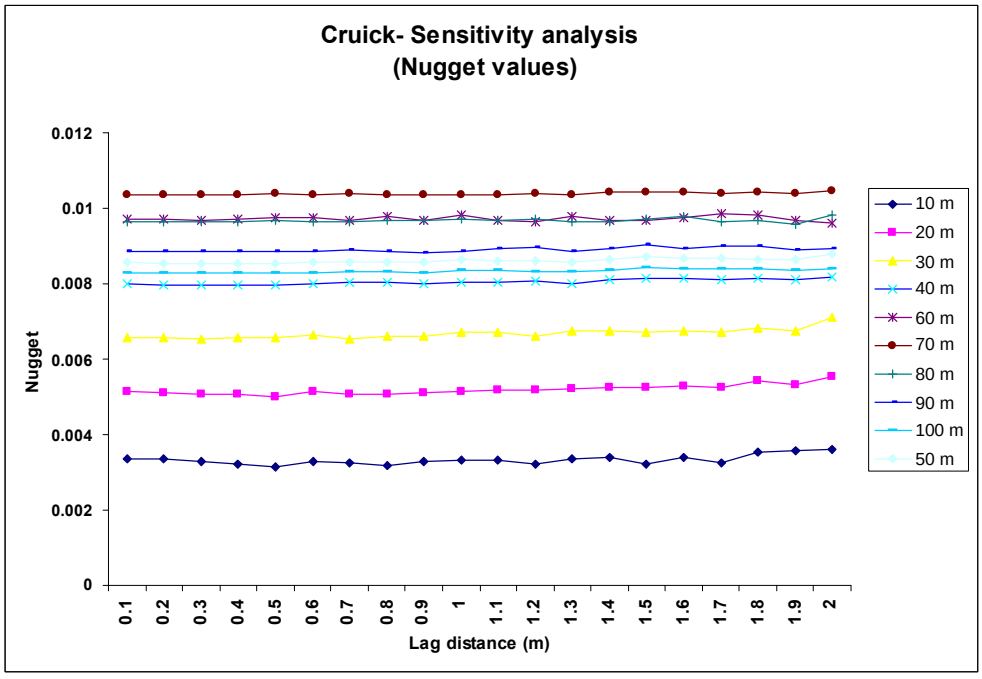
Cruick- Sensitivity analysis
(Nugget values)
Nugget
Lag distance (m)
10 m
20 m
30 m
40 m
60 m
70 m
80 m
90 m
100 m
50 m

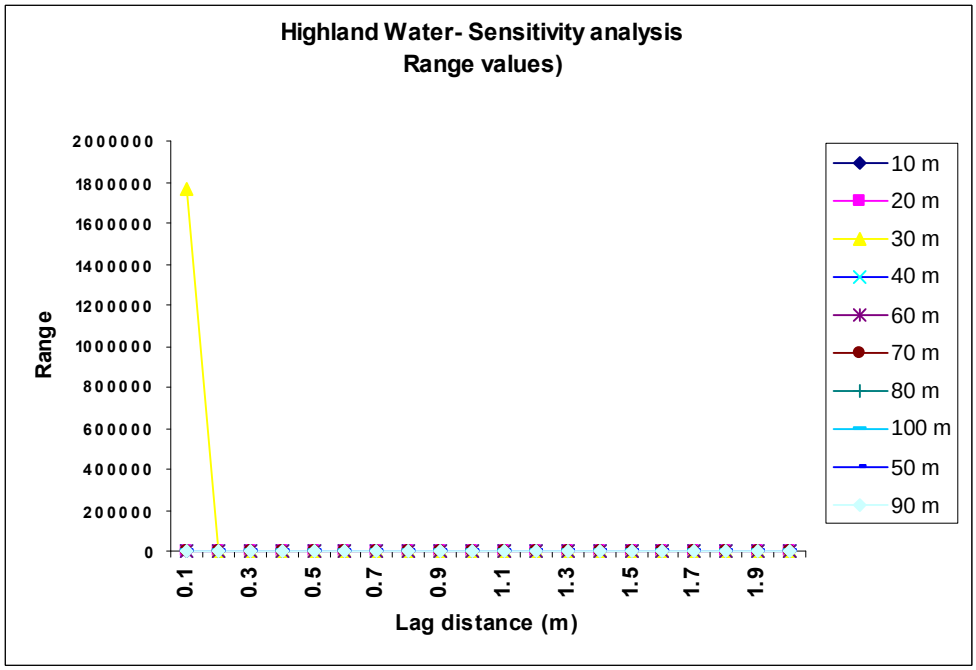
Highland Water- Sensitivity analysis
Range values)
Range
2000000
1800000
1600000
1400000
1200000
1000000
800000
600000
400000
200000
0
0.1
0.3
0.5
0.7
0.9
1.1
1.3
1.5
1.7
1.9
Lag distance (m)
10 m
20 m
30 m
40 m
60 m
70 m
80 m
100 m
50 m
90 m

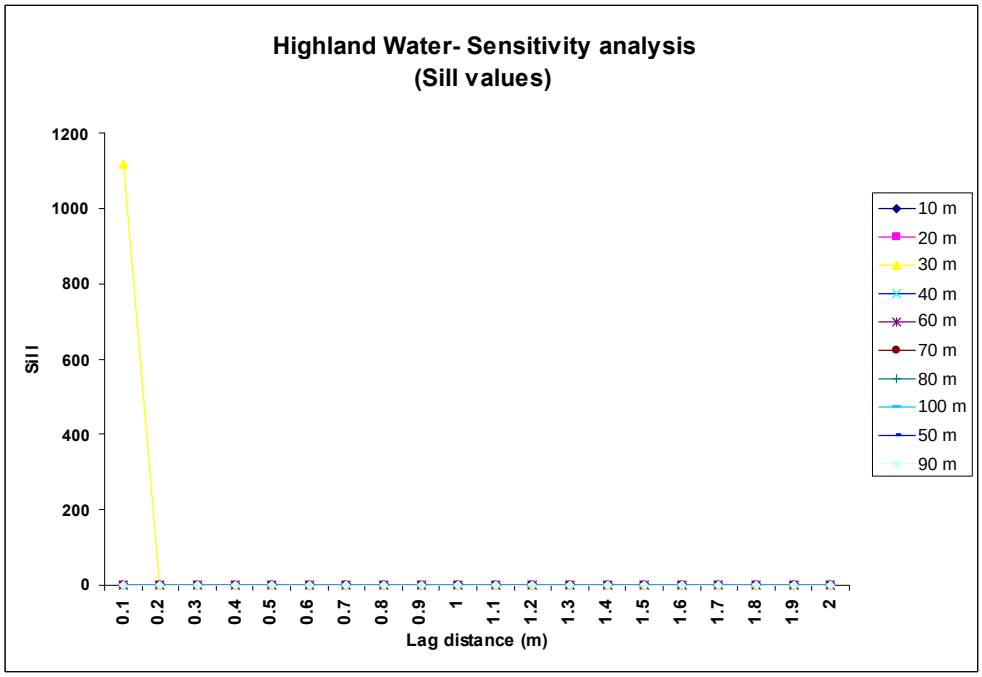
Highland Water- Sensitivity analysis
(Sill values)
Sill
1200
1000
800
600
400
200
0
0.1
0.2
0.3
0.4
0.5
0.6
0.7
0.8
0.9
1
1.1
1.2
1.3
1.4
1.5
1.6
1.7
1.8
1.9
2
Lag distance (m)
10 m
20 m
30 m
40 m
60 m
70 m
80 m
100 m
50 m
90 m

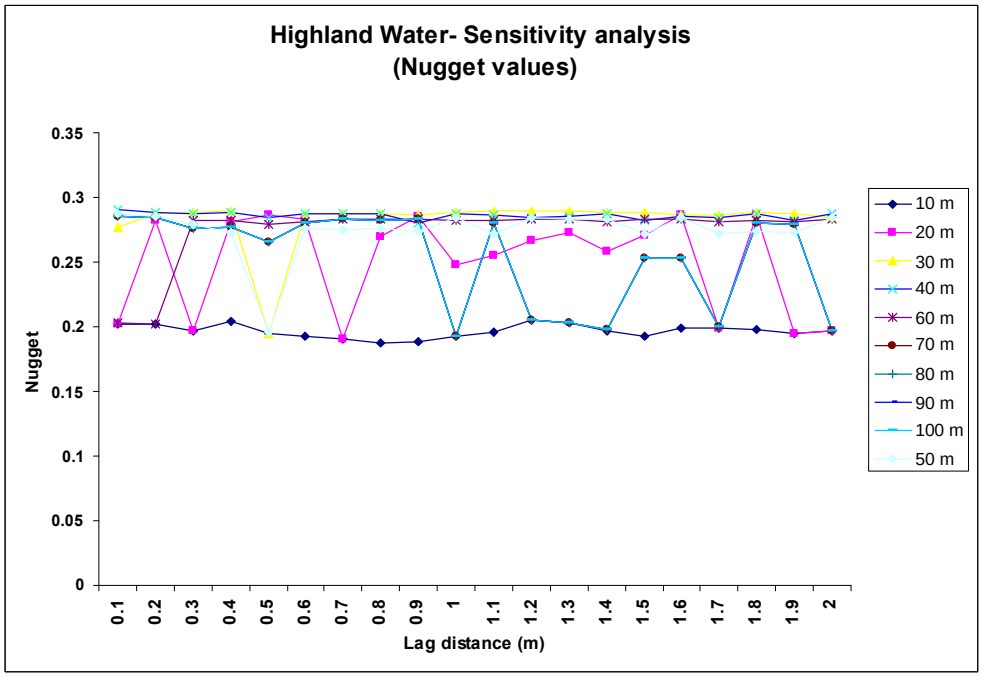
Highland Water- Sensitivity analysis
(Nugget values)
Nugget
0.35
0.3
0.25
0.2
0.15
0.1
0.05
0
0.1
0.2
0.3
0.4
0.5
0.6
0.7
0.8
0.9
1
1.1
1.2
1.3
1.4
1.5
1.6
1.7
1.8
1.9
2
Lag distance (m)
10 m
20 m
30 m
40 m
60 m
70 m
80 m
90 m
100 m
50 m

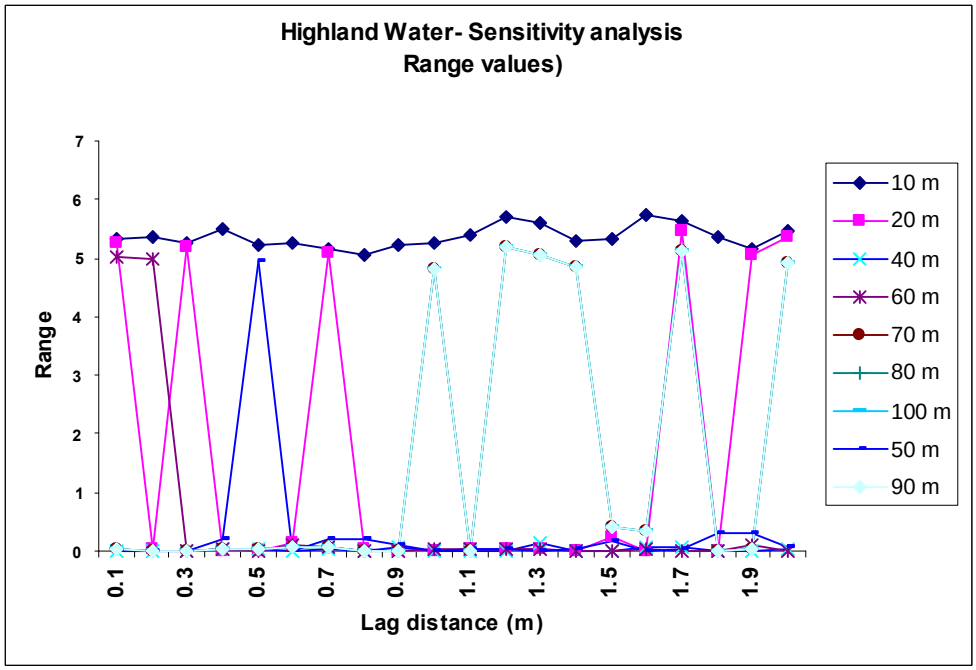
Highland Water- Sensitivity analysis
Range values)
Range
Lag distance (m)
10 m
20 m
40 m
60 m
70 m
80 m
100 m
50 m
90 m

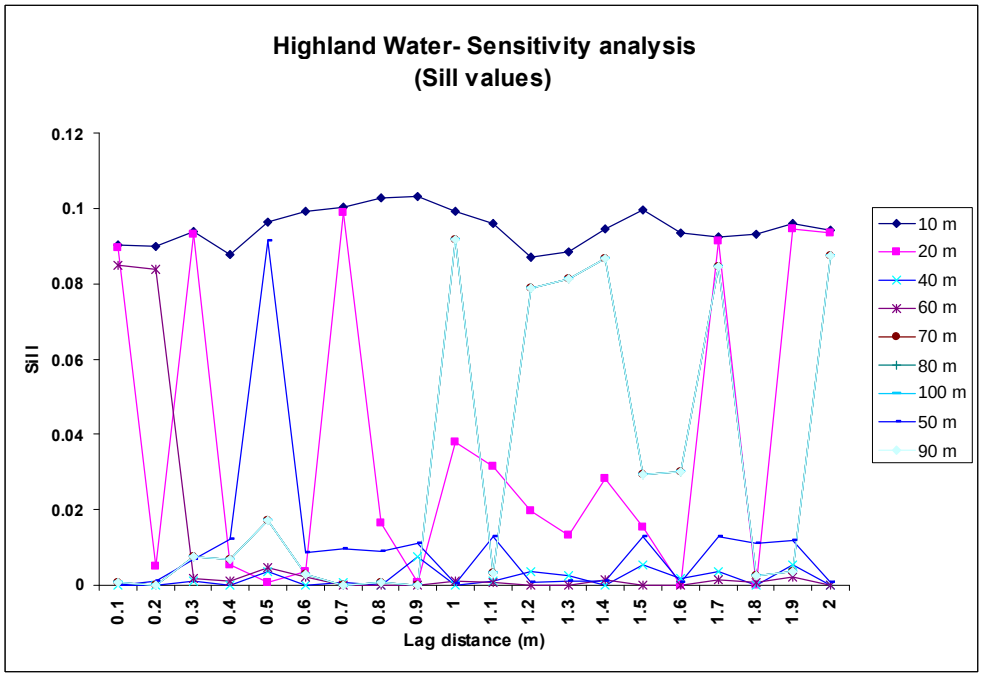
Highland Water- Sensitivity analysis
(Sill values)
Sill
Lag distance (m)
10 m
20 m
40 m
60 m
70 m
80 m
100 m
50 m
90 m

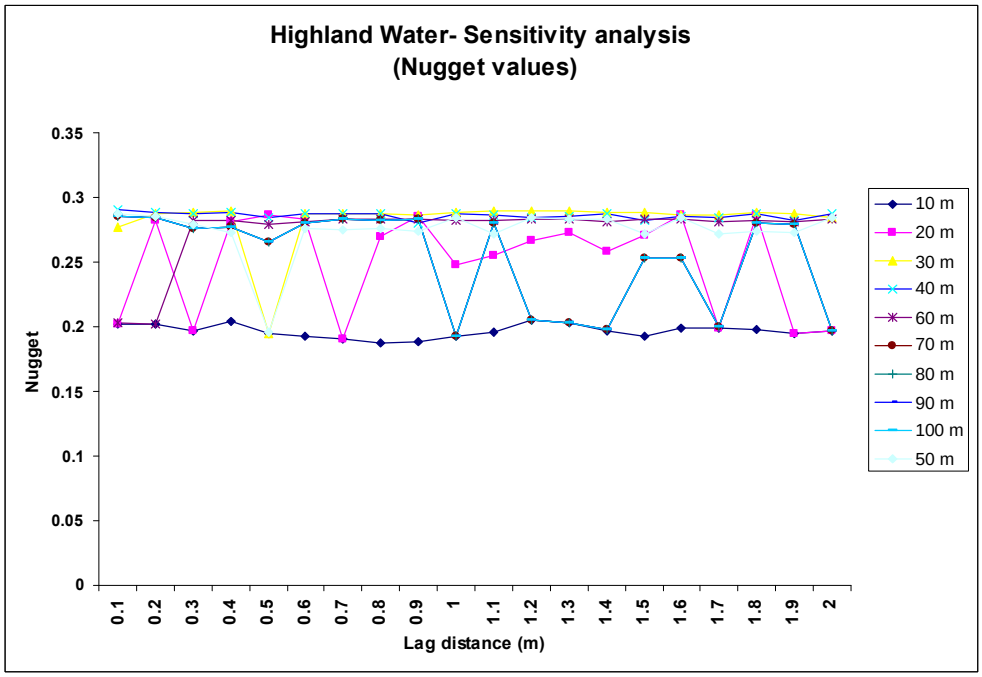
Highland Water- Sensitivity analysis
(Nugget values)
Nugget
Lag distance (m)
10 m
20 m
30 m
40 m
60 m
70 m
80 m
90 m
100 m
50 m

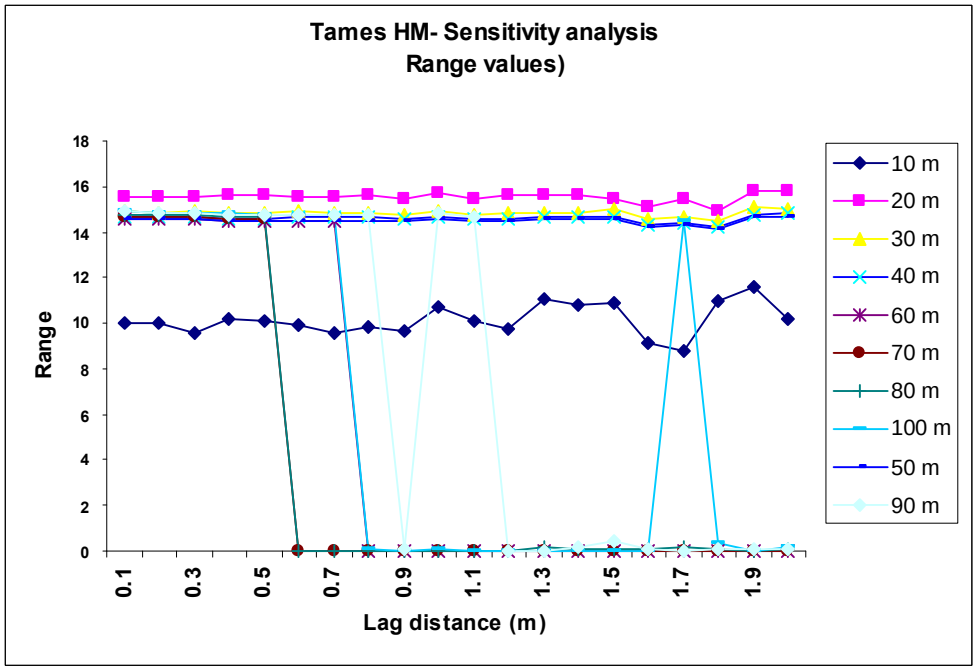
Tames HM- Sensitivity analysis
Range values)
Range
Lag distance (m)
10 m
20 m
30 m
40 m
60 m
70 m
80 m
100 m
50 m
90 m

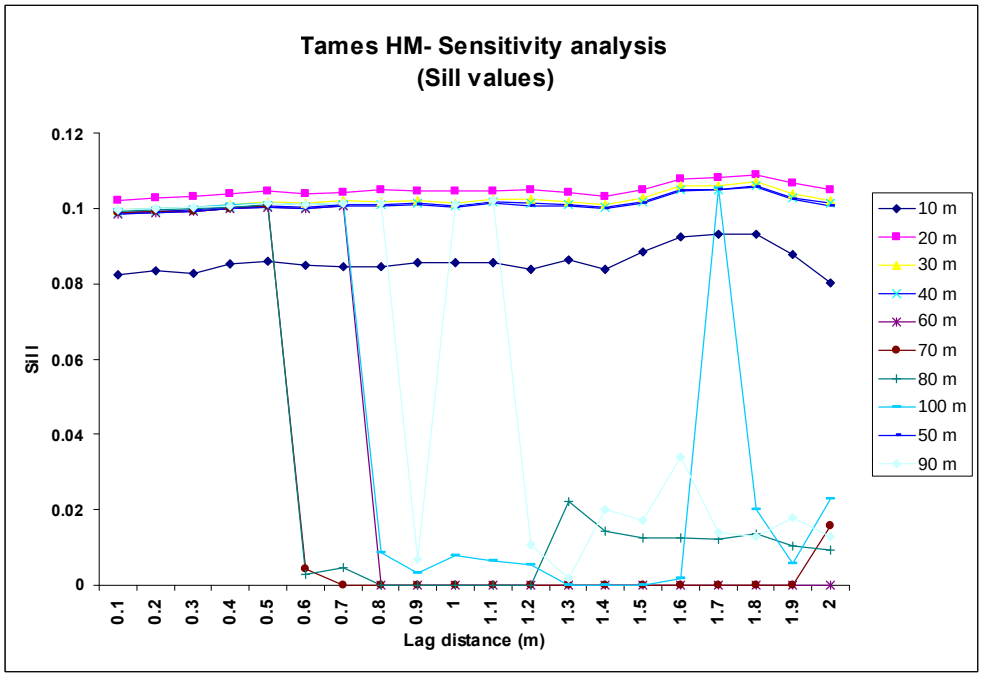
Tames HM- Sensitivity analysis
(Sill values)
Sill
Lag distance (m)
10 m
20 m
30 m
40 m
60 m
70 m
80 m
100 m
50 m
90 m

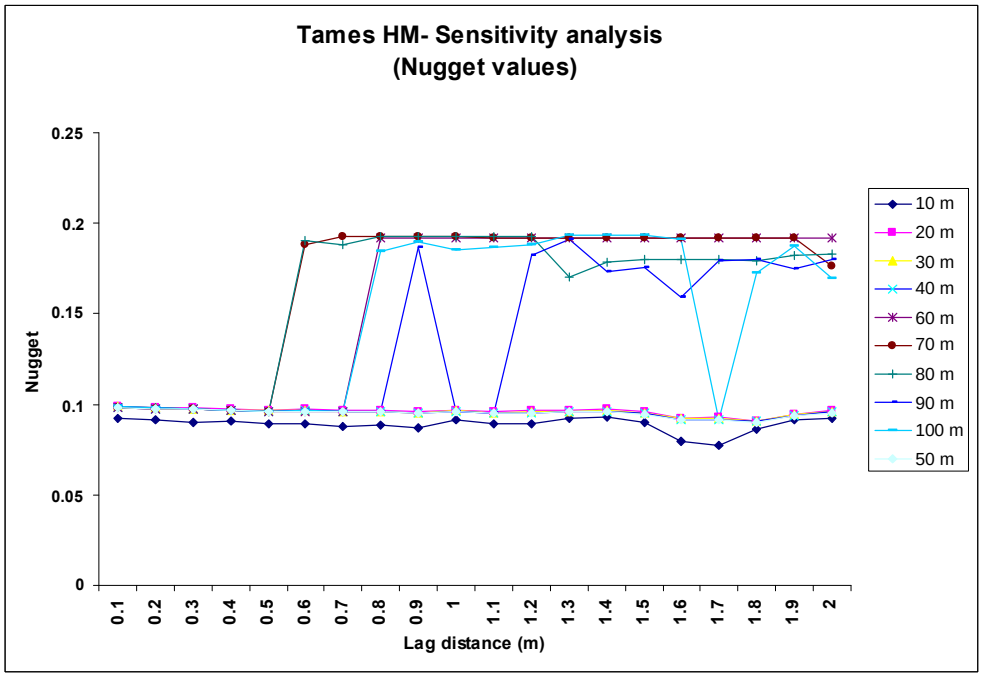
Tames HM- Sensitivity analysis
(Nugget values)
Nugget
Lag distance (m)
10 m
20 m
30 m
40 m
60 m
70 m
80 m
90 m
100 m
50 m

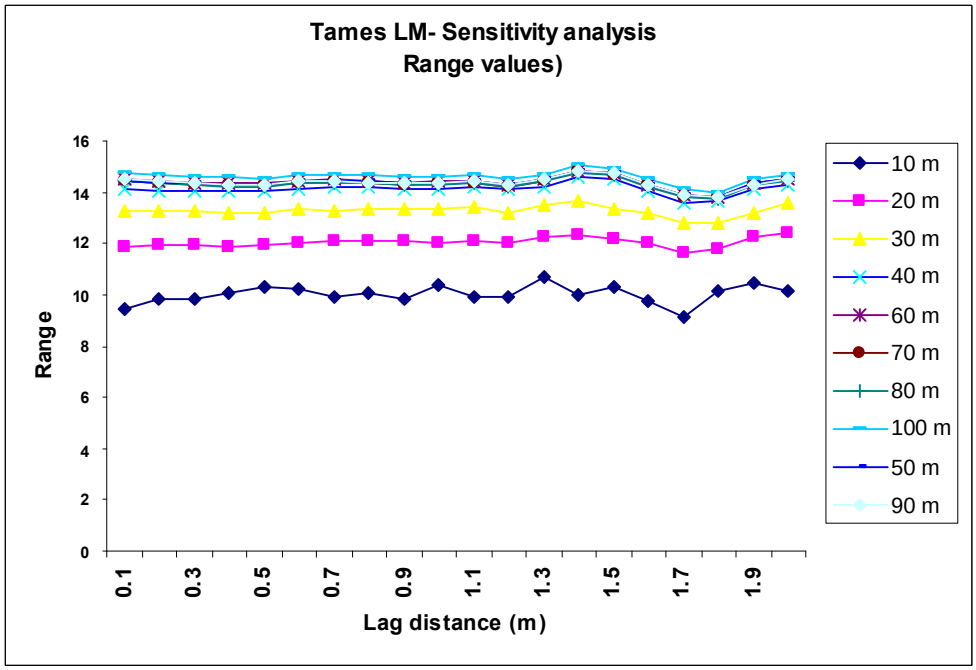
Tames LM- Sensitivity analysis
Range values)
Range
Lag distance (m)
10 m
20 m
30 m
40 m
60 m
70 m
80 m
100 m
50 m
90 m

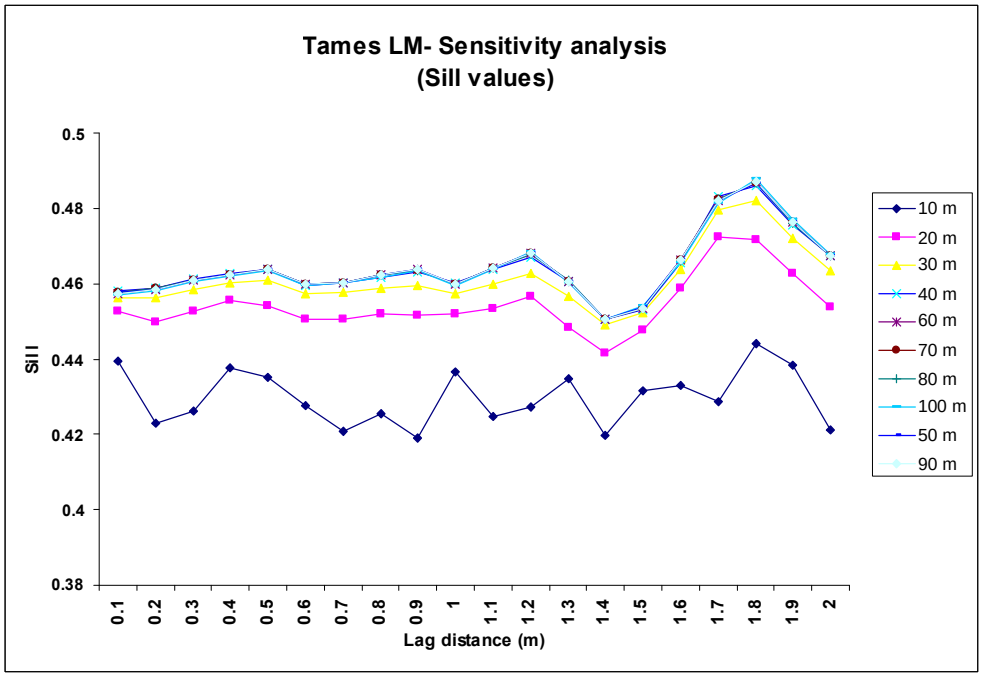
Tames LM- Sensitivity analysis
(Sill values)
Sill
Lag distance (m)
10 m
20 m
30 m
40 m
60 m
70 m
80 m
100 m
50 m
90 m

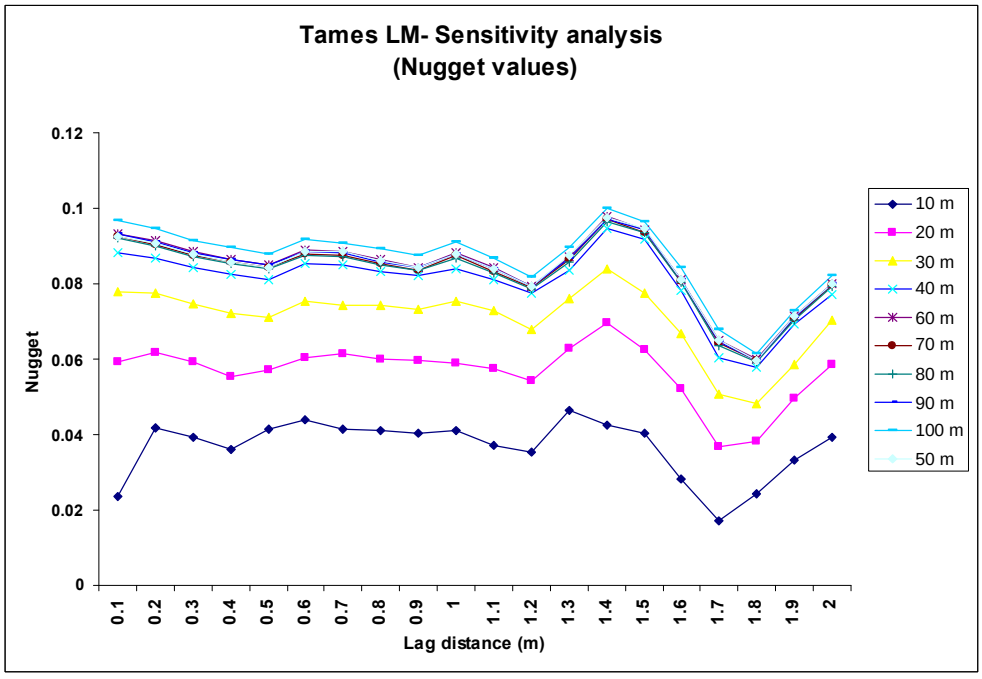
Tames LM- Sensitivity analysis
(Nugget values)
Nugget
Lag distance (m)
10 m
20 m
30 m
40 m
60 m
70 m
80 m
90 m
100 m
50 m

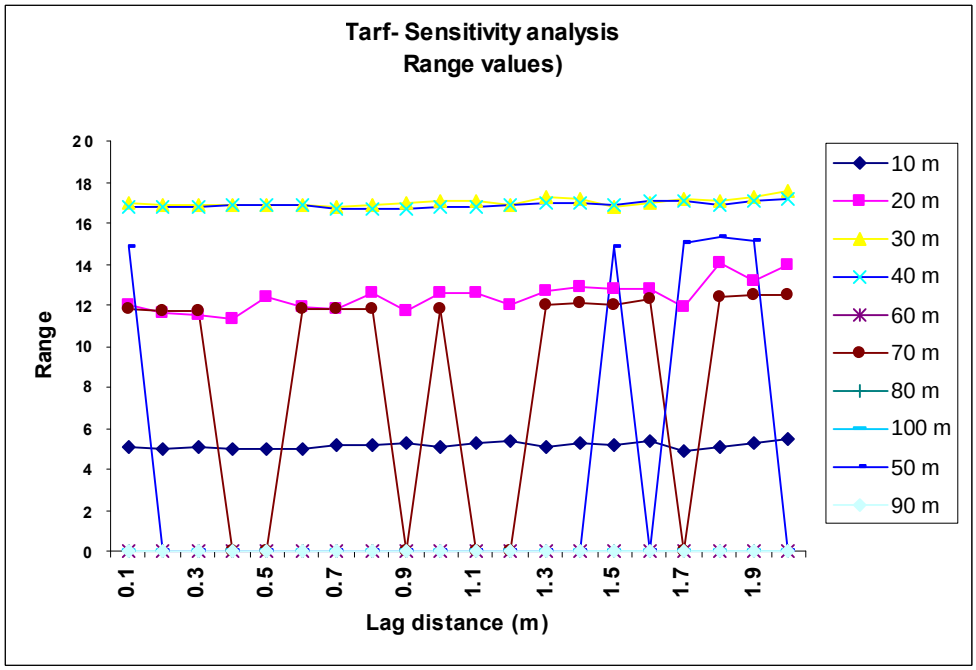
Tarf- Sensitivity analysis
Range values)
Range
Lag distance (m)
10 m
20 m
30 m
40 m
60 m
70 m
80 m
100 m
50 m
90 m

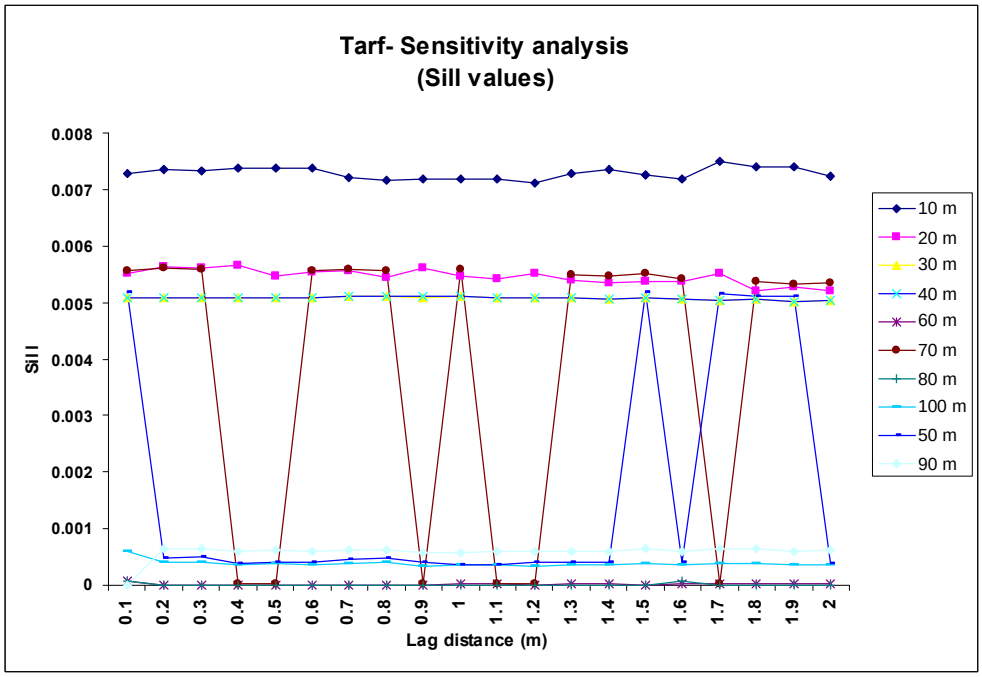
Tarf- Sensitivity analysis
(Sill values)
Sill
Lag distance (m)
10 m
20 m
30 m
40 m
60 m
70 m
80 m
100 m
50 m
90 m

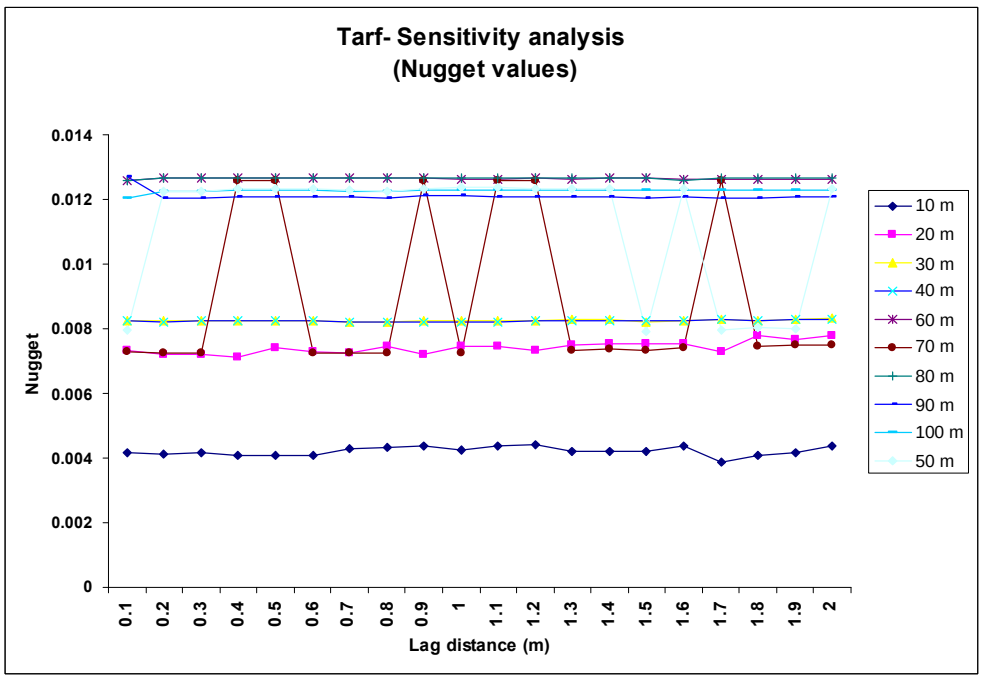
Tarf- Sensitivity analysis
(Nugget values)
Nugget
Lag distance (m)
10 m
20 m
30 m
40 m
60 m
70 m
80 m
90 m
100 m
50 m

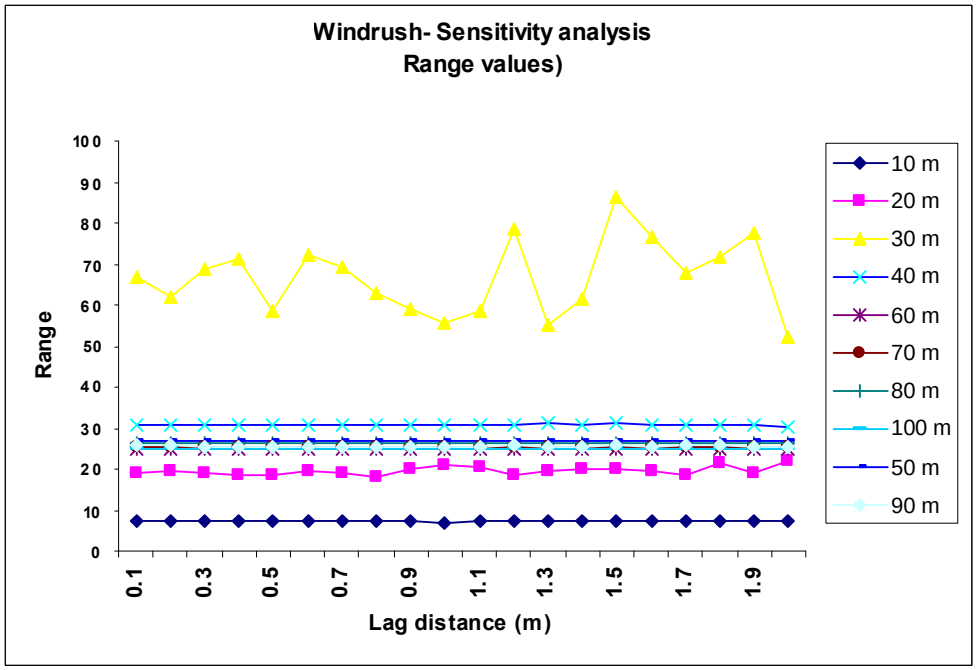
Windrush- Sensitivity analysis
Range values)
Range
Lag distance (m)
10 m
20 m
30 m
40 m
60 m
70 m
80 m
100 m
50 m
90 m

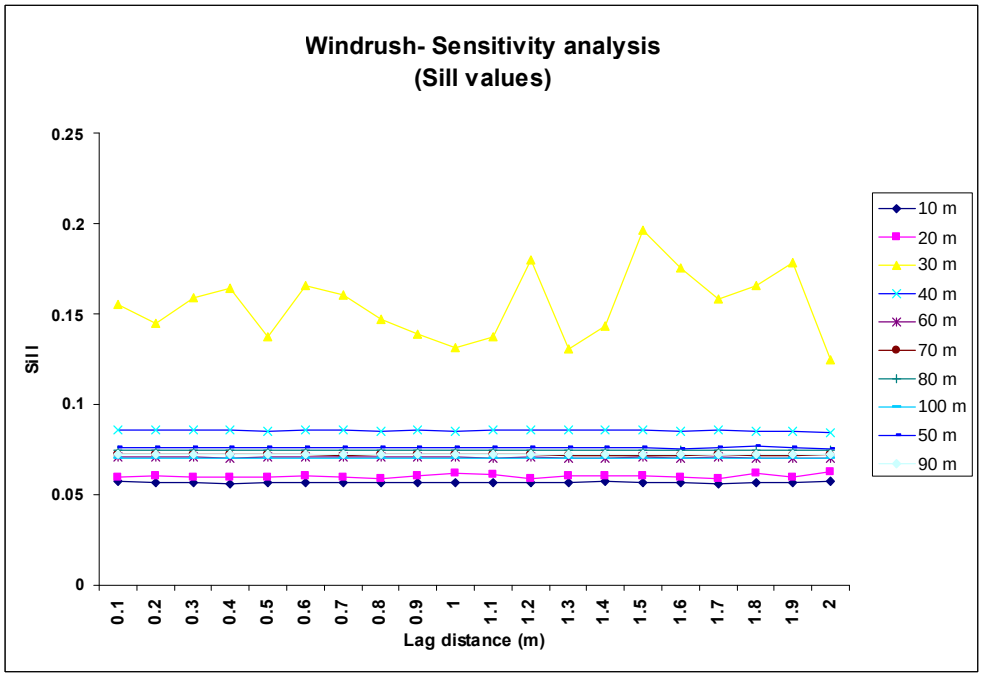
Windrush- Sensitivity analysis
(Sill values)
Sill
Lag distance (m)
10 m
20 m
30 m
40 m
60 m
70 m
80 m
100 m
50 m
90 m

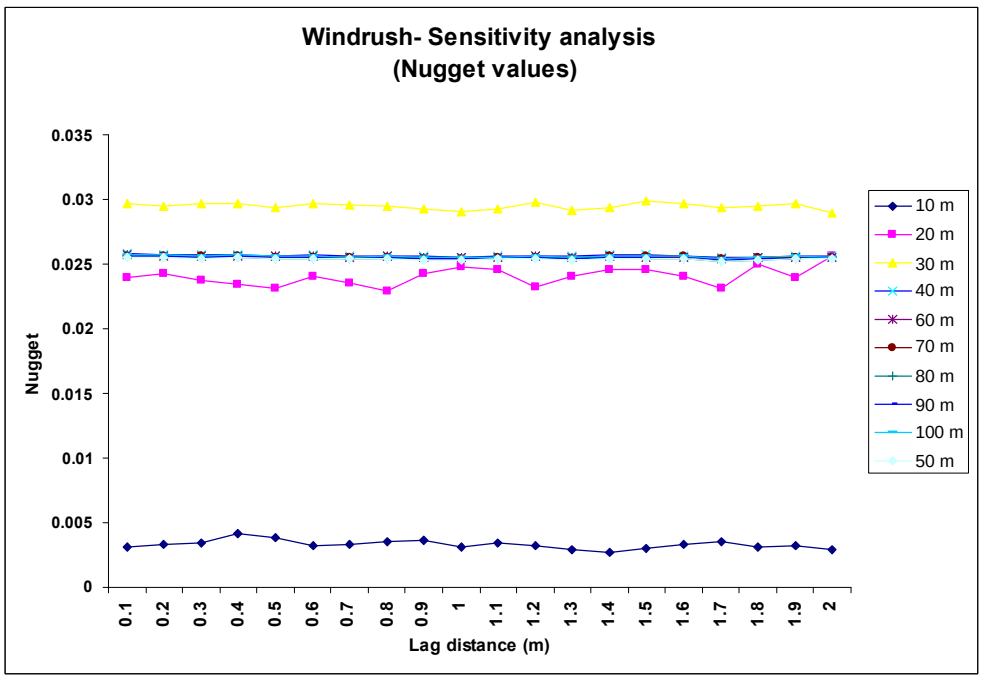
Windrush- Sensitivity analysis
(Nugget values)
Nugget
Lag distance (m)
10 m
20 m
30 m
40 m
60 m
70 m
80 m
90 m
100 m
50 m

Appendix 3.5.2

Results obtained for the analysis in Chapter 5 –Sensitivity Analysis – Variogram values for combinations of lag and maximum distance considered: exponential variogram for dry and wet points.

This appendix summarises the results obtained for the sensitivity analysis developed in section 5.4.3. for the combination of lag distances and maximum distances selected. Results presented in this section only include the graphical output for the data sets analysed with dry and wet points. The variogram model analysed is the exponential one. Three different outputs, one for each variogram variable analysed (i.e. range, sill and nugget) are presented for each river site. Those river sites that had extreme variogram values are included twice: the graphical output is presented with two different axis scales so results can be better analysed.

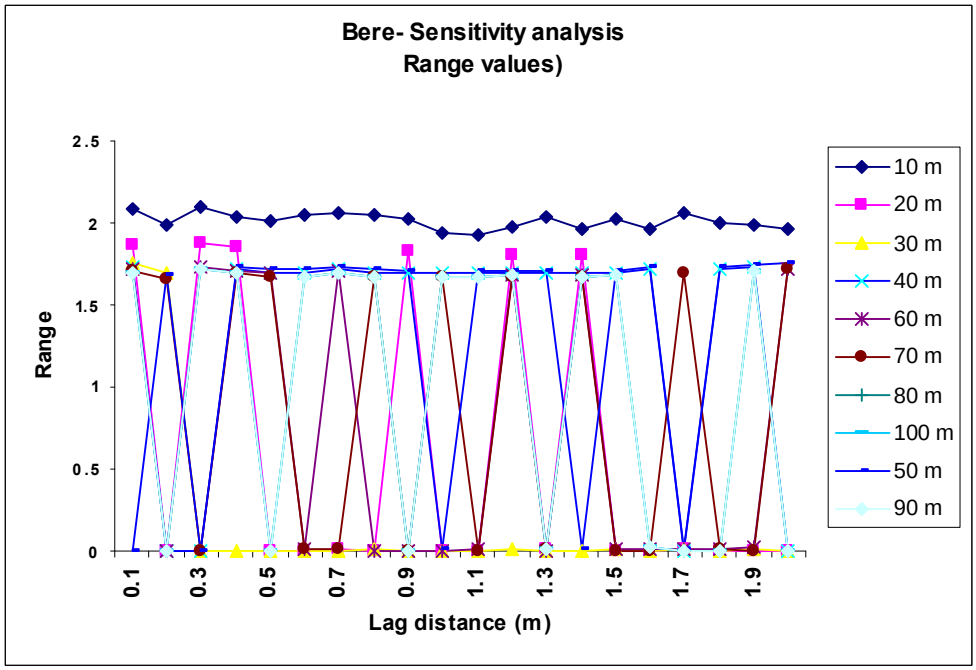
Bere- Sensitivity analysis
Range values)
Range
Lag distance (m)
10 m
20 m
30 m
40 m
60 m
70 m
80 m
100 m
50 m
90 m

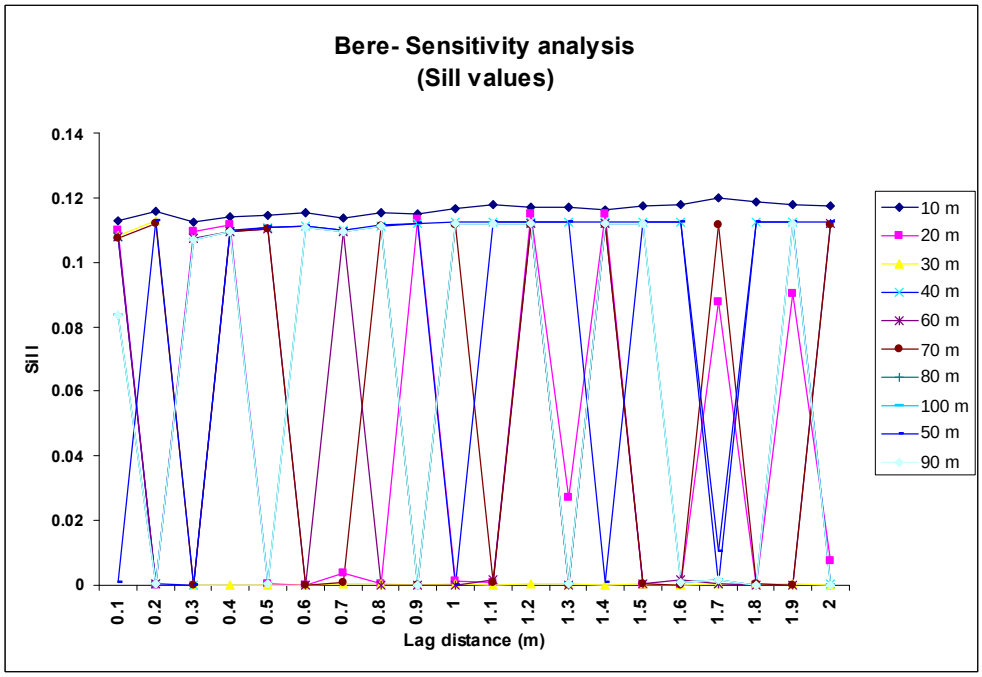
Bere- Sensitivity analysis
(Sill values)
Sill
Lag distance (m)
10 m
20 m
30 m
40 m
60 m
70 m
80 m
100 m
50 m
90 m

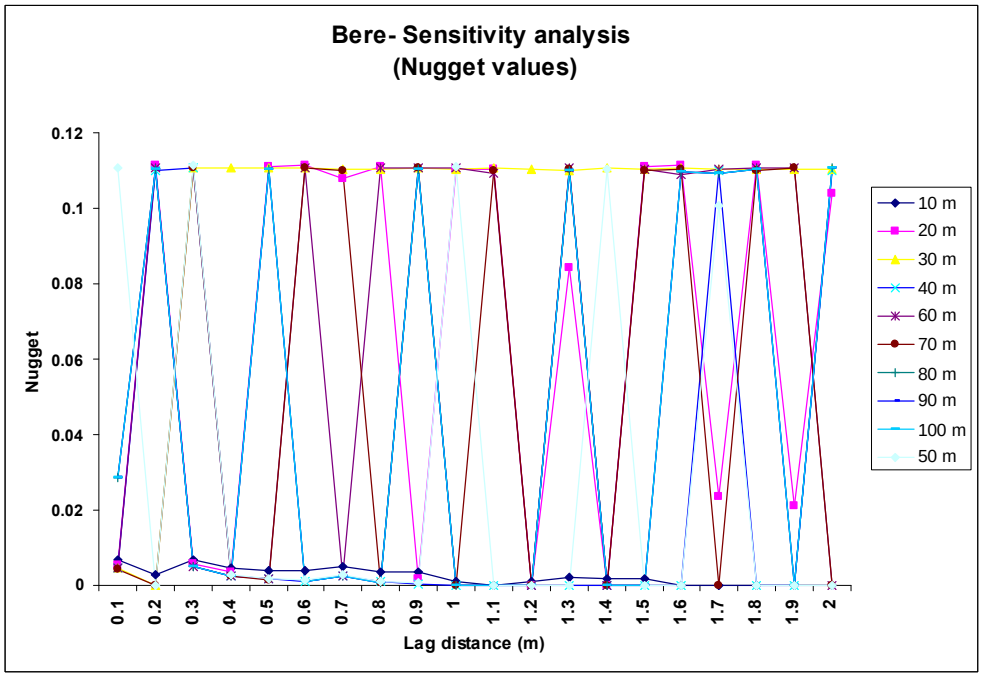
Bere- Sensitivity analysis
(Nugget values)
Nugget
Lag distance (m)
10 m
20 m
30 m
40 m
60 m
70 m
80 m
90 m
100 m
50 m

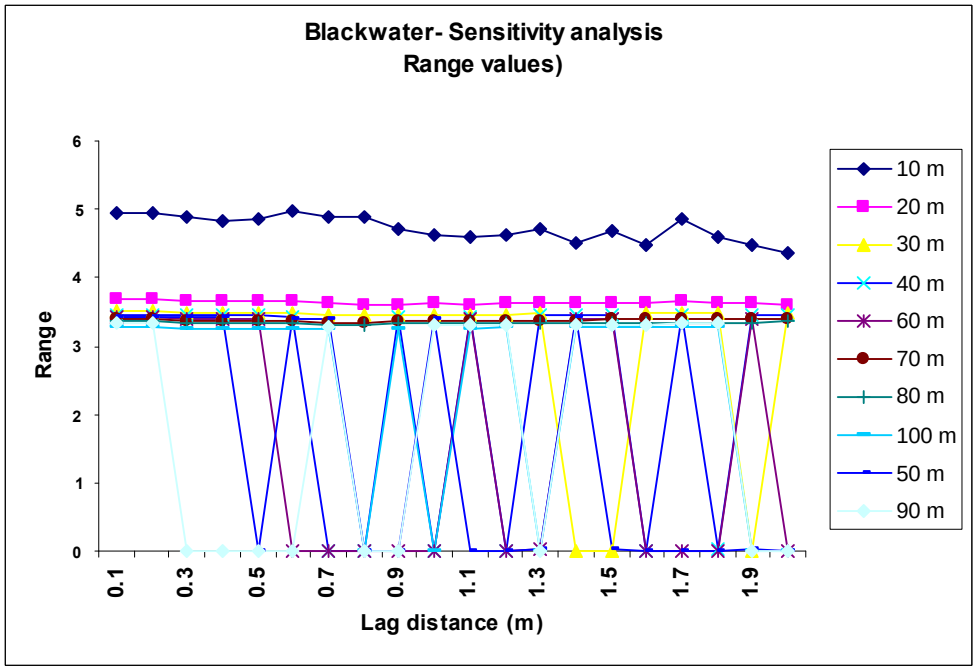
Blackwater- Sensitivity analysis
Range values)
Range
Lag distance (m)
10 m
20 m
30 m
40 m
60 m
70 m
80 m
100 m
50 m
90 m

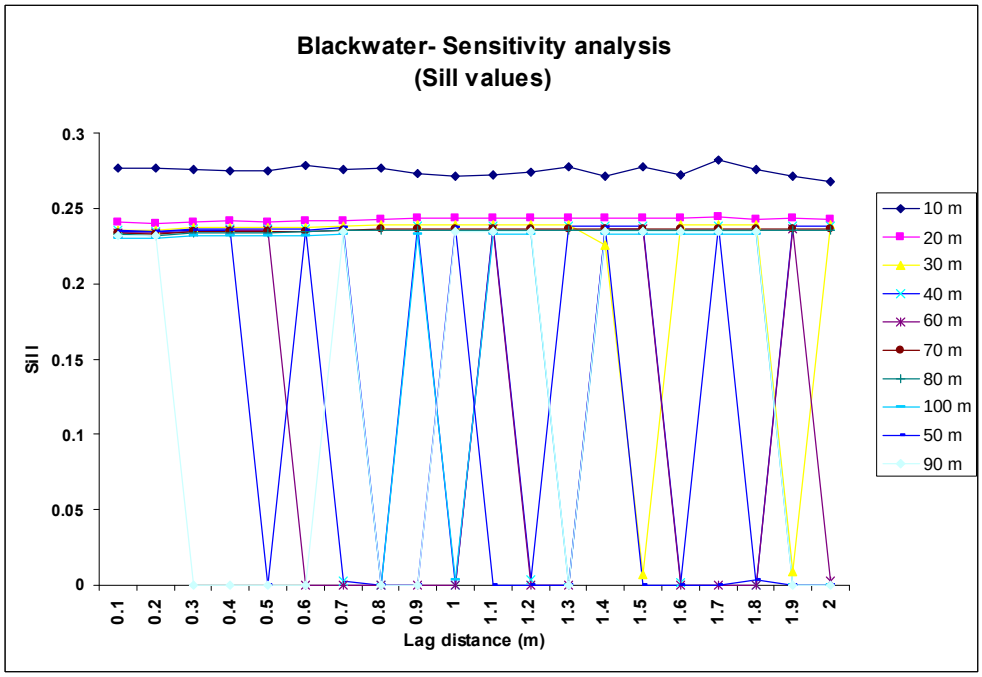
Blackwater- Sensitivity analysis
(Sill values)
Sill
Lag distance (m)
10 m
20 m
30 m
40 m
60 m
70 m
80 m
100 m
50 m
90 m

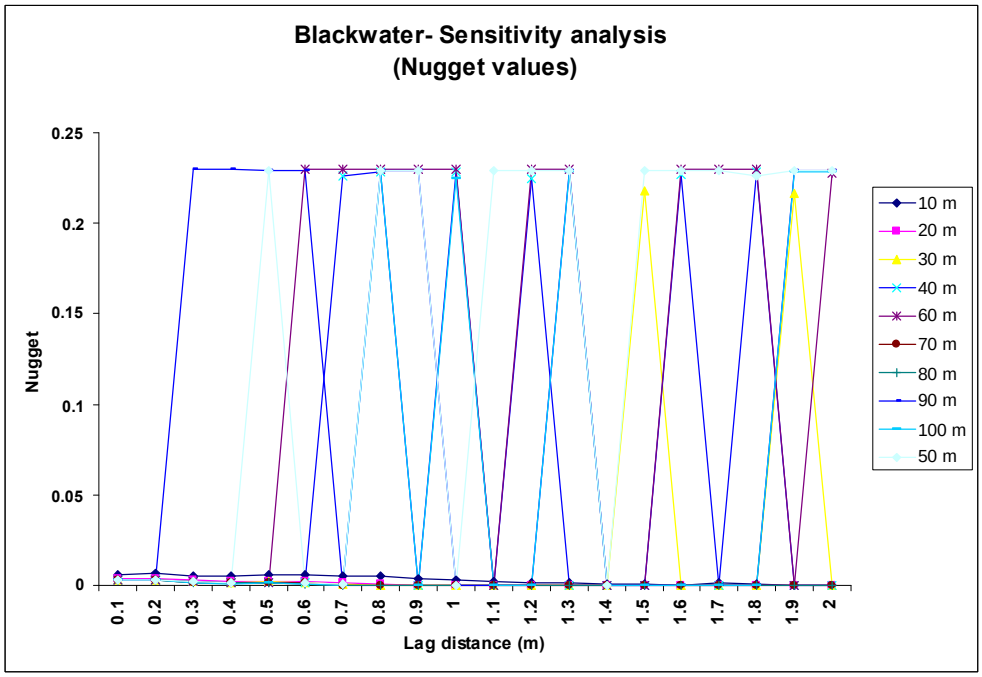
Blackwater- Sensitivity analysis
(Nugget values)
Nugget
Lag distance (m)
10 m
20 m
30 m
40 m
60 m
70 m
80 m
90 m
100 m
50 m

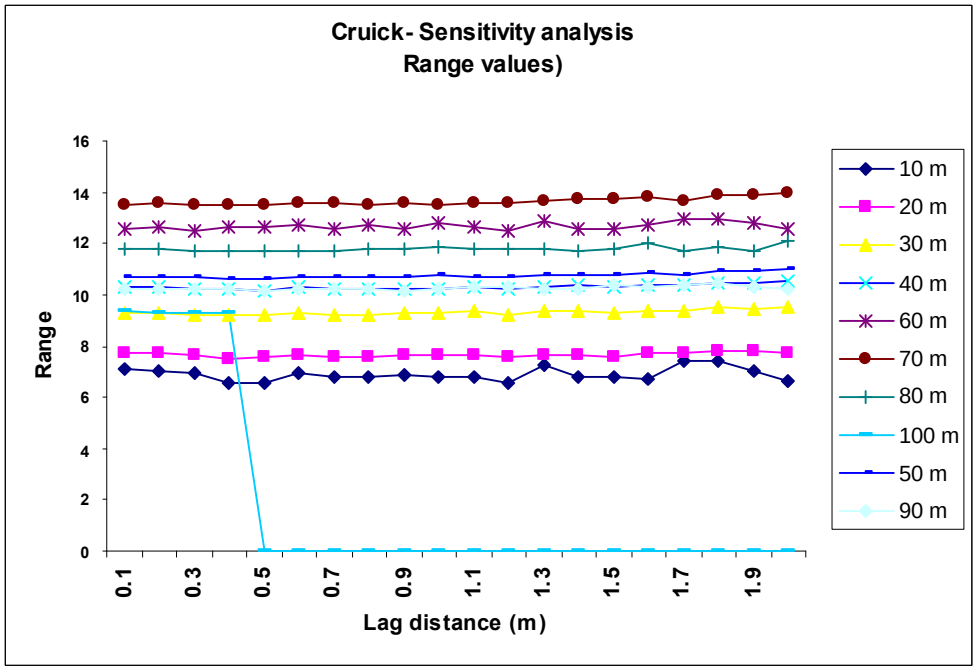
Cruick- Sensitivity analysis
Range values)
Range
Lag distance (m)
10 m
20 m
30 m
40 m
60 m
70 m
80 m
100 m
50 m
90 m

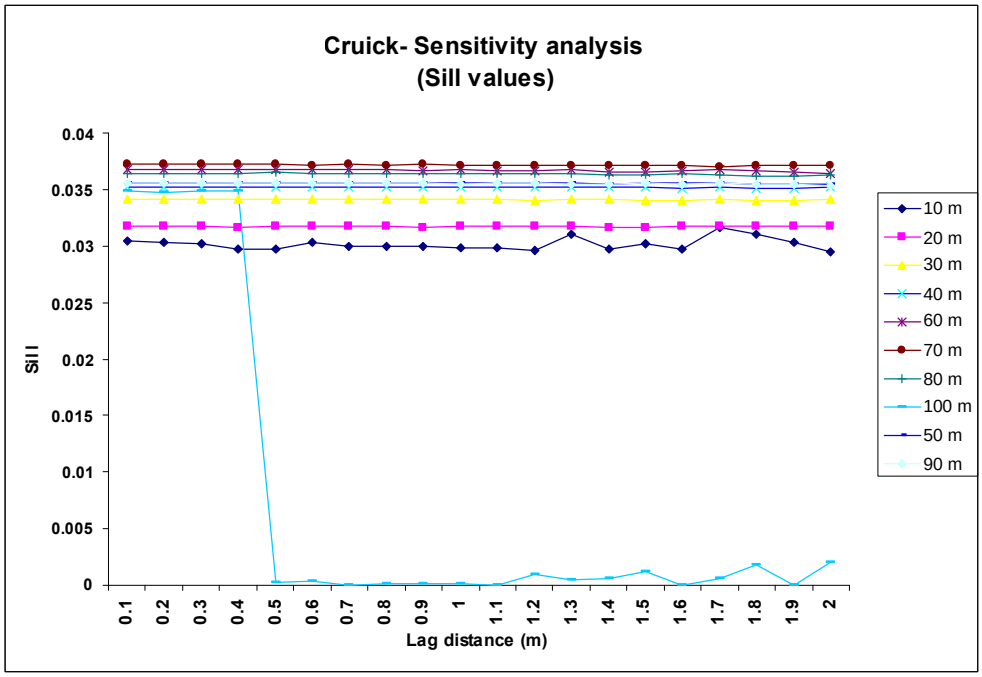
Cruick- Sensitivity analysis
(Sill values)
Sill
Lag distance (m)
10 m
20 m
30 m
40 m
60 m
70 m
80 m
100 m
50 m
90 m

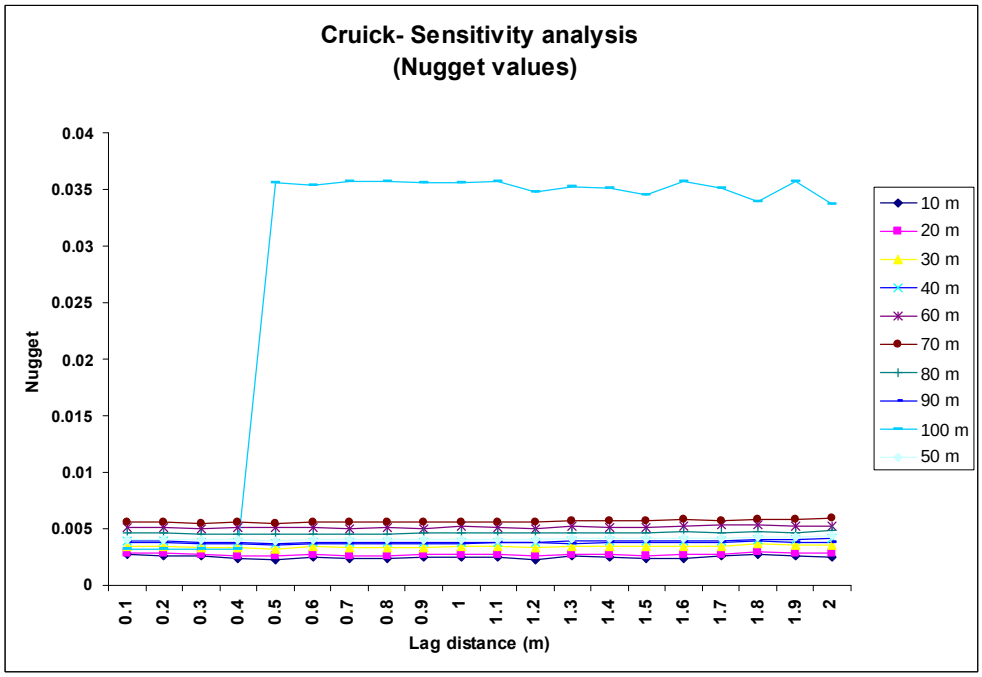
Cruick- Sensitivity analysis
(Nugget values)
Nugget
Lag distance (m)
10 m
20 m
30 m
40 m
60 m
70 m
80 m
90 m
100 m
50 m

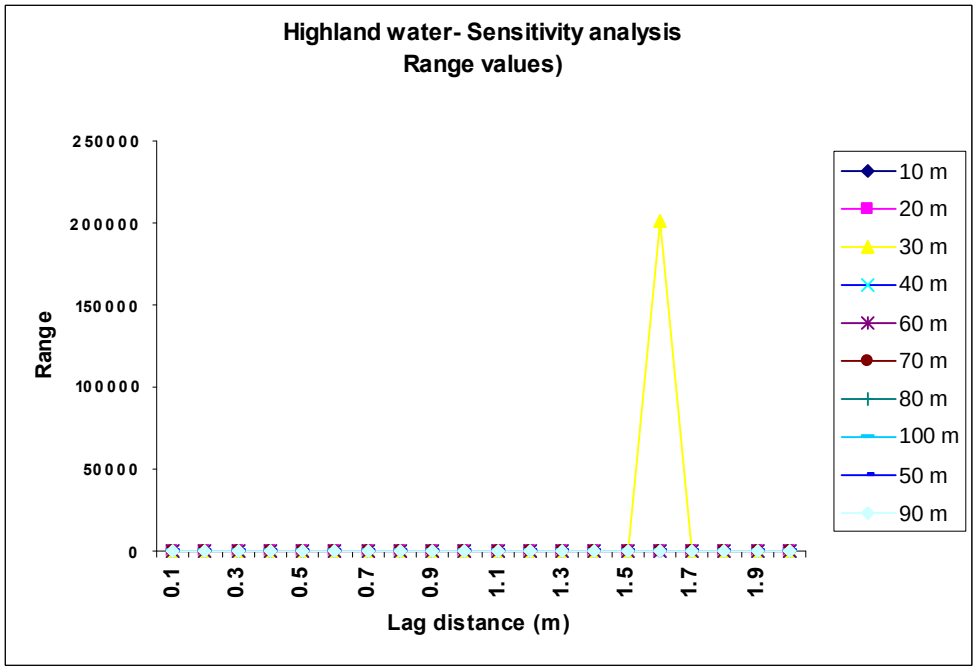
Highland water- Sensitivity analysis
Range values)
250000
200000
150000
100000
50000
0
Range
0.1
0.3
0.5
0.7
0.9
1.1
1.3
1.5
1.7
1.9
Lag distance (m)
10 m
20 m
30 m
40 m
60 m
70 m
80 m
100 m
50 m
90 m

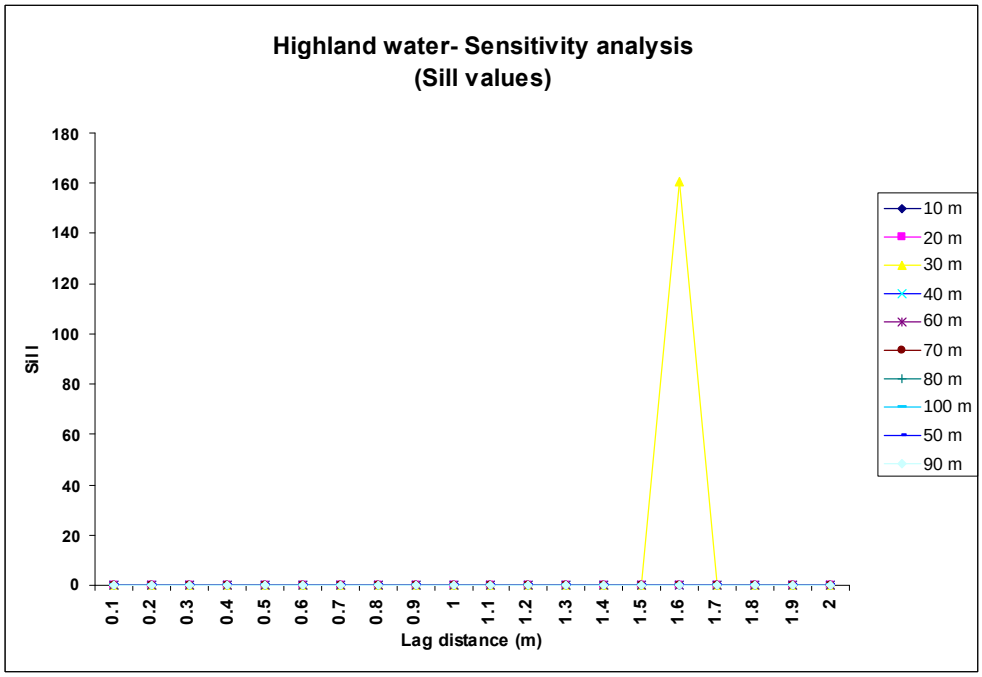
Highland water- Sensitivity analysis
(Sill values)
180
160
140
120
100
80
60
40
20
0
Sill
0.1
0.2
0.3
0.4
0.5
0.6
0.7
0.8
0.9
1
1.1
1.2
1.3
1.4
1.5
1.6
1.7
1.8
1.9
2
Lag distance (m)
10 m
20 m
30 m
40 m
60 m
70 m
80 m
100 m
50 m
90 m

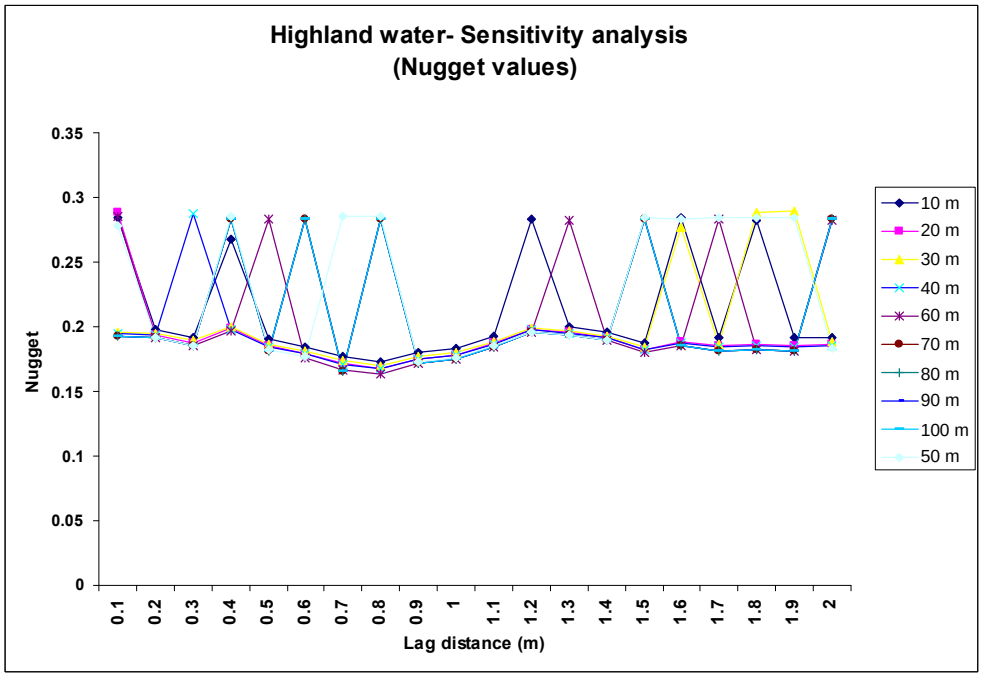
Highland water- Sensitivity analysis
(Nugget values)
0.35
0.3
0.25
0.2
0.15
0.1
0.05
0
Nugget
0.1
0.2
0.3
0.4
0.5
0.6
0.7
0.8
0.9
1
1.1
1.2
1.3
1.4
1.5
1.6
1.7
1.8
1.9
2
Lag distance (m)
10 m
20 m
30 m
40 m
60 m
70 m
80 m
90 m
100 m
50 m

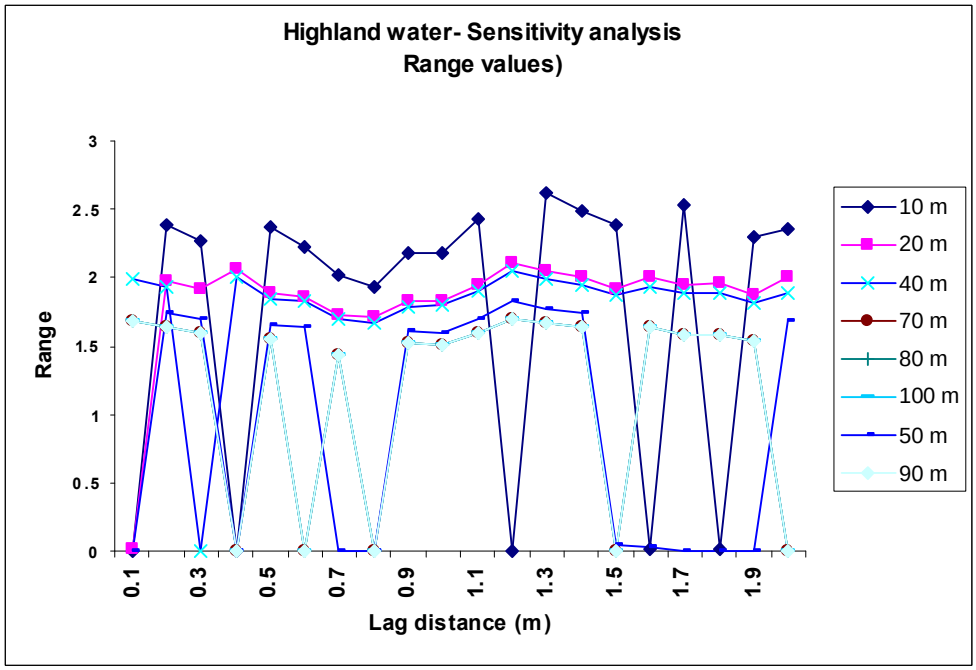
Highland water- Sensitivity analysis
Range values)
Range
Lag distance (m)
10 m
20 m
40 m
70 m
80 m
100 m
50 m
90 m

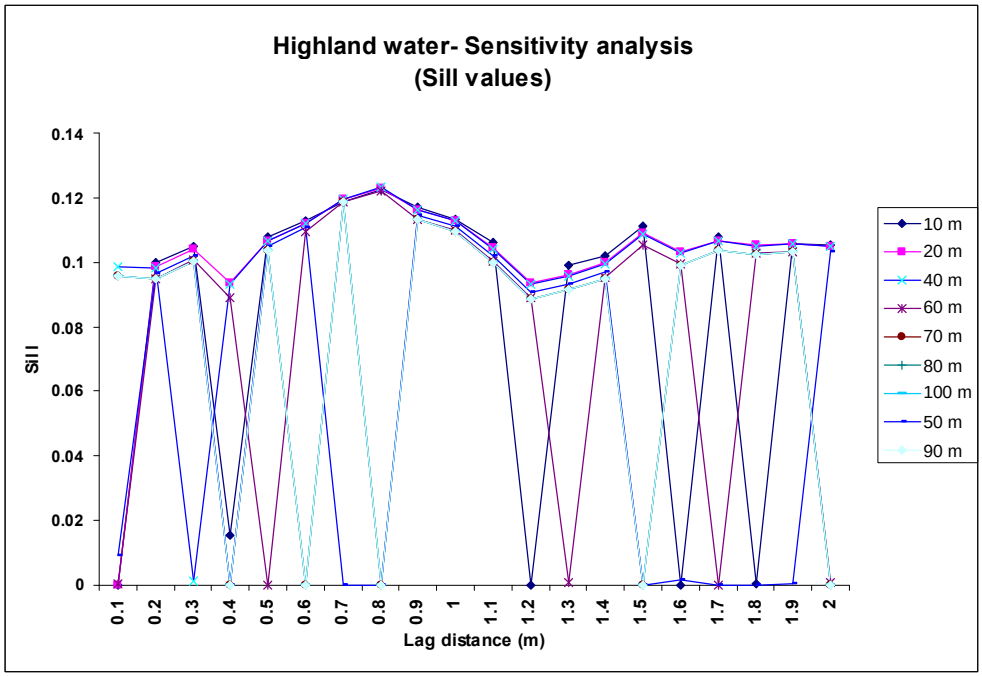
Highland water- Sensitivity analysis
(Sill values)
Sill
Lag distance (m)
10 m
20 m
40 m
60 m
70 m
80 m
100 m
50 m
90 m

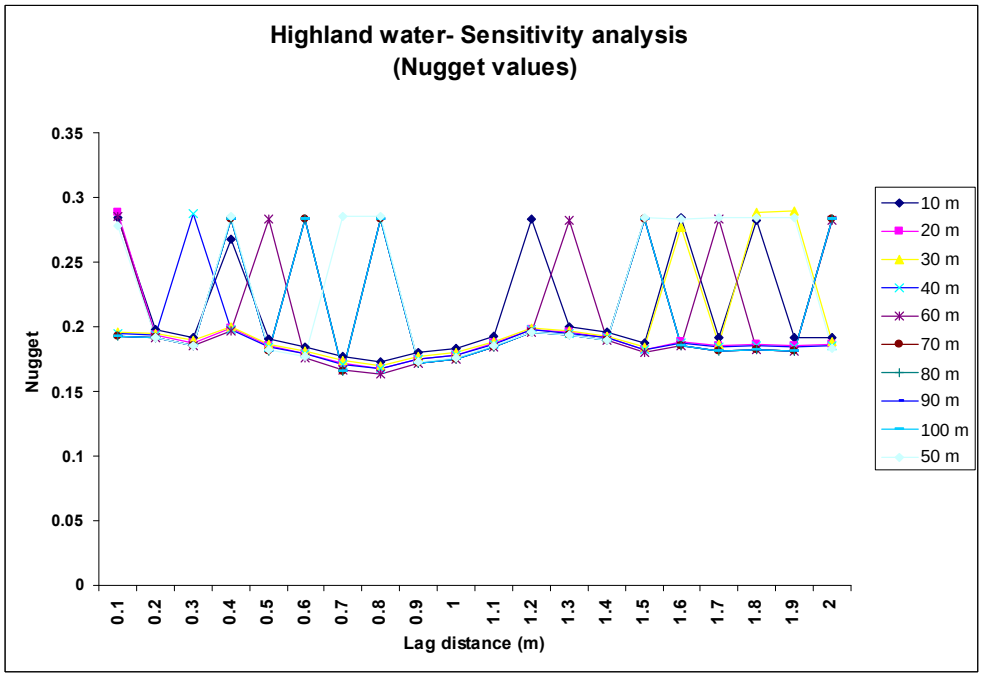
Highland water- Sensitivity analysis
(Nugget values)
Nugget
Lag distance (m)
10 m
20 m
30 m
40 m
60 m
70 m
80 m
90 m
100 m
50 m

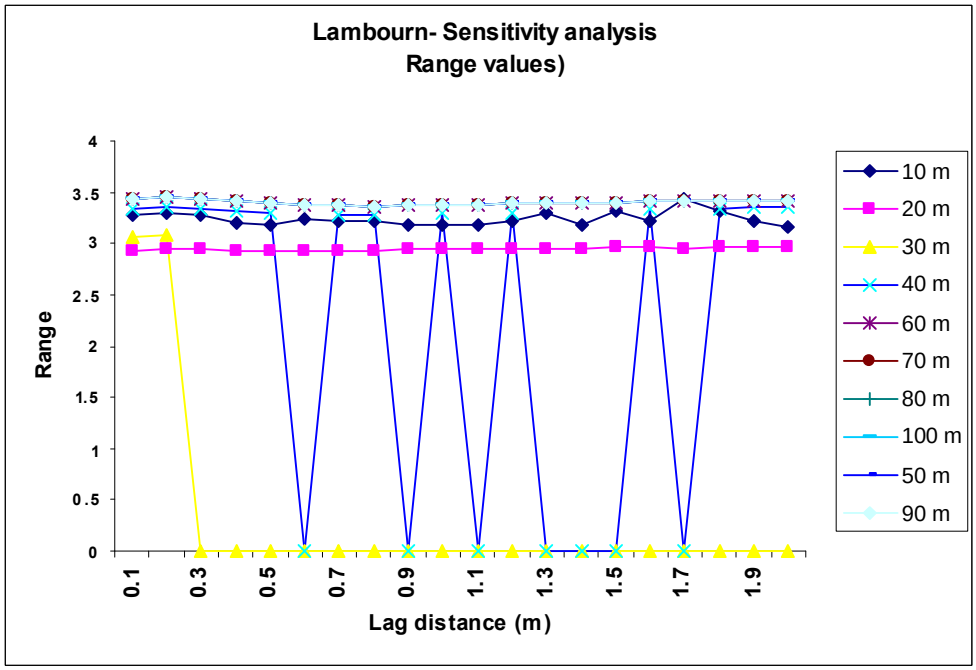
Lambourn- Sensitivity analysis
Range values)
Range
Lag distance (m)
10 m
20 m
30 m
40 m
60 m
70 m
80 m
100 m
50 m
90 m

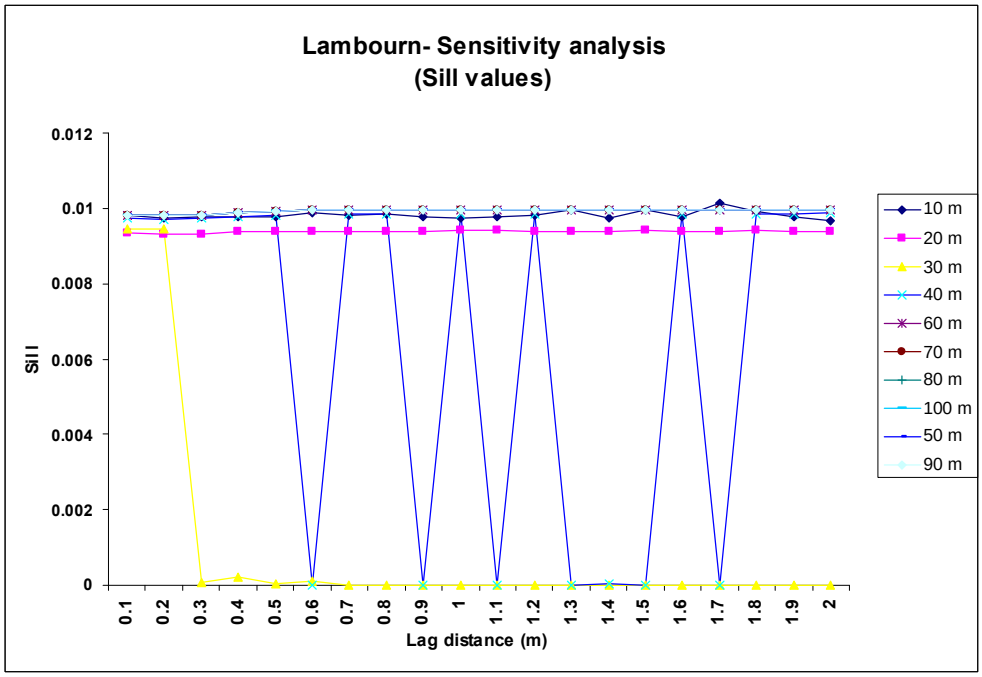
Lambourn- Sensitivity analysis
(Sill values)
Sill
Lag distance (m)
10 m
20 m
30 m
40 m
60 m
70 m
80 m
100 m
50 m
90 m

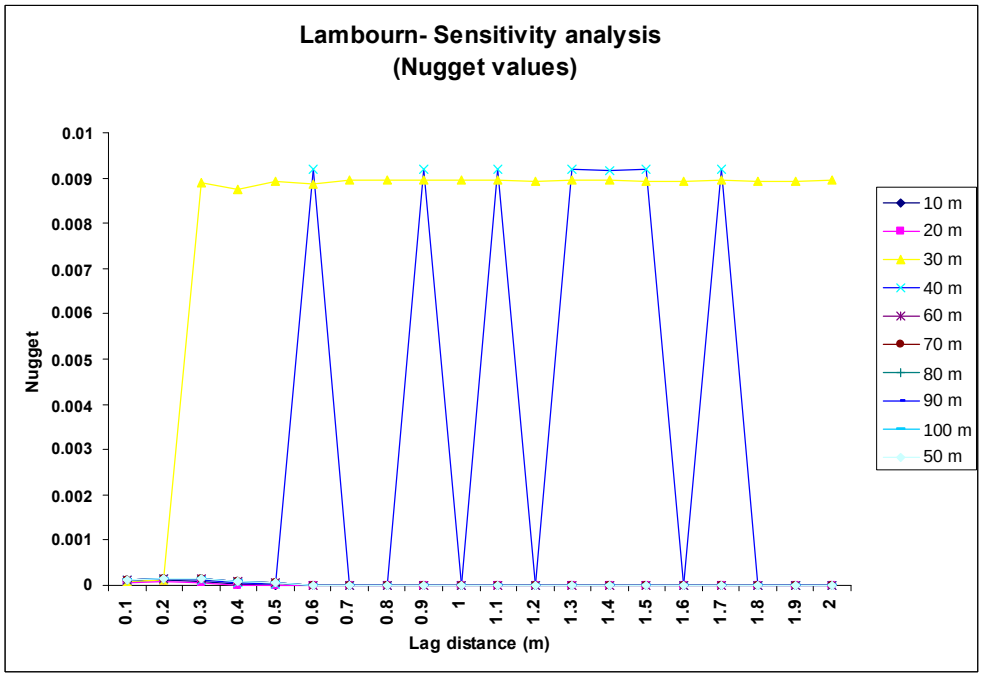
Lambourn- Sensitivity analysis
(Nugget values)
Nugget
Lag distance (m)
10 m
20 m
30 m
40 m
60 m
70 m
80 m
90 m
100 m
50 m

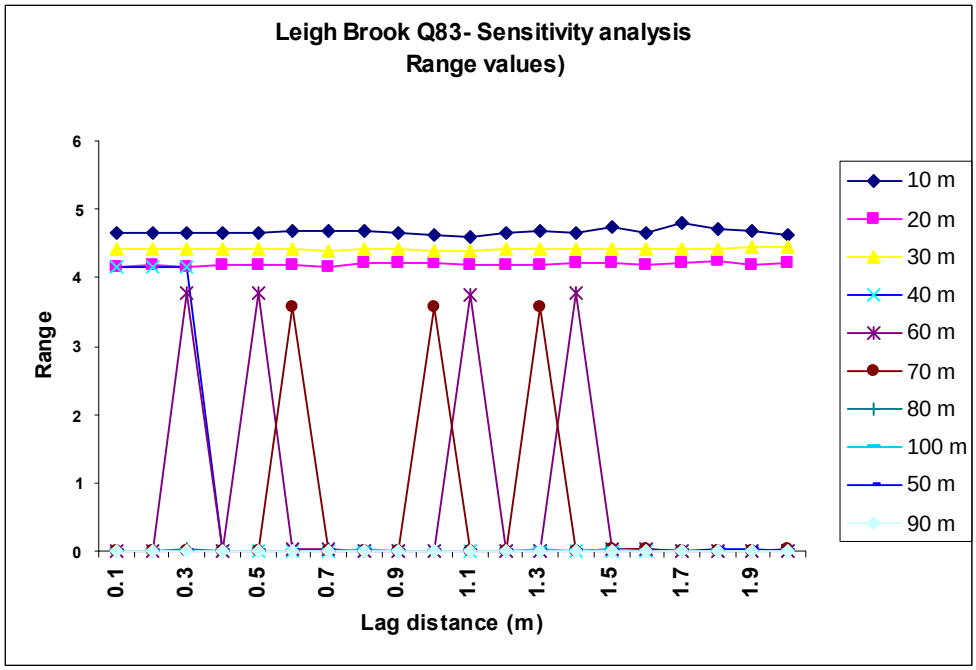
Leigh Brook Q83- Sensitivity analysis
Range values)
Range
Lag distance (m)
10 m
20 m
30 m
40 m
60 m
70 m
80 m
100 m
50 m
90 m

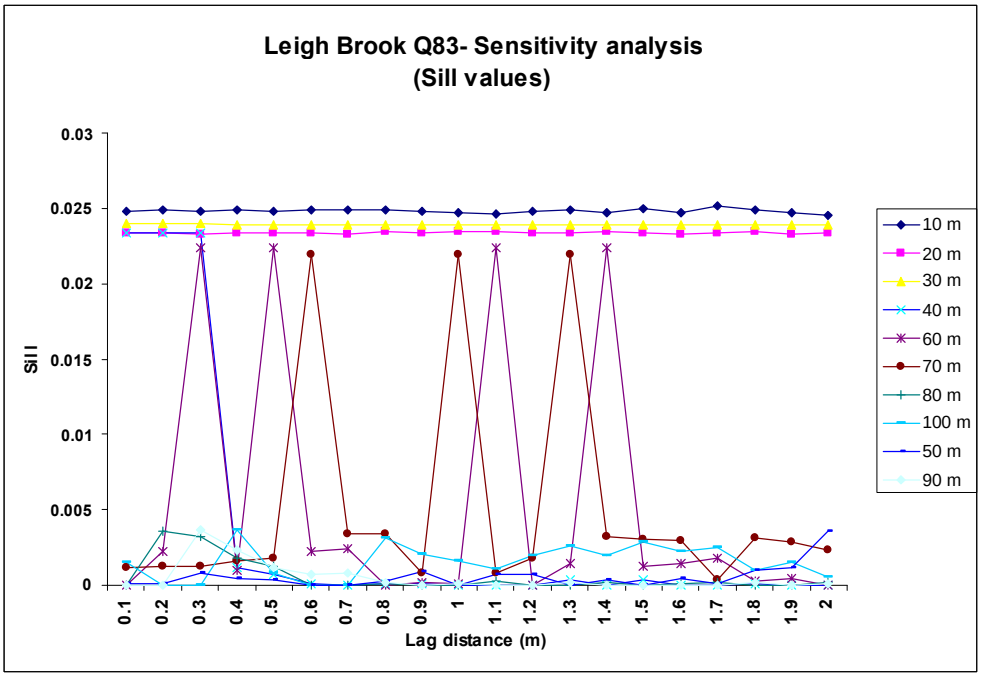
Leigh Brook Q83- Sensitivity analysis
(Sill values)
Sill
Lag distance (m)
10 m
20 m
30 m
40 m
60 m
70 m
80 m
100 m
50 m
90 m

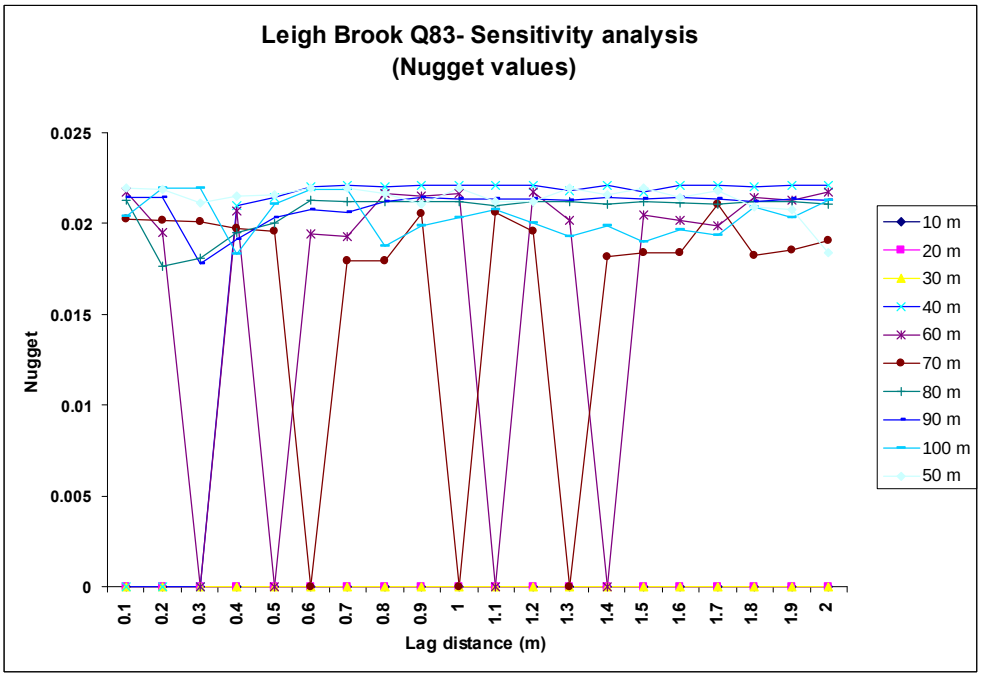
Leigh Brook Q83- Sensitivity analysis
(Nugget values)
Nugget
Lag distance (m)
10 m
20 m
30 m
40 m
60 m
70 m
80 m
90 m
100 m
50 m

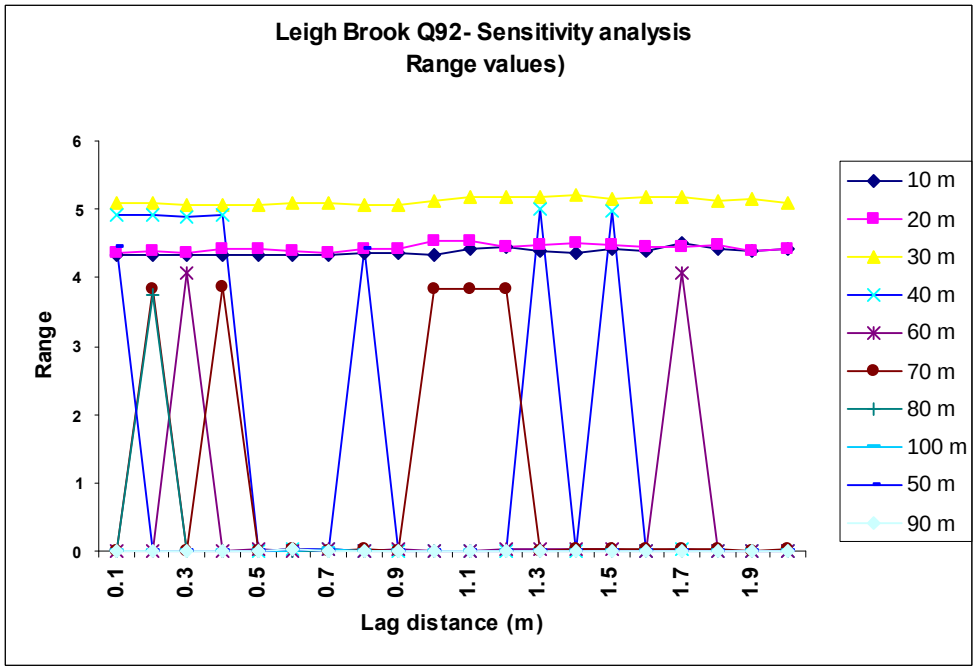
Leigh Brook Q92- Sensitivity analysis
Range values)
Range
Lag distance (m)
10 m
20 m
30 m
40 m
60 m
70 m
80 m
100 m
50 m
90 m

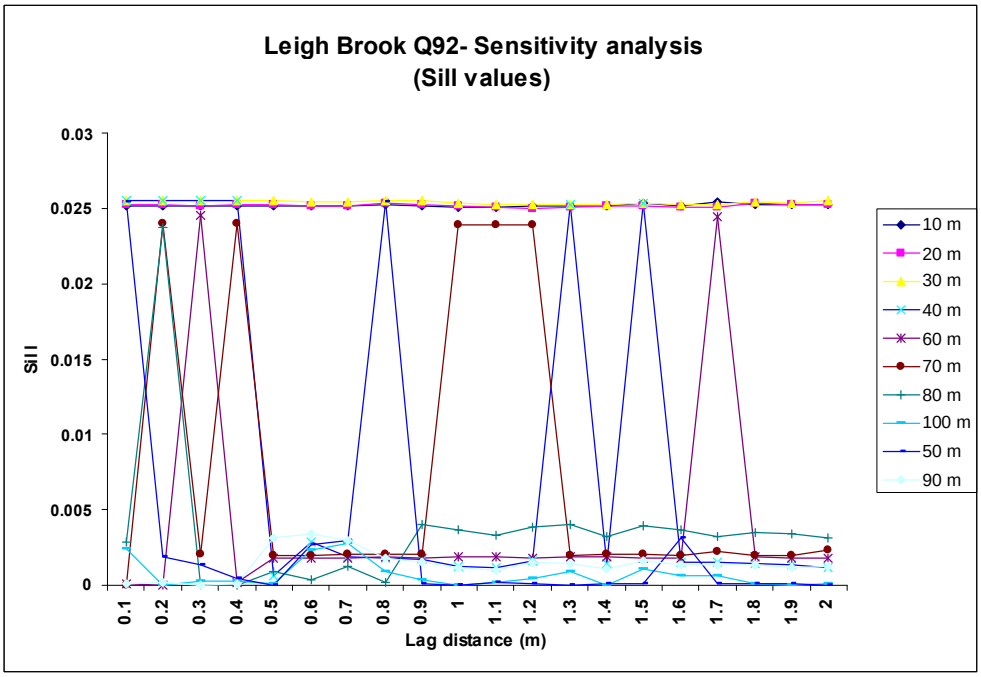
Leigh Brook Q92- Sensitivity analysis
(Sill values)
Sill
Lag distance (m)
10 m
20 m
30 m
40 m
60 m
70 m
80 m
100 m
50 m
90 m

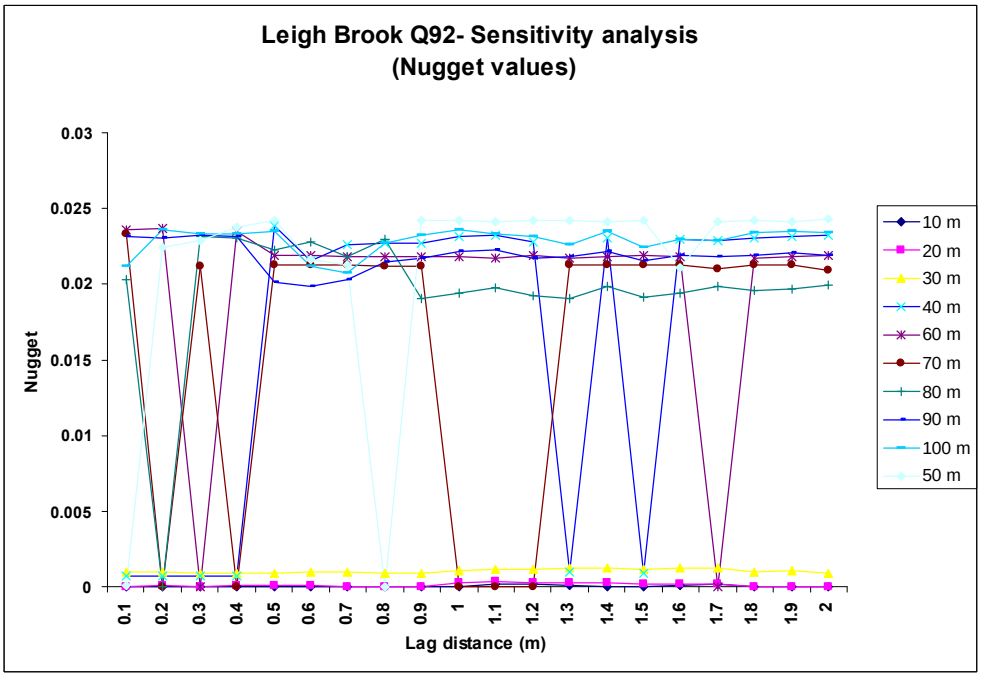
Leigh Brook Q92- Sensitivity analysis
(Nugget values)
Nugget
Lag distance (m)
10 m
20 m
30 m
40 m
60 m
70 m
80 m
90 m
100 m
50 m

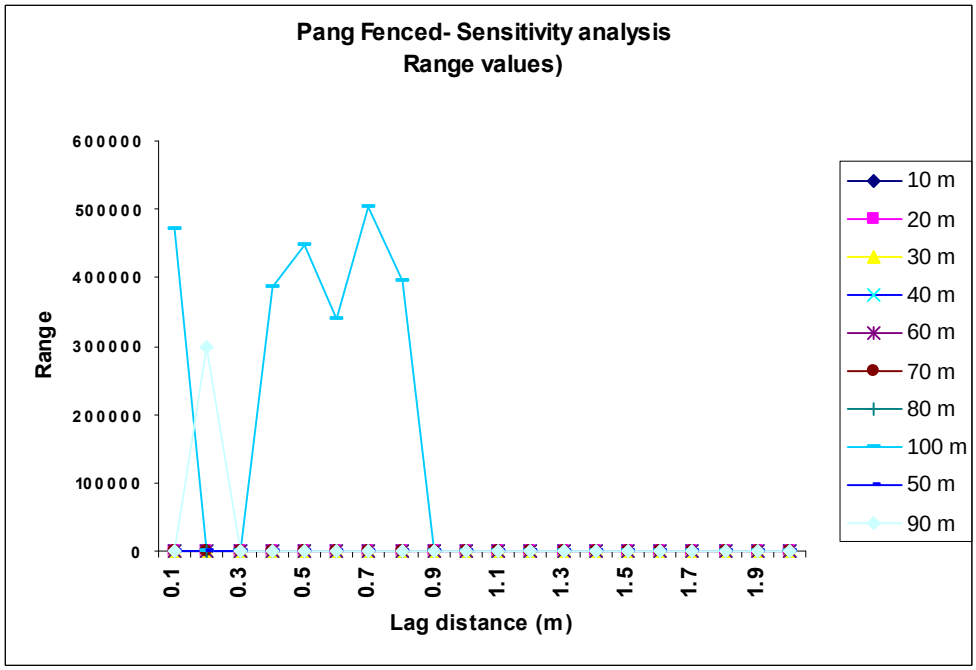
Pang Fenced- Sensitivity analysis
Range values)
Range
600000
500000
400000
300000
200000
100000
0
0.1
0.3
0.5
0.7
0.9
1.1
1.3
1.5
1.7
1.9
Lag distance (m)
10 m
20 m
30 m
40 m
60 m
70 m
80 m
100 m
50 m
90 m

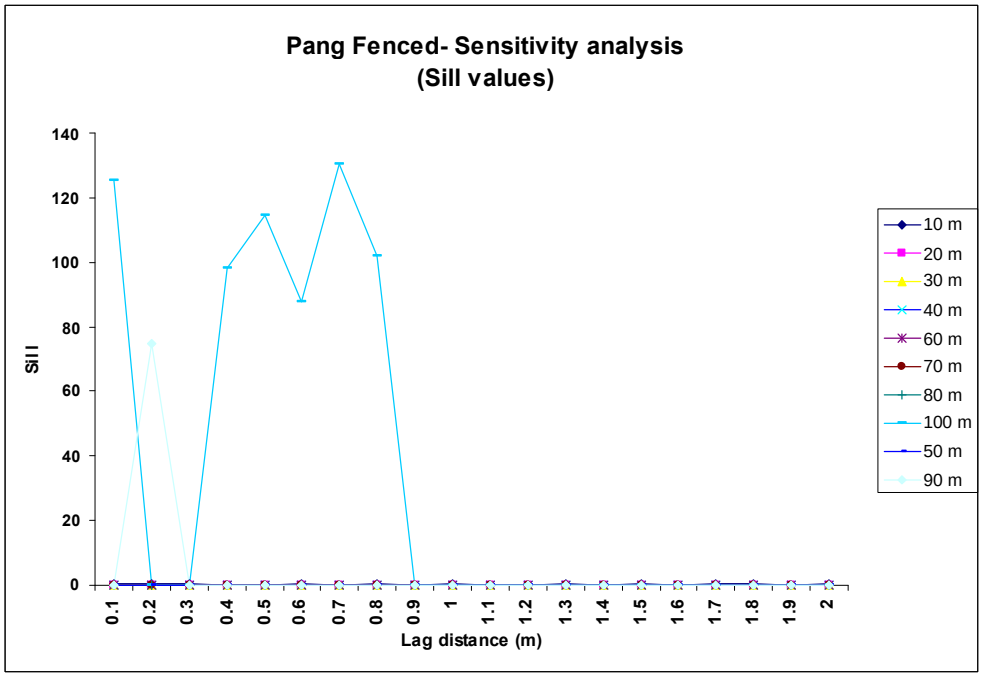
Pang Fenced- Sensitivity analysis
(Sill values)
Sill
140
120
100
80
60
40
20
0
0.1
0.2
0.3
0.4
0.5
0.6
0.7
0.8
0.9
1
1.1
1.2
1.3
1.4
1.5
1.6
1.7
1.8
1.9
2
Lag distance (m)
10 m
20 m
30 m
40 m
60 m
70 m
80 m
100 m
50 m
90 m

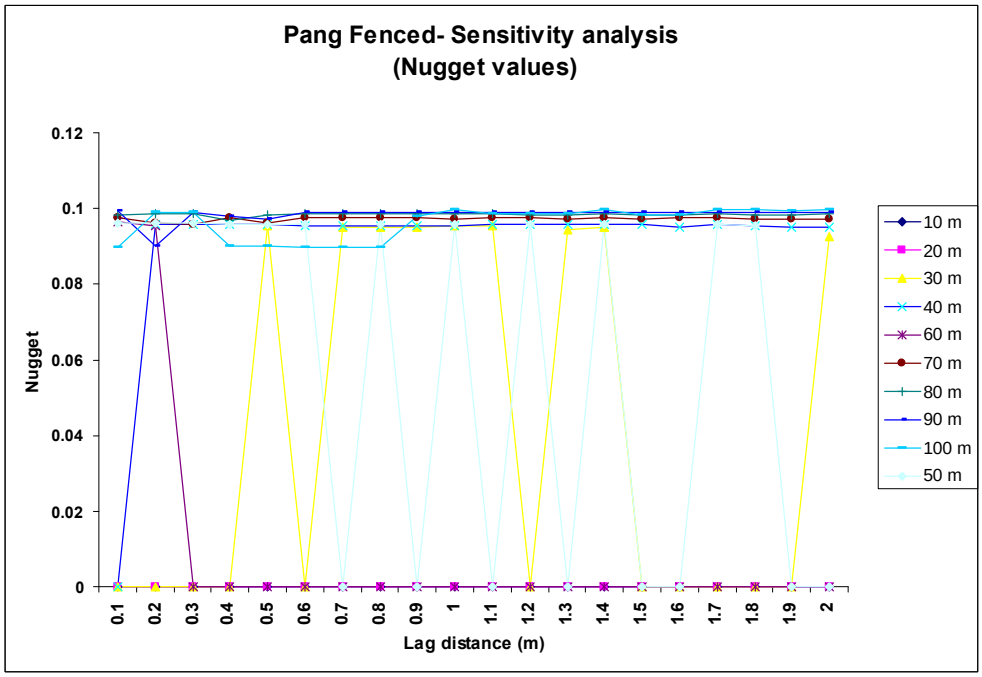
Pang Fenced- Sensitivity analysis
(Nugget values)
Nugget
0.12
0.1
0.08
0.06
0.04
0.02
0
0.1
0.2
0.3
0.4
0.5
0.6
0.7
0.8
0.9
1
1.1
1.2
1.3
1.4
1.5
1.6
1.7
1.8
1.9
2
Lag distance (m)
10 m
20 m
30 m
40 m
60 m
70 m
80 m
90 m
100 m
50 m

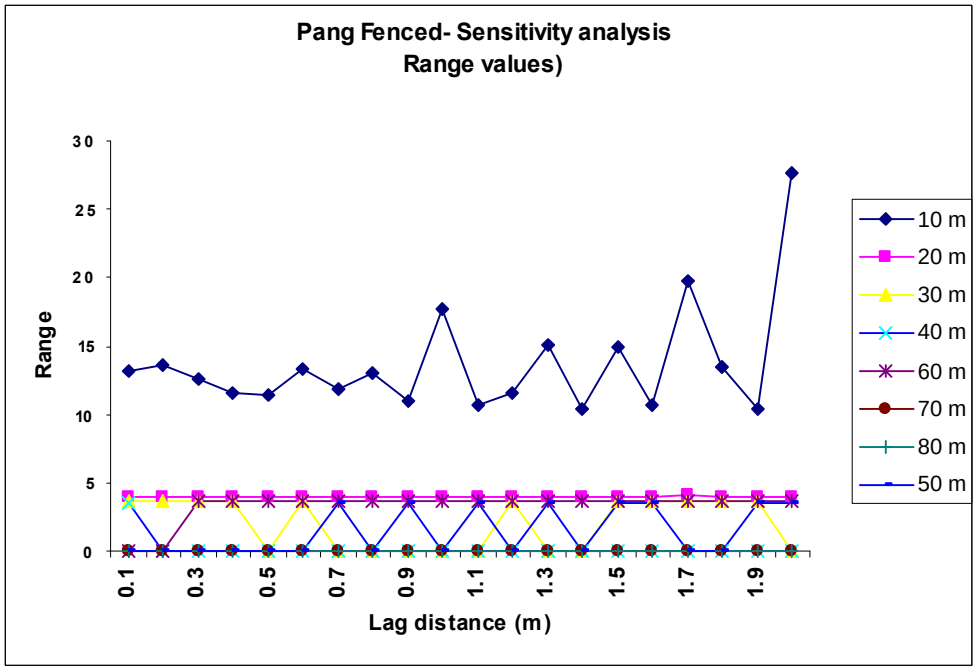
Pang Fenced- Sensitivity analysis
Range values)
Range
Lag distance (m)
10 m
20 m
30 m
40 m
60 m
70 m
80 m
50 m

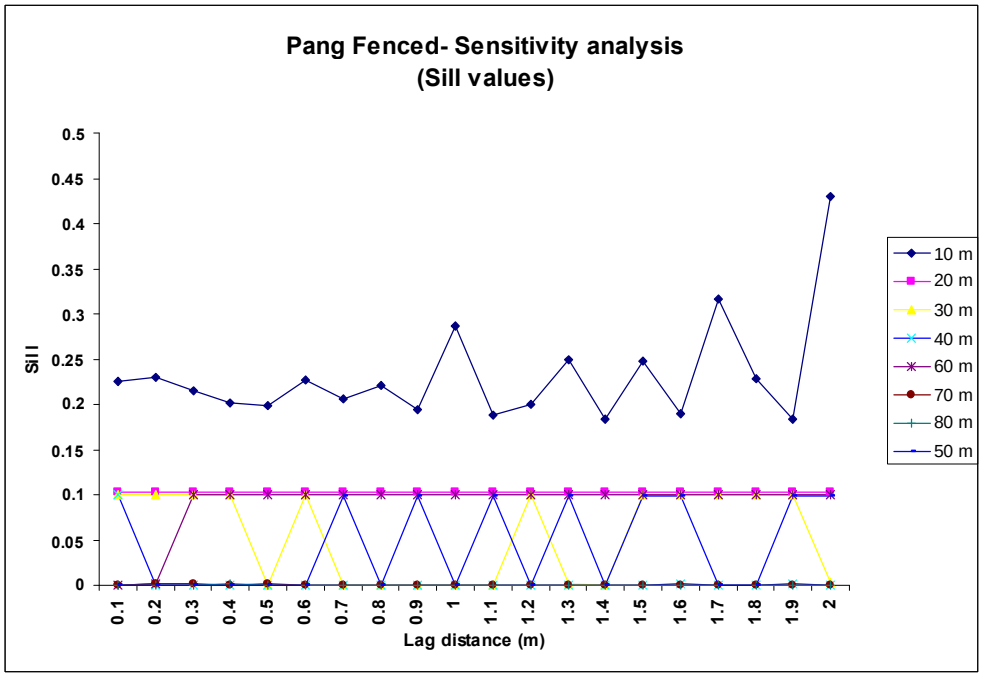
Pang Fenced- Sensitivity analysis
(Sill values)
Sill
Lag distance (m)
10 m
20 m
30 m
40 m
60 m
70 m
80 m
50 m

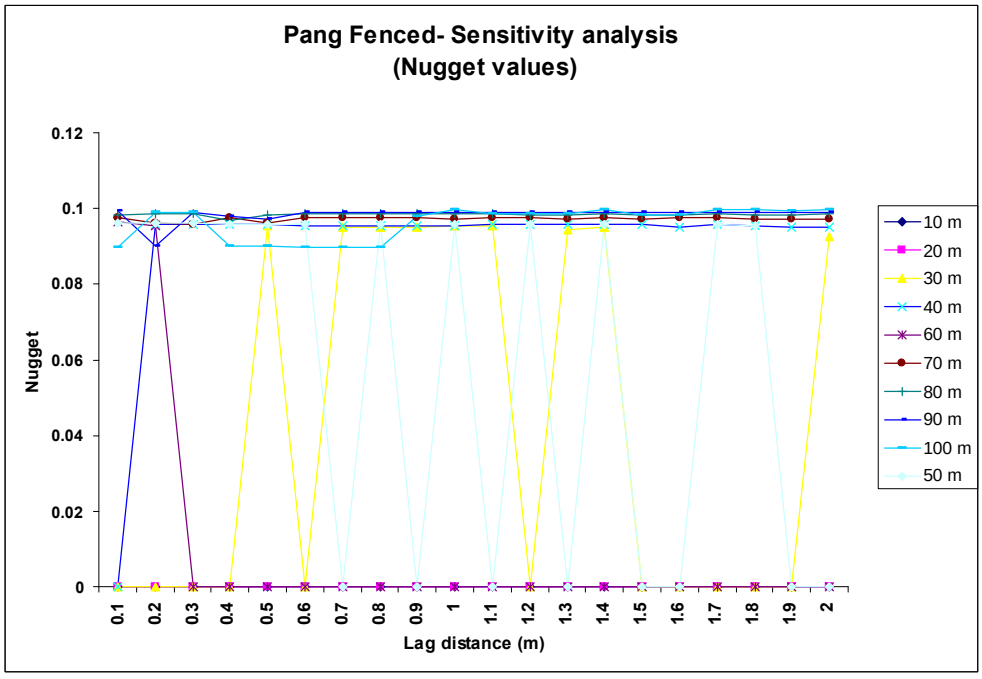
Pang Fenced- Sensitivity analysis
(Nugget values)
Nugget
Lag distance (m)
10 m
20 m
30 m
40 m
60 m
70 m
80 m
90 m
100 m
50 m

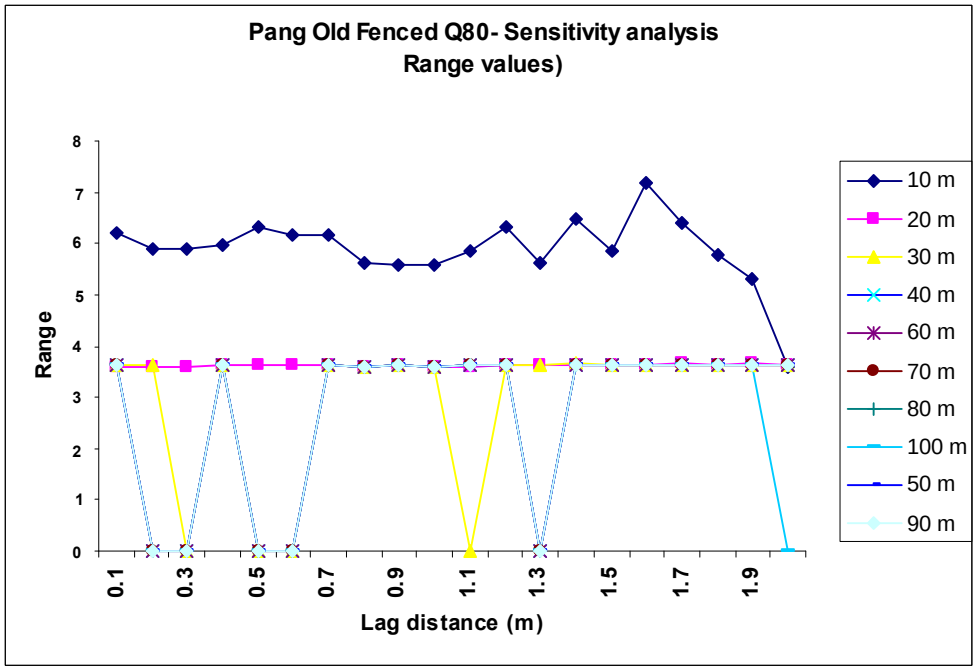
Pang Old Fenced Q80- Sensitivity analysis
Range values)
Range
Lag distance (m)
10 m
20 m
30 m
40 m
60 m
70 m
80 m
100 m
50 m
90 m

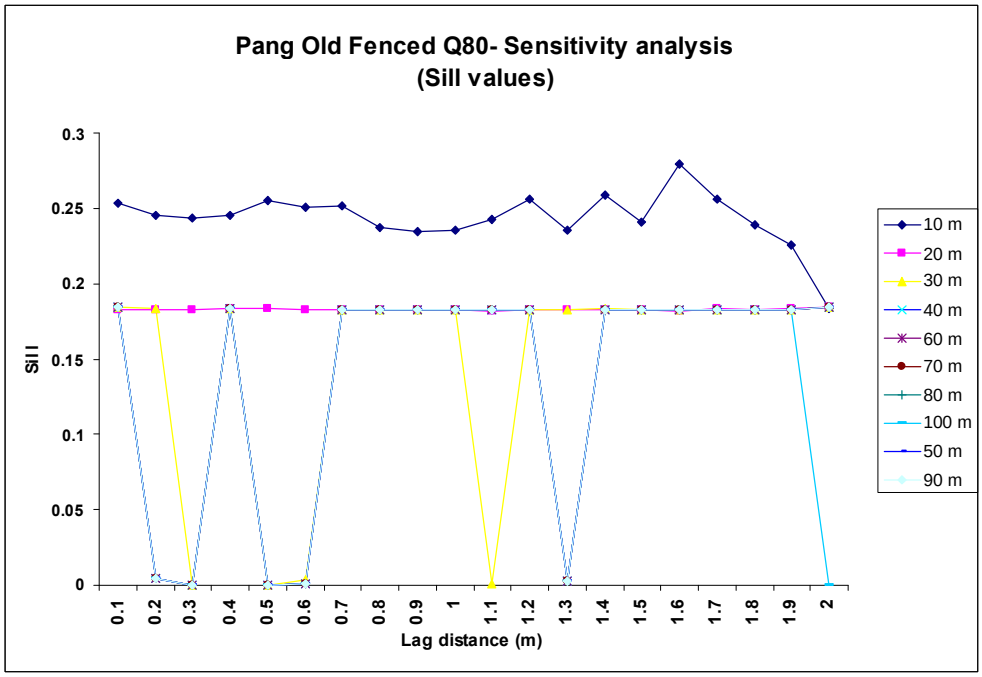
Pang Old Fenced Q80- Sensitivity analysis
(Sill values)
Sill
Lag distance (m)
10 m
20 m
30 m
40 m
60 m
70 m
80 m
100 m
50 m
90 m

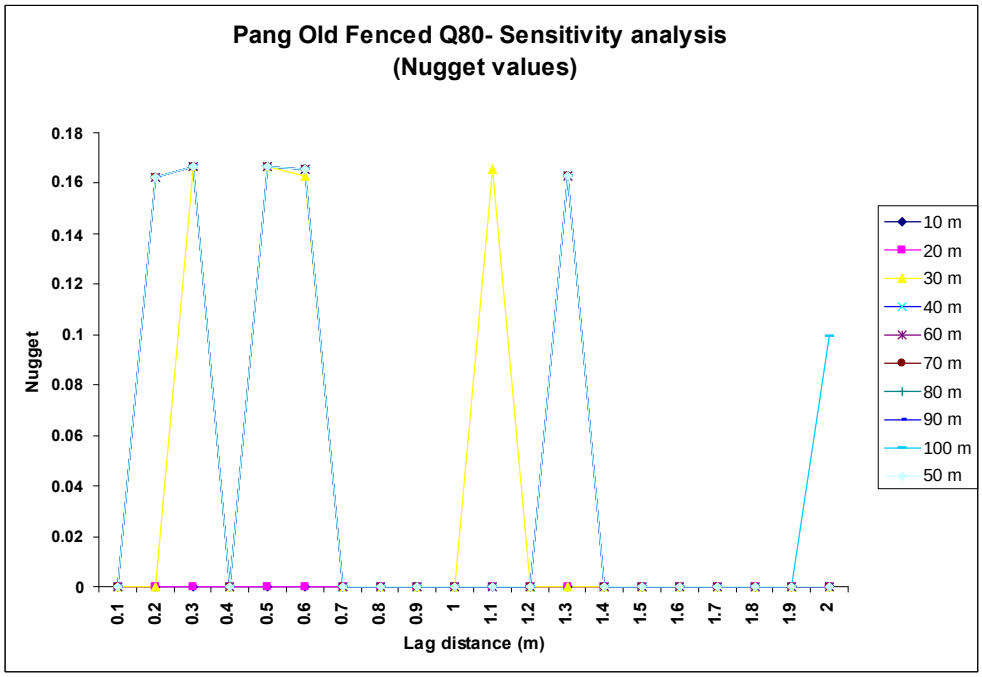
Pang Old Fenced Q80- Sensitivity analysis
(Nugget values)
Nugget
Lag distance (m)
10 m
20 m
30 m
40 m
60 m
70 m
80 m
90 m
100 m
50 m

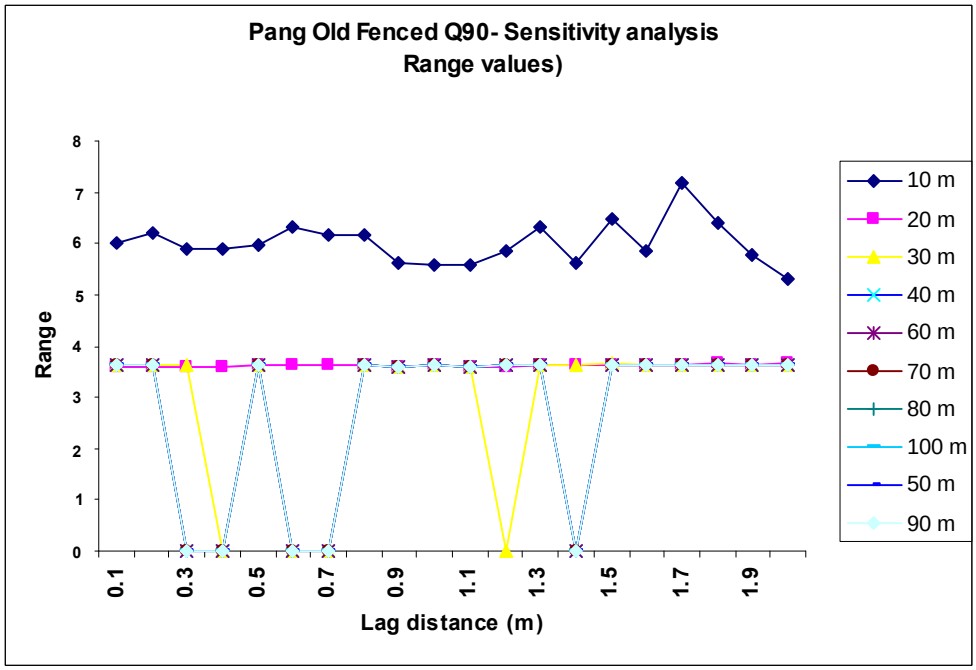
Pang Old Fenced Q90- Sensitivity analysis
Range values)
Range
Lag distance (m)
10 m
20 m
30 m
40 m
60 m
70 m
80 m
100 m
50 m
90 m

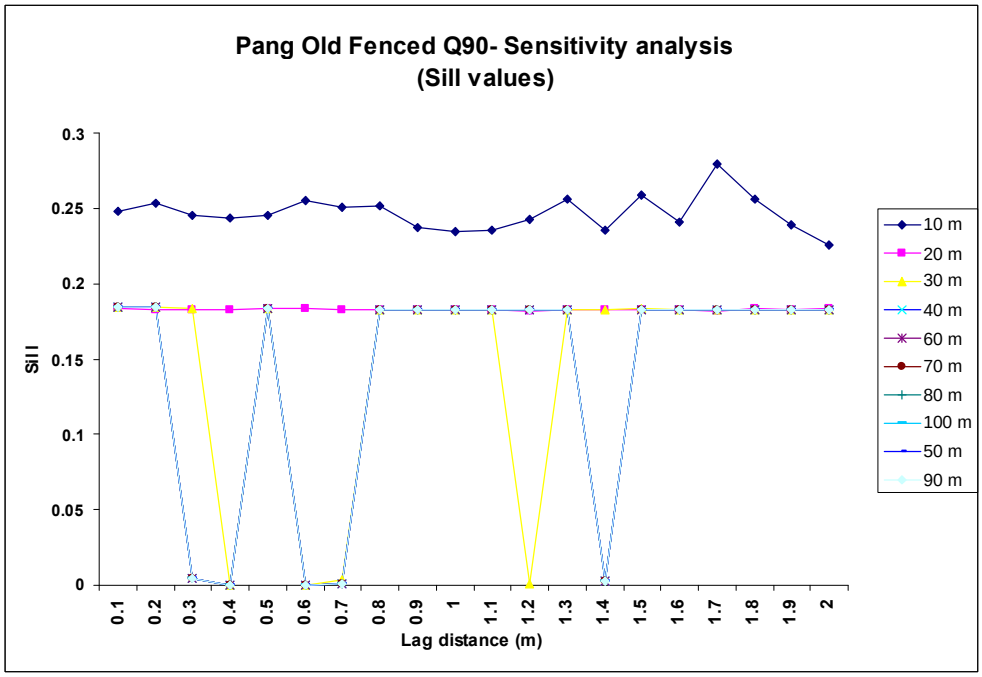
Pang Old Fenced Q90- Sensitivity analysis
(Sill values)
Sill
Lag distance (m)
10 m
20 m
30 m
40 m
60 m
70 m
80 m
100 m
50 m
90 m

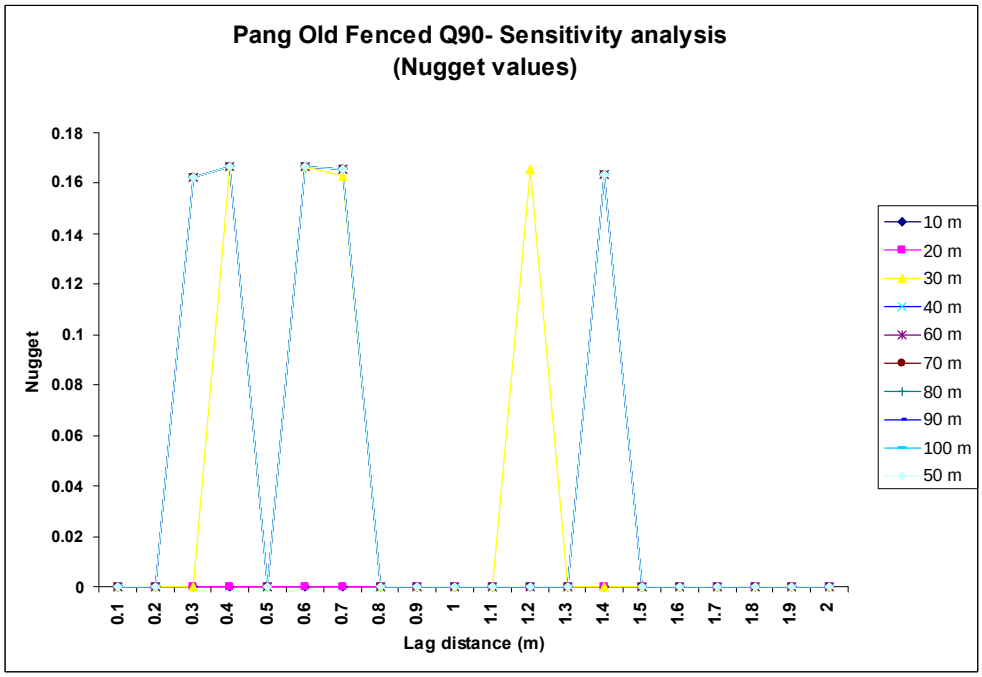
Pang Old Fenced Q90- Sensitivity analysis
(Nugget values)
Nugget
Lag distance (m)
10 m
20 m
30 m
40 m
60 m
70 m
80 m
90 m
100 m
50 m

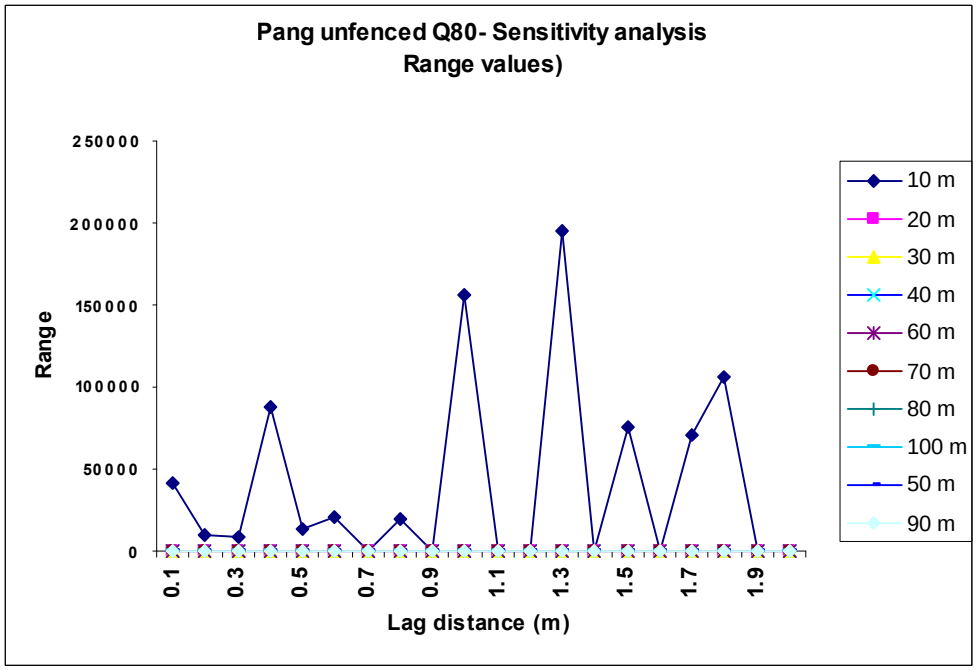
Pang unfenced Q80- Sensitivity analysis
Range values)
Range
250000
200000
150000
100000
50000
0
0.1
0.3
0.5
0.7
0.9
1.1
1.3
1.5
1.7
1.9
Lag distance (m)
10 m
20 m
30 m
40 m
60 m
70 m
80 m
100 m
50 m
90 m

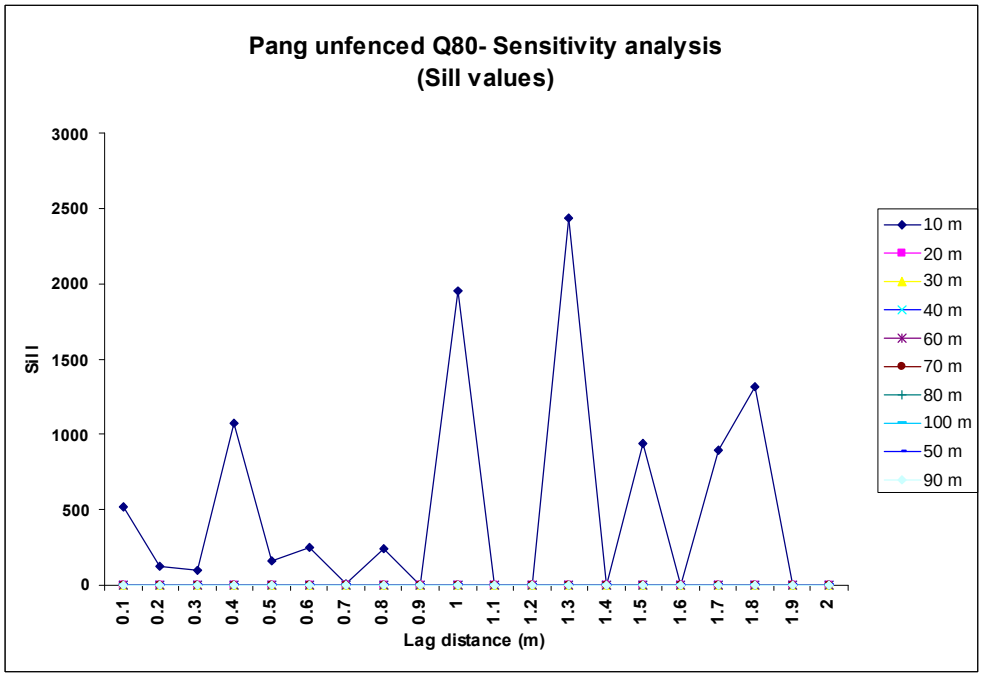
Pang unfenced Q80- Sensitivity analysis
(Sill values)
Sill
3000
2500
2000
1500
1000
500
0
0.1
0.2
0.3
0.4
0.5
0.6
0.7
0.8
0.9
1
1.1
1.2
1.3
1.4
1.5
1.6
1.7
1.8
1.9
2
Lag distance (m)
10 m
20 m
30 m
40 m
60 m
70 m
80 m
100 m
50 m
90 m

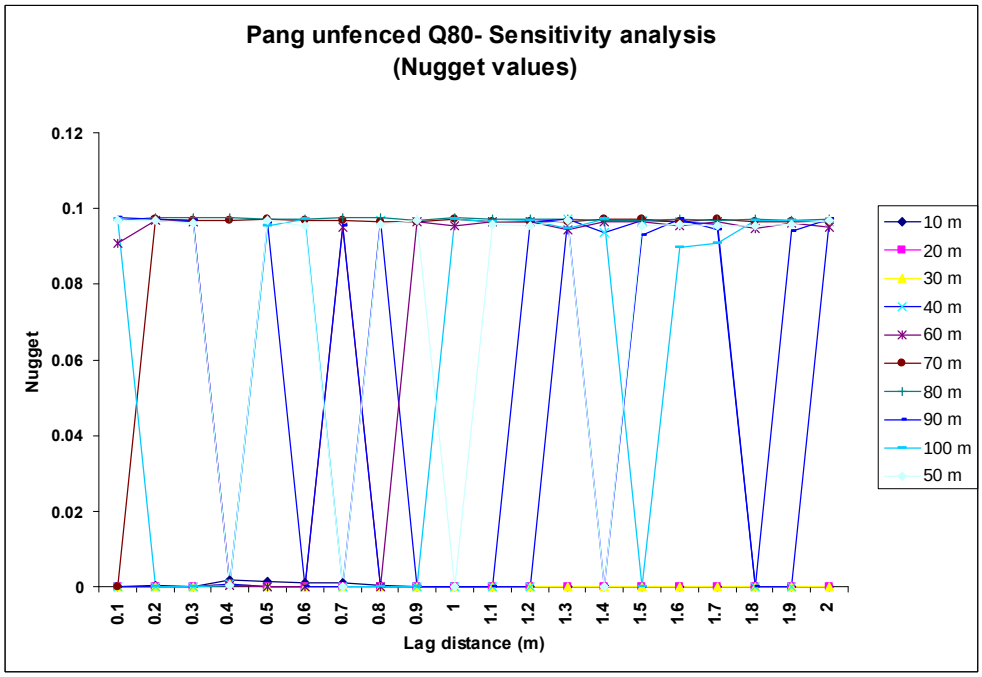
Pang unfenced Q80- Sensitivity analysis
(Nugget values)
Nugget
0.12
0.1
0.08
0.06
0.04
0.02
0
0.1
0.2
0.3
0.4
0.5
0.6
0.7
0.8
0.9
1
1.1
1.2
1.3
1.4
1.5
1.6
1.7
1.8
1.9
2
Lag distance (m)
10 m
20 m
30 m
40 m
60 m
70 m
80 m
90 m
100 m
50 m

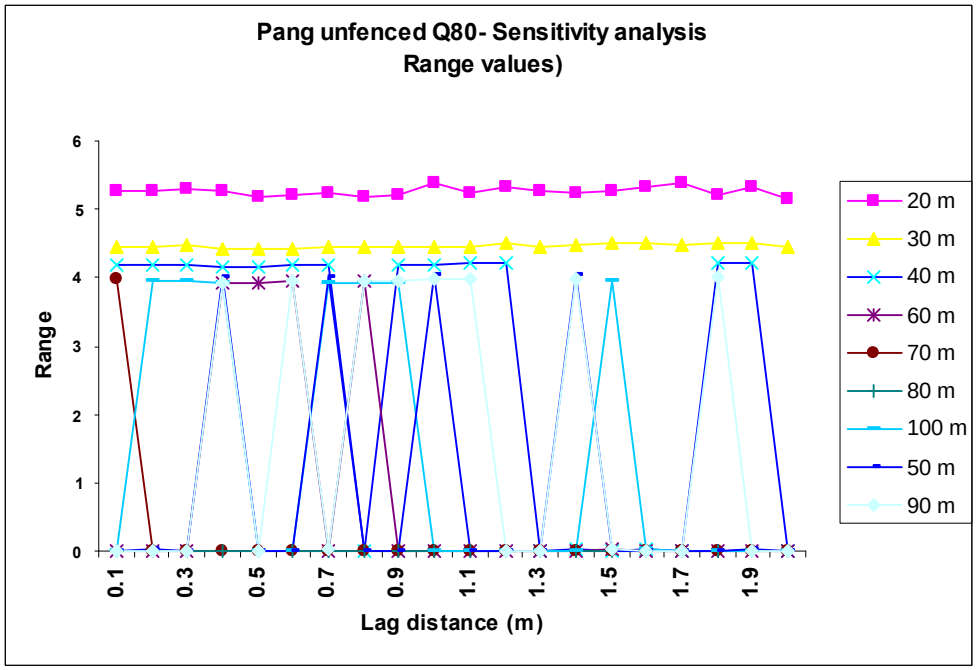
Pang unfenced Q80- Sensitivity analysis
Range values)
Range
Lag distance (m)
20 m
30 m
40 m
60 m
70 m
80 m
100 m
50 m
90 m

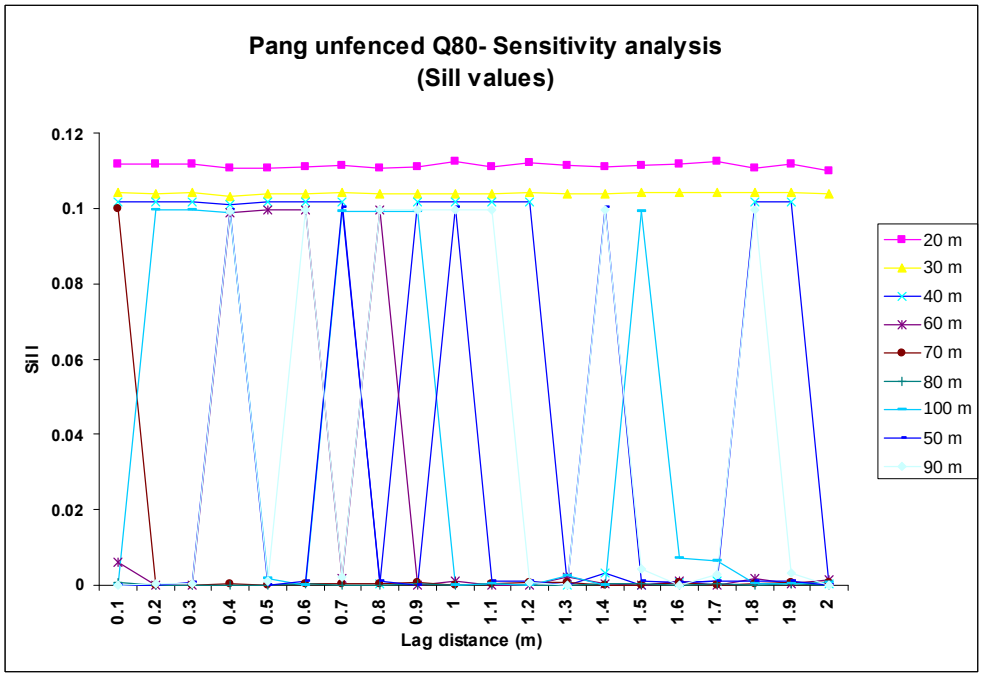
Pang unfenced Q80- Sensitivity analysis
(Sill values)
Sill
Lag distance (m)
20 m
30 m
40 m
60 m
70 m
80 m
100 m
50 m
90 m

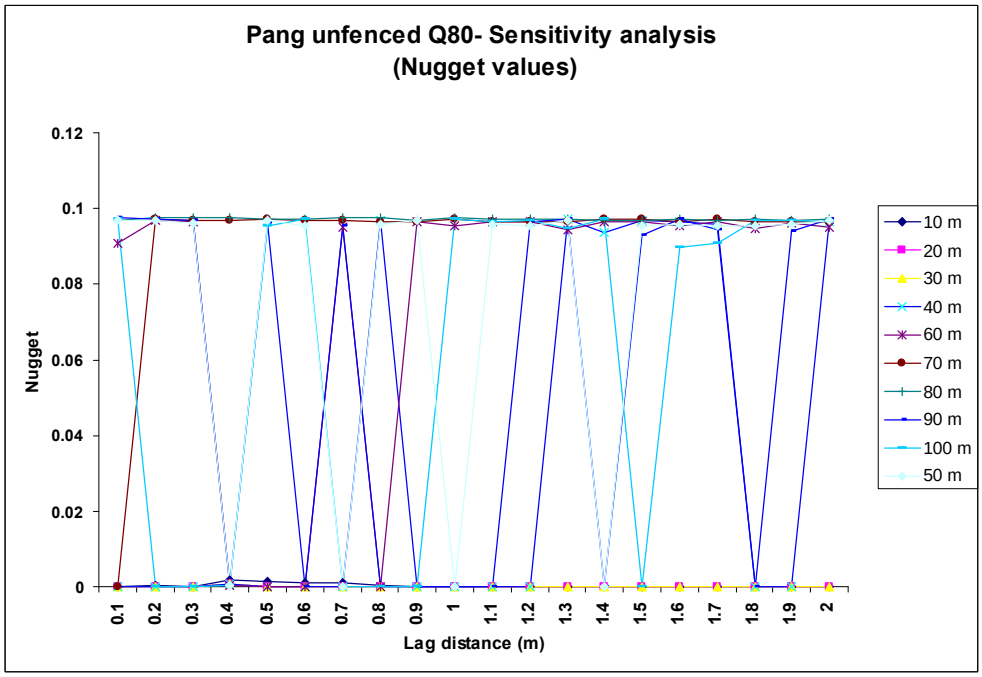
Pang unfenced Q80- Sensitivity analysis
(Nugget values)
Nugget
Lag distance (m)
10 m
20 m
30 m
40 m
60 m
70 m
80 m
90 m
100 m
50 m

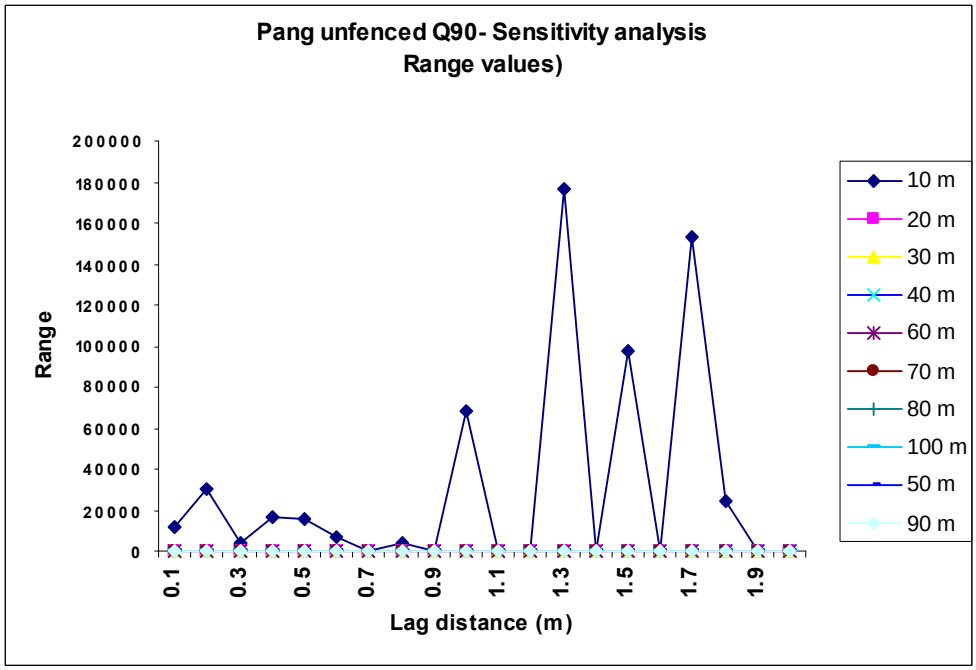
Pang unfenced Q90- Sensitivity analysis
Range values)
Range
200000
180000
160000
140000
120000
100000
80000
60000
40000
20000
0
0.1
0.3
0.5
0.7
0.9
1.1
1.3
1.5
1.7
1.9
Lag distance (m)
10 m
20 m
30 m
40 m
60 m
70 m
80 m
100 m
50 m
90 m

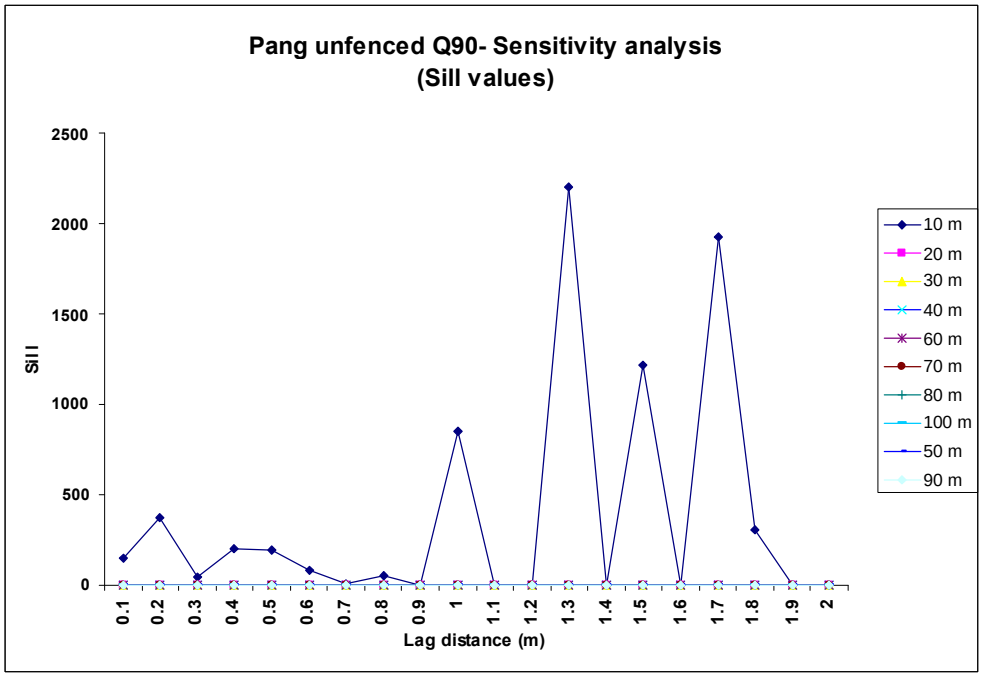
Pang unfenced Q90- Sensitivity analysis
(Sill values)
Sill
2500
2000
1500
1000
500
0
0.1
0.2
0.3
0.4
0.5
0.6
0.7
0.8
0.9
1
1.1
1.2
1.3
1.4
1.5
1.6
1.7
1.8
1.9
2
Lag distance (m)
10 m
20 m
30 m
40 m
60 m
70 m
80 m
100 m
50 m
90 m

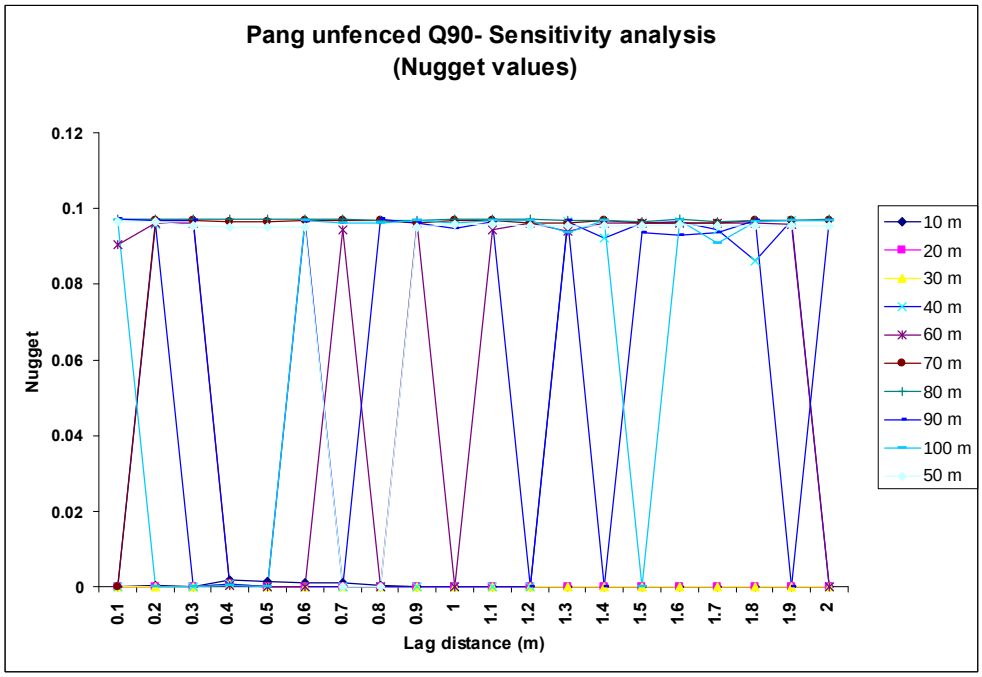
Pang unfenced Q90- Sensitivity analysis
(Nugget values)
Nugget
0.12
0.1
0.08
0.06
0.04
0.02
0
0.1
0.2
0.3
0.4
0.5
0.6
0.7
0.8
0.9
1
1.1
1.2
1.3
1.4
1.5
1.6
1.7
1.8
1.9
2
Lag distance (m)
10 m
20 m
30 m
40 m
60 m
70 m
80 m
90 m
100 m
50 m

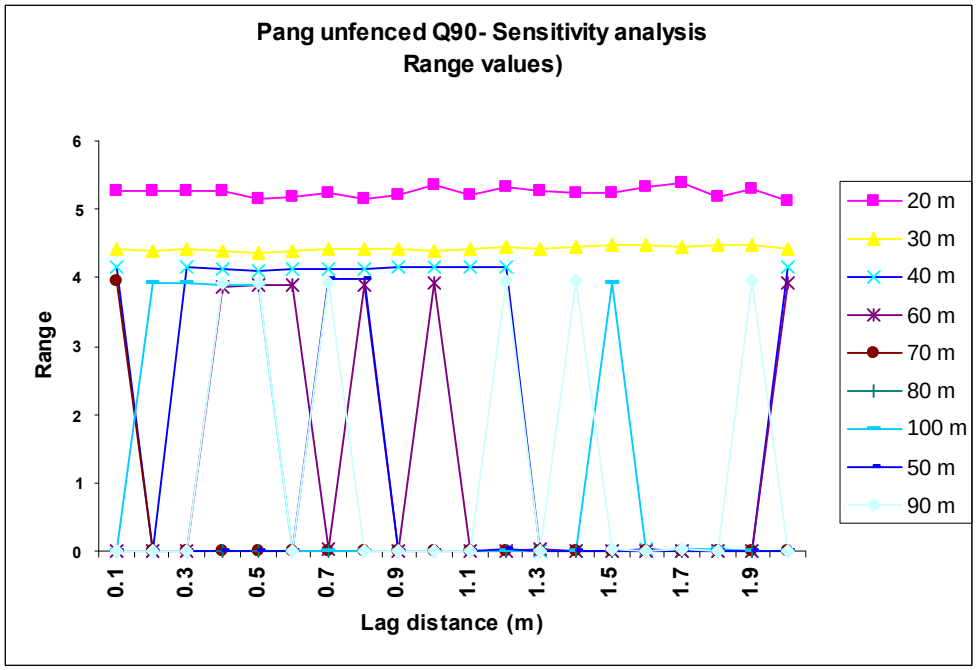
Pang unfenced Q90- Sensitivity analysis
Range values)
Range
Lag distance (m)
20 m
30 m
40 m
60 m
70 m
80 m
100 m
50 m
90 m

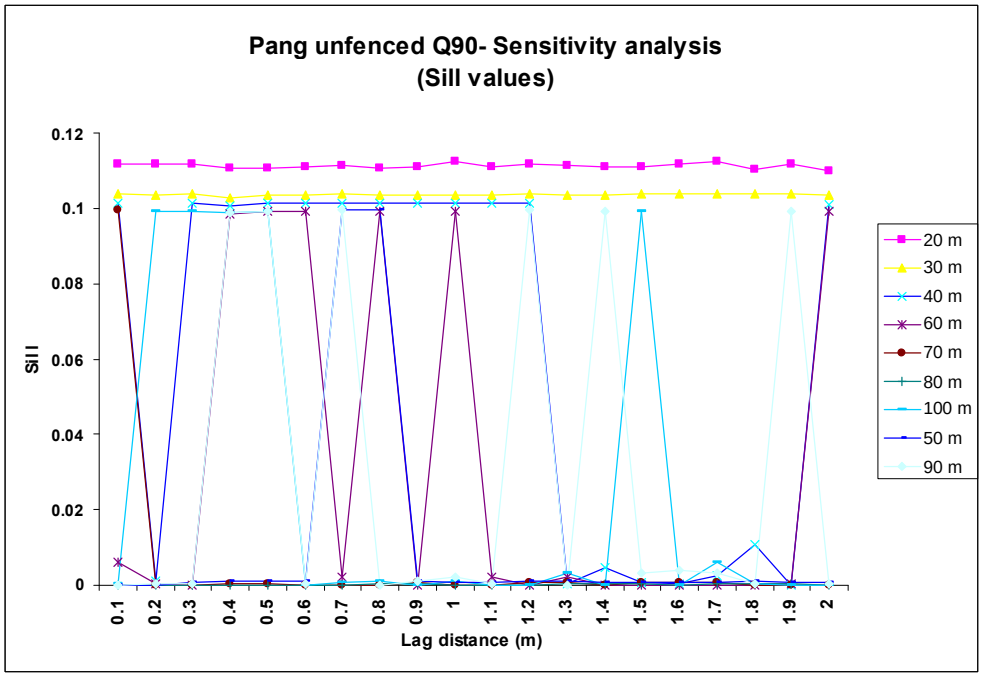
Pang unfenced Q90- Sensitivity analysis
(Sill values)
Sill
Lag distance (m)
20 m
30 m
40 m
60 m
70 m
80 m
100 m
50 m
90 m

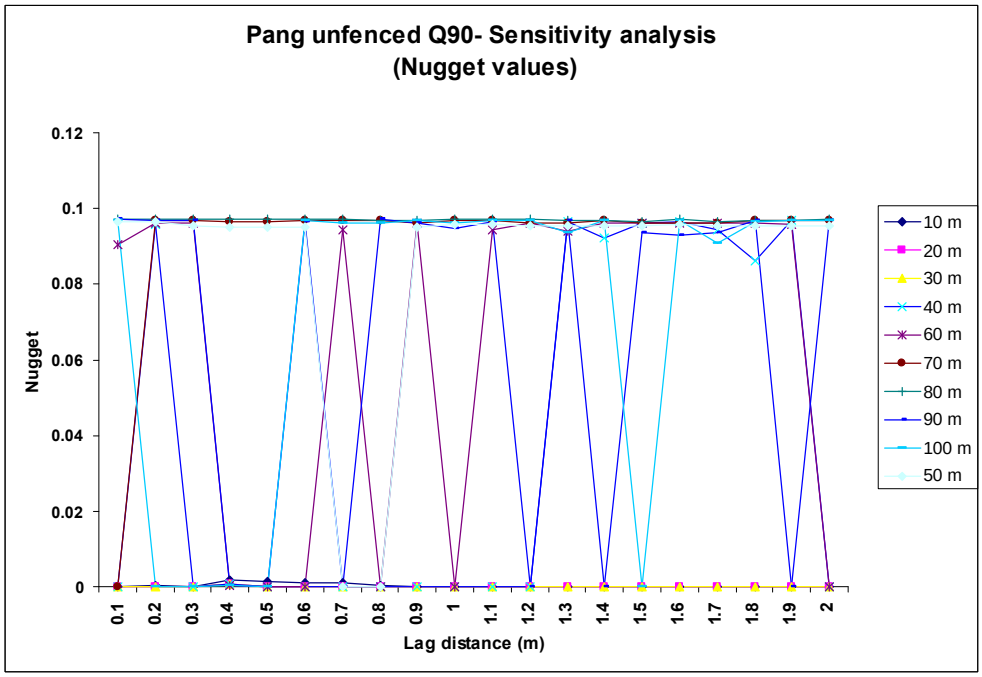
Pang unfenced Q90- Sensitivity analysis
(Nugget values)
Nugget
Lag distance (m)
10 m
20 m
30 m
40 m
60 m
70 m
80 m
90 m
100 m
50 m

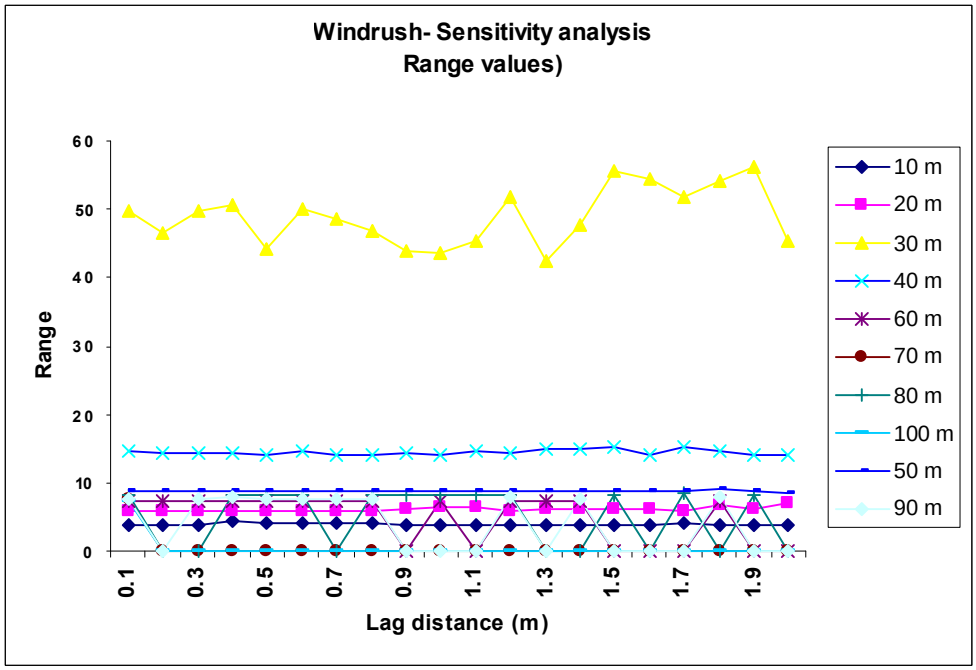
Windrush- Sensitivity analysis
Range values)
Range
Lag distance (m)
10 m
20 m
30 m
40 m
60 m
70 m
80 m
100 m
50 m
90 m

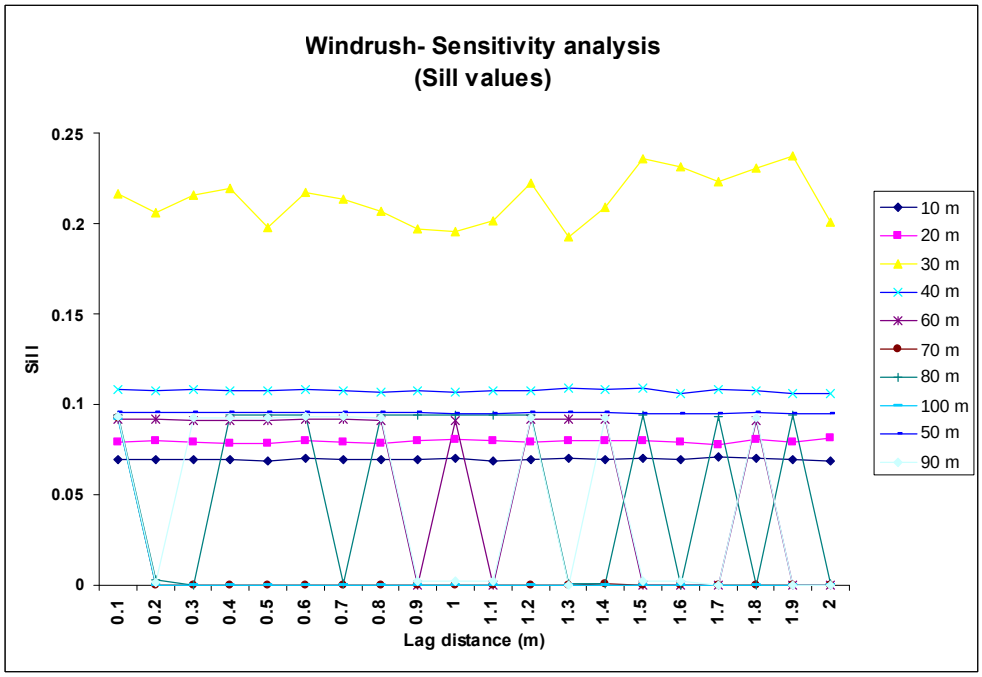
Windrush- Sensitivity analysis
(Sill values)
Sill
Lag distance (m)
10 m
20 m
30 m
40 m
60 m
70 m
80 m
100 m
50 m
90 m

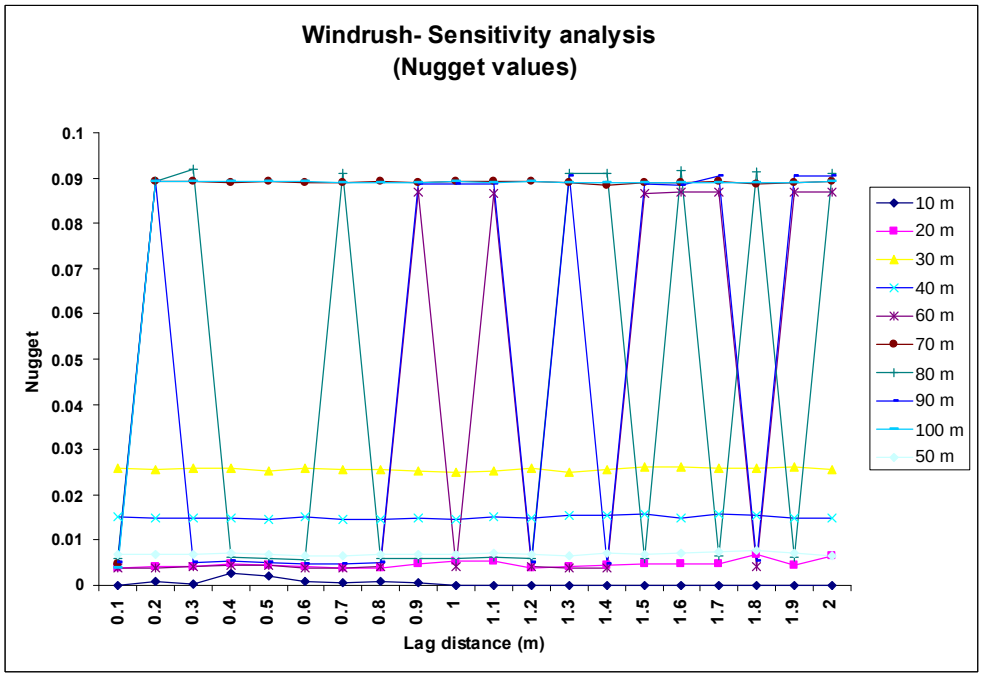
Windrush- Sensitivity analysis
(Nugget values)
Nugget
Lag distance (m)
10 m
20 m
30 m
40 m
60 m
70 m
80 m
90 m
100 m
50 m

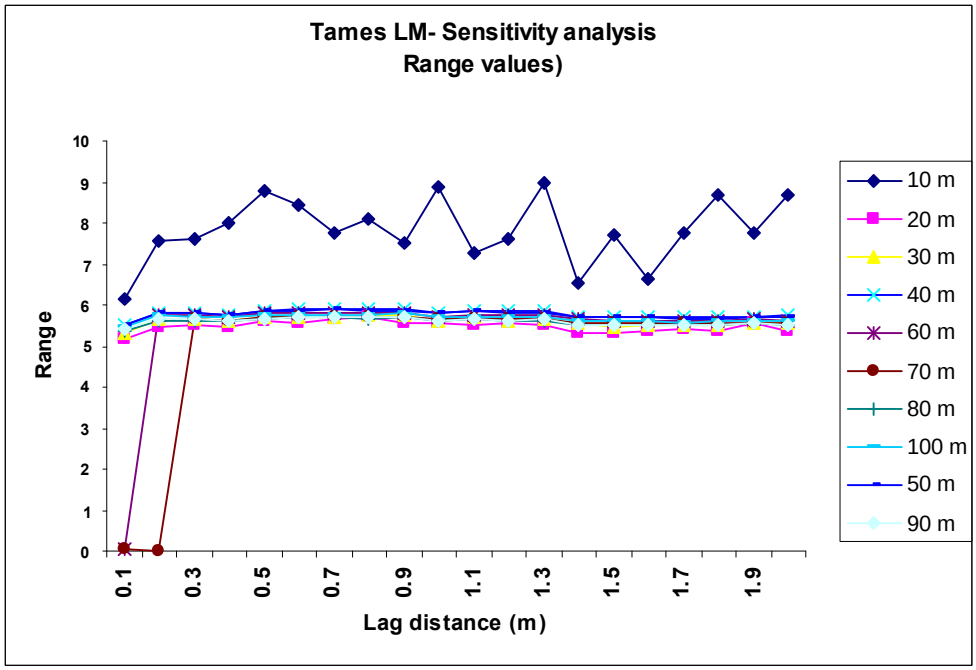
Tames LM- Sensitivity analysis
Range values)
Range
Lag distance (m)
10 m
20 m
30 m
40 m
60 m
70 m
80 m
100 m
50 m
90 m

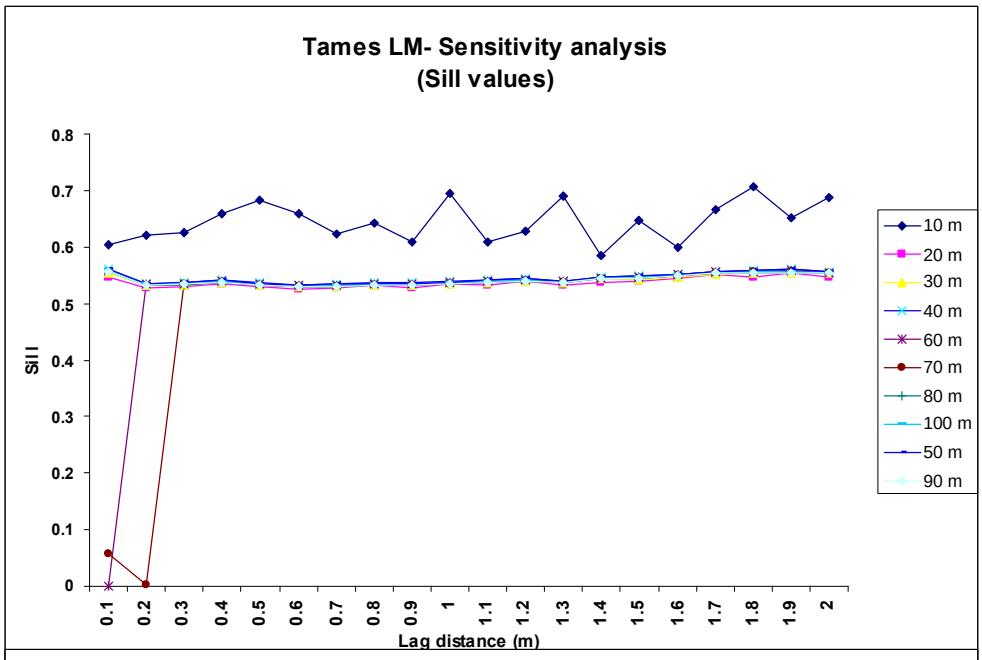
Tames LM- Sensitivity analysis
(Sill values)
Sill
Lag distance (m)
10 m
20 m
30 m
40 m
60 m
70 m
80 m
100 m
50 m
90 m

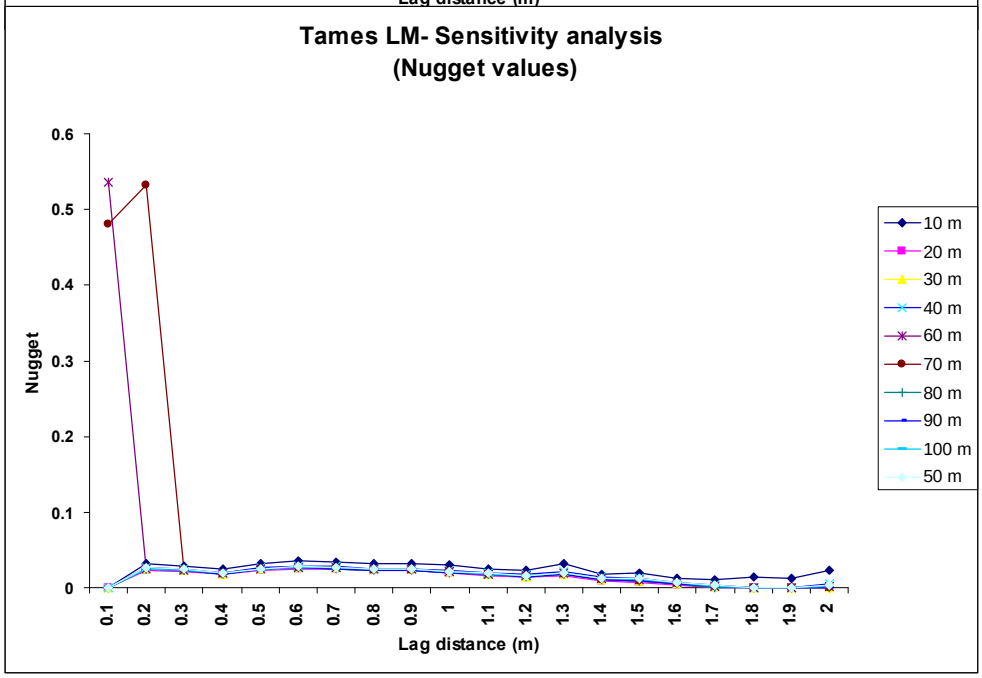
Tames LM- Sensitivity analysis
(Nugget values)
Nugget
Lag distance (m)
10 m
20 m
30 m
40 m
60 m
70 m
80 m
90 m
100 m
50 m

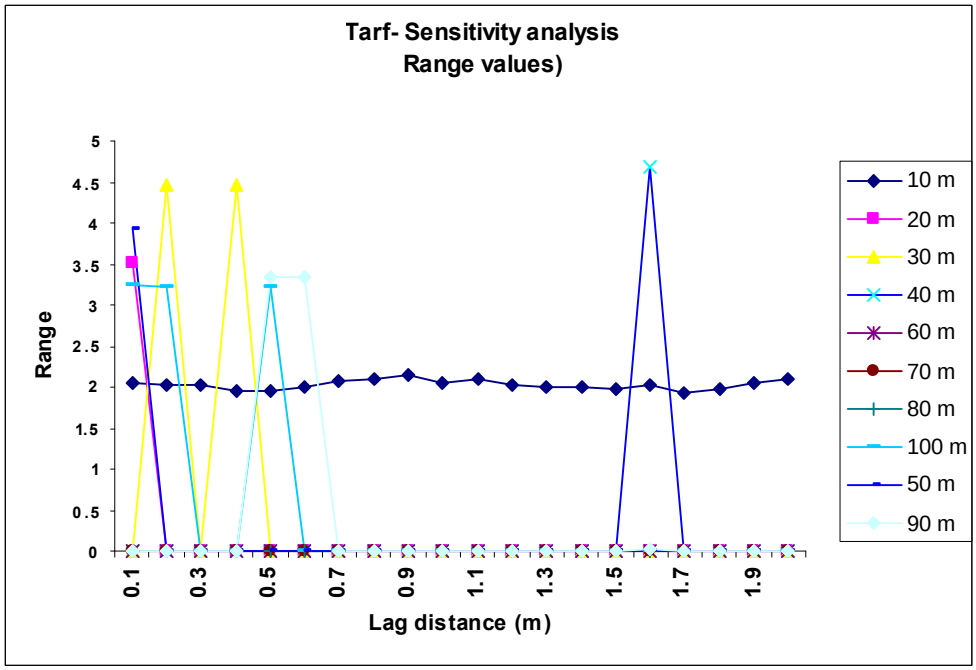
Tarf- Sensitivity analysis
Range values)
Range
Lag distance (m)
10 m
20 m
30 m
40 m
60 m
70 m
80 m
100 m
50 m
90 m

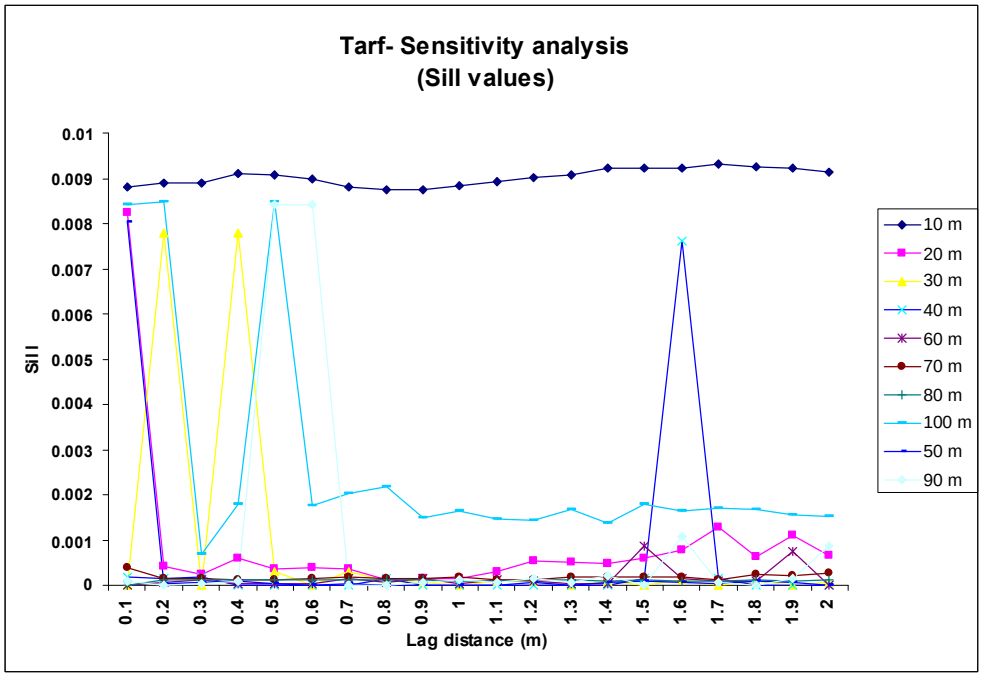
Tarf- Sensitivity analysis
(Sill values)
Sill
Lag distance (m)
10 m
20 m
30 m
40 m
60 m
70 m
80 m
100 m
50 m
90 m

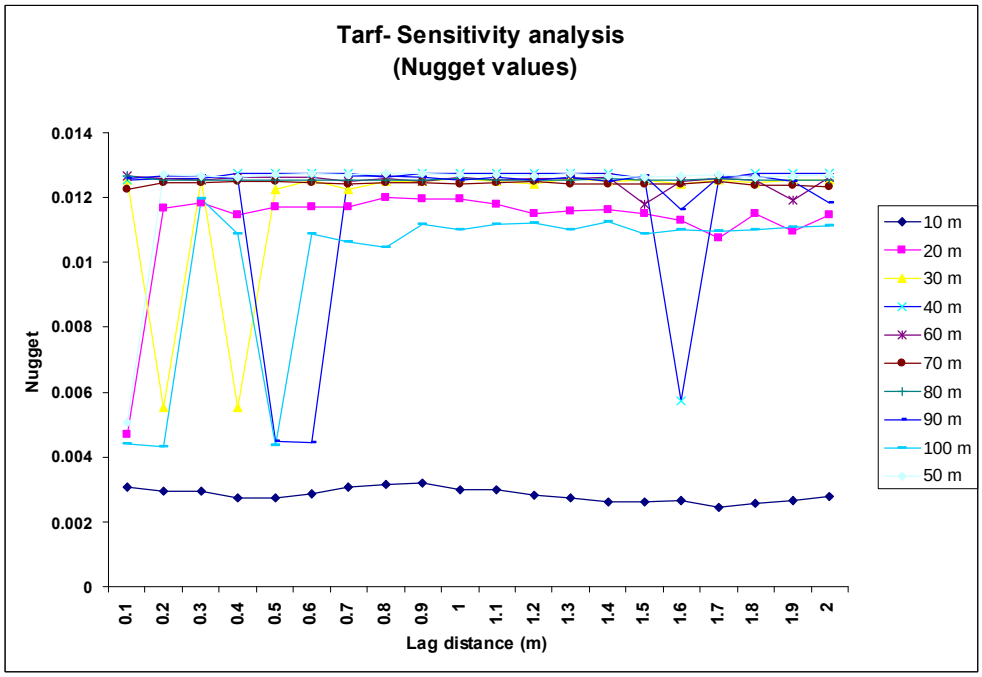
Tarf- Sensitivity analysis
(Nugget values)
Nugget
Lag distance (m)
10 m
20 m
30 m
40 m
60 m
70 m
80 m
90 m
100 m
50 m

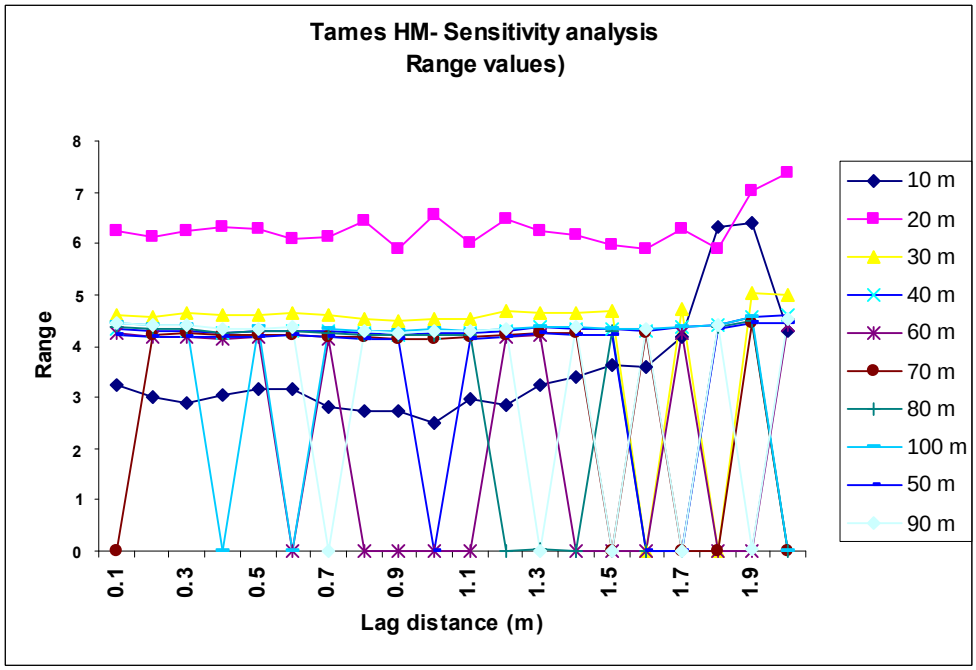
Tames HM- Sensitivity analysis
Range values)
Range
Lag distance (m)
10 m
20 m
30 m
40 m
60 m
70 m
80 m
100 m
50 m
90 m

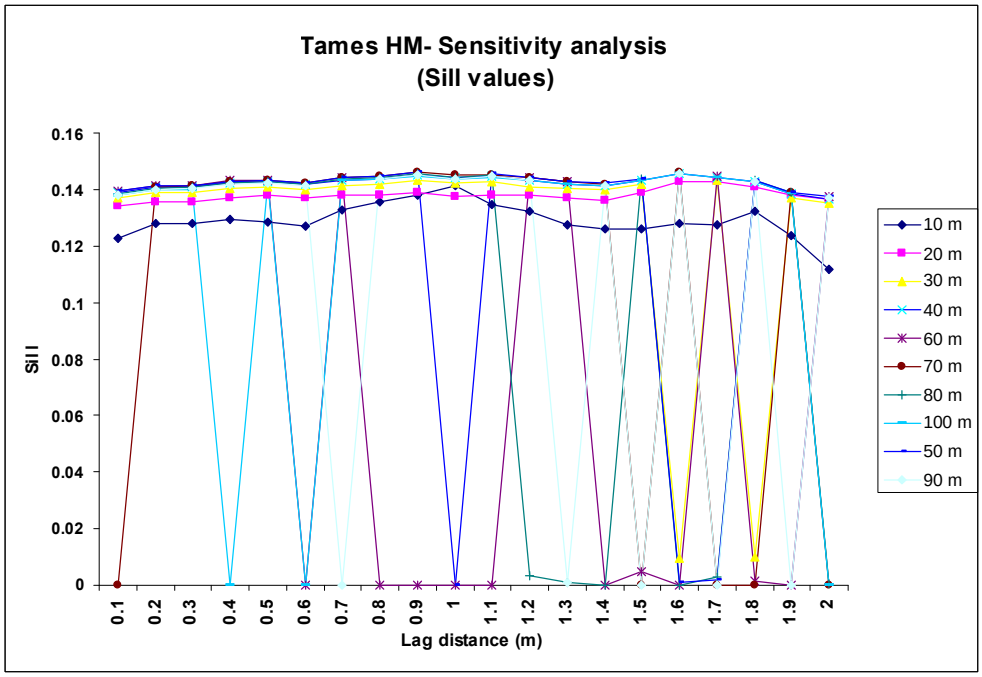
Tames HM- Sensitivity analysis
(Sill values)
Sill
Lag distance (m)
10 m
20 m
30 m
40 m
60 m
70 m
80 m
100 m
50 m
90 m

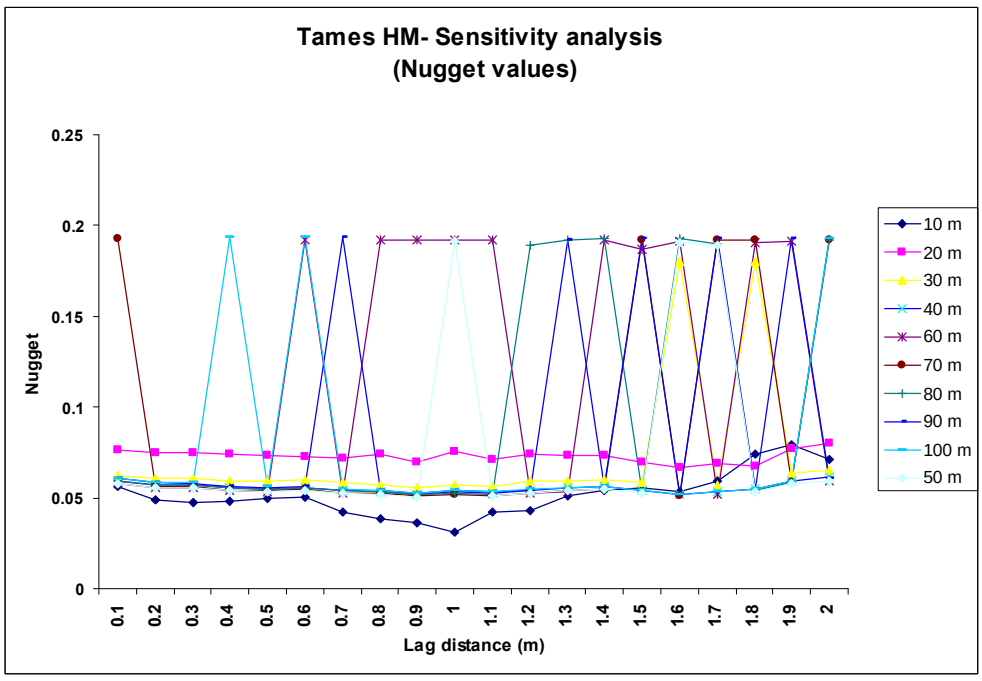
Tames HM- Sensitivity analysis
(Nugget values)
Nugget
Lag distance (m)
10 m
20 m
30 m
40 m
60 m
70 m
80 m
90 m
100 m
50 m

Appendix 3.5.3

Results obtained for the analysis in Chapter 5 –Sensitivity Analysis – Variogram values for combinations of lag and maximum distance considered: exponential variogram for wet points.

This appendix summarises the results obtained for the sensitivity analysis developed in section 5.4.3. for the combination of lag distances and maximum distances selected. Results presented in this section only include the graphical output for the data sets analysed with wet points. The variogram model analysed is the spherical one. Three different outputs, one for each variogram variable analysed (i.e. range, sill and nugget) are presented for each river site. Those river sites that had extreme variogram values are included twice: the graphical output is presented with two different axis scales so results can be better analysed. The horizontal axis represents the selected lag distance.

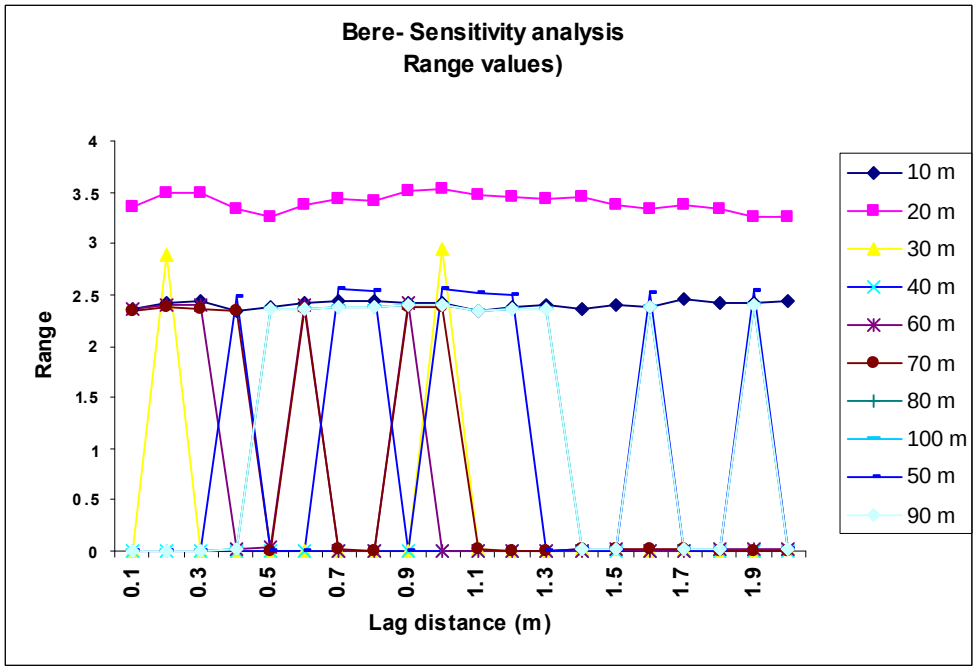
Bere- Sensitivity analysis
Range values)
Range
Lag distance (m)
10 m
20 m
30 m
40 m
60 m
70 m
80 m
100 m
50 m
90 m

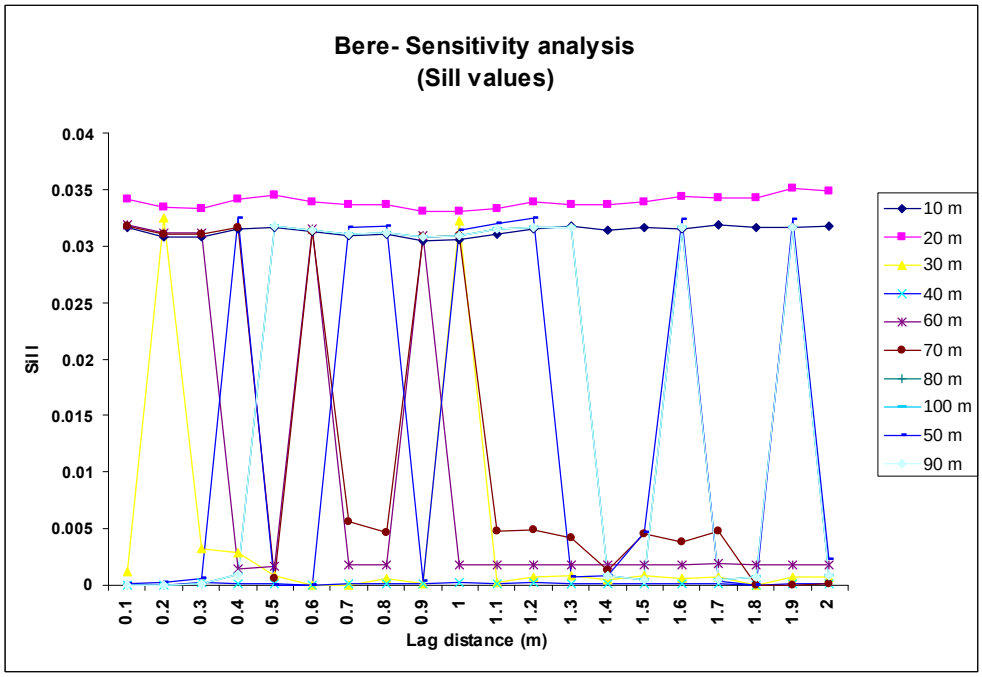
Bere- Sensitivity analysis
(Sill values)
Sill
Lag distance (m)
10 m
20 m
30 m
40 m
60 m
70 m
80 m
100 m
50 m
90 m

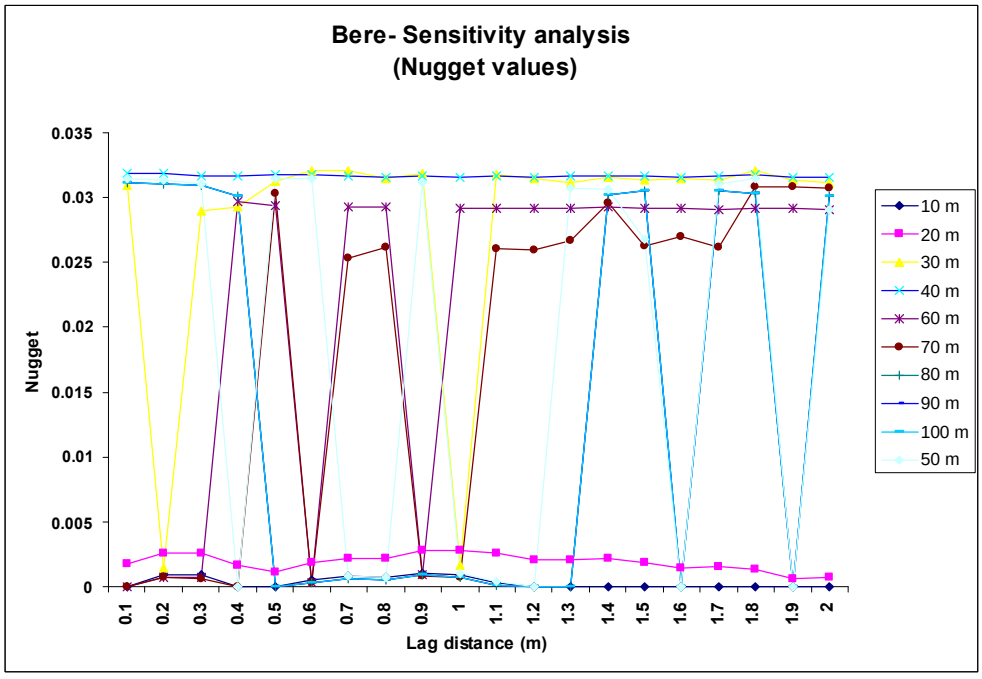
Bere- Sensitivity analysis
(Nugget values)
Nugget
Lag distance (m)
10 m
20 m
30 m
40 m
60 m
70 m
80 m
90 m
100 m
50 m

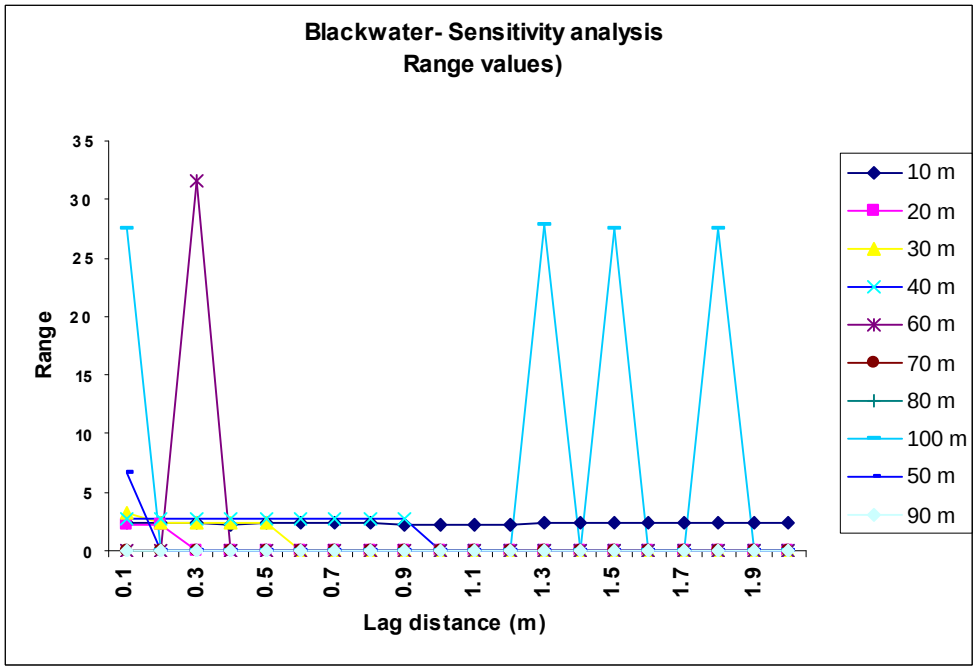
Blackwater- Sensitivity analysis
Range values)
Range
Lag distance (m)
10 m
20 m
30 m
40 m
60 m
70 m
80 m
100 m
50 m
90 m

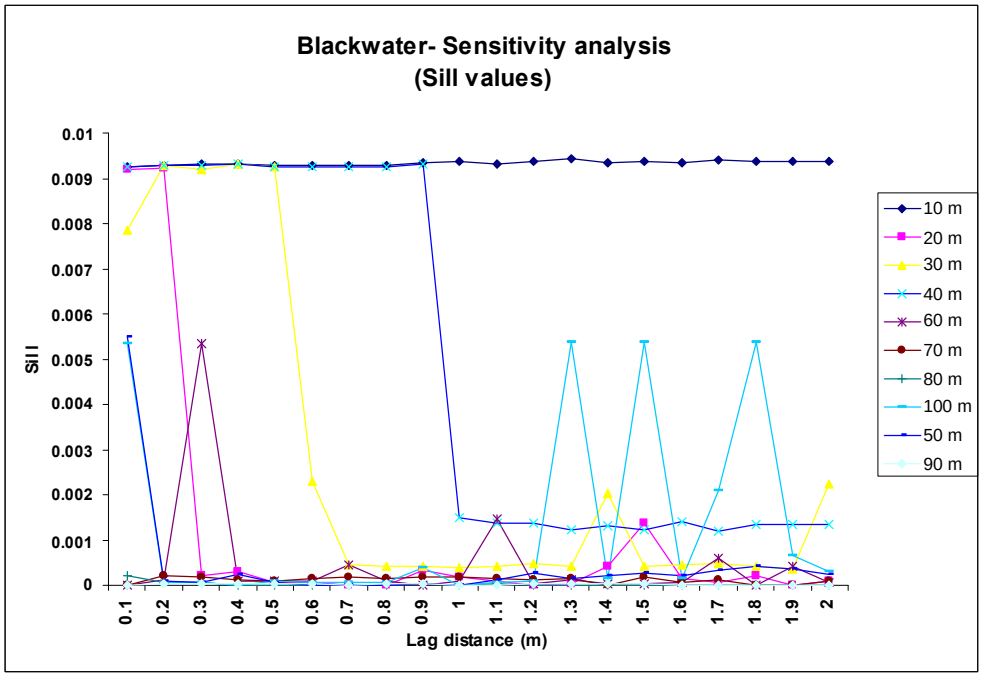
Blackwater- Sensitivity analysis
(Sill values)
Sill
Lag distance (m)
10 m
20 m
30 m
40 m
60 m
70 m
80 m
100 m
50 m
90 m

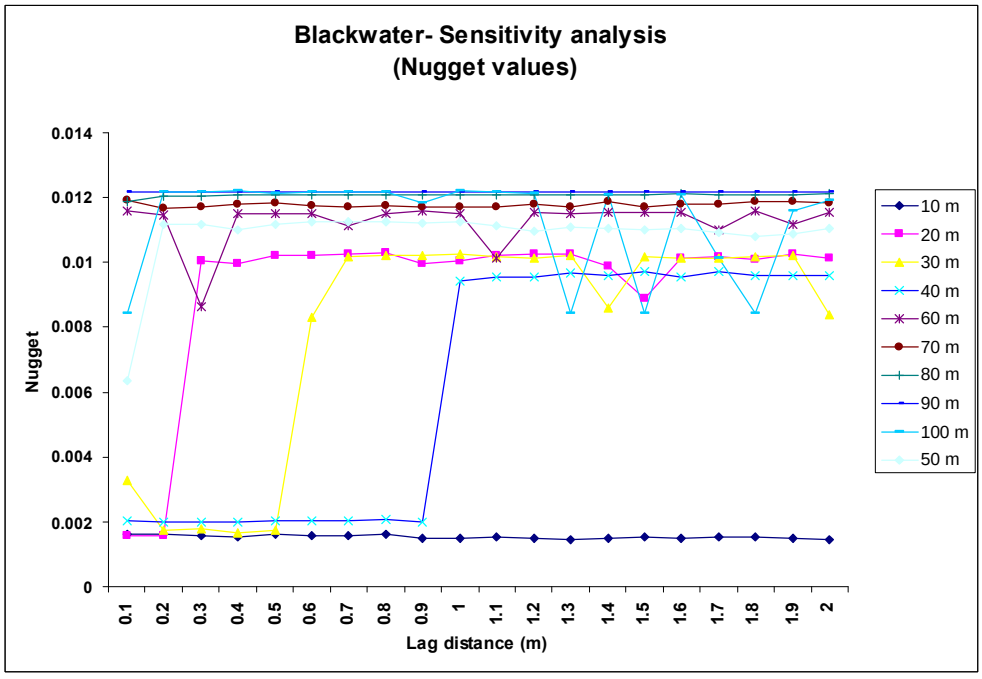
Blackwater- Sensitivity analysis
(Nugget values)
Nugget
Lag distance (m)
10 m
20 m
30 m
40 m
60 m
70 m
80 m
90 m
100 m
50 m

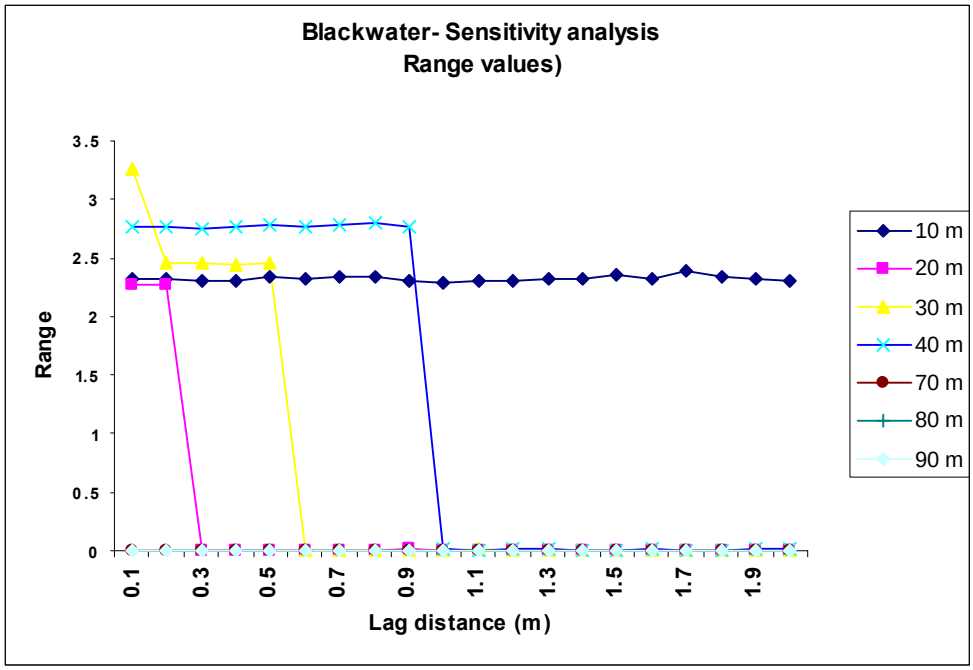
Blackwater- Sensitivity analysis
Range values)
Range
Lag distance (m)
10 m
20 m
30 m
40 m
70 m
80 m
90 m

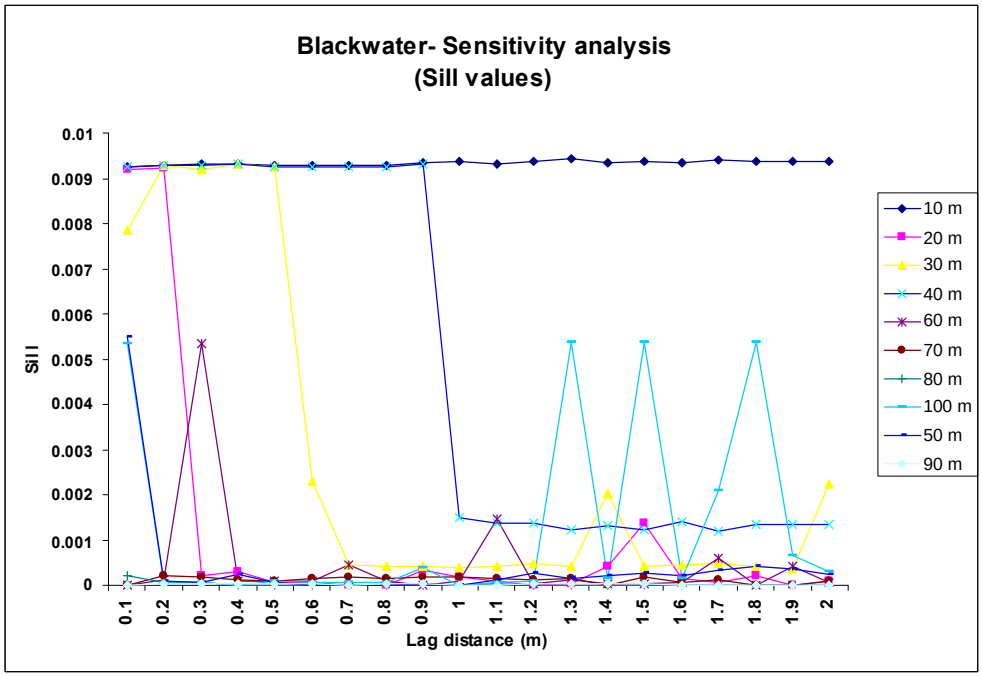
Blackwater- Sensitivity analysis
(Sill values)
Sill
Lag distance (m)
10 m
20 m
30 m
40 m
60 m
70 m
80 m
100 m
50 m
90 m

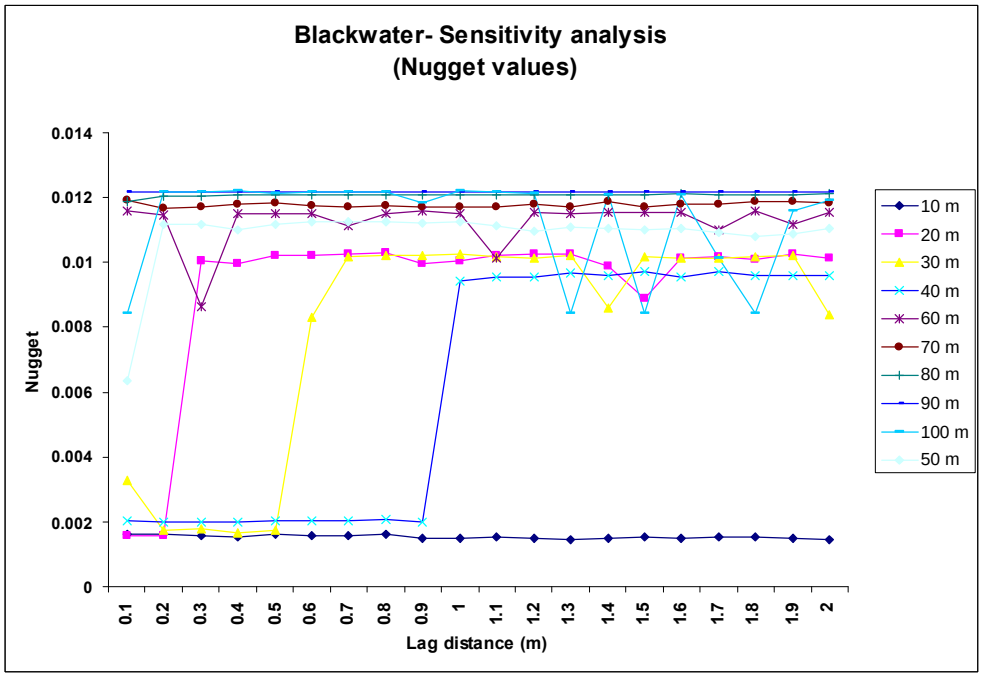
Blackwater- Sensitivity analysis
(Nugget values)
Nugget
Lag distance (m)
10 m
20 m
30 m
40 m
60 m
70 m
80 m
90 m
100 m
50 m

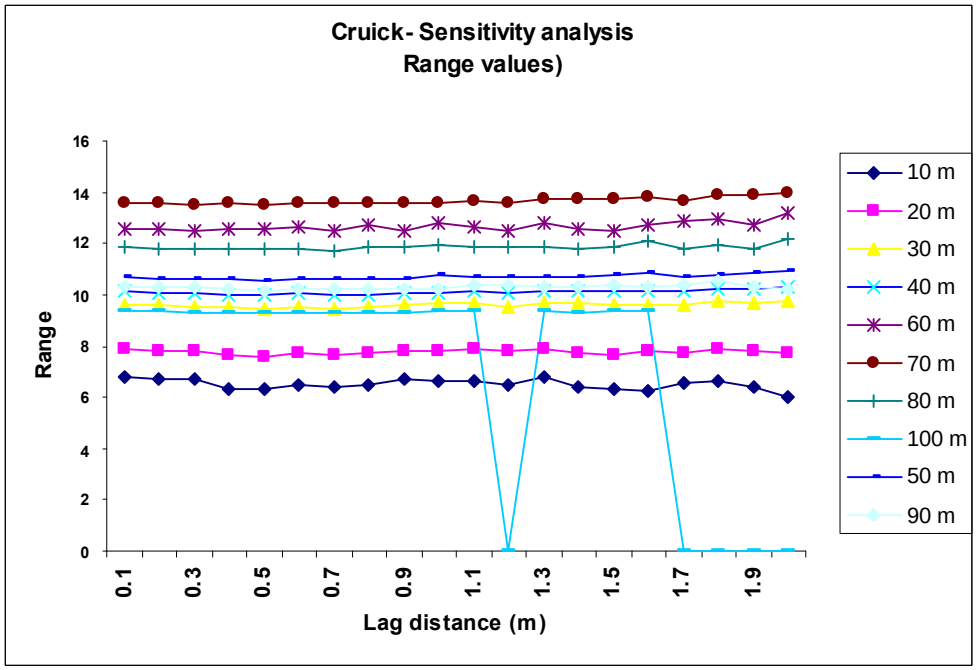
Cruick- Sensitivity analysis
Range values)
Range
Lag distance (m)
10 m
20 m
30 m
40 m
60 m
70 m
80 m
100 m
50 m
90 m

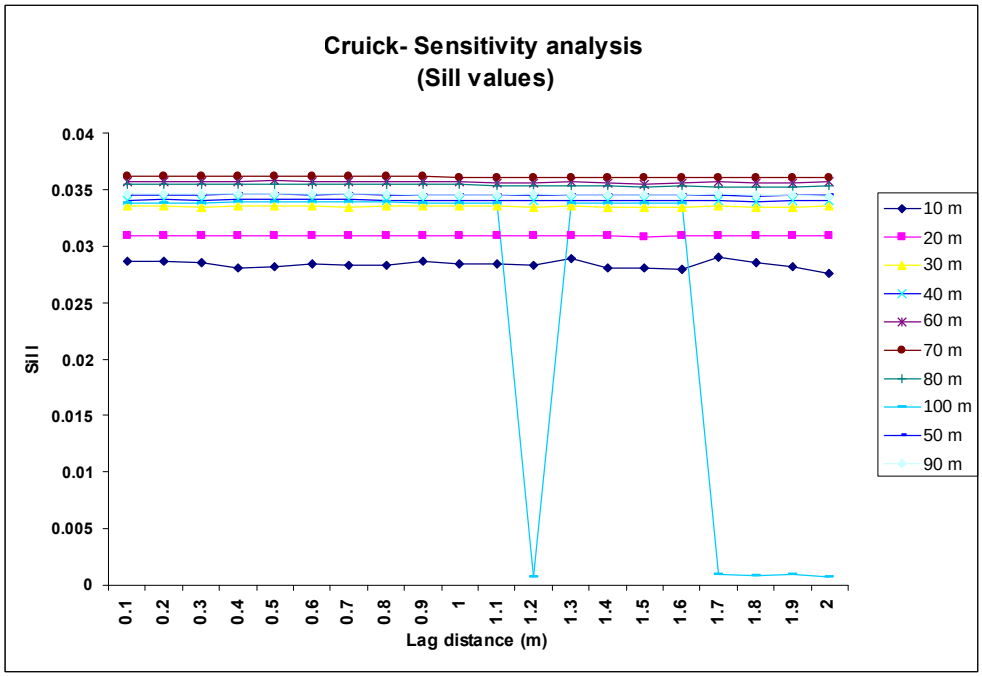
Cruick- Sensitivity analysis
(Sill values)
Sill
Lag distance (m)
10 m
20 m
30 m
40 m
60 m
70 m
80 m
100 m
50 m
90 m

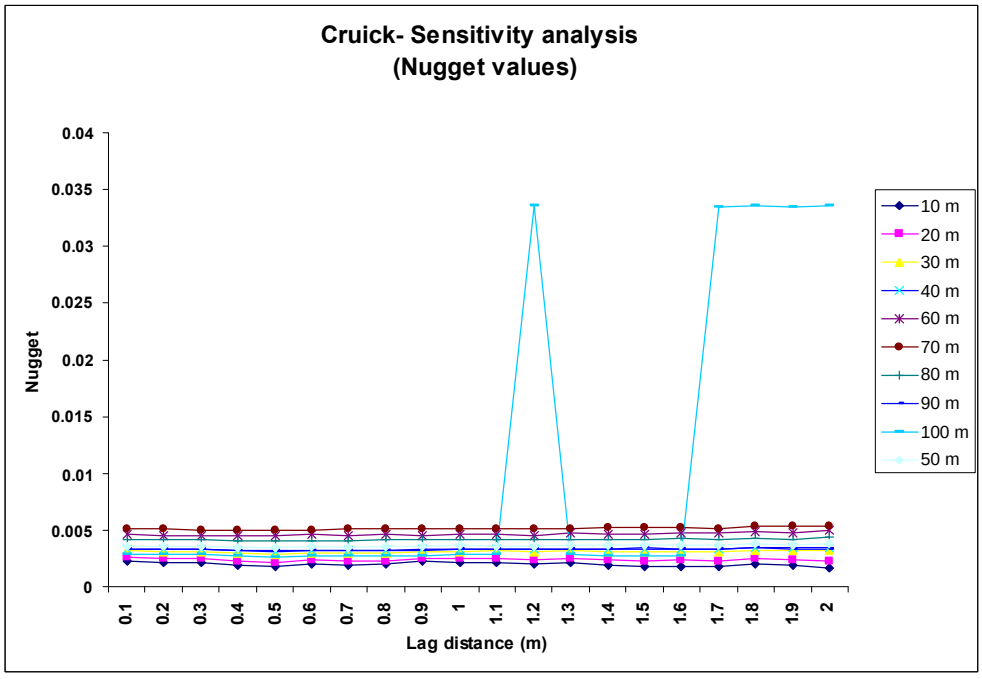
Cruick- Sensitivity analysis
(Nugget values)
Nugget
Lag distance (m)
10 m
20 m
30 m
40 m
60 m
70 m
80 m
90 m
100 m
50 m

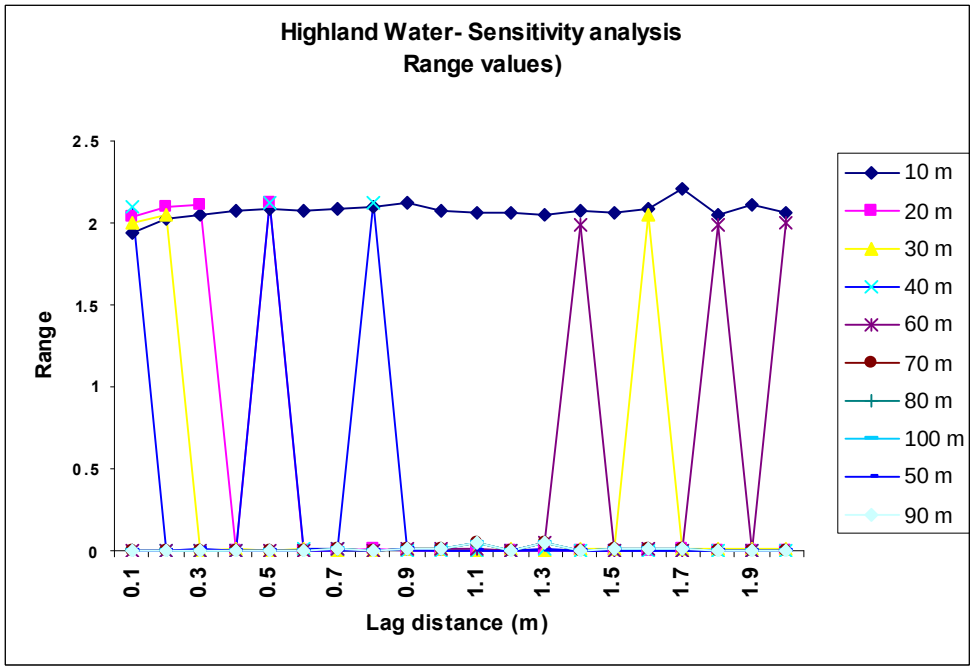
Highland Water- Sensitivity analysis
Range values)
Range
Lag distance (m)
10 m
20 m
30 m
40 m
60 m
70 m
80 m
100 m
50 m
90 m

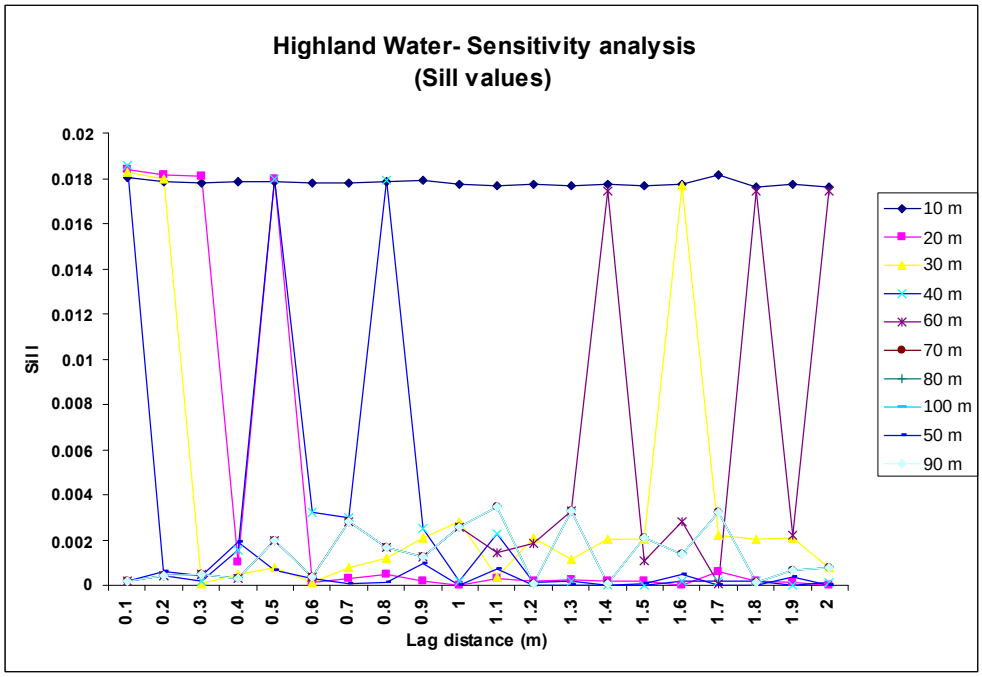
Highland Water- Sensitivity analysis
(Sill values)
Sill
Lag distance (m)
10 m
20 m
30 m
40 m
60 m
70 m
80 m
100 m
50 m
90 m

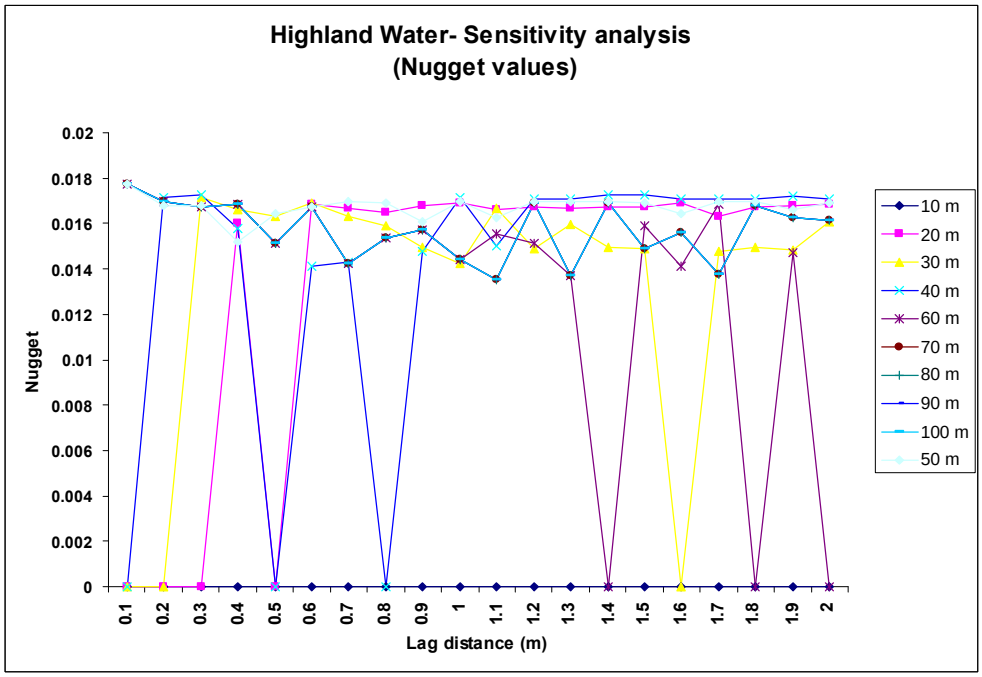
Highland Water- Sensitivity analysis
(Nugget values)
Nugget
Lag distance (m)
10 m
20 m
30 m
40 m
60 m
70 m
80 m
90 m
100 m
50 m

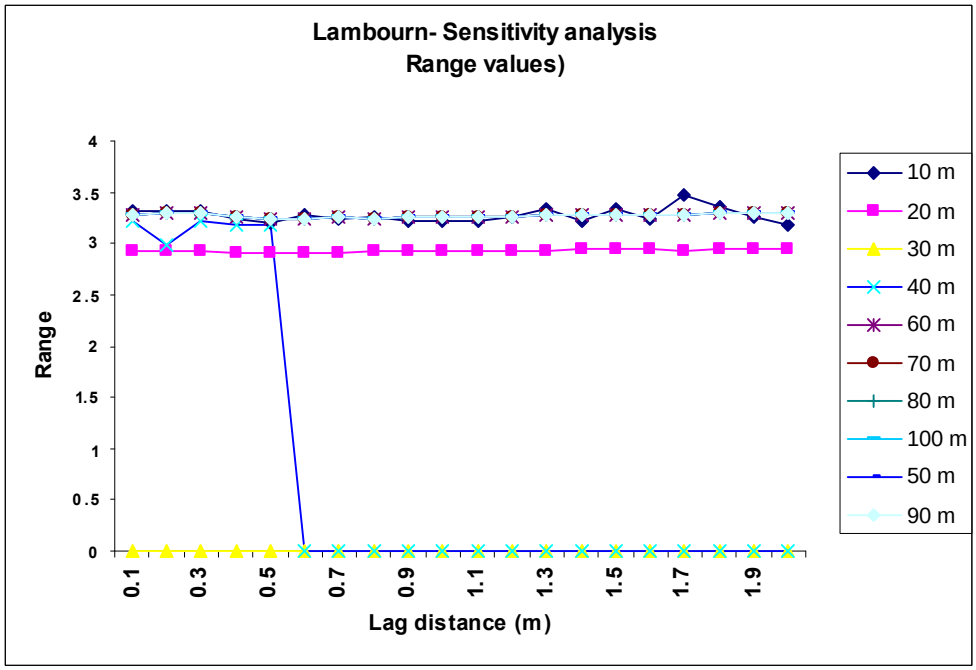
Lambourn- Sensitivity analysis
Range values)
Range
Lag distance (m)
10 m
20 m
30 m
40 m
60 m
70 m
80 m
100 m
50 m
90 m

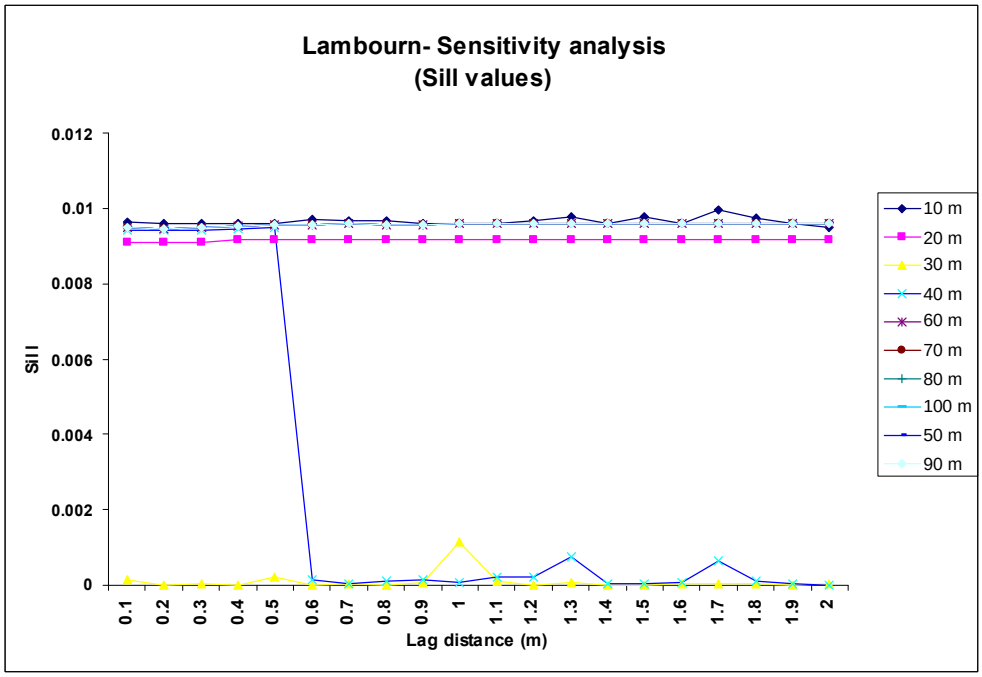
Lambourn- Sensitivity analysis
(Sill values)
Sill
Lag distance (m)
10 m
20 m
30 m
40 m
60 m
70 m
80 m
100 m
50 m
90 m

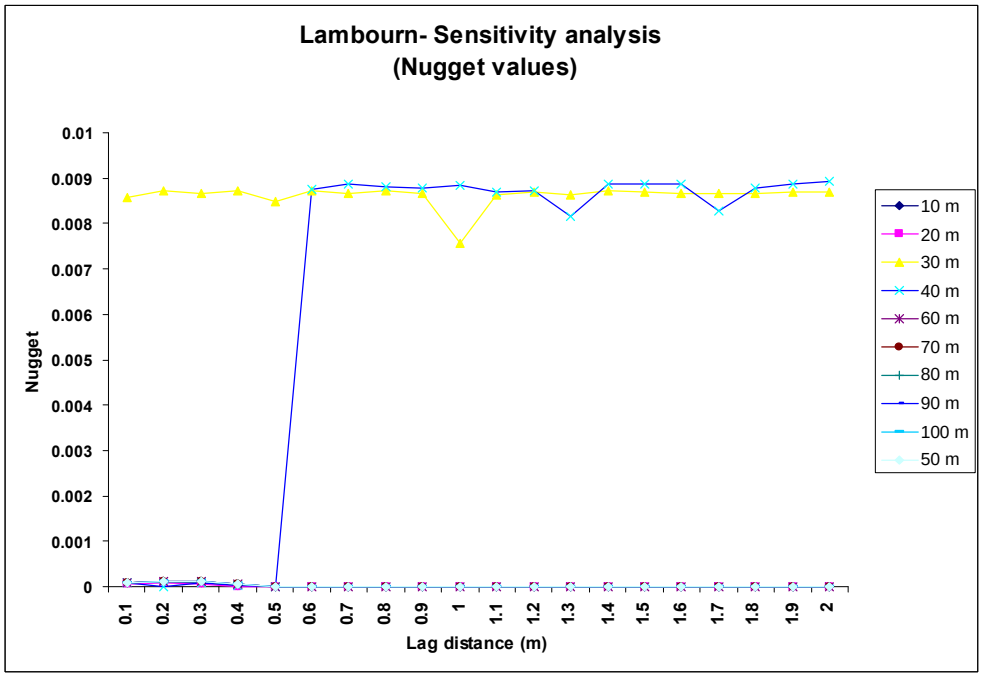
Lambourn- Sensitivity analysis
(Nugget values)
Nugget
Lag distance (m)
10 m
20 m
30 m
40 m
60 m
70 m
80 m
90 m
100 m
50 m

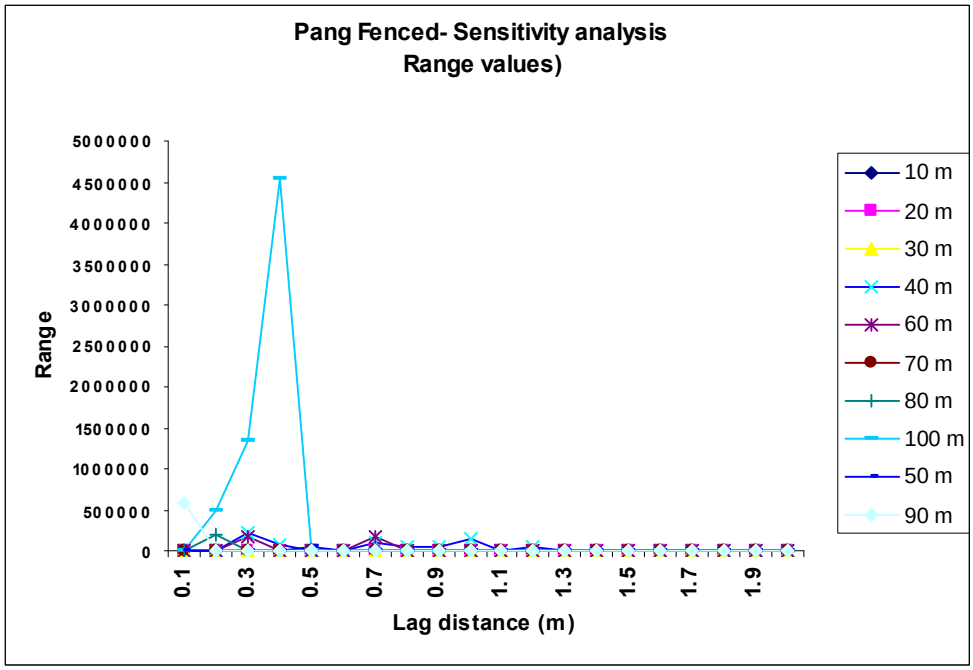
Pang Fenced- Sensitivity analysis
Range values)
Range
5000000
4500000
4000000
3500000
3000000
2500000
2000000
1500000
1000000
500000
0
0.1
0.3
0.5
0.7
0.9
1.1
1.3
1.5
1.7
1.9
Lag distance (m)
10 m
20 m
30 m
40 m
60 m
70 m
80 m
100 m
50 m
90 m

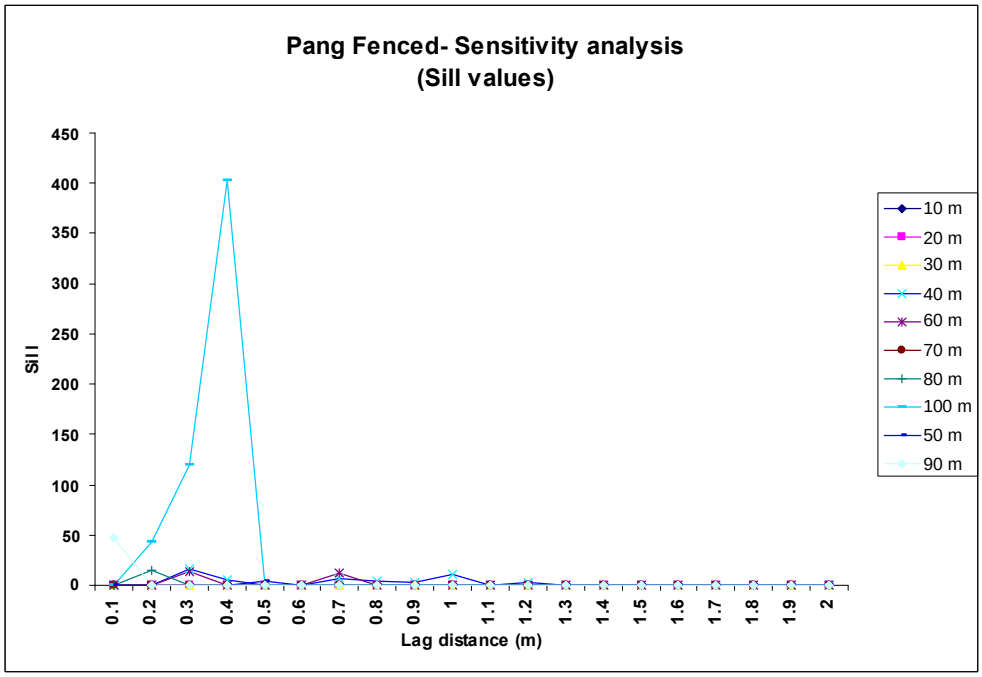
Pang Fenced- Sensitivity analysis
(Sill values)
Sill
450
400
350
300
250
200
150
100
50
0
0.1
0.2
0.3
0.4
0.5
0.6
0.7
0.8
0.9
1
1.1
1.2
1.3
1.4
1.5
1.6
1.7
1.8
1.9
2
Lag distance (m)
10 m
20 m
30 m
40 m
60 m
70 m
80 m
100 m
50 m
90 m

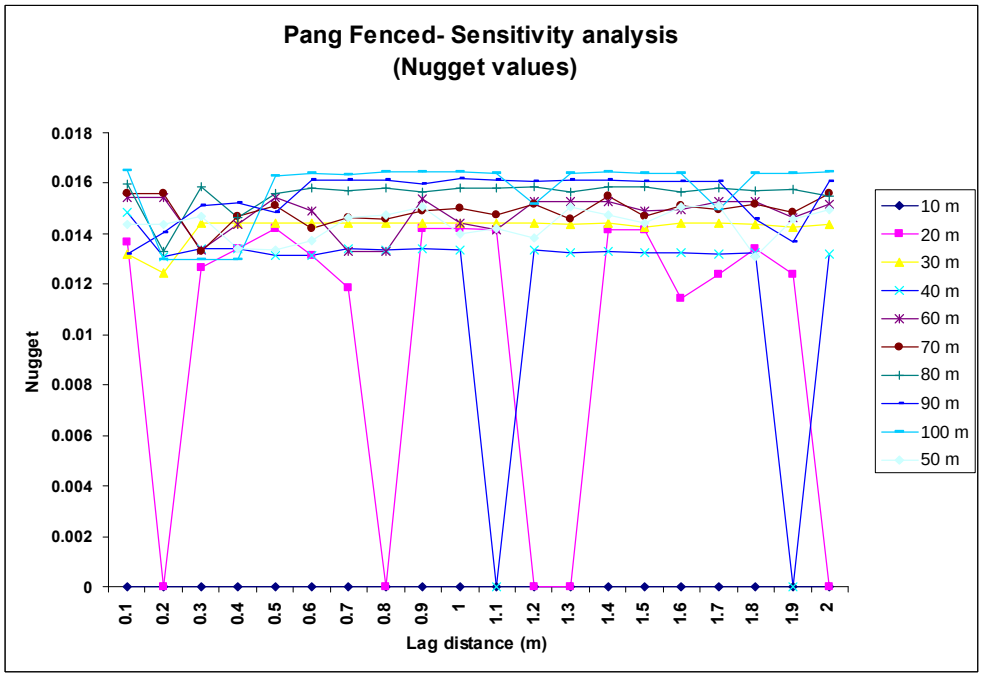
Pang Fenced- Sensitivity analysis
(Nugget values)
Nugget
0.018
0.016
0.014
0.012
0.01
0.008
0.006
0.004
0.002
0
0.1
0.2
0.3
0.4
0.5
0.6
0.7
0.8
0.9
1
1.1
1.2
1.3
1.4
1.5
1.6
1.7
1.8
1.9
2
Lag distance (m)
10 m
20 m
30 m
40 m
60 m
70 m
80 m
90 m
100 m
50 m

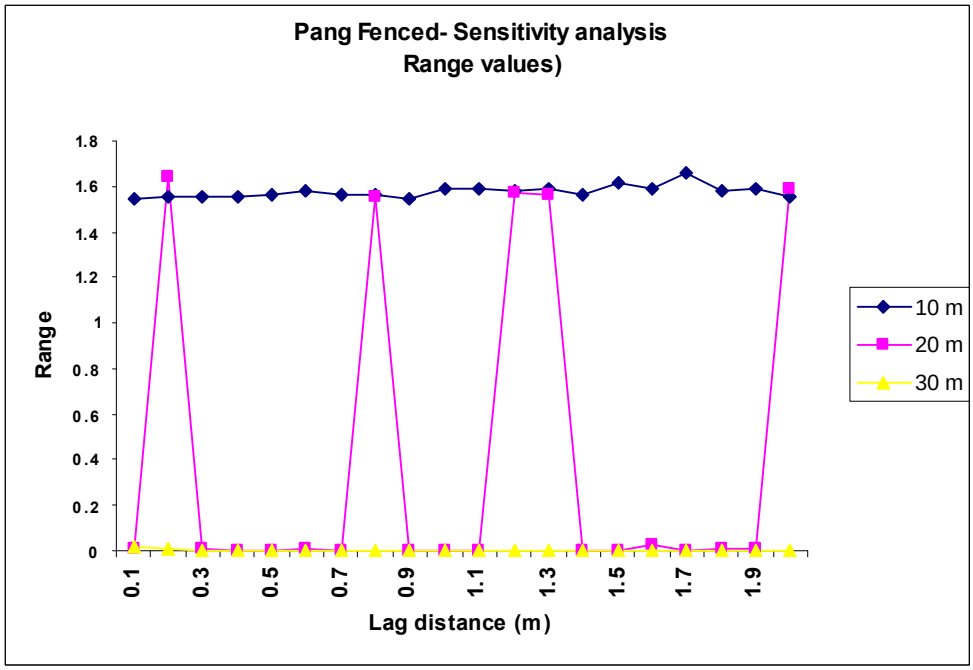
Pang Fenced- Sensitivity analysis
Range values)
Range
Lag distance (m)
10 m
20 m
30 m

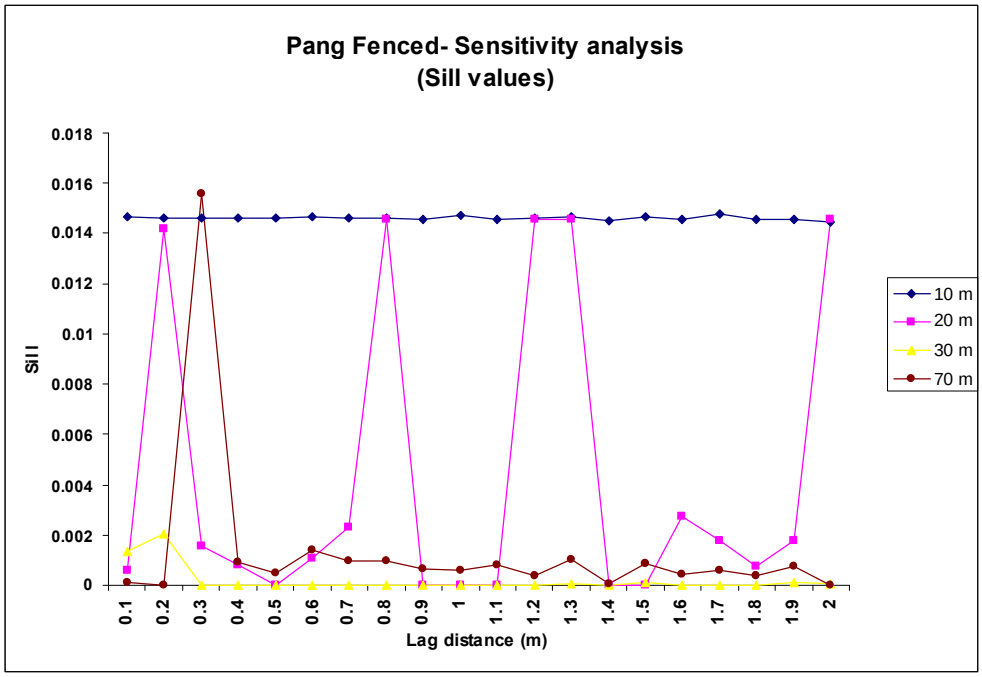
Pang Fenced- Sensitivity analysis
(Sill values)
Sill
Lag distance (m)
10 m
20 m
30 m
70 m

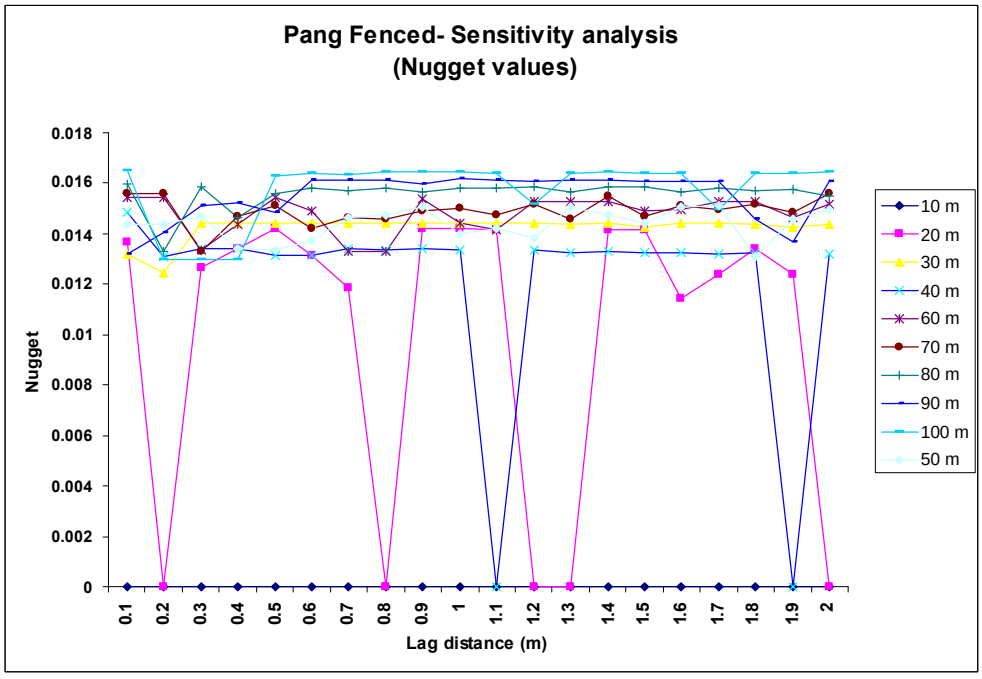
Pang Fenced- Sensitivity analysis
(Nugget values)
Nugget
Lag distance (m)
10 m
20 m
30 m
40 m
60 m
70 m
80 m
90 m
100 m
50 m

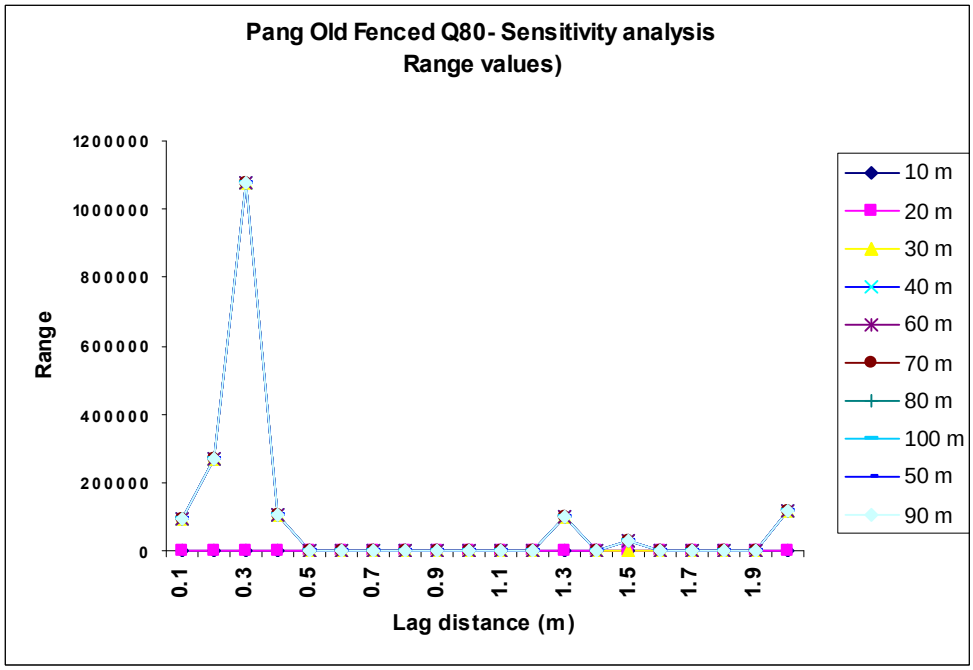
Pang Old Fenced Q80- Sensitivity analysis
Range values)
Range
1200000
1000000
800000
600000
400000
200000
0
0.1
0.3
0.5
0.7
0.9
1.1
1.3
1.5
1.7
1.9
Lag distance (m)
10 m
20 m
30 m
40 m
60 m
70 m
80 m
100 m
50 m
90 m

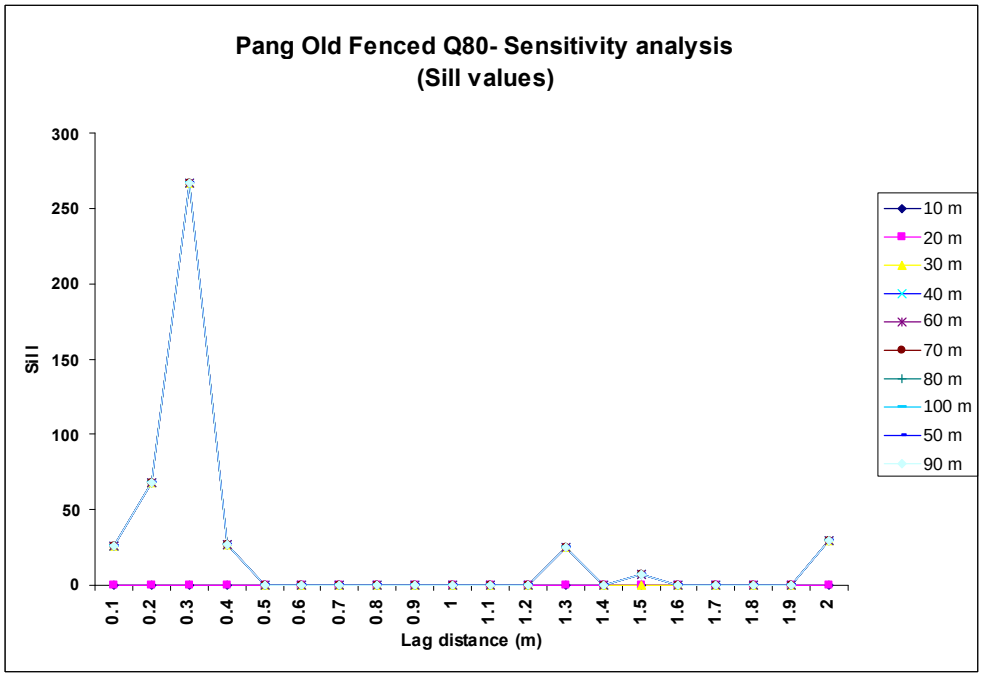
Pang Old Fenced Q80- Sensitivity analysis
(Sill values)
Sill
300
250
200
150
100
50
0
0.1
0.2
0.3
0.4
0.5
0.6
0.7
0.8
0.9
1
1.1
1.2
1.3
1.4
1.5
1.6
1.7
1.8
1.9
2
Lag distance (m)
10 m
20 m
30 m
40 m
60 m
70 m
80 m
100 m
50 m
90 m

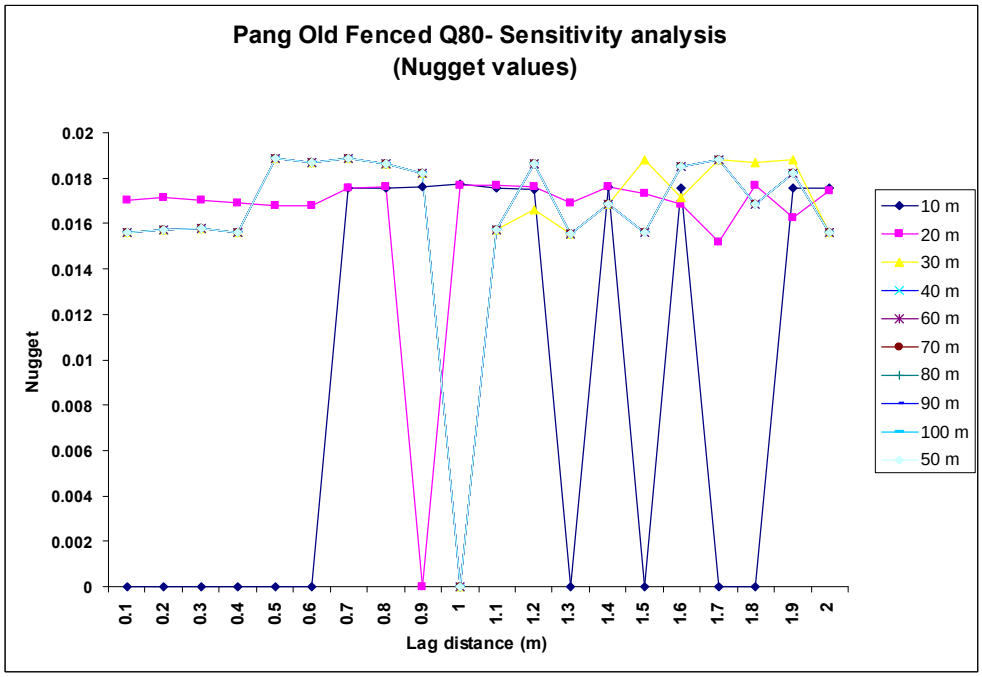
Pang Old Fenced Q80- Sensitivity analysis
(Nugget values)
Nugget
0.02
0.018
0.016
0.014
0.012
0.01
0.008
0.006
0.004
0.002
0
0.1
0.2
0.3
0.4
0.5
0.6
0.7
0.8
0.9
1
1.1
1.2
1.3
1.4
1.5
1.6
1.7
1.8
1.9
2
Lag distance (m)
10 m
20 m
30 m
40 m
60 m
70 m
80 m
90 m
100 m
50 m

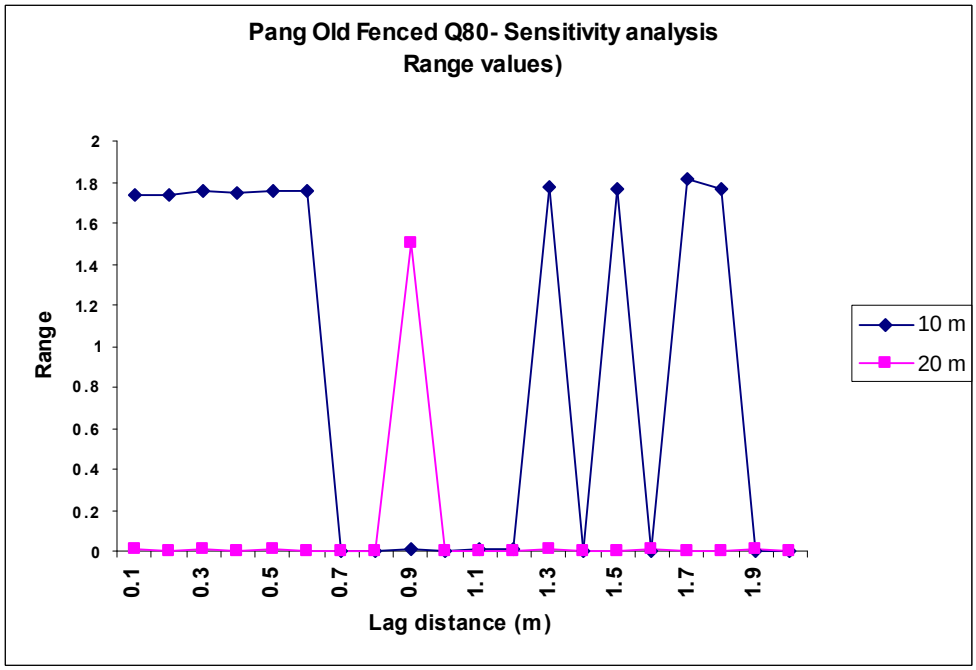
Pang Old Fenced Q80- Sensitivity analysis
Range values)
Range
Lag distance (m)
10 m
20 m

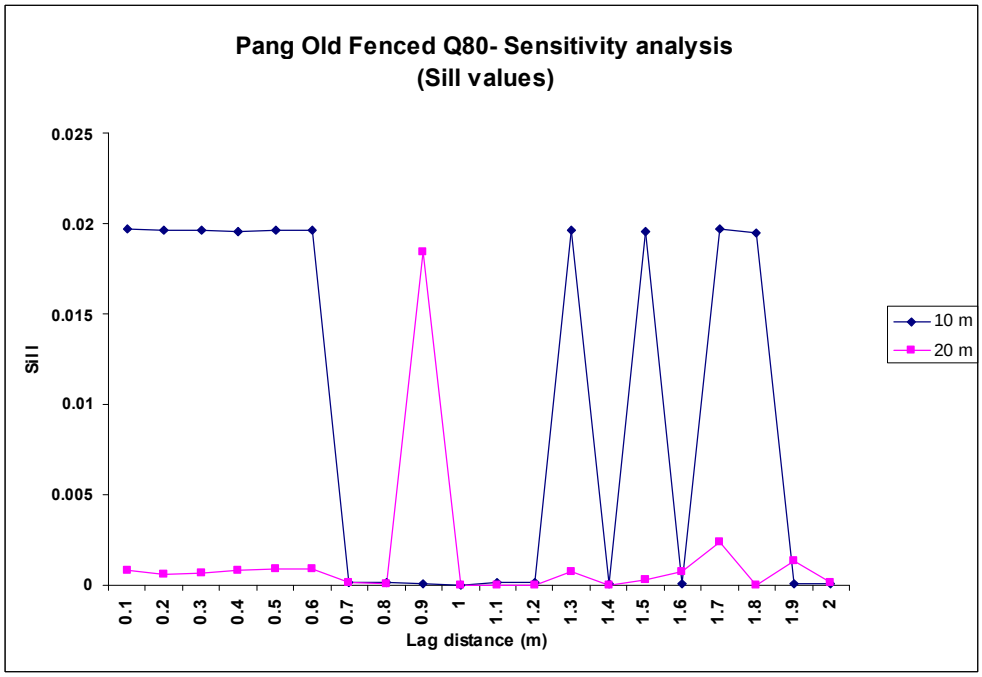
Pang Old Fenced Q80- Sensitivity analysis
(Sill values)
Sill
Lag distance (m)
10 m
20 m

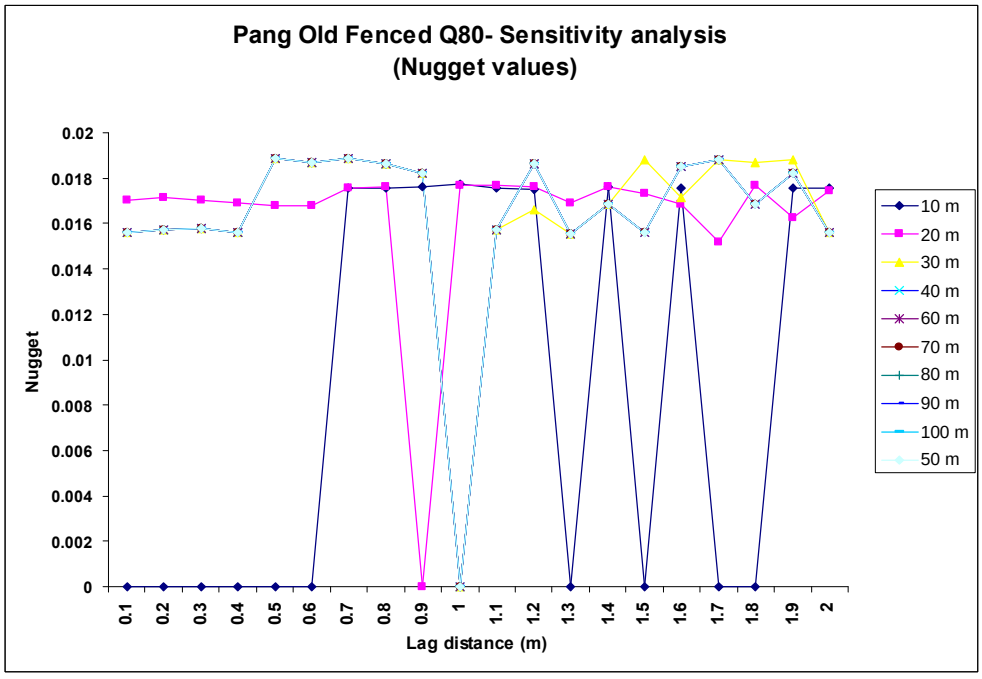
Pang Old Fenced Q80- Sensitivity analysis
(Nugget values)
Nugget
Lag distance (m)
10 m
20 m
30 m
40 m
60 m
70 m
80 m
90 m
100 m
50 m

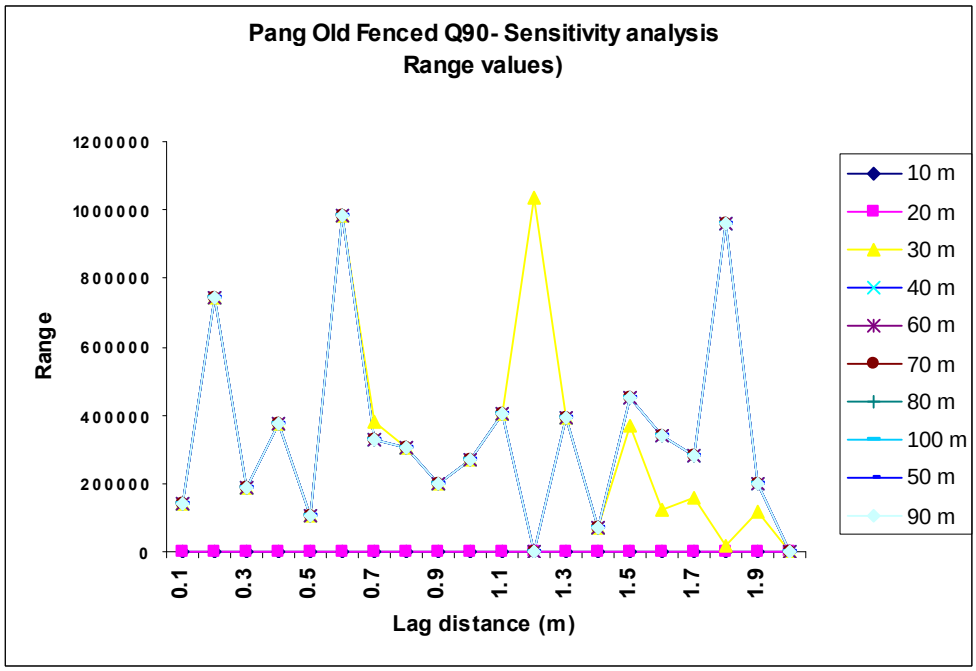
Pang Old Fenced Q90- Sensitivity analysis
Range values)
Range
1200000
1000000
800000
600000
400000
200000
0
0.1
0.3
0.5
0.7
0.9
1.1
1.3
1.5
1.7
1.9
Lag distance (m)
10 m
20 m
30 m
40 m
60 m
70 m
80 m
100 m
50 m
90 m

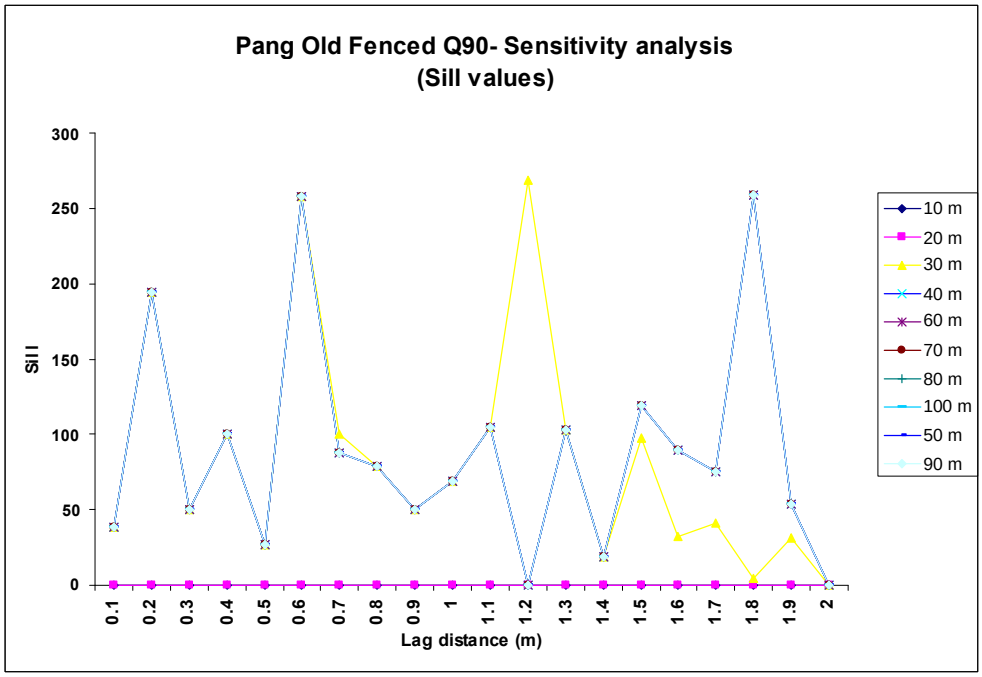
Pang Old Fenced Q90- Sensitivity analysis
(Sill values)
Sill
300
250
200
150
100
50
0
0.1
0.2
0.3
0.4
0.5
0.6
0.7
0.8
0.9
1
1.1
1.2
1.3
1.4
1.5
1.6
1.7
1.8
1.9
2
Lag distance (m)
10 m
20 m
30 m
40 m
60 m
70 m
80 m
100 m
50 m
90 m

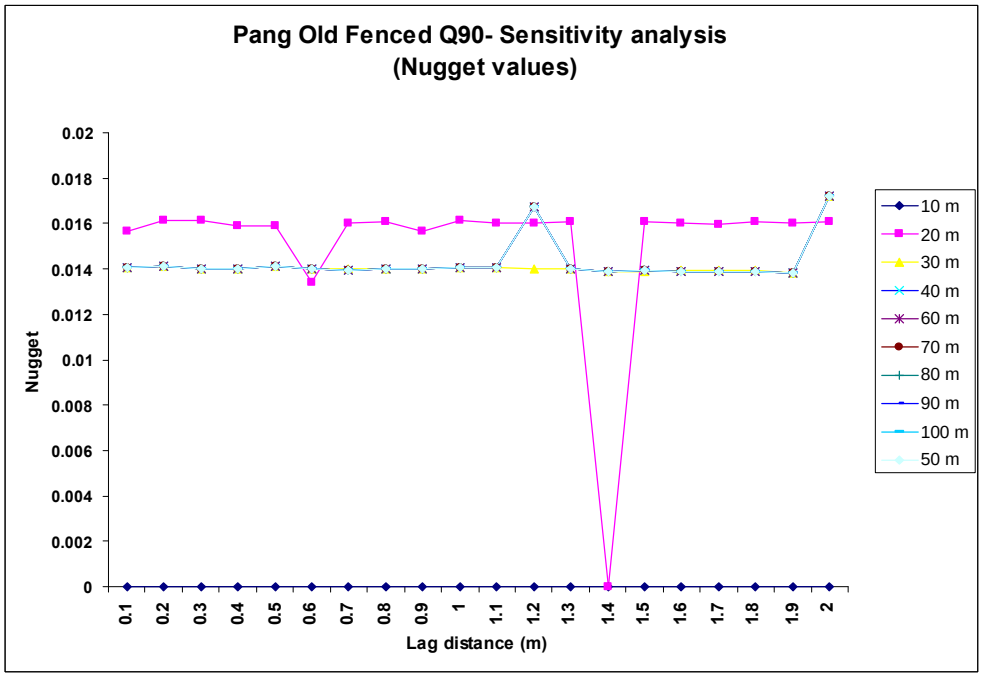
Pang Old Fenced Q90- Sensitivity analysis
(Nugget values)
Nugget
0.02
0.018
0.016
0.014
0.012
0.01
0.008
0.006
0.004
0.002
0
0.1
0.2
0.3
0.4
0.5
0.6
0.7
0.8
0.9
1
1.1
1.2
1.3
1.4
1.5
1.6
1.7
1.8
1.9
2
Lag distance (m)
10 m
20 m
30 m
40 m
60 m
70 m
80 m
90 m
100 m
50 m

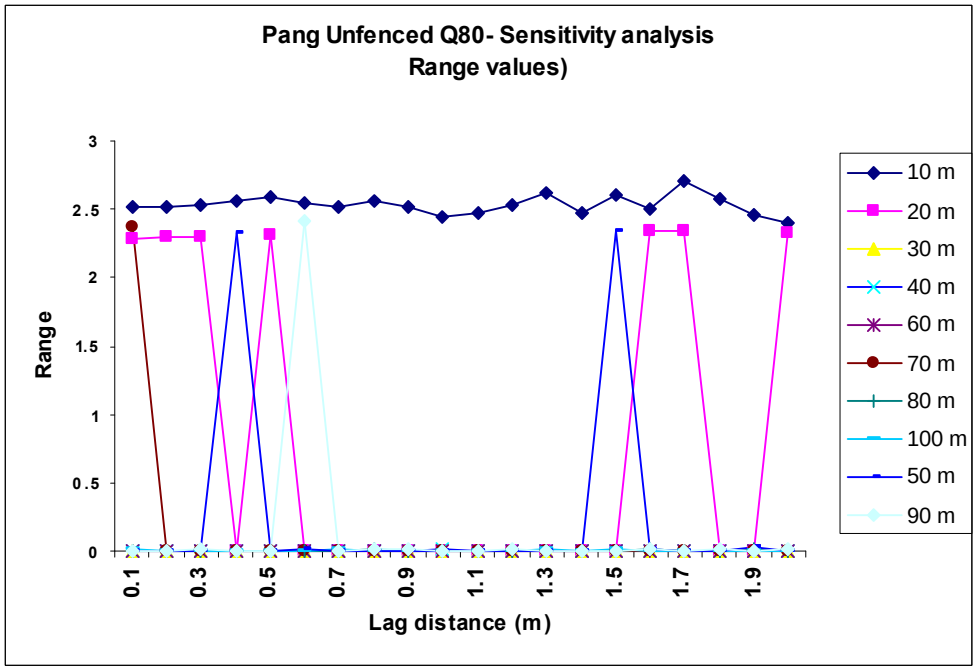
Pang Unfenced Q80- Sensitivity analysis
Range values)
Range
Lag distance (m)
10 m
20 m
30 m
40 m
60 m
70 m
80 m
100 m
50 m
90 m

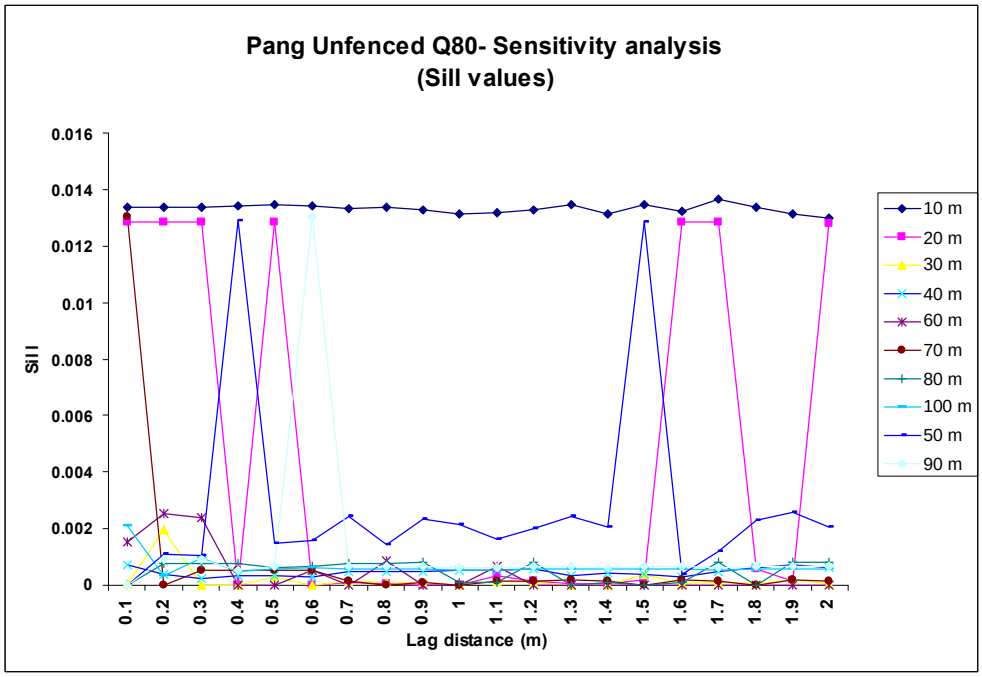
Pang Unfenced Q80- Sensitivity analysis
(Sill values)
Sill
Lag distance (m)
10 m
20 m
30 m
40 m
60 m
70 m
80 m
100 m
50 m
90 m

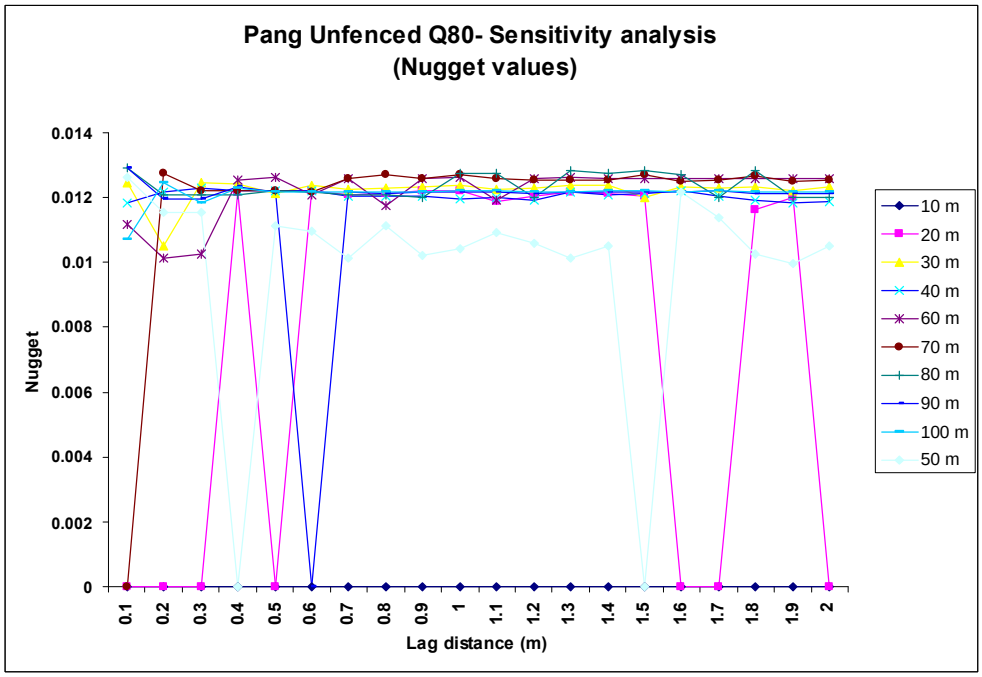
Pang Unfenced Q80- Sensitivity analysis
(Nugget values)
Nugget
Lag distance (m)
10 m
20 m
30 m
40 m
60 m
70 m
80 m
90 m
100 m
50 m

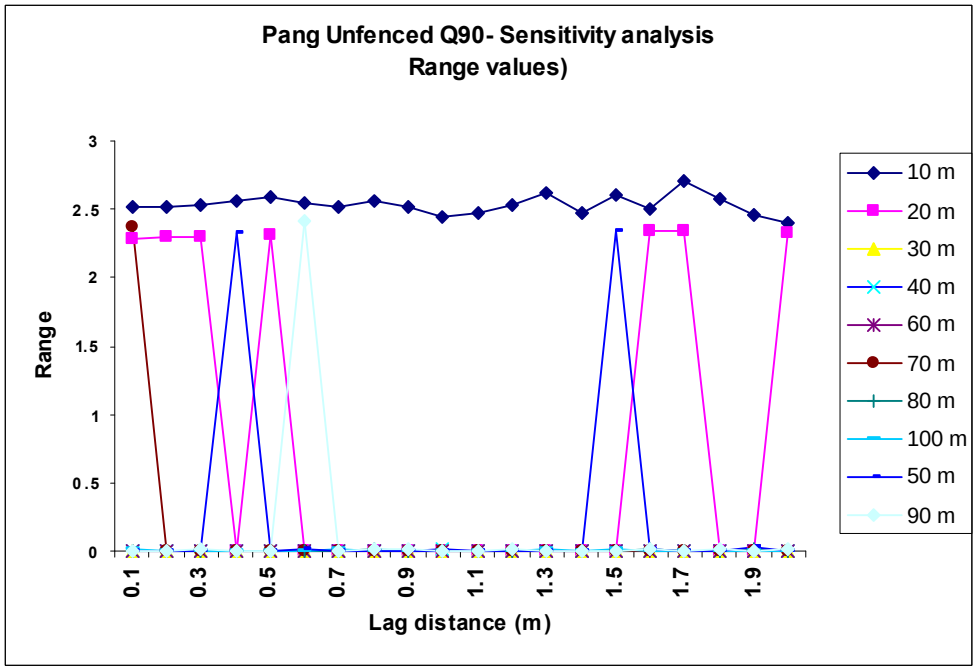
Pang Unfenced Q90- Sensitivity analysis
Range values)
Range
Lag distance (m)
10 m
20 m
30 m
40 m
60 m
70 m
80 m
100 m
50 m
90 m

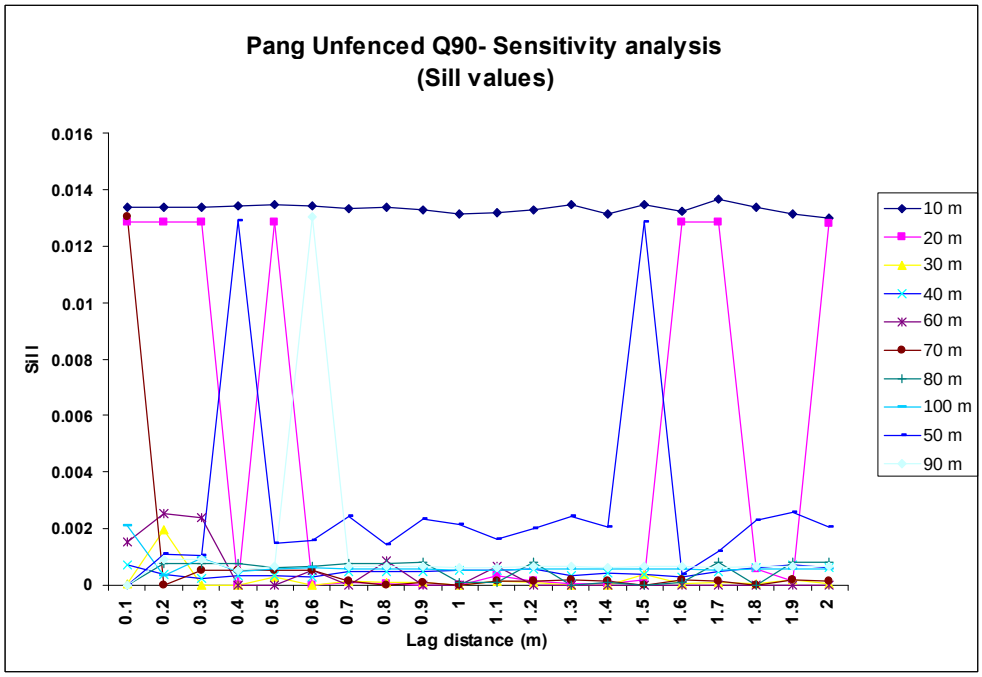
Pang Unfenced Q90- Sensitivity analysis
(Sill values)
Sill
Lag distance (m)
10 m
20 m
30 m
40 m
60 m
70 m
80 m
100 m
50 m
90 m

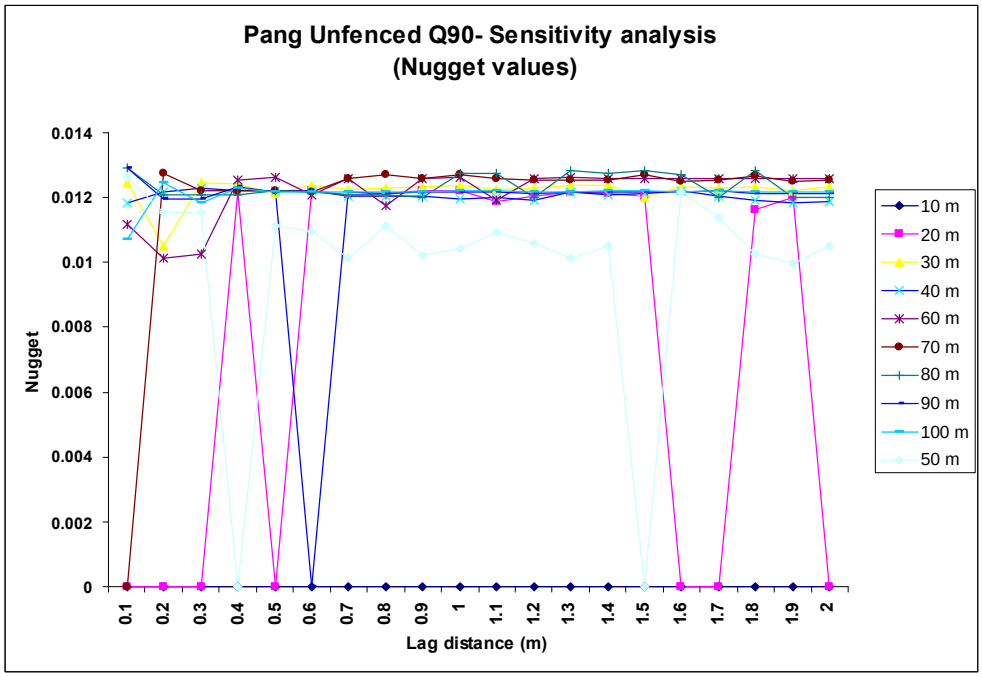
Pang Unfenced Q90- Sensitivity analysis
(Nugget values)
Nugget
Lag distance (m)
10 m
20 m
30 m
40 m
60 m
70 m
80 m
90 m
100 m
50 m

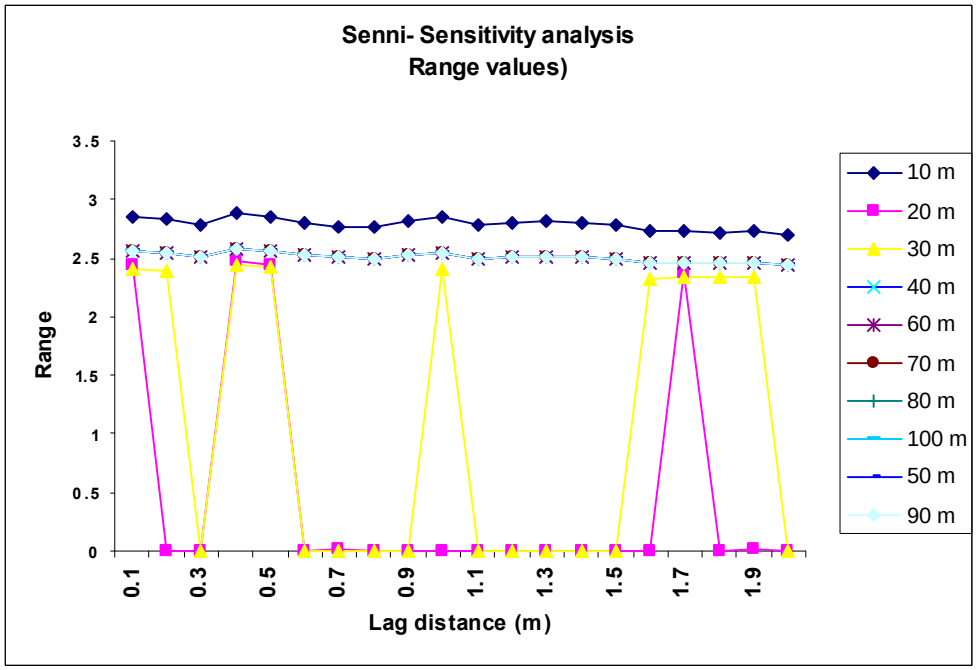
Senni- Sensitivity analysis
Range values)
Range
Lag distance (m)
10 m
20 m
30 m
40 m
60 m
70 m
80 m
100 m
50 m
90 m

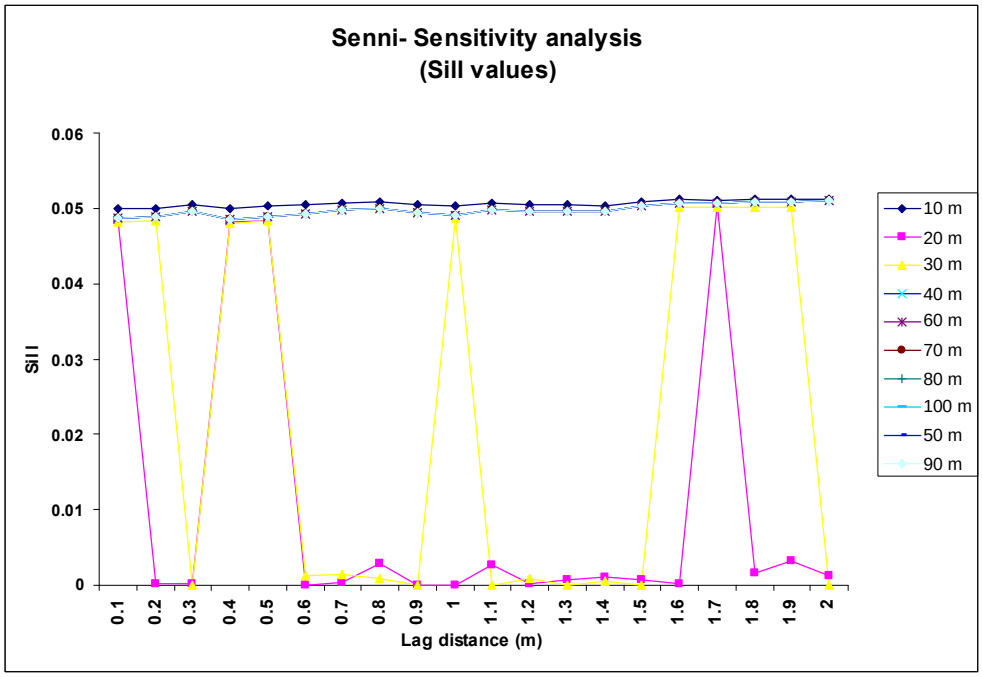
Senni- Sensitivity analysis
(Sill values)
Sill
Lag distance (m)
10 m
20 m
30 m
40 m
60 m
70 m
80 m
100 m
50 m
90 m

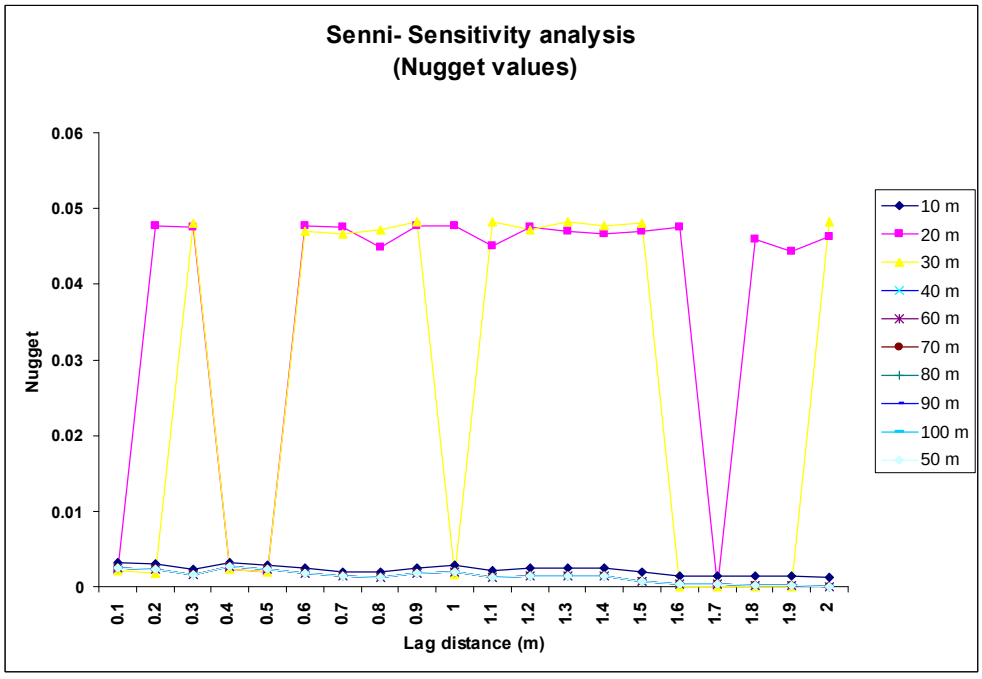
Senni- Sensitivity analysis
(Nugget values)
Nugget
Lag distance (m)
10 m
20 m
30 m
40 m
60 m
70 m
80 m
90 m
100 m
50 m

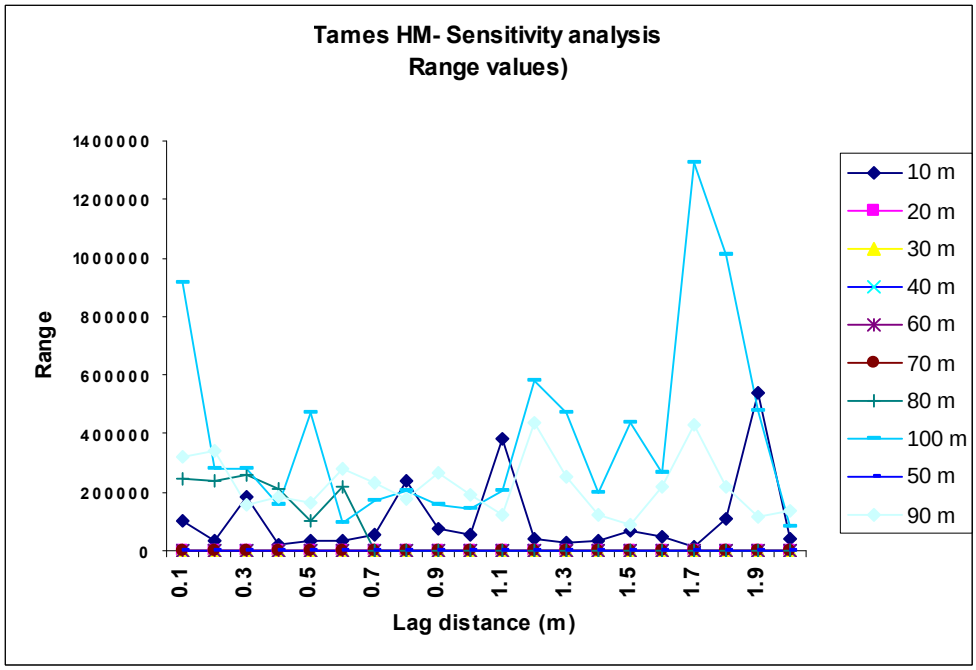
Tames HM- Sensitivity analysis
Range values)
Range
1400000
1200000
1000000
800000
600000
400000
200000
0
0.1
0.3
0.5
0.7
0.9
1.1
1.3
1.5
1.7
1.9
Lag distance (m)
10 m
20 m
30 m
40 m
60 m
70 m
80 m
100 m
50 m
90 m

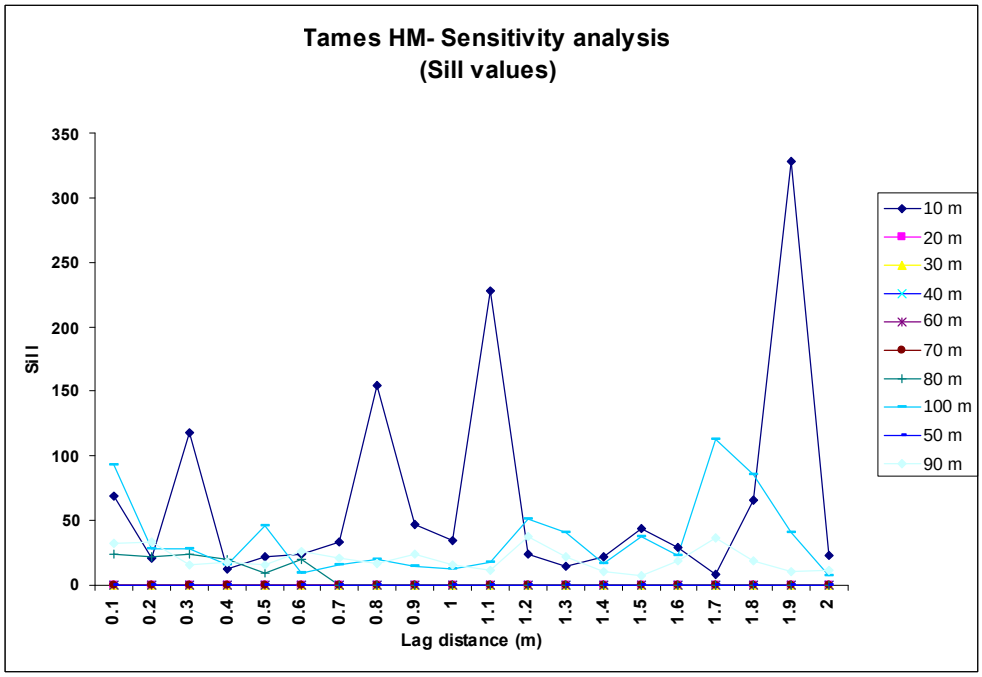
Tames HM- Sensitivity analysis
(Sill values)
Sill
350
300
250
200
150
100
50
0
0.1
0.2
0.3
0.4
0.5
0.6
0.7
0.8
0.9
1
1.1
1.2
1.3
1.4
1.5
1.6
1.7
1.8
1.9
2
Lag distance (m)
10 m
20 m
30 m
40 m
60 m
70 m
80 m
100 m
50 m
90 m

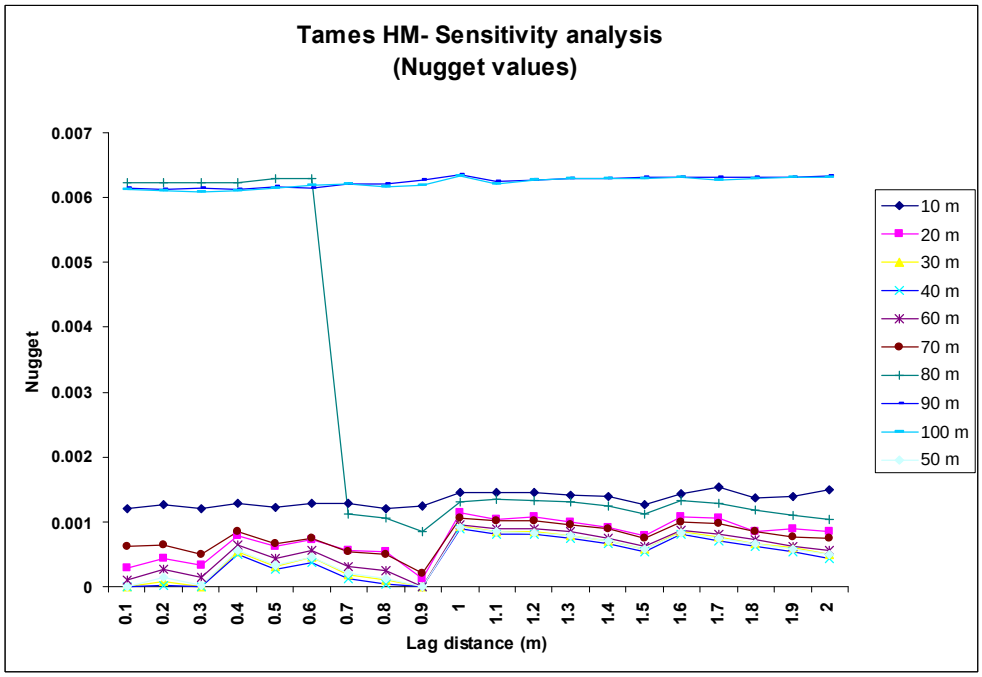
Tames HM- Sensitivity analysis
(Nugget values)
Nugget
0.007
0.006
0.005
0.004
0.003
0.002
0.001
0
0.1
0.2
0.3
0.4
0.5
0.6
0.7
0.8
0.9
1
1.1
1.2
1.3
1.4
1.5
1.6
1.7
1.8
1.9
2
Lag distance (m)
10 m
20 m
30 m
40 m
60 m
70 m
80 m
90 m
100 m
50 m

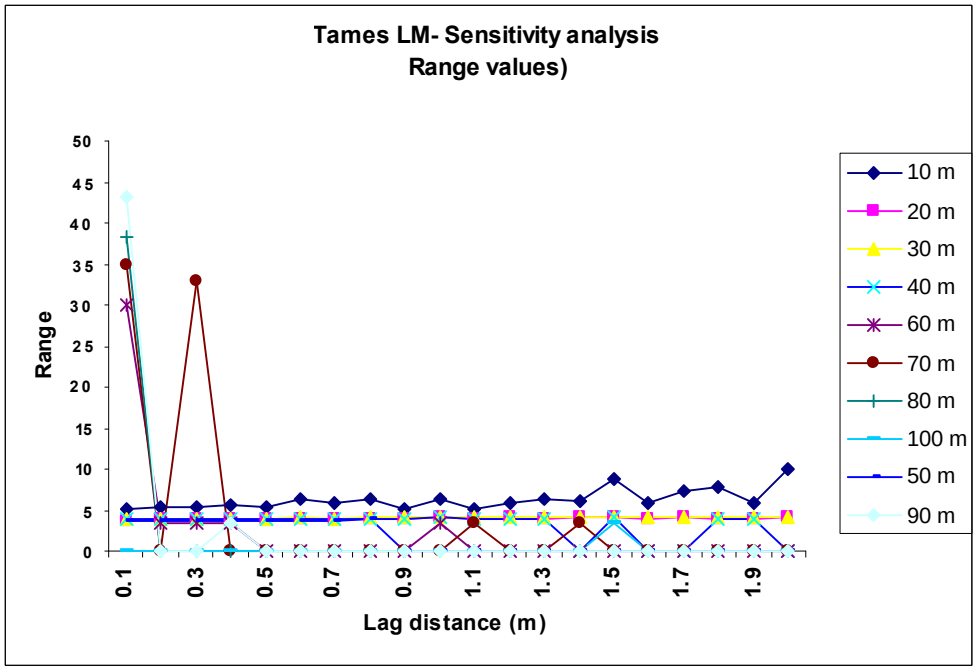
Tames LM- Sensitivity analysis
Range values)
Range
Lag distance (m)
10 m
20 m
30 m
40 m
60 m
70 m
80 m
100 m
50 m
90 m

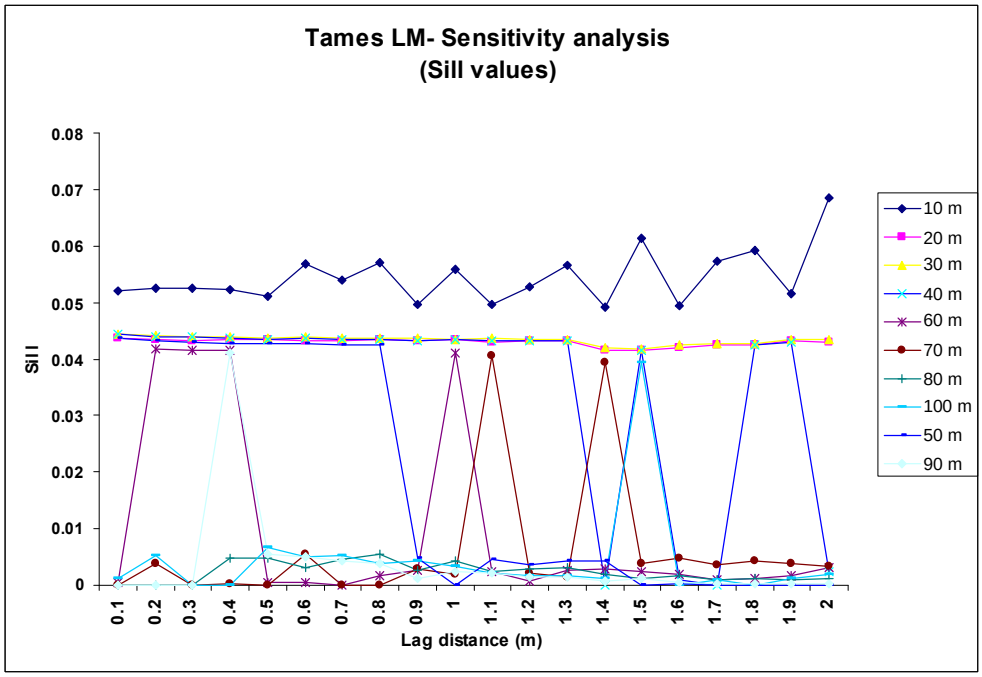
Tames LM- Sensitivity analysis
(Sill values)
Sill
Lag distance (m)
10 m
20 m
30 m
40 m
60 m
70 m
80 m
100 m
50 m
90 m

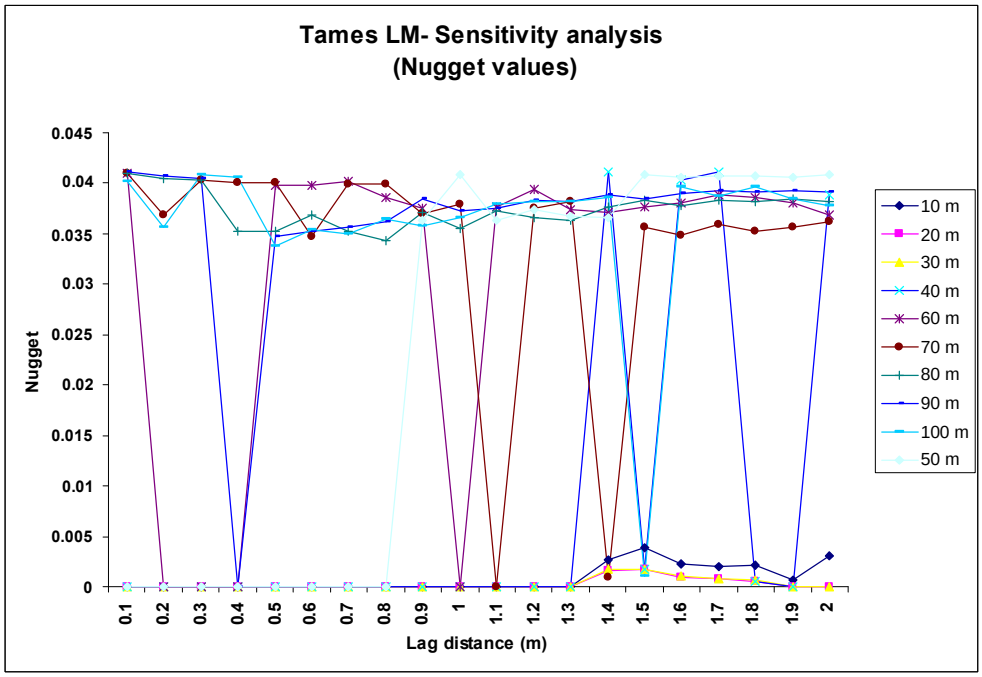
Tames LM- Sensitivity analysis
(Nugget values)
Nugget
Lag distance (m)
10 m
20 m
30 m
40 m
60 m
70 m
80 m
90 m
100 m
50 m

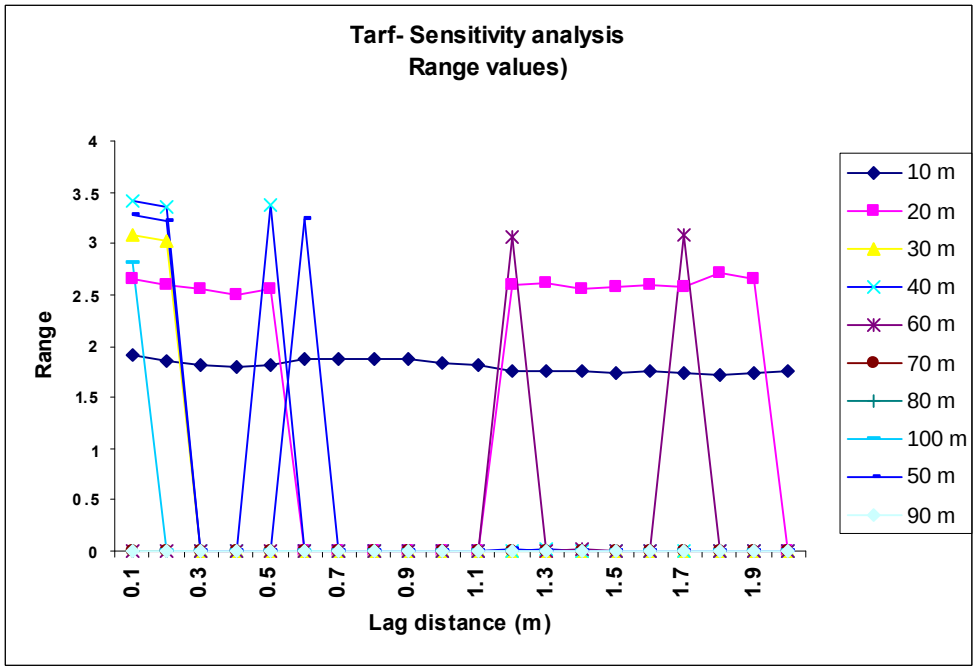
Tarf- Sensitivity analysis
Range values)
Range
Lag distance (m)
10 m
20 m
30 m
40 m
60 m
70 m
80 m
100 m
50 m
90 m

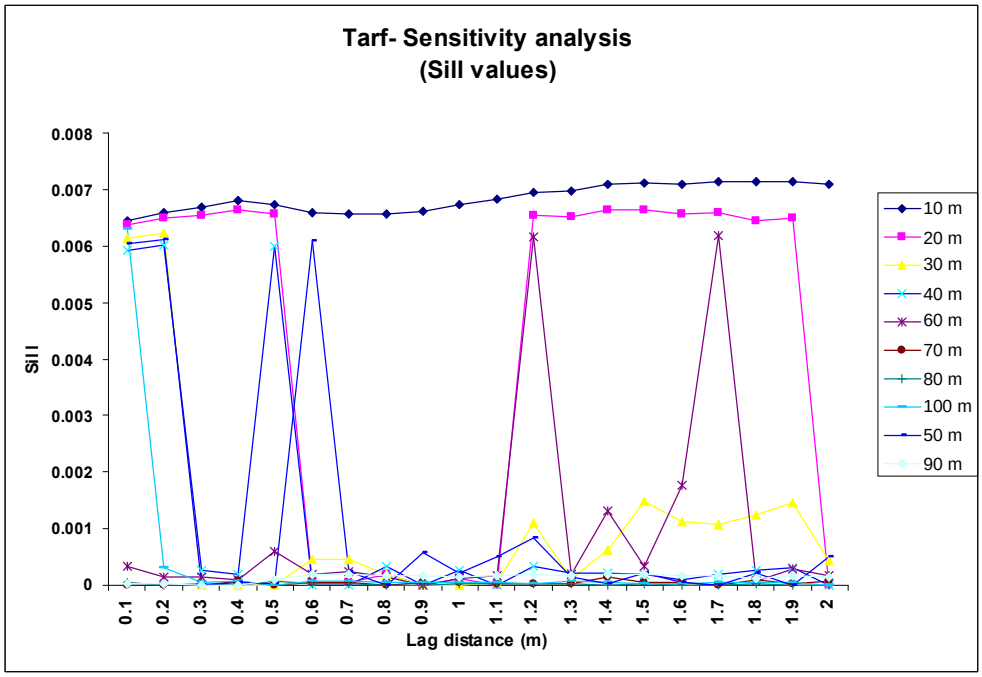
Tarf- Sensitivity analysis
(Sill values)
Sill
Lag distance (m)
10 m
20 m
30 m
40 m
60 m
70 m
80 m
100 m
50 m
90 m

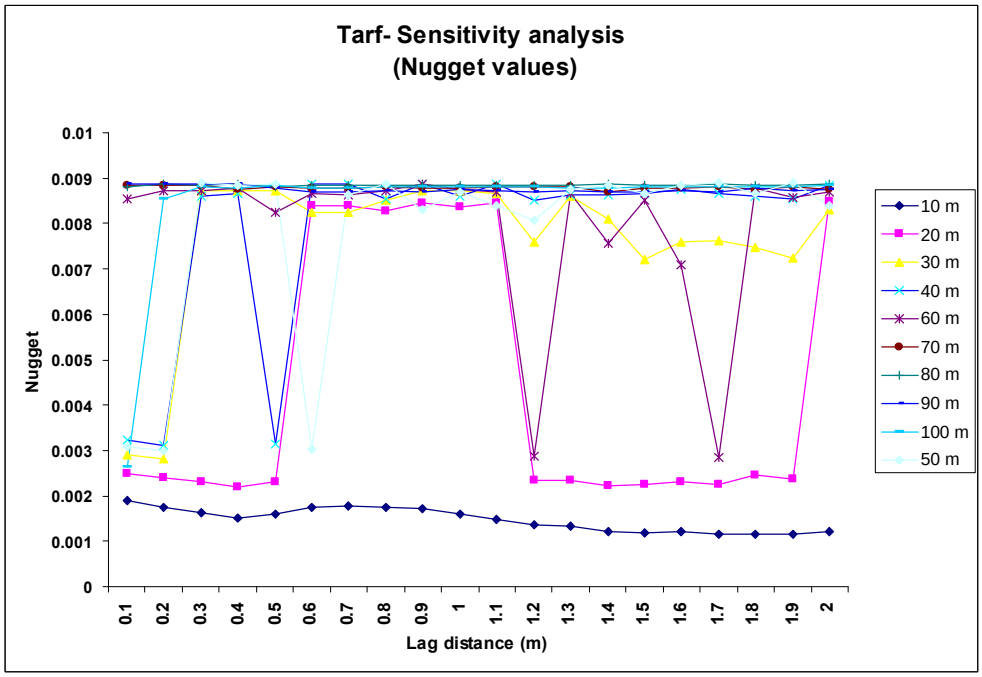
Tarf- Sensitivity analysis
(Nugget values)
Nugget
Lag distance (m)
10 m
20 m
30 m
40 m
60 m
70 m
80 m
90 m
100 m
50 m

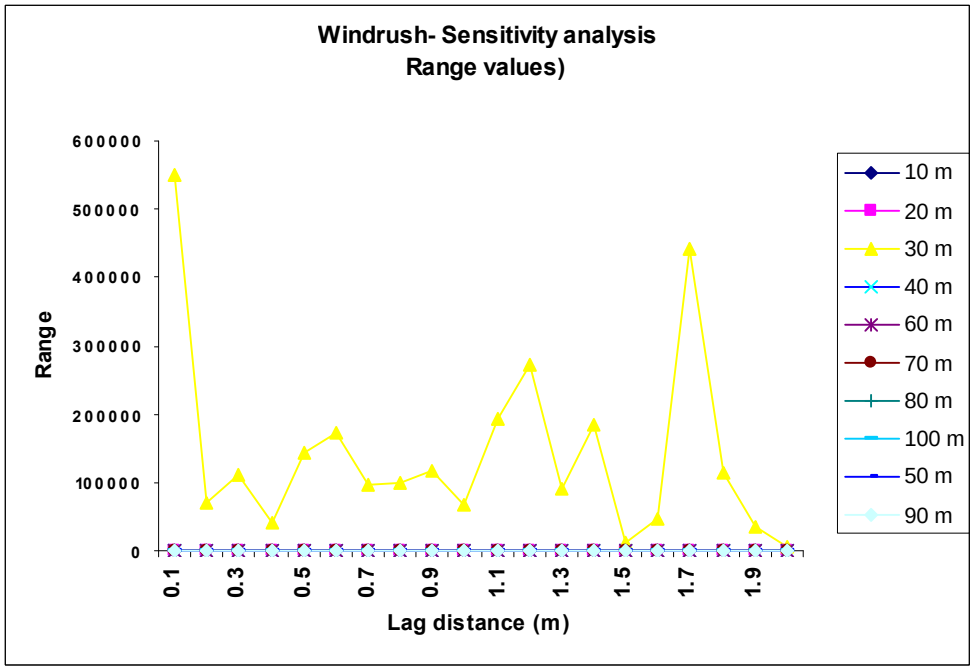
Windrush- Sensitivity analysis
Range values)
Range
600000
500000
400000
300000
200000
100000
0
0.1
0.3
0.5
0.7
0.9
1.1
1.3
1.5
1.7
1.9
Lag distance (m)
10 m
20 m
30 m
40 m
60 m
70 m
80 m
100 m
50 m
90 m

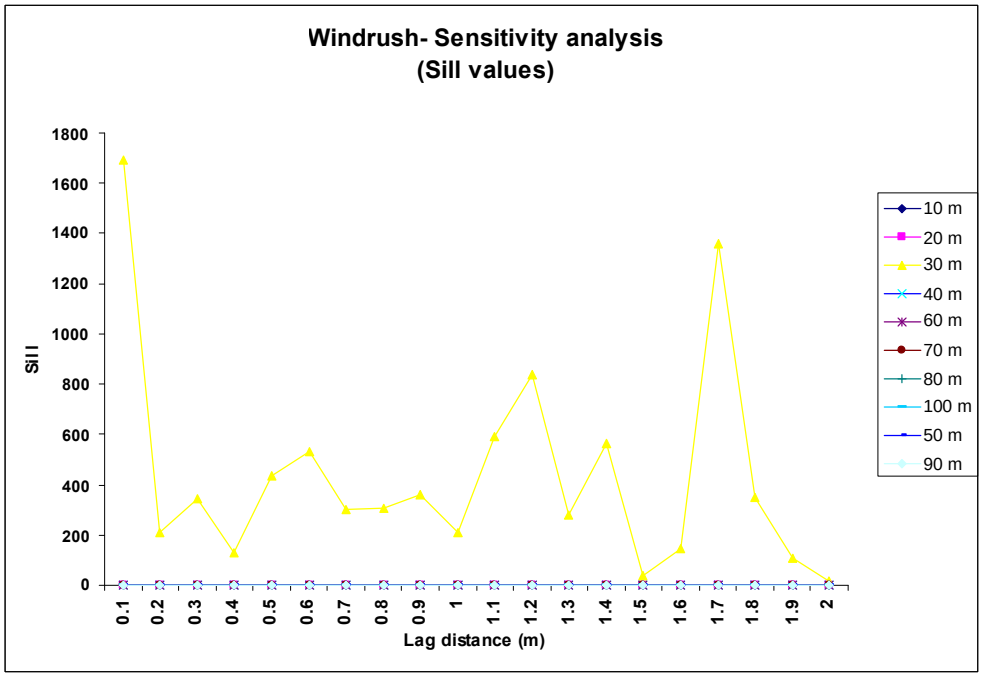
Windrush- Sensitivity analysis
(Sill values)
Sill
1800
1600
1400
1200
1000
800
600
400
200
0
0.1
0.2
0.3
0.4
0.5
0.6
0.7
0.8
0.9
1
1.1
1.2
1.3
1.4
1.5
1.6
1.7
1.8
1.9
2
Lag distance (m)
10 m
20 m
30 m
40 m
60 m
70 m
80 m
100 m
50 m
90 m

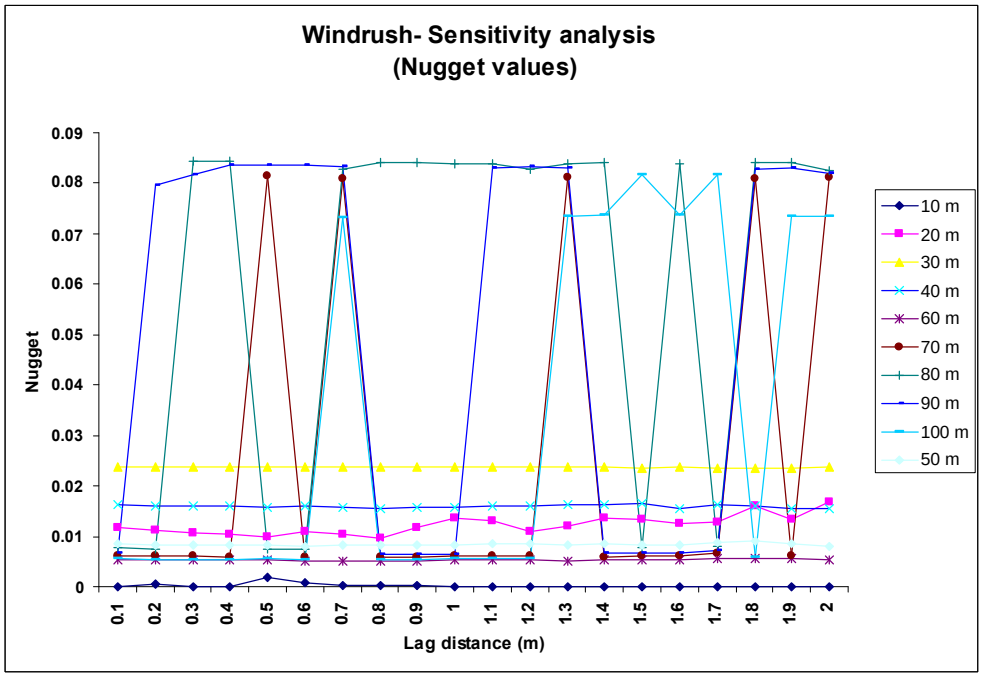
Windrush- Sensitivity analysis
(Nugget values)
Nugget
0.09
0.08
0.07
0.06
0.05
0.04
0.03
0.02
0.01
0
0.1
0.2
0.3
0.4
0.5
0.6
0.7
0.8
0.9
1
1.1
1.2
1.3
1.4
1.5
1.6
1.7
1.8
1.9
2
Lag distance (m)
10 m
20 m
30 m
40 m
60 m
70 m
80 m
90 m
100 m
50 m

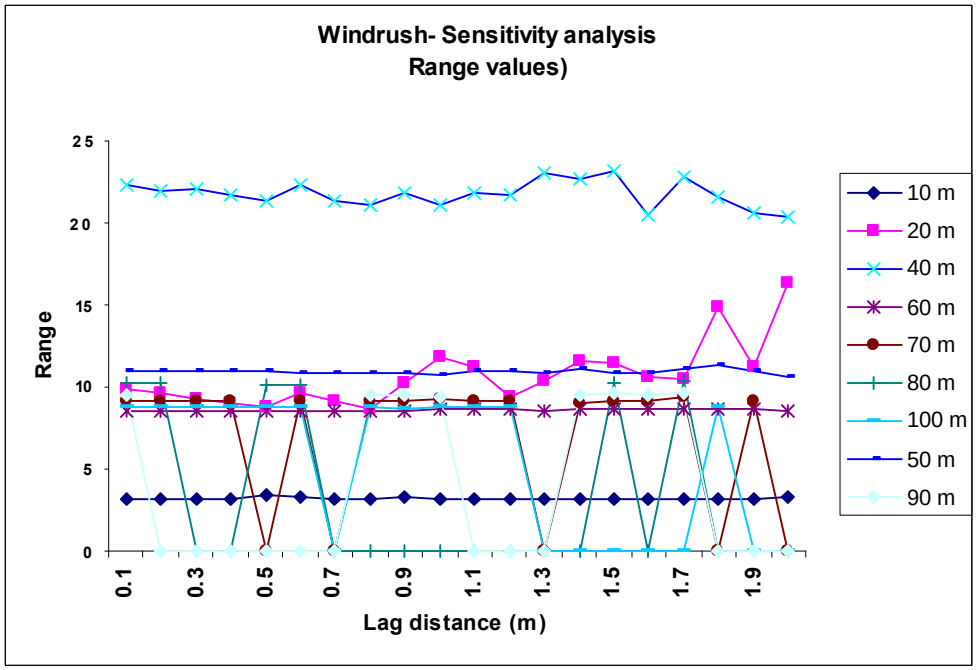
Windrush- Sensitivity analysis
Range values)
Range
Lag distance (m)
10 m
20 m
40 m
60 m
70 m
80 m
100 m
50 m
90 m

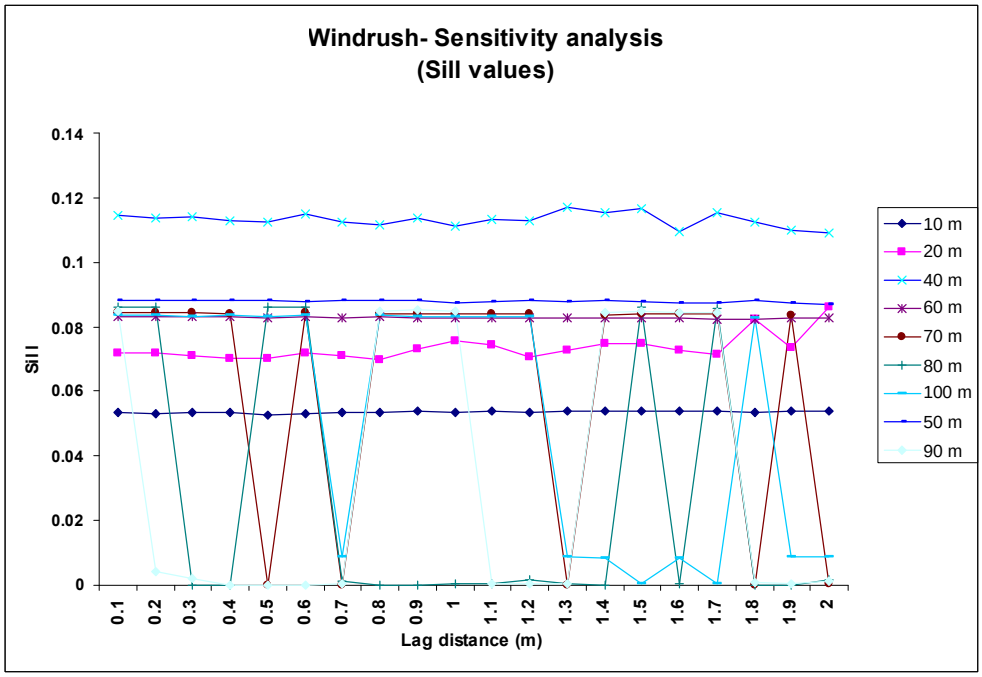
Windrush- Sensitivity analysis
(Sill values)
Sill
Lag distance (m)
10 m
20 m
40 m
60 m
70 m
80 m
100 m
50 m
90 m

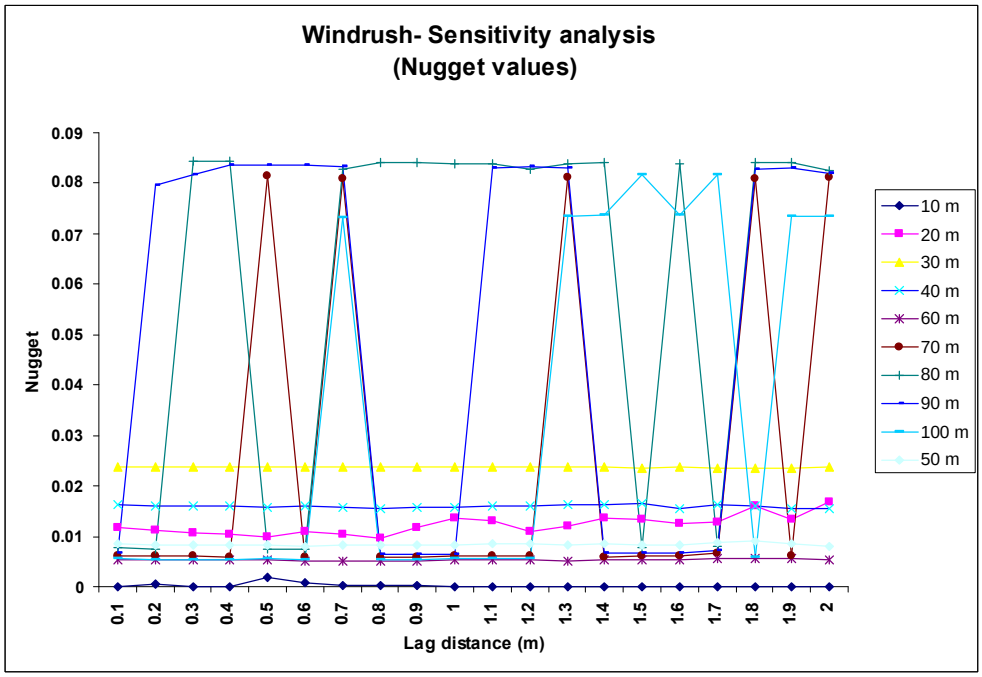
Windrush- Sensitivity analysis
(Nugget values)
Nugget
Lag distance (m)
10 m
20 m
30 m
40 m
60 m
70 m
80 m
90 m
100 m
50 m

Appendix 3.5.4

Results obtained for the analysis in Chapter 5 –Sensitivity Analysis – Variogram values for combinations of lag and maximum distance considered: spherical variogram for wet points.

This appendix summarises the results obtained for the sensitivity analysis developed in section 5.4.3. for the combination of lag distances and maximum distances selected. Results presented in this section only include the graphical output for the data sets analysed with wet points. The horizontal axis represents the selected lag distance. The variogram model analysed is the spherical one. Three different outputs, one for each variogram variable analysed (i.e. range, sill and nugget) are presented for each river site. Those river sites that had extreme variogram values are included twice: the graphical output is presented with two different axis scales so results can be better analysed.

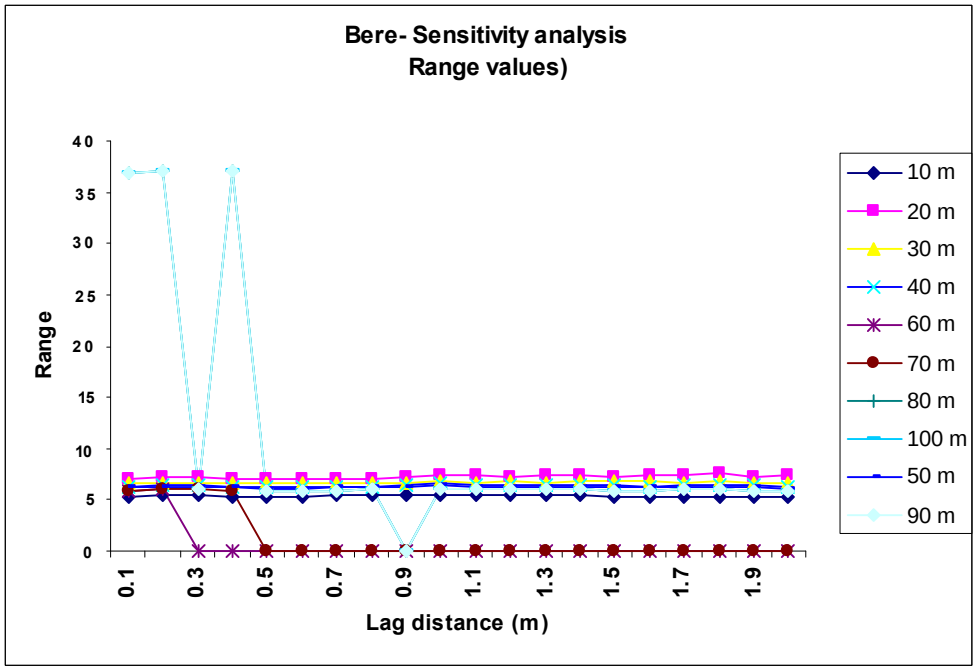
Bere- Sensitivity analysis
Range values)
Range
Lag distance (m)
10 m
20 m
30 m
40 m
60 m
70 m
80 m
100 m
50 m
90 m

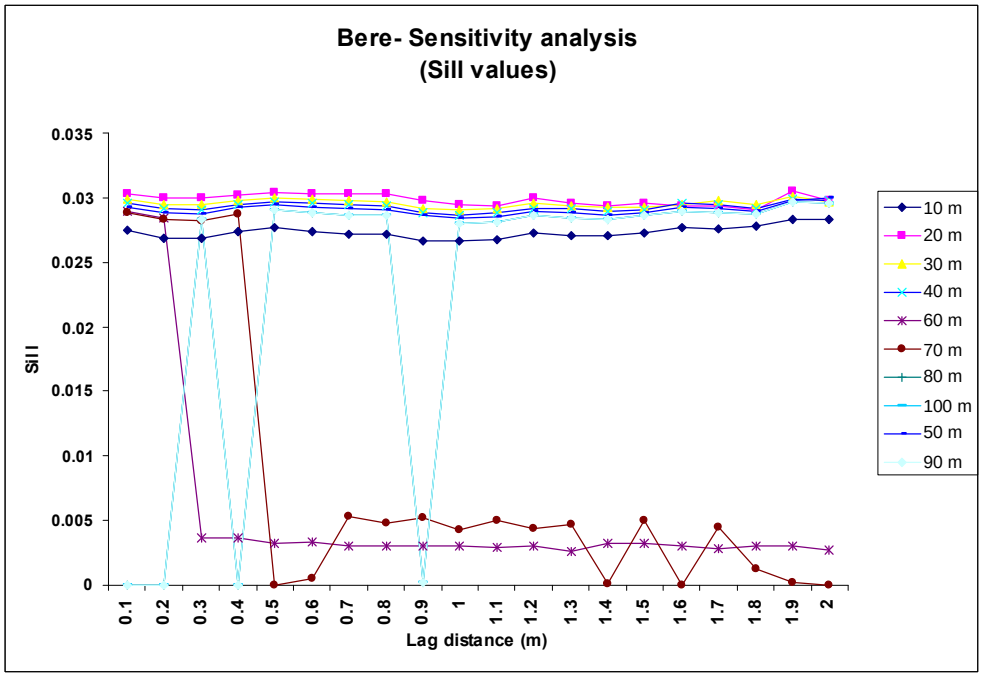
Bere- Sensitivity analysis
(Sill values)
Sill
Lag distance (m)
10 m
20 m
30 m
40 m
60 m
70 m
80 m
100 m
50 m
90 m

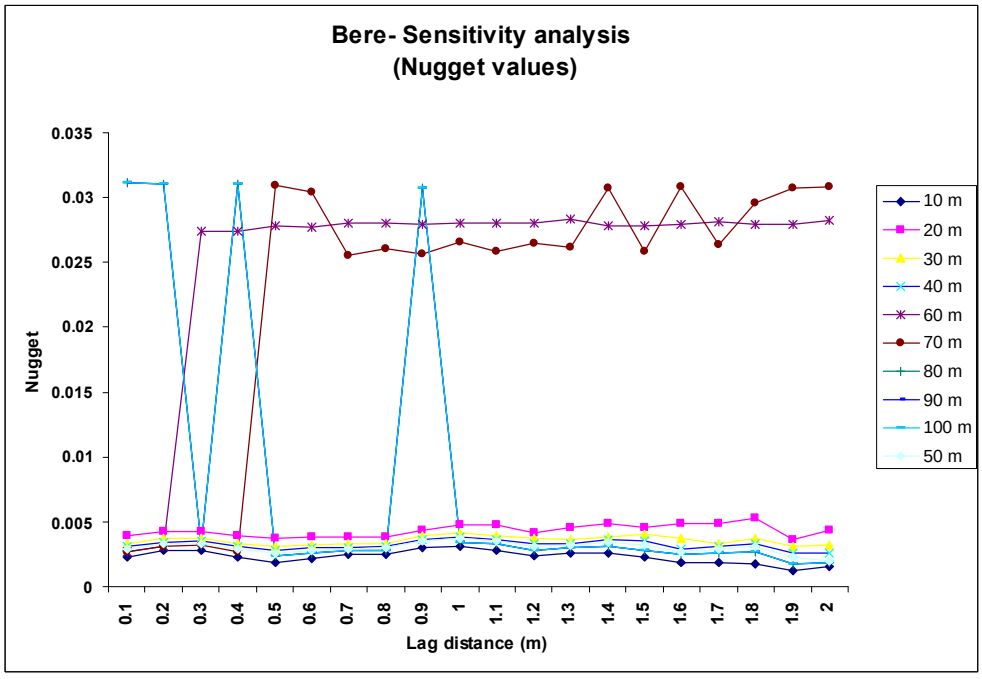
Bere- Sensitivity analysis
(Nugget values)
Nugget
Lag distance (m)
10 m
20 m
30 m
40 m
60 m
70 m
80 m
90 m
100 m
50 m

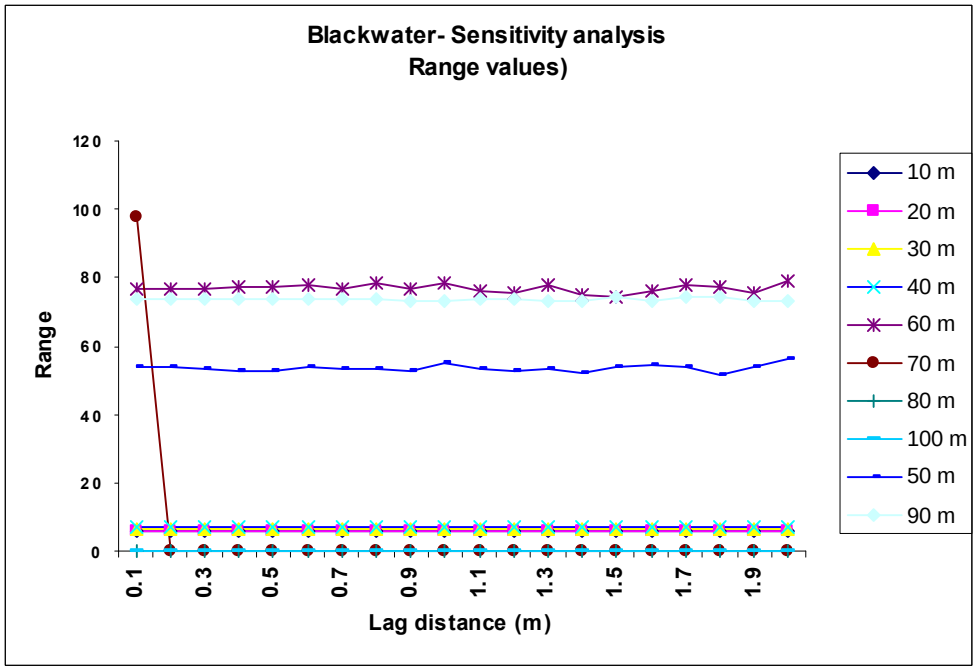
Blackwater- Sensitivity analysis
Range values)
Range
120
100
80
60
40
20
0
0.1
0.3
0.5
0.7
0.9
1.1
1.3
1.5
1.7
1.9
Lag distance (m)
10 m
20 m
30 m
40 m
60 m
70 m
80 m
100 m
50 m
90 m

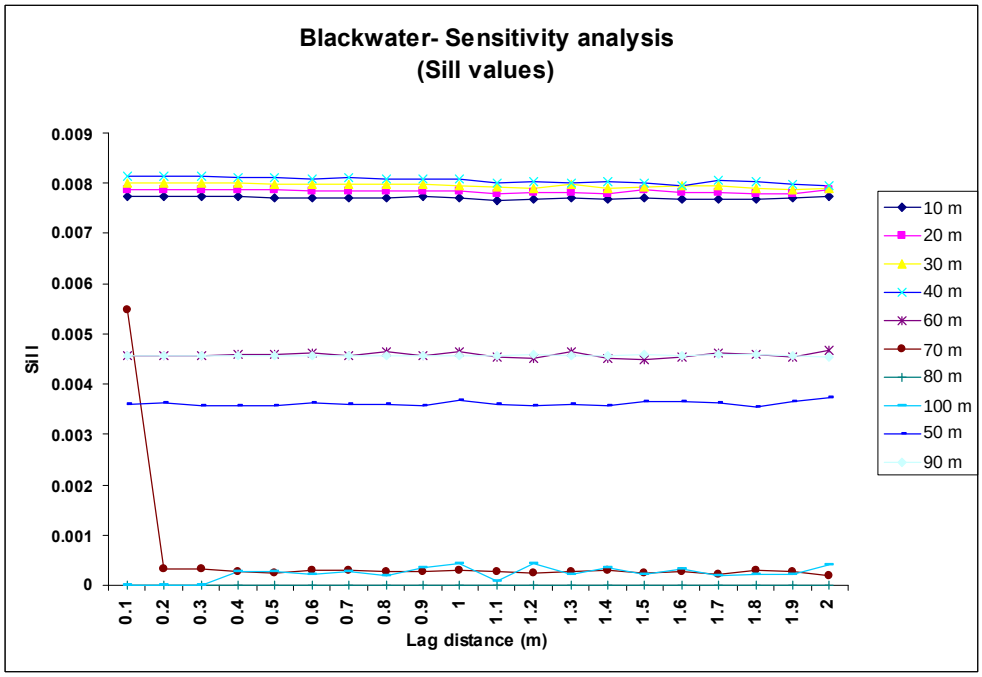
Blackwater- Sensitivity analysis
(Sill values)
Sill
0.009
0.008
0.007
0.006
0.005
0.004
0.003
0.002
0.001
0
0.1
0.2
0.3
0.4
0.5
0.6
0.7
0.8
0.9
1
1.1
1.2
1.3
1.4
1.5
1.6
1.7
1.8
1.9
2
Lag distance (m)
10 m
20 m
30 m
40 m
60 m
70 m
80 m
100 m
50 m
90 m

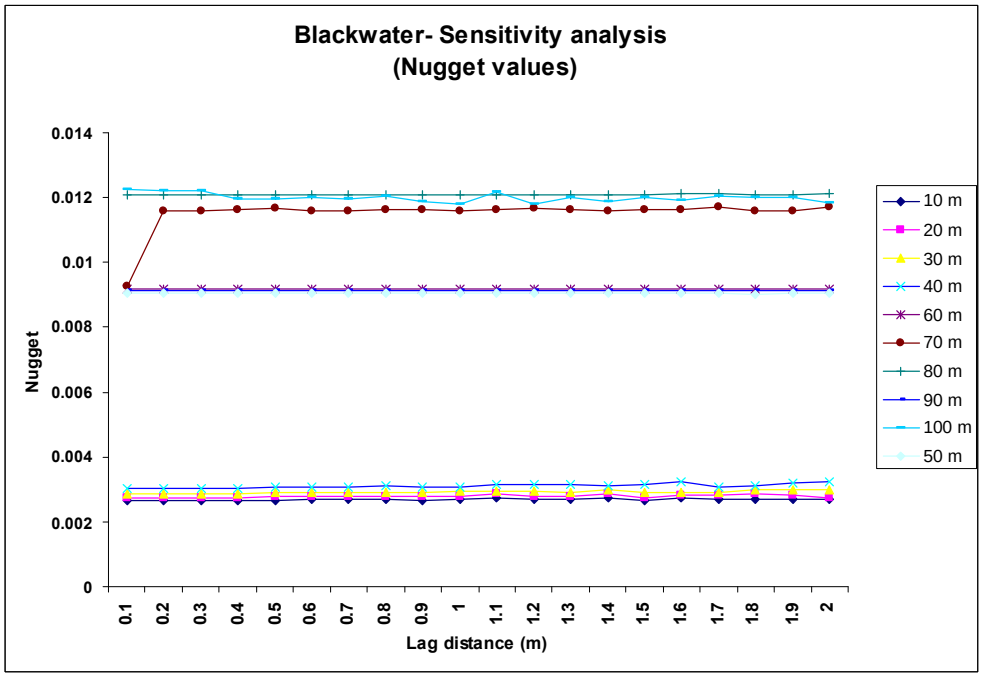
Blackwater- Sensitivity analysis
(Nugget values)
Nugget
0.014
0.012
0.01
0.008
0.006
0.004
0.002
0
0.1
0.2
0.3
0.4
0.5
0.6
0.7
0.8
0.9
1
1.1
1.2
1.3
1.4
1.5
1.6
1.7
1.8
1.9
2
Lag distance (m)
10 m
20 m
30 m
40 m
60 m
70 m
80 m
90 m
100 m
50 m

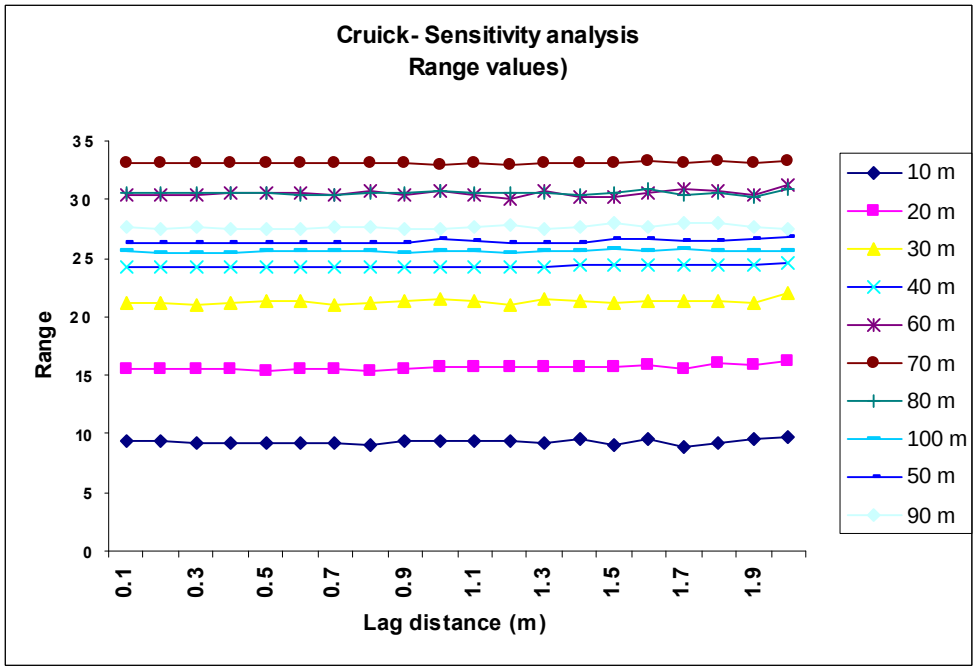
Cruick- Sensitivity analysis
Range values)
Range
Lag distance (m)
10 m
20 m
30 m
40 m
60 m
70 m
80 m
100 m
50 m
90 m

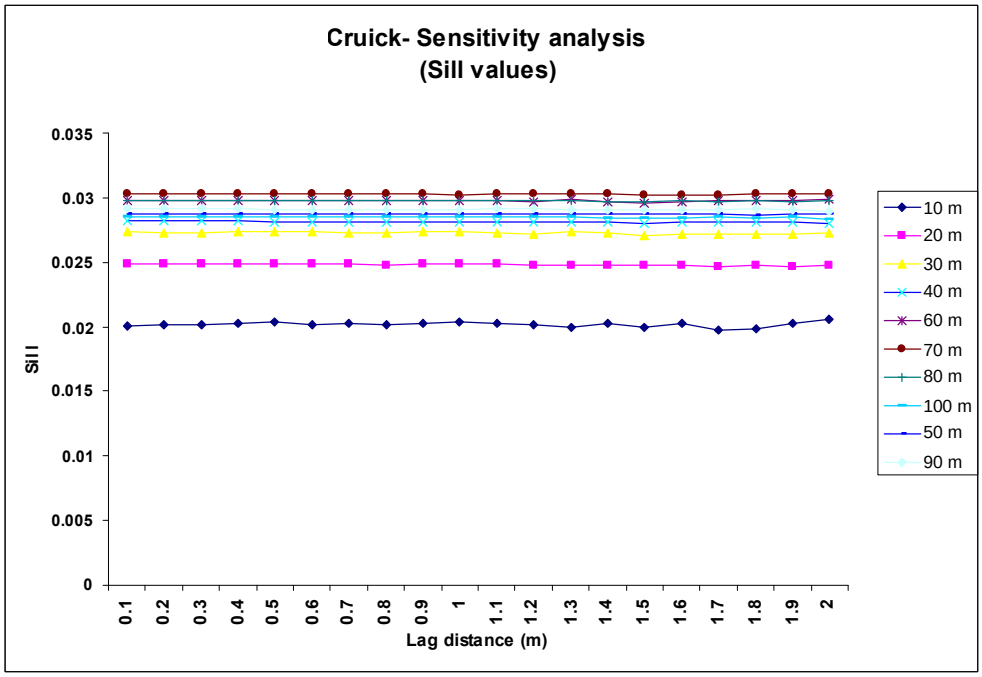
Cruick- Sensitivity analysis
(Sill values)
Sill
Lag distance (m)
10 m
20 m
30 m
40 m
60 m
70 m
80 m
100 m
50 m
90 m

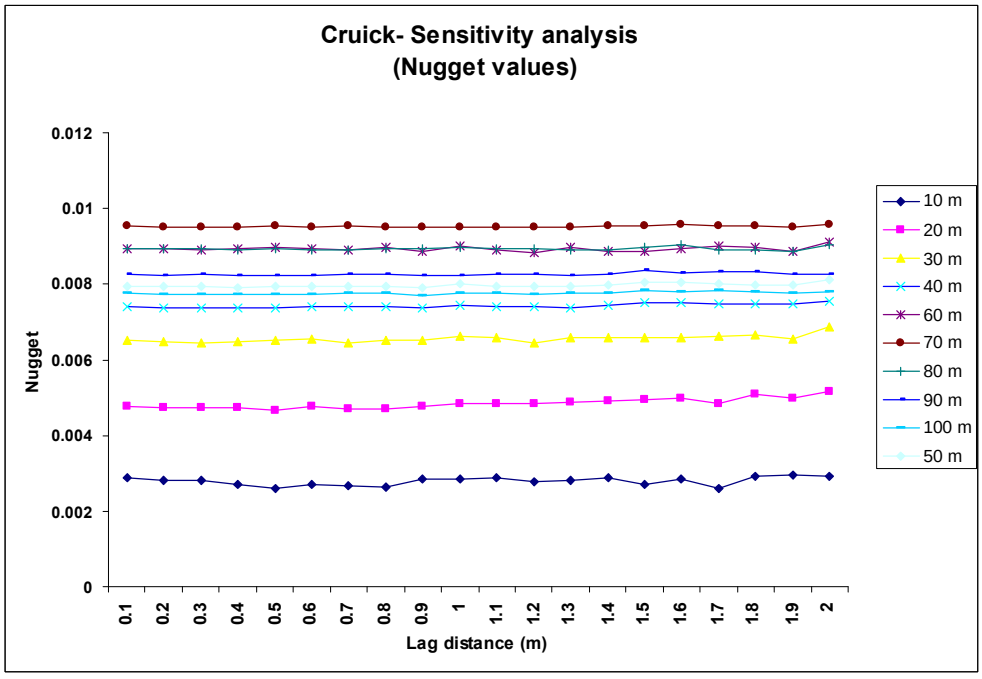
Cruick- Sensitivity analysis
(Nugget values)
Nugget
Lag distance (m)
10 m
20 m
30 m
40 m
60 m
70 m
80 m
90 m
100 m
50 m

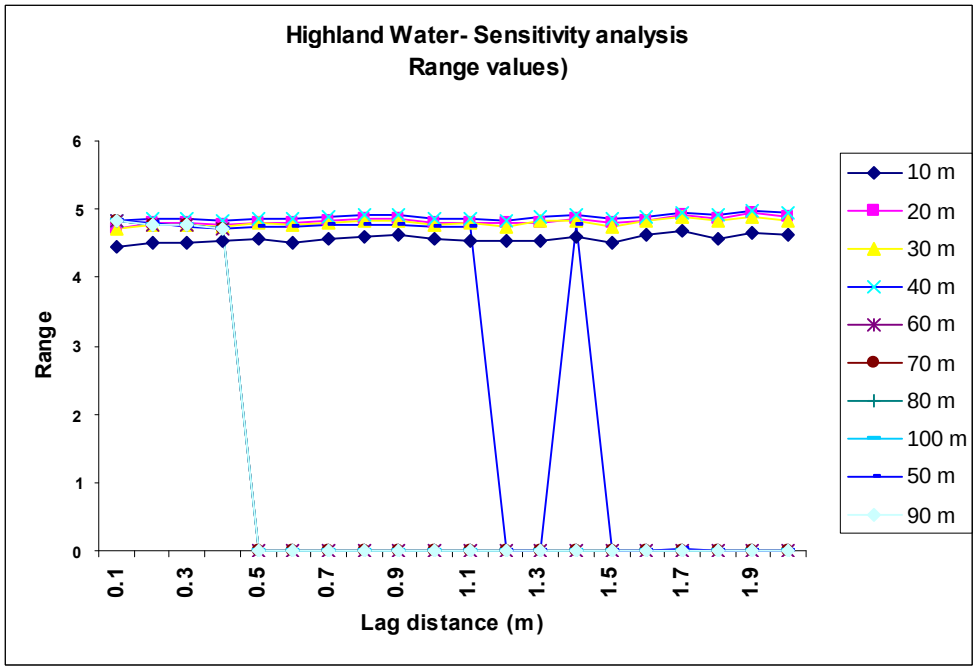
Highland Water- Sensitivity analysis
Range values)
Range
Lag distance (m)
10 m
20 m
30 m
40 m
60 m
70 m
80 m
100 m
50 m
90 m

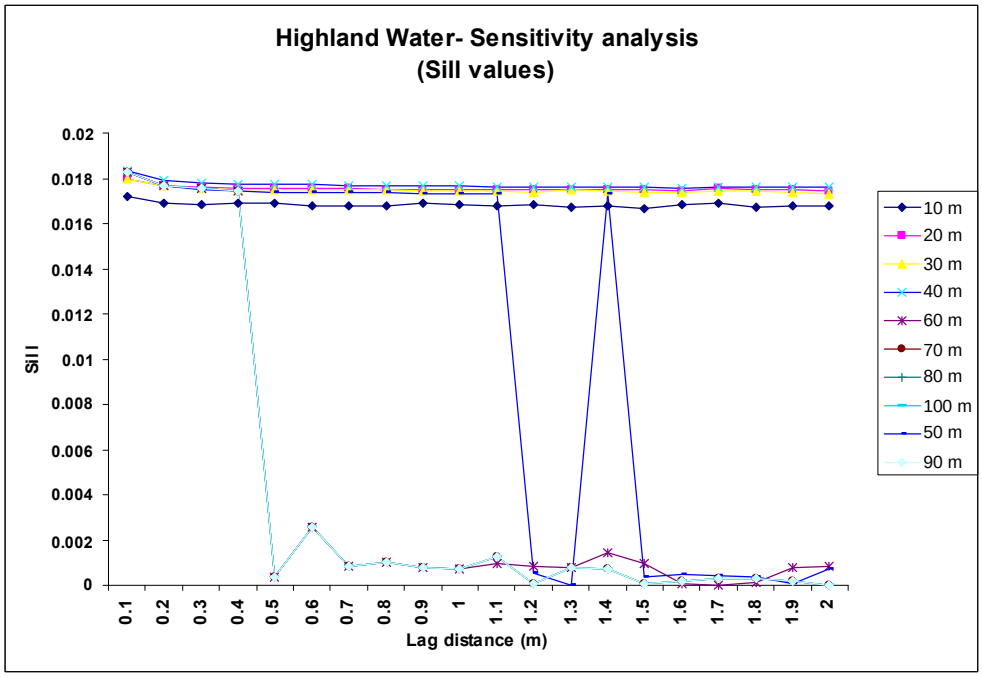
Highland Water- Sensitivity analysis
(Sill values)
Sill
Lag distance (m)
10 m
20 m
30 m
40 m
60 m
70 m
80 m
100 m
50 m
90 m

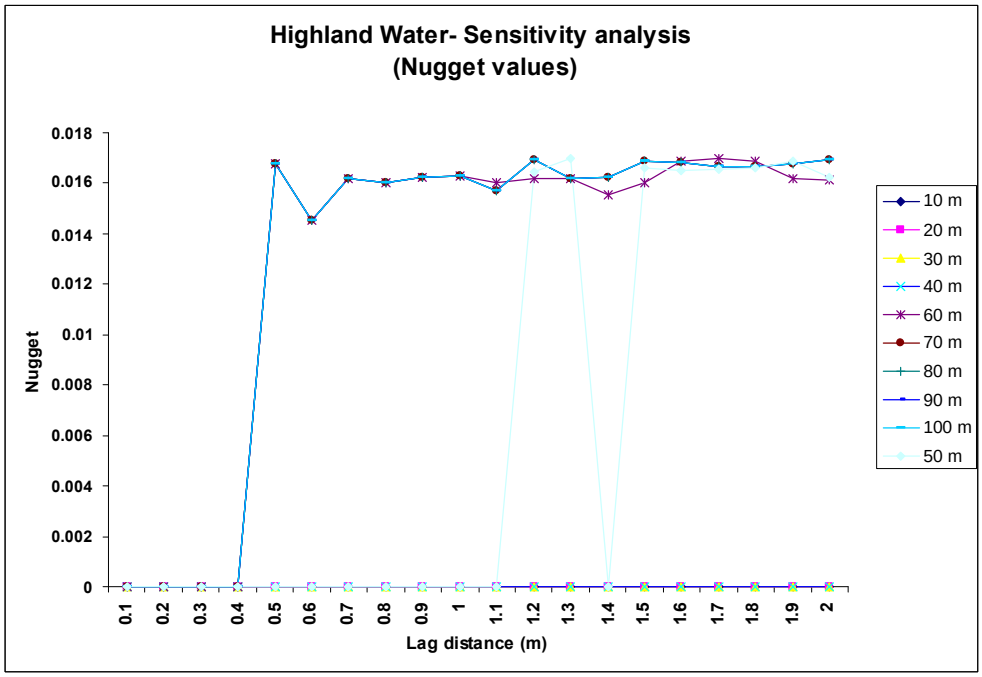
Highland Water- Sensitivity analysis
(Nugget values)
Nugget
Lag distance (m)
10 m
20 m
30 m
40 m
60 m
70 m
80 m
90 m
100 m
50 m

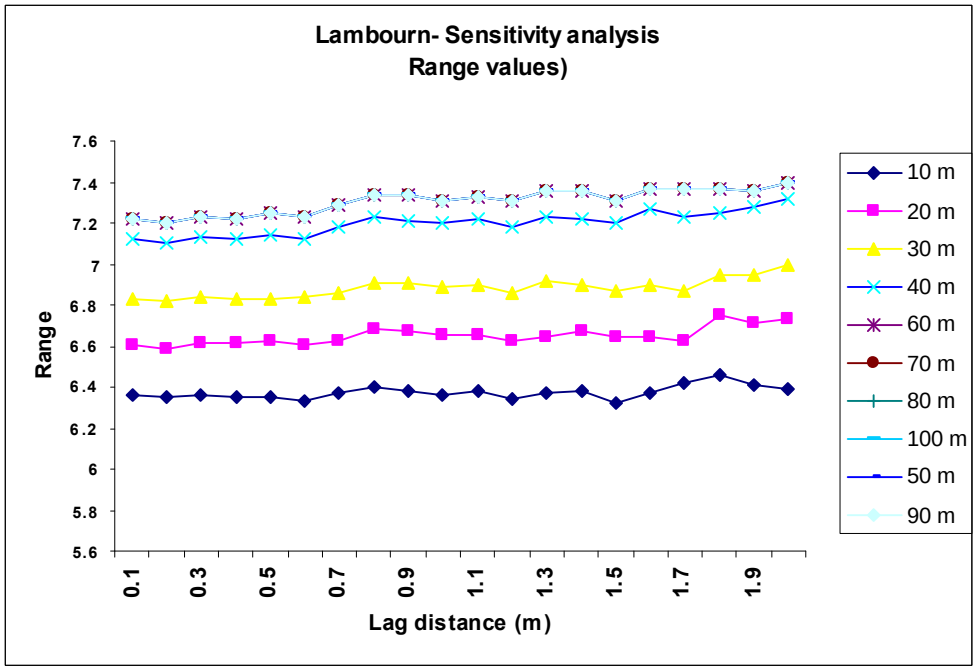
Lambourn- Sensitivity analysis
Range values)
Range
7.6
7.4
7.2
7
6.8
6.6
6.4
6.2
6
5.8
5.6
0.1
0.3
0.5
0.7
0.9
1.1
1.3
1.5
1.7
1.9
Lag distance (m)
10 m
20 m
30 m
40 m
60 m
70 m
80 m
100 m
50 m
90 m

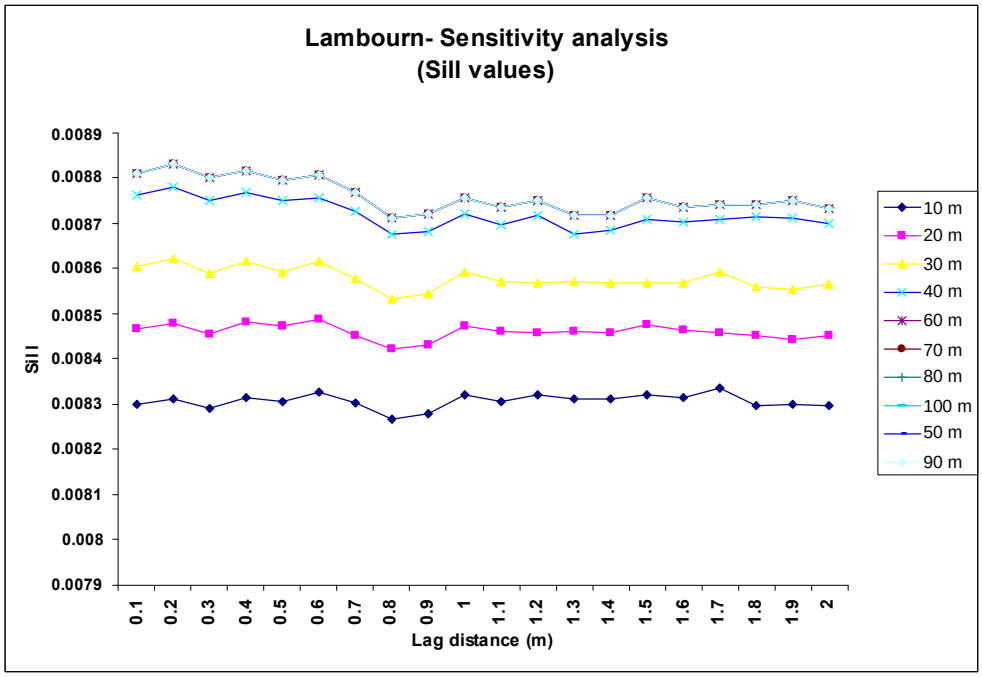
Lambourn- Sensitivity analysis
(Sill values)
Sill
0.0089
0.0088
0.0087
0.0086
0.0085
0.0084
0.0083
0.0082
0.0081
0.008
0.0079
0.1
0.2
0.3
0.4
0.5
0.6
0.7
0.8
0.9
1
1.1
1.2
1.3
1.4
1.5
1.6
1.7
1.8
1.9
2
Lag distance (m)
10 m
20 m
30 m
40 m
60 m
70 m
80 m
100 m
50 m
90 m

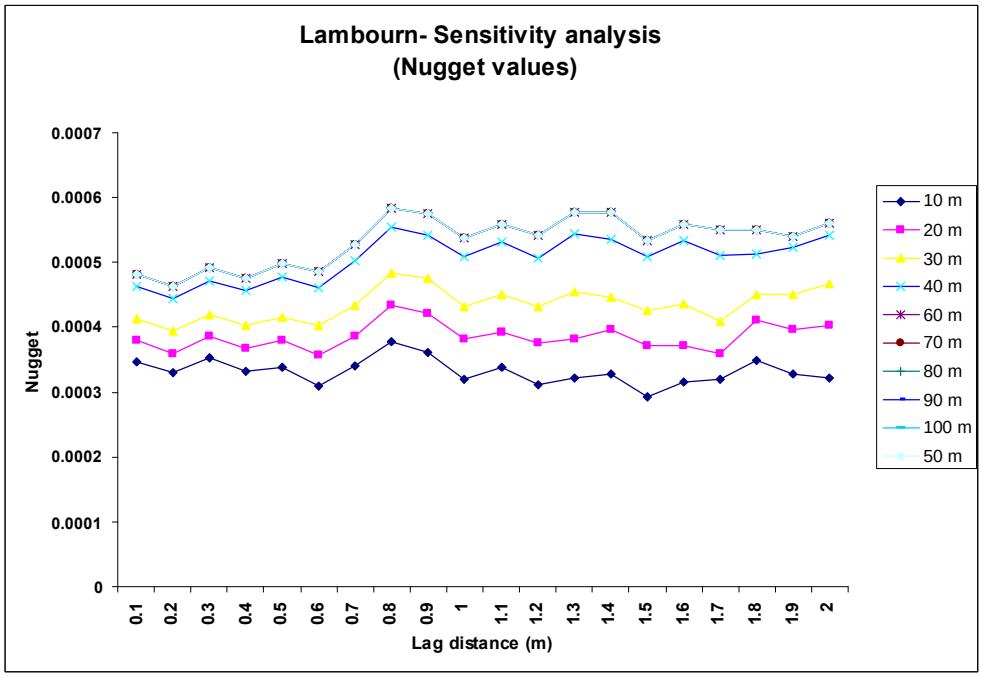
Lambourn- Sensitivity analysis
(Nugget values)
Nugget
0.0007
0.0006
0.0005
0.0004
0.0003
0.0002
0.0001
0
0.1
0.2
0.3
0.4
0.5
0.6
0.7
0.8
0.9
1
1.1
1.2
1.3
1.4
1.5
1.6
1.7
1.8
1.9
2
Lag distance (m)
10 m
20 m
30 m
40 m
60 m
70 m
80 m
90 m
100 m
50 m

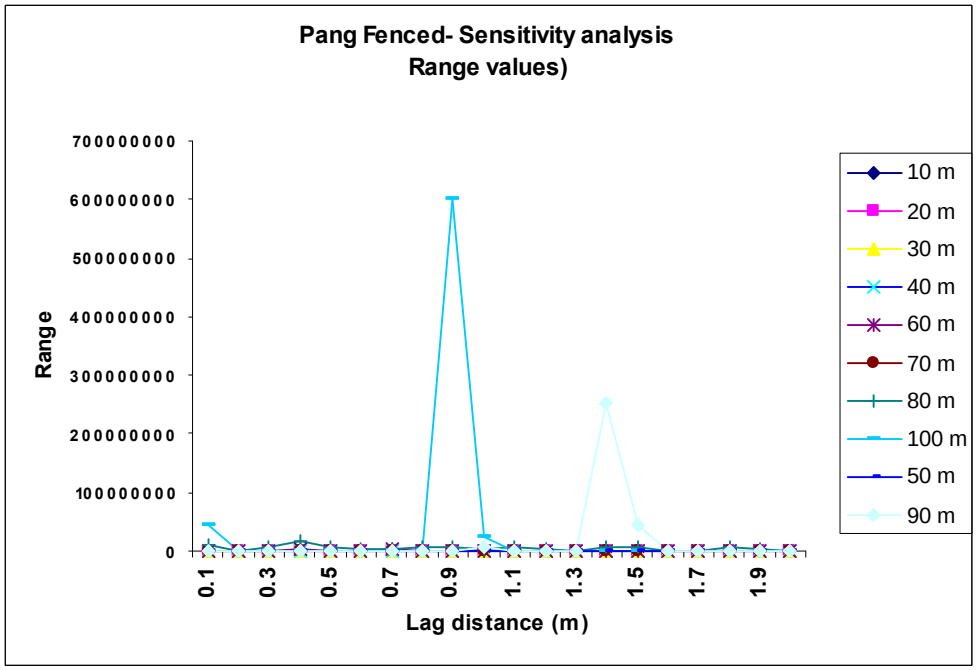
Pang Fenced- Sensitivity analysis
Range values)
Range
700000000
600000000
500000000
400000000
300000000
200000000
100000000
0
0.1
0.3
0.5
0.7
0.9
1.1
1.3
1.5
1.7
1.9
Lag distance (m)
10 m
20 m
30 m
40 m
60 m
70 m
80 m
100 m
50 m
90 m

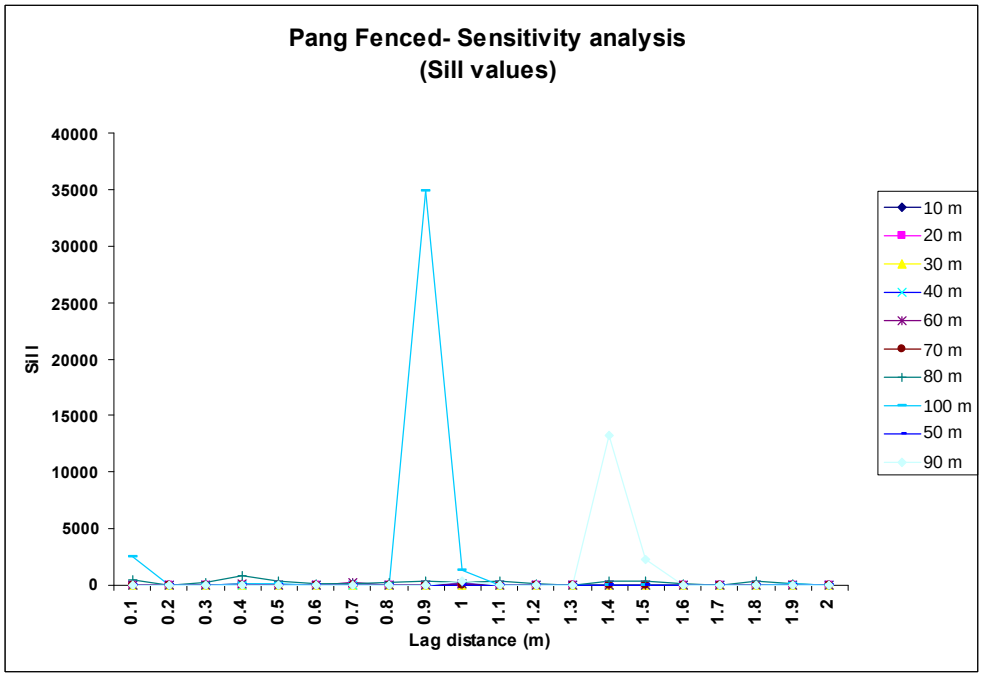
Pang Fenced- Sensitivity analysis
(Sill values)
Sill
40000
35000
30000
25000
20000
15000
10000
5000
0
0.1
0.2
0.3
0.4
0.5
0.6
0.7
0.8
0.9
1
1.1
1.2
1.3
1.4
1.5
1.6
1.7
1.8
1.9
2
Lag distance (m)
10 m
20 m
30 m
40 m
60 m
70 m
80 m
100 m
50 m
90 m

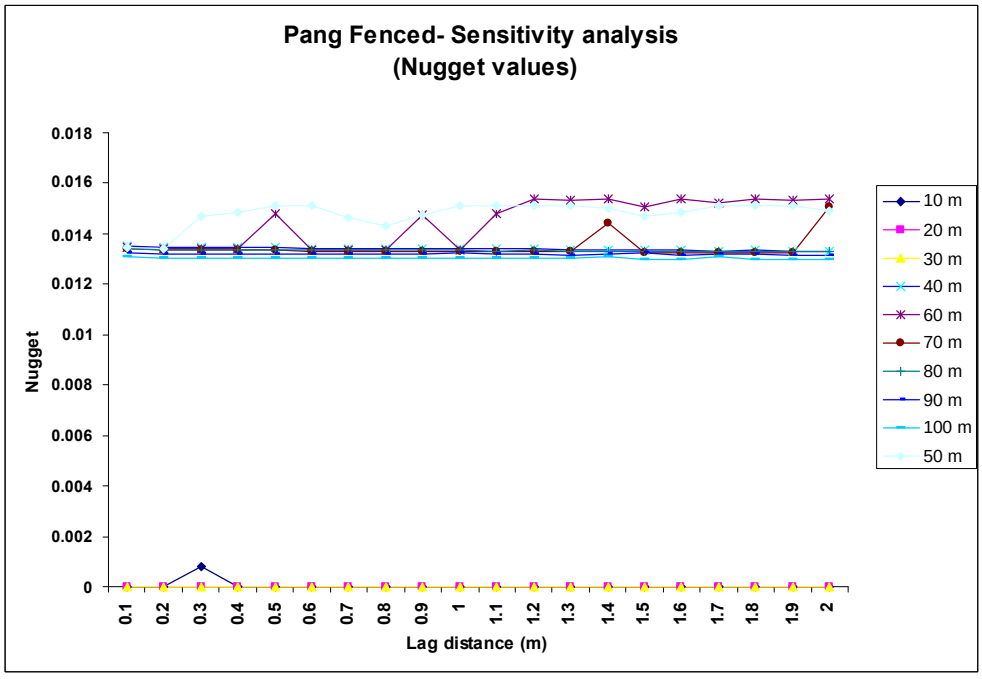
Pang Fenced- Sensitivity analysis
(Nugget values)
Nugget
0.018
0.016
0.014
0.012
0.01
0.008
0.006
0.004
0.002
0
0.1
0.2
0.3
0.4
0.5
0.6
0.7
0.8
0.9
1
1.1
1.2
1.3
1.4
1.5
1.6
1.7
1.8
1.9
2
Lag distance (m)
10 m
20 m
30 m
40 m
60 m
70 m
80 m
90 m
100 m
50 m

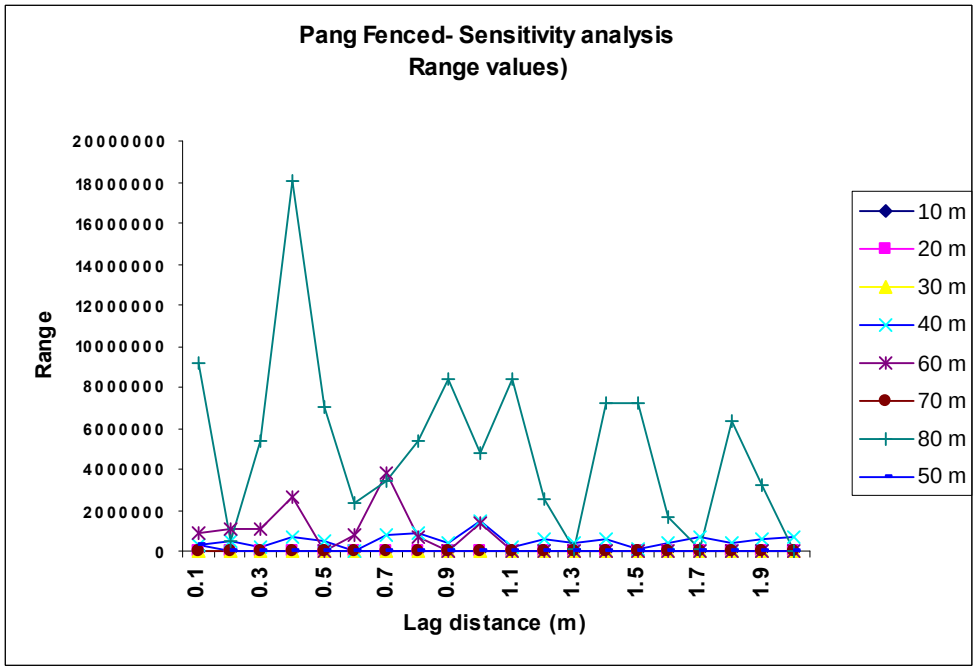
Pang Fenced- Sensitivity analysis
Range values)
Range
20000000
18000000
16000000
14000000
12000000
10000000
8000000
6000000
4000000
2000000
0
0.1
0.3
0.5
0.7
0.9
1.1
1.3
1.5
1.7
1.9
Lag distance (m)
10 m
20 m
30 m
40 m
60 m
70 m
80 m
50 m

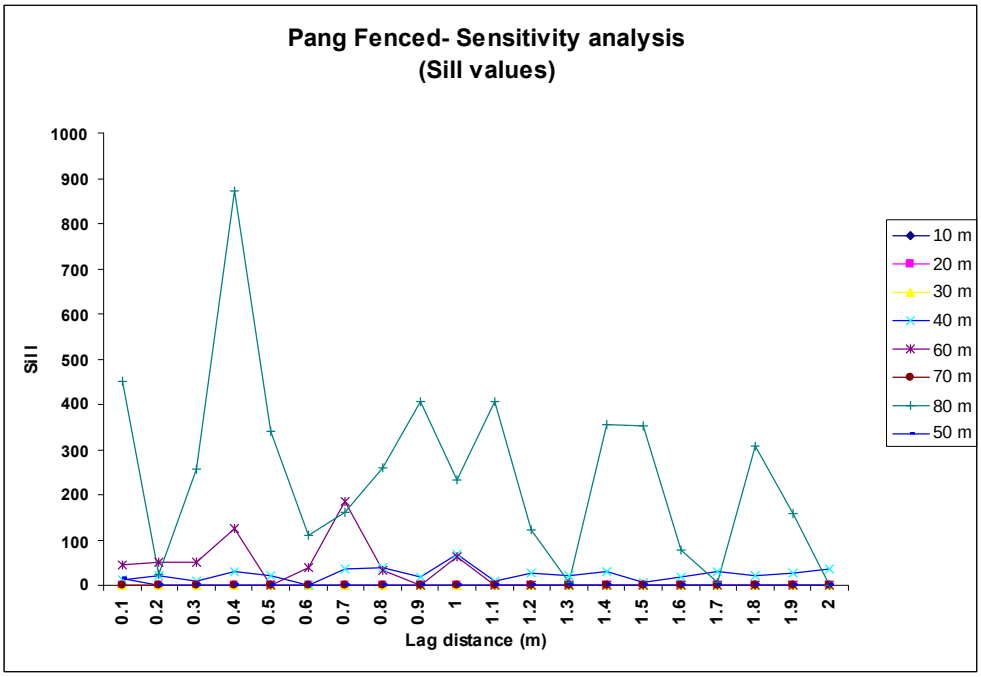
Pang Fenced- Sensitivity analysis
(Sill values)
Sill
1000
900
800
700
600
500
400
300
200
100
0
0.1
0.2
0.3
0.4
0.5
0.6
0.7
0.8
0.9
1
1.1
1.2
1.3
1.4
1.5
1.6
1.7
1.8
1.9
2
Lag distance (m)
10 m
20 m
30 m
40 m
60 m
70 m
80 m
50 m

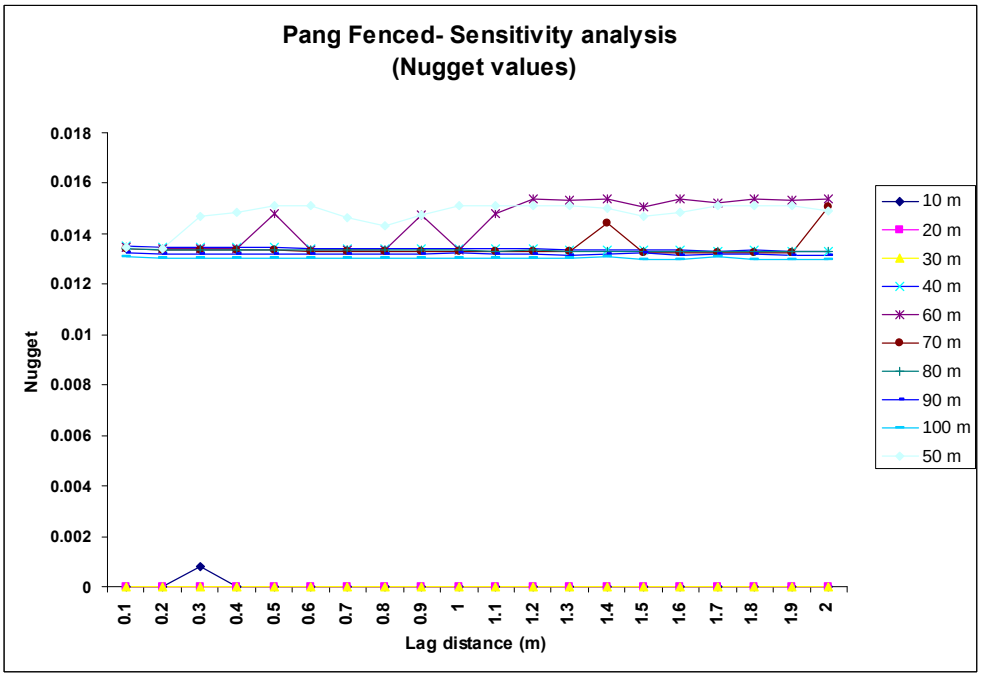
Pang Fenced- Sensitivity analysis
(Nugget values)
Nugget
0.018
0.016
0.014
0.012
0.01
0.008
0.006
0.004
0.002
0
0.1
0.2
0.3
0.4
0.5
0.6
0.7
0.8
0.9
1
1.1
1.2
1.3
1.4
1.5
1.6
1.7
1.8
1.9
2
Lag distance (m)
10 m
20 m
30 m
40 m
60 m
70 m
80 m
90 m
100 m
50 m

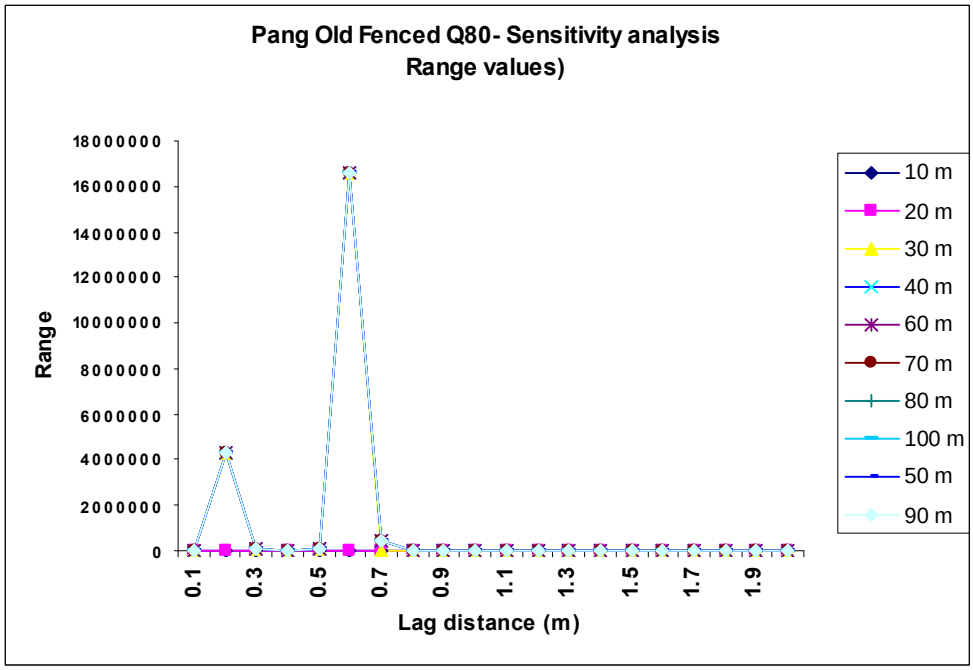
Pang Old Fenced Q80- Sensitivity analysis
Range values)
Range
18000000
16000000
14000000
12000000
10000000
8000000
6000000
4000000
2000000
0
0.1
0.3
0.5
0.7
0.9
1.1
1.3
1.5
1.7
1.9
Lag distance (m)
10 m
20 m
30 m
40 m
60 m
70 m
80 m
100 m
50 m
90 m

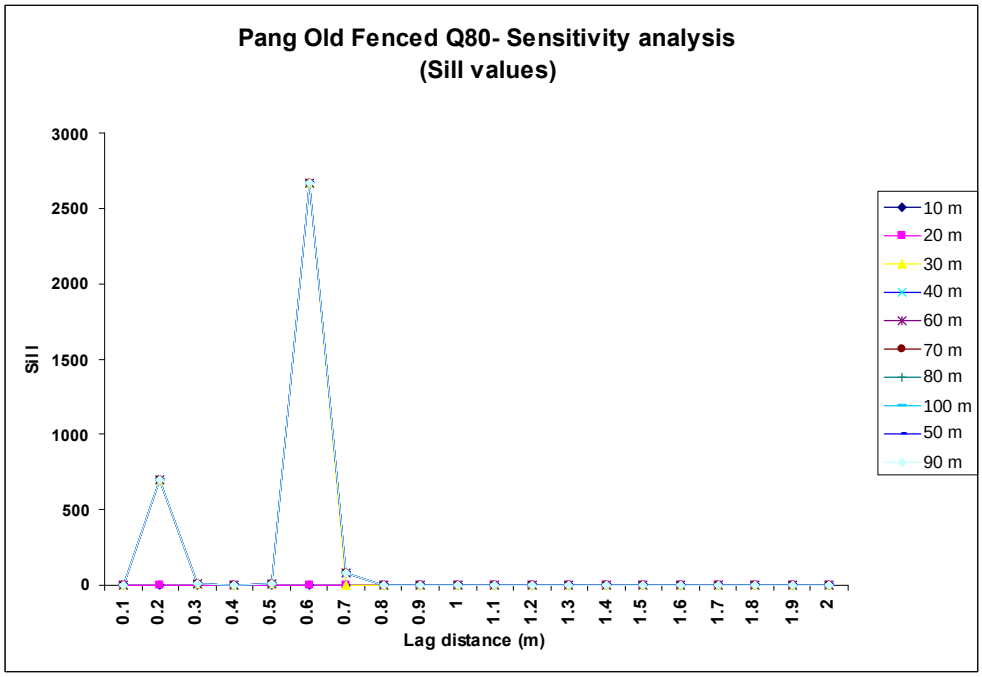
Pang Old Fenced Q80- Sensitivity analysis
(Sill values)
Sill
3000
2500
2000
1500
1000
500
0
0.1
0.2
0.3
0.4
0.5
0.6
0.7
0.8
0.9
1
1.1
1.2
1.3
1.4
1.5
1.6
1.7
1.8
1.9
2
Lag distance (m)
10 m
20 m
30 m
40 m
60 m
70 m
80 m
100 m
50 m
90 m

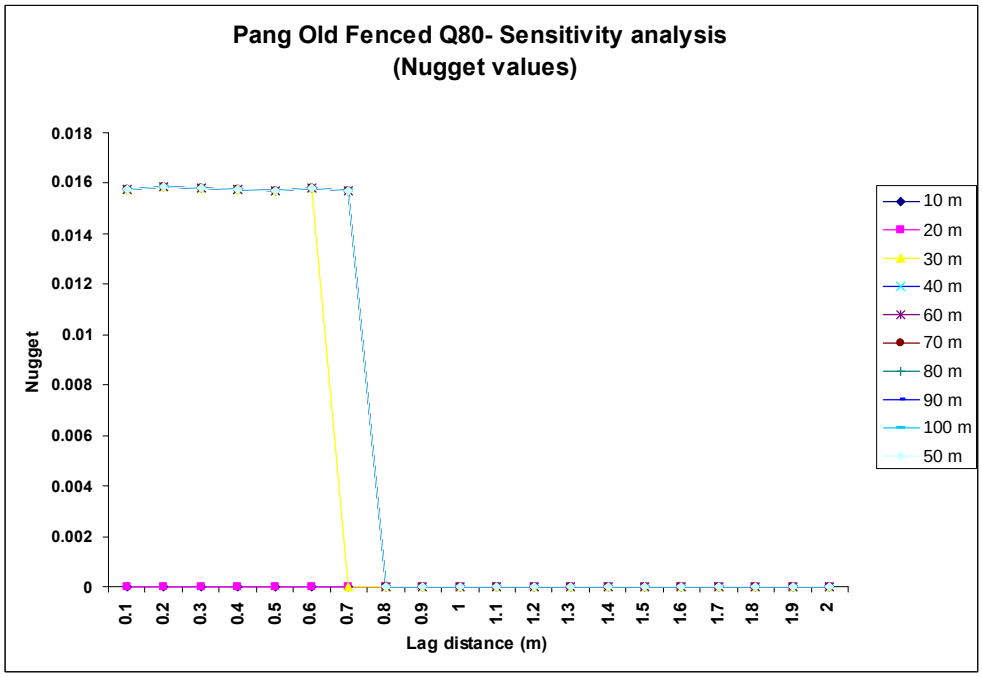
Pang Old Fenced Q80- Sensitivity analysis
(Nugget values)
Nugget
0.018
0.016
0.014
0.012
0.01
0.008
0.006
0.004
0.002
0
0.1
0.2
0.3
0.4
0.5
0.6
0.7
0.8
0.9
1
1.1
1.2
1.3
1.4
1.5
1.6
1.7
1.8
1.9
2
Lag distance (m)
10 m
20 m
30 m
40 m
60 m
70 m
80 m
90 m
100 m
50 m

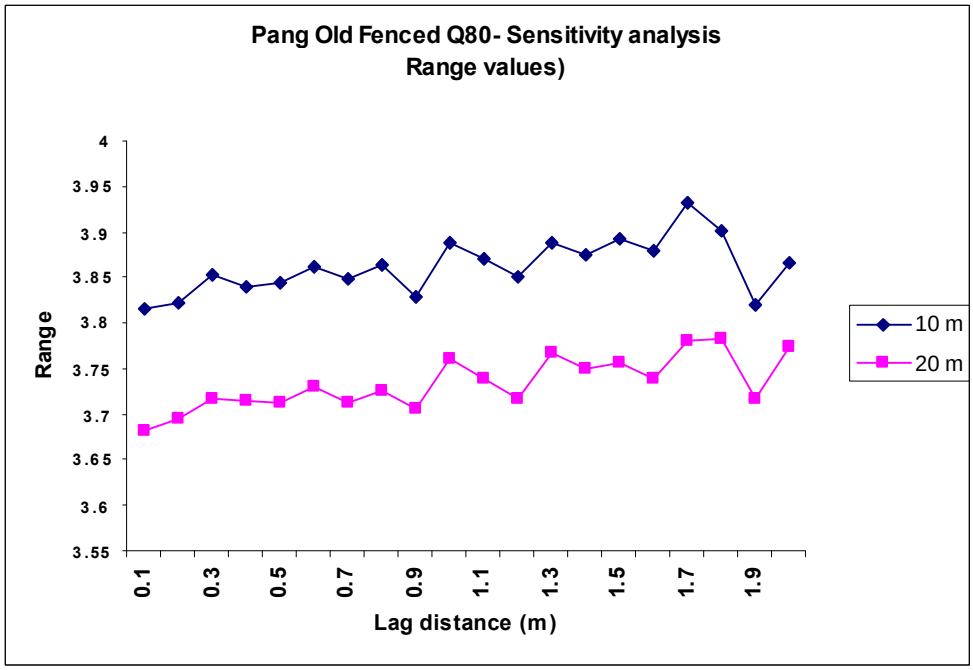
Pang Old Fenced Q80- Sensitivity analysis
Range values)
Range
4
3.95
3.9
3.85
3.8
3.75
3.7
3.65
3.6
3.55
0.1
0.3
0.5
0.7
0.9
1.1
1.3
1.5
1.7
1.9
Lag distance (m)
10 m
20 m

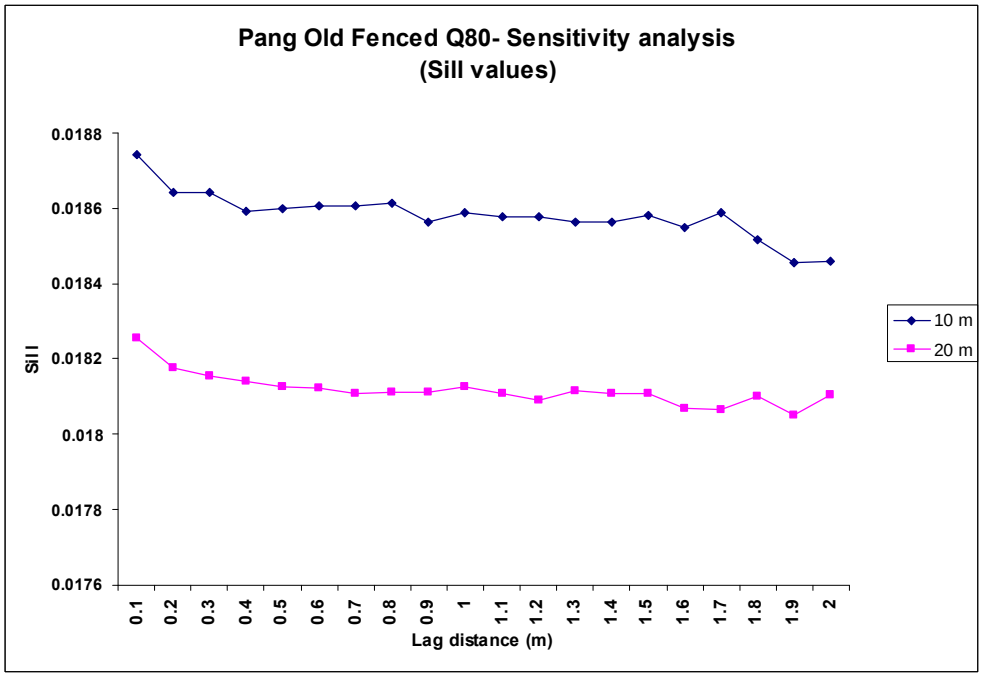
Pang Old Fenced Q80- Sensitivity analysis
(Sill values)
Sill
0.0188
0.0186
0.0184
0.0182
0.018
0.0178
0.0176
0.1
0.2
0.3
0.4
0.5
0.6
0.7
0.8
0.9
1
1.1
1.2
1.3
1.4
1.5
1.6
1.7
1.8
1.9
2
Lag distance (m)
10 m
20 m

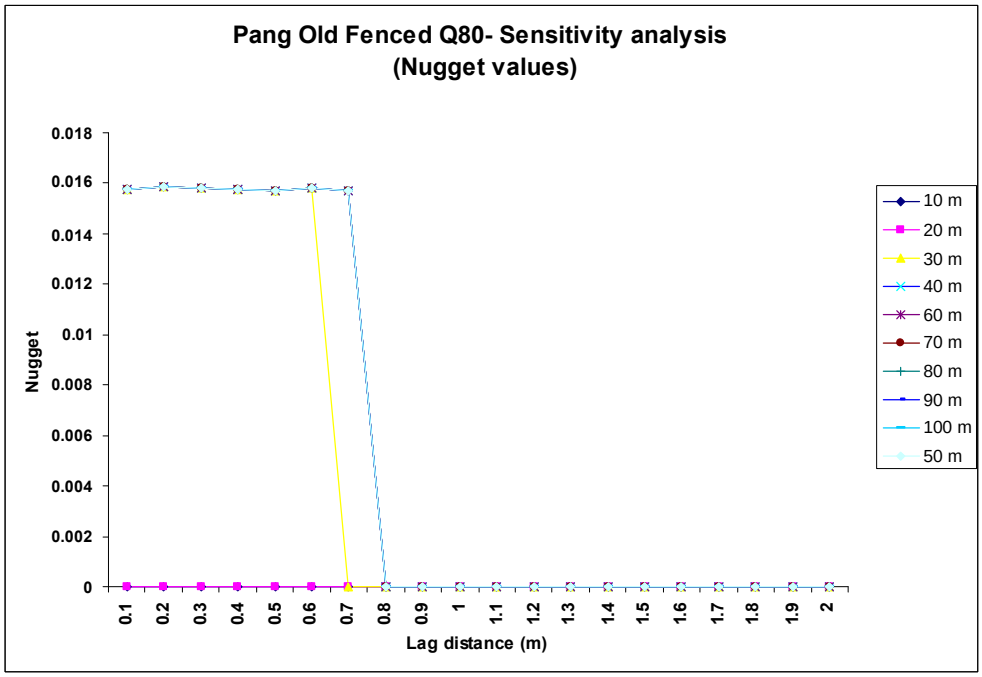
Pang Old Fenced Q80- Sensitivity analysis
(Nugget values)
Nugget
0.018
0.016
0.014
0.012
0.01
0.008
0.006
0.004
0.002
0
0.1
0.2
0.3
0.4
0.5
0.6
0.7
0.8
0.9
1
1.1
1.2
1.3
1.4
1.5
1.6
1.7
1.8
1.9
2
Lag distance (m)
10 m
20 m
30 m
40 m
60 m
70 m
80 m
90 m
100 m
50 m

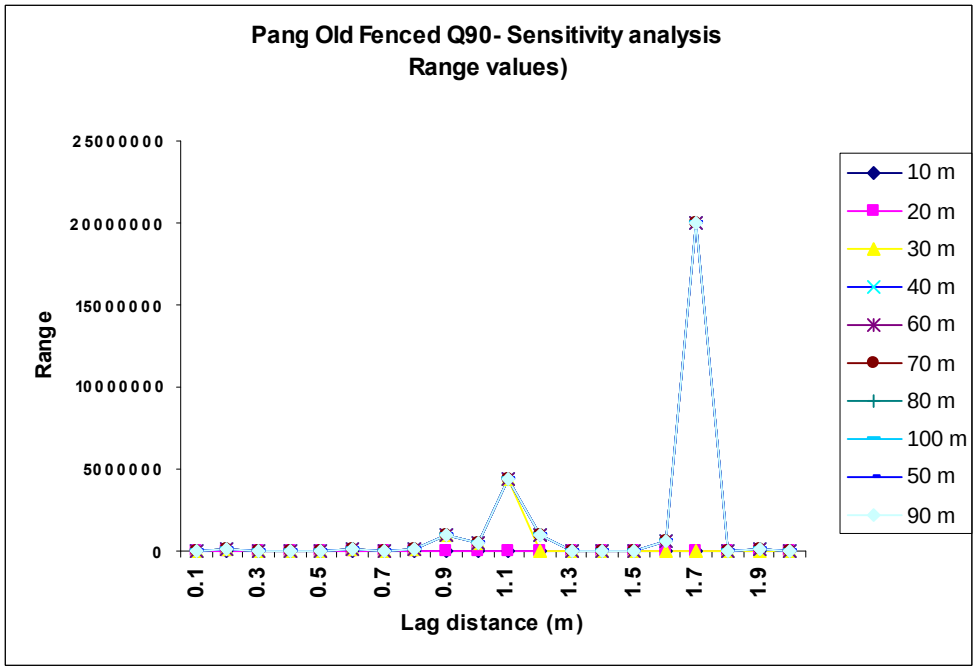
Pang Old Fenced Q90- Sensitivity analysis
Range values)
Range
25000000
20000000
15000000
10000000
5000000
0
0.1
0.3
0.5
0.7
0.9
1.1
1.3
1.5
1.7
1.9
Lag distance (m)
10 m
20 m
30 m
40 m
60 m
70 m
80 m
100 m
50 m
90 m

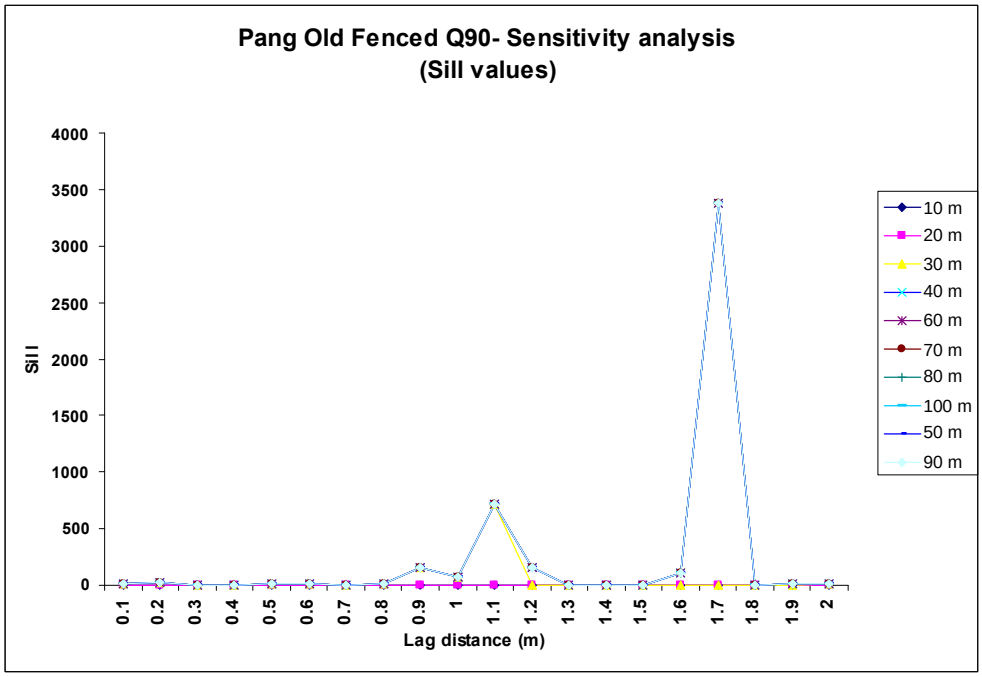
Pang Old Fenced Q90- Sensitivity analysis
(Sill values)
Sill
4000
3500
3000
2500
2000
1500
1000
500
0
0.1
0.2
0.3
0.4
0.5
0.6
0.7
0.8
0.9
1
1.1
1.2
1.3
1.4
1.5
1.6
1.7
1.8
1.9
2
Lag distance (m)
10 m
20 m
30 m
40 m
60 m
70 m
80 m
100 m
50 m
90 m

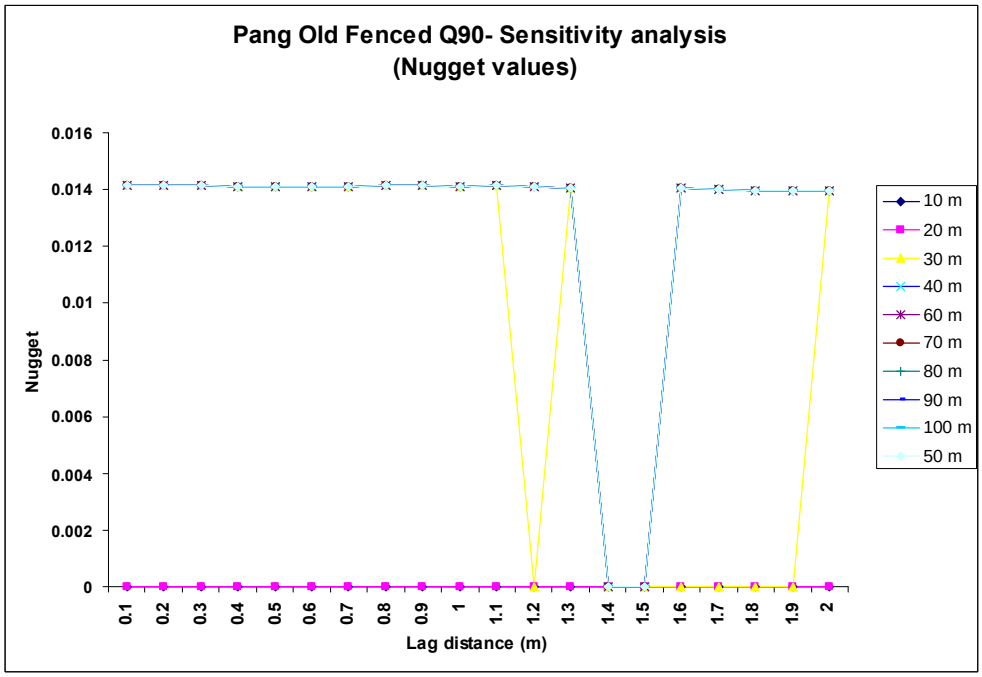
Pang Old Fenced Q90- Sensitivity analysis
(Nugget values)
Nugget
0.016
0.014
0.012
0.01
0.008
0.006
0.004
0.002
0
0.1
0.2
0.3
0.4
0.5
0.6
0.7
0.8
0.9
1
1.1
1.2
1.3
1.4
1.5
1.6
1.7
1.8
1.9
2
Lag distance (m)
10 m
20 m
30 m
40 m
60 m
70 m
80 m
90 m
100 m
50 m

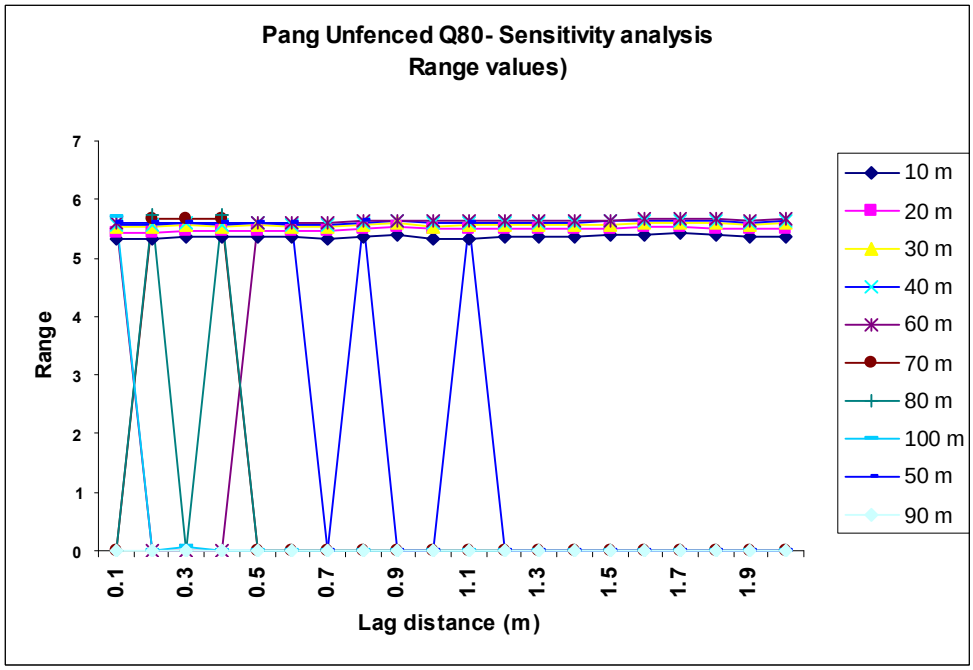
Pang Unfenced Q80- Sensitivity analysis
Range values)
Range
Lag distance (m)
10 m
20 m
30 m
40 m
60 m
70 m
80 m
100 m
50 m
90 m

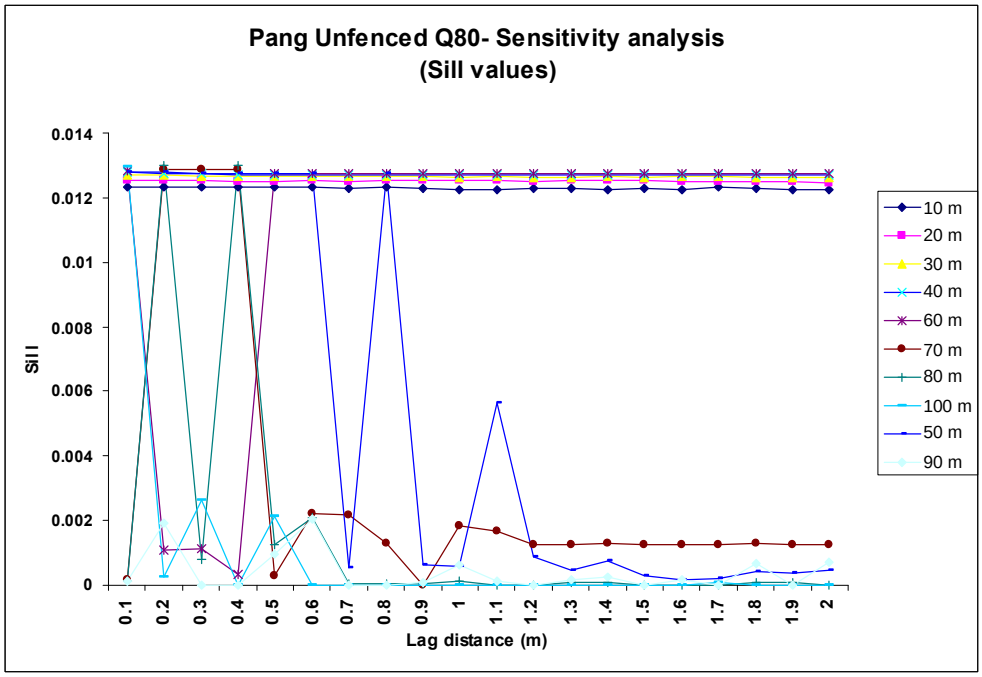
Pang Unfenced Q80- Sensitivity analysis
(Sill values)
Sill
Lag distance (m)
10 m
20 m
30 m
40 m
60 m
70 m
80 m
100 m
50 m
90 m

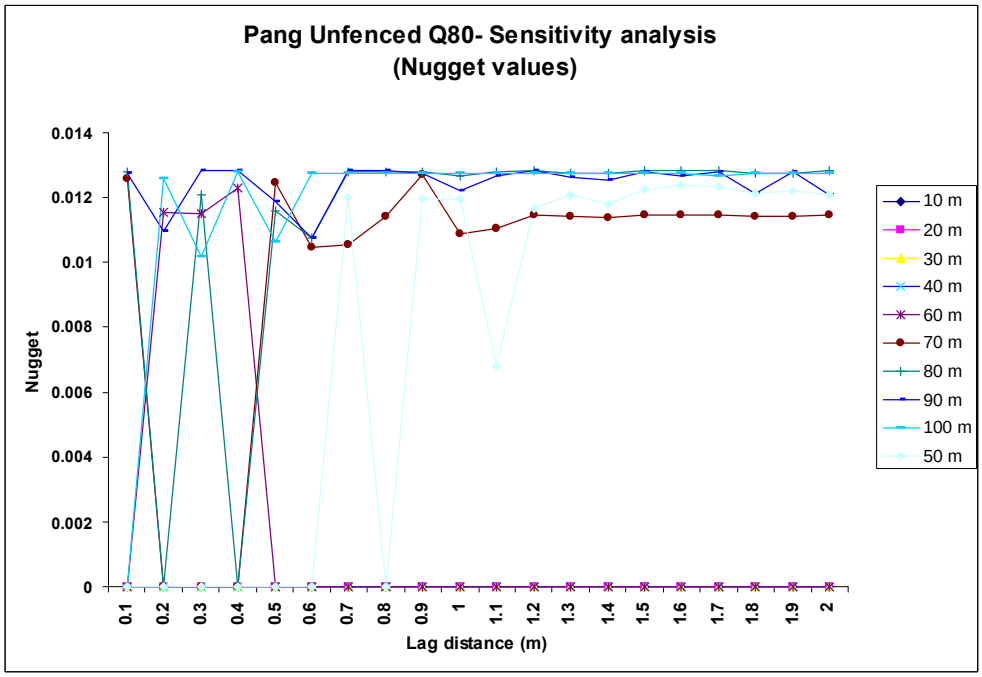
Pang Unfenced Q80- Sensitivity analysis
(Nugget values)
Nugget
Lag distance (m)
10 m
20 m
30 m
40 m
60 m
70 m
80 m
90 m
100 m
50 m

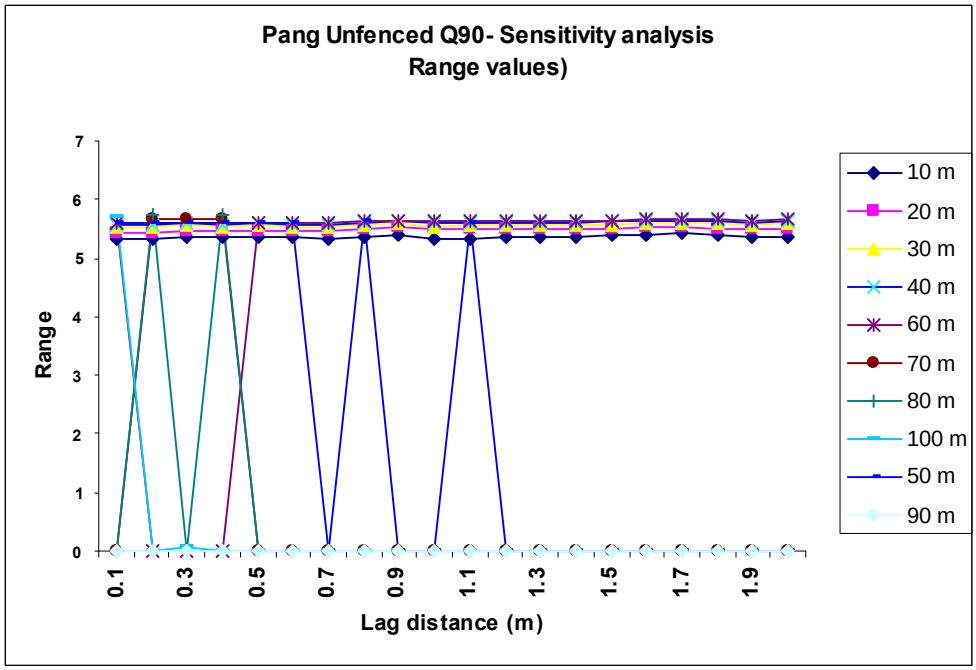
Pang Unfenced Q90- Sensitivity analysis
Range values)
Range
Lag distance (m)
10 m
20 m
30 m
40 m
60 m
70 m
80 m
100 m
50 m
90 m

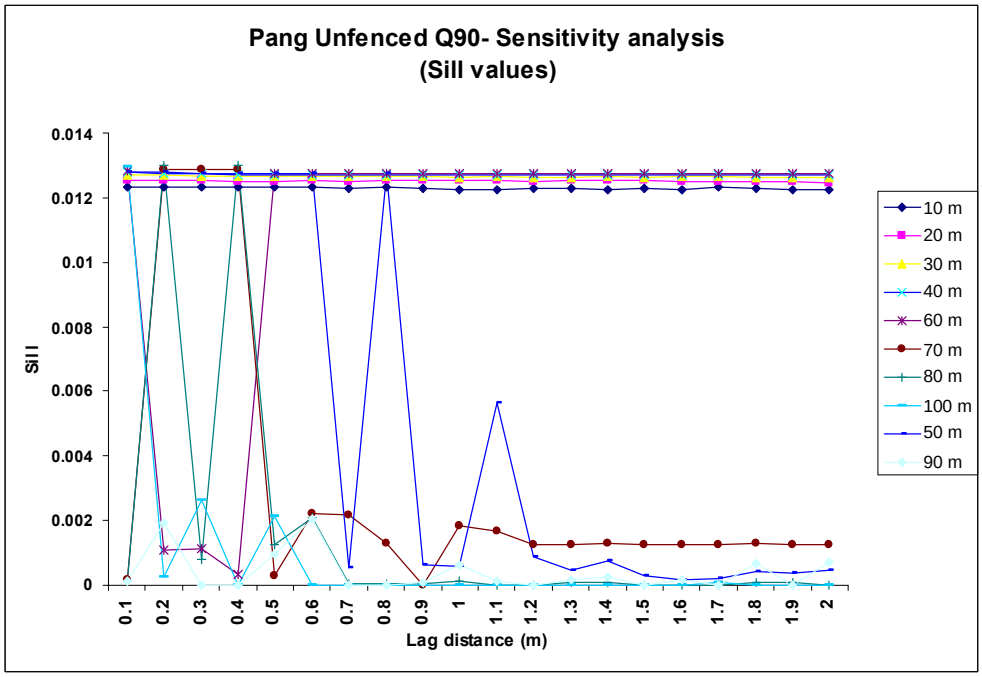
Pang Unfenced Q90- Sensitivity analysis
(Sill values)
Sill
Lag distance (m)
10 m
20 m
30 m
40 m
60 m
70 m
80 m
100 m
50 m
90 m

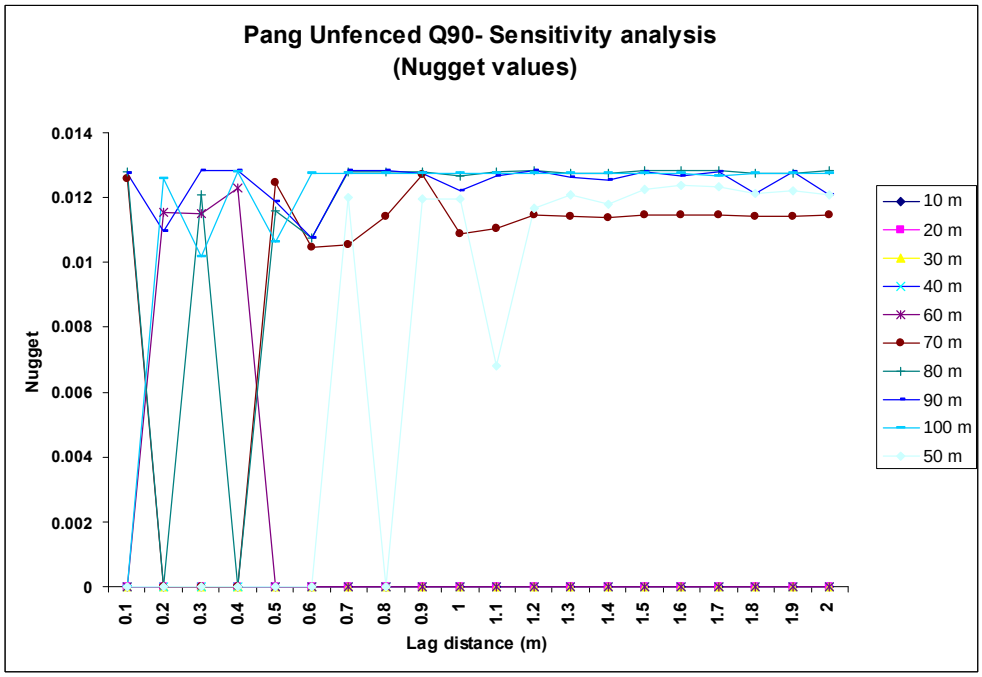
Pang Unfenced Q90- Sensitivity analysis
(Nugget values)
Nugget
Lag distance (m)
10 m
20 m
30 m
40 m
60 m
70 m
80 m
90 m
100 m
50 m

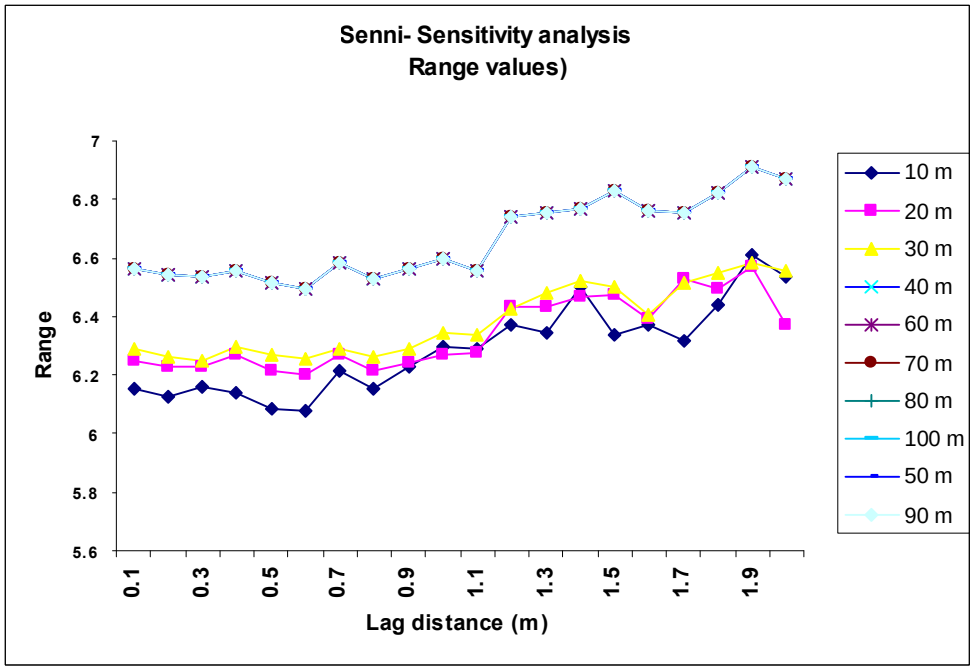
Senni- Sensitivity analysis
Range values)
Range
Lag distance (m)
10 m
20 m
30 m
40 m
60 m
70 m
80 m
100 m
50 m
90 m

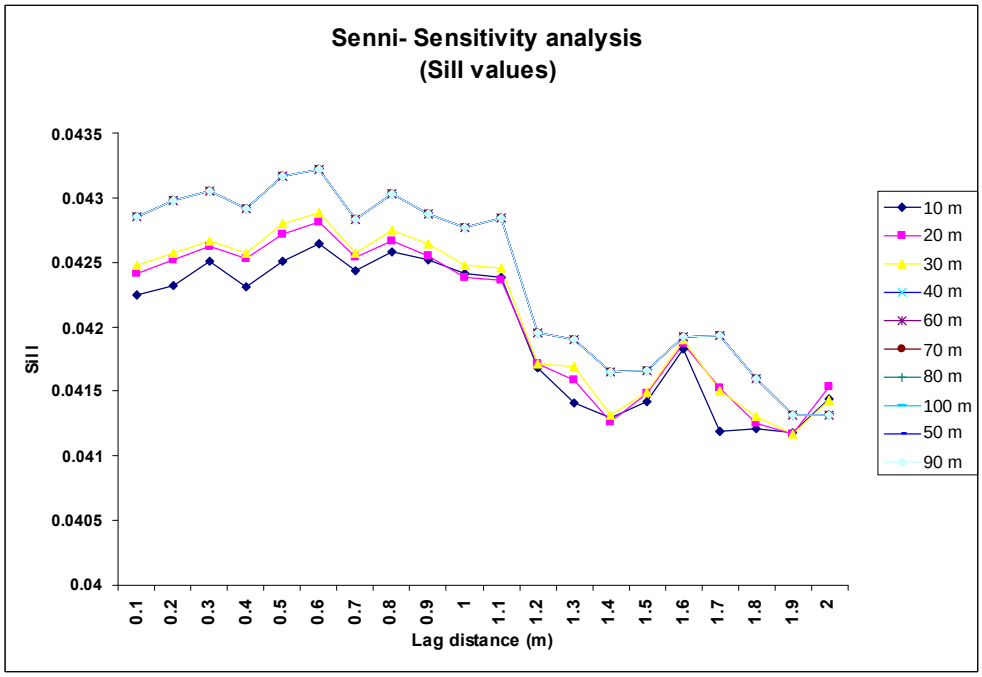
Senni- Sensitivity analysis
(Sill values)
Sill
Lag distance (m)
10 m
20 m
30 m
40 m
60 m
70 m
80 m
100 m
50 m
90 m

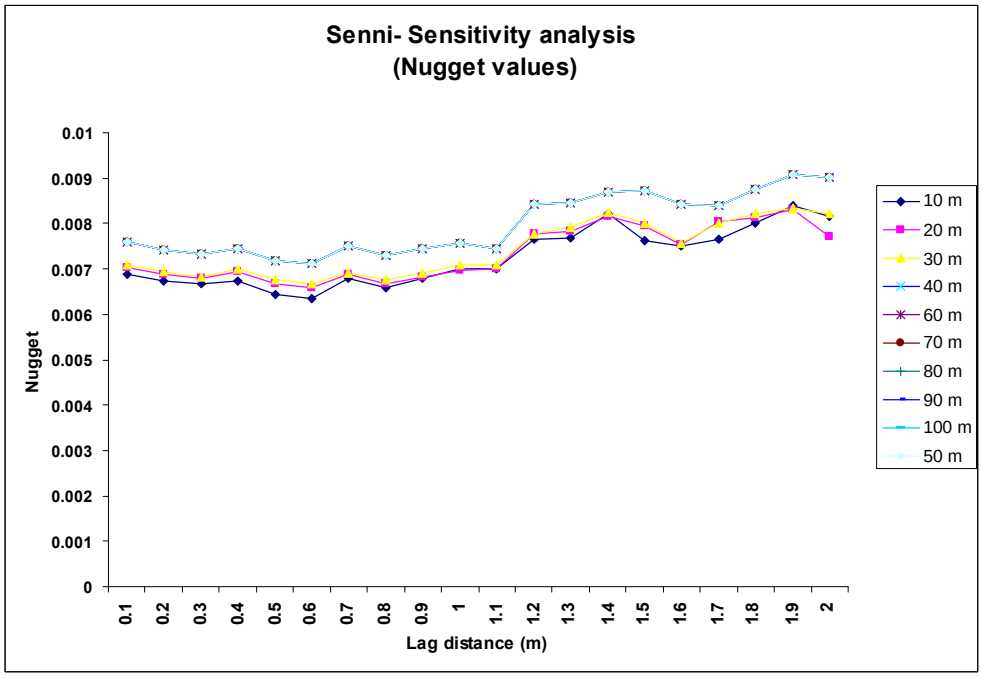
Senni- Sensitivity analysis
(Nugget values)
Nugget
Lag distance (m)
10 m
20 m
30 m
40 m
60 m
70 m
80 m
90 m
100 m
50 m

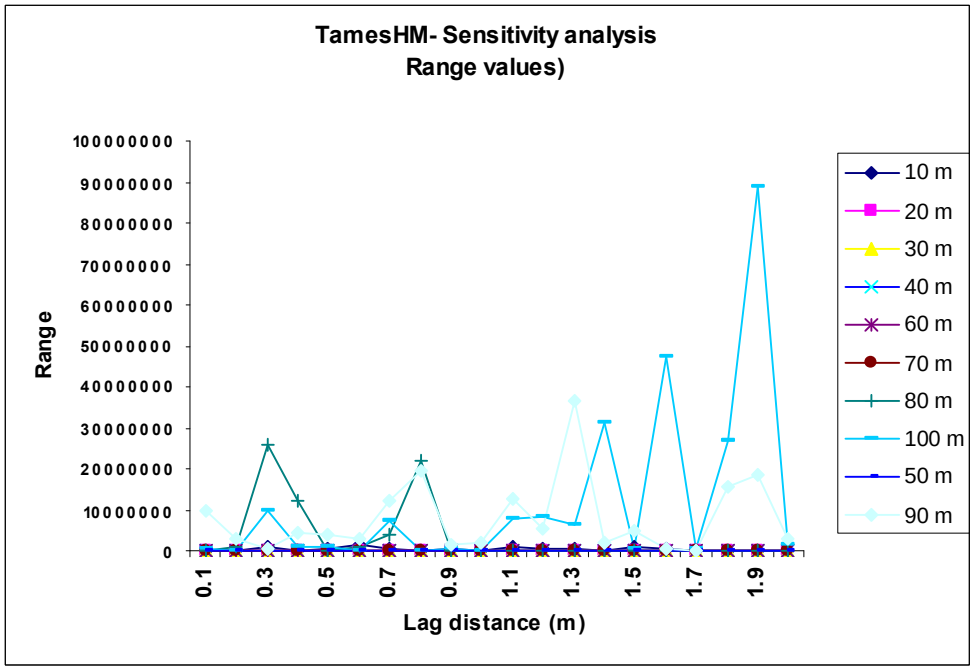
TamesHM- Sensitivity analysis
Range values)
Range
100000000
90000000
80000000
70000000
60000000
50000000
40000000
30000000
20000000
10000000
0
0.1
0.3
0.5
0.7
0.9
1.1
1.3
1.5
1.7
1.9
Lag distance (m)
10 m
20 m
30 m
40 m
60 m
70 m
80 m
100 m
50 m
90 m

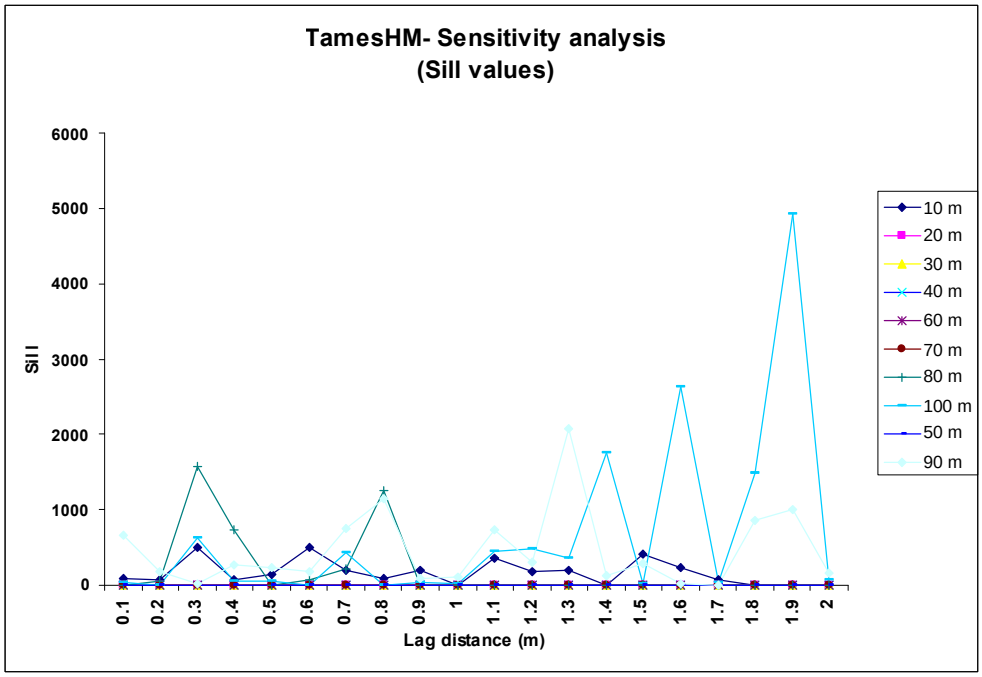
TamesHM- Sensitivity analysis
(Sill values)
Sill
6000
5000
4000
3000
2000
1000
0
0.1
0.2
0.3
0.4
0.5
0.6
0.7
0.8
0.9
1
1.1
1.2
1.3
1.4
1.5
1.6
1.7
1.8
1.9
2
Lag distance (m)
10 m
20 m
30 m
40 m
60 m
70 m
80 m
100 m
50 m
90 m

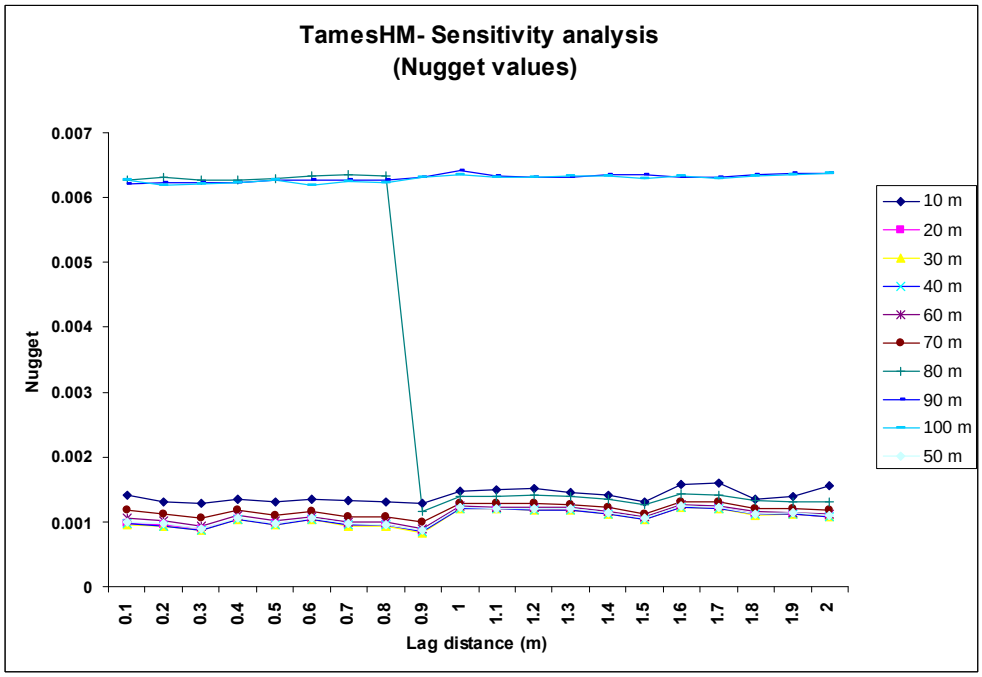
TamesHM- Sensitivity analysis
(Nugget values)
Nugget
0.007
0.006
0.005
0.004
0.003
0.002
0.001
0
0.1
0.2
0.3
0.4
0.5
0.6
0.7
0.8
0.9
1
1.1
1.2
1.3
1.4
1.5
1.6
1.7
1.8
1.9
2
Lag distance (m)
10 m
20 m
30 m
40 m
60 m
70 m
80 m
90 m
100 m
50 m

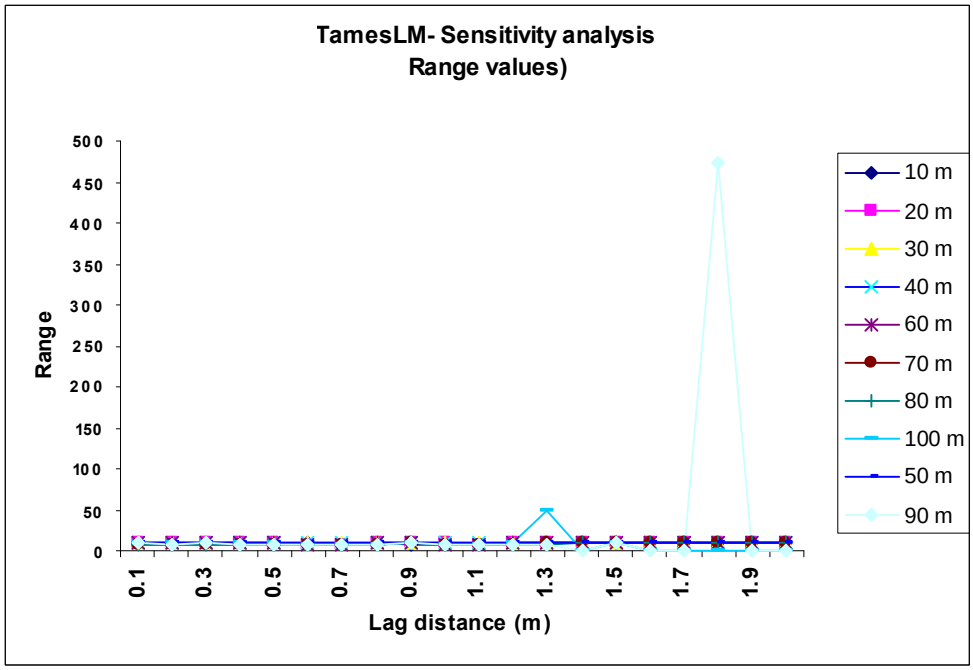
TamesLM- Sensitivity analysis
Range values)
Range
Lag distance (m)
10 m
20 m
30 m
40 m
60 m
70 m
80 m
100 m
50 m
90 m

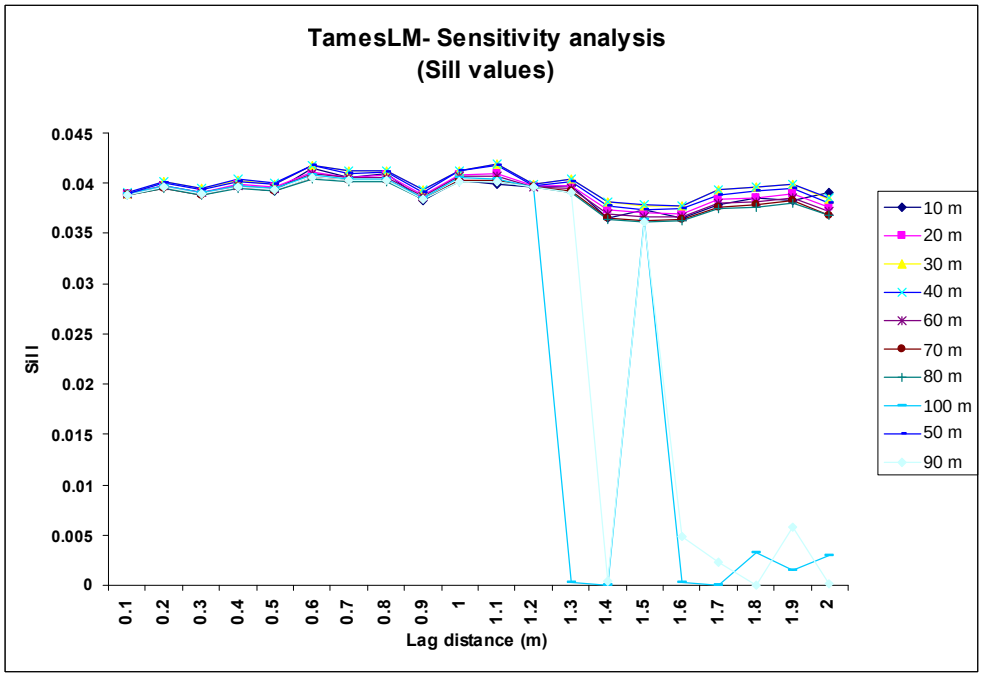
TamesLM- Sensitivity analysis
(Sill values)
Sill
Lag distance (m)
10 m
20 m
30 m
40 m
60 m
70 m
80 m
100 m
50 m
90 m

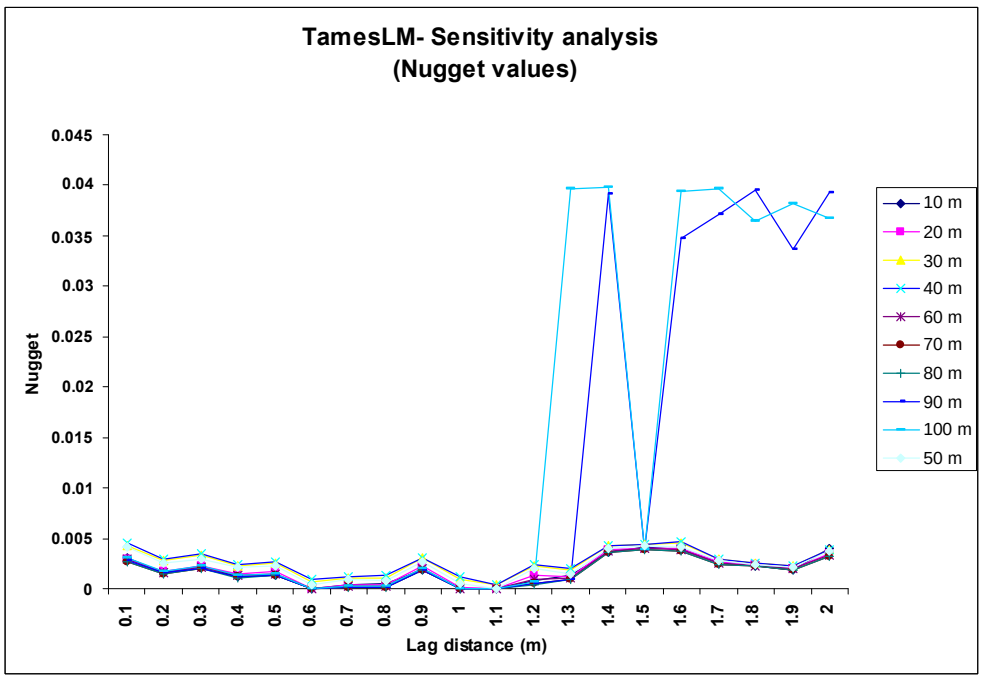
TamesLM- Sensitivity analysis
(Nugget values)
Nugget
Lag distance (m)
10 m
20 m
30 m
40 m
60 m
70 m
80 m
90 m
100 m
50 m

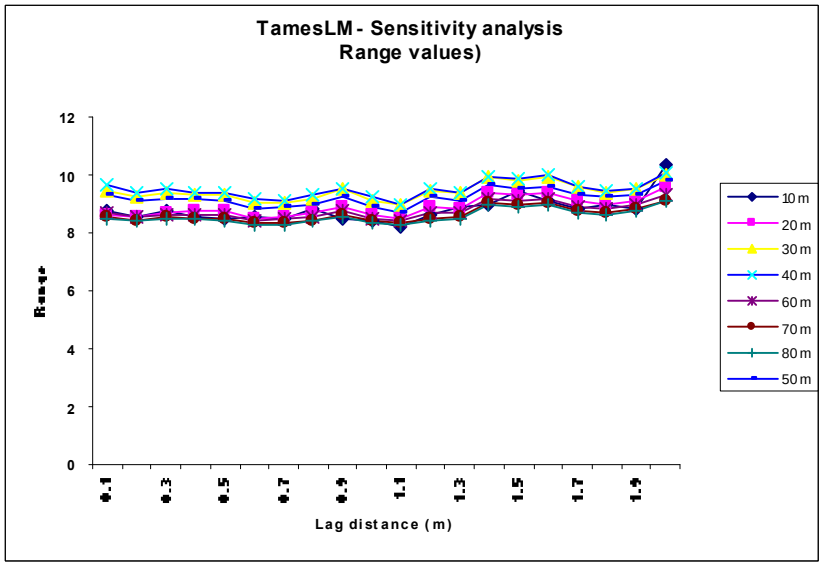
TamesLM - Sensitivity analysis
Range values)
Range
Lag distance (m)
10 m
20 m
30 m
40 m
60 m
70 m
80 m
50 m

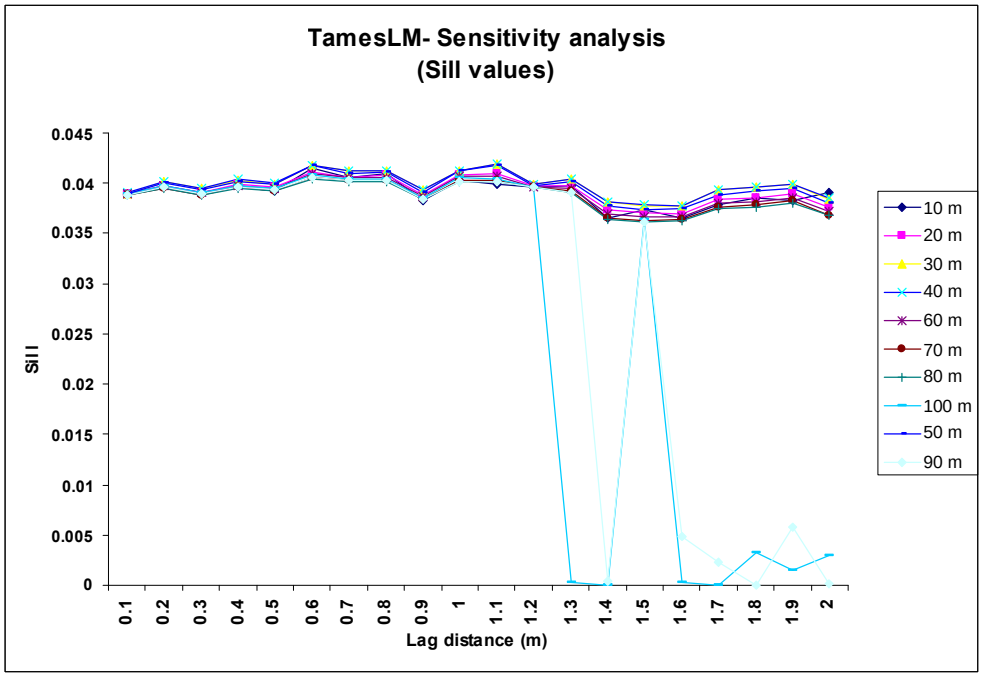
TamesLM- Sensitivity analysis
(Sill values)
Sill
Lag distance (m)
10 m
20 m
30 m
40 m
60 m
70 m
80 m
100 m
50 m
90 m

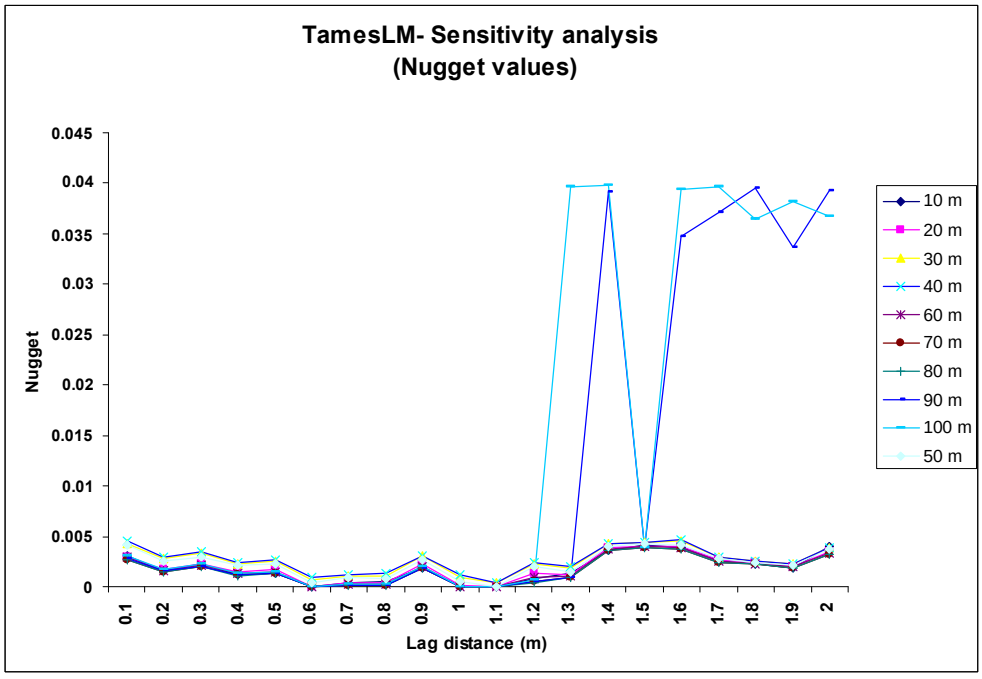
TamesLM- Sensitivity analysis
(Nugget values)
Nugget
Lag distance (m)
10 m
20 m
30 m
40 m
60 m
70 m
80 m
90 m
100 m
50 m

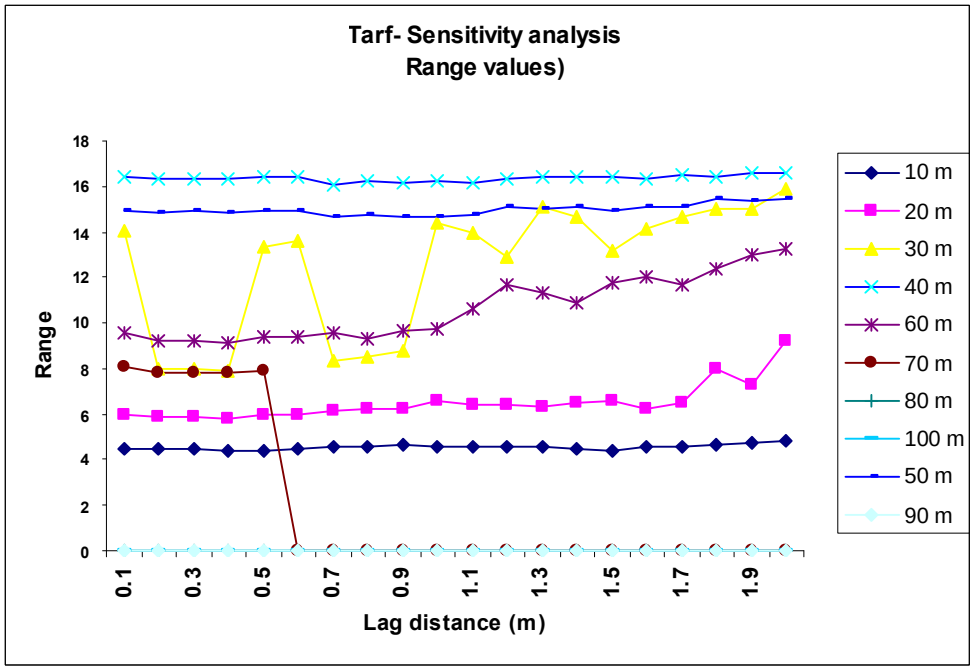
Tarf- Sensitivity analysis
Range values)
Range
Lag distance (m)
10 m
20 m
30 m
40 m
60 m
70 m
80 m
100 m
50 m
90 m

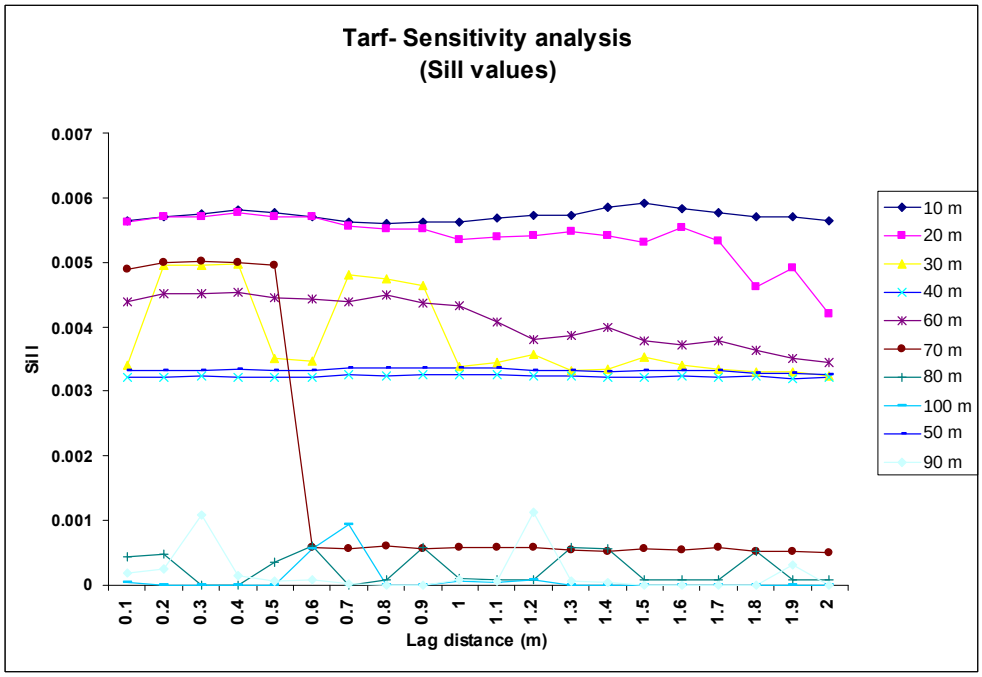
Tarf- Sensitivity analysis
(Sill values)
Sill
Lag distance (m)
10 m
20 m
30 m
40 m
60 m
70 m
80 m
100 m
50 m
90 m

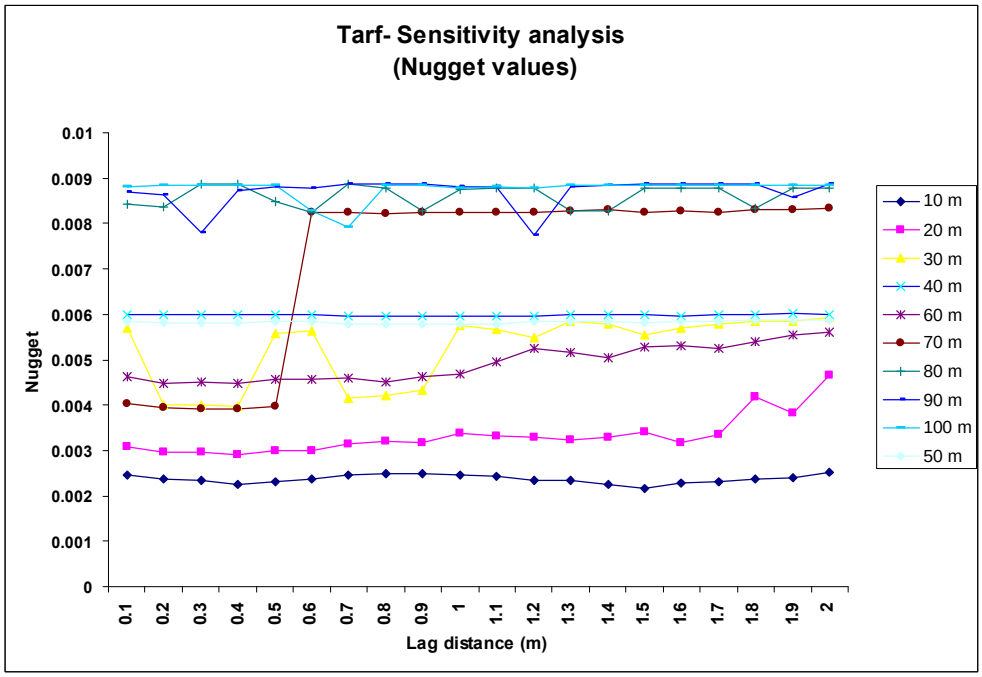
Tarf- Sensitivity analysis
(Nugget values)
Nugget
Lag distance (m)
10 m
20 m
30 m
40 m
60 m
70 m
80 m
90 m
100 m
50 m

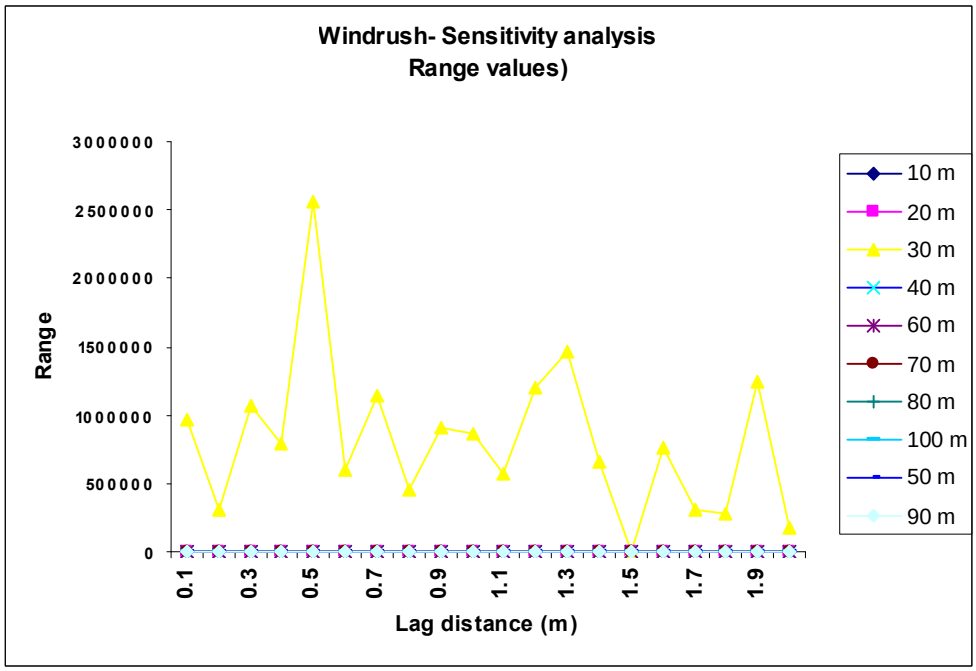
Windrush- Sensitivity analysis
Range values)
Range
3000000
2500000
2000000
1500000
1000000
500000
0
0.1
0.3
0.5
0.7
0.9
1.1
1.3
1.5
1.7
1.9
Lag distance (m)
10 m
20 m
30 m
40 m
60 m
70 m
80 m
100 m
50 m
90 m

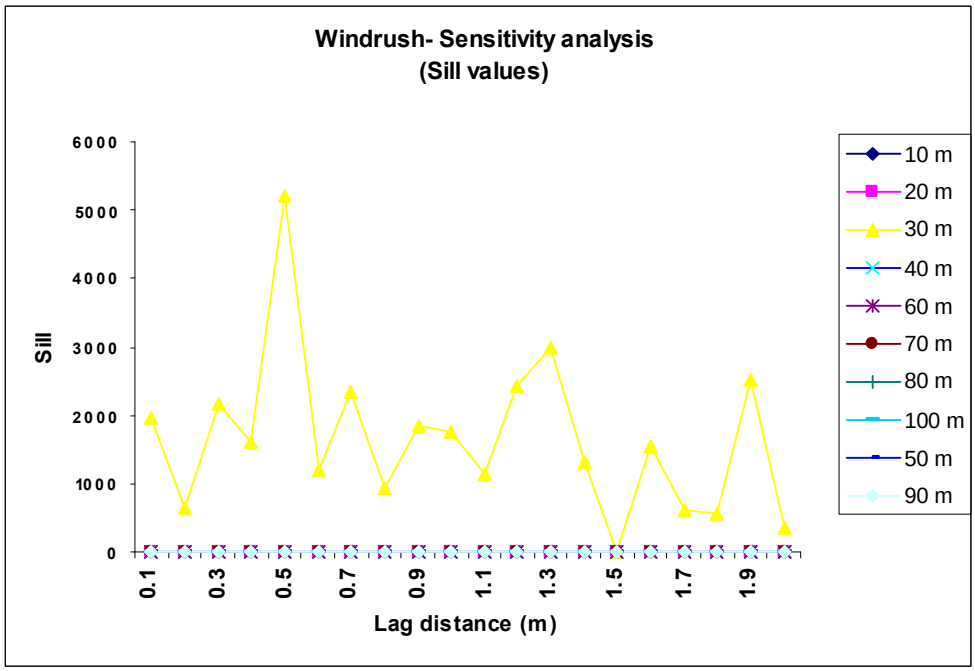
Windrush- Sensitivity analysis
(Sill values)
Sill
6000
5000
4000
3000
2000
1000
0
0.1
0.3
0.5
0.7
0.9
1.1
1.3
1.5
1.7
1.9
Lag distance (m)
10 m
20 m
30 m
40 m
60 m
70 m
80 m
100 m
50 m
90 m

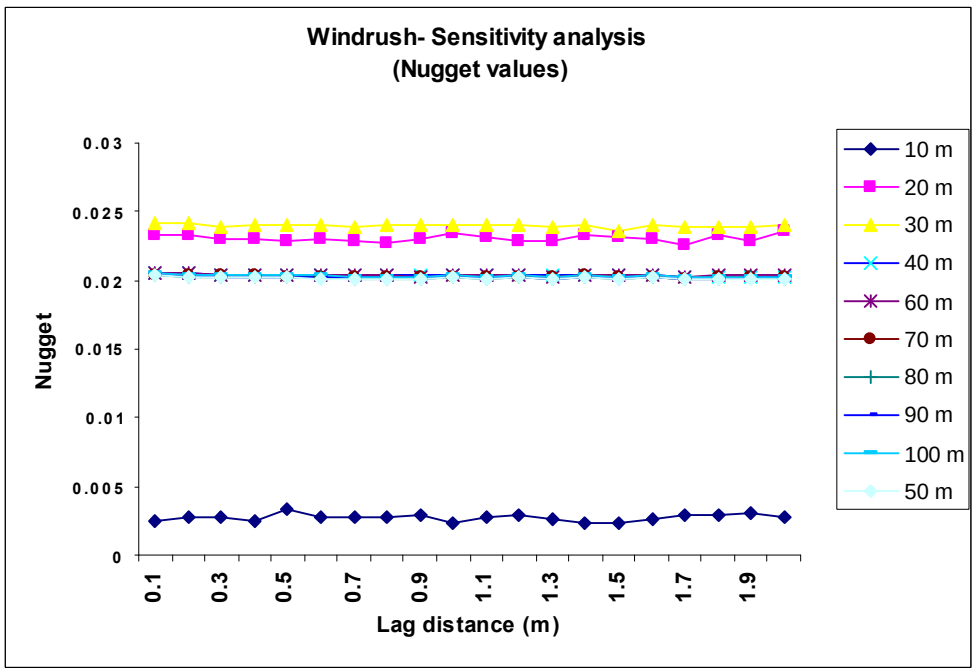
Windrush- Sensitivity analysis
(Nugget values)
Nugget
0.03
0.025
0.02
0.015
0.01
0.005
0
0.1
0.3
0.5
0.7
0.9
1.1
1.3
1.5
1.7
1.9
Lag distance (m)
10 m
20 m
30 m
40 m
60 m
70 m
80 m
90 m
100 m
50 m

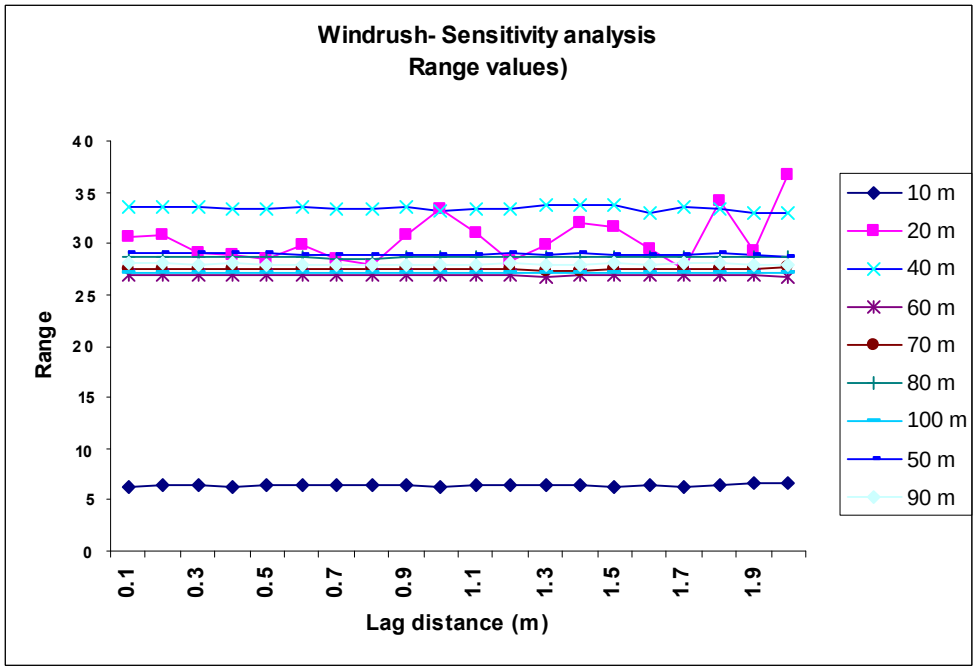
Windrush- Sensitivity analysis
Range values)
Range
Lag distance (m)
10 m
20 m
40 m
60 m
70 m
80 m
100 m
50 m
90 m

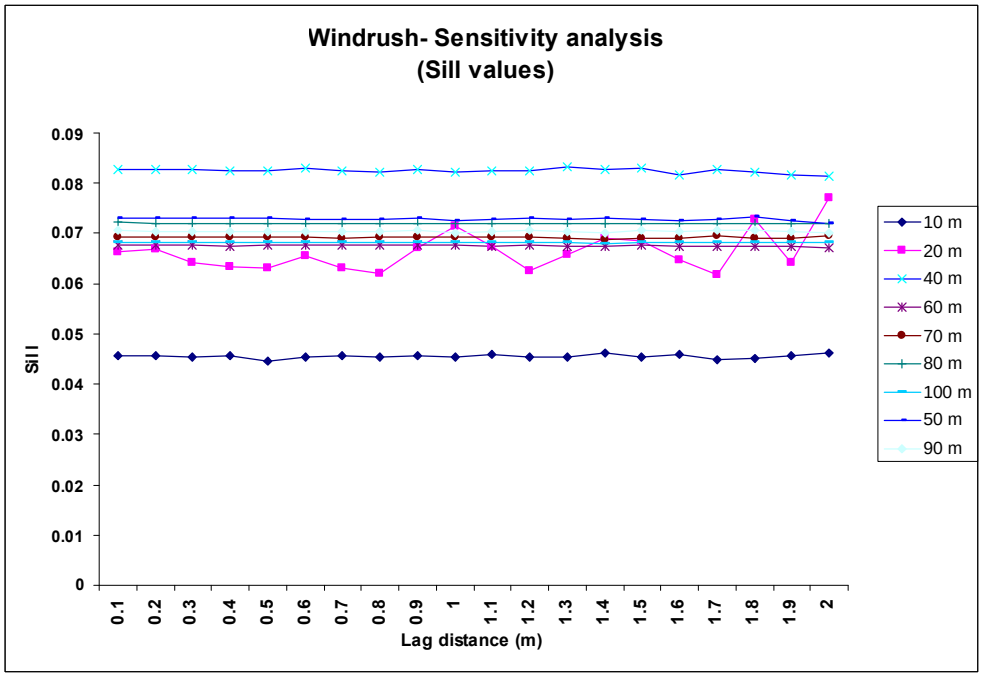
Windrush- Sensitivity analysis
(Sill values)
Sill
Lag distance (m)
10 m
20 m
40 m
60 m
70 m
80 m
100 m
50 m
90 m

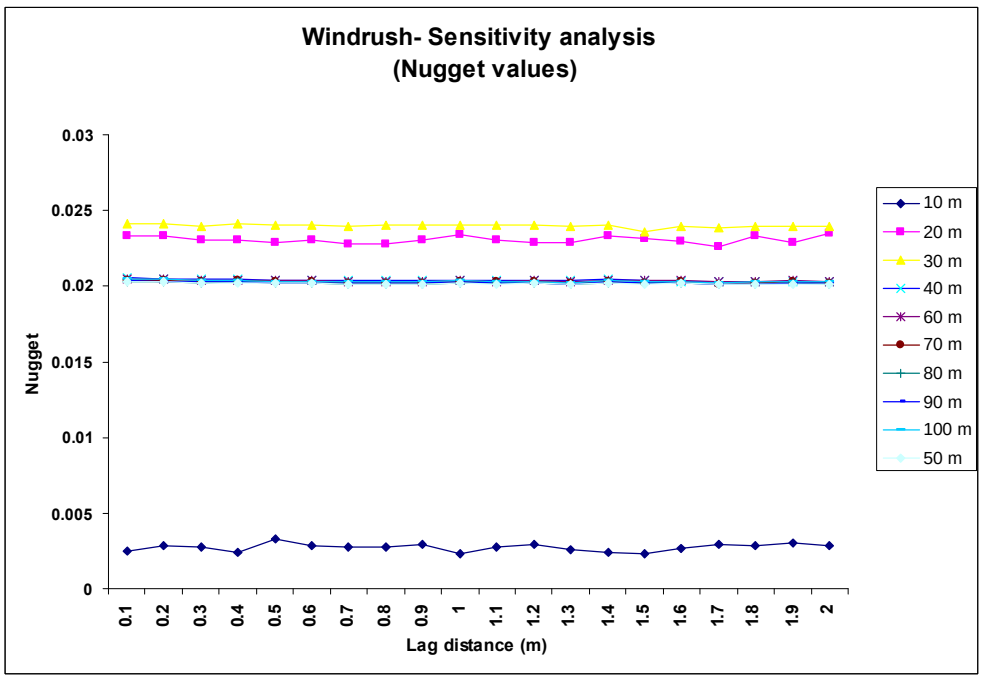
Windrush- Sensitivity analysis
(Nugget values)
Nugget
Lag distance (m)
10 m
20 m
30 m
40 m
60 m
70 m
80 m
90 m
100 m
50 m

Appendix 3.5.5

Results obtained for the analysis in Chapter 5 –Sensitivity Analysis – Variogram values for combinations of lag and maximum distance considered: spherical variogram for dry and wet points.

This appendix summarises the results obtained for the sensitivity analysis developed in section 5.4.3. for the combination of lag distances and maximum distances selected. Results presented in this section only include the graphical output for the data sets analysed with dry and wet points. The horizontal axis represents the selected maximum distance. The variogram model analysed is the spherical one. Three different outputs, one for each variogram variable analysed (i.e. range, sill and nugget) are presented for each river site. Those river sites that had extreme variogram values are included twice: the graphical output is presented with two different axis scales so results can be better analysed.

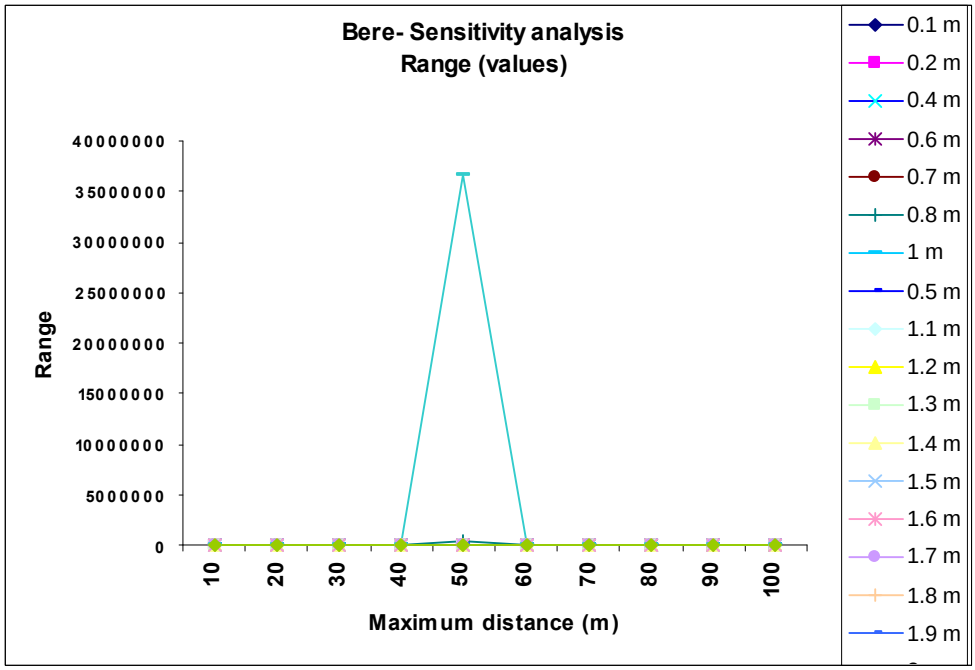
Bere- Sensitivity analysis
Range (values)
Range
40000000
35000000
30000000
25000000
20000000
15000000
10000000
5000000
0
10
20
30
40
50
60
70
80
90
100
Maximum distance (m)
0.1 m
0.2 m
0.4 m
0.6 m
0.7 m
0.8 m
1 m
0.5 m
1.1 m
1.2 m
1.3 m
1.4 m
1.5 m
1.6 m
1.7 m
1.8 m
1.9 m

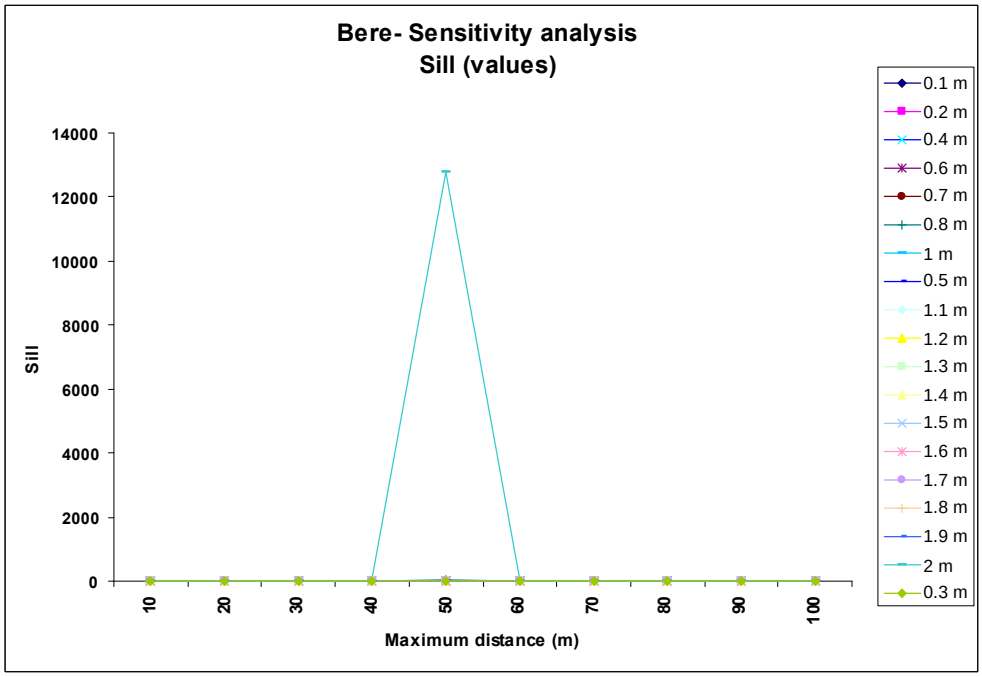
Bere- Sensitivity analysis
Sill (values)
Sill
14000
12000
10000
8000
6000
4000
2000
0
10
20
30
40
50
60
70
80
90
100
Maximum distance (m)
0.1 m
0.2 m
0.4 m
0.6 m
0.7 m
0.8 m
1 m
0.5 m
1.1 m
1.2 m
1.3 m
1.4 m
1.5 m
1.6 m
1.7 m
1.8 m
1.9 m
2 m
0.3 m

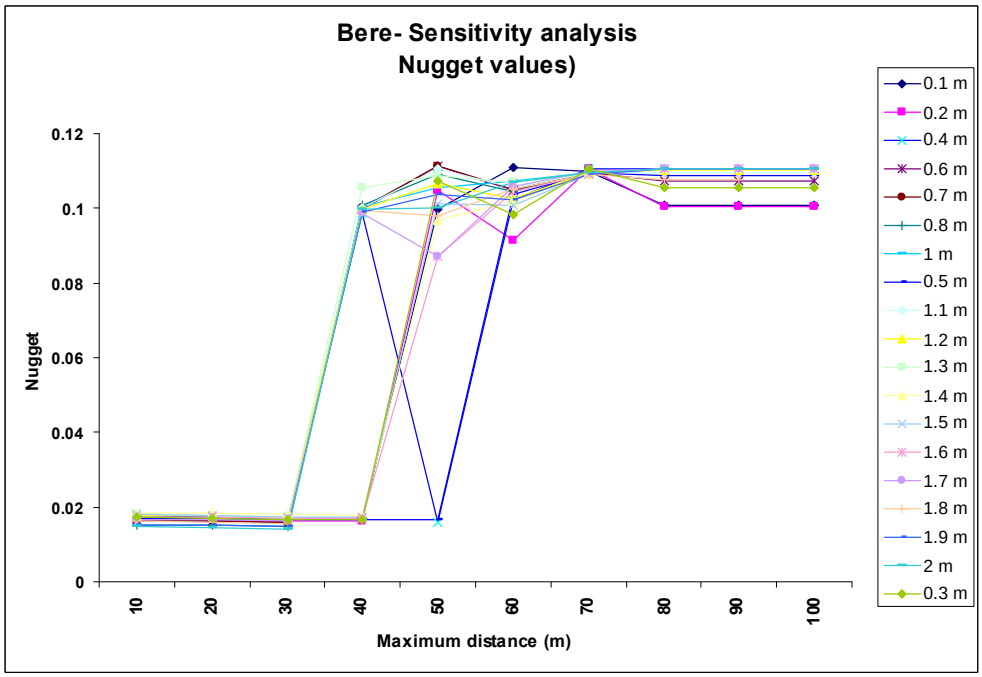
Bere- Sensitivity analysis
Nugget values)
Nugget
0.12
0.1
0.08
0.06
0.04
0.02
0
10
20
30
40
50
60
70
80
90
100
Maximum distance (m)
0.1 m
0.2 m
0.4 m
0.6 m
0.7 m
0.8 m
1 m
0.5 m
1.1 m
1.2 m
1.3 m
1.4 m
1.5 m
1.6 m
1.7 m
1.8 m
1.9 m
2 m
0.3 m

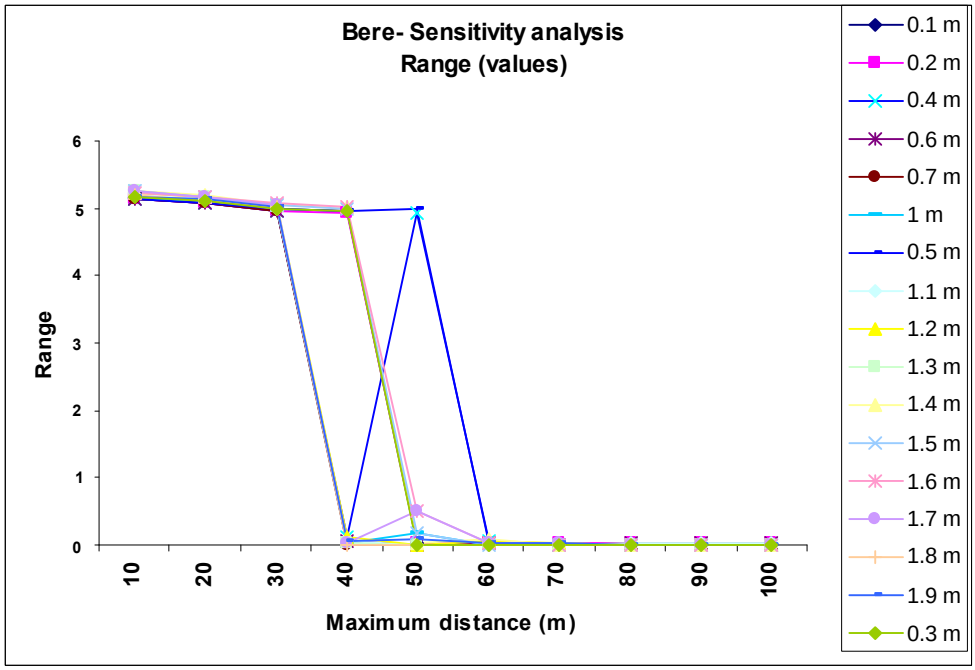
Bere- Sensitivity analysis
Range (values)
Range
Maximum distance (m)
0.1 m
0.2 m
0.4 m
0.6 m
0.7 m
1 m
0.5 m
1.1 m
1.2 m
1.3 m
1.4 m
1.5 m
1.6 m
1.7 m
1.8 m
1.9 m
0.3 m

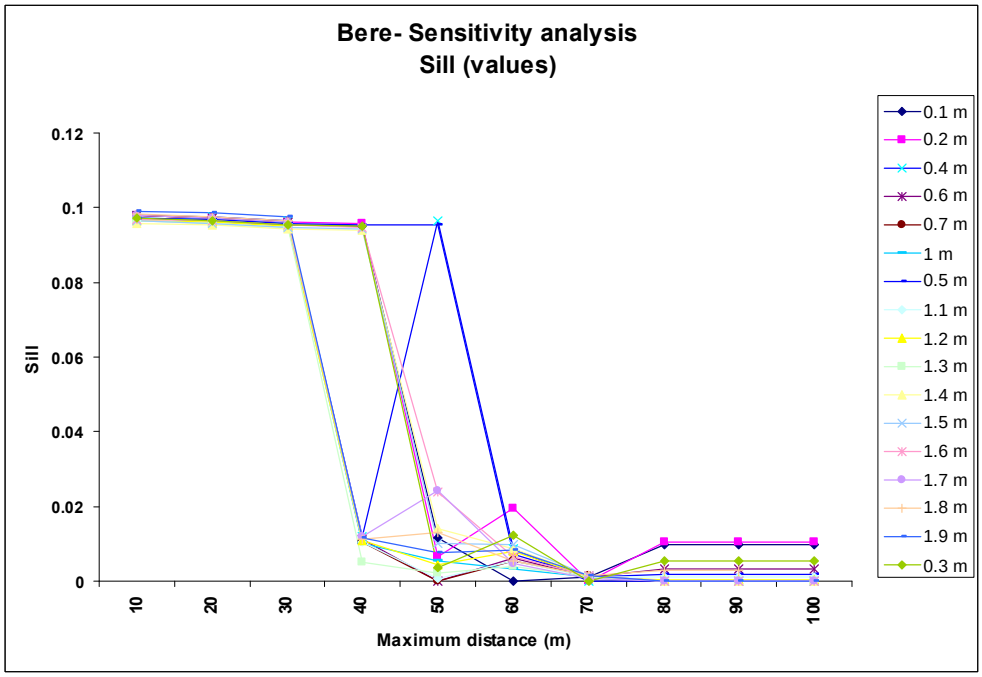
Bere- Sensitivity analysis
Sill (values)
Sill
Maximum distance (m)
0.1 m
0.2 m
0.4 m
0.6 m
0.7 m
1 m
0.5 m
1.1 m
1.2 m
1.3 m
1.4 m
1.5 m
1.6 m
1.7 m
1.8 m
1.9 m
0.3 m

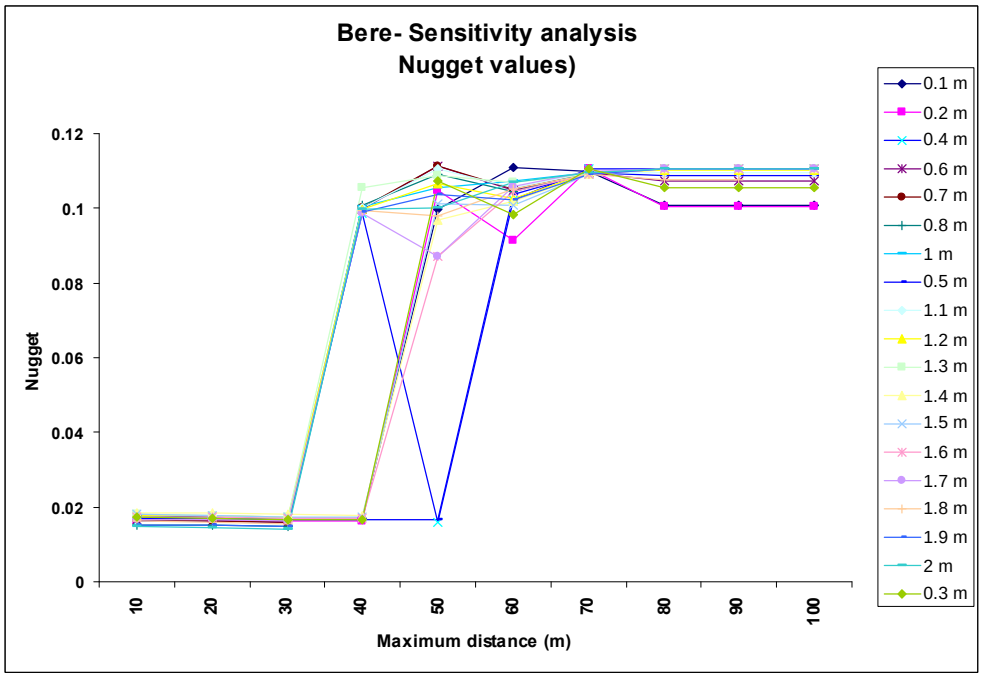
Bere- Sensitivity analysis
Nugget values)
Nugget
Maximum distance (m)
0.1 m
0.2 m
0.4 m
0.6 m
0.7 m
0.8 m
1 m
0.5 m
1.1 m
1.2 m
1.3 m
1.4 m
1.5 m
1.6 m
1.7 m
1.8 m
1.9 m
2 m
0.3 m

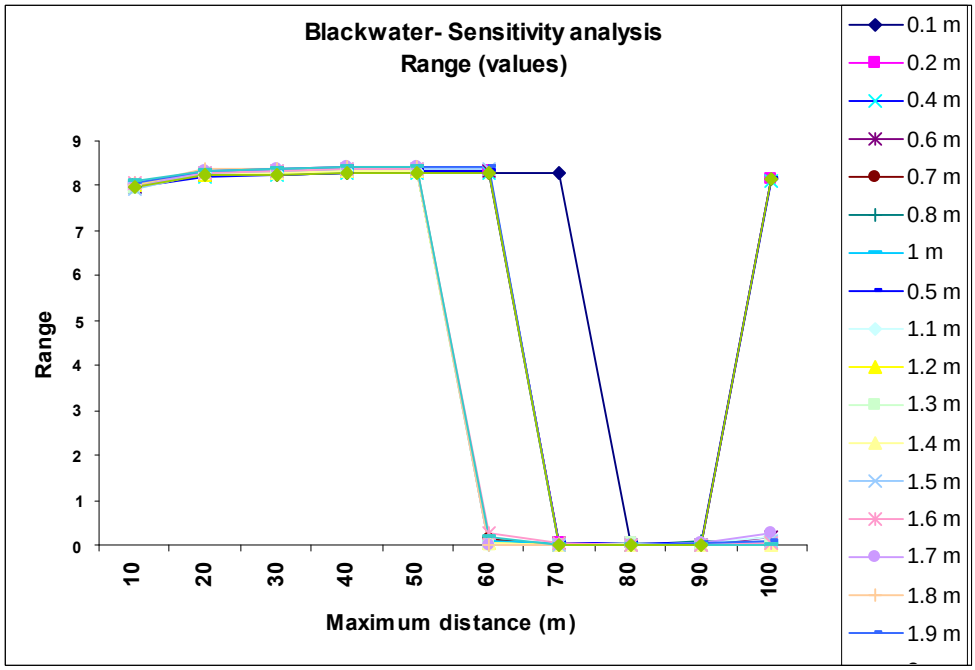
Blackwater- Sensitivity analysis
Range (values)
Range
Maximum distance (m)
0.1 m
0.2 m
0.4 m
0.6 m
0.7 m
0.8 m
1 m
0.5 m
1.1 m
1.2 m
1.3 m
1.4 m
1.5 m
1.6 m
1.7 m
1.8 m
1.9 m

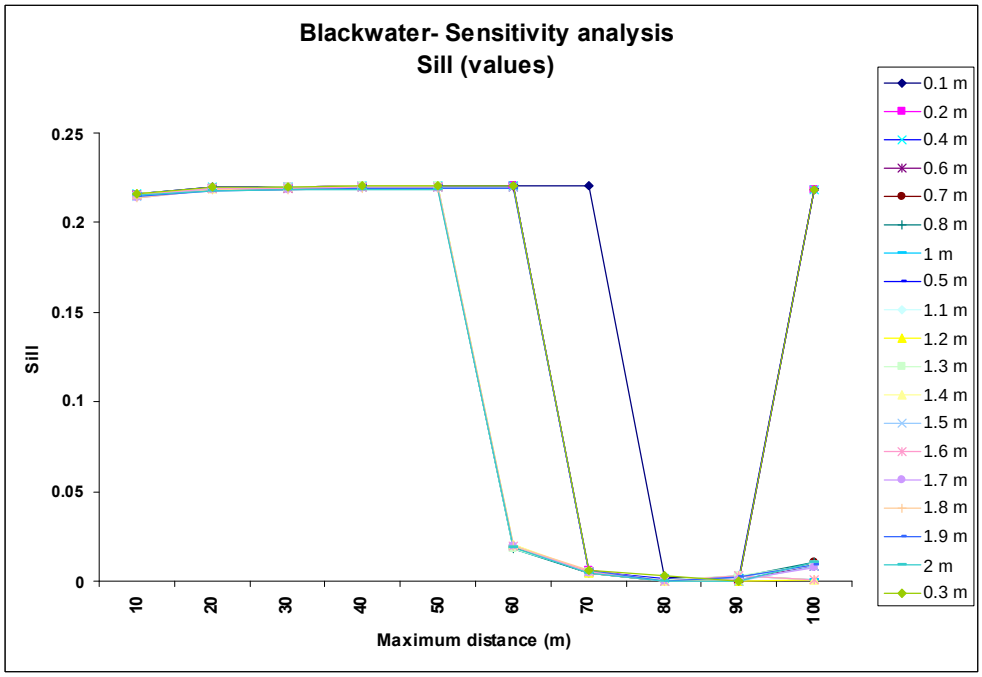
Blackwater- Sensitivity analysis
Sill (values)
Sill
Maximum distance (m)
0.1 m
0.2 m
0.4 m
0.6 m
0.7 m
0.8 m
1 m
0.5 m
1.1 m
1.2 m
1.3 m
1.4 m
1.5 m
1.6 m
1.7 m
1.8 m
1.9 m
2 m
0.3 m

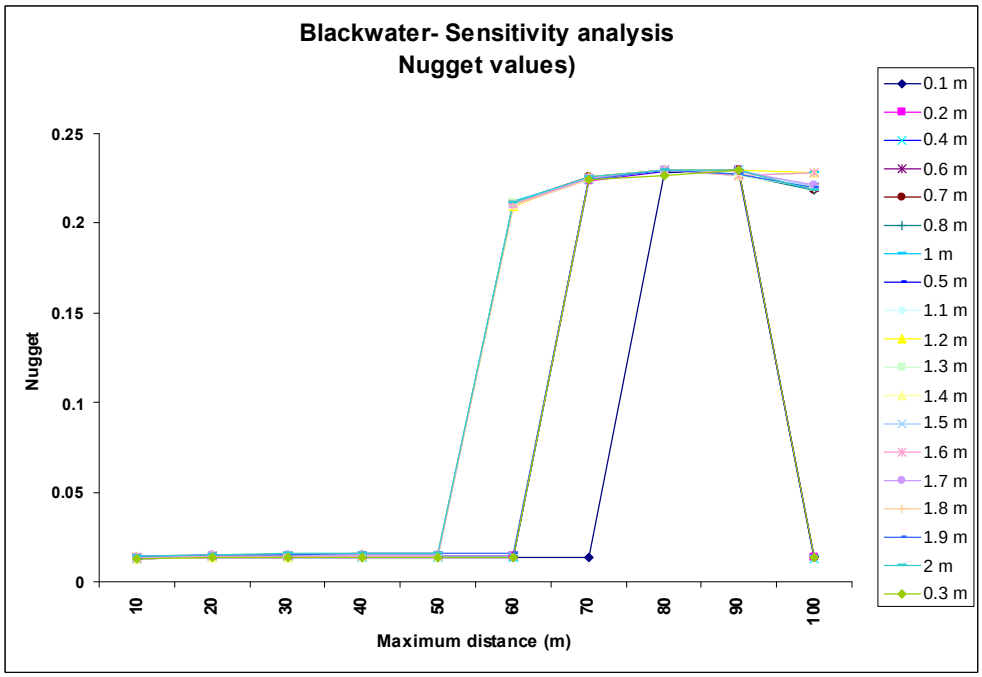
Blackwater- Sensitivity analysis
Nugget values)
Nugget
Maximum distance (m)
0.1 m
0.2 m
0.4 m
0.6 m
0.7 m
0.8 m
1 m
0.5 m
1.1 m
1.2 m
1.3 m
1.4 m
1.5 m
1.6 m
1.7 m
1.8 m
1.9 m
2 m
0.3 m

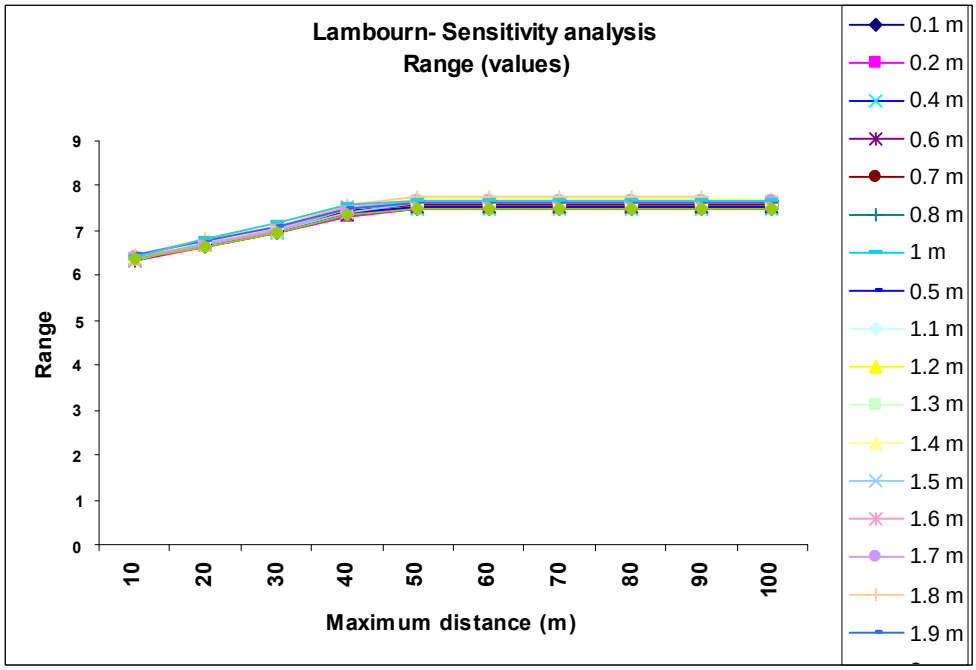
Lambourn- Sensitivity analysis
Range (values)
Range
Maximum distance (m)
0.1 m
0.2 m
0.4 m
0.6 m
0.7 m
0.8 m
1 m
0.5 m
1.1 m
1.2 m
1.3 m
1.4 m
1.5 m
1.6 m
1.7 m
1.8 m
1.9 m

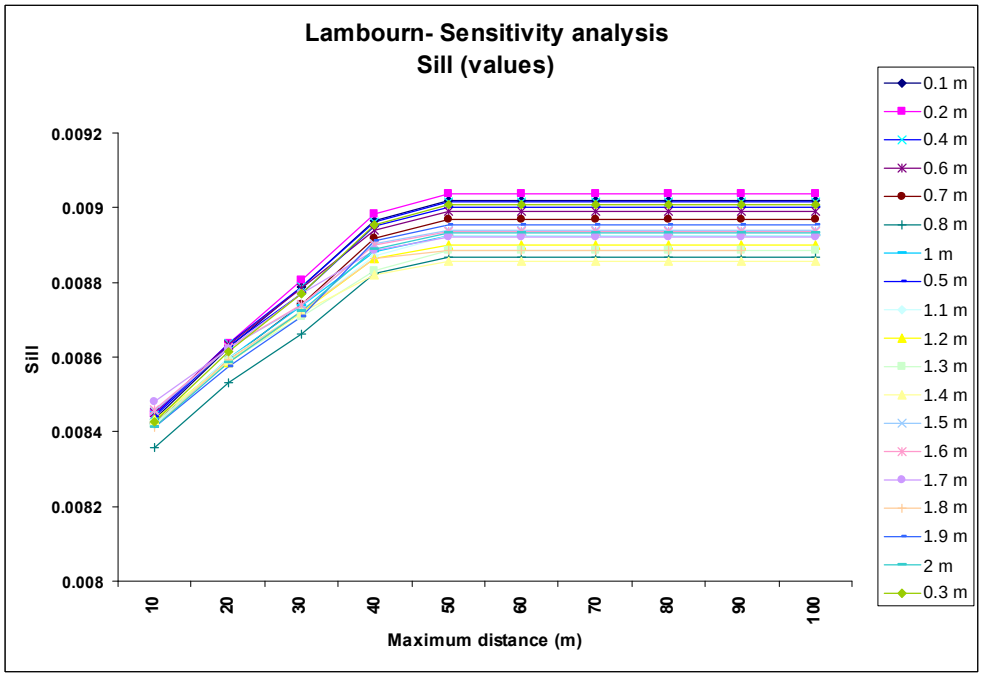
Lambourn- Sensitivity analysis
Sill (values)
Sill
Maximum distance (m)
0.1 m
0.2 m
0.4 m
0.6 m
0.7 m
0.8 m
1 m
0.5 m
1.1 m
1.2 m
1.3 m
1.4 m
1.5 m
1.6 m
1.7 m
1.8 m
1.9 m
2 m
0.3 m

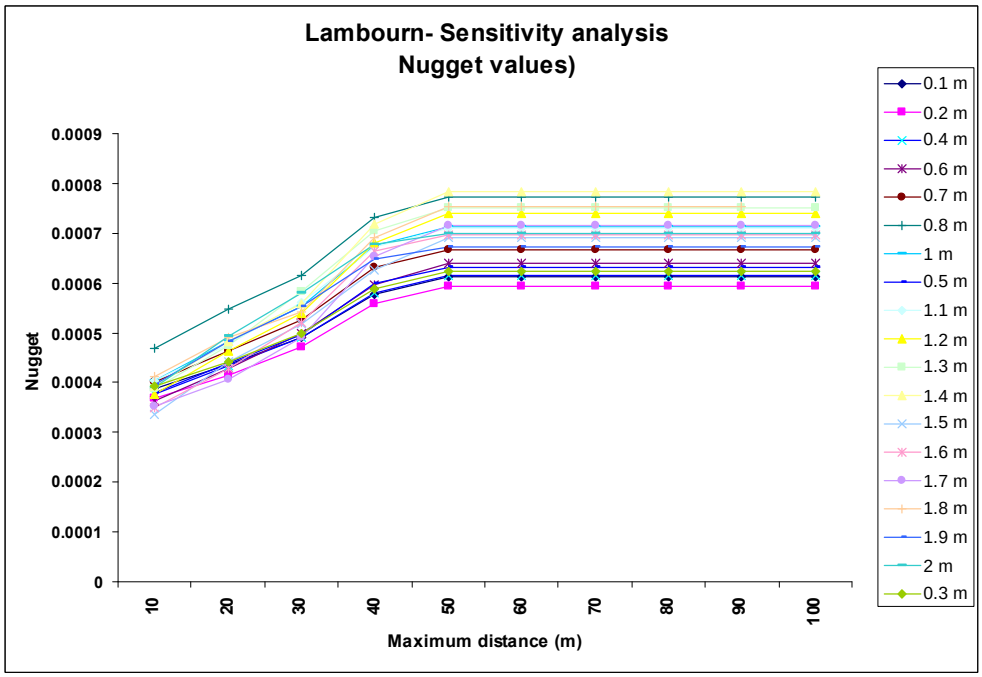
Lambourn- Sensitivity analysis
Nugget values)
Nugget
Maximum distance (m)
0.1 m
0.2 m
0.4 m
0.6 m
0.7 m
0.8 m
1 m
0.5 m
1.1 m
1.2 m
1.3 m
1.4 m
1.5 m
1.6 m
1.7 m
1.8 m
1.9 m
2 m
0.3 m

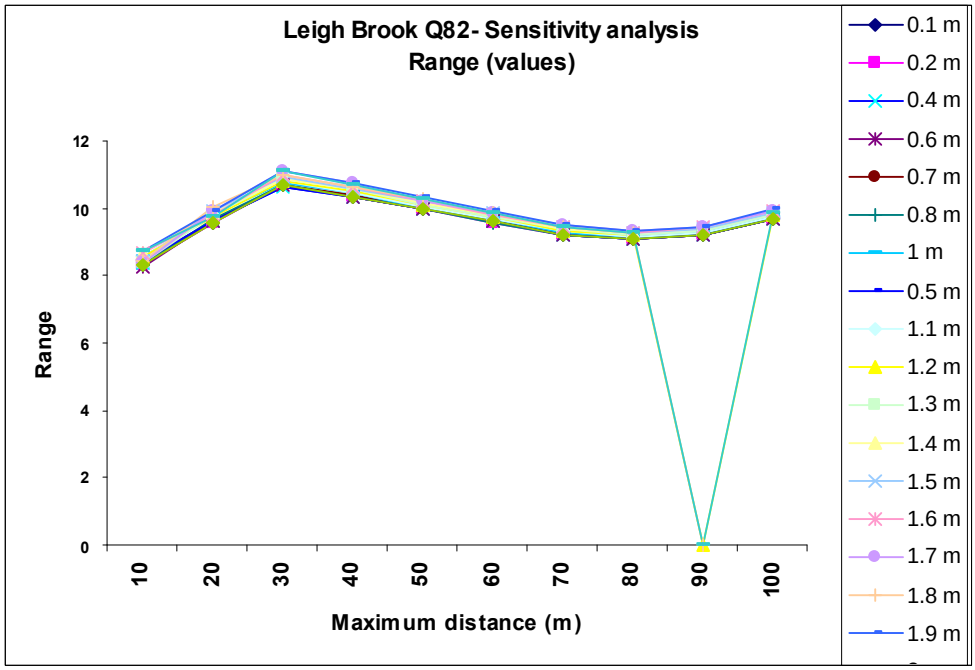
Leigh Brook Q82- Sensitivity analysis
Range (values)
Range
Maximum distance (m)
0.1 m
0.2 m
0.4 m
0.6 m
0.7 m
0.8 m
1 m
0.5 m
1.1 m
1.2 m
1.3 m
1.4 m
1.5 m
1.6 m
1.7 m
1.8 m
1.9 m

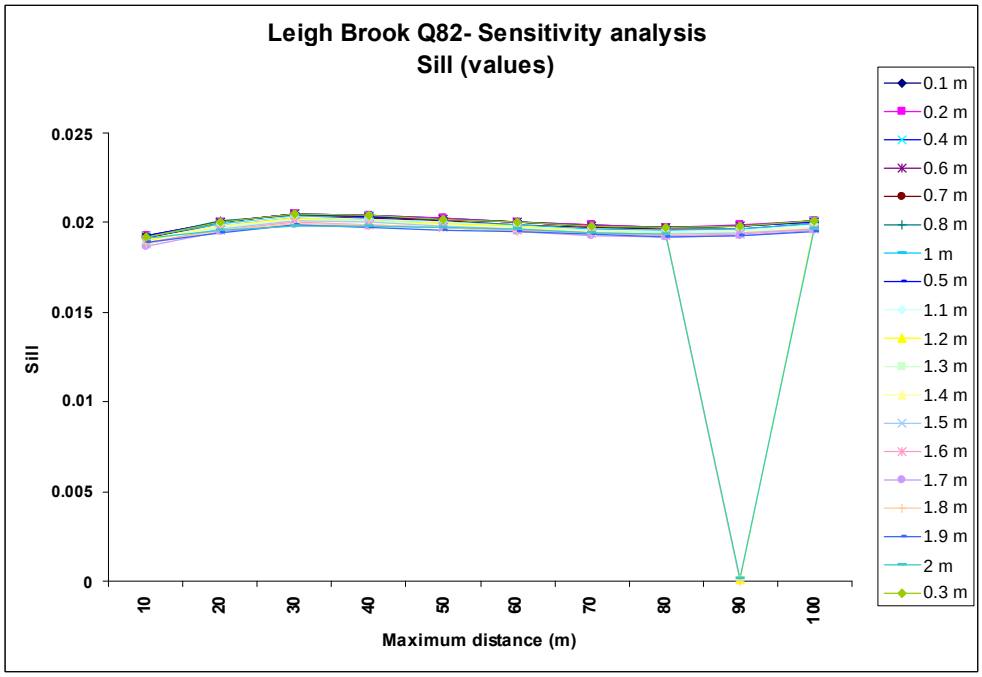
Leigh Brook Q82- Sensitivity analysis
Sill (values)
Sill
Maximum distance (m)
0.1 m
0.2 m
0.4 m
0.6 m
0.7 m
0.8 m
1 m
0.5 m
1.1 m
1.2 m
1.3 m
1.4 m
1.5 m
1.6 m
1.7 m
1.8 m
1.9 m
2 m
0.3 m

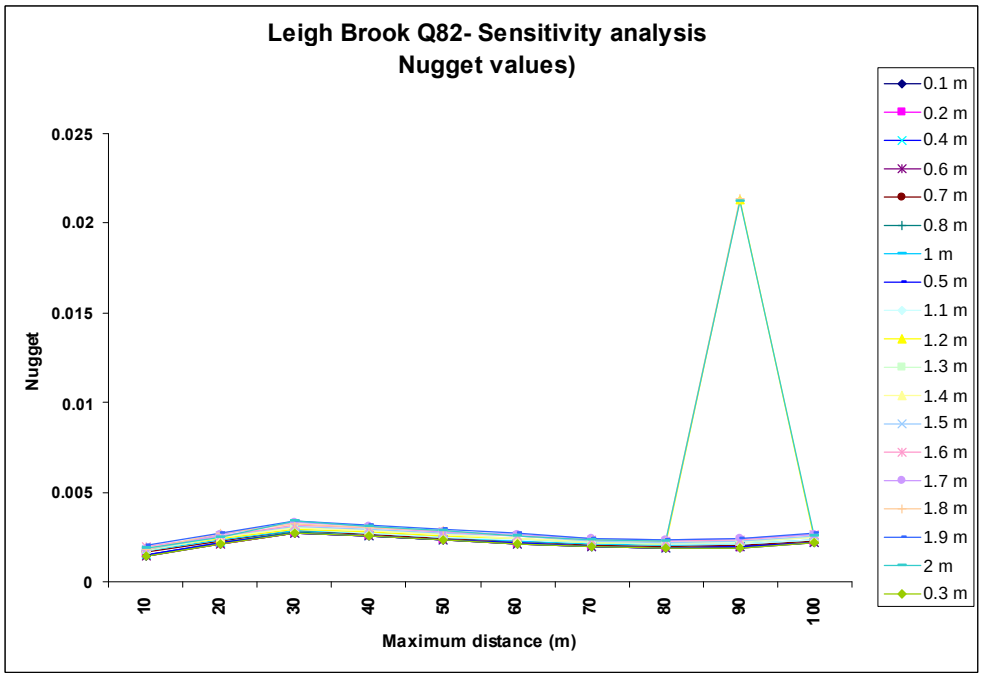
Leigh Brook Q82- Sensitivity analysis
Nugget values)
Nugget
Maximum distance (m)
0.1 m
0.2 m
0.4 m
0.6 m
0.7 m
0.8 m
1 m
0.5 m
1.1 m
1.2 m
1.3 m
1.4 m
1.5 m
1.6 m
1.7 m
1.8 m
1.9 m
2 m
0.3 m

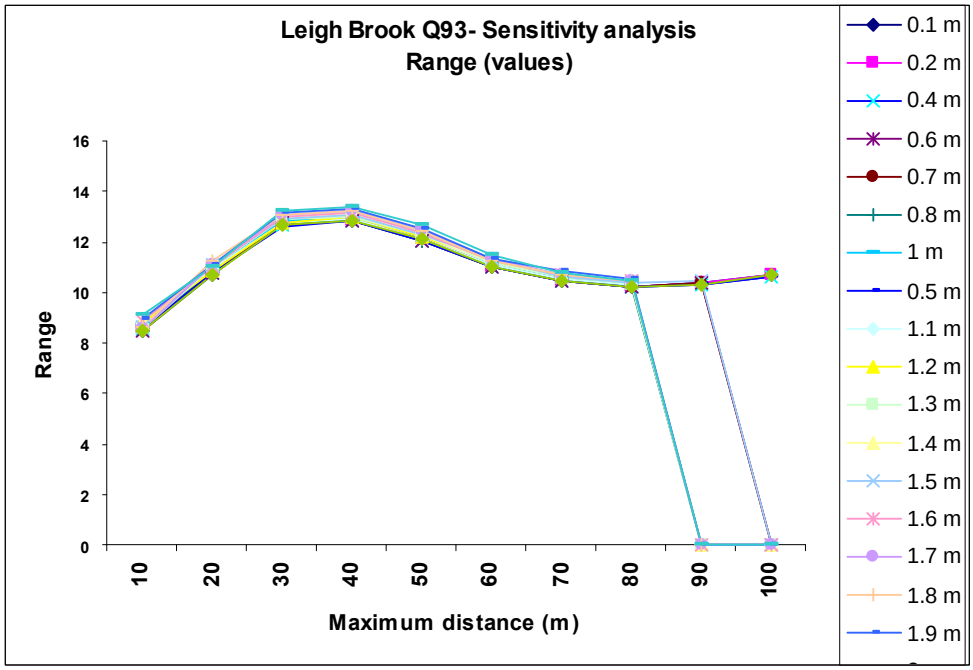
Leigh Brook Q93- Sensitivity analysis
Range (values)
Range
Maximum distance (m)
0.1 m
0.2 m
0.4 m
0.6 m
0.7 m
0.8 m
1 m
0.5 m
1.1 m
1.2 m
1.3 m
1.4 m
1.5 m
1.6 m
1.7 m
1.8 m
1.9 m

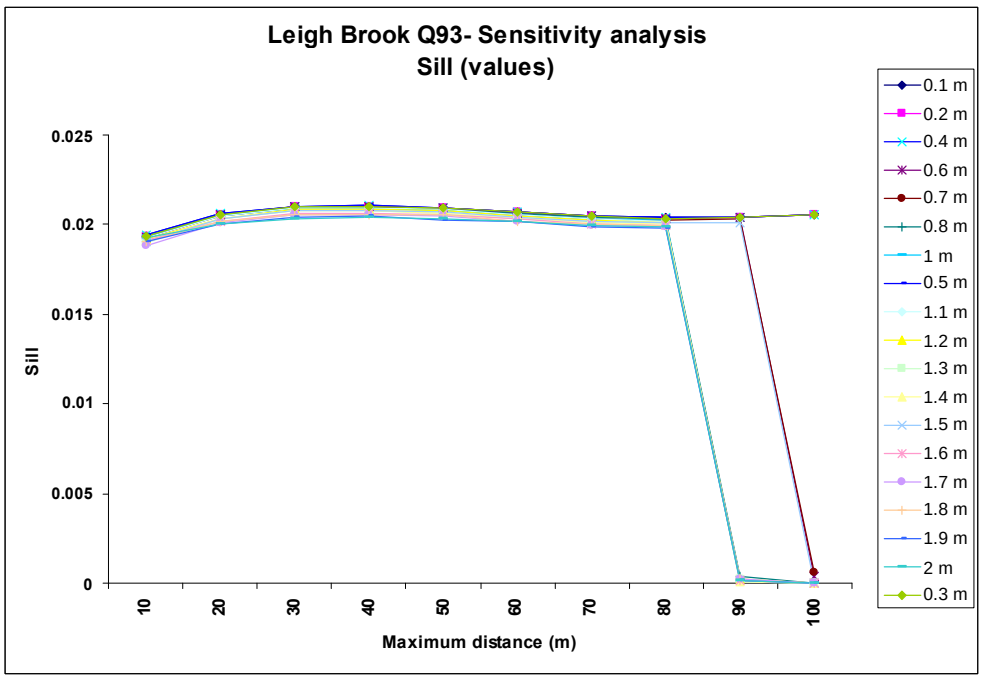
Leigh Brook Q93- Sensitivity analysis
Sill (values)
Sill
Maximum distance (m)
0.1 m
0.2 m
0.4 m
0.6 m
0.7 m
0.8 m
1 m
0.5 m
1.1 m
1.2 m
1.3 m
1.4 m
1.5 m
1.6 m
1.7 m
1.8 m
1.9 m
2 m
0.3 m

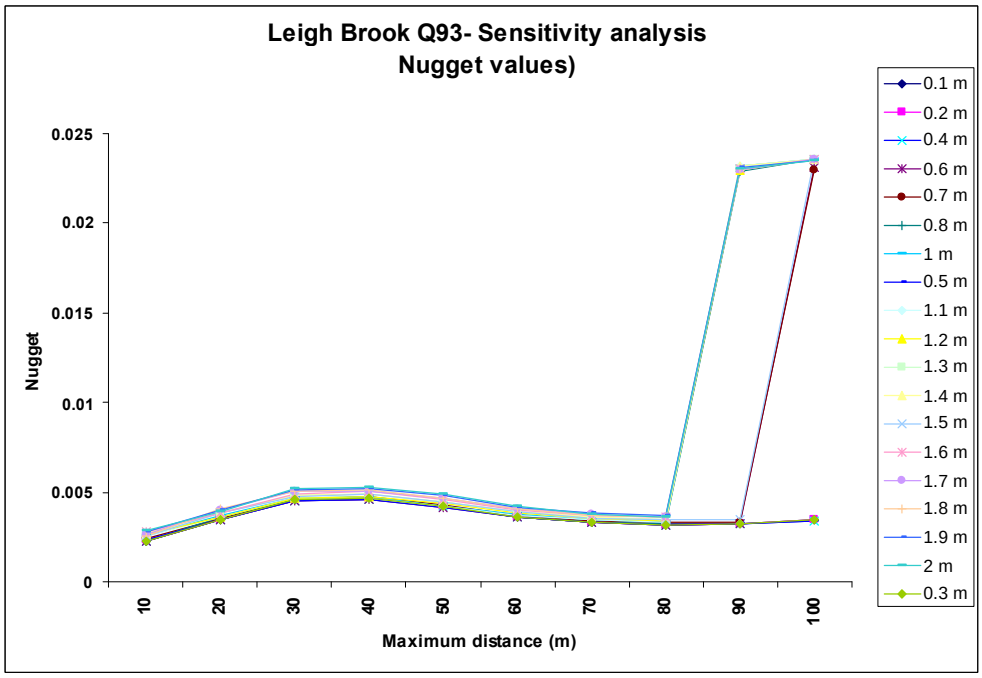
Leigh Brook Q93- Sensitivity analysis
Nugget values)
Nugget
Maximum distance (m)
0.1 m
0.2 m
0.4 m
0.6 m
0.7 m
0.8 m
1 m
0.5 m
1.1 m
1.2 m
1.3 m
1.4 m
1.5 m
1.6 m
1.7 m
1.8 m
1.9 m
2 m
0.3 m

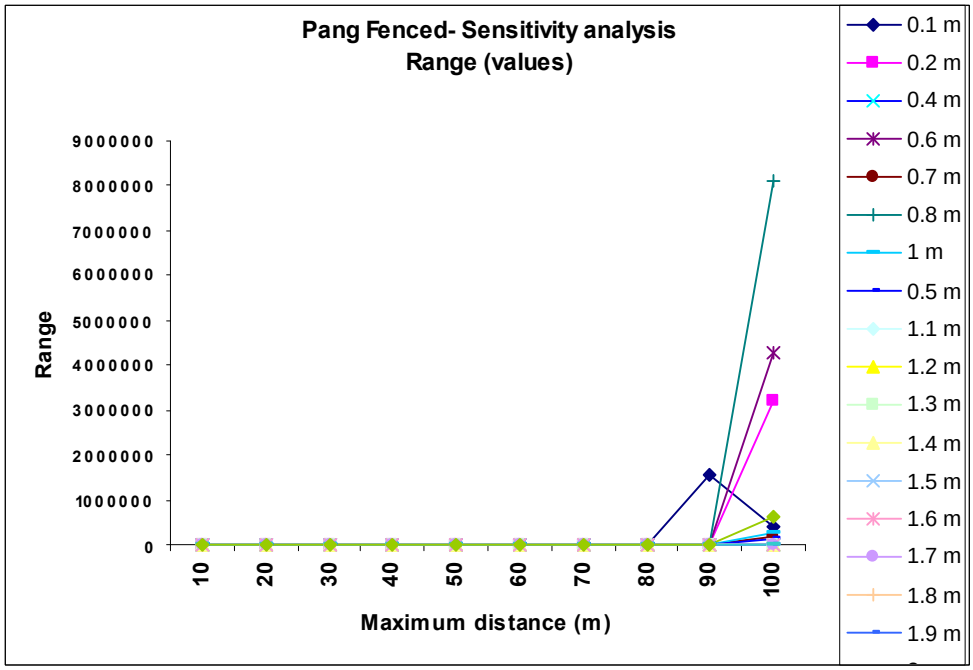
Pang Fenced- Sensitivity analysis
Range (values)
Range
9000000
8000000
7000000
6000000
5000000
4000000
3000000
2000000
1000000
0
10
20
30
40
50
60
70
80
90
100
Maximum distance (m)
0.1 m
0.2 m
0.4 m
0.6 m
0.7 m
0.8 m
1 m
0.5 m
1.1 m
1.2 m
1.3 m
1.4 m
1.5 m
1.6 m
1.7 m
1.8 m
1.9 m

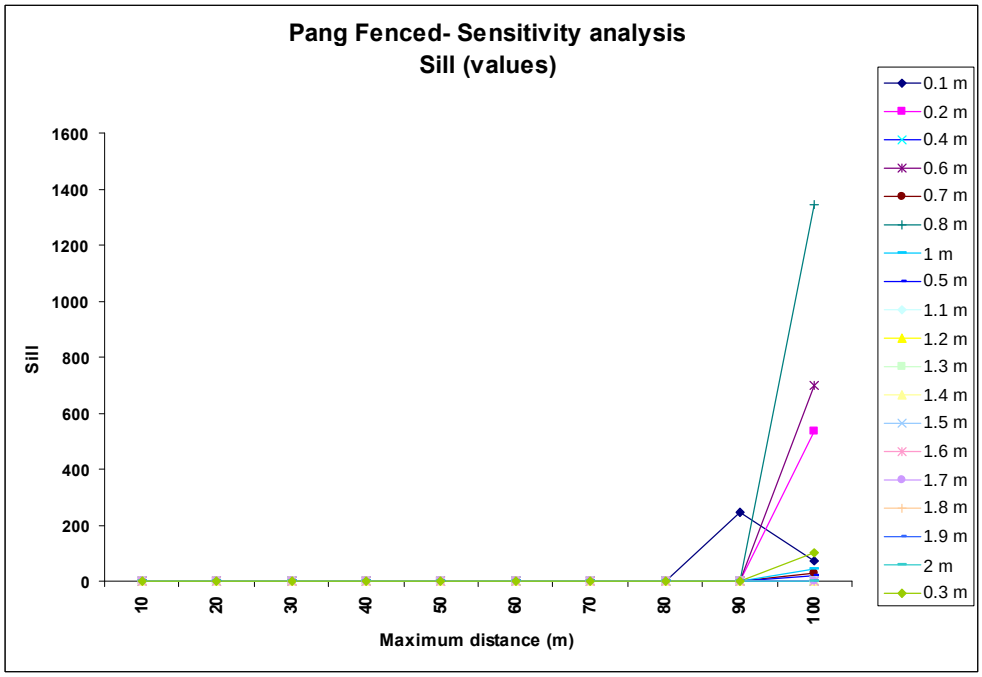
Pang Fenced- Sensitivity analysis
Sill (values)
Sill
1600
1400
1200
1000
800
600
400
200
0
10
20
30
40
50
60
70
80
90
100
Maximum distance (m)
0.1 m
0.2 m
0.4 m
0.6 m
0.7 m
0.8 m
1 m
0.5 m
1.1 m
1.2 m
1.3 m
1.4 m
1.5 m
1.6 m
1.7 m
1.8 m
1.9 m
2 m
0.3 m

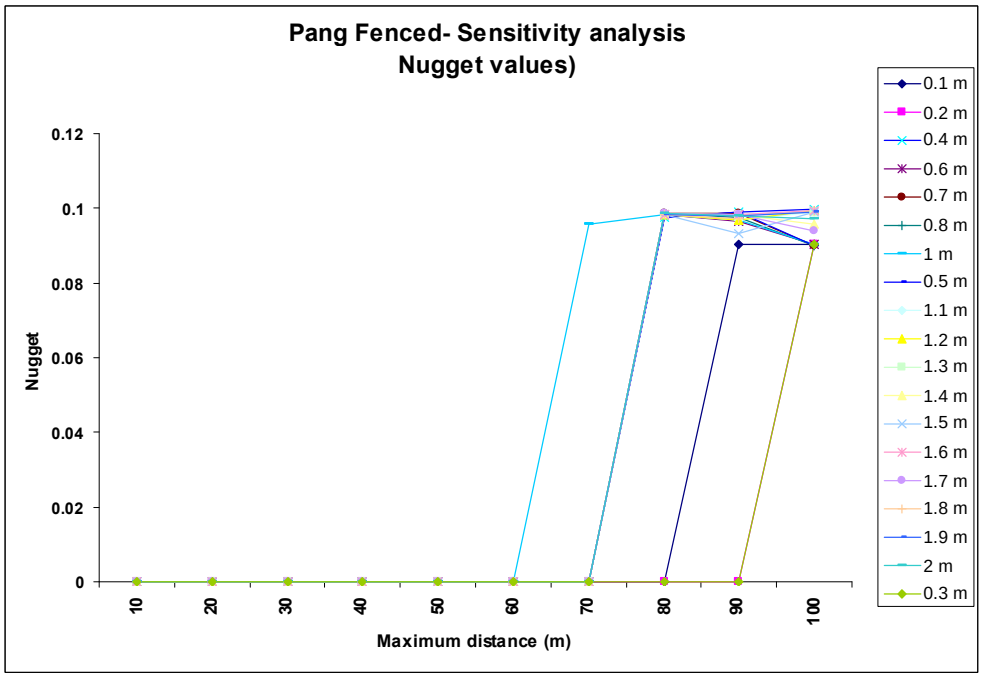
Pang Fenced- Sensitivity analysis
Nugget values)
Nugget
0.12
0.1
0.08
0.06
0.04
0.02
0
10
20
30
40
50
60
70
80
90
100
Maximum distance (m)
0.1 m
0.2 m
0.4 m
0.6 m
0.7 m
0.8 m
1 m
0.5 m
1.1 m
1.2 m
1.3 m
1.4 m
1.5 m
1.6 m
1.7 m
1.8 m
1.9 m
2 m
0.3 m

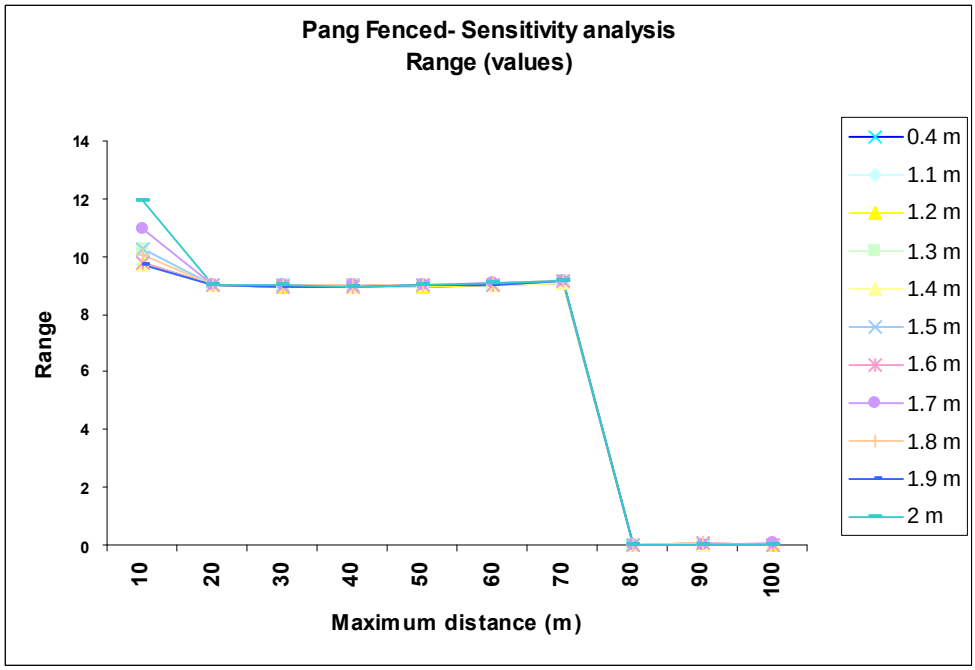
Pang Fenced- Sensitivity analysis
Range (values)
Range
Maximum distance (m)
0.4 m
1.1 m
1.2 m
1.3 m
1.4 m
1.5 m
1.6 m
1.7 m
1.8 m
1.9 m
2 m

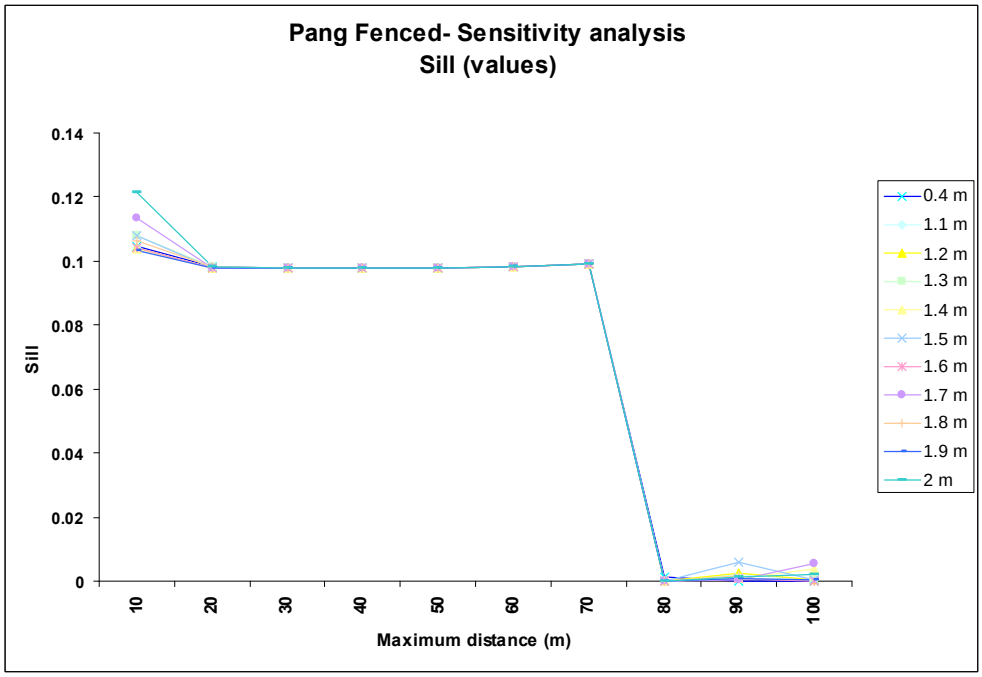
Pang Fenced- Sensitivity analysis
Sill (values)
Sill
Maximum distance (m)
0.4 m
1.1 m
1.2 m
1.3 m
1.4 m
1.5 m
1.6 m
1.7 m
1.8 m
1.9 m
2 m

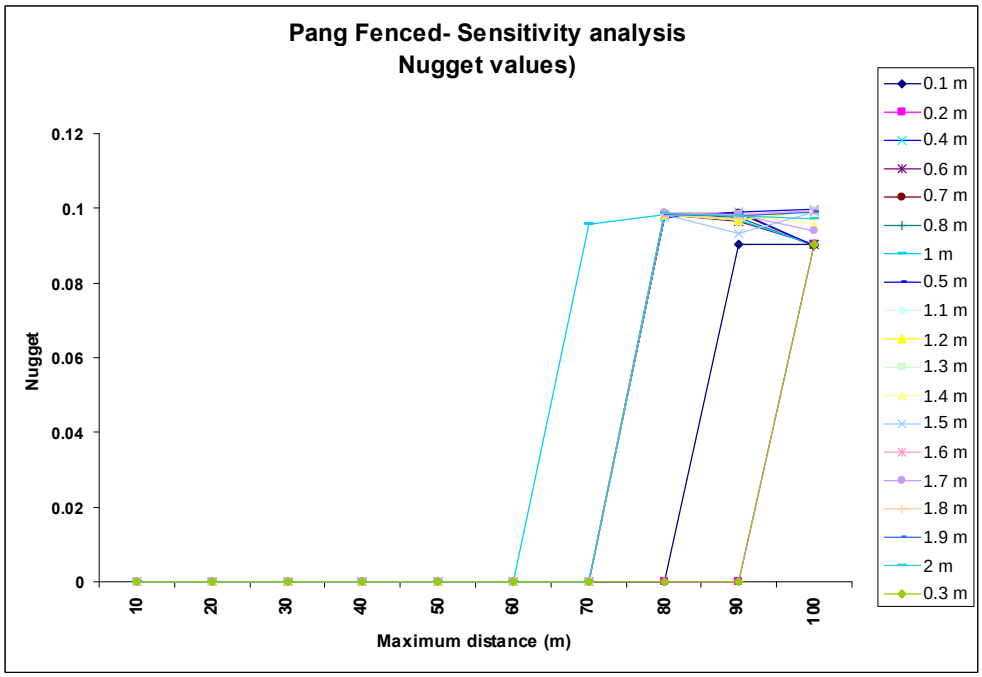
Pang Fenced- Sensitivity analysis
Nugget values)
Nugget
Maximum distance (m)
0.1 m
0.2 m
0.4 m
0.6 m
0.7 m
0.8 m
1 m
0.5 m
1.1 m
1.2 m
1.3 m
1.4 m
1.5 m
1.6 m
1.7 m
1.8 m
1.9 m
2 m
0.3 m

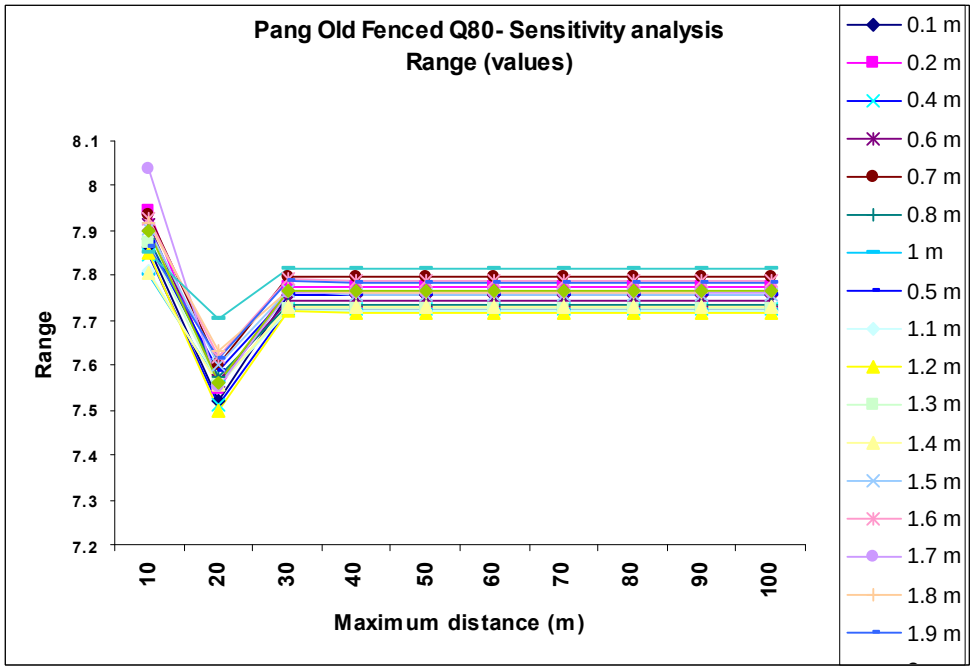
Pang Old Fenced Q80- Sensitivity analysis
Range (values)
Range
8.1
8
7.9
7.8
7.7
7.6
7.5
7.4
7.3
7.2
10
20
30
40
50
60
70
80
90
100
Maximum distance (m)
0.1 m
0.2 m
0.4 m
0.6 m
0.7 m
0.8 m
1 m
0.5 m
1.1 m
1.2 m
1.3 m
1.4 m
1.5 m
1.6 m
1.7 m
1.8 m
1.9 m

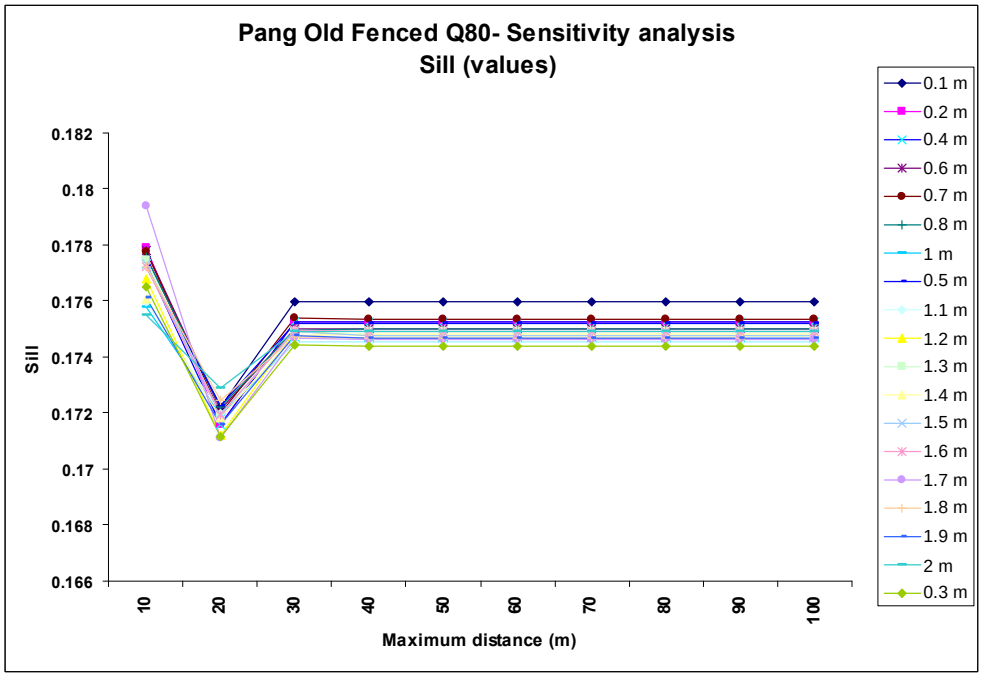
Pang Old Fenced Q80- Sensitivity analysis
Sill (values)
Sill
0.182
0.18
0.178
0.176
0.174
0.172
0.17
0.168
0.166
10
20
30
40
50
60
70
80
90
100
Maximum distance (m)
0.1 m
0.2 m
0.4 m
0.6 m
0.7 m
0.8 m
1 m
0.5 m
1.1 m
1.2 m
1.3 m
1.4 m
1.5 m
1.6 m
1.7 m
1.8 m
1.9 m
2 m
0.3 m

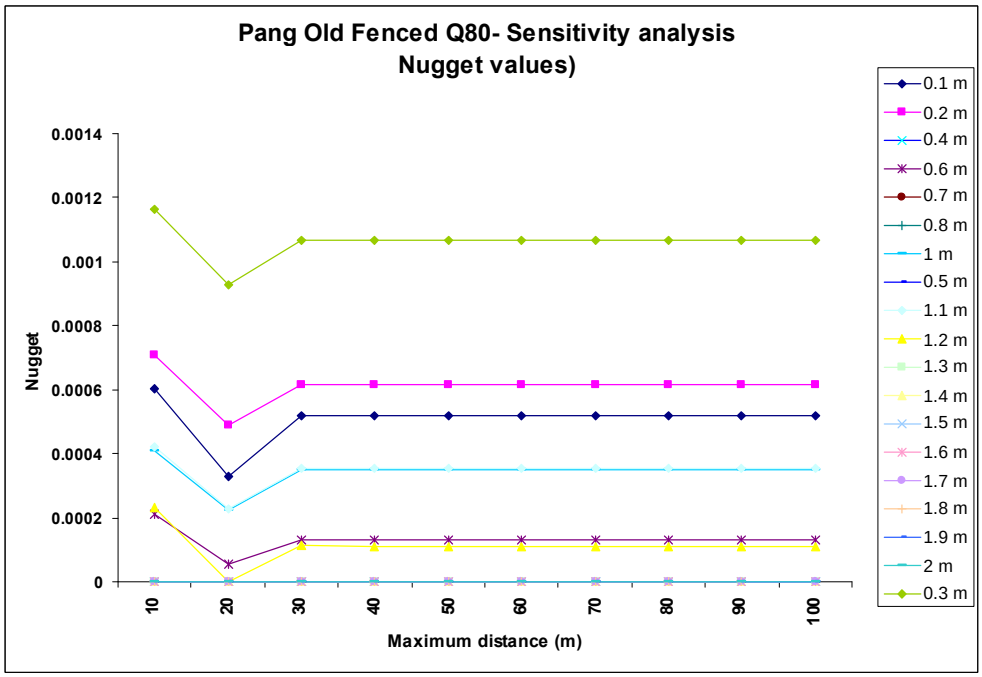
Pang Old Fenced Q80- Sensitivity analysis
Nugget values)
Nugget
0.0014
0.0012
0.001
0.0008
0.0006
0.0004
0.0002
0
10
20
30
40
50
60
70
80
90
100
Maximum distance (m)
0.1 m
0.2 m
0.4 m
0.6 m
0.7 m
0.8 m
1 m
0.5 m
1.1 m
1.2 m
1.3 m
1.4 m
1.5 m
1.6 m
1.7 m
1.8 m
1.9 m
2 m
0.3 m

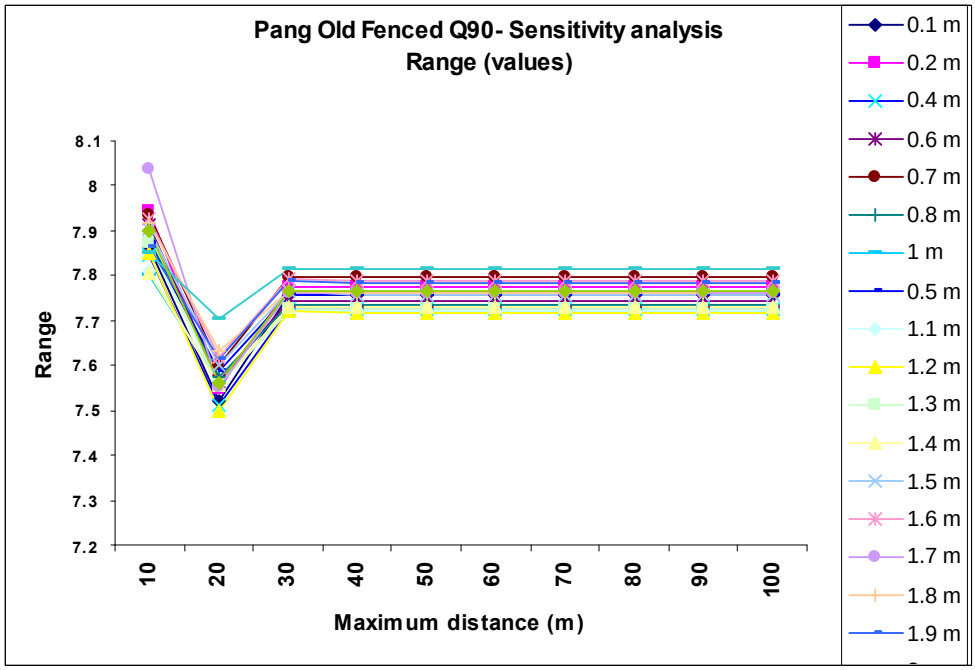
Pang Old Fenced Q90- Sensitivity analysis
Range (values)
Range
8.1
8
7.9
7.8
7.7
7.6
7.5
7.4
7.3
7.2
10
20
30
40
50
60
70
80
90
100
Maximum distance (m)
0.1 m
0.2 m
0.4 m
0.6 m
0.7 m
0.8 m
1 m
0.5 m
1.1 m
1.2 m
1.3 m
1.4 m
1.5 m
1.6 m
1.7 m
1.8 m
1.9 m

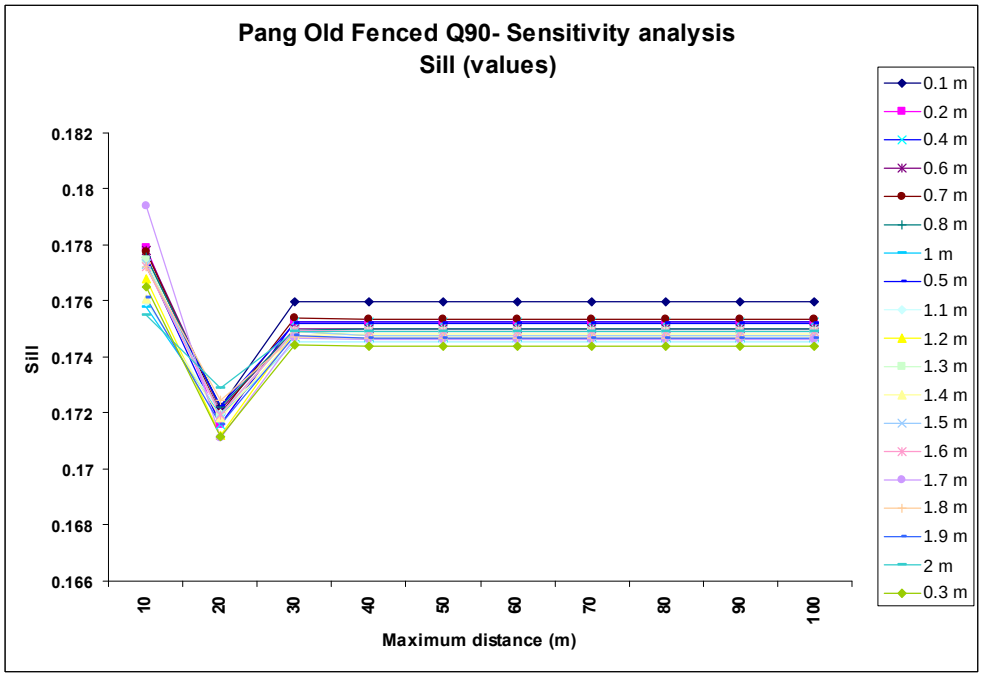
Pang Old Fenced Q90- Sensitivity analysis
Sill (values)
Sill
0.182
0.18
0.178
0.176
0.174
0.172
0.17
0.168
0.166
10
20
30
40
50
60
70
80
90
100
Maximum distance (m)
0.1 m
0.2 m
0.4 m
0.6 m
0.7 m
0.8 m
1 m
0.5 m
1.1 m
1.2 m
1.3 m
1.4 m
1.5 m
1.6 m
1.7 m
1.8 m
1.9 m
2 m
0.3 m

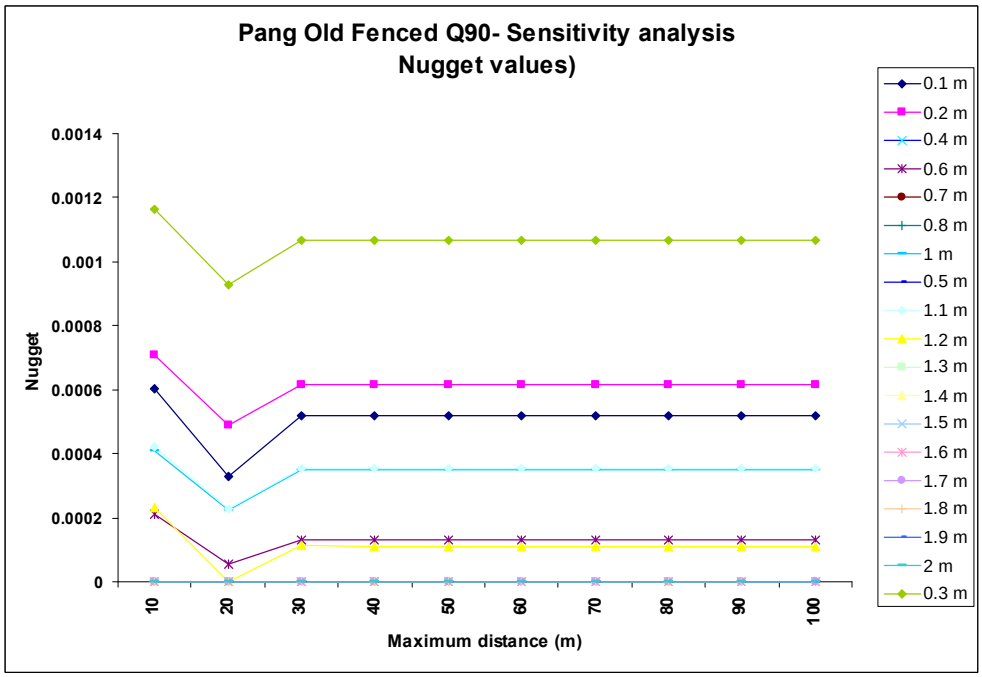
Pang Old Fenced Q90- Sensitivity analysis
Nugget values)
Nugget
0.0014
0.0012
0.001
0.0008
0.0006
0.0004
0.0002
0
10
20
30
40
50
60
70
80
90
100
Maximum distance (m)
0.1 m
0.2 m
0.4 m
0.6 m
0.7 m
0.8 m
1 m
0.5 m
1.1 m
1.2 m
1.3 m
1.4 m
1.5 m
1.6 m
1.7 m
1.8 m
1.9 m
2 m
0.3 m

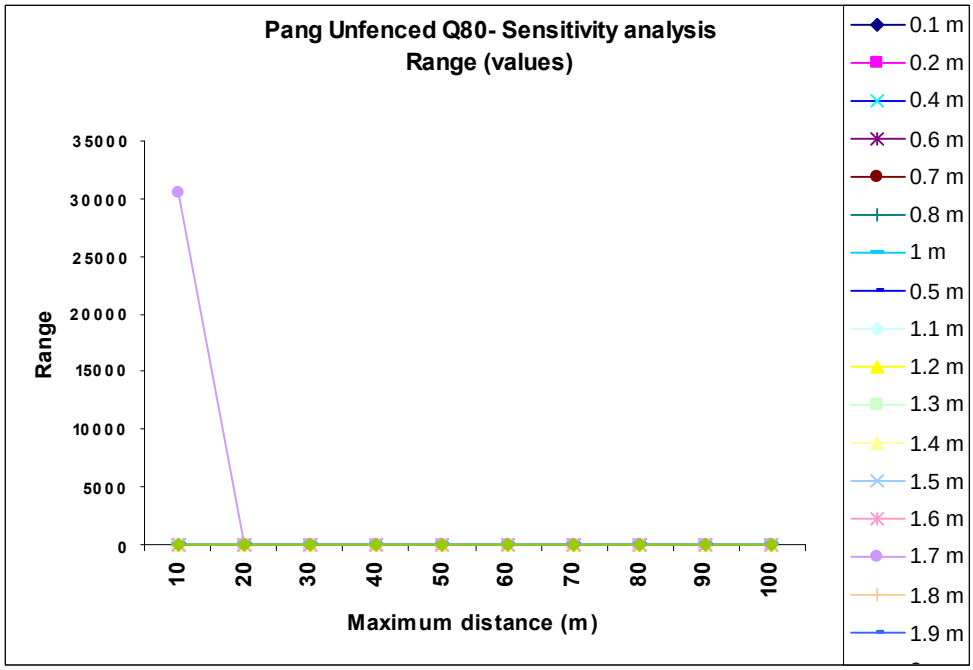
Pang Unfenced Q80- Sensitivity analysis
Range (values)
Range
35000
30000
25000
20000
15000
10000
5000
0
10
20
30
40
50
60
70
80
90
100
Maximum distance (m)
0.1 m
0.2 m
0.4 m
0.6 m
0.7 m
0.8 m
1 m
0.5 m
1.1 m
1.2 m
1.3 m
1.4 m
1.5 m
1.6 m
1.7 m
1.8 m
1.9 m

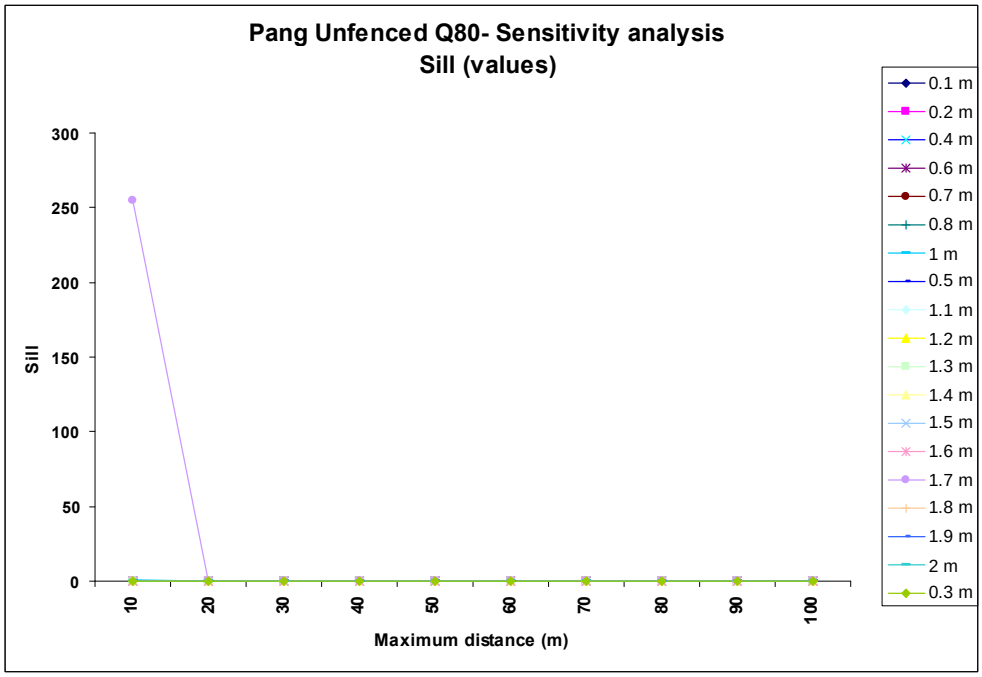
Pang Unfenced Q80- Sensitivity analysis
Sill (values)
Sill
300
250
200
150
100
50
0
10
20
30
40
50
60
70
80
90
100
Maximum distance (m)
0.1 m
0.2 m
0.4 m
0.6 m
0.7 m
0.8 m
1 m
0.5 m
1.1 m
1.2 m
1.3 m
1.4 m
1.5 m
1.6 m
1.7 m
1.8 m
1.9 m
2 m
0.3 m

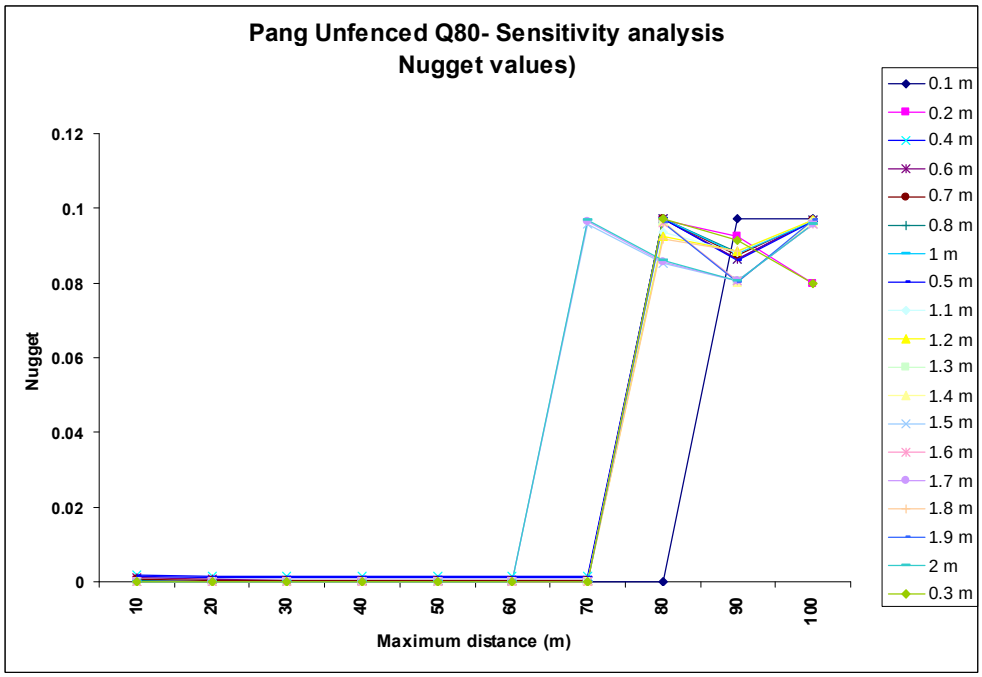
Pang Unfenced Q80- Sensitivity analysis
Nugget values)
Nugget
0.12
0.1
0.08
0.06
0.04
0.02
0
10
20
30
40
50
60
70
80
90
100
Maximum distance (m)
0.1 m
0.2 m
0.4 m
0.6 m
0.7 m
0.8 m
1 m
0.5 m
1.1 m
1.2 m
1.3 m
1.4 m
1.5 m
1.6 m
1.7 m
1.8 m
1.9 m
2 m
0.3 m

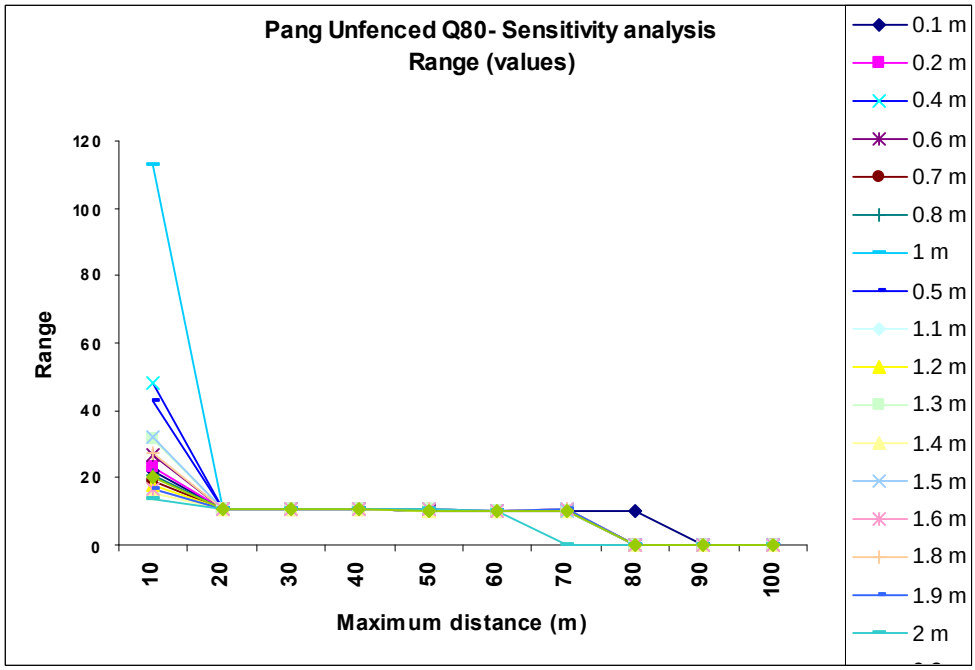
Pang Unfenced Q80- Sensitivity analysis
Range (values)
Range
Maximum distance (m)
0.1 m
0.2 m
0.4 m
0.6 m
0.7 m
0.8 m
1 m
0.5 m
1.1 m
1.2 m
1.3 m
1.4 m
1.5 m
1.6 m
1.8 m
1.9 m
2 m

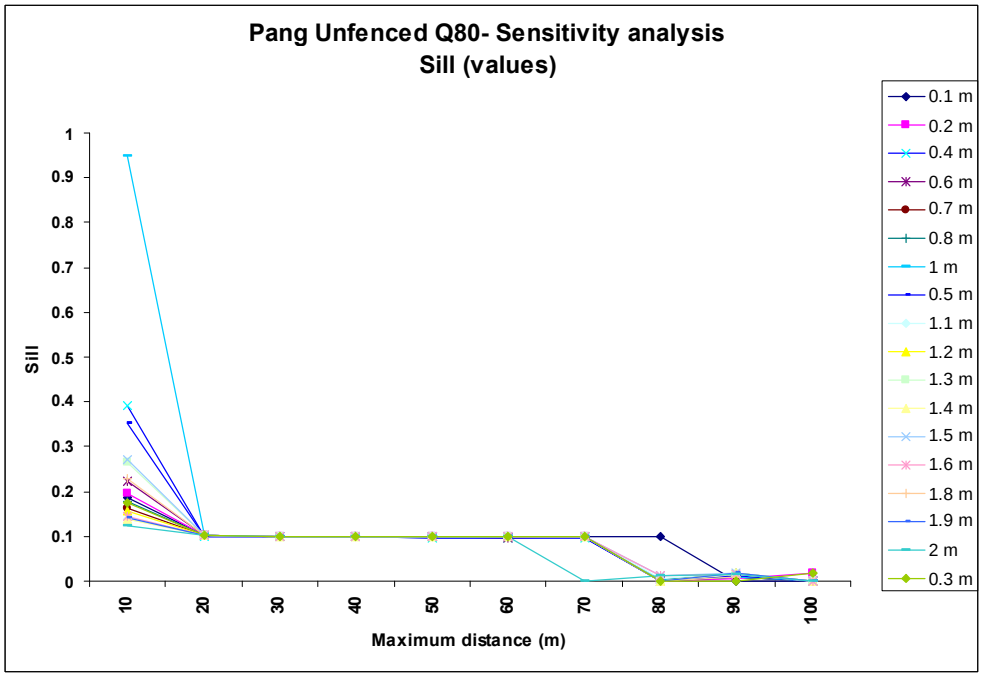
Pang Unfenced Q80- Sensitivity analysis
Sill (values)
Sill
Maximum distance (m)
0.1 m
0.2 m
0.4 m
0.6 m
0.7 m
0.8 m
1 m
0.5 m
1.1 m
1.2 m
1.3 m
1.4 m
1.5 m
1.6 m
1.8 m
1.9 m
2 m
0.3 m

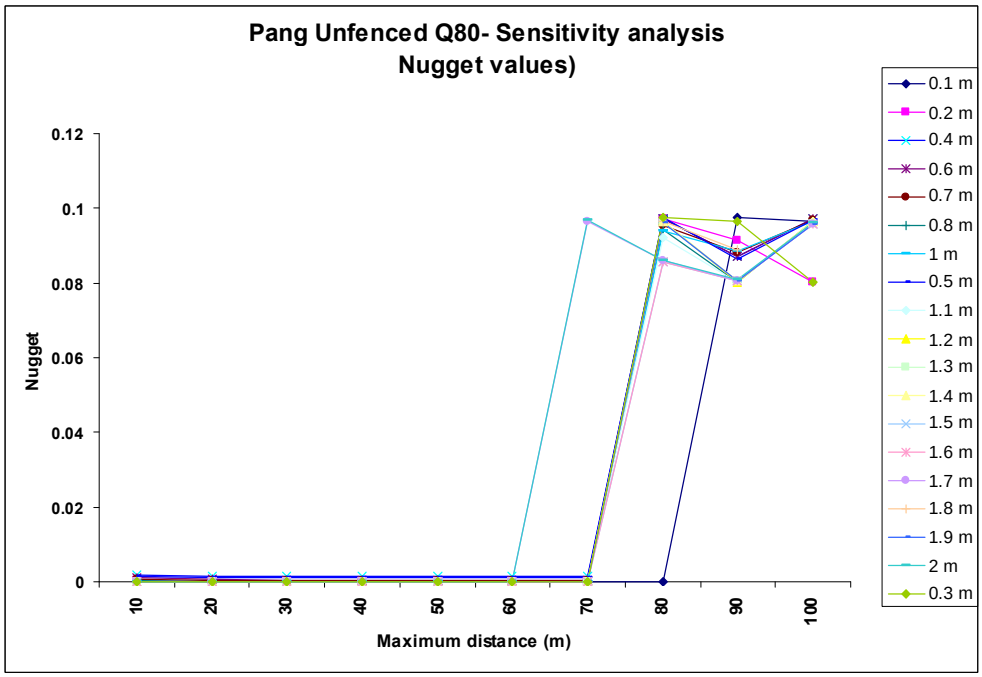
Pang Unfenced Q80- Sensitivity analysis
Nugget values)
Nugget
Maximum distance (m)
0.1 m
0.2 m
0.4 m
0.6 m
0.7 m
0.8 m
1 m
0.5 m
1.1 m
1.2 m
1.3 m
1.4 m
1.5 m
1.6 m
1.7 m
1.8 m
1.9 m
2 m
0.3 m

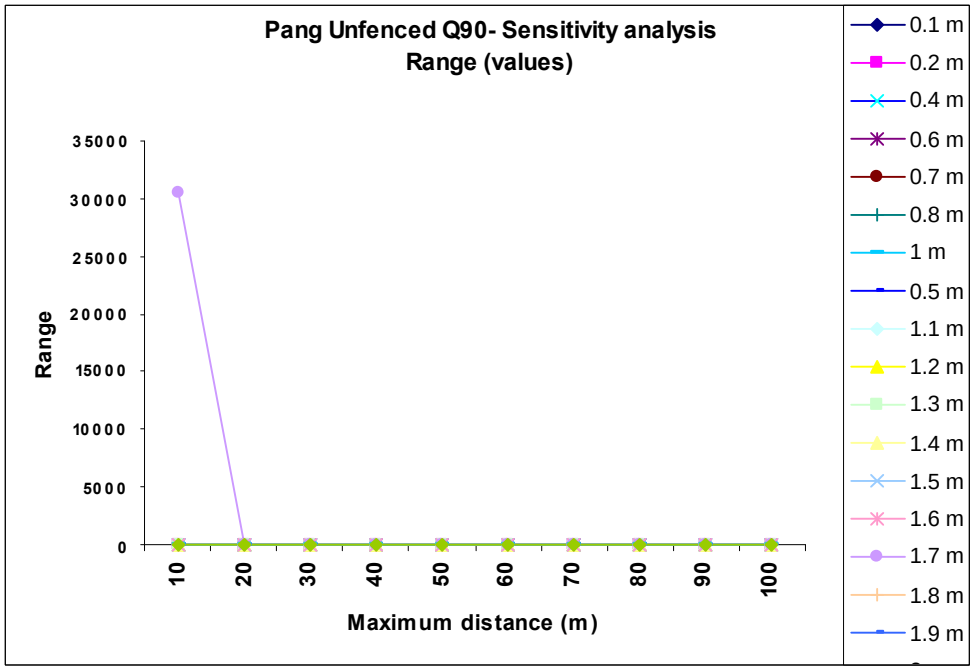
Pang Unfenced Q90- Sensitivity analysis
Range (values)
Range
35000
30000
25000
20000
15000
10000
5000
0
10
20
30
40
50
60
70
80
90
100
Maximum distance (m)
0.1 m
0.2 m
0.4 m
0.6 m
0.7 m
0.8 m
1 m
0.5 m
1.1 m
1.2 m
1.3 m
1.4 m
1.5 m
1.6 m
1.7 m
1.8 m
1.9 m

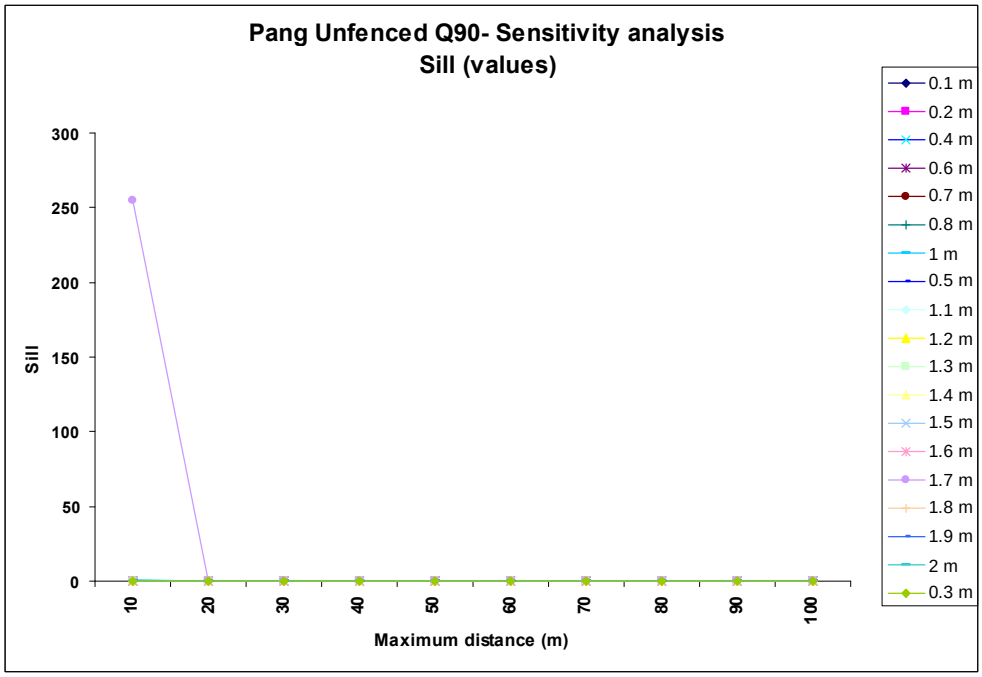
Pang Unfenced Q90- Sensitivity analysis
Sill (values)
Sill
300
250
200
150
100
50
0
10
20
30
40
50
60
70
80
90
100
Maximum distance (m)
0.1 m
0.2 m
0.4 m
0.6 m
0.7 m
0.8 m
1 m
0.5 m
1.1 m
1.2 m
1.3 m
1.4 m
1.5 m
1.6 m
1.7 m
1.8 m
1.9 m
2 m
0.3 m

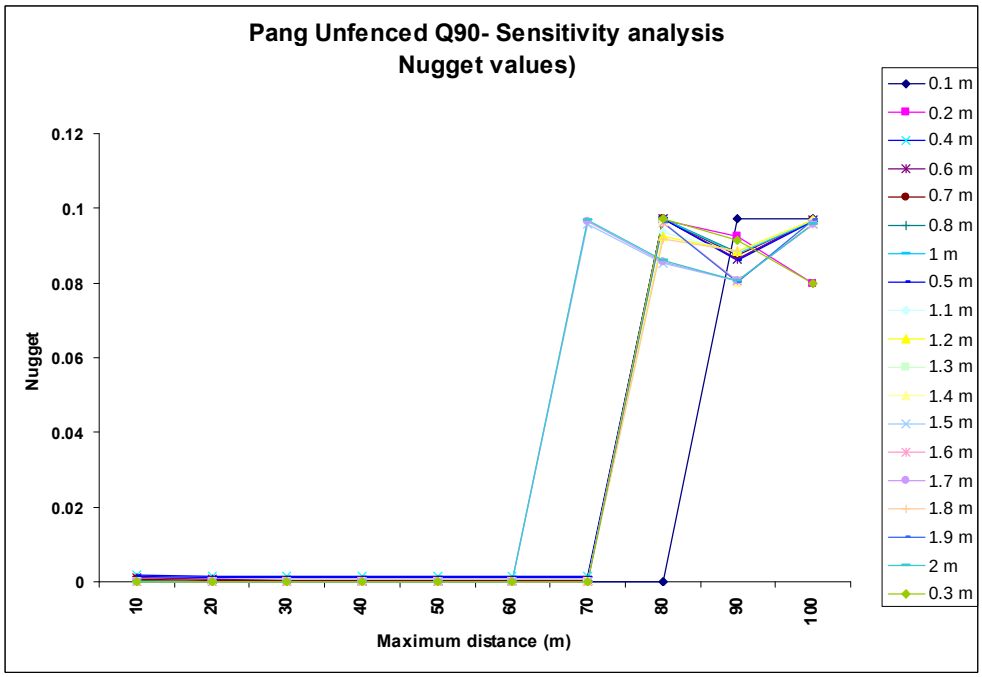
Pang Unfenced Q90- Sensitivity analysis
Nugget values)
Nugget
0.12
0.1
0.08
0.06
0.04
0.02
0
10
20
30
40
50
60
70
80
90
100
Maximum distance (m)
0.1 m
0.2 m
0.4 m
0.6 m
0.7 m
0.8 m
1 m
0.5 m
1.1 m
1.2 m
1.3 m
1.4 m
1.5 m
1.6 m
1.7 m
1.8 m
1.9 m
2 m
0.3 m

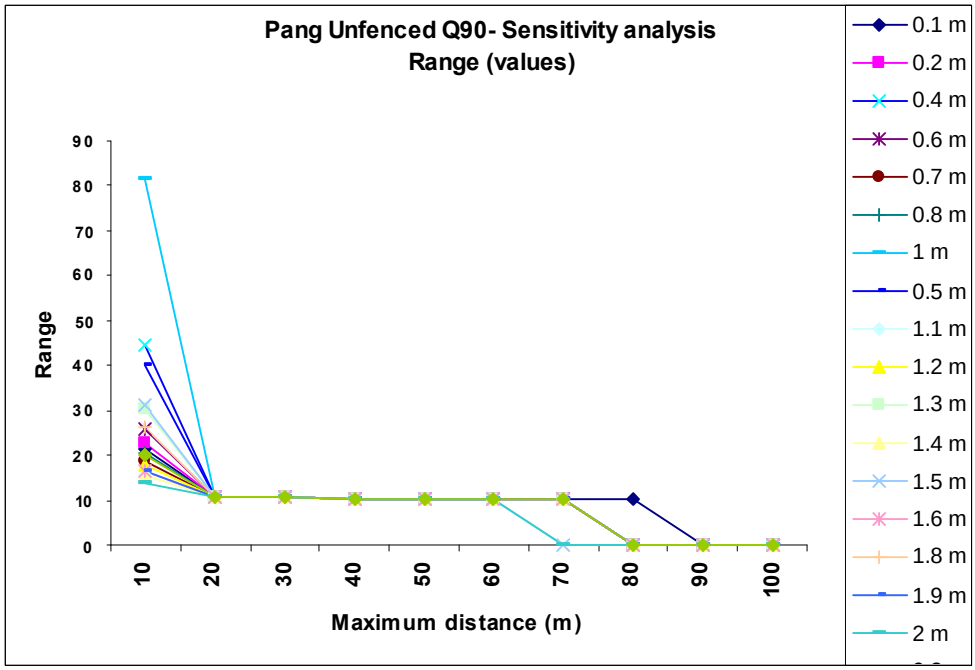
Pang Unfenced Q90- Sensitivity analysis
Range (values)
Range
Maximum distance (m)
0.1 m
0.2 m
0.4 m
0.6 m
0.7 m
0.8 m
1 m
0.5 m
1.1 m
1.2 m
1.3 m
1.4 m
1.5 m
1.6 m
1.8 m
1.9 m
2 m

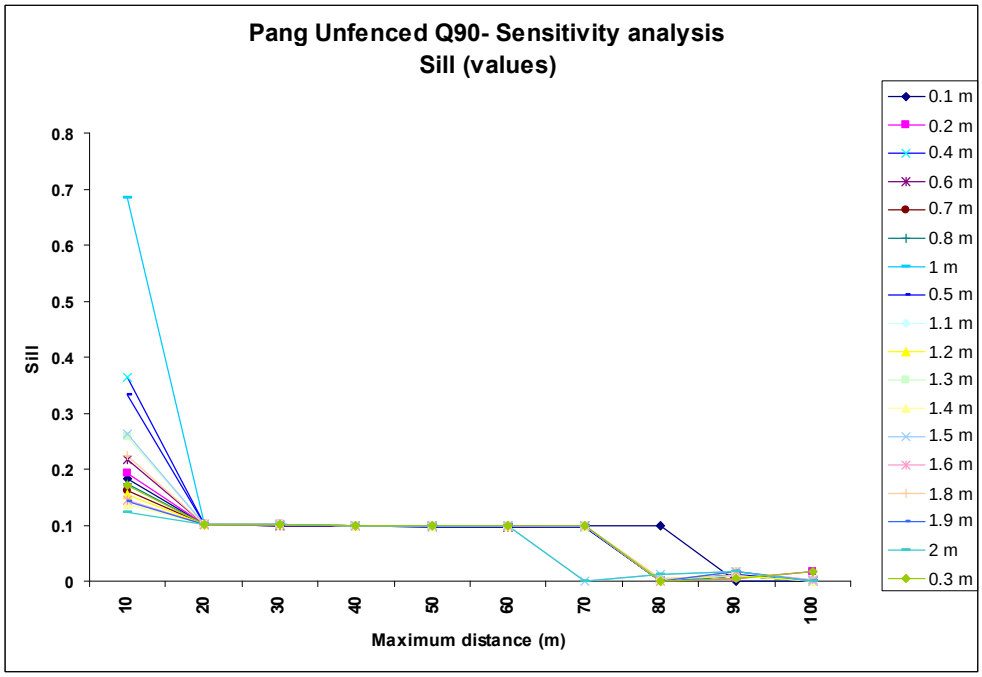
Pang Unfenced Q90- Sensitivity analysis
Sill (values)
Sill
Maximum distance (m)
0.1 m
0.2 m
0.4 m
0.6 m
0.7 m
0.8 m
1 m
0.5 m
1.1 m
1.2 m
1.3 m
1.4 m
1.5 m
1.6 m
1.8 m
1.9 m
2 m
0.3 m

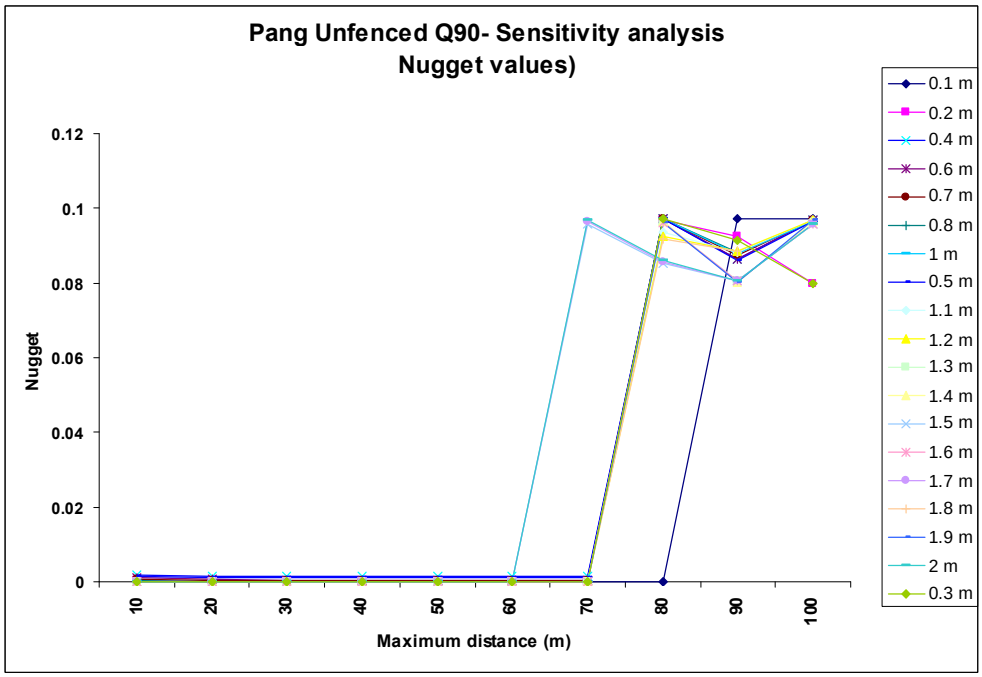
Pang Unfenced Q90- Sensitivity analysis
Nugget values)
Nugget
Maximum distance (m)
0.1 m
0.2 m
0.4 m
0.6 m
0.7 m
0.8 m
1 m
0.5 m
1.1 m
1.2 m
1.3 m
1.4 m
1.5 m
1.6 m
1.7 m
1.8 m
1.9 m
2 m
0.3 m

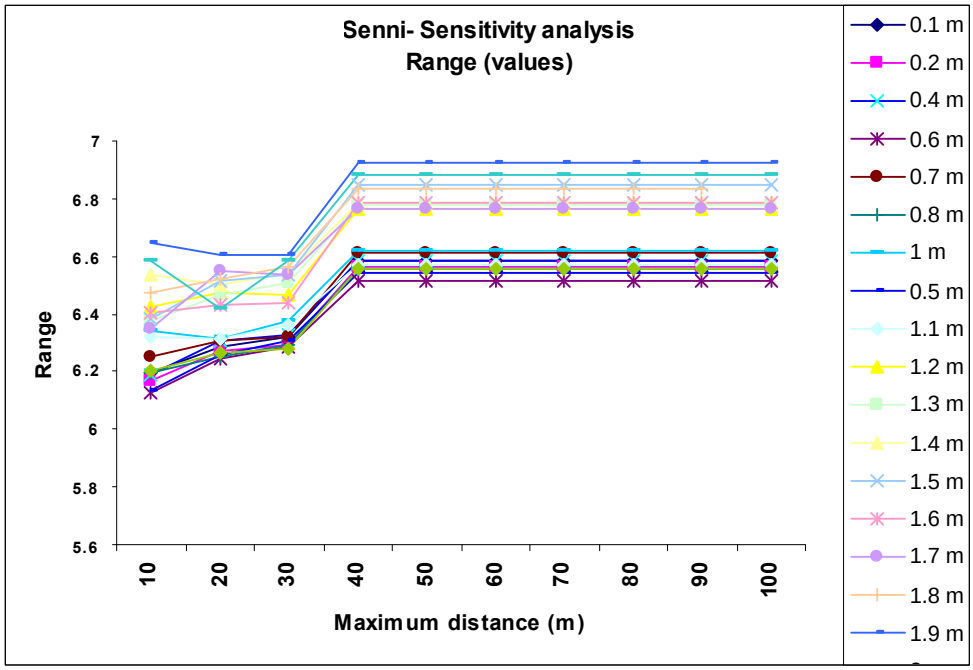
Senni- Sensitivity analysis
Range (values)
Range
Maximum distance (m)
0.1 m
0.2 m
0.4 m
0.6 m
0.7 m
0.8 m
1 m
0.5 m
1.1 m
1.2 m
1.3 m
1.4 m
1.5 m
1.6 m
1.7 m
1.8 m
1.9 m

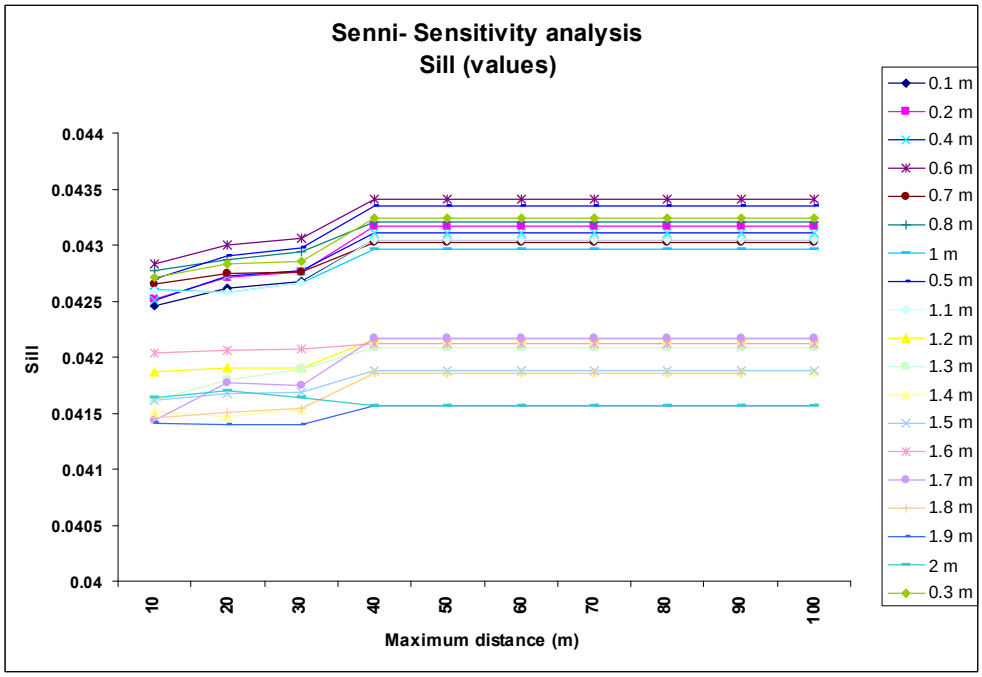
Senni- Sensitivity analysis
Sill (values)
Sill
Maximum distance (m)
0.1 m
0.2 m
0.4 m
0.6 m
0.7 m
0.8 m
1 m
0.5 m
1.1 m
1.2 m
1.3 m
1.4 m
1.5 m
1.6 m
1.7 m
1.8 m
1.9 m
2 m
0.3 m

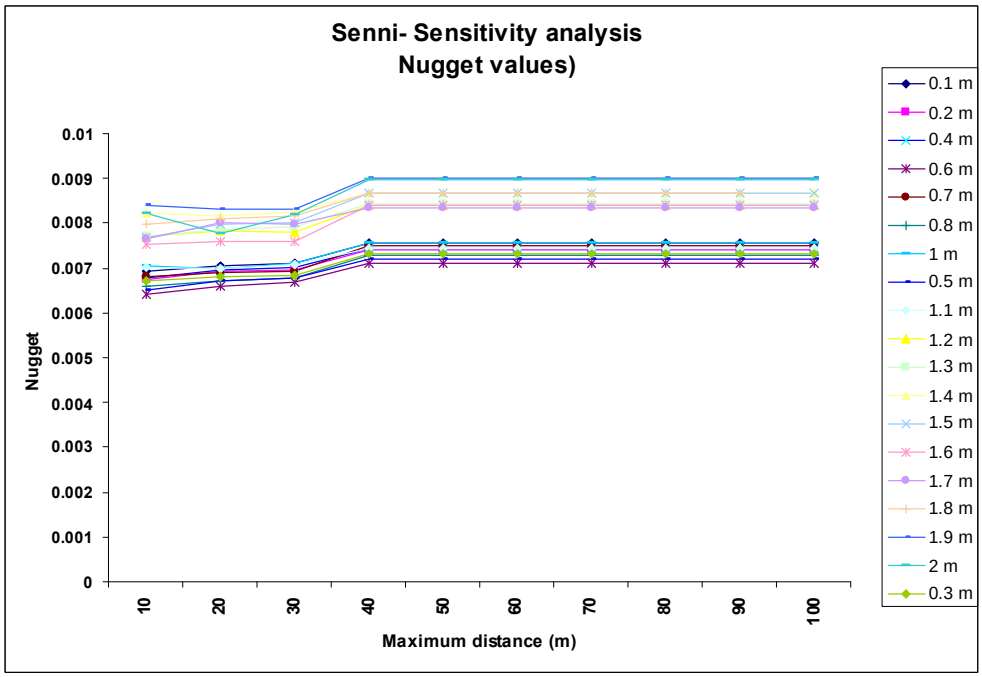
Senni- Sensitivity analysis
Nugget values)
Nugget
Maximum distance (m)
0.1 m
0.2 m
0.4 m
0.6 m
0.7 m
0.8 m
1 m
0.5 m
1.1 m
1.2 m
1.3 m
1.4 m
1.5 m
1.6 m
1.7 m
1.8 m
1.9 m
2 m
0.3 m

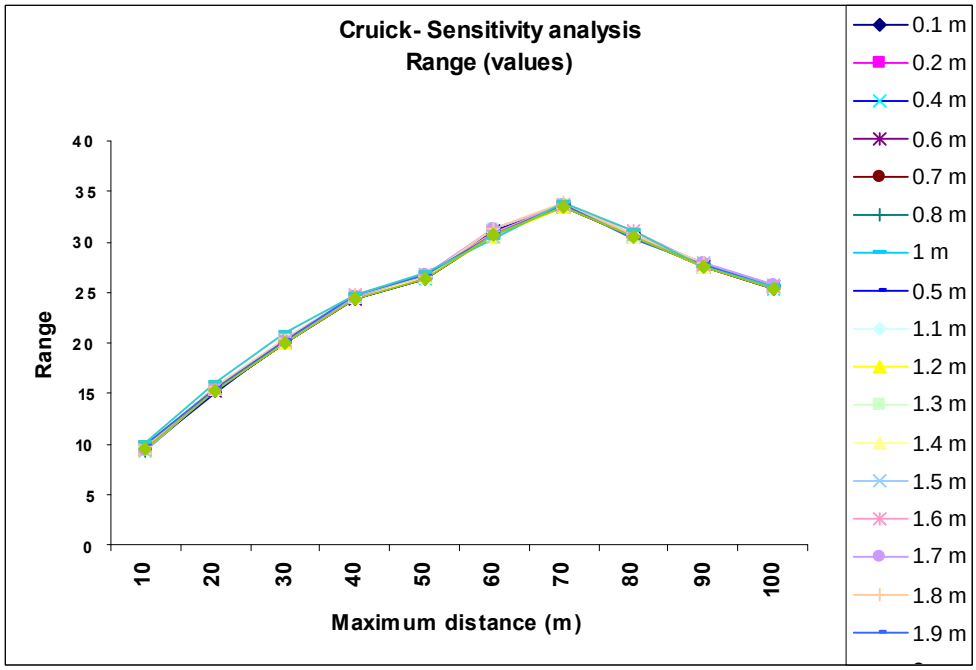
Cruick- Sensitivity analysis
Range (values)
Range
Maximum distance (m)
0.1 m
0.2 m
0.4 m
0.6 m
0.7 m
0.8 m
1 m
0.5 m
1.1 m
1.2 m
1.3 m
1.4 m
1.5 m
1.6 m
1.7 m
1.8 m
1.9 m

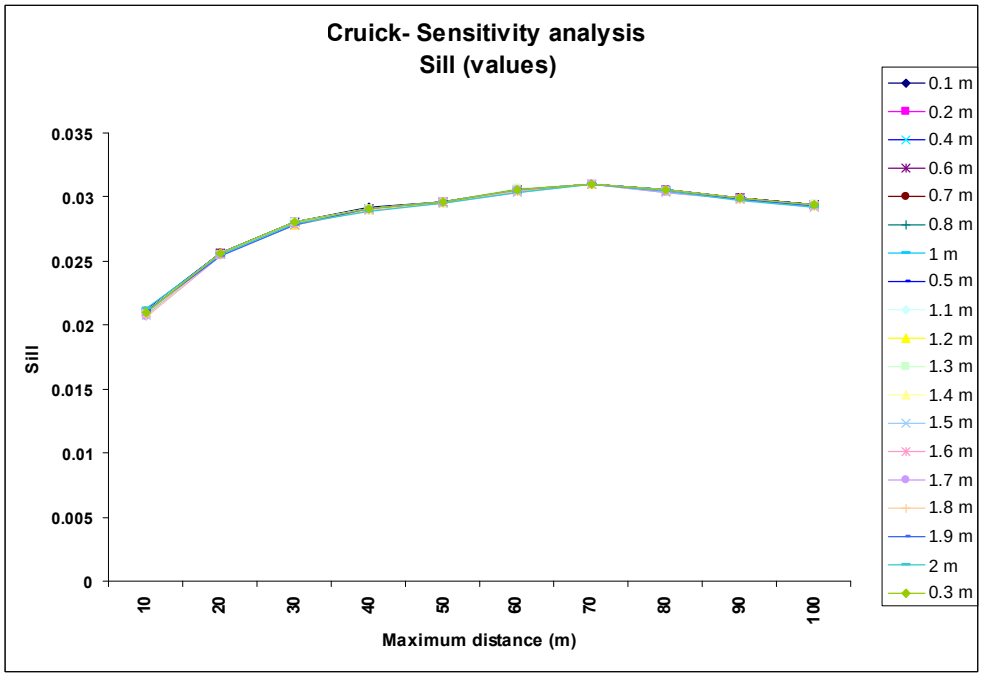
Cruick- Sensitivity analysis
Sill (values)
Sill
Maximum distance (m)
0.1 m
0.2 m
0.4 m
0.6 m
0.7 m
0.8 m
1 m
0.5 m
1.1 m
1.2 m
1.3 m
1.4 m
1.5 m
1.6 m
1.7 m
1.8 m
1.9 m
2 m
0.3 m

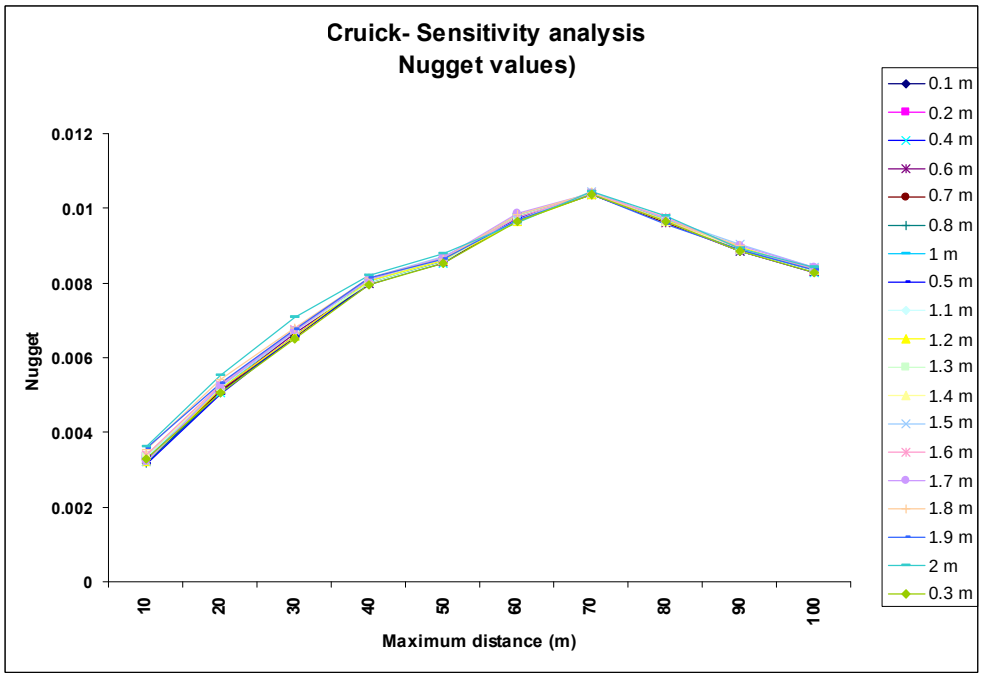
Cruick- Sensitivity analysis
Nugget values)
Nugget
Maximum distance (m)
0.1 m
0.2 m
0.4 m
0.6 m
0.7 m
0.8 m
1 m
0.5 m
1.1 m
1.2 m
1.3 m
1.4 m
1.5 m
1.6 m
1.7 m
1.8 m
1.9 m
2 m
0.3 m

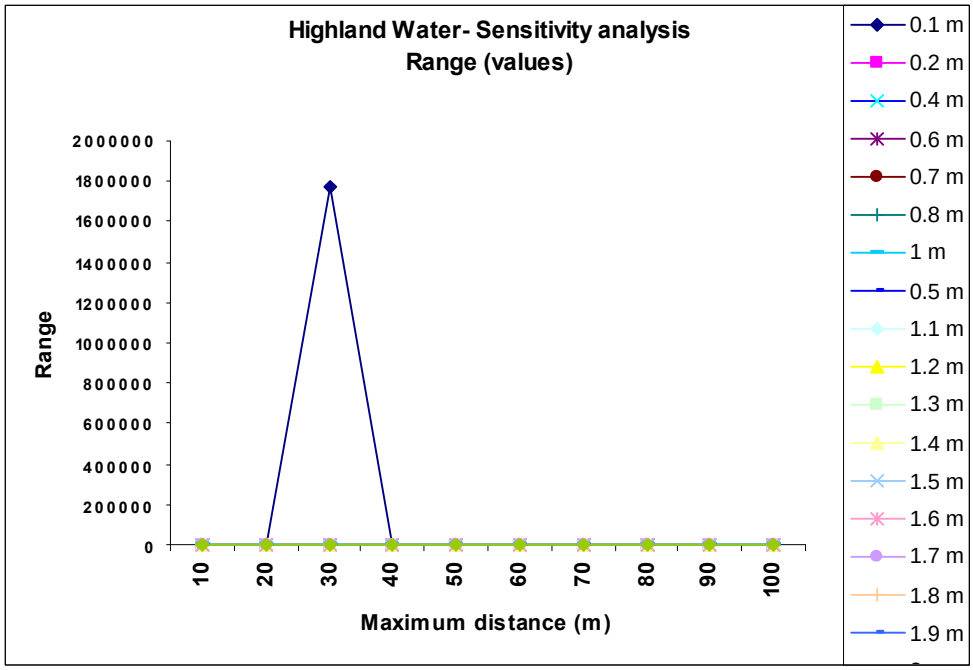
Highland Water- Sensitivity analysis
Range (values)
Range
2000000
1800000
1600000
1400000
1200000
1000000
800000
600000
400000
200000
0
10
20
30
40
50
60
70
80
90
100
Maximum distance (m)
0.1 m
0.2 m
0.4 m
0.6 m
0.7 m
0.8 m
1 m
0.5 m
1.1 m
1.2 m
1.3 m
1.4 m
1.5 m
1.6 m
1.7 m
1.8 m
1.9 m

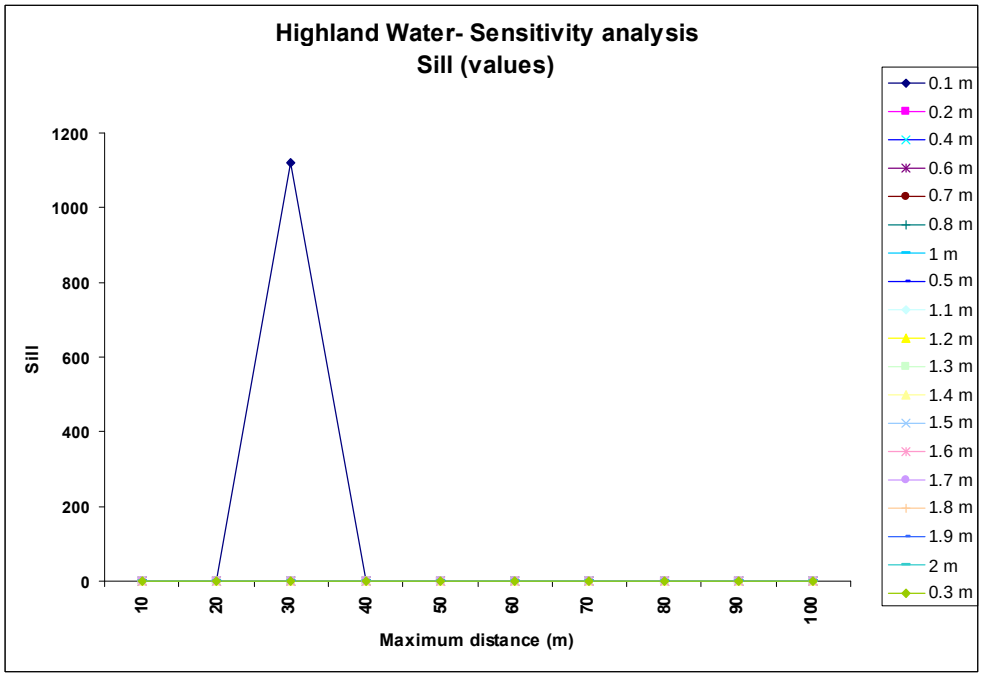
Highland Water- Sensitivity analysis
Sill (values)
Sill
1200
1000
800
600
400
200
0
10
20
30
40
50
60
70
80
90
100
Maximum distance (m)
0.1 m
0.2 m
0.4 m
0.6 m
0.7 m
0.8 m
1 m
0.5 m
1.1 m
1.2 m
1.3 m
1.4 m
1.5 m
1.6 m
1.7 m
1.8 m
1.9 m
2 m
0.3 m

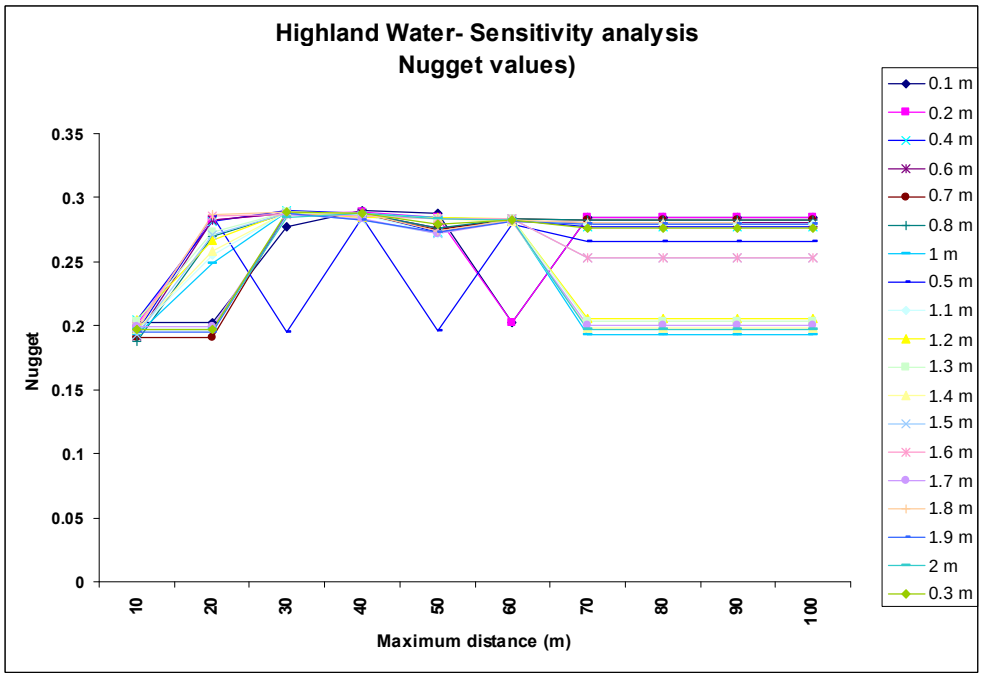
Highland Water- Sensitivity analysis
Nugget values)
Nugget
0.35
0.3
0.25
0.2
0.15
0.1
0.05
0
10
20
30
40
50
60
70
80
90
100
Maximum distance (m)
0.1 m
0.2 m
0.4 m
0.6 m
0.7 m
0.8 m
1 m
0.5 m
1.1 m
1.2 m
1.3 m
1.4 m
1.5 m
1.6 m
1.7 m
1.8 m
1.9 m
2 m
0.3 m

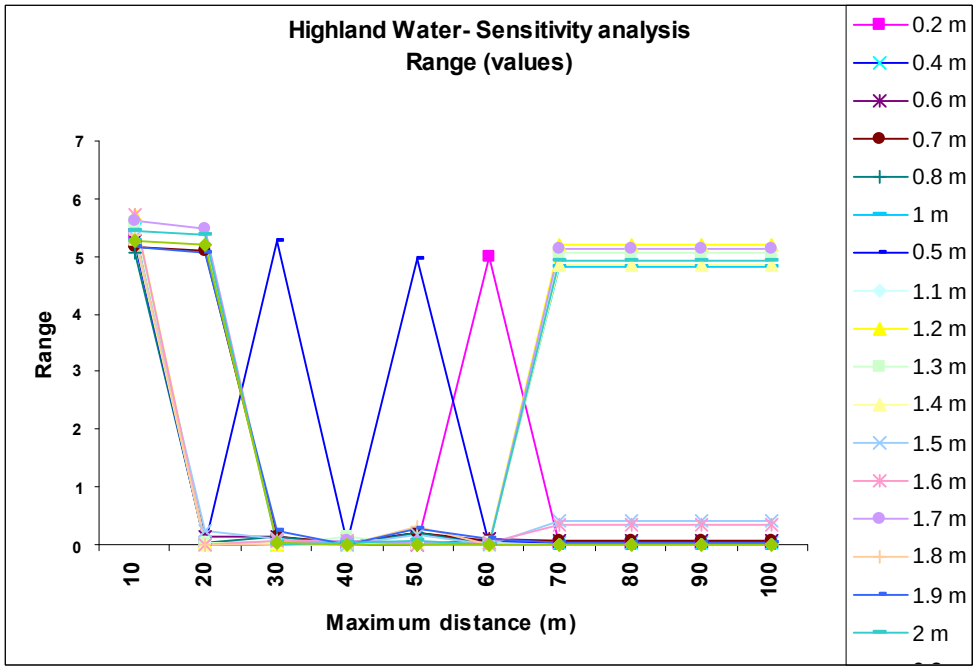
Highland Water- Sensitivity analysis
Range (values)
Range
Maximum distance (m)
0.2 m
0.4 m
0.6 m
0.7 m
0.8 m
1 m
0.5 m
1.1 m
1.2 m
1.3 m
1.4 m
1.5 m
1.6 m
1.7 m
1.8 m
1.9 m
2 m

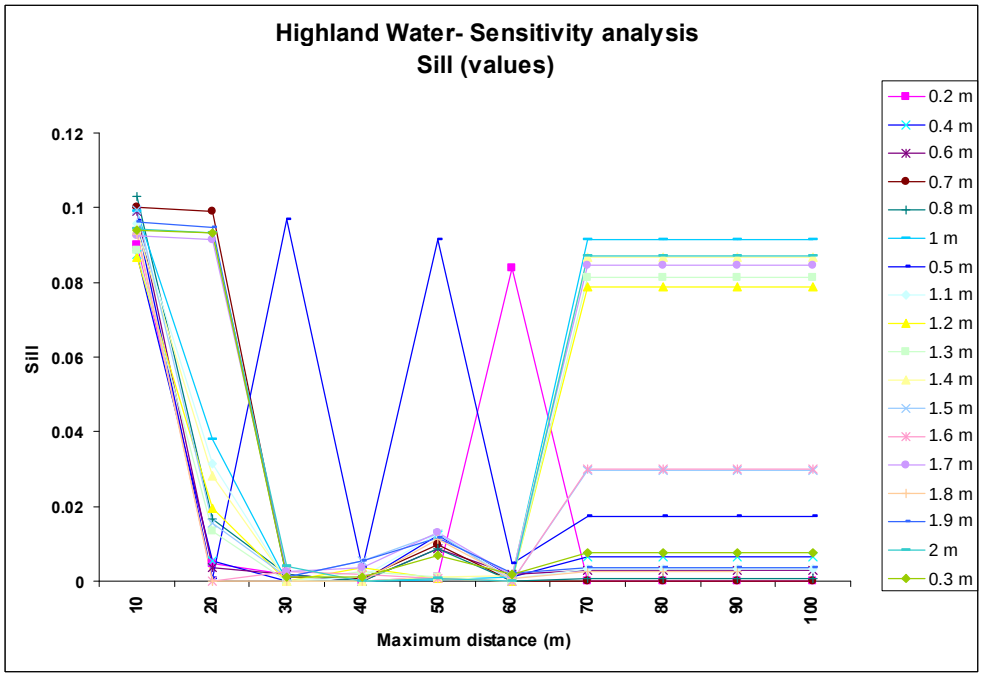
Highland Water- Sensitivity analysis
Sill (values)
Sill
Maximum distance (m)
0.2 m
0.4 m
0.6 m
0.7 m
0.8 m
1 m
0.5 m
1.1 m
1.2 m
1.3 m
1.4 m
1.5 m
1.6 m
1.7 m
1.8 m
1.9 m
2 m
0.3 m

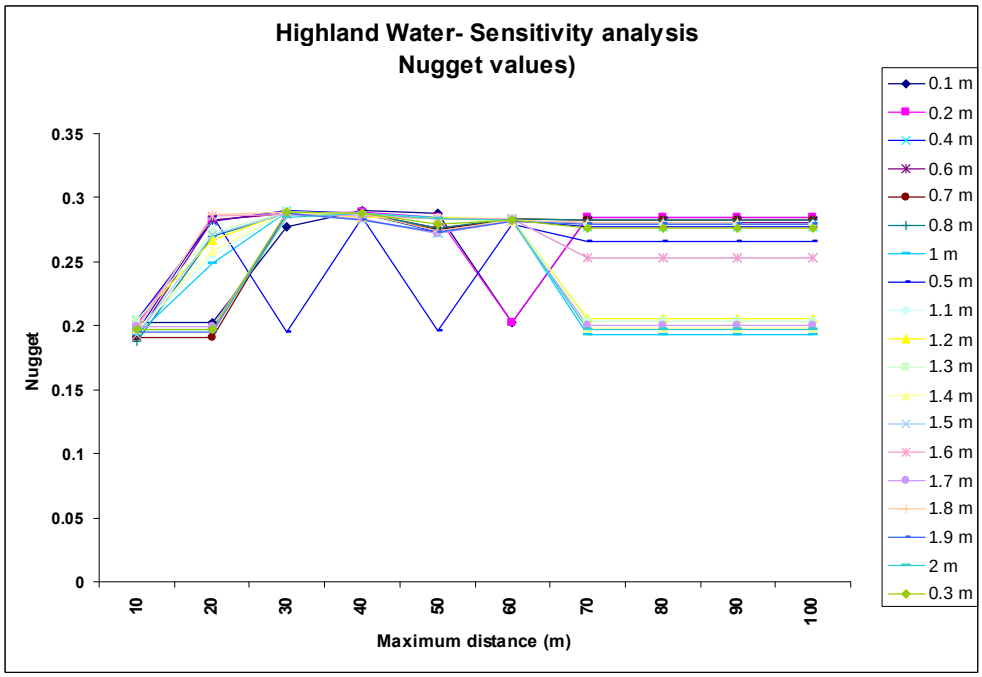
Highland Water- Sensitivity analysis
Nugget values)
Nugget
Maximum distance (m)
0.1 m
0.2 m
0.4 m
0.6 m
0.7 m
0.8 m
1 m
0.5 m
1.1 m
1.2 m
1.3 m
1.4 m
1.5 m
1.6 m
1.7 m
1.8 m
1.9 m
2 m
0.3 m

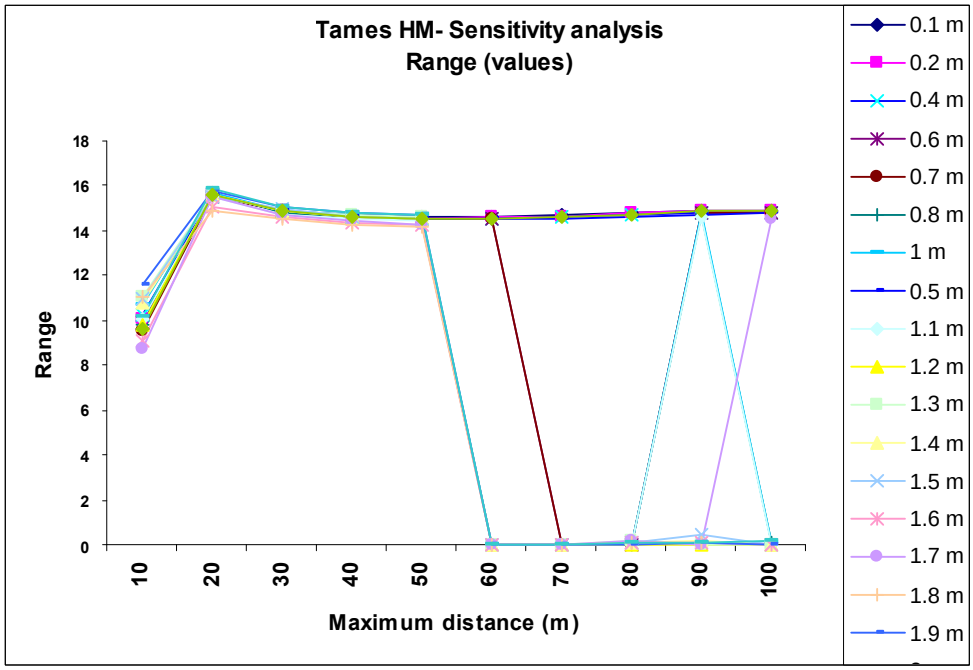
Tames HM- Sensitivity analysis
Range (values)
Range
Maximum distance (m)
0.1 m
0.2 m
0.4 m
0.6 m
0.7 m
0.8 m
1 m
0.5 m
1.1 m
1.2 m
1.3 m
1.4 m
1.5 m
1.6 m
1.7 m
1.8 m
1.9 m

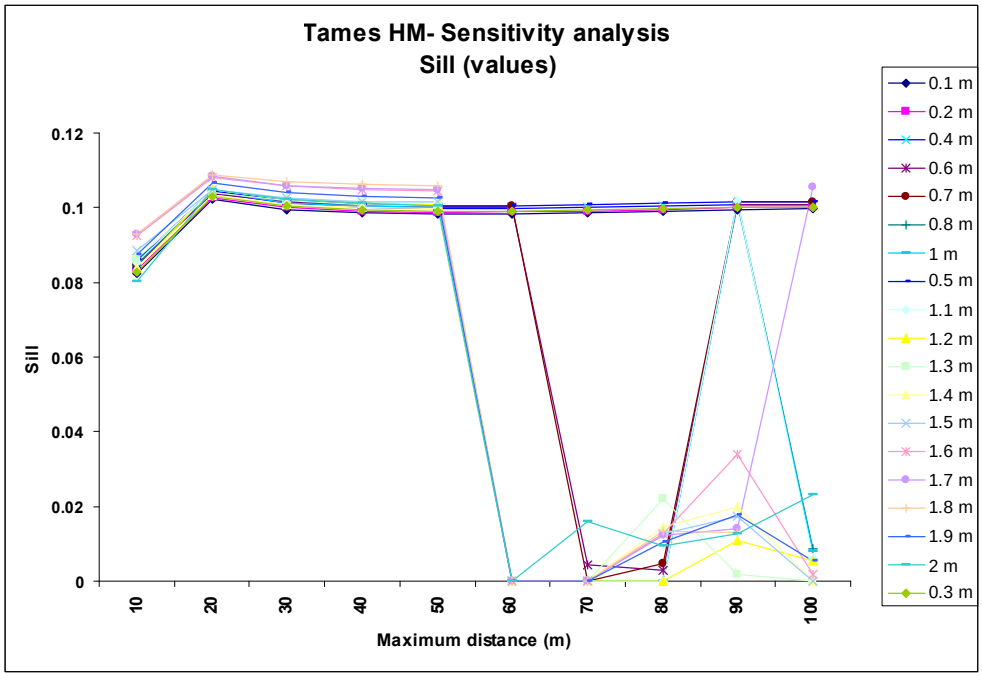
Tames HM- Sensitivity analysis
Sill (values)
Sill
Maximum distance (m)
0.1 m
0.2 m
0.4 m
0.6 m
0.7 m
0.8 m
1 m
0.5 m
1.1 m
1.2 m
1.3 m
1.4 m
1.5 m
1.6 m
1.7 m
1.8 m
1.9 m
2 m
0.3 m

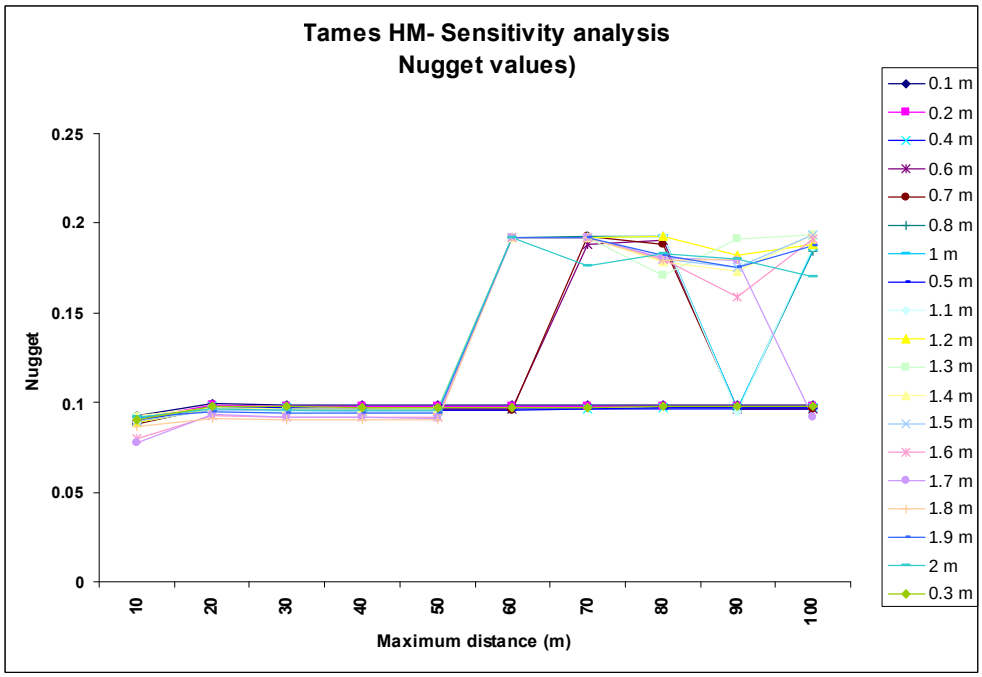
Tames HM- Sensitivity analysis
Nugget values)
Nugget
Maximum distance (m)
0.1 m
0.2 m
0.4 m
0.6 m
0.7 m
0.8 m
1 m
0.5 m
1.1 m
1.2 m
1.3 m
1.4 m
1.5 m
1.6 m
1.7 m
1.8 m
1.9 m
2 m
0.3 m

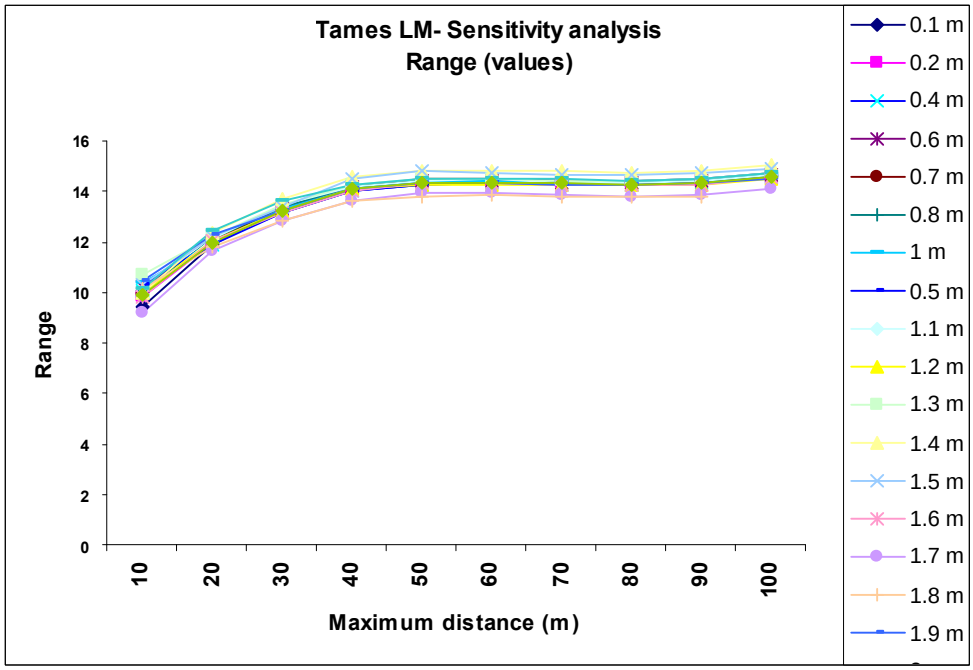
Tames LM- Sensitivity analysis
Range (values)
Range
Maximum distance (m)
0.1 m
0.2 m
0.4 m
0.6 m
0.7 m
0.8 m
1 m
0.5 m
1.1 m
1.2 m
1.3 m
1.4 m
1.5 m
1.6 m
1.7 m
1.8 m
1.9 m

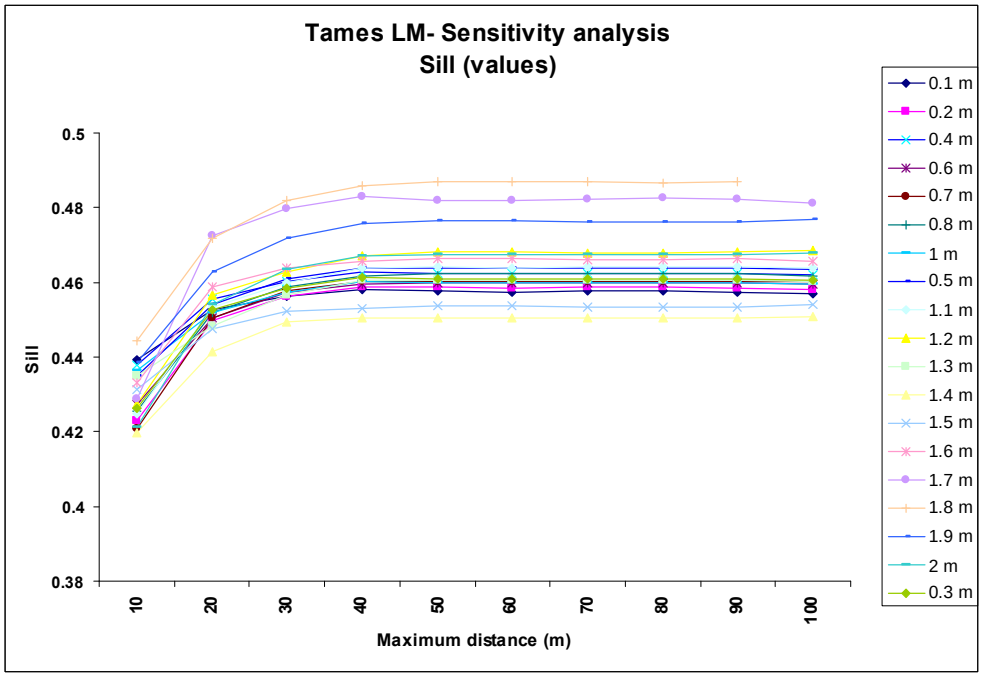
Tames LM- Sensitivity analysis
Sill (values)
Sill
Maximum distance (m)
0.1 m
0.2 m
0.4 m
0.6 m
0.7 m
0.8 m
1 m
0.5 m
1.1 m
1.2 m
1.3 m
1.4 m
1.5 m
1.6 m
1.7 m
1.8 m
1.9 m
2 m
0.3 m

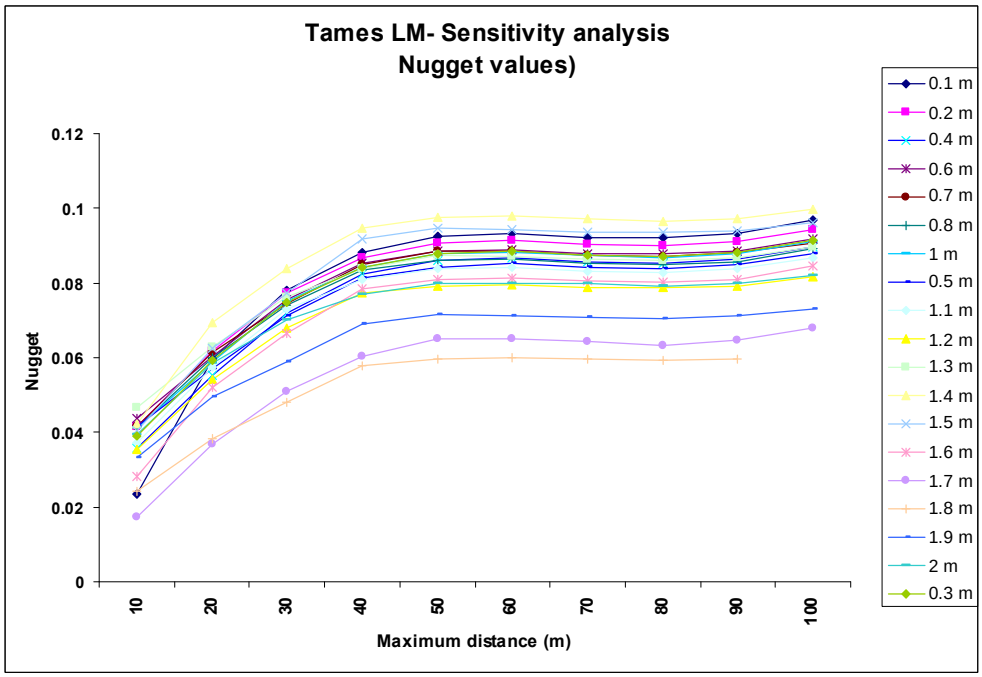
Tames LM- Sensitivity analysis
Nugget values)
Nugget
Maximum distance (m)
0.1 m
0.2 m
0.4 m
0.6 m
0.7 m
0.8 m
1 m
0.5 m
1.1 m
1.2 m
1.3 m
1.4 m
1.5 m
1.6 m
1.7 m
1.8 m
1.9 m
2 m
0.3 m

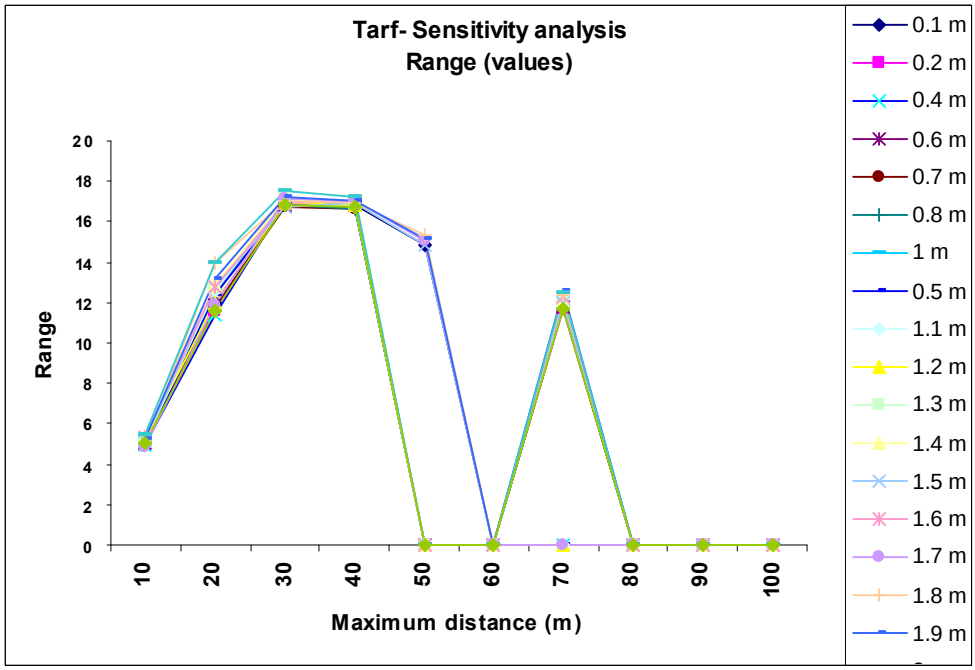
Tarf- Sensitivity analysis
Range (values)
Range
Maximum distance (m)
0.1 m
0.2 m
0.4 m
0.6 m
0.7 m
0.8 m
1 m
0.5 m
1.1 m
1.2 m
1.3 m
1.4 m
1.5 m
1.6 m
1.7 m
1.8 m
1.9 m

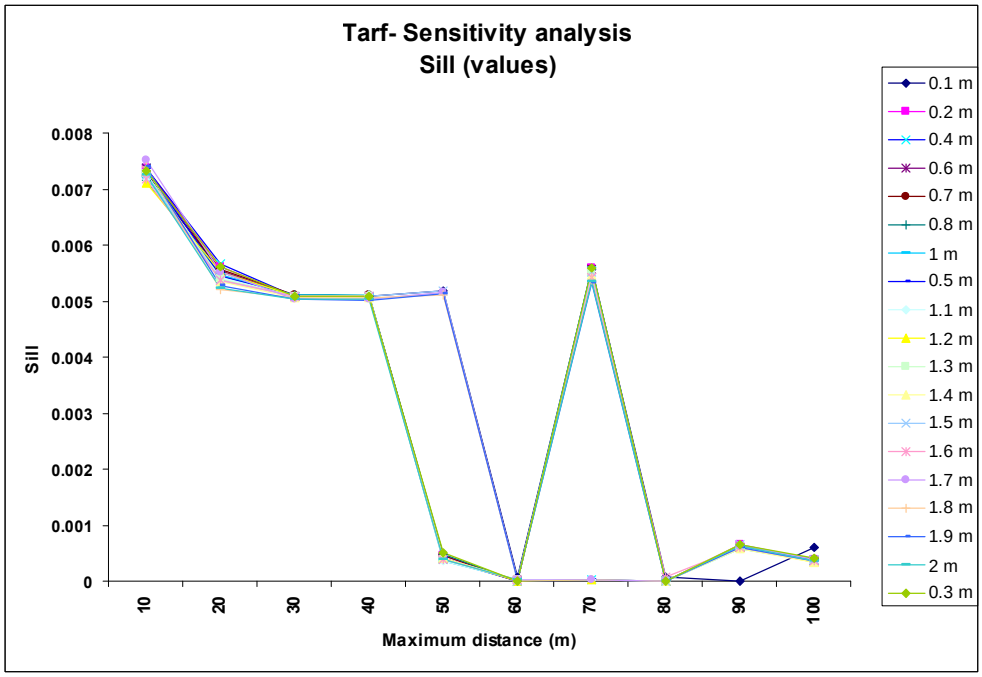
Tarf- Sensitivity analysis
Sill (values)
Sill
Maximum distance (m)
0.1 m
0.2 m
0.4 m
0.6 m
0.7 m
0.8 m
1 m
0.5 m
1.1 m
1.2 m
1.3 m
1.4 m
1.5 m
1.6 m
1.7 m
1.8 m
1.9 m
2 m
0.3 m

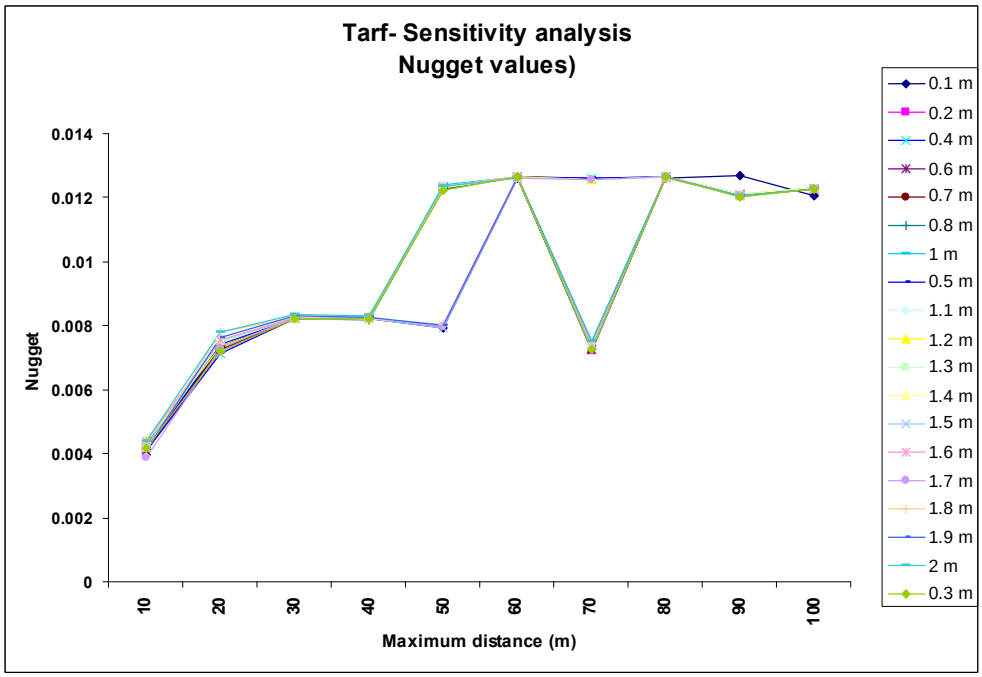
Tarf- Sensitivity analysis
Nugget values)
Nugget
Maximum distance (m)
0.1 m
0.2 m
0.4 m
0.6 m
0.7 m
0.8 m
1 m
0.5 m
1.1 m
1.2 m
1.3 m
1.4 m
1.5 m
1.6 m
1.7 m
1.8 m
1.9 m
2 m
0.3 m

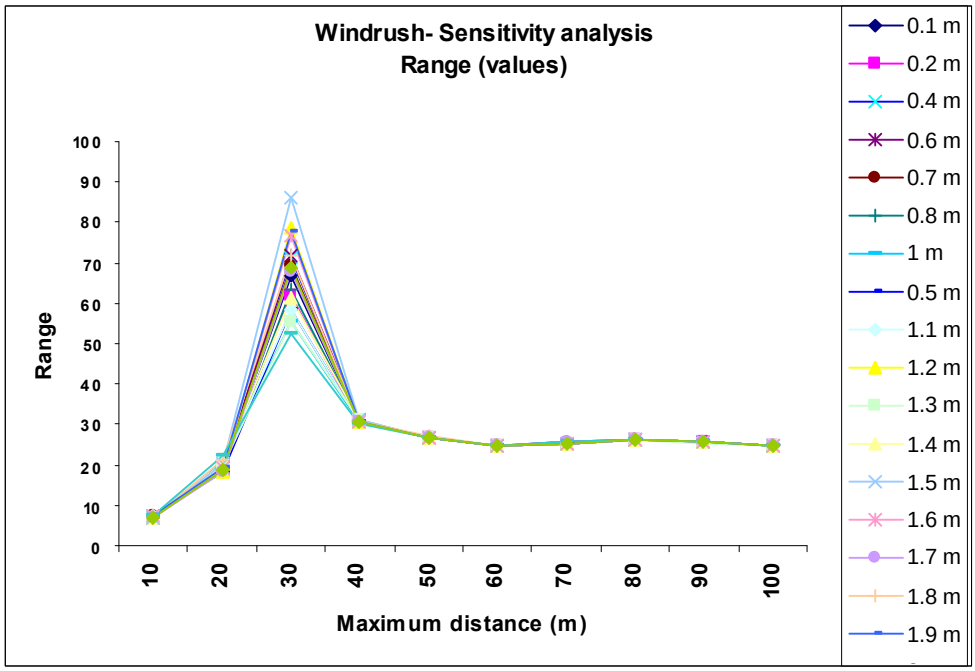
Windrush- Sensitivity analysis
Range (values)
Range
Maximum distance (m)
0.1 m
0.2 m
0.4 m
0.6 m
0.7 m
0.8 m
1 m
0.5 m
1.1 m
1.2 m
1.3 m
1.4 m
1.5 m
1.6 m
1.7 m
1.8 m
1.9 m

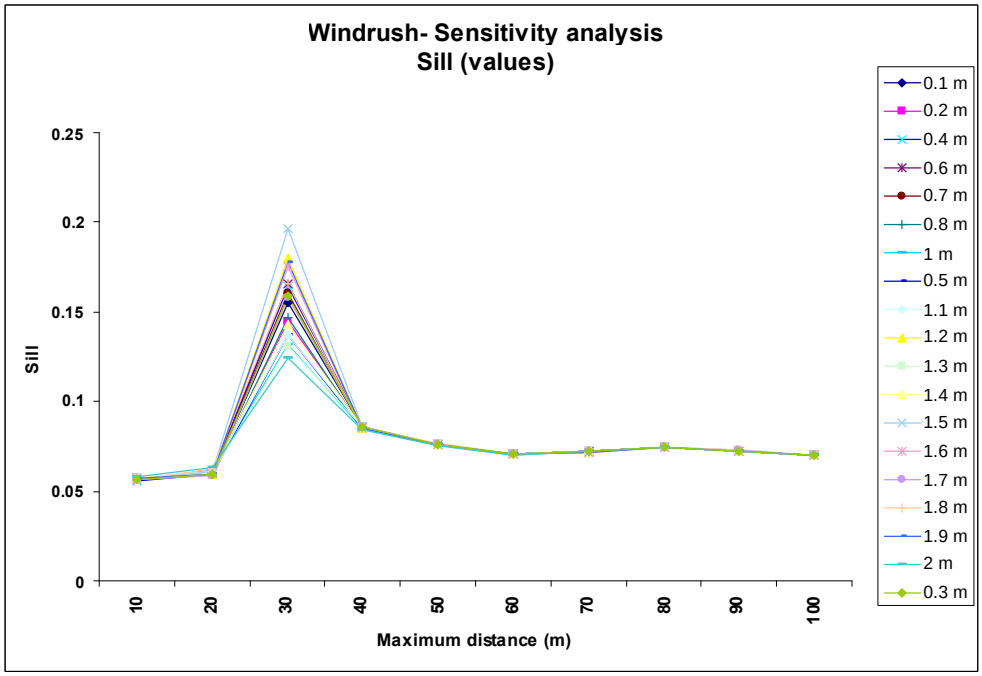
Windrush- Sensitivity analysis
Sill (values)
Sill
Maximum distance (m)
0.1 m
0.2 m
0.4 m
0.6 m
0.7 m
0.8 m
1 m
0.5 m
1.1 m
1.2 m
1.3 m
1.4 m
1.5 m
1.6 m
1.7 m
1.8 m
1.9 m
2 m
0.3 m

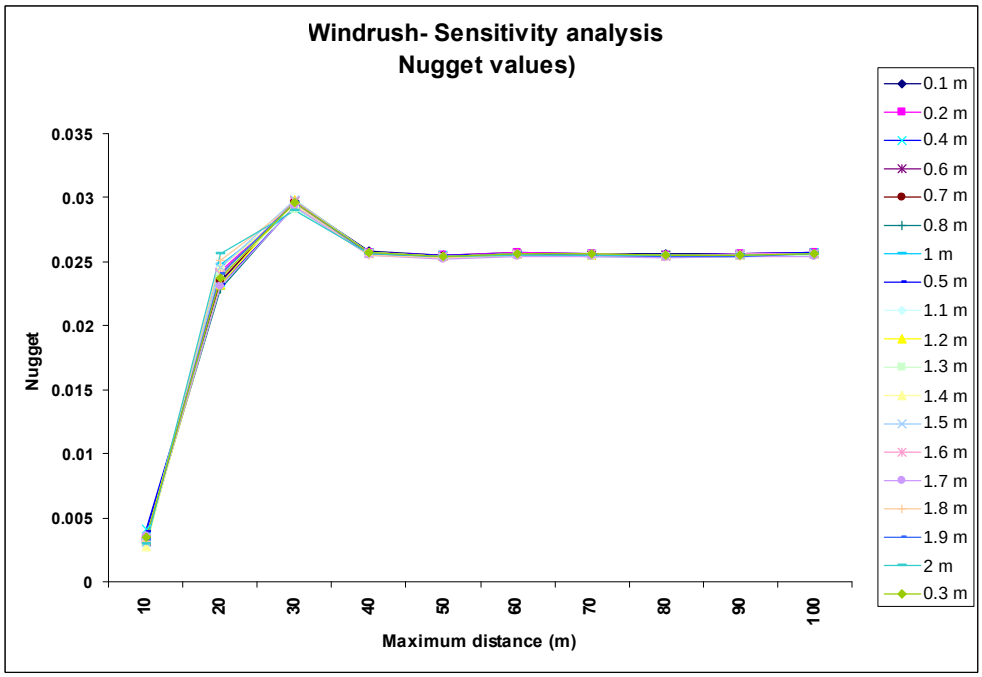
Windrush- Sensitivity analysis
Nugget values)
Nugget
Maximum distance (m)
0.1 m
0.2 m
0.4 m
0.6 m
0.7 m
0.8 m
1 m
0.5 m
1.1 m
1.2 m
1.3 m
1.4 m
1.5 m
1.6 m
1.7 m
1.8 m
1.9 m
2 m
0.3 m

Appendix 3.6

Results obtained for the analysis in Chapter 5 –sensitivity analysis: variogram cloud comparison for the wet & dry points.

This Appendix includes the graphical outputs obtained for the variogram cloud analysis developed in section 5.4.4. Each plots presents three different variogram clouds: (i) one representing the total variogram cloud calculated with the wet and dry points of each data sets (blue colour), (ii) a second one representing the variogram cloud obtained for the data sets with only dry points (pink colour) and (ii) a third one showing the variogram cloud for the wet points (green colour). The comparison of these three variogram clouds allow us to determine the information that is being introduced by each data sets in terms of spatial structure.

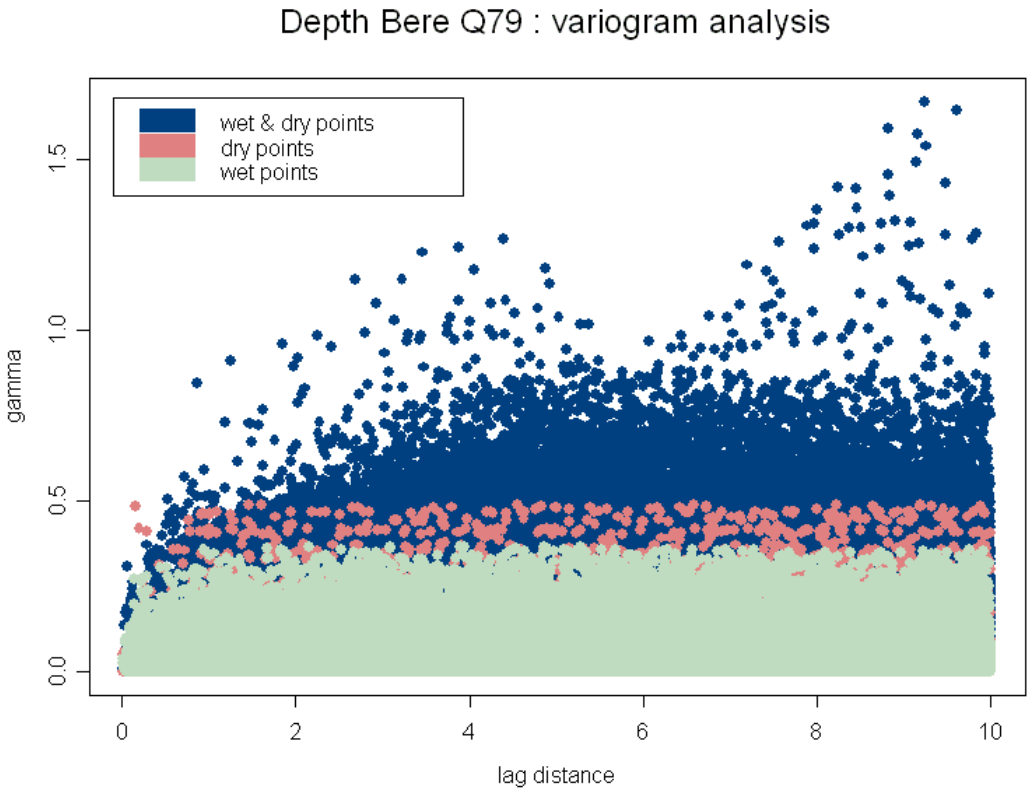
Depth Bere Q79 : variogram analysis
wet & dry points
dry points
wet points
gamma
0.0
0.5
1.0
1.5
0
2
4
6
8
10
lag distance

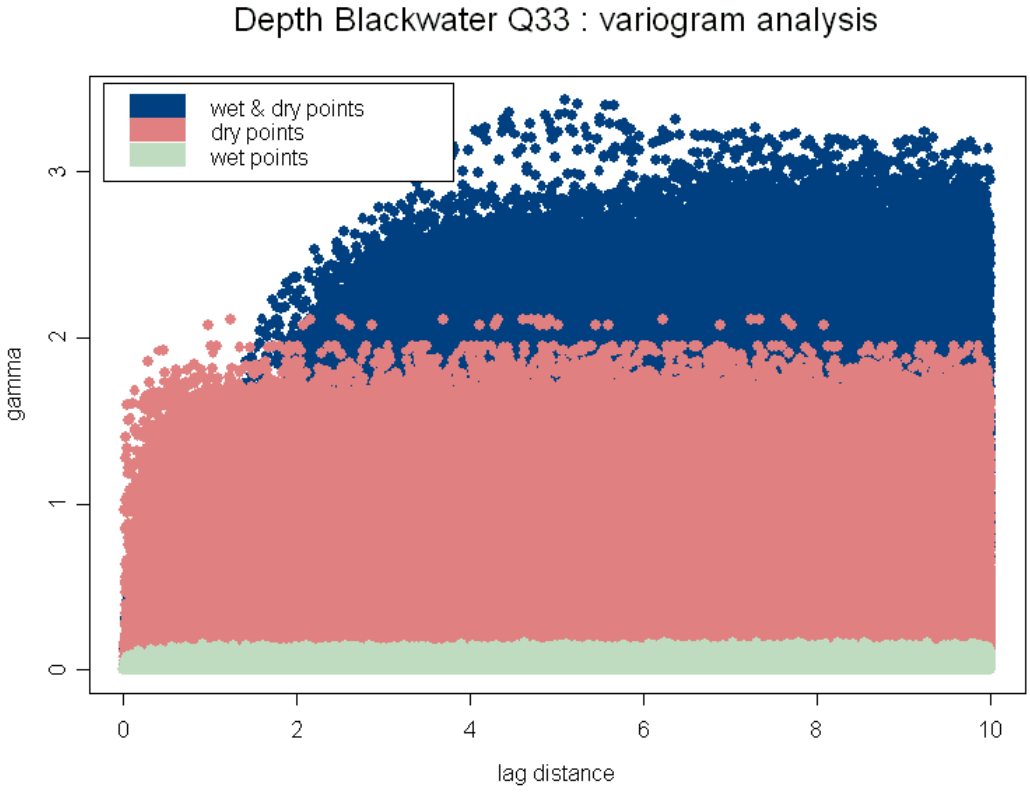
Depth Blackwater Q33 : variogram analysis
wet & dry points
dry points
wet points
gamma
0
1
2
3
0
2
4
6
8
10
lag distance

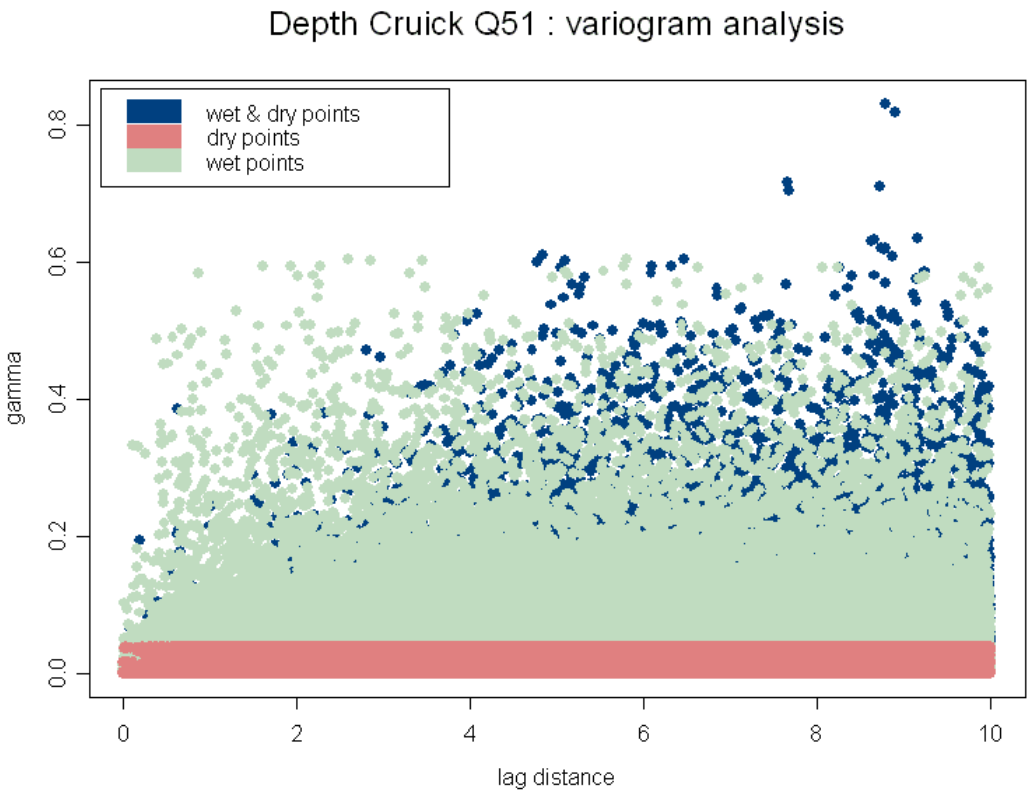
Depth Cruick Q51 : variogram analysis
wet & dry points
dry points
wet points
gamma
0.0
0.2
0.4
0.6
0.8
0
2
4
6
8
10
lag distance

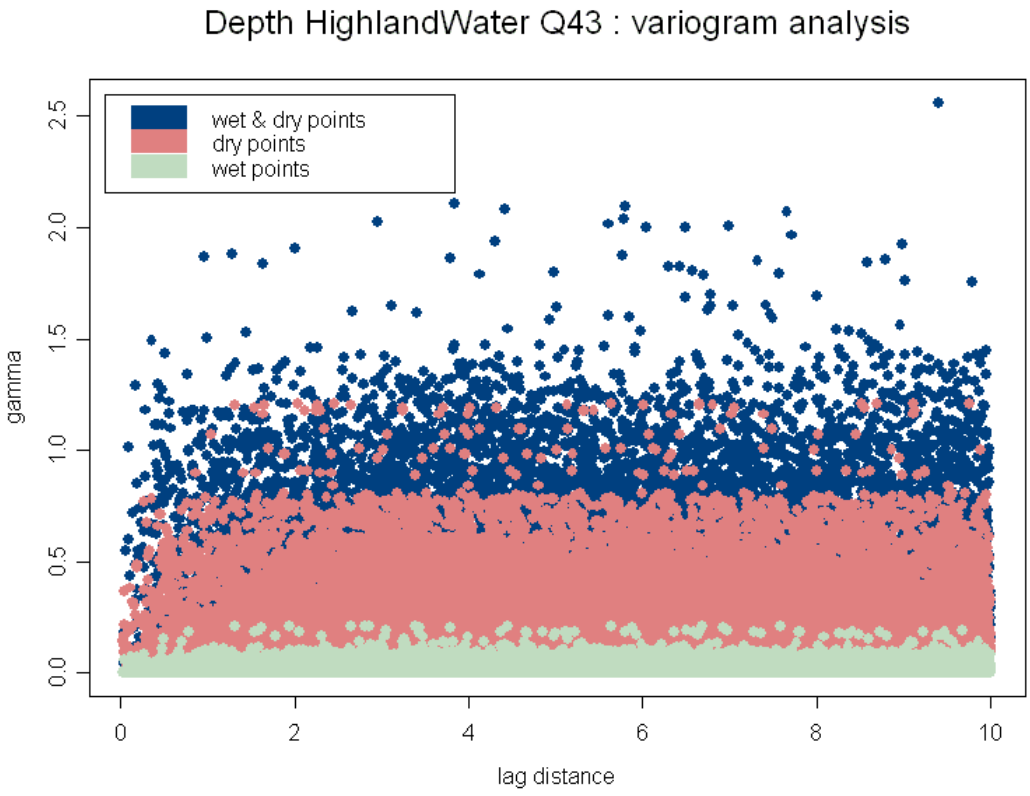
Depth HighlandWater Q43 : variogram analysis
wet & dry points
dry points
wet points
gamma
0.0
0.5
1.0
1.5
2.0
2.5
0
2
4
6
8
10
lag distance

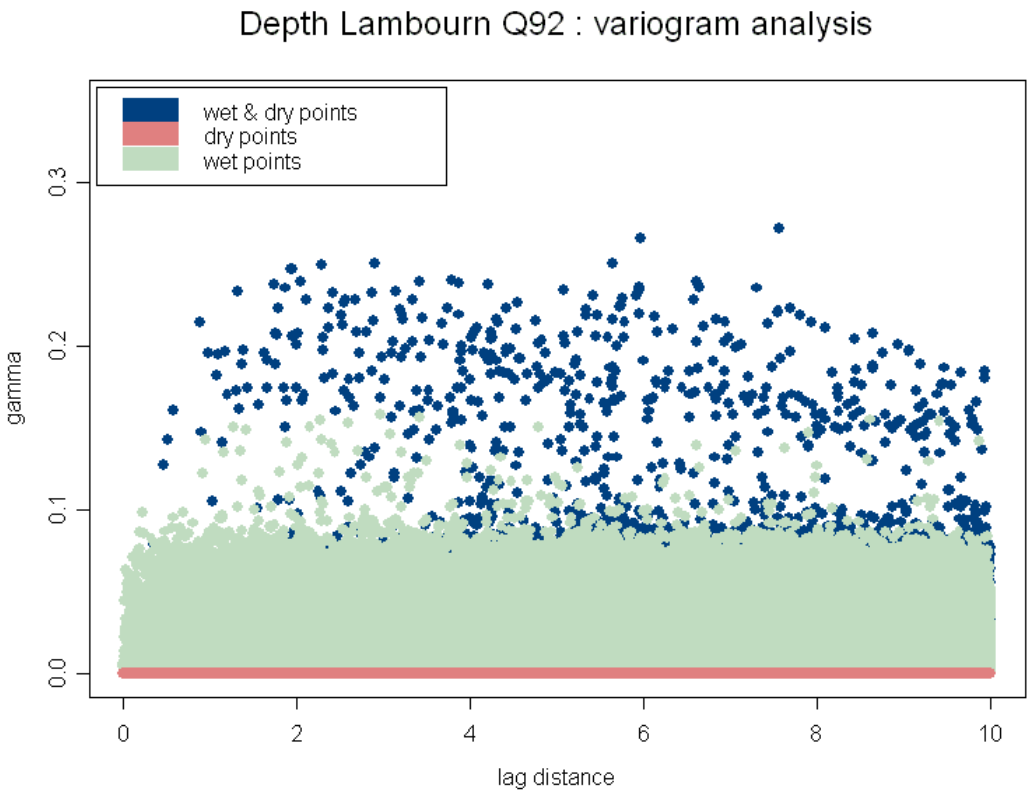
Depth Lambourn Q92 : variogram analysis
wet & dry points
dry points
wet points
gamma
0.0
0.1
0.2
0.3
0
2
4
6
8
10
lag distance

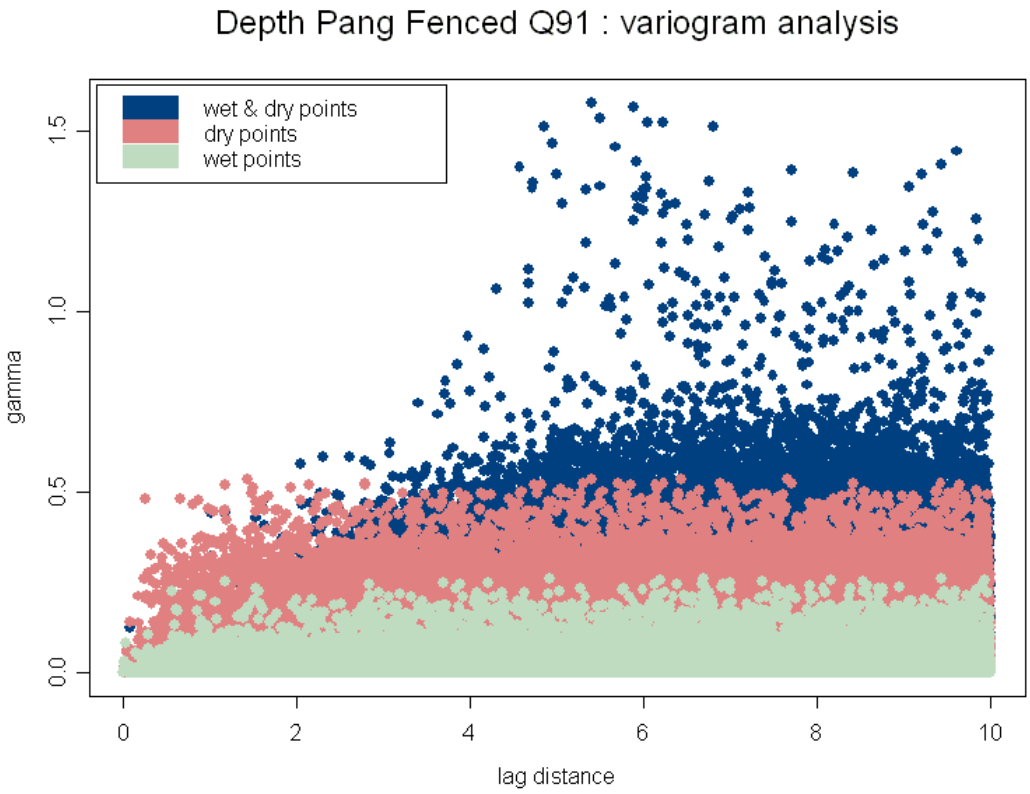
Depth Pang Fenced Q91 : variogram analysis
wet & dry points
dry points
wet points
gamma
0.0
0.5
1.0
1.5
0
2
4
6
8
10
lag distance

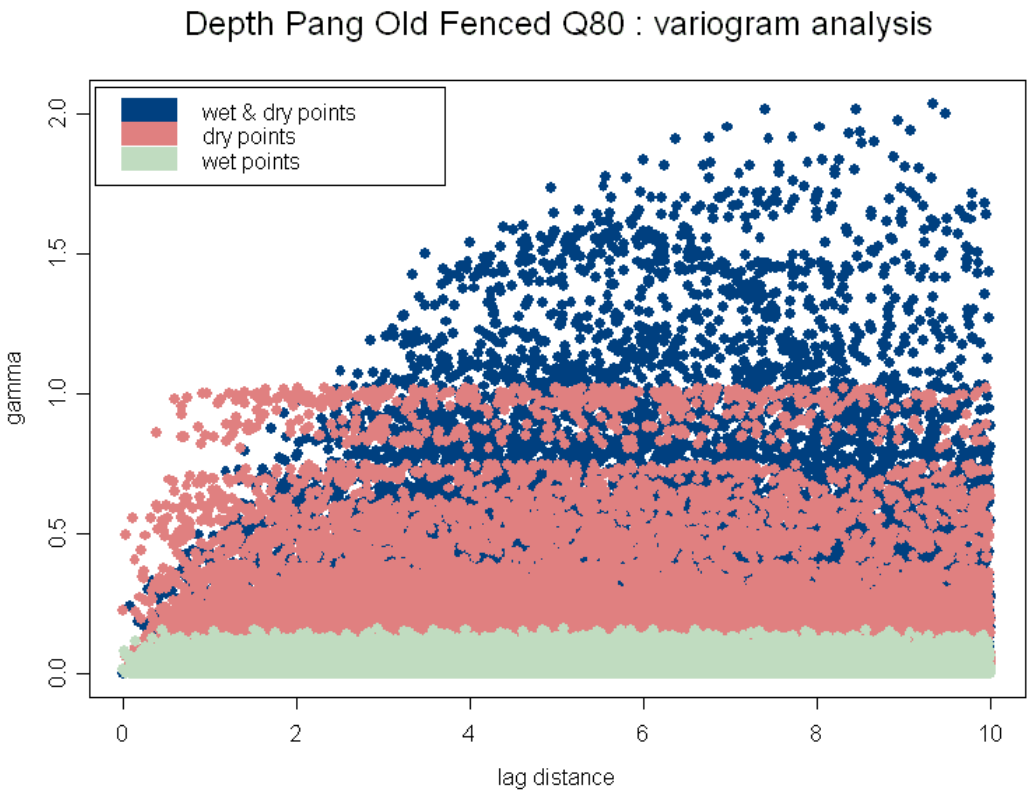
Depth Pang Old Fenced Q80 : variogram analysis
wet & dry points
dry points
wet points
gamma
0.0
0.5
1.0
1.5
2.0
0
2
4
6
8
10
lag distance

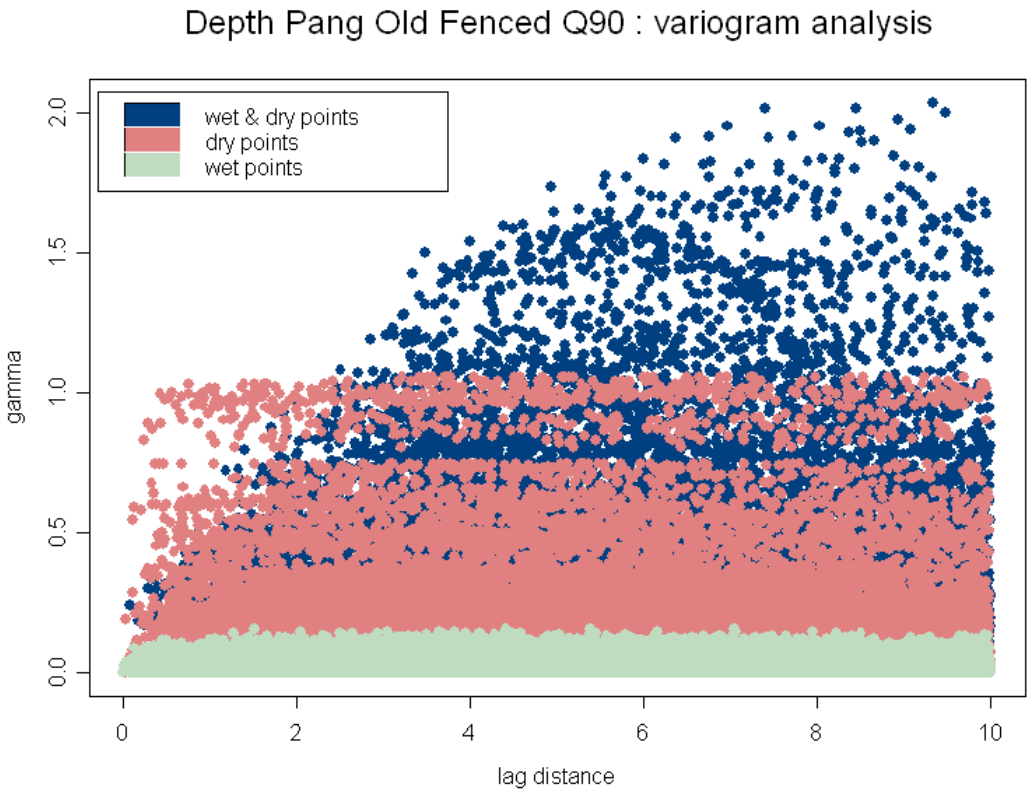
Depth Pang Old Fenced Q90 : variogram analysis
wet & dry points
dry points
wet points
gamma
0.0
0.5
1.0
1.5
2.0
0
2
4
6
8
10
lag distance

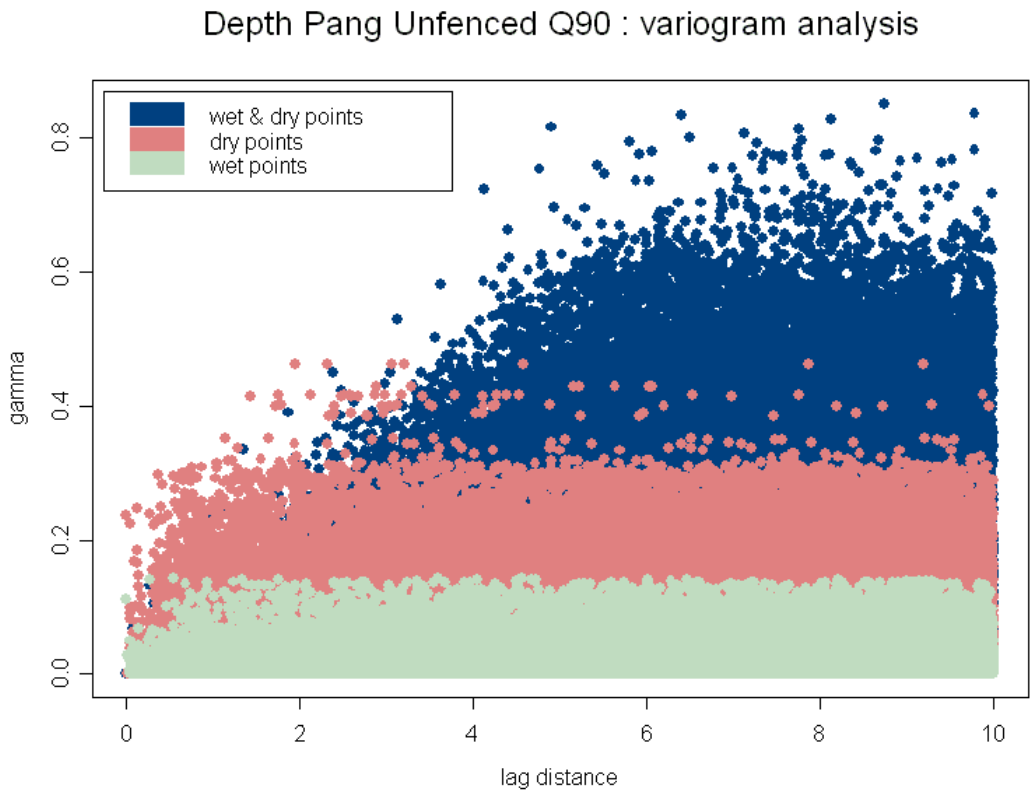
Depth Pang Unfenced Q90 : variogram analysis
wet & dry points
dry points
wet points
gamma
0.0
0.2
0.4
0.6
0.8
0
2
4
6
8
10
lag distance

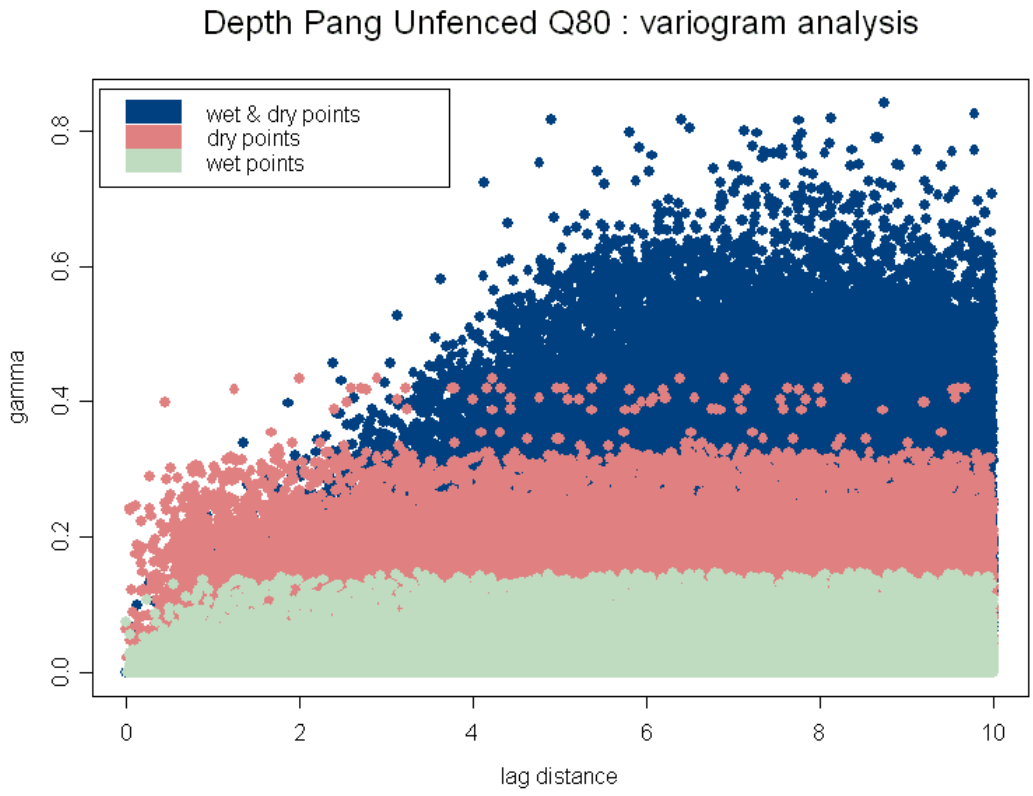
Depth Pang Unfenced Q80 : variogram analysis
wet & dry points
dry points
wet points
gamma
0.0
0.2
0.4
0.6
0.8
0
2
4
6
8
10
lag distance

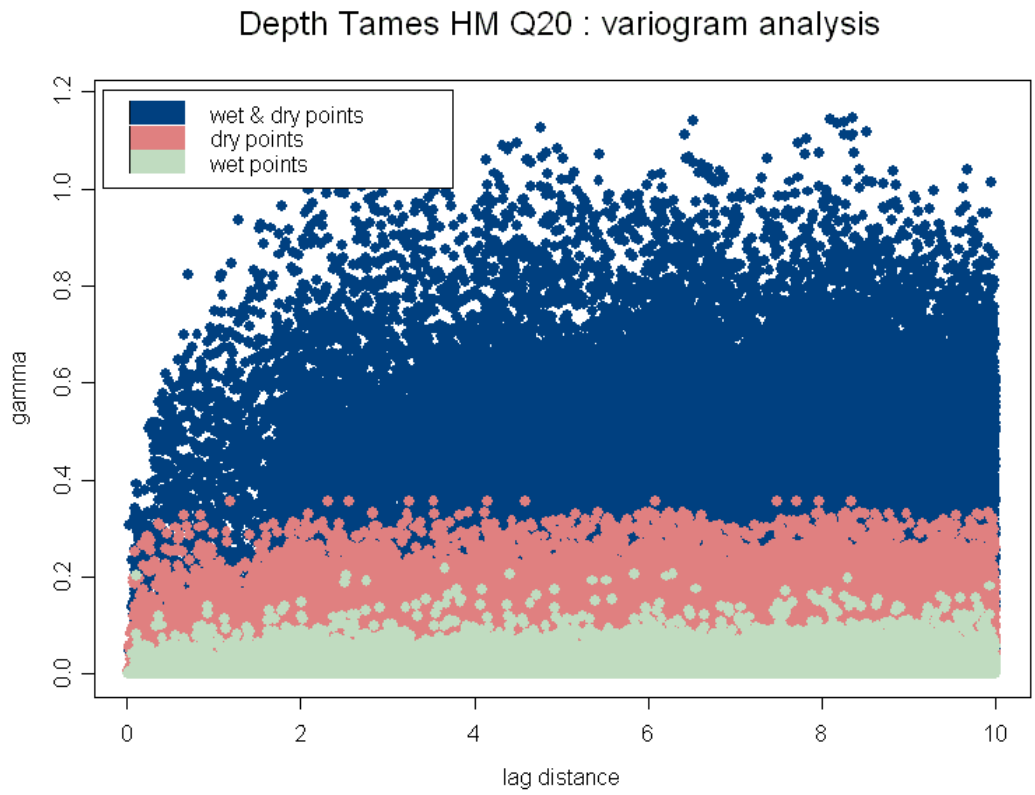
Depth Tames HM Q20 : variogram analysis
wet & dry points
dry points
wet points
gamma
0.0
0.2
0.4
0.6
0.8
1.0
1.2
0
2
4
6
8
10
lag distance

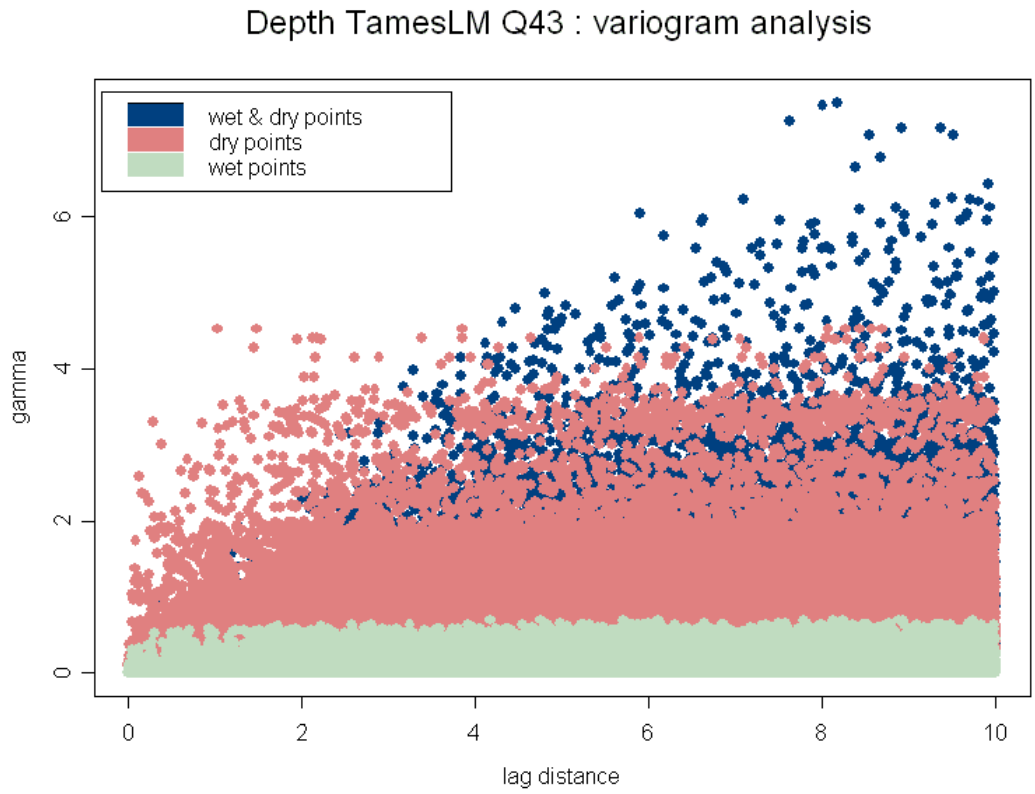
Depth TamesLM Q43 : variogram analysis
wet & dry points
dry points
wet points
gamma
0
2
4
6
0
2
4
6
8
10
lag distance

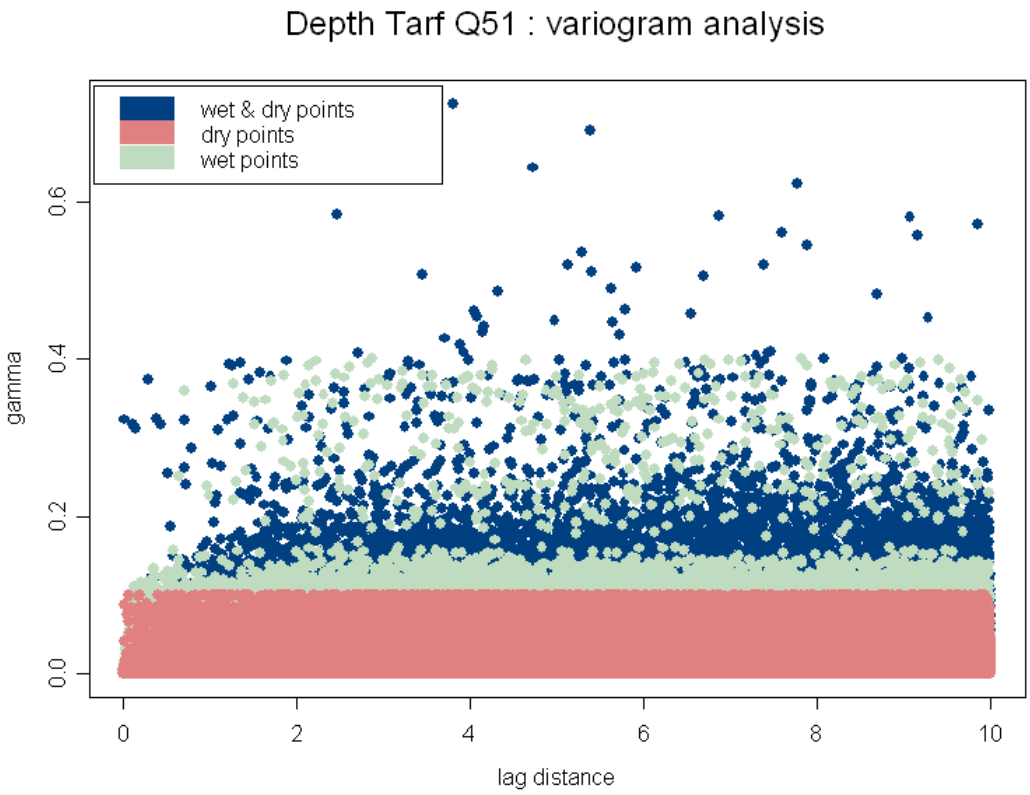
Depth Tarf Q51 : variogram analysis
wet & dry points
dry points
wet points
gamma
0.0
0.2
0.4
0.6
0
2
4
6
8
10
lag distance

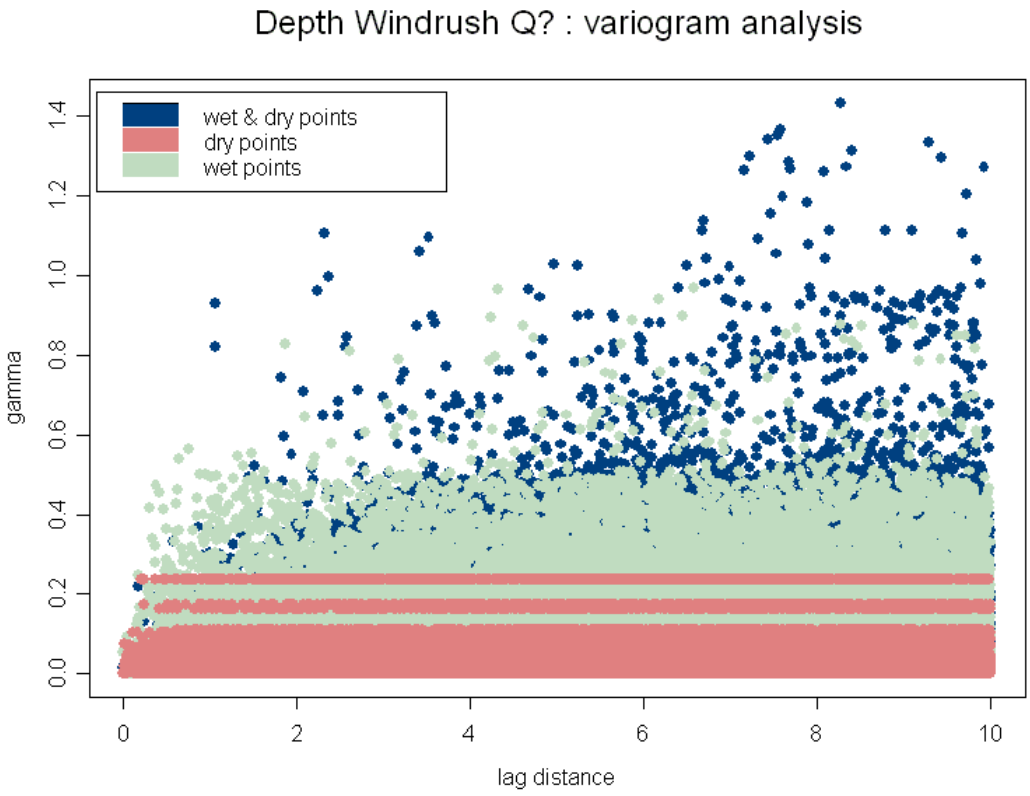
Depth Windrush Q? : variogram analysis
wet & dry points
dry points
wet points
gamma
0.0
0.2
0.4
0.6
0.8
1.0
1.2
1.4
0
2
4
6
8
10
lag distance

Appendix 3.7

Results obtained for the analysis in Chapter 5 –geostatistical analysis – modelling the variogram

This Appendix includes the graphical outputs obtained when modelling the variograms in section 5.4.5. The output show the final variogram selected after analysing the good of fitness of the spherical and exponential variogram models. Two sections can be identified: a former including the results for those data sets with wet and dry data points and a second including the results obtained for the data sets with just wet points.

Geostatistical Analysis: variogram fit dry and wet points

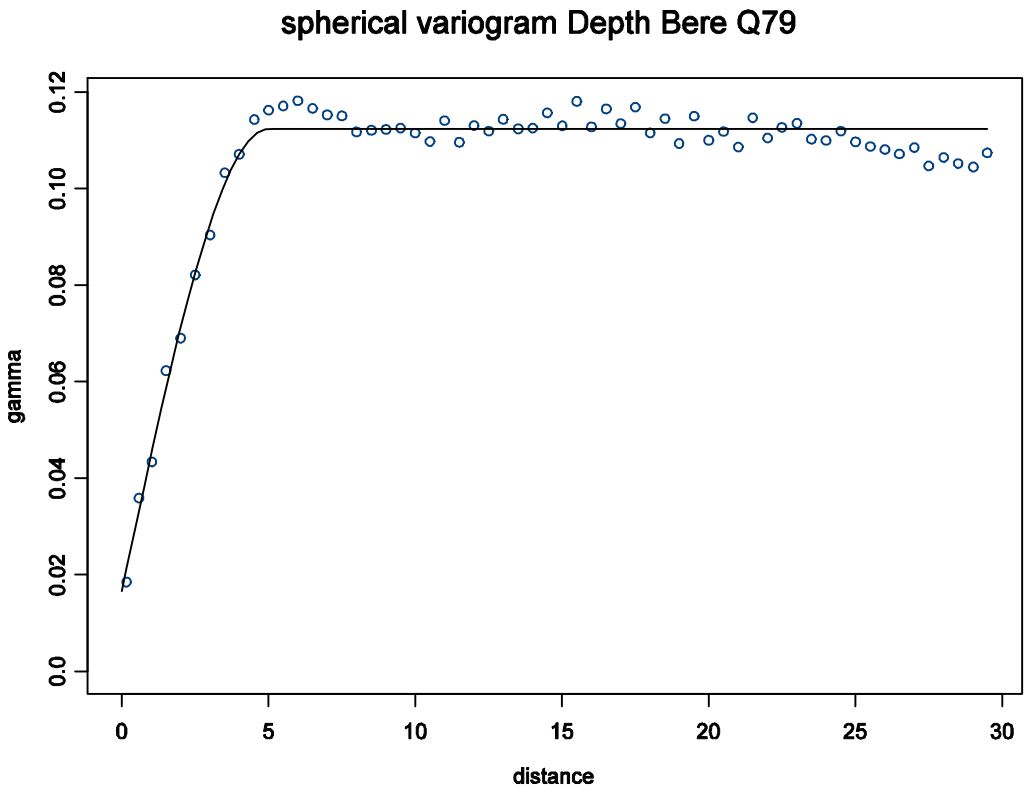

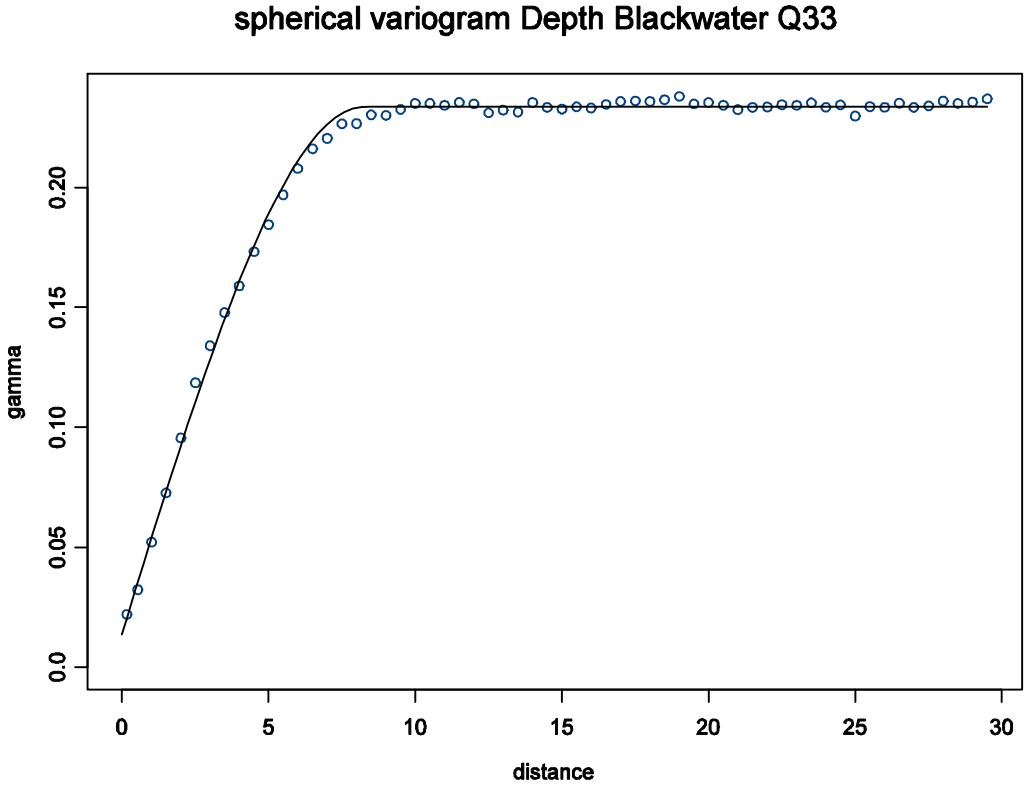

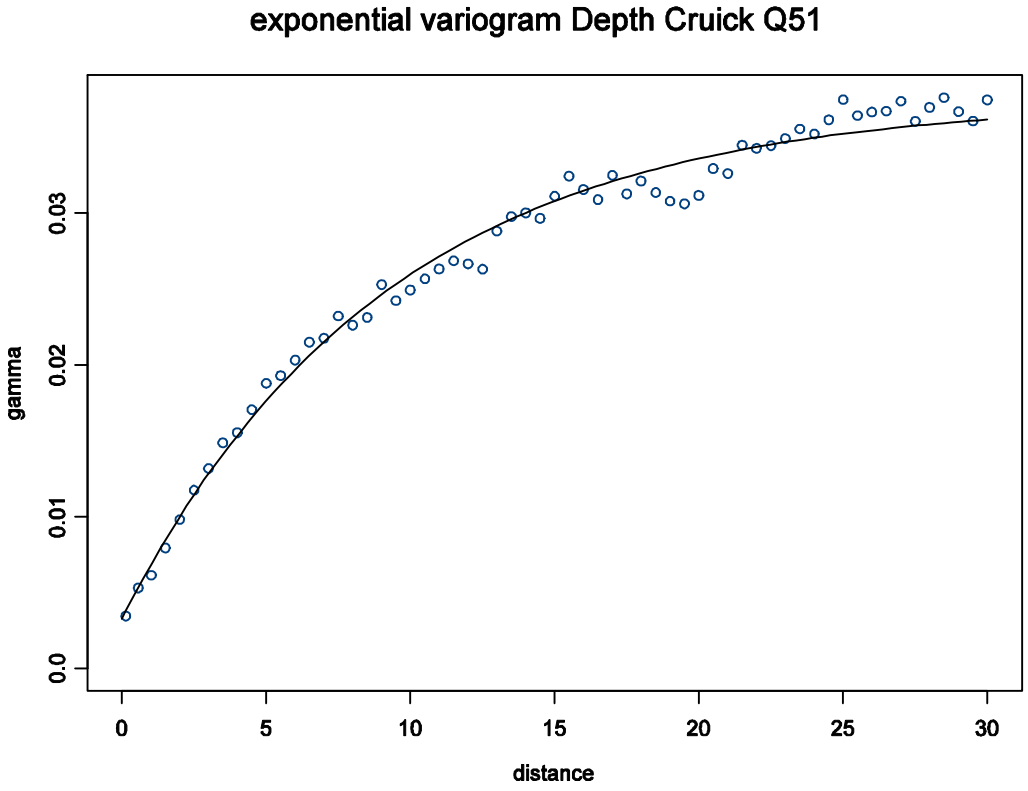
exponential variogram Depth Cruick Q51
gamma
0.0
0.01
0.02
0.03
0
5
10
15
20
25
30
distance

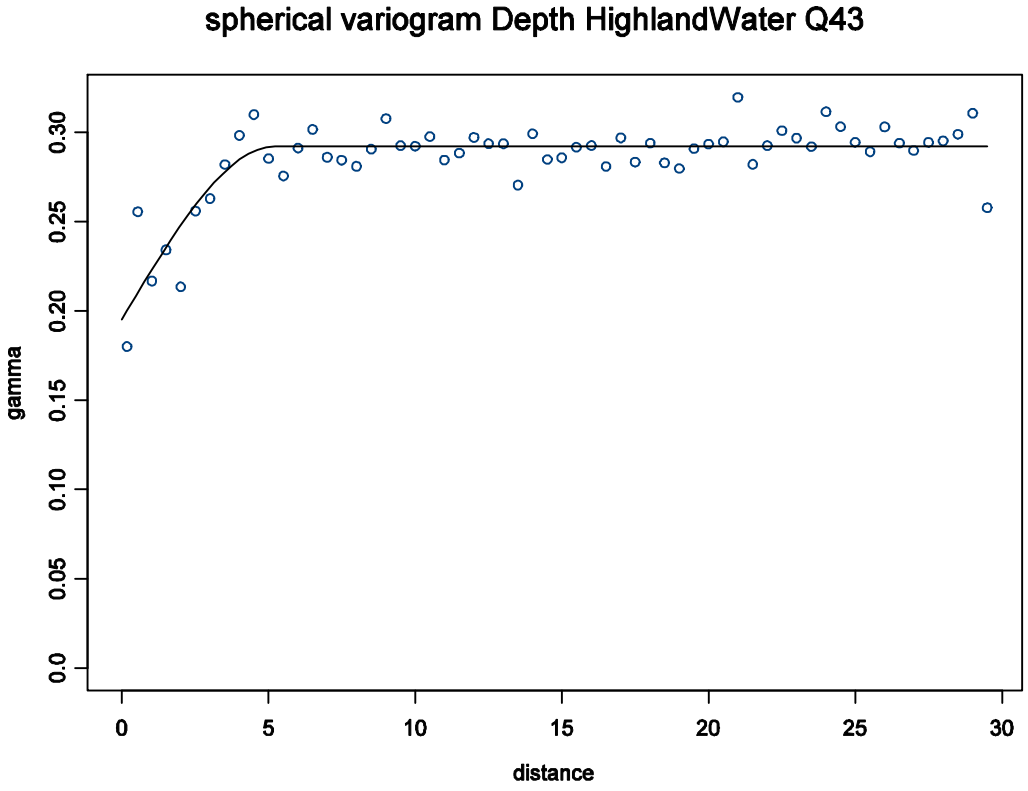
spherical variogram Depth HighlandWater Q43
gamma
0.0
0.05
0.10
0.15
0.20
0.25
0.30
0
5
10
15
20
25
30
distance

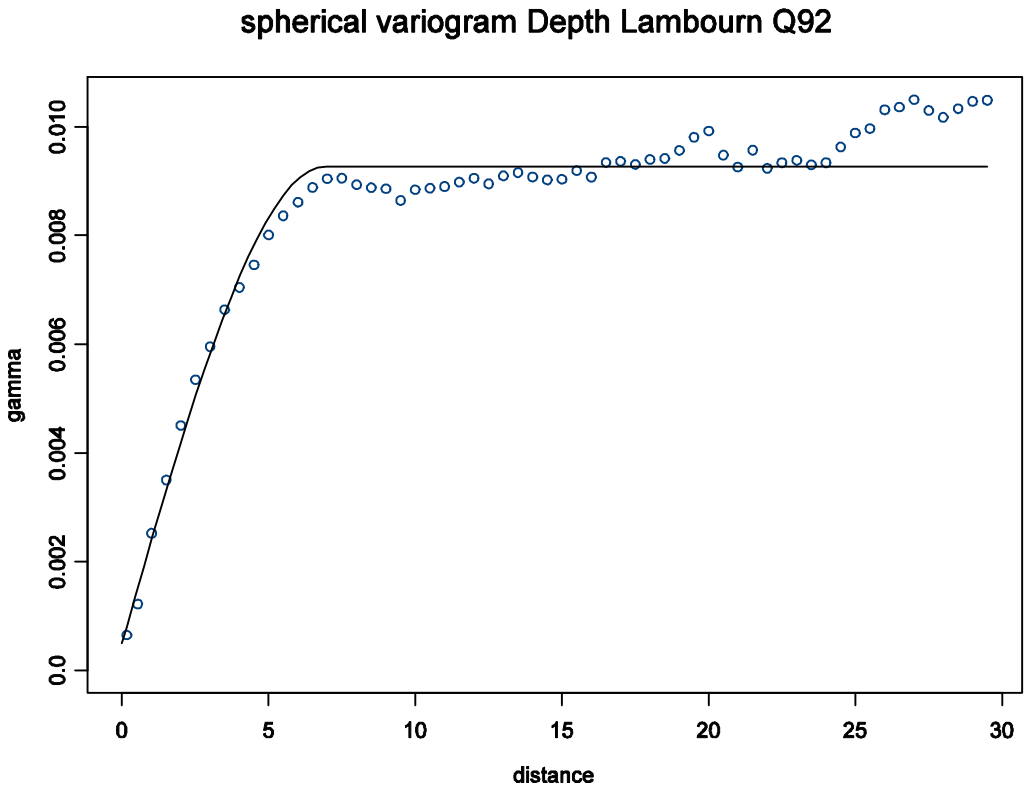
spherical variogram Depth Lambourn Q92
gamma
0.0
0.002
0.004
0.006
0.008
0.010
0
5
10
15
20
25
30
distance

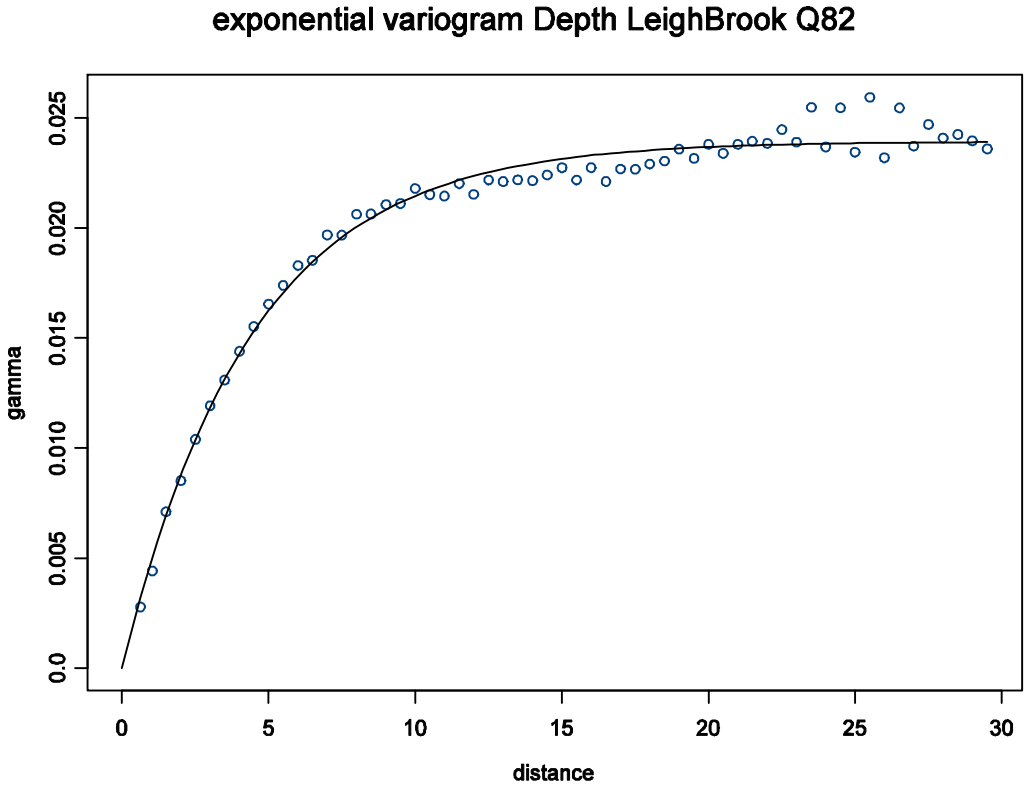
exponential variogram Depth LeighBrook Q82
gamma
0.0
0.005
0.010
0.015
0.020
0.025
0
5
10
15
20
25
30
distance

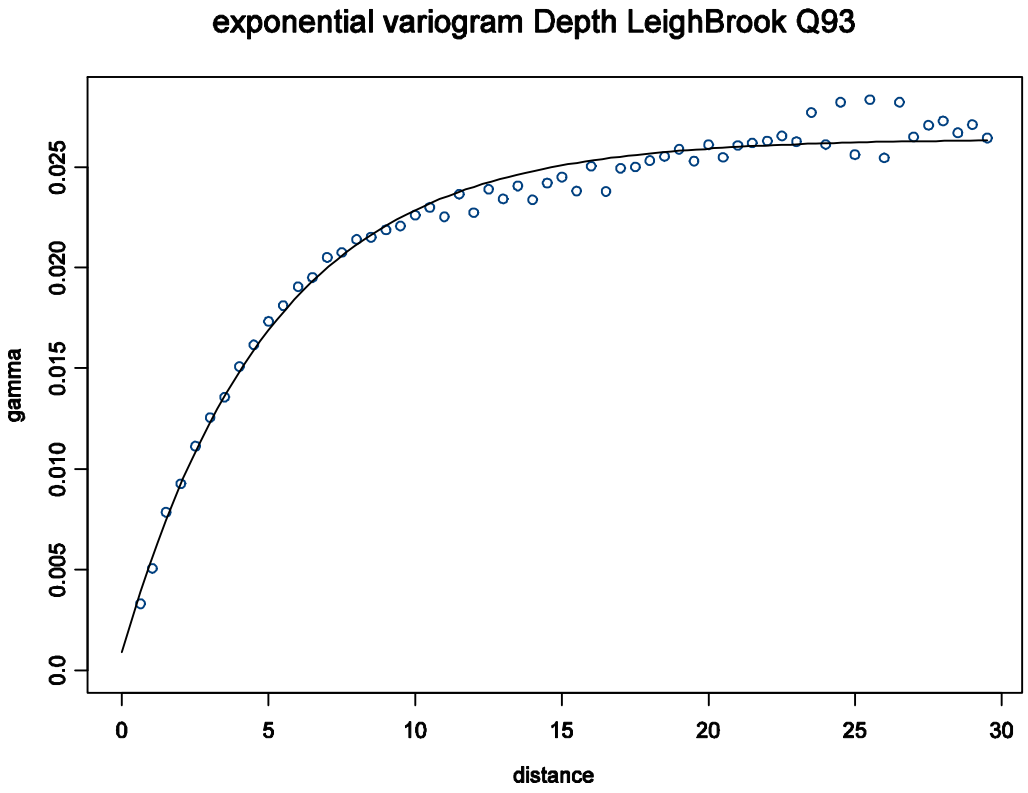
exponential variogram Depth LeighBrook Q93
gamma
0.0
0.005
0.010
0.015
0.020
0.025
0
5
10
15
20
25
30
distance

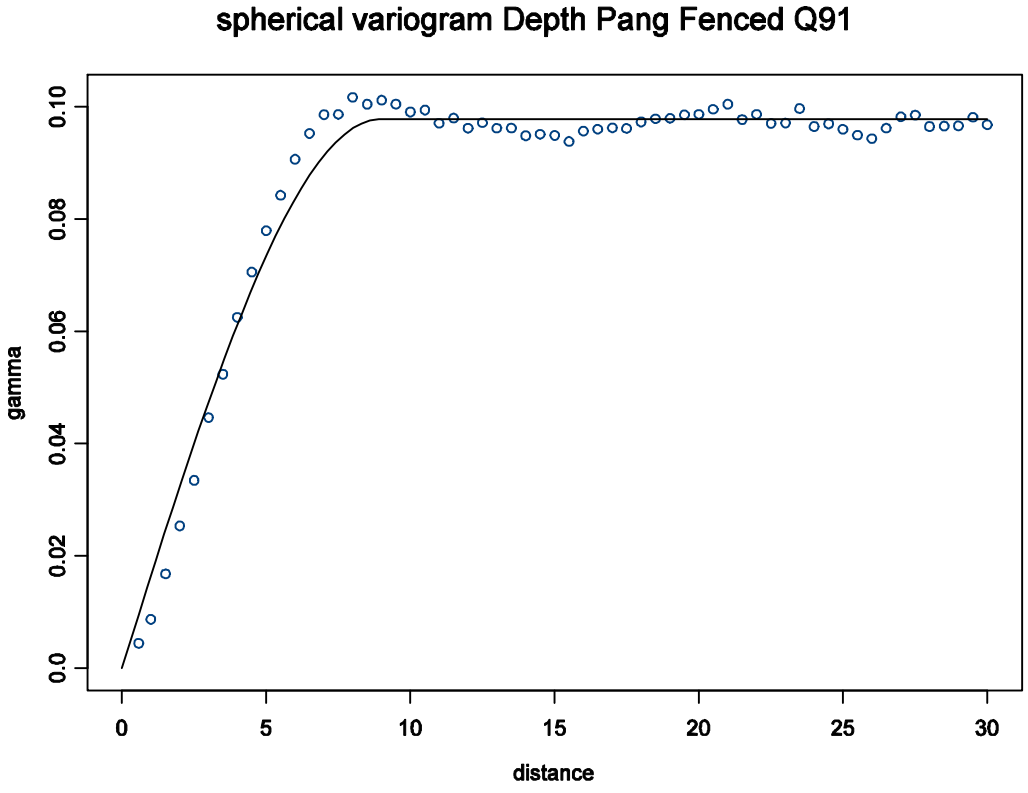
spherical variogram Depth Pang Fenced Q91
gamma
0.0
0.02
0.04
0.06
0.08
0.10
0
5
10
15
20
25
30
distance

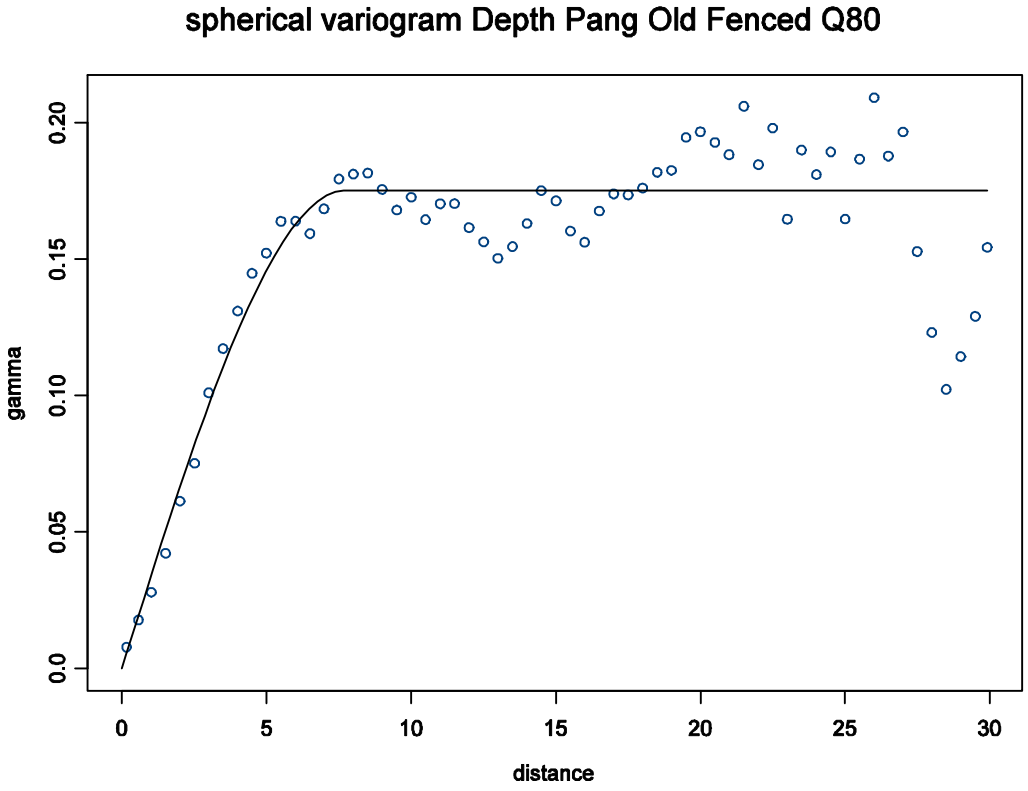
spherical variogram Depth Pang Old Fenced Q80
gamma
0.0
0.05
0.10
0.15
0.20
0
5
10
15
20
25
30
distance

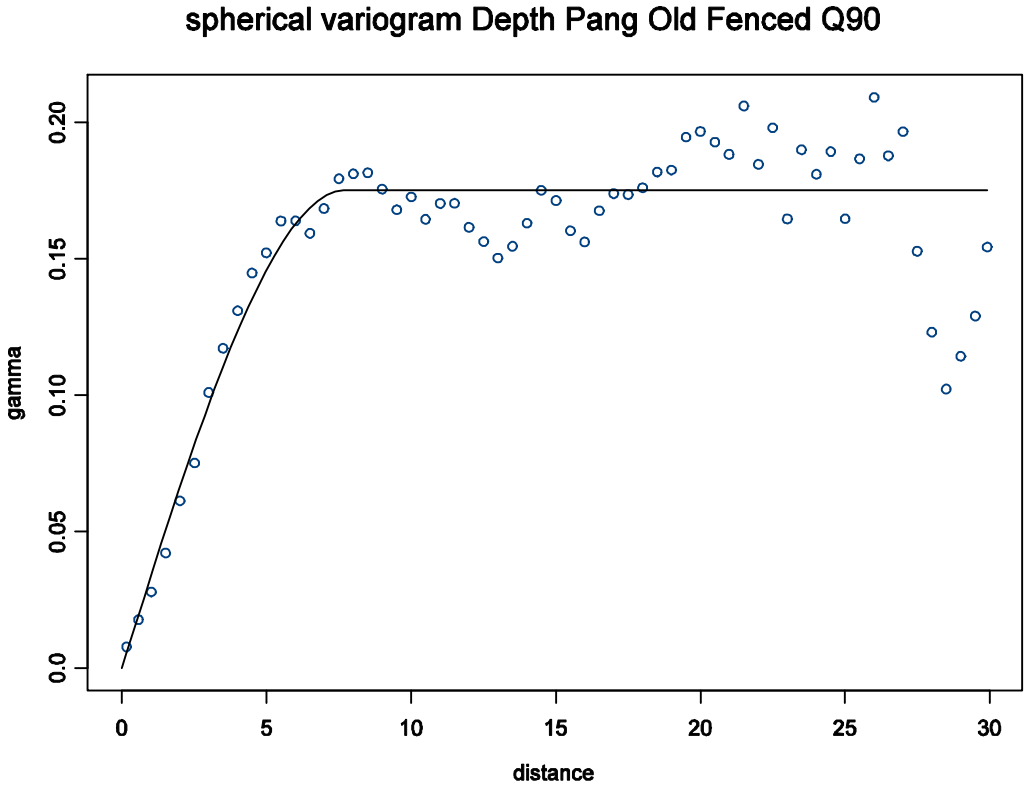
spherical variogram Depth Pang Old Fenced Q90
gamma
0.0
0.05
0.10
0.15
0.20
0
5
10
15
20
25
30
distance

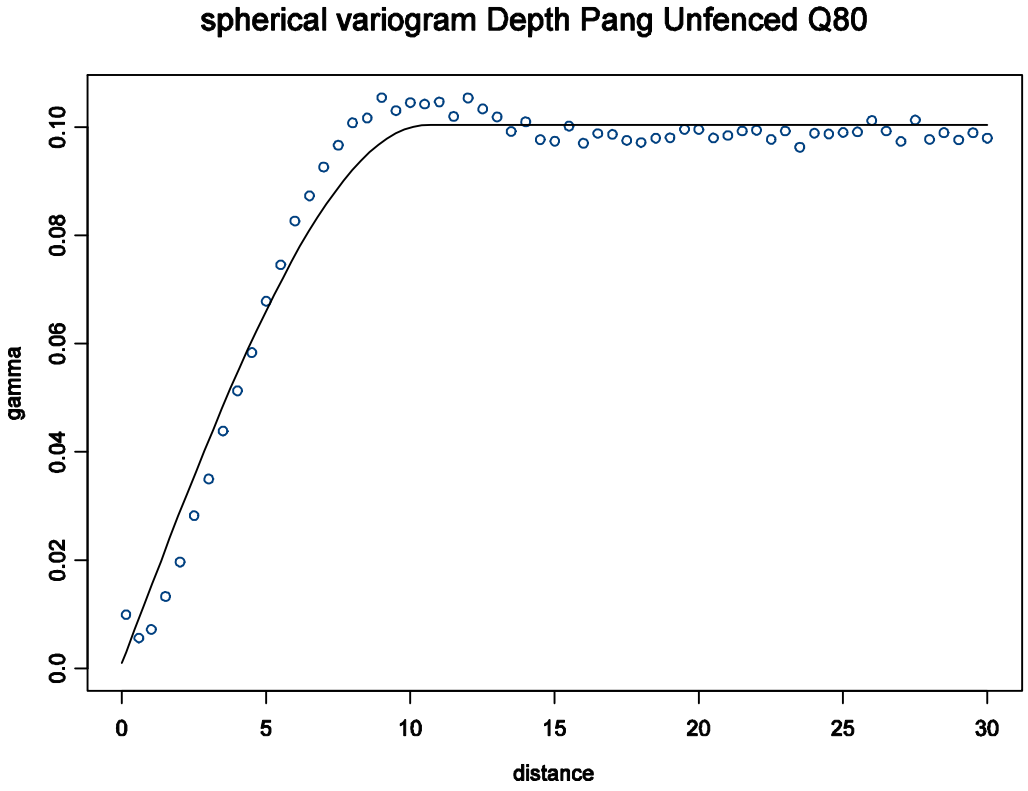
spherical variogram Depth Pang Unfenced Q80
gamma
0.0
0.02
0.04
0.06
0.08
0.10
0
5
10
15
20
25
30
distance

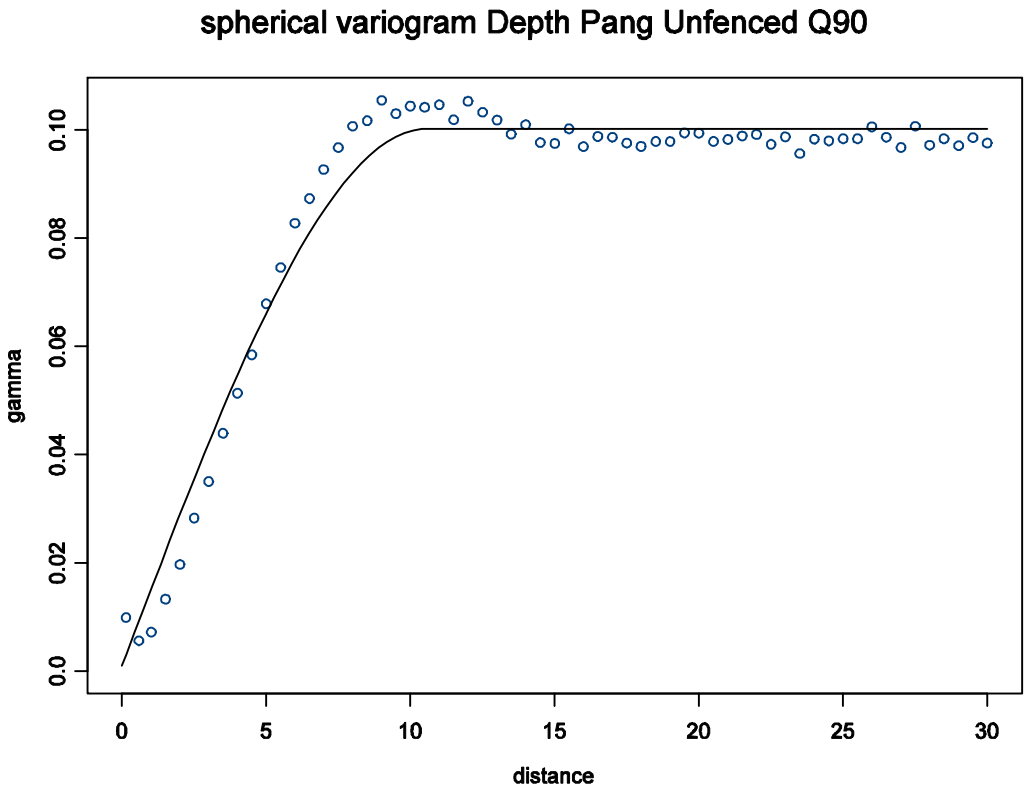
spherical variogram Depth Pang Unfenced Q90
gamma
0.0
0.02
0.04
0.06
0.08
0.10
0
5
10
15
20
25
30
distance

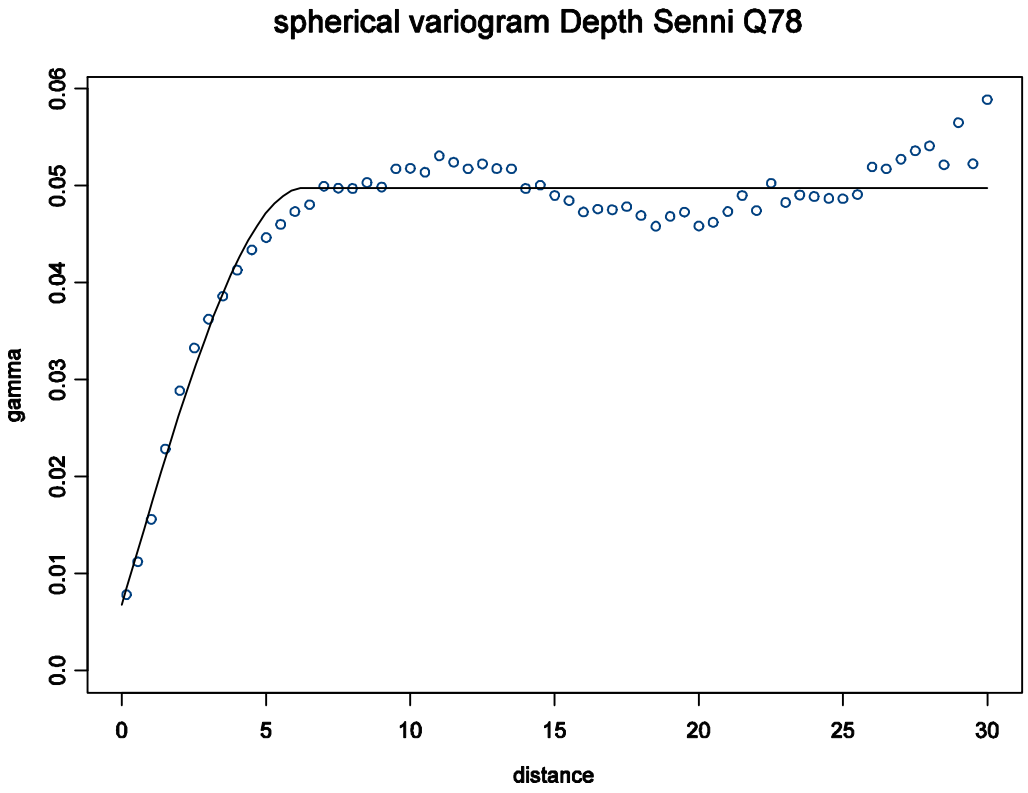
spherical variogram Depth Senni Q78
gamma
0.0
0.01
0.02
0.03
0.04
0.05
0.06
0
5
10
15
20
25
30
distance

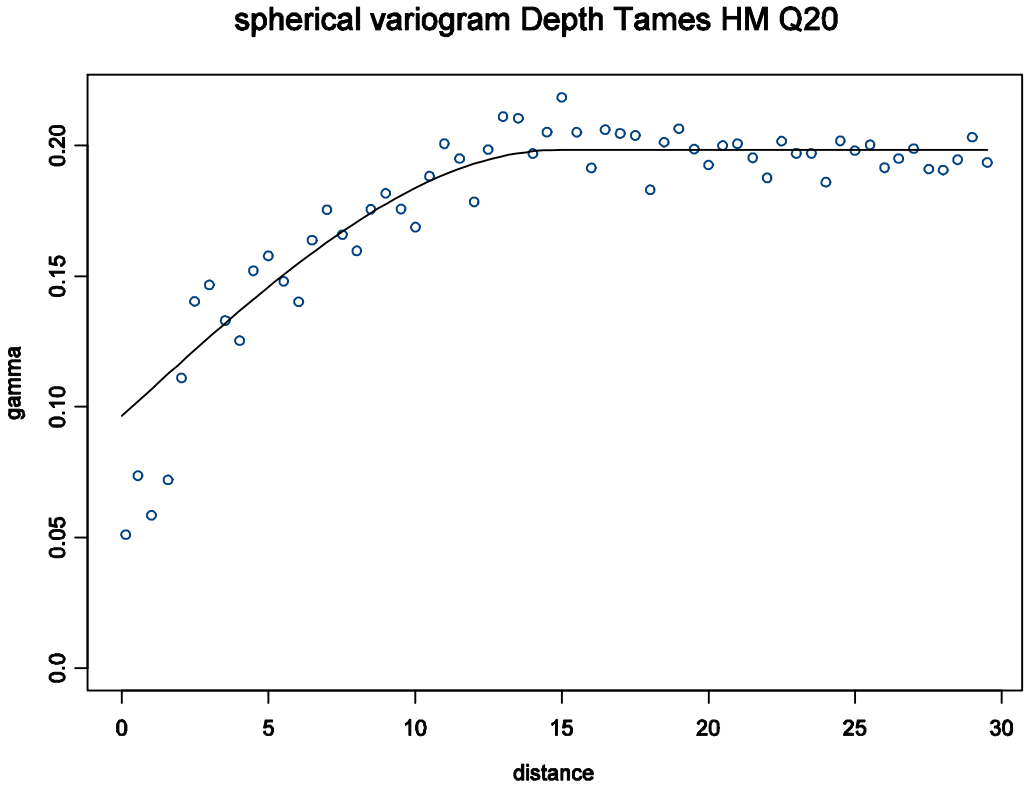
spherical variogram Depth Tames HM Q20
gamma
0.0
0.05
0.10
0.15
0.20
0
5
10
15
20
25
30
distance

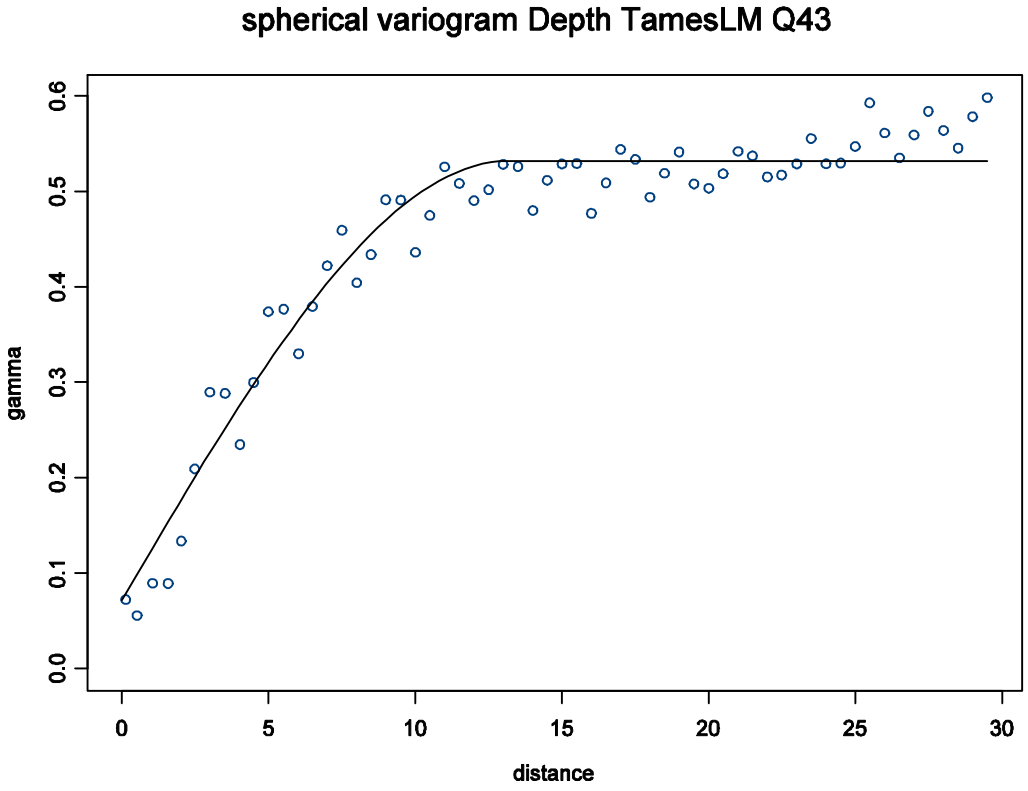
spherical variogram Depth TamesLM Q43
gamma
0.0
0.1
0.2
0.3
0.4
0.5
0.6
0
5
10
15
20
25
30
distance

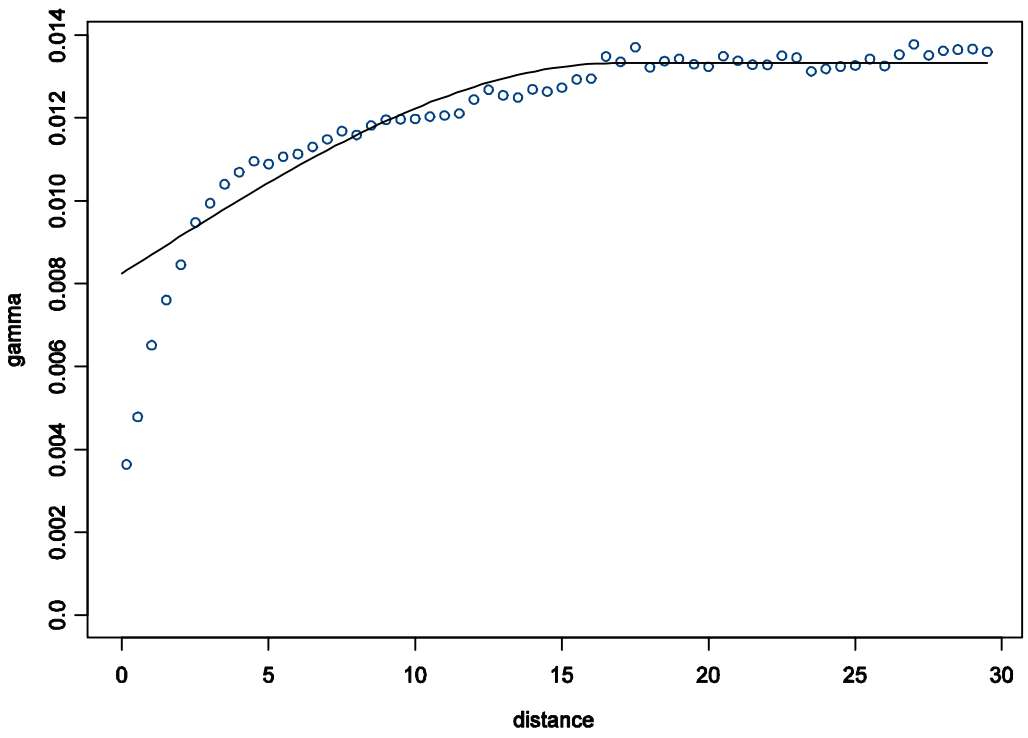
spherical variogram Depth Tarf Q51
gamma
0.0
0.002
0.004
0.006
0.008
0.010
0.012
0.014
0
5
10
15
20
25
30
distance

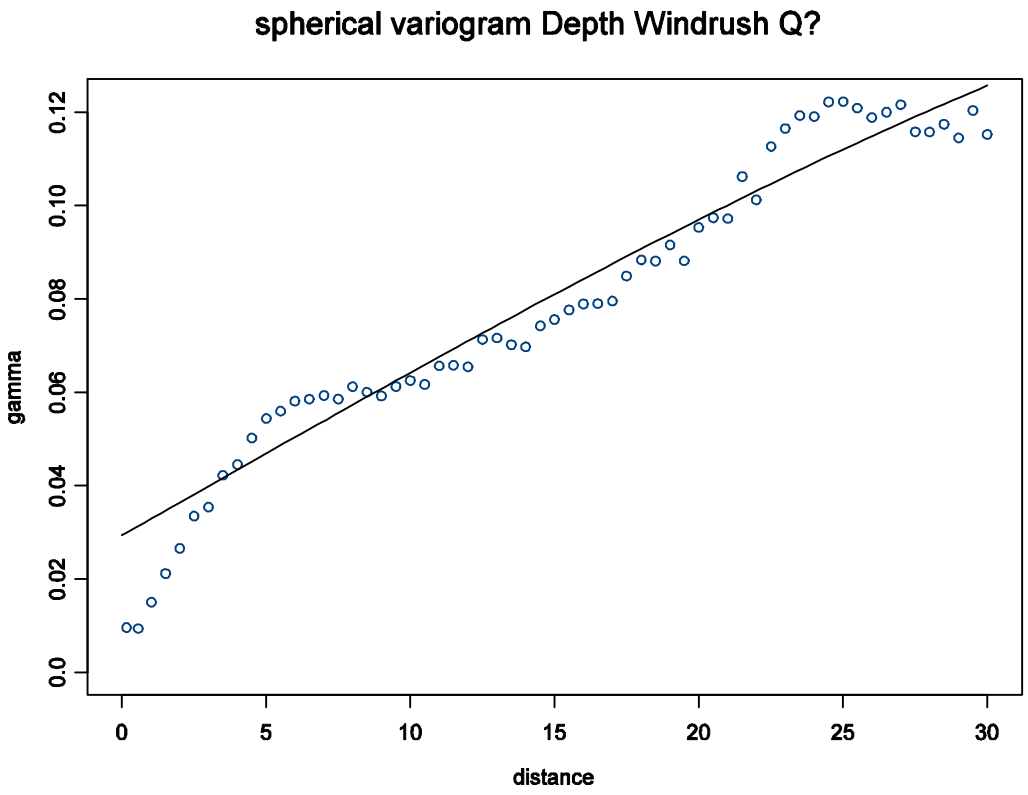

Geostatistical Analysis: variogram fit dry and wet points

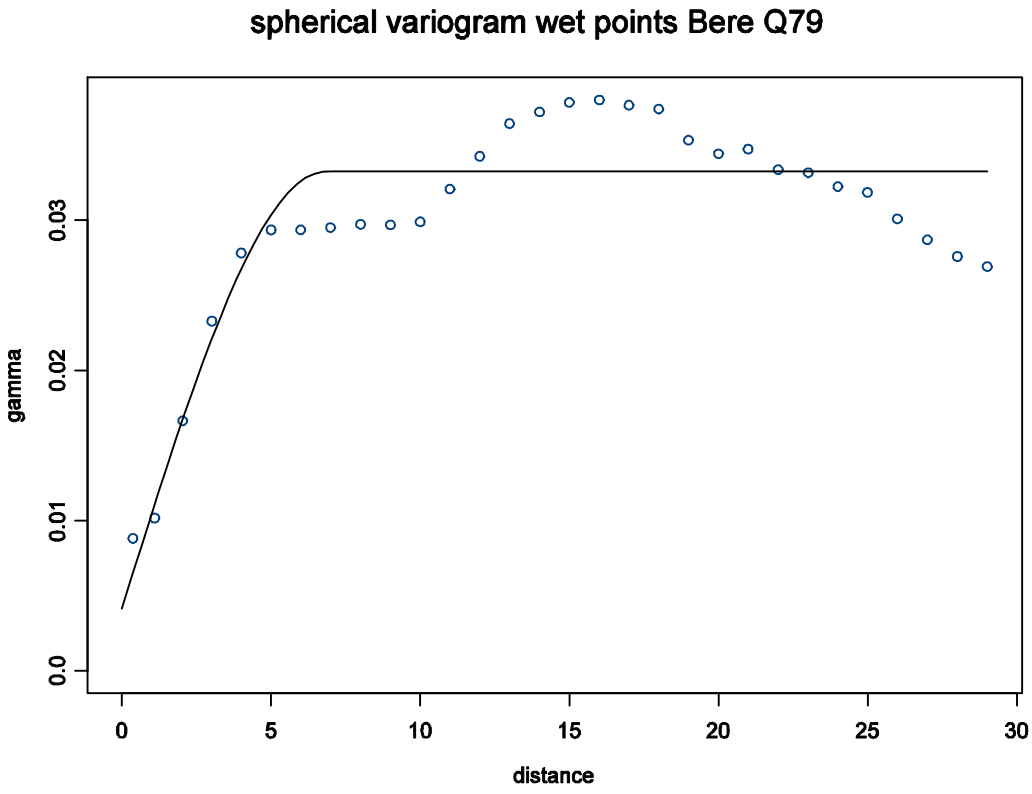

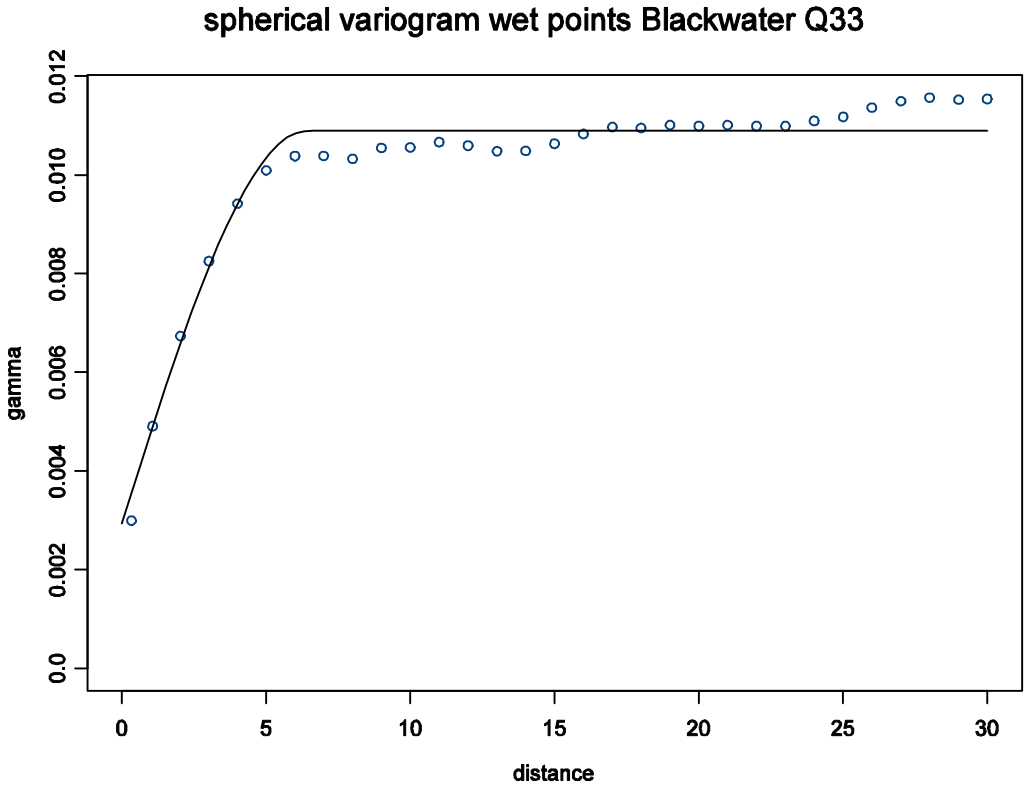
spherical variogram wet points Blackwater Q33
gamma
0.0
0.002
0.004
0.006
0.008
0.010
0.012
0
5
10
15
20
25
30
distance

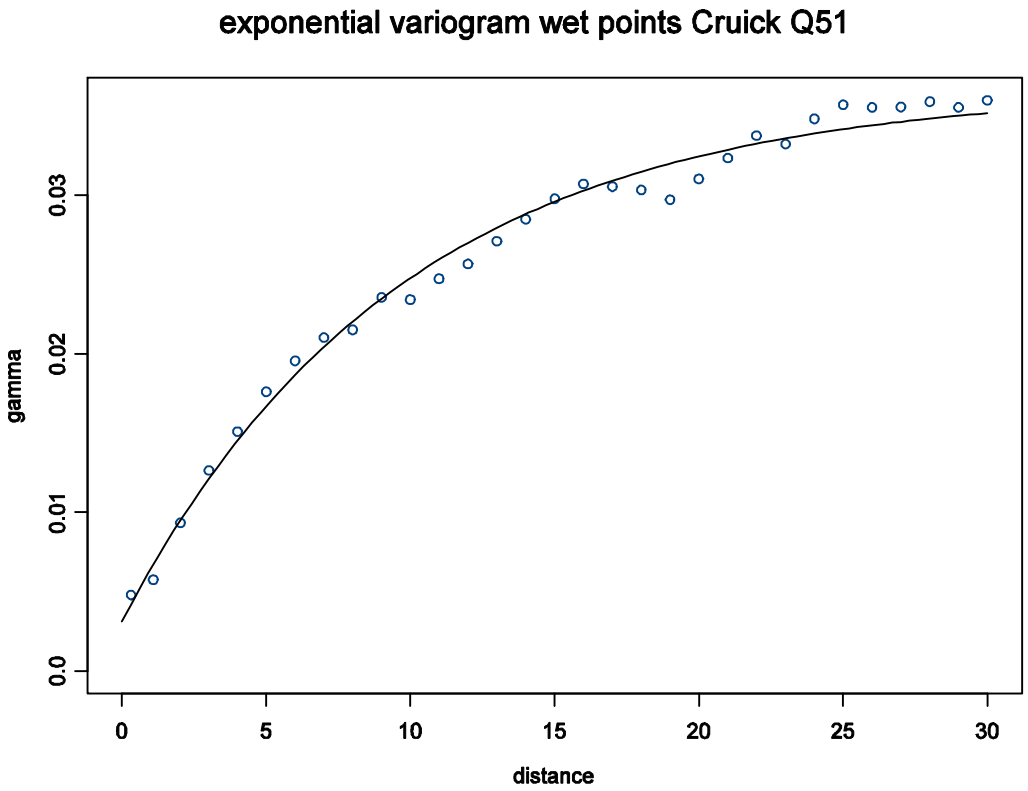
exponential variogram wet points Cruick Q51
gamma
0.0
0.01
0.02
0.03
0
5
10
15
20
25
30
distance

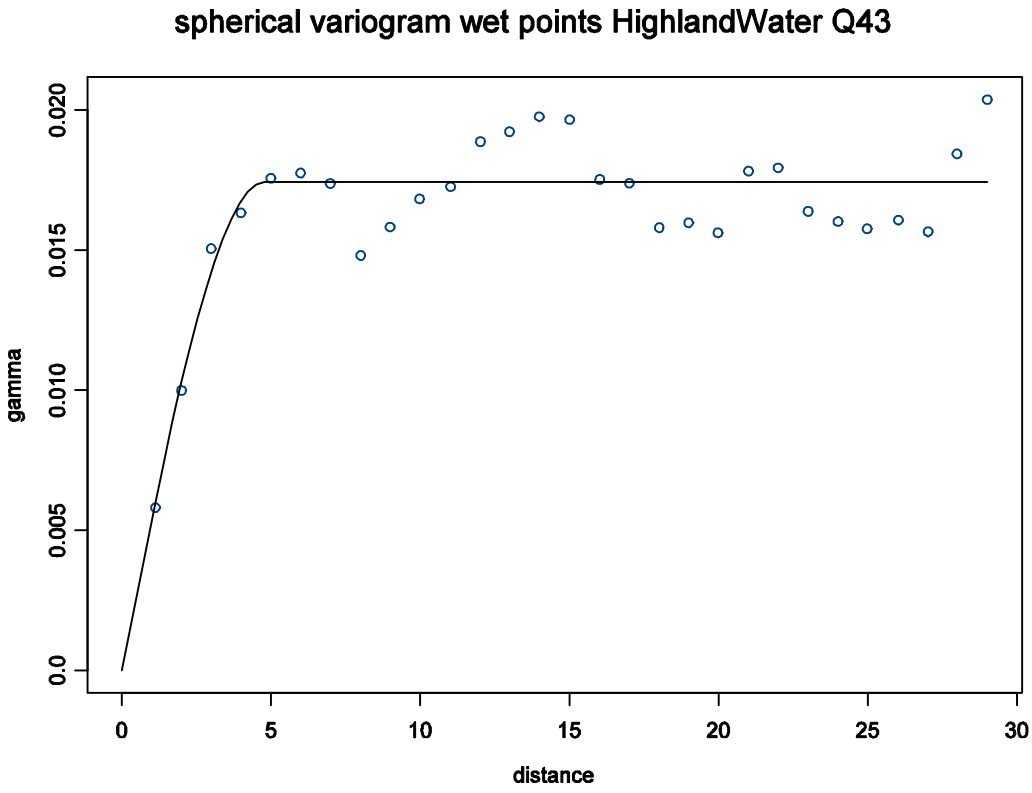
spherical variogram wet points HighlandWater Q43
gamma
0.0
0.005
0.010
0.015
0.020
0
5
10
15
20
25
30
distance

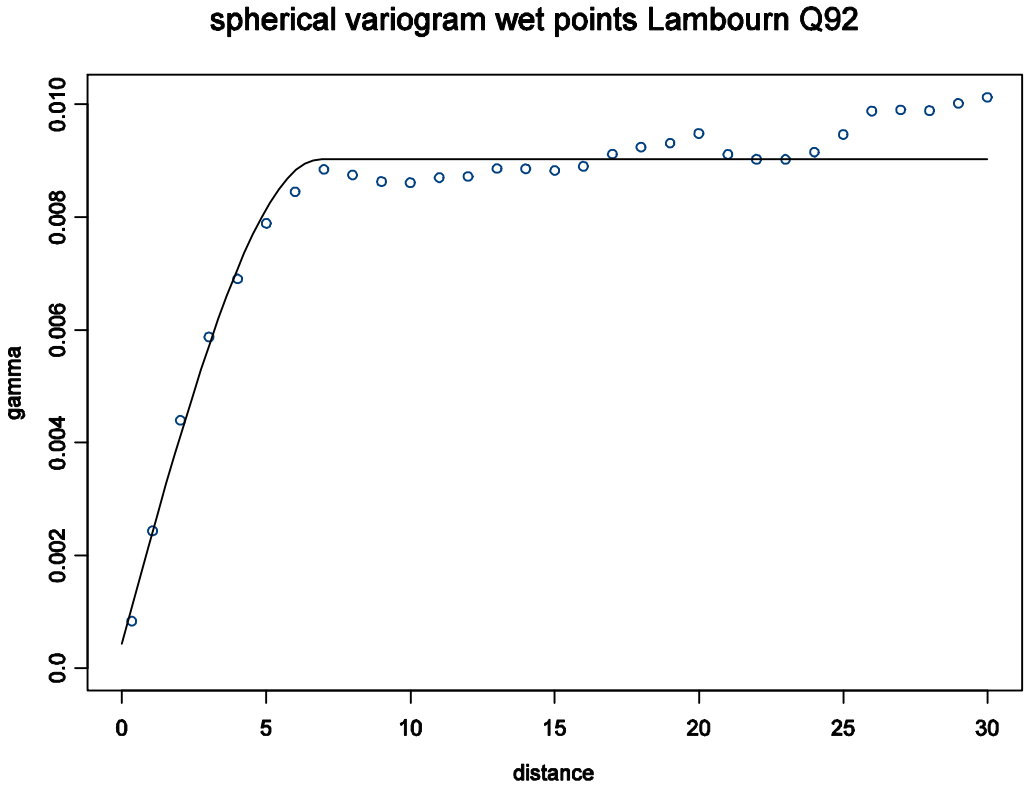
spherical variogram wet points Lambourn Q92
gamma
0.0
0.002
0.004
0.006
0.008
0.010
0
5
10
15
20
25
30
distance

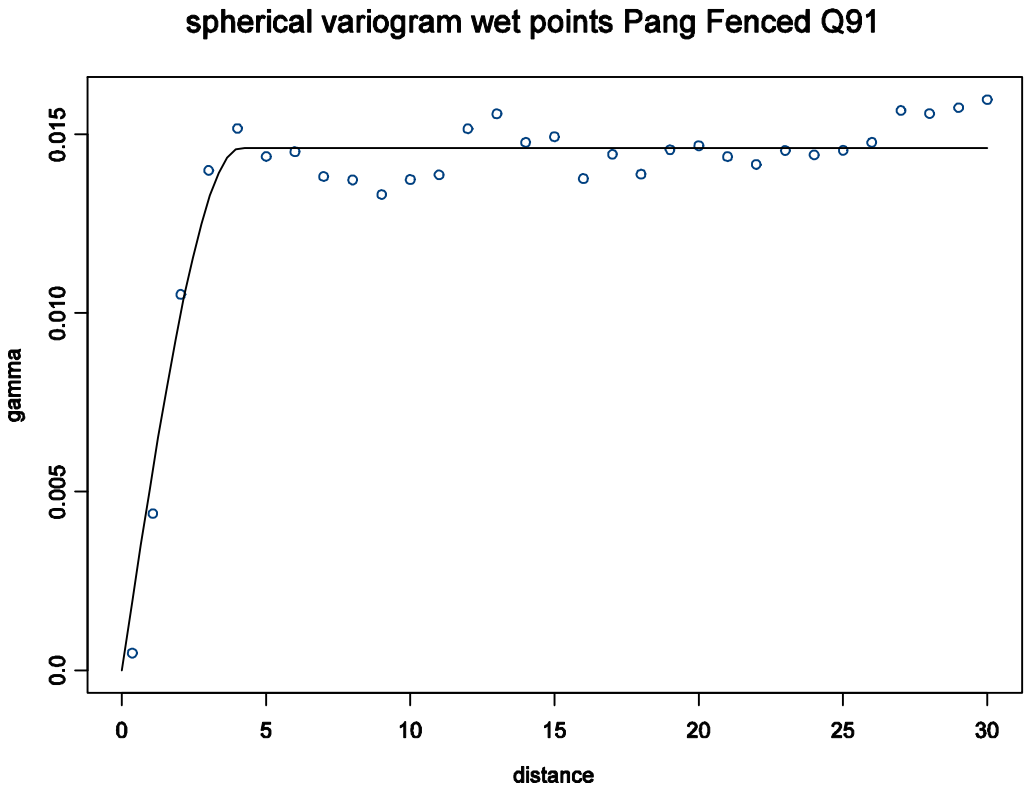
spherical variogram wet points Pang Fenced Q91
gamma
0.0
0.005
0.010
0.015
0
5
10
15
20
25
30
distance

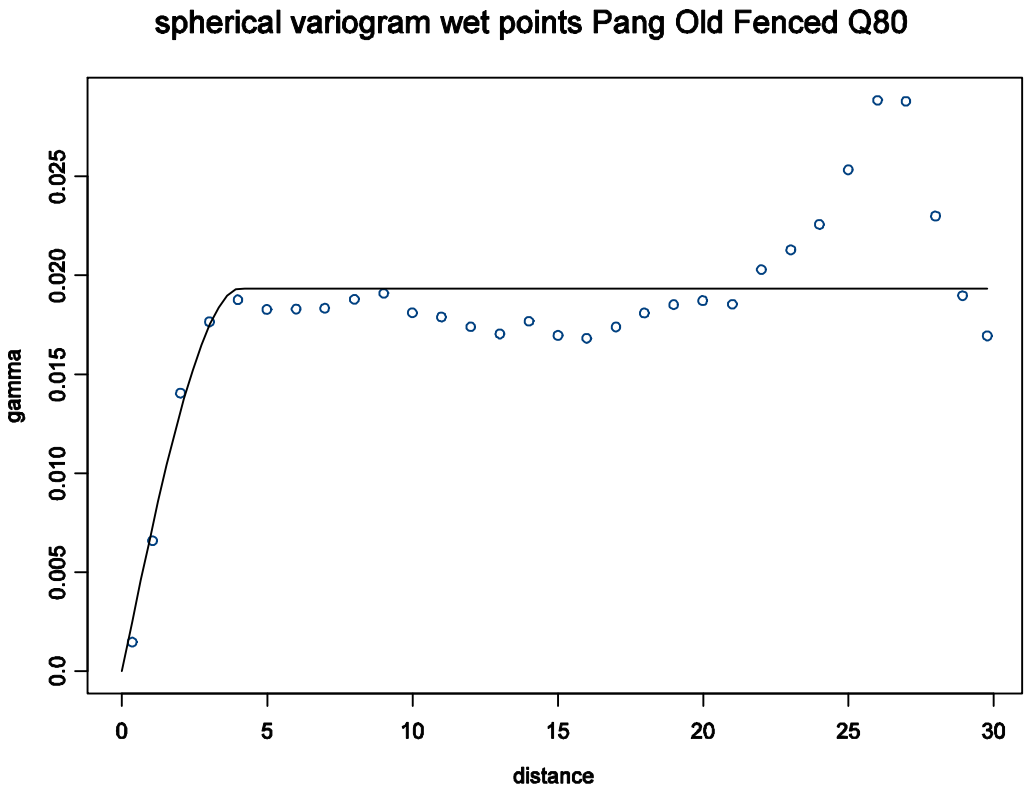
spherical variogram wet points Pang Old Fenced Q80
gamma
0.0
0.005
0.010
0.015
0.020
0.025
0
5
10
15
20
25
30
distance

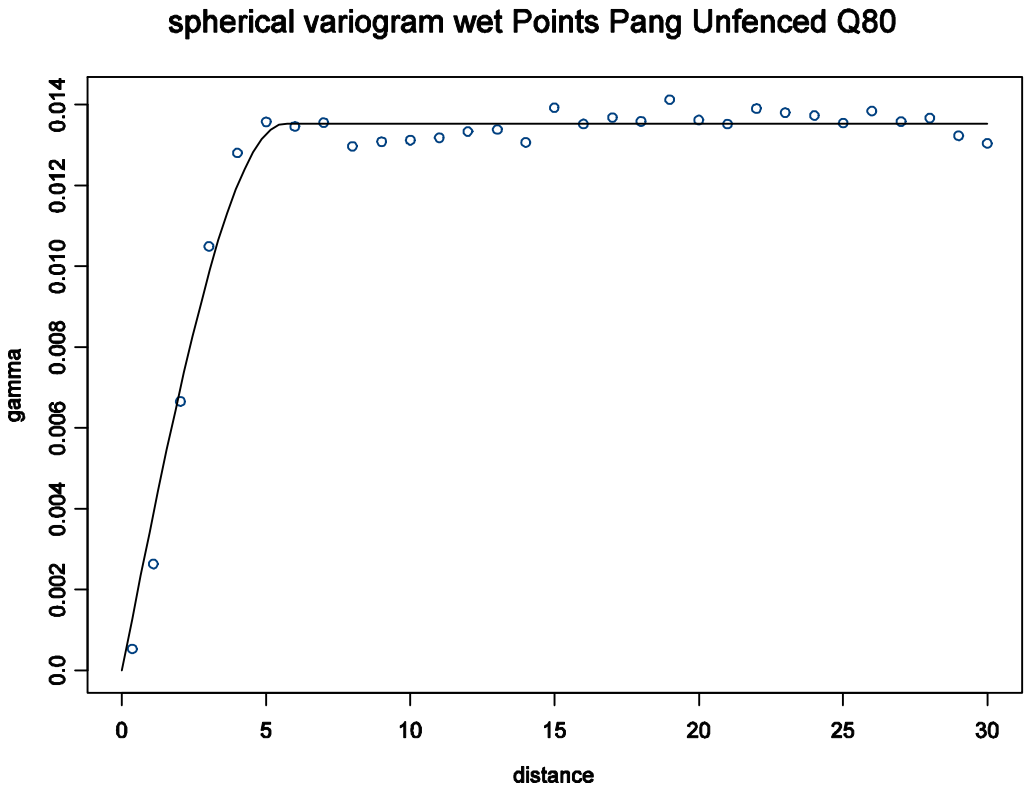
spherical variogram wet Points Pang Unfenced Q80
gamma
0.0
0.002
0.004
0.006
0.008
0.010
0.012
0.014
0
5
10
15
20
25
30
distance

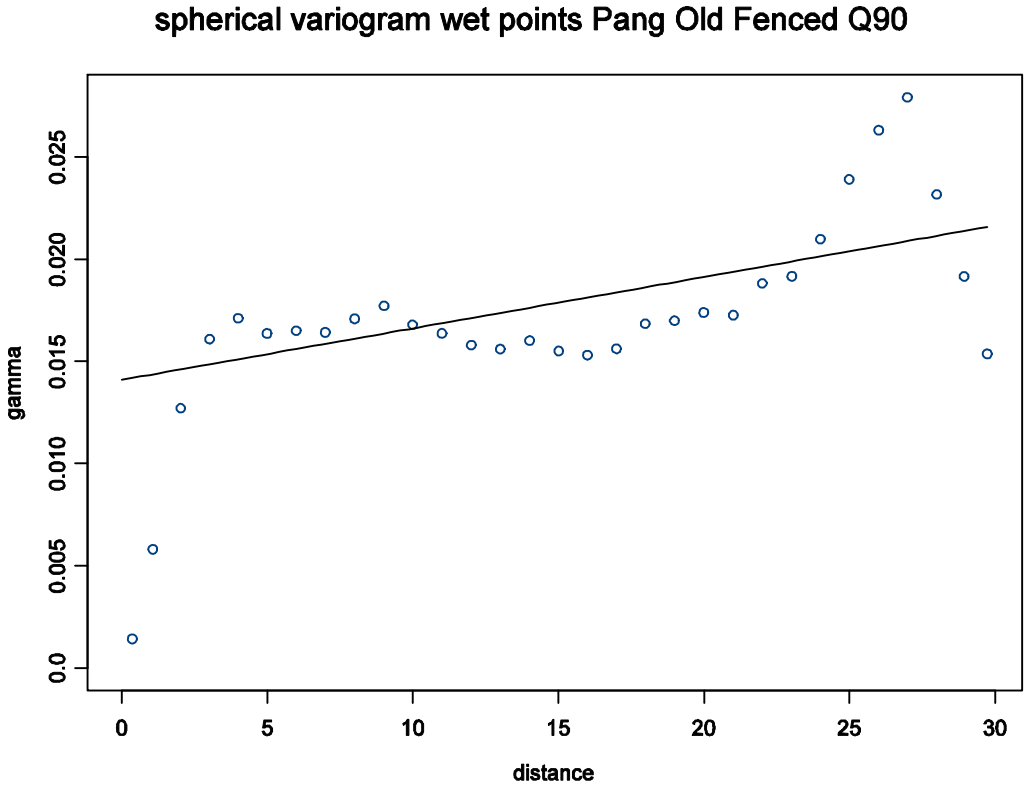
spherical variogram wet points Pang Old Fenced Q90
gamma
0.0
0.005
0.010
0.015
0.020
0.025
0
5
10
15
20
25
30
distance

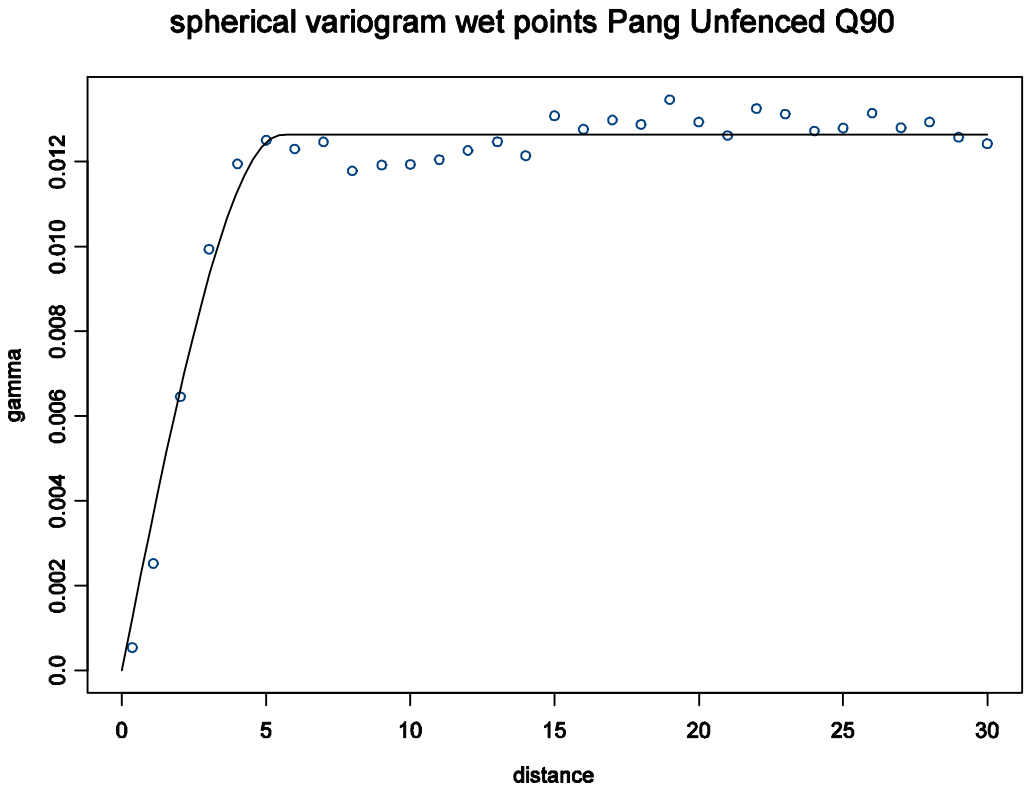
spherical variogram wet points Pang Unfenced Q90
gamma
0.0
0.002
0.004
0.006
0.008
0.010
0.012
0
5
10
15
20
25
30
distance

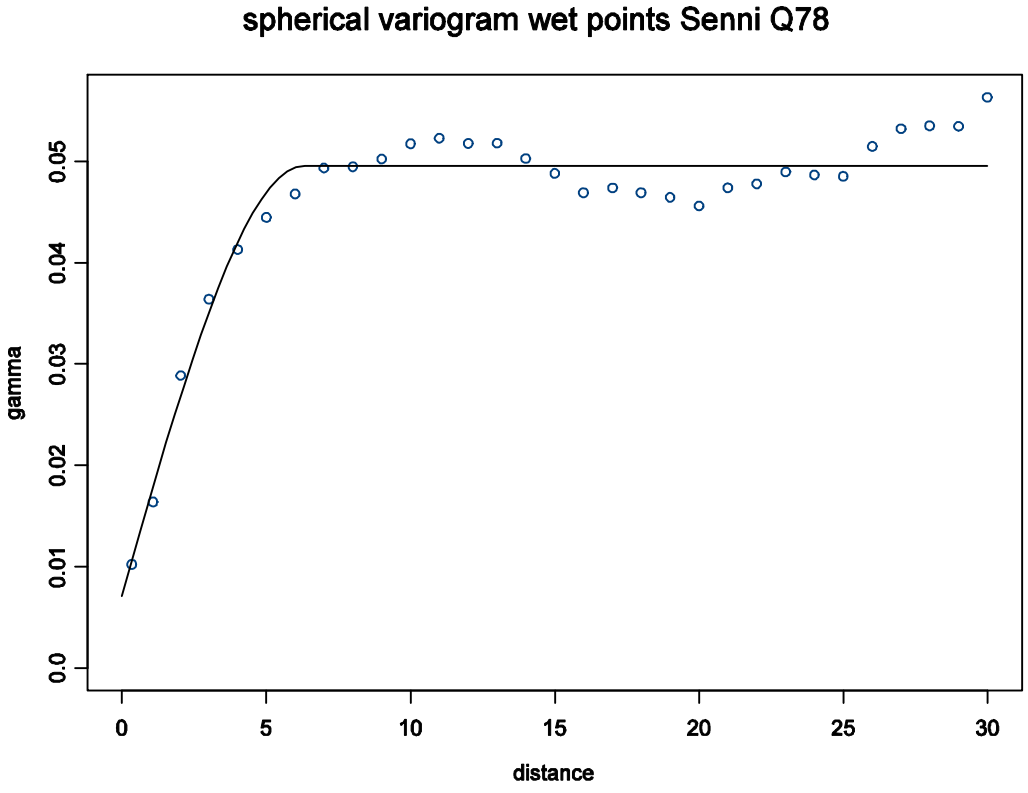
spherical variogram wet points Senni Q78
gamma
0.0
0.01
0.02
0.03
0.04
0.05
0
5
10
15
20
25
30
distance

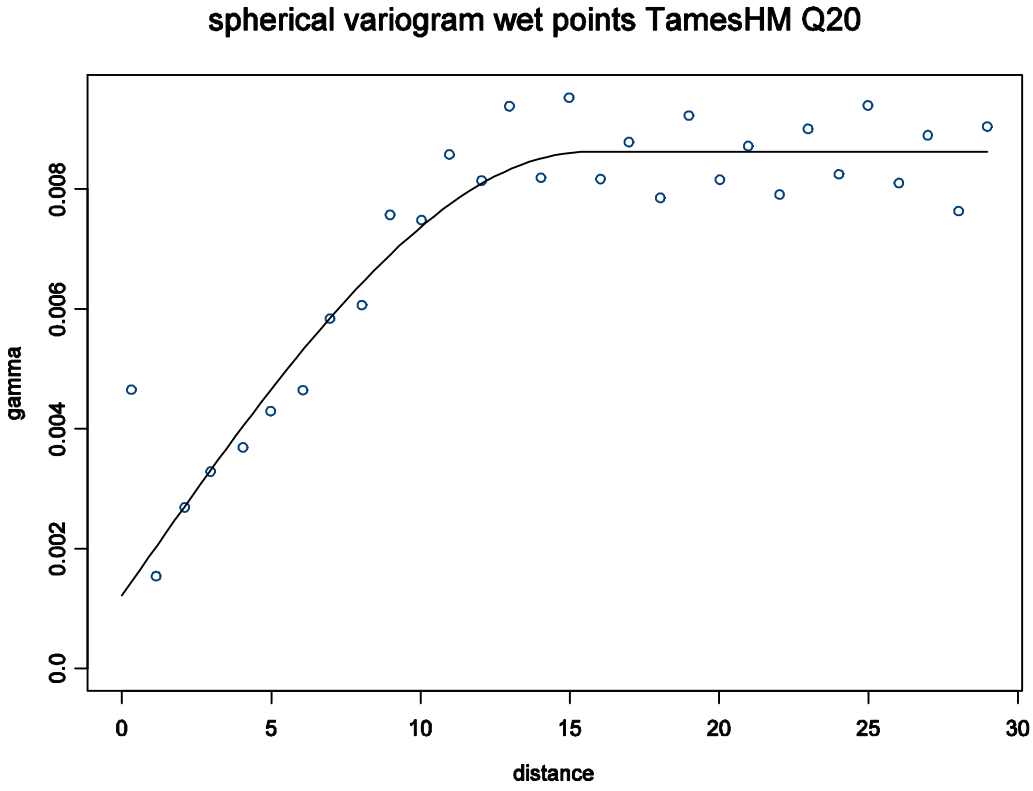
spherical variogram wet points TamesHM Q20
gamma
0.0
0.002
0.004
0.006
0.008
0
5
10
15
20
25
30
distance

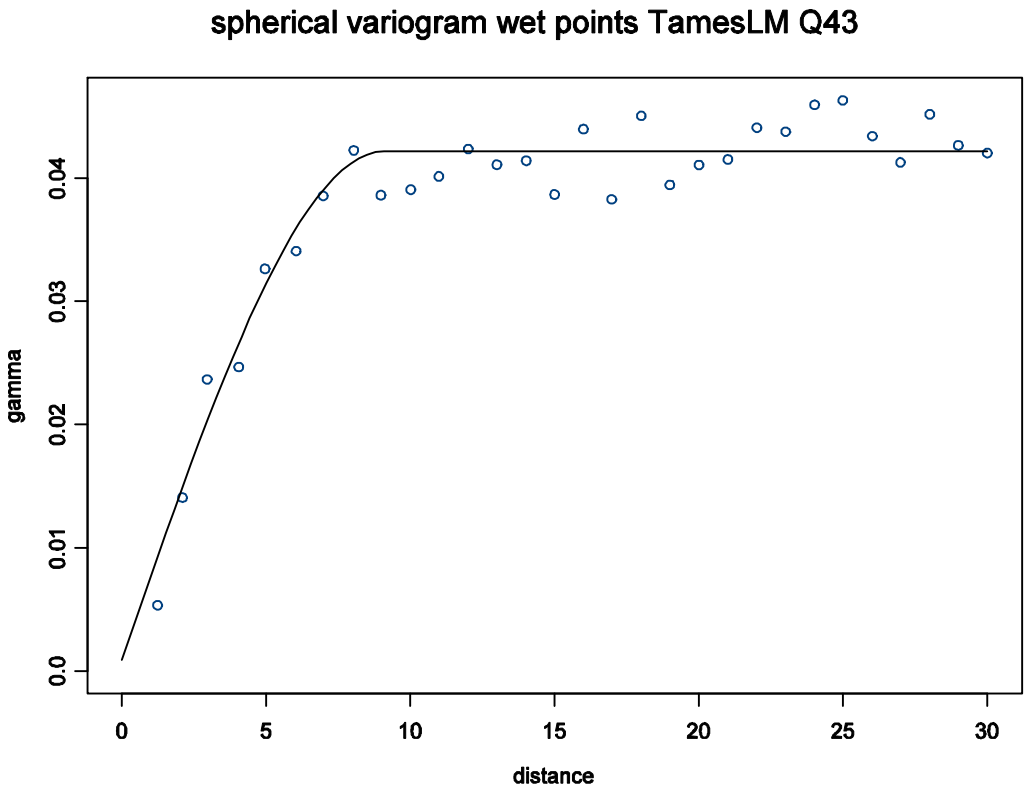
spherical variogram wet points TamesLM Q43
gamma
0.0
0.01
0.02
0.03
0.04
0
5
10
15
20
25
30
distance

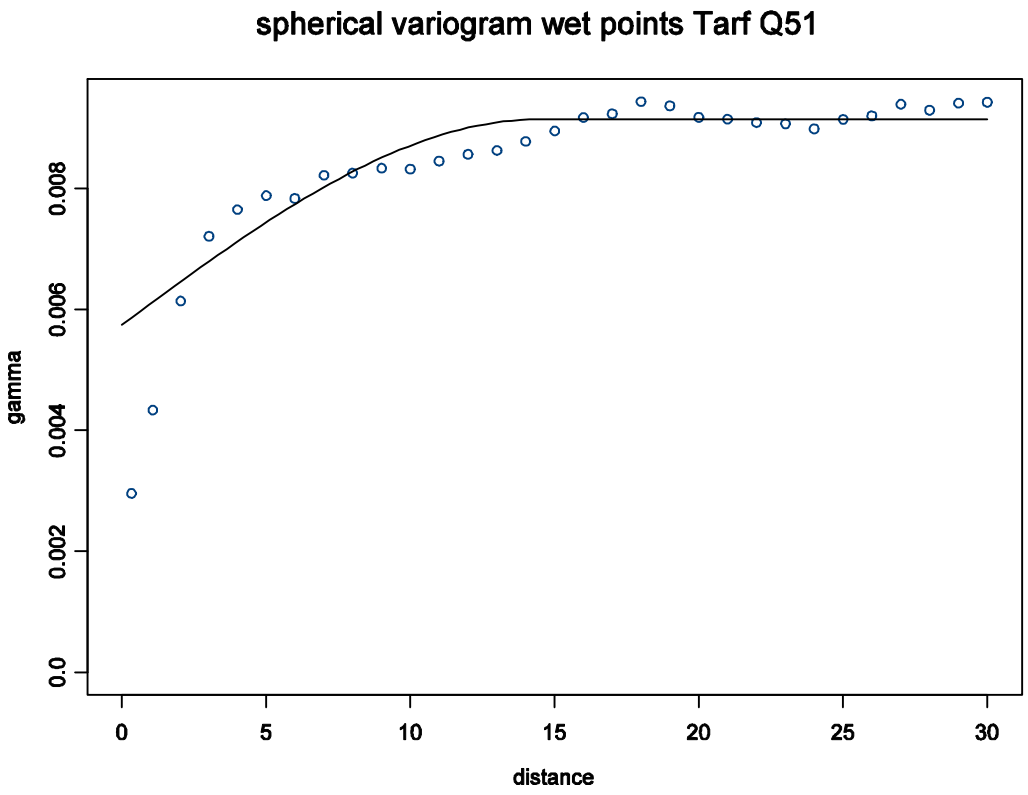
spherical variogram wet points Tarf Q51
gamma
0.0
0.002
0.004
0.006
0.008
0
5
10
15
20
25
30
distance

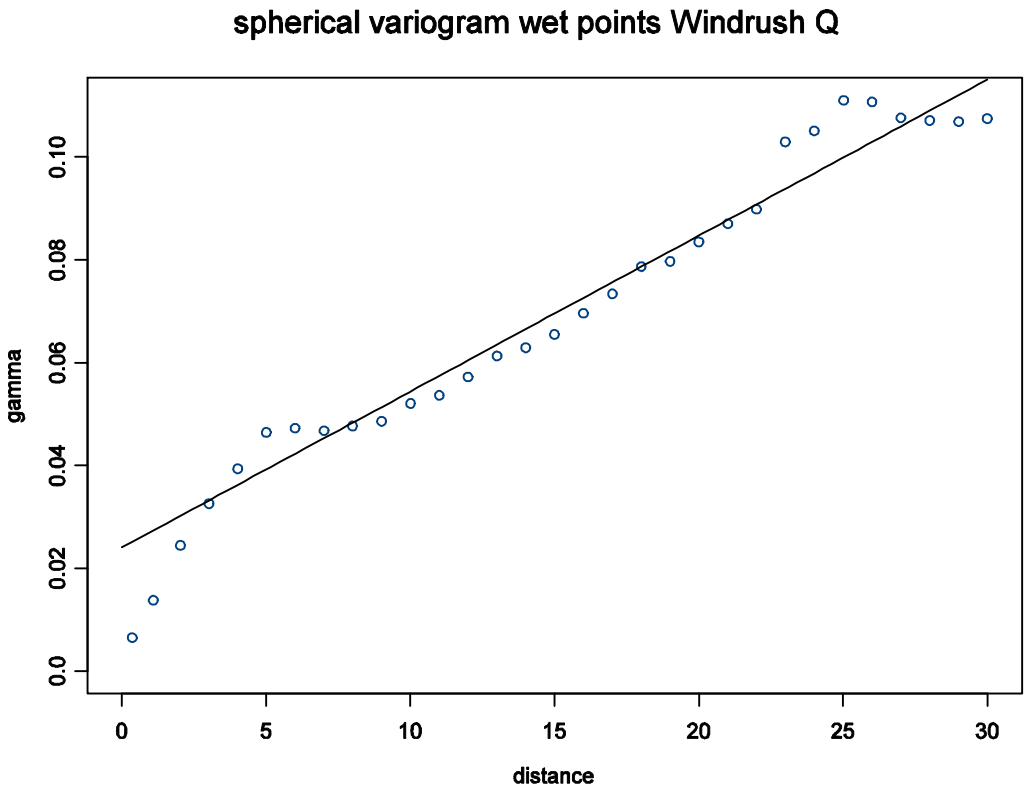
spherical variogram wet points Windrush Q
gamma
0.0
0.02
0.04
0.06
0.08
0.10
0
5
10
15
20
25
30
distance

Appendix 4.1

Equations relating sampling density with indicator values – Chapter 6

This appendix summarises the equations obtained for those indicators that showed a pattern of change when decreasing the sampling density. The equations have been calculated independently for each river site. The "x" and "y" in the equations refer to the sampling density (points/m^2) and the indicator value (in the units shown in the tables), respectively. It is recommended to use these equations in combination with the information provided in Annex 6.2 and Annex 6.3. Maximum, minimum and mean difference refer to the difference between predicted and observed values.

Indicator	Mean Squared Error	P-value	R-squared	Objective function
Bere	0.0222*exp(-2.3136*x)	-0.3934+0.9306*x-0.1491*x^2	0.862+0.3364*log10(x)	365.8153*exp(1.0684*x)
Blackwater	0.0089*exp(-1.5487*x)	-0.2174+0.3167*x+0.0082*x^2	0.796+0.4956*log10(x)	151.5419*exp(0.8739*x)
Cruick	0.0039*exp(-1.3909*x)	-0.2114+0.9363*x-0.1668*x^2	0.9668+0.0718*log10(x)	506.3296*exp(0.9166*x)
HighlandWater	0.0096*exp(-2.1908*x)	-0.4975+1.1048*x-0.1908*x^2	0.8963+0.2342*log10(x)	83.6897*exp(1.0442*x)
Lambourn	0.0045*exp(-1.8274*x)	-0.3672+0.9009*x-0.1429*x^2	0.8862+0.2493*log10(x)	88.369*exp(0.9664*x)
LeighQ82	0.0073*exp(-1.5932*x)	-0.2688+0.391*x-0.0076*x^2	0.9207+0.1752*log10(x)	214.5544*exp(1.1506*x)
LeighQ90	0.0072*exp(-1.5837*x)	-0.2771+0.4167*x-0.014*x^2	0.9212+0.1738*log10(x)	211.4321*exp(1.1481*x)
PangFenced	0.0353*exp(-2.6885*x)	-0.426+0.7103*x-0.0828*x^2	0.732+0.4873*log10(x)	351.1401*exp(0.8724*x)
PangUFQ80	0.0018*exp(-1.8587*x)	-0.3778+0.9894*x-0.1675*x^2	0.9606+0.0987*log10(x)	306.5785*exp(1.076*x)
PangUFQ90	0.0016*exp(-1.8407*x)	-0.3462+0.9823*x-0.1682*x^2	0.9614+0.0966*log10(x)	303.2993*exp(1.0693*x)
Senni	0.012*exp(-2.0318*x)	-0.2166+0.9336*x-0.1656*x^2	0.9427+0.1432*log10(x)	210.7293*exp(1.1844*x)
TameLM	0.0009*exp(-1.9265*x)	0.243+0.6704*x-0.1288*x^2	0.988+0.0314*log10(x)	721.3967*exp(1.1546*x)
TameHM	0.0043*exp(-2.1344*x)	-0.2938+0.8229*x-0.1268*x^2	0.979+0.0524*log10(x)	499.6575*exp(1.0834*x)
Tarf	0.0009*exp(-0.5893*x)	0.012-0.0248*x+0.0089*x^2	0.8774+0.2104*log10(x)	582.7786*exp(1.1735*x)
Windrush	0.0014*exp(-2.3819*x)	0.4794+0.4702*x-0.0919*x^2	0.9911+0.0241*log10(x)	621.7147*exp(1.1872*x)

Indicator	Maximum Difference (m)	Minimum Difference (m)	Mean Difference (m)	Maximum Squared Error
Bere	0.6391*exp(-0.8158*x)	0.3534*exp(-0.6962*x)	0.107*exp(-3.6255*x)	0.4024*exp(-1.5588*x)
Blackwater	0.435*exp(-0.5212*x)	0.289*exp(-0.4621*x)	0.0326*exp(-3.2724*x)	0.1799*exp(-1.004*x)
Cruick	0.4965*exp(-0.3988*x)	0.3764*exp(-0.4075*x)	0.0074*exp(-2.8216*x)	0.2479*exp(-0.7987*x)
HighlandWater	0.3494*exp(-0.8503*x)	0.4338*exp(-0.8502*x)	0.2455*exp(-3.8518*x)	0.2091*exp(-1.6641*x)
Lambourn	0.2939*exp(-0.6612*x)	0.167*exp(-0.5728*x)	0.0588*exp(-3.1641*x)	0.0864*exp(-1.3224*x)
LeighQ82	0.6204*exp(-0.5859*x)	0.5179*exp(-0.6324*x)	0.0419*exp(-2.7832*x)	0.4529*exp(-1.2292*x)
LeighQ90	0.6182*exp(-0.5809*x)	0.5075*exp(-0.6195*x)	0.0635*exp(-2.93*x)	0.4632*exp(-1.2299*x)
PangFenced	0.4896*exp(-0.9492*x)	0.5855*exp(-0.8536*x)	0.0786*exp(-3.5831*x)	0.3435*exp(-1.7037*x)
PangUFQ80	0.1798*exp(-0.6322*x)	0.23*exp(-0.6827*x)	0.0131*exp(-2.9141*x)	0.0558*exp(-1.3647*x)
PangUFQ90	0.1632*exp(-0.5931*x)	0.2245*exp(-0.6738*x)	0.015*exp(-3.1068*x)	0.0513*exp(-1.3335*x)
Senni	0.4258*exp(-0.8267*x)	0.4889*exp(-0.8427*x)	0.0989*exp(-3.2997*x)	0.2475*exp(-1.6318*x)
TameLM	0.2775*exp(-0.6625*x)	0.2347*exp(-0.7375*x)	0.0186*exp(-3.4503*x)	0.0845*exp(-1.35*x)
TameHM	0.5165*exp(-0.848*x)	0.1749*exp(-0.6988*x)	0.1592*exp(-3.7773*x)	0.2667*exp(-1.696*x)
Tarf	0.1658*exp(-0.1476*x)	0.1592*exp(-0.0904*x)	0.025*exp(-3.0844*x)	0.0295*exp(-0.2291*x)
Windrush	0.2823*exp(-0.9561*x)	0.2339*exp(-0.9176*x)	0.0062*exp(-3.1087*x)	0.0796*exp(-1.8819*x)

Appendix 4.2

Tables relating sampling density with indicator values for each river type – Chapter 6

This Appendix presents the results obtained at different sampling densities for the indicators analysed. The Appendix has been structured in two main blocks of information: (i) a first section on the morphological characteristics of the river site analysed and the results obtained and (ii) a graphical representation of the results obtained. The user can, in this way, identify which river site is most similar to the site to be monitored and select the sampling density that is needed for the characterisation of the indicator required.

A set of tables with the catchment and reach descriptors described in Chapter 5 has been included to provide information on the morphological characteristics of the river sites analysed (see Chapter 5 for more information on how to calculate each descriptor).

Note that the original sampling density describing the river characteristics of the river site is 4 points per square metre. To determine the effect of decreasing the sampling density for each indicator it is necessary to compare this value with the one obtained for the highest sampling density considered, which describes the original data set. The values of maximum, mean and minimum differences, as well as the values of maximum, minimum and mean predicted and observed depth are given in metres.

Table Appendix 4.2.1: values obtained for the catchment and reach physical descriptors (Chapter 5). Codes for substrate are: 1-GravelCobble &Pebble, Category 2- Gravel-Cobble & Sand, Category 3-Gravel and Category 4-Gravel, Silt & Sand.

RIVER	Substrate type	Mean Width (m)	Minimum Width (m)	Maximum Width (m)	Mean Width wetted channel (m)	Minimum Width wetted channel (m)	Maximum Width wetted channel (m)	Variation for the depth data set collected (only for the points in the wet channel)	Variation for the depth data set collected (including wet channel and banks)	Number of habitat types encountered	Sampled length (m)	Sinuosity coefficient	Space between consecutive pool-riffles (m)	Mean depth wetted channel (m)	Maximum depth (m)	Minimum depth (m)	Mean Depth (m)
Lambourn	1	7.5	5	7.6	7.5	5	7.6	0.008	0.009	2	46	1.1	31	0.272	0.569	-0.264	0.271
Highland	2	6.5	2	6.5	4	2	3.5	0.016	0.282	2	50	1.15	18	0.196	0.668	-1.594	-0.305
Bere	1	6.9	3.6	5.1	5.8	3.4	4.2	0.030	0.1109	2	80	1.33	60	0.332	0.857	-0.995	0.094
Tame modified	2	14.5	13.5	15.2	12	13	15	0.009	0.1944	1	93	1.01	0	0.359	0.681	-0.851	0.066
Tame less mod	1	9.5	13.1	28.3	9.5	8.2	10	0.038	0.551	2	142	1	50	0.340	1.191	-3.669	-0.198
Senni	1	8.8	6.9	11.5	8.8	6.9	11.5	0.047	0.048	3	40	1.01	25	0.424	1.042	-0.040	0.423
Pang old fenced Q80	3	7.5	5	10	5	3	5.6	0.018	0.166	1	31	1.01	0	0.292	0.575	-1.442	0.038
Pang fenced	3	10.5	9	13.6	5.5	4.5	7	0.016	0.099	2	110	1.06	90	0.193	0.726	-1.051	-0.064
Pang unfenced Q80	3	12.5	9	18.5	6.7	6.3	10.6	0.013	0.097	2	107	1.17	70	0.222	0.544	-0.956	-0.016
Blackwater	1	7.8	2.6	10.7	5.8	2.1	5.6	0.012	0.226	1	155	1.14	0	0.344	0.578	-2.055	0.099
Cruick	1	5.6	4.2	12	5.6	4.2	12	0.032	0.033	3	246	1.01	70	0.309	1.102	-0.283	0.302
Tarf	1	5.5	7	14	5.5	4.3	14	0.008	0.012	2	212	1.97	200	0.158	0.897	-0.450	0.138
Windrush	4	9.7	6	14.3	9.7	6	14	0.069	0.076	3	126	2.48	50	0.398	1.449	-0.766	0.386
Leigh Brook Q82	1	8.1	1	11.5	8.1	1	11.5	0.022	0.022	4	200	1.05	45	0.205	0.850	0	0.205
Leigh Brook Q93	1	8.1	1	11.5	8.1	1	11.5	0.023	0.023	4	200	1.05	45	0.244	0.940	0	0.244
Pang old fenced Q90	3	7.5	5	10	5	3.2	6	0.0168	0.166	1	31	1.01	0	0.286	0.562	-1.455	0.025
Pang unfenced Q90	3	12.5	9	18.5	6.7	6.3	10.6	0.012	0.096	2	107	1.17	70	0.213	0.534	-0.969	-0.030

Table Appendix 4.2.1: values obtained for the catchment and reach physical descriptors (Chapter 5). Codes for substrate are: 1-GravelCobble &Pebble, Category 2- Gravel-Cobble & Sand, Category 3-Gravel and Category 4-Gravel, Silt & Sand (continuation).

RIVER	AREA	ALTBAR	ASPBAR	BFIHOST	DPLBAR	DPSBAR	LDP	SPRHOST	Distance from the origin to the river site Source (m)	Stream order	Height at river source (m)	Height at river site (m)	Discharge during the data collection (m^3s^{-1})	Percentage Flow exceedance during the data collection	Averaged annual mean flow (m^3s^{-1})
Lambourn	185	169	127	0.86	18.3	62.7	31.01	14.4	16	1	140	90	0.67	92	1.58
Highland	13.2	73	163	0.4	4.06	56.1	8.25	38.9	5.75	2	107	30	0.09	43	0.17
Bere	48.22	105	152	0.908	10.98	82.5	22.04	9.7	7.5	1	41	25	0.36	79	0.71
Tame modified	183.2	147	97	0.399	13.97	28.1	24.07	38.2	30	5	150	100	2.52	20	1.90
Tame less mod	187.8	147	88	0.399	14.16	28.5	24.57	38.2	30	5	150	100	1.46	43	1.94
Senni	28.26	367	324	0.554	6.09	177.4	11.22	35.2	4.3	2	518	240	0.44	78	1.33
Pang old fenced Q80	84.77	146	125	0.886	11.07	56.4	22.39	12.2	4	2	95	80	0.32	80	0.64
Pang fenced	84.54	146	125	0.886	10.71	56.5	21.97	12.2	4	2	95	80	0.27	91	0.63
Pang unfenced Q80	84.93	145	125	0.885	11.22	56.4	22.56	12.2	4	2	95	80	0.32	80	0.64
Blackwater	46.15	89	345	0.648	8.51	34.4	14.5	26.6	3	1	85	80	0.46	33	0.39
Cruick	72.02	159	123	0.57	11.47	73	24.42	40.9	18.5	3	450	50	0.61	51	0.17
Tarf	21.52	528	163	0.338	5.3	184.2	9.46	50.9	7	4	650	240	0.34	50	0.63
Windrush	173.7	210	131	0.795	16.42	70.6	29.75	16.6	18.5	2	250	110	#	#	1.81
Leigh Brook Q82	70.41	124	319	0.551	9.68	90.7	18.32	35.4	7.3	3	140	60	0.517	82	0.51
Leigh Brook Q93	70.41	124	319	0.551	9.68	90.7	18.32	35.4	7.3	3	140	60	0.344	93	0.51
Pang old fenced Q90	84.77	146	125	0.886	11.07	56.4	22.39	12.2	4	2	95	80	0.27	90	0.64
Pang unfenced Q90	84.93	145	125	0.885	11.22	56.4	22.56	12.2	4	2	95	80	0.27	90	0.64

THE BERE

The Bere

The geology of the catchment is composed of Jurassic limestone, Upper Greensand, Chalk, sands of the Tertiary deposits, superficial sands or gravels, which provide the likelihood of large groundwater storage, and clay with flints. The dominant substrate is a combination of sands, gravels and clay. The proximity of the Piddle catchment to the Frome and the chalk character of the geology point towards the possibility of groundwater interchange between these two areas. In addition, the chalk aquifer presents extensive karst development that contributes to the water interchange. The existence of faults provides constraints on groundwater and influences the contributions to outflows. Mean annual rainfall in the Bere area is around 800 mm.

Table Appendix 4.2.2: results obtained for each indicator at different sampling densities for the Bere river site. Note that the original sampling density is 4 points per square metre. The abbreviations for each indicator are as follows: MaxTran=maximum depth of the data set to be interpolated, MinTran=minimum depth of the data set to be interpolated, Mean Tran= mean depth of the data set to be interpolated, StdTran=standard deviation of the reach to be interpolated, MaxDiff=maximum difference between predicted and observed values, MinDiff=minimum difference between predicted and observed values, MeanDiff= mean difference between predicted and observed values, MaxSE=Maximum Squared Error, MSE=Mean Squared Error, MaxPred=Maximum value predicted, MinPred=Minimum value predicted, MeanPred= Mean value predicted, Std Pred=Standard deviation of the predicted values, P-value=p-value of the non parametric Kolmogorov-Smirnov test and R-squared = linear regression coefficient between predicted and observed values. Range, Sill, Nugget and Objective refer to the characteristics of the variogram obtained for each sampling density considered.

Points per Square metre	Max Tran	Min Tran	Mean Tran	Std Tran	Max Dif	Min Dif	Mean Dif	Max SE	MSE	Max Pred	Min Pred	Mean Pred	Std Pred	P-value	R-squared	Range	Sill	Nugget	Objective
0.20	0.81	0.02	0.32	0.17	0.29	-0.39	-0.01	0.15	0.02	0.59	0.15	0.33	0.08	0.00	0.47	16.68	0.02	0.01	99.10
0.40	0.85	0.02	0.33	0.16	0.29	-0.27	0.00	0.08	0.01	0.61	0.14	0.34	0.09	0.00	0.69	15.26	0.02	0.01	317.37
0.60	0.85	0.02	0.33	0.17	0.27	-0.19	0.00	0.08	0.01	0.71	0.09	0.34	0.11	0.00	0.84	14.47	0.03	0.01	663.59
0.80	0.85	0.01	0.34	0.17	0.26	-0.19	0.00	0.07	0.00	0.78	0.09	0.34	0.12	0.00	0.87	13.70	0.03	0.01	1102.51
1.00	0.85	0.01	0.34	0.17	0.22	-0.13	0.00	0.05	0.00	0.86	0.01	0.34	0.16	0.47	0.97	8.33	0.03	0.00	1329.75
1.20	0.85	0.01	0.35	0.17	0.24	-0.11	0.00	0.06	0.00	0.82	0.06	0.34	0.14	0.00	0.93	13.06	0.03	0.01	2112.32
1.40	0.85	0.01	0.34	0.17	0.22	-0.11	0.00	0.05	0.00	0.86	0.01	0.34	0.16	0.76	0.98	8.33	0.03	0.00	2444.16
1.60	0.85	0.01	0.34	0.17	0.22	-0.09	0.00	0.05	0.00	0.86	0.01	0.34	0.16	0.92	0.99	8.18	0.03	0.00	3104.31
1.80	0.85	0.01	0.34	0.16	0.22	-0.09	0.00	0.05	0.00	0.86	0.01	0.34	0.16	0.97	0.99	7.93	0.03	0.00	3756.48
2.00	0.85	0.01	0.34	0.16	0.22	-0.09	0.00	0.05	0.00	0.86	0.01	0.34	0.16	0.99	0.99	7.88	0.03	0.00	4581.62
2.20	0.85	0.01	0.34	0.16	0.21	-0.09	0.00	0.05	0.00	0.86	0.01	0.34	0.16	0.99	0.99	7.98	0.03	0.00	5481.25
2.40	0.86	0.01	0.34	0.16	0.14	-0.09	0.00	0.02	0.00	0.86	0.01	0.34	0.16	1.00	1.00	7.94	0.03	0.00	6977.81
2.60	0.86	0.01	0.34	0.17	0.14	-0.08	0.00	0.02	0.00	0.86	0.01	0.34	0.16	1.00	1.00	7.61	0.03	0.00	8118.70
2.80	0.86	0.01	0.34	0.16	0.14	-0.07	0.00	0.02	0.00	0.86	0.01	0.34	0.16	1.00	1.00	7.56	0.03	0.00	9013.18
3.00	0.86	0.01	0.34	0.16	0.07	-0.07	0.00	0.00	0.00	0.86	0.01	0.34	0.16	1.00	1.00	7.32	0.03	0.00	8475.14
3.20	0.86	0.01	0.34	0.16	0.07	-0.07	0.00	0.00	0.00	0.86	0.01	0.34	0.16	1.00	1.00	7.30	0.03	0.00	9827.70
3.40	0.86	0.01	0.34	0.16	0.03	-0.07	0.00	0.00	0.00	0.86	0.01	0.34	0.16	1.00	1.00	7.25	0.03	0.00	11030.16
3.60	0.86	0.01	0.34	0.16	0.03	-0.04	0.00	0.00	0.00	0.86	0.01	0.34	0.16	1.00	1.00	7.37	0.03	0.00	12345.36
3.80	0.86	0.01	0.34	0.16	0.03	-0.04	0.00	0.00	0.00	0.86	0.01	0.34	0.16	1.00	1.00	7.36	0.03	0.00	13634.86
4.00	0.86	0.01	0.34	0.16	0.00	0.00	0.00	0.00	0.00	0.86	0.01	0.34	0.16	1.00	1.00	7.47	0.03	0.00	15491.54

THE BLACKWATER

The Blackwater

The Blackwater river rises in Rowhill Nature Reserve, which is on the Surrey and Hampshire border between Aldershot and Farnham. The Blackwater river is the centre piece of the Blackwater Valley. The main tributaries are Cove Brook and the Whitewater.

The geology of the valley is defined at the southern end by the Hogs Back, a ridge of chalk that forms the southern limit of the London Basin. Tertiary deposits of London Clays, Bagshot formation, Bracklesham Beds and Barton Beds are found in the surrounding valley. The current land uses for the catchment area include gravel and sand extraction and urban expansion.

Table Appendix 4.2.3: results obtained for each indicator at different sampling densities for the Blackwater river site. Note that the original sampling density is 4 points per square metre. The abbreviations for each indicator are as follows: MaxTran=maximum depth of the data set to be interpolated, MinTran=minimum depth of the data set to be interpolated, Mean Tran= mean depth of the data set to be interpolated, StdTran=standard deviation of the reach to be interpolated, MaxDiff=maximum difference between predicted and observed values, MinDiff=minimum difference between predicted and observed values, MeanDiff= mean difference between predicted and observed values, MaxSE=Maximum Squared Error, MSE=Mean Squared Error, MaxPred=Maximum value predicted, MinPred=Minimum value predicted, MeanPred= Mean value predicted, Std Pred=Standard deviation of the predicted values, P-value=p-value of the non parametric Kolmogorov-Smirnov test and R-squared = linear regression coefficient between predicted and observed values. Range, Sill, Nugget and Objective refer to the characteristics of the variogram obtained for each sampling density considered.

Points per Square metre	Max Tran	Min Tran	Mean Tran	Std Tran	Max Dif	Min Dif	Mean Dif	Max SE	MSE	Max Pred	Min Pred	Mean Pred	Std Pred	P-value	R-squared	Range	Sill	Nugget	Objective
0.20	0.55	-0.01	0.32	0.13	0.38	-0.25	0.00	0.15	0.01	0.32	0.32	0.32	0.00	0.00	0.00	14.76	0.00	0.02	238.92
0.40	0.55	-0.01	0.32	0.12	0.34	-0.19	0.00	0.11	0.00	0.54	-0.01	0.33	0.09	0.00	0.75	5.45	0.01	0.00	232.97
0.60	0.56	-0.01	0.33	0.13	0.28	-0.17	0.00	0.08	0.00	0.57	-0.06	0.33	0.11	0.00	0.86	5.29	0.01	0.00	230.60
0.80	0.56	-0.04	0.33	0.12	0.27	-0.20	0.00	0.07	0.00	0.57	-0.08	0.33	0.11	0.00	0.89	5.15	0.01	0.00	222.36
1.00	0.56	-0.04	0.32	0.12	0.27	-0.16	0.00	0.07	0.00	0.58	-0.07	0.32	0.11	0.00	0.92	5.38	0.01	0.00	297.25
1.20	0.56	-0.04	0.33	0.12	0.20	-0.17	0.00	0.04	0.00	0.58	-0.08	0.32	0.12	0.04	0.94	5.17	0.01	0.00	344.91
1.40	0.56	-0.04	0.32	0.12	0.18	-0.15	0.00	0.03	0.00	0.58	-0.08	0.32	0.12	0.10	0.95	5.10	0.01	0.00	527.98
1.60	0.56	-0.04	0.32	0.12	0.16	-0.15	0.00	0.03	0.00	0.57	-0.08	0.32	0.12	0.25	0.96	5.09	0.01	0.00	527.08
1.80	0.56	-0.04	0.32	0.12	0.16	-0.13	0.00	0.02	0.00	0.57	-0.08	0.33	0.12	0.41	0.96	5.10	0.01	0.00	780.50
2.00	0.56	-0.04	0.32	0.12	0.15	-0.12	0.00	0.02	0.00	0.56	-0.08	0.32	0.12	0.28	0.97	5.11	0.01	0.00	984.36
2.20	0.56	-0.04	0.32	0.12	0.14	-0.11	0.00	0.02	0.00	0.56	-0.05	0.32	0.12	0.38	0.98	5.09	0.01	0.00	1269.14
2.40	0.56	-0.04	0.32	0.12	0.14	-0.11	0.00	0.02	0.00	0.56	-0.06	0.32	0.12	0.61	0.98	5.10	0.01	0.00	1525.84
2.60	0.56	-0.04	0.32	0.12	0.14	-0.11	0.00	0.02	0.00	0.56	-0.06	0.32	0.12	0.84	0.98	5.14	0.01	0.00	1783.33
2.80	0.56	-0.04	0.32	0.12	0.14	-0.11	0.00	0.02	0.00	0.56	-0.06	0.32	0.12	0.99	0.99	5.17	0.01	0.00	2034.07
3.00	0.57	-0.05	0.32	0.12	0.16	-0.09	0.00	0.03	0.00	0.57	-0.06	0.33	0.12	0.99	0.99	5.34	0.01	0.00	2209.81
3.20	0.57	-0.05	0.32	0.12	0.16	-0.09	0.00	0.02	0.00	0.57	-0.05	0.32	0.12	1.00	0.99	5.31	0.01	0.00	2570.47
3.40	0.57	-0.05	0.32	0.12	0.11	-0.08	0.00	0.01	0.00	0.57	-0.05	0.32	0.12	1.00	0.99	5.31	0.01	0.00	2819.04
3.60	0.57	-0.06	0.32	0.12	0.10	-0.08	0.00	0.01	0.00	0.57	-0.06	0.32	0.12	1.00	1.00	5.31	0.01	0.00	3201.89
3.80	0.57	-0.06	0.32	0.12	0.06	-0.08	0.00	0.01	0.00	0.57	-0.06	0.32	0.12	1.00	1.00	5.28	0.01	0.00	3739.24
4.00	0.57	-0.06	0.32	0.12	0.01	-0.01	0.00	0.00	0.00	0.57	-0.06	0.32	0.12	1.00	1.00	5.31	0.01	0.00	4215.03

THE CRUICK

The Cruick

The geology of the Cruick catchment is mainly composed of a combination of highly permeable aquifer at the surface (with areas overlain by a clay layer of unknown thickness) and weakly permeable rocks. Thick beds of marine and estuarine clay overlie Devonian sandstone and form an effective barrier between the aquifer and the surface activities. The Lower Devonian sandstone aquifer forms part of an elongate structural feature in which the strata have been extensively folded. Mudstones and igneous rocks can be found between the sandstone layers. The Cruick Water catchment area is considered to be at high risk due to the combination of a high permeable aquifer system and a high level of water abstraction.

Table Appendix 4.2.4: results obtained for each indicator at different sampling densities for the Cruick river site. Note that the original sampling density is 4 points per square metre. The abbreviations for each indicator are as follows: MaxTran=maximum depth of the data set to be interpolated, MinTran=minimum depth of the data set to be interpolated, Mean Tran= mean depth of the data set to be interpolated, StdTran=standard deviation of the reach to be interpolated, MaxDiff=maximum difference between predicted and observed values, MinDiff=minimum difference between predicted and observed values, MeanDiff= mean difference between predicted and observed values, MaxSE=Maximum Squared Error, MSE=Mean Squared Error, MaxPred=Maximum value predicted, MinPred=Minimum value predicted, MeanPred= Mean value predicted, Std Pred=Standard deviation of the predicted values, P-value=p-value of the non parametric Kolmogorov-Smirnov test and R-squared = linear regression coefficient between predicted and observed values. Range, Sill, Nugget and Objective refer to the characteristics of the variogram obtained for each sampling density considered.

Points per Square metre	Max Tran	Min Tran	Mean Tran	Std Tran	Max Dif	Min Dif	Mean Dif	Max SE	MSE	Max Pred	Min Pred	Mean Pred	Std Pred	P-value	R-squared	Range	Sill	Nugget	Objective
0.20	1.00	0.00	0.30	0.18	0.44	-0.26	0.00	0.20	0.00	1.00	0.00	0.32	0.18	0.00	0.89	12.67	0.03	0.00	293.23
0.40	1.00	0.00	0.31	0.19	0.42	-0.21	0.00	0.17	0.00	1.00	0.00	0.32	0.18	0.04	0.94	12.35	0.03	0.00	453.32
0.60	1.00	0.00	0.32	0.19	0.33	-0.20	0.00	0.11	0.00	1.00	0.00	0.32	0.18	0.08	0.96	13.15	0.03	0.00	899.46
0.80	1.00	0.00	0.32	0.19	0.30	-0.18	0.00	0.09	0.00	1.00	0.00	0.32	0.18	0.30	0.97	13.46	0.03	0.00	1433.82
1.00	1.00	0.00	0.32	0.19	0.30	-0.28	0.00	0.09	0.00	1.00	0.00	0.32	0.18	0.77	0.98	13.37	0.03	0.00	1546.40
1.20	1.00	0.00	0.32	0.18	0.29	-0.28	0.00	0.09	0.00	1.00	0.00	0.32	0.18	0.85	0.98	13.19	0.03	0.00	1748.59
1.40	1.02	0.00	0.32	0.19	0.27	-0.28	0.00	0.08	0.00	1.01	0.00	0.32	0.18	0.94	0.99	13.05	0.03	0.00	2096.82
1.60	1.02	0.00	0.32	0.19	0.27	-0.26	0.00	0.07	0.00	1.01	0.00	0.32	0.18	0.98	0.99	12.90	0.03	0.00	2605.41
1.80	1.02	0.00	0.32	0.18	0.27	-0.26	0.00	0.07	0.00	1.01	0.00	0.32	0.18	1.00	0.99	13.02	0.03	0.00	3271.49
2.00	1.02	0.00	0.32	0.19	0.26	-0.22	0.00	0.07	0.00	1.02	0.00	0.32	0.18	1.00	0.99	13.02	0.03	0.00	3986.57
2.20	1.02	0.00	0.32	0.19	0.19	-0.20	0.00	0.04	0.00	1.02	0.00	0.32	0.19	0.99	0.99	12.90	0.03	0.00	4530.27
2.40	1.02	0.00	0.32	0.19	0.20	-0.14	0.00	0.04	0.00	1.02	0.00	0.32	0.19	1.00	1.00	12.90	0.03	0.00	5490.82
2.60	1.02	0.00	0.32	0.19	0.20	-0.14	0.00	0.04	0.00	1.02	0.00	0.32	0.19	1.00	1.00	12.92	0.03	0.00	6096.99
2.80	1.04	0.00	0.32	0.19	0.18	-0.12	0.00	0.03	0.00	1.04	0.00	0.32	0.19	1.00	1.00	12.86	0.03	0.00	7450.78
3.00	1.02	0.00	0.32	0.19	0.19	-0.18	0.00	0.04	0.00	1.02	0.00	0.32	0.19	1.00	1.00	12.84	0.03	0.00	8053.79
3.20	1.06	0.00	0.32	0.19	0.20	-0.18	0.00	0.04	0.00	1.06	0.00	0.32	0.19	1.00	1.00	12.95	0.03	0.00	9040.25
3.40	1.06	0.00	0.32	0.19	0.19	-0.18	0.00	0.04	0.00	1.06	0.00	0.32	0.19	1.00	1.00	12.76	0.03	0.00	10754.18
3.60	1.06	0.00	0.32	0.19	0.19	-0.07	0.00	0.04	0.00	1.06	0.00	0.32	0.19	1.00	1.00	12.88	0.03	0.00	11499.76
3.80	1.06	0.00	0.32	0.19	0.12	-0.07	0.00	0.01	0.00	1.06	0.00	0.32	0.19	1.00	1.00	12.97	0.03	0.00	13025.24
4.00	1.06	0.00	0.32	0.19	0.02	-0.02	0.00	0.00	0.00	1.06	0.00	0.32	0.19	1.00	1.00	12.91	0.03	0.00	14660.04

THE HIGHLAND WATER

The Highland Water

The Highland Water is located in the New Forest in Hampshire and is a meandering gravel-bed river with an active bedload of fine-coarse gravels, and a suspended load of silts and clays. The river is characterised by a large number of organic debris dams and a damp riparian forest floodplain that regulates the equilibrium between sedimentation and erosion, storing bedload upstream and forcing water and suspended sediments downstream (floodplain).

The extension of the New Forest catchment area is 12km^2 approximately and is located to the Northwest of the town of Lyndhurst. The geology is composed of an underlying Eocene Barton group (marine clays and sands) capped by older River Gravels. In the valley floor, the deposits bordering the channels are dominated by sands and gravels laid down as alluvium, that sometimes are overlain by peat.

The Highland Water river site is located at 30 m AOD and 6.5 km from the river origin, with a length of 50 m and width of approximately 6.5 m. The mean width of the wetted cross-section is 4 m. The selected stream presents a smooth curvature with a distance between pool and riffles of ≅18 m. Maximum depth observed is ≅ 66 cm whilst mean depth is 18 cm.

Table Appendix 4.2.5: results obtained for each indicator at different sampling densities for the Highland Water river site. Note that the original sampling density is 4 points per square metre. The abbreviations for each indicator are as follows: MaxTran=maximum depth of the data set to be interpolated, MinTran=minimum depth of the data set to be interpolated, Mean Tran= mean depth of the data set to be interpolated, StdTran=standard deviation of the reach to be interpolated, MaxDiff=maximum difference between predicted and observed values, MinDiff=minimum difference between predicted and observed values, MeanDiff= mean difference between predicted and observed values, MaxSE=Maximum Squared Error, MSE=Mean Squared Error, MaxPred=Maximum value predicted, MinPred=Minimum value predicted, MeanPred= Mean value predicted, Std Pred=Standard deviation of the predicted values, P-value=p-value of the non parametric Kolmogorov-Smirnov test and R-squared = linear regression coefficient between predicted and observed values. Range, Sill, Nugget and Objective refer to the characteristics of the variogram obtained for each sampling density considered.

Points per Square metre	Max Tran	Min Tran	Mean Tran	Std Tran	Max Dif	Min Dif	Mean Dif	Max SE	MSE	Max Pred	Min Pred	Mean Pred	Std Pred	P-value	R-squared	Range	Sill	Nugget	Objective
0.40	0.45	0.01	0.20	0.13	0.21	-0.24	0.01	0.06	0.00	0.45	0.01	0.20	0.09	0.00	0.74	5.23	0.02	0.00	82.46
0.60	0.45	0.01	0.20	0.13	0.21	-0.24	0.01	0.06	0.00	0.45	0.01	0.20	0.09	0.00	0.74	5.23	0.02	0.00	82.46
0.80	0.45	0.01	0.20	0.12	0.22	-0.28	0.00	0.08	0.00	0.45	0.01	0.19	0.09	0.00	0.79	5.21	0.02	0.00	128.28
1.00	0.46	-0.03	0.18	0.11	0.05	-0.09	0.00	0.01	0.00	0.46	-0.03	0.18	0.11	0.97	0.99	4.81	0.01	0.00	684.46
1.20	0.45	-0.01	0.19	0.12	0.22	-0.27	0.00	0.07	0.00	0.45	-0.01	0.18	0.10	0.04	0.87	5.21	0.02	0.00	210.05
1.40	0.46	-0.03	0.18	0.12	0.08	-0.10	0.00	0.01	0.00	0.46	-0.03	0.18	0.11	0.65	0.97	5.21	0.01	0.00	261.91
1.60	0.46	-0.03	0.18	0.12	0.08	-0.10	0.00	0.01	0.00	0.46	-0.03	0.18	0.11	0.93	0.98	4.94	0.01	0.00	404.40
1.80	0.46	-0.03	0.18	0.12	0.07	-0.09	0.00	0.01	0.00	0.46	-0.03	0.18	0.11	0.99	0.98	4.86	0.01	0.00	530.26
2.00	0.49	-0.03	0.18	0.11	0.04	-0.08	0.00	0.01	0.00	0.49	-0.03	0.18	0.11	1.00	1.00	5.04	0.01	0.00	1404.36
2.20	0.46	-0.01	0.19	0.11	0.22	-0.10	0.00	0.05	0.00	0.46	-0.01	0.19	0.10	0.26	0.95	5.05	0.01	0.00	208.82
2.40	0.49	-0.03	0.19	0.11	0.04	-0.09	0.00	0.01	0.00	0.49	-0.03	0.18	0.11	1.00	0.99	4.85	0.01	0.00	1049.05
2.60	0.49	-0.03	0.18	0.11	0.05	-0.08	0.00	0.01	0.00	0.49	-0.03	0.18	0.11	1.00	0.99	4.89	0.01	0.00	1205.84
2.80	0.49	-0.03	0.18	0.11	0.05	-0.08	0.00	0.01	0.00	0.49	-0.03	0.18	0.11	1.00	1.00	4.92	0.01	0.00	1400.96
3.00	0.49	-0.02	0.18	0.11	0.01	-0.02	0.00	0.00	0.00	0.49	-0.03	0.18	0.11	1.00	1.00	5.13	0.01	0.00	3745.95
3.20	0.46	-0.03	0.18	0.11	0.05	-0.09	0.00	0.01	0.00	0.46	-0.03	0.18	0.11	0.99	0.99	4.83	0.01	0.00	909.29
3.40	0.49	-0.02	0.18	0.11	0.06	-0.05	0.00	0.00	0.00	0.49	-0.03	0.18	0.11	1.00	1.00	5.23	0.01	0.00	2750.39
3.60	0.49	-0.02	0.18	0.11	0.04	-0.04	0.00	0.00	0.00	0.49	-0.03	0.18	0.11	1.00	1.00	5.11	0.01	0.00	2986.64
3.80	0.49	-0.02	0.18	0.11	0.04	-0.04	0.00	0.00	0.00	0.49	-0.03	0.18	0.11	1.00	1.00	5.09	0.01	0.00	3234.42
4.00	0.49	-0.03	0.18	0.11	0.00	0.00	0.00	0.00	0.00	0.49	-0.03	0.18	0.11	1.00	1.00	5.13	0.01	0.00	3550.67

THE LAMBOURN

The Lambourn

The river Lambourn is located in the Thames Region and rises near the village of Lambourn, in the chalk of the Berkshire Downs at an altitude of about 152m.

The catchment is mainly rural characterised by farming activities, with deciduous woods along the catchment boundary. The river Lambourn is considered to have one of the least modified catchments in southern England, with one of the lowest rates of abstraction. Most of the river has been designated a Site of Special Scientific Interest (SSSI) and Special Area of Conservation (SAC).

Table Appendix 4.2.6: results obtained for each indicator at different sampling densities for the Lambourn river site. Note that the original sampling density is 4 points per square metre. The abbreviations for each indicator are as follows: MaxTran=maximum depth of the data set to be interpolated, MinTran=minimum depth of the data set to be interpolated, Mean Tran= mean depth of the data set to be interpolated, StdTran=standard deviation of the reach to be interpolated, MaxDiff=maximum difference between predicted and observed values, MinDiff=minimum difference between predicted and observed values, MeanDiff= mean difference between predicted and observed values, MaxSE=Maximum Squared Error, MSE=Mean Squared Error, MaxPred=Maximum value predicted, MinPred=Minimum value predicted, MeanPred= Mean value predicted, Std Pred=Standard deviation of the predicted values, P-value=p-value of the non parametric Kolmogorov-Smirnov test and R-squared = linear regression coefficient between predicted and observed values. Range, Sill, Nugget and Objective refer to the characteristics of the variogram obtained for each sampling density considered.

Points per Square metre	Max Tran	Min Tran	Mean Tran	Std Tran	Max Dif	Min Dif	Mean Dif	Max SE	MSE	Max Pred	Min Pred	Mean Pred	Std Pred	P-value	R-squared	Range	Sill	Nugget	Objective
0.20	0.43	0.02	0.29	0.08	0.00	0.00	0.00	0.00	0.00	0.43	0.02	0.29	0.08	1.00	1.00	7.38	0.01	0.00	3259.27
0.40	0.40	0.09	0.29	0.07	0.21	-0.12	0.01	0.04	0.00	0.40	0.09	0.30	0.06	0.00	0.62	8.50	0.01	0.00	38.05
0.60	0.42	0.03	0.29	0.08	0.23	-0.10	0.00	0.05	0.00	0.42	0.02	0.29	0.07	0.00	0.78	7.12	0.01	0.00	278.07
0.80	0.42	0.03	0.28	0.08	0.18	-0.09	0.00	0.03	0.00	0.42	0.02	0.29	0.07	0.01	0.86	7.13	0.01	0.00	225.82
1.00	0.43	0.03	0.29	0.08	0.09	-0.06	0.00	0.01	0.00	0.43	0.03	0.29	0.08	0.94	0.97	6.65	0.01	0.00	481.40
1.20	0.42	0.03	0.29	0.08	0.13	-0.08	0.00	0.02	0.00	0.42	0.02	0.29	0.07	0.13	0.91	6.50	0.01	0.00	166.58
1.40	0.43	0.03	0.29	0.07	0.12	-0.08	0.00	0.01	0.00	0.43	0.02	0.29	0.07	0.48	0.94	6.66	0.01	0.00	242.91
1.60	0.43	0.03	0.29	0.08	0.12	-0.07	0.00	0.01	0.00	0.43	0.03	0.29	0.08	0.72	0.95	6.38	0.01	0.00	397.27
1.80	0.43	0.03	0.29	0.08	0.10	-0.07	0.00	0.01	0.00	0.43	0.03	0.29	0.08	0.69	0.96	6.64	0.01	0.00	553.77
2.00	0.43	0.02	0.29	0.08	0.07	-0.07	0.00	0.01	0.00	0.43	0.02	0.29	0.08	1.00	0.99	7.24	0.01	0.00	1223.56
2.20	0.43	0.03	0.29	0.07	0.12	-0.08	0.00	0.01	0.00	0.43	0.02	0.29	0.07	0.14	0.92	6.46	0.01	0.00	194.27
2.40	0.43	0.02	0.29	0.08	0.08	-0.06	0.00	0.01	0.00	0.43	0.02	0.29	0.08	0.99	0.98	6.89	0.01	0.00	743.01
2.60	0.43	0.02	0.29	0.08	0.07	-0.06	0.00	0.00	0.00	0.43	0.02	0.29	0.08	1.00	0.99	7.17	0.01	0.00	895.26
2.80	0.43	0.02	0.29	0.08	0.07	-0.07	0.00	0.00	0.00	0.43	0.02	0.29	0.08	1.00	0.99	7.13	0.01	0.00	1151.27
3.00	0.43	0.02	0.29	0.08	0.05	-0.03	0.00	0.00	0.00	0.43	0.02	0.29	0.08	1.00	1.00	7.44	0.01	0.00	3076.79
3.20	0.43	0.02	0.29	0.08	0.08	-0.06	0.00	0.01	0.00	0.43	0.02	0.29	0.08	0.99	0.98	6.89	0.01	0.00	665.08
3.40	0.43	0.02	0.29	0.08	0.06	-0.03	0.00	0.00	0.00	0.43	0.02	0.29	0.08	1.00	0.99	7.36	0.01	0.00	2040.30
3.60	0.43	0.02	0.29	0.08	0.06	-0.03	0.00	0.00	0.00	0.43	0.02	0.29	0.08	1.00	1.00	7.55	0.01	0.00	2587.10
3.80	0.43	0.02	0.29	0.08	0.05	-0.04	0.00	0.00	0.00	0.43	0.02	0.29	0.08	1.00	1.00	7.52	0.01	0.00	2854.93
4.00	0.49	-0.02	0.18	0.11	0.06	-0.05	0.00	0.00	0.00	0.49	-0.03	0.18	0.11	1.00	1.00	5.26	0.01	0.00	2152.67

THE LEIGH BROOK








The Leigh Brook

The Leigh Brook is a tributary of the river Teme and rises on the Malvern Hills in Worcestershire. Data were collected in a 198 m reach within the Knapp and Papermill Nature reserve. The reach is 10 m to 15 m wide and 2 m to 3 m deep at bankfull discharge. The catchment area upstream of the reach is approximately 80 km^2 (Maddock and Lander 2002). The Leigh Brook is characterised by a sandstone-dominated geology. River banks have been eroded over time due to the type of geology present at the river.

Table Appendix 4.2.7: results obtained for each indicator at different sampling densities for the Leigh Brook river site. Note that the original sampling density is 4 points per square metre. The abbreviations for each indicator are as follows: MaxTran=maximum depth of the data set to be interpolated, MinTran=minimum depth of the data set to be interpolated, Mean Tran= mean depth of the data set to be interpolated, StdTran=standard deviation of the reach to be interpolated, MaxDiff=maximum difference between predicted and observed values, MinDiff=minimum difference between predicted and observed values, MeanDiff= mean difference between predicted and observed values, MaxSE=Maximum Squared Error, MSE=Mean Squared Error, MaxPred=Maximum value predicted, MinPred=Minimum value predicted, MeanPred= Mean value predicted, Std Pred=Standard deviation of the predicted values, P-value=p-value of the non parametric Kolmogorov-Smirnov test and R-squared = linear regression coefficient between predicted and observed values. Range, Sill, Nugget and Objective refer to the characteristics of the variogram obtained for each sampling density considered.

Points per Square metre	Max Tran	Min Tran	Mean Tran	Std Tran	Max Dif	Min Dif	Mean Dif	Max SE	MSE	Max Pred	Min Pred	Mean Pred	Std Pred	P-value	R-squared	Range	Sill	Nugget	Objective
0.20	0.89	-0.09	0.23	0.15	0.01	-0.01	0.00	0.00	0.00	0.88	-0.09	0.23	0.15	1.00	1.00	9.25	0.02	0.00	13121.02
0.40	0.84	-0.03	0.23	0.15	0.36	-0.46	0.00	0.21	0.01	0.84	-0.04	0.23	0.12	0.00	0.73	8.22	0.02	0.00	166.20
0.60	0.87	-0.03	0.23	0.15	0.40	-0.48	0.00	0.23	0.00	0.85	-0.03	0.23	0.13	0.00	0.85	9.11	0.02	0.00	145.24
0.80	0.87	-0.04	0.23	0.15	0.42	-0.27	0.00	0.18	0.00	0.86	-0.05	0.23	0.14	0.00	0.91	9.57	0.02	0.00	512.90
1.00	0.89	-0.09	0.23	0.15	0.20	-0.19	0.00	0.04	0.00	0.88	-0.09	0.23	0.15	0.25	0.98	9.31	0.02	0.00	2112.47
1.20	0.87	-0.09	0.23	0.15	0.41	-0.25	0.00	0.17	0.00	0.87	-0.09	0.23	0.14	0.00	0.93	9.07	0.02	0.00	670.24
1.40	0.89	-0.09	0.23	0.15	0.40	-0.19	0.00	0.16	0.00	0.88	-0.09	0.23	0.14	0.02	0.96	9.52	0.02	0.00	1007.86
1.60	0.89	-0.09	0.23	0.15	0.21	-0.20	0.00	0.05	0.00	0.88	-0.09	0.23	0.14	0.05	0.97	9.26	0.02	0.00	1179.75
1.80	0.89	-0.09	0.23	0.15	0.22	-0.18	0.00	0.05	0.00	0.88	-0.09	0.23	0.15	0.14	0.98	9.33	0.02	0.00	1572.97
2.00	0.89	-0.09	0.23	0.15	0.18	-0.10	0.00	0.03	0.00	0.88	-0.09	0.23	0.15	0.90	0.99	9.48	0.02	0.00	6143.13
2.20	0.87	-0.09	0.23	0.15	0.41	-0.25	0.00	0.17	0.00	0.86	-0.08	0.23	0.14	0.00	0.94	9.14	0.02	0.00	768.09
2.40	0.89	-0.09	0.23	0.15	0.19	-0.13	0.00	0.04	0.00	0.88	-0.09	0.23	0.15	0.65	0.99	9.31	0.02	0.00	3128.68
2.60	0.89	-0.09	0.23	0.15	0.19	-0.11	0.00	0.04	0.00	0.88	-0.09	0.23	0.15	0.82	0.99	9.52	0.02	0.00	4543.33
2.80	0.89	-0.09	0.23	0.15	0.18	-0.10	0.00	0.03	0.00	0.88	-0.09	0.23	0.15	0.91	0.99	9.53	0.02	0.00	5311.45
3.00	0.89	-0.09	0.23	0.15	0.10	-0.06	0.00	0.01	0.00	0.88	-0.09	0.23	0.15	1.00	1.00	9.24	0.02	0.00	11610.73
3.20	0.89	-0.09	0.23	0.15	0.20	-0.19	0.00	0.04	0.00	0.88	-0.09	0.23	0.15	0.42	0.98	9.27	0.02	0.00	2763.72
3.40	0.89	-0.09	0.23	0.15	0.12	-0.10	0.00	0.01	0.00	0.88	-0.09	0.23	0.15	1.00	1.00	9.29	0.02	0.00	8742.89
3.60	0.89	-0.09	0.23	0.15	0.12	-0.10	0.00	0.01	0.00	0.88	-0.09	0.23	0.15	1.00	1.00	9.29	0.02	0.00	8742.89
3.80	0.89	-0.09	0.23	0.15	0.12	-0.11	0.00	0.01	0.00	0.88	-0.09	0.23	0.15	1.00	1.00	9.31	0.02	0.00	10671.42
4.00	0.43	0.02	0.29	0.08	0.06	-0.04	0.00	0.00	0.00	0.43	0.02	0.29	0.08	1.00	0.99	7.35	0.01	0.00	1907.39

THE PANG FENCED

The Pang Fenced

The Pang is a small tributary of the Thames and rises south of Compton. The catchment is located in central southern England and is characterised by a gentle slope and a maximum height of 186m (Lowbury Hill).

The Pang has its origins in the Chalk aquifer of the West Berkshire Downs and thus, the river presents the characteristics of a chalk groundwater dominated river system, with slow, damped responses to rainfall and 'bourne' behaviour of headwater reaches when the water table is low. Water pumping for water supply has been one of the main activities in the catchment. The annual rainfall for the Pang area is close to 700 mm.

Table Appendix 4.2.8: results obtained for each indicator at different sampling densities for the Pang Fenced river site. Note that the original sampling density is 4 points per square metre. The abbreviations for each indicator are as follows: MaxTran=maximum depth of the data set to be interpolated, MinTran=minimum depth of the data set to be interpolated, Mean Tran= mean depth of the data set to be interpolated, StdTran=standard deviation of the reach to be interpolated, MaxDiff=maximum difference between predicted and observed values, MinDiff=minimum difference between predicted and observed values, MeanDiff= mean difference between predicted and observed values, MaxSE=Maximum Squared Error, MSE=Mean Squared Error, MaxPred=Maximum value predicted, MinPred=Minimum value predicted, MeanPred= Mean value predicted, Std Pred=Standard deviation of the predicted values, P-value=p-value of the non parametric Kolmogorov-Smirnov test and R-squared = linear regression coefficient between predicted and observed values. Range, Sill, Nugget and Objective refer to the characteristics of the variogram obtained for each sampling density considered.

Points per Square metre	Max Tran	Min Tran	Mean Tran	Std Tran	Max Dif	Min Dif	Mean Dif	Max SE	MSE	Max Pred	Min Pred	Mean Pred	Std Pred	P-value	R-squared	Range	Sill	Nugget	Objective
0.20	0.87	-0.03	0.23	0.15	0.13	-0.11	0.00	0.02	0.00	0.86	-0.04	0.23	0.15	1.00	1.00	9.38	0.02	0.00	7118.21
0.40	0.74	-0.01	0.18	0.12	0.00	0.00	0.00	0.00	0.00	0.74	-0.01	0.18	0.12	1.00	1.00	4.68	0.01	0.00	8101.35
0.60	0.66	0.01	0.19	0.12	0.24	-0.42	0.01	0.18	0.01	0.33	0.08	0.19	0.05	0.00	0.27	12.09	0.00	0.01	135.79
0.80	0.66	0.01	0.19	0.12	0.19	-0.19	0.01	0.04	0.00	0.66	0.01	0.19	0.10	0.00	0.88	4.56	0.01	0.00	285.73
1.00	0.74	0.00	0.19	0.12	0.27	-0.34	0.00	0.11	0.01	0.41	0.06	0.18	0.05	0.00	0.66	12.79	0.00	0.01	3170.32
1.20	0.67	0.00	0.18	0.12	0.16	-0.18	0.00	0.03	0.00	0.67	0.00	0.18	0.10	0.00	0.94	4.12	0.01	0.00	327.22
1.40	0.74	0.00	0.19	0.12	0.26	-0.37	0.00	0.14	0.01	0.38	0.07	0.19	0.05	0.00	0.47	13.39	0.00	0.01	851.52
1.60	0.74	0.00	0.18	0.12	0.27	-0.38	0.00	0.14	0.01	0.38	0.08	0.18	0.05	0.00	0.51	13.70	0.00	0.01	1908.15
1.80	0.74	0.00	0.18	0.12	0.27	-0.36	0.00	0.13	0.01	0.39	0.07	0.18	0.05	0.00	0.59	13.29	0.00	0.01	2448.07
2.00	0.74	0.00	0.18	0.12	0.05	-0.04	0.00	0.00	0.00	0.74	-0.02	0.18	0.12	1.00	1.00	4.72	0.01	0.00	3532.74
2.20	0.74	0.00	0.19	0.12	0.06	-0.09	0.00	0.01	0.00	0.74	0.00	0.18	0.11	0.85	1.00	4.55	0.01	0.00	1852.72
2.40	0.74	0.00	0.18	0.12	0.26	-0.39	0.00	0.15	0.01	0.37	0.08	0.18	0.05	0.00	0.49	13.55	0.00	0.01	1391.37
2.60	0.74	0.00	0.19	0.12	0.05	-0.06	0.00	0.00	0.00	0.74	0.00	0.18	0.12	1.00	1.00	4.67	0.01	0.00	2616.67
2.80	0.74	0.00	0.18	0.12	0.05	-0.06	0.00	0.00	0.00	0.74	-0.02	0.18	0.12	1.00	1.00	4.69	0.01	0.00	3175.86
3.00	0.74	-0.01	0.18	0.12	0.03	-0.05	0.00	0.00	0.00	0.74	-0.01	0.18	0.12	1.00	1.00	4.63	0.01	0.00	6581.02
3.20	0.74	0.00	0.18	0.12	0.03	-0.04	0.00	0.00	0.00	0.74	-0.02	0.18	0.12	1.00	1.00	4.64	0.01	0.00	4179.28
3.40	0.74	0.00	0.19	0.12	0.06	-0.08	0.00	0.01	0.00	0.74	0.00	0.18	0.11	0.97	1.00	4.69	0.01	0.00	2242.57
3.60	0.74	-0.01	0.18	0.12	0.03	-0.07	0.00	0.00	0.00	0.74	-0.01	0.18	0.12	1.00	1.00	4.67	0.01	0.00	5518.81
3.80	0.74	-0.01	0.18	0.12	0.03	-0.05	0.00	0.00	0.00	0.74	-0.01	0.18	0.12	1.00	1.00	4.65	0.01	0.00	5982.58
4.00	0.89	-0.03	0.23	0.15	0.10	-0.07	0.00	0.01	0.00	0.89	-0.03	0.23	0.15	1.00	1.00	9.26	0.02	0.00	12198.01

THE PANG UNFENCED

The Pang Unfenced

The Pang is a small tributary of the Thames and rises south of Compton. The catchment is located in central southern England and is characterised by a gentle slope and a maximum height of 186m (Lowbury Hill).

The Pang has its origins in the Chalk aquifer of the West Berkshire Downs and thus, the river presents the characteristics of a chalk groundwater dominated river system, with slow, damped responses to rainfall and 'bourne' behaviour of headwater reaches when the water table is low. Water pumping for water supply has been one of the main activities in the catchment. The annual rainfall for the Pang area is close to 700 mm.

Table Appendix 4.2.9: results obtained for each indicator at different sampling densities for the Pang Unfenced river site. Note that the original sampling density is 4 points per square metre. The abbreviations for each indicator are as follows: MaxTran=maximum depth of the data set to be interpolated, MinTran=minimum depth of the data set to be interpolated, Mean Tran= mean depth of the data set to be interpolated, StdTran=standard deviation of the reach to be interpolated, MaxDiff=maximum difference between predicted and observed values, MinDiff=minimum difference between predicted and observed values, MeanDiff= mean difference between predicted and observed values, MaxSE=Maximum Squared Error, MSE=Mean Squared Error, MaxPred=Maximum value predicted, MinPred=Minimum value predicted, MeanPred= Mean value predicted, Std Pred=Standard deviation of the predicted values, P-value=p-value of the non parametric Kolmogorov-Smirnov test and R-squared = linear regression coefficient between predicted and observed values. Range, Sill, Nugget and Objective refer to the characteristics of the variogram obtained for each sampling density considered.

Points per Square metre	Max Tran	Min Tran	Mean Tran	Std Tran	Max Dif	Min Dif	Mean Dif	Max SE	MSE	Max Pred	Min Pred	Mean Pred	Std Pred	P-value	R-squared	Range	Sill	Nugget	Objective
0.20	0.74	-0.01	0.18	0.12	0.03	-0.07	0.00	0.00	0.00	0.74	-0.01	0.18	0.12	1.00	1.00	4.66	0.01	0.00	4623.22
0.40	0.56	-0.01	0.26	0.13	0.00	0.00	0.00	0.00	0.00	0.56	-0.01	0.26	0.13	1.00	1.00	4.88	0.02	0.00	2154.82
0.60	0.54	-0.03	0.21	0.11	0.00	0.00	0.00	0.00	0.00	0.54	-0.03	0.21	0.11	1.00	1.00	6.50	0.01	0.00	13901.67
0.80	0.54	-0.03	0.21	0.11	0.00	0.00	0.00	0.00	0.00	0.54	-0.03	0.21	0.11	1.00	1.00	6.50	0.01	0.00	13901.67
1.00	0.54	-0.03	0.20	0.11	0.09	-0.17	0.00	0.03	0.00	0.54	-0.03	0.21	0.10	0.00	0.97	6.64	0.01	0.00	491.64
1.20	0.47	-0.03	0.20	0.12	0.20	-0.18	0.00	0.04	0.00	0.47	-0.03	0.21	0.08	0.00	0.82	5.80	0.01	0.00	118.10
1.40	0.47	-0.03	0.20	0.12	0.20	-0.18	0.00	0.04	0.00	0.47	-0.03	0.21	0.08	0.00	0.82	5.80	0.01	0.00	118.10
1.60	0.54	-0.03	0.20	0.11	0.15	-0.17	0.00	0.03	0.00	0.54	-0.04	0.21	0.10	0.00	0.94	6.12	0.01	0.00	305.04
1.80	0.54	-0.03	0.20	0.11	0.15	-0.17	0.00	0.03	0.00	0.54	-0.04	0.21	0.10	0.00	0.94	6.12	0.01	0.00	305.04
2.00	0.54	-0.03	0.20	0.11	0.05	-0.09	0.00	0.01	0.00	0.54	-0.03	0.21	0.11	0.91	0.99	6.05	0.01	0.00	1869.16
2.20	0.54	-0.03	0.20	0.11	0.09	-0.17	0.00	0.03	0.00	0.54	-0.03	0.21	0.10	0.00	0.97	6.64	0.01	0.00	491.64
2.40	0.54	-0.03	0.21	0.11	0.09	-0.16	0.00	0.03	0.00	0.54	-0.03	0.21	0.11	0.02	0.98	6.56	0.01	0.00	840.09
2.60	0.54	-0.03	0.21	0.11	0.09	-0.16	0.00	0.03	0.00	0.54	-0.03	0.21	0.11	0.02	0.98	6.56	0.01	0.00	840.09
2.80	0.54	-0.03	0.20	0.11	0.06	-0.09	0.00	0.01	0.00	0.54	-0.03	0.21	0.11	0.57	0.99	6.10	0.01	0.00	1492.02
3.00	0.54	-0.03	0.20	0.11	0.05	-0.04	0.00	0.00	0.00	0.54	-0.03	0.21	0.11	1.00	1.00	6.44	0.01	0.00	5382.35
3.20	0.54	-0.03	0.20	0.11	0.05	-0.05	0.00	0.00	0.00	0.54	-0.03	0.21	0.11	0.99	1.00	6.17	0.01	0.00	2508.32
3.40	0.54	-0.03	0.20	0.12	0.05	-0.05	0.00	0.00	0.00	0.54	-0.03	0.21	0.11	1.00	1.00	6.26	0.01	0.00	3086.10
3.60	0.54	-0.03	0.20	0.11	0.10	-0.09	0.00	0.01	0.00	0.54	-0.03	0.21	0.11	0.29	0.99	6.26	0.01	0.00	1158.40
3.80	0.54	-0.03	0.20	0.12	0.05	-0.05	0.00	0.00	0.00	0.54	-0.03	0.21	0.11	1.00	1.00	6.39	0.01	0.00	4599.26
4.00	0.74	-0.01	0.18	0.12	0.03	-0.05	0.00	0.00	0.00	0.74	-0.01	0.18	0.12	1.00	1.00	4.67	0.01	0.00	7189.44

THE SENNI

The Senni

The Senni is a small tributary of the river Usk which is located in Wales and has been declared a Special Area of Conservation.The Senni catchment is fully contained in the Brecon Beacons National Park. The geology of the Senni catchment is composed of Old Red Sandstone. The uses of the land are mainly restricted to livestock farming, with approximately 5% of the surface occupied by forest. The dominant soils in the area are peat and the bed channel is composed of a combination of gravel-pebble-cobble with marginal areas composed of sand and silt.

Table Appendix 4.2.10: results obtained for each indicator at different sampling densities for the Senni river site. Note that the original sampling density is 4 points per square metre. The abbreviations for each indicator are as follows: MaxTran=maximum depth of the data set to be interpolated, MinTran=minimum depth of the data set to be interpolated, Mean Tran= mean depth of the data set to be interpolated, StdTran=standard deviation of the reach to be interpolated, MaxDiff=maximum difference between predicted and observed values, MinDiff=minimum difference between predicted and observed values, MeanDiff= mean difference between predicted and observed values, MaxSE=Maximum Squared Error, MSE=Mean Squared Error, MaxPred=Maximum value predicted, MinPred=Minimum value predicted, MeanPred= Mean value predicted, Std Pred=Standard deviation of the predicted values, P-value=p-value of the non parametric Kolmogorov-Smirnov test and R-squared = linear regression coefficient between predicted and observed values. Range, Sill, Nugget and Objective refer to the characteristics of the variogram obtained for each sampling density considered.

Points per Square metre	Max Tran	Min Tran	Mean Tran	Std Tran	Max Dif	Min Dif	Mean Dif	Max SE	MSE	Max Pred	Min Pred	Mean Pred	Std Pred	P-value	R-squared	Range	Sill	Nugget	Objective
0.20	0.53	-0.03	0.19	0.11	0.04	-0.04	0.00	0.00	0.00	0.53	-0.04	0.19	0.11	1.00	1.00	6.37	0.01	0.00	6927.53
0.40	0.53	-0.03	0.19	0.11	0.05	-0.05	0.00	0.00	0.00	0.53	-0.03	0.19	0.11	1.00	1.00	6.17	0.01	0.00	3839.05
0.60	0.53	-0.03	0.19	0.11	0.04	-0.04	0.00	0.00	0.00	0.53	-0.03	0.19	0.11	1.00	1.00	6.29	0.01	0.00	8689.46
0.80	0.53	-0.03	0.19	0.11	0.03	-0.04	0.00	0.00	0.00	0.53	-0.03	0.19	0.11	1.00	1.00	6.26	0.01	0.00	9643.14
1.00	0.90	0.05	0.43	0.21	0.45	-0.39	0.01	0.20	0.01	0.86	0.07	0.43	0.16	0.00	0.72	12.11	0.04	0.00	74.23
1.20	0.53	-0.03	0.19	0.11	0.02	-0.03	0.00	0.00	0.00	0.53	-0.03	0.19	0.11	1.00	1.00	6.33	0.01	0.00	11103.66
1.40	0.53	-0.03	0.19	0.11	0.02	-0.03	0.00	0.00	0.00	0.53	-0.03	0.19	0.11	1.00	1.00	6.29	0.01	0.00	12109.81
1.60	0.53	-0.03	0.19	0.11	0.05	-0.06	0.00	0.00	0.00	0.53	-0.03	0.19	0.11	1.00	1.00	6.39	0.01	0.00	7909.99
1.80	0.98	0.03	0.42	0.21	0.00	0.00	0.00	0.00	0.00	0.98	0.03	0.42	0.21	1.00	1.00	8.44	0.05	0.00	14079.47
2.00	0.98	0.03	0.43	0.22	0.12	-0.18	0.00	0.03	0.00	0.98	0.03	0.42	0.21	0.95	0.99	7.50	0.05	0.00	1370.55
2.20	0.91	0.05	0.44	0.21	0.22	-0.25	0.00	0.06	0.00	0.91	-0.01	0.43	0.19	0.00	0.93	8.44	0.05	0.00	300.71
2.40	0.91	0.04	0.43	0.21	0.25	-0.20	0.00	0.06	0.00	0.91	0.04	0.43	0.20	0.06	0.95	8.38	0.05	0.00	450.53
2.60	0.98	0.03	0.43	0.22	0.23	-0.19	0.00	0.05	0.00	0.98	0.03	0.42	0.21	0.45	0.97	8.03	0.05	0.00	589.07
2.80	0.98	0.03	0.43	0.22	0.12	-0.18	0.00	0.03	0.00	0.98	0.03	0.42	0.21	0.81	0.99	7.71	0.05	0.00	1000.81
3.00	0.98	0.03	0.42	0.22	0.07	-0.08	0.00	0.01	0.00	0.98	0.03	0.42	0.21	1.00	1.00	7.85	0.05	0.00	4205.85
3.20	0.98	0.03	0.43	0.22	0.12	-0.12	0.00	0.02	0.00	0.98	0.03	0.42	0.21	0.95	0.99	7.77	0.05	0.00	1629.51
3.40	0.98	0.03	0.43	0.22	0.09	-0.12	0.00	0.01	0.00	0.98	0.03	0.42	0.21	0.99	0.99	8.12	0.05	0.00	2320.24
3.60	0.98	0.03	0.43	0.22	0.18	-0.19	0.00	0.03	0.00	0.98	0.03	0.42	0.21	0.66	0.98	8.25	0.05	0.00	1072.35
3.80	0.98	0.03	0.42	0.22	0.06	-0.08	0.00	0.01	0.00	0.98	0.03	0.42	0.21	1.00	1.00	7.90	0.05	0.00	3499.47
4.00	0.53	-0.03	0.19	0.11	0.04	-0.04	0.00	0.00	0.00	0.53	-0.04	0.19	0.11	1.00	1.00	6.27	0.01	0.00	5879.55

THE TAME: HIGH MODIFIED

The Tame: High Modified

The river Tame catchment covers an area of 1490 km^2 at its confluence with the Trent river. The geology of the Tame catchments is composed of Lower, Middle and Upper Carboniferous Coal Measures in the upper area of the catchment. Triassic Mercia Mudstones and Triassic Sherwood Sandstones are also present in lower down the Tame catchment. The substrate for the majority of the river Tame is composed of a gravel-pebble combination, with limited presence of vegetation in the banks and channel. The straightening of several parts of the river, pollution of running waters, flow alteration and the separation of the floodplain from the river are consequences of the activities in the Tame catchment over time.

The mean annual rainfall in the Tame catchment is 740 mm of which approximately 450 mm constitutes runoff. The catchment is characterised by a flashy response to rainfall events due to the geology, the amount of water imported from outside the catchment (Wales) and the presence of several navigable waterways.

Table Appendix 4.2.11: results obtained for each indicator at different sampling densities for the Tame High Modified river site. Note that the original sampling density is 4 points per square metre. The abbreviations for each indicator are as follows: MaxTran=maximum depth of the data set to be interpolated, MinTran=minimum depth of the data set to be interpolated, Mean Tran= mean depth of the data set to be interpolated, StdTran=standard deviation of the reach to be interpolated, MaxDiff=maximum difference between predicted and observed values, MinDiff=minimum difference between predicted and observed values, MeanDiff= mean difference between predicted and observed values, MaxSE=Maximum Squared Error, MSE=Mean Squared Error, MaxPred=Maximum value predicted, MinPred=Minimum value predicted, MeanPred= Mean value predicted, Std Pred=Standard deviation of the predicted values, P-value=p-value of the non parametric Kolmogorov-Smirnov test and R-squared = linear regression coefficient between predicted and observed values. Range, Sill, Nugget and Objective refer to the characteristics of the variogram obtained for each sampling density considered.

Points per Square metre	Max Tran	Min Tran	Mean Tran	Std Tran	Max Dif	Min Dif	Mean Dif	Max SE	MSE	Max Pred	Min Pred	Mean Pred	Std Pred	P-value	R-squared	Range	Sill	Nugget	Objective
0.20	1.16	-0.01	0.31	0.17	0.04	-0.03	0.00	0.00	0.00	1.16	-0.01	0.31	0.16	1.00	1.00	10.86	0.03	0.00	18518.86
0.40	1.16	-0.01	0.31	0.17	0.04	-0.03	0.00	0.00	0.00	1.16	-0.01	0.31	0.16	1.00	1.00	10.87	0.03	0.00	21551.24
0.60	1.16	-0.01	0.31	0.16	0.08	-0.06	0.00	0.01	0.00	1.16	-0.01	0.31	0.16	1.00	1.00	10.80	0.03	0.00	10560.38
0.80	1.16	-0.01	0.31	0.16	0.07	-0.04	0.00	0.01	0.00	1.16	-0.01	0.31	0.17	1.00	1.00	10.85	0.03	0.00	26874.12
1.00	0.58	-0.34	0.26	0.21	0.49	-0.15	0.01	0.24	0.00	0.58	-0.34	0.27	0.18	0.00	0.90	10.86	0.04	0.00	207.10
1.20	1.16	-0.01	0.31	0.17	0.07	-0.04	0.00	0.01	0.00	1.16	-0.01	0.31	0.17	1.00	1.00	10.87	0.03	0.00	30834.08
1.40	1.16	-0.01	0.31	0.17	0.07	-0.03	0.00	0.01	0.00	1.16	-0.01	0.31	0.17	1.00	1.00	10.90	0.03	0.00	34916.60
1.60	1.16	-0.01	0.31	0.17	0.04	-0.01	0.00	0.00	0.00	1.16	-0.01	0.31	0.17	1.00	1.00	10.84	0.03	0.00	39141.35
1.80	0.59	-0.37	0.26	0.20	0.00	0.00	0.00	0.00	0.00	0.59	-0.37	0.26	0.20	1.00	1.00	11.11	0.04	0.00	22935.21
2.00	0.58	-0.37	0.26	0.20	0.14	-0.04	0.00	0.02	0.00	0.59	-0.37	0.26	0.20	0.58	1.00	11.39	0.04	0.00	3375.77
2.20	0.58	-0.35	0.26	0.21	0.29	-0.11	0.00	0.08	0.00	0.59	-0.35	0.26	0.19	0.04	0.97	12.24	0.04	0.00	448.54
2.40	0.58	-0.37	0.26	0.21	0.25	-0.09	0.00	0.06	0.00	0.58	-0.37	0.26	0.19	0.12	0.98	12.20	0.04	0.00	795.12
2.60	0.58	-0.37	0.26	0.21	0.19	-0.08	0.00	0.03	0.00	0.59	-0.37	0.26	0.20	0.22	0.99	11.94	0.04	0.00	1364.33
2.80	0.58	-0.37	0.26	0.20	0.14	-0.08	0.00	0.02	0.00	0.59	-0.37	0.26	0.20	0.35	0.99	11.39	0.04	0.00	2422.43
3.00	0.58	-0.37	0.26	0.20	0.11	-0.04	0.00	0.01	0.00	0.59	-0.37	0.26	0.20	1.00	1.00	11.02	0.04	0.00	8744.38
3.20	0.58	-0.37	0.26	0.20	0.13	-0.06	0.00	0.02	0.00	0.59	-0.37	0.26	0.20	0.67	1.00	11.16	0.04	0.00	4049.53
3.40	0.58	-0.37	0.26	0.20	0.13	-0.06	0.00	0.02	0.00	0.59	-0.37	0.26	0.20	0.90	1.00	11.12	0.04	0.00	5134.01
3.60	0.58	-0.37	0.26	0.21	0.16	-0.08	0.00	0.02	0.00	0.59	-0.37	0.26	0.20	0.29	0.99	11.66	0.04	0.00	1915.26
3.80	0.58	-0.37	0.26	0.20	0.11	-0.06	0.00	0.01	0.00	0.59	-0.37	0.26	0.20	0.99	1.00	11.15	0.04	0.00	7886.10
4.00	1.16	-0.01	0.31	0.16	0.04	-0.04	0.00	0.00	0.00	1.16	-0.01	0.31	0.16	1.00	1.00	10.85	0.03	0.00	16193.41

THE TAME: LOW MODIFIED

The Tame LM

The river Tame catchment covers an area of 1490 km^2 at its confluence with the Trent river. The geology of the Tame catchments is composed of Lower, Middle and Upper Carboniferous Coal Measures in the upper area of the catchment. Triassic Mercia Mudstones and Triassic Sherwood Sandstones are also present in lower down the Tame catchment. The substrate for the majority of the river Tame is composed of a gravel-pebble combination, with limited presence of vegetation in the banks and channel. The straightening of several parts of the river, pollution of running waters, flow alteration and the separation of the floodplain from the river are consequences of the activities in the Tame catchment over time.

The mean annual rainfall in the Tame catchment is 740 mm of which approximately 450 mm constitutes runoff. The catchment is characterised by a flashy response to rainfall events due to the geology, the amount of water imported from outside the catchment (Wales) and the presence of several navigable waterways.

Table Appendix 4.2.12: results obtained for each indicator at different sampling densities for the Tame Low Modified river site. Note that the original sampling density is 4 points per square metre. The abbreviations for each indicator are as follows: MaxTran=maximum depth of the data set to be interpolated, MinTran=minimum depth of the data set to be interpolated, Mean Tran= mean depth of the data set to be interpolated, StdTran=standard deviation of the reach to be interpolated, MaxDiff=maximum difference between predicted and observed values, MinDiff=minimum difference between predicted and observed values, MeanDiff= mean difference between predicted and observed values, MaxSE=Maximum Squared Error, MSE=Mean Squared Error, MaxPred=Maximum value predicted, MinPred=Minimum value predicted, MeanPred= Mean value predicted, Std Pred=Standard deviation of the predicted values, P-value=p-value of the non parametric Kolmogorov-Smirnov test and R-squared = linear regression coefficient between predicted and observed values. Range, Sill, Nugget and Objective refer to the characteristics of the variogram obtained for each sampling density considered.

Points per Square metre	Max Tran	Min Tran	Mean Tran	Std Tran	Max Dif	Min Dif	Mean Dif	Max SE	MSE	Max Pred	Min Pred	Mean Pred	Std Pred	P-value	R-squared	Range	Sill	Nugget	Objective
0.20	0.98	0.03	0.42	0.22	0.04	-0.07	0.00	0.00	0.00	0.98	0.03	0.42	0.21	1.00	1.00	8.04	0.05	0.00	6855.11
0.40	0.98	0.03	0.42	0.22	0.06	-0.11	0.00	0.01	0.00	0.98	0.03	0.42	0.21	1.00	1.00	8.09	0.05	0.00	3078.46
0.60	0.98	0.03	0.42	0.21	0.05	-0.06	0.00	0.00	0.00	0.98	0.03	0.42	0.21	1.00	1.00	8.64	0.05	0.00	9538.66
0.80	0.98	0.03	0.42	0.21	0.05	-0.05	0.00	0.00	0.00	0.98	0.03	0.42	0.21	1.00	1.00	8.58	0.05	0.00	11637.51
1.00	1.15	-0.01	0.30	0.16	0.39	-0.22	0.00	0.15	0.00	1.15	-0.01	0.31	0.15	0.00	0.94	10.21	0.03	0.00	299.73
1.20	0.98	0.03	0.42	0.21	0.05	-0.04	0.00	0.00	0.00	0.98	0.03	0.42	0.21	1.00	1.00	8.49	0.05	0.00	12984.64
1.40	0.98	0.03	0.42	0.22	0.04	-0.03	0.00	0.00	0.00	0.98	0.03	0.42	0.21	1.00	1.00	8.32	0.05	0.00	12765.13
1.60	0.96	0.03	0.42	0.21	0.06	-0.08	0.00	0.01	0.00	0.96	0.03	0.42	0.21	1.00	1.00	8.63	0.05	0.00	8670.47
1.80	1.16	-0.01	0.31	0.17	0.00	0.00	0.00	0.00	0.00	1.16	-0.01	0.31	0.17	1.00	1.00	10.83	0.03	0.00	43566.13
2.00	1.16	-0.01	0.31	0.16	0.08	-0.10	0.00	0.01	0.00	1.16	-0.01	0.31	0.16	1.00	1.00	10.80	0.03	0.00	5154.24
2.20	1.16	-0.01	0.31	0.16	0.29	-0.18	0.00	0.08	0.00	1.16	-0.01	0.31	0.16	0.22	0.98	10.64	0.03	0.00	677.80
2.40	1.16	-0.01	0.31	0.16	0.30	-0.12	0.00	0.09	0.00	1.16	-0.01	0.31	0.16	0.93	0.99	10.66	0.03	0.00	1287.92
2.60	1.16	-0.01	0.31	0.17	0.11	-0.12	0.00	0.01	0.00	1.16	-0.01	0.31	0.16	0.99	1.00	11.04	0.03	0.00	2020.41
2.80	1.16	-0.01	0.31	0.16	0.10	-0.11	0.00	0.01	0.00	1.16	-0.01	0.31	0.16	1.00	1.00	10.98	0.03	0.00	3849.27
3.20	1.16	-0.01	0.31	0.16	0.08	-0.06	0.00	0.01	0.00	1.16	-0.01	0.31	0.16	1.00	1.00	10.88	0.03	0.00	6671.34
3.40	1.16	-0.01	0.31	0.16	0.08	-0.06	0.00	0.01	0.00	1.16	-0.01	0.31	0.16	1.00	1.00	10.68	0.03	0.00	8712.73
3.60	1.16	-0.01	0.31	0.16	0.11	-0.12	0.00	0.01	0.00	1.16	-0.01	0.31	0.16	1.00	1.00	11.15	0.03	0.00	2686.34
3.80	1.16	-0.01	0.31	0.16	0.04	-0.04	0.00	0.00	0.00	1.16	-0.01	0.31	0.16	1.00	1.00	10.79	0.03	0.00	13172.49
4.00	0.98	0.03	0.42	0.22	0.04	-0.07	0.00	0.01	0.00	0.98	0.03	0.42	0.21	1.00	1.00	8.01	0.05	0.00	5205.85

THE TARF

The Tarf

The site is located upstream of Tarfside and lies at around 248 m above sea level. It is a tributary of the North Esk, which is on the northern edge of the Tayside region of Scotland. The geology is intrusive igneous, although the river runs over metamorphic rocks and old red sandstone in the lower reaches. There are no artificial influences to the flow regime. The main land uses in the catchment area are rough grazing with little tree cover.

Table Appendix 4.2.13: results obtained for each indicator at different sampling densities for the Tarf river site. Note that the original sampling density is 4 points per square metre. The abbreviations for each indicator are as follows: MaxTran=maximum depth of the data set to be interpolated, MinTran=minimum depth of the data set to be interpolated, Mean Tran= mean depth of the data set to be interpolated, StdTran=standard deviation of the reach to be interpolated, MaxDiff=maximum difference between predicted and observed values, MinDiff=minimum difference between predicted and observed values, MeanDiff= mean difference between predicted and observed values, MaxSE=Maximum Squared Error, MSE=Mean Squared Error, MaxPred=Maximum value predicted, MinPred=Minimum value predicted, MeanPred= Mean value predicted, Std Pred=Standard deviation of the predicted values, P-value=p-value of the non parametric Kolmogorov-Smirnov test and R-squared = linear regression coefficient between predicted and observed values. Range, Sill, Nugget and Objective refer to the characteristics of the variogram obtained for each sampling density considered.

Points per Square metre	Max Tran	Min Tran	Mean Tran	Std Tran	Max Dif	Min Dif	Mean Dif	Max SE	MSE	Max Pred	Min Pred	Mean Pred	Std Pred	P-value	R-squared	Range	Sill	Nugget	Objective
0.20	0.58	-0.37	0.26	0.20	0.06	-0.03	0.00	0.00	0.00	0.59	-0.37	0.26	0.20	1.00	1.00	10.96	0.04	0.00	11703.72
0.40	0.58	-0.37	0.26	0.20	0.13	-0.06	0.00	0.02	0.00	0.59	-0.37	0.26	0.20	0.97	1.00	11.15	0.04	0.00	6454.21
0.60	0.59	-0.37	0.26	0.20	0.04	-0.02	0.00	0.00	0.00	0.59	-0.37	0.26	0.20	1.00	1.00	11.07	0.04	0.00	14900.13
0.80	0.59	-0.37	0.26	0.20	0.04	-0.02	0.00	0.00	0.00	0.59	-0.37	0.26	0.20	1.00	1.00	11.07	0.04	0.00	16778.42
1.00	0.45	0.02	0.16	0.06	0.17	-0.17	0.00	0.03	0.00	0.28	0.05	0.16	0.05	0.00	0.65	29.10	0.00	0.00	225.17
1.20	0.59	-0.37	0.26	0.20	0.04	-0.02	0.00	0.00	0.00	0.59	-0.37	0.26	0.20	1.00	1.00	11.09	0.04	0.00	18900.80
1.40	0.59	-0.37	0.26	0.20	0.04	-0.02	0.00	0.00	0.00	0.59	-0.37	0.26	0.20	1.00	1.00	11.10	0.04	0.00	21164.88
1.60	0.59	-0.37	0.26	0.20	0.06	-0.02	0.00	0.00	0.00	0.59	-0.37	0.26	0.20	1.00	1.00	11.08	0.04	0.00	13155.46
1.80	0.45	0.02	0.16	0.07	0.10	-0.11	0.00	0.01	0.00	0.35	0.03	0.16	0.06	0.06	0.98	27.15	0.00	0.00	36619.33
2.00	0.45	0.02	0.16	0.07	0.13	-0.13	0.00	0.02	0.00	0.34	0.03	0.16	0.06	0.00	0.94	27.02	0.00	0.00	4433.13
2.20	0.45	0.02	0.16	0.06	0.18	-0.17	0.00	0.03	0.00	0.31	0.04	0.16	0.05	0.00	0.81	28.86	0.00	0.00	473.22
2.40	0.45	0.02	0.16	0.07	0.19	-0.15	0.00	0.04	0.00	0.32	0.03	0.16	0.06	0.00	0.85	28.94	0.00	0.00	1076.86
2.60	0.45	0.02	0.16	0.07	0.14	-0.15	0.00	0.02	0.00	0.33	0.03	0.16	0.06	0.00	0.88	27.69	0.00	0.00	1634.73
2.80	0.45	0.02	0.16	0.07	0.14	-0.12	0.00	0.02	0.00	0.34	0.03	0.16	0.06	0.00	0.92	27.64	0.00	0.00	3351.57
3.00	0.45	0.02	0.16	0.07	0.11	-0.13	0.00	0.02	0.00	0.34	0.03	0.16	0.06	0.00	0.96	27.40	0.00	0.00	12962.72
3.20	0.45	0.02	0.16	0.07	0.11	-0.13	0.00	0.02	0.00	0.34	0.03	0.16	0.06	0.00	0.94	27.09	0.00	0.00	5729.96
3.40	0.45	0.02	0.16	0.07	0.11	-0.13	0.00	0.02	0.00	0.34	0.03	0.16	0.06	0.00	0.95	26.47	0.00	0.00	7292.62
3.60	0.45	0.02	0.16	0.07	0.14	-0.15	0.00	0.02	0.00	0.34	0.03	0.16	0.06	0.00	0.91	28.95	0.00	0.00	2659.62
3.80	0.45	0.02	0.16	0.07	0.11	-0.13	0.00	0.02	0.00	0.34	0.03	0.16	0.06	0.00	0.96	26.73	0.00	0.00	10789.15
4.00	0.58	-0.37	0.26	0.20	0.11	-0.04	0.00	0.01	0.00	0.59	-0.37	0.26	0.20	1.00	1.00	11.07	0.04	0.00	10519.25

THE WINDRUSH








The Windrush

The river Windrush is a meandering river whose source is the Cotswold limestone. It originates approximately 4 km from Temple Guiting and is joined by a number of small tributaries (notably the River Dikler at Bourton-on-the-Water and the Sherborne Brook at Little Barrington). At the study area in Sherborne Park Estate, between Bourton-on the Water and Burford in Gloucestershire, the river flows through a water meadow system, belonging to the National Trust.

Water abstraction is a major issue; water is abstracted from the river Windrush at Worsham and studies (Environment Agency, 2001) have been carried out to investigate the low flow problems on the Windrush. The mean, Q_{10} and Q_{95} flows are equal to 2.17 m^3s^{-1}, 0.647 m^3s^{-1} and 4.28 m^3s^{-1}, respectively.

The river site is located in an area of meandering 18 km from the river source. The river site defines a catchment area of 17 km^2 and is located at an altitude of 250 m. The length of river surveyed is approximately 126 m, with a mean width of 9.7 m. The meander area is characterised by pools which are deep enough to make the measurement of the water surface level impossible with the total station. Mean and maximum depth measured are 37 cm and 1.44 m, respectively.

Table Appendix 4.2.14: results obtained for each indicator at different sampling densities for the Windrush river site. Note that the original sampling density is 4 points per square metre. The abbreviations for each indicator are as follows: MaxTran=maximum depth of the data set to be interpolated, MinTran=minimum depth of the data set to be interpolated, Mean Tran= mean depth of the data set to be interpolated, StdTran=standard deviation of the reach to be interpolated, MaxDiff=maximum difference between predicted and observed values, MinDiff=minimum difference between predicted and observed values, MeanDiff= mean difference between predicted and observed values, MaxSE=Maximum Squared Error, MSE=Mean Squared Error, MaxPred=Maximum value predicted, MinPred=Minimum value predicted, MeanPred= Mean value predicted, Std Pred=Standard deviation of the predicted values, P-value=p-value of the non parametric Kolmogorov-Smirnov test and R-squared = linear regression coefficient between predicted and observed values. Range, Sill, Nugget and Objective refer to the characteristics of the variogram obtained for each sampling density considered.

Points per Square metre	Max Tran	Min Tran	Mean Tran	Std Tran	Max Dif	Min Dif	Mean Dif	Max SE	MSE	Max Pred	Min Pred	Mean Pred	Std Pred	P-value	R-squared	Range	Sill	Nugget	Objective
0.20	0.45	0.02	0.16	0.07	0.11	-0.13	0.00	0.02	0.00	0.34	0.03	0.16	0.06	0.00	0.96	27.69	0.00	0.00	18595.23
0.40	0.45	0.02	0.16	0.07	0.11	-0.13	0.00	0.02	0.00	0.34	0.03	0.16	0.06	0.00	0.95	26.70	0.00	0.00	9020.42
0.60	0.45	0.02	0.16	0.07	0.10	-0.12	0.00	0.01	0.00	0.35	0.03	0.16	0.06	0.02	0.97	27.55	0.00	0.00	22951.41
0.80	0.45	0.02	0.16	0.07	0.10	-0.12	0.00	0.01	0.00	0.35	0.03	0.16	0.06	0.03	0.97	27.40	0.00	0.00	26393.76
1.20	0.45	0.02	0.16	0.07	0.10	-0.11	0.00	0.01	0.00	0.35	0.03	0.16	0.06	0.04	0.97	27.17	0.00	0.00	30026.22
1.40	0.45	0.02	0.16	0.07	0.10	-0.12	0.00	0.01	0.00	0.35	0.03	0.16	0.06	0.05	0.97	27.64	0.00	0.00	33459.43
1.60	0.45	0.02	0.16	0.07	0.11	-0.12	0.00	0.02	0.00	0.35	0.03	0.16	0.06	0.01	0.97	27.85	0.00	0.00	20351.66
4.00	0.45	0.02	0.16	0.07	0.11	-0.13	0.00	0.02	0.00	0.34	0.03	0.16	0.06	0.00	0.96	27.31	0.00	0.00	15752.69
1.80	1.16	0.02	0.37	0.23	0.00	0.00	0.00	0.00	0.00	1.16	0.02	0.37	0.23	1.00	1.00	30.34	0.08	0.00	41015.55
1.00	1.05	0.02	0.37	0.23	0.31	-0.35	0.00	0.12	0.00	1.02	0.04	0.37	0.21	0.00	0.95	33.05	0.08	0.00	206.62
2.20	1.16	0.02	0.37	0.24	0.15	-0.11	0.00	0.02	0.00	1.16	0.02	0.37	0.23	0.82	0.99	31.60	0.09	0.00	629.87
2.40	1.16	0.02	0.37	0.24	0.12	-0.10	0.00	0.01	0.00	1.16	0.02	0.37	0.23	0.97	1.00	30.50	0.09	0.00	1094.32
2.60	1.16	0.02	0.37	0.24	0.11	-0.09	0.00	0.01	0.00	1.16	0.02	0.37	0.23	1.00	1.00	31.83	0.09	0.00	1578.95
2.80	1.16	0.02	0.38	0.23	0.08	-0.07	0.00	0.01	0.00	1.16	0.02	0.37	0.23	1.00	1.00	30.50	0.08	0.00	3620.74
2.00	1.16	0.02	0.37	0.23	0.07	-0.06	0.00	0.01	0.00	1.16	0.02	0.37	0.23	1.00	1.00	31.31	0.08	0.00	5023.68
3.20	1.16	0.02	0.37	0.23	0.07	-0.05	0.00	0.01	0.00	1.16	0.02	0.37	0.23	1.00	1.00	30.64	0.08	0.00	6496.36
3.40	1.16	0.02	0.37	0.23	0.04	-0.05	0.00	0.00	0.00	1.16	0.02	0.37	0.23	1.00	1.00	29.72	0.08	0.00	8615.61
3.60	1.16	0.02	0.37	0.23	0.08	-0.07	0.00	0.01	0.00	1.16	0.02	0.37	0.23	1.00	1.00	31.28	0.08	0.00	2497.90
3.80	1.16	0.02	0.37	0.23	0.04	-0.03	0.00	0.00	0.00	1.16	0.02	0.37	0.23	1.00	1.00	29.04	0.08	0.00	13245.28
3.00	1.16	0.02	0.37	0.23	0.04	-0.03	0.00	0.00	0.00	1.16	0.02	0.37	0.23	1.00	1.00	28.95	0.08	0.00	15854.82

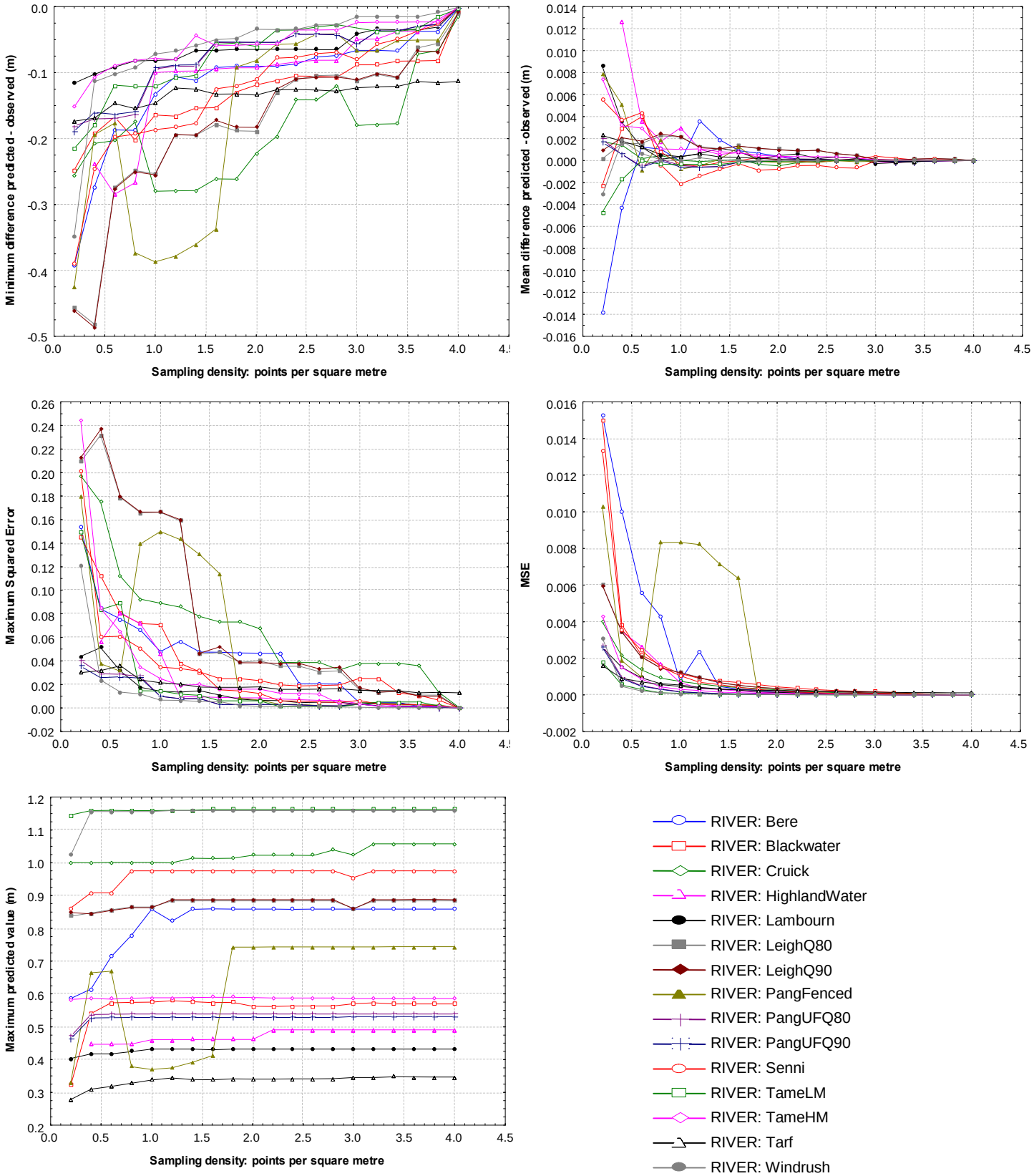

Figure Appendix 4.2.1: graphs representing the results obtained for each indicator at different sampling densities for all the river sites analysed.

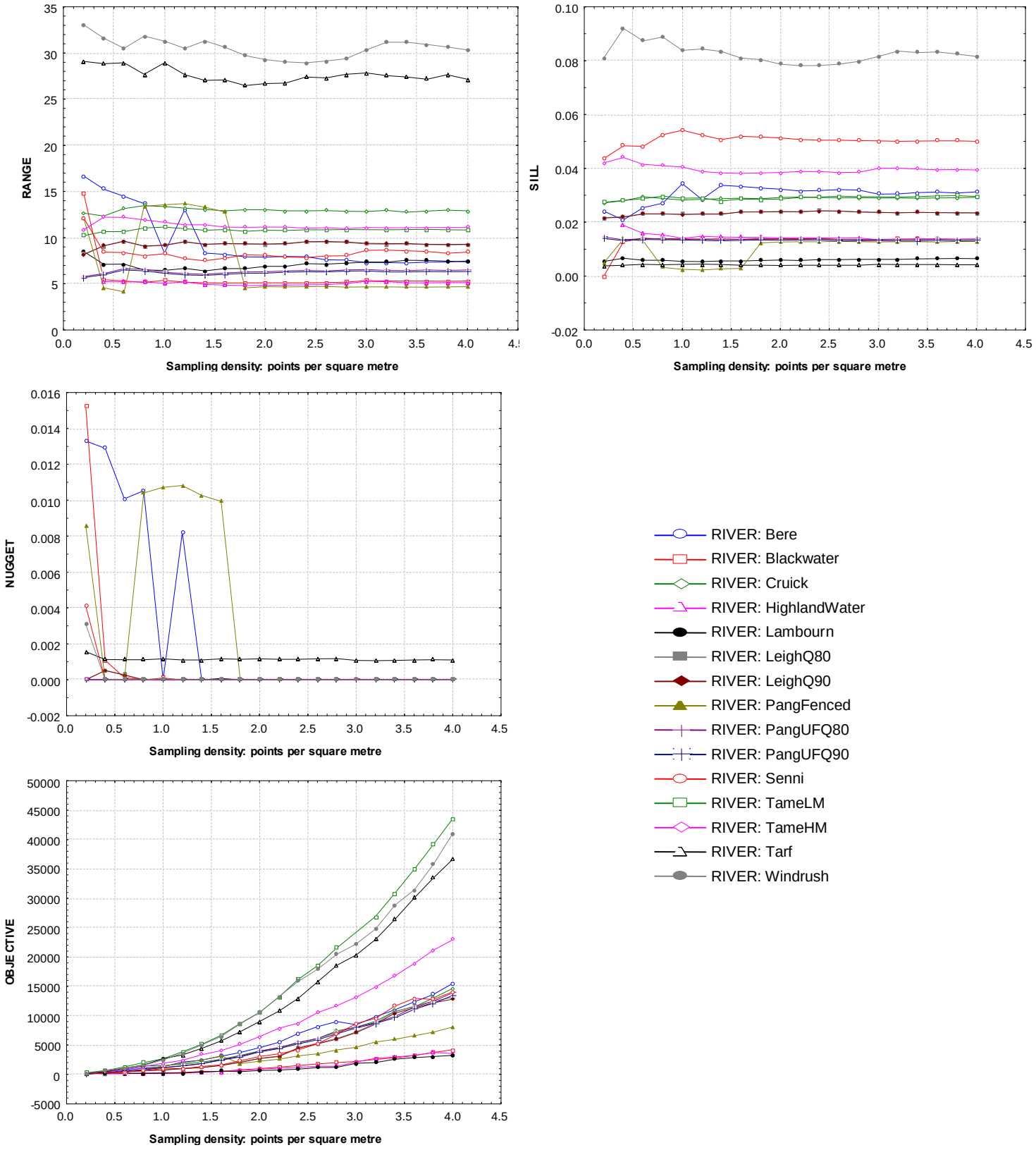

Figure Appendix 4.2.2: graphs representing the results obtained for each indicator at different sampling densities for all the river sites analysed.

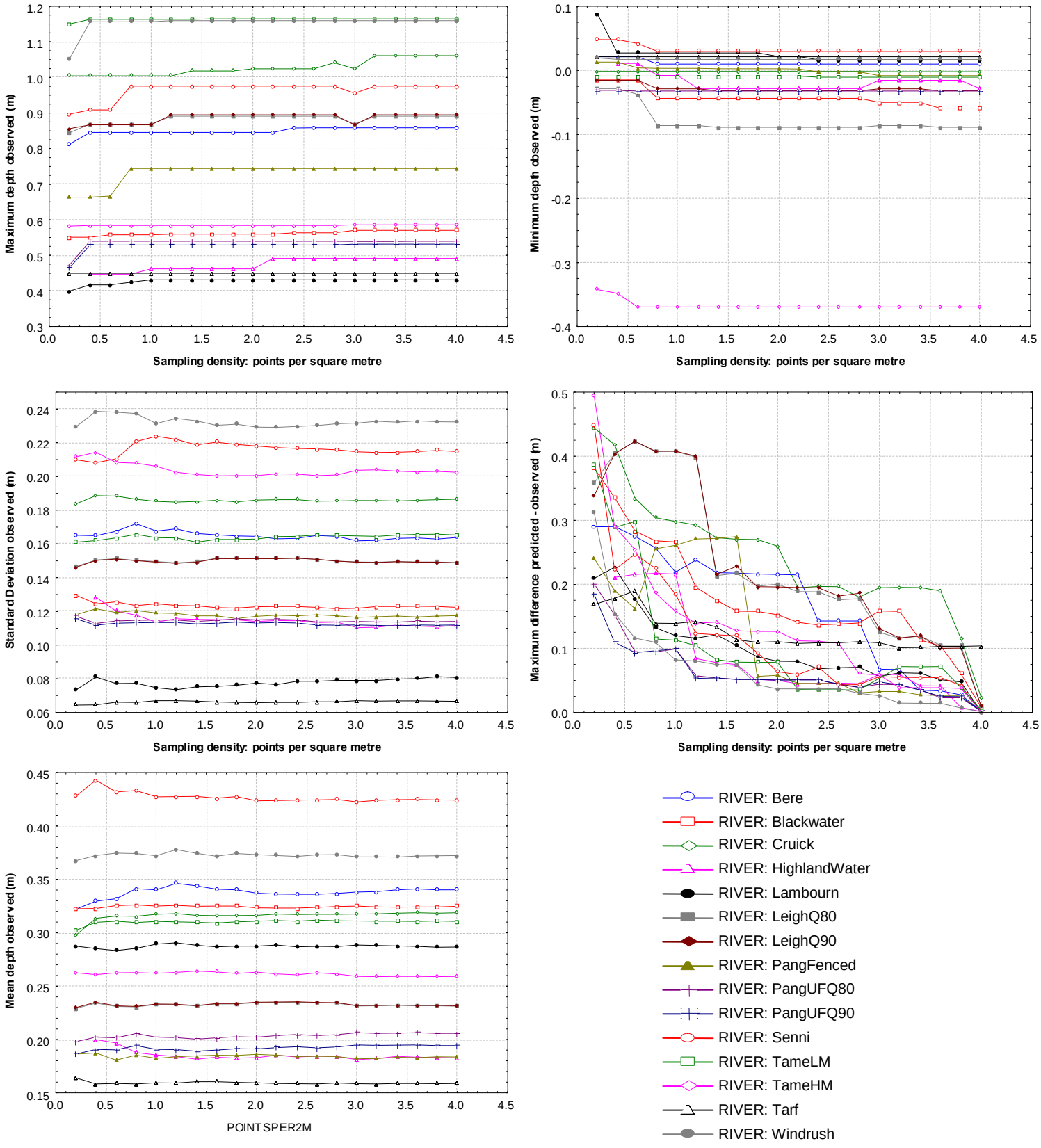

Figure Appendix 4.2.3: graphs representing the results obtained for each indicator at different sampling densities for all the river sites analysed.

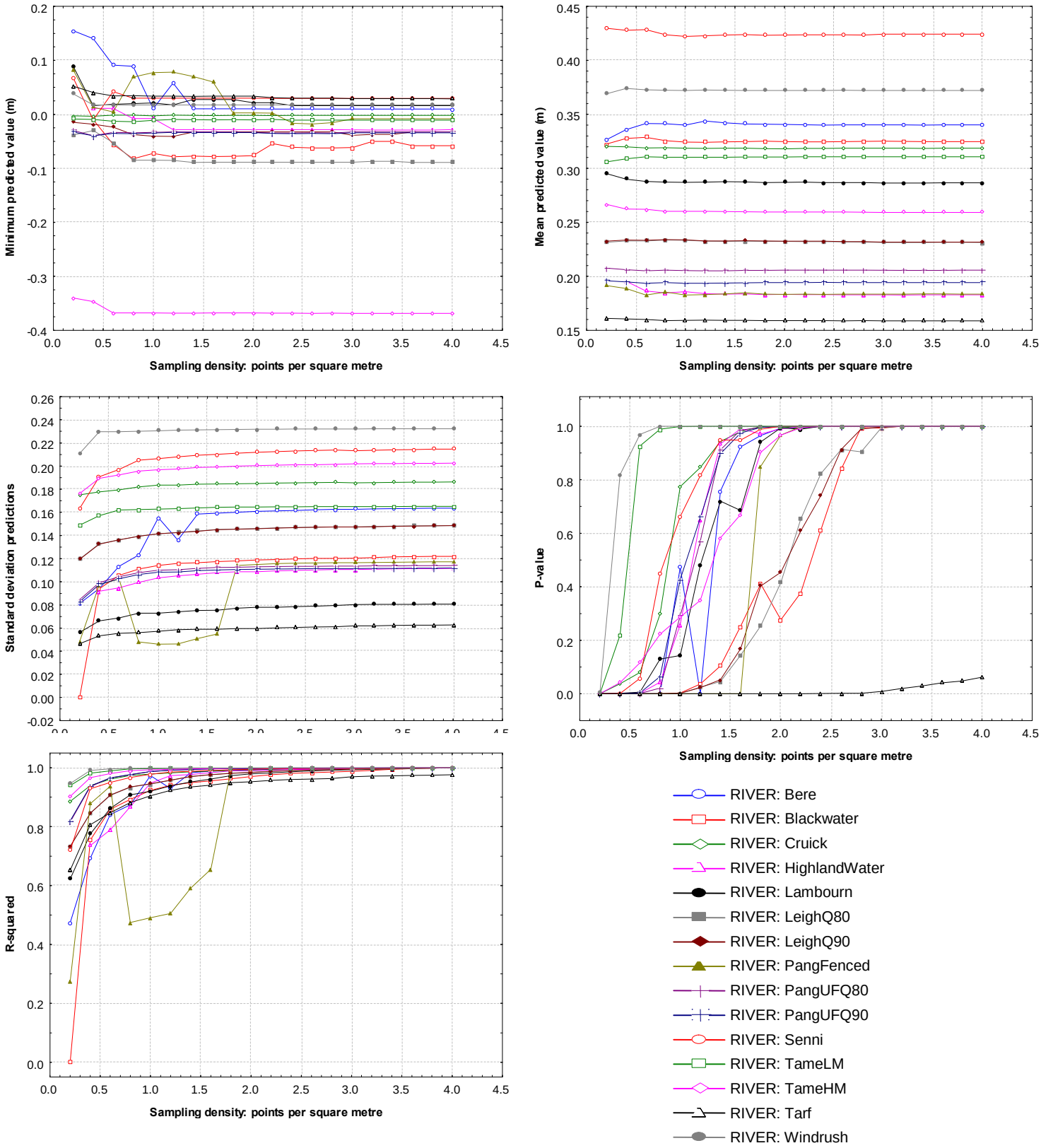

Figure Appendix 4.2.4: graphs representing the results obtained for each indicator at different sampling densities for all the river sites analysed

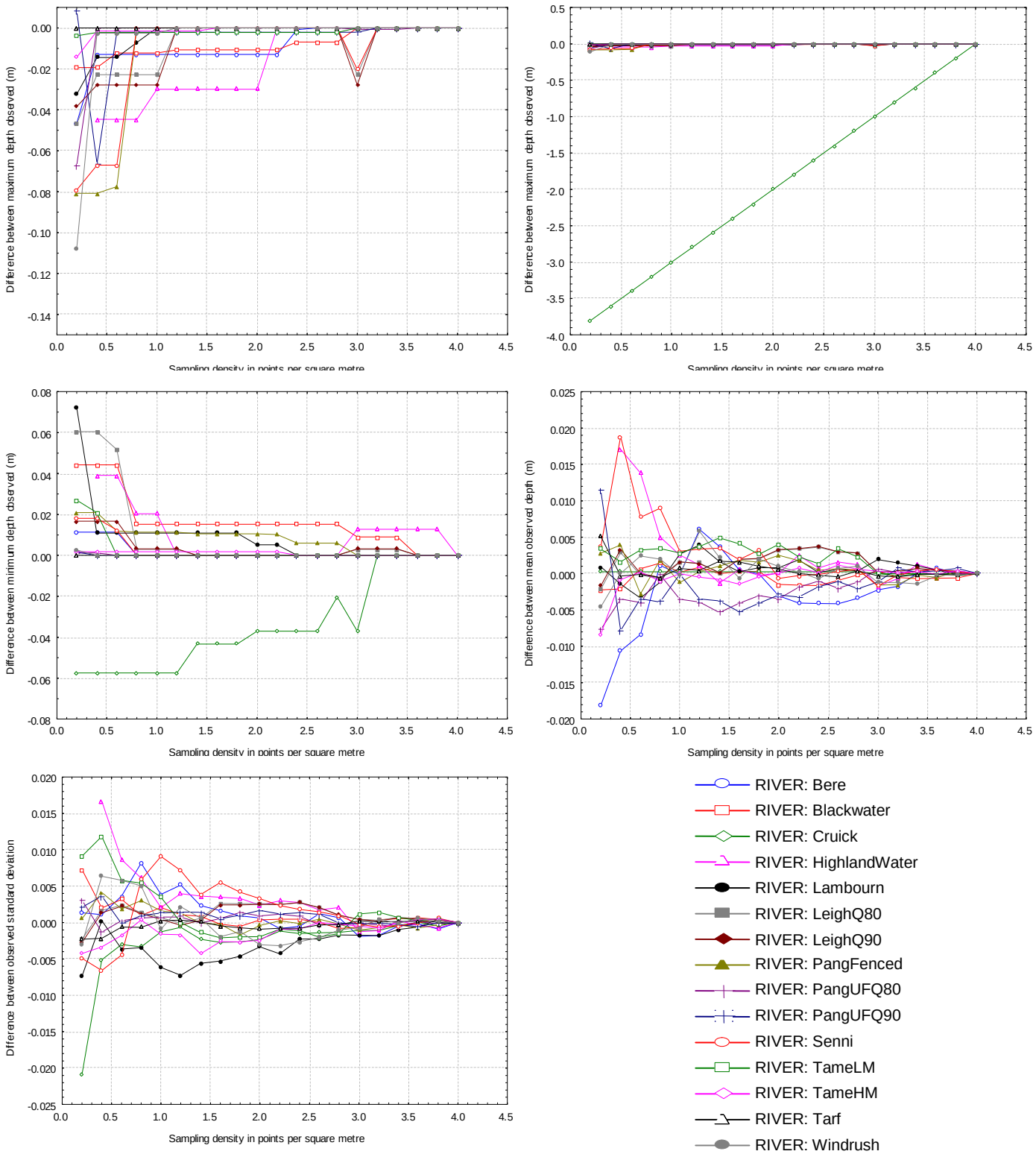

Figure Appendix 4.2.5: graphs representing the results obtained for each indicator at different sampling densities for all the river sites analysed

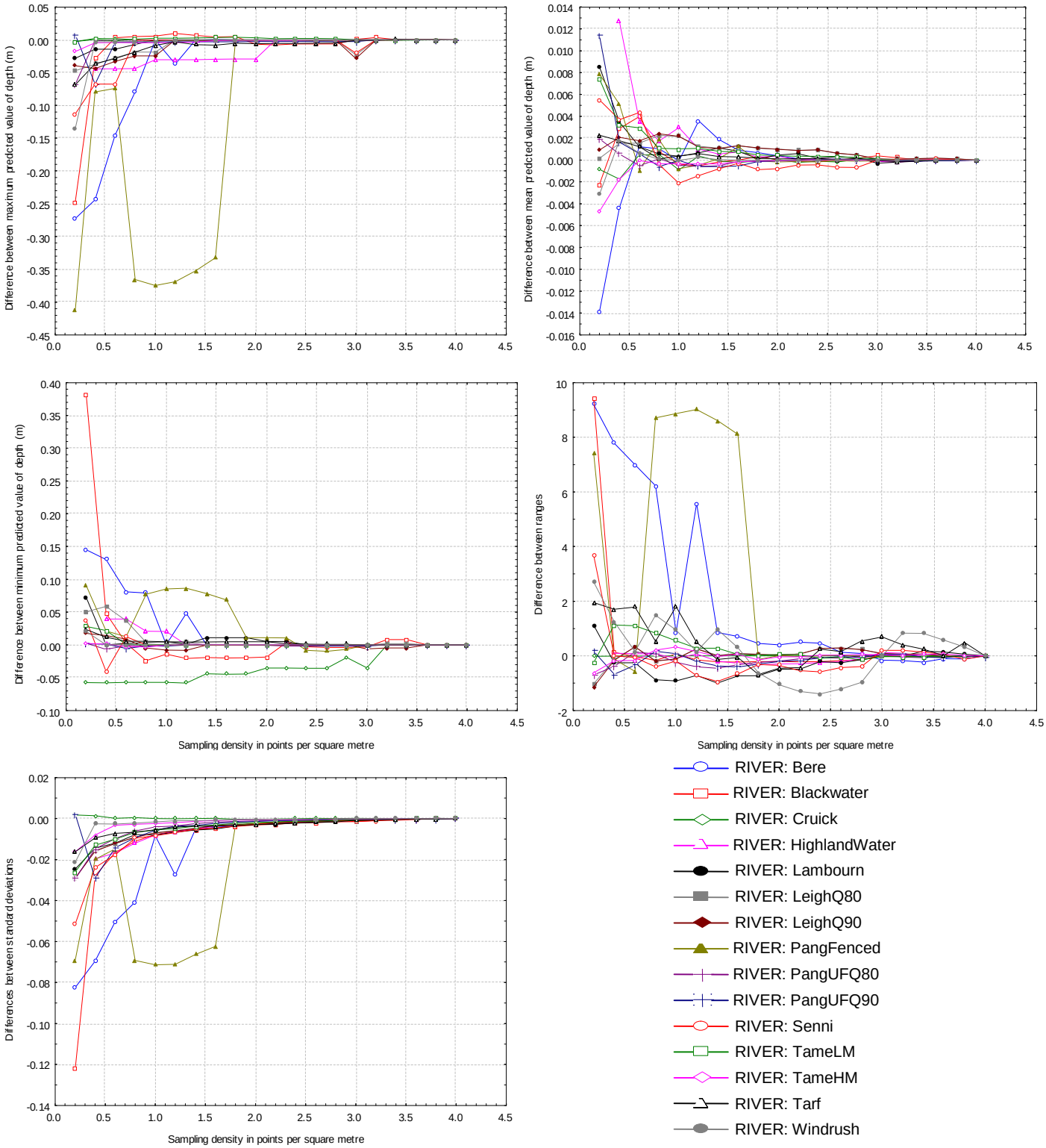

Figure Appendix 4.2.6: graphs representing the results obtained for each indicator at different sampling densities for all the river sites analysed

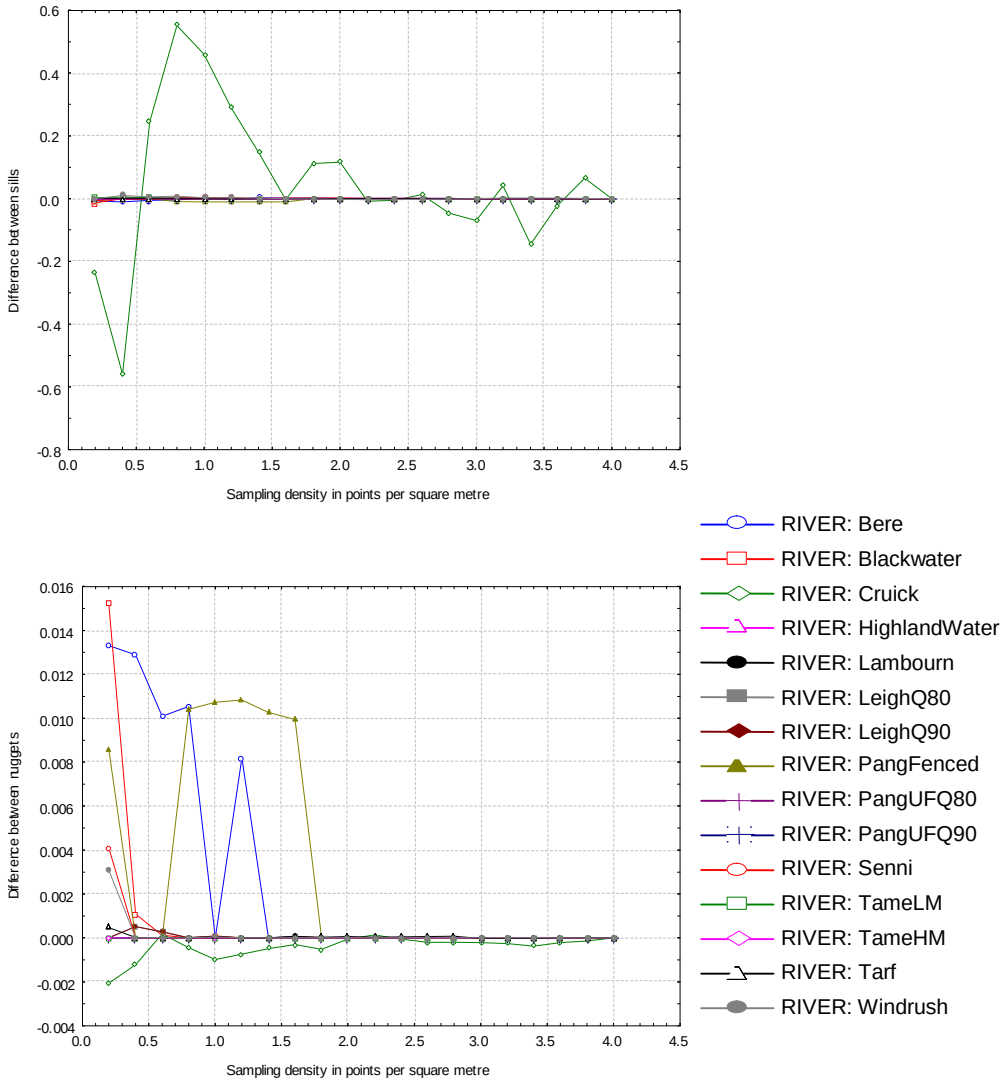

Figure Appendix 4.2.7: graphs representing the results obtained for each indicator at different sampling densities for all the river sites analysed

Appendix 4.3

Confidence Intervals for different sampling densities and indicators analysed – Chapter 6

This appendix presents the confidence intervals obtained for the river sites and sampling strategies analysed. The confidence intervals (CI) have been calculated according to the methodology explained in Chapter 6. Each value in the table represents the ±CI that needs to be added to the indicator calculated to obtain a specific interval of confidence. Those indicators that provided information on the characteristics of the data set (e.g. mean predicted depth) have been transformed into differences between the value of the indicator at a specific sampling density and density equal to 4 points per square metre. If this transformation were not used, the CI error for these indicators would have represented the dispersion between values of the indicator for different river sites instead of the dispersion between the value of the indicator for original and reduced sampling strategies. Depth values and corresponding confidence intervals are given in metres.

Maximum depth observed (m)

CONFIDENCE INTERVAL %																			
SAMPLING DENSITY points per square metre		99.90	99.00	98.50	97.50	95.00	90.00	85.00	80.00	75.00	70.00	65.00	60.00	55.00	50.00	40.00	30.00	20.00	10.00
	0.2	0.88664	0.69239	0.65343	0.60211	0.52661	0.44198	0.38663	0.34418	0.30925	0.27835	0.25095	0.22596	0.20285	0.18109	0.14079	0.10344	0.06798	0.03385
	0.4	0.78664	0.61429	0.57973	0.53420	0.46721	0.39213	0.34302	0.30536	0.27437	0.24696	0.22264	0.20047	0.17997	0.16066	0.12491	0.09177	0.06031	0.03004
	0.6	0.74377	0.58082	0.54814	0.50509	0.44175	0.37076	0.32433	0.28872	0.25942	0.23350	0.21051	0.18955	0.17017	0.15191	0.11810	0.08677	0.05702	0.02840
	0.8	0.70195	0.54816	0.51732	0.47669	0.41692	0.34991	0.30609	0.27248	0.24483	0.22037	0.19867	0.17889	0.16060	0.14337	0.11146	0.08189	0.05382	0.02680
	1	0.65827	0.51405	0.48512	0.44702	0.39097	0.32814	0.28705	0.25553	0.22960	0.20666	0.18631	0.16776	0.15060	0.13445	0.10453	0.07680	0.05047	0.02513
	1.2	0.61511	0.48034	0.45331	0.41771	0.36534	0.30662	0.26822	0.23877	0.21454	0.19311	0.17409	0.15676	0.14073	0.12563	0.09767	0.07176	0.04716	0.02349
	1.4	0.57111	0.44598	0.42089	0.38783	0.33920	0.28469	0.24904	0.22169	0.19920	0.17929	0.16164	0.14555	0.13066	0.11664	0.09069	0.06663	0.04379	0.02181
	1.6	0.52714	0.41165	0.38848	0.35797	0.31309	0.26277	0.22986	0.20462	0.18386	0.16549	0.14920	0.13434	0.12060	0.10766	0.08370	0.06150	0.04041	0.02013
	1.8	0.48314	0.37729	0.35606	0.32810	0.28696	0.24084	0.21068	0.18755	0.16851	0.15168	0.13674	0.12313	0.11054	0.09868	0.07672	0.05637	0.03704	0.01845
	2	0.43915	0.34293	0.32364	0.29822	0.26083	0.21891	0.19149	0.17047	0.15317	0.13787	0.12429	0.11192	0.10047	0.08969	0.06973	0.05123	0.03367	0.01677
	2.2	0.39558	0.30891	0.29153	0.26863	0.23495	0.19719	0.17249	0.15356	0.13797	0.12419	0.11196	0.10081	0.09050	0.08079	0.06281	0.04615	0.03033	0.01510
	2.4	0.35182	0.27474	0.25928	0.23891	0.20896	0.17537	0.15341	0.13657	0.12271	0.11045	0.09957	0.08966	0.08049	0.07186	0.05586	0.04105	0.02697	0.01343
	2.6	0.30783	0.24039	0.22686	0.20904	0.18283	0.15345	0.13423	0.11949	0.10737	0.09664	0.08712	0.07845	0.07043	0.06287	0.04888	0.03591	0.02360	0.01175
	2.8	0.26383	0.20603	0.19443	0.17916	0.15670	0.13151	0.11505	0.10241	0.09202	0.08283	0.07467	0.06724	0.06036	0.05389	0.04189	0.03078	0.02023	0.01007
	3	0.23454	0.18316	0.17285	0.15928	0.13930	0.11692	0.10228	0.09105	0.08181	0.07363	0.06638	0.05977	0.05366	0.04790	0.03724	0.02736	0.01798	0.00896
	3.2	0.17599	0.13743	0.12970	0.11951	0.10453	0.08773	0.07674	0.06832	0.06138	0.05525	0.04981	0.04485	0.04026	0.03594	0.02795	0.02053	0.01349	0.00672
	3.4	0.13199	0.10307	0.09727	0.08963	0.07839	0.06579	0.05756	0.05124	0.04604	0.04144	0.03736	0.03364	0.03020	0.02696	0.02096	0.01540	0.01012	0.00504
	3.6	0.08800	0.06872	0.06485	0.05976	0.05227	0.04387	0.03837	0.03416	0.03069	0.02763	0.02491	0.02243	0.02013	0.01797	0.01397	0.01027	0.00675	0.00336
	3.8	0.04400	0.03436	0.03243	0.02988	0.02613	0.02193	0.01919	0.01708	0.01535	0.01381	0.01245	0.01121	0.01007	0.00899	0.00699	0.00513	0.00337	0.00168
	4	0.00000	0.00000	0.00000	0.00000	0.00000	0.00000	0.00000	0.00000	0.00000	0.00000	0.00000	0.00000	0.00000	0.00000	0.00000	0.00000	0.00000	0.00000

Minimum depth observed (m)

SAMPLING DENSITY points per square metre	CONFIDENCE INTERVAL %																	
		99.90	**99.00**	**98.50**	**97.50**	**95.00**	**90.00**	**85.00**	**80.00**	**75.00**	**70.00**	**65.00**	**60.00**	**55.00**	**50.00**	**40.00**	**30.00**	**20.00**	**10.00**
	0.2	0.02742	0.02141	0.02021	0.01862	0.01628	0.01367	0.01196	0.01064	0.00956	0.00861	0.00776	0.00699	0.00627	0.00560	0.00435	0.00320	0.00210	0.00105
	0.4	0.02257	0.01763	0.01663	0.01533	0.01341	0.01125	0.00984	0.00876	0.00787	0.00709	0.00639	0.00575	0.00516	0.00461	0.00358	0.00263	0.00173	0.00086
	0.6	0.02153	0.01681	0.01587	0.01462	0.01279	0.01073	0.00939	0.00836	0.00751	0.00676	0.00609	0.00549	0.00493	0.00440	0.00342	0.00251	0.00165	0.00082
	0.8	0.01478	0.01154	0.01089	0.01004	0.00878	0.00737	0.00645	0.00574	0.00516	0.00464	0.00418	0.00377	0.00338	0.00302	0.00235	0.00172	0.00113	0.00056
	1	0.01478	0.01154	0.01089	0.01004	0.00878	0.00737	0.00645	0.00574	0.00516	0.00464	0.00418	0.00377	0.00338	0.00302	0.00235	0.00172	0.00113	0.00056
	1.2	0.01403	0.01095	0.01034	0.00952	0.00833	0.00699	0.00612	0.00544	0.00489	0.00440	0.00397	0.00357	0.00321	0.00286	0.00223	0.00164	0.00108	0.00054
	1.4	0.01100	0.00859	0.00811	0.00747	0.00653	0.00548	0.00480	0.00427	0.00384	0.00345	0.00311	0.00280	0.00252	0.00225	0.00175	0.00128	0.00084	0.00042
	1.6	0.01100	0.00859	0.00811	0.00747	0.00653	0.00548	0.00480	0.00427	0.00384	0.00345	0.00311	0.00280	0.00252	0.00225	0.00175	0.00128	0.00084	0.00042
	1.8	0.01100	0.00859	0.00811	0.00747	0.00653	0.00548	0.00480	0.00427	0.00384	0.00345	0.00311	0.00280	0.00252	0.00225	0.00175	0.00128	0.00084	0.00042
	2	0.00951	0.00743	0.00701	0.00646	0.00565	0.00474	0.00415	0.00369	0.00332	0.00299	0.00269	0.00242	0.00218	0.00194	0.00151	0.00111	0.00073	0.00036
	2.2	0.00949	0.00741	0.00700	0.00645	0.00564	0.00473	0.00414	0.00369	0.00331	0.00298	0.00269	0.00242	0.00217	0.00194	0.00151	0.00111	0.00073	0.00036
	2.4	0.00917	0.00716	0.00676	0.00623	0.00545	0.00457	0.00400	0.00356	0.00320	0.00288	0.00260	0.00234	0.00210	0.00187	0.00146	0.00107	0.00070	0.00035
	2.6	0.00917	0.00716	0.00676	0.00623	0.00545	0.00457	0.00400	0.00356	0.00320	0.00288	0.00260	0.00234	0.00210	0.00187	0.00146	0.00107	0.00070	0.00035
	2.8	0.00594	0.00464	0.00438	0.00403	0.00353	0.00296	0.00259	0.00231	0.00207	0.00186	0.00168	0.00151	0.00136	0.00121	0.00094	0.00069	0.00046	0.00023
	3	0.00987	0.00771	0.00728	0.00670	0.00586	0.00492	0.00431	0.00383	0.00344	0.00310	0.00279	0.00252	0.00226	0.00202	0.00157	0.00115	0.00076	0.00038
	3.2	0.00330	0.00258	0.00243	0.00224	0.00196	0.00164	0.00144	0.00128	0.00115	0.00104	0.00093	0.00084	0.00075	0.00067	0.00052	0.00038	0.00025	0.00013
	3.4	0.00330	0.00258	0.00243	0.00224	0.00196	0.00164	0.00144	0.00128	0.00115	0.00104	0.00093	0.00084	0.00075	0.00067	0.00052	0.00038	0.00025	0.00013
	3.6	0.00280	0.00219	0.00206	0.00190	0.00166	0.00140	0.00122	0.00109	0.00098	0.00088	0.00079	0.00071	0.00064	0.00057	0.00044	0.00033	0.00021	0.00011
	3.8	0.00280	0.00219	0.00206	0.00190	0.00166	0.00140	0.00122	0.00109	0.00098	0.00088	0.00079	0.00071	0.00064	0.00057	0.00044	0.00033	0.00021	0.00011
	4	0.00000	0.00000	0.00000	0.00000	0.00000	0.00000	0.00000	0.00000	0.00000	0.00000	0.00000	0.00000	0.00000	0.00000	0.00000	0.00000	0.00000	0.00000

Standard deviation of the observed values

		CONFIDENCE INTERVAL %																	
SAMPLING DENSITY points per square metre		**99.90**	**99.00**	**98.50**	**97.50**	**95.00**	**90.00**	**85.00**	**80.00**	**75.00**	**70.00**	**65.00**	**60.00**	**55.00**	**50.00**	**40.00**	**30.00**	**20.00**	**10.00**
	0.2	0.00633	0.00494	0.00466	0.00430	0.00376	0.00315	0.00276	0.00246	0.00221	0.00199	0.00179	0.00161	0.00145	0.00129	0.00100	0.00074	0.00049	0.00024
	0.4	0.00522	0.00407	0.00385	0.00354	0.00310	0.00260	0.00228	0.00203	0.00182	0.00164	0.00148	0.00133	0.00119	0.00107	0.00083	0.00061	0.00040	0.00020
	0.6	0.00321	0.00251	0.00237	0.00218	0.00191	0.00160	0.00140	0.00125	0.00112	0.00101	0.00091	0.00082	0.00073	0.00066	0.00051	0.00037	0.00025	0.00012
	0.8	0.00292	0.00228	0.00215	0.00198	0.00173	0.00145	0.00127	0.00113	0.00102	0.00092	0.00083	0.00074	0.00067	0.00060	0.00046	0.00034	0.00022	0.00011
	1	0.00280	0.00218	0.00206	0.00190	0.00166	0.00139	0.00122	0.00109	0.00098	0.00088	0.00079	0.00071	0.00064	0.00057	0.00044	0.00033	0.00021	0.00011
	1.2	0.00277	0.00216	0.00204	0.00188	0.00164	0.00138	0.00121	0.00107	0.00097	0.00087	0.00078	0.00071	0.00063	0.00057	0.00044	0.00032	0.00021	0.00011
	1.4	0.00221	0.00173	0.00163	0.00150	0.00131	0.00110	0.00096	0.00086	0.00077	0.00069	0.00063	0.00056	0.00051	0.00045	0.00035	0.00026	0.00017	0.00008
	1.6	0.00238	0.00186	0.00175	0.00161	0.00141	0.00119	0.00104	0.00092	0.00083	0.00075	0.00067	0.00061	0.00054	0.00049	0.00038	0.00028	0.00018	0.00009
	1.8	0.00215	0.00168	0.00158	0.00146	0.00127	0.00107	0.00094	0.00083	0.00075	0.00067	0.00061	0.00055	0.00049	0.00044	0.00034	0.00025	0.00016	0.00008
	2	0.00191	0.00149	0.00141	0.00129	0.00113	0.00095	0.00083	0.00074	0.00066	0.00060	0.00054	0.00049	0.00044	0.00039	0.00030	0.00022	0.00015	0.00007
	2.2	0.00180	0.00140	0.00132	0.00122	0.00107	0.00090	0.00078	0.00070	0.00063	0.00056	0.00051	0.00046	0.00041	0.00037	0.00029	0.00021	0.00014	0.00007
	2.4	0.00153	0.00120	0.00113	0.00104	0.00091	0.00076	0.00067	0.00059	0.00053	0.00048	0.00043	0.00039	0.00035	0.00031	0.00024	0.00018	0.00012	0.00006
	2.6	0.00129	0.00101	0.00095	0.00087	0.00076	0.00064	0.00056	0.00050	0.00045	0.00040	0.00036	0.00033	0.00029	0.00026	0.00020	0.00015	0.00010	0.00005
	2.8	0.00092	0.00072	0.00068	0.00063	0.00055	0.00046	0.00040	0.00036	0.00032	0.00029	0.00026	0.00024	0.00021	0.00019	0.00015	0.00011	0.00007	0.00004
	3	0.00078	0.00061	0.00058	0.00053	0.00046	0.00039	0.00034	0.00030	0.00027	0.00025	0.00022	0.00020	0.00018	0.00016	0.00012	0.00009	0.00006	0.00003
	3.2	0.00075	0.00058	0.00055	0.00051	0.00044	0.00037	0.00033	0.00029	0.00026	0.00024	0.00021	0.00019	0.00017	0.00015	0.00012	0.00009	0.00006	0.00003
	3.4	0.00044	0.00035	0.00033	0.00030	0.00026	0.00022	0.00019	0.00017	0.00015	0.00014	0.00013	0.00011	0.00010	0.00009	0.00007	0.00005	0.00003	0.00002
	3.6	0.00040	0.00031	0.00029	0.00027	0.00023	0.00020	0.00017	0.00015	0.00014	0.00012	0.00011	0.00010	0.00009	0.00008	0.00006	0.00005	0.00003	0.00002
	3.8	0.00040	0.00031	0.00029	0.00027	0.00024	0.00020	0.00017	0.00016	0.00014	0.00013	0.00011	0.00010	0.00009	0.00008	0.00006	0.00005	0.00003	0.00002
	4	0.00004	0.00003	0.00003	0.00003	0.00003	0.00002	0.00002	0.00002	0.00001	0.00001	0.00001	0.00001	0.00001	0.00001	0.00001	0.00000	0.00000	0.00000

Mean depth observed (m)

SAMPLING DENSITY points per square metre	CONFIDENCE INTERVAL %																	
		99.90	99.00	98.50	97.50	95.00	90.00	85.00	80.00	75.00	70.00	65.00	60.00	55.00	50.00	40.00	30.00	20.00	10.00
	0.2	0.00628	0.00490	0.00463	0.00426	0.00373	0.00313	0.00274	0.00244	0.00219	0.00197	0.00178	0.00160	0.00144	0.00128	0.00100	0.00073	0.00048	0.00024
	0.4	0.00663	0.00518	0.00489	0.00450	0.00394	0.00331	0.00289	0.00257	0.00231	0.00208	0.00188	0.00169	0.00152	0.00135	0.00105	0.00077	0.00051	0.00025
	0.6	0.00445	0.00348	0.00328	0.00302	0.00264	0.00222	0.00194	0.00173	0.00155	0.00140	0.00126	0.00113	0.00102	0.00091	0.00071	0.00052	0.00034	0.00017
	0.8	0.00260	0.00203	0.00191	0.00176	0.00154	0.00129	0.00113	0.00101	0.00091	0.00082	0.00073	0.00066	0.00059	0.00053	0.00041	0.00030	0.00020	0.00010
	1	0.00150	0.00117	0.00111	0.00102	0.00089	0.00075	0.00066	0.00058	0.00052	0.00047	0.00043	0.00038	0.00034	0.00031	0.00024	0.00018	0.00012	0.00006
	1.2	0.00246	0.00192	0.00181	0.00167	0.00146	0.00122	0.00107	0.00095	0.00086	0.00077	0.00070	0.00063	0.00056	0.00050	0.00039	0.00029	0.00019	0.00009
	1.4	0.00231	0.00180	0.00170	0.00157	0.00137	0.00115	0.00101	0.00090	0.00080	0.00072	0.00065	0.00059	0.00053	0.00047	0.00037	0.00027	0.00018	0.00009
	1.6	0.00204	0.00159	0.00150	0.00139	0.00121	0.00102	0.00089	0.00079	0.00071	0.00064	0.00058	0.00052	0.00047	0.00042	0.00032	0.00024	0.00016	0.00008
	1.8	0.00170	0.00133	0.00125	0.00115	0.00101	0.00085	0.00074	0.00066	0.00059	0.00053	0.00048	0.00043	0.00039	0.00035	0.00027	0.00020	0.00013	0.00006
	2	0.00200	0.00157	0.00148	0.00136	0.00119	0.00100	0.00087	0.00078	0.00070	0.00063	0.00057	0.00051	0.00046	0.00041	0.00032	0.00023	0.00015	0.00008
	2.2	0.00195	0.00152	0.00143	0.00132	0.00116	0.00097	0.00085	0.00076	0.00068	0.00061	0.00055	0.00050	0.00044	0.00040	0.00031	0.00023	0.00015	0.00007
	2.4	0.00168	0.00131	0.00124	0.00114	0.00100	0.00084	0.00073	0.00065	0.00059	0.00053	0.00047	0.00043	0.00038	0.00034	0.00027	0.00020	0.00013	0.00006
	2.6	0.00170	0.00133	0.00126	0.00116	0.00101	0.00085	0.00074	0.00066	0.00059	0.00053	0.00048	0.00043	0.00039	0.00035	0.00027	0.00020	0.00013	0.00007
	2.8	0.00144	0.00112	0.00106	0.00098	0.00085	0.00072	0.00063	0.00056	0.00050	0.00045	0.00041	0.00037	0.00033	0.00029	0.00023	0.00017	0.00011	0.00005
	3	0.00102	0.00080	0.00075	0.00069	0.00061	0.00051	0.00044	0.00040	0.00036	0.00032	0.00029	0.00026	0.00023	0.00021	0.00016	0.00012	0.00008	0.00004
	3.2	0.00072	0.00056	0.00053	0.00049	0.00042	0.00036	0.00031	0.00028	0.00025	0.00022	0.00020	0.00018	0.00016	0.00015	0.00011	0.00008	0.00005	0.00003
	3.4	0.00056	0.00044	0.00041	0.00038	0.00033	0.00028	0.00024	0.00022	0.00019	0.00018	0.00016	0.00014	0.00013	0.00011	0.00009	0.00007	0.00004	0.00002
	3.6	0.00037	0.00029	0.00028	0.00025	0.00022	0.00019	0.00016	0.00014	0.00013	0.00012	0.00011	0.00010	0.00009	0.00008	0.00006	0.00004	0.00003	0.00001
	3.8	0.00028	0.00022	0.00021	0.00019	0.00017	0.00014	0.00012	0.00011	0.00010	0.00009	0.00008	0.00007	0.00006	0.00006	0.00004	0.00003	0.00002	0.00001
	4	0.00001	0.00001	0.00001	0.00001	0.00001	0.00001	0.00001	0.00001	0.00000	0.00000	0.00000	0.00000	0.00000	0.00000	0.00000	0.00000	0.00000	0.00000

Maximum difference between predicted and observed values (m)

	CONFIDENCE INTERVAL %																	
SAMPLING DENSITY points per square metre	**99.90**	**99.00**	**98.50**	**97.50**	**95.00**	**90.00**	**85.00**	**80.00**	**75.00**	**70.00**	**65.00**	**60.00**	**55.00**	**50.00**	**40.00**	**30.00**	**20.00**	**10.00**
0.2	0.09391	0.07333	0.06921	0.06377	0.05577	0.04681	0.04095	0.03645	0.03275	0.02948	0.02658	0.02393	0.02148	0.01918	0.01491	0.01096	0.00720	0.00359
0.4	0.08417	0.06573	0.06203	0.05716	0.04999	0.04196	0.03670	0.03267	0.02936	0.02643	0.02382	0.02145	0.01926	0.01719	0.01337	0.00982	0.00645	0.00321
0.6	0.08930	0.06974	0.06581	0.06064	0.05304	0.04452	0.03894	0.03467	0.03115	0.02804	0.02528	0.02276	0.02043	0.01824	0.01418	0.01042	0.00685	0.00341
0.8	0.08865	0.06923	0.06533	0.06020	0.05265	0.04419	0.03866	0.03441	0.03092	0.02783	0.02509	0.02259	0.02028	0.01811	0.01408	0.01034	0.00680	0.00338
1	0.09064	0.07078	0.06680	0.06155	0.05383	0.04518	0.03952	0.03518	0.03161	0.02846	0.02565	0.02310	0.02074	0.01851	0.01439	0.01057	0.00695	0.00346
1.2	0.09849	0.07691	0.07258	0.06688	0.05850	0.04910	0.04295	0.03823	0.03435	0.03092	0.02788	0.02510	0.02253	0.02012	0.01564	0.01149	0.00755	0.00376
1.4	0.06418	0.05012	0.04730	0.04359	0.03812	0.03199	0.02799	0.02491	0.02239	0.02015	0.01817	0.01636	0.01468	0.01311	0.01019	0.00749	0.00492	0.00245
1.6	0.06661	0.05201	0.04909	0.04523	0.03956	0.03320	0.02904	0.02586	0.02323	0.02091	0.01885	0.01697	0.01524	0.01360	0.01058	0.00777	0.00511	0.00254
1.8	0.06158	0.04809	0.04538	0.04182	0.03657	0.03070	0.02685	0.02390	0.02148	0.01933	0.01743	0.01569	0.01409	0.01258	0.00978	0.00718	0.00472	0.00235
2	0.06172	0.04820	0.04549	0.04191	0.03666	0.03077	0.02691	0.02396	0.02153	0.01938	0.01747	0.01573	0.01412	0.01261	0.00980	0.00720	0.00473	0.00236
2.2	0.05657	0.04417	0.04169	0.03841	0.03360	0.02820	0.02467	0.02196	0.01973	0.01776	0.01601	0.01442	0.01294	0.01155	0.00898	0.00660	0.00434	0.00216
2.4	0.05104	0.03986	0.03762	0.03466	0.03031	0.02544	0.02226	0.01981	0.01780	0.01602	0.01445	0.01301	0.01168	0.01042	0.00810	0.00595	0.00391	0.00195
2.6	0.05049	0.03943	0.03721	0.03429	0.02999	0.02517	0.02202	0.01960	0.01761	0.01585	0.01429	0.01287	0.01155	0.01031	0.00802	0.00589	0.00387	0.00193
2.8	0.05161	0.04030	0.03804	0.03505	0.03065	0.02573	0.02251	0.02003	0.01800	0.01620	0.01461	0.01315	0.01181	0.01054	0.00820	0.00602	0.00396	0.00197
3	0.04521	0.03531	0.03332	0.03070	0.02685	0.02254	0.01972	0.01755	0.01577	0.01419	0.01280	0.01152	0.01034	0.00923	0.00718	0.00527	0.00347	0.00173
3.2	0.04258	0.03325	0.03138	0.02891	0.02529	0.02122	0.01857	0.01653	0.01485	0.01337	0.01205	0.01085	0.00974	0.00870	0.00676	0.00497	0.00326	0.00163
3.4	0.04199	0.03279	0.03095	0.02852	0.02494	0.02093	0.01831	0.01630	0.01465	0.01318	0.01188	0.01070	0.00961	0.00858	0.00667	0.00490	0.00322	0.00160
3.6	0.04030	0.03147	0.02970	0.02737	0.02393	0.02009	0.01757	0.01564	0.01406	0.01265	0.01141	0.01027	0.00922	0.00823	0.00640	0.00470	0.00309	0.00154
3.8	0.03154	0.02463	0.02324	0.02142	0.01873	0.01572	0.01375	0.01224	0.01100	0.00990	0.00893	0.00804	0.00721	0.00644	0.00501	0.00368	0.00242	0.00120
4	0.02235	0.01746	0.01647	0.01518	0.01328	0.01114	0.00975	0.00868	0.00780	0.00702	0.00633	0.00570	0.00511	0.00457	0.00355	0.00261	0.00171	0.00085

Minimum difference between predicted and observed values (m)

	CONFIDENCE INTERVAL %																	
SAMPLING DENSITY points per square metre	**99.90**	**99.00**	**98.50**	**97.50**	**95.00**	**90.00**	**85.00**	**80.00**	**75.00**	**70.00**	**65.00**	**60.00**	**55.00**	**50.00**	**40.00**	**30.00**	**20.00**	**10.00**
0.2	0.10736	0.08384	0.07912	0.07291	0.06377	0.05352	0.04682	0.04168	0.03745	0.03370	0.03039	0.02736	0.02456	0.02193	0.01705	0.01253	0.00823	0.00410
0.4	0.10001	0.07810	0.07371	0.06792	0.05940	0.04985	0.04361	0.03882	0.03488	0.03140	0.02831	0.02549	0.02288	0.02043	0.01588	0.01167	0.00767	0.00382
0.6	0.05440	0.04248	0.04009	0.03695	0.03231	0.02712	0.02372	0.02112	0.01898	0.01708	0.01540	0.01386	0.01245	0.01111	0.00864	0.00635	0.00417	0.00208
0.8	0.06709	0.05239	0.04944	0.04556	0.03985	0.03344	0.02925	0.02604	0.02340	0.02106	0.01899	0.01710	0.01535	0.01370	0.01065	0.00783	0.00514	0.00256
1	0.07877	0.06151	0.05805	0.05349	0.04678	0.03926	0.03435	0.03058	0.02747	0.02473	0.02229	0.02007	0.01802	0.01609	0.01251	0.00919	0.00604	0.00301
1.2	0.07378	0.05761	0.05437	0.05010	0.04382	0.03678	0.03217	0.02864	0.02573	0.02316	0.02088	0.01880	0.01688	0.01507	0.01171	0.00861	0.00566	0.00282
1.4	0.07406	0.05784	0.05458	0.05030	0.04399	0.03692	0.03230	0.02875	0.02583	0.02325	0.02096	0.01887	0.01694	0.01513	0.01176	0.00864	0.00568	0.00283
1.6	0.07193	0.05617	0.05301	0.04884	0.04272	0.03585	0.03136	0.02792	0.02509	0.02258	0.02036	0.01833	0.01646	0.01469	0.01142	0.00839	0.00551	0.00275
1.8	0.05296	0.04135	0.03903	0.03596	0.03145	0.02640	0.02309	0.02056	0.01847	0.01662	0.01499	0.01350	0.01212	0.01082	0.00841	0.00618	0.00406	0.00202
2	0.04819	0.03763	0.03551	0.03272	0.02862	0.02402	0.02101	0.01870	0.01681	0.01513	0.01364	0.01228	0.01102	0.00984	0.00765	0.00562	0.00369	0.00184
2.2	0.03772	0.02945	0.02780	0.02561	0.02240	0.01880	0.01645	0.01464	0.01316	0.01184	0.01068	0.00961	0.00863	0.00770	0.00599	0.00440	0.00289	0.00144
2.4	0.03050	0.02382	0.02248	0.02071	0.01811	0.01520	0.01330	0.01184	0.01064	0.00957	0.00863	0.00777	0.00698	0.00623	0.00484	0.00356	0.00234	0.00116
2.6	0.03143	0.02454	0.02316	0.02134	0.01867	0.01567	0.01370	0.01220	0.01096	0.00987	0.00890	0.00801	0.00719	0.00642	0.00499	0.00367	0.00241	0.00120
2.8	0.02977	0.02325	0.02194	0.02022	0.01768	0.01484	0.01298	0.01156	0.01038	0.00935	0.00843	0.00759	0.00681	0.00608	0.00473	0.00347	0.00228	0.00114
3	0.03862	0.03016	0.02846	0.02623	0.02294	0.01925	0.01684	0.01499	0.01347	0.01212	0.01093	0.00984	0.00884	0.00789	0.00613	0.00451	0.00296	0.00147
3.2	0.03744	0.02924	0.02759	0.02543	0.02224	0.01866	0.01633	0.01453	0.01306	0.01175	0.01060	0.00954	0.00857	0.00765	0.00595	0.00437	0.00287	0.00143
3.4	0.03837	0.02996	0.02828	0.02606	0.02279	0.01913	0.01673	0.01489	0.01338	0.01205	0.01086	0.00978	0.00878	0.00784	0.00609	0.00448	0.00294	0.00147
3.6	0.02243	0.01752	0.01653	0.01523	0.01332	0.01118	0.00978	0.00871	0.00782	0.00704	0.00635	0.00572	0.00513	0.00458	0.00356	0.00262	0.00172	0.00086
3.8	0.02491	0.01945	0.01836	0.01692	0.01480	0.01242	0.01086	0.00967	0.00869	0.00782	0.00705	0.00635	0.00570	0.00509	0.00396	0.00291	0.00191	0.00095
4	0.02432	0.01900	0.01793	0.01652	0.01445	0.01213	0.01061	0.00944	0.00848	0.00764	0.00688	0.00620	0.00557	0.00497	0.00386	0.00284	0.00186	0.00093

Mean difference between predicted and observed values (m)

CONFIDENCE INTERVAL %																		
SAMPLING DENSITY points per square metre		99.90	99.00	98.50	97.50	95.00	90.00	85.00	80.00	75.00	70.00	65.00	60.00	55.00	50.00	40.00	30.00	20.00	10.00
	0.2	0.00520	0.00406	0.00383	0.00353	0.00309	0.00259	0.00227	0.00202	0.00181	0.00163	0.00147	0.00132	0.00119	0.00106	0.00083	0.00061	0.00040	0.00020
	0.4	0.00312	0.00244	0.00230	0.00212	0.00186	0.00156	0.00136	0.00121	0.00109	0.00098	0.00088	0.00080	0.00071	0.00064	0.00050	0.00036	0.00024	0.00012
	0.6	0.00144	0.00113	0.00106	0.00098	0.00086	0.00072	0.00063	0.00056	0.00050	0.00045	0.00041	0.00037	0.00033	0.00029	0.00023	0.00017	0.00011	0.00006
	0.8	0.00079	0.00062	0.00058	0.00054	0.00047	0.00039	0.00034	0.00031	0.00027	0.00025	0.00022	0.00020	0.00018	0.00016	0.00013	0.00009	0.00006	0.00003
	1	0.00112	0.00087	0.00082	0.00076	0.00066	0.00056	0.00049	0.00043	0.00039	0.00035	0.00032	0.00028	0.00026	0.00023	0.00018	0.00013	0.00009	0.00004
	1.2	0.00102	0.00079	0.00075	0.00069	0.00060	0.00051	0.00044	0.00040	0.00036	0.00032	0.00029	0.00026	0.00023	0.00021	0.00016	0.00012	0.00008	0.00004
	1.4	0.00065	0.00051	0.00048	0.00044	0.00039	0.00032	0.00028	0.00025	0.00023	0.00020	0.00018	0.00017	0.00015	0.00013	0.00010	0.00008	0.00005	0.00002
	1.6	0.00050	0.00039	0.00036	0.00034	0.00029	0.00025	0.00022	0.00019	0.00017	0.00016	0.00014	0.00013	0.00011	0.00010	0.00008	0.00006	0.00004	0.00002
	1.8	0.00044	0.00035	0.00033	0.00030	0.00026	0.00022	0.00019	0.00017	0.00015	0.00014	0.00013	0.00011	0.00010	0.00009	0.00007	0.00005	0.00003	0.00002
	2	0.00041	0.00032	0.00030	0.00028	0.00024	0.00020	0.00018	0.00016	0.00014	0.00013	0.00012	0.00010	0.00009	0.00008	0.00006	0.00005	0.00003	0.00002
	2.2	0.00032	0.00025	0.00024	0.00022	0.00019	0.00016	0.00014	0.00013	0.00011	0.00010	0.00009	0.00008	0.00007	0.00007	0.00005	0.00004	0.00002	0.00001
	2.4	0.00031	0.00025	0.00023	0.00021	0.00019	0.00016	0.00014	0.00012	0.00011	0.00010	0.00009	0.00008	0.00007	0.00006	0.00005	0.00004	0.00002	0.00001
	2.6	0.00026	0.00020	0.00019	0.00018	0.00015	0.00013	0.00011	0.00010	0.00009	0.00008	0.00007	0.00007	0.00006	0.00005	0.00004	0.00003	0.00002	0.00001
	2.8	0.00023	0.00018	0.00017	0.00015	0.00013	0.00011	0.00010	0.00009	0.00008	0.00007	0.00006	0.00006	0.00005	0.00005	0.00004	0.00003	0.00002	0.00001
	3	0.00013	0.00010	0.00010	0.00009	0.00008	0.00007	0.00006	0.00005	0.00005	0.00004	0.00004	0.00003	0.00003	0.00003	0.00002	0.00002	0.00001	0.00001
	3.2	0.00009	0.00007	0.00007	0.00006	0.00006	0.00005	0.00004	0.00004	0.00003	0.00003	0.00003	0.00002	0.00002	0.00002	0.00002	0.00001	0.00001	0.00000
	3.4	0.00007	0.00005	0.00005	0.00005	0.00004	0.00003	0.00003	0.00003	0.00002	0.00002	0.00002	0.00002	0.00002	0.00001	0.00001	0.00001	0.00001	0.00000
	3.6	0.00006	0.00005	0.00005	0.00004	0.00004	0.00003	0.00003	0.00002	0.00002	0.00002	0.00002	0.00002	0.00001	0.00001	0.00001	0.00001	0.00000	0.00000
	3.8	0.00004	0.00003	0.00003	0.00003	0.00002	0.00002	0.00002	0.00002	0.00001	0.00001	0.00001	0.00001	0.00001	0.00001	0.00001	0.00000	0.00000	0.00000
	4	0.00000	0.00000	0.00000	0.00000	0.00000	0.00000	0.00000	0.00000	0.00000	0.00000	0.00000	0.00000	0.00000	0.00000	0.00000	0.00000	0.00000	0.00000

Maximum square error

SAMPLING DENSITY points per square metre	CONFIDENCE INTERVAL %																	
	99.90	**99.00**	**98.50**	**97.50**	**95.00**	**90.00**	**85.00**	**80.00**	**75.00**	**70.00**	**65.00**	**60.00**	**55.00**	**50.00**	**40.00**	**30.00**	**20.00**	**10.00**
0.2	0.06585	0.05143	0.04853	0.04472	0.03911	0.03283	0.02872	0.02556	0.02297	0.02067	0.01864	0.01678	0.01507	0.01345	0.01046	0.00768	0.00505	0.00251
0.4	0.06078	0.04746	0.04479	0.04127	0.03610	0.03030	0.02650	0.02359	0.02120	0.01908	0.01720	0.01549	0.01391	0.01241	0.00965	0.00709	0.00466	0.00232
0.6	0.04384	0.03423	0.03231	0.02977	0.02604	0.02185	0.01912	0.01702	0.01529	0.01376	0.01241	0.01117	0.01003	0.00895	0.00696	0.00511	0.00336	0.00167
0.8	0.04568	0.03568	0.03367	0.03102	0.02713	0.02277	0.01992	0.01773	0.01593	0.01434	0.01293	0.01164	0.01045	0.00933	0.00725	0.00533	0.00350	0.00174
1	0.04952	0.03867	0.03650	0.03363	0.02941	0.02469	0.02160	0.01922	0.01727	0.01555	0.01402	0.01262	0.01133	0.01011	0.00786	0.00578	0.00380	0.00189
1.2	0.04886	0.03815	0.03600	0.03318	0.02902	0.02435	0.02130	0.01896	0.01704	0.01534	0.01383	0.01245	0.01118	0.00998	0.00776	0.00570	0.00375	0.00187
1.4	0.02862	0.02235	0.02109	0.01944	0.01700	0.01427	0.01248	0.01111	0.00998	0.00898	0.00810	0.00729	0.00655	0.00585	0.00454	0.00334	0.00219	0.00109
1.6	0.02693	0.02103	0.01985	0.01829	0.01599	0.01342	0.01174	0.01045	0.00939	0.00845	0.00762	0.00686	0.00616	0.00550	0.00428	0.00314	0.00206	0.00103
1.8	0.01734	0.01354	0.01278	0.01178	0.01030	0.00864	0.00756	0.00673	0.00605	0.00544	0.00491	0.00442	0.00397	0.00354	0.00275	0.00202	0.00133	0.00066
2	0.01674	0.01307	0.01233	0.01137	0.00994	0.00834	0.00730	0.00650	0.00584	0.00525	0.00474	0.00427	0.00383	0.00342	0.00266	0.00195	0.00128	0.00064
2.2	0.01352	0.01056	0.00996	0.00918	0.00803	0.00674	0.00589	0.00525	0.00471	0.00424	0.00383	0.00344	0.00309	0.00276	0.00215	0.00158	0.00104	0.00052
2.4	0.01163	0.00909	0.00857	0.00790	0.00691	0.00580	0.00507	0.00452	0.00406	0.00365	0.00329	0.00297	0.00266	0.00238	0.00185	0.00136	0.00089	0.00044
2.6	0.01090	0.00851	0.00803	0.00740	0.00647	0.00543	0.00475	0.00423	0.00380	0.00342	0.00308	0.00278	0.00249	0.00223	0.00173	0.00127	0.00084	0.00042
2.8	0.01070	0.00836	0.00789	0.00727	0.00636	0.00533	0.00467	0.00415	0.00373	0.00336	0.00303	0.00273	0.00245	0.00219	0.00170	0.00125	0.00082	0.00041
3	0.00945	0.00738	0.00697	0.00642	0.00562	0.00471	0.00412	0.00367	0.00330	0.00297	0.00268	0.00241	0.00216	0.00193	0.00150	0.00110	0.00072	0.00036
3.2	0.00898	0.00702	0.00662	0.00610	0.00534	0.00448	0.00392	0.00349	0.00313	0.00282	0.00254	0.00229	0.00206	0.00183	0.00143	0.00105	0.00069	0.00034
3.4	0.00842	0.00657	0.00620	0.00572	0.00500	0.00420	0.00367	0.00327	0.00294	0.00264	0.00238	0.00215	0.00193	0.00172	0.00134	0.00098	0.00065	0.00032
3.6	0.00783	0.00611	0.00577	0.00532	0.00465	0.00390	0.00341	0.00304	0.00273	0.00246	0.00222	0.00199	0.00179	0.00160	0.00124	0.00091	0.00060	0.00030
3.8	0.00421	0.00329	0.00310	0.00286	0.00250	0.00210	0.00184	0.00164	0.00147	0.00132	0.00119	0.00107	0.00096	0.00086	0.00067	0.00049	0.00032	0.00016
4	0.00283	0.00221	0.00208	0.00192	0.00168	0.00141	0.00123	0.00110	0.00099	0.00089	0.00080	0.00072	0.00065	0.00058	0.00045	0.00033	0.00022	0.00011

Mean Square Error

	CONFIDENCE INTERVAL %																	
SAMPLING DENSITY points per square metre	**99.90**	**99.00**	**98.50**	**97.50**	**95.00**	**90.00**	**85.00**	**80.00**	**75.00**	**70.00**	**65.00**	**60.00**	**55.00**	**50.00**	**40.00**	**30.00**	**20.00**	**10.00**
0.2	0.004398	0.003435	0.003241	0.002987	0.002612	0.002193	0.001918	0.001707	0.001534	0.001381	0.001245	0.001121	0.001006	0.000898	0.000698	0.000513	0.000337	0.000168
0.4	0.002041	0.001594	0.001504	0.001386	0.001212	0.001017	0.000890	0.000792	0.000712	0.000641	0.000578	0.000520	0.000467	0.000417	0.000324	0.000238	0.000156	0.000078
0.6	0.001184	0.000924	0.000872	0.000804	0.000703	0.000590	0.000516	0.000459	0.000413	0.000372	0.000335	0.000302	0.000271	0.000242	0.000188	0.000138	0.000091	0.000045
0.8	0.001822	0.001423	0.001343	0.001237	0.001082	0.000908	0.000794	0.000707	0.000635	0.000572	0.000516	0.000464	0.000417	0.000372	0.000289	0.000213	0.000140	0.000070
1	0.001733	0.001354	0.001277	0.001177	0.001030	0.000864	0.000756	0.000673	0.000605	0.000544	0.000491	0.000442	0.000397	0.000354	0.000275	0.000202	0.000133	0.000066
1.2	0.001751	0.001367	0.001290	0.001189	0.001040	0.000873	0.000763	0.000680	0.000611	0.000550	0.000495	0.000446	0.000400	0.000358	0.000278	0.000204	0.000134	0.000067
1.4	0.001516	0.001184	0.001118	0.001030	0.000901	0.000756	0.000661	0.000589	0.000529	0.000476	0.000429	0.000386	0.000347	0.000310	0.000241	0.000177	0.000116	0.000058
1.6	0.001349	0.001053	0.000994	0.000916	0.000801	0.000672	0.000588	0.000524	0.000471	0.000424	0.000382	0.000344	0.000309	0.000276	0.000214	0.000157	0.000103	0.000052
1.8	0.000145	0.000113	0.000107	0.000099	0.000086	0.000072	0.000063	0.000056	0.000051	0.000046	0.000041	0.000037	0.000033	0.000030	0.000023	0.000017	0.000011	0.000006
2	0.000118	0.000092	0.000087	0.000080	0.000070	0.000059	0.000051	0.000046	0.000041	0.000037	0.000033	0.000030	0.000027	0.000024	0.000019	0.000014	0.000009	0.000005
2.2	0.000093	0.000073	0.000069	0.000063	0.000055	0.000046	0.000041	0.000036	0.000032	0.000029	0.000026	0.000024	0.000021	0.000019	0.000015	0.000011	0.000007	0.000004
2.4	0.000077	0.000060	0.000057	0.000052	0.000046	0.000038	0.000034	0.000030	0.000027	0.000024	0.000022	0.000020	0.000018	0.000016	0.000012	0.000009	0.000006	0.000003
2.6	0.000065	0.000051	0.000048	0.000044	0.000039	0.000032	0.000028	0.000025	0.000023	0.000020	0.000018	0.000017	0.000015	0.000013	0.000010	0.000008	0.000005	0.000002
2.8	0.000057	0.000044	0.000042	0.000039	0.000034	0.000028	0.000025	0.000022	0.000020	0.000018	0.000016	0.000014	0.000013	0.000012	0.000009	0.000007	0.000004	0.000002
3	0.000050	0.000039	0.000037	0.000034	0.000030	0.000025	0.000022	0.000019	0.000018	0.000016	0.000014	0.000013	0.000011	0.000010	0.000008	0.000006	0.000004	0.000002
3.2	0.000039	0.000030	0.000028	0.000026	0.000023	0.000019	0.000017	0.000015	0.000013	0.000012	0.000011	0.000010	0.000009	0.000008	0.000006	0.000005	0.000003	0.000001
3.4	0.000031	0.000024	0.000023	0.000021	0.000019	0.000016	0.000014	0.000012	0.000011	0.000010	0.000009	0.000008	0.000007	0.000006	0.000005	0.000004	0.000002	0.000001
3.6	0.000027	0.000021	0.000020	0.000019	0.000016	0.000014	0.000012	0.000011	0.000010	0.000009	0.000008	0.000007	0.000006	0.000006	0.000004	0.000003	0.000002	0.000001
3.8	0.000026	0.000021	0.000019	0.000018	0.000016	0.000013	0.000011	0.000010	0.000009	0.000008	0.000007	0.000007	0.000006	0.000005	0.000004	0.000003	0.000002	0.000001
4	0.000026	0.000020	0.000019	0.000017	0.000015	0.000013	0.000011	0.000010	0.000009	0.000008	0.000007	0.000007	0.000006	0.000005	0.000004	0.000003	0.000002	0.000001

Maximum predicted depth (m)

SAMPLING DENSITY points per square metre	CONFIDENCE INTERVAL %																	
	99.90	**99.00**	**98.50**	**97.50**	**95.00**	**90.00**	**85.00**	**80.00**	**75.00**	**70.00**	**65.00**	**60.00**	**55.00**	**50.00**	**40.00**	**30.00**	**20.00**	**10.00**
0.2	0.10974	0.08570	0.08088	0.07452	0.06518	0.05470	0.04785	0.04260	0.03828	0.03445	0.03106	0.02797	0.02511	0.02241	0.01743	0.01280	0.00841	0.00419
0.4	0.05225	0.04080	0.03851	0.03548	0.03103	0.02605	0.02278	0.02028	0.01822	0.01640	0.01479	0.01332	0.01195	0.01067	0.00830	0.00610	0.00401	0.00199
0.6	0.03445	0.02690	0.02539	0.02340	0.02046	0.01717	0.01502	0.01337	0.01202	0.01082	0.00975	0.00878	0.00788	0.00704	0.00547	0.00402	0.00264	0.00132
0.8	0.07961	0.06217	0.05867	0.05406	0.04728	0.03968	0.03471	0.03090	0.02777	0.02499	0.02253	0.02029	0.01821	0.01626	0.01264	0.00929	0.00610	0.00304
1	0.08148	0.06363	0.06005	0.05533	0.04839	0.04062	0.03553	0.03163	0.02842	0.02558	0.02306	0.02076	0.01864	0.01664	0.01294	0.00951	0.00625	0.00311
1.2	0.08076	0.06306	0.05952	0.05484	0.04796	0.04026	0.03521	0.03135	0.02817	0.02535	0.02286	0.02058	0.01848	0.01649	0.01282	0.00942	0.00619	0.00308
1.4	0.07724	0.06032	0.05693	0.05246	0.04588	0.03851	0.03368	0.02998	0.02694	0.02425	0.02186	0.01969	0.01767	0.01578	0.01227	0.00901	0.00592	0.00295
1.6	0.07286	0.05689	0.05369	0.04948	0.04327	0.03632	0.03177	0.02828	0.02541	0.02287	0.02062	0.01857	0.01667	0.01488	0.01157	0.00850	0.00559	0.00278
1.8	0.00671	0.00524	0.00494	0.00456	0.00399	0.00334	0.00293	0.00260	0.00234	0.00211	0.00190	0.00171	0.00154	0.00137	0.00107	0.00078	0.00051	0.00026
2	0.00655	0.00512	0.00483	0.00445	0.00389	0.00327	0.00286	0.00254	0.00229	0.00206	0.00186	0.00167	0.00150	0.00134	0.00104	0.00076	0.00050	0.00025
2.2	0.00208	0.00162	0.00153	0.00141	0.00124	0.00104	0.00091	0.00081	0.00073	0.00065	0.00059	0.00053	0.00048	0.00042	0.00033	0.00024	0.00016	0.00008
2.4	0.00191	0.00149	0.00141	0.00130	0.00113	0.00095	0.00083	0.00074	0.00067	0.00060	0.00054	0.00049	0.00044	0.00039	0.00030	0.00022	0.00015	0.00007
2.6	0.00186	0.00145	0.00137	0.00126	0.00110	0.00093	0.00081	0.00072	0.00065	0.00058	0.00053	0.00047	0.00043	0.00038	0.00030	0.00022	0.00014	0.00007
2.8	0.00180	0.00141	0.00133	0.00122	0.00107	0.00090	0.00079	0.00070	0.00063	0.00057	0.00051	0.00046	0.00041	0.00037	0.00029	0.00021	0.00014	0.00007
3	0.00902	0.00705	0.00665	0.00613	0.00536	0.00450	0.00394	0.00350	0.00315	0.00283	0.00255	0.00230	0.00206	0.00184	0.00143	0.00105	0.00069	0.00034
3.2	0.00087	0.00068	0.00064	0.00059	0.00052	0.00044	0.00038	0.00034	0.00031	0.00027	0.00025	0.00022	0.00020	0.00018	0.00014	0.00010	0.00007	0.00003
3.4	0.00030	0.00024	0.00022	0.00020	0.00018	0.00015	0.00013	0.00012	0.00010	0.00009	0.00009	0.00008	0.00007	0.00006	0.00005	0.00004	0.00002	0.00001
3.6	0.00019	0.00015	0.00014	0.00013	0.00011	0.00009	0.00008	0.00007	0.00007	0.00006	0.00005	0.00005	0.00004	0.00004	0.00003	0.00002	0.00001	0.00001
3.8	0.00009	0.00007	0.00007	0.00006	0.00006	0.00005	0.00004	0.00004	0.00003	0.00003	0.00003	0.00002	0.00002	0.00002	0.00001	0.00001	0.00001	0.00000
4	0.00000	0.00000	0.00000	0.00000	0.00000	0.00000	0.00000	0.00000	0.00000	0.00000	0.00000	0.00000	0.00000	0.00000	0.00000	0.00000	0.00000	0.00000

Minimum depth predicted (m)

CONFIDENCE INTERVAL %																		
SAMPLING DENSITY points per square metre		99.90	99.00	98.50	97.50	95.00	90.00	85.00	80.00	75.00	70.00	65.00	60.00	55.00	50.00	40.00	30.00	20.00	10.00
	0.2	0.09194	0.07180	0.06776	0.06244	0.05461	0.04583	0.04009	0.03569	0.03207	0.02886	0.02602	0.02343	0.02103	0.01878	0.01460	0.01073	0.00705	0.00351
	0.4	0.03716	0.02902	0.02739	0.02524	0.02207	0.01852	0.01620	0.01443	0.01296	0.01167	0.01052	0.00947	0.00850	0.00759	0.00590	0.00434	0.00285	0.00142
	0.6	0.02494	0.01948	0.01838	0.01694	0.01481	0.01243	0.01088	0.00968	0.00870	0.00783	0.00706	0.00636	0.00571	0.00509	0.00396	0.00291	0.00191	0.00095
	0.8	0.02878	0.02248	0.02121	0.01955	0.01709	0.01435	0.01255	0.01117	0.01004	0.00904	0.00815	0.00734	0.00659	0.00588	0.00457	0.00336	0.00221	0.00110
	1	0.02409	0.01881	0.01775	0.01636	0.01431	0.01201	0.01050	0.00935	0.00840	0.00756	0.00682	0.00614	0.00551	0.00492	0.00382	0.00281	0.00185	0.00092
	1.2	0.02646	0.02066	0.01950	0.01797	0.01572	0.01319	0.01154	0.01027	0.00923	0.00831	0.00749	0.00674	0.00605	0.00540	0.00420	0.00309	0.00203	0.00101
	1.4	0.02107	0.01646	0.01553	0.01431	0.01252	0.01050	0.00919	0.00818	0.00735	0.00662	0.00596	0.00537	0.00482	0.00430	0.00335	0.00246	0.00162	0.00080
	1.6	0.01931	0.01508	0.01423	0.01311	0.01147	0.00963	0.00842	0.00750	0.00673	0.00606	0.00547	0.00492	0.00442	0.00394	0.00307	0.00225	0.00148	0.00074
	1.8	0.01145	0.00894	0.00844	0.00777	0.00680	0.00571	0.00499	0.00444	0.00399	0.00359	0.00324	0.00292	0.00262	0.00234	0.00182	0.00134	0.00088	0.00044
	2	0.00937	0.00732	0.00691	0.00636	0.00556	0.00467	0.00409	0.00364	0.00327	0.00294	0.00265	0.00239	0.00214	0.00191	0.00149	0.00109	0.00072	0.00036
	2.2	0.00852	0.00665	0.00628	0.00579	0.00506	0.00425	0.00372	0.00331	0.00297	0.00268	0.00241	0.00217	0.00195	0.00174	0.00135	0.00099	0.00065	0.00033
	2.4	0.00782	0.00611	0.00577	0.00531	0.00465	0.00390	0.00341	0.00304	0.00273	0.00246	0.00221	0.00199	0.00179	0.00160	0.00124	0.00091	0.00060	0.00030
	2.6	0.00794	0.00620	0.00585	0.00539	0.00472	0.00396	0.00346	0.00308	0.00277	0.00249	0.00225	0.00202	0.00182	0.00162	0.00126	0.00093	0.00061	0.00030
	2.8	0.00436	0.00341	0.00321	0.00296	0.00259	0.00217	0.00190	0.00169	0.00152	0.00137	0.00123	0.00111	0.00100	0.00089	0.00069	0.00051	0.00033	0.00017
	3	0.00816	0.00637	0.00601	0.00554	0.00485	0.00407	0.00356	0.00317	0.00285	0.00256	0.00231	0.00208	0.00187	0.00167	0.00130	0.00095	0.00063	0.00031
	3.2	0.00217	0.00169	0.00160	0.00147	0.00129	0.00108	0.00094	0.00084	0.00076	0.00068	0.00061	0.00055	0.00050	0.00044	0.00034	0.00025	0.00017	0.00008
	3.4	0.00219	0.00171	0.00161	0.00148	0.00130	0.00109	0.00095	0.00085	0.00076	0.00069	0.00062	0.00056	0.00050	0.00045	0.00035	0.00026	0.00017	0.00008
	3.6	0.00017	0.00013	0.00013	0.00012	0.00010	0.00009	0.00007	0.00007	0.00006	0.00005	0.00005	0.00004	0.00004	0.00004	0.00003	0.00002	0.00001	0.00001
	3.8	0.00015	0.00012	0.00011	0.00010	0.00009	0.00007	0.00007	0.00006	0.00005	0.00005	0.00004	0.00004	0.00003	0.00003	0.00002	0.00002	0.00001	0.00001
	4	0.00001	0.00000	0.00000	0.00000	0.00000	0.00000	0.00000	0.00000	0.00000	0.00000	0.00000	0.00000	0.00000	0.00000	0.00000	0.00000	0.00000	0.00000

Mean predicted depth (m)

	CONFIDENCE INTERVAL %																	
SAMPLING DENSITY points per square metre		99.90	99.00	98.50	97.50	95.00	90.00	85.00	80.00	75.00	70.00	65.00	60.00	55.00	50.00	40.00	30.00	20.00	10.00
	0.2	0.00578	0.00452	0.00426	0.00393	0.00343	0.00288	0.00252	0.00224	0.00202	0.00182	0.00164	0.00147	0.00132	0.00118	0.00092	0.00067	0.00044	0.00022
	0.4	0.00323	0.00252	0.00238	0.00219	0.00192	0.00161	0.00141	0.00125	0.00113	0.00101	0.00091	0.00082	0.00074	0.00066	0.00051	0.00038	0.00025	0.00012
	0.6	0.00137	0.00107	0.00101	0.00093	0.00081	0.00068	0.00060	0.00053	0.00048	0.00043	0.00039	0.00035	0.00031	0.00028	0.00022	0.00016	0.00010	0.00005
	0.8	0.00083	0.00065	0.00061	0.00056	0.00049	0.00041	0.00036	0.00032	0.00029	0.00026	0.00023	0.00021	0.00019	0.00017	0.00013	0.00010	0.00006	0.00003
	1	0.00113	0.00089	0.00084	0.00077	0.00067	0.00057	0.00049	0.00044	0.00040	0.00036	0.00032	0.00029	0.00026	0.00023	0.00018	0.00013	0.00009	0.00004
	1.2	0.00101	0.00079	0.00075	0.00069	0.00060	0.00050	0.00044	0.00039	0.00035	0.00032	0.00029	0.00026	0.00023	0.00021	0.00016	0.00012	0.00008	0.00004
	1.4	0.00066	0.00051	0.00048	0.00045	0.00039	0.00033	0.00029	0.00025	0.00023	0.00021	0.00019	0.00017	0.00015	0.00013	0.00010	0.00008	0.00005	0.00003
	1.6	0.00054	0.00042	0.00040	0.00037	0.00032	0.00027	0.00024	0.00021	0.00019	0.00017	0.00015	0.00014	0.00012	0.00011	0.00009	0.00006	0.00004	0.00002
	1.8	0.00043	0.00034	0.00032	0.00029	0.00026	0.00022	0.00019	0.00017	0.00015	0.00014	0.00012	0.00011	0.00010	0.00009	0.00007	0.00005	0.00003	0.00002
	2	0.00038	0.00030	0.00028	0.00026	0.00023	0.00019	0.00017	0.00015	0.00013	0.00012	0.00011	0.00010	0.00009	0.00008	0.00006	0.00004	0.00003	0.00001
	2.2	0.00033	0.00025	0.00024	0.00022	0.00019	0.00016	0.00014	0.00013	0.00011	0.00010	0.00009	0.00008	0.00007	0.00007	0.00005	0.00004	0.00003	0.00001
	2.4	0.00032	0.00025	0.00023	0.00021	0.00019	0.00016	0.00014	0.00012	0.00011	0.00010	0.00009	0.00008	0.00007	0.00006	0.00005	0.00004	0.00002	0.00001
	2.6	0.00026	0.00021	0.00019	0.00018	0.00016	0.00013	0.00012	0.00010	0.00009	0.00008	0.00007	0.00007	0.00006	0.00005	0.00004	0.00003	0.00002	0.00001
	2.8	0.00023	0.00018	0.00017	0.00015	0.00013	0.00011	0.00010	0.00009	0.00008	0.00007	0.00006	0.00006	0.00005	0.00005	0.00004	0.00003	0.00002	0.00001
	3	0.00013	0.00010	0.00010	0.00009	0.00008	0.00006	0.00006	0.00005	0.00005	0.00004	0.00004	0.00003	0.00003	0.00003	0.00002	0.00002	0.00001	0.00000
	3.2	0.00009	0.00007	0.00007	0.00006	0.00006	0.00005	0.00004	0.00004	0.00003	0.00003	0.00003	0.00002	0.00002	0.00002	0.00001	0.00001	0.00001	0.00000
	3.4	0.00007	0.00005	0.00005	0.00005	0.00004	0.00003	0.00003	0.00003	0.00002	0.00002	0.00002	0.00002	0.00002	0.00001	0.00001	0.00001	0.00001	0.00000
	3.6	0.00006	0.00005	0.00005	0.00004	0.00004	0.00003	0.00003	0.00002	0.00002	0.00002	0.00002	0.00002	0.00001	0.00001	0.00001	0.00001	0.00000	0.00000
	3.8	0.00004	0.00003	0.00003	0.00003	0.00003	0.00002	0.00002	0.00002	0.00002	0.00001	0.00001	0.00001	0.00001	0.00001	0.00001	0.00001	0.00000	0.00000
	4	0.00000	0.00000	0.00000	0.00000	0.00000	0.00000	0.00000	0.00000	0.00000	0.00000	0.00000	0.00000	0.00000	0.00000	0.00000	0.00000	0.00000	0.00000

Standard deviation of the predicted values

SAMPLING DENSITY points per square metre	CONFIDENCE INTERVAL %																	
		99.90	99.00	98.50	97.50	95.00	90.00	85.00	80.00	75.00	70.00	65.00	60.00	55.00	50.00	40.00	30.00	20.00	10.00
	0.2	0.03008	0.02349	0.02217	0.02042	0.01786	0.01499	0.01312	0.01168	0.01049	0.00944	0.00851	0.00766	0.00688	0.00614	0.00478	0.00351	0.00231	0.00115
	0.4	0.01397	0.01091	0.01030	0.00949	0.00830	0.00696	0.00609	0.00542	0.00487	0.00439	0.00395	0.00356	0.00320	0.00285	0.00222	0.00163	0.00107	0.00053
	0.6	0.00987	0.00771	0.00727	0.00670	0.00586	0.00492	0.00430	0.00383	0.00344	0.00310	0.00279	0.00252	0.00226	0.00202	0.00157	0.00115	0.00076	0.00038
	0.8	0.01536	0.01199	0.01132	0.01043	0.00912	0.00766	0.00670	0.00596	0.00536	0.00482	0.00435	0.00391	0.00351	0.00314	0.00244	0.00179	0.00118	0.00059
	1	0.01461	0.01141	0.01077	0.00992	0.00868	0.00728	0.00637	0.00567	0.00510	0.00459	0.00414	0.00372	0.00334	0.00298	0.00232	0.00170	0.00112	0.00056
	1.2	0.01530	0.01195	0.01127	0.01039	0.00909	0.00763	0.00667	0.00594	0.00534	0.00480	0.00433	0.00390	0.00350	0.00312	0.00243	0.00178	0.00117	0.00058
	1.4	0.01387	0.01083	0.01022	0.00942	0.00824	0.00691	0.00605	0.00538	0.00484	0.00435	0.00393	0.00354	0.00317	0.00283	0.00220	0.00162	0.00106	0.00053
	1.6	0.01314	0.01026	0.00969	0.00893	0.00781	0.00655	0.00573	0.00510	0.00458	0.00413	0.00372	0.00335	0.00301	0.00268	0.00209	0.00153	0.00101	0.00050
	1.8	0.00104	0.00081	0.00077	0.00071	0.00062	0.00052	0.00045	0.00040	0.00036	0.00033	0.00029	0.00027	0.00024	0.00021	0.00017	0.00012	0.00008	0.00004
	2	0.00083	0.00065	0.00061	0.00056	0.00049	0.00041	0.00036	0.00032	0.00029	0.00026	0.00023	0.00021	0.00019	0.00017	0.00013	0.00010	0.00006	0.00003
	2.2	0.00074	0.00058	0.00054	0.00050	0.00044	0.00037	0.00032	0.00029	0.00026	0.00023	0.00021	0.00019	0.00017	0.00015	0.00012	0.00009	0.00006	0.00003
	2.4	0.00060	0.00047	0.00044	0.00041	0.00035	0.00030	0.00026	0.00023	0.00021	0.00019	0.00017	0.00015	0.00014	0.00012	0.00009	0.00007	0.00005	0.00002
	2.6	0.00052	0.00040	0.00038	0.00035	0.00031	0.00026	0.00022	0.00020	0.00018	0.00016	0.00015	0.00013	0.00012	0.00011	0.00008	0.00006	0.00004	0.00002
	2.8	0.00041	0.00032	0.00030	0.00028	0.00024	0.00020	0.00018	0.00016	0.00014	0.00013	0.00012	0.00010	0.00009	0.00008	0.00007	0.00005	0.00003	0.00002
	3	0.00041	0.00032	0.00030	0.00028	0.00024	0.00020	0.00018	0.00016	0.00014	0.00013	0.00012	0.00010	0.00009	0.00008	0.00006	0.00005	0.00003	0.00002
	3.2	0.00028	0.00022	0.00021	0.00019	0.00017	0.00014	0.00012	0.00011	0.00010	0.00009	0.00008	0.00007	0.00006	0.00006	0.00004	0.00003	0.00002	0.00001
	3.4	0.00016	0.00012	0.00011	0.00011	0.00009	0.00008	0.00007	0.00006	0.00005	0.00005	0.00004	0.00004	0.00004	0.00003	0.00002	0.00002	0.00001	0.00001
	3.6	0.00009	0.00007	0.00007	0.00006	0.00006	0.00005	0.00004	0.00004	0.00003	0.00003	0.00003	0.00002	0.00002	0.00002	0.00002	0.00001	0.00001	0.00000
	3.8	0.00006	0.00005	0.00005	0.00004	0.00004	0.00003	0.00003	0.00002	0.00002	0.00002	0.00002	0.00002	0.00001	0.00001	0.00001	0.00001	0.00000	0.00000
	4	0.00001	0.00001	0.00001	0.00001	0.00001	0.00001	0.00001	0.00001	0.00001	0.00000	0.00000	0.00000	0.00000	0.00000	0.00000	0.00000	0.00000	0.00000

p-Value

SAMPLING DENSITY points per square metre	CONFIDENCE INTERVAL %																	
		99.90	**99.00**	**98.50**	**97.50**	**95.00**	**90.00**	**85.00**	**80.00**	**75.00**	**70.00**	**65.00**	**60.00**	**55.00**	**50.00**	**40.00**	**30.00**	**20.00**	**10.00**
	0.2	0.00116	0.00091	0.00086	0.00079	0.00069	0.00058	0.00051	0.00045	0.00041	0.00037	0.00033	0.00030	0.00027	0.00024	0.00018	0.00014	0.00009	0.00004
	0.4	0.18182	0.14198	0.13400	0.12347	0.10799	0.09063	0.07928	0.07058	0.06342	0.05708	0.05146	0.04634	0.04160	0.03714	0.02887	0.02121	0.01394	0.00694
	0.6	0.27973	0.21844	0.20615	0.18996	0.16614	0.13944	0.12198	0.10858	0.09756	0.08782	0.07917	0.07129	0.06400	0.05713	0.04442	0.03263	0.02145	0.01068
	0.8	0.29245	0.22837	0.21552	0.19860	0.17369	0.14578	0.12752	0.11352	0.10200	0.09181	0.08277	0.07453	0.06691	0.05973	0.04644	0.03412	0.02242	0.01117
	1	0.30626	0.23916	0.22570	0.20798	0.18190	0.15267	0.13355	0.11888	0.10682	0.09615	0.08668	0.07805	0.07007	0.06255	0.04863	0.03573	0.02348	0.01169
	1.2	0.33295	0.26000	0.24538	0.22610	0.19775	0.16597	0.14519	0.12925	0.11613	0.10453	0.09424	0.08485	0.07618	0.06800	0.05287	0.03884	0.02553	0.01271
	1.4	0.35768	0.27932	0.26360	0.24290	0.21244	0.17830	0.15597	0.13885	0.12476	0.11229	0.10123	0.09115	0.08183	0.07305	0.05680	0.04173	0.02742	0.01366
	1.6	0.34857	0.27220	0.25688	0.23671	0.20703	0.17375	0.15200	0.13531	0.12158	0.10943	0.09865	0.08883	0.07975	0.07119	0.05535	0.04067	0.02672	0.01331
	1.8	0.28455	0.22221	0.20971	0.19324	0.16901	0.14185	0.12408	0.11046	0.09925	0.08933	0.08054	0.07252	0.06510	0.05812	0.04518	0.03320	0.02182	0.01086
	2	0.28663	0.22383	0.21124	0.19465	0.17024	0.14288	0.12499	0.11126	0.09997	0.08998	0.08112	0.07305	0.06558	0.05854	0.04551	0.03344	0.02197	0.01094
	2.2	0.25731	0.20094	0.18963	0.17474	0.15283	0.12827	0.11220	0.09988	0.08975	0.08078	0.07283	0.06558	0.05887	0.05255	0.04086	0.03002	0.01973	0.00982
	2.4	0.23052	0.18001	0.16988	0.15654	0.13691	0.11491	0.10052	0.08948	0.08040	0.07237	0.06524	0.05875	0.05274	0.04708	0.03660	0.02689	0.01767	0.00880
	2.6	0.21819	0.17039	0.16080	0.14817	0.12959	0.10876	0.09514	0.08470	0.07610	0.06850	0.06175	0.05561	0.04992	0.04456	0.03465	0.02546	0.01673	0.00833
	2.8	0.21868	0.17077	0.16116	0.14850	0.12988	0.10901	0.09536	0.08489	0.07627	0.06865	0.06189	0.05573	0.05003	0.04466	0.03472	0.02551	0.01677	0.00835
	3	0.23322	0.18213	0.17188	0.15838	0.13852	0.11626	0.10170	0.09053	0.08135	0.07322	0.06601	0.05944	0.05336	0.04763	0.03703	0.02721	0.01788	0.00890
	3.2	0.21566	0.16841	0.15893	0.14645	0.12809	0.10750	0.09404	0.08371	0.07522	0.06770	0.06104	0.05496	0.04934	0.04405	0.03424	0.02516	0.01653	0.00823
	3.4	0.21354	0.16676	0.15737	0.14501	0.12683	0.10645	0.09312	0.08289	0.07448	0.06704	0.06044	0.05442	0.04886	0.04361	0.03391	0.02491	0.01637	0.00815
	3.6	0.21105	0.16481	0.15554	0.14332	0.12535	0.10521	0.09203	0.08193	0.07361	0.06626	0.05973	0.05379	0.04829	0.04311	0.03351	0.02462	0.01618	0.00806
	3.8	0.20951	0.16361	0.15441	0.14228	0.12444	0.10444	0.09136	0.08133	0.07308	0.06577	0.05930	0.05339	0.04793	0.04279	0.03327	0.02444	0.01606	0.00800
	4	0.20644	0.16121	0.15214	0.14019	0.12261	0.10291	0.09002	0.08014	0.07200	0.06481	0.05843	0.05261	0.04723	0.04216	0.03278	0.02408	0.01583	0.00788

R-squared

		CONFIDENCE INTERVAL %																	
SAMPLING DENSITY points per square metre		**99.90**	**99.00**	**98.50**	**97.50**	**95.00**	**90.00**	**85.00**	**80.00**	**75.00**	**70.00**	**65.00**	**60.00**	**55.00**	**50.00**	**40.00**	**30.00**	**20.00**	**10.00**
	0.2	0.23834	0.18612	0.17565	0.16186	0.14156	0.11881	0.10393	0.09252	0.08313	0.07483	0.06746	0.06074	0.05453	0.04868	0.03785	0.02781	0.01827	0.00910
	0.4	0.08225	0.06423	0.06061	0.05585	0.04885	0.04100	0.03587	0.03193	0.02869	0.02582	0.02328	0.02096	0.01882	0.01680	0.01306	0.00960	0.00631	0.00314
	0.6	0.05457	0.04262	0.04022	0.03706	0.03241	0.02720	0.02380	0.02118	0.01903	0.01713	0.01545	0.01391	0.01249	0.01115	0.00867	0.00637	0.00418	0.00208
	0.8	0.10991	0.08583	0.08100	0.07464	0.06528	0.05479	0.04793	0.04267	0.03834	0.03451	0.03111	0.02801	0.02515	0.02245	0.01745	0.01282	0.00843	0.00420
	1	0.10699	0.08355	0.07885	0.07266	0.06355	0.05333	0.04666	0.04153	0.03732	0.03359	0.03028	0.02727	0.02448	0.02185	0.01699	0.01248	0.00820	0.00409
	1.2	0.10440	0.08153	0.07694	0.07090	0.06201	0.05204	0.04553	0.04053	0.03641	0.03278	0.02955	0.02661	0.02389	0.02132	0.01658	0.01218	0.00800	0.00399
	1.4	0.08673	0.06773	0.06392	0.05890	0.05151	0.04323	0.03782	0.03367	0.03025	0.02723	0.02455	0.02210	0.01984	0.01771	0.01377	0.01012	0.00665	0.00331
	1.6	0.07338	0.05731	0.05408	0.04983	0.04359	0.03658	0.03200	0.02849	0.02560	0.02304	0.02077	0.01870	0.01679	0.01499	0.01165	0.00856	0.00563	0.00280
	1.8	0.01254	0.00979	0.00924	0.00851	0.00745	0.00625	0.00547	0.00487	0.00437	0.00394	0.00355	0.00319	0.00287	0.00256	0.00199	0.00146	0.00096	0.00048
	2	0.01104	0.00862	0.00814	0.00750	0.00656	0.00550	0.00482	0.00429	0.00385	0.00347	0.00313	0.00281	0.00253	0.00226	0.00175	0.00129	0.00085	0.00042
	2.2	0.00978	0.00764	0.00721	0.00664	0.00581	0.00488	0.00427	0.00380	0.00341	0.00307	0.00277	0.00249	0.00224	0.00200	0.00155	0.00114	0.00075	0.00037
	2.4	0.00890	0.00695	0.00656	0.00605	0.00529	0.00444	0.00388	0.00346	0.00311	0.00280	0.00252	0.00227	0.00204	0.00182	0.00141	0.00104	0.00068	0.00034
	2.6	0.00833	0.00650	0.00614	0.00566	0.00495	0.00415	0.00363	0.00323	0.00290	0.00261	0.00236	0.00212	0.00191	0.00170	0.00132	0.00097	0.00064	0.00032
	2.8	0.00791	0.00618	0.00583	0.00537	0.00470	0.00394	0.00345	0.00307	0.00276	0.00248	0.00224	0.00202	0.00181	0.00162	0.00126	0.00092	0.00061	0.00030
	3	0.00703	0.00549	0.00518	0.00478	0.00418	0.00351	0.00307	0.00273	0.00245	0.00221	0.00199	0.00179	0.00161	0.00144	0.00112	0.00082	0.00054	0.00027
	3.2	0.00608	0.00475	0.00448	0.00413	0.00361	0.00303	0.00265	0.00236	0.00212	0.00191	0.00172	0.00155	0.00139	0.00124	0.00097	0.00071	0.00047	0.00023
	3.4	0.00579	0.00452	0.00427	0.00393	0.00344	0.00289	0.00252	0.00225	0.00202	0.00182	0.00164	0.00148	0.00132	0.00118	0.00092	0.00068	0.00044	0.00022
	3.6	0.00554	0.00433	0.00409	0.00376	0.00329	0.00276	0.00242	0.00215	0.00193	0.00174	0.00157	0.00141	0.00127	0.00113	0.00088	0.00065	0.00043	0.00021
	3.8	0.00549	0.00428	0.00404	0.00373	0.00326	0.00273	0.00239	0.00213	0.00191	0.00172	0.00155	0.00140	0.00126	0.00112	0.00087	0.00064	0.00042	0.00021
	4	0.00528	0.00412	0.00389	0.00359	0.00314	0.00263	0.00230	0.00205	0.00184	0.00166	0.00149	0.00135	0.00121	0.00108	0.00084	0.00062	0.00040	0.00020

Range

CONFIDENCE INTERVAL %																			
SAMPLING DENSITY points per square metre		99.90	99.00	98.50	97.50	95.00	90.00	85.00	80.00	75.00	70.00	65.00	60.00	55.00	50.00	40.00	30.00	20.00	10.00
	0.2	3.327499	2.598474	2.452266	2.259675	1.976333	1.658708	1.450991	1.291675	1.160591	1.044633	0.941783	0.848008	0.761292	0.679617	0.528367	0.388208	0.255108	0.12705
	0.4	1.768384	1.380947	1.303245	1.200894	1.050313	0.881513	0.771123	0.686455	0.616791	0.555165	0.500506	0.45067	0.404585	0.361179	0.280798	0.206311	0.135576	0.06752
	0.6	1.578987	1.233045	1.163665	1.072276	0.937822	0.787101	0.688534	0.612934	0.550731	0.495706	0.446901	0.402402	0.361253	0.322496	0.250724	0.184215	0.121056	0.060289
	0.8	2.285417	1.784703	1.684283	1.552006	1.357399	1.139246	0.99658	0.887157	0.797126	0.717483	0.646842	0.582435	0.522876	0.466779	0.362897	0.266632	0.175215	0.087261
	1	1.979299	1.545653	1.458684	1.344124	1.175584	0.986651	0.863094	0.768328	0.690356	0.62138	0.560202	0.504421	0.45284	0.404257	0.314289	0.230918	0.151746	0.075573
	1.2	2.288422	1.78705	1.686498	1.554047	1.359184	1.140744	0.997891	0.888324	0.798174	0.718426	0.647693	0.583201	0.523563	0.467393	0.363374	0.266983	0.175446	0.087376
	1.4	1.965682	1.535019	1.448648	1.334877	1.167496	0.979863	0.857157	0.763042	0.685606	0.617105	0.556348	0.500951	0.449724	0.401476	0.312126	0.22933	0.150702	0.075053
	1.6	1.832118	1.430718	1.350215	1.244175	1.088167	0.913283	0.798914	0.711195	0.639021	0.575174	0.518545	0.466912	0.419166	0.374196	0.290918	0.213747	0.140462	0.069954
	1.8	0.266401	0.208035	0.196329	0.18091	0.158226	0.132797	0.116167	0.103412	0.092917	0.083634	0.0754	0.067892	0.060949	0.05441	0.042301	0.03108	0.020424	0.010172
	2	0.283282	0.221218	0.20877	0.192374	0.168252	0.141212	0.123528	0.109965	0.098805	0.088933	0.080177	0.072194	0.064812	0.057858	0.044982	0.03305	0.021718	0.010816
	2.2	0.343219	0.268023	0.252942	0.233077	0.203852	0.17109	0.149664	0.133232	0.119711	0.10775	0.097141	0.087469	0.078524	0.0701	0.054499	0.040042	0.026313	0.013105
	2.4	0.37551	0.293239	0.27674	0.255006	0.22303	0.187186	0.163745	0.145766	0.130973	0.117887	0.106281	0.095698	0.085912	0.076695	0.059626	0.04381	0.028789	0.014338
	2.6	0.310644	0.242585	0.228935	0.210956	0.184504	0.154851	0.13546	0.120586	0.108349	0.097523	0.087922	0.079167	0.071072	0.063447	0.049327	0.036242	0.023816	0.011861
	2.8	0.281867	0.220113	0.207728	0.191414	0.167412	0.140507	0.122911	0.109416	0.098312	0.088489	0.079777	0.071833	0.064488	0.057569	0.044757	0.032885	0.02161	0.010762
	3	0.173182	0.13524	0.12763	0.117606	0.10286	0.086329	0.075518	0.067226	0.060404	0.054369	0.049016	0.044135	0.039622	0.035371	0.027499	0.020205	0.013277	0.006612
	3.2	0.205266	0.160294	0.151275	0.139394	0.121916	0.102322	0.089508	0.079681	0.071594	0.064441	0.058097	0.052312	0.046962	0.041924	0.032594	0.023948	0.015737	0.007837
	3.4	0.200555	0.156615	0.147803	0.136195	0.119118	0.099974	0.087454	0.077852	0.069951	0.062962	0.056763	0.051111	0.045885	0.040962	0.031846	0.023398	0.015376	0.007658
	3.6	0.137522	0.107392	0.101349	0.09339	0.08168	0.068553	0.059968	0.053383	0.047966	0.043173	0.038923	0.035047	0.031463	0.028088	0.021837	0.016044	0.010543	0.005251
	3.8	0.137105	0.107066	0.101042	0.093106	0.081432	0.068345	0.059786	0.053221	0.04782	0.043043	0.038805	0.034941	0.031368	0.028003	0.021771	0.015996	0.010511	0.005235
	4	0.008165	0.006376	0.006017	0.005545	0.004849	0.00407	0.00356	0.003169	0.002848	0.002563	0.002311	0.002081	0.001868	0.001668	0.001296	0.000953	0.000626	0.000312

Sill

CONFIDENCE INTERVAL %																		
SAMPLING DENSITY points per square metre		99.90	99.00	98.50	97.50	95.00	90.00	85.00	80.00	75.00	70.00	65.00	60.00	55.00	50.00	40.00	30.00	20.00	10.00
	0.2	0.05572	0.04351	0.04107	0.03784	0.03310	0.02778	0.02430	0.02163	0.01944	0.01749	0.01577	0.01420	0.01275	0.01138	0.00885	0.00650	0.00427	0.00213
	0.4	0.12314	0.09616	0.09075	0.08362	0.07314	0.06138	0.05370	0.04780	0.04295	0.03866	0.03485	0.03138	0.02817	0.02515	0.01955	0.01437	0.00944	0.00470
	0.6	0.05377	0.04199	0.03963	0.03651	0.03194	0.02680	0.02345	0.02087	0.01875	0.01688	0.01522	0.01370	0.01230	0.01098	0.00854	0.00627	0.00412	0.00205
	0.8	0.12145	0.09484	0.08950	0.08247	0.07213	0.06054	0.05296	0.04714	0.04236	0.03813	0.03437	0.03095	0.02779	0.02480	0.01928	0.01417	0.00931	0.00464
	1	0.10129	0.07910	0.07465	0.06878	0.06016	0.05049	0.04417	0.03932	0.03533	0.03180	0.02867	0.02581	0.02317	0.02069	0.01608	0.01182	0.00777	0.00387
	1.2	0.06364	0.04970	0.04690	0.04322	0.03780	0.03172	0.02775	0.02470	0.02220	0.01998	0.01801	0.01622	0.01456	0.01300	0.01011	0.00742	0.00488	0.00243
	1.4	0.03265	0.02549	0.02406	0.02217	0.01939	0.01627	0.01424	0.01267	0.01139	0.01025	0.00924	0.00832	0.00747	0.00667	0.00518	0.00381	0.00250	0.00125
	1.6	0.00242	0.00189	0.00178	0.00164	0.00144	0.00121	0.00105	0.00094	0.00084	0.00076	0.00068	0.00062	0.00055	0.00049	0.00038	0.00028	0.00019	0.00009
	1.8	0.02460	0.01921	0.01813	0.01670	0.01461	0.01226	0.01073	0.00955	0.00858	0.00772	0.00696	0.00627	0.00563	0.00502	0.00391	0.00287	0.00189	0.00094
	2	0.02555	0.01995	0.01883	0.01735	0.01517	0.01273	0.01114	0.00992	0.00891	0.00802	0.00723	0.00651	0.00584	0.00522	0.00406	0.00298	0.00196	0.00098
	2.2	0.00210	0.00164	0.00155	0.00143	0.00125	0.00105	0.00092	0.00082	0.00073	0.00066	0.00060	0.00054	0.00048	0.00043	0.00033	0.00025	0.00016	0.00008
	2.4	0.00136	0.00106	0.00100	0.00092	0.00081	0.00068	0.00059	0.00053	0.00047	0.00043	0.00038	0.00035	0.00031	0.00028	0.00022	0.00016	0.00010	0.00005
	2.6	0.00300	0.00234	0.00221	0.00204	0.00178	0.00150	0.00131	0.00116	0.00105	0.00094	0.00085	0.00076	0.00069	0.00061	0.00048	0.00035	0.00023	0.00011
	2.8	0.01015	0.00793	0.00748	0.00689	0.00603	0.00506	0.00443	0.00394	0.00354	0.00319	0.00287	0.00259	0.00232	0.00207	0.00161	0.00118	0.00078	0.00039
	3	0.01650	0.01288	0.01216	0.01120	0.00980	0.00822	0.00719	0.00640	0.00575	0.00518	0.00467	0.00420	0.00377	0.00337	0.00262	0.00192	0.00126	0.00063
	3.2	0.00894	0.00698	0.00659	0.00607	0.00531	0.00446	0.00390	0.00347	0.00312	0.00281	0.00253	0.00228	0.00205	0.00183	0.00142	0.00104	0.00069	0.00034
	3.4	0.03199	0.02498	0.02357	0.02172	0.01900	0.01595	0.01395	0.01242	0.01116	0.01004	0.00905	0.00815	0.00732	0.00653	0.00508	0.00373	0.00245	0.00122
	3.6	0.00493	0.00385	0.00364	0.00335	0.00293	0.00246	0.00215	0.00191	0.00172	0.00155	0.00140	0.00126	0.00113	0.00101	0.00078	0.00058	0.00038	0.00019
	3.8	0.01435	0.01120	0.01057	0.00974	0.00852	0.00715	0.00626	0.00557	0.00500	0.00450	0.00406	0.00366	0.00328	0.00293	0.00228	0.00167	0.00110	0.00055
	4	0.00001	0.00001	0.00001	0.00001	0.00001	0.00001	0.00001	0.00001	0.00000	0.00000	0.00000	0.00000	0.00000	0.00000	0.00000	0.00000	0.00000	0.00000

Nugget

	CONFIDENCE INTERVAL %																	
SAMPLING DENSITY points per square metre		99.90	99.00	98.50	97.50	95.00	90.00	85.00	80.00	75.00	70.00	65.00	60.00	55.00	50.00	40.00	30.00	20.00	10.00
	0.2	0.00479	0.00374	0.00353	0.00325	0.00285	0.00239	0.00209	0.00186	0.00167	0.00150	0.00136	0.00122	0.00110	0.00098	0.00076	0.00056	0.00037	0.00018
	0.4	0.00285	0.00223	0.00210	0.00194	0.00169	0.00142	0.00124	0.00111	0.00099	0.00090	0.00081	0.00073	0.00065	0.00058	0.00045	0.00033	0.00022	0.00011
	0.6	0.00221	0.00172	0.00163	0.00150	0.00131	0.00110	0.00096	0.00086	0.00077	0.00069	0.00062	0.00056	0.00050	0.00045	0.00035	0.00026	0.00017	0.00008
	0.8	0.00315	0.00246	0.00232	0.00214	0.00187	0.00157	0.00137	0.00122	0.00110	0.00099	0.00089	0.00080	0.00072	0.00064	0.00050	0.00037	0.00024	0.00012
	1	0.00238	0.00186	0.00176	0.00162	0.00141	0.00119	0.00104	0.00092	0.00083	0.00075	0.00067	0.00061	0.00054	0.00049	0.00038	0.00028	0.00018	0.00009
	1.2	0.00290	0.00227	0.00214	0.00197	0.00172	0.00145	0.00127	0.00113	0.00101	0.00091	0.00082	0.00074	0.00066	0.00059	0.00046	0.00034	0.00022	0.00011
	1.4	0.00227	0.00177	0.00167	0.00154	0.00135	0.00113	0.00099	0.00088	0.00079	0.00071	0.00064	0.00058	0.00052	0.00046	0.00036	0.00026	0.00017	0.00009
	1.6	0.00219	0.00171	0.00162	0.00149	0.00130	0.00109	0.00096	0.00085	0.00076	0.00069	0.00062	0.00056	0.00050	0.00045	0.00035	0.00026	0.00017	0.00008
	1.8	0.00012	0.00009	0.00009	0.00008	0.00007	0.00006	0.00005	0.00005	0.00004	0.00004	0.00003	0.00003	0.00003	0.00002	0.00002	0.00001	0.00001	0.00000
	2	0.00002	0.00001	0.00001	0.00001	0.00001	0.00001	0.00001	0.00001	0.00001	0.00001	0.00001	0.00000	0.00000	0.00000	0.00000	0.00000	0.00000	0.00000
	2.2	0.00003	0.00002	0.00002	0.00002	0.00002	0.00002	0.00001	0.00001	0.00001	0.00001	0.00001	0.00001	0.00001	0.00001	0.00000	0.00000	0.00000	0.00000
	2.4	0.00001	0.00001	0.00001	0.00001	0.00001	0.00001	0.00001	0.00001	0.00001	0.00000	0.00000	0.00000	0.00000	0.00000	0.00000	0.00000	0.00000	0.00000
	2.6	0.00005	0.00004	0.00003	0.00003	0.00003	0.00002	0.00002	0.00002	0.00002	0.00001	0.00001	0.00001	0.00001	0.00001	0.00001	0.00001	0.00000	0.00000
	2.8	0.00005	0.00004	0.00004	0.00003	0.00003	0.00002	0.00002	0.00002	0.00002	0.00002	0.00001	0.00001	0.00001	0.00001	0.00001	0.00001	0.00000	0.00000
	3	0.00005	0.00004	0.00004	0.00003	0.00003	0.00003	0.00002	0.00002	0.00002	0.00002	0.00001	0.00001	0.00001	0.00001	0.00001	0.00001	0.00000	0.00000
	3.2	0.00006	0.00004	0.00004	0.00004	0.00003	0.00003	0.00002	0.00002	0.00002	0.00002	0.00002	0.00001	0.00001	0.00001	0.00001	0.00001	0.00000	0.00000
	3.4	0.00008	0.00006	0.00006	0.00006	0.00005	0.00004	0.00004	0.00003	0.00003	0.00003	0.00002	0.00002	0.00002	0.00002	0.00001	0.00001	0.00001	0.00000
	3.6	0.00005	0.00004	0.00003	0.00003	0.00003	0.00002	0.00002	0.00002	0.00002	0.00001	0.00001	0.00001	0.00001	0.00001	0.00001	0.00001	0.00000	0.00000
	3.8	0.00003	0.00003	0.00002	0.00002	0.00002	0.00002	0.00001	0.00001	0.00001	0.00001	0.00001	0.00001	0.00001	0.00001	0.00001	0.00000	0.00000	0.00000
	4	0.00000	0.00000	0.00000	0.00000	0.00000	0.00000	0.00000	0.00000	0.00000	0.00000	0.00000	0.00000	0.00000	0.00000	0.00000	0.00000	0.00000	0.00000

Appendix 4.4

Effect of random selection of points on the variogram model parameter – Chapter 6

This appendix is divided into two main sections: a first section containing numerical results (tables) for values of range, sill and nugget obtained for depth at different river sites and a second section with a set of graphical output for the mean values of range, sill and nugget obtained at three specific river sites.

The tables show the range, sill and nugget obtained for the spherical variogram model for the points selected randomly from the 0.5 m x 0.5 m regular grid (for sampling densities equal to 0.2 points/m^2 and 3.8 points/m^2). The values shown in the tables were the results of repeating the random selection process ten times for each river site listed. Descriptive statistics were calculated.

The plots show the mean and the Standard Error on the variogram model parameters obtained for all the sampling densities considered at three river sites. The river sites where selected according to the rate of variance encountered in the first section of this Appendix. The variogram was modelled for ten different data sets obtained by random selection of points from the 0.5 m x 0.5 m regular grid.

Results showed that the change on the variogram model parameters depended on the river site that was being analysed. High values of range, sill and nugget were the result of a bad fitting of the variogram model. Those river sites with high values of variogram model parameters were not considered for the analysis carried out in the second section of this Appendix.

The plots showed that nugget presented the highest Standard Errors (in relation to the mean), followed by the sill and the range. The Standard Error increases when decreasing the sampling density since (i) a smaller number of points is being selected for the variogram calculation and (ii) the ten randomly selected data sets have a

smaller chance to include the same points in each of these ten replications. Therefore, the decrease in Standard Error value observed when increasing the sampling density needs to be carefully analysed. Low Standard Error encountered for high sampling densities (> 3.2. points/m^2) might not indicate high stability of the variogram model parameters since higher Standard Errors could be encountered for these sampling densities when repeating the experiment for more detailed data sets. Further research is required to determine the effect that the observed variability of the variogram model parameters has on the value of the depth predictions.

River sites such as the Tame Highly Modified presented smaller Standard Errors than those encountered for the Tarf and the Bere. This was associated to the variability of depth that could be observed at each river site.

River	Number of points of the original data set	Number of points for the selected sampling strategy	Sampling density (points/m^2)	Range							
				Minimum	1stQu	Median	Mean	3rdQu	Maximum	SE	Variance
Cruick	5552	278	0.2	10.28	12.31	12.87	13.29	14.63	16.35	2.135	4.57
		5275	3.8	12.87	12.89	12.95	12.95	13.01	12.059	0.0655	0.004
Bere	1660	83	0.2	9.5	12.07	16.02	15.66	17.68	22.76	4.215	17.8
		1577	3.8	7.34	7.42	7.48	7.47	7.52	7.62	0.08	0.0069
Blackwater	3636	181	0.2	5.15	5.6	6.8	8.16	8.38	14.76	3.68	13.56
		3454	3.8	5.28	5.3	5.34	5.33	5.35	5.38	0.034	0.0011
HighlandWater	811	122	0.6	4.49	5.11	5.3	5.41	5.81	6.42	0.58	0.339
		770	3.8	5.01	5.12	5.13	5.13	5.18	5.19	0.063	0.0039
LeighBrook	6490	324	0.2	7.95	8.37	8.63	10.24	10.87	17.62	3.045	9.28
		6165	3.8	9.07	9.2	9.27	9.26	9.34	9.38	0.0955	0.0092
PangFenced	2444	122	0.2	4.9	12.7	16.8	24861.2	35975.2	118345.9	401063.15	1605056350
		2321	3.8	4.61	4.67	4.69	4.68	4.7	4.72	0.032	0.001
Senni	1409	71	0.2	6	8	10	1101221	12	10650066	3357051	1.12698E+13
		1338	3.8	8.26	8.35	8.45	8.46	8.56	8.68	0.1395	0.0194
TameLM	6168	308	0.2	9.1	10.37	11.15	11.16	11.8	12.56	1.06	1.12
		5859	3.8	10.82	10.82	10.82	10.82	10.82	10.82	5.41	0.000000001
TameHM	4625	231	0.2	9.83	9.95	10.65	10.8	11.54	12.41	0.945	0.89
		4393	3.8	11.05	11.08	11.12	11.12	11.15	11.22	0.0505	0.00259
Tarf	5450	272	0.2	20.7	24.07	28.19	27	30.2	30.9	4.005	16.06
		5177	3.8	14.76	14.76	14.76	14.76	14.76	14.76	0.00004	0.000000002
Windrush	4913	245	27.63	31.87		36.02	1794.13	41.87	17614.66	5558.77	3089964.06
		4667	29.81	30.07	30.27	30.28	30.48	30.79	0.64	0.051	0.08

River	Number of points of the original data set	Number of points for the selected sampling strategy	Sampling density (points/m^2)	Sill							
				Minimum	1stQu	Median	Mean	3rdQu	Maximum	SE	Variance
Cruick	5552	278	0.2	0.019	0.024	0.028	0.028	0.03	0.037	0.0055	0.000033
		5275	3.8	0.029	0.029	0.029	0.029	0.029	0.029	0.0002	0.00000004
Bere	1660	83	0.2	0.0032	0.015	0.021	0.021	0.03	0.036	0.011	0.0001
		1577	3.8	0.03	0.031	0.031	0.031	0.031	0.031	0.0002	0.00000004
Blackwater	3636	181	0.2	0	0.005	0.008	0.008	0.013	0.014	0.0054	0.0000294
		3454	3.8	0.013	0.013	0.013	0.013	0.013	0.013	0.0000625	0
HighlandWater	811	122	0.6	0.012	0.013	0.014	0.014	0.015	0.015	0.00115	0
		770	3.8	0.013	0.013	0.013	0.013	0.013	0.013	0.0001	0.00000002
LeighBrook	6490	324	0.2	0.019	0.02	0.023	0.0229	0.024	0.025	0.0018	0
		6165	3.8	0.023	0.023	0.023	0.023	0.023	0.023	0.000143	0.00000002
PangFenced	2444	122	0.2	0	0.005	0.01	1.35	1.75	8.23	2.57	6.61
		2321	3.8	0.0126	0.0128	0.0128	0.0128	0.0129	0.0129	0.000085	0.000000007
Senni	1409	71	0.2	0	0.04	0.05	1636.82	0.05	15901.8	5014.3705	25143915.44
		1338	3.8	0.049	0.049	0.05	0.049	0.05	0.05	0.0003615	0.00000013
TameLM	6168	308	0.2	0.025	0.027	0.03	0.03	0.031	0.034	0.003125	0.000009
		5859	3.8	0	0.029	0.029	0.029	0.029	0.029	0	0
TameHM	4625	231	0.2	0.036	0.037	0.04	0.04	0.04	0.04	0.0035	0.000015
		4393	3.8	0.039	0.039	0.039	0.039	0.09	0.039	0.0002	0.00000005
Tarf	5450	272	0.2	0.003	0.004	0.004	0.004	0.005	0.005	0.00085	0.0000007
		5177	3.8	0.004	0.004	0.004	0.004	0.004	0.004	0.0000225	5E-10
Windrush	4913	245	27.63	0.063	0.07	0.08	4.02	0.12	39.45	12.4	154.96
		4667	29.81	0.08	0.08	0.08	0.08	0.08	0.001	2.05E-07	0

River	Number of points of the original data set	Number of points for the selected sampling strategy	Sampling density (points/m^2)	Nugget							
				Minimum	1stQu	Median	Mean	3rdQu	Maximum	SE	Variance
Cruick	5552	278	0.2	0	0	0	0	0	0	0	0
		5275	3.8	0	0	0	0	0	0	0	0
Bere	1660	83	0.2	0.0009	0.008	0.013	0.013	0.018	0.024	0.0075	0.00000005
		1577	3.8	0	0	0	0	0	0	0	0
Blackwater	3636	181	0.2	0	0	0.004	0.0055	0.008	0.015	0.006115	0.0000374
		3454	3.8	0	0	0	0	0	0	0	0
HighlandWater	811	122	0.6	0	0	0	0	0	0	0	0
		770	3.8	0	0	0	0	0	0	0	0
LeighBrook	6490	324	0.2	0	0	0	0	0	0	0.0015	0.000006
		6165	3.8	0	0	0	0	0	0	0	0
PangFenced	2444	122	0.2	0	0.008	0.01	0.008	0.01	0.01	0.005	0.00002
		2321	3.8	0	0	0	0	0	0	0	0
Senni	1409	71	0.2	0	0	0.003	0.01	0.01	0.04	0.015	0.00025
		1338	3.8	0	0	0	0	0	0	0	0
TameLM	6168	308	0.2	0	0	0	0	0	0	0	0
		5859	3.8	0	0	0	0	0	0	0	0
TameHM	4625	231	0.2	0	0	0	0	0	0	0	0
		4393	3.8	0	0	0	0	0	0	0	0
Tarf	5450	272	0.2	0	0.0002	0.0005	0.0005	0.0009	0.001	0.0004	0.0000001
		5177	3.8	0	0	0	0	0	0	0	0
Windrush	4913	245	27.63	0	0	0	0.0017	0.0027	0.007	0.0025	0.000007
		4667	29.81	0	0	0	0	0	0	0	0

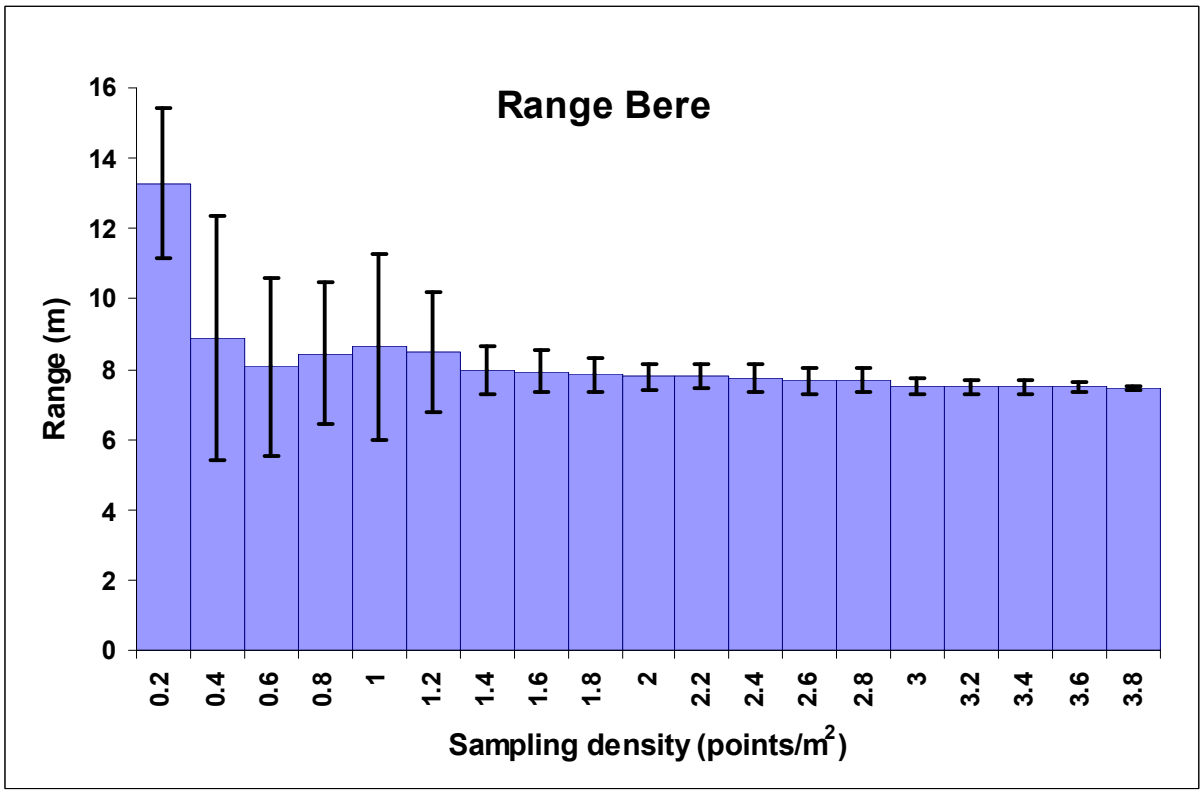
Range Bere
Range (m)
16
14
12
10
8
6
4
2
0
0.2
0.4
0.6
0.8
1
1.2
1.4
1.6
1.8
2
2.2
2.4
2.6
2.8
3
3.2
3.4
3.6
3.8
Sampling density (points/m2)

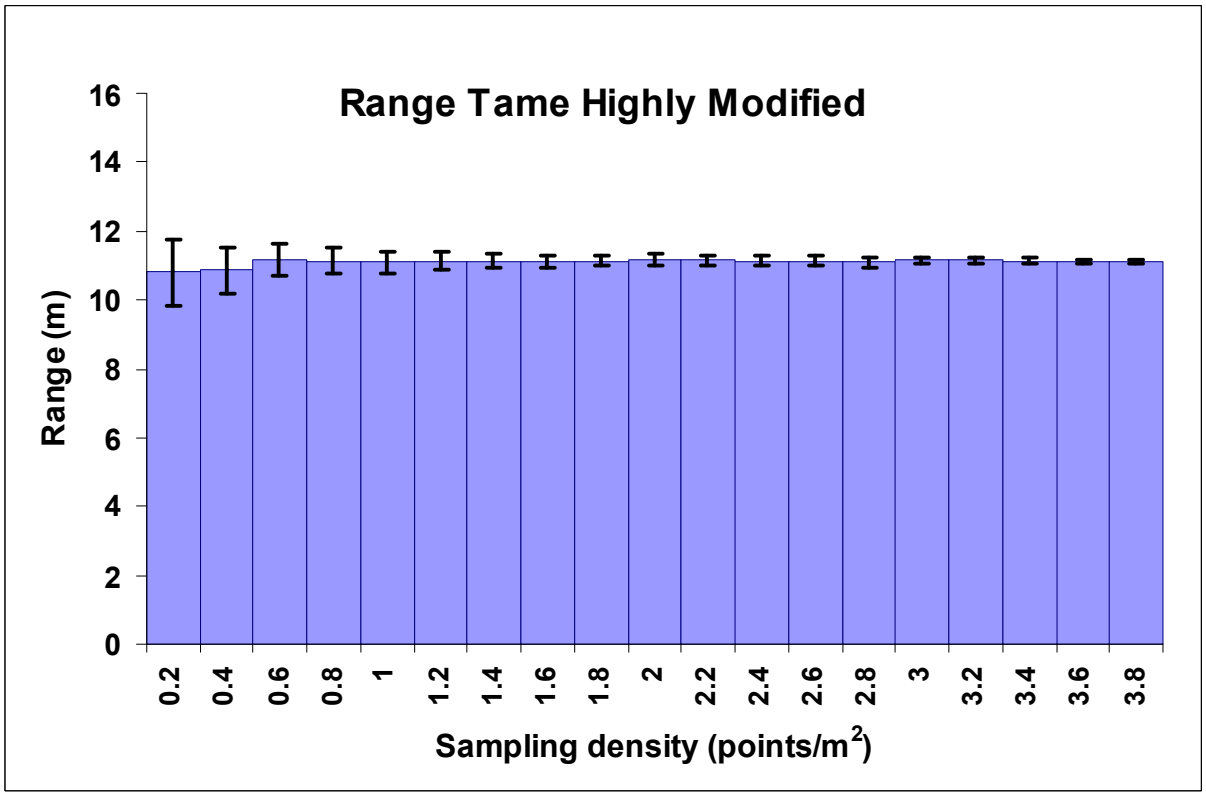
Range Tame Highly Modified
Range (m)
16
14
12
10
8
6
4
2
0
0.2
0.4
0.6
0.8
1
1.2
1.4
1.6
1.8
2
2.2
2.4
2.6
2.8
3
3.2
3.4
3.6
3.8
Sampling density (points/m2)

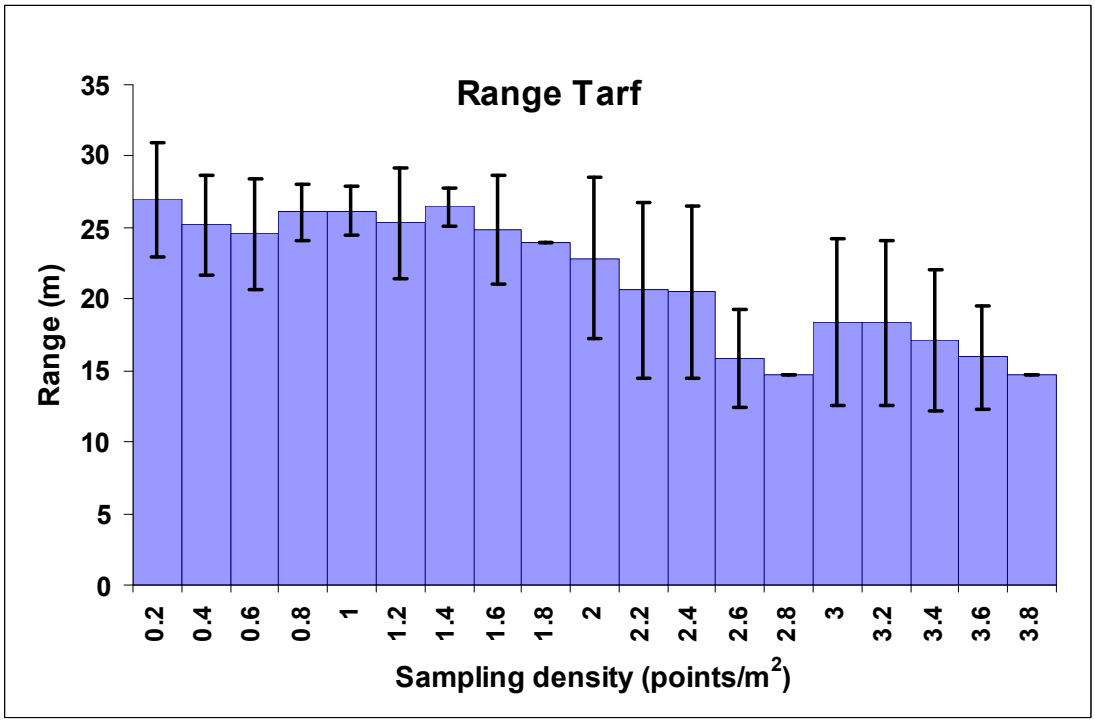
Range Tarf
Range (m)
35
30
25
20
15
10
5
0
0.2
0.4
0.6
0.8
1
1.2
1.4
1.6
1.8
2
2.2
2.4
2.6
2.8
3
3.2
3.4
3.6
3.8
Sampling density (points/m2)

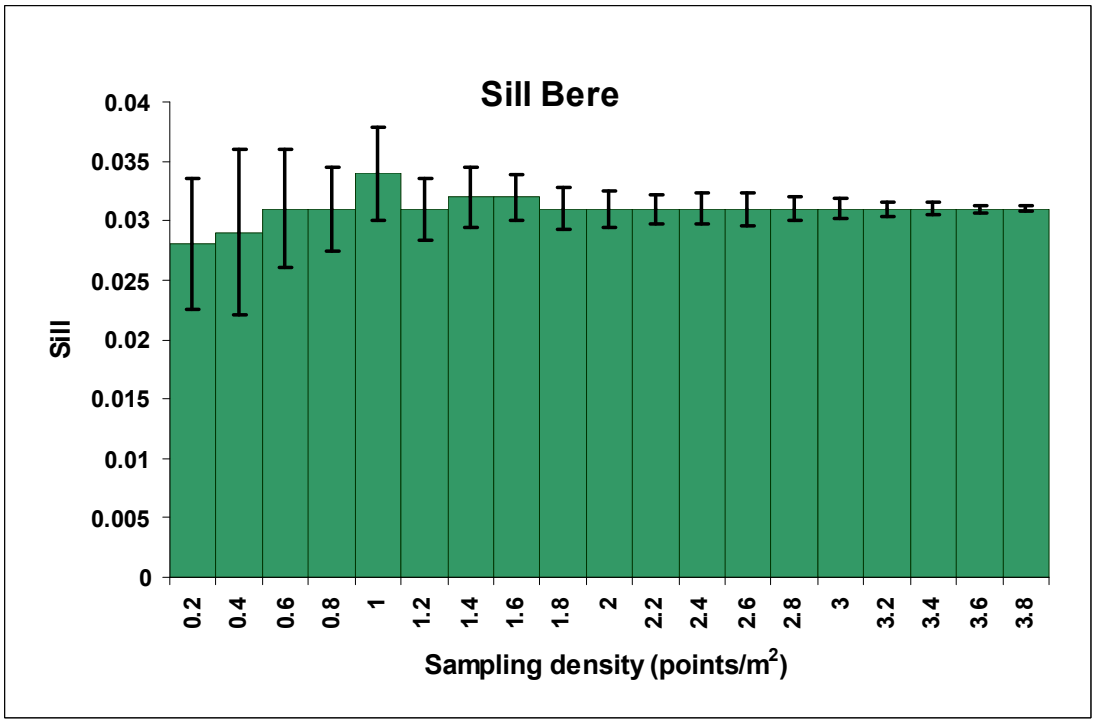
Sill Bere
Sill
0.04
0.035
0.03
0.025
0.02
0.015
0.01
0.005
0
0.2
0.4
0.6
0.8
1
1.2
1.4
1.6
1.8
2
2.2
2.4
2.6
2.8
3
3.2
3.4
3.6
3.8
Sampling density (points/m2)

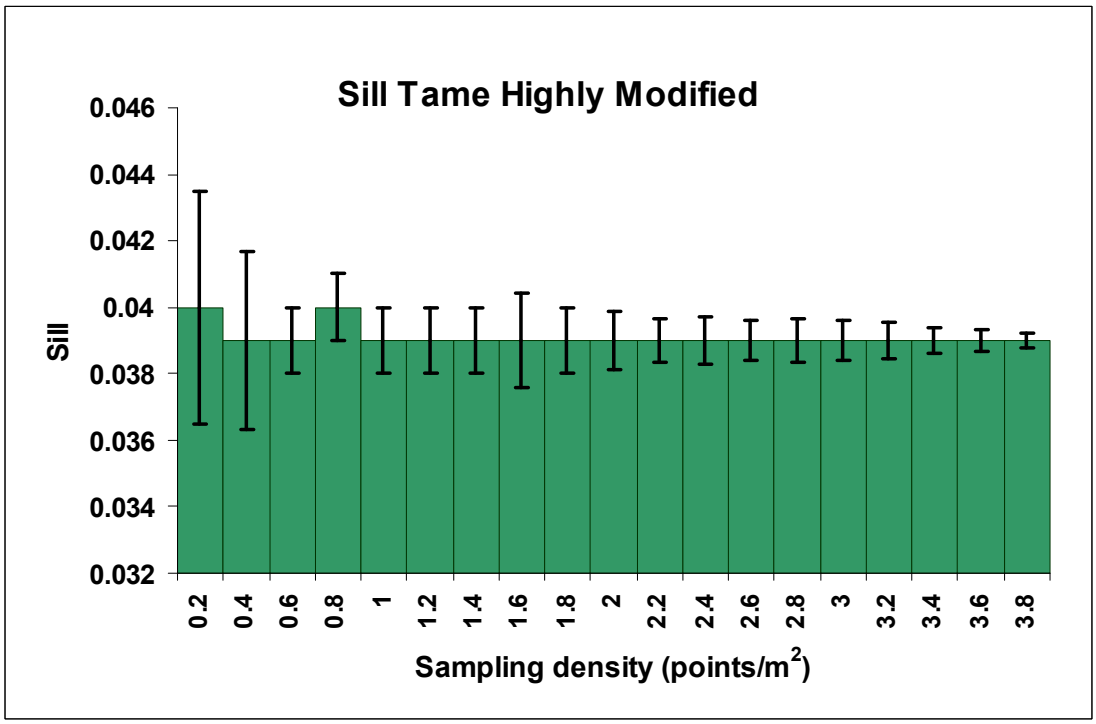
Sill Tame Highly Modified
Sill
0.046
0.044
0.042
0.04
0.038
0.036
0.034
0.032
0.2
0.4
0.6
0.8
1
1.2
1.4
1.6
1.8
2
2.2
2.4
2.6
2.8
3
3.2
3.4
3.6
3.8
Sampling density (points/m2)

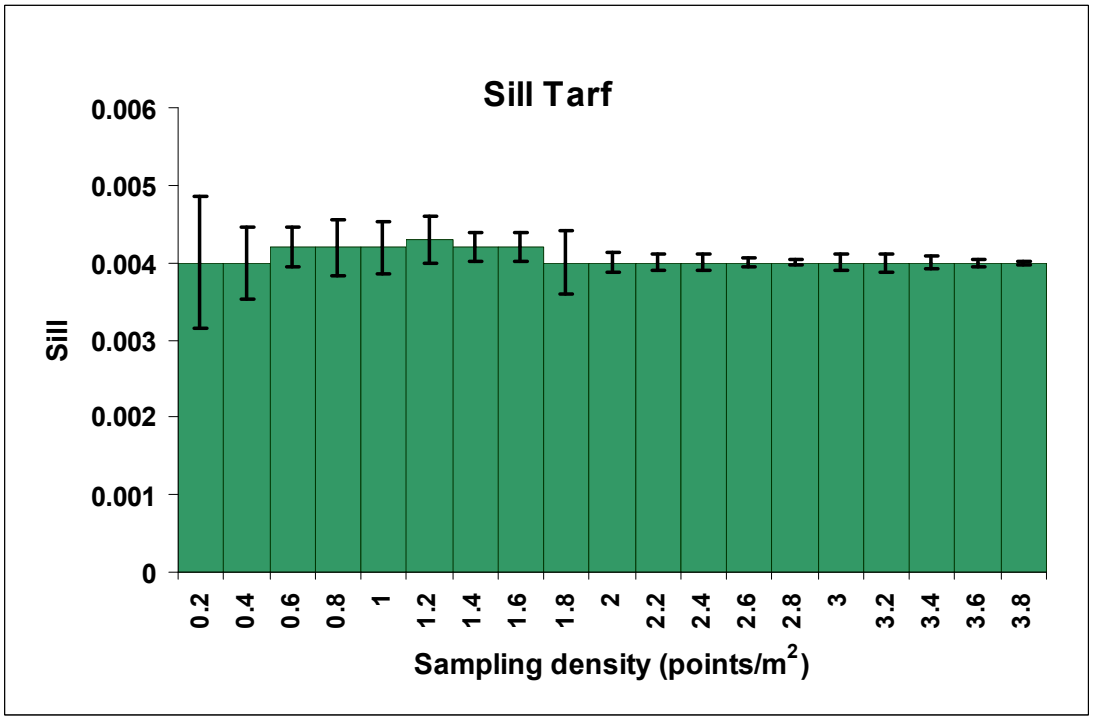
Sill Tarf
Sill
0.006
0.005
0.004
0.003
0.002
0.001
0
0.2
0.4
0.6
0.8
1
1.2
1.4
1.6
1.8
2
2.2
2.4
2.6
2.8
3
3.2
3.4
3.6
3.8
Sampling density (points/m2)

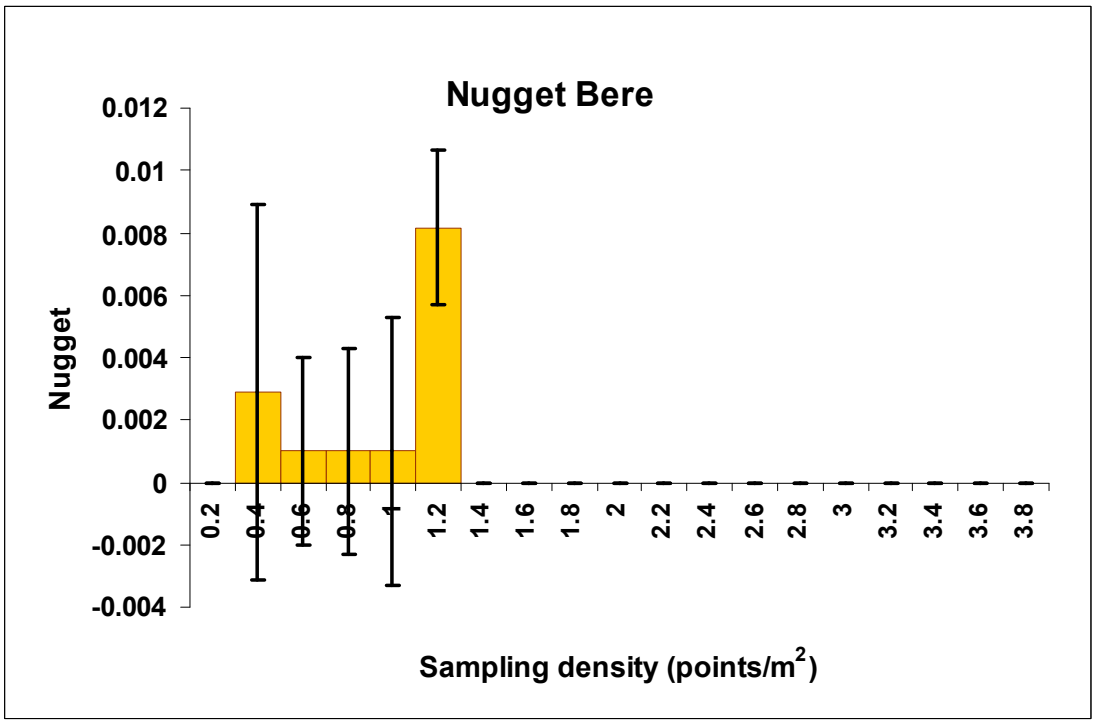
Nugget Bere
0.012
0.01
0.008
0.006
0.004
0.002
0
-0.002
-0.004
Nugget
0.2
0.4
0.6
0.8
1
1.2
1.4
1.6
1.8
2
2.2
2.4
2.6
2.8
3
3.2
3.4
3.6
3.8
Sampling density (points/m2)

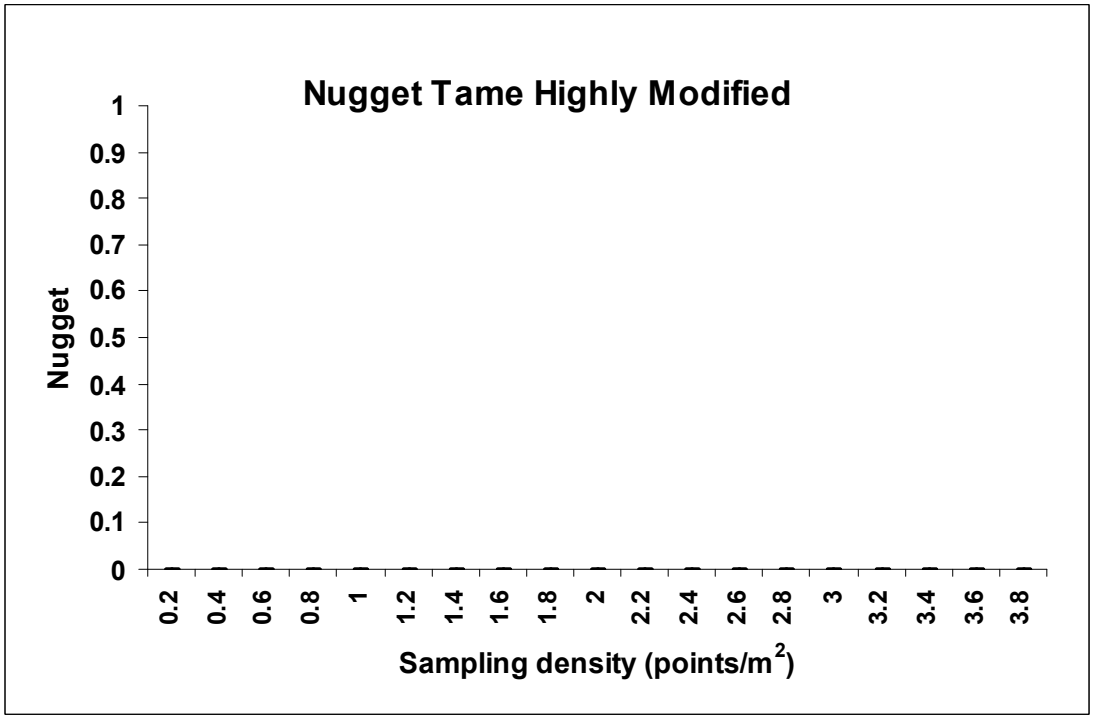
Nugget Tame Highly Modified
1
0.9
0.8
0.7
0.6
0.5
0.4
0.3
0.2
0.1
0
Nugget
0.2
0.4
0.6
0.8
1
1.2
1.4
1.6
1.8
2
2.2
2.4
2.6
2.8
3
3.2
3.4
3.6
3.8
Sampling density (points/m2)

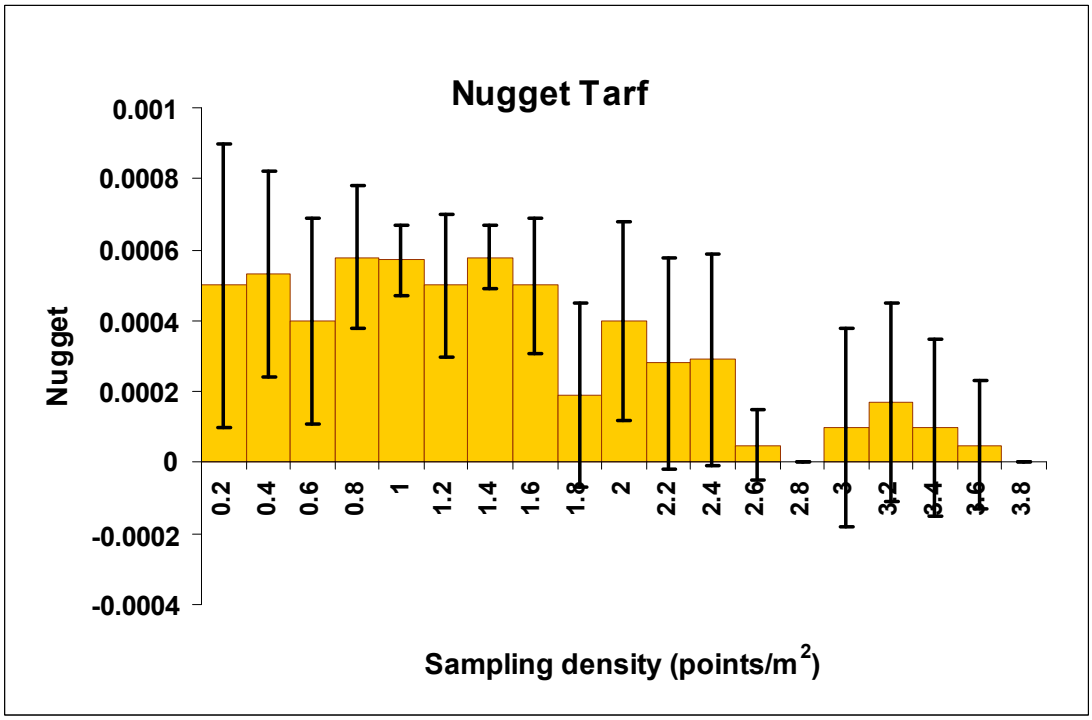

Sampling Density (points/m^2)	Number of points		
	Bere	Tame Highly Modified	Tarf
0.2	83	231	272
0.4	166	462	545
0.6	249	693	817
0.8	332	925	1090
1	415	1156	1362
1.2	498	1387	1635
1.4	581	1618	1907
1.6	664	1850	2180
1.8	747	2081	2452
2	830	2312	2725
2.2	913	2543	2997
2.4	996	2775	3270
2.6	1079	3006	3542
2.8	1162	3237	3815
3	1245	3468	4087
3.2	1328	3700	4360
3.4	1411	3931	4632
3.6	1494	4162	4905
3.8	1577	4393	5177
4	1660	4625	5450